

Averages of b -hadron, c -hadron, and τ -lepton properties as of 2018

Heavy Flavor Averaging Group (HFLAV):

Y. Amhis¹, Sw. Banerjee², E. Ben-Haim³, F. U. Bernlochner⁴, M. Bona⁵,
 A. Bozek⁶, C. Bozzi⁷, J. Brodzicka⁶, M. Chrzaszcz⁶, J. Dingfelder⁴, S. Duell⁴,
 U. Egede⁸, M. Gersabeck⁹, T. Gershon¹⁰, P. Goldenzweig¹¹, K. Hayasaka¹²,
 H. Hayashii¹³, D. Johnson¹⁴, M. Kenzie¹⁵, T. Kuhr¹⁶, O. Leroy¹⁷, H.-B. Li^{18,19},
 A. Lusiani^{20,21}, H.-L. Ma¹⁸, K. Miyabayashi¹³, P. Naik²², T. Nanut²³, M. Patel²⁴,
 A. Pompili^{25,26}, M. Rama²¹, M. Roney²⁷, M. Rotondo²⁸, O. Schneider²³,
 C. Schwanda²⁹, A. J. Schwartz³⁰, B. Shwartz^{31,32}, J. Serrano¹⁷, A. Soffer³³,
 D. Tonelli³⁴, P. Urquijo³⁵, R. Van Kooten³⁶, and J. Yelton³⁷

¹*LAL, Université Paris-Sud, CNRS/IN2P3, Orsay, France*

²*University of Louisville, Louisville, Kentucky, USA*

³*LPNHE, Sorbonne Université, Paris Diderot Sorbonne Paris Cité, CNRS/IN2P3, Paris, France*

⁴*University of Bonn, Bonn, Germany*

⁵*School of Physics and Astronomy, Queen Mary University of London, London, UK*

⁶*H. Niewodniczanski Institute of Nuclear Physics, Kraków, Poland*

⁷*INFN Sezione di Ferrara, Ferrara, Italy*

⁸*School of Physics and Astronomy, Monash University, Melbourne, Australia*

⁹*School of Physics and Astronomy, University of Manchester, Manchester, UK*

¹⁰*Department of Physics, University of Warwick, Coventry, UK*

¹¹*Institut für Experimentelle Teilchenphysik, Karlsruher Institut für Technologie, Karlsruhe, Germany*

¹²*Niigata University, Niigata, Japan*

¹³*Nara Women's University, Nara, Japan*

¹⁴*European Organization for Nuclear Research (CERN), Geneva, Switzerland*

¹⁵*Cavendish Laboratory, University of Cambridge, Cambridge, UK*

¹⁶*Ludwig-Maximilians-University, Munich, Germany*

¹⁷*Aix Marseille Univ, CNRS/IN2P3, CPPM, Marseille, France*

¹⁸*Institute of High Energy Physics, Beijing 100049, People's Republic of China*

¹⁹*University of Chinese Academy of Sciences, Beijing 100049, People's Republic of China*

²⁰*Scuola Normale Superiore, Pisa, Italy*

²¹*INFN Sezione di Pisa, Pisa, Italy*

²²*H.H. Wills Physics Laboratory, University of Bristol, Bristol, UK*

²³*Institute of Physics, Ecole Polytechnique Fédérale de Lausanne (EPFL), Lausanne, Switzerland*

²⁴*Imperial College London, London, UK*

²⁵*Università di Bari Aldo Moro, Bari, Italy*

²⁶*INFN Sezione di Bari, Bari, Italy*

²⁷*University of Victoria, Victoria, British Columbia, Canada*

²⁸*Laboratori Nazionali dell'INFN di Frascati, Frascati, Italy*

²⁹*Institute of High Energy Physics, Vienna, Austria*

³⁰*University of Cincinnati, Cincinnati, Ohio, USA*

³¹*Budker Institute of Nuclear Physics (SB RAS), Novosibirsk, Russia*

³²*Novosibirsk State University, Novosibirsk, Russia*

³³*Tel Aviv University, Tel Aviv, Israel*

³⁴*INFN Sezione di Trieste, Trieste, Italy*

³⁵*School of Physics, University of Melbourne, Melbourne, Victoria, Australia*

³⁶*Indiana University, Bloomington, Indiana, USA*

³⁷*University of Florida, Gainesville, Florida, USA*

November 5, 2019

Abstract

This paper reports world averages of measurements of b -hadron, c -hadron, and τ -lepton properties obtained by the Heavy Flavor Averaging Group using results available through September 2018. In rare cases, significant results obtained several months later are also used. For the averaging, common input parameters used in the various analyses are adjusted (rescaled) to common values, and known correlations are taken into account. The averages include branching fractions, lifetimes, neutral meson mixing parameters, CP violation parameters, parameters of semileptonic decays, and Cabibbo-Kobayashi-Maskawa matrix elements.

Contents

1 Executive Summary	8
2 Introduction	13
3 Averaging methodology	15
3.1 Treatment of correlated systematic uncertainties	16
3.2 Treatment of non-Gaussian likelihood functions	19
4 Production fractions, lifetimes and mixing parameters of b hadrons	22
4.1 b -hadron production fractions	22
4.1.1 b -hadron production fractions in $\Upsilon(4S)$ decays	23
4.1.2 b -hadron production fractions at the $\Upsilon(5S)$ energy	25
4.1.3 b -hadron production fractions at high energy	27
4.2 b -hadron lifetimes	32
4.2.1 Overview of lifetime measurements	33
4.2.2 Inclusive b -hadron lifetimes	35
4.2.3 B^0 and B^+ lifetimes and their ratio	36
4.2.4 B_s^0 lifetimes	38
4.2.5 B_c^+ lifetime	43
4.2.6 Λ_b^0 and b -baryon lifetimes	43
4.2.7 Summary and comparison with theoretical predictions	44
4.3 Neutral B -meson mixing	47
4.3.1 B^0 mixing parameters $\Delta\Gamma_d$ and Δm_d	48
4.3.2 B_s^0 mixing parameters $\Delta\Gamma_s$ and Δm_s	50
4.3.3 CP violation in B^0 and B_s^0 mixing	56
4.3.4 Mixing-induced CP violation in B_s^0 decays	60
5 Measurements related to Unitarity Triangle angles	64
5.1 Introduction	64
5.2 Notations	66
5.2.1 CP asymmetries	66
5.2.2 Time-dependent CP asymmetries in decays to CP eigenstates	67
5.2.3 Time-dependent distributions with non-zero decay width difference	69
5.2.4 Time-dependent CP asymmetries in decays to vector-vector final states	70
5.2.5 Time-dependent asymmetries: self-conjugate multiparticle final states	71
5.2.6 Time-dependent CP asymmetries in decays to non- CP eigenstates	74
5.2.7 Asymmetries in $B \rightarrow D^{(*)} K^{(*)}$ decays	79
5.3 Common inputs and uncertainty treatment	84
5.4 Time-dependent asymmetries in $b \rightarrow c\bar{s}$ transitions	84
5.4.1 Time-dependent CP asymmetries in $b \rightarrow c\bar{s}$ decays to CP eigenstates	84
5.4.2 Time-dependent transversity analysis of $B^0 \rightarrow J/\psi K^{*0}$ decays	86
5.4.3 Time-dependent CP asymmetries in $B^0 \rightarrow D^{*+} D^{*-} K_s^0$ decays	88
5.4.4 Time-dependent analysis of B_s^0 decays through the $b \rightarrow c\bar{s}$ transition	88
5.5 Time-dependent CP asymmetries in colour-suppressed $b \rightarrow c\bar{u}\bar{d}$ transitions	89
5.5.1 Time-dependent CP asymmetries: $b \rightarrow c\bar{u}\bar{d}$ decays to CP eigenstates	89

5.5.2	Time-dependent Dalitz-plot analyses of $b \rightarrow c\bar{u}d$ decays	89
5.6	Time-dependent CP asymmetries in $b \rightarrow c\bar{c}d$ transitions	91
5.6.1	Time-dependent CP asymmetries in B_s^0 decays mediated by $b \rightarrow c\bar{c}d$ transitions	93
5.7	Time-dependent CP asymmetries in charmless $b \rightarrow q\bar{q}s$ transitions	94
5.7.1	Time-dependent CP asymmetries: $b \rightarrow q\bar{q}s$ decays to CP eigenstates	96
5.7.2	Time-dependent Dalitz plot analyses: $B^0 \rightarrow K^+K^-K^0$ and $B^0 \rightarrow \pi^+\pi^-K_s^0$	99
5.7.3	Time-dependent analyses of $B^0 \rightarrow \phi K_s^0\pi^0$	105
5.7.4	Time-dependent CP asymmetries in $B_s^0 \rightarrow K^+K^-$	105
5.7.5	Time-dependent CP asymmetries in $B_s^0 \rightarrow \phi\phi$	106
5.8	Time-dependent CP asymmetries in $b \rightarrow q\bar{q}d$ transitions	106
5.9	Time-dependent asymmetries in $b \rightarrow s\gamma$ transitions	106
5.10	Time-dependent asymmetries in $b \rightarrow d\gamma$ transitions	109
5.11	Time-dependent CP asymmetries in $b \rightarrow u\bar{u}d$ transitions	109
5.11.1	Constraints on $\alpha \equiv \phi_2$	117
5.12	Time-dependent CP asymmetries in $b \rightarrow c\bar{u}d/u\bar{c}d$ transitions	119
5.13	Time-dependent CP asymmetries in $b \rightarrow c\bar{u}s/u\bar{c}s$ transitions	122
5.13.1	Time-dependent CP asymmetries in $B^0 \rightarrow D^\mp K_s^0\pi^\pm$	122
5.13.2	Time-dependent CP asymmetries in $B_s^0 \rightarrow D_s^\mp K^\pm$	122
5.14	Rates and asymmetries in $B \rightarrow D^{(*)}K^{(*)}$ decays	122
5.14.1	D decays to CP eigenstates	122
5.14.2	D decays to quasi- CP eigenstates	125
5.14.3	D decays to suppressed final states	125
5.14.4	D decays to multiparticle self-conjugate final states (model-dependent analysis)	130
5.14.5	D decays to multiparticle self-conjugate final states (model-independent analysis)	133
5.14.6	D decays to multiparticle non-self-conjugate final states (model-independent analysis)	138
5.14.7	Combinations of results on rates and asymmetries in $B \rightarrow D^{(*)}K^{(*)}$ decays to obtain constraints on $\gamma \equiv \phi_3$	138
5.15	Summary of the constraints on the angles of the Unitarity Triangle	145
6	Semileptonic B decays	146
6.1	Exclusive CKM-favoured decays	146
6.1.1	$\overline{B} \rightarrow D^*\ell^-\bar{\nu}_\ell$	146
6.1.2	$\overline{B} \rightarrow D\ell^-\bar{\nu}_\ell$	150
6.1.3	$\overline{B} \rightarrow D^{(*)}\pi\ell^-\bar{\nu}_\ell$	154
6.1.4	$\overline{B} \rightarrow D^{**}\ell^-\bar{\nu}_\ell$	154
6.2	Inclusive CKM-favored decays	157
6.2.1	Global analysis of $\overline{B} \rightarrow X_c\ell^-\bar{\nu}_\ell$	157
6.2.2	Analysis in the kinetic scheme	159
6.2.3	Analysis in the 1S scheme	160
6.3	Exclusive CKM-suppressed decays	162
6.3.1	$B \rightarrow \pi\ell\nu$ branching fraction and q^2 spectrum	163
6.3.2	$ V_{ub} $ from $B \rightarrow \pi\ell\nu$	164

6.3.3	Combined extraction of $ V_{ub} $ and $ V_{cb} $	166
6.3.4	Other exclusive charmless semileptonic B decays	167
6.4	Inclusive CKM-suppressed decays	172
6.4.1	BLNP	173
6.4.2	DGE	174
6.4.3	GGOU	174
6.4.4	ADFR	175
6.4.5	BLL	176
6.4.6	Summary	177
6.5	$B \rightarrow D^{(*)}\tau\nu_\tau$ decays	177
7	Decays of b-hadrons into open or hidden charm hadrons	182
7.1	Decays of \bar{B}^0 mesons	183
7.1.1	Decays to a single open charm meson	183
7.1.2	Decays to two open charm mesons	190
7.1.3	Decays to charmonium states	194
7.1.4	Decays to charm baryons	200
7.1.5	Decays to XYZ states	201
7.2	Decays of B^- mesons	204
7.2.1	Decays to a single open charm meson	204
7.2.2	Decays to two open charm mesons	209
7.2.3	Decays to charmonium states	212
7.2.4	Decays to charm baryons	217
7.2.5	Decays to other (XYZ) states	218
7.3	Decays of admixtures of \bar{B}^0/B^- mesons	221
7.3.1	Decays to two open charm mesons	221
7.3.2	Decays to charmonium states	221
7.3.3	Decays to other (XYZ) states	222
7.4	Decays of \bar{B}_s^0 mesons	223
7.4.1	Decays to a single open charm meson	223
7.4.2	Decays to two open charm mesons	225
7.4.3	Decays to charmonium states	226
7.4.4	Decays to charm baryons	228
7.5	Decays of B_c^- mesons	229
7.5.1	Decays to a single open charm meson	229
7.5.2	Decays to two open charm mesons	229
7.5.3	Decays to charmonium states	230
7.5.4	Decays to a B meson	232
7.6	Decays of b baryons	232
7.6.1	Decays to a single open charm meson	232
7.6.2	Decays to charmonium states	232
7.6.3	Decays to charm baryons	234
7.6.4	Decays to other (XYZ) states	235

8	<i>B</i> decays to charmless final states	236
8.1	Mesonic decays of B^0 and B^+ mesons	237
8.2	Baryonic decays of B^+ and B^0 mesons	248
8.3	Decays of b baryons	251
8.4	Decays of B_s^0 mesons	254
8.5	Radiative and leptonic decays of B^0 and B^+ mesons.	257
8.6	Charge asymmetries in b -hadron decays	270
8.7	Polarization measurements in b -hadron decays	276
8.8	Decays of B_c^+ mesons	281
9	Charm physics	282
9.1	D^0 - \bar{D}^0 mixing and CP violation	282
9.1.1	Introduction	282
9.1.2	Input observables	283
9.1.3	Fit results	285
9.1.4	Conclusions	289
9.2	CP asymmetries	297
9.3	T -odd asymmetries	307
9.4	Interplay of direct and indirect CP violation	309
9.5	Semileptonic decays	312
9.5.1	Introduction	312
9.5.2	$D \rightarrow P \bar{\ell} \nu_\ell$ decays	312
9.5.3	Form factor parameterizations	312
9.5.4	Simple pole	313
9.5.5	z expansion	313
9.5.6	Three-pole formalism	314
9.5.7	Experimental techniques and results	315
9.5.8	Combined results for the $D \rightarrow K \ell \nu_\ell$ and $D \rightarrow \pi \ell \nu_\ell$ channels	316
9.5.9	Form factors of other $D_{(s)} \rightarrow P \ell \nu_\ell$ decays	316
9.5.10	Determinations of $ V_{cs} $ and $ V_{cd} $	320
9.5.11	Test of e - μ lepton flavor universality	322
9.5.12	$D \rightarrow V \ell \nu_\ell$ decays	323
9.5.13	Vector form factor measurements	324
9.5.14	$D \rightarrow S \ell^+ \nu_\ell$ decays	326
9.5.15	$D \rightarrow A \ell^+ \nu_\ell$ decays	327
9.6	Leptonic decays	328
9.6.1	$D^+ \rightarrow \ell^+ \nu_\ell$ decays and $ V_{cd} $	329
9.6.2	$D_s^+ \rightarrow \ell^+ \nu_\ell$ decays and $ V_{cs} $	329
9.6.3	Comparison with other determinations of $ V_{cd} $ and $ V_{cs} $	331
9.6.4	Extraction of $D_{(s)}$ meson decay constants	333
9.7	Hadronic D^0 decays and final state radiation	335
9.7.1	Updates to the branching fractions	336
9.7.2	Average branching fractions for $D^0 \rightarrow K^- \pi^+$, $D^0 \rightarrow \pi^+ \pi^-$ and $D^0 \rightarrow K^+ K^-$	340
9.7.3	Average branching fraction for $D^0 \rightarrow K^+ \pi^-$	341
9.7.4	Consideration of PHOTOS++	342

9.8	Hadronic D_s decays	344
9.9	Excited $D_{(s)}$ mesons	347
9.10	Excited charm baryons	357
9.11	Rare and forbidden decays	362
10	Tau lepton properties	373
10.1	Branching fraction fit	373
10.1.1	Technical implementation of the fit procedure	373
10.1.2	Fit results	375
10.1.3	Changes with respect to the previous report	375
10.1.4	Differences between the HFLAV 2018 fit and the PDG 2018 fit	375
10.1.5	Branching ratio fit results and experimental inputs	376
10.1.6	Correlation terms between basis branching fractions uncertainties	391
10.1.7	Equality constraints	394
10.2	Tests of lepton universality	400
10.3	Universality-improved $\mathcal{B}(\tau \rightarrow e\nu\bar{\nu})$ and R_{had}	401
10.4	$ V_{us} $ measurement	402
10.4.1	$ V_{us} $ from $\mathcal{B}(\tau \rightarrow X_s\nu)$	402
10.4.2	$ V_{us} $ from $\mathcal{B}(\tau \rightarrow K\nu)/\mathcal{B}(\tau \rightarrow \pi\nu)$	403
10.4.3	$ V_{us} $ from $\mathcal{B}(\tau \rightarrow K\nu)$	404
10.4.4	$ V_{us} $ from τ summary	405
10.5	Combination of upper limits on τ lepton-flavour-violating branching fractions . .	406
11	Acknowledgments	412
References		415

1 Executive Summary

This paper provides updated world averages of measurements of b -hadron, c -hadron, and τ -lepton properties using results available by September 2018. In a few cases, later important results are included and clearly labelled as such. While new measurements since the previous version of this paper [1] have been dominated by the LHCb and the BESIII experiment in, there are new results from many other experiments, and the older results from previous generations of experiments are still very important. The future will provide updated results, with the most important change being that Belle II has started data taking in 2019.

Since the previous version of the paper, the b -hadron fraction, lifetime and mixing averages have mostly made small incremental progress in precision, with the most significant improvements in several effective B_s^0 lifetimes. In total 14 new results (of which 12 from the LHC data and 2 from the KEKB data) have been incorporated in these averages.

The lifetime hierarchy for the most abundant weakly decaying b -hadron species is well established, with impressive precisions of 4 fs for the most common B^0 , B^+ and B_s^0 mesons, and compatible with the expectations from the Heavy Quark Expansion. However, small sample sizes still limit the precision for b baryons heavier than Λ_b^0 (Ξ_b^- , Ξ_b^0 , Ω_b , and all other yet-to-be-discovered b baryons). A sizable value of the decay width difference in the B_s^0 – \bar{B}_s^0 system is measured with a relative precision of 6% and is well predicted by the Standard Model (SM). In contrast, the experimental results for the decay width difference in the B^0 – \bar{B}^0 system are not yet precise enough to distinguish the small (expected) value from zero. The mass differences in both systems are known very accurately, to the (few) per mil level. On the other hand, CP violation in the mixing of either system has not been observed yet, with asymmetries known within a couple per mil but still consistent both with zero and their SM predictions. A similar conclusion holds for the CP violation induced by B_s^0 mixing in the $b \rightarrow c\bar{c}s$ transition, although in this case the experimental uncertainty on the corresponding weak phase is an order of magnitude larger, but now smaller than the SM central value. Many measurements are still dominated by statistical uncertainties and will improve once new results from the LHC Run 2 become available, and later from LHC Run 3 and Belle II.

The measurement of $\sin 2\beta \equiv \sin 2\phi_1$ from $b \rightarrow c\bar{c}s$ transitions such as $B^0 \rightarrow J/\psi K_s^0$ has reached better than 2.5 % precision: $\sin 2\beta \equiv \sin 2\phi_1 = 0.699 \pm 0.017$. Measurements of the same parameter using different quark-level processes provide a consistency test of the SM and allow insight into possible beyond the Standard Model effects. All results among hadronic $b \rightarrow s$ penguin dominated decays of B^0 mesons are currently consistent with the SM expectations. Measurements of CP violation parameters in $B_s^0 \rightarrow \phi\phi$ allow a similar comparison to the value of $\phi_s^{c\bar{c}s}$; where results again are consistent with the close to zero SM expectation. Among measurements related to the Unitarity Triangle angle $\alpha \equiv \phi_2$, results from B decays to $\pi\pi$, $\rho\pi$ and $\rho\rho$ are combined to obtain a world average value of $(84.9^{+5.1}_{-4.5})^\circ$. Knowledge of the third angle $\gamma \equiv \phi_3$ also continues to improve, with the current world average being $(71.1^{+4.6}_{-5.3})^\circ$. The constraints on the angles of the Unitarity Triangle are summarized in Fig. 49.

In semileptonic B meson decays, the anomalies in the magnitudes of the CKM elements $|V_{cb}|$ and $|V_{ub}|$ remain at about the same level compared to the previous update: the discrepancy between $|V_{cb}|$ measured with inclusive and exclusive decays is of the order of 3σ (3.3σ for $|V_{cb}|$ from $\bar{B} \rightarrow D^*\ell^-\bar{\nu}_\ell$, 2.0σ for $|V_{cb}|$ from $\bar{B} \rightarrow D\ell^-\bar{\nu}_\ell$). The difference between $|V_{ub}|$ measured with inclusive decays $\bar{B} \rightarrow X_u\ell^-\bar{\nu}_\ell$ and $|V_{ub}|$ from $\bar{B} \rightarrow \pi\ell^-\bar{\nu}_\ell$ has fallen to 2.8σ . Some decrease is observed in the size of the $B \rightarrow D^{(*)}\tau\nu_\tau$ decays anomaly: the combined discrepancy of

the measured values of $\mathcal{R}(D^*)$ and $\mathcal{R}(D)$ to their SM expectations is found to be 3.1σ .

The most important new measurements of rare b -hadron decays are coming from the LHC. Precision measurements of B_s^0 decays are particularly noteworthy, including several measurements of the longitudinal polarisation fraction from LHCb. ATLAS and LHCb have updated their measurements of the branching fractions of $B_{(s)}^0 \rightarrow \mu^+\mu^-$ decays, improving the sensitivity. There are more and more measurements of observables related to $b \rightarrow sll$ transitions. One of the observables measured by LHCb, P'_5 , differs from the SM prediction by 3.7σ in one of the squared dimuon mass intervals; results from Belle on this observable are consistent but less precise. Improved measurements from LHCb and other experiments are keenly anticipated. A measurement of the ratio of branching fractions of $B^+ \rightarrow K^+\mu^+\mu^-$ and $B^+ \rightarrow K^+e^+e^-$ decays (R_K) has been made by LHCb. In the low squared dilepton mass region, it differs from the SM prediction by 2.6σ . Among the CP violating observables in rare decays, the “ $K\pi$ puzzle” persists, and important new results have appeared in three-body decays. LHCb has produced many other results on a wide variety of decays, including b -baryon and B_c^+ -meson decays.

About 800 b to charm results from *BABAR*, Belle, CDF, D0, LHCb, CMS, and ATLAS reported in more than 200 papers are compiled in a list of over 600 averages. The large samples of b hadrons that are available in contemporary experiments allows measurements of decays to states with open or hidden charm content with unprecedented precision. In addition to improvements in precision for branching fractions of \bar{B}^0 and B^- mesons, many new decay modes have been discovered. In addition, the set of measurements available for \bar{B}_s^0 and B_c^- mesons as well as for b baryon decays is rapidly increasing.

In the charm sector, the main highlight is the discovery of CP violation. A global fit to measurements of $D^0 \rightarrow K^+K^-/\pi^+\pi^-$ decays gives $\Delta a_{CP}^{\text{dir}} = (-0.164 \pm 0.028)\%$, confirming the observation of direct CP violation with indirect CP violation being compatible with zero. Measurements of 49 observables from the E791, FOCUS, Belle, *BABAR*, CLEO, BESIII, CDF, and LHCb experiments are input into a global fit for 10 underlying parameters, and the no-mixing hypothesis is excluded at a confidence level above 11σ . The mixing parameters x and y individually differ from zero by 3.1σ and above 11σ , respectively. This is the first time that x has been found to be non-zero at a significance exceeding 3σ . The world average value for the observable y_{CP} is positive, indicating that the CP -even state is shorter-lived as in the $K^0-\bar{K}^0$ system; however, the CP -even state also appears to be the heavier one, which differs from the $K^0-\bar{K}^0$ system. The CP violation parameters $|q/p|$ and ϕ are consistent with the CP symmetry hypothesis within 1σ . Thus there is no evidence for CP violation arising from mixing ($|q/p| \neq 1$) or from a phase difference between the mixing amplitude and a direct decay amplitude ($\phi \neq 0$). The world’s most precise measurements of $|V_{cd}|$ and $|V_{cs}|$ are obtained from leptonic $D^+ \rightarrow \mu^+\nu$ and $D_s^+ \rightarrow \mu^+\nu/\tau^+\nu$ decays, respectively. These measurements have theoretical uncertainties arising from decay constants. However, calculations of decay constants within lattice QCD have improved such that the theory error is below 15% of the experimental uncertainties of the measurements.

The τ branching fraction fit has been updated using 7 new branching fraction measurements by *BABAR* that were released in 2018. With respect to the HFLAV Spring 2017 report, there are no significant changes to the lepton universality tests. The precision of $|V_{us}|$ from $\mathcal{B}(\tau \rightarrow X_s\nu)$ improved by about 10%. There is no significant variation of the significance of the about 3σ discrepancy between $|V_{us}|$ from $\mathcal{B}(\tau \rightarrow X_s\nu)$ and $|V_{us}|$ from $|V_{ud}|$ and the CKM matrix unitarity. No additional upper limit on τ lepton-flavour-violating branching fractions has been added.

A small selection of highlights of the results described in Sections 4–10 is given in Table 1.

Table 1: Selected world averages. Where two uncertainties are given the first is statistical and the second is systematic, except where indicated otherwise.

<i>b</i>-hadron lifetimes	
$\tau(B^0)$	1.519 ± 0.004 ps
$\tau(B^+)$	1.638 ± 0.004 ps
$\bar{\tau}(B_s^0) = 1/\Gamma_s$	1.510 ± 0.004 ps
$\tau(B_{sL}^0)$	1.414 ± 0.006 ps
$\tau(B_{sH}^0)$	1.619 ± 0.009 ps
$\tau(B_c^+)$	0.510 ± 0.009 ps
$\tau(\Lambda_b^0)$	1.471 ± 0.009 ps
$\tau(\Xi_b^-)$	1.572 ± 0.040 ps
$\tau(\Xi_b^0)$	1.480 ± 0.030 ps
$\tau(\Omega_b^-)$	$1.64^{+0.18}_{-0.17}$ ps
B^0 and B_s^0 mixing / CP violation parameters	
Δm_d	0.5065 ± 0.0019 ps $^{-1}$
$\Delta\Gamma_d/\Gamma_d$	0.001 ± 0.010
$ q_d/p_d $	1.0009 ± 0.0013
Δm_s	17.757 ± 0.021 ps $^{-1}$
$\Delta\Gamma_s$	$+0.090 \pm 0.005$ ps $^{-1}$
$ q_s/p_s $	1.0003 ± 0.0014
$\phi_s^{c\bar{c}s}$	-0.021 ± 0.031 rad
Parameters related to Unitarity Triangle angles	
$\sin 2\beta \equiv \sin 2\phi_1$	0.699 ± 0.017
$\beta \equiv \phi_1$	$(22.2 \pm 0.7)^\circ$
$-\eta S_{\phi K_S^0}$	$0.74^{+0.11}_{-0.13}$
$-\eta S_{\eta' K^0}$	0.63 ± 0.06
$-\eta S_{K_S^0 K_S^0 K_S^0}$	0.72 ± 0.19
$\phi_s(\phi\phi)$	$-0.06 \pm 0.13 \pm 0.03$ rad
$-\eta S_{J/\psi \pi^0}$	0.86 ± 0.14
$-\eta S_{D^+ D^-}$	0.84 ± 0.12
$-\eta S_{J/\psi \rho^0}$	$0.66^{+0.13}_{-0.12}{}^{+0.09}_{-0.03}$
$S_{K^* \gamma}$	-0.16 ± 0.22
$(S_{\pi^+ \pi^-}, C_{\pi^+ \pi^-})$	$(-0.63 \pm 0.04, -0.32 \pm 0.04)$
$(S_{\rho^+ \rho^-}, C_{\rho^+ \rho^-})$	$(-0.14 \pm 0.13, 0.00 \pm 0.09)$
$\alpha \equiv \phi_2$	$(84.9^{+5.1}_{-4.5})^\circ$
$a(D^\mp \pi^\pm), a(D^{*\mp} \pi^\pm)$	$-0.038 \pm 0.013, -0.039 \pm 0.010$
$A_{CP}(B \rightarrow D_{CP+} K)$	0.129 ± 0.012
$A_{ADS}(B \rightarrow D_{K\pi} K)$	-0.415 ± 0.055
$\gamma \equiv \phi_3$	$(71.1^{+4.6}_{-5.3})^\circ$
Semileptonic B decay parameters	
$\mathcal{B}(\bar{B}^0 \rightarrow D^{*+} \ell^- \bar{\nu}_\ell)$	$(5.06 \pm 0.12)\%$

Selected world averages – continued from previous page.

$\mathcal{B}(B^- \rightarrow D^{*0} \ell^- \bar{\nu}_\ell)$	$(5.66 \pm 0.22)\%$
$\eta_{\text{EW}} \mathcal{F}(1) V_{cb} $	$(35.27 \pm 0.38) \times 10^{-3}$
$ V_{cb} $ from $\bar{B} \rightarrow D^* \ell^- \bar{\nu}_\ell$	$(38.76 \pm 0.42_{\text{exp}} \pm 0.55_{\text{th}}) \times 10^{-3}$
$\mathcal{B}(\bar{B}^0 \rightarrow D^+ \ell^- \bar{\nu}_\ell)$	$(2.31 \pm 0.10)\%$
$\mathcal{B}(B^- \rightarrow D^0 \ell^- \bar{\nu}_\ell)$	$(2.35 \pm 0.09)\%$
$\eta_{\text{EW}} \mathcal{G}(1) V_{cb} $	$(42.00 \pm 1.00) \times 10^{-3}$
$ V_{cb} $ from $\bar{B} \rightarrow D \ell^- \bar{\nu}_\ell$	$(39.58 \pm 0.94_{\text{exp}} \pm 0.37_{\text{th}}) \times 10^{-3}$
$\mathcal{B}(\bar{B} \rightarrow X_c \ell^- \bar{\nu}_\ell)$	$(10.65 \pm 0.16)\%$
$\mathcal{B}(\bar{B} \rightarrow X \ell^- \bar{\nu}_\ell)$	$(10.86 \pm 0.16)\%$
$ V_{cb} $ from $\bar{B} \rightarrow X \ell^- \bar{\nu}_\ell$	$(42.19 \pm 0.78) \times 10^{-3}$
$\mathcal{B}(\bar{B}^0 \rightarrow \pi^+ \ell^- \bar{\nu}_\ell)$	$(1.50 \pm 0.06) \times 10^{-4}$
$ V_{ub} $ from $\bar{B} \rightarrow \pi \ell^- \bar{\nu}_\ell$	$(3.67 \pm 0.15) \times 10^{-3}$
$ V_{ub} $ from $\bar{B} \rightarrow X_u \ell^- \bar{\nu}_\ell$	$(4.32 \pm 0.12_{\text{exp}} \pm 0.13_{\text{th}}) \times 10^{-3}$
$ V_{ub} / V_{cb} $ from $\Lambda_b^0 \rightarrow p \mu^- \bar{\nu}_\mu / \Lambda_b^0 \rightarrow \Lambda_c^+ \mu^- \bar{\nu}_\mu$	$0.079 \pm 0.004_{\text{exp}} \pm 0.004_{\text{th}}$
$\mathcal{R}(D) = \mathcal{B}(B \rightarrow D \tau \nu_\tau) / \mathcal{B}(B \rightarrow D \ell \nu_\ell)$	0.340 ± 0.030
$\mathcal{R}(D^*) = \mathcal{B}(B \rightarrow D^* \tau \nu_\tau) / \mathcal{B}(B \rightarrow D^* \ell \nu_\ell)$	0.295 ± 0.014
b-hadron to charmed hadron decays	
$\mathcal{B}(\bar{B}^0 \rightarrow D^+ \pi^-)$	$(2.65 \pm 0.15) \times 10^{-3}$
$\mathcal{B}(B^- \rightarrow D^0 \pi^-)$	$(4.75 \pm 0.19) \times 10^{-3}$
$\mathcal{B}(\bar{B}_s^0 \rightarrow D_s^+ \pi^-)$	$(3.03 \pm 0.25) \times 10^{-3}$
$\mathcal{B}(\Lambda_b^0 \rightarrow \Lambda_c^+ \pi^-)$	$(4.30_{-0.35}^{+0.36}) \times 10^{-3}$
$\mathcal{B}(\bar{B}^0 \rightarrow J/\psi \bar{K}^0)$	$(0.863 \pm 0.035) \times 10^{-3}$
$\mathcal{B}(B^- \rightarrow J/\psi K^-)$	$(1.028 \pm 0.040) \times 10^{-3}$
$\mathcal{B}(\bar{B}_s^0 \rightarrow J/\psi \phi)$	$(1.00 \pm 0.09) \times 10^{-3}$
$\mathcal{B}(\Lambda_b^0 \rightarrow J/\psi \Lambda^0)$	$(0.47 \pm 0.28) \times 10^{-3}$
$\mathcal{B}(B_c^- \rightarrow J/\psi D_s^-) / \mathcal{B}(B_c^- \rightarrow J/\psi \pi^-)$	3.09 ± 0.55
b-hadron to charmless final states	
$\mathcal{B}(B_s^0 \rightarrow \mu^+ \mu^-)$	$(3.1 \pm 0.6) \times 10^{-9}$
$\mathcal{B}(B^0 \rightarrow \mu^+ \mu^-)$	$< 0.34 \times 10^{-9}$ (CL=90%)
$\mathcal{B}(B_s^0 \rightarrow \tau^+ \tau^-)$	$< 5.2 \times 10^{-3}$ (CL=90%)
$\mathcal{B}(B \rightarrow X_s \gamma)$ ($E_\gamma > 1.6$ GeV)	$(3.32 \pm 0.15) \times 10^{-4}$
$\mathcal{B}(B^+ \rightarrow \tau^+ \nu)$	$(1.06 \pm 0.19) \times 10^{-4}$
$R_K = \mathcal{B}(B^+ \rightarrow K^+ \mu^+ \mu^-) / \mathcal{B}(B^+ \rightarrow K^+ e^+ e^-)$ in $1.0 < m_{\ell^+ \ell^-}^2 < 6.0$ GeV $^2/c^4$	$0.745_{-0.074}^{+0.090} \pm 0.036$
$R_{K^*} = \mathcal{B}(B^+ \rightarrow K^{*0} \mu^+ \mu^-) / \mathcal{B}(B^+ \rightarrow K^{*0} e^+ e^-)$ in $1.1 < m_{\ell^+ \ell^-}^2 < 6.0$ GeV $^2/c^4$	$0.69_{-0.09}^{+0.12}$
$A_{CP}(B^0 \rightarrow K^+ \pi^-)$, $A_{CP}(B^+ \rightarrow K^+ \pi^0)$	-0.084 ± 0.004 , 0.040 ± 0.021
$A_{CP}(B_s^0 \rightarrow K^- \pi^+)$	0.213 ± 0.017
Longitudinal polarisation of $B^0 \rightarrow \phi K^{*0}$	0.497 ± 0.017
Longitudinal polarisation of $B_s^0 \rightarrow \phi \phi$	0.379 ± 0.013
Observables in $B^0 \rightarrow K^{*0} \mu^+ \mu^-$ decays	See Sec. 8.5

Selected world averages – continued from previous page.

in bins of $q^2 = m^2(\mu^+\mu^-)$	
D^0 mixing and CP violation parameters	
x	$(0.32 \pm 0.14)\%$
y	$(0.69^{+0.06}_{-0.07})\%$
$\delta_{K\pi}$	$(15.2^{+7.6}_{-10.0})^\circ$
A_D	$(-0.88 \pm 0.99)\%$
$ q/p $	$0.89^{+0.08}_{-0.07}$
ϕ	$(-12.9^{+9.9}_{-8.7})^\circ$
x_{12} (no direct CP violation)	$(0.41^{+0.14}_{-0.15})\%$
y_{12} (no direct CP violation)	$(0.61 \pm 0.07)\%$
ϕ_{12} (no direct CP violation)	$(-0.17 \pm 1.8)^\circ$
a_{CP}^{ind}	$(0.030 \pm 0.026)\%$
$\Delta a_{CP}^{\text{dir}}$	$(-0.134 \pm 0.070)\%$
Leptonic D decays	
f_D	(203.7 ± 4.9) MeV
f_{D_s}	(257.1 ± 4.6) MeV
$ V_{cd} $	$0.2164 \pm 0.0050_{\text{exp}} \pm 0.0015_{\text{LQCD}}$
$ V_{cs} $	$1.006 \pm 0.018_{\text{exp}} \pm 0.005_{\text{LQCD}}$
Benchmark charm branching fractions	
$\mathcal{B}(D^0 \rightarrow K^-\pi^+)$	$(3.962 \pm 0.017 \pm 0.038 \pm 0.027_{\text{FSR}})\%$
$\mathcal{B}(D^0 \rightarrow K^+\pi^-)/\mathcal{B}(D^0 \rightarrow K^-\pi^+)$	$(0.349^{+0.004}_{-0.003})\%$
$\mathcal{B}(D_s^+ \rightarrow K^+K^-\pi^+)$	$(5.44 \pm 0.09 \pm 0.11)\%$
τ parameters, lepton universality, and V_{us}	
g_τ/g_μ	1.0010 ± 0.0014
g_τ/g_e	1.0029 ± 0.0014
g_μ/g_e	1.0018 ± 0.0014
$\mathcal{B}_e^{\text{uni}}$	$(17.814 \pm 0.022)\%$
R_{had}	3.6355 ± 0.0081
$ V_{us} $ from $\mathcal{B}(\tau^- \rightarrow X_s \nu_\tau)$	0.2195 ± 0.0019
$ V_{us} $ from $\mathcal{B}(\tau^- \rightarrow K^-\nu_\tau)/\mathcal{B}(\tau^- \rightarrow \pi^-\nu_\tau)$	0.2236 ± 0.0015
$ V_{us} $ from $\mathcal{B}(\tau^- \rightarrow K^-\nu_\tau)$	0.2234 ± 0.0015
$ V_{us} $ τ average	0.2221 ± 0.0013

2 Introduction

Flavor dynamics plays an important role in elementary particle interactions. The accurate knowledge of properties of heavy flavor hadrons, especially b hadrons, plays an essential role in determination of the elements of the Cabibbo-Kobayashi-Maskawa (CKM) quark-mixing matrix [2, 3]. The operation of the Belle and *BABAR* e^+e^- B factory experiments led to a large increase in the size of available B -meson, D -hadron and τ -lepton samples, enabling dramatic improvement in the accuracies of related measurements. The CDF and D0 experiments at the Fermilab Tevatron have also provided important results in heavy flavour physics, most notably in the B_s^0 sector. In the D -meson sector, the dedicated e^+e^- charm factory experiments CLEO-c and BESIII have made significant contributions. Run I and Run II of the CERN Large Hadron Collider delivered high luminosity, enabling the collection of even larger samples of b and c hadrons, and thus a further leap in precision in many areas, at the ATLAS, CMS, and (especially) LHCb experiments. With ongoing analyses of the LHC Run II data, further improvements are anticipated.

The Heavy Flavor Averaging Group (HFLAV)¹ was formed in 2002 to continue the activities of the LEP Heavy Flavor Steering Group [4], which was responsible for calculating averages of measurements of b -flavor related quantities. HFLAV has evolved since its inception and currently consists of seven subgroups:

- the “ B Lifetime and Oscillations” subgroup provides averages for b -hadron lifetimes, b -hadron fractions in $\Upsilon(4S)$ decay and pp or $p\bar{p}$ collisions, and various parameters governing $B^0-\bar{B}^0$ and $B_s^0-\bar{B}_s^0$ mixing and CP violation;
- the “Unitarity Triangle Angles” subgroup provides averages for parameters associated with time-dependent CP asymmetries and $B \rightarrow DK$ decays, and resulting determinations of the angles of the CKM unitarity triangle;
- the “Semileptonic B Decays” subgroup provides averages for inclusive and exclusive measurements of B -decay branching fractions, and subsequent determinations of the CKM matrix element magnitudes $|V_{cb}|$ and $|V_{ub}|$;
- the “ B to Charm Decays” subgroup provides averages of branching fractions for b -hadron decays to final states involving open charm or charmonium mesons;
- the “Rare Decays” subgroup provides averages of branching fractions and CP asymmetries for charmless, radiative, leptonic, and baryonic B -meson and b -baryon decays;
- the “Charm Physics” subgroup provides averages of numerous quantities in the charm sector, including branching fractions, properties of excited D^{**} and D_{sJ} mesons, properties of charm baryons, mixing, CP -, and T -violation parameters in the $D^0-\bar{D}^0$ system, and the D^+ and D_s^+ decay constants f_D and f_{D_s} ;
- the “Tau Physics” subgroup provides averages for τ branching fractions using a global fit, elaborates on the results to test lepton universality and to determine the CKM matrix element magnitude $|V_{us}|$, and lists and combines branching-fraction upper limits for τ lepton-flavor-violating decays.

¹ The group was originally known by the acronym “HFAG.” Following feedback from the community, this was changed to HFLAV in 2017.

Subgroups consist of representatives from experiments producing relevant results in that area, *i.e.*, representatives from *BABAR*, Belle, Belle II, BESIII, CLEO(c), CDF, D0, LHCb, ATLAS, and CMS.

This article is an update of the last HFLAV publication, which used results available by summer 2016 [1]. Here we report world averages using results available by September 2018. In some cases, important new results made available later are included, and in others, minor revisions in the September 2018 averages have been made. All plots carry a timestamp indicating approximately when the results shown were published. In general, we use all publicly available results, including preliminary results that are supported by written documentation, such as conference proceedings or publicly available reports from the collaborations. However, we do not use preliminary results that remain unpublished for an extended period of time, or for which no publication is planned. Since HFLAV members are also members of the different collaborations, we exploit our close contact with analyzers to ensure that the results are prepared in a form suitable for combinations.

Section 3 describes the methodology used for calculating averages. In the averaging procedure, common input parameters used in the various analyses are adjusted (rescaled) to common values, and, where possible, known correlations are taken into account. Sections 4–10 present world average values from each of the subgroups listed above. A complete listing of the averages and plots, including updates since this document was prepared, is available on the HFLAV web site:

<https://hflav.web.cern.ch>

3 Averaging methodology

The main task of HFLAV is to combine independent but possibly correlated measurements of a parameter to obtain the world’s best estimate of that parameter’s value and uncertainty. These measurements are typically made by different experiments, or by the same experiment using different data sets, or by the same experiment using the same data but using different analysis methods. In this section, the general approach adopted by HFLAV is outlined. For some cases, somewhat simplified or more complex algorithms are used; these are noted in the corresponding sections.

Our methodology focuses on the problem of combining measurements obtained with different assumptions about external (or “nuisance”) parameters and with potentially correlated systematic uncertainties. It is important for any averaging procedure that the quantities measured by experiments be statistically well-behaved, which in this context means having a (one- or multi-dimensional) Gaussian likelihood function that is described by the central value(s) \mathbf{x}_i and covariance matrix \mathbf{V}_i . In what follows we assume that \mathbf{x} does not contain redundant information, *i.e.*, if it contains n elements then n is the number of parameters being determined. A χ^2 statistic is constructed as

$$\chi^2(\mathbf{x}) = \sum_i^N (\mathbf{x}_i - \mathbf{x})^T \mathbf{V}_i^{-1} (\mathbf{x}_i - \mathbf{x}) , \quad (1)$$

where the sum is over the N independent determinations of the quantities \mathbf{x} , typically coming from different experiments; possible correlations of the systematic uncertainties are discussed below. The results of the average are the central values $\hat{\mathbf{x}}$, which are the values of \mathbf{x} at the minimum of $\chi^2(\mathbf{x})$, and their covariance matrix

$$\hat{\mathbf{V}}^{-1} = \sum_i^N \mathbf{V}_i^{-1} . \quad (2)$$

We report the covariance matrices or the correlation matrices derived from the averages whenever possible. In some cases where the matrices are large, it is inconvenient to report them in this document, and they can instead be found on the HFLAV web pages.

The value of $\chi^2(\hat{\mathbf{x}})$ provides a measure of the consistency of the independent measurements of \mathbf{x} after accounting for the number of degrees of freedom (dof), which is the difference between the number of measurements and the number of fitted parameters: $N \cdot n - n$. The values of $\chi^2(\hat{\mathbf{x}})$ and dof are typically converted to a confidence level (C.L.) and reported together with the averages. In cases where $\chi^2/\text{dof} > 1$, we do not usually scale the resulting uncertainty, in contrast to what is done by the Particle Data Group [5]. Rather, we examine the systematic uncertainties of each measurement to better understand them. Unless we find systematic discrepancies among the measurements, we do not apply any additional correction to the calculated uncertainty. If special treatment is necessary in order to calculate an average, or if an approximation used in the calculation might not be sufficiently accurate (*e.g.*, assuming Gaussian uncertainties when the likelihood function exhibits non-Gaussian behavior), we point this out. Further modifications to the averaging procedures for non-Gaussian situations are discussed in Sec. 3.2.

For observables such as branching fractions, experiments typically report upper limits when the signal is not significant. Sometimes there is insufficient information available to combine

upper limits on a parameter obtained by different experiments; in this case we usually report only the most restrictive upper limit. For branching fractions of lepton-flavor-violating decays of tau leptons, we calculate combined upper limits as discussed in Sec. 10.5.

3.1 Treatment of correlated systematic uncertainties

Consider two hypothetical measurements of a parameter x , which can be summarized as

$$\begin{aligned} x_1 &\pm \delta x_1 \pm \Delta x_{1,1} \pm \Delta x_{1,2} \dots \\ x_2 &\pm \delta x_2 \pm \Delta x_{2,1} \pm \Delta x_{2,2} \dots , \end{aligned}$$

where the δx_k are statistical uncertainties and the $\Delta x_{k,i}$ are contributions to the systematic uncertainty. The simplest approach is to combine statistical and systematic uncertainties in quadrature:

$$\begin{aligned} x_1 &\pm (\delta x_1 \oplus \Delta x_{1,1} \oplus \Delta x_{1,2} \oplus \dots) \\ x_2 &\pm (\delta x_2 \oplus \Delta x_{2,1} \oplus \Delta x_{2,2} \oplus \dots) , \end{aligned}$$

and then perform a weighted average of x_1 and x_2 using their combined uncertainties, treating the measurements as independent. This approach suffers from two potential problems that we try to address. First, the values x_k may have been obtained using different assumptions for nuisance parameters; *e.g.*, different values of the B^0 lifetime may have been used for different measurements of the oscillation frequency Δm_d . The second potential problem is that some systematic uncertainties may be correlated between measurements. For example, different measurements of Δm_d may depend on the same branching fraction used to model a common background.

The above two problems are related, as any quantity y_i upon which x_k depends gives a contribution $\Delta x_{k,i}$ to the systematic uncertainty, arising from the uncertainty Δy_i on y_i . We thus use the values of y_i and Δy_i assumed by each measurement in our averaging (we refer to these values as $y_{k,i}$ and $\Delta y_{k,i}$). To properly treat correlated systematic uncertainties among measurements, requires decomposing the overall systematic uncertainties into correlated and uncorrelated components. As different measurements often quote different types of systematic uncertainties, achieving consistent definitions in order to properly treat correlations requires close coordination between HFLAV and the experiments. In some cases, a group of systematic uncertainties must be combined into a coarser description in order to obtain an average that is consistent among measurements. Systematic uncertainties that are uncorrelated with any other source of uncertainty are combined together with the statistical uncertainty, so that the only systematic uncertainties treated explicitly are those that are correlated with at least one other measurement via a consistently-defined external parameter y_i . When asymmetric statistical or systematic uncertainties are quoted by experiments, we symmetrize them, since our combination method implicitly assumes Gaussian likelihoods (or parabolic log likelihoods) for each measurement.

The fact that a measurement of x is sensitive to y_i indicates that, in principle, the data used to measure x could also be used for a simultaneous measurement of x and y_i . This is illustrated by the large contour in Fig. 1(a). However, there often exists an external constraint Δy_i on y_i (represented by the horizontal band in Fig. 1(a)) that is more precise than the constraint $\sigma(y_i)$ from the x data alone. In this case one can perform a simultaneous fit to x and y_i , including the

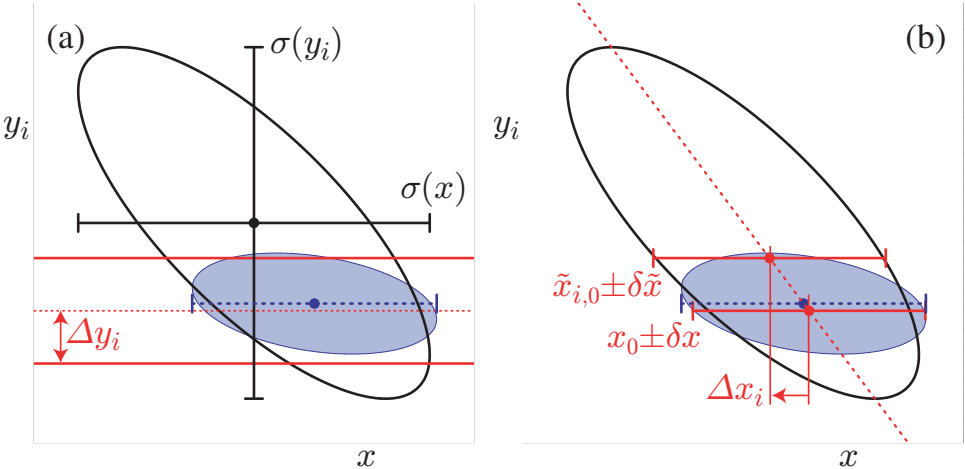


Figure 1: Illustration of the possible dependence of a measured quantity x on a nuisance parameter y_i . The left-hand plot (a) compares the 68% confidence level contours of a hypothetical measurement's unconstrained (large ellipse) and constrained (filled ellipse) likelihoods, using the Gaussian constraint on y_i represented by the horizontal band. The solid error bars represent the statistical uncertainties $\sigma(x)$ and $\sigma(y_i)$ of the unconstrained likelihood. The dashed error bar shows the statistical uncertainty on x from a constrained simultaneous fit to x and y_i . The right-hand plot (b) illustrates the method described in the text of performing fits to x with y_i fixed at different values. The dashed diagonal line between these fit results has the slope $\rho(x, y_i)\sigma(y_i)/\sigma(x)$ in the limit of an unconstrained parabolic log likelihood. The result of the constrained simultaneous fit from (a) is shown as a dashed error bar on x .

external constraint, and obtain the filled (x, y) contour and dashed one-dimensional estimate of x shown in Fig. 1(a). For this procedure one usually takes the external constraint Δy_i to be Gaussian.

When the external constraints Δy_i are significantly more precise than the sensitivity $\sigma(y_i)$ of the data alone, the additional complexity of a constrained fit with extra free parameters may not be justified by the resulting increase in sensitivity. In this case the usual procedure is to perform a baseline fit with all y_i fixed to nominal values $y_{i,0}$, obtaining $x = x_0 \pm \delta x$. This baseline fit neglects the uncertainty due to Δy_i , but this uncertainty is subsequently recovered by repeating the fit separately for each external parameter y_i , with its value fixed to $y_i = y_{i,0} \pm \Delta y_i$. This gives the result $x = \tilde{x}_{0,i} \pm \delta \tilde{x}$ as illustrated in Fig. 1(b). The shift in the central value $\Delta x_i = \tilde{x}_{0,i} - x_0$ is usually quoted as the systematic uncertainty due to the unknown value of y_i . If the unconstrained data can be represented by a Gaussian likelihood function, the shift will equal

$$\Delta x_i = \rho(x, y_i) \frac{\sigma(x)}{\sigma(y_i)} \Delta y_i, \quad (3)$$

where $\sigma(x)$ and $\rho(x, y_i)$ are the statistical uncertainty on x and the correlation between x and y_i in the unconstrained data, respectively. This procedure gives very similar results to that of the constrained fit with extra parameters: the central values x_0 agree to $\mathcal{O}(\Delta y_i/\sigma(y_i))^2$, and the uncertainties $\delta x \oplus \Delta x_i$ agree to $\mathcal{O}(\Delta y_i/\sigma(y_i))^4$.

To combine two or more measurements that share systematic uncertainty due to the same external parameter(s) y_i , we try to perform a constrained simultaneous fit of all measurements

to obtain values of x and y_i . When this is not practical, *e.g.* if we do not have sufficient information to reconstruct the likelihoods corresponding to each measurement, we perform the two-step approximate procedure described below.

Consider two statistically-independent measurements, $x_1 \pm (\delta x_1 \oplus \Delta x_{1,i})$ and $x_2 \pm (\delta x_2 \oplus \Delta x_{2,i})$, of the quantity x as shown in Figs. 2(a,b). For simplicity we consider only one correlated systematic uncertainty for each external parameter y_i . As our knowledge of the y_i improves, the measurements of x will shift to different central values and uncertainties. The first step of our procedure is to adjust the values of each measurement to reflect the current best knowledge of the external parameters y'_i and their ranges $\Delta y'_i$, as illustrated in Figs. 2(c,d). We adjust the central values x_k and correlated systematic uncertainties $\Delta x_{k,i}$ linearly for each measurement (indexed by k) and each external parameter (indexed by i):

$$x'_k = x_k + \sum_i \frac{\Delta x_{k,i}}{\Delta y_{k,i}} (y'_i - y_{k,i}) \quad (4)$$

$$\Delta x'_{k,i} = \Delta x_{k,i} \frac{\Delta y'_i}{\Delta y_{k,i}}. \quad (5)$$

This procedure is exact in the limit that the unconstrained likelihood of each measurement is Gaussian.

The second step is to combine the adjusted measurements, $x'_k \pm (\delta x_k \oplus \Delta x'_{k,1} \oplus \Delta x'_{k,2} \oplus \dots)$ by constructing the goodness-of-fit statistic

$$\chi^2_{\text{comb}}(x, y_1, y_2, \dots) \equiv \sum_k \frac{1}{\delta x_k^2} \left[x'_k - \left(x + \sum_i (y_i - y'_i) \frac{\Delta x'_{k,i}}{\Delta y'_i} \right) \right]^2 + \sum_i \left(\frac{y_i - y'_i}{\Delta y'_i} \right)^2. \quad (6)$$

We minimize this χ^2 to obtain the best values of x and y_i and their uncertainties, as shown in Fig. 3. Although this method determines new values for the y_i , we typically do not report them.

For comparison, the exact method we perform if the unconstrained likelihoods $\mathcal{L}_k(x, y_1, y_2, \dots)$ are available is to minimize the simultaneous likelihood

$$\mathcal{L}_{\text{comb}}(x, y_1, y_2, \dots) \equiv \prod_k \mathcal{L}_k(x, y_1, y_2, \dots) \prod_i \mathcal{L}_i(y_i), \quad (7)$$

with an independent Gaussian constraint for each y_i :

$$\mathcal{L}_i(y_i) = \exp \left[-\frac{1}{2} \left(\frac{y_i - y'_i}{\Delta y'_i} \right)^2 \right]. \quad (8)$$

The results of this exact method agree with those of the approximate method when the \mathcal{L}_k are Gaussian and $\Delta y'_i \ll \sigma(y_i)$. If the likelihoods are non-Gaussian, experiments need to provide \mathcal{L}_k in order to perform a combination. If $\sigma(y_i) \approx \Delta y'_i$, experiments are encouraged to perform a simultaneous measurement of x and y_i so that their data will improve the world knowledge of y_i .

For averages where common sources of systematic uncertainty are important, central values and uncertainties are rescaled to a common set of input parameters following the prescription above. We use the most up-to-date values for common inputs, consistently across subgroups, taking values from within HFLAV or from the Particle Data Group when possible. The parameters and values used are listed in each subgroup section.

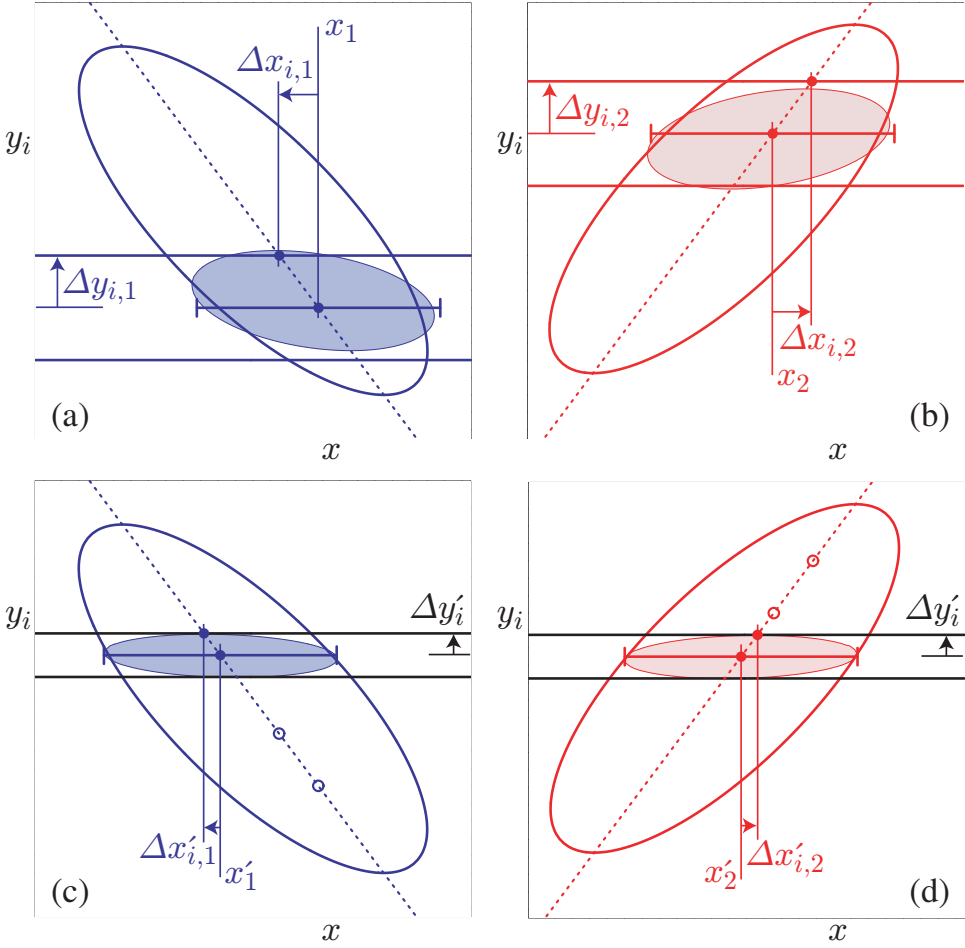


Figure 2: Illustration of the HFLAV combination procedure for correlated systematic uncertainties. Upper plots (a) and (b) show examples of two individual measurements to be combined. The large (filled) ellipses represent their unconstrained (constrained) likelihoods, while horizontal bands indicate the different assumptions about the value and uncertainty of y_i used by each measurement. The error bars show the results of the method described in the text for obtaining x by performing fits with y_i fixed to different values. Lower plots (c) and (d) illustrate the adjustments to accommodate updated and consistent knowledge of y_i . Open circles mark the central values of the unadjusted fits to x with y fixed; these determine the dashed line used to obtain the adjusted values.

3.2 Treatment of non-Gaussian likelihood functions

For measurements with Gaussian uncertainties, the usual estimator for the average of a set of measurements is obtained by minimizing

$$\chi^2(x) = \sum_k^N \frac{(x_k - x)^2}{\sigma_k^2}, \quad (9)$$

where x_k is the k -th measured value of x and σ_k^2 is the variance of the distribution from which x_k was drawn. The value \hat{x} at minimum χ^2 is the estimate for the parameter x . The true σ_k are unknown but typically the uncertainty as assigned by the experiment σ_k^{raw} is used as an

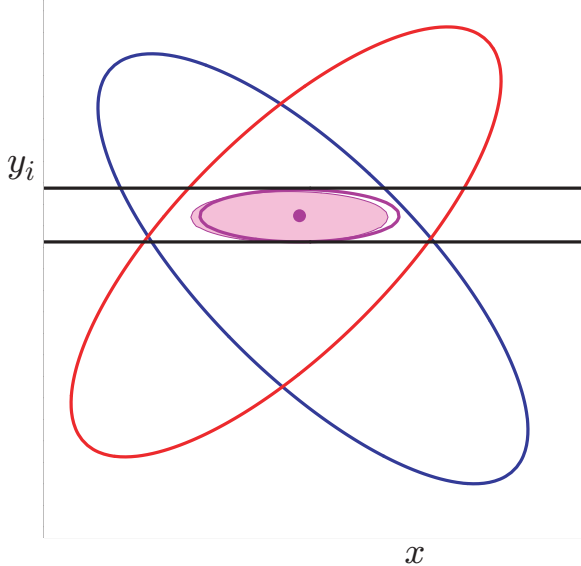


Figure 3: Illustration of the combination of two hypothetical measurements of x using the method described in the text. The ellipses represent the unconstrained likelihoods of each measurement, and the horizontal band represents the latest knowledge about y_i that is used to adjust the individual measurements. The filled small ellipse shows the result of the exact method using $\mathcal{L}_{\text{comb}}$, and the hollow small ellipse and dot show the result of the approximate method using χ^2_{comb} .

estimator for it. However, caution is advised when σ_k^{raw} depends on the measured value x_k . Examples of this are multiplicative systematic uncertainties such as those due to acceptance, or the \sqrt{N} dependence of Poisson statistics for which $x_k \propto N$ and $\sigma_k \propto \sqrt{N}$. Failing to account for this type of dependence when averaging leads to a biased average. Such biases can be avoided by minimizing

$$\chi^2(x) = \sum_k^N \frac{(x_k - x)^2}{\sigma_k^2(\hat{x})}, \quad (10)$$

where $\sigma_k(\hat{x})$ is the uncertainty on x_k that includes the dependence of the uncertainty on the value measured. As an example, consider the uncertainty due to acceptance for which $\sigma_k(\hat{x}) = (\hat{x}/x_k) \times \sigma_k^{\text{raw}}$. Inserting this into Eq. (10) leads to

$$\hat{x} = \frac{\sum_k^N x_k^3 / (\sigma_k^{\text{raw}})^2}{\sum_k^N x_k^2 / (\sigma_k^{\text{raw}})^2},$$

which is the correct behavior, *i.e.*, weighting by the inverse square of the fractional uncertainty $\sigma_k^{\text{raw}}/x_k$. It is sometimes difficult to assess the dependence of σ_k^{raw} on \hat{x} from the uncertainties quoted by the experiments.

Another issue that needs careful treatment is that of correlations among measurements, *e.g.*, due to using the same decay model for intermediate states to calculate acceptances. A common practice is to set the correlation coefficient to unity to indicate full correlation. However, this is not necessarily conservative and can result in underestimated uncertainty on the average. The most conservative choice of correlation coefficient between two measurements i and j is that

which maximizes the uncertainty on \hat{x} due to the pair of measurements,

$$\sigma_{\hat{x}(i,j)}^2 = \frac{\sigma_i^2 \sigma_j^2 (1 - \rho_{ij}^2)}{\sigma_i^2 + \sigma_j^2 - 2 \rho_{ij} \sigma_i \sigma_j}, \quad (11)$$

namely

$$\rho_{ij} = \min \left(\frac{\sigma_i}{\sigma_j}, \frac{\sigma_j}{\sigma_i} \right). \quad (12)$$

This corresponds to setting $\sigma_{\hat{x}(i,j)}^2 = \min(\sigma_i^2, \sigma_j^2)$. Setting $\rho_{ij} = 1$ when $\sigma_i \neq \sigma_j$ can lead to a significant underestimate of the uncertainty on \hat{x} , as can be seen from Eq. (11).

Finally, we carefully consider the various uncertainties contributing to the overall uncertainty of an average. The covariance matrix describing the uncertainties of different measurements and their correlations is constructed, *i.e.*, $\mathbf{V} = \mathbf{V}_{\text{stat}} + \mathbf{V}_{\text{sys}} + \mathbf{V}_{\text{theory}}$. If the measurements are from independent data samples, then \mathbf{V}_{stat} is diagonal, but \mathbf{V}_{sys} and $\mathbf{V}_{\text{theory}}$ may contain correlations. The variance on the average \hat{x} can be written

$$\sigma_{\hat{x}}^2 = \frac{\sum_{i,j} (\mathbf{V}^{-1} [\mathbf{V}_{\text{stat}} + \mathbf{V}_{\text{sys}} + \mathbf{V}_{\text{theory}}] \mathbf{V}^{-1})_{ij}}{\left(\sum_{i,j} \mathbf{V}_{ij}^{-1} \right)^2} = \sigma_{\text{stat}}^2 + \sigma_{\text{sys}}^2 + \sigma_{\text{th}}^2. \quad (13)$$

This breakdown of uncertainties is used in certain cases, but usually only a single, total uncertainty is quoted for an average.

4 Production fractions, lifetimes and mixing parameters of b hadrons

Quantities such as b -hadron production fractions, b -hadron lifetimes, and neutral B -meson oscillation frequencies were studied in the 1990's at LEP and SLC (e^+e^- colliders at $\sqrt{s} = m_Z$) as well as at the first version of the Tevatron ($p\bar{p}$ collider at $\sqrt{s} = 1.8$ TeV). This was followed by precise measurements of the B^0 and B^+ mesons performed at the asymmetric B factories, KEKB and PEPII (e^+e^- colliders at $\sqrt{s} = m_{T(4S)}$), as well as measurements related to the other b hadrons, in particular B_s^0 , B_c^+ and Λ_b^0 , performed at the upgraded Tevatron ($\sqrt{s} = 1.96$ TeV). Nowadays, the most precise measurements are coming from the LHC (pp collider at $\sqrt{s} = 7$, 8 TeV and 13 TeV), in particular the LHCb experiment.

In most cases, these basic quantities, in addition to being interesting by themselves, are necessary ingredients for more refined measurements, such as those of decay-time-dependent CP -violating asymmetries. It is therefore important that the best experimental values of these quantities continue to be kept up-to-date and improved.

In several cases, the averages presented in this chapter are needed and used as input for the results given in the subsequent sections. Some averages need the knowledge of other averages in a circular way. This coupling, which appears through the b -hadron fractions whenever inclusive or semi-exclusive measurements have to be considered, has been reduced drastically in the past several years with increasingly precise exclusive measurements becoming available and dominating practically all averages.

In addition to b -hadron fractions, lifetimes and oscillation frequencies, this section also deals with CP violation in the B^0 and B_s^0 mixing amplitudes, as well as the CP -violating phase $\phi_s^{c\bar{c}s} \simeq -2\beta_s$, which is the phase difference between the $B_s^0 - \bar{B}_s^0$ mixing amplitude and the $b \rightarrow c\bar{c}s$ decay amplitude. The angle β , which is the equivalent of β_s for the B^0 system, is discussed in Section 5.

Throughout this section, published results that have been superseded by subsequent publications are ignored (*i.e.*, excluded from the averages) and are only referred to if necessary.

4.1 b -hadron production fractions

We consider here the relative fractions of the different b -hadron species found in an unbiased sample of weakly decaying b hadrons produced in a specific process. The knowledge of these fractions is useful to characterize the signal composition in inclusive b -hadron analyses, to predict the background composition in exclusive analyses, and to convert (relative) observed event yields into (relative) branching fraction measurements. We distinguish here the following three b -hadron production processes: $\Upsilon(4S)$ decays, $\Upsilon(5S)$ decays, and high-energy collisions (including Z^0 decays).

Table 2: Published measurements of the B^+/B^0 production ratio in $\Upsilon(4S)$ decays, together with their average (see text). Systematic uncertainties due to the imperfect knowledge of $\tau(B^+)/\tau(B^0)$ are included.

Experiment, year	Ref.	Decay modes or method	Published value of $R^{+-/00} = f^{+-}/f^{00}$	Assumed value of $\tau(B^+)/\tau(B^0)$
CLEO, 2001	[6]	$J/\psi K^{(*)}$	$1.04 \pm 0.07 \pm 0.04$	1.066 ± 0.024
CLEO, 2002	[7]	$D^*\ell\nu$	$1.058 \pm 0.084 \pm 0.136$	1.074 ± 0.028
Belle, 2003	[8]	Dilepton events	$1.01 \pm 0.03 \pm 0.09$	1.083 ± 0.017
<i>BABAR</i> , 2005	[9]	$(c\bar{c})K^{(*)}$	$1.06 \pm 0.02 \pm 0.03$	1.086 ± 0.017
Average			1.059 ± 0.027 (tot)	1.076 ± 0.004

4.1.1 b -hadron production fractions in $\Upsilon(4S)$ decays

Only pairs of the two lightest (charged and neutral) B mesons can be produced in $\Upsilon(4S)$ decays. Therefore, only the following two branching fractions must be considered:

$$f^{+-} = \frac{\Gamma(\Upsilon(4S) \rightarrow B^+ B^-)}{\Gamma_{\text{tot}}(\Upsilon(4S))}, \quad (14)$$

$$f^{00} = \frac{\Gamma(\Upsilon(4S) \rightarrow B^0 \overline{B}^0)}{\Gamma_{\text{tot}}(\Upsilon(4S))}. \quad (15)$$

In practice, most analyses measure their ratio

$$R^{+-/00} = \frac{f^{+-}}{f^{00}} = \frac{\Gamma(\Upsilon(4S) \rightarrow B^+ B^-)}{\Gamma(\Upsilon(4S) \rightarrow B^0 \overline{B}^0)}, \quad (16)$$

which is easier to access experimentally. An inclusive (but separate) reconstruction of B^+ and B^0 is difficult. Therefore, $R^{+-/00}$ is measured with exclusive decays $B^+ \rightarrow f^+$ and $B^0 \rightarrow f^0$ to specific final states f^+ and f^0 that are related by isospin symmetry. Under the assumption that $\Gamma(B^+ \rightarrow f^+) = \Gamma(B^0 \rightarrow f^0)$, *i.e.*, that isospin invariance holds in relating these B decays, the ratio of the number of reconstructed $B^+ \rightarrow f^+$ and $B^0 \rightarrow f^0$ mesons, after correcting for efficiency, is proportional to

$$\frac{f^{+-} \mathcal{B}(B^+ \rightarrow f^+)}{f^{00} \mathcal{B}(B^0 \rightarrow f^0)} = \frac{f^{+-} \Gamma(B^+ \rightarrow f^+) \tau(B^+)}{f^{00} \Gamma(B^0 \rightarrow f^0) \tau(B^0)} = \frac{f^{+-}}{f^{00}} \frac{\tau(B^+)}{\tau(B^0)}, \quad (17)$$

where $\tau(B^+)$ and $\tau(B^0)$ are the B^+ and B^0 lifetimes, respectively. Hence the primary quantity measured in these analyses is $R^{+-/00} \tau(B^+)/\tau(B^0)$, and the extraction of $R^{+-/00}$ with this method therefore requires the knowledge of the $\tau(B^+)/\tau(B^0)$ lifetime ratio.

The published measurements of $R^{+-/00}$ are listed² in Table 2 together with the corresponding values of $\tau(B^+)/\tau(B^0)$ assumed in each measurement. All measurements are based on the above-mentioned method, except the one from Belle, which is a by-product of the B^0 mixing frequency analysis using dilepton events (but note that it too assumes isospin invariance, namely

²An old and imprecise R measurement from CLEO [10] is included in neither Table 2 nor the average.

$\Gamma(B^+ \rightarrow \ell^+ X) = \Gamma(B^0 \rightarrow \ell^+ X)$. The latter is therefore treated in a slightly different manner in the following procedure used to combine these measurements:

- each published value of $R^{+-/00}$ from CLEO and *BABAR* is first converted back to the original measurement of $R^{+-/00} \tau(B^+)/\tau(B^0)$, using the value of the lifetime ratio assumed in the corresponding analysis;
- a simple weighted average of these original measurements of $R^{+-/00} \tau(B^+)/\tau(B^0)$ from CLEO and *BABAR* is then computed, assuming no statistical or systematic correlations between them;
- the weighted average of $R^{+-/00} \tau(B^+)/\tau(B^0)$ is converted into a value of $R^{+-/00}$, using the latest average of the lifetime ratios, $\tau(B^+)/\tau(B^0) = 1.076 \pm 0.004$ (see Sec. 4.2.3);
- the Belle measurement of $R^{+-/00}$ is adjusted to the current values of $\tau(B^0) = 1.519 \pm 0.004$ ps and $\tau(B^+)/\tau(B^0) = 1.076 \pm 0.004$ (see Sec. 4.2.3), using the procedure described in Sec. 3.1;
- the combined value of $R^{+-/00}$ from CLEO and *BABAR* is averaged with the adjusted value of $R^{+-/00}$ from Belle, assuming a 100% correlation of the systematic uncertainty due to the limited knowledge on $\tau(B^+)/\tau(B^0)$; no other correlation is considered.

The resulting global average,

$$R^{+-/00} = \frac{f^{+-}}{f^{00}} = 1.059 \pm 0.027, \quad (18)$$

is consistent with equal production rate of charged and neutral B mesons, although only at the 2.2σ level.

On the other hand, the *BABAR* collaboration has performed a direct measurement of the f^{00} fraction using an original method, which neither relies on isospin symmetry nor requires the knowledge of $\tau(B^+)/\tau(B^0)$. Rather, the method is based on comparing the number of events where a single $B^0 \rightarrow D^{*-} \ell^+ \nu$ decay is reconstructed to the number of events where two such decays are reconstructed. The result of this measurement is [11]

$$f^{00} = 0.487 \pm 0.010 \text{ (stat)} \pm 0.008 \text{ (syst)}. \quad (19)$$

The results of Eqs. (18) and (19) are obtained with very different methods and are completely independent of each other. Their product yields $f^{+-} = 0.516 \pm 0.019$, and combining them into the sum of the charged and neutral fractions gives $f^{+-} + f^{00} = 1.003 \pm 0.029$, compatible with unity.

The precision of the fractions can be further improved by setting $f^{+-} + f^{00} = 1$. This approximation is justified by the small branching fractions, of order 10^{-4} , that have been measured for $\Upsilon(4S)$ decays to several non- $B\bar{B}$ final states, specifically $\Upsilon(1S)\pi^+\pi^-$, $\Upsilon(2S)\pi^+\pi^-$, $\Upsilon(1S)\eta$ and $\Upsilon(1S)\eta'$ [12–15]. These branching fractions correspond to a sum of partial widths that is several times larger than $\Gamma(\Upsilon(4S) \rightarrow e^+e^-)$, yet are much smaller than the uncertainties in the measurements of f^{+-} and f^{00} . The approximation is also consistent with CLEO’s observation that $\mathcal{B}(\Upsilon(4S) \rightarrow B\bar{B}) > 0.96$ at 95% CL [16]. Assuming $f^{+-} + f^{00} = 1$, the results

Table 3: Published measurements of $f_s^{\Upsilon(5S)}$, obtained assuming $f_{\beta}^{\Upsilon(5S)} = 0$. The results are quoted as in the original publications, except for the 2010 Belle measurement, which is quoted as $1 - f_{u,d}^{\Upsilon(5S)}$ with $f_{u,d}^{\Upsilon(5S)}$ from Ref. [17]. The 2012 Belle measurement, reported and used in Ref. [18], is an undocumented update of the analysis of Ref. [19] with the full $\Upsilon(5S)$ dataset.

Experiment, year, dataset	Decay mode or method	Value of $f_s^{\Upsilon(5S)}$
CLEO, 2006, 0.42 fb^{-1} [20]	$\Upsilon(5S) \rightarrow D_s X$	$0.168 \pm 0.026 {}^{+0.067}_{-0.034}$
	$\Upsilon(5S) \rightarrow \phi X$	$0.246 \pm 0.029 {}^{+0.110}_{-0.053}$
	$\Upsilon(5S) \rightarrow B\bar{B} X$	$0.411 \pm 0.100 \pm 0.092$
	CLEO average of above 3	$0.21 {}^{+0.06}_{-0.03}$
Belle, 2006, 1.86 fb^{-1} [19]	$\Upsilon(5S) \rightarrow D_s X$	$0.179 \pm 0.014 \pm 0.041$
	$\Upsilon(5S) \rightarrow D^0 X$	$0.181 \pm 0.036 \pm 0.075$
	Belle average of above 2	$0.180 \pm 0.013 \pm 0.032$
Belle, 2010, 23.6 fb^{-1} [17]	$\Upsilon(5S) \rightarrow B\bar{B} X$	$0.263 \pm 0.032 \pm 0.051$
Belle, 2012, 121.4 fb^{-1} [18]	$\Upsilon(5S) \rightarrow D_s X, D^0 X$	0.172 ± 0.030

of Eqs. (18) and (19) are averaged (first converting Eq. (18) into a value of $f^{00} = 1/(R^{+-/00} + 1)$) to yield the following more precise estimates:

$$f^{00} = 0.486 \pm 0.006, \quad f^{+-} = 1 - f^{00} = 0.514 \pm 0.006, \quad \frac{f^{+-}}{f^{00}} = 1.058 \pm 0.024. \quad (20)$$

The latter ratio differs from unity by 2.4σ .

4.1.2 b -hadron production fractions at the $\Upsilon(5S)$ energy

Hadronic events produced in e^+e^- collisions at the $\Upsilon(5S)$ (also known as $\Upsilon(10860)$) energy can be classified into three categories: light-quark (u, d, s, c) continuum events, $b\bar{b}$ continuum events, and $\Upsilon(5S)$ events. The latter two cannot be distinguished and will be called $b\bar{b}$ events in the following. These $b\bar{b}$ events, including $b\bar{b}\gamma$ where the photon arises from initial-state radiation, can hadronize into different final states. We define $f_{u,d}^{\Upsilon(5S)}$ to be the fraction of $b\bar{b}$ events with a pair of non-strange bottom mesons, namely, $B\bar{B}$, $B\bar{B}^*$, $B^*\bar{B}$, $B^*\bar{B}^*$, $B\bar{B}\pi$, $B\bar{B}^*\pi$, $B^*\bar{B}\pi$, $B^*\bar{B}^*\pi$, and $B\bar{B}\pi\pi$, where B denotes a B^0 or B^+ meson and \bar{B} denotes a \bar{B}^0 or B^- meson. Similarly, we define $f_s^{\Upsilon(5S)}$ to be the fraction of $b\bar{b}$ events that hadronize into a pair of strange bottom mesons ($B_s^0\bar{B}_s^0$, $B_s^0\bar{B}_s^{*0}$, $B_s^{*0}\bar{B}_s^0$, and $B_s^{*0}\bar{B}_s^{*0}$). Note that the excited bottom-meson states decay via $B^* \rightarrow B\gamma$ and $B_s^{*0} \rightarrow B_s^0\gamma$. Lastly, $f_{\beta}^{\Upsilon(5S)}$ is defined to be the fraction of $b\bar{b}$ events without open-bottom mesons (but with a light bottomonium instead) in the final state. By construction, these fractions satisfy

$$f_{u,d}^{\Upsilon(5S)} + f_s^{\Upsilon(5S)} + f_{\beta}^{\Upsilon(5S)} = 1. \quad (21)$$

The CLEO and Belle collaborations have published measurements of several inclusive $\Upsilon(5S)$ branching fractions, $\mathcal{B}(\Upsilon(5S) \rightarrow D_s X)$, $\mathcal{B}(\Upsilon(5S) \rightarrow \phi X)$ and $\mathcal{B}(\Upsilon(5S) \rightarrow D^0 X)$, from which

Table 4: External inputs on which the $f_s^{\Upsilon(5S)}$ averages are based.

Branching fraction	Value	Explanation and reference
$\mathcal{B}(B \rightarrow D_s X) \times \mathcal{B}(D_s \rightarrow \phi\pi)$	0.00374 ± 0.00014	Derived from [21]
$\mathcal{B}(B_s^0 \rightarrow D_s X)$	0.92 ± 0.11	Model-dependent estimate [22]
$\mathcal{B}(D_s \rightarrow \phi\pi)$	0.045 ± 0.004	[21]
$\mathcal{B}(B \rightarrow D^0 X) \times \mathcal{B}(D^0 \rightarrow K\pi)$	0.0242 ± 0.0011	Derived from [21]
$\mathcal{B}(B_s^0 \rightarrow D^0 X)$	0.08 ± 0.07	Model-dependent estimate [19, 22]
$\mathcal{B}(D^0 \rightarrow K\pi)$	0.03954 ± 0.00031	[21]
$\mathcal{B}(B \rightarrow \phi X)$	0.0343 ± 0.0012	[21]
$\mathcal{B}(B_s^0 \rightarrow \phi X)$	0.161 ± 0.024	Model-dependent estimate [20]

they extracted the model-dependent estimates of $f_s^{\Upsilon(5S)}$ reported in Table 3. This extraction was performed under the implicit assumption $f_{\mathcal{B}}^{\Upsilon(5S)} = 0$, using the relation

$$\frac{1}{2} \mathcal{B}(\Upsilon(5S) \rightarrow D_s X) = f_s^{\Upsilon(5S)} \times \mathcal{B}(B_s^0 \rightarrow D_s X) + \left(1 - f_s^{\Upsilon(5S)} - f_{\mathcal{B}}^{\Upsilon(5S)}\right) \times \mathcal{B}(B \rightarrow D_s X), \quad (22)$$

and similar relations for $\mathcal{B}(\Upsilon(5S) \rightarrow D^0 X)$ and $\mathcal{B}(\Upsilon(5S) \rightarrow \phi X)$.

However, the assumption $f_{\mathcal{B}}^{\Upsilon(5S)} = 0$ is known to be incorrect, given the observed production in e^+e^- collisions at the $\Upsilon(5S)$ energy of the final states $\Upsilon(1S)\pi^+\pi^-$, $\Upsilon(2S)\pi^+\pi^-$, $\Upsilon(3S)\pi^+\pi^-$ and $\Upsilon(1S)K^+K^-$ [23, 24], $h_b(1P)\pi^+\pi^-$ and $h_b(2P)\pi^+\pi^-$ [25], $\Upsilon(1S)\pi^0\pi^0$, $\Upsilon(2S)\pi^0\pi^0$ and $\Upsilon(3S)\pi^0\pi^0$ [26], and more recently $\Upsilon_J(1D)\eta$ and $\Upsilon(2S)\eta$ [27]. The sum of the visible (i.e., uncorrected for initial-state radiation) cross-sections into these final states, plus those of the unmeasured final states $\Upsilon(1S)K^0\bar{K}^0$, $h_b(1P)\pi^0\pi^0$ and $h_b(2P)\pi^0\pi^0$, which are obtained by assuming isospin conservation, amounts to

$$\sigma^{\text{vis}}(e^+e^- \rightarrow (b\bar{b})X) = 15.0 \pm 1.4 \text{ pb},$$

where $(b\bar{b}) = \Upsilon(1S, 2S, 3S)$, $\Upsilon_J(1D)$, $h_b(1P, 2P)$, and $X = \pi\pi$, KK , η . We divide this by the $b\bar{b}$ production cross section, $\sigma(e^+e^- \rightarrow b\bar{b}X) = 337 \pm 15$ pb, obtained as the average of the CLEO [22] and Belle [18] measurements, to obtain

$$\mathcal{B}(\Upsilon(5S) \rightarrow (b\bar{b})X) = 0.045 \pm 0.005.$$

This should be taken as a lower bound for $f_{\mathcal{B}}^{\Upsilon(5S)}$.

To simultaneously extract the fractions under the exact constraints of Eqs. (21) and (22) and the one-sided Gaussian constraint $f_{\mathcal{B}}^{\Upsilon(5S)} \geq \mathcal{B}(\Upsilon(5S) \rightarrow (b\bar{b})X)$, we follow the method described in Ref. [28], performing a χ^2 fit of the measurements of the $\Upsilon(5S)$ branching fractions of Refs. [17, 19, 20]. The latest Belle measurement of $f_s^{\Upsilon(5S)}$ Ref. [18] lacks the information needed for the averaging, and is therefore not included. Taking the inputs of Table 4 and all known correlations into account, the best fit values are

$$f_{u,d}^{\Upsilon(5S)} = 0.758^{+0.027}_{-0.037}, \quad (23)$$

$$f_s^{\Upsilon(5S)} = 0.198^{+0.030}_{-0.029}, \quad (24)$$

$$f_{\mathcal{B}}^{\Upsilon(5S)} = 0.044^{+0.044}_{-0.005}, \quad (25)$$

where the strongly asymmetric uncertainty on $f_{\mathcal{B}}^{\Upsilon(5S)}$ is due to the one-sided constraint from the observed $(b\bar{b})X$ decays. These results, together with their correlations, imply

$$f_s^{\Upsilon(5S)} / f_{u,d}^{\Upsilon(5S)} = 0.261^{+0.051}_{-0.043}. \quad (26)$$

This is in fair agreement with *BABAR* results [29], obtained as a function of centre-of-mass energy and as a by-product of another measurement, and which are not used in our average due to insufficient information.

The production of B_s^0 mesons at the $\Upsilon(5S)$ is observed to be dominated by the $B_s^{*0}\bar{B}_s^{*0}$ channel, with $\sigma(e^+e^- \rightarrow B_s^{*0}\bar{B}_s^{*0})/\sigma(e^+e^- \rightarrow B_s^{(*)0}\bar{B}_s^{(*)0}) = (87.0 \pm 1.7)\%$ [30] measured as described in Ref. [31]. The proportions of the various production channels for non-strange B mesons have also been measured [17].

4.1.3 b -hadron production fractions at high energy

At high energy, all species of weakly decaying b hadrons may be produced, either directly or in strong and electromagnetic decays of excited b hadrons. Before 2010, it was assumed that the fractions of different species in unbiased samples of high- p_T b -hadron jets were independent of whether they originated from Z^0 decays, $p\bar{p}$ collisions at the Tevatron, or pp collisions at the LHC. This hypothesis was plausible under the condition $Q^2 \gg \Lambda_{\text{QCD}}^2$, namely, that the square of the momentum transfer to the produced b quarks is large compared with the square of the hadronization energy scale. However, this is only a weak argument. In fact, the available data show that the fractions depend on the kinematics of the produced b hadron. Both CDF and LHCb report a p_T dependence of the fractions, with the fraction of Λ_b^0 baryons observed at low p_T being enhanced with respect to that seen at LEP at higher p_T .

We present here two sets of averages: one set includes only measurements performed at LEP, and the second set includes only measurements performed by CDF at the Tevatron.³ While the first set is well defined and is basically related to branching fractions of inclusive Z^0 decays, the other set is somewhat ill-defined, since it depends on the kinematic region covered by the experiment and over which the measurements are integrated.

Contrary to what happens in the charm sector, where the fractions of D^+ and D^0 are different, the relative production rate of B^+ and B^0 is not affected by the electromagnetic decays of excited B^{*+} and B^{*0} states and strong decays of excited B^{**+} and B^{**0} states. Decays of the type $B_s^{*0} \rightarrow B^{(*)}K$ also contribute to the B^+ and B^0 rates, but with the same magnitude if mass effects can be neglected. We therefore assume equal production of B^+ and B^0 mesons. We also neglect the production of weakly decaying states made of several heavy quarks (such as B_c^+ or doubly heavy baryons) which is much smaller. Hence, for the purpose of determining the b -hadron fractions, we use the constraints

$$f_u = f_d \quad \text{and} \quad f_u + f_d + f_s + f_{\text{baryon}} = 1, \quad (27)$$

where f_u , f_d , f_s and f_{baryon} are the unbiased fractions of B^+ , B^0 , B_s^0 and b baryons, respectively.

³The LHC production fractions results are still incomplete, lacking measurements of the production of weakly-decaying baryons heavier than Λ_b^0 . In Ref [1], we provided also a third set of averages including measurements performed at LEP, Tevatron and LHC, but this was mostly for comparison with previous averages. We have decided to discontinue these “world averages”, because they mix environments with different fractions.

We note that there are many measurements of the production cross-sections of different species of b hadrons. In principle, these could be included in a global fit to determine the production fractions. We do not use these inputs at the current time, and instead average only the explicit measurements of the production fractions.

The LEP experiments have measured $f_s \times \mathcal{B}(B_s^0 \rightarrow D_s^- \ell^+ \nu_\ell X)$ [32–34], $\mathcal{B}(b \rightarrow \Lambda_b^0) \times \mathcal{B}(\Lambda_b^0 \rightarrow \Lambda_c^+ \ell^- \bar{\nu}_\ell X)$ [35, 36] and $\mathcal{B}(b \rightarrow \Xi_b^-) \times \mathcal{B}(\Xi_b^- \rightarrow \Xi^- \ell^- \bar{\nu}_\ell X)$ [37, 38] using partially reconstructed hadronic final states and a lepton to identify the b hadron. They have also measured f_{baryon} using protons identified in b -hadron decays [39], as well as the production rate of charged b hadrons [40].

Ratios of b -hadron fractions have been measured by CDF using lepton+charm final states [41–43] and double semileptonic decays with $K^* \mu \mu$ and $\phi \mu \mu$ final states [44]. In our determination of f_{baryon} at the Tevatron, we include measurements of the production of Ξ_b and Ω_b^- relative to that of the Λ_b^0 [45–47] by applying the constraint

$$\begin{aligned} f_{\text{baryon}} &= f_{\Lambda_b^0} + f_{\Xi_b^0} + f_{\Xi_b^-} + f_{\Omega_b^-} \\ &= f_{\Lambda_b^0} \left(1 + 2 \frac{f_{\Xi_b^-}}{f_{\Lambda_b^0}} + \frac{f_{\Omega_b^-}}{f_{\Lambda_b^0}} \right), \end{aligned} \quad (28)$$

where isospin invariance in the production of Ξ_b^0 and Ξ_b^- is assumed. Excited b baryons are expected to decay strongly or electromagnetically to the baryons listed in Eq. (28). Both CDF [47] and D0 [45, 46] reconstruct their b baryons exclusively to final states that include a J/ψ and a hyperon, namely, $\Lambda_b^0 \rightarrow J/\psi \Lambda$, $\Xi_b^- \rightarrow J/\psi \Xi^-$ and $\Omega_b^- \rightarrow J/\psi \Omega^-$. We assume that the partial decay width of a b baryon to a J/ψ and the corresponding hyperon is equal to the partial width of any other b baryon to a J/ψ and the corresponding hyperon. We use the CDF+D0 average of $f_{\Xi_b^-}/f_{\Lambda_b^0}$ to obtain $f_{\Omega_b^-}/f_{\Lambda_b^0}$ from the D0 measurement of $f_{\Omega_b^-}/f_{\Xi_b^-}$, which we combine with the CDF measurement of $f_{\Omega_b^-}/f_{\Lambda_b^0}$ for input into Eq. (28).

LHCb has also measured ratios of b -hadron fractions in charm+lepton final states [48] and in the fully reconstructed hadronic two-body decays $B^0 \rightarrow D^- \pi^+$, $B_s^0 \rightarrow D_s^- \pi^+$ and $\Lambda_b^0 \rightarrow \Lambda_c^+ \pi^-$ [49, 50].

Both CDF [43] and LHCb [48] observe that the ratio $f_{\Lambda_b^0}/f_d$ depends on the p_T of the charm+lepton system.⁴ In Ref. [43], CDF chose to correct an older result [41] to account for the p_T dependence. In a second result, CDF binned their data in p_T of the charm+electron system [42]. In their more recent measurement using hadronic decays [50], LHCb obtain the scale for $R_{\Lambda_b^0} = f_{\Lambda_b^0}/f_d$ from their previous charm + lepton data [48], bin the data in pseudo-rapidity (η) and see a linear dependence of $R_{\Lambda_b^0}$. Since η is not entirely independent of p_T , it is impossible to tell at this time whether this dependence is just an artifact of the p_T dependence. Figure 4 shows the ratio $R_{\Lambda_b^0}$ as a function of p_T for the b hadron, as measured by LHCb.⁵ LHCb fit their scaled results using hadronic decays to obtain [50]

$$R_{\Lambda_b^0} = (0.151 \pm 0.030) + \exp \{ -(0.57 \pm 0.11) - (0.095 \pm 0.016)[\text{GeV}/c]^{-1} \times p_T \}. \quad (29)$$

⁴ CDF compare the p_T distribution of fully reconstructed $\Lambda_b^0 \rightarrow \Lambda_c^+ \pi^-$ with that of $\bar{B}^0 \rightarrow D^+ \pi^-$, which gives $f_{\Lambda_b^0}/f_d$ up to a scale factor. LHCb compares the p_T of the charm+lepton system in Λ_b^0 , B^0 and B^+ decays, giving $R_{\Lambda_b^0}/2 = f_{\Lambda_b^0}/(f_u + f_d) = f_{\Lambda_b^0}/(2f_d)$.

⁵ The CDF results from semileptonic decays [42] would require significant corrections to obtain the p_T of the b hadron and be included on the same plot with the LHCb data. We do not have these corrections at this time.

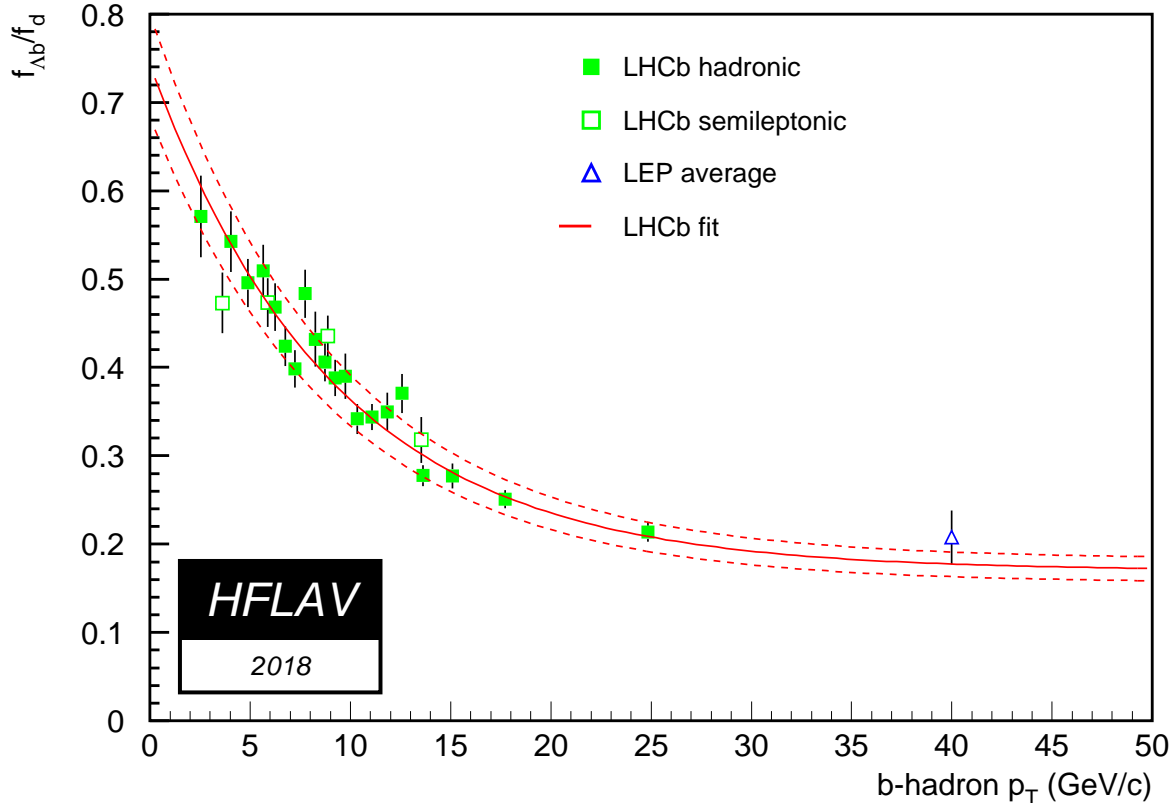


Figure 4: Ratio of production fractions $f_{\Lambda_b^0}/f_d$ as a function of p_T of the b hadron from LHCb data for b hadrons decaying semileptonically [48] and fully reconstructed in hadronic decays [50]. The curve represents a fit to the LHCb hadronic data [50]. Our LEP average (derived from Table 6) is displayed at an approximate p_T in Z decays, but is not used in the fit.

Since the two LHCb results for $R_{\Lambda_b^0}$ are not independent, we use only the results with semileptonic final states for the averages. Note that the p_T dependence of $R_{\Lambda_b^0}$ combined with the constraint from Eq. (27) implies a compensating p_T dependence in one or more of the production fractions, f_u , f_d , or f_s .

LHCb and ATLAS have investigated the p_T dependence of the ratio $R_s = f_s/f_d$, shown in Figure 5, using fully reconstructed B_s^0 and B^0 decays. LHCb reported 3σ evidence that R_s decreases with p_T using theoretical predictions for branching fractions [49]. The results from the ATLAS experiment [51] use theoretical predictions for branching fractions [52] and indicate that R_s is consistent with no p_T dependence. From Figure 5, we perform two fits for R_s . The first fit, using a linear parameterization, yields $R_s = (0.2701 \pm 0.0058) - (0.00139 \pm 0.00044)[\text{GeV}/c]^{-1} \times p_T$. The second fit, using a simple exponential, yields

$$R_s = \exp \left\{ (-1.304 \pm 0.024) - (0.0058 \pm 0.0019)[\text{GeV}/c]^{-1} \times p_T \right\}. \quad (30)$$

The two fits are nearly indistinguishable over the p_T range of the results, but the second fit

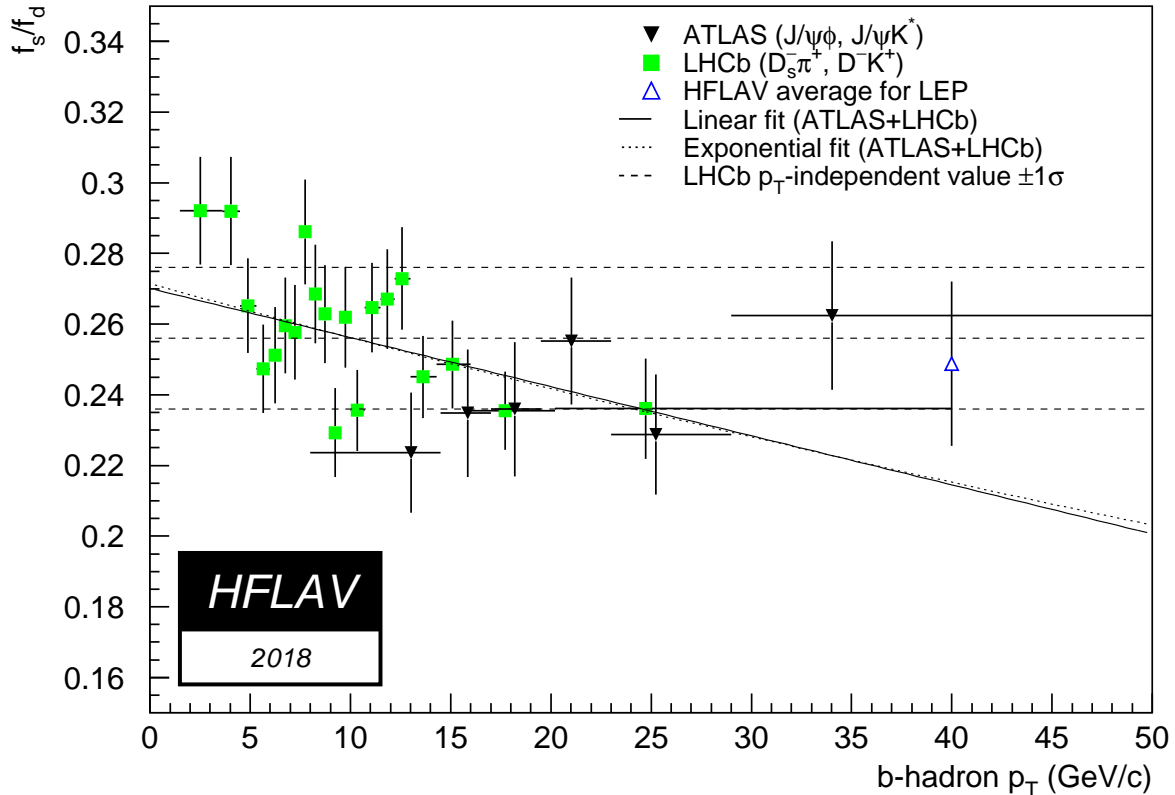


Figure 5: Ratio of production fractions f_s/f_d as a function of p_T of the reconstructed b hadrons for the LHCb [49] (green solid points) and ATLAS [51] (black solid points) data. Note the suppressed zero for the vertical axis. The curves represent fits to these data: a linear fit (solid curve), and an exponential fit described in the text (dotted curve). The p_T -independent value of R_s published by LHCb [49] (dashed lines) and our LEP average of Table 6 (open blue point at an approximate p_T in Z decays) are shown for comparison, but not used in any fit.

gives a physical value for all p_T . The p_T -independent value of R_s published by LHCb [49] and our LEP average are also shown in Figure 5.

For comparison purposes, a weighted average of the LHCb measurements in bins of p_T and η is computed, both for $f_s/(f_u + f_d)$ and $f_{\Lambda_b^0}/(f_u + f_d)$.⁶ As shown in Table 5, the weighted LHCb data and similar averages from CDF appear to be still compatible, at the current level of precision, despite the b hadrons being produced in different kinematic regimes.

Ignoring the p_T and η dependence, we have adjusted the published results to the latest branching fraction averages [21] and combined them under the constraints of Eq. (27), following the procedure and assumptions described in Ref. [4]. This yield $f_u = f_d = 0.412 \pm 0.008$, $f_s =$

⁶ In practice, the LHCb data are given in 14 bins in p_T and η with a full covariance matrix [48]. The weighted average is calculated as $D^T C^{-1} M / \sigma$, where $\sigma = D^T C^{-1} D$, M is a vector of measurements, C^{-1} is the inverse covariance matrix and D^T is the transpose of the design matrix (vector of 1's).

Table 5: Comparison of average production fraction ratios from CDF [42, 43] and LHCb [48]. The kinematic regime of the charm+lepton system reconstructed in each experiment is also shown.

Quantity	CDF	LHCb
$f_s/(f_u + f_d)$	0.224 ± 0.057	0.134 ± 0.009
$f_{\Lambda_b^0}/(f_u + f_d)$	0.229 ± 0.062	0.240 ± 0.022
Average charm+lepton p_T	$\sim 13 \text{ GeV}/c$	$\sim 7 \text{ GeV}/c$
Pseudorapidity range	$-1 < \eta < 1$	$2 < \eta < 5$

0.087 ± 0.013 and $f_{\text{baryon}} = 0.089 \pm 0.012$ when using LEP data only, and $f_u = f_d = 0.340 \pm 0.021$, $f_s = 0.101 \pm 0.015$ and $f_{\text{baryon}} = 0.220 \pm 0.048$ when using Tevatron data only. As noted previously, the LHC data are insufficient to determine a complete set of b -hadron production fractions. For these combinations other external inputs are used, *e.g.*, the branching fractions of B mesons to final states with a D or D^* in semileptonic decays, which are needed to evaluate the fraction of semileptonic B_s^0 decays with a D_s^- in the final state.

Time-integrated mixing analyses performed with lepton pairs from $b\bar{b}$ events produced at high-energy colliders measure the quantity

$$\bar{\chi} = f'_d \chi_d + f'_s \chi_s, \quad (31)$$

where f'_d and f'_s are the fractions of B^0 and B_s^0 hadrons in a sample of semileptonic b -hadron decays, and where χ_d and χ_s are the B^0 and B_s^0 time-integrated mixing probabilities. Assuming that all b hadrons have the same semileptonic decay width implies $f'_i = f_i R_i$, where $R_i = \tau_i / \tau_b$ is the ratio of the lifetime τ_i of species i to the average b -hadron lifetime $\tau_b = \sum_i f_i \tau_i$. Hence measurements of the mixing probabilities $\bar{\chi}$, χ_d and χ_s can be used to improve our knowledge of f_u , f_d , f_s and f_{baryon} . In practice, the above relations yield another determination of f_s obtained from f_{baryon} and mixing information,

$$f_s = \frac{1}{R_s} \frac{(1+r)\bar{\chi} - (1-f_{\text{baryon}}R_{\text{baryon}})\chi_d}{(1+r)\chi_s - \chi_d}, \quad (32)$$

where $r = R_u/R_d = \tau(B^+)/\tau(B^0)$.

The published measurements of $\bar{\chi}$ performed by the LEP experiments have been combined by the LEP Electroweak Working Group to yield $\bar{\chi} = 0.1259 \pm 0.0042$ [53].⁷ This can be compared with the our Tevatron average, $\bar{\chi} = 0.147 \pm 0.011$, obtained from D0 [54] and CDF [55] measurements. The two averages deviate from each other by 1.8σ ; this could be an indication that the production fractions of b hadrons at the Z peak or at the Tevatron are not the same.

Using the $\bar{\chi}$ average in Eq. (32) together with our world average $\chi_d = 0.1858 \pm 0.0011$ (see Eq. (68) of Sec. 4.3.1), the assumption $\chi_s = 1/2$ (justified by Eq. (77) in Sec. 4.3.2), the best knowledge of the lifetimes (see Sec. 4.2) and the estimate of f_{baryon} given above, yields $f_s = 0.111 \pm 0.011$ using only LEP data, or $f_s = 0.165 \pm 0.029$ using only Tevatron data. Taking

⁷We use the $\bar{\chi}$ average of Eq. 5.39 in Ref. [53], obtained from a 10-parameter global fit of all electroweak data where the asymmetry measurements have been excluded.

Table 6: Time-integrated mixing probability $\bar{\chi}$ (defined in Eq. (31)), and fractions of the different b -hadron species in an unbiased sample of weakly decaying b hadrons, obtained from both direct and mixing measurements. The correlation coefficients between the fractions are also given.

Quantity		Z decays	Tevatron	ATLAS [51]	LHCb [49]
Mixing probability	$\bar{\chi}$	0.1259 ± 0.0042	0.147 ± 0.011		
B^+ or B^0 fraction	$f_u = f_d$	0.407 ± 0.007	0.344 ± 0.021		
B_s^0 fraction	f_s	0.101 ± 0.008	0.115 ± 0.013		
b -baryon fraction	f_{baryon}	0.085 ± 0.011	0.198 ± 0.046		
B_s^0/B^0 ratio	f_s/f_d	0.249 ± 0.023	0.334 ± 0.040	0.240 ± 0.020	0.256 ± 0.020^u
$\rho(f_s, f_u) = \rho(f_s, f_d)$		-0.628	$+0.159$		
$\rho(f_{\text{baryon}}, f_u) = \rho(f_{\text{baryon}}, f_d)$		-0.817	-0.960		
$\rho(f_{\text{baryon}}, f_s)$		$+0.065$	-0.429		

^u This value has been updated with new inputs by LHCb to yield 0.259 ± 0.015 [56].

into account all known correlations (including that introduced by f_{baryon}), this result is then combined with the set of fractions obtained from direct measurements (given above), to yield the improved estimates of Table 6, still under the constraints of Eq. (27). As can be seen, our knowledge on the mixing parameters reduces the uncertainty on f_s , quite substantially in the case of LEP data.

4.2 b -hadron lifetimes

In the spectator model the decay of a b hadron H_b is governed entirely by the flavour changing $b \rightarrow Wq$ transition ($q = c, u$). For this reason, lifetimes of all b hadrons with light spectators are the same in the spectator approximation regardless of the (spectator) quark content of the H_b . However, in the early 1990's experiments became sensitive enough to start seeing the differences of the lifetimes among various H_b species. The first theoretical calculations of the spectator quark effects on H_b lifetime emerged only a few years earlier [57].

Lifetime calculations are performed in the framework of the Heavy Quark Expansion (HQE) [57–59], using the assumption of quark-hadron duality [60, 61].⁸ In these calculations, the total decay rate of a hadron H_b is expressed as a series of expectation values of operators of increasing dimension, multiplied by the correspondingly higher powers of Λ_{QCD}/m_b :

$$\Gamma_{H_b} = |\text{CKM}|^2 \sum_n c_n \left(\frac{\Lambda_{\text{QCD}}}{m_b} \right)^n \langle H_b | O_n | H_b \rangle, \quad (33)$$

where $|\text{CKM}|^2$ is the relevant combination of CKM matrix elements. The coefficients c_n are calculated perturbatively [63], with the precision of current experiments requiring expansion up to the next-to-leading order in QCD, *i.e.*, order $\alpha_s(m_b)$. Hence, the HQE predicts Γ_{H_b} in the form of an expansion in both Λ_{QCD}/m_b and $\alpha_s(m_b)$. The non-perturbative parts of the calculation are grouped into the expectation values $\langle H_b | O_n | H_b \rangle$ of operators O_n . The

⁸Possible violation of quark-hadron duality has been shown to be severely constrained by experimental results [62].

expectation values can be calculated using lattice QCD or QCD sum rules, or can be related to other observables via the HQE. One may reasonably expect that powers of Λ_{QCD}/m_b provide enough suppression that only the first few terms of the sum in Eq. (33) matter.

Theoretical predictions are usually made for the ratios of the lifetimes (with $\tau(B^0)$ often chosen as the common denominator) rather than for the individual lifetimes, since this leads to cancellation of several uncertainties. The precision of the HQE calculations (see Refs. [64–69], and Ref. [70, 71] for the latest updates) is in some instances already surpassed by the measurements, *e.g.*, in the case of $\tau(B^+)/\tau(B^0)$. Improvement in the precision of calculations is now a matter of progress in the evaluation of the non-perturbative hadronic matrix elements, in particular using lattice QCD, where significant advances have been made in the last decade. However, the following important conclusions, which are in agreement with experimental observation, can be drawn from the HQE, even in its present state:

- The larger the mass of the heavy quark, the smaller the variation in the lifetimes among different hadrons containing this quark, which is to say that, as $m_b \rightarrow \infty$, we retrieve the spectator picture in which the lifetimes of all H_b states are the same. This is well illustrated by the fact that lifetimes are rather similar in the b sector, while they differ by large factors in the charm sector ($m_c < m_b$).
- The non-perturbative corrections to differences between meson and baryon lifetimes arise only at the order of $\Lambda_{\text{QCD}}^2/m_b^2$, which translates into differences among H_b lifetimes of only a few percent.
- The splitting of the meson lifetimes occurs at the $\Lambda_{\text{QCD}}^3/m_b^3$ level.

4.2.1 Overview of lifetime measurements

This section gives an overview of the types of b -hadron lifetime measurements, with details given in subsequent sections. In most cases, the decay time of an H_b state is estimated by measuring its flight distance and dividing it by $\beta\gamma c$. Methods of accessing lifetime information can roughly be divided into the following five categories:

1. ***Inclusive (flavour-blind) measurements.*** Early, low-statistics measurements were aimed at extracting the lifetime from a mixture of b -hadron decays, without distinguishing the decaying species. Often, knowledge of the H_b composition was limited, which made the measurements experiment-specific. Also, Monte Carlo simulation was used for estimating the $\beta\gamma$ factor, because the decaying hadrons were not fully reconstructed. These were usually the largest-statistics b -hadron lifetime measurements accessible to a given experiment, and could therefore serve as an important performance benchmark.
2. ***Measurements in semileptonic decays of a specific H_b .*** The W boson from $b \rightarrow Wc$ produces a $\ell\nu_\ell$ pair ($\ell = e, \mu$) in about 21% of the cases. The electron or muon from such decays provides a clean and efficient trigger signature. The c quark and the spectator quark(s) combine into a charm hadron H_c , which is reconstructed in one or more exclusive decay channels. Identification of the H_c species allows one to separate, at least statistically, different H_b species. The advantage of these measurements is in the sample size, which is usually larger than in the case of exclusively reconstructed hadronic H_b decays (described next). The main disadvantages are related to the difficulty of

estimating the lepton+charm sample composition and to the Monte Carlo reliance for the momentum (and hence $\beta\gamma$ factor) estimate.

3. ***Measurements in exclusively reconstructed hadronic decays.*** These have the advantage of complete reconstruction of the decaying H_b state, which allows one to infer the decaying species, as well as to perform precise measurement of the $\beta\gamma$ factor. Both lead to generally smaller systematic uncertainties than in the above two categories. The downsides are smaller branching fractions and larger combinatorial backgrounds in the case of multi-hadron decays, such as $H_b \rightarrow H_c\pi(\pi\pi)$ with multi-body H_c decays. This problem is often more serious in a hadron collider environment, which has many hadrons and a non-trivial underlying event. Decays of the type $H_b \rightarrow J/\psi H_s$ are often used, as they are relatively clean and easy to trigger on due to the $J/\psi \rightarrow \ell^+\ell^-$ signature.
4. ***Measurements at asymmetric B factories.*** In the $\Upsilon(4S) \rightarrow B\bar{B}$ decay, the B mesons (B^+ or B^0) are essentially at rest in the $\Upsilon(4S)$ frame. This makes direct lifetime measurements impossible in experiments at symmetric-energy colliders, which produce the $\Upsilon(4S)$ at rest. At asymmetric B factories the $\Upsilon(4S)$ meson is boosted, resulting in the B and \bar{B} moving nearly parallel to each other with similar boosts. The lifetime is inferred from the distance Δz separating the B and \bar{B} decay vertices along the beam axis and from the $\Upsilon(4S)$ boost, which is known from the beam energies. This boost was $\beta\gamma \approx 0.55$ (0.43) in the *BABAR* (Belle) experiment, resulting in an average B decay length of approximately 250 (190) μm .

While one B^0 or B^+ meson is fully reconstructed in a semileptonic or hadronic decay mode, the other B in the event is typically not fully reconstructed, in order to avoid loss of efficiency. Rather, only the position of its decay vertex is determined from the remaining tracks in the event. These measurements benefit from large sample sizes, but suffer from poor proper time resolution, comparable to the B lifetime itself. The resolution is dominated by the uncertainty on the decay-vertex positions, which is typically 50 (100) μm for a fully (partially) reconstructed B meson. With much larger samples in the future, the resolution and purity could be improved (and hence the systematics reduced) by fully reconstructing both B mesons in the event.

5. ***Measurement of lifetime ratios.*** This method, initially applied in the measurement of $\tau(B^+)/\tau(B^0)$, is now also used for other b -hadron species at the LHC. The ratio of the lifetimes is extracted from the proper-time dependence of the ratio of the observed yields of two different b -hadron species, both reconstructed in decay modes with similar topologies. The advantage of this method is that subtle efficiency effects and systematic uncertainties (partially) cancel in the ratio.

In some analyses, measurements of two (*e.g.*, $\tau(B^+)$ and $\tau(B^+)/\tau(B^0)$) or three (*e.g.* $\tau(B^+)$, $\tau(B^+)/\tau(B^0)$, and Δm_d) quantities are combined. This introduces correlations among measurements. Another source of correlations among the measurements is systematic effects, which could be common to a number of measurements in the same experiment or to an analysis technique across different experiments. When calculating the averages presented below, such known correlations are taken into account.

Table 7: Measurements of average b -hadron lifetimes.

Experiment	Method	Data set	τ_b (ps)	Ref.
ALEPH	Dipole	91	$1.511 \pm 0.022 \pm 0.078$	[72]
DELPHI	All track i.p. (2D)	91–92	$1.542 \pm 0.021 \pm 0.045$	[73] ^a
DELPHI	Sec. vtx	91–93	$1.582 \pm 0.011 \pm 0.027$	[74] ^a
DELPHI	Sec. vtx	94–95	$1.570 \pm 0.005 \pm 0.008$	[75]
L3	Sec. vtx + i.p.	91–94	$1.556 \pm 0.010 \pm 0.017$	[76] ^b
OPAL	Sec. vtx	91–94	$1.611 \pm 0.010 \pm 0.027$	[77]
SLD	Sec. vtx	93	$1.564 \pm 0.030 \pm 0.036$	[78]
Average set 1 (b vertex)			1.572 ± 0.009	
ALEPH	Lepton i.p. (3D)	91–93	$1.533 \pm 0.013 \pm 0.022$	[79]
L3	Lepton i.p. (2D)	91–94	$1.544 \pm 0.016 \pm 0.021$	[76] ^b
OPAL	Lepton i.p. (2D)	90–91	$1.523 \pm 0.034 \pm 0.038$	[80]
Average set 2 ($b \rightarrow \ell$)			1.537 ± 0.020	
CDF1	J/ψ vtx	92–95	$1.533 \pm 0.015^{+0.035}_{-0.031}$	[81]
Average set 3 ($b \rightarrow J/\psi$)			1.533 ± 0.036	

^a The combined DELPHI result quoted in [74] is $1.575 \pm 0.010 \pm 0.026$ ps.

^b The combined L3 result quoted in [76] is $1.549 \pm 0.009 \pm 0.015$ ps.

4.2.2 Inclusive b -hadron lifetimes

The inclusive b -hadron lifetime is defined as $\tau_b = \sum_i f_i \tau_i$ where τ_i are the individual species lifetimes and f_i are the fractions of the various species present in an unbiased sample of weakly decaying b hadrons produced at a high-energy collider. This quantity is experiment-dependent and certainly less fundamental than the lifetimes of the individual species, which are much more useful for comparison with the theoretical predictions. Nonetheless, we perform the averaging of the inclusive lifetime measurements for completeness and because they might be of interest as “technical numbers.”

In practice, an unbiased measurement of the inclusive lifetime is difficult to achieve, because it would imply that the efficiency is guaranteed to be identical across H_b species. As a result, most of the measurements are biased. In an attempt to group analyses that are expected to select the same mixture of b hadrons, the available results (given in Table 7) are divided into the following three sets:

1. measurements at LEP and SLD that include any b -hadron decay, based on topological reconstruction (secondary vertex or track impact parameters);
2. measurements at LEP based on the identification of a lepton from a b decay; and
3. measurements at hadron colliders based on inclusive $H_b \rightarrow J/\psi X$ reconstruction, where the J/ψ is fully reconstructed.

The mixtures corresponding to Sets 2 and 3 are better defined than for Set 1, in the limit where the reconstruction and selection efficiency of a lepton or a J/ψ from an H_b does not

depend on the decaying hadron type. These mixtures are given by the production fractions and the inclusive branching fractions for each H_b species to give a lepton or a J/ψ . In particular, under the assumption that all b hadrons have the same semileptonic decay width, the analyses of the second set should measure $\tau(b \rightarrow \ell) = (\sum_i f_i \tau_i^3) / (\sum_i f_i \tau_i^2)$ which is necessarily larger than τ_b if lifetime differences exist. Given the present knowledge on τ_i and f_i , $\tau(b \rightarrow \ell) - \tau_b$ is expected to be of the order of 0.003 ps. On the other hand, the third set measuring $\tau(b \rightarrow J/\psi)$ is expected to give an average smaller than τ_b because of the B_c^+ meson, which has a significantly larger probability to decay to a J/ψ than other b -hadron species.

Measurements by SLC and LEP experiments are subject to a number of common systematic uncertainties, such as those due to (lack of knowledge of) b and c fragmentation, b and c decay models, $\mathcal{B}(B \rightarrow \ell)$, $\mathcal{B}(B \rightarrow c \rightarrow \ell)$, $\mathcal{B}(c \rightarrow \ell)$, τ_c , and H_b decay multiplicity. In the averaging, these systematic uncertainties are assumed to be 100% correlated among the experiments. The averages for the sets defined above (also given in Table 7) are

$$\tau(b \text{ vertex}) = 1.572 \pm 0.009 \text{ ps}, \quad (34)$$

$$\tau(b \rightarrow \ell) = 1.537 \pm 0.020 \text{ ps}, \quad (35)$$

$$\tau(b \rightarrow J/\psi) = 1.533 \pm 0.036 \text{ ps}. \quad (36)$$

The differences between these averages are consistent with zero within less than 2σ .

4.2.3 B^0 and B^+ lifetimes and their ratio

After a number of years of dominating these averages, the LEP experiments yielded the scene to the asymmetric B factories and the Tevatron experiments. The B factories have been very successful in utilizing their potential – in only a few years of running, *BABAR* and, to a greater extent, *Belle*, have struck a balance between the statistical and the systematic uncertainties, with both being close to (or even better than) an impressive 1% level. In the meanwhile, CDF and D0 have emerged as significant contributors to the field as the Tevatron Run II data flowed in. In more recent years, the LHCb experiment reached a further step in precision, improving by a factor ~ 2 over the previous best measurements.

At the present time we are in an interesting position of having three sets of measurements (from LEP/SLC, B factories and Tevatron/LHC) that originate from different environments, are obtained using substantially different techniques and are precise enough for cross-checking and comparison.

The $\tau(B^+)$, $\tau(B^0)$ and $\tau(B^+)/\tau(B^0)$ measurements, and their averages, are summarized in Tables 8, 9, and 10. For the average of $\tau(B^+)/\tau(B^0)$ we use only direct measurements of this ratio and not separate measurements of $\tau(B^+)$ and $\tau(B^0)$. The following sources of correlated (within experiment/machine) systematic uncertainties have been considered in the averaging:

- for the SLC and LEP measurements – D^{**} branching fraction uncertainties [4], estimation of the momentum of b mesons produced in Z^0 decays (b -quark fragmentation parameter $\langle X_E \rangle = 0.702 \pm 0.008$ [4]), B_s^0 and b -baryon lifetimes (see Secs. 4.2.4 and 4.2.6), and b -hadron fractions at high energy (see Table 6);
- for the B -factory measurements – alignment, z scale, machine boost (separately within each experiment), sample composition (where applicable);
- for the Tevatron and LHC measurements – alignment (separately within each experiment).

Table 8: Measurements of the B^0 lifetime.

Experiment	Method	Data set	$\tau(B^0)$ (ps)	Ref.
ALEPH	$D^{(*)}\ell$	91–95	$1.518 \pm 0.053 \pm 0.034$	[82]
ALEPH	Exclusive	91–94	$1.25_{-0.13}^{+0.15} \pm 0.05$	[83]
ALEPH	Partial rec. $\pi^+\pi^-$	91–94	$1.49_{-0.15}^{+0.17+0.08}$	[83]
DELPHI	$D^{(*)}\ell$	91–93	$1.61_{-0.13}^{+0.14} \pm 0.08$	[84]
DELPHI	Charge sec. vtx	91–93	$1.63 \pm 0.14 \pm 0.13$	[85]
DELPHI	Inclusive $D^*\ell$	91–93	$1.532 \pm 0.041 \pm 0.040$	[86]
DELPHI	Charge sec. vtx	94–95	$1.531 \pm 0.021 \pm 0.031$	[75]
L3	Charge sec. vtx	94–95	$1.52 \pm 0.06 \pm 0.04$	[87]
OPAL	$D^{(*)}\ell$	91–93	$1.53 \pm 0.12 \pm 0.08$	[88]
OPAL	Charge sec. vtx	93–95	$1.523 \pm 0.057 \pm 0.053$	[89]
OPAL	Inclusive $D^*\ell$	91–00	$1.541 \pm 0.028 \pm 0.023$	[90]
SLD	Charge sec. vtx ℓ	93–95	$1.56_{-0.13}^{+0.14} \pm 0.10$	[91] ^a
SLD	Charge sec. vtx	93–95	$1.66 \pm 0.08 \pm 0.08$	[91] ^a
CDF1	$D^{(*)}\ell$	92–95	$1.474 \pm 0.039_{-0.051}^{+0.052}$	[92]
CDF1	Excl. $J/\psi K^{*0}$	92–95	$1.497 \pm 0.073 \pm 0.032$	[93]
CDF2	Excl. $J/\psi K_S^0, J/\psi K^{*0}$	02–09	$1.507 \pm 0.010 \pm 0.008$	[94]
D0	Excl. $J/\psi K^{*0}$	03–07	$1.414 \pm 0.018 \pm 0.034$	[95]
D0	Excl. $J/\psi K_S^0$	02–11	$1.508 \pm 0.025 \pm 0.043$	[96]
D0	Inclusive $D^-\mu^+$	02–11	$1.534 \pm 0.019 \pm 0.021$	[97]
BABAR	Exclusive	99–00	$1.546 \pm 0.032 \pm 0.022$	[98]
BABAR	Inclusive $D^*\ell$	99–01	$1.529 \pm 0.012 \pm 0.029$	[99]
BABAR	Exclusive $D^*\ell$	99–02	$1.523_{-0.023}^{+0.024} \pm 0.022$	[100]
BABAR	Incl. $D^*\pi, D^*\rho$	99–01	$1.533 \pm 0.034 \pm 0.038$	[101]
BABAR	Inclusive $D^*\ell$	99–04	$1.504 \pm 0.013_{-0.013}^{+0.018}$	[102]
Belle	Exclusive	00–03	$1.534 \pm 0.008 \pm 0.010$	[103]
ATLAS	Excl. $J/\psi K_S^0$	2011	$1.509 \pm 0.012 \pm 0.018$	[104]
CMS	Excl. $J/\psi K^{*0}$	2012	$1.511 \pm 0.005 \pm 0.006$	[105] ^b
CMS	Excl. $J/\psi K_S^0$	2012	$1.527 \pm 0.009 \pm 0.009$	[105] ^b
LHCb	Excl. $J/\psi K^{*0}$	2011	$1.524 \pm 0.006 \pm 0.004$	[106]
LHCb	Excl. $J/\psi K_S^0$	2011	$1.499 \pm 0.013 \pm 0.005$	[106]
LHCb	$K^+\pi^-$	2011	$1.524 \pm 0.011 \pm 0.004$	[107]
Average			1.519 ± 0.004	

^a The combined SLD result quoted in Ref. [91] is $1.64 \pm 0.08 \pm 0.08$ ps.

^b The combined CMS result quoted in Ref. [105] is $1.515 \pm 0.005 \pm 0.006$ ps.

The resultant averages are:

$$\tau(B^0) = 1.519 \pm 0.004 \text{ ps}, \quad (37)$$

$$\tau(B^+) = 1.638 \pm 0.004 \text{ ps}, \quad (38)$$

$$\tau(B^+)/\tau(B^0) = 1.076 \pm 0.004. \quad (39)$$

4.2.4 B_s^0 lifetimes

Like neutral kaons, neutral B mesons contain short- and long-lived components, since the light (L) and heavy (H) eigenstates differ not only in their masses, but also in their total decay widths. While the decay width difference $\Delta\Gamma_d$ can be neglected in the B^0 system, the B_s^0 system exhibits a significant value of $\Delta\Gamma_s = \Gamma_{sL} - \Gamma_{sH}$, where Γ_{sL} and Γ_{sH} are the total decay widths of the light eigenstate B_{sL}^0 and the heavy eigenstate B_{sH}^0 , respectively. The sign of $\Delta\Gamma_s$ is measured to be positive [110], *i.e.*, B_{sH}^0 has a longer lifetime than B_{sL}^0 . Specific measurements of $\Delta\Gamma_s$ and $\Gamma_s = (\Gamma_{sL} + \Gamma_{sH})/2$ are explained and averaged in Sec. 4.3.2, but the results for $1/\Gamma_{sL} = 1/(\Gamma_s + \Delta\Gamma_s/2)$, $1/\Gamma_{sH} = 1/(\Gamma_s - \Delta\Gamma_s/2)$ and the mean B_s^0 lifetime, defined as $\tau(B_s^0) = 1/\Gamma_s$, are also quoted at the end of this section. Neglecting CP violation in $B_s^0 - \bar{B}_s^0$ mixing, which is expected to be very small [62, 111–114] (see also Sec. 4.3.3), the mass eigenstates are also CP eigenstates, with the short-lived (light) state being CP -even and the long-lived (heavy) state being CP -odd [110].

Many B_s^0 lifetime analyses, in particular the early ones performed before the non-zero value of $\Delta\Gamma_s$ was firmly established, ignore $\Delta\Gamma_s$ and fit the proper time distribution of a sample of B_s^0 candidates reconstructed in a certain final state f with a model assuming a single exponential function for the signal. Such *effective lifetime* measurements, which we denote as $\tau_{\text{single}}(B_s^0 \rightarrow f)$, are estimates of the expectation value $\int_0^\infty t \Gamma(B_s(t) \rightarrow f) dt / \int_0^\infty \Gamma(B_s(t) \rightarrow f) dt$ of the total untagged time-dependent decay rate $\Gamma(B_s(t) \rightarrow f)$ [115]; this expectation value may lie *a priori* anywhere between $1/\Gamma_{sL}$ and $1/\Gamma_{sH}$, depending on the proportion of B_{sL}^0 and B_{sH}^0 in the final state f . More recent determinations of effective lifetimes may be interpreted as measurements of the relative composition of B_{sL}^0 and B_{sH}^0 decaying to the final state f . Table 11 summarizes the effective lifetime measurements.

Averaging measurements of $\tau_{\text{single}}(B_s^0 \rightarrow f)$ over several final states f will yield a result corresponding to an ill-defined observable when the proportions of B_{sL}^0 and B_{sH}^0 differ. Therefore, the effective B_s^0 lifetime measurements are broken down into the following categories and averaged separately.

- **$B_s^0 \rightarrow D_s^\mp X$ decays** include mostly flavour-specific decays but also decays with an unknown mixture of light and heavy components. Measurements performed with such inclusive states are no longer used in averages.
- **Decays to flavour-specific final states**, *i.e.*, decays to final states f with decay amplitudes satisfying $A(B_s^0 \rightarrow f) \neq 0$, $A(\bar{B}_s^0 \rightarrow \bar{f}) \neq 0$, $A(B_s^0 \rightarrow \bar{f}) = 0$ and $A(\bar{B}_s^0 \rightarrow f) = 0$, have equal fractions of B_{sL}^0 and B_{sH}^0 at time zero. The corresponding effective lifetime, called the *flavour-specific lifetime*, is equal to [136]

$$\tau_{\text{single}}(B_s^0 \rightarrow \text{flavour specific}) = \frac{1/\Gamma_{sL}^2 + 1/\Gamma_{sH}^2}{1/\Gamma_{sL} + 1/\Gamma_{sH}} = \frac{1}{\Gamma_s} \frac{1 + \left(\frac{\Delta\Gamma_s}{2\Gamma_s}\right)^2}{1 - \left(\frac{\Delta\Gamma_s}{2\Gamma_s}\right)^2}. \quad (40)$$

Because of the fast $B_s^0 - \bar{B}_s^0$ oscillations, possible biases of the flavour-specific lifetime due to a combination of B_s^0/\bar{B}_s^0 production asymmetry, CP violation in the decay amplitudes ($|A(B_s^0 \rightarrow f)| \neq |A(\bar{B}_s^0 \rightarrow \bar{f})|$), and CP violation in $B_s^0 - \bar{B}_s^0$ mixing ($|q_s/p_s| \neq 1$) are strongly suppressed, by a factor $\sim x_s^2$ (given in Eq. (76)). The B_s^0/\bar{B}_s^0 production

Table 9: Measurements of the B^+ lifetime.

Experiment	Method	Data set	$\tau(B^+)$ (ps)	Ref.
ALEPH	$D^{(*)}\ell$	91–95	$1.648 \pm 0.049 \pm 0.035$	[82]
ALEPH	Exclusive	91–94	$1.58^{+0.21+0.04}_{-0.18-0.03}$	[83]
DELPHI	$D^{(*)}\ell$	91–93	$1.61 \pm 0.16 \pm 0.12$	[84] ^a
DELPHI	Charge sec. vtx	91–93	$1.72 \pm 0.08 \pm 0.06$	[85] ^a
DELPHI	Charge sec. vtx	94–95	$1.624 \pm 0.014 \pm 0.018$	[75]
L3	Charge sec. vtx	94–95	$1.66 \pm 0.06 \pm 0.03$	[87]
OPAL	$D^{(*)}\ell$	91–93	$1.52 \pm 0.14 \pm 0.09$	[88]
OPAL	Charge sec. vtx	93–95	$1.643 \pm 0.037 \pm 0.025$	[89]
SLD	Charge sec. vtx ℓ	93–95	$1.61^{+0.13}_{-0.12} \pm 0.07$	[91] ^b
SLD	Charge sec. vtx	93–95	$1.67 \pm 0.07 \pm 0.06$	[91] ^b
CDF1	$D^{(*)}\ell$	92–95	$1.637 \pm 0.058^{+0.045}_{-0.043}$	[92]
CDF1	Excl. $J/\psi K$	92–95	$1.636 \pm 0.058 \pm 0.025$	[93]
CDF2	Excl. $J/\psi K$	02–09	$1.639 \pm 0.009 \pm 0.009$	[94]
CDF2	Excl. $D^0\pi$	02–06	$1.663 \pm 0.023 \pm 0.015$	[108]
<i>BABAR</i>	Exclusive	99–00	$1.673 \pm 0.032 \pm 0.023$	[98]
Belle	Exclusive	00–03	$1.635 \pm 0.011 \pm 0.011$	[103]
LHCb	Excl. $J/\psi K$	2011	$1.637 \pm 0.004 \pm 0.003$	[106]
Average			1.638 ± 0.004	

^a The combined DELPHI result quoted in [85] is 1.70 ± 0.09 ps.

^b The combined SLD result quoted in [91] is $1.66 \pm 0.06 \pm 0.05$ ps.

Table 10: Measurements of the ratio $\tau(B^+)/\tau(B^0)$.

Experiment	Method	Data set	Ratio $\tau(B^+)/\tau(B^0)$	Ref.
ALEPH	$D^{(*)}\ell$	91–95	$1.085 \pm 0.059 \pm 0.018$	[82]
ALEPH	Exclusive	91–94	$1.27^{+0.23+0.03}_{-0.19-0.02}$	[83]
DELPHI	$D^{(*)}\ell$	91–93	$1.00^{+0.17}_{-0.15} \pm 0.10$	[84]
DELPHI	Charge sec. vtx	91–93	$1.06^{+0.13}_{-0.11} \pm 0.10$	[85]
DELPHI	Charge sec. vtx	94–95	$1.060 \pm 0.021 \pm 0.024$	[75]
L3	Charge sec. vtx	94–95	$1.09 \pm 0.07 \pm 0.03$	[87]
OPAL	$D^{(*)}\ell$	91–93	$0.99 \pm 0.14^{+0.05}_{-0.04}$	[88]
OPAL	Charge sec. vtx	93–95	$1.079 \pm 0.064 \pm 0.041$	[89]
SLD	Charge sec. vtx ℓ	93–95	$1.03^{+0.16}_{-0.14} \pm 0.09$	[91] ^a
SLD	Charge sec. vtx	93–95	$1.01^{+0.09}_{-0.08} \pm 0.05$	[91] ^a
CDF1	$D^{(*)}\ell$	92–95	$1.110 \pm 0.056^{+0.033}_{-0.030}$	[92]
CDF1	Excl. $J/\psi K$	92–95	$1.093 \pm 0.066 \pm 0.028$	[93]
CDF2	Excl. $J/\psi K^{(*)}$	02–09	$1.088 \pm 0.009 \pm 0.004$	[94]
D0	$D^{*+}\mu D^0\mu$ ratio	02–04	$1.080 \pm 0.016 \pm 0.014$	[109]
BABAR	Exclusive	99–00	$1.082 \pm 0.026 \pm 0.012$	[98]
Belle	Exclusive	00–03	$1.066 \pm 0.008 \pm 0.008$	[103]
LHCb	Excl. $J/\psi K^{(*)}$	2011	$1.074 \pm 0.005 \pm 0.003$	[106]
Average			1.076 ± 0.004	

^a The combined SLD result quoted in [91] is $1.01 \pm 0.07 \pm 0.06$.

Table 11: Measurements of the effective B_s^0 lifetimes obtained from single exponential fits.

Experiment	Final state f	Data set	$\tau_{\text{single}}(B_s^0 \rightarrow f)$ (ps)	Ref.
ALEPH	$D_s h$	ill-defined	$91\text{--}95$	$1.47 \pm 0.14 \pm 0.08$ [116]
DELPHI	$D_s h$	ill-defined	$91\text{--}95$	$1.53^{+0.16}_{-0.15} \pm 0.07$ [117]
OPAL	D_s incl.	ill-defined	$90\text{--}95$	$1.72^{+0.20+0.18}_{-0.19-0.17}$ [118]
ALEPH	$D_s^- \ell^+$	flavour-specific	$91\text{--}95$	$1.54^{+0.14}_{-0.13} \pm 0.04$ [119]
CDF1	$D_s^- \ell^+$	flavour-specific	$92\text{--}96$	$1.36 \pm 0.09^{+0.06}_{-0.05}$ [120]
DELPHI	$D_s^- \ell^+$	flavour-specific	$92\text{--}95$	$1.42^{+0.14}_{-0.13} \pm 0.03$ [121]
OPAL	$D_s^- \ell^+$	flavour-specific	$90\text{--}95$	$1.50^{+0.16}_{-0.15} \pm 0.04$ [122]
D0	$D_s^- \mu^+ X$	flavour-specific	Run II	10.4 fb^{-1} $1.479 \pm 0.010 \pm 0.021$ [97]
CDF2	$D_s^- \pi^+(X)$	flavour-specific	$02\text{--}06$	1.3 fb^{-1} $1.518 \pm 0.041 \pm 0.027$ [123]
LHCb	$D_s^- D^+$	flavour-specific	$11\text{--}12$	3 fb^{-1} $1.52 \pm 0.15 \pm 0.01$ [124]
LHCb	$D_s^- \pi^+$	flavour-specific	11	1 fb^{-1} $1.535 \pm 0.015 \pm 0.014$ [125]
LHCb	$\pi^+ K^-$	flavour-specific	11	1.0 fb^{-1} $1.60 \pm 0.06 \pm 0.01$ [107]
LHCb	$D_s^{(*)-} \mu^+ \nu_\mu$	flavour-specific	$11\text{--}12$	3.0 fb^{-1} $1.547 \pm 0.013 \pm 0.011$ [126]
Average of above 10 flavour-specific lifetime measurements				1.527 ± 0.011
CDF1	$J/\psi \phi$	CP even+odd	$92\text{--}95$	$1.34^{+0.23}_{-0.19} \pm 0.05$ [81]
D0	$J/\psi \phi$	CP even+odd	$02\text{--}04$	$1.444^{+0.098}_{-0.090} \pm 0.02$ [127]
LHCb	$J/\psi \phi$	CP even+odd	11	1 fb^{-1} $1.480 \pm 0.011 \pm 0.005$ [106]
CMS	$J/\psi \phi$	CP even+odd	12	19.7 fb^{-1} $1.481 \pm 0.007 \pm 0.005$ [105]
Average of above 4 $J/\psi \phi$ lifetime measurements				1.480 ± 0.007
LHCb	$\mu^+ \mu^-$	CP even+odd	$11\text{--}16$	4.4 fb^{-1} $2.04 \pm 0.44 \pm 0.05$ [128]
ALEPH	$D_s^{(*)+} D_s^{(*)-}$	mostly CP even	$91\text{--}95$	$1.27 \pm 0.33 \pm 0.08$ [129]
LHCb	$K^+ K^-$	CP -even	10	0.037 fb^{-1} $1.440 \pm 0.096 \pm 0.009$ [130]
LHCb	$K^+ K^-$	CP -even	11	1.0 fb^{-1} $1.407 \pm 0.016 \pm 0.007$ [107]
Average of above 2 $K^+ K^-$ lifetime measurements				1.408 ± 0.017
LHCb	$D_s^+ D_s^-$	CP -even	$11\text{--}12$	3 fb^{-1} $1.379 \pm 0.026 \pm 0.017$ [124]
LHCb	$J/\psi \eta$	CP -even	$11\text{--}12$	3 fb^{-1} $1.479 \pm 0.034 \pm 0.011$ [131]
Average of above 2 measurements of $1/\Gamma_{sL}$				1.422 ± 0.023
LHCb	$J/\psi K_S^0$	CP -odd	11	1.0 fb^{-1} $1.75 \pm 0.12 \pm 0.07$ [132]
CDF2	$J/\psi f_0(980)$	CP -odd	$02\text{--}08$	3.8 fb^{-1} $1.70^{+0.12}_{-0.11} \pm 0.03$ [133]
D0	$J/\psi f_0(980)$	CP -odd	Run II	10.4 fb^{-1} $1.70 \pm 0.14 \pm 0.05$ [134]
LHCb	$J/\psi \pi^+ \pi^-$	CP -odd	11	1.0 fb^{-1} $1.652 \pm 0.024 \pm 0.024$ [135]
CMS	$J/\psi \pi^+ \pi^-$	CP -odd	12	19.7 fb^{-1} $1.677 \pm 0.034 \pm 0.011$ [105]
Average of above 4 measurements of $1/\Gamma_{sH}$				1.666 ± 0.024

asymmetry at LHCb and the CP asymmetry due to mixing have been measured to be compatible with zero with a precision below 3% [137] and 0.3% (see Eq. (84)), respectively. The corresponding effects on the flavour-specific lifetime, which therefore have a relative size of the order of 10^{-5} or smaller, can be neglected at the current level of experimental precision. Under the assumption of no production asymmetry and no CP violation in mixing, Eq. (40) is exact even for a flavour-specific decay with CP violation in the decay amplitudes. Hence any flavour-specific decay mode can be used to measure the flavour-specific lifetime.

The average of all flavour-specific B_s^0 lifetime measurements [97, 107, 119–126] is

$$\tau_{\text{single}}(B_s^0 \rightarrow \text{flavour specific}) = 1.527 \pm 0.011 \text{ ps}. \quad (41)$$

- **$B_s^0 \rightarrow J/\psi \phi$ decays** contain a well-measured mixture of CP -even and CP -odd states. The published $B_s^0 \rightarrow J/\psi \phi$ effective lifetime measurements [81, 105, 106, 127] are combined into the average $\tau_{\text{single}}(B_s^0 \rightarrow J/\psi \phi) = 1.480 \pm 0.007$ ps. Analyses that separate the CP -even and CP -odd components in this decay through a full angular study, outlined in Sec. 4.3.2, provide directly precise measurements of $1/\Gamma_s$ and $\Delta\Gamma_s$ (see Table 22).
- **$B_s^0 \rightarrow \mu^+ \mu^-$ decays** contain an as-yet unknown mixture of CP -even and CP -odd states. A first measurement has been published by LHCb [128].
- **Decays to CP eigenstates** have also been measured, in the CP -even modes $B_s^0 \rightarrow D_s^{(*)+} D_s^{(*)-}$ by ALEPH [129], $B_s^0 \rightarrow K^+ K^-$ by LHCb [107, 130], $B_s^0 \rightarrow D_s^+ D_s^-$ by LHCb [124] and $B_s^0 \rightarrow J/\psi \eta$ by LHCb [131], as well as in the CP -odd modes $B_s^0 \rightarrow J/\psi f_0(980)$ by CDF [133] and D0 [134], $B_s^0 \rightarrow J/\psi \pi^+ \pi^-$ by LHCb [135] and CMS [105], and $B_s^0 \rightarrow J/\psi K_S^0$ by LHCb [132]. If these decays are dominated by a single weak phase and if CP violation can be neglected, then $\tau_{\text{single}}(B_s^0 \rightarrow CP\text{-even}) = 1/\Gamma_{sL}$ and $\tau_{\text{single}}(B_s^0 \rightarrow CP\text{-odd}) = 1/\Gamma_{sH}$ (see Eqs. (71) and (72) for approximate relations in the presence of mixing-induced CP violation). However, not all these modes can be considered as pure CP eigenstates: a small CP -odd component is most probably present in $B_s^0 \rightarrow D_s^{(*)+} D_s^{(*)-}$ decays. Furthermore, the decays $B_s^0 \rightarrow K^+ K^-$ and $B_s^0 \rightarrow J/\psi K_S^0$ may suffer from direct CP violation due to interfering tree and loop amplitudes. The averages for the effective lifetimes obtained for decays to pure CP -even ($D_s^+ D_s^-$, $J/\psi \eta$) and CP -odd ($J/\psi f_0(980)$, $J/\psi \pi^+ \pi^-$) final states where CP conservation can be assumed are

$$\tau_{\text{single}}(B_s^0 \rightarrow CP\text{-even}) = 1.422 \pm 0.023 \text{ ps}, \quad (42)$$

$$\tau_{\text{single}}(B_s^0 \rightarrow CP\text{-odd}) = 1.666 \pm 0.024 \text{ ps}. \quad (43)$$

As described in Sec. 4.3.2, the effective lifetime averages of Eqs. (41), (42), and (43) are used as ingredients to improve the determination of $1/\Gamma_s$ and $\Delta\Gamma_s$ obtained from the full angular analyses of $B_s^0 \rightarrow J/\psi \phi$ and $B_s^0 \rightarrow J/\psi K^+ K^-$ decays. The resulting world averages for the B_s^0 lifetimes are

$$\tau(B_{sL}^0) = \frac{1}{\Gamma_{sL}} = \frac{1}{\Gamma_s + \Delta\Gamma_s/2} = 1.414 \pm 0.006 \text{ ps}, \quad (44)$$

$$\tau(B_{sH}^0) = \frac{1}{\Gamma_{sH}} = \frac{1}{\Gamma_s - \Delta\Gamma_s/2} = 1.619 \pm 0.009 \text{ ps}, \quad (45)$$

$$\tau(B_s^0) = \frac{1}{\Gamma_s} = \frac{2}{\Gamma_{sL} + \Gamma_{sH}} = 1.510 \pm 0.004 \text{ ps}. \quad (46)$$

Table 12: Measurements of the B_c^+ lifetime.

Experiment	Method	Data set		$\tau(B_c^+)$ (ps)	Ref.
CDF1	$J/\psi \ell$	92–95	0.11 fb^{-1}	$0.46^{+0.18}_{-0.16} \pm 0.03$	[138]
CDF2	$J/\psi e$	02–04	0.36 fb^{-1}	$0.463^{+0.073}_{-0.065} \pm 0.036$	[139]
D0	$J/\psi \mu$	02–06	1.3 fb^{-1}	$0.448^{+0.038}_{-0.036} \pm 0.032$	[140]
CDF2	$J/\psi \pi$		6.7 fb^{-1}	$0.452 \pm 0.048 \pm 0.027$	[141]
LHCb	$J/\psi \mu$	12	2 fb^{-1}	$0.509 \pm 0.008 \pm 0.012$	[142]
LHCb	$J/\psi \pi$	11–12	3 fb^{-1}	$0.5134 \pm 0.0110 \pm 0.0057$	[143]
CMS	$J/\psi \pi$	12	19.7 fb^{-1}	$0.541 \pm 0.026 \pm 0.014$	[105]
Average				0.510 ± 0.009	

4.2.5 B_c^+ lifetime

Early measurements of the B_c^+ meson lifetime, from CDF [138, 139] and D0 [140], use the semileptonic decay mode $B_c^+ \rightarrow J/\psi \ell^+ \nu$ and are based on a simultaneous fit to the mass and lifetime using the vertex formed with the leptons from the decay of the J/ψ and the third lepton. Correction factors to estimate the boost due to the missing neutrino are used. Correlated systematic uncertainties include the impact of the uncertainty of the B_c^+ transverse-momentum spectrum on the correction factors, the level of feed-down from $\psi(2S)$ decays, Monte Carlo modeling of the decay (estimated by varying the decay model from phase space to the ISGW model), and uncertainties in the B_c^+ mass. With more statistics, CDF2 was able to perform the first B_c^+ lifetime based on fully reconstructed $B_c^+ \rightarrow J/\psi \pi^+$ decays [141], which does not suffer from a missing neutrino. More recent measurements at the LHC, both with $B_c^+ \rightarrow J/\psi \mu^+ \nu$ decays from LHCb [142] and $B_c^+ \rightarrow J/\psi \pi^+$ decays from LHCb [143] and CMS [105], achieve the highest level of precision. Two of them [105, 143] are made relative to the B^+ lifetime. Before averaging, they are scaled to our latest B^+ lifetime average, and the induced correlation is taken into account.

All the measurements are summarized in Table 12 and the world average, dominated by the LHCb measurements, is determined to be

$$\tau(B_c^+) = 0.510 \pm 0.009 \text{ ps}. \quad (47)$$

4.2.6 Λ_b^0 and b -baryon lifetimes

The first measurements of b -baryon lifetimes, performed at LEP, originate from two classes of partially reconstructed decays. In the first class, decays with a fully reconstructed Λ_c^+ baryon and a lepton of opposite charge are used. These products are likely to occur in the decay of Λ_b^0 baryons. In the second class, more inclusive final states with a baryon (p , \bar{p} , Λ , or $\bar{\Lambda}$) and a lepton have been used, and these final states can generally arise from any b baryon. With the large b -hadron samples available at the Tevatron and the LHC, the most precise measurements of b baryons now come from fully reconstructed exclusive decays.

The following sources of correlated systematic uncertainties have been accounted for when averaging these measurements: experimental time resolution within a given experiment, b -quark fragmentation distribution into weakly decaying b baryons, Λ_b^0 polarisation, decay model, and

evaluation of the b -baryon purity in the selected event samples. In computing the averages, the central values of the masses are scaled to $M(\Lambda_b^0) = 5619.60 \pm 0.17 \text{ MeV}/c^2$ [21].

For measurements with partially reconstructed decays, the meaning of the decay model systematic uncertainties and the correlation of these uncertainties between measurements are not always clear. Uncertainties related to the decay model are dominated by assumptions on the fraction of n -body semileptonic decays. To be conservative, it is assumed that these are 100% correlated whenever given as an uncertainty. DELPHI varies the fraction of four-body decays from 0.0 to 0.3. In computing the average, the DELPHI result is scaled to a value of 0.2 ± 0.2 for this fraction. Furthermore the semileptonic decay results from LEP are scaled to a Λ_b^0 polarisation of $-0.45^{+0.19}_{-0.17}$ [4] and a b fragmentation parameter $\langle x_E \rangle_b = 0.702 \pm 0.008$ [53].

The list of all measurements are given in Table 13. We do not attempt to average measurements performed with $p\ell$ or $\Lambda\ell$ combinations, which select unknown mixtures of b baryons. Measurements performed with $\Lambda_c^+\ell$ or $\Lambda\ell^+\ell^-$ combinations can be assumed to correspond to semileptonic Λ_b^0 decays. Their average ($1.247^{+0.071}_{-0.069} \text{ ps}$) is significantly different from the average using only measurements performed with exclusively reconstructed hadronic Λ_b^0 decays ($1.471 \pm 0.009 \text{ ps}$). The latter is much more precise and less prone to potential biases than the former. The discrepancy between the two averages is at the level of 3.1σ and assumed to be due to an experimental systematic effect in the semileptonic measurements or to a rare statistical fluctuation. The best estimate of the Λ_b^0 lifetime is therefore taken as the average of the exclusive measurements only. The CDF $\Lambda_b^0 \rightarrow J/\psi \Lambda$ lifetime result [150] is larger than the average of all other exclusive measurements by 2.4σ . It is nonetheless kept in the average without adjustment of input uncertainties. The world average Λ_b^0 lifetime is then

$$\tau(\Lambda_b^0) = 1.471 \pm 0.009 \text{ ps}. \quad (48)$$

For the strange b baryons, we do not include the measurements based on inclusive $\Xi^\mp\ell^\mp$ final states, which consist of a mixture of Ξ_b^- and Ξ_b^0 baryons. Rather, we only average results obtained with fully reconstructed Ξ_b^- , Ξ_b^0 and Ω_b^- baryons, and obtain

$$\tau(\Xi_b^-) = 1.572 \pm 0.040 \text{ ps}, \quad (49)$$

$$\tau(\Xi_b^0) = 1.480 \pm 0.030 \text{ ps}, \quad (50)$$

$$\tau(\Omega_b^-) = 1.64^{+0.18}_{-0.17} \text{ ps}. \quad (51)$$

It should be noted that several b -baryon lifetime measurements from LHCb [152, 155–157] were made with respect to the lifetime of another b hadron (*i.e.*, the original measurement is that of a decay width difference). Before these measurements are included in the averages quoted above, we rescale them according to our latest lifetime average of that reference b hadron. This introduces correlations between our averages, in particular between the Ξ_b^- and Ξ_b^0 lifetimes. Taking this correlation into account leads to

$$\tau(\Xi_b^0)/\tau(\Xi_b^-) = 0.929 \pm 0.028. \quad (52)$$

4.2.7 Summary and comparison with theoretical predictions

Averages of lifetimes of specific b -hadron species are collected in Table 14. As described in the introduction to Sec. 4.2, the HQE can be employed to explain the hierarchy of $\tau(B_c^+) \ll \tau(\Lambda_b^0) < \tau(B_s^0) \approx \tau(B^0) < \tau(B^+)$, and used to predict the ratios between lifetimes. Recent predictions are compared to the measured lifetime ratios in Table 15.

Table 13: Measurements of the b -baryon lifetimes.

Experiment	Method	Data set	Lifetime (ps)	Ref.
ALEPH	$\Lambda\ell$	91–95	$1.20 \pm 0.08 \pm 0.06$	[36]
DELPHI	$\Lambda\ell\pi$ vtx	91–94	$1.16 \pm 0.20 \pm 0.08$	[144] ^b
DELPHI	$\Lambda\mu$ i.p.	91–94	$1.10_{-0.17}^{+0.19} \pm 0.09$	[145] ^b
DELPHI	$p\ell$	91–94	$1.19 \pm 0.14 \pm 0.07$	[144] ^b
OPAL	$\Lambda\ell$ i.p.	90–94	$1.21_{-0.13}^{+0.15} \pm 0.10$	[146] ^c
OPAL	$\Lambda\ell$ vtx	90–94	$1.15 \pm 0.12 \pm 0.06$	[146] ^c
ALEPH	$\Lambda_c^+\ell$	91–95	$1.18_{-0.12}^{+0.13} \pm 0.03$	[36] ^a
ALEPH	$\Lambda\ell^-\ell^+$	91–95	$1.30_{-0.21}^{+0.26} \pm 0.04$	[36] ^a
DELPHI	$\Lambda_c^+\ell$	91–94	$1.11_{-0.18}^{+0.19} \pm 0.05$	[144] ^b
OPAL	$\Lambda_c^+\ell, \Lambda\ell^-\ell^+$	90–95	$1.29_{-0.22}^{+0.24} \pm 0.06$	[122]
CDF1	$\Lambda_c^+\ell$	91–95	$1.32 \pm 0.15 \pm 0.07$	[147]
D0	$\Lambda_c^+\mu$	02–06	$1.290_{-0.110-0.091}^{+0.119+0.087}$	[148]
Average of above 6			$1.247_{-0.069}^{+0.071}$	
CDF2	$\Lambda_c^+\pi$	02–06	$1.401 \pm 0.046 \pm 0.035$	[149]
CDF2	$J/\psi\Lambda$	02–11	$1.565 \pm 0.035 \pm 0.020$	[150]
D0	$J/\psi\Lambda$	02–11	$1.303 \pm 0.075 \pm 0.035$	[96]
ATLAS	$J/\psi\Lambda$	2011	$1.449 \pm 0.036 \pm 0.017$	[104]
CMS	$J/\psi\Lambda$	2011	$1.503 \pm 0.052 \pm 0.031$	[151]
CMS	$J/\psi\Lambda$	2012	$1.477 \pm 0.027 \pm 0.009$	[105]
LHCb	$J/\psi\Lambda$	2011	$1.415 \pm 0.027 \pm 0.006$	[106]
LHCb	$J/\psi pK$ (w.r.t. B^0)	11–12	$1.479 \pm 0.009 \pm 0.010$	[152]
Average of above 8:		Λ_b^0 lifetime =	1.471 ± 0.009	
ALEPH	$\Xi^-\ell^-X$	90–95	$1.35_{-0.28-0.17}^{+0.37+0.15}$	[37]
DELPHI	$\Xi^-\ell^-X$	91–93	$1.5_{-0.4}^{+0.7} \pm 0.3$	[153] ^d
DELPHI	$\Xi^-\ell^-X$	92–95	$1.45_{-0.43}^{+0.55} \pm 0.13$	[38] ^d
CDF2	$J/\psi\Xi^-$	02–11	$1.32 \pm 0.14 \pm 0.02$	[150]
LHCb	$J/\psi\Xi^-$	11–12	$1.55_{-0.09}^{+0.10} \pm 0.03$	[154]
LHCb	$\Xi_c^0\pi^-$ (w.r.t. Λ_b^0)	11–12	$1.599 \pm 0.041 \pm 0.022$	[155]
Average of above 3:		Ξ_b^- lifetime =	1.572 ± 0.040	
LHCb	$\Xi_c^+\pi^-$ (w.r.t. Λ_b^0)	11–12	$1.477 \pm 0.026 \pm 0.019$	[156]
Average of above 1:		Ξ_b^0 lifetime =	1.480 ± 0.030	
CDF2	$J/\psi\Omega^-$	02–11	$1.66_{-0.40}^{+0.53} \pm 0.02$	[150]
LHCb	$J/\psi\Omega^-$	11–12	$1.54_{-0.21}^{+0.26} \pm 0.05$	[154]
LHCb	$\Omega_c^0\pi^-$ (w.r.t. Ξ_b^-)	11–12	$1.78 \pm 0.26 \pm 0.05 \pm 0.06$	[157]
Average of above 3:		Ω_b^- lifetime =	$1.64_{-0.17}^{+0.18}$	

^a The combined ALEPH result quoted in [36] is 1.21 ± 0.11 ps.

^b The combined DELPHI result quoted in [144] is $1.14 \pm 0.08 \pm 0.04$ ps.

^c The combined OPAL result quoted in [146] is $1.16 \pm 0.11 \pm 0.06$ ps.

^d The combined DELPHI result quoted in [38] is $1.48_{-0.31}^{+0.40} \pm 0.12$ ps.

Table 14: Summary of the lifetime averages for the different b -hadron species.

b -hadron species	Measured lifetime
B^+	1.638 ± 0.004 ps
B^0	1.519 ± 0.004 ps
B_s^0	$1/\Gamma_s = 1.510 \pm 0.004$ ps
B_{sL}^0	$1/\Gamma_{sL} = 1.414 \pm 0.006$ ps
B_{sH}^0	$1/\Gamma_{sH} = 1.619 \pm 0.009$ ps
B_c^+	0.510 ± 0.009 ps
Λ_b^0	1.471 ± 0.009 ps
Ξ_b^-	1.572 ± 0.040 ps
Ξ_b^0	1.480 ± 0.030 ps
Ω_b^-	$1.64^{+0.18}_{-0.17}$ ps

 Table 15: Experimental averages of b -hadron lifetime ratios and Heavy-Quark Expansion (HQE) predictions [70, 71].

Lifetime ratio	Experimental average	HQE prediction
$\tau(B^+)/\tau(B^0)$	1.076 ± 0.004	$1.04^{+0.05}_{-0.01} \pm 0.02 \pm 0.01$
$\tau(B_s^0)/\tau(B^0)$	0.994 ± 0.004	1.001 ± 0.002
$\tau(\Lambda_b^0)/\tau(B^0)$	0.969 ± 0.006	0.935 ± 0.054
$\tau(\Xi_b^0)/\tau(\Xi_b^-)$	0.929 ± 0.028	0.95 ± 0.06

The predictions of the ratio between the B^+ and B^0 lifetimes, 1.06 ± 0.02 [67, 68] or $1.04^{+0.05}_{-0.01} \pm 0.02 \pm 0.01$ [70, 71], are in good agreement with experiment.

The total widths of the B_s^0 and B^0 mesons are expected to be very close and differ by at most 1% [69–71, 158, 159]. This prediction is consistent with the experimental ratio $\tau(B_s^0)/\tau(B^0) = \Gamma_d/\Gamma_s$, which is smaller than 1 by $(0.6 \pm 0.4)\%$. The authors of Ref. [62, 111] predict $\tau(B_s^0)/\tau(B^0) = 1.00050 \pm 0.00108 \pm 0.0225 \times \delta$, where δ quantifies a possible breaking of the quark-hadron duality. In this context, they interpret the 2.5σ difference between theory and experiment as being due to either new physics or a sizable duality violation. The key message is that improved experimental precision on this ratio is very welcome.

The ratio $\tau(\Lambda_b^0)/\tau(B^0)$ has particularly been the source of theoretical scrutiny since earlier calculations using the HQE [57–59, 160] predicted a value larger than 0.90, almost 2σ above the world average at the time. Many predictions cluster around a most likely central value of 0.94 [161]. Calculations of this ratio that include higher-order effects predict a lower ratio between the Λ_b^0 and B^0 lifetimes [67–69] and reduce this difference. Since then, the experimental average has settled at a value significantly larger than initially, in agreement with the latest theoretical predictions. A recent review [70, 71] concludes that the long-standing Λ_b^0 lifetime puzzle is resolved, with a nice agreement between the precise experimental determination of $\tau(\Lambda_b^0)/\tau(B^0)$ and the less precise HQE prediction, which needs new lattice calculations. There is also good agreement for the $\tau(\Xi_b^0)/\tau(\Xi_b^-)$ ratio.

The lifetimes of the most abundant b -hadron species are now all known to sub-percent precision. Neglecting the contributions of the rarer species (B_c^+ meson and b baryons other than the Λ_b^0), one can compute the average b -hadron lifetime from the individual lifetimes and

production fractions as

$$\tau_b = \frac{f_d\tau(B^0)^2 + f_u\tau(B^+)^2 + 0.5f_s\tau(B_{sH}^0)^2 + 0.5f_s\tau(B_{sL}^0)^2 + f_{\text{baryon}}\tau(A_b^0)^2}{f_d\tau(B^0) + f_u\tau(B^+) + 0.5f_s\tau(B_{sH}^0) + 0.5f_s\tau(B_{sL}^0) + f_{\text{baryon}}\tau(A_b^0)}. \quad (53)$$

Using the lifetimes of Table 14 and the fractions in Z decays of Table 6, taking into account the correlations between the fractions (Table 6) as well as the correlation between $\tau(B_{sH})$ and $\tau(B_{sL})$ (-0.398), one obtains

$$\tau_b(Z) = 1.5662 \pm 0.0029 \text{ ps}. \quad (54)$$

This is in very good agreement with (and three times more precise than) the average of Eq. (34) for the inclusive measurements performed at LEP.

4.3 Neutral B -meson mixing

The $B^0 - \bar{B}^0$ and $B_s^0 - \bar{B}_s^0$ systems both exhibit the phenomenon of particle-antiparticle mixing. For each of them, there are two mass eigenstates which are linear combinations of the two flavour states, B_q^0 and \bar{B}_q^0 ,

$$|B_{qL}^0\rangle = p_q|B_q^0\rangle + q_q|\bar{B}_q^0\rangle, \quad (55)$$

$$|B_{qH}^0\rangle = p_q|B_q^0\rangle - q_q|\bar{B}_q^0\rangle, \quad (56)$$

where the subscript $q = d$ is used for the B_d^0 ($= B^0$) meson and $q = s$ for the B_s^0 meson. The heaviest (lightest) of these mass states is denoted B_{qH}^0 (B_{qL}^0), with mass m_{qH} (m_{qL}) and total decay width Γ_{qH} (Γ_{qL}). We define

$$\Delta m_q = m_{qH} - m_{qL}, \quad x_q = \Delta m_q/\Gamma_q, \quad (57)$$

$$\Delta\Gamma_q = \Gamma_{qL} - \Gamma_{qH}, \quad y_q = \Delta\Gamma_q/(2\Gamma_q), \quad (58)$$

where $\Gamma_q = (\Gamma_{qH} + \Gamma_{qL})/2 = 1/\bar{\tau}(B_q^0)$ is the average decay width. Δm_q is positive by definition, and $\Delta\Gamma_q$ is expected to be positive within the Standard Model.⁹

Four different time-dependent probabilities are needed to describe the evolution of a neutral B meson that is produced as a flavour state and decays without CP violation to a flavour-specific final state. If CPT is conserved (which will be assumed throughout), they can be written as

$$\left\{ \begin{array}{lcl} \mathcal{P}(B_q^0 \rightarrow B_q^0) & = & \frac{1}{2}e^{-\Gamma_q t} [\cosh(\frac{1}{2}\Delta\Gamma_q t) + \cos(\Delta m_q t)] \\ \mathcal{P}(B_q^0 \rightarrow \bar{B}_q^0) & = & \frac{1}{2}e^{-\Gamma_q t} [\cosh(\frac{1}{2}\Delta\Gamma_q t) - \cos(\Delta m_q t)] |q_q/p_q|^2 \\ \mathcal{P}(\bar{B}_q^0 \rightarrow B_q^0) & = & \frac{1}{2}e^{-\Gamma_q t} [\cosh(\frac{1}{2}\Delta\Gamma_q t) - \cos(\Delta m_q t)] |p_q/q_q|^2 \\ \mathcal{P}(\bar{B}_q^0 \rightarrow \bar{B}_q^0) & = & \frac{1}{2}e^{-\Gamma_q t} [\cosh(\frac{1}{2}\Delta\Gamma_q t) + \cos(\Delta m_q t)] \end{array} \right., \quad (59)$$

where t is the proper time of the system (*i.e.*, the time interval between the production and the decay in the rest frame of the B meson). At the B factories, only the proper-time difference Δt between the decays of the two neutral B mesons from the $\Upsilon(4S)$ can be determined. However,

⁹ For reasons of symmetry in Eqs. (57) and (58), $\Delta\Gamma$ is sometimes defined with the opposite sign. The definition adopted in Eq. (58) is the one used by most experimentalists and many phenomenologists in B physics.

since the two B mesons evolve coherently (keeping opposite flavours as long as neither of them has decayed), the above formulae remain valid if t is replaced with Δt and the production flavour is replaced by the flavour at the time of the decay of the accompanying B meson into a flavour-specific state. As can be seen in the above expressions, the mixing probabilities depend on three mixing observables: Δm_q , $\Delta\Gamma_q$, and $|q_q/p_q|^2$. In particular, CP violation in mixing exists if $|q_q/p_q|^2 \neq 1$. Another (non independent) observable often used to characterize CP violation in the mixing is the so-called semileptonic asymmetry, defined as

$$\mathcal{A}_{\text{SL}}^q = \frac{|p_q/q_q|^2 - |q_q/p_q|^2}{|p_q/q_q|^2 + |q_q/p_q|^2}. \quad (60)$$

All mixing observables depend on two complex numbers, M_{12}^q and Γ_{12}^q , which are the off-diagonal elements of the 2×2 mass and decay matrices describing the evolution of the $B_q^0 - \bar{B}_q^0$ system. In the Standard Model the quantity $|\Gamma_{12}^q/M_{12}^q|$ is small, of the order of $(m_b/m_t)^2$, where m_b and m_t are the bottom and top quark masses. The following relations hold to first order in $|\Gamma_{12}^q/M_{12}^q|$:

$$\Delta m_q = 2|M_{12}^q| [1 + \mathcal{O}(|\Gamma_{12}^q/M_{12}^q|^2)], \quad (61)$$

$$\Delta\Gamma_q = 2|\Gamma_{12}^q| \cos \phi_{12}^q [1 + \mathcal{O}(|\Gamma_{12}^q/M_{12}^q|^2)], \quad (62)$$

$$\mathcal{A}_{\text{SL}}^q = \text{Im}(\Gamma_{12}^q/M_{12}^q) + \mathcal{O}(|\Gamma_{12}^q/M_{12}^q|^2) = \frac{\Delta\Gamma_q}{\Delta m_q} \tan \phi_{12}^q + \mathcal{O}(|\Gamma_{12}^q/M_{12}^q|^2), \quad (63)$$

where

$$\phi_{12}^q = \arg(-M_{12}^q/\Gamma_{12}^q) \quad (64)$$

is the observable phase difference between $-M_{12}^q$ and Γ_{12}^q (often called the mixing phase). It should be noted that the theoretical predictions for Γ_{12}^q are based on the same HQE as the lifetime predictions.

In the next sections we review in turn the experimental knowledge on the B^0 decay-width and mass differences, the B_s^0 decay-width and mass differences, CP violation in B^0 and B_s^0 mixing, and mixing-induced CP violation in B_s^0 decays.

4.3.1 B^0 mixing parameters $\Delta\Gamma_d$ and Δm_d

A large number of time-dependent $B^0 - \bar{B}^0$ oscillation analyses have been performed in the past 20 years by the ALEPH, DELPHI, L3, OPAL, CDF, D0, *BABAR*, Belle and LHCb collaborations. The corresponding measurements of Δm_d are summarized in Table 16. It is notable that the systematic uncertainties are comparable to the statistical uncertainties; they are often dominated by sample composition, mistag probability, or b -hadron lifetime contributions. Before being combined, the measurements are adjusted on the basis of a common set of input values, including the averages of the b -hadron fractions and lifetimes given in this report (see Secs. 4.1 and 4.2). Some measurements are statistically correlated. Systematic correlations arise both from common physics sources (fractions, lifetimes, branching fractions of b hadrons), and from purely experimental or algorithmic effects (efficiency, resolution, flavour tagging, background description). Combining all published measurements listed in Table 16 and accounting for all identified correlations as described in Ref. [4] yields $\Delta m_d = 0.5065 \pm 0.0016 \pm 0.0011 \text{ ps}^{-1}$.

On the other hand, ARGUS and CLEO have published measurements of the time-integrated mixing probability χ_d [181–183], which average to $\chi_d = 0.182 \pm 0.015$. Following Ref. [183],

Table 16: Time-dependent measurements included in the Δm_d average. The results obtained from multi-dimensional fits involving also the B^0 (and B^+) lifetime(s) as free parameter(s) [100, 102, 103] have been converted into one-dimensional measurements of Δm_d . All measurements have then been adjusted to a common set of physics parameters before being combined.

Experiment and Ref.	Method rec.	Method tag	Δm_d in ps $^{-1}$ before adjustment	Δm_d in ps $^{-1}$ after adjustment
ALEPH [162]	ℓ	Q_{jet}	$0.404 \pm 0.045 \pm 0.027$	
ALEPH [162]	ℓ	ℓ	$0.452 \pm 0.039 \pm 0.044$	
ALEPH [162]	above two combined		$0.422 \pm 0.032 \pm 0.026$	$0.440 \pm 0.032 \pm^{+0.020}_{-0.019}$
ALEPH [162]	D^*	ℓ, Q_{jet}	$0.482 \pm 0.044 \pm 0.024$	$0.482 \pm 0.044 \pm 0.024$
DELPHI [163]	ℓ	Q_{jet}	$0.493 \pm 0.042 \pm 0.027$	$0.500 \pm 0.042 \pm 0.024$
DELPHI [163]	$\pi^* \ell$	Q_{jet}	$0.499 \pm 0.053 \pm 0.015$	$0.500 \pm 0.053 \pm 0.015$
DELPHI [163]	ℓ	ℓ	$0.480 \pm 0.040 \pm 0.051$	$0.495 \pm 0.040 \pm^{+0.042}_{-0.040}$
DELPHI [163]	D^*	Q_{jet}	$0.523 \pm 0.072 \pm 0.043$	$0.518 \pm 0.072 \pm 0.043$
DELPHI [164]	vtx	comb	$0.531 \pm 0.025 \pm 0.007$	$0.525 \pm 0.025 \pm 0.006$
L3 [165]	ℓ	ℓ	$0.458 \pm 0.046 \pm 0.032$	$0.467 \pm 0.046 \pm 0.028$
L3 [165]	ℓ	Q_{jet}	$0.427 \pm 0.044 \pm 0.044$	$0.439 \pm 0.044 \pm 0.042$
L3 [165]	ℓ	$\ell(\text{IP})$	$0.462 \pm 0.063 \pm 0.053$	$0.471 \pm 0.063 \pm 0.044$
OPAL [166]	ℓ	ℓ	$0.430 \pm 0.043 \pm^{+0.028}_{-0.030}$	$0.467 \pm 0.043 \pm^{+0.017}_{-0.016}$
OPAL [167]	ℓ	Q_{jet}	$0.444 \pm 0.029 \pm^{+0.020}_{-0.017}$	$0.481 \pm 0.029 \pm 0.013$
OPAL [168]	$D^* \ell$	Q_{jet}	$0.539 \pm 0.060 \pm 0.024$	$0.544 \pm 0.060 \pm 0.023$
OPAL [168]	D^*	ℓ	$0.567 \pm 0.089 \pm^{+0.029}_{-0.023}$	$0.572 \pm 0.089 \pm^{+0.028}_{-0.022}$
OPAL [90]	$\pi^* \ell$	Q_{jet}	$0.497 \pm 0.024 \pm 0.025$	$0.496 \pm 0.024 \pm 0.025$
CDF1 [169]	$D\ell$	SST	$0.471 \pm^{+0.078}_{-0.068} \pm^{+0.033}_{-0.034}$	$0.470 \pm^{+0.078}_{-0.068} \pm^{+0.033}_{-0.034}$
CDF1 [170]	μ	μ	$0.503 \pm 0.064 \pm 0.071$	$0.514 \pm 0.064 \pm^{+0.070}_{-0.069}$
CDF1 [171]	ℓ	ℓ, Q_{jet}	$0.500 \pm 0.052 \pm 0.043$	$0.546 \pm 0.052 \pm 0.036$
CDF1 [172]	$D^* \ell$	ℓ	$0.516 \pm 0.099 \pm^{+0.029}_{-0.035}$	$0.523 \pm 0.099 \pm^{+0.028}_{-0.035}$
D0 [173]	$D^{(*)} \mu$	OST	$0.506 \pm 0.020 \pm 0.016$	$0.506 \pm 0.020 \pm 0.016$
BABAR [174]	B^0	ℓ, K, NN	$0.516 \pm 0.016 \pm 0.010$	$0.521 \pm 0.016 \pm 0.008$
BABAR [175]	ℓ	ℓ	$0.493 \pm 0.012 \pm 0.009$	$0.487 \pm 0.012 \pm 0.006$
BABAR [100]	$D^* \ell \nu$	ℓ, K, NN	$0.492 \pm 0.018 \pm 0.014$	$0.493 \pm 0.018 \pm 0.013$
BABAR [102]	$D^* \ell \nu(\text{part})$	ℓ	$0.511 \pm 0.007 \pm 0.007$	$0.513 \pm 0.007 \pm 0.007$
Belle [103]	$B^0, D^* \ell \nu$	comb	$0.511 \pm 0.005 \pm 0.006$	$0.514 \pm 0.005 \pm 0.006$
Belle [176]	$D^* \pi(\text{part})$	ℓ	$0.509 \pm 0.017 \pm 0.020$	$0.514 \pm 0.017 \pm 0.019$
Belle [8]	ℓ	ℓ	$0.503 \pm 0.008 \pm 0.010$	$0.506 \pm 0.008 \pm 0.008$
LHCb [177]	B^0	OST	$0.499 \pm 0.032 \pm 0.003$	$0.499 \pm 0.032 \pm 0.003$
LHCb [178]	B^0	OST,SST	$0.5156 \pm 0.0051 \pm 0.0033$	$0.5156 \pm 0.0051 \pm 0.0033$
LHCb [179]	$D\mu$	OST,SST	$0.503 \pm 0.011 \pm 0.013$	$0.503 \pm 0.011 \pm 0.013$
LHCb [180]	$D^{(*)} \mu$	OST	$0.5050 \pm 0.0021 \pm 0.0010$	$0.5050 \pm 0.0021 \pm 0.0010$

World average (all above measurements included):	$0.5065 \pm 0.0016 \pm 0.0011$
– ALEPH, DELPHI, L3 and OPAL only:	$0.493 \pm 0.011 \pm 0.009$
– CDF and D0 only:	$0.509 \pm 0.017 \pm 0.013$
– BABAR and Belle only:	$0.509 \pm 0.003 \pm 0.003$
– LHCb only:	$0.5063 \pm 0.0019 \pm 0.0010$

the decay width difference $\Delta\Gamma_d$ could in principle be extracted from the measured value of $\Gamma_d = 1/\tau(B^0)$ and the above averages for Δm_d and χ_d (provided that $\Delta\Gamma_d$ has a negligible impact on the Δm_d and $\tau(B^0)$ analyses that have assumed $\Delta\Gamma_d = 0$), using the relation

$$\chi_d = \frac{x_d^2 + y_d^2}{2(x_d^2 + 1)}. \quad (65)$$

However, direct time-dependent studies provide much stronger constraints: $|\Delta\Gamma_d|/\Gamma_d < 18\%$ at 95% CL from DELPHI [164], $-6.8\% < \text{sign}(\text{Re}\lambda_{CP})\Delta\Gamma_d/\Gamma_d < 8.4\%$ at 90% CL from *BABAR* [184], and $\text{sign}(\text{Re}\lambda_{CP})\Delta\Gamma_d/\Gamma_d = (1.7 \pm 1.8 \pm 1.1)\%$ [185] from Belle, where $\lambda_{CP} = (q_d/p_d)(\bar{A}_{CP}/A_{CP})$ is defined for a *CP*-even final state. The sensitivity to the overall sign of $\text{sign}(\text{Re}\lambda_{CP})\Delta\Gamma_d/\Gamma_d$ comes from the use of B^0 decays to *CP* eigenstates. In addition, LHCb has obtained $\Delta\Gamma_d/\Gamma_d = (-4.4 \pm 2.5 \pm 1.1)\%$ [106] by comparing measurements of the lifetime for $B^0 \rightarrow J/\psi K^{*0}$ and $B^0 \rightarrow J/\psi K_S^0$ decays, following the method of Ref. [186]. Using a similar method, ATLAS and CMS have measured $\Delta\Gamma_d/\Gamma_d = (-0.1 \pm 1.1 \pm 0.9)\%$ [187] and $\Delta\Gamma_d/\Gamma_d = (+3.4 \pm 2.3 \pm 2.4)\%$ [105], respectively. Assuming $\text{Re}\lambda_{CP} > 0$, as expected from the global fits of the Unitarity Triangle within the Standard Model [188], a combination of these six results (after adjusting the DELPHI and *BABAR* results to $1/\Gamma_d = \tau(B^0) = 1.519 \pm 0.004$ ps) yields

$$\Delta\Gamma_d/\Gamma_d = 0.001 \pm 0.010, \quad (66)$$

an average consistent with zero and with the Standard Model prediction of $(3.97 \pm 0.90) \times 10^{-3}$ [111]. An independent result, $\Delta\Gamma_d/\Gamma_d = (0.50 \pm 1.38)\%$ [189], was obtained by the D0 collaboration from their measurements of the single muon and same-sign dimuon charge asymmetries, under the interpretation that the observed asymmetries are due to *CP* violation in neutral *B*-meson mixing and interference. This indirect determination was called into question [190] and is therefore not included in the above average, as explained in Sec. 4.3.3.

Assuming $\Delta\Gamma_d = 0$ and using $1/\Gamma_d = \tau(B^0) = 1.519 \pm 0.004$ ps, the Δm_d and χ_d results are combined through Eq. (65) to yield the world average

$$\Delta m_d = 0.5065 \pm 0.0019 \text{ ps}^{-1}, \quad (67)$$

or, equivalently,

$$x_d = 0.769 \pm 0.004 \quad \text{and} \quad \chi_d = 0.1858 \pm 0.0011. \quad (68)$$

Figure 6 compares the Δm_d values obtained by the different experiments.

The B^0 mixing averages given in Eqs. (67) and (68) and the *b*-hadron fractions of Table 6 have been obtained in a fully consistent way, taking into account the fact that the fractions are computed using the χ_d value of Eq. (68) and that many individual measurements of Δm_d at high energy depend on the assumed values for the *b*-hadron fractions. Furthermore, this set of averages is consistent with the lifetime averages of Sec. 4.2.

4.3.2 B_s^0 mixing parameters $\Delta\Gamma_s$ and Δm_s

The best sensitivity to $\Delta\Gamma_s$ is currently achieved by the recent time-dependent measurements of the $B_s^0 \rightarrow J/\psi \phi$ (or more generally $B_s^0 \rightarrow (c\bar{c})K^+K^-$) decay rates performed at CDF [191], D0 [192], ATLAS [193, 194] CMS [195] and LHCb [196–198], where the *CP*-even and *CP*-odd amplitudes are statistically separated through a full angular analysis. These studies use both

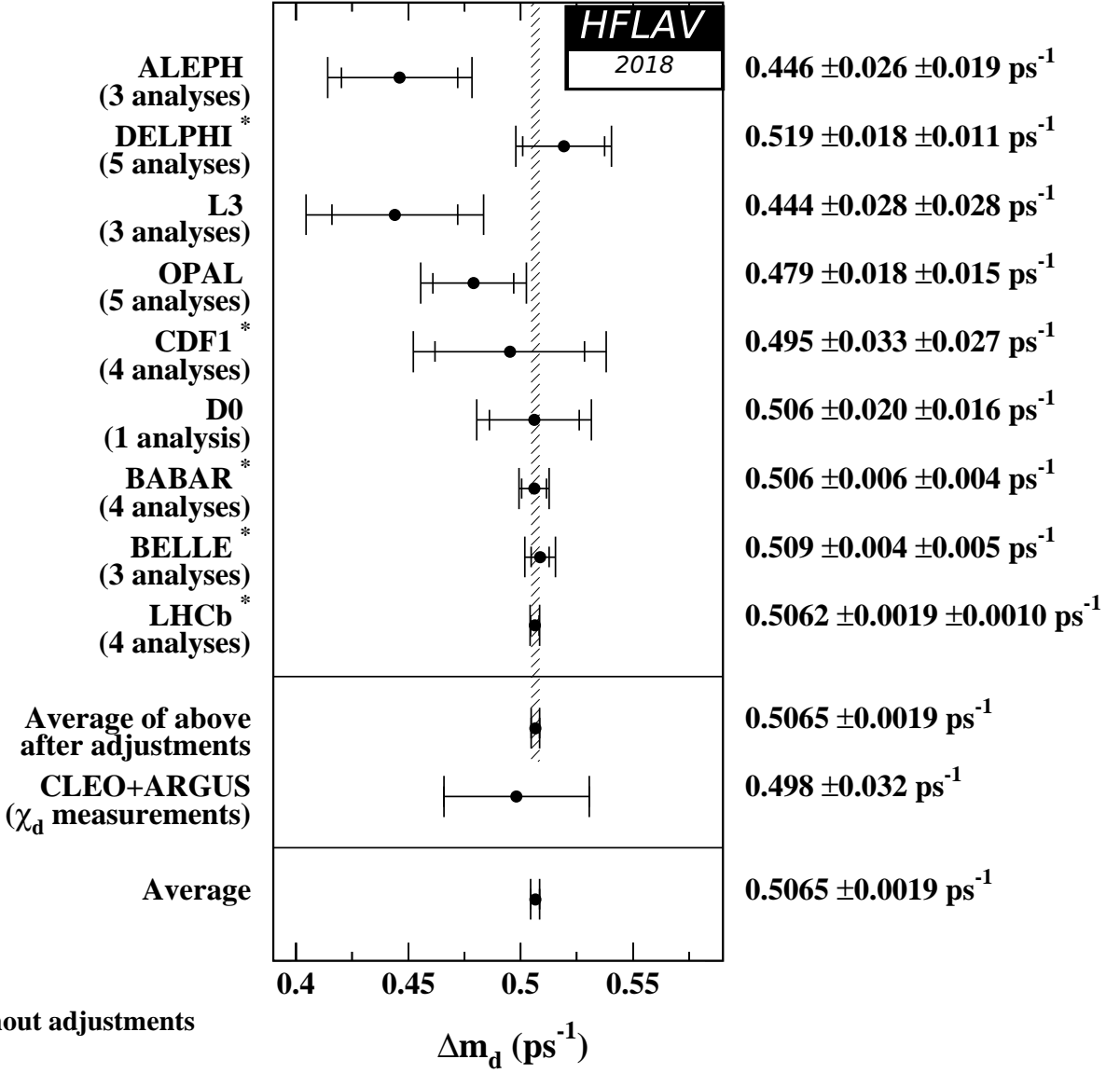


Figure 6: The $B^0-\overline{B}^0$ oscillation frequency Δm_d as measured by the different experiments. The averages quoted for ALEPH, L3 and OPAL are taken from the original publications, while the ones for DELPHI, CDF, BABAR, Belle and LHCb are computed from the individual results listed in Table 16 without performing any adjustments. The time-integrated measurements of χ_d from the symmetric B factory experiments ARGUS and CLEO are converted to a Δm_d value using $\tau(B^0) = 1.519 \pm 0.004$ ps. The two global averages are obtained after adjustments of all the individual Δm_d results of Table 16 (see text).

Table 17: Measurements of $\Delta\Gamma_s$ and Γ_s using $B_s^0 \rightarrow J/\psi\phi$, $B_s^0 \rightarrow J/\psi K^+K^-$ and $B_s^0 \rightarrow \psi(2S)\phi$ decays. Only the solution with $\Delta\Gamma_s > 0$ is shown, since the two-fold ambiguity has been resolved in Ref. [110]. The first error is due to statistics, the second one to systematics. The last line gives our average.

Exp.	Mode	Dataset	$\Delta\Gamma_s$ (ps $^{-1}$)	Γ_s (ps $^{-1}$)	Ref.
CDF	$J/\psi\phi$	9.6 fb $^{-1}$	$+0.068 \pm 0.026 \pm 0.009$	$0.654 \pm 0.008 \pm 0.004$	[191]
D0	$J/\psi\phi$	8.0 fb $^{-1}$	$+0.163^{+0.065}_{-0.064}$	$0.693^{+0.018}_{-0.017}$	[192]
ATLAS	$J/\psi\phi$	4.9 fb $^{-1}$	$+0.053 \pm 0.021 \pm 0.010$	$0.677 \pm 0.007 \pm 0.004$	[193]
ATLAS	$J/\psi\phi$	14.3 fb $^{-1}$	$+0.101 \pm 0.013 \pm 0.007$	$0.676 \pm 0.004 \pm 0.004$	[194]
ATLAS	above 2 combined		$+0.085 \pm 0.011 \pm 0.007$	$0.675 \pm 0.003 \pm 0.003$	[194]
CMS	$J/\psi\phi$	19.7 fb $^{-1}$	$+0.095 \pm 0.013 \pm 0.007$	$0.6704 \pm 0.0043 \pm 0.0055$	[195]
LHCb	$J/\psi K^+K^-$	3.0 fb $^{-1}$	$+0.0805 \pm 0.0091 \pm 0.0032$	$0.6603 \pm 0.0027 \pm 0.0015$	[196]
LHCb	$J/\psi K^+K^-$ ^a	3.0 fb $^{-1}$	$+0.066 \pm 0.018 \pm 0.010$	$0.650 \pm 0.006 \pm 0.004$	[197]
LHCb	above 2 combined		$+0.0813 \pm 0.0073 \pm 0.0036$	$0.6588 \pm 0.0022 \pm 0.0015$	[197]
LHCb	$\psi(2S)\phi$	3.0 fb $^{-1}$	$+0.066^{+0.041}_{-0.044} \pm 0.007$	$0.668 \pm 0.011 \pm 0.006$	[198]
All combined			$+0.085 \pm 0.006$	0.6640 ± 0.0020	

^a $m(K^+K^-) > 1.05$ GeV/ c^2 .

untagged and tagged B_s^0 candidates and are optimized for the measurement of the CP -violating phase $\phi_s^{c\bar{c}s}$, defined later in Sec. 4.3.4. The LHCb collaboration analyzed the $B_s^0 \rightarrow J/\psi K^+K^-$ decay, considering that the K^+K^- system can be in a P -wave or S -wave state, and measured the dependence of the strong phase difference between the P -wave and S -wave amplitudes as a function of the K^+K^- invariant mass [110]. This allowed, for the first time, the unambiguous determination of the sign of $\Delta\Gamma_s$, which was found to be positive at the 4.7σ level. The following averages present only the $\Delta\Gamma_s > 0$ solutions.

The published results [191–198] are shown in Table 17. They are combined taking into account, in each analysis, the correlation between $\Delta\Gamma_s$ and Γ_s . The results, displayed as the red contours labelled “ $B_s^0 \rightarrow (c\bar{c})KK$ measurements” in the plots of Fig. 7, are given in the first column of numbers of Table 18.

An alternative approach, which is directly sensitive to first order in $\Delta\Gamma_s/\Gamma_s$, is to determine the effective lifetime of untagged B_s^0 candidates decaying to pure CP eigenstates; we use here measurements with $B_s^0 \rightarrow D_s^+D_s^-$ [124], $B_s^0 \rightarrow J/\psi\eta$ [131], $B_s^0 \rightarrow J/\psi f_0(980)$ [133, 134] and $B_s^0 \rightarrow J/\psi\pi^+\pi^-$ [135] decays. The precise extraction of $1/\Gamma_s$ and $\Delta\Gamma_s$ from such measurements, discussed in detail in Ref. [115], requires additional information in the form of theoretical assumptions or external inputs on weak phases and hadronic parameters. If f denotes a final state into which both B_s^0 and \bar{B}_s^0 can decay, the ratio of the effective B_s^0 lifetime decaying to f relative to the mean B_s^0 lifetime is [115]¹⁰

$$\frac{\tau_{\text{single}}(B_s^0 \rightarrow f)}{\tau(B_s^0)} = \frac{1}{1 - y_s^2} \left[\frac{1 - 2A_f^{\Delta\Gamma}y_s + y_s^2}{1 - A_f^{\Delta\Gamma}y_s} \right], \quad (69)$$

¹⁰ The definition of $A_f^{\Delta\Gamma}$ given in Eq. (70) has the sign opposite to that given in Ref. [115].

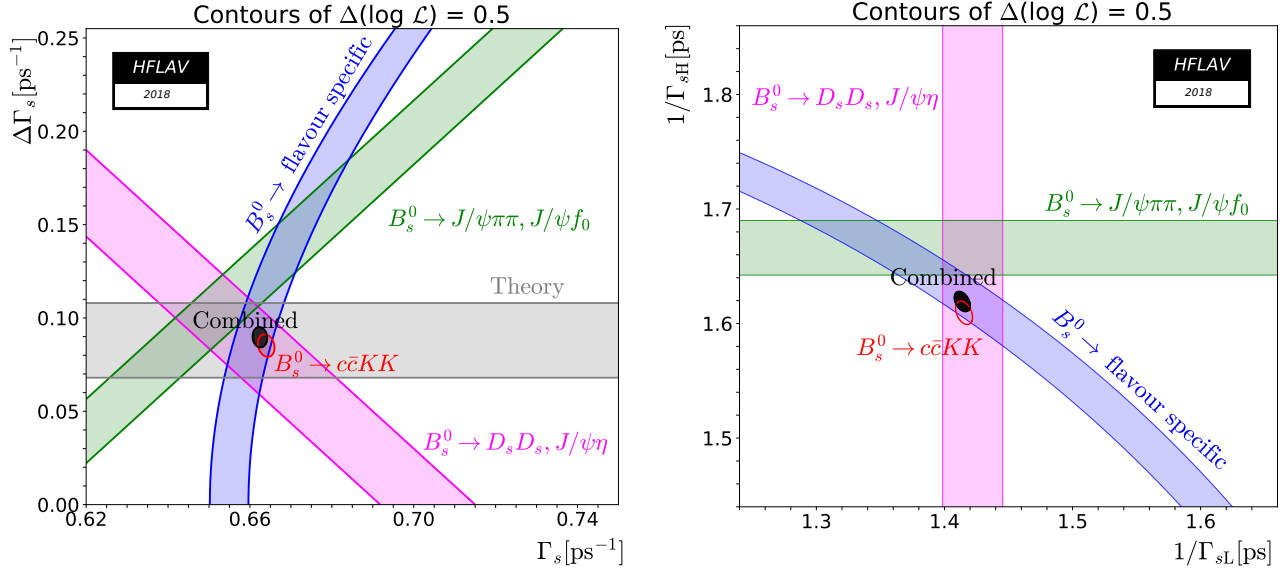


Figure 7: Contours of $\Delta \ln L = 0.5$ (39% CL for the enclosed 2D regions, 68% CL for the bands) shown in the $(\Gamma_s, \Delta\Gamma_s)$ plane on the left and in the $(1/\Gamma_{sL}, 1/\Gamma_{sH})$ plane on the right. The average of all the $B_s^0 \rightarrow J/\psi\phi$, $B_s^0 \rightarrow J/\psi K^+K^-$ and $B_s^0 \rightarrow \psi(2S)\phi$ results is shown as the red contour, and the constraints given by the effective lifetime measurements of B_s^0 to flavour-specific, pure CP -odd and pure CP -even final states are shown as the blue, green and purple bands, respectively. The average taking all constraints into account is shown as the dark-filled contour. The light-grey band is a theory prediction $\Delta\Gamma_s = 0.088 \pm 0.020 \text{ ps}^{-1}$ [62, 111] that assumes no new physics in B_s^0 mixing.

Table 18: Averages of $\Delta\Gamma_s$, Γ_s and related quantities, obtained from $B_s^0 \rightarrow J/\psi\phi$, $B_s^0 \rightarrow J/\psi K^+K^-$ and $B_s^0 \rightarrow \psi(2S)\phi$ alone (first column), adding the constraints from the effective lifetimes measured in pure CP modes $B_s^0 \rightarrow D_s^+D_s^-, J/\psi\eta$ and $B_s^0 \rightarrow J/\psi f_0(980), J/\psi\pi^+\pi^-$ (second column), and adding the constraint from the effective lifetime measured in flavour-specific modes $B_s^0 \rightarrow D_s^-\ell^+\nu X, D_s^-\pi^+, D_s^-D^+$ (third column, recommended world averages).

	$B_s^0 \rightarrow (c\bar{c})K^+K^-$ modes only (see Table 17)	$B_s^0 \rightarrow (c\bar{c})K^+K^-$ modes + pure CP modes	$B_s^0 \rightarrow (c\bar{c})K^+K^-$ modes + pure CP modes + flavour-specific modes
Γ_s	$0.6640 \pm 0.0020 \text{ ps}^{-1}$	$0.6627 \pm 0.0019 \text{ ps}^{-1}$	$0.6624 \pm 0.0018 \text{ ps}^{-1}$
$1/\Gamma_s$	$1.506 \pm 0.005 \text{ ps}$	$1.509 \pm 0.004 \text{ ps}$	$1.510 \pm 0.004 \text{ ps}$
$1/\Gamma_{sL}$	$1.415 \pm 0.007 \text{ ps}$	$1.414 \pm 0.006 \text{ ps}$	$1.414 \pm 0.006 \text{ ps}$
$1/\Gamma_{sH}$	$1.609 \pm 0.010 \text{ ps}$	$1.618 \pm 0.009 \text{ ps}$	$1.619 \pm 0.009 \text{ ps}$
$\Delta\Gamma_s$	$+0.085 \pm 0.006 \text{ ps}^{-1}$	$+0.089 \pm 0.006 \text{ ps}^{-1}$	$+0.090 \pm 0.005 \text{ ps}^{-1}$
$\Delta\Gamma_s/\Gamma_s$	$+0.128 \pm 0.009$	$+0.135 \pm 0.008$	$+0.135 \pm 0.008$
$\rho(\Gamma_s, \Delta\Gamma_s)$	-0.193	-0.151	-0.080

where

$$A_f^{\Delta\Gamma} = -\frac{2\text{Re}(\lambda_f)}{1+|\lambda_f|^2}. \quad (70)$$

To include the measurements of the effective $B_s^0 \rightarrow D_s^+ D_s^-$ (CP -even), $B_s^0 \rightarrow J/\psi f_0(980)$ (CP -odd) and $B_s^0 \rightarrow J/\psi \pi^+ \pi^-$ (CP -odd) lifetimes as constraints in the $\Delta\Gamma_s$ fit,¹¹ we neglect sub-leading penguin contributions and possible direct CP violation. Explicitly, in Eq. (70), we set $A_{CP\text{-even}}^{\Delta\Gamma} = \cos\phi_s^{c\bar{c}s}$ and $A_{CP\text{-odd}}^{\Delta\Gamma} = -\cos\phi_s^{c\bar{c}s}$. Given the small value of $\phi_s^{c\bar{c}s}$, we have, to first order in y_s :

$$\tau_{\text{single}}(B_s^0 \rightarrow CP\text{-even}) \approx \frac{1}{\Gamma_{sL}} \left(1 + \frac{(\phi_s^{c\bar{c}s})^2 y_s}{2} \right), \quad (71)$$

$$\tau_{\text{single}}(B_s^0 \rightarrow CP\text{-odd}) \approx \frac{1}{\Gamma_{sH}} \left(1 - \frac{(\phi_s^{c\bar{c}s})^2 y_s}{2} \right). \quad (72)$$

The numerical inputs are taken from Eqs. (42) and (43), and the resulting averages, combined with the $B_s^0 \rightarrow J/\psi K^+ K^-$ information, are indicated in the second column of numbers of Table 18. These averages assume $\phi_s^{c\bar{c}s} = 0$, which is compatible with the $\phi_s^{c\bar{c}s}$ average presented in Sec. 4.3.4.

Information on $\Delta\Gamma_s$ can also be obtained from the study of the proper time distribution of untagged samples of flavour-specific B_s^0 decays [136], where the flavour (*i.e.*, B_s^0 or \bar{B}_s^0) at the time of decay can be determined by the decay products. In such decays, *e.g.* semileptonic B_s^0 decays, there is an equal mix of the heavy and light mass eigenstates at time zero. The proper time distribution is then a superposition of two exponential functions with decay constants Γ_{sL} and Γ_{sH} . This provides sensitivity to both $1/\Gamma_s$ and $(\Delta\Gamma_s/\Gamma_s)^2$. Ignoring $\Delta\Gamma_s$ and fitting for a single exponential leads to an estimate of Γ_s with a relative bias proportional to $(\Delta\Gamma_s/\Gamma_s)^2$, as shown in Eq. (40). Including the constraint from the world-average flavour-specific B_s^0 lifetime, given in Eq. (41), leads to the results shown in the last column of Table 18. These world averages are displayed as the dark-filled contours labelled ‘‘Combined’’ in the plots of Fig. 7. They correspond to the lifetime averages $1/\Gamma_s = 1.510 \pm 0.004$ ps, $1/\Gamma_{sL} = 1.414 \pm 0.006$ ps, $1/\Gamma_{sH} = 1.619 \pm 0.009$ ps, and to the decay-width difference

$$\Delta\Gamma_s = +0.090 \pm 0.005 \text{ ps}^{-1} \quad \text{and} \quad \Delta\Gamma_s/\Gamma_s = +0.135 \pm 0.008. \quad (73)$$

The good agreement with the Standard Model prediction $\Delta\Gamma_s = 0.088 \pm 0.020 \text{ ps}^{-1}$ [62, 111] excludes significant quark-hadron duality violation in the HQE [199]. Estimates of $\Delta\Gamma_s/\Gamma_s$ obtained from measurements of the $B_s^0 \rightarrow D_s^{(*)+} D_s^{*-}$ branching fraction [129, 200–202] are not used in the average, since they are based on the questionable [203] assumption that these decays account for all CP -even final states. The results of early lifetime analyses that attempted to measure $\Delta\Gamma_s/\Gamma_s$ [81, 87, 117, 121] are not used either.

The strength of B_s^0 mixing has been known to be large for more than 20 years. Indeed the time-integrated measurements of $\bar{\chi}$ (see Sec. 4.1.3), when compared to our knowledge of χ_d and the b -hadron fractions, indicated that χ_s should be close to its maximal possible value of $1/2$. Many searches of the time dependence of this mixing have been performed by ALEPH [204], DELPHI [117, 121, 164, 205], OPAL [206, 207], SLD [208, 209], CDF (Run I) [210] and D0 [211]

¹¹The effective lifetimes measured in $B_s^0 \rightarrow K^+ K^-$ (mostly CP -even) and $B_s^0 \rightarrow J/\psi K_S^0$ (mostly CP -odd) are not used because we can not quantify the penguin contributions in those modes.

Table 19: Measurements of Δm_s .

Experiment	Method	Data set	Δm_s (ps $^{-1}$)	Ref.	
CDF2	$D_s^{(*)-}\ell^+\nu, D_s^{(*)-}\pi^+, D_s^-\rho^+$	1 fb $^{-1}$	17.77 $\pm 0.10 \pm 0.07$	[212]	
LHCb	$D_s^-\pi^+, D_s^-\pi^+\pi^-\pi^+$	2010	0.034 fb $^{-1}$	17.63 $\pm 0.11 \pm 0.02$	[177]
LHCb	$D_s^-\mu^+X$	2011	1.0 fb $^{-1}$	17.93 $\pm 0.22 \pm 0.15$	[179]
LHCb	$D_s^-\pi^+$	2011	1.0 fb $^{-1}$	17.768 $\pm 0.023 \pm 0.006$	[213]
LHCb	$J/\psi K^+K^-$	2011–2012	3.0 fb $^{-1}$	17.711 $^{+0.055}_{-0.057} \pm 0.011$	[196]
Average			17.757 $\pm 0.020 \pm 0.007$		

but did not have enough statistical power and proper time resolution to resolve the small period of the B_s^0 oscillations.

B_s^0 oscillations were observed for the first time in 2006 by the CDF collaboration [212], based on samples of flavour-tagged hadronic and semileptonic B_s^0 decays (in flavour-specific final states), partially or fully reconstructed in 1 fb $^{-1}$ of data collected during Tevatron’s Run II. More recently, the LHCb collaboration obtained the most precise results using fully reconstructed $B_s^0 \rightarrow D_s^-\pi^+$ and $B_s^0 \rightarrow D_s^-\pi^+\pi^-\pi^+$ decays [177, 213]. LHCb has also observed B_s^0 oscillations with $B_s^0 \rightarrow J/\psi K^+K^-$ decays [196] and with semileptonic $B_s^0 \rightarrow D_s^-\mu^+X$ decays [179]. The measurements of Δm_s are summarized in Table 19.

A simple average of the CDF and LHCb results, taking into account the correlated systematic uncertainties between the three LHCb measurements, yields

$$\Delta m_s = 17.757 \pm 0.020 \pm 0.007 \text{ ps}^{-1} = 17.757 \pm 0.021 \text{ ps}^{-1} \quad (74)$$

and is illustrated in Figure 8. The Standard Model prediction $\Delta m_s = 18.3 \pm 2.7 \text{ ps}^{-1}$ [62, 111] is consistent with the experimental value, but has a much larger uncertainty dominated by the uncertainty on the hadronic matrix elements. The ratio $\Delta\Gamma_s/\Delta m_s$ can be predicted more accurately to be 0.0048 ± 0.0008 [62, 111], in good agreement with the experimental determination of

$$\Delta\Gamma_s/\Delta m_s = 0.00505 \pm 0.00031. \quad (75)$$

Multiplying the Δm_s result of Eq. (74) by the mean B_s^0 lifetime of Eq. (46), $1/\Gamma_s = 1.510 \pm 0.004 \text{ ps}$, yields

$$x_s = 26.81 \pm 0.08. \quad (76)$$

With $2y_s = +0.135 \pm 0.008$ (see Eq. (73)) and under the assumption of no CP violation in B_s^0 mixing, this corresponds to

$$\chi_s = \frac{x_s^2 + y_s^2}{2(x_s^2 + 1)} = 0.499308 \pm 0.000004. \quad (77)$$

The ratio

$$\frac{\Delta m_d}{\Delta m_s} = 0.02852 \pm 0.00011, \quad (78)$$

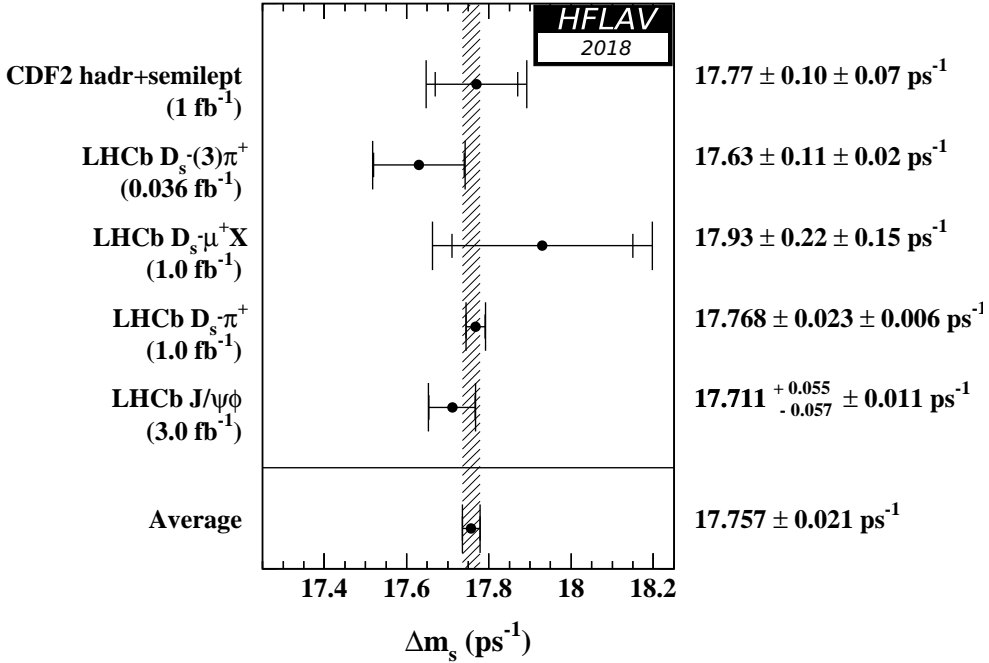


Figure 8: Published measurements of Δm_s , together with their average.

of the B^0 and B_s^0 oscillation frequencies, obtained from Eqs. (67) and (74), can be used to extract the following magnitude of the ratio of CKM matrix elements,

$$\left| \frac{V_{td}}{V_{ts}} \right| = \xi \sqrt{\frac{\Delta m_d}{\Delta m_s} \frac{m(B_s^0)}{m(B^0)}} = 0.2053 \pm 0.0004 \pm 0.0029 , \quad (79)$$

where the first uncertainty is from experimental uncertainties (with the masses $m(B_s^0)$ and $m(B^0)$ taken from Ref. [21]), and the second uncertainty arises from theoretical uncertainties in the estimation of the SU(3) flavour-symmetry breaking factor $\xi = 1.206 \pm 0.017$ [214], an average of three-flavour lattice QCD calculations dominated by the results of Ref. [215]. Note that Eq. (79) assumes that Δm_s and Δm_d only receive Standard Model contributions.

4.3.3 CP violation in B^0 and B_s^0 mixing

Evidence for CP violation in B^0 mixing has been searched for, both with flavour-specific and inclusive B^0 decays, in samples where the initial flavour state is tagged. In the case of semileptonic (or other flavour-specific) decays, where the final state tag is also available, the asymmetry

$$\mathcal{A}_{\text{SL}}^d = \frac{N(\bar{B}^0(t) \rightarrow \ell^+ \nu_\ell X) - N(B^0(t) \rightarrow \ell^- \bar{\nu}_\ell X)}{N(\bar{B}^0(t) \rightarrow \ell^+ \nu_\ell X) + N(B^0(t) \rightarrow \ell^- \bar{\nu}_\ell X)} \quad (80)$$

has been measured, either in decay-time-integrated analyses at CLEO [183, 216], *BABAR* [217], *CDF* [218] and *D0* [189], or in decay-time-dependent analyses at *OPAL* [167], *ALEPH* [219],

Table 20: Measurements¹² of CP violation in B^0 mixing and their average in terms of both $\mathcal{A}_{\text{SL}}^d$ and $|q_d/p_d|$. The individual results are listed as quoted in the original publications, or converted¹⁴ to an $\mathcal{A}_{\text{SL}}^d$ value. When two errors are quoted, the first one is statistical and the second one systematic. The ALEPH and OPAL results assume no CP violation in B_s^0 mixing.

Exp. & Ref.	Method	Measured $\mathcal{A}_{\text{SL}}^d$	Measured $ q_d/p_d $
CLEO [183]	Partial hadronic rec.	+0.017 $\pm 0.070 \pm 0.014$	
CLEO [216]	Dileptons	+0.013 $\pm 0.050 \pm 0.005$	
CLEO [216]	Average of above two	+0.014 $\pm 0.041 \pm 0.006$	
BABAR [184]	Full hadronic rec.		1.029 $\pm 0.013 \pm 0.011$
BABAR [220]	Part. rec. $D^* X \ell \nu$	+0.0006 $\pm 0.0017^{+0.0038}_{-0.0032}$	0.99971 $\pm 0.00084 \pm 0.00175$
BABAR [217]	Dileptons	-0.0039 $\pm 0.0035 \pm 0.0019$	
Belle [222]	Dileptons	-0.0011 $\pm 0.0079 \pm 0.0085$	1.0005 $\pm 0.0040 \pm 0.0043$
Average of above 6 B -factory results		-0.0019 ± 0.0027 (tot)	1.0009 ± 0.0013 (tot)
D0 [224]	$B^0 \rightarrow D^{(*)-} \mu^+ \nu X$	+0.0068 $\pm 0.0045 \pm 0.0014$	
LHCb [225]	$B^0 \rightarrow D^{(*)-} \mu^+ \nu X$	-0.0002 $\pm 0.0019 \pm 0.0030$	
Average of above 8 pure B^0 results		+0.0001 ± 0.0020 (tot)	1.0000 ± 0.0010 (tot)
D0 [189]	Muons & dimuons	-0.0062 ± 0.0043 (tot)	
Average of above 9 direct measurements		-0.0010 ± 0.0018 (tot)	1.0005 ± 0.0009 (tot)
OPAL [167]	Leptons	+0.008 $\pm 0.028 \pm 0.012$	
OPAL [89]	Inclusive (Eq. (81))	+0.005 $\pm 0.055 \pm 0.013$	
ALEPH [219]	Leptons	-0.037 $\pm 0.032 \pm 0.007$	
ALEPH [219]	Inclusive (Eq. (81))	+0.016 $\pm 0.034 \pm 0.009$	
ALEPH [219]	Average of above two	-0.013 ± 0.026 (tot)	
Average of above 13 results		-0.0010 ± 0.0018 (tot)	1.0005 ± 0.0009 (tot)
Best fit value from 2D combination of $\mathcal{A}_{\text{SL}}^d$ and $\mathcal{A}_{\text{SL}}^s$ results (see Eq. (83))		-0.0021 ± 0.0017 (tot)	1.0010 ± 0.0008 (tot)

BABAR [184, 220, 221] and Belle [222]. Note that the asymmetry of time-dependent decay rates in Eq. (80) is related to $|q_d/p_d|$ through Eq. (60) and is therefore time-independent. In the inclusive case, also investigated and published by ALEPH [219] and OPAL [89], no final state tag is used, and the asymmetry [223]

$$\frac{N(B^0(t) \rightarrow \text{all}) - N(\bar{B}^0(t) \rightarrow \text{all})}{N(B^0(t) \rightarrow \text{all}) + N(\bar{B}^0(t) \rightarrow \text{all})} \simeq \mathcal{A}_{\text{SL}}^d \left[\frac{\Delta m_d}{2\Gamma_d} \sin(\Delta m_d t) - \sin^2 \left(\frac{\Delta m_d t}{2} \right) \right] \quad (81)$$

must be measured as a function of the proper time to extract information on CP violation.

On the other hand, D0 [224] and LHCb [225] have studied the time-dependence of the charge asymmetry of $B^0 \rightarrow D^{(*)-} \mu^+ \nu_\mu X$ decays without tagging the initial state, which would be equal to

$$\frac{N(D^{(*)-} \mu^+ \nu_\mu X) - N(D^{(*)+} \mu^- \bar{\nu}_\mu X)}{N(D^{(*)-} \mu^+ \nu_\mu X) + N(D^{(*)+} \mu^- \bar{\nu}_\mu X)} = \mathcal{A}_{\text{SL}}^d \frac{1 - \cos(\Delta m_d t)}{2} \quad (82)$$

in absence of detection and production asymmetries.

Table 20 summarizes the different measurements¹² of $\mathcal{A}_{\text{SL}}^d$ and $|q_d/p_d|$. In all cases asymmetries compatible with zero have been found, with precision limited by the available statistics.

A simple average of all measurements performed at the B factories [183, 184, 216, 217, 220, 222] yields $\mathcal{A}_{\text{SL}}^d = -0.0019 \pm 0.0027$. Adding also the D0 [224] and LHCb [225] measurements obtained with reconstructed semileptonic B^0 decays yields $\mathcal{A}_{\text{SL}}^d = +0.0001 \pm 0.0020$. As discussed in more detail later in this section, the D0 analysis with single muons and like-sign dimuons [189] separates the B^0 and B_s^0 contributions by exploiting the dependence on the muon impact parameter cut; including the $\mathcal{A}_{\text{SL}}^d$ result quoted by D0 in the average yields $\mathcal{A}_{\text{SL}}^d = -0.0010 \pm 0.0018$. All the other B^0 analyses performed at high energy, either at LEP or at the Tevatron, did not separate the contributions from the B^0 and B_s^0 mesons. Under the assumption of no CP violation in B_s^0 mixing ($\mathcal{A}_{\text{SL}}^s = 0$), a number of these early analyses [54, 89, 167, 219] quote a measurement of $\mathcal{A}_{\text{SL}}^d$ or $|q_d/p_d|$ for the B^0 meson. However, these imprecise determinations no longer improve the world average of $\mathcal{A}_{\text{SL}}^d$. Furthermore, the assumption makes sense within the Standard Model, since $\mathcal{A}_{\text{SL}}^s$ is predicted to be much smaller than $\mathcal{A}_{\text{SL}}^d$ [62, 111], but may not be suitable in the presence of new physics.

The Tevatron experiments have measured linear combinations of $\mathcal{A}_{\text{SL}}^d$ and $\mathcal{A}_{\text{SL}}^s$ using inclusive semileptonic decays of b hadrons. CDF (Run I) finds $\mathcal{A}_{\text{SL}}^b = +0.0015 \pm 0.0038(\text{stat}) \pm 0.0020(\text{syst})$ [218], and D0 obtains $\mathcal{A}_{\text{SL}}^b = -0.00496 \pm 0.00153(\text{stat}) \pm 0.00072(\text{syst})$ [189]. While the imprecise CDF result is compatible with no CP violation, the D0 result, obtained by measuring the single muon and like-sign dimuon charge asymmetries, differs by 2.8 standard deviations from the Standard Model expectation of $\mathcal{A}_{\text{SL}}^{b,\text{SM}} = (-2.3 \pm 0.4) \times 10^{-4}$ [189, 203]. With a more sophisticated analysis in bins of the muon impact parameters, D0 conclude that the overall deviation of their measurements from the SM is at the level of 3.6σ . Interpreting the observed asymmetries in bins of the muon impact parameters in terms of CP violation in B -meson mixing and in interference, and using the mixing parameters and the world b -hadron fractions of Ref. [226], the D0 collaboration extracts [189] values for $\mathcal{A}_{\text{SL}}^d$ and $\mathcal{A}_{\text{SL}}^s$ and their correlation coefficient¹³, as shown in Table 21. However, the various contributions to the total quoted uncertainties from this analysis and from the external inputs are not given, so the adjustment of these results to different or more recent values of the external inputs cannot (easily) be done.

Finally, direct determinations of $\mathcal{A}_{\text{SL}}^s$, also shown in Table 21, have been obtained by D0 [227] and LHCb [228] from the time-integrated charge asymmetry of untagged $B_s^0 \rightarrow D_s^- \mu^+ \nu X$ decays.

Using a two-dimensional fit, all measurements of $\mathcal{A}_{\text{SL}}^s$ and $\mathcal{A}_{\text{SL}}^d$ obtained by D0 and LHCb are combined with the B -factory average of Table 20. Correlations are taken into account as shown in Table 21. The results, displayed graphically in Fig. 9, are

¹² A low-statistics result published by CDF using the Run I data [218] is not included in our averages, nor in Table 20.

¹³ In each impact parameter bin i the measured same-sign dimuon asymmetry is interpreted as $A_i = K_i^s \mathcal{A}_{\text{SL}}^s + K_i^d \mathcal{A}_{\text{SL}}^d + \lambda K_i^{\text{int}} \Delta \Gamma_d / \Gamma_d$, where the factors K_i^s , K_i^d and K_i^{int} are obtained by D0 from Monte Carlo simulation. The D0 publication [189] assumes $\lambda = 1$, but it has been demonstrated subsequently that $\lambda \leq 0.49$ [190]. This particular point invalidates the $\Delta \Gamma_d / \Gamma_d$ result published by D0, but not the $\mathcal{A}_{\text{SL}}^d$ and $\mathcal{A}_{\text{SL}}^s$ results. As stated by D0, their $\mathcal{A}_{\text{SL}}^d$ and $\mathcal{A}_{\text{SL}}^s$ results assume the above expression for A_i , *i.e.* that the observed asymmetries are due to CP violation in B mixing. As long as this assumption is not shown to be wrong (or withdrawn by D0), we include the $\mathcal{A}_{\text{SL}}^d$ and $\mathcal{A}_{\text{SL}}^s$ results in our world average.

Table 21: Measurements of CP violation in B_s^0 and B^0 mixing, together with their correlations $\rho(\mathcal{A}_{\text{SL}}^s, \mathcal{A}_{\text{SL}}^d)$ and their two-dimensional average. Only total errors are quoted.

Exp. & Ref.	Method	Measured $\mathcal{A}_{\text{SL}}^s$	Measured $\mathcal{A}_{\text{SL}}^d$	$\rho(\mathcal{A}_{\text{SL}}^s, \mathcal{A}_{\text{SL}}^d)$
<i>B</i> -factory average of Table 20			-0.0019 ± 0.0027	
D0 [224, 227]	$B_{(s)}^0 \rightarrow D_{(s)}^{(*)-} \mu^+ \nu X$	-0.0112 ± 0.0076	$+0.0068 \pm 0.0047$	+0.
LHCb [225, 228]	$B_{(s)}^0 \rightarrow D_{(s)}^{(*)-} \mu^+ \nu X$	$+0.0039 \pm 0.0033$	-0.0002 ± 0.0036	+0.13
Average of above		$+0.0016 \pm 0.0030$	$+0.0000 \pm 0.0019$	+0.066
D0 [189]	muons & dimuons	-0.0082 ± 0.0099	-0.0062 ± 0.0043	-0.61
Average of all above		-0.0006 ± 0.0028	-0.0021 ± 0.0017	-0.054

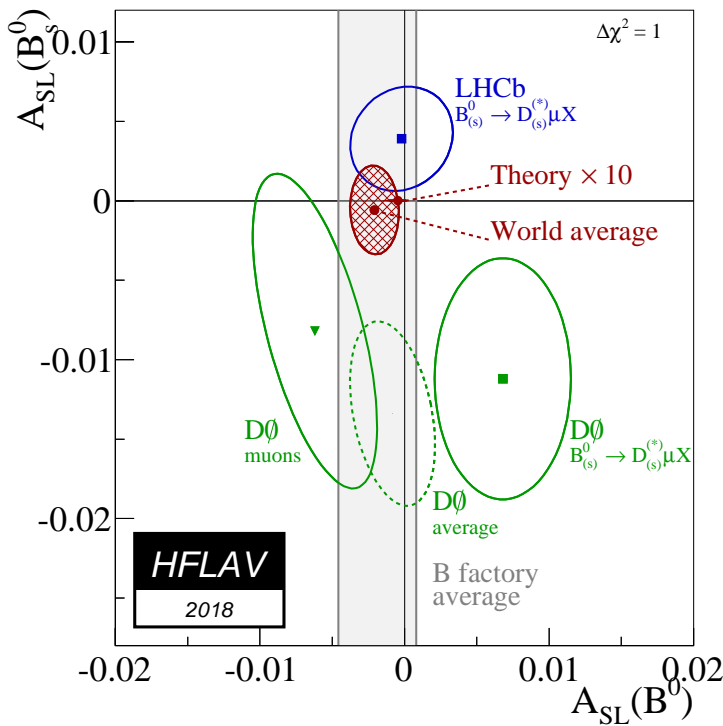


Figure 9: Measurements of $\mathcal{A}_{\text{SL}}^s$ and $\mathcal{A}_{\text{SL}}^d$ listed in Table 21 (B -factory average as the grey band, D0 measurements as the green ellipses, LHCb measurements as the blue ellipse) together with their two-dimensional average (red hatched ellipse). The red point close to $(0,0)$ is the Standard Model prediction of Ref. [62, 111] with error bars multiplied by 10. The prediction and the experimental world average deviate from each other by 0.5σ .

$$\mathcal{A}_{\text{SL}}^d = -0.0021 \pm 0.0017 \iff |q_d/p_d| = 1.0010 \pm 0.0008, \quad (83)$$

$$\mathcal{A}_{\text{SL}}^s = -0.0006 \pm 0.0028 \iff |q_s/p_s| = 1.0003 \pm 0.0014, \quad (84)$$

$$\rho(\mathcal{A}_{\text{SL}}^d, \mathcal{A}_{\text{SL}}^s) = -0.054, \quad (85)$$

where the relation between $\mathcal{A}_{\text{SL}}^q$ and $|q_q/p_q|$ is given in Eq. (60).¹⁴ However, the fit χ^2 probability is only 4.5%. This is mostly due to an overall discrepancy between the D0 and LHCb averages at the level of 2.2σ . Since the assumptions underlying the inclusion of the D0 muon results in the average¹³ are somewhat controversial [229], we also provide in Table 21 an average excluding these results.

The above averages show no evidence of CP violation in B^0 or B_s^0 mixing. They deviate by 0.5σ from the very small predictions of the Standard Model (SM), $\mathcal{A}_{\text{SL}}^{d,\text{SM}} = -(4.7 \pm 0.6) \times 10^{-4}$ and $\mathcal{A}_{\text{SL}}^{s,\text{SM}} = +(2.22 \pm 0.27) \times 10^{-5}$ [62, 111]. Given the current experimental uncertainties, there is still significant room for a possible new physics contribution, in particular in the B_s^0 system. In this respect, the deviation of the D0 dimuon asymmetry [189] from expectation has generated significant interest. However, the recent $\mathcal{A}_{\text{SL}}^s$ and $\mathcal{A}_{\text{SL}}^d$ results from LHCb are not precise enough yet to settle the issue. It was pointed out [230] that the D0 dimuon result can be reconciled with the SM expectations of $\mathcal{A}_{\text{SL}}^s$ and $\mathcal{A}_{\text{SL}}^d$ if there were non-SM sources of CP violation in the semileptonic decays of the b and c quarks. A Run 1 ATLAS study [231] of charge asymmetries in muon+jets $t\bar{t}$ events, in which a b -hadron decays semileptonically to a soft muon, yields results with limited statistical precision, compatible both with the D0 dimuon asymmetry and with the SM predictions.

At the more fundamental level, CP violation in B_s^0 mixing is caused by the weak phase difference ϕ_{12}^s defined in Eq. (64). The SM prediction for this phase is tiny [62, 111],

$$\phi_{12}^{s,\text{SM}} = 0.0046 \pm 0.0012. \quad (86)$$

However, new physics in B_s^0 mixing could change the observed phase to

$$\phi_{12}^s = \phi_{12}^{s,\text{SM}} + \phi_{12}^{s,\text{NP}}. \quad (87)$$

Using Eq. (63), the current knowledge of $\mathcal{A}_{\text{SL}}^s$, $\Delta\Gamma_s$ and Δm_s , given in Eqs. (84), (73), and (74) respectively, yields an experimental determination of ϕ_{12}^s ,

$$\tan \phi_{12}^s = \mathcal{A}_{\text{SL}}^s \frac{\Delta m_s}{\Delta\Gamma_s} = -0.1 \pm 0.6, \quad (88)$$

which represents only a very weak constraint at present.

4.3.4 Mixing-induced CP violation in B_s^0 decays

CP violation induced by $B_s^0 - \overline{B}_s^0$ mixing has been a field of very active study and fast experimental progress in the past several years. The main observable is the CP -violating phase

¹⁴ Early analyses and the PDG use the complex parameter $\epsilon_B = (p_q - q_q)/(p_q + q_q)$ for the B^0 ; if CP violation in the mixing is small, $\mathcal{A}_{\text{SL}}^d \cong 4\text{Re}(\epsilon_B)/(1+|\epsilon_B|^2)$ and the average of Eq. (83) corresponds to $\text{Re}(\epsilon_B)/(1+|\epsilon_B|^2) = -0.0005 \pm 0.0004$.

Table 22: Direct experimental measurements of $\phi_s^{c\bar{s}s}$, $\Delta\Gamma_s$ and Γ_s using $B_s^0 \rightarrow J/\psi\phi$, $J/\psi K^+K^-$, $\psi(2S)\phi$, $J/\psi\pi^+\pi^-$ and $D_s^+D_s^-$ decays. Only the solution with $\Delta\Gamma_s > 0$ is shown, since the two-fold ambiguity has been resolved in Ref. [110]. The first error is due to statistics, and the second one is due to systematics. The last line gives our average.

Exp.	Mode	Dataset	$\phi_s^{c\bar{s}s}$	$\Delta\Gamma_s$ (ps $^{-1}$)	Ref.
CDF	$J/\psi\phi$	9.6 fb $^{-1}$	-0.60 ± 0.12 , 68% CL	$+0.068 \pm 0.026 \pm 0.009$	[191]
D0	$J/\psi\phi$	8.0 fb $^{-1}$	$-0.55^{+0.38}_{-0.36}$	$+0.163^{+0.065}_{-0.064}$	[192]
ATLAS	$J/\psi\phi$	4.9 fb $^{-1}$	$+0.12 \pm 0.25 \pm 0.05$	$+0.053 \pm 0.021 \pm 0.010$	[193]
ATLAS	$J/\psi\phi$	14.3 fb $^{-1}$	$-0.110 \pm 0.082 \pm 0.042$	$+0.101 \pm 0.013 \pm 0.007$	[194]
ATLAS	above 2 combined		$-0.090 \pm 0.078 \pm 0.041$	$+0.085 \pm 0.011 \pm 0.007$	[194]
CMS	$J/\psi\phi$	19.7 fb $^{-1}$	$-0.075 \pm 0.097 \pm 0.031$	$+0.095 \pm 0.013 \pm 0.007$	[195]
LHCb	$J/\psi K^+K^-$	3.0 fb $^{-1}$	$-0.058 \pm 0.049 \pm 0.006$	$+0.0805 \pm 0.0091 \pm 0.0032$	[196]
LHCb	$J/\psi\pi^+\pi^-$	3.0 fb $^{-1}$	$+0.070 \pm 0.068 \pm 0.008$	—	[232]
LHCb	$J/\psi K^+K^-$ ^a	3.0 fb $^{-1}$	$+0.119 \pm 0.107 \pm 0.034$	$+0.066 \pm 0.018 \pm 0.010$	[197]
LHCb	above 3 combined		$+0.001 \pm 0.037$ (tot)	$+0.0813 \pm 0.0073 \pm 0.0036$	[197]
LHCb	$\psi(2S)\phi$	3.0 fb $^{-1}$	$+0.23^{+0.29}_{-0.28} \pm 0.02$	$+0.066^{+0.41}_{-0.44} \pm 0.007$	[198]
LHCb	$D_s^+D_s^-$	3.0 fb $^{-1}$	$+0.02 \pm 0.17 \pm 0.02$	—	[234]
All combined			-0.021 ± 0.031	$+0.085 \pm 0.006$	

^a $m(K^+K^-) > 1.05$ GeV/c 2 .

$\phi_s^{c\bar{s}s}$, defined as the weak phase difference between the $B_s^0 - \bar{B}_s^0$ mixing amplitude M_{12}^s and the $b \rightarrow c\bar{s}s$ decay amplitude.

The golden mode for such studies is $B_s^0 \rightarrow J/\psi\phi$, followed by $J/\psi \rightarrow \mu^+\mu^-$ and $\phi \rightarrow K^+K^-$, for which a full angular analysis of the decay products is performed to statistically separate the CP -even and CP -odd contributions in the final state. As already mentioned in Sec. 4.3.2, CDF [191], D0 [192], ATLAS [193, 194], CMS [195] and LHCb [196–198] have used both untagged and tagged $B_s^0 \rightarrow J/\psi\phi$ (and more generally $B_s^0 \rightarrow (c\bar{c})K^+K^-$) decays for the measurement of $\phi_s^{c\bar{s}s}$. LHCb [232] has used $B_s^0 \rightarrow J/\psi\pi^+\pi^-$ events, analyzed with a full amplitude model including several $\pi^+\pi^-$ resonances (*e.g.*, $f_0(980)$), although the $J/\psi\pi^+\pi^-$ final state had already been shown to be almost CP pure with a CP -odd fraction larger than 0.977 at 95% CL [233]. In addition, LHCb has used the $B_s^0 \rightarrow D_s^+D_s^-$ channel [234] to measure $\phi_s^{c\bar{s}s}$.

All CDF, D0, ATLAS and CMS analyses provide two mirror solutions related by the transformation $(\Delta\Gamma_s, \phi_s^{c\bar{s}s}) \rightarrow (-\Delta\Gamma_s, \pi - \phi_s^{c\bar{s}s})$. However, the LHCb analysis of $B_s^0 \rightarrow J/\psi K^+K^-$ resolves this ambiguity and rules out the solution with negative $\Delta\Gamma_s$ [110], a result in agreement with the Standard Model expectation. Therefore, in what follows, we only consider the solution with $\Delta\Gamma_s > 0$.

We perform a combination of the CDF [191], D0 [192], ATLAS [193, 194], CMS [195] and LHCb [196–198, 232] results summarized in Table 22. This is done by adding the two-dimensional log profile-likelihood scans of $\Delta\Gamma_s$ and $\phi_s^{c\bar{s}s}$ from all $B_s^0 \rightarrow (c\bar{c})K^+K^-$ analyses and a one-dimensional log profile-likelihood of $\phi_s^{c\bar{s}s}$ from the $B_s^0 \rightarrow J/\psi\pi^+\pi^-$ and $B_s^0 \rightarrow D_s^+D_s^-$ analyses; the combined likelihood is then maximized with respect to $\Delta\Gamma_s$ and $\phi_s^{c\bar{s}s}$.

In the $B_s^0 \rightarrow J/\psi\phi$ and $B_s^0 \rightarrow J/\psi K^+K^-$ analyses, $\phi_s^{c\bar{s}s}$ and $\Delta\Gamma_s$ come from a simultaneous

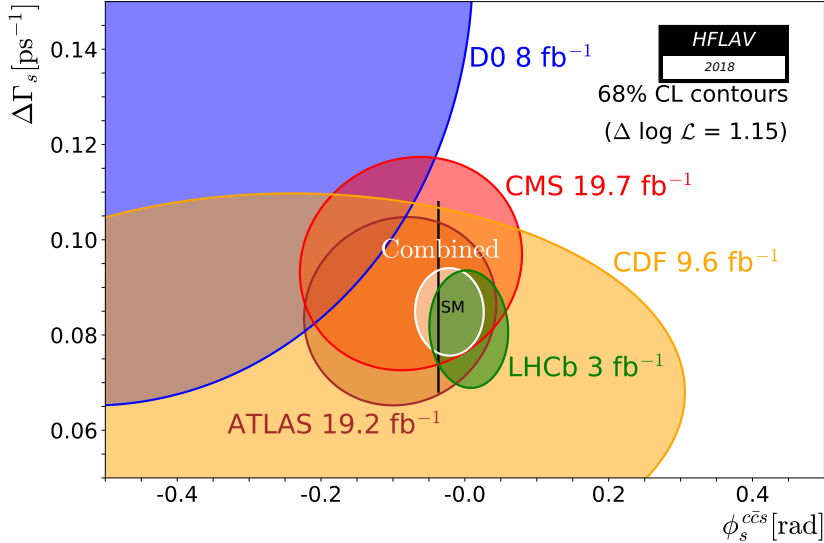


Figure 10: 68% CL regions in B_s^0 width difference $\Delta\Gamma_s$ and weak phase $\phi_s^{c\bar{c}s}$ obtained from individual and combined CDF [191], D0 [192], ATLAS [193, 194], CMS [195] and LHCb [196–198, 232, 234] likelihoods of $B_s^0 \rightarrow J/\psi \phi$, $B_s^0 \rightarrow J/\psi K^+ K^-$, $B_s^0 \rightarrow \psi(2S) \phi$, $B_s^0 \rightarrow J/\psi \pi^+ \pi^-$ and $B_s^0 \rightarrow D_s^+ D_s^-$ samples. The expectation within the Standard Model [62, 111, 188] is shown as the black rectangle.

fit that determines also the B_s^0 lifetime, the polarisation amplitudes, and the strong phases. While the correlation between $\phi_s^{c\bar{c}s}$ and all other parameters is small, the correlations between $\Delta\Gamma_s$ and the polarisation amplitudes are sizable. However, since the various experiments use different conventions for the amplitudes and phases, a full combination including all correlations is not performed. Instead, our average only takes into account the correlation between $\phi_s^{c\bar{c}s}$ and $\Delta\Gamma_s$.

In the LHCb $B_s^0 \rightarrow J/\psi K^+ K^-$ analysis [196], $\phi_s^{c\bar{c}s}$ is measured for the first time separately for each polarisation of the final state. Since the measured values for the different polarisations are compatible, we use the average value of $\phi_s^{c\bar{c}s}$ from Ref. [196] for our world average. In the same analysis, the statistical correlation coefficient between $\phi_s^{c\bar{c}s}$ and $|\lambda|$ (which signals CP violation in the decay if $|\lambda| \neq 1$) is measured to be very small (-0.02). We neglect this correlation in our average. Furthermore, the statistical correlation coefficient between $\phi_s^{c\bar{c}s}$ and $\Delta\Gamma_s$, measured to be -0.08 , is also neglected when averaging the $B_s^0 \rightarrow J/\psi K^+ K^-$, $B_s^0 \rightarrow J/\psi \pi^+ \pi^-$ and $B_s^0 \rightarrow D_s^+ D_s^-$ results of LHCb. Given the increasing experimental precision of the LHC results, we have stopped using the two-dimensional $\Delta\Gamma_s - \phi_s^{c\bar{c}s}$ histograms provided by the CDF and D0 collaborations, and are now approximating them with two-dimensional Gaussian likelihoods.

We obtain the individual and combined contours shown in Fig. 10. Maximizing the likelihood, we find, as summarized in Table 22:

$$\Delta\Gamma_s = +0.085 \pm 0.006 \text{ ps}^{-1}, \quad (89)$$

$$\phi_s^{c\bar{c}s} = -0.021 \pm 0.031. \quad (90)$$

This $\Delta\Gamma_s$ average is consistent but highly correlated with the average of Eq. (73). Our final recommended average for $\Delta\Gamma_s$ is the one of Eq. (73), which includes all available information

on this quantity.

In the Standard Model and ignoring sub-leading penguin contributions, $\phi_s^{c\bar{c}s}$ is expected to be equal to $-2\beta_s$, where $\beta_s = \arg [-(V_{ts}V_{tb}^*) / (V_{cs}V_{cb}^*)]$ is a phase analogous to the angle β of the usual CKM unitarity triangle (aside from a sign change). An indirect determination via global fits to experimental data gives [188]

$$(\phi_s^{c\bar{c}s})^{\text{SM}} = -2\beta_s = -0.0369_{-0.0010}^{+0.0007}. \quad (91)$$

The average value of $\phi_s^{c\bar{c}s}$ from Eq. (90) is consistent with this Standard Model expectation.

From its measurements of time-dependent CP violation in $B_s^0 \rightarrow K^+K^-$ decays, the LHCb collaboration has determined the B_s^0 mixing phase to be $-2\beta_s = -0.12_{-0.12}^{+0.14}$ [235], assuming a U-spin relation (with up to 50% breaking effects) between the decay amplitudes of $B_s^0 \rightarrow K^+K^-$ and $B^0 \rightarrow \pi^+\pi^-$, and a value of the CKM angle γ of $(70.1 \pm 7.1)^\circ$. This determination is compatible with, and less precise than, the world average of $\phi_s^{c\bar{c}s}$ from Eq. (90).

New physics could contribute to $\phi_s^{c\bar{c}s}$. Assuming that new physics only enters in M_{12}^s (rather than in Γ_{12}^s), one can write [203]

$$\phi_s^{c\bar{c}s} = -2\beta_s + \phi_{12}^{s,\text{NP}}, \quad (92)$$

where the new physics phase $\phi_{12}^{s,\text{NP}}$ is the same as that appearing in Eq. (87). In this case

$$\phi_{12}^s = \phi_{12}^{s,\text{SM}} + 2\beta_s + \phi_s^{c\bar{c}s} = 0.020 \pm 0.032, \quad (93)$$

where the numerical estimation was performed with the values of Eqs. (86), (91), and (90). Keeping in mind the approximation and assumption mentioned above, this can serve as a reference value to which the measurement of Eq. (88) can be compared.

5 Measurements related to Unitarity Triangle angles

We provide averages of measurements obtained from analyses of decay-time-dependent asymmetries and other quantities that are related to the angles of the Unitarity Triangle (UT). Straightforward interpretations of the averages are given, where possible. However, no attempt to extract the angles is made in cases where considerable theoretical input is required to do so.

In Sec. 5.1 a brief introduction to the relevant phenomenology is given. In Sec. 5.2 an attempt is made to clarify the various different notations in use. In Sec. 5.3 the common inputs to which experimental results are rescaled in the averaging procedure are listed. We also briefly introduce the treatment of experimental uncertainties. In the remainder of this section, the experimental results and their averages are given, divided into subsections based on the underlying quark-level decays. All the measurements reported are quantities determined from decay-time-dependent analyses, with the exception of several in Sec. 5.14, which are related to the UT angle γ and are obtained from decay-time-integrated analyses. In the compilations of measurements, indications of the sizes of the data samples used by each experiment are given. For the $e^+e^- B$ factory experiments, this is quoted in terms of the number of $B\bar{B}$ pairs in the data sample, while the integrated luminosity is given for experiments at hadron colliders.

5.1 Introduction

In the Standard Model, the Cabibbo-Kobayashi-Maskawa (CKM) quark-mixing matrix is a unitary matrix, conventionally written as the product of three (complex) rotation matrices [236]. The rotations are parametrised by the Euler mixing angles between the generations, θ_{12} , θ_{13} and θ_{23} , and one overall phase δ ,

$$V = \begin{pmatrix} V_{ud} & V_{us} & V_{ub} \\ V_{cd} & V_{cs} & V_{cb} \\ V_{td} & V_{ts} & V_{tb} \end{pmatrix} = \begin{pmatrix} c_{12}c_{13} & s_{12}c_{13} & s_{13}e^{-i\delta} \\ -s_{12}c_{23} - c_{12}s_{23}s_{13}e^{i\delta} & c_{12}c_{23} - s_{12}s_{23}s_{13}e^{i\delta} & s_{23}c_{13} \\ s_{12}s_{23} - c_{12}c_{23}s_{13}e^{i\delta} & -c_{12}s_{23} - s_{12}c_{23}s_{13}e^{i\delta} & c_{23}c_{13} \end{pmatrix}, \quad (94)$$

where $c_{ij} = \cos \theta_{ij}$, $s_{ij} = \sin \theta_{ij}$ for $i < j = 1, 2, 3$.

The often used Wolfenstein parametrisation [237] involves the replacements [238]

$$\begin{aligned} s_{12} &\equiv \lambda, \\ s_{23} &\equiv A\lambda^2, \\ s_{13}e^{-i\delta} &\equiv A\lambda^3(\rho - i\eta). \end{aligned} \quad (95)$$

The observed hierarchy among the CKM matrix elements is captured by the small value of λ , in which a Taylor expansion of V leads to the familiar approximation

$$V = \begin{pmatrix} 1 - \lambda^2/2 & \lambda & A\lambda^3(\rho - i\eta) \\ -\lambda & 1 - \lambda^2/2 & A\lambda^2 \\ A\lambda^3(1 - \rho - i\eta) & -A\lambda^2 & 1 \end{pmatrix} + \mathcal{O}(\lambda^4). \quad (96)$$

At order λ^5 , the CKM matrix in this parametrisation is

$$V = \begin{pmatrix} 1 - \frac{1}{2}\lambda^2 - \frac{1}{8}\lambda^4 & \lambda & A\lambda^3(\rho - i\eta) \\ -\lambda + \frac{1}{2}A^2\lambda^5[1 - 2(\rho + i\eta)] & 1 - \frac{1}{2}\lambda^2 - \frac{1}{8}\lambda^4(1 + 4A^2) & A\lambda^2 \\ A\lambda^3[1 - (1 - \frac{1}{2}\lambda^2)(\rho + i\eta)] & -A\lambda^2 + \frac{1}{2}A\lambda^4[1 - 2(\rho + i\eta)] & 1 - \frac{1}{2}A^2\lambda^4 \end{pmatrix} + \mathcal{O}(\lambda^6). \quad (97)$$

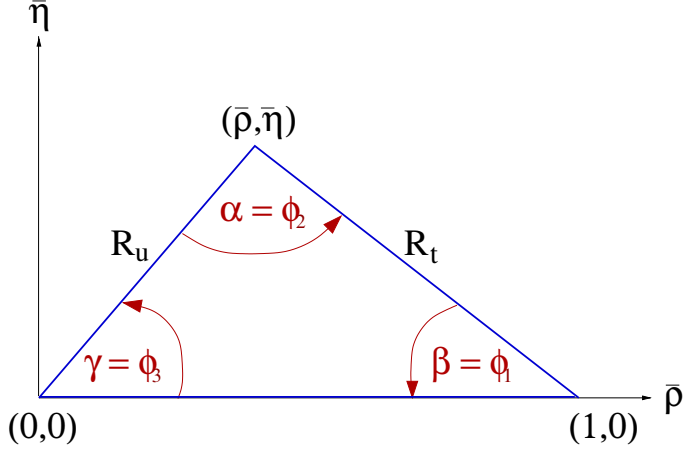


Figure 11: The Unitarity Triangle.

A non-zero value of η implies that the CKM matrix is not purely real, and is the source of CP violation in the Standard Model. This is encapsulated in a parametrisation-invariant way through the Jarlskog parameter $J = \text{Im} (V_{us} V_{cb} V_{ub}^* V_{cs}^*)$ [239], which is non-zero if and only if CP violation exists.

The unitarity relation $V^\dagger V = 1$ results in a total of nine equations, which can be written as $\sum_{i=u,c,t} V_{ij}^* V_{ik} = \delta_{jk}$, where δ_{jk} is the Kronecker symbol. Of the off-diagonal expressions ($j \neq k$), three can be transformed into the other three (under $j \leftrightarrow k$, corresponding to complex conjugation). This leaves three relations in which three complex numbers sum to zero, which therefore can be expressed as triangles in the complex plane. The diagonal terms yield three relations, in which the squares of the elements in each column of the CKM matrix sum to unity. Similar relations are obtained for the rows of the matrix from $V V^\dagger = 1$. Thus, there are in total six triangle relations and six sums to unity. More details about unitarity triangles can be found in Refs. [240–243].

One of the triangle relations,

$$V_{ud} V_{ub}^* + V_{cd} V_{cb}^* + V_{td} V_{tb}^* = 0, \quad (98)$$

is of particular importance to the B system, being specifically related to flavour-changing neutral-current $b \rightarrow d$ transitions, and since the three terms in Eq. (98) are of the same order, $\mathcal{O}(\lambda^3)$. This relation is commonly known as the Unitarity Triangle (UT). For presentational purposes, it is convenient to rescale the triangle by $(V_{cd} V_{cb}^*)^{-1}$, so that one of its sides becomes 1, as shown in Fig. 11.

Two popular naming conventions for the UT angles exist in the literature,

$$\alpha \equiv \phi_2 = \arg \left[-\frac{V_{td} V_{tb}^*}{V_{ud} V_{ub}^*} \right], \quad \beta \equiv \phi_1 = \arg \left[-\frac{V_{cd} V_{cb}^*}{V_{td} V_{tb}^*} \right], \quad \gamma \equiv \phi_3 = \arg \left[-\frac{V_{ud} V_{ub}^*}{V_{cd} V_{cb}^*} \right]. \quad (99)$$

In this document the (α, β, γ) set is used. The sides R_u and R_t of the UT (see Fig. 11) are given by

$$R_u = \left| \frac{V_{ud} V_{ub}^*}{V_{cd} V_{cb}^*} \right| = \sqrt{\bar{\rho}^2 + \bar{\eta}^2}, \quad R_t = \left| \frac{V_{td} V_{tb}^*}{V_{cd} V_{cb}^*} \right| = \sqrt{(1 - \bar{\rho})^2 + \bar{\eta}^2}. \quad (100)$$

Determinations of R_u rely on measurements of semileptonic B decays and are discussed in Sec. 6, while R_t is constrained by measurements of B meson oscillation frequencies (Sec. 4) and of rare decays (Sec. 8). The parameters $\bar{\rho}$ and $\bar{\eta}$ define the apex of the UT, and are given by [238]

$$\bar{\rho} + i\bar{\eta} \equiv -\frac{V_{ud}V_{ub}^*}{V_{cd}V_{cb}^*} \equiv 1 + \frac{V_{td}V_{tb}^*}{V_{cd}V_{cb}^*} = \frac{\sqrt{1-\lambda^2}(\rho+i\eta)}{\sqrt{1-A^2\lambda^4}+\sqrt{1-\lambda^2}A^2\lambda^4(\rho+i\eta)}. \quad (101)$$

The inverse relation between (ρ, η) and $(\bar{\rho}, \bar{\eta})$ is

$$\rho + i\eta = \frac{\sqrt{1-A^2\lambda^4}(\bar{\rho}+i\bar{\eta})}{\sqrt{1-\lambda^2}[1-A^2\lambda^4(\bar{\rho}+i\bar{\eta})]}. \quad (102)$$

By expanding in powers of λ , several useful approximate expressions can be obtained, including

$$\bar{\rho} = \rho \left(1 - \frac{1}{2}\lambda^2\right) + \mathcal{O}(\lambda^4), \quad \bar{\eta} = \eta \left(1 - \frac{1}{2}\lambda^2\right) + \mathcal{O}(\lambda^4), \quad V_{td} = A\lambda^3(1-\bar{\rho}-i\bar{\eta}) + \mathcal{O}(\lambda^6). \quad (103)$$

Recent world-average values for the Wolfenstein parameters, evaluated using many of the measurements reported in this document, are [244]

$$A = 0.8403^{+0.0056}_{-0.0201}, \quad \lambda = 0.224747^{+0.000254}_{-0.000059}, \quad \bar{\rho} = 0.1577^{+0.0096}_{-0.0074}, \quad \bar{\eta} = 0.3493^{+0.0095}_{-0.0071}. \quad (104)$$

The relevant unitarity triangle for the $b \rightarrow s$ transition is obtained by replacing $d \leftrightarrow s$ in Eq. (98). Definitions of the set of angles $(\alpha_s, \beta_s, \gamma_s)$ can be obtained using equivalent relations to those of Eq. (99). However, this gives a value of β_s that is negative in the Standard Model, so that the sign is usually flipped in the literature; this convention, *i.e.* $\beta_s = \arg[-(V_{ts}V_{tb}^*)/(V_{cs}V_{cb}^*)]$, is also followed here and in Sec. 4. Since the sides of the $b \rightarrow s$ unitarity triangle are not all of the same order of λ , the triangle is squashed, and $\beta_s \sim \lambda^2\eta$.

5.2 Notations

Several different notations for CP violation parameters are commonly used. This section reviews those found in the experimental literature, in the hope of reducing the potential for confusion, and to define the frame that is used for the averages.

In some cases, when B mesons decay into multibody final states via broad resonances (ρ , K^* , *etc.*), the experimental analyses ignore the effects of interference between the overlapping structures. This is referred to as the quasi-two-body (Q2B) approximation in the following.

5.2.1 CP asymmetries

The CP asymmetry is defined as the difference between the rate of a decay involving a b quark and that involving a \bar{b} quark, divided by the sum. For example, the partial rate asymmetry for a charged B decay would be given as

$$\mathcal{A}_f \equiv \frac{\Gamma(B^- \rightarrow f) - \Gamma(B^+ \rightarrow \bar{f})}{\Gamma(B^- \rightarrow f) + \Gamma(B^+ \rightarrow \bar{f})}, \quad (105)$$

where f and \bar{f} are CP -conjugate final states.

5.2.2 Time-dependent CP asymmetries in decays to CP eigenstates

If the amplitudes for B^0 and \bar{B}^0 to decay to a final state f , which is a CP eigenstate with eigenvalue η_f , are given by A_f and \bar{A}_f , respectively, then the decay distributions for neutral B mesons, with known (*i.e.* “tagged”) flavour at time $\Delta t = 0$, are given by

$$\Gamma_{\bar{B}^0 \rightarrow f}(\Delta t) = \frac{e^{-|\Delta t|/\tau(B^0)}}{4\tau(B^0)} \left[1 + \frac{2 \operatorname{Im}(\lambda_f)}{1 + |\lambda_f|^2} \sin(\Delta m \Delta t) - \frac{1 - |\lambda_f|^2}{1 + |\lambda_f|^2} \cos(\Delta m \Delta t) \right], \quad (106)$$

$$\Gamma_{B^0 \rightarrow f}(\Delta t) = \frac{e^{-|\Delta t|/\tau(B^0)}}{4\tau(B^0)} \left[1 - \frac{2 \operatorname{Im}(\lambda_f)}{1 + |\lambda_f|^2} \sin(\Delta m \Delta t) + \frac{1 - |\lambda_f|^2}{1 + |\lambda_f|^2} \cos(\Delta m \Delta t) \right]. \quad (107)$$

Here the term

$$\lambda_f = \frac{q}{p} \frac{\bar{A}_f}{A_f} \quad (108)$$

contains factors related to the decay amplitudes and to B^0 – \bar{B}^0 mixing, which originates from the fact that the Hamiltonian eigenstates with physical masses and lifetimes are $|B_\pm\rangle = p|B^0\rangle \pm q|\bar{B}^0\rangle$ (see Sec. 4.3, where the mass difference Δm is also defined). This formulation assumes CPT invariance and neglects a possible lifetime difference between the two physical states. The case where non-zero lifetime differences are taken into account is discussed in Sec. 5.2.3.

The definition of λ_f in Eq. (108) allows three different categories of CP violation to be distinguished.

- CP violation in mixing, where $\left| \frac{q}{p} \right| \neq 1$. The strongest constraints on the associated parameters are obtained using semileptonic decays, and are discussed in Sec. 4. There is currently no evidence for CP violation in either B^0 – \bar{B}^0 or B_s^0 – \bar{B}_s^0 mixing, and therefore this is assumed to be absent throughout the discussion in this Section.
- CP violation in decay, where $\left| \frac{\bar{A}_f}{A_f} \right| \neq 1$. This is the only possible category of CP violation for charged B mesons and b baryons (see, for example, results reported in Sec. 8). Several parameters measured in time-dependent analyses are also sensitive to CP violation and are discussed in this Section.
- CP violation in the interference between mixing and decay, where $\operatorname{Im}(\lambda_f) \neq 0$. Results related to this category, also referred to as mixing-induced CP violation, are reported in this Section.

The notation and normalisation used in Eqs. (106) and (107) are relevant for the e^+e^- B factory experiments. In this case, neutral B mesons are produced via the $e^+e^- \rightarrow \Upsilon(4S) \rightarrow B\bar{B}$ process, and the wavefunction of the produced $B\bar{B}$ pair evolves coherently until one meson decays. When one of the pair decays into a final state that tags its flavour, the flavour of the other at that instant is known. The evolution of the other neutral B meson is therefore described in terms of Δt , the difference between the decay times of the two mesons in the pair. At hadron collider experiments, t is usually used in place of Δt , since the flavour tagging is done at production ($t = 0$); due to the nature of the production in hadron colliders (incoherent $b\bar{b}$ quark pair production with many additional associated particles), very different methods are used for tagging compared to those in e^+e^- experiments. Moreover, since negative values of t

are not possible, the normalisation is such that $\int_0^{+\infty} (\Gamma_{\bar{B}^0 \rightarrow f}(t) + \Gamma_{B^0 \rightarrow f}(t)) dt = 1$, rather than the $\int_{-\infty}^{+\infty} (\Gamma_{\bar{B}^0 \rightarrow f}(\Delta t) + \Gamma_{B^0 \rightarrow f}(\Delta t)) d(\Delta t) = 1$ normalization in Eqs. (106) and (107).

The time-dependent CP asymmetry, again defined as the normalized difference between the decay rate involving a b quark and that involving a \bar{b} quark, is then given by

$$\mathcal{A}_f(\Delta t) \equiv \frac{\Gamma_{\bar{B}^0 \rightarrow f}(\Delta t) - \Gamma_{B^0 \rightarrow f}(\Delta t)}{\Gamma_{\bar{B}^0 \rightarrow f}(\Delta t) + \Gamma_{B^0 \rightarrow f}(\Delta t)} = \frac{2 \operatorname{Im}(\lambda_f)}{1 + |\lambda_f|^2} \sin(\Delta m \Delta t) - \frac{1 - |\lambda_f|^2}{1 + |\lambda_f|^2} \cos(\Delta m \Delta t). \quad (109)$$

While the coefficient of the $\sin(\Delta m \Delta t)$ term in Eq. (109) is customarily¹⁵ denoted S_f :

$$S_f \equiv \frac{2 \operatorname{Im}(\lambda_f)}{1 + |\lambda_f|^2}, \quad (110)$$

different notations are in use for the coefficient of the $\cos(\Delta m \Delta t)$ term:

$$C_f \equiv -A_f \equiv \frac{1 - |\lambda_f|^2}{1 + |\lambda_f|^2}. \quad (111)$$

The C notation has been used by the *BABAR* collaboration (see *e.g.* Ref. [245]), and subsequently by the *LHCb* collaboration (see *e.g.* Ref. [246]), and is also adopted in this document. The A notation has been used by the *Belle* collaboration (see *e.g.* Ref. [247]). When the final state is a CP eigenstate, the notation S_{CP} and C_{CP} is widely used, including in this document, instead of specifying the final state f . In addition, the S , C notation with a subscript indicating the transition is used, particularly when grouping together measurements with different final states mediated by the same quark-level transition.

Neglecting effects due to CP violation in mixing, if the decay amplitude contains terms with a single weak (*i.e.* CP -violating) phase then $|\lambda_f| = 1$, and one finds $S_f = -\eta_f \sin(\phi_{\text{mix}} + \phi_{\text{dec}})$, $C_f = 0$, where $\phi_{\text{mix}} = \arg(q/p)$ and $\phi_{\text{dec}} = \arg(\bar{A}_f/A_f)$. The B^0 – \bar{B}^0 mixing phase ϕ_{mix} is approximately equal to 2β in the Standard Model (in the usual phase convention) [248, 249].

If amplitudes with different weak phases contribute to the decay, no clean interpretation of S_f in terms of UT angles is possible without further input. In this document, only the theoretically cleanest channels are interpreted as measurements of the weak phase (*e.g.* $b \rightarrow c\bar{c}s$ transitions for $\sin(2\beta)$), although even in these cases some care is necessary. In channels in which a second amplitude with a different weak phase to the leading amplitude contributes but is expected to be suppressed, the concept of an effective weak phase difference is sometimes used, *e.g.* $\sin(2\beta^{\text{eff}})$ in $b \rightarrow q\bar{q}s$ transitions.

If, in addition to having a weak phase difference, two contributing decay amplitudes have different strong (*i.e.* CP -conserving) phases, then $|\lambda_f| \neq 1$. Additional input is required for interpretation of the results. The coefficient of the cosine term becomes non-zero, indicating CP violation in decay.

Due to the fact that $\sin(\Delta m \Delta t)$ and $\cos(\Delta m \Delta t)$ are, respectively, odd and even functions of Δt , only small correlations (that can be induced by backgrounds, for example) between S_f and C_f are expected at an e^+e^- B factory experiment, where the range of Δt is $-\infty < \Delta t < +\infty$. The situation is different for measurements at hadron collider experiments, where the range of the time variable is $0 < t < +\infty$, so that more sizable correlations can be expected. We include the correlations in the averages where available.

¹⁵ Occasionally one also finds Eq. (109) written as $\mathcal{A}_f(\Delta t) = \mathcal{A}_f^{\text{mix}} \sin(\Delta m \Delta t) + \mathcal{A}_f^{\text{dir}} \cos(\Delta m \Delta t)$, or similar.

Frequently, we are interested in combining measurements governed by similar or identical short-distance physics, but with different final states (*e.g.*, $B^0 \rightarrow J/\psi K_s^0$ and $B^0 \rightarrow J/\psi K_L^0$). In this case, we remove the dependence on the CP eigenvalue of the final state by quoting $-\eta S_f$. In cases where the final state is not a CP eigenstate but has an effective CP content (see Sec. 5.2.4), the reported $-\eta S$ is corrected by the effective CP .

5.2.3 Time-dependent distributions with non-zero decay width difference

A complete analysis of the time-dependent decay rates of neutral B mesons must also take into account the difference between the widths of the Hamiltonian eigenstates, denoted $\Delta\Gamma$. This is particularly important in the B_s^0 system, where a non-negligible value of $\Delta\Gamma_s$ has been established (see Sec. 4.3). The formalism given here is appropriate for measurements of B_s^0 decays to a CP eigenstate f as studied at hadron colliders, but appropriate modifications for B^0 mesons or for the e^+e^- environment are straightforward to make.

Neglecting CP violation in mixing, the relevant replacements for Eqs. (106) and (107) are [250]

$$\Gamma_{\bar{B}_s^0 \rightarrow f}(t) = \mathcal{N} \frac{e^{-t/\tau(B_s^0)}}{2\tau(B_s^0)} \left[\cosh\left(\frac{\Delta\Gamma_s t}{2}\right) + S_f \sin(\Delta m_s t) - C_f \cos(\Delta m_s t) + A_f^{\Delta\Gamma} \sinh\left(\frac{\Delta\Gamma_s t}{2}\right) \right] \quad (112)$$

and

$$\Gamma_{B_s^0 \rightarrow f}(t) = \mathcal{N} \frac{e^{-t/\tau(B_s^0)}}{2\tau(B_s^0)} \left[\cosh\left(\frac{\Delta\Gamma_s t}{2}\right) - S_f \sin(\Delta m_s t) + C_f \cos(\Delta m_s t) + A_f^{\Delta\Gamma} \sinh\left(\frac{\Delta\Gamma_s t}{2}\right) \right], \quad (113)$$

where S_f and C_f are as defined in Eqs. (110) and (111), respectively, $\tau(B_s^0) = 1/\Gamma_s$ is defined in Sec. 4.2.4, and the coefficient of the sinh term is¹⁶

$$A_f^{\Delta\Gamma} = -\frac{2 \operatorname{Re}(\lambda_f)}{1 + |\lambda_f|^2}. \quad (114)$$

With the requirement $\int_0^{+\infty} [\Gamma_{\bar{B}_s^0 \rightarrow f}(t) + \Gamma_{B_s^0 \rightarrow f}(t)] dt = 1$, the normalisation factor is fixed to $\mathcal{N} = \left(1 - (\frac{\Delta\Gamma_s}{2\Gamma_s})^2\right) / \left(1 + \frac{A_f^{\Delta\Gamma} \Delta\Gamma_s}{2\Gamma_s}\right)$.¹⁷

A time-dependent analysis of CP asymmetries in flavour-tagged B_s^0 decays to a CP eigenstate f can thus determine the parameters S_f , C_f and $A_f^{\Delta\Gamma}$. Note that, by definition,

$$(S_f)^2 + (C_f)^2 + (A_f^{\Delta\Gamma})^2 = 1, \quad (115)$$

and this constraint may or may not be imposed in the fits. Since these parameters have sensitivity to both $\operatorname{Im}(\lambda_f)$ and $\operatorname{Re}(\lambda_f)$, alternative choices of parametrisation, including those

¹⁶ As ever, alternative and conflicting notations appear in the literature. One popular alternative notation for this parameter is $\mathcal{A}_{\Delta\Gamma}$. Particular care must be taken over the signs.

¹⁷ The prefactor of $\mathcal{N}/2\tau(B_s^0)$ in Eqs. (110) and (111) has been chosen so that $\mathcal{N} = 1$ in the limit $\Delta\Gamma_s = 0$. In the e^+e^- environment, where the range is $-\infty < \Delta t < \infty$, the prefactor should be $\mathcal{N}/4\tau(B_s^0)$ and $\mathcal{N} = 1 - (\frac{\Delta\Gamma_s}{2\Gamma_s})^2$.

directly involving CP violating phases (such as β_s), are possible. These can also be adopted for vector-vector final states (see Sec. 5.2.4).

The *un>tagged* time-dependent decay rate is given by

$$\Gamma_{\bar{B}_s^0 \rightarrow f}(t) + \Gamma_{B_s^0 \rightarrow f}(t) = \mathcal{N} \frac{e^{-t/\tau(B_s^0)}}{\tau(B_s^0)} \left[\cosh\left(\frac{\Delta\Gamma_s t}{2}\right) + A_f^{\Delta\Gamma} \sinh\left(\frac{\Delta\Gamma_s t}{2}\right) \right]. \quad (116)$$

Thus, an untagged time-dependent analysis can probe λ_f , through the dependence of $A_f^{\Delta\Gamma}$ on $\text{Re}(\lambda_f)$, given that $\Delta\Gamma_s \neq 0$. This is equivalent to determining the “*effective lifetime*” [115], as discussed in Sec. 4.2.4. The analysis of flavour-tagged B_s^0 mesons is, of course, more sensitive.

The discussion in this and the previous section is relevant for decays to CP eigenstates. In the following sections, various cases of time-dependent CP asymmetries in decays to non- CP eigenstates are considered. For brevity, these will be given assuming that the decay width difference $\Delta\Gamma$ is negligible. Modifications similar to those described here can be made to take into account a non-zero decay width difference.

5.2.4 Time-dependent CP asymmetries in decays to vector-vector final states

Consider B decays to states consisting of two spin-1 particles, such as $J/\psi K^{*0} (\rightarrow K_s^0 \pi^0)$, $J/\psi \phi$, $D^{*+} D^{*-}$ and $\rho^+ \rho^-$, which are eigenstates of charge conjugation but not of parity.¹⁸ For such a system, there are three possible final states. In the helicity basis, these are denoted h_{-1}, h_0, h_{+1} . The h_0 state is an eigenstate of parity, and hence of CP . By contrast, CP transforms $h_{+1} \leftrightarrow h_{-1}$ (up to an unobservable phase). These states are transformed into the transversity basis states $h_{\parallel} = (h_{+1} + h_{-1})/2$ and $h_{\perp} = (h_{+1} - h_{-1})/2$. In this basis all three states are CP eigenstates, and h_{\perp} has the opposite CP to the others.

The amplitude for decays to the transversity basis states are usually given by $A_{0,\perp,\parallel}$, with normalisation such that $|A_0|^2 + |A_{\perp}|^2 + |A_{\parallel}|^2 = 1$. Given the relation between the CP eigenvalues of the states, the effective CP content of the vector-vector state is known if $|A_{\perp}|^2$ is measured. An alternative strategy is to measure just the longitudinally polarised component, $|A_0|^2$ (sometimes denoted by f_{long}), which allows a limit to be set on the effective CP content, since $|A_{\perp}|^2 \leq |A_{\perp}|^2 + |A_{\parallel}|^2 = 1 - |A_0|^2$. The value of the effective CP content can be used to treat the decay with the same formalism as for CP eigenstates. The most complete treatment for neutral B decays to vector-vector final states is, however, time-dependent angular analysis (also known as time-dependent transversity analysis). In such an analysis, interference between CP -even and CP -odd states provides additional sensitivity to the weak and strong phases involved.

In most analyses of time-dependent CP asymmetries in decays to vector-vector final states carried out to date, an assumption has been made that each helicity (or transversity) amplitude has the same weak phase. This is a good approximation for decays that are dominated by amplitudes with a single weak phase, such $B^0 \rightarrow J/\psi K^{*0}$, and is a reasonable approximation in any mode for which only small sample sizes are available. However, for modes that have contributions from amplitudes with different weak phases, the relative size of these contributions can be different for each helicity (or transversity) amplitude, and therefore the time-dependent CP asymmetry parameters can also differ. The most generic analysis, suitable for analyses with

¹⁸ This is not true for all vector-vector final states, *e.g.*, $D^{*\pm} \rho^{\mp}$ is clearly not an eigenstate of charge conjugation.

sufficiently large samples, allows for this effect; such an analysis has been carried out by LHCb for the $B^0 \rightarrow J/\psi \rho^0$ decay [251]. An intermediate analysis can allow different parameters for the CP -even and CP -odd components; such an analysis has been carried out by *BABAR* for the decay $B^0 \rightarrow D^{*+} D^{*-}$ [252]. The independent treatment of each helicity (or transversity) amplitude, as in the study of $B_s^0 \rightarrow J/\psi \phi$ [196] (discussed in Sec. 4), becomes increasingly important for high precision measurements.

5.2.5 Time-dependent asymmetries: self-conjugate multiparticle final states

Amplitudes for neutral B decays into self-conjugate multiparticle final states such as $\pi^+\pi^-\pi^0$, $K^+K^-K_s^0$, $\pi^+\pi^-K_s^0$, $J/\psi\pi^+\pi^-$ or $D\pi^0$ with $D \rightarrow K_s^0\pi^+\pi^-$ may be written in terms of CP -even and CP -odd amplitudes. As above, the interference between these terms provides additional sensitivity to the weak and strong phases involved in the decay, and the time-dependence depends on both the sine and cosine of the weak phase difference. In order to perform unbinned maximum likelihood fits, and thereby extract as much information as possible from the distributions, it is necessary to choose a model for the multiparticle decay, and therefore the results acquire some model dependence. In certain cases, model-independent methods are also possible, but the resulting need to bin the Dalitz plot leads to some loss of statistical precision. The number of observables depends on the final state (and on the model used); the key feature is that as long as there are kinematic regions where both CP -even and CP -odd amplitudes contribute, the interference terms will be sensitive to the cosine of the weak phase difference. Therefore, these measurements allow distinction between multiple solutions for, *e.g.*, the two values of 2β from the measurement of $\sin(2\beta)$.

In model-dependent analysis of multibody decays, the decay amplitude is typically described as a coherent sum of contributions from contributions that proceed via different intermediate resonances and through nonresonant interactions. It is therefore of interest to present results in terms of the CP violation parameters associated with each resonant amplitude, *e.g.* $\rho^0 K_s^0$ in the case of the $\pi^+\pi^-K_s^0$ final state. These are referred to as Q2B parameters, since in the limit that there was no other contribution to the multibody decay, the amplitude analysis and the Q2B analysis would give the same results.

We now consider the various notations that have been used in experimental studies of time-dependent asymmetries in decays to self-conjugate multiparticle final states.

$B^0 \rightarrow D^{(*)}h^0$ with $D \rightarrow K_s^0\pi^+\pi^-$

The states $D\pi^0$, $D^*\pi^0$, $D\eta$, $D^*\eta$, $D\omega$ are collectively denoted $D^{(*)}h^0$. When the D decay model is fixed, fits to the time-dependent decay distributions can be performed to extract the weak phase difference. However, it is experimentally advantageous to use the sine and cosine of this phase as fit parameters, since these behave as essentially independent parameters, with low correlations and (potentially) rather different uncertainties. A parameter representing CP violation in the B decay can be simultaneously determined. For consistency with other analyses, this could be chosen to be C_f , but could equally well be $|\lambda_f|$, or other possibilities.

Belle performed an analysis of these channels with $\sin(2\phi_1)$ and $\cos(2\phi_1)$ as free parameters [253]. *BABAR* has performed an analysis in which $|\lambda_f|$ was also determined [254]. A joint analysis of the final *BABAR* and Belle data samples supersedes these earlier measurements, and uses $\sin(2\beta)$ and $\cos(2\beta)$ as free parameters [255, 256]. Belle has in addition performed a model-independent analysis [257] using as input information about the average strong phase difference

between symmetric bins of the Dalitz plot determined by CLEO-c [258].¹⁹ The results of this analysis are measurements of $\sin(2\phi_1)$ and $\cos(2\phi_1)$.

$$B^0 \rightarrow D^{*+} D^{*-} K_s^0$$

The hadronic structure of the $B^0 \rightarrow D^{*+} D^{*-} K_s^0$ decay is not sufficiently well understood to perform a full time-dependent Dalitz-plot analysis. Instead, following Ref. [259], *BABAR* [260] and *Belle* [261] divide the Dalitz plane in two regions: $m(D^{*+} K_s^0)^2 > m(D^{*-} K_s^0)^2$ (labelled $\eta_y = +1$) and $m(D^{*+} K_s^0)^2 < m(D^{*-} K_s^0)^2$ ($\eta_y = -1$); and then fit to a decay time distribution with asymmetry given by

$$\mathcal{A}_f(\Delta t) = \eta_y \frac{J_c}{J_0} \cos(\Delta m \Delta t) - \left[\frac{2J_{s1}}{J_0} \sin(2\beta) + \eta_y \frac{2J_{s2}}{J_0} \cos(2\beta) \right] \sin(\Delta m \Delta t). \quad (117)$$

The fitted observables are $\frac{J_c}{J_0}$, $\frac{2J_{s1}}{J_0} \sin(2\beta)$ and $\frac{2J_{s2}}{J_0} \cos(2\beta)$, where the parameters J_0 , J_c , J_{s1} and J_{s2} are the integrals over the half Dalitz plane $m(D^{*+} K_s^0)^2 < m(D^{*-} K_s^0)^2$ of the functions $|a|^2 + |\bar{a}|^2$, $|a|^2 - |\bar{a}|^2$, $\text{Re}(\bar{a}a^*)$ and $\text{Im}(\bar{a}a^*)$, respectively, where a and \bar{a} are the decay amplitudes of $B^0 \rightarrow D^{*+} D^{*-} K_s^0$ and $\bar{B}^0 \rightarrow D^{*+} D^{*-} K_s^0$, respectively. The parameter J_{s2} (and hence J_{s2}/J_0) is predicted to be positive [259]; assuming this prediction to be correct, it is possible to determine the sign of $\cos(2\beta)$.

$$B^0 \rightarrow J/\psi \pi^+ \pi^-$$

Amplitude analyses of $B^0 \rightarrow J/\psi \pi^+ \pi^-$ decays [251, 262] show large contributions from the $\rho(770)^0$ and $f_0(500)$ states, together with smaller contributions from higher resonances. Since modelling the $f_0(500)$ structure is challenging [263], it is difficult to determine reliably its associated CP violation parameters. Corresponding parameters for the $J/\psi \rho^0$ decay can, however, be determined. In the LHCb analysis [251], $2\beta^{\text{eff}}$ is determined from the fit; results are then converted into values for S_{CP} and C_{CP} to allow comparison with other modes. Here, the notation S_{CP} and C_{CP} denotes parameters obtained for the $J/\psi \rho^0$ final state accounting for the composition of CP -even and CP -odd amplitudes (while assuming that all amplitudes involve the same phases), so that no dilution occurs. Possible CP violation effects in the other amplitudes contributing to the Dalitz plot are treated as a source of systematic uncertainty.

Amplitude analyses have also been done for the $B_s^0 \rightarrow J/\psi \pi^+ \pi^-$ decay, where the final state is dominated by scalar resonances, including the $f_0(980)$ [232, 233]. Time-dependent analyses of this B_s^0 decay allow a determination of $2\beta_s$, as discussed in Sec. 4

$$B^0 \rightarrow K^+ K^- K^0$$

Studies of $B^0 \rightarrow K^+ K^- K^0$ [264–266] and of the related decay $B^+ \rightarrow K^+ K^- K^+$ [266–268], show that the decay is dominated by a large nonresonant contribution with significant components from the intermediate $K^+ K^-$ resonances $\phi(1020)$, $f_0(980)$, and other higher resonances, as well as a contribution from χ_{c0} .

The full time-dependent Dalitz plot analysis allows the complex amplitudes of each contributing term to be determined from data, including CP violation effects (*i.e.* allowing the complex amplitude for the B^0 decay to be independent from that for \bar{B}^0 decay), although one

¹⁹ The external input needed for this analysis is the same as in the model-independent analysis of $B^+ \rightarrow DK^+$ with $D \rightarrow K_s^0 \pi^+ \pi^-$, discussed in Sec. 5.14.5.

amplitude must be fixed to serve as a reference. There are several choices for parametrisation of the complex amplitudes (*e.g.* real and imaginary part, or magnitude and phase). Similarly, there are various approaches to the inclusion of CP violation effects. Note that the use of positive definite parameters such as magnitudes are disfavoured in certain circumstances (it inevitably leads to biases for small values). In order to compare results between analyses, it is useful for each experiment to present results in terms of the parameters that can be measured in a Q2B analysis (such as \mathcal{A}_f , S_f , C_f , $\sin(2\beta^{\text{eff}})$, $\cos(2\beta^{\text{eff}})$, *etc.*)

In the *BABAR* analysis of the $B^0 \rightarrow K^+ K^- K^0$ decay [266], the complex amplitude for each resonant contribution was written as

$$A_f = c_f(1 + b_f)e^{i(\phi_f + \delta_f)} , \quad \bar{A}_f = c_f(1 - b_f)e^{i(\phi_f - \delta_f)} , \quad (118)$$

where b_f and δ_f parametrize CP violation in the magnitude and phase, respectively. *Belle* [265] used the same parametrisation but with a different notation for the parameters.²⁰ The Q2B parameter of CP violation in decay is directly related to b_f ,

$$\mathcal{A}_f = \frac{-2b_f}{1 + b_f^2} \approx C_f , \quad (119)$$

and the mixing-induced CP violation parameter can be used to obtain $\sin(2\beta^{\text{eff}})$,

$$-\eta_f S_f \approx \frac{1 - b_f^2}{1 + b_f^2} \sin(2\beta_f^{\text{eff}}) , \quad (120)$$

where the approximations are exact in the case that $|q/p| = 1$.

Both *BABAR* [266] and *Belle* [265] present results for c_f and ϕ_f , for each resonant contribution, and in addition present results for \mathcal{A}_f and β_f^{eff} for $\phi(1020)K^0$, $f_0(980)K^0$ and for the remainder of the contributions to the $K^+ K^- K^0$ Dalitz plot combined. *BABAR* also present results for the Q2B parameter S_f for these channels. The models used to describe the resonant structure of the Dalitz plot differ, however. Both analyses suffer from symmetries in the likelihood that lead to multiple solutions, from which we select only one for averaging.

$B^0 \rightarrow \pi^+ \pi^- K_s^0$

Studies of $B^0 \rightarrow \pi^+ \pi^- K_s^0$ [269, 270] and of the related decay $B^+ \rightarrow \pi^+ \pi^- K^+$ [267, 271–273] show that the decay is dominated by components from intermediate resonances in the $K\pi$ ($K^*(892)$, $K_0^*(1430)$) and $\pi\pi$ ($\rho(770)$, $f_0(980)$, $f_2(1270)$) spectra, together with a poorly understood scalar structure that peaks near $m(\pi\pi) \sim 1300$ MeV/ c^2 and is denoted f_X ,²¹ as well as a large nonresonant component. There is also a contribution from the χ_{c0} state.

The full time-dependent Dalitz plot analysis allows the complex amplitudes of each contributing term to be determined from data, including CP violation effects. In the *BABAR* analysis [269], the magnitude and phase of each component (for both B^0 and \bar{B}^0 decays) are measured relative to $B^0 \rightarrow f_0(980)K_s^0$, using the following parametrisation:

$$A_f = |A_f| e^{i \arg(A_f)} , \quad \bar{A}_f = |\bar{A}_f| e^{i \arg(\bar{A}_f)} . \quad (121)$$

²⁰ $(c, b, \phi, \delta) \leftrightarrow (a, c, b, d)$. See Eq. (122).

²¹ The f_X component may originate from either the $f_0(1370)$ or $f_0(1500)$ resonances, or from interference between those or other states and nonresonant amplitudes in this region.

In the Belle analysis [270], the $B^0 \rightarrow K^{*+}\pi^-$ amplitude is chosen as the reference, and the amplitudes are parametrised as

$$A_f = a_f(1 + c_f)e^{i(b_f + d_f)} , \quad \bar{A}_f = a_f(1 - c_f)e^{i(b_f - d_f)} . \quad (122)$$

In both cases, the results are translated into Q2B parameters such as $2\beta_f^{\text{eff}}$, S_f , C_f for each CP eigenstate f , and parameters of CP violation in decay for each flavour-specific state. Relative phase differences between resonant terms are also extracted.

$B^0 \rightarrow \pi^+\pi^-\pi^0$

The $B^0 \rightarrow \pi^+\pi^-\pi^0$ decay is dominated by intermediate ρ resonances. Although it is possible, as above, to directly determine the complex amplitudes for each component, an alternative approach [274, 275] has been used by both *BABAR* [276, 277] and *Belle* [278, 279]. The amplitudes for B^0 and \bar{B}^0 decays to $\pi^+\pi^-\pi^0$ are written as

$$A_{3\pi} = f_+ A_+ + f_- A_- + f_0 A_0 , \quad \bar{A}_{3\pi} = f_+ \bar{A}_+ + f_- \bar{A}_- + f_0 \bar{A}_0 , \quad (123)$$

respectively. The symbols A_+ , A_- and A_0 represent the complex decay amplitudes for $B^0 \rightarrow \rho^+\pi^-$, $B^0 \rightarrow \rho^-\pi^+$ and $B^0 \rightarrow \rho^0\pi^0$ while \bar{A}_+ , \bar{A}_- and \bar{A}_0 represent those for $\bar{B}^0 \rightarrow \rho^+\pi^-$, $\bar{B}^0 \rightarrow \rho^-\pi^+$ and $\bar{B}^0 \rightarrow \rho^0\pi^0$, respectively. The terms f_+ , f_- and f_0 incorporate kinematic and dynamical factors and depend on the Dalitz plot coordinates. The full time-dependent decay distribution can then be written in terms of 27 free parameters, one for each coefficient of the form factor bilinears, as listed in Table 23. These parameters are sometimes referred to as “the *Us* and *Is*”, and can be expressed in terms of A_+ , A_- , A_0 , \bar{A}_+ , \bar{A}_- and \bar{A}_0 . If the full set of parameters is determined, together with their correlations, other parameters, such as weak and strong phases, parameters of CP violation in decay, *etc.*, can be subsequently extracted. Note that one of the parameters (typically U_+^+) is often fixed to unity to provide a reference; this does not affect the analysis.

5.2.6 Time-dependent CP asymmetries in decays to non- CP eigenstates

Consider a non- CP eigenstate f , and its conjugate \bar{f} . For neutral B decays to these final states, there are four amplitudes to consider: those for B^0 to decay to f and \bar{f} (A_f and $A_{\bar{f}}$, respectively), and the equivalents for \bar{B}^0 (\bar{A}_f and $\bar{A}_{\bar{f}}$). If CP is conserved in the decay, then $A_f = \bar{A}_{\bar{f}}$ and $A_{\bar{f}} = \bar{A}_f$.

The time-dependent decay distributions can be written in many different ways. Here, we follow Sec. 5.2.2 and define $\lambda_f = \frac{q}{p} \frac{\bar{A}_f}{A_f}$ and $\lambda_{\bar{f}} = \frac{q}{p} \frac{\bar{A}_{\bar{f}}}{A_{\bar{f}}}$. The time-dependent CP asymmetries that are sensitive to mixing-induced CP violation effects then follow Eq. (109):

$$\mathcal{A}_f(\Delta t) \equiv \frac{\Gamma_{\bar{B}^0 \rightarrow f}(\Delta t) - \Gamma_{B^0 \rightarrow f}(\Delta t)}{\Gamma_{\bar{B}^0 \rightarrow f}(\Delta t) + \Gamma_{B^0 \rightarrow f}(\Delta t)} = S_f \sin(\Delta m \Delta t) - C_f \cos(\Delta m \Delta t), \quad (124)$$

$$\mathcal{A}_{\bar{f}}(\Delta t) \equiv \frac{\Gamma_{\bar{B}^0 \rightarrow \bar{f}}(\Delta t) - \Gamma_{B^0 \rightarrow \bar{f}}(\Delta t)}{\Gamma_{\bar{B}^0 \rightarrow \bar{f}}(\Delta t) + \Gamma_{B^0 \rightarrow \bar{f}}(\Delta t)} = S_{\bar{f}} \sin(\Delta m \Delta t) - C_{\bar{f}} \cos(\Delta m \Delta t), \quad (125)$$

with the definitions of the parameters C_f , S_f , $C_{\bar{f}}$ and $S_{\bar{f}}$, following Eqs. (110) and (111).

Table 23: Definitions of the U and I coefficients. Modified from Ref. [276].

Parameter	Description
U_+^+	Coefficient of $ f_+ ^2$
U_0^+	Coefficient of $ f_0 ^2$
U_-^+	Coefficient of $ f_- ^2$
U_0^-	Coefficient of $ f_0 ^2 \cos(\Delta m \Delta t)$
U_-^-	Coefficient of $ f_- ^2 \cos(\Delta m \Delta t)$
U_+^-	Coefficient of $ f_+ ^2 \cos(\Delta m \Delta t)$
I_0	Coefficient of $ f_0 ^2 \sin(\Delta m \Delta t)$
I_-	Coefficient of $ f_- ^2 \sin(\Delta m \Delta t)$
I_+	Coefficient of $ f_+ ^2 \sin(\Delta m \Delta t)$
$U_{+-}^{+, \text{Im}}$	Coefficient of $\text{Im}[f_+ f_-^*]$
$U_{+-}^{+, \text{Re}}$	Coefficient of $\text{Re}[f_+ f_-^*]$
$U_{+-}^{-, \text{Im}}$	Coefficient of $\text{Im}[f_+ f_-^*] \cos(\Delta m \Delta t)$
$U_{+-}^{-, \text{Re}}$	Coefficient of $\text{Re}[f_+ f_-^*] \cos(\Delta m \Delta t)$
I_{+-}^{Im}	Coefficient of $\text{Im}[f_+ f_-^*] \sin(\Delta m \Delta t)$
I_{+-}^{Re}	Coefficient of $\text{Re}[f_+ f_-^*] \sin(\Delta m \Delta t)$
$U_{+0}^{+, \text{Im}}$	Coefficient of $\text{Im}[f_+ f_0^*]$
$U_{+0}^{+, \text{Re}}$	Coefficient of $\text{Re}[f_+ f_0^*]$
$U_{+0}^{-, \text{Im}}$	Coefficient of $\text{Im}[f_+ f_0^*] \cos(\Delta m \Delta t)$
$U_{+0}^{-, \text{Re}}$	Coefficient of $\text{Re}[f_+ f_0^*] \cos(\Delta m \Delta t)$
I_{+0}^{Im}	Coefficient of $\text{Im}[f_+ f_0^*] \sin(\Delta m \Delta t)$
I_{+0}^{Re}	Coefficient of $\text{Re}[f_+ f_0^*] \sin(\Delta m \Delta t)$
$U_{-0}^{+, \text{Im}}$	Coefficient of $\text{Im}[f_- f_0^*]$
$U_{-0}^{+, \text{Re}}$	Coefficient of $\text{Re}[f_- f_0^*]$
$U_{-0}^{-, \text{Im}}$	Coefficient of $\text{Im}[f_- f_0^*] \cos(\Delta m \Delta t)$
$U_{-0}^{-, \text{Re}}$	Coefficient of $\text{Re}[f_- f_0^*] \cos(\Delta m \Delta t)$
I_{-0}^{Im}	Coefficient of $\text{Im}[f_- f_0^*] \sin(\Delta m \Delta t)$
I_{-0}^{Re}	Coefficient of $\text{Re}[f_- f_0^*] \sin(\Delta m \Delta t)$

The time-dependent decay rates are given by

$$\Gamma_{\bar{B}^0 \rightarrow f}(\Delta t) = \frac{e^{-|\Delta t|/\tau(B^0)}}{8\tau(B^0)} (1 + \langle \mathcal{A}_{f\bar{f}} \rangle) [1 + S_f \sin(\Delta m \Delta t) - C_f \cos(\Delta m \Delta t)], \quad (126)$$

$$\Gamma_{B^0 \rightarrow f}(\Delta t) = \frac{e^{-|\Delta t|/\tau(B^0)}}{8\tau(B^0)} (1 + \langle \mathcal{A}_{f\bar{f}} \rangle) [1 - S_f \sin(\Delta m \Delta t) + C_f \cos(\Delta m \Delta t)], \quad (127)$$

$$\Gamma_{\bar{B}^0 \rightarrow \bar{f}}(\Delta t) = \frac{e^{-|\Delta t|/\tau(B^0)}}{8\tau(B^0)} (1 - \langle \mathcal{A}_{f\bar{f}} \rangle) [1 + S_{\bar{f}} \sin(\Delta m \Delta t) - C_{\bar{f}} \cos(\Delta m \Delta t)], \quad (128)$$

$$\Gamma_{B^0 \rightarrow \bar{f}}(\Delta t) = \frac{e^{-|\Delta t|/\tau(B^0)}}{8\tau(B^0)} (1 - \langle \mathcal{A}_{f\bar{f}} \rangle) [1 - S_{\bar{f}} \sin(\Delta m \Delta t) + C_{\bar{f}} \cos(\Delta m \Delta t)], \quad (129)$$

where the time-independent parameter $\langle \mathcal{A}_{f\bar{f}} \rangle$ represents an overall asymmetry in the production of the f and \bar{f} final states,²²

$$\langle \mathcal{A}_{f\bar{f}} \rangle = \frac{\left(|A_f|^2 + |\bar{A}_f|^2\right) - \left(|A_{\bar{f}}|^2 + |\bar{A}_{\bar{f}}|^2\right)}{\left(|A_f|^2 + |\bar{A}_f|^2\right) + \left(|A_{\bar{f}}|^2 + |\bar{A}_{\bar{f}}|^2\right)}. \quad (130)$$

Assuming $|q/p| = 1$, *i.e.* absence of CP violation in mixing, the parameters C_f and $C_{\bar{f}}$ can also be written in terms of the decay amplitudes as

$$C_f = \frac{|A_f|^2 - |\bar{A}_f|^2}{|A_f|^2 + |\bar{A}_f|^2} \quad \text{and} \quad C_{\bar{f}} = \frac{|A_{\bar{f}}|^2 - |\bar{A}_{\bar{f}}|^2}{|A_{\bar{f}}|^2 + |\bar{A}_{\bar{f}}|^2}, \quad (131)$$

giving rise to asymmetries in the decay amplitudes for the final states f and \bar{f} . In this notation, the conditions for absence of CP violation in decay are $\langle \mathcal{A}_{f\bar{f}} \rangle = 0$ and $C_f = -C_{\bar{f}}$. Note that C_f and $C_{\bar{f}}$ are typically non-zero; *e.g.*, for a flavour-specific final state where $\bar{A}_f = A_{\bar{f}} = 0$, they take the values $C_f = -C_{\bar{f}} = 1$.

The coefficients of the sine terms contain information about the weak phase. In the case that each decay amplitude contains only a single weak phase (*i.e.*, no CP violation in decay as well as none in mixing), these terms can be written as

$$S_f = \frac{-2 |A_f| |\bar{A}_f| \sin(\phi_{\text{mix}} + \phi_{\text{dec}} - \delta_f)}{|A_f|^2 + |\bar{A}_f|^2} \quad \text{and} \quad S_{\bar{f}} = \frac{-2 |A_{\bar{f}}| |\bar{A}_{\bar{f}}| \sin(\phi_{\text{mix}} + \phi_{\text{dec}} + \delta_f)}{|A_{\bar{f}}|^2 + |\bar{A}_{\bar{f}}|^2}, \quad (132)$$

where δ_f is the strong phase difference between the decay amplitudes. If there is no CP violation, the condition $S_f = -S_{\bar{f}}$ holds. If decay amplitudes with different weak and strong phases contribute, no straightforward interpretation of S_f and $S_{\bar{f}}$ is possible.

The conditions for CP invariance $C_f = -C_{\bar{f}}$ and $S_f = -S_{\bar{f}}$ motivate a rotation of the parameters:

$$S_{f\bar{f}} = \frac{S_f + S_{\bar{f}}}{2}, \quad \Delta S_{f\bar{f}} = \frac{S_f - S_{\bar{f}}}{2}, \quad C_{f\bar{f}} = \frac{C_f + C_{\bar{f}}}{2}, \quad \Delta C_{f\bar{f}} = \frac{C_f - C_{\bar{f}}}{2}. \quad (133)$$

With these parameters, the CP invariance conditions become $S_{f\bar{f}} = 0$ and $C_{f\bar{f}} = 0$. The parameter $\Delta C_{f\bar{f}}$ gives a measure of the “flavour-specificity” of the decay: $\Delta C_{f\bar{f}} = \pm 1$ corresponds to a completely flavour-specific decay, in which no interference between decays with and without mixing can occur, while $\Delta C_{f\bar{f}} = 0$ results in maximum sensitivity to mixing-induced CP violation. The parameter $\Delta S_{f\bar{f}}$ is related to the strong phase difference between the decay amplitudes of the B^0 meson to the f and to \bar{f} final states. We note that the observables of Eq. (133) exhibit experimental correlations (typically of $\sim 20\%$, depending on the tagging purity, and other effects) between $S_{f\bar{f}}$ and $\Delta S_{f\bar{f}}$, and between $C_{f\bar{f}}$ and $\Delta C_{f\bar{f}}$. On the other hand, the final-state-specific observables of Eqs. (126)–(129) tend to have low correlations.

Alternatively, if we recall that the CP invariance conditions at the decay amplitude level are $A_f = \bar{A}_{\bar{f}}$ and $A_{\bar{f}} = \bar{A}_f$, we are led to consider the parameters [244]

$$\mathcal{A}_{f\bar{f}} = \frac{|\bar{A}_{\bar{f}}|^2 - |A_f|^2}{|\bar{A}_{\bar{f}}|^2 + |A_f|^2} \quad \text{and} \quad \mathcal{A}_{\bar{f}f} = \frac{|\bar{A}_f|^2 - |A_{\bar{f}}|^2}{|\bar{A}_f|^2 + |A_{\bar{f}}|^2}. \quad (134)$$

²² This parameter is often denoted \mathcal{A}_f (or \mathcal{A}_{CP}), but here we avoid this notation to prevent confusion with the time-dependent CP asymmetry.

These are sometimes considered more physically intuitive parameters, since they characterise CP violation in decay in decays with particular topologies. For example, in the case of $B^0 \rightarrow \rho^\pm \pi^\mp$ (choosing $f = \rho^+ \pi^-$ and $\bar{f} = \rho^- \pi^+$), $\mathcal{A}_{f\bar{f}}$ (also denoted $\mathcal{A}_{\rho\pi}^{+-}$) parametrises CP violation in decays in which the produced ρ meson does not contain the spectator quark, while $\mathcal{A}_{\bar{f}f}$ (also denoted $\mathcal{A}_{\rho\pi}^{-+}$) parametrises CP violation in decays in which it does. Note that we have again followed the sign convention that the asymmetry is the difference between the rate involving a b quark and that involving a \bar{b} quark, *cf.* Eq. (105). Of course, these parameters are not independent of the other sets of parameters given above, and can be written as

$$\mathcal{A}_{f\bar{f}} = -\frac{\langle \mathcal{A}_{f\bar{f}} \rangle + C_{f\bar{f}} + \langle \mathcal{A}_{f\bar{f}} \rangle \Delta C_{f\bar{f}}}{1 + \Delta C_{f\bar{f}} + \langle \mathcal{A}_{f\bar{f}} \rangle C_{f\bar{f}}} \quad \text{and} \quad \mathcal{A}_{\bar{f}f} = \frac{-\langle \mathcal{A}_{f\bar{f}} \rangle + C_{f\bar{f}} + \langle \mathcal{A}_{f\bar{f}} \rangle \Delta C_{f\bar{f}}}{-1 + \Delta C_{f\bar{f}} + \langle \mathcal{A}_{f\bar{f}} \rangle C_{f\bar{f}}}. \quad (135)$$

They usually exhibit strong correlations.

We now consider the various notations used in experimental studies of time-dependent CP asymmetries in decays to non- CP eigenstates.

$B^0 \rightarrow D^{*\pm} D^\mp$

The $(\langle \mathcal{A}_{f\bar{f}} \rangle, C_f, S_f, C_{\bar{f}}, S_{\bar{f}})$ set of parameters was used in early publications by both *BABAR* [280] and *Belle* [281] (albeit with slightly different notations), with $f = D^{*+} D^-$, $\bar{f} = D^{*-} D^+$. In their most recent paper on this topic, *Belle* [282] instead use the parametrisation $(A_{D^{*}D}, S_{D^{*}D}, \Delta S_{D^{*}D}, C_{D^{*}D}, \Delta C_{D^{*}D})$, while *BABAR* [252] give results in both sets of parameters. We therefore use the $(A_{D^{*}D}, S_{D^{*}D}, \Delta S_{D^{*}D}, C_{D^{*}D}, \Delta C_{D^{*}D})$ set.

$B^0 \rightarrow \rho^\pm \pi^\mp$

In the $\rho^\pm \pi^\mp$ system, the $(\langle \mathcal{A}_{f\bar{f}} \rangle, C_{f\bar{f}}, S_{f\bar{f}}, \Delta C_{f\bar{f}}, \Delta S_{f\bar{f}})$ set of parameters was originally used by *BABAR* [283] and *Belle* [284] in the Q2B approximation; the exact names²³ used in this case were $(\mathcal{A}_{CP}^{\rho\pi}, C_{\rho\pi}, S_{\rho\pi}, \Delta C_{\rho\pi}, \Delta S_{\rho\pi})$, and these names are also used in this document.

Since $\rho^\pm \pi^\mp$ is reconstructed in the final state $\pi^+ \pi^- \pi^0$, the interference between the ρ resonances can provide additional information about the phases (see Sec. 5.2.5). Both *BABAR* [276] and *Belle* [278, 279] have performed time-dependent Dalitz-plot analyses, from which the weak phase α is directly extracted. In such an analysis, the measured Q2B parameters are also naturally corrected for interference effects.

$B^0 \rightarrow D^\mp \pi^\pm, D^{*\mp} \pi^\pm, D^\mp \rho^\pm$

Time-dependent CP analyses have also been performed for the final states $D^\mp \pi^\pm$, $D^{*\mp} \pi^\pm$ and $D^\mp \rho^\pm$. In these theoretically clean cases, no penguin contributions are possible, so there is no CP violation in decay. Furthermore, due to the smallness of the ratio of the magnitudes of the suppressed ($b \rightarrow u$) and favoured ($b \rightarrow c$) amplitudes (denoted R_f), to a very good approximation, $C_f = -C_{\bar{f}} = 1$ (using $f = D^{(*)-} h^+$, $\bar{f} = D^{(*)+} h^-$ $h = \pi, \rho$), and the coefficients of the sine terms are given by

$$S_f = -2R_f \sin(\phi_{\text{mix}} + \phi_{\text{dec}} - \delta_f) \quad \text{and} \quad S_{\bar{f}} = -2R_f \sin(\phi_{\text{mix}} + \phi_{\text{dec}} + \delta_f). \quad (136)$$

Thus, weak phase information can be obtained from measurements of S_f and $S_{\bar{f}}$, although external information on at least one of R_f or δ_f is necessary, constituting a source of theoretical

²³ *BABAR* has used the notations $A_{CP}^{\rho\pi}$ [283] and $\mathcal{A}_{\rho\pi}$ [276] in place of $\mathcal{A}_{CP}^{\rho\pi}$.

uncertainty. Note that $\phi_{\text{mix}} + \phi_{\text{dec}} = 2\beta + \gamma \equiv 2\phi_1 + \phi_3$ for all the decay modes in question, while R_f and δ_f depend on the decay mode.

Again, different notations have been used in the literature. *BABAR* [285, 286] defines the time-dependent probability function by

$$f^\pm(\eta, \Delta t) = \frac{e^{-|\Delta t|/\tau}}{4\tau} [1 \mp S_\zeta \sin(\Delta m \Delta t) \mp \eta C_\zeta \cos(\Delta m \Delta t)], \quad (137)$$

where the upper (lower) sign corresponds to the tagging meson being a B^0 (\bar{B}^0). The parameters η and ζ take the values +1 and + (−1 and −) when the final state is, *e.g.*, $D^- \pi^+$ ($D^+ \pi^-$). However, in the fit, the substitutions $C_\zeta = 1$ and $S_\zeta = a \mp \eta b_i - \eta c_i$ are made, where the subscript i denotes the flavor tagging category. Neglecting b terms,

$$S_+ = a - c \quad \text{and} \quad S_- = a + c \Leftrightarrow a = (S_+ + S_-)/2 \quad \text{and} \quad c = (S_- - S_+)/2, \quad (138)$$

in analogy to the parameters of Eq. (133). These are motivated by the possibility of CP violation on the tag side [287]. The parameter a is not affected by tag-side CP violation. The parameter b only depends on tag-side CP violation parameters and is not directly useful for determining UT angles. A clean interpretation of the c parameter is only possible for lepton-tagged events, which are not affected by tag-side CP violation effects, so the *BABAR* measurements report c measured with those events only.

The parameters used by *Belle* in the analysis using partially reconstructed B decays [288], are similar to the S_ζ parameters defined above. However, in the *Belle* convention, a tagging B^0 corresponds to a + sign in front of the sine coefficient; furthermore the correspondence between the super/subscript and the final state is opposite, so that S_\pm (*BABAR*) = $-S^\mp$ (*Belle*). In this analysis, only lepton tags are used, so there is no effect from tag-side CP violation. In the *Belle* analysis that used fully reconstructed B decays [289], this effect is measured and taken into account using $D^* \ell \nu$ decays; in neither *Belle* analysis are the a , b and c parameters used. The parameters measured by *Belle* are $2R_{D^{(*)}\pi} \sin(2\phi_1 + \phi_3 \pm \delta_{D^{(*)}\pi})$; the definition is such that S^\pm (*Belle*) = $-2R_{D^*\pi} \sin(2\phi_1 + \phi_3 \pm \delta_{D^*\pi})$. This definition includes an angular momentum factor $(-1)^L$ [290], and so for the results in the $D\pi$ system, there is an additional factor of -1 in the conversion.

LHCb has also measured the parameters of $B^0 \rightarrow D^\mp \pi^\pm$ decays [291]. The convention used is essentially the same as *Belle*, but with the notation $(S_f, S_{\bar{f}}) = (S_-, S_+)$. For the averages in this document, we use the a and c parameters. Correlations are taken into account in the *LHCb* case, where significant correlations are reported. Explicitly, the conversion reads: $a = -(S_+ + S_-)/2$, $c = -(S_+ - S_-)/2$.

$B_s^0 \rightarrow D_s^\mp K^\pm$

The phenomenology of $B_s^0 \rightarrow D_s^\mp K^\pm$ decays is similar to that of $B^0 \rightarrow D^\mp \pi^\pm$, with some important caveats. The two amplitudes $b \rightarrow u$ and $b \rightarrow c$ amplitudes have the same level of Cabibbo-suppression (*i.e.* are of the same order in λ) though the former is suppressed by $\sqrt{\rho^2 + \eta^2}$. The large value of the ratio R of their magnitudes allows it to be determined from data, as the deviation of $|C_f|$ and $|C_{\bar{f}}|$ from unity can be observed. Moreover, the non-zero value of $\Delta\Gamma_s$ allows the determination of additional terms, $A_f^{\Delta\Gamma}$ and $A_{\bar{f}}^{\Delta\Gamma}$ (see Sec. 5.2.3), that break ambiguities in the solutions for $\phi_{\text{mix}} + \phi_{\text{dec}}$, which for $B_s^0 \rightarrow D_s^\mp K^\pm$ decays is equal to $\gamma - 2\beta_s$.

LHCb [292, 293] has performed such an analysis with $B_s^0 \rightarrow D_s^\mp K^\pm$ decays. The absence of CP violation in decay was assumed, and the parameters determined from the fit were labelled C , $A^{\Delta\Gamma}$, $\bar{A}^{\Delta\Gamma}$, S , \bar{S} . These are trivially related to the definitions used in this section.

Time-dependent asymmetries in radiative B decays

As a special case of decays to non- CP eigenstates, let us consider radiative B decays. Here, the emitted photon has a distinct helicity, which is in principle observable, but in practice is not usually measured. Thus, the measured time-dependent decay rates for neutral B meson decays are given by [294, 295]

$$\begin{aligned}\Gamma_{\bar{B}^0 \rightarrow X\gamma}(\Delta t) &= \Gamma_{\bar{B}^0 \rightarrow X\gamma_L}(\Delta t) + \Gamma_{\bar{B}^0 \rightarrow X\gamma_R}(\Delta t) \\ &= \frac{e^{-|\Delta t|/\tau(B^0)}}{4\tau(B^0)} [1 + (S_L + S_R) \sin(\Delta m\Delta t) - (C_L + C_R) \cos(\Delta m\Delta t)],\end{aligned}\tag{139}$$

$$\begin{aligned}\Gamma_{B^0 \rightarrow X\gamma}(\Delta t) &= \Gamma_{B^0 \rightarrow X\gamma_L}(\Delta t) + \Gamma_{B^0 \rightarrow X\gamma_R}(\Delta t) \\ &= \frac{e^{-|\Delta t|/\tau(B^0)}}{4\tau(B^0)} [1 - (S_L + S_R) \sin(\Delta m\Delta t) + (C_L + C_R) \cos(\Delta m\Delta t)],\end{aligned}\tag{140}$$

where in place of the subscripts f and \bar{f} we have used L and R to indicate the photon helicity. In order for interference between decays with and without B^0 - \bar{B}^0 mixing to occur, the X system must not be flavour-specific, *e.g.*, in the case of $B^0 \rightarrow K^{*0}\gamma$, the final state must be $K_s^0\pi^0\gamma$. The sign of the sine term depends on the C eigenvalue of the X system. At leading order, the photons from $b \rightarrow q\gamma$ ($\bar{b} \rightarrow \bar{q}\gamma$) are predominantly left (right) polarised, with corrections of order of m_q/m_b , and thus interference effects are suppressed. Higher-order effects can lead to corrections of order Λ_{QCD}/m_b [296, 297], although explicit calculations indicate that such corrections may be small for exclusive final states [298, 299]. The predicted smallness of the S terms in the Standard Model results in sensitivity to new physics contributions.

The formalism discussed above is valid for any radiative decay to a final state where the hadronic system is an eigenstate of C . In addition to $K_s^0\pi^0\gamma$, experiments have presented results using B^0 decays to $K_s^0\eta\gamma$, $K_s^0\rho^0\gamma$ and $K_s^0\phi\gamma$. For the case of the $K_s^0\rho^0\gamma$ final state, particular care is needed, as due to the non-negligible width of the ρ^0 meson, decays selected as $B^0 \rightarrow K_s^0\rho^0\gamma$ can include a significant contribution from $K^{*\pm}\pi^\mp\gamma$ decays, which are flavour-specific and do not have the same oscillation phenomenology. It is therefore necessary to correct the fitted asymmetry parameter for a “dilution factor”.

In the case of radiative B_s^0 decays, the time-dependent decay rates of Eqs. (139) and (140) must be modified, in a similar way to that discussed in Sec. 5.2.3, to account for the non-zero value of $\Delta\Gamma_s$. Thus, for decays such as $B_s^0 \rightarrow \phi\gamma$, there is an additional observable, $A_{\phi\gamma}^{\Delta\Gamma}$, which can be determined from an untagged effective lifetime measurement [300].

5.2.7 Asymmetries in $B \rightarrow D^{(*)}K^{(*)}$ decays

CP asymmetries in $B \rightarrow D^{(*)}K^{(*)}$ decays are sensitive to γ . The neutral $D^{(*)}$ meson produced is an admixture of $D^{(*)0}$ (produced by a $b \rightarrow c$ transition) and $\bar{D}^{(*)0}$ (produced by a colour-suppressed $b \rightarrow u$ transition) states. If the final state is chosen so that both $D^{(*)0}$ and $\bar{D}^{(*)0}$ can contribute, the two amplitudes interfere, and the resulting observables are sensitive to γ , the relative weak phase between the two B decay amplitudes [301]. Various methods have been

proposed to exploit this interference, including those where the neutral D meson is reconstructed as a CP eigenstate (GLW) [302, 303], in a suppressed final state (ADS) [304, 305], or in a self-conjugate three-body final state, such as $K_S^0\pi^+\pi^-$ (GGSZ or Dalitz) [306, 307]. While each method differs in the choice of D decay, they are all sensitive to the same parameters of the B decay, and can be considered as variations of the same technique.

Consider the case of $B^\mp \rightarrow DK^\mp$, with D decaying to a final state f , which is accessible from both D^0 and \bar{D}^0 . We can write the decay rates Γ_\mp for B^- and B^+ , the charge averaged rate $\Gamma = (\Gamma_- + \Gamma_+)/2$, and the charge asymmetry $A = (\Gamma_- - \Gamma_+)/(\Gamma_- + \Gamma_+)$ (see Eq. (105)) as

$$\Gamma_\mp \propto r_B^2 + r_D^2 + 2r_B r_D \cos(\delta_B + \delta_D \mp \gamma), \quad (141)$$

$$\Gamma \propto r_B^2 + r_D^2 + 2r_B r_D \cos(\delta_B + \delta_D) \cos(\gamma), \quad (142)$$

$$A = \frac{2r_B r_D \sin(\delta_B + \delta_D) \sin(\gamma)}{r_B^2 + r_D^2 + 2r_B r_D \cos(\delta_B + \delta_D) \cos(\gamma)}, \quad (143)$$

where the ratio

$$r_B = \left| \frac{A(B^- \rightarrow \bar{D}^0 K^-)}{A(B^- \rightarrow D^0 K^-)} \right| = \left| \frac{A(B^+ \rightarrow D^0 K^+)}{A(B^+ \rightarrow \bar{D}^0 K^+)} \right|, \quad (144)$$

of B decay amplitudes²⁴ is usually defined to be less than one, and the ratio of D decay amplitudes is correspondingly defined by

$$r_D = \left| \frac{A(D^0 \rightarrow f)}{A(\bar{D}^0 \rightarrow f)} \right|. \quad (145)$$

The relation between B^- and B^+ amplitudes given in Eq. (144) is a result of there being only one weak phase contributing to each amplitude in the Standard Model, which is the source of the theoretical cleanliness of this approach for measuring γ [308]. The strong phase differences between the B and D decay amplitudes are denoted by δ_B and δ_D , respectively. The values of r_D and δ_D depend on the final state f : for the GLW analysis, $r_D = 1$ and δ_D is trivial (either zero or π); for other modes, values of r_D and δ_D are not trivial, and for multibody final states they vary across the phase space. This can be quantified either by an explicit D decay amplitude model or by model-independent information. In the case that the multibody final state is treated inclusively, the formalism is modified by the inclusion of a coherence factor, usually denoted κ , while r_D and δ_D become effective parameters corresponding to amplitude-weighted averages across the phase space.

Note that, for given values of r_B and r_D , the maximum size of A (at $\sin(\delta_B + \delta_D) = 1$) is $2r_B r_D \sin(\gamma) / (r_B^2 + r_D^2)$. Thus, even for D decay modes with small r_D , large asymmetries, and hence sensitivity to γ , may occur for B decay modes with similar values of r_B . For this reason, the ADS analysis of the decay $B^\mp \rightarrow D\pi^\mp$ is also of interest.

The expressions of Eq. (141)–(145) are for a specific point in phase space, and therefore are relevant where both B and D decays are to two-body final states. Additional coherence factors enter the expressions when the B decay is to a multibody final state (further discussion of multibody D decays can be found below). In particular, experiments have studied $B^+ \rightarrow$

²⁴ Note that here we use the notation r_B to denote the ratio of B decay amplitudes, whereas in Sec. 5.2.6 we used, *e.g.*, $R_{D\pi}$, for a rather similar quantity. The reason is that here we need to be concerned also with D decay amplitudes, and so it is convenient to use the subscript to denote the decaying particle. Hopefully, using r in place of R will reduce the potential for confusion.

$DK^*(892)^+$, $B^0 \rightarrow DK^*(892)^0$ and $B^+ \rightarrow DK^+\pi^+\pi^-$ decays. Considering, for concreteness, the $B \rightarrow DK^*(892)$ case, the non-negligible width of the $K^*(892)$ resonance implies that contributions from other $B \rightarrow DK\pi$ decays can pass the selection requirements. Their effect on the Q2B analysis can be accounted for with a coherence factor [309], usually denoted κ , which tends to unity in the limit that the $K^*(892)$ resonance is the only signal amplitude contributing in the selected region of phase space. In this case, the hadronic parameters r_B and δ_B become effectively weighted averages across the selected phase space of the magnitude ratio and relative strong phase between the CKM-suppressed and -favoured amplitudes; these effective parameters are denoted \bar{r}_B and $\bar{\delta}_B$ (the notations r_s , δ_s and r_S , δ_S are also found in the literature). An alternative, and in certain cases more advantageous, approach is Dalitz plot analysis of the full $B \rightarrow DK\pi$ phase space [310–312].

We now consider the various notations used in experimental studies of CP asymmetries in $B \rightarrow D^{(*)}K^{(*)}$ decays. To simplify the notation the $B^+ \rightarrow DK^+$ decay is considered; the extension to other modes mediated by the same quark-level transitions is straightforward.

$B \rightarrow D^{(*)}K^{(*)}$ with $D \rightarrow CP$ eigenstate decays

In the GLW analysis, the measured quantities are the partial rate asymmetry

$$A_{CP} = \frac{\Gamma(B^- \rightarrow D_{CP}K^-) - \Gamma(B^+ \rightarrow D_{CP}K^+)}{\Gamma(B^- \rightarrow D_{CP}K^-) + \Gamma(B^+ \rightarrow D_{CP}K^+)} \quad (146)$$

and the charge-averaged rate

$$R_{CP} = \frac{2\Gamma(B^+ \rightarrow D_{CP}K^+)}{\Gamma(B^+ \rightarrow \bar{D}^0K^+)}, \quad (147)$$

which are measured for D decays to both CP -even and CP -odd final states. It is often experimentally convenient to measure R_{CP} using a double ratio,

$$R_{CP} = \frac{\Gamma(B^+ \rightarrow D_{CP}K^+) / \Gamma(B^+ \rightarrow \bar{D}^0K^+)}{\Gamma(B^+ \rightarrow D_{CP}\pi^+) / \Gamma(B^+ \rightarrow \bar{D}^0\pi^+)} \quad (148)$$

that is normalised both to the rate for the favoured $\bar{D}^0 \rightarrow K^+\pi^-$ decay, and to the equivalent quantities for $B^+ \rightarrow D\pi^+$ decays (charge conjugate processes are implicitly included in Eqs. (147) and (148)). In this way the constant of proportionality drops out of Eq. (142). Eq. (148) is exact in the limit that the contribution of the $b \rightarrow u$ decay amplitude to $B^+ \rightarrow D\pi^+$ vanishes and when the flavour-specific rates $\Gamma(B^+ \rightarrow \bar{D}^0h^+)$ ($h = \pi, K$) are determined using appropriately flavour-specific D decays. In reality, the Cabibbo-favoured $D \rightarrow K\pi$ decay is used, leading to a small source of systematic uncertainty.

$B \rightarrow D^{(*)}K^{(*)}$ with $D \rightarrow$ non- CP eigenstate two-body decays

For the ADS analysis, which is based on a suppressed $D \rightarrow f$ decay, the measured quantities are again the partial rate asymmetry and the charge-averaged rate. In this case it is sufficient to measure the rate in a single ratio (normalised to the favoured $D \rightarrow \bar{f}$ decay) since potential systematic uncertainties related to detection cancel naturally; the observed charge-averaged rate is then

$$R_{ADS} = \frac{\Gamma(B^- \rightarrow [f]_D K^-) + \Gamma(B^+ \rightarrow [\bar{f}]_D K^+)}{\Gamma(B^- \rightarrow [\bar{f}]_D K^-) + \Gamma(B^+ \rightarrow [f]_D K^+)}, \quad (149)$$

where the inclusion of charge-conjugate modes has been made explicit. The CP asymmetry is defined as

$$A_{\text{ADS}} = \frac{\Gamma(B^- \rightarrow [f]_D K^-) - \Gamma(B^+ \rightarrow [f]_D K^+)}{\Gamma(B^- \rightarrow [f]_D K^-) + \Gamma(B^+ \rightarrow [f]_D K^+)}. \quad (150)$$

Since the uncertainty of A_{ADS} depends on the central value of R_{ADS} , for some statistical treatments it is preferable to use an alternative pair of parameters [313]

$$R_- = \frac{\Gamma(B^- \rightarrow [f]_D K^-)}{\Gamma(B^- \rightarrow [\bar{f}]_D K^-)} \quad R_+ = \frac{\Gamma(B^+ \rightarrow [\bar{f}]_D K^+)}{\Gamma(B^+ \rightarrow [f]_D K^+)}, \quad (151)$$

where there is no implied inclusion of charge-conjugate processes. These parameters are statistically uncorrelated but may be affected by common sources of systematic uncertainty. We use the $(R_{\text{ADS}}, A_{\text{ADS}})$ set in our compilation where available.

In the ADS analysis, there are two additional unknowns (r_D and δ_D) compared to the GLW case. Additional constraints are therefore required in order to obtain sensitivity to γ . Generally, one needs access to two different linear admixtures of D^0 and \bar{D}^0 states in order to determine the relative phase: one such sample can be flavour tagged D mesons, which are available in abundant quantities in many experiments; the other can be CP -tagged D mesons from $\psi(3770)$ decays, or a superposition of D^0 and \bar{D}^0 from $D^0-\bar{D}^0$ mixing or from production in $B \rightarrow DK$ decays. In fact, the most precise information on both r_D and δ_D for $D \rightarrow K\pi$ currently comes from global fits to charm mixing data, as discussed in Sec. 9.1.

The relation of A_{ADS} to the underlying parameters given in Eq. (143) and Table 24 is exact for a two-body D decay. For multibody decays, a similar formalism can be used with the introduction of a coherence factor [314]. This is most appropriate for doubly-Cabibbo-suppressed decays to non-self-conjugate final states, but can also be modified for use with singly-Cabibbo-suppressed decays [315]. For multibody self-conjugate final states, such as $K_s^0\pi^+\pi^-$, a Dalitz plot analysis (discussed below) is often more appropriate. However, in certain cases where the final state can be approximated as a CP eigenstate, a modified version of the GLW formalism can be used [316]. In such cases the observables are denoted $A_{q\text{GLW}}$ and $R_{q\text{GLW}}$ to indicate that the final state is not a pure CP eigenstate.

$B \rightarrow D^{(*)}K^{(*)}$ with $D \rightarrow$ multibody final state decays

In the model-dependent Dalitz-plot (or GGSZ) analysis of D decays to multibody self-conjugate final states, the values of r_D and δ_D across the Dalitz plot are given by an amplitude model (with parameters typically obtained from data). A simultaneous fit to the B^+ and B^- samples can then be used to obtain γ , r_B and δ_B directly. The uncertainties on the phases depend approximately inversely on r_B , which is positive definite and therefore tends to be overestimated leading to an underestimation of the uncertainty on γ that must be corrected statistically (unless $\sigma(r_B) \ll r_B$). An alternative approach is to fit for the ‘‘Cartesian’’ variables

$$(x_\pm, y_\pm) = (\text{Re}(r_B e^{i(\delta_B \pm \gamma)}), \text{Im}(r_B e^{i(\delta_B \pm \gamma)})) = (r_B \cos(\delta_B \pm \gamma), r_B \sin(\delta_B \pm \gamma)). \quad (152)$$

These variables tend to be statistically well-behaved, and are therefore appropriate for combination of results obtained from independent B^\pm data samples.

The assumption of a model for the D decay leads to a non-negligible, and hard to quantify, source of uncertainty. To obviate this, it is possible to use instead a model-independent approach, in which the Dalitz plot (or, more generally, the phase space) is binned [306, 317, 318].

In this case, hadronic parameters describing the average strong phase difference in each bin between the interfering decay amplitudes enter the equations. These parameters can be determined from interference effects in decays of quantum-correlated $D\bar{D}$ pairs produced at the $\psi(3770)$ resonance. Measurements of such parameters have been made for several hadronic D decays by CLEO-c and BESIII.

When a multibody D decay is dominated by one CP state, additional sensitivity to γ is obtained from the relative widths of the $B^+ \rightarrow DK^+$ and $B^- \rightarrow DK^-$ decays. This can be taken into account in various ways. One possibility is to perform a GLW-like analysis, as mentioned above. An alternative approach proceeds by defining

$$z_{\pm} = x_{\pm} + iy_{\pm}, \quad x_0 = - \int \text{Re}[f(s_1, s_2)f^*(s_2, s_1)] ds_1 ds_2, \quad (153)$$

where s_1, s_2 are the coordinates of invariant mass squared that define the Dalitz plot and f is the complex amplitude for D decay as a function of the Dalitz plot coordinates.²⁵ The fitted parameters $(\rho^{\pm}, \theta^{\pm})$ are then defined by

$$\rho^{\pm} e^{i\theta^{\pm}} = z_{\pm} - x_0. \quad (154)$$

Note that the yields of B^{\pm} decays are proportional to $1 + (\rho^{\pm})^2 - (x_0)^2$. This choice of variables has been used by *BABAR* in the analysis of $B^+ \rightarrow DK^+$ with $D \rightarrow \pi^+\pi^-\pi^0$ [320]; for this D decay, and with the assumed amplitude model, a value of $x_0 = 0.850$ is obtained.

The relations between the measured quantities and the underlying parameters are summarised in Table 24. It must be emphasised that the hadronic factors r_B and δ_B are different, in general, for each B decay mode.

Table 24: Summary of relations between measured and physical parameters in GLW, ADS and Dalitz analyses of $B \rightarrow D^{(*)}K^{(*)}$ decays.

GLW analysis	
$R_{CP\pm}$	$1 + r_B^2 \pm 2r_B \cos(\delta_B) \cos(\gamma)$
$A_{CP\pm}$	$\pm 2r_B \sin(\delta_B) \sin(\gamma) / R_{CP\pm}$
ADS analysis	
R_{ADS}	$r_B^2 + r_D^2 + 2r_B r_D \cos(\delta_B + \delta_D) \cos(\gamma)$
A_{ADS}	$2r_B r_D \sin(\delta_B + \delta_D) \sin(\gamma) / R_{ADS}$
GGSZ Dalitz analysis ($D \rightarrow K_s^0 \pi^+ \pi^-$)	
x_{\pm}	$r_B \cos(\delta_B \pm \gamma)$
y_{\pm}	$r_B \sin(\delta_B \pm \gamma)$
Dalitz analysis ($D \rightarrow \pi^+ \pi^- \pi^0$)	
ρ^{\pm}	$ z_{\pm} - x_0 $
θ^{\pm}	$\tan^{-1}(\text{Im}(z_{\pm}) / (\text{Re}(z_{\pm}) - x_0))$

²⁵ The x_0 parameter gives a model-dependent measure of the net CP content of the final state [316, 319]. It is closely related to the c_i parameters of the model dependent Dalitz plot analysis [306, 317, 318], and the coherence factor of inclusive ADS-type analyses [314], integrated over the entire Dalitz plot.

5.3 Common inputs and uncertainty treatment

As described in Sec. 3, where measurements combined in an average depend on external parameters, it can be important to rescale to the latest values of those parameters in order to obtain the most precise and accurate results. In practice, this is only necessary for modes with reasonably small statistical errors, so that the systematic uncertainty associated with the knowledge of the external parameter is not negligible. Among the averages in this section, rescaling to common inputs is only done for $b \rightarrow c\bar{c}s$ transitions of B^0 mesons. Correlated sources of systematic uncertainty are also taken into account in these averages. For most other modes, the effects of common inputs and sources of systematic uncertainty are currently negligible, however similar considerations are applied when combining results to obtain constraints on $\alpha \equiv \phi_2$ and $\gamma \equiv \phi_3$ as discussed in Sec. 5.11.1 and 5.14.7, respectively.

The common inputs used for calculating the averages are listed in Table 25. The average values for the B^0 lifetime ($\tau(B^0)$), mixing parameter (Δm_d) and relative width difference ($\Delta\Gamma_d/\Gamma_d$) averages are discussed in Sec. 4. The fraction of the perpendicularly polarised component ($|A_\perp|^2$) in $B \rightarrow J/\psi K^*(892)$ decays, which determines the CP composition in these decays, is averaged from results by *BABAR* [321], *Belle* [322], *CDF* [323], *D0* [95] and *LHCb* [324] (see also Sec. 7).

Table 25: Common inputs used in calculating the averages.

$\tau(B^0)$ (ps)	1.520 ± 0.004
Δm_d (ps $^{-1}$)	0.5065 ± 0.0019
$\Delta\Gamma_d/\Gamma_d$	-0.002 ± 0.010
$ A_\perp ^2 (J/\psi K^*)$	0.209 ± 0.006

As explained in Sec. 2, we do not apply a rescaling factor on the uncertainty of an average that has $\chi^2/\text{dof} > 1$ (unlike the procedure currently used by the PDG [21]). We provide a confidence level of the fit so that one can know the consistency of the measurements included in the average, and attach comments in case some care needs to be taken in the interpretation. Note that, in general, results obtained from small data samples will exhibit some non-Gaussian behaviour. We average measurements with asymmetric uncertainties using the PDG [21] prescription. In cases where several measurements are correlated (*e.g.* S_f and C_f in measurements of time-dependent CP violation in B decays to a particular CP eigenstate) we take these into account in the averaging procedure if the uncertainties are sufficiently Gaussian. For measurements where one uncertainty is given, it represents the total error, where statistical and systematic uncertainties have been added in quadrature. If two uncertainties are given, the first is statistical and the second systematic. If more than two errors are given, the origin of the additional uncertainty will be explained in the text.

5.4 Time-dependent asymmetries in $b \rightarrow c\bar{c}s$ transitions

5.4.1 Time-dependent CP asymmetries in $b \rightarrow c\bar{c}s$ decays to CP eigenstates

In the Standard Model, the time-dependent parameters for B^0 decays governed by $b \rightarrow c\bar{c}s$ transitions are predicted to be $S_{b \rightarrow c\bar{c}s} = -\eta \sin(2\beta)$ and $C_{b \rightarrow c\bar{c}s} = 0$ to very good accuracy.

Deviations from this relation are currently limited to the level of $\lesssim 1^\circ$ on 2β [325–327]. The averages for $-\eta S_{b \rightarrow c\bar{c}s}$ and $C_{b \rightarrow c\bar{c}s}$ are provided in Table 26. The averages for $-\eta S_{b \rightarrow c\bar{c}s}$ are shown in Fig. 12.

Both *BABAR* and *Belle* have used the $\eta = -1$ modes $J/\psi K_s^0$, $\psi(2S)K_s^0$, $\chi_{c1}K_s^0$ and $\eta_c K_s^0$, as well as $J/\psi K_L^0$, which has $\eta = +1$ and $J/\psi K^{*0}(892)$, which is found to have η close to +1 based on the measurement of $|A_\perp|$ (see Sec. 5.3). The most recent *Belle* result does not use $\eta_c K_s^0$ or $J/\psi K^{*0}(892)$ decays.²⁶ *LHCb* have used $J/\psi K_s^0$ (data with $J/\psi \rightarrow \mu^+\mu^-$ and e^+e^- are reported in different publications) and $\psi(2S)K_s^0$ decays. *ALEPH*, *OPAL*, and *CDF* have used only the $J/\psi K_s^0$ final state. *BABAR* has also determined the CP violation parameters of the $B^0 \rightarrow \chi_{c0}K_s^0$ decay from the time-dependent Dalitz-plot analysis of the $B^0 \rightarrow \pi^+\pi^-K_s^0$ mode (see Sec. 5.7.2). In addition, *Belle* has performed a measurement with data accumulated at the $\Upsilon(5S)$ resonance, using the $J/\psi K_s^0$ final state – this involves a different flavour tagging method compared to the measurements performed with data accumulated at the $\Upsilon(4S)$ resonance. A breakdown of results in each charmonium-kaon final state is given in Table 27.

Table 26: Results and averages for $S_{b \rightarrow c\bar{c}s}$ and $C_{b \rightarrow c\bar{c}s}$. The averages are given from a combination of the most precise results only, and also including less precise measurements.

Experiment		Sample size	$-\eta S_{b \rightarrow c\bar{c}s}$	$C_{b \rightarrow c\bar{c}s}$
<i>BABAR</i> $b \rightarrow c\bar{c}s$	[328]	$N(B\bar{B}) = 465\text{M}$	$0.687 \pm 0.028 \pm 0.012$	$0.024 \pm 0.020 \pm 0.016$
<i>Belle</i> $b \rightarrow c\bar{c}s$	[329]	$N(B\bar{B}) = 772\text{M}$	$0.667 \pm 0.023 \pm 0.012$	$-0.006 \pm 0.016 \pm 0.012$
<i>LHCb</i> $J/\psi K_s^0$	[330,331]	$\int \mathcal{L} dt = 3 \text{ fb}^{-1}$	0.75 ± 0.04	-0.014 ± 0.030
<i>LHCb</i> $\psi(2S)K_s^0$	[331]	$\int \mathcal{L} dt = 3 \text{ fb}^{-1}$	$0.84 \pm 0.10 \pm 0.01$	$-0.05 \pm 0.10 \pm 0.01$
Average			0.698 ± 0.017	-0.005 ± 0.015
Confidence level			$0.09 \text{ (} 1.7\sigma \text{)}$	$0.54 \text{ (} 0.6\sigma \text{)}$
<i>BABAR</i> $\chi_{c0}K_s^0$	[269]	$N(B\bar{B}) = 383\text{M}$	$0.69 \pm 0.52 \pm 0.04 \pm 0.07$	$-0.29^{+0.53}_{-0.44} \pm 0.03 \pm 0.05$
<i>BABAR</i> $J/\psi K_s^0$ (*)	[332]	$N(B\bar{B}) = 88\text{M}$	$1.56 \pm 0.42 \pm 0.21$	–
<i>ALEPH</i>	[333]	$N(Z \rightarrow \text{hadrons}) = 4\text{M}$	$0.84^{+0.82}_{-1.04} \pm 0.16$	–
<i>OPAL</i>	[334]	$N(Z \rightarrow \text{hadrons}) = 4.4\text{M}$	$3.2^{+1.8}_{-2.0} \pm 0.5$	–
<i>CDF</i>	[335]	$\int \mathcal{L} dt = 110 \text{ pb}^{-1}$	$0.79^{+0.41}_{-0.44}$	–
<i>Belle</i> $\Upsilon(5S)$	[336]	$\int \mathcal{L} dt = 121 \text{ fb}^{-1}$	$0.57 \pm 0.58 \pm 0.06$	–
Average			0.699 ± 0.017	-0.005 ± 0.015

(*) This result uses “hadronic and previously unused muonic decays of the J/ψ ”. We neglect a small possible correlation of this result with the main *BABAR* result [328] that could be caused by reprocessing of the data.

While the uncertainty in the average for $-\eta S_{b \rightarrow c\bar{c}s}$ is limited by statistical error, the precision for $C_{b \rightarrow c\bar{c}s}$ is close to being dominated by the systematic uncertainty, particularly for measurements from the e^+e^- *B* factory experiments. This occurs due to the possible effect of tag-side interference [287] on the $C_{b \rightarrow c\bar{c}s}$ measurement, an effect which is correlated between different $e^+e^- \rightarrow \Upsilon(4S) \rightarrow B\bar{B}$ experiments. Understanding of this effect may continue to improve in future, allowing the uncertainty to reduce.

From the average for $-\eta S_{b \rightarrow c\bar{c}s}$ above, we obtain the following solutions for β (in $[0, \pi]$):

$$\beta = (22.2 \pm 0.7)^\circ \quad \text{or} \quad \beta = (67.8 \pm 0.7)^\circ . \quad (155)$$

²⁶ Previous analyses from *Belle* did include these channels [103], but it is not possible to obtain separate results for those modes from the published information.

Table 27: Breakdown of results on $S_{b \rightarrow c\bar{s}s}$ and $C_{b \rightarrow c\bar{s}s}$.

Mode		Sample size	$-\eta S_{b \rightarrow c\bar{s}s}$	$C_{b \rightarrow c\bar{s}s}$
BABAR				
$J/\psi K_s^0$	[328]	$N(B\bar{B}) = 465M$	$0.657 \pm 0.036 \pm 0.012$	$0.026 \pm 0.025 \pm 0.016$
$J/\psi K_L^0$	[328]	$N(B\bar{B}) = 465M$	$0.694 \pm 0.061 \pm 0.031$	$-0.033 \pm 0.050 \pm 0.027$
$J/\psi K^0$	[328]	$N(B\bar{B}) = 465M$	$0.666 \pm 0.031 \pm 0.013$	$0.016 \pm 0.023 \pm 0.018$
$\psi(2S)K_s^0$	[328]	$N(B\bar{B}) = 465M$	$0.897 \pm 0.100 \pm 0.036$	$0.089 \pm 0.076 \pm 0.020$
$\chi_{c1}K_s^0$	[328]	$N(B\bar{B}) = 465M$	$0.614 \pm 0.160 \pm 0.040$	$0.129 \pm 0.109 \pm 0.025$
$\eta_c K_s^0$	[328]	$N(B\bar{B}) = 465M$	$0.925 \pm 0.160 \pm 0.057$	$0.080 \pm 0.124 \pm 0.029$
$J/\psi K^{*0}(892)$	[328]	$N(B\bar{B}) = 465M$	$0.601 \pm 0.239 \pm 0.087$	$0.025 \pm 0.083 \pm 0.054$
All	[328]	$N(B\bar{B}) = 465M$	$0.687 \pm 0.028 \pm 0.012$	$0.024 \pm 0.020 \pm 0.016$
Belle				
$J/\psi K_s^0$	[329]	$N(B\bar{B}) = 772M$	$0.670 \pm 0.029 \pm 0.013$	$0.015 \pm 0.021 {}^{+0.023}_{-0.045}$
$J/\psi K_L^0$	[329]	$N(B\bar{B}) = 772M$	$0.642 \pm 0.047 \pm 0.021$	$-0.019 \pm 0.026 {}^{+0.041}_{-0.017}$
$\psi(2S)K_s^0$	[329]	$N(B\bar{B}) = 772M$	$0.738 \pm 0.079 \pm 0.036$	$-0.104 \pm 0.055 {}^{+0.027}_{-0.047}$
$\chi_{c1}K_s^0$	[329]	$N(B\bar{B}) = 772M$	$0.640 \pm 0.117 \pm 0.040$	$0.017 \pm 0.083 {}^{+0.026}_{-0.046}$
All	[329]	$N(B\bar{B}) = 772M$	$0.667 \pm 0.023 \pm 0.012$	$-0.006 \pm 0.016 \pm 0.012$
LHCb				
$J/\psi(\rightarrow \mu^+\mu^-)K_s^0$	[330]	$\int \mathcal{L} dt = 3 \text{ fb}^{-1}$	$0.731 \pm 0.035 \pm 0.020$	$-0.038 \pm 0.032 \pm 0.005$
$J/\psi(\rightarrow e^+e^-)K_s^0$	[331]	$\int \mathcal{L} dt = 3 \text{ fb}^{-1}$	$0.83 \pm 0.08 \pm 0.01$	$0.12 \pm 0.07 \pm 0.02$
$\psi(2S)K_s^0$	[331]	$\int \mathcal{L} dt = 3 \text{ fb}^{-1}$	$0.84 \pm 0.10 \pm 0.01$	$-0.05 \pm 0.10 \pm 0.01$
Averages				
$J/\psi K_s^0$			0.695 ± 0.019	0.000 ± 0.020
$J/\psi K_L^0$			0.663 ± 0.041	-0.023 ± 0.030
$\psi(2S)K_s^0$			0.817 ± 0.056	-0.019 ± 0.048
$\chi_{c1}K_s^0$			0.632 ± 0.099	0.066 ± 0.074

This result gives a precise constraint on the $(\bar{\rho}, \bar{\eta})$ plane, as shown in Fig. 12. The measurement is in remarkable agreement with other constraints from CP -conserving quantities, and with CP violation in the kaon system, in the form of the parameter ϵ_K . Such comparisons have been performed by various phenomenological groups, such as CKMfitter [244] and UTfit [337] (see also Refs. [338, 339]).

5.4.2 Time-dependent transversity analysis of $B^0 \rightarrow J/\psi K^{*0}$ decays

B meson decays to the vector-vector final state $J/\psi K^{*0}$ are also mediated by the $b \rightarrow c\bar{s}s$ transition. When a final state that is not flavour-specific ($K^{*0} \rightarrow K_s^0\pi^0$) is used, a time-dependent transversity analysis can be performed, yielding sensitivity to both $\sin(2\beta)$ and $\cos(2\beta)$ [340]. Such analyses have been performed by both B factory experiments. In principle, the strong phases between the transversity amplitudes are not uniquely determined by such an analysis, leading to a discrete ambiguity in the sign of $\cos(2\beta)$. The *BABAR* collaboration

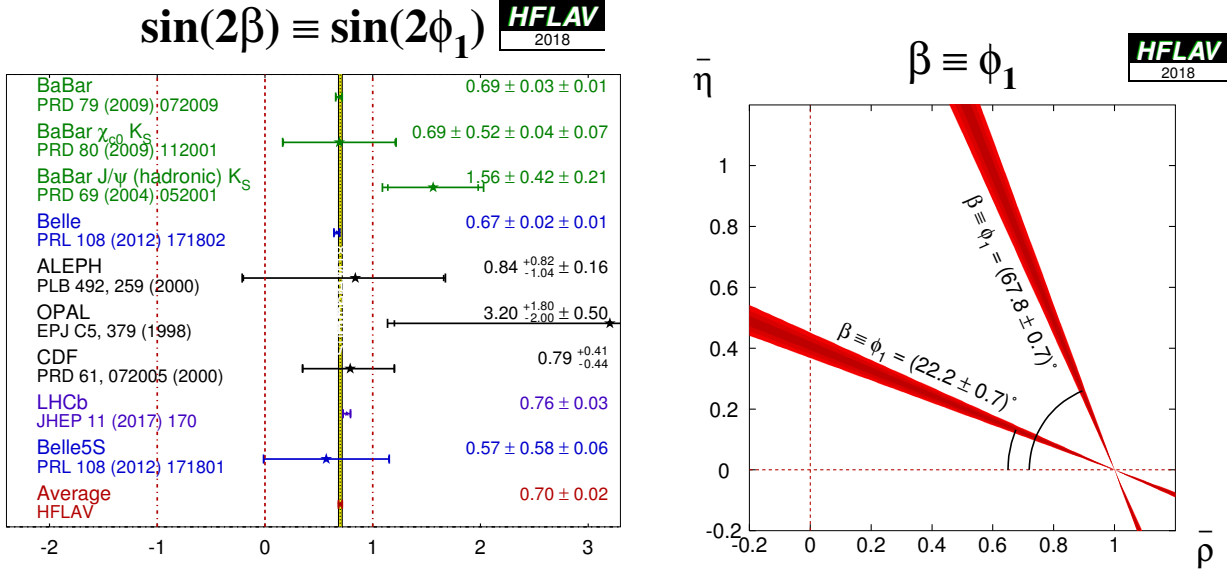


Figure 12: (Left) Average of measurements of $S_{b \rightarrow c\bar{c}s}$, interpreted as $\sin(2\beta)$. (Right) Constraints on the $(\bar{\rho}, \bar{\eta})$ plane, obtained from the average of $-\eta S_{b \rightarrow c\bar{c}s}$ and Eq. (155). Note that the solution with the smaller (larger) value of β has $\cos(2\beta) > 0$ (< 0).

resolves this ambiguity using the known variation [341] of the P-wave phase (fast) relative to that of the S-wave phase (slow) with the invariant mass of the $K\pi$ system in the vicinity of the $K^*(892)$ resonance. The result is in agreement with the prediction from s quark helicity conservation, and corresponds to Solution II defined by Suzuki [342]. We include only the solutions consistent with this phase variation in Table 28 and Fig. 13.

Table 28: Averages from $B^0 \rightarrow J/\psi K^{*0}$ transversity analyses.

Experiment	$N(B\bar{B})$	$\sin 2\beta$	$\cos 2\beta$	Correlation
BABAR [343]	88M	$-0.10 \pm 0.57 \pm 0.14$	$3.32^{+0.76}_{-0.96} \pm 0.27$	-0.37
Belle [322]	275M	$0.24 \pm 0.31 \pm 0.05$	$0.56 \pm 0.79 \pm 0.11$	0.22
Average	0.16 ± 0.28		1.64 ± 0.62	uncorrelated averages
Confidence level	0.61 (0.5 σ)		0.03 (2.2 σ)	

At present, the results are dominated by large and non-Gaussian statistical uncertainties, and exhibit significant correlations. We perform uncorrelated averages, which necessitates care in the interpretation of these averages. Nonetheless, it is clear that $\cos(2\beta) > 0$ is preferred by the experimental data in $J/\psi K^{*0}$ (for example, BABAR [343] find a confidence level for $\cos(2\beta) > 0$ of 89%).

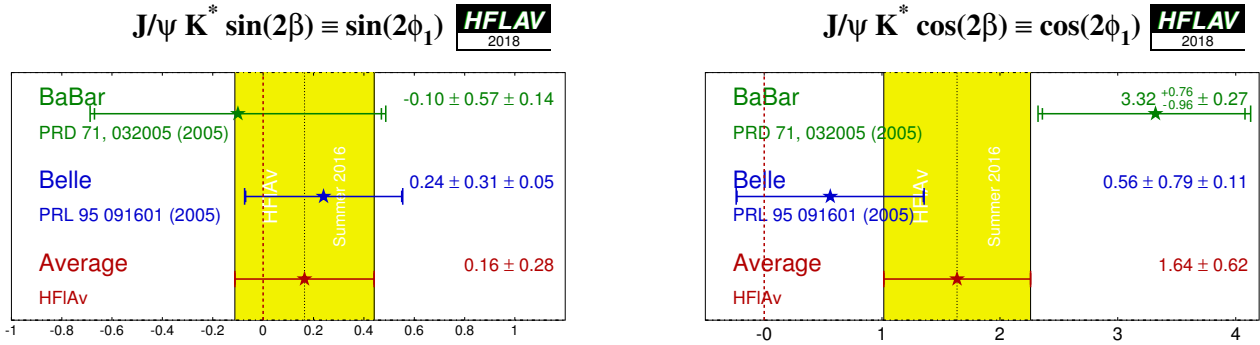


Figure 13: Averages of (left) $\sin(2\beta) \equiv \sin(2\phi_1)$ and (right) $\cos(2\beta) \equiv \cos(2\phi_1)$ from time-dependent analyses of $B^0 \rightarrow J/\psi K^{*0}$ decays.

5.4.3 Time-dependent CP asymmetries in $B^0 \rightarrow D^{*+} D^{*-} K_s^0$ decays

Both *BABAR* [260] and *Belle* [261] have performed time-dependent analyses of the $B^0 \rightarrow D^{*+} D^{*-} K_s^0$ decay, to obtain information on the sign of $\cos(2\beta)$. More information can be found in Sec. 5.2.5. The results are given in Table 29, and shown in Fig. 14.

Table 29: Results from time-dependent analysis of $B^0 \rightarrow D^{*+} D^{*-} K_s^0$.

Experiment	$N(B\bar{B})$	$\frac{J_c}{J_0}$	$\frac{2J_{s1}}{J_0} \sin(2\beta)$	$\frac{2J_{s2}}{J_0} \cos(2\beta)$
<i>BABAR</i> [260]	230M	$0.76 \pm 0.18 \pm 0.07$	$0.10 \pm 0.24 \pm 0.06$	$0.38 \pm 0.24 \pm 0.05$
<i>Belle</i> [261]	449M	$0.60^{+0.25}_{-0.28} \pm 0.08$	$-0.17 \pm 0.42 \pm 0.09$	$-0.23^{+0.43}_{-0.41} \pm 0.13$
Average		0.71 ± 0.16	0.03 ± 0.21	0.24 ± 0.22
Confidence level		$0.63 (0.5\sigma)$	$0.59 (0.5\sigma)$	$0.23 (1.2\sigma)$

From the above result and the assumption that $J_{s2} > 0$, *BABAR* infer that $\cos(2\beta) > 0$ at the 94% confidence level [260].

5.4.4 Time-dependent analysis of B_s^0 decays through the $b \rightarrow c\bar{s}$ transition

As described in Sec. 5.2.3, time-dependent analysis of decays such as $B_s^0 \rightarrow J/\psi \phi$ probes the CP violating phase of $B_s^0 - \bar{B}_s^0$ oscillations, ϕ_s .²⁷ The combination of results on $B_s^0 \rightarrow J/\psi \phi$ decays, including also results from channels such as $B_s^0 \rightarrow J/\psi \pi^+ \pi^-$ and $B_s^0 \rightarrow D_s^+ D_s^-$ decays, is discussed in Sec. 4.

²⁷ We use ϕ_s here to denote the same quantity labelled $\phi_s^{c\bar{s}}$ in Sec. 4. It should not be confused with the parameter $\phi_{12} \equiv \arg[-M_{12}/\Gamma_{12}]$, which historically was also often referred to as ϕ_s .

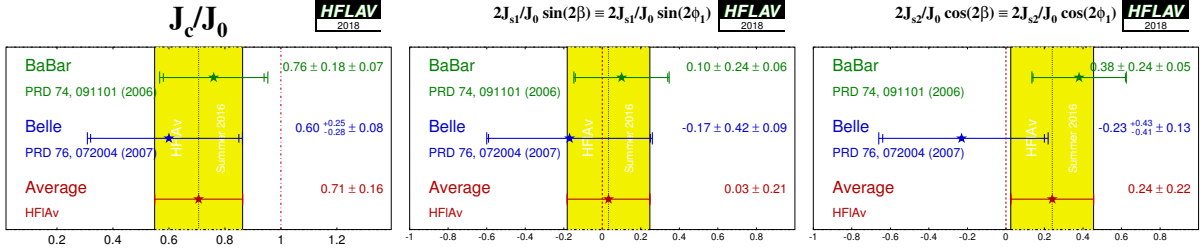


Figure 14: Averages of (left) (J_c/J_0) , (middle) $(2J_{s1}/J_0) \sin(2\beta) \equiv 2J_{s1}/J_0 \sin(2\phi_1)$ and (right) $(2J_{s2}/J_0) \cos(2\beta) \equiv 2J_{s2}/J_0 \cos(2\phi_1)$ from time-dependent analyses of $B^0 \rightarrow D^{*+} D^{*-} K_S^0$ decays.

5.5 Time-dependent CP asymmetries in colour-suppressed $b \rightarrow c\bar{u}d$ transitions

5.5.1 Time-dependent CP asymmetries: $b \rightarrow c\bar{u}d$ decays to CP eigenstates

Decays of B mesons to final states such as $D\pi^0$ are governed by $b \rightarrow c\bar{u}d$ transitions. If the final state is a CP eigenstate, *e.g.* $D_{CP}\pi^0$, the usual time-dependence formulae are recovered, with the sine coefficient sensitive to $\sin(2\beta)$. Since there is no penguin contribution to these decays, there is even less associated theoretical uncertainty than for $b \rightarrow c\bar{c}s$ decays such as $B \rightarrow J/\psi K_S^0$. Such measurements therefore allow to test the Standard Model prediction that the CP violation parameters in $b \rightarrow c\bar{u}d$ transitions are the same as those in $b \rightarrow c\bar{c}s$ [344]. Although there is an additional contribution from CKM suppressed $b \rightarrow u\bar{c}d$ amplitudes, which have a different weak phase compared to the leading $b \rightarrow c\bar{u}d$ transition, the effect is small and can be taken into account in the analysis [345, 346].

Results are available from a joint analysis of *BABAR* and *Belle* data [347]. The following CP -even final states are included: $D\pi^0$ and $D\eta$ with $D \rightarrow K_S^0\pi^0$ and $D \rightarrow K_S^0\omega$; $D\omega$ with $D \rightarrow K_S^0\pi^0$; $D^*\pi^0$ and $D^*\eta$ with $D^* \rightarrow D\pi^0$ and $D \rightarrow K^+K^-$. The following CP -odd final states are included: $D\pi^0$, $D\eta$ and $D\omega$ with $D \rightarrow K^+K^-$, $D^*\pi^0$ and $D^*\eta$ with $D^* \rightarrow D\pi^0$ and $D \rightarrow K_S^0\pi^0$. All $B^0 \rightarrow D^{(*)}h^0$ decays are analysed together, taking into account the different CP factors (denoted $D_{CP}^{(*)}h^0$). The results are summarised in Table 30.

Table 30: Results from analyses of $B^0 \rightarrow D^{(*)}h^0$, $D \rightarrow CP$ eigenstates decays.

Experiment	$N(B\bar{B})$	S_{CP}	C_{CP}	Correlation
<i>BABAR</i> & <i>Belle</i> [347]	1243M	$0.66 \pm 0.10 \pm 0.06$	$-0.02 \pm 0.07 \pm 0.03$	-0.05

5.5.2 Time-dependent Dalitz-plot analyses of $b \rightarrow c\bar{u}d$ decays

When multibody D decays, such as $D \rightarrow K_S^0\pi^+\pi^-$ are used, a time-dependent analysis of the Dalitz plot of the neutral D decay allows for a direct determination of the weak phase 2β or, equivalently, of both $\sin(2\beta)$ and $\cos(2\beta)$. This information can be used to resolve the ambiguity in the measurement of 2β from $\sin(2\beta)$ [348].

Results are available from a joint analysis of *BABAR* and *Belle* data [255, 256]. The decays $B \rightarrow D\pi^0$, $B \rightarrow D\eta$, $B \rightarrow D\omega$, $B \rightarrow D^*\pi^0$ and $B \rightarrow D^*\eta$ are used. (This collection of states is denoted by $D^{(*)}h^0$.) The daughter decays are $D^* \rightarrow D\pi^0$ and $D \rightarrow K_s^0\pi^+\pi^-$. These results supersede those from previous analyses done separately by *Belle* [253] and *BABAR* [254] and are given in Table 31. Treating β as a free parameter in the fit, the result $\beta = (22.5 \pm 4.4 \pm 1.2 \pm 0.6)^\circ$ is obtained. This corresponds to an observation of CP violation ($\beta \neq 0$) at 5.1σ significance, and evidence for $\cos(2\beta) > 0$ at 3.7σ . The ambiguous solution with $\cos(2\beta) < 0$, corresponding to the solution for $\sin(2\beta)$ from $b \rightarrow c\bar{c}s$ transitions, is ruled out at 7.3σ .

A comparison of the results for $\sin(2\beta)$ from $B^0 \rightarrow D^{(*)}h^0$ decays, with D decays to CP eigenstates or to $D \rightarrow K_s^0\pi^+\pi^-$, is shown in Fig. 15. Averaging these results gives $\sin(2\beta) = 0.71 \pm 0.09$, which is consistent with, but not as precise as, the value from $b \rightarrow c\bar{c}s$ transitions.

Table 31: Averages from $B^0 \rightarrow D^{(*)}h^0$, $D \rightarrow K_s^0\pi^+\pi^-$ analyses.

Experiment	$N(B\bar{B})$	$\sin 2\beta$	$\cos 2\beta$
Model-dependent			
<i>BABAR</i> & <i>Belle</i> [255, 256]	1240M	$0.80 \pm 0.14 \pm 0.06 \pm 0.03$	$0.91 \pm 0.22 \pm 0.09 \pm 0.07$
Model-independent			
<i>Belle</i> [257]	772M	$0.43 \pm 0.27 \pm 0.08$	$1.06 \pm 0.33^{+0.21}_{-0.15}$

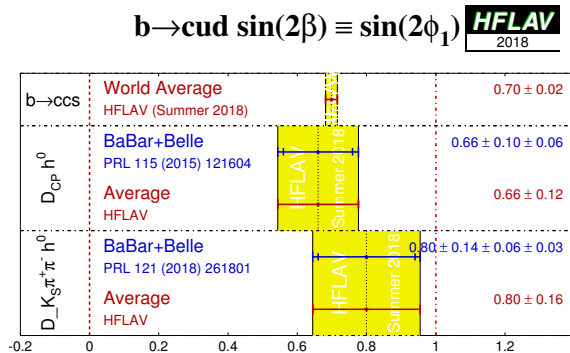


Figure 15: Averages of $\sin(2\beta)$ measured in colour-suppressed $b \rightarrow c\bar{u}d$ transitions.

A model-independent time-dependent analysis of $B^0 \rightarrow D^{(*)}h^0$ decays, with $D \rightarrow K_s^0\pi^+\pi^-$, has been performed by *Belle* [257]. The decays $B^0 \rightarrow D\pi^0$, $B^0 \rightarrow D\eta$, $B^0 \rightarrow D\eta'$, $B^0 \rightarrow D\omega$, $B^0 \rightarrow D^*\pi^0$ and $B^0 \rightarrow D^*\eta$ are used. The results are also included in Table 31. From these results, *Belle* disfavour the $\cos(2\phi_1) < 0$ solution that corresponds to the $\sin(2\phi_1)$ results from $b \rightarrow c\bar{c}s$ transitions at 5.1σ significance. The solution $\cos(2\phi_1) > 0$ solution is consistent with the data at the level of 1.3σ . Note that due to the strong statistical and systematic correlations, model-dependent results and model-independent results from the same experiment cannot be combined.

5.6 Time-dependent CP asymmetries in $b \rightarrow c\bar{c}d$ transitions

The transition $b \rightarrow c\bar{c}d$ can occur via either a $b \rightarrow c$ tree or a $b \rightarrow d$ penguin amplitude. The flavour changing neutral current $b \rightarrow d$ penguin can be mediated by any up-type quark in the loop, and hence the amplitude can be written as

$$\begin{aligned} A_{b \rightarrow d} &= F_u V_{ub} V_{ud}^* + F_c V_{cb} V_{cd}^* + F_t V_{tb} V_{td}^* \\ &= (F_u - F_c) V_{ub} V_{ud}^* + (F_t - F_c) V_{tb} V_{td}^*, \end{aligned} \quad (156)$$

where $F_{u,c,t}$ describe all factors, except CKM suppression, in each quark loop diagram. In the last line, both terms are $\mathcal{O}(\lambda^3)$, exposing that the $b \rightarrow d$ penguin amplitude contains terms with different weak phases at the same order of CKM suppression.

In Eq. (156), we have chosen to eliminate the F_c term using unitarity. However, we could equally well write

$$\begin{aligned} A_{b \rightarrow d} &= (F_u - F_t) V_{ub} V_{ud}^* + (F_c - F_t) V_{cb} V_{cd}^* \\ &= (F_c - F_u) V_{cb} V_{cd}^* + (F_t - F_u) V_{tb} V_{td}^*. \end{aligned} \quad (157)$$

Since the $b \rightarrow c\bar{c}d$ tree amplitude has the weak phase of $V_{cb} V_{cd}^*$, either of the above expressions allows the penguin amplitude to be decomposed into a part with the same weak phase as the tree amplitude and a part with another weak phase, which can be chosen to be either β or γ . The choice of parametrisation cannot, of course, affect the physics [349]. In any case, if the tree amplitude dominates, there is little sensitivity to any phase other than that from $B^0 - \bar{B}^0$ mixing.

The $b \rightarrow c\bar{c}d$ transitions can be investigated with studies of various different final states. Results are available from both *BABAR* and *Belle* using the final states $J/\psi \pi^0$, $D^+ D^-$, $D^{*+} D^{*-}$ and $D^{*\pm} D^\mp$, and from *LHCb* using the final states $J/\psi \rho^0$ and $D^+ D^-$; the averages of these results are given in Tables 32 and 33. The results using the CP -even modes $J/\psi \pi^0$ and $D^+ D^-$ are shown in Fig. 16 and Fig. 17 respectively, with two-dimensional constraints shown in Fig. 18.

Table 32: Averages for the $b \rightarrow c\bar{c}d$ modes, $B^0 \rightarrow J/\psi \pi^0$ and $D^+ D^-$.

Experiment		Sample size	S_{CP}	C_{CP}	Correlation
$J/\psi \pi^0$					
<i>BABAR</i>	[350]	$N(B\bar{B}) = 466M$	$-1.23 \pm 0.21 \pm 0.04$	$-0.20 \pm 0.19 \pm 0.03$	0.20
<i>Belle</i>	[351]	$N(B\bar{B}) = 772M$	$-0.59 \pm 0.19 \pm 0.03$	$0.15 \pm 0.14^{+0.03}_{-0.04}$	0.01
Average			-0.86 ± 0.14	0.04 ± 0.12	0.08
Confidence level			0.04 (2.0 σ)		
$D^+ D^-$					
<i>BABAR</i>	[252]	$N(B\bar{B}) = 467M$	$-0.65 \pm 0.36 \pm 0.05$	$-0.07 \pm 0.23 \pm 0.03$	-0.01
<i>Belle</i>	[282]	$N(B\bar{B}) = 772M$	$-1.06^{+0.21}_{-0.14} \pm 0.08$	$-0.43 \pm 0.16 \pm 0.05$	-0.12
<i>LHCb</i>	[352]	$\int \mathcal{L} dt = 3 \text{ fb}^{-1}$	$-0.54^{+0.17}_{-0.16} \pm 0.05$	$0.26^{+0.18}_{-0.17} \pm 0.02$	0.48
Average			-0.84 ± 0.12	-0.13 ± 0.10	0.18
Confidence level			0.027 (2.2 σ)		

Table 33: Averages for the $b \rightarrow c\bar{c}d$ modes, $J/\psi \rho^0$, $D^{*+}D^{*-}$ and $D^{*\pm}D^\mp$.

Experiment	$N(B\bar{B})$	S_{CP}	C_{CP}	R_\perp
LHCb	[251]	3 fb^{-1}	$J/\psi \rho^0$	
		$-0.66^{+0.13}_{-0.12}{}^{+0.09}_{-0.03}$	$-0.06 \pm 0.06^{+0.02}_{-0.01}$	0.198 ± 0.017
		$D^{*+}D^{*-}$		
BABAR	[252]	467M	$-0.70 \pm 0.16 \pm 0.03$	$0.05 \pm 0.09 \pm 0.02$
BABAR part. rec.	[353]	471M	$-0.49 \pm 0.18 \pm 0.07 \pm 0.04$	$0.15 \pm 0.09 \pm 0.04$
Belle	[354]	772M	$-0.79 \pm 0.13 \pm 0.03$	$-0.15 \pm 0.08 \pm 0.02$
Average		-0.71 ± 0.09	-0.01 ± 0.05	$0.14 \pm 0.02 \pm 0.01$
Confidence level			$0.72 (0.4\sigma)$	0.15 ± 0.02
Experiment	$N(B\bar{B})$	S_{CP+}	C_{CP+}	R_\perp
		$D^{*+}D^{*-}$	S_{CP-}	
BABAR	[252]	467M	$-0.76 \pm 0.16 \pm 0.04$	$0.02 \pm 0.12 \pm 0.02$
			$-1.81 \pm 0.71 \pm 0.16$	$0.41 \pm 0.50 \pm 0.08$
				0.15 ± 0.03
Experiment	$N(B\bar{B})$	S	C	ΔS
			$D^{*\pm}D^\mp$	ΔC
BABAR	[252]	467M	$-0.68 \pm 0.15 \pm 0.04$	$0.04 \pm 0.12 \pm 0.03$
Belle	[282]	772M	$-0.78 \pm 0.15 \pm 0.05$	$-0.01 \pm 0.11 \pm 0.04$
Average		-0.73 ± 0.11	0.01 ± 0.09	-0.04 ± 0.11
Confidence level		$0.65 (0.5\sigma)$	$0.77 (0.3\sigma)$	$0.41 (0.8\sigma)$
				$0.63 (0.5\sigma)$
				$0.48 (0.7\sigma)$

Results for the vector-vector mode $J/\psi \rho^0$ are obtained from a full time-dependent amplitude analysis of $B^0 \rightarrow J/\psi \pi^+ \pi^-$ decays. LHCb [251] find a $J/\psi \rho^0$ fit fraction of $65.6 \pm 1.9\%$ and a longitudinal polarisation fraction of $56.7 \pm 1.8\%$ (uncertainties are statistical only; both results are consistent with those from a time-integrated amplitude analysis [262] where systematic uncertainties were also evaluated). Fits are performed to obtain $2\beta_s^{\text{eff}}$ in the cases that all transversity amplitudes are assumed to have the same CP violation parameter. A separate fit is performed allowing different parameters. The results in the former case are presented in terms of S_{CP} and C_{CP} in Table 33.

The vector-vector mode $D^{*+} D^{*-}$ is found to be dominated by the CP -even, longitudinally polarised component. *BABAR* measures a CP -odd fraction of $0.158 \pm 0.028 \pm 0.006$ [252], and Belle measures $0.138 \pm 0.024 \pm 0.006$ [354]. These values are listed as R_\perp in Table 33, and are included in the averages so that correlations are taken into account.²⁸ *BABAR* has also performed an additional fit in which the CP -even and CP -odd components have independent pairs of CP violation parameters S and C . These results are included in Table 33. Results using $D^{*+} D^{*-}$ are shown in Fig. 19.

As discussed in Sec. 5.2.6, the most recent papers on the non- CP eigenstate mode $D^{*\pm} D^\mp$ use the $(A, S, \Delta S, C, \Delta C)$ set of parameters. Therefore, we perform the averages with this choice, with results presented in Table 33.

In the absence of the penguin contribution (so-called tree dominance), the time-dependent parameters are given by $S_{b \rightarrow c\bar{c}d} = -\eta \sin(2\beta)$, $C_{b \rightarrow c\bar{c}d} = 0$, $S_{+-} = \sin(2\beta + \delta)$, $S_{-+} = \sin(2\beta - \delta)$, $C_{+-} = -C_{-+}$ and $A = 0$, where δ is the strong phase difference between the $D^{*+} D^-$ and $D^{*-} D^+$ decay amplitudes. In the presence of the penguin contribution, there is no straightforward interpretation in terms of CKM parameters; however, CP violation in decay may be observed through any of $C_{b \rightarrow c\bar{c}d} \neq 0$, $C_{+-} \neq -C_{-+}$ or $A_{+-} \neq 0$.

The averages for the $b \rightarrow c\bar{c}d$ modes are shown in Figs. 20 and 21. Results are consistent with tree dominance and with the Standard Model, although the Belle results in $B^0 \rightarrow D^+ D^-$ [355] show an indication of CP violation in decay, and hence a non-zero penguin contribution. The average of $S_{b \rightarrow c\bar{c}d}$ in each of the $J/\psi \pi^0$, $D^+ D^-$ and $D^{*+} D^{*-}$ final states is more than 5σ away from zero, corresponding to observations of CP violation in these decay channels. Possible non-Gaussian effects due to some of the input measurements being outside the physical region ($S_{CP}^2 + C_{CP}^2 \leq 1$) should, however, be borne in mind.

5.6.1 Time-dependent CP asymmetries in B_s^0 decays mediated by $b \rightarrow c\bar{c}d$ transitions

Time-dependent CP asymmetries in B_s^0 decays mediated by $b \rightarrow c\bar{c}d$ transitions provide a determination of $2\beta_s^{\text{eff}}$, where possible effects from penguin amplitudes may cause a shift from the value of $2\beta_s$ seen in $b \rightarrow c\bar{c}s$ transitions. Results in the $b \rightarrow c\bar{c}d$ case, with larger penguin effects, can be used together with flavour symmetries to derive limits on the possible size of penguin effects in the $b \rightarrow c\bar{c}s$ transitions [356, 357].

The parameters have been measured in $B_s^0 \rightarrow J/\psi K_s^0$ decays by LHCb, as summarised in Table 34. The results supersede an earlier measurement of the effective lifetime, which is directly related to $A^{\Delta\Gamma}$, in the same mode [132].

²⁸ Note that the *BABAR* value given in Table 33 differs from the value quoted here, since that in the table is not corrected for efficiency.

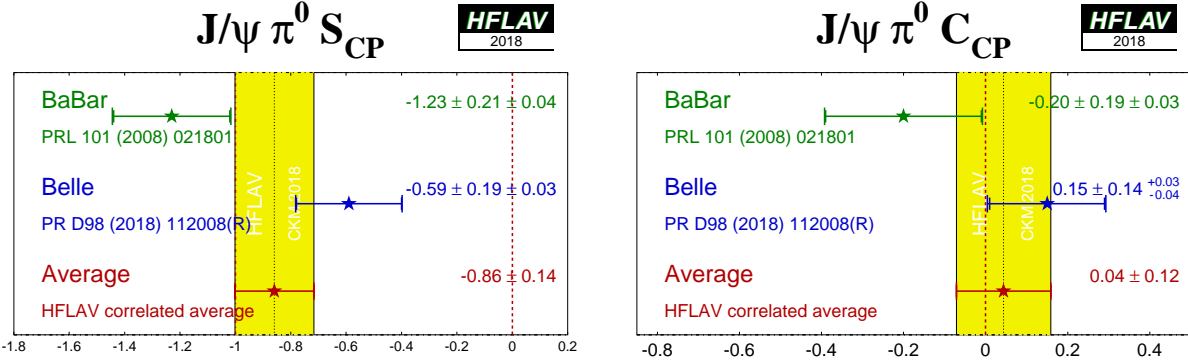


Figure 16: Averages of (left) $S_{b \rightarrow c\bar{c}d}$ and (right) $C_{b \rightarrow c\bar{c}d}$ for the mode $B^0 \rightarrow J/\psi \pi^0$.

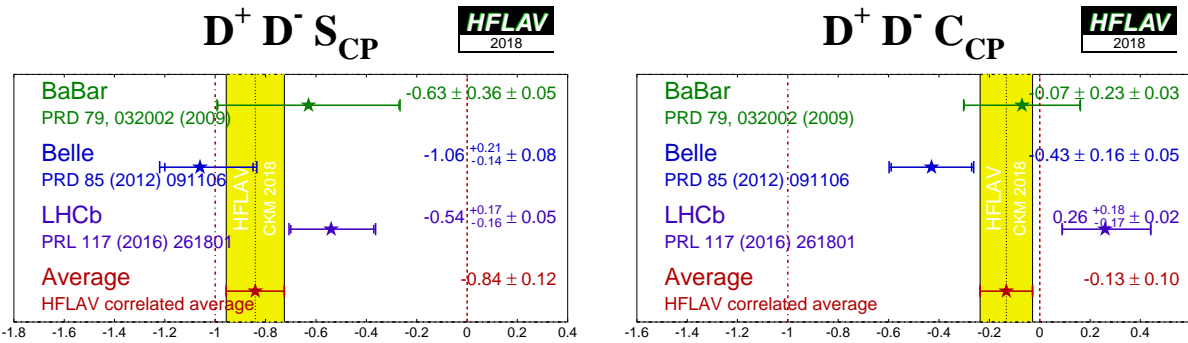


Figure 17: Averages of (left) $S_{b \rightarrow c\bar{c}d}$ and (right) $C_{b \rightarrow c\bar{c}d}$ for the mode $B^0 \rightarrow D^+ D^-$.

Table 34: Measurements of CP violation parameters from $B_s^0 \rightarrow J/\psi K_s^0$.

Experiment	$\int \mathcal{L} dt$	S_{CP}	C_{CP}	$A^{\Delta\Gamma}$
LHCb [358]	3 fb^{-1}	$0.49^{+0.77}_{-0.65} \pm 0.06$	$-0.28 \pm 0.41 \pm 0.08$	$-0.08 \pm 0.40 \pm 0.08$

5.7 Time-dependent CP asymmetries in charmless $b \rightarrow q\bar{q}s$ transitions

Similarly to Eq. (156), the $b \rightarrow s$ penguin amplitude can be written as

$$\begin{aligned} A_{b \rightarrow s} &= F_u V_{ub} V_{us}^* + F_c V_{cb} V_{cs}^* + F_t V_{tb} V_{ts}^* \\ &= (F_u - F_c) V_{ub} V_{us}^* + (F_t - F_c) V_{tb} V_{ts}^*, \end{aligned} \quad (158)$$

using the unitarity of the CKM matrix to eliminate the F_c term. In this case, the first term in the last line is $\mathcal{O}(\lambda^4)$ while the second is $\mathcal{O}(\lambda^2)$. Therefore, in the Standard Model, this amplitude is dominated by $V_{tb} V_{ts}^*$, and to within a few degrees ($|\delta\beta^{\text{eff}}| \equiv |\beta^{\text{eff}} - \beta| \lesssim 2^\circ$ for

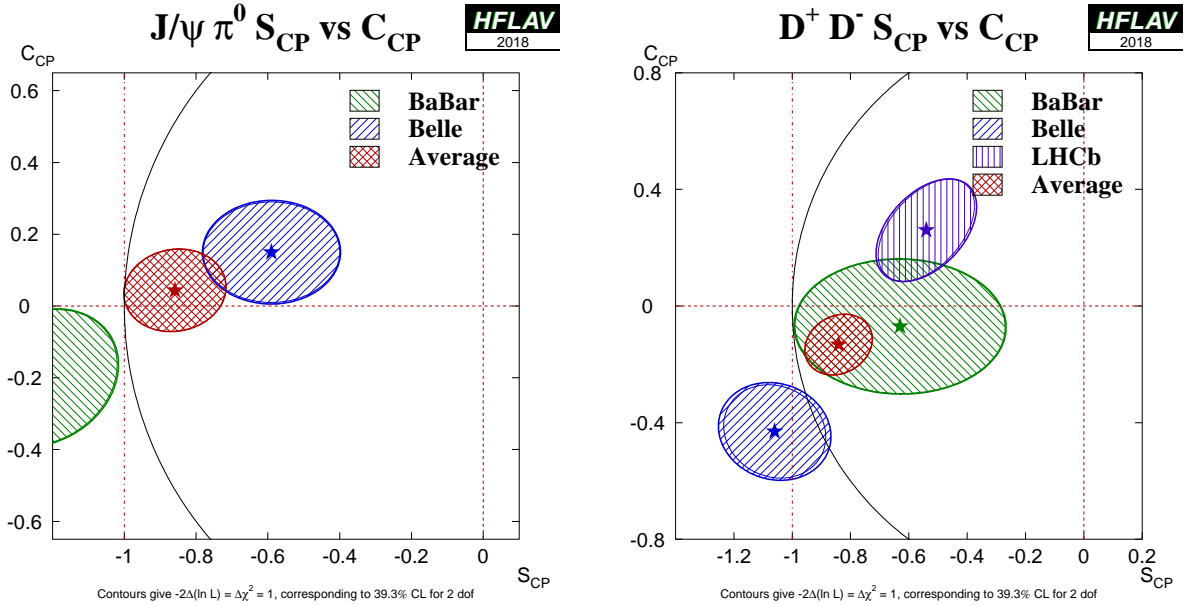


Figure 18: Averages of two $b \rightarrow c\bar{c}d$ dominated channels, for which correlated averages are performed, in the S_{CP} vs. C_{CP} plane. (Left) $B^0 \rightarrow J/\psi\pi^0$ and (right) $B^0 \rightarrow D^+D^-$.

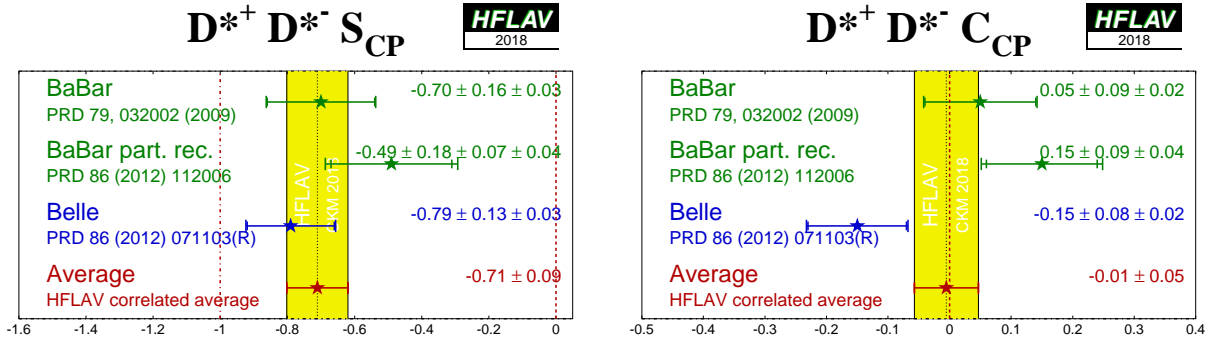


Figure 19: Averages of (left) $S_{b \rightarrow c\bar{c}d}$ and (right) $C_{b \rightarrow c\bar{c}d}$ for the mode $B^0 \rightarrow D^{*+}D^{*-}$.

$\beta \approx 20^\circ$) the time-dependent parameters can be written as²⁹ $S_{b \rightarrow q\bar{q}s} \approx -\eta \sin(2\beta)$, $C_{b \rightarrow q\bar{q}s} \approx 0$, assuming $b \rightarrow s$ penguin contributions only ($q = u, d, s$).

Due to the suppression of the Standard Model amplitude, contributions of additional diagrams from physics beyond the Standard Model, with heavy virtual particles in the penguin loops, may have observable effects. In general, these contributions will affect the values of $S_{b \rightarrow c\bar{c}s}$ and $C_{b \rightarrow q\bar{q}s}$. A discrepancy between the values of $S_{b \rightarrow c\bar{c}s}$ and $S_{b \rightarrow q\bar{q}s}$ can therefore provide a solid indication of non-Standard Model physics [344, 359–361].

However, there is an additional consideration to take into account. The above argument

²⁹ The presence of a small ($\mathcal{O}(\lambda^2)$) weak phase in the dominant amplitude of the s penguin decays introduces a phase shift given by $S_{b \rightarrow q\bar{q}s} = -\eta \sin(2\beta)(1 + \Delta)$. Using the CKMfitter results for the Wolfenstein parameters [244], one finds $\Delta \simeq 0.033$, which corresponds to a shift of 2β of $+2.1^\circ$. Nonperturbative contributions can alter this result.

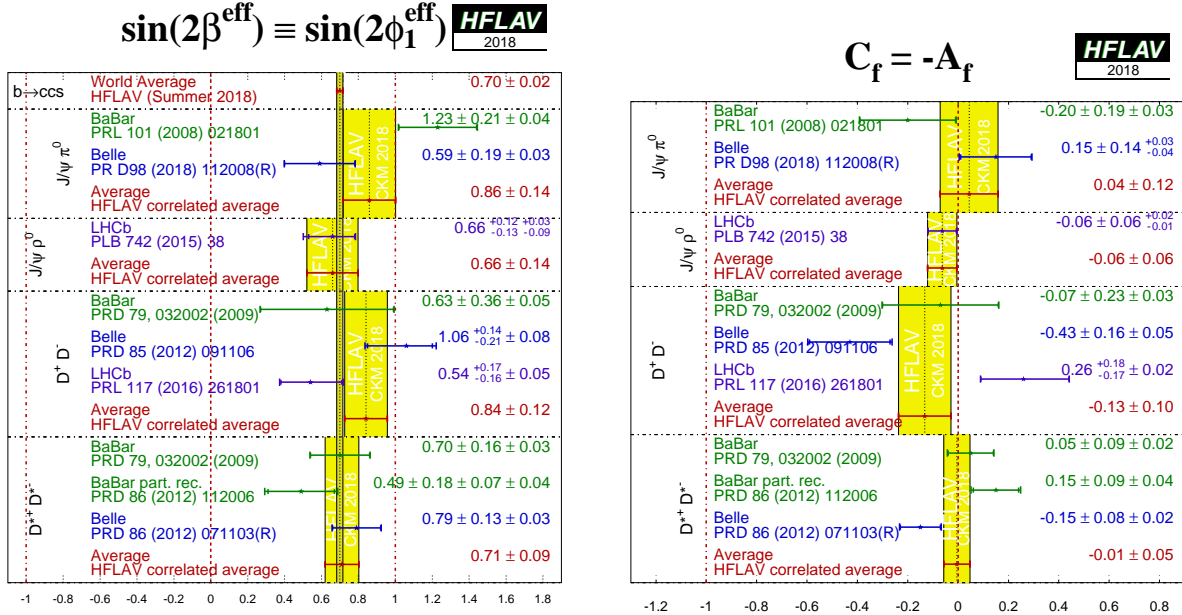


Figure 20: Averages of (left) $-\eta S_{b \rightarrow c\bar{c}s}$ interpreted as $\sin(2\beta^{\text{eff}})$ and (right) $C_{b \rightarrow c\bar{c}s}$. The $-\eta S_{b \rightarrow c\bar{c}s}$ figure compares the results to the world average for $-\eta S_{b \rightarrow c\bar{c}s}$ (see Sec. 5.4.1).

assumes that only the $b \rightarrow s$ penguin contributes to the $b \rightarrow q\bar{q}s$ transition. For $q = s$ this is a good assumption, which neglects only rescattering effects. However, for $q = u$ there is a colour-suppressed $b \rightarrow u$ tree diagram (of order $\mathcal{O}(\lambda^4)$), which has a different weak (and possibly strong) phase. In the case $q = d$, any light neutral meson that is formed from $d\bar{d}$ also has a $u\bar{u}$ component, and so again there is ‘‘tree pollution’’. The B^0 decays to $\pi^0 K_s^0$, $\rho^0 K_s^0$ and ωK_s^0 belong to this category. The mesons ϕ , f_0 and η' are expected to have predominant $s\bar{s}$ composition, which reduces the relative size of the possible tree pollution. If the inclusive decay $B^0 \rightarrow K^+ K^- K^0$ (excluding ϕK^0) is dominated by a nonresonant three-body transition, an Okubo-Zweig-Iizuka-suppressed [362–364] tree-level diagram can occur through insertion of an $s\bar{s}$ pair. The corresponding penguin-type transition proceeds via insertion of a $u\bar{u}$ pair, which is expected to be favoured over the $s\bar{s}$ insertion by fragmentation models. Neglecting rescattering, the final state $K^0 \bar{K}^0 K^0$ (reconstructed as $K_s^0 K_s^0 K_s^0$) has no tree pollution [365]. Various estimates, using different theoretical approaches, of the values of $\Delta S = S_{b \rightarrow q\bar{q}s} - S_{b \rightarrow c\bar{c}s}$ exist in the literature [366–379]. In general, there is agreement that the modes ϕK^0 , $\eta' K^0$ and $K^0 \bar{K}^0 K^0$ are the cleanest, with values of $|\Delta S|$ at or below the few percent level, with ΔS usually predicted to be positive. Nonetheless, the uncertainty is sufficient that interpretation is given here in terms of $\sin(2\beta^{\text{eff}})$.

5.7.1 Time-dependent \mathcal{CP} asymmetries: $b \rightarrow q\bar{q}s$ decays to \mathcal{CP} eigenstates

The averages for $-\eta S_{b \rightarrow q\bar{q}s}$ and $C_{b \rightarrow q\bar{q}s}$ can be found in Tables 35 and 36, and are shown in Figs. 22, 23 and 24. Results from both *BABAR* and *Belle* are averaged for the modes $\eta' K^0$

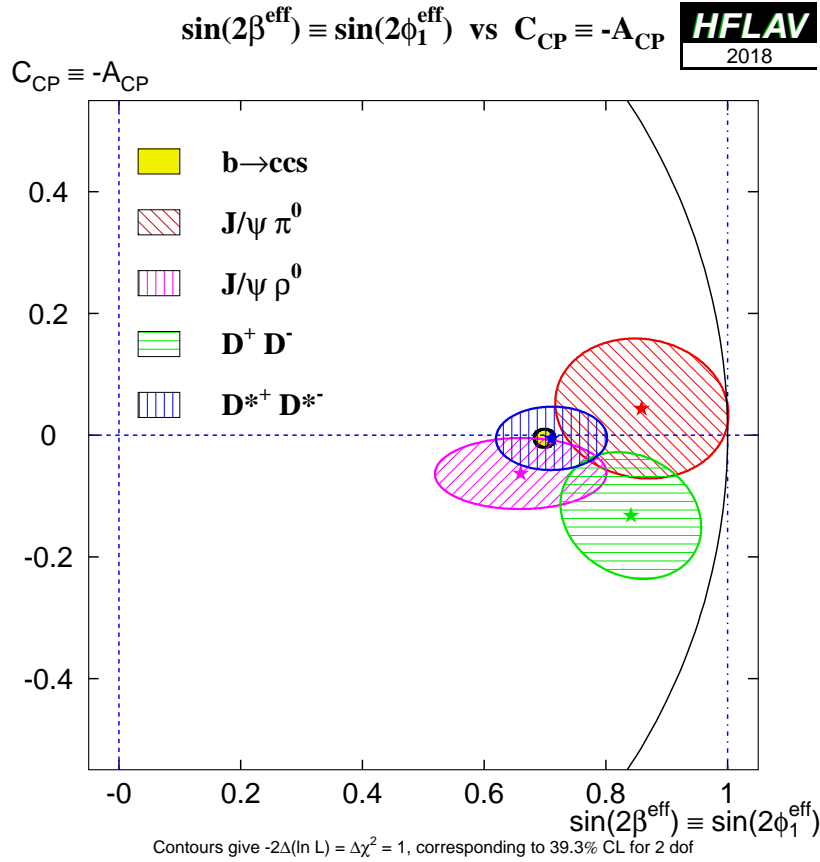


Figure 21: Compilation of constraints in the $-\eta S_{b \rightarrow c\bar{c}d}$, interpreted as $\sin(2\beta^{\text{eff}})$, vs. $C_{b \rightarrow c\bar{c}d}$ plane.

(K^0 indicates that both K_s^0 and K_L^0 are used) $K_s^0 K_s^0 K_s^0$, $\pi^0 K_s^0$ and ωK_s^0 .³⁰ Results on ϕK_s^0 and $K^+ K^- K_s^0$ (implicitly excluding ϕK_s^0 and $f_0 K_s^0$) are taken from time-dependent Dalitz plot analyses of $K^+ K^- K_s^0$; results on $\rho^0 K_s^0$, $f_2 K_s^0$, $f_X K_s^0$ and $\pi^+ \pi^- K_s^0$ nonresonant are taken from time-dependent Dalitz-plot analyses of $\pi^+ \pi^- K_s^0$ (see Sec. 5.7.2).³¹ The results on $f_0 K_s^0$ are from combinations of both Dalitz plot analyses. *BABAR* has also presented results with the final states $\pi^0 \pi^0 K_s^0$ and $\phi K_s^0 \pi^0$.

Of these final states, ϕK_s^0 , $\eta' K_s^0$, $\pi^0 K_s^0$, $\rho^0 K_s^0$, ωK_s^0 and $f_0 K_L^0$ have CP eigenvalue $\eta = -1$, while ϕK_L^0 , $\eta' K_L^0$, $K_s^0 K_s^0 K_s^0$, $f_0 K_s^0$, $f_2 K_s^0$, $f_X K_s^0$, $\pi^0 \pi^0 K_s^0$ and $\pi^+ \pi^- K_s^0$ nonresonant have $\eta = +1$. The final state $K^+ K^- K_s^0$ (with ϕK_s^0 and $f_0 K_s^0$ implicitly excluded) is not a CP eigenstate, but the CP content can be absorbed in the amplitude analysis to allow the determination of a single effective S parameter. (In earlier analyses of the $K^+ K^- K^0$ final state, its CP composition was determined using an isospin argument [381] and a moments analysis [382].)

The final state $\phi K_s^0 \pi^0$ is also not a CP eigenstate but its CP -composition can be deter-

³⁰ Belle [380] include the $\pi^0 K_L^0$ final state together with $\pi^0 K_s^0$ in order to improve the constraint on the parameter of CP violation in decay; these events cannot be used for time-dependent analysis.

³¹ Throughout this section, $f_0 \equiv f_0(980)$ and $f_2 \equiv f_2(1270)$. Details of the assumed lineshapes of these states, and of the f_X (which is taken to have even spin), can be found in the relevant experimental papers [265, 266, 269, 270].

Table 35: Averages of $-\eta S_{b \rightarrow q\bar{q}s}$ and $C_{b \rightarrow q\bar{q}s}$. Where a third source of uncertainty is given, it is due to model uncertainties arising in Dalitz plot analyses.

Experiment		$N(B\bar{B})$	$-\eta S_{b \rightarrow q\bar{q}s}$	$C_{b \rightarrow q\bar{q}s}$	Correlation
ϕK^0					
BABAR	[266]	470M	$0.66 \pm 0.17 \pm 0.07$	$0.05 \pm 0.18 \pm 0.05$	–
Belle	[265]	657M	$0.90^{+0.09}_{-0.19}$	$-0.04 \pm 0.20 \pm 0.10 \pm 0.02$	–
Average			$0.74^{+0.11}_{-0.13}$	0.01 ± 0.14	uncorrelated averages
$\eta' K^0$					
BABAR	[383]	467M	$0.57 \pm 0.08 \pm 0.02$	$-0.08 \pm 0.06 \pm 0.02$	0.03
Belle	[384]	772M	$0.68 \pm 0.07 \pm 0.03$	$-0.03 \pm 0.05 \pm 0.03$	0.03
Average			0.63 ± 0.06	-0.05 ± 0.04	0.02
Confidence level			$0.53 (0.6\sigma)$		
$K_S^0 K_S^0 K_S^0$					
BABAR	[385]	468M	$0.94^{+0.21}_{-0.24} \pm 0.06$	$-0.17 \pm 0.18 \pm 0.04$	0.16
Belle	[386]	535M	$0.30 \pm 0.32 \pm 0.08$	$-0.31 \pm 0.20 \pm 0.07$	–
Average			0.72 ± 0.19	-0.24 ± 0.14	0.09
Confidence level			$0.26 (1.1\sigma)$		
$\pi^0 K^0$					
BABAR	[383]	467M	$0.55 \pm 0.20 \pm 0.03$	$0.13 \pm 0.13 \pm 0.03$	0.06
Belle	[380]	657M	$0.67 \pm 0.31 \pm 0.08$	$-0.14 \pm 0.13 \pm 0.06$	–0.04
Average			0.57 ± 0.17	0.01 ± 0.10	0.02
Confidence level			$0.37 (0.9\sigma)$		
$\rho^0 K_S^0$					
BABAR	[269]	383M	$0.35^{+0.26}_{-0.31} \pm 0.06 \pm 0.03$	$-0.05 \pm 0.26 \pm 0.10 \pm 0.03$	–
Belle	[270]	657M	$0.64^{+0.19}_{-0.25} \pm 0.09 \pm 0.10$	$-0.03^{+0.24}_{-0.23} \pm 0.11 \pm 0.10$	–
Average			$0.54^{+0.18}_{-0.21}$	-0.06 ± 0.20	uncorrelated averages
ωK_S^0					
BABAR	[383]	467M	$0.55^{+0.26}_{-0.29} \pm 0.02$	$-0.52^{+0.22}_{-0.20} \pm 0.03$	0.03
Belle	[387]	772M	$0.91 \pm 0.32 \pm 0.05$	$0.36 \pm 0.19 \pm 0.05$	–0.00
Average			0.71 ± 0.21	-0.04 ± 0.14	0.01
Confidence level			$0.007 (2.7\sigma)$		
$f_0 K^0$					
BABAR	[266, 269]	–	$0.74^{+0.12}_{-0.15}$	0.15 ± 0.16	–
Belle	[265, 270]	–	$0.63^{+0.16}_{-0.19}$	0.13 ± 0.17	–
Average			$0.69^{+0.10}_{-0.12}$	0.14 ± 0.12	uncorrelated averages
$f_2 K_S^0$					
BABAR	[269]	383M	$0.48 \pm 0.52 \pm 0.06 \pm 0.10$	$0.28^{+0.35}_{-0.40} \pm 0.08 \pm 0.07$	–
$f_X K_S^0$					
BABAR	[269]	383M	$0.20 \pm 0.52 \pm 0.07 \pm 0.07$	$0.13^{+0.33}_{-0.35} \pm 0.04 \pm 0.09$	–

mined from an angular analysis. Since the parameters are common to the $B^0 \rightarrow \phi K_S^0 \pi^0$ and $B^0 \rightarrow \phi K^+ \pi^-$ decays (because only $K\pi$ resonances contribute), *BABAR* perform a simultaneous analysis of the two final states [390] (see Sec. 5.7.3).

It must be noted that Q2B parameters extracted from Dalitz-plot analyses are constrained to lie within the physical boundary ($S_{CP}^2 + C_{CP}^2 < 1$). Consequently, the obtained uncertainties are highly non-Gaussian when the central value is close to the boundary. This is particularly

Table 36: Averages of $-\eta S_{b \rightarrow q\bar{q}s}$ and $C_{b \rightarrow q\bar{q}s}$ (continued). Where a third source of uncertainty is given, it is due to model uncertainties arising in Dalitz plot analyses.

Experiment	$N(B\bar{B})$	$-\eta S_{b \rightarrow q\bar{q}s}$	$C_{b \rightarrow q\bar{q}s}$	Correlation
		$\pi^0 \pi^0 K_s^0$		
BABAR [388]	227M	$-0.72 \pm 0.71 \pm 0.08$	$0.23 \pm 0.52 \pm 0.13$	-0.02
Belle [389]	772M	$0.92^{+0.27}_{-0.31} \pm 0.11$	$-0.28 \pm 0.21 \pm 0.04$	0.00
Average		0.66 ± 0.28	-0.21 ± 0.20	0.00
Confidence level		0.08 (1.8 σ)		
		$\phi K_s^0 \pi^0$		
BABAR [390]	465M	$0.97^{+0.03}_{-0.52}$	$-0.20 \pm 0.14 \pm 0.06$	-
		$\pi^+ \pi^- K_s^0$ nonresonant		
BABAR [269]	383M	$0.01 \pm 0.31 \pm 0.05 \pm 0.09$	$0.01 \pm 0.25 \pm 0.06 \pm 0.05$	-
		$K^+ K^- K^0$		
BABAR [266]	470M	$0.65 \pm 0.12 \pm 0.03$	$0.02 \pm 0.09 \pm 0.03$	-
Belle [265]	657M	$0.76^{+0.14}_{-0.18}$	$0.14 \pm 0.11 \pm 0.08 \pm 0.03$	-
Average		$0.68^{+0.09}_{-0.10}$	0.06 ± 0.08	uncorrelated averages

evident in the *BABAR* results for $B^0 \rightarrow f_0 K^0$ with $f_0 \rightarrow \pi^+ \pi^-$ [269]. These results must be treated with caution.

As explained above, each of the modes listed in Tables 35 and 36 has potentially different subleading contributions within the Standard Model, and thus each may have a different value of $-\eta S_{b \rightarrow q\bar{q}s}$. Therefore, there is no strong motivation to make a combined average over the different modes. We refer to such an average as a “naïve s -penguin average.” It is naïve not only because the theoretical uncertainties are neglected, but also since possible correlations of systematic effects between different modes are not included. In spite of these caveats, there remains interest in the value of this quantity and therefore it is given here: $\langle -\eta S_{b \rightarrow q\bar{q}s} \rangle = 0.648 \pm 0.038$, with confidence level 0.63 (0.5 σ). This value is in agreement with the average $-\eta S_{b \rightarrow c\bar{c}s}$ given in Sec. 5.4.1. The average for $C_{b \rightarrow q\bar{q}s}$ is $\langle C_{b \rightarrow q\bar{q}s} \rangle = -0.003 \pm 0.029$ with a confidence level of 0.43 (0.8 σ).

From Table 35 it may be noted that the averages for $-\eta S_{b \rightarrow q\bar{q}s}$ in ϕK_s^0 , $\eta' K^0$, $f_0 K_s^0$ and $K^+ K^- K_s^0$ are all now more than 5 σ away from zero, so that CP violation in these modes can be considered well established. There is no evidence (above 2 σ) for CP violation in decay in any of these $b \rightarrow q\bar{q}s$ transitions.

5.7.2 Time-dependent Dalitz plot analyses: $B^0 \rightarrow K^+ K^- K^0$ and $B^0 \rightarrow \pi^+ \pi^- K_s^0$

As mentioned in Sec. 5.2.5 and above, both *BABAR* and Belle have performed time-dependent Dalitz plot analysis of $B^0 \rightarrow K^+ K^- K^0$ and $B^0 \rightarrow \pi^+ \pi^- K_s^0$ decays. The results are summarised in Tables 37 and 38. Averages for the $B^0 \rightarrow f_0 K_s^0$ decay, which contributes to both Dalitz plots, are shown in Fig. 25. Results are presented in terms of the effective weak phase (from mixing and decay) difference β^{eff} and the parameter of CP violation in decay \mathcal{A} ($\mathcal{A} = -C$) for each of the resonant contributions. Note that Dalitz-plot analyses, including all those included in



Figure 22: (Top) Averages of (left) $-\eta S_{b \rightarrow q\bar{q}s}$, interpreted as $\sin(2\beta^{\text{eff}}$ and (right) $C_{b \rightarrow q\bar{q}s}$. The $-\eta S_{b \rightarrow q\bar{q}s}$ figure compares the results to the world average for $-\eta S_{b \rightarrow c\bar{c}s}$ (see Sec. 5.4.1). (Bottom) Same, but only averages for each mode are shown. More figures are available from the HFLAV web pages.

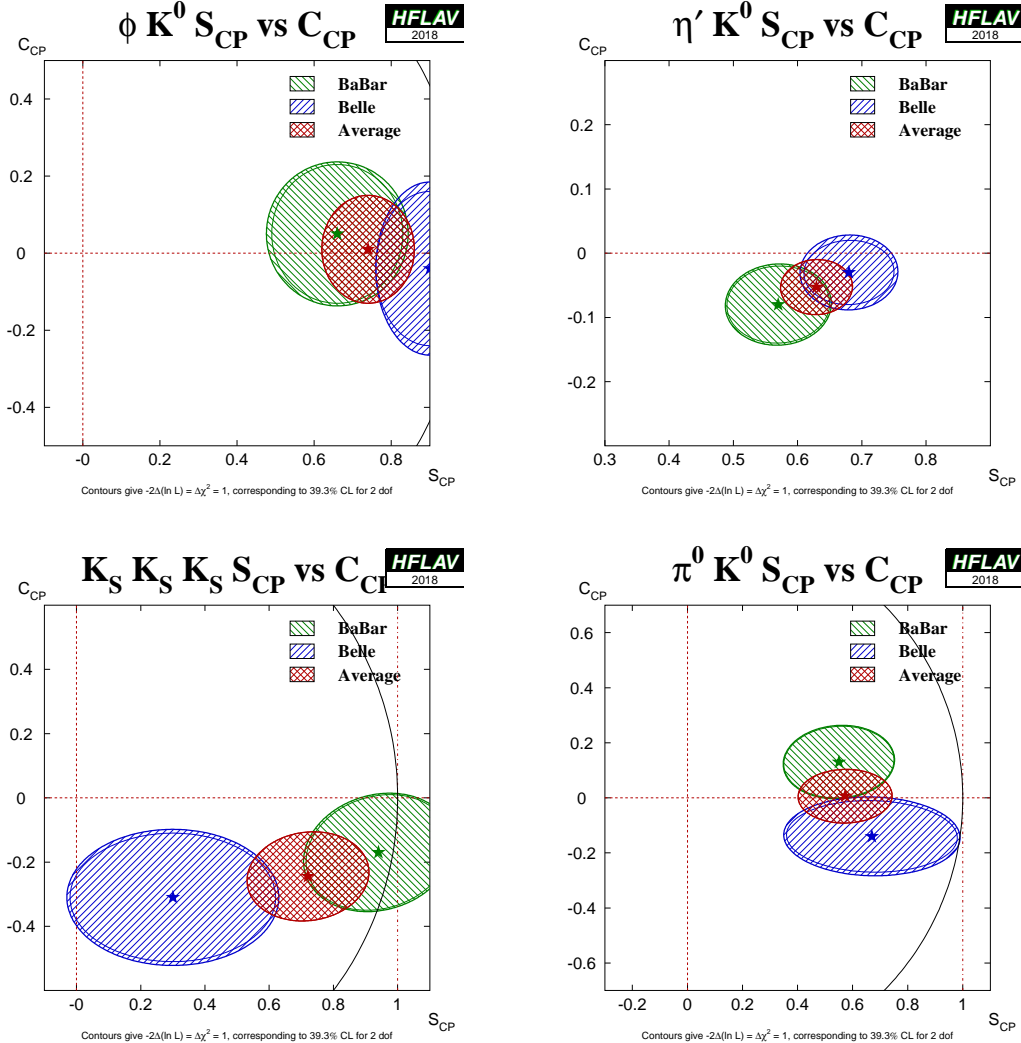


Figure 23: Averages of four $b \rightarrow q\bar{q}s$ dominated channels, for which correlated averages are performed, in the S_{CP} vs. C_{CP} plane, where S_{CP} has been corrected by the CP eigenvalue to give $\sin(2\beta^{\text{eff}})$. (Top left) $B^0 \rightarrow \phi K^0$, (top right) $B^0 \rightarrow \eta' K^0$, (bottom left) $B^0 \rightarrow K_S^0 K_S^0 K_S^0$, (bottom right) $B^0 \rightarrow \pi^0 K_S^0$. More figures are available from the HFLAV web pages.

these averages, often suffer from ambiguous solutions – we quote the results corresponding to those presented as "solution 1" in all cases. Results on flavour-specific amplitudes that may contribute to these Dalitz plots (such as $K^{*+}\pi^-$) are given in Sec. 8.

For the $B^0 \rightarrow K^+ K^- K^0$ decay, both *BABAR* and *Belle* measure the CP violation parameters for the ϕK^0 , $f_0 K^0$ and "other $K^+ K^- K^0$ " amplitudes, where the latter includes all remaining resonant and nonresonant contributions to the charmless three-body decay. For the $B^0 \rightarrow \pi^+ \pi^- K_S^0$ decay, *BABAR* reports CP violation parameters for all of the CP eigenstate components in the Dalitz plot model ($\rho^0 K_S^0$, $f_0 K_S^0$, $f_2 K_S^0$, $f_X K_S^0$ and nonresonant decays; see Sec. 5.2.5), while *Belle* reports the CP violation parameters for only the $\rho^0 K_S^0$ and $f_0 K_S^0$ amplitudes, although the Dalitz-plot models used by the two collaborations are rather similar.

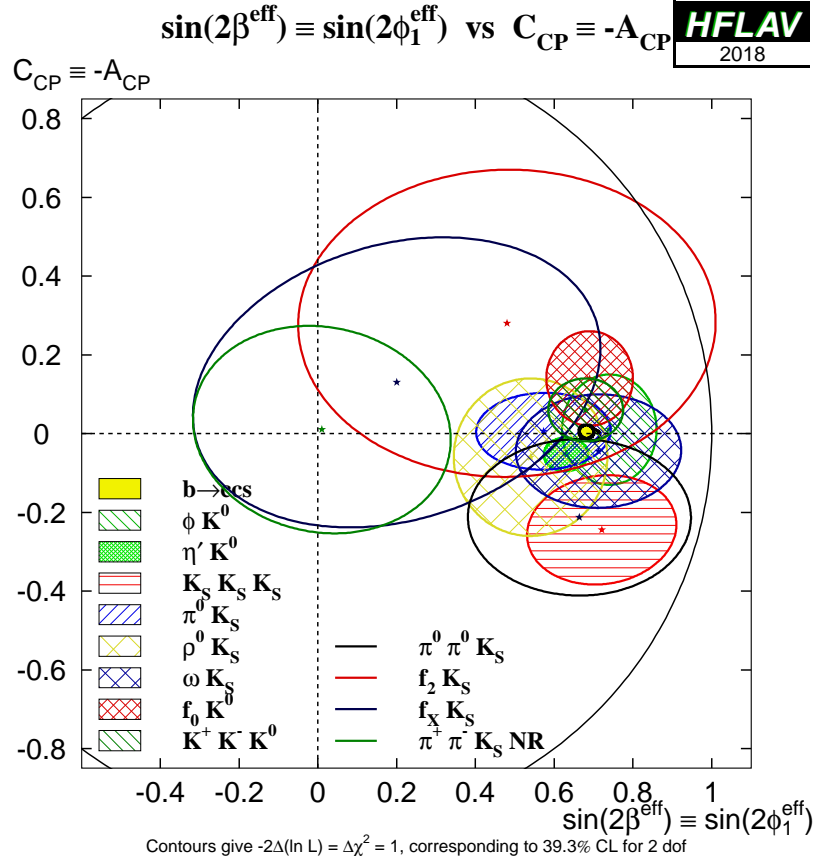


Figure 24: Compilation of constraints in the $-\eta S_{b \rightarrow q\bar{q}s}$, interpreted as $\sin(2\beta^{\text{eff}})$, vs. $C_{b \rightarrow q\bar{q}s}$ plane.

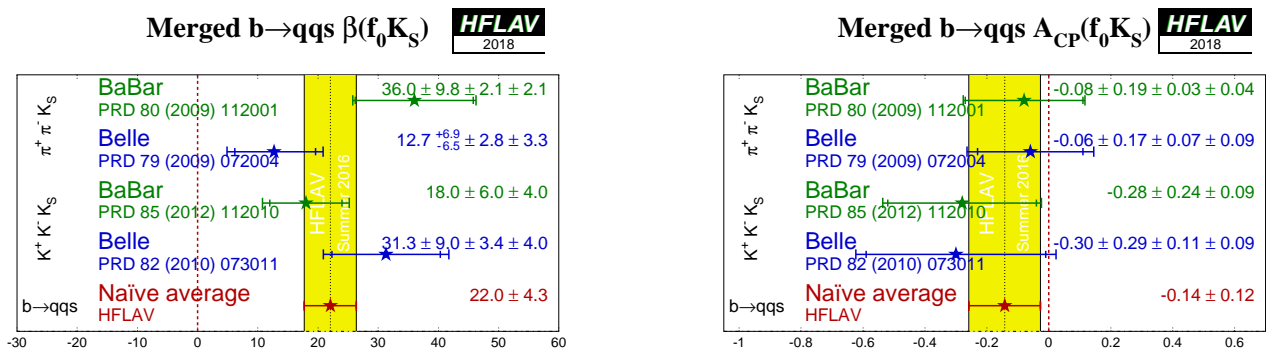


Figure 25: Averages of (left) $\beta^{\text{eff}} \equiv \phi_1^{\text{eff}}$ and (right) A_{CP} for the $B^0 \rightarrow f_0 K_S^0$ decay including measurements from Dalitz plot analyses of both $B^0 \rightarrow K^+ K^- K_S^0$ and $B^0 \rightarrow \pi^+ \pi^- K_S^0$.

Table 37: Results from time-dependent Dalitz plot analyses of the $B^0 \rightarrow K^+ K^- K^0$ decay. Correlations (not shown) are taken into account in the average.

Experiment	$N(B\bar{B})$	ϕK_s^0			$f_0 K_s^0$			$K^+ K^- K_s^0$		
		$\beta^{\text{eff}} (\circ)$	A	$\beta^{\text{eff}} (\circ)$	A	$\beta^{\text{eff}} (\circ)$	A	$\beta^{\text{eff}} (\circ)$	A	$\beta^{\text{eff}} (\circ)$
BABAR [266]	470M	21 ± 6 ± 2	-0.05 ± 0.18 ± 0.05	18 ± 6 ± 4	-0.28 ± 0.24 ± 0.09	20.3 ± 4.3 ± 1.2	-0.02 ± 0.09 ± 0.03			
Belle [265]	657M	32.2 ± 9.0 ± 2.6 ± 1.4	0.04 ± 0.20 ± 0.10 ± 0.02	31.3 ± 9.0 ± 3.4 ± 4.0	-0.30 ± 0.29 ± 0.11 ± 0.09	24.9 ± 6.4 ± 2.1 ± 2.5	-0.14 ± 0.11 ± 0.08 ± 0.03			
Average		24 ± 5	-0.01 ± 0.14	22 ± 6	-0.29 ± 0.20	21.6 ± 3.7	-0.06 ± 0.08			
Confidence level				0.93 (0.1 σ)						

Table 38: Results from time-dependent Dalitz plot analysis of the $B^0 \rightarrow \pi^+ \pi^- K_s^0$ decay. Correlations (not shown) are taken into account in the average.

Experiment	$N(B\bar{B})$	$\rho^0 K_s^0$			$f_0 K_s^0$		
		β_{eff}	\mathcal{A}	β_{eff}	\mathcal{A}	β_{eff}	\mathcal{A}
BABAR [269]	383M	$(10.2 \pm 8.9 \pm 3.0 \pm 1.9)^\circ$	$0.05 \pm 0.26 \pm 0.10 \pm 0.03$	$(36.0 \pm 9.8 \pm 2.1 \pm 2.1)^\circ$	$-0.08 \pm 0.19 \pm 0.03 \pm 0.04$		
Belle [270]	657M	$(20.0^{+8.6}_{-8.5} \pm 3.2 \pm 3.5)^\circ$	$0.03^{+0.23}_{-0.24} \pm 0.11 \pm 0.10$	$(12.7^{+6.9}_{-6.5} \pm 2.8 \pm 3.3)^\circ$	$-0.06 \pm 0.17 \pm 0.07 \pm 0.09$		
Average		16.4 ± 6.8	0.06 ± 0.20	20.6 ± 6.2	-0.07 ± 0.14		
Confidence level				$0.39 \text{ (} 0.9\sigma \text{)}$			
Experiment	$N(B\bar{B})$	$f_2 K_s^0$			$f_X K_s^0$		
		β_{eff}	\mathcal{A}	β_{eff}	\mathcal{A}	β_{eff}	\mathcal{A}
BABAR [269]	383M	$(14.9 \pm 17.9 \pm 3.1 \pm 5.2)^\circ$	$-0.28^{+0.40}_{-0.35} \pm 0.08 \pm 0.07$	$(5.8 \pm 15.2 \pm 2.2 \pm 2.3)^\circ$	$-0.13^{+0.35}_{-0.33} \pm 0.04 \pm 0.09$		
Experiment	$N(B\bar{B})$	$B^0 \rightarrow \pi^+ \pi^- K_s^0$ nonresonant			$\chi_{c0} K_s^0$		
		β_{eff}	\mathcal{A}	β_{eff}	\mathcal{A}	β_{eff}	\mathcal{A}
BABAR [269]	383M	$(0.4 \pm 8.8 \pm 1.9 \pm 3.8)^\circ$	$-0.01 \pm 0.25 \pm 0.06 \pm 0.05$	$(23.2 \pm 22.4 \pm 2.3 \pm 4.2)^\circ$	$0.29^{+0.44}_{-0.53} \pm 0.03 \pm 0.05$		

5.7.3 Time-dependent analyses of $B^0 \rightarrow \phi K_s^0 \pi^0$

The final state in the decay $B^0 \rightarrow \phi K_s^0 \pi^0$ is a mixture of CP -even and CP -odd amplitudes. However, since only ϕK^{*0} resonant states contribute (in particular, $\phi K^{*0}(892)$, $\phi K_0^{*0}(1430)$ and $\phi K_2^{*0}(1430)$ are seen), the composition can be determined from the analysis of $B \rightarrow \phi K^+ \pi^-$ decays, assuming only that the ratio of branching fractions $\mathcal{B}(K^{*0} \rightarrow K_s^0 \pi^0)/\mathcal{B}(K^{*0} \rightarrow K^+ \pi^-)$ is the same for each excited kaon state.

BABAR [390] has performed a simultaneous analysis of $B^0 \rightarrow \phi K_s^0 \pi^0$ and $B^0 \rightarrow \phi K^+ \pi^-$ decays that is time-dependent for the former mode and time-integrated for the latter. Such an analysis allows, in principle, all parameters of the $B^0 \rightarrow \phi K^{*0}$ system to be determined, including mixing-induced CP violation effects. The latter is determined to be $\Delta\phi_{00} = 0.28 \pm 0.42 \pm 0.04$, where $\Delta\phi_{00}$ is half the weak phase difference between B^0 and \bar{B}^0 decays to the $\phi K_0^{*0}(1430)$ final state. As discussed above, this can also be presented in terms of the Q2B parameter $\sin(2\beta_{00}^{\text{eff}}) = \sin(2\beta + 2\Delta\phi_{00}) = 0.97^{+0.03}_{-0.52}$. The highly asymmetric uncertainty arises due to the conversion from the phase to the sine of the phase, and the proximity of the physical boundary.

Similar $\sin(2\beta^{\text{eff}})$ parameters can be defined for each of the helicity amplitudes for both $\phi K^{*0}(892)$ and $\phi K_2^{*0}(1430)$. However, the relative phases between these decays are constrained due to the nature of the simultaneous analysis of $B^0 \rightarrow \phi K_s^0 \pi^0$ and $B^0 \rightarrow \phi K^+ \pi^-$, decays and therefore these measurements are highly correlated. Instead of quoting all these results, *BABAR* provide an illustration of their measurements with the following differences:

$$\sin(2\beta - 2\Delta\delta_{01}) - \sin(2\beta) = -0.42^{+0.26}_{-0.34}, \quad (159)$$

$$\sin(2\beta - 2\Delta\phi_{||1}) - \sin(2\beta) = -0.32^{+0.22}_{-0.30}, \quad (160)$$

$$\sin(2\beta - 2\Delta\phi_{\perp1}) - \sin(2\beta) = -0.30^{+0.23}_{-0.32}, \quad (161)$$

$$\sin(2\beta - 2\Delta\phi_{\perp1}) - \sin(2\beta - 2\Delta\phi_{||1}) = 0.02 \pm 0.23, \quad (162)$$

$$\sin(2\beta - 2\Delta\delta_{02}) - \sin(2\beta) = -0.10^{+0.18}_{-0.29}, \quad (163)$$

where the first subscript indicates the helicity amplitude and the second indicates the spin of the kaon resonance. For the complete definitions of the $\Delta\delta$ and $\Delta\phi$ parameters, refer to the *BABAR* paper [390].

Parameters of CP violation in decay for each of the contributing helicity amplitudes can also be measured. Again, these are determined from a simultaneous fit of $B^0 \rightarrow \phi K_s^0 \pi^0$ and $B^0 \rightarrow \phi K^+ \pi^-$ decays, with the precision being dominated by the statistics of the latter mode. Measurements of CP violation in decay, obtained from decay-time-integrated analyses, are tabulated in Sec. 8.

5.7.4 Time-dependent CP asymmetries in $B_s^0 \rightarrow K^+ K^-$

The decay $B_s^0 \rightarrow K^+ K^-$ involves a $b \rightarrow u\bar{s}$ transition, and hence has both penguin and tree contributions. Both mixing-induced and CP violation in decay effects may arise, and additional input is needed to disentangle the contributions and determine γ and β_s^{eff} . For example, the observables in $B^0 \rightarrow \pi^+ \pi^-$ can be related using U-spin, as proposed in Refs. [391, 392].

The observables are $A_{\text{mix}} = S_{CP}$, $A_{\text{dir}} = -C_{CP}$, and $A_{\Delta\Gamma}$. They are related by $A_{\text{mix}}^2 + A_{\text{dir}}^2 + A_{\Delta\Gamma}^2 = 1$, but are usually treated as independent (albeit correlated) free parameters in experimental analyses, since this approach yields results with better statistical behavior. Note that the untagged decay distribution, from which an “effective lifetime” can be measured,

retains sensitivity to $A_{\Delta\Gamma}$; measurements of the $B_s^0 \rightarrow K^+K^-$ effective lifetime have been made by LHCb [107, 130]. Compilations and averages of effective lifetimes are performed by the HFLAV Lifetimes and Oscillations subgroup, see Sec. 4.

The observables in $B_s^0 \rightarrow K^+K^-$ have been measured by LHCb [393]. The results are shown in Table 39, and correspond to evidence for CP violation both in the interference between mixing and decay, and in the $B_s^0 \rightarrow K^+K^-$ decay.

Table 39: Results from time-dependent analysis of the $B_s^0 \rightarrow K^+K^-$ decay.

Experiment	Sample size	S_{CP}	C_{CP}	$A^{\Delta\Gamma}$
LHCb [393]	$\int \mathcal{L} dt = 3.0 \text{ fb}^{-1}$	$0.18 \pm 0.06 \pm 0.02$	$0.20 \pm 0.06 \pm 0.02$	$-0.79 \pm 0.07 \pm 0.10$

Interpretations of an earlier set of results [394], in terms of constraints on γ and $2\beta_s$, have been separately published by LHCb [235].

5.7.5 Time-dependent CP asymmetries in $B_s^0 \rightarrow \phi\phi$

The decay $B_s^0 \rightarrow \phi\phi$ involves a $b \rightarrow s\bar{s}s$ transition, and hence is a “pure penguin” mode (in the limit that the ϕ meson is considered a pure $s\bar{s}$ state). Since the mixing phase and the decay phase are expected to cancel in the Standard Model, the phase from the interference of mixing and decay is predicted to be $\phi_s(\phi\phi) = 0$ with low uncertainty [395]. Due to the vector-vector nature of the final state, angular analysis is needed to separate the CP -even and CP -odd contributions. Such an analysis also makes it possible to fit directly for $\phi_s(\phi\phi)$.

A constraint on $\phi_s(\phi\phi)$ has been obtained by LHCb using 5 fb^{-1} [396]. The result is $\phi_s(\phi\phi) = -0.06 \pm 0.13 \pm 0.03 \text{ rad}$, where the first uncertainty is statistical and the second is systematic.

5.8 Time-dependent CP asymmetries in $b \rightarrow q\bar{q}d$ transitions

Decays such as $B^0 \rightarrow K_S^0 K_S^0$ are pure $b \rightarrow q\bar{q}d$ penguin transitions. As shown in Eq. (156), this diagram has different contributing weak phases, and therefore the observables are sensitive to their difference (which can be chosen to be either β or γ). Note that if the contribution with the top quark in the loop dominates, the weak phase from the decay amplitudes should cancel that from mixing, so that no CP violation (neither mixing-induced nor in decay) occurs. Non-zero contributions from loops with intermediate up and charm quarks can result in both types of effect (as usual, a strong phase difference is required for CP violation in decay to occur).

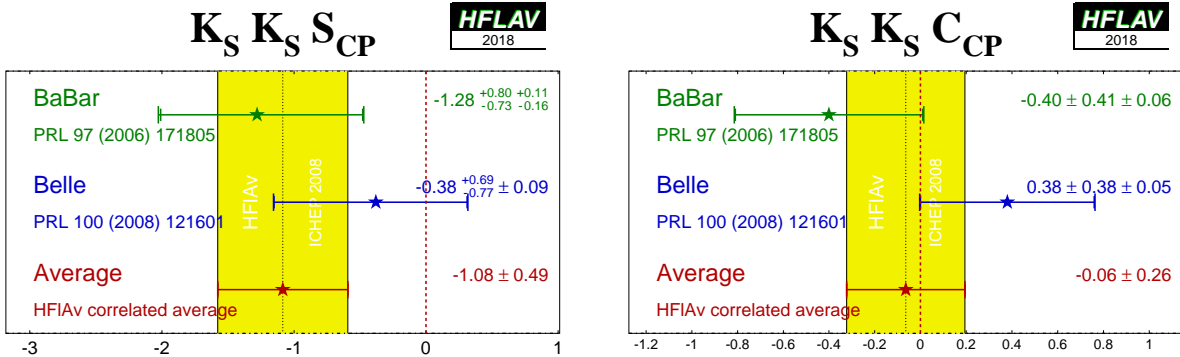
Both *BABAR* [397] and *Belle* [398] have performed time-dependent analyses of $B^0 \rightarrow K_S^0 K_S^0$ decays. The results are given in Table 40 and shown in Fig. 26.

5.9 Time-dependent asymmetries in $b \rightarrow s\gamma$ transitions

The radiative decays $b \rightarrow s\gamma$ produce photons that are highly polarised in the Standard Model. The decays $B^0 \rightarrow F\gamma$ and $\bar{B}^0 \rightarrow F\gamma$, where F is a strange hadronic system, produce photons with opposite helicities, and since the polarisation is, in principle, observable, these final states cannot interfere. The finite mass of the s quark introduces small corrections to the limit of maximum polarisation, but any large mixing-induced CP violation would be a signal for new

Table 40: Results for $B^0 \rightarrow K_s^0 K_s^0$.

Experiment	$N(B\bar{B})$	S_{CP}	C_{CP}	Correlation
<i>BABAR</i> [397]	350M	$-1.28^{+0.80}_{-0.73}{}^{+0.11}_{-0.16}$	$-0.40 \pm 0.41 \pm 0.06$	-0.32
<i>Belle</i> [398]	657M	$-0.38^{+0.69}_{-0.77} \pm 0.09$	$0.38 \pm 0.38 \pm 0.05$	0.48
Average		-1.08 ± 0.49	-0.06 ± 0.26	0.14
Confidence level		0.29 (1.1 σ)		


 Figure 26: Averages of (left) S_{CP} and (right) C_{CP} for the mode $B^0 \rightarrow K_s^0 K_s^0$.

physics. Since a single weak phase dominates the $b \rightarrow s\gamma$ transition in the Standard Model, the cosine term is also expected to be small.

Atwood *et al.* [295] have shown that an inclusive analysis of $K_s^0 \pi^0 \gamma$ can be performed, since the properties of the decay amplitudes are independent of the angular momentum of the $K_s^0 \pi^0$ system. However, if non-dipole operators contribute significantly to the amplitudes, then the Standard Model mixing-induced CP violation could be larger than the naïve expectation $S \simeq -2(m_s/m_b) \sin(2\beta)$ [296, 297]. In this case, the CP parameters may vary over the $K_s^0 \pi^0 \gamma$ Dalitz plot, for example, as a function of the $K_s^0 \pi^0$ invariant mass.

With the above in mind, we quote two averages: one for the final state $K^*(892)\gamma$ only, and one for the inclusive $K_s^0 \pi^0 \gamma$ final state (including $K^*(892)\gamma$). If the Standard Model dipole operator is dominant, both should give the same CP -violation parameters (the latter, naturally, with smaller statistical uncertainties). If not, care needs to be taken in interpretation of the inclusive parameters, while the results on the $K^*(892)$ resonance remain relatively clean. Results from *BABAR* and *Belle* are used for both averages; both experiments use the invariant-mass range $0.60 < M_{K_s^0 \pi^0} < 1.80$ GeV/ c^2 in the inclusive analysis.

In addition to the $K_s^0 \pi^0 \gamma$ decay, both *BABAR* and *Belle* have presented results using the $K_s^0 \rho \gamma$ mode, while *BABAR* (*Belle*) has in addition presented results using the $K_s^0 \eta \gamma$ ($K_s^0 \phi \gamma$) channel. For the $K_s^0 \rho \gamma$ case, due to the non-negligible width of the ρ^0 meson, decays selected as $B^0 \rightarrow K_s^0 \rho^0 \gamma$ can include a significant contribution from $K^{*\pm} \pi^\mp \gamma$ decays, which are flavour-specific and do not have the same oscillation phenomenology. Both *BABAR* and *Belle* measure S_{eff} for all B decay candidates with the ρ^0 selection being $0.6 < m(\pi^+ \pi^-) < 0.9$ GeV/ c^2 , obtaining $0.14 \pm 0.25^{+0.04}_{-0.03}$ (*BABAR*) and $0.09 \pm 0.27^{+0.04}_{-0.07}$ (*Belle*). These values are then corrected for a

“dilution factor”, that is evaluated with different methods in the two experiments: *BABAR* [399, 400] obtains a dilution factor of $-0.78^{+0.19}_{-0.17}$, while *Belle* [401] obtains $+0.83^{+0.19}_{-0.03}$. Until the discrepancy between these values is understood, the average of the results should be treated with caution.

Table 41: Averages for $b \rightarrow s\gamma$ modes.

Experiment		$N(B\bar{B})$	$S_{CP}(b \rightarrow s\gamma)$	$C_{CP}(b \rightarrow s\gamma)$	Correlation
			$K^*(892)\gamma$		
<i>BABAR</i>	[402]	467M	$-0.03 \pm 0.29 \pm 0.03$	$-0.14 \pm 0.16 \pm 0.03$	0.05
<i>Belle</i>	[403]	535M	$-0.32^{+0.36}_{-0.33} \pm 0.05$	$0.20 \pm 0.24 \pm 0.05$	0.08
Average			-0.16 ± 0.22	-0.04 ± 0.14	0.06
Confidence level			0.40 (0.9 σ)		
			$K_s^0\pi^0\gamma$ (including $K^*(892)\gamma$)		
<i>BABAR</i>	[402]	467M	$-0.17 \pm 0.26 \pm 0.03$	$-0.19 \pm 0.14 \pm 0.03$	0.04
<i>Belle</i>	[403]	535M	$-0.10 \pm 0.31 \pm 0.07$	$0.20 \pm 0.20 \pm 0.06$	0.08
Average			-0.15 ± 0.20	-0.07 ± 0.12	0.05
Confidence level			0.30 (1.0 σ)		
			$K_s^0\eta\gamma$		
<i>BABAR</i>	[404]	465M	$-0.18^{+0.49}_{-0.46} \pm 0.12$	$-0.32^{+0.40}_{-0.39} \pm 0.07$	-0.17
<i>Belle</i>	[405]	772M	$-1.32 \pm 0.77 \pm 0.36$	$0.48 \pm 0.41 \pm 0.07$	-0.15
Average			-0.49 ± 0.42	0.06 ± 0.29	-0.15
Confidence level			0.24 (1.2 σ)		
			$K_s^0\rho^0\gamma$		
<i>BABAR</i>	[400]	471M	$-0.18 \pm 0.32^{+0.06}_{-0.05}$	$-0.39 \pm 0.20^{+0.03}_{-0.02}$	-0.09
<i>Belle</i>	[401]	657M	$0.11 \pm 0.33^{+0.05}_{-0.09}$	$-0.05 \pm 0.18 \pm 0.06$	0.04
Average			-0.06 ± 0.23	-0.22 ± 0.14	-0.02
Confidence level			0.38 (0.9 σ)		
			$K_s^0\phi\gamma$		
<i>Belle</i>	[406]	772M	$0.74^{+0.72}_{-1.05}{}^{+0.10}_{-0.24}$	$-0.35 \pm 0.58^{+0.10}_{-0.23}$	-

The results are given in Table 41, and shown in Figs. 27 and 28. No significant CP violation is seen; the results are consistent with the Standard Model and with other measurements in the $b \rightarrow s\gamma$ system (see Sec. 8).

A similar analysis can be performed for radiative B_s^0 decays to, for example, the $\phi\gamma$ final state. As for other observables determined with self-conjugate final states produced in B_s^0 decays, the effective lifetime also provides sensitivity to the underlying amplitudes, and can be determined without tagging the initial flavour of the decaying meson. The LHCb collaboration has determined the associated parameter $A_{\Delta\Gamma}(\phi\gamma) = -0.98^{+0.46}_{-0.52}{}^{+0.23}_{-0.20}$ [407].

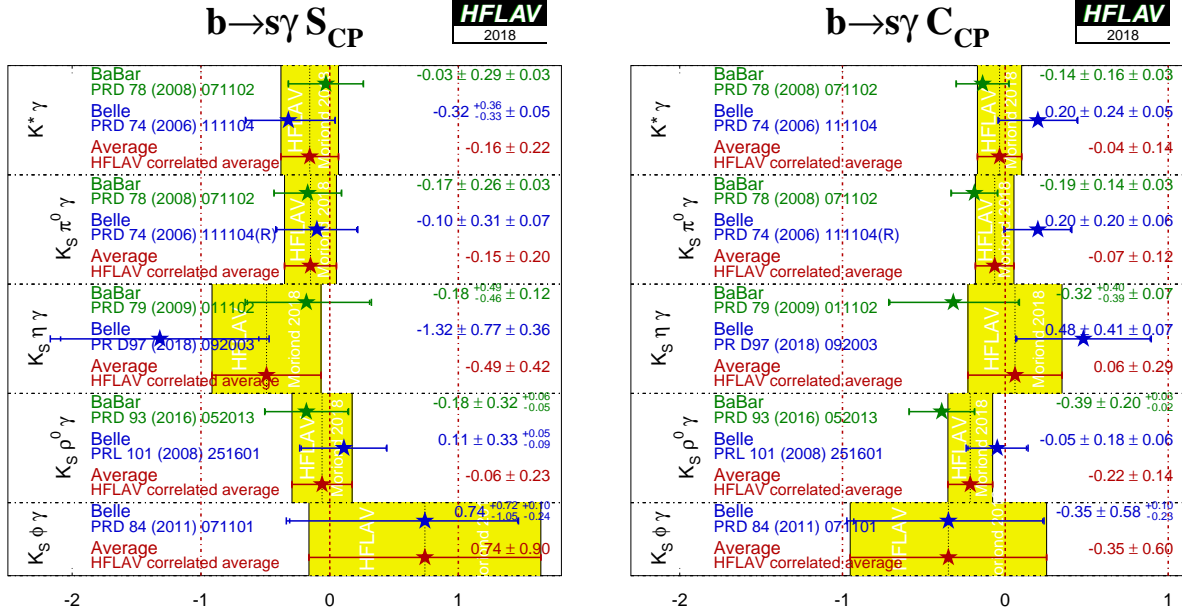


Figure 27: Averages of (left) $S_{b \rightarrow s\gamma}$ and (right) $C_{b \rightarrow s\gamma}$. Recall that the data for $K^*\gamma$ is a subset of that for $K_s^0\pi^0\gamma$.

5.10 Time-dependent asymmetries in $b \rightarrow d\gamma$ transitions

The formalism for the radiative decays $b \rightarrow d\gamma$ is much the same as that for $b \rightarrow s\gamma$ discussed above. Assuming dominance of the top quark in the loop, the weak phase in decay should cancel with that from mixing, so that the mixing-induced CP violation parameter S_{CP} should be very small. Corrections due to the finite light-quark mass are smaller compared to $b \rightarrow s\gamma$, since $m_d < m_s$, but QCD corrections of $\mathcal{O}(\Lambda_{\text{QCD}}/m_b)$ may be sizable [296]. Large CP violation effects could be seen through a non-zero value of $C_{b \rightarrow d\gamma}$, since the top loop is not the only contribution.

Results using the mode $B^0 \rightarrow \rho^0\gamma$ are available from Belle and are given in Table 42.

Table 42: Averages for $B^0 \rightarrow \rho^0\gamma$.

Experiment	$N(B\bar{B})$	S_{CP}	C_{CP}	Correlation
Belle [408]	657M	$-0.83 \pm 0.65 \pm 0.18$	$0.44 \pm 0.49 \pm 0.14$	-0.08

5.11 Time-dependent CP asymmetries in $b \rightarrow u\bar{u}d$ transitions

The $b \rightarrow u\bar{u}d$ transition can be mediated by either a $b \rightarrow u$ tree amplitude or a $b \rightarrow d$ penguin amplitude. These transitions can be investigated using the time dependence of B^0 decays to final states containing light mesons. Results are available from both *BABAR* and Belle for the CP eigenstate ($\eta = +1$) $\pi^+\pi^-$ final state and for the vector-vector final state $\rho^+\rho^-$, which is found to be dominated by the CP -even longitudinally polarised component (*BABAR* measures

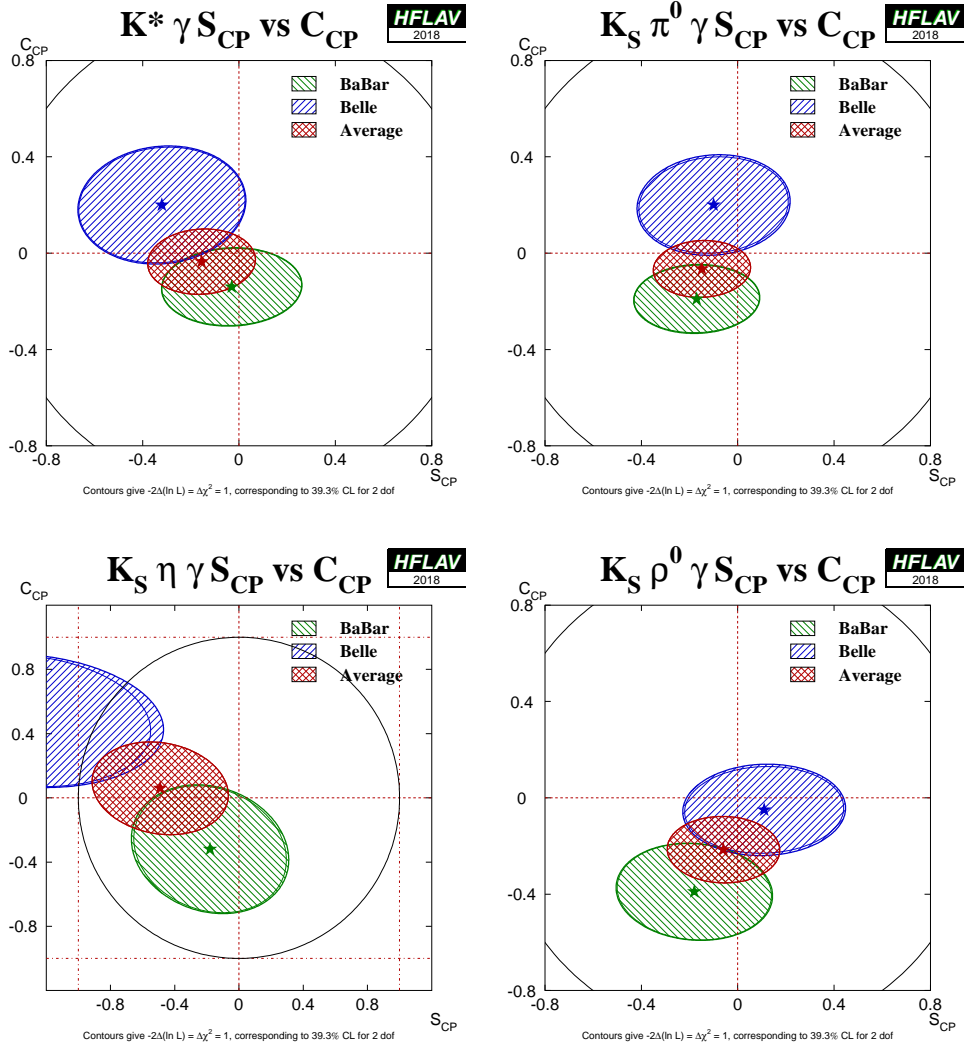


Figure 28: Averages of four $b \rightarrow s\gamma$ dominated channels in the S_{CP} vs. C_{CP} plane. (Top left) $B^0 \rightarrow K^*\gamma$, (top right) $B^0 \rightarrow K_s^0\pi^0\gamma$ (including $K^*\gamma$), (bottom left) $B^0 \rightarrow K_s^0\eta\gamma$, (bottom right) $B^0 \rightarrow K_s^0\rho^0\gamma$.

$f_{\text{long}} = 0.992 \pm 0.024^{+0.026}_{-0.013}$ [409], and Belle measures $f_{\text{long}} = 0.988 \pm 0.012 \pm 0.023$ [410]). *BABAR* has also performed a time-dependent analysis of the vector-vector final state $\rho^0\rho^0$ [411], in which they measure $f_{\text{long}} = 0.70 \pm 0.14 \pm 0.05$; Belle measure a smaller branching fraction than *BABAR* for $B^0 \rightarrow \rho^0\rho^0$ [412] with corresponding signal yields too small to perform a time-dependent analysis; for the longitudinal polarisation they measure $f_{\text{long}} = 0.21^{+0.18}_{-0.22} \pm 0.13$. *LHCb* has measured the branching fraction and longitudinal polarisation for $B^0 \rightarrow \rho^0\rho^0$, and for the latter finds $f_{\text{long}} = 0.745^{+0.048}_{-0.058} \pm 0.034$ [413], but has not yet performed a time-dependent analysis of this decay. The Belle measurement for f_{long} is thus in some tension with the other results. Both *BABAR* and Belle have furthermore performed time-dependent analyses of the $B^0 \rightarrow a_1^\pm\pi^\mp$ decay [414, 415]; *BABAR* in addition reported further experimental input for the extraction of α from this channel in a later publication [416].

Results and averages of time-dependent CP violation parameters in $b \rightarrow u\bar{u}d$ transitions are listed in Table 43. The averages for $\pi^+\pi^-$ are shown in Fig. 29, and those for $\rho^+\rho^-$ are shown

in Fig. 30, with the averages in the S_{CP} vs. C_{CP} plane shown in Fig. 31, and averages of CP violation parameters in $B^0 \rightarrow a_1^\pm \pi^\mp$ decay shown in Fig. 32.

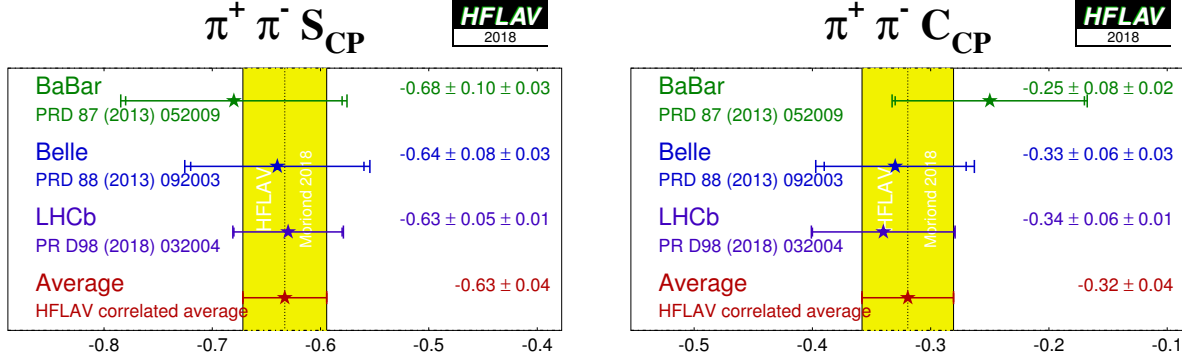


Figure 29: Averages of (left) S_{CP} and (right) C_{CP} for the mode $B^0 \rightarrow \pi^+ \pi^-$.

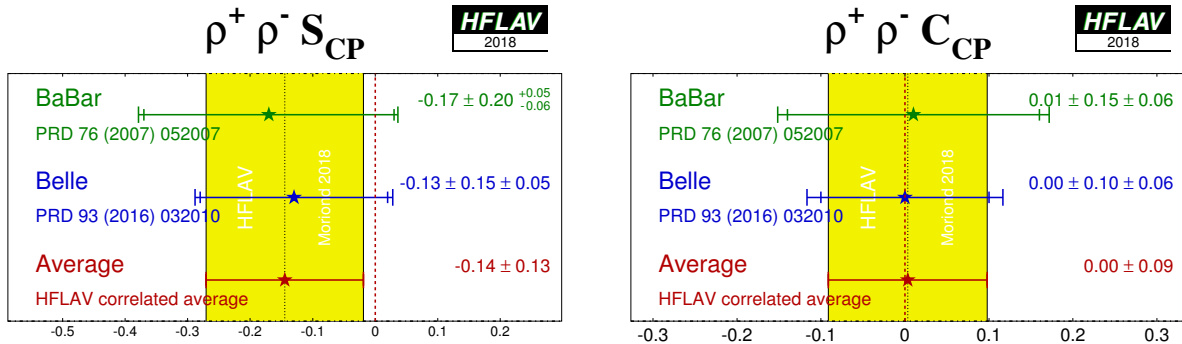


Figure 30: Averages of (left) S_{CP} and (right) C_{CP} for the mode $B^0 \rightarrow \rho^+ \rho^-$.

If the penguin contribution is negligible, the time-dependent parameters for $B^0 \rightarrow \pi^+ \pi^-$ and $B^0 \rightarrow \rho^+ \rho^-$ are given by $S_{b \rightarrow u\bar{u}d} = \eta \sin(2\alpha)$ and $C_{b \rightarrow u\bar{u}d} = 0$. In the presence of the penguin contribution, CP violation in decay may arise, and there is no straightforward interpretation of $S_{b \rightarrow u\bar{u}d}$ and $C_{b \rightarrow u\bar{u}d}$. An isospin analysis [419] can be used to disentangle the contributions and extract α , as discussed further in Sec. 5.11.1.

For the non- CP eigenstate $\rho^\pm \pi^\mp$, both *BABAR* [276] and *Belle* [278, 279] have performed time-dependent Dalitz-plot analyses of the $\pi^+ \pi^- \pi^0$ final state [274]; such analyses allow direct measurements of the phases. Both experiments have measured the U and I parameters discussed in Sec. 5.2.5 and defined in Table 23. We have performed a full correlated average of these parameters, the results of which are summarised in Fig. 33.

Both experiments have also extracted the Q2B parameters for the $\rho\pi$ channels. We have performed a full correlated average of these parameters, which is equivalent to determining the values from the averaged U and I parameters. The results are given in Table 44.³² Averages of the $B^0 \rightarrow \rho^0 \pi^0$ Q2B parameters are shown in Figs. 34 and 35.

³² The $B^0 \rightarrow \rho^\pm \pi^\mp$ Q2B parameters are comparable to the parameters used for $B^0 \rightarrow a_1^\pm \pi^\mp$ decays, reported

Table 43: Averages for $b \rightarrow u\bar{u}d$ modes.

Experiment		Sample size	S_{CP}	C_{CP}	Correlation
<i>BABAR</i>	[417]	$N(B\bar{B}) = 467M$	$\pi^+\pi^-$		
Belle	[418]	$N(B\bar{B}) = 772M$	$-0.68 \pm 0.10 \pm 0.03$	$-0.25 \pm 0.08 \pm 0.02$	-0.06
LHCb	[393]	$\int \mathcal{L} dt = 3.0 \text{ fb}^{-1}$	$-0.64 \pm 0.08 \pm 0.03$	$-0.33 \pm 0.06 \pm 0.03$	-0.10
Average			$-0.63 \pm 0.05 \pm 0.01$	$-0.34 \pm 0.06 \pm 0.01$	0.45
Confidence level			-0.63 ± 0.04	-0.32 ± 0.04	0.21
				0.90 (0.1 σ)	
<i>BABAR</i>	[409]	$N(B\bar{B}) = 387M$	$\rho^+ \rho^-$		
Belle	[410]	$N(B\bar{B}) = 772M$	$-0.17 \pm 0.20^{+0.05}_{-0.06}$	$0.01 \pm 0.15 \pm 0.06$	-0.04
Average			$-0.13 \pm 0.15 \pm 0.05$	$0.00 \pm 0.10 \pm 0.06$	-0.02
Confidence level			-0.14 ± 0.13	0.00 ± 0.09	-0.02
			0.99 (0.02 σ)		
<i>BABAR</i>	[411]	$N(B\bar{B}) = 465M$	$\rho^0 \rho^0$		
			$0.3 \pm 0.7 \pm 0.2$	$0.2 \pm 0.8 \pm 0.3$	-0.04
Experiment	$N(B\bar{B})$	$A_{CP}^{a_1\pi}$	$C_{a_1\pi}$	$a_1^\pm \pi^\mp$	$\Delta S_{a_1\pi}$
<i>BABAR</i>	[414]	384M	$-0.07 \pm 0.07 \pm 0.02$	$-0.10 \pm 0.15 \pm 0.09$	$0.37 \pm 0.21 \pm 0.07$
Belle	[415]	772M	$-0.06 \pm 0.05 \pm 0.07$	$-0.01 \pm 0.11 \pm 0.09$	$0.26 \pm 0.15 \pm 0.07$
Average			-0.06 ± 0.06	-0.05 ± 0.11	$-0.14 \pm 0.21 \pm 0.06$
Confidence level					
				0.20 \pm 0.13	$-0.14 \pm 0.14 \pm 0.06$
				0.43 \pm 0.10	$-0.09 \pm 0.07 \pm 0.06$
				0.03 (2.1 σ)	$-0.09 \pm 0.12 \pm 0.06$
Experiment		$N(B\bar{B})$	$\mathcal{A}_{a_1\pi}^{-+}$	$\mathcal{A}_{a_1\pi}^{+-}$	Correlation
<i>BABAR</i>	[414]	384M	$0.07 \pm 0.21 \pm 0.15$	$0.15 \pm 0.15 \pm 0.07$	0.63
Belle	[415]	772M	$-0.04 \pm 0.26 \pm 0.19$	$0.07 \pm 0.08 \pm 0.10$	0.61
Average			0.02 ± 0.20	0.10 ± 0.10	0.38
Confidence level				0.92 (0.1 σ)	

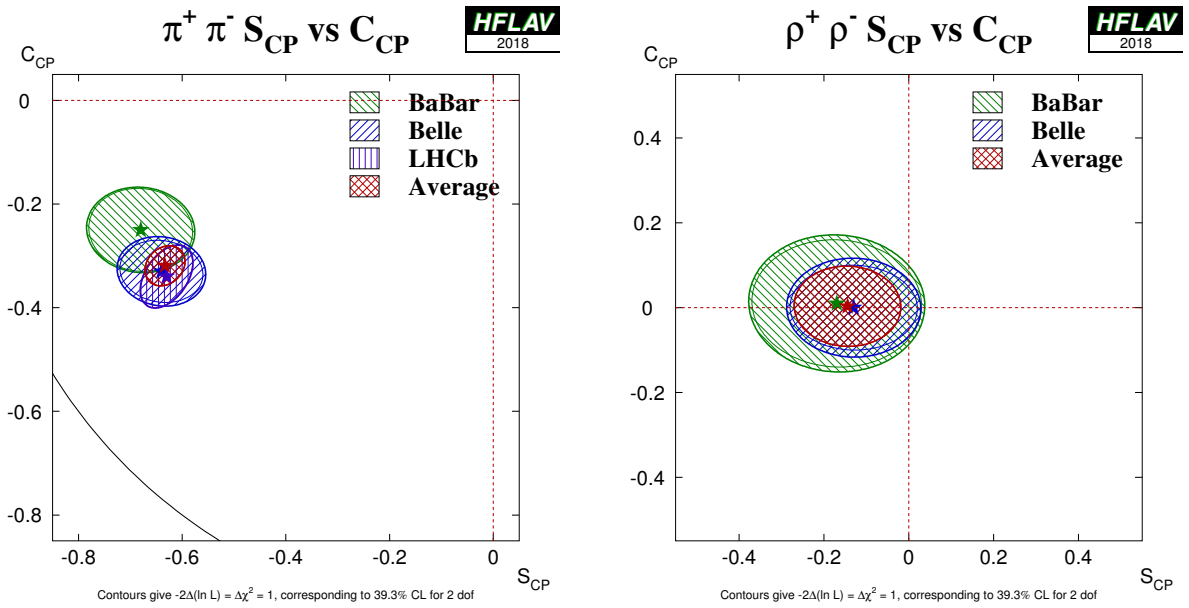


Figure 31: Averages of $b \rightarrow u\bar{u}d$ dominated channels, for which correlated averages are performed, in the S_{CP} vs. C_{CP} plane. (Left) $B^0 \rightarrow \pi^+\pi^-$ and (right) $B^0 \rightarrow \rho^+\rho^-$.

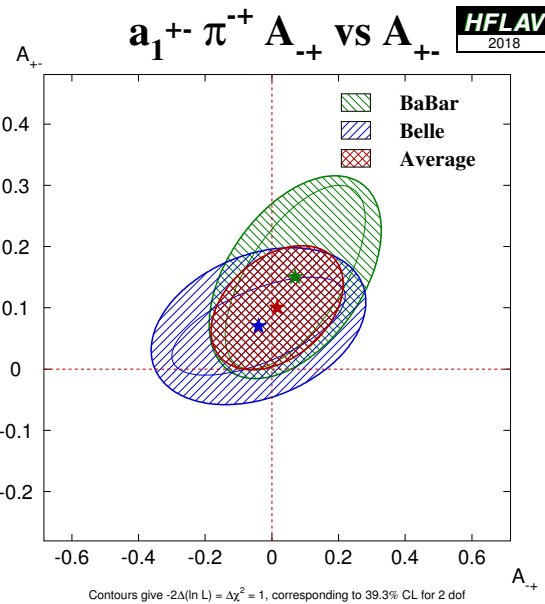


Figure 32: Averages of CP violation parameters in $B^0 \rightarrow a_1^\pm \pi^\mp$ in $\mathcal{A}_{a_1\pi}^{-+}$ vs. $\mathcal{A}_{a_1\pi}^{+-}$ space.

Table 44: Averages of quasi-two-body parameters extracted from time-dependent Dalitz plot analysis of $B^0 \rightarrow \pi^+ \pi^- \pi^0$.

Experiment	$N(B\bar{B})$	$\mathcal{A}_{CP}^{\rho\pi}$	$C_{\rho\pi}$	$S_{\rho\pi}$	$\Delta C_{\rho\pi}$	$\Delta S_{\rho\pi}$
<i>BABAR</i>	[277]	471M	$-0.10 \pm 0.03 \pm 0.02$	$0.02 \pm 0.06 \pm 0.04$	$0.05 \pm 0.08 \pm 0.03$	$0.23 \pm 0.06 \pm 0.05$
Belle	[278,279]	449M	$-0.12 \pm 0.05 \pm 0.04$	$-0.13 \pm 0.09 \pm 0.05$	$0.06 \pm 0.13 \pm 0.05$	$0.36 \pm 0.10 \pm 0.05$
Average			-0.11 ± 0.03	-0.03 ± 0.06	0.06 ± 0.07	0.27 ± 0.06
Confidence level					0.63 (0.5 σ)	0.01 ± 0.08

Experiment	$N(B\bar{B})$	$\mathcal{A}_{\rho\pi}^{-+}$	$\mathcal{A}_{\rho\pi}^{+-}$	$\mathcal{A}_{\rho\pi}^{+-}$	Correlation
<i>BABAR</i>	[277]	471M	$-0.12 \pm 0.08^{+0.04}_{-0.05}$	$0.09^{+0.05}_{-0.06} \pm 0.04$	0.55
Belle	[278,279]	449M	$0.08 \pm 0.16 \pm 0.11$	$0.21 \pm 0.08 \pm 0.04$	0.47
Average			-0.08 ± 0.08	0.13 ± 0.05	0.37
Confidence level				0.47 (0.7 σ)	

Experiment	$N(B\bar{B})$	$C_{\rho^0\pi^0}$	$C_{\rho^0\pi^0}$	$S_{\rho^0\pi^0}$	Correlation
<i>BABAR</i>	[277]	471M	$0.19 \pm 0.23 \pm 0.15$	$-0.37 \pm 0.34 \pm 0.20$	0.00
Belle	[278,279]	449M	$0.49 \pm 0.36 \pm 0.28$	$0.17 \pm 0.57 \pm 0.35$	0.08
Average			0.27 ± 0.24	-0.23 ± 0.34	0.02
Confidence level				0.68 (0.4 σ)	

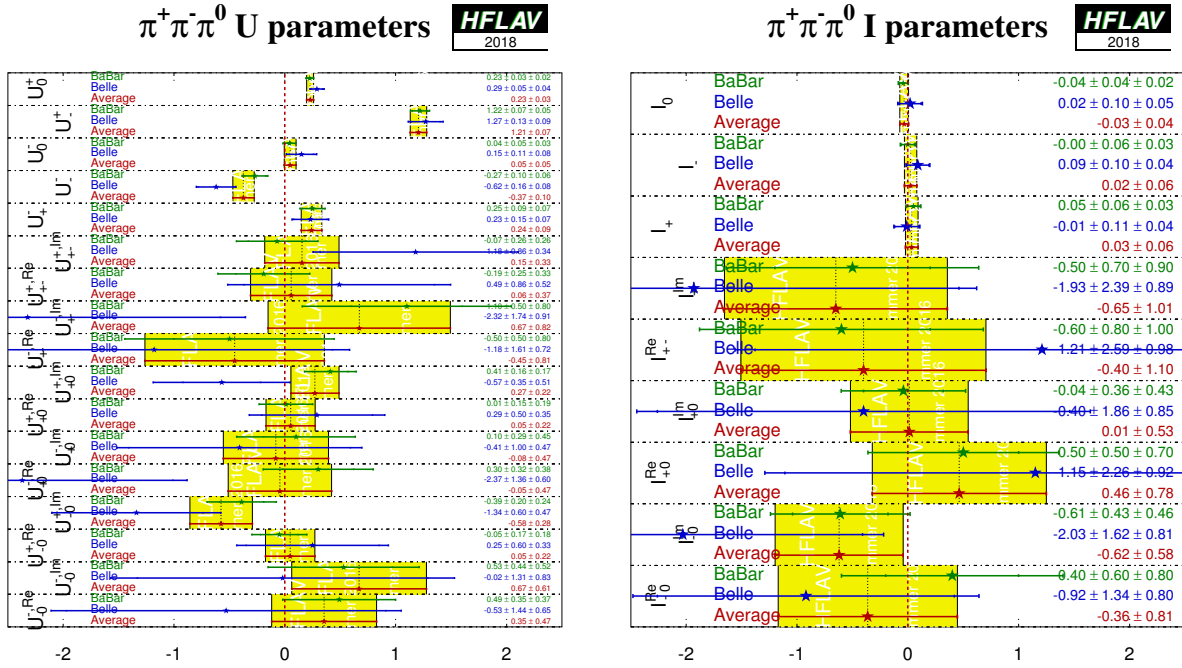


Figure 33: Summary of the U and I parameters measured in the time-dependent $B^0 \rightarrow \pi^+\pi^-\pi^0$ Dalitz plot analysis.

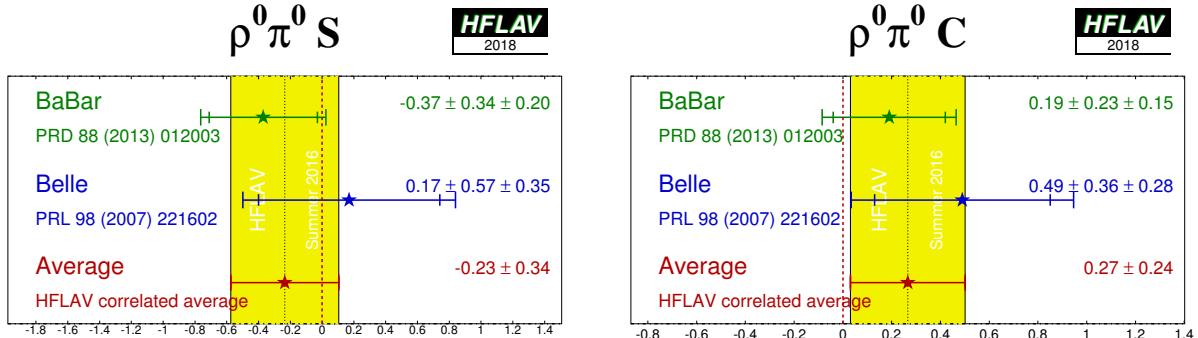


Figure 34: Averages of (left) $S_{b \rightarrow u\bar{u}d}$ and (right) $C_{b \rightarrow u\bar{u}d}$ for the mode $B^0 \rightarrow \rho^0\pi^0$.

With the notation described in Sec. 5.2 (Eq. (133)), the time-dependent parameters for the Q2B $B^0 \rightarrow \rho^\pm\pi^\mp$ analysis are, neglecting penguin contributions, given by

$$S_{\rho\pi} = \sqrt{1 - \left(\frac{\Delta C}{2}\right)^2} \sin(2\alpha) \cos(\delta), \quad \Delta S_{\rho\pi} = \sqrt{1 - \left(\frac{\Delta C}{2}\right)^2} \cos(2\alpha) \sin(\delta) \quad (164)$$

and $C_{\rho\pi} = \mathcal{A}_{CP}^{\rho\pi} = 0$, where $\delta = \arg(A_{-+}A_{+-}^*)$ is the strong phase difference between the $\rho^-\pi^+$ and $\rho^+\pi^-$ decay amplitudes. In the presence of penguin contributions, there is no straight-

in Table 43. For the $B^0 \rightarrow a_1^\pm\pi^\mp$ case there has not yet been a full amplitude analysis of $B^0 \rightarrow \pi^+\pi^-\pi^+\pi^-$ and therefore only the Q2B parameters are available.

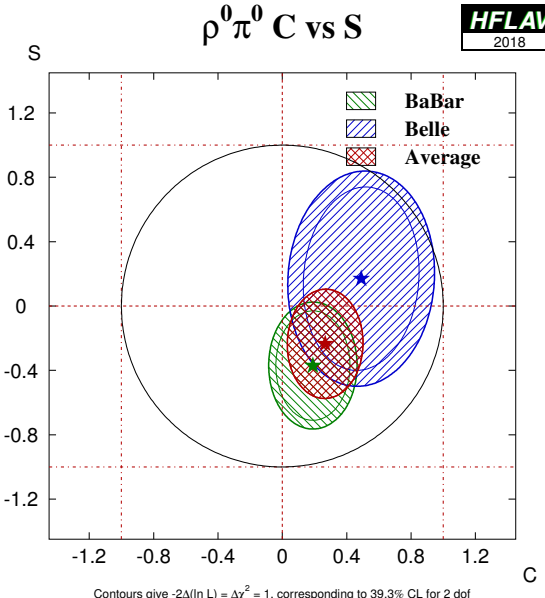


Figure 35: Averages of $b \rightarrow u\bar{u}d$ dominated channels, for the mode $B^0 \rightarrow \rho^0\pi^0$ in the S_{CP} vs. C_{CP} plane.

forward interpretation of the Q2B observables in the $B^0 \rightarrow \rho^\pm\pi^\mp$ system in terms of CKM parameters. However, CP violation in decay may arise, resulting in either or both of $C_{\rho\pi} \neq 0$ and $\mathcal{A}_{CP}^{\rho\pi} \neq 0$. Equivalently, CP violation in decay may be detected via deviation from zero of either of the decay-type-specific observables $\mathcal{A}_{\rho\pi}^{+-}$ and $\mathcal{A}_{\rho\pi}^{-+}$, defined in Eq. (134). Results and averages for these parameters are also given in Table 44. Averages of CP violation parameters in $B^0 \rightarrow \rho^\pm\pi^\mp$ decays are shown in Fig. 36, both in $\mathcal{A}_{CP}^{\rho\pi}$ vs. $C_{\rho\pi}$ space and in $\mathcal{A}_{\rho\pi}^{-+}$ vs. $\mathcal{A}_{\rho\pi}^{+-}$ space.

The averages for $S_{b \rightarrow u\bar{u}d}$ and $C_{b \rightarrow u\bar{u}d}$ in $B^0 \rightarrow \pi^+\pi^-$ decays are both more than 5σ away from zero, suggesting that both mixing-induced and CP violation in decay are well-established in this channel. The discrepancy between results from *BABAR* and *Belle* that used to exist in this channel (see, for example, Ref. [420]) is no longer apparent, and the results from *LHCb* are also fully consistent with other measurements. Some difference is, however, seen between the *BABAR* and *Belle* measurements in the $a_1^\pm\pi^\mp$ system. The confidence level of the five-dimensional average is 0.03, which corresponds to a 2.1σ discrepancy. As seen in Table 43, this discrepancy is primarily in the values of $S_{a_1\pi}$, and is not evident in the $\mathcal{A}_{a_1\pi}^{-+}$ vs. $\mathcal{A}_{a_1\pi}^{+-}$ projection shown in Fig. 32. Since there is no evidence of underestimation of uncertainties in either analysis, we do not rescale the uncertainties of the averages.

In $B^0 \rightarrow \rho^\pm\pi^\mp$ decays, both experiments see an indication of CP violation in the $\mathcal{A}_{CP}^{\rho\pi}$ parameter (as seen in Fig. 36). The average is more than 3σ from zero, providing evidence of CP violation in decay in this channel. In $B^0 \rightarrow \rho^+\rho^-$ decays there is no evidence for CP violation, either mixing-induced or in decay. The absence of evidence of penguin contributions in this mode leads to strong constraints on $\alpha \equiv \phi_2$.

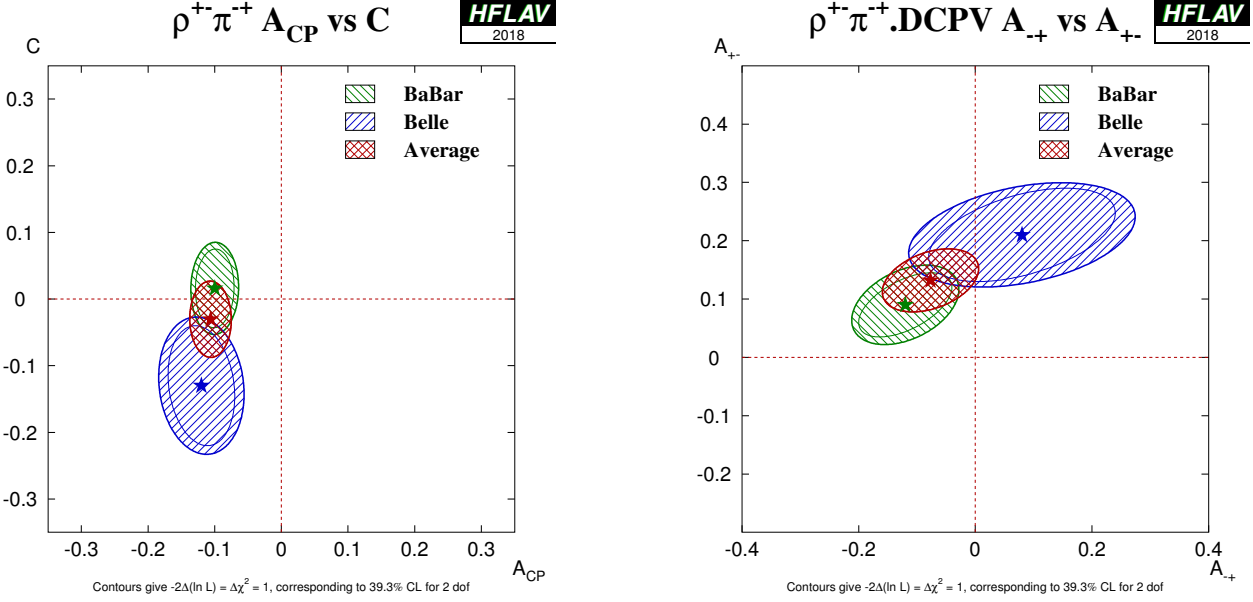


Figure 36: CP violation in $B^0 \rightarrow \rho^\pm \pi^\mp$ decays. (Left) $A_{CP}^{\rho\pi}$ vs. $C_{\rho\pi}$ space, (right) $A_{\rho\pi}^{+-}$ vs. $A_{\rho\pi}^{+-}$ space.

5.11.1 Constraints on $\alpha \equiv \phi_2$

The precision of the measured CP violation parameters in $b \rightarrow u\bar{u}d$ transitions allows constraints to be set on the UT angle $\alpha \equiv \phi_2$. Constraints have been obtained with various methods:

- Both *BABAR* [417] and *Belle* [418] have performed isospin analyses in the $\pi\pi$ system. *Belle* exclude $23.8^\circ < \phi_2 < 66.8^\circ$ at 68% CL while *BABAR* give a confidence level interpretation for α , and constrain $\alpha \in [71^\circ, 109^\circ]$ at 68% CL. Values in the range $[23^\circ, 67^\circ]$ are excluded at 90% CL. In both cases, only solutions in 0° – 180° are quoted.
- Both experiments have also performed isospin analyses in the $\rho\rho$ system. The most recent result from *BABAR* is given in an update of the measurements of the $B^+ \rightarrow \rho^+\rho^0$ decay [421], and sets the constraint $\alpha = (92.4^{+6.0}_{-6.5})^\circ$. The most recent result from *Belle* is given in their paper on time-dependent CP violation parameters in $B^0 \rightarrow \rho^+\rho^-$ decays, and sets the constraint $\phi_2 = (93.7 \pm 10.6)^\circ$ [410].
- The time-dependent Dalitz-plot analysis of the $B^0 \rightarrow \pi^+\pi^-\pi^0$ decay allows a determination of α without input from any other channels. *BABAR* [277] present a scan, but not an interval, for α , since their studies indicate that the scan is not statistically robust and cannot be interpreted in terms of 1–CL. *Belle* [278, 279] have obtained a constraint on α using additional information from SU(2) relations between $B \rightarrow \rho\pi$ decay amplitudes, which can be used to constrain α via an isospin pentagon relation [422]. With this analysis, *Belle* obtain the constraint $\phi_2 = (83^{+12}_{-23})^\circ$.
- The results from *BABAR* on $B^0 \rightarrow a_1^\pm \pi^\mp$ [414] can be combined with results from modes related by flavour symmetries ($a_1 K$ and $K_1 \pi$) [423]. This has been done by *BABAR* [416], resulting in the constraint $\alpha = (79 \pm 7 \pm 11)^\circ$, where the first uncertainty is from the analysis of $B^0 \rightarrow a_1^\pm \pi^\mp$ that obtains α^{eff} , and the second is due to the constraint on

$|\alpha^{\text{eff}} - \alpha|$. This approach gives a result with several ambiguous solutions; only the one that is consistent with other determinations of α and with global fits to the CKM matrix parameters is quoted here.

- The CKMfitter [244] and UTfit [337] groups use the measurements from Belle and *BABAR* given above with other branching fractions and CP asymmetries in $B \rightarrow \pi\pi$, $\pi\pi\pi^0$ and $\rho\rho$ modes to perform isospin analyses for each system, and to obtain combined constraints on α .
- The *BABAR* and Belle collaborations have combined their results on $B \rightarrow \pi\pi$, $\pi\pi\pi^0$ and $\rho\rho$ decays to obtain [424]

$$\alpha \equiv \phi_2 = (88 \pm 5)^\circ. \quad (165)$$

The above solution is that consistent with the Standard Model (there exists an ambiguous solution, shifted by 180°). The strongest constraint currently comes from the $B \rightarrow \rho\rho$ system. The inclusion of results from $B^0 \rightarrow a_1^\pm \pi^\mp$ does not significantly affect the average.

- All results for $\alpha \equiv \phi_2$ based on isospin symmetry have a theoretical uncertainty due to possible isospin-breaking effects. This is expected to be small, $\lesssim 1^\circ$ [425–427], but is hard to quantify reliably and is usually not included in the quoted uncertainty.

Note that methods based on isospin symmetry make extensive use of measurements of branching fractions and CP asymmetries, for which averages are reported in Sec. 8. Note also that each method suffers from discrete ambiguities in the solutions. The model assumption in the $B^0 \rightarrow \pi^+\pi^-\pi^0$ analysis helps resolve some of the multiple solutions, and results in a single preferred value for α in $[0, \pi]$. All the above measurements correspond to the choice that is in agreement with the global CKM fit.

Independently from the constraints on $\alpha \equiv \phi_2$ obtained by the experiments, the results summarised in Sec. 5.11 are statistically combined to produce world average constraints on $\alpha \equiv \phi_2$. The combination is performed with the GAMMACOMBO framework [428] and follows a frequentist procedure, similar to that used by *BABAR* and Belle [424], and described in detail in Ref. [427].

The input measurements used in the combination are those listed above and are summarised in Table 45. Additional inputs, summarised in Table 46, for the branching fractions and (for $\rho\rho$) polarisation fractions, for the relevant modes and their isospin partners are taken from Sec. 8, whilst the ratio of B^+ to B^0 lifetimes is taken from Sec. 4. Individual measurements are used as inputs, rather than the HFLAV averages, in order to facilitate cross-checks and to ensure the most appropriate treatment of correlations. A combination based on HFLAV averages gives consistent results. Results on $B^0 \rightarrow a_1^\pm \pi^\mp$ decays are not included, as to do so requires additional theoretical assumptions, but as shown in Ref. [424] this does not significantly affect the average.

The fit has a χ^2 of 16.4 with 51 observables and 24 parameters. Using the χ^2 distribution, this corresponds to a p-value of 94.4% (or 0.1σ). A coverage check with pseudoexperiments gives a p-value of $(92.9 \pm 0.3)\%$.

The obtained world average for the Unitarity Triangle angle $\alpha \equiv \phi_2$ is

$$\alpha \equiv \phi_2 = (84.9 \pm 5.1)^\circ. \quad (166)$$

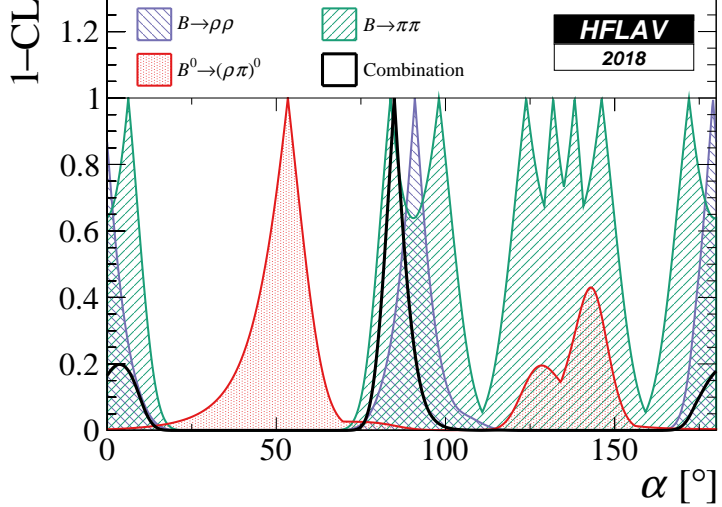


Figure 37: World average of $\alpha \equiv \phi_2$, in terms of $1-\text{CL}$, split by decay mode.

An ambiguous solution also exists at $\alpha \equiv \phi_2 \Leftrightarrow \alpha + \pi \equiv \phi_2 + \pi$. The quoted uncertainty does not include effects due to isospin-breaking. A secondary minimum close to zero is disfavoured, as discussed in Ref. [427]. Results split by decay mode are shown in Table 47 and Fig. 37.

5.12 Time-dependent CP asymmetries in $b \rightarrow c\bar{u}d/u\bar{c}d$ transitions

Non- CP eigenstates such as $D^\mp\pi^\pm$, $D^{*\mp}\pi^\pm$ and $D^\mp\rho^\pm$ can be produced in decays of B^0 mesons either via Cabibbo favoured ($b \rightarrow c$) or doubly Cabibbo suppressed ($b \rightarrow u$) tree amplitudes. Since no penguin contribution is possible, these modes are theoretically clean. The ratio of the magnitudes of the suppressed and favoured amplitudes, R , is sufficiently small (predicted to be about 0.02), that $\mathcal{O}(R^2)$ terms can be neglected, and the sine terms give sensitivity to the combination of UT angles $2\beta + \gamma$.

As described in Sec. 5.2.6, the averages are given in terms of the parameters a and c of Eq. (138). CP violation would appear as $a \neq 0$. Results for the $D^\mp\pi^\pm$ mode are available from *BABAR*, *Belle* and *LHCb*, while for $D^{*\mp}\pi^\pm$ *BABAR* and *Belle* have results with both full and partial reconstruction techniques. Results are also available from *BABAR* using $D^\mp\rho^\pm$. These results, and their averages, are listed in Table 48 and shown in Fig. 38. It is notable that the average value of a from $D^*\pi$ is more than 3σ from zero, providing evidence of CP violation in this channel.

For each mode, $D\pi$, $D^*\pi$ and $D\rho$, there are two measurements (a and c , or S^+ and S^-) that depend on three unknowns (R , δ and $2\beta + \gamma$), of which two are different for each decay mode. Therefore, there is not enough information to solve directly for $2\beta + \gamma$. Constraints can be obtained if one is willing to use theoretical input on the values of R and/or δ . One popular choice is the use of SU(3) symmetry to obtain R by relating the suppressed decay mode to B decays involving D_s mesons. More details can be found in Refs. [290, 430–433].

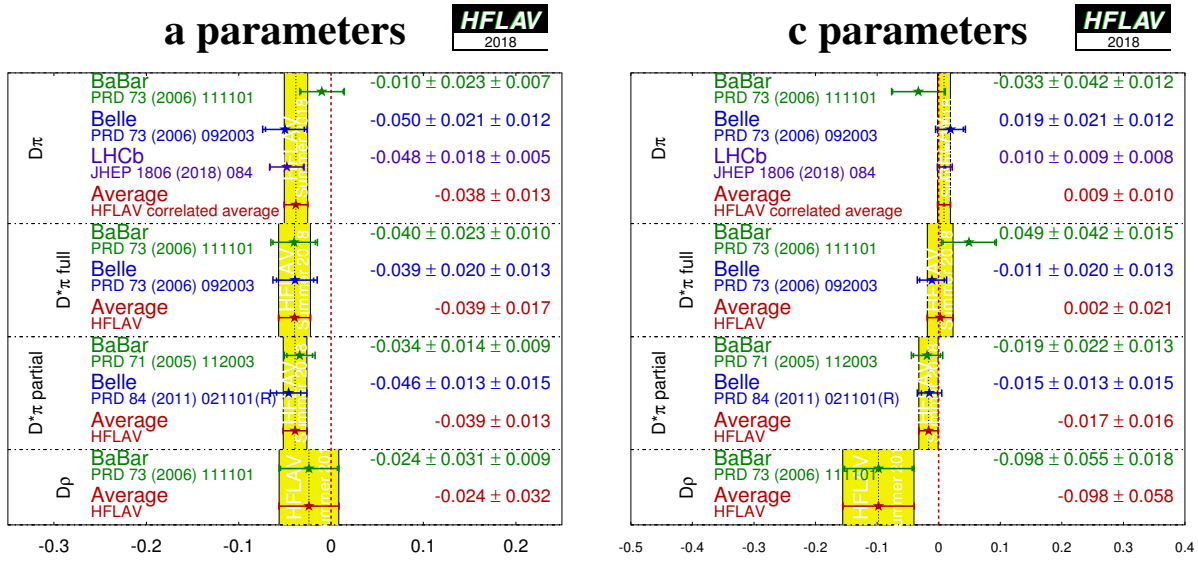


Figure 38: Averages for $b \rightarrow c\bar{u}d/u\bar{c}d$ modes.

Table 45: List of measurements used in the α combination. Results are obtained from either time-dependent (TD) CP asymmetries of decays to CP eigenstates or vector-vector final states, or time-integrated CP asymmetry measurements (CP). Results from time-dependent asymmetries in decays to self-conjugate three-body final states (TD-Dalitz) are also used in the form of the U and I parameters defined in Tab. 23.

B decay	Method	Parameters	Experiment	Ref.
$B^0 \rightarrow \pi^+ \pi^-$	TD	S_{CP}, C_{CP}	$BABAR$	[417]
			Belle	[418]
			LHCb	[393]
$B^0 \rightarrow \pi^0 \pi^0$	CP	C_{CP}	$BABAR$	[417]
			Belle	[429]
$B^0 \rightarrow \rho^+ \rho^-$	TD	S_{CP}, C_{CP}	$BABAR$	[409]
			Belle	[410]
$B^0 \rightarrow \rho^0 \rho^0$	TD	S_{CP}, C_{CP}	$BABAR$	[411]
$B^0 \rightarrow \pi^+ \pi^- \pi^0$	TD-Dalitz	$\{U, I\}$	$BABAR$	[277]
			Belle	[278]

Table 46: List of the auxiliary inputs used in the α combination.

Particle / Decay	Parameters	Source	Ref.
B^+/B^0	$\tau(B^+)/\tau(B^0)$	HFLAV	Sec. 4
$B^0 \rightarrow \pi^+ \pi^-$	BR	HFLAV	Sec. 8
$B^0 \rightarrow \pi^0 \pi^0$	BR	HFLAV	Sec. 8
$B^\pm \rightarrow \pi^\pm \pi^0$	BR	HFLAV	Sec. 8
$B^0 \rightarrow \rho^+ \rho^-$	BR, f_L	HFLAV	Sec. 8
$B^0 \rightarrow \rho^0 \rho^0$	BR, f_L	HFLAV	Sec. 8
$B^\pm \rightarrow \rho^\pm \rho^0$	BR, f_L	HFLAV	Sec. 8

 Table 47: Averages of $\alpha \equiv \phi_2$ split by B meson decay mode. Only solutions consistent with the obtained world average are shown.

Decay Mode	Value
$B \rightarrow \pi\pi$	$(84^{+21}_{-6})^\circ$
	$(98^{+7}_{-20})^\circ$
$B \rightarrow \rho\rho$	$(91 \pm 6)^\circ$
$B^0 \rightarrow (\rho\pi)^0$	$(53^{+8}_{-10})^\circ$

 Table 48: Averages for $b \rightarrow c\bar{u}d/u\bar{c}d$ modes.

Experiment	Sample size	a	c	Correlation
$D^\mp \pi^\pm$				
<i>BABAR</i> (full rec.)	[285] $N(B\bar{B}) = 232M$	$-0.010 \pm 0.023 \pm 0.007$	$-0.033 \pm 0.042 \pm 0.012$	—
<i>Belle</i> (full rec.)	[289] $N(B\bar{B}) = 386M$	$-0.050 \pm 0.021 \pm 0.012$	$0.019 \pm 0.021 \pm 0.012$	—
LHCb	[291] $\int \mathcal{L} dt = 3.0 \text{ fb}^{-1}$	$-0.048 \pm 0.018 \pm 0.005$	$0.010 \pm 0.009 \pm 0.008$	-0.46 (syst)
Average		-0.038 ± 0.013	0.009 ± 0.010	-0.05
Confidence level		0.56 (0.6 σ)		
$D^{*\mp} \pi^\pm$				
<i>BABAR</i> (full rec.)	[285] $N(B\bar{B}) = 232M$	$-0.040 \pm 0.023 \pm 0.010$	$0.049 \pm 0.042 \pm 0.015$	
<i>BABAR</i> (partial rec.)	[286] $N(B\bar{B}) = 232M$	$-0.034 \pm 0.014 \pm 0.009$	$-0.019 \pm 0.022 \pm 0.013$	
<i>Belle</i> (full rec.)	[289] $N(B\bar{B}) = 386M$	$-0.039 \pm 0.020 \pm 0.013$	$-0.011 \pm 0.020 \pm 0.013$	
<i>Belle</i> (partial rec.)	[288] $N(B\bar{B}) = 657M$	$-0.046 \pm 0.013 \pm 0.015$	$-0.015 \pm 0.013 \pm 0.015$	
Average		-0.039 ± 0.010	-0.010 ± 0.013	
Confidence level		0.97 (0.03 σ)		
$D^\mp \rho^\pm$				
<i>BABAR</i> (full rec.)	[285] $N(B\bar{B}) = 232M$	$-0.024 \pm 0.031 \pm 0.009$	$-0.098 \pm 0.055 \pm 0.018$	

5.13 Time-dependent CP asymmetries in $b \rightarrow c\bar{u}s/u\bar{c}s$ transitions

5.13.1 Time-dependent CP asymmetries in $B^0 \rightarrow D^\mp K_s^0 \pi^\pm$

Time-dependent analyses of transitions such as $B^0 \rightarrow D^\mp K_s^0 \pi^\pm$ can be used to probe $\sin(2\beta + \gamma)$ in a similar way to that discussed above (Sec. 5.12). Since the final state contains three particles, a Dalitz-plot analysis is necessary to maximise the sensitivity. *BABAR* [434] has carried out such an analysis. They obtain $2\beta + \gamma = (83 \pm 53 \pm 20)^\circ$ (with an ambiguity $2\beta + \gamma \leftrightarrow 2\beta + \gamma + \pi$) assuming the ratio of the $b \rightarrow u$ and $b \rightarrow c$ amplitude to be constant across the Dalitz plot at 0.3.

5.13.2 Time-dependent CP asymmetries in $B_s^0 \rightarrow D_s^\mp K^\pm$

Time-dependent analysis of $B_s^0 \rightarrow D_s^\mp K^\pm$ decays can be used to determine $\gamma - 2\beta_s$ [435, 436]. Compared to the situation for $B^0 \rightarrow D^{(*)\mp} \pi^\pm$ decays discussed in Sec. 5.12, the larger value of the ratio R of the magnitudes of the suppressed and favoured amplitudes allows it to be determined from the data. Moreover, the non-zero value of $\Delta\Gamma_s$ allows the determination of additional terms, labelled $A^{\Delta\Gamma}$ and $\bar{A}^{\Delta\Gamma}$, that break ambiguities in the solutions for $\gamma - 2\beta_s$.

LHCb [293] has measured the time-dependent CP violation parameters in $B_s^0 \rightarrow D_s^\mp K^\pm$ decays, using 3.0 fb^{-1} of data. The results are given in Table 49, and correspond to 3.8σ evidence for CP violation in the interference between mixing and $B_s^0 \rightarrow D_s^\mp K^\pm$ decays. From these results, and the world average constraint on $2\beta_s$ [1], LHCb determine $\gamma = (128_{-22}^{+17})^\circ$, $\delta_{D_s K} = (358_{-14}^{+13})^\circ$ and $R_{D_s K} = 0.37_{-0.09}^{+0.10}$.

Table 49: Results for $B_s^0 \rightarrow D_s^\mp K^\pm$.

Experiment	$\int \mathcal{L} dt$	C	$A^{\Delta\Gamma}$	$\bar{A}^{\Delta\Gamma}$	S	\bar{S}
LHCb [293]	3 fb^{-1}	$0.73 \pm 0.14 \pm 0.05$	$0.39 \pm 0.28 \pm 0.15$	$0.31 \pm 0.28 \pm 0.15$	$-0.52 \pm 0.20 \pm 0.07$	$-0.49 \pm 0.20 \pm 0.07$

5.14 Rates and asymmetries in $B \rightarrow D^{(*)} K^{(*)}$ decays

As explained in Sec. 5.2.7, rates and asymmetries in $B^+ \rightarrow D^{(*)} K^{(*)+}$ decays are sensitive to γ , and have negligible theoretical uncertainty [308]. Various methods using different $D^{(*)}$ final states have been used.

5.14.1 D decays to CP eigenstates

Results are available from *BABAR*, *Belle*, *CDF* and *LHCb* on GLW analyses in the decay mode $B^+ \rightarrow DK^+$. All experiments use the CP -even D decay final states K^+K^- and $\pi^+\pi^-$; *BABAR* and *Belle* in addition use the CP -odd decay modes $K_s^0\pi^0$, $K_s^0\omega$ and $K_s^0\phi$, though care is taken to avoid statistical overlap with the $K_s^0K^+K^-$ sample used for Dalitz plot analyses (see Sec. 5.14.4). *BABAR* and *Belle* also have results in the decay mode $B^+ \rightarrow D^*K^+$, using both the $D^* \rightarrow D\pi^0$ decay, for which $CP(D^*) = CP(D)$, and the $D^* \rightarrow D\gamma$ decay, for which $CP(D^*) = -CP(D)$. *LHCb* also have results in the $B^+ \rightarrow D^*K^+$ decay mode, exploiting a partial reconstruction technique in which the π^0 or γ produced in the D^* decay is not explicitly reconstructed. Results obtained with this technique have significant correlations, and therefore

a correlated average is performed for the $B^+ \rightarrow D^* K^+$ observables. In addition, *BABAR* and *LHCb* have results in the decay mode $B^+ \rightarrow DK^{*+}$, and *LHCb* has results in the decay mode $B^+ \rightarrow DK^+ \pi^+ \pi^-$. In many cases *LHCb* presents results separately for the cases of D decay to $K^+ K^-$ and $\pi^+ \pi^-$ to allow for possible effects related to $D^0 - \bar{D}^0$ mixing and CP violation in charm decays [437], which, however, are known to be small and are neglected in our averages. These separate results are presented together with their combination, as provided in the *LHCb* publications, where possible. The results and averages are given in Table 50 and shown in Fig. 39. *LHCb* has performed a GLW analysis using the $B^0 \rightarrow DK^{*0}$ decay with the CP -even $D \rightarrow K^+ K^-$ and $D \rightarrow \pi^+ \pi^-$ channels, which are also included in Table 50.

Table 50: Averages from GLW analyses of $b \rightarrow c\bar{s}/u\bar{s}$ modes. The sample size is given in terms of number of $B\bar{B}$ pairs, $N(B\bar{B})$, for the e^+e^- B factory experiments *BABAR* and *Belle*, and in terms of integrated luminosity, $\int \mathcal{L} dt$, for the hadron collider experiments *CDF* and *LHCb*.

Experiment		Sample size $N(B\bar{B})$ or $\int \mathcal{L} dt$	A_{CP+}	A_{CP-}	R_{CP+}	R_{CP-}
$B^+ \rightarrow D_{CP} K^+$						
<i>BABAR</i>	[438]	467M	$0.25 \pm 0.06 \pm 0.02$	$-0.09 \pm 0.07 \pm 0.02$	$1.18 \pm 0.09 \pm 0.05$	$1.07 \pm 0.08 \pm 0.04$
<i>Belle</i>	[439]	275M	$0.06 \pm 0.14 \pm 0.05$	$-0.12 \pm 0.14 \pm 0.05$	$1.13 \pm 0.16 \pm 0.08$	$1.17 \pm 0.14 \pm 0.14$
<i>CDF</i>	[440]	1 fb^{-1}	$0.39 \pm 0.17 \pm 0.04$	–	$1.30 \pm 0.24 \pm 0.12$	–
<i>LHCb KK</i>	[441]	5 fb^{-1}	$0.126 \pm 0.014 \pm 0.002$	–	$0.988 \pm 0.015 \pm 0.011$	–
<i>LHCb $\pi\pi$</i>	[441]	5 fb^{-1}	$0.115 \pm 0.025 \pm 0.007$	–	$0.992 \pm 0.027 \pm 0.015$	–
<i>LHCb average</i>	[441]	5 fb^{-1}	$0.124 \pm 0.012 \pm 0.002$	–	$0.989 \pm 0.013 \pm 0.010$	–
Average			0.129 ± 0.012	-0.10 ± 0.07	0.996 ± 0.016	1.09 ± 0.08
Confidence level			$0.17 (1.4\sigma)$	$0.86 (0.2\sigma)$	$0.26 (1.1\sigma)$	$0.65 (0.5\sigma)$
$B^+ \rightarrow D_{CP}^* K^+$						
<i>BABAR</i>	[442]	383M	$-0.11 \pm 0.09 \pm 0.01$	$0.06 \pm 0.10 \pm 0.02$	$1.31 \pm 0.13 \pm 0.03$	$1.09 \pm 0.12 \pm 0.04$
<i>Belle</i>	[439]	275M	$-0.20 \pm 0.22 \pm 0.04$	$0.13 \pm 0.30 \pm 0.08$	$1.41 \pm 0.25 \pm 0.06$	$1.15 \pm 0.31 \pm 0.12$
<i>LHCb</i>	[441]	5 fb^{-1}	$-0.151 \pm 0.033 \pm 0.011$	$0.276 \pm 0.094 \pm 0.047$	$1.138 \pm 0.029 \pm 0.016$	$0.902 \pm 0.087 \pm 0.112$
Average			-0.142 ± 0.032	0.15 ± 0.07	1.140 ± 0.031	1.03 ± 0.09
Confidence level				$0.67 (0.4\sigma)$		
$B^+ \rightarrow D_{CP} K^{*+}$						
<i>BABAR</i>	[443]	379M	$0.09 \pm 0.13 \pm 0.06$	$-0.23 \pm 0.21 \pm 0.07$	$2.17 \pm 0.35 \pm 0.09$	$1.03 \pm 0.27 \pm 0.13$
<i>LHCb KK</i>	[444]	4.8 fb^{-1}	$0.06 \pm 0.07 \pm 0.01$	–	$1.22 \pm 0.09 \pm 0.01$	–
<i>LHCb $\pi\pi$</i>	[444]	4.8 fb^{-1}	$0.15 \pm 0.13 \pm 0.02$	–	$1.08 \pm 0.14 \pm 0.03$	–
<i>LHCb average</i>	[444]	4.8 fb^{-1}	$0.08 \pm 0.06 \pm 0.01$	–	$1.18 \pm 0.08 \pm 0.02$	–
Average			0.08 ± 0.06	-0.23 ± 0.22	1.22 ± 0.07	1.03 ± 0.30
Confidence level			$0.83 (0.2\sigma)$		$0.02 (2.3\sigma)$	
$B^+ \rightarrow D_{CP} K^+ \pi^+ \pi^-$						
<i>LHCb KK</i>	[445]	3 fb^{-1}	$-0.045 \pm 0.064 \pm 0.011$	–	$1.043 \pm 0.069 \pm 0.034$	–
<i>LHCb $\pi\pi$</i>	[445]	3 fb^{-1}	$-0.054 \pm 0.101 \pm 0.011$	–	$1.035 \pm 0.108 \pm 0.038$	–
<i>LHCb average</i>	[445]	3 fb^{-1}	-0.048 ± 0.055	–	1.040 ± 0.064	–
$B^0 \rightarrow D_{CP} K^{*0}$						
<i>LHCb KK</i>	[446]	3 fb^{-1}	$-0.20 \pm 0.15 \pm 0.02$	–	$1.05^{+0.17}_{-0.15} \pm 0.04$	–
<i>LHCb $\pi\pi$</i>	[446]	3 fb^{-1}	$-0.09 \pm 0.22 \pm 0.02$	–	$1.21^{+0.28}_{-0.25} \pm 0.05$	–
Average			-0.16 ± 0.12	–	1.10 ± 0.14	–

As pointed out in Refs. [311, 312], a Dalitz plot analysis of $B^0 \rightarrow DK^+ \pi^-$ decays provides

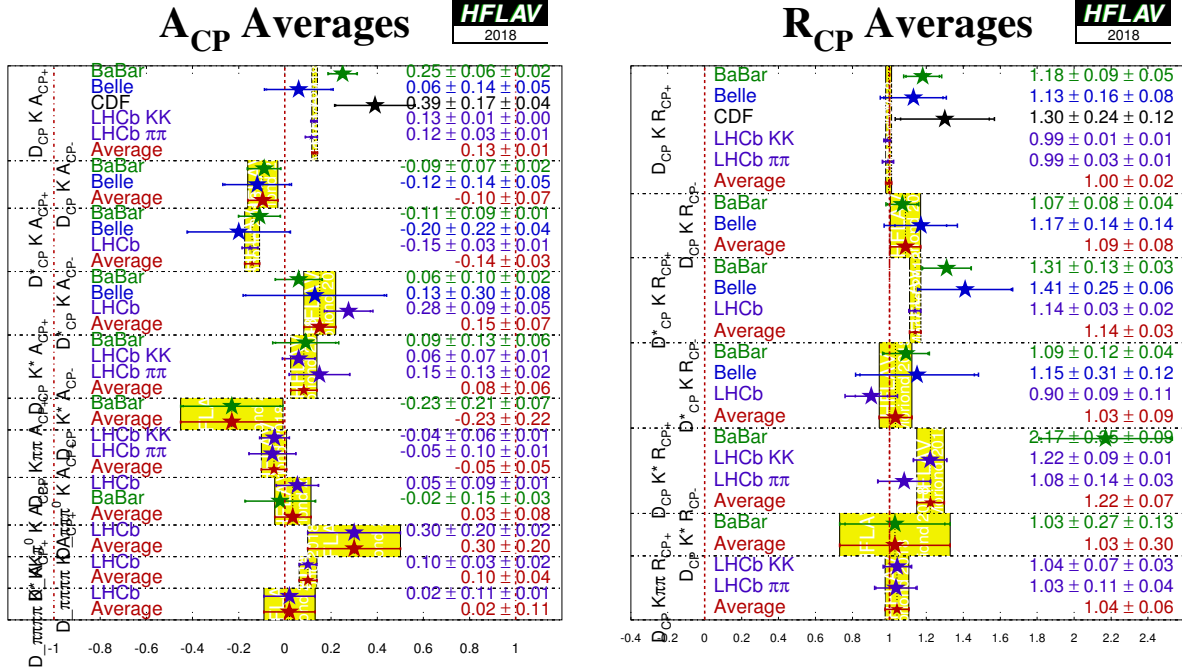


Figure 39: Averages of A_{CP} and R_{CP} from GLW analyses.

more sensitivity to $\gamma \equiv \phi_3$ than the Q2B DK^{*0} approach. The analysis provides direct sensitivity to the hadronic parameters r_B and δ_B associated with the $B^0 \rightarrow DK^{*0}$ decay amplitudes, rather than effective hadronic parameters averaged over the K^{*0} selection window as in the Q2B case.

Such an analysis has been performed by LHCb. A simultaneous fit is performed to the $B^0 \rightarrow DK^+\pi^-$ Dalitz plots with the neutral D meson reconstructed in the $K^+\pi^-$, K^+K^- and $\pi^+\pi^-$ final states. The reported results in Table 51 are for the Cartesian parameters, defined in Eq. (152) associated with the $B^0 \rightarrow DK^*(892)^0$ decay. Note that, since the measurements use overlapping data samples, these results cannot be combined with the LHCb results for GLW observables in $B^0 \rightarrow DK^*(892)^0$ decays reported in Table 50.

Table 51: Results from Dalitz plot analysis of $B^0 \rightarrow DK^+\pi^-$ decays with $D \rightarrow K^+K^-$ and $\pi^+\pi^-$.

Experiment	$\int \mathcal{L} dt$	x_+	y_+	x_-	y_-
LHCb [447]	3 fb^{-1}	$0.04 \pm 0.16 \pm 0.11$	$-0.47 \pm 0.28 \pm 0.22$	$-0.02 \pm 0.13 \pm 0.14$	$-0.35 \pm 0.26 \pm 0.41$

LHCb use these results to obtain confidence levels for γ , $r_B(DK^{*0})$ and $\delta_B(DK^{*0})$. In addition, results are reported for the hadronic parameters needed to relate these results to Q2B measurements of $B^0 \rightarrow DK^*(892)^0$ decays, where a selection window of $m(K^+\pi^-)$ within $50 \text{ MeV}/c^2$ of the pole mass and helicity angle satisfying $|\cos(\theta_{K^{*0}})| > 0.4$ is assumed. These parameters are the coherence factor κ , the ratio of Q2B and amplitude level r_B values, $\bar{R}_B = \bar{r}_B/r_B$, and

the difference between Q2B and amplitude level δ_B values, $\Delta\bar{\delta}_B = \bar{\delta}_B - \delta_B$. LHCb [447] obtain

$$\gamma = 0.958^{+0.005}_{-0.010}{}^{+0.002}_{-0.045}, \quad \bar{R}_B = 1.02^{+0.03}_{-0.01} \pm 0.06, \quad \Delta\bar{\delta}_B = 0.02^{+0.03}_{-0.02} \pm 0.11. \quad (167)$$

5.14.2 D decays to quasi- CP eigenstates

As discussed in Sec. 5.2.7, if a multibody neutral D meson decay can be shown to be dominated by one CP eigenstate, it can be used in a “GLW-like” (sometimes called “quasi-GLW”) analysis [316]. The same observables R_{CP} , A_{CP} as for the GLW case are measured, but an additional factor of $(2F_+ - 1)$, where F_+ is the fractional CP -even content, enters the expressions relating these observables to $\gamma \equiv \phi_3$. The F_+ factors have been measured using CLEO-c data to be $F_+(\pi^+\pi^-\pi^0) = 0.973 \pm 0.017$, $F_+(K^+K^-\pi^0) = 0.732 \pm 0.055$, $F_+(\pi^+\pi^-\pi^+\pi^-) = 0.737 \pm 0.028$ [448].

The GLW-like observables for $B^+ \rightarrow DK^+$ with $D \rightarrow \pi^+\pi^-\pi^0$, $K^+K^-\pi^0$ and $D \rightarrow \pi^+\pi^-\pi^+\pi^-$ have been measured by LHCb. The $A_{q\text{GLW}}$ observable for $B^+ \rightarrow DK^+$ with $D \rightarrow \pi^+\pi^-\pi^0$ was measured in an earlier analysis by *BABAR*, from which additional observables, discussed in Sec. 5.2.7 and reported in Table 56 below, were reported. The observables for $B^+ \rightarrow DK^{*+}$ with $D \rightarrow \pi^+\pi^-\pi^+\pi^-$ have also been measured by LHCb. The results are given in Table 52.

Table 52: Averages from GLW-like analyses of $b \rightarrow c\bar{s}/u\bar{s}$ modes.

Experiment		Sample size	$A_{q\text{GLW}}$	$R_{q\text{GLW}}$
		$D_{\pi^+\pi^-\pi^0} K^+$		
LHCb	[449]	$\int \mathcal{L} dt = 3 \text{ fb}^{-1}$	$0.05 \pm 0.09 \pm 0.01$	$0.98 \pm 0.11 \pm 0.05$
<i>BABAR</i>	[320]	$N(B\bar{B}) = 324\text{M}$	$-0.02 \pm 0.15 \pm 0.03$	–
Average			0.03 ± 0.08	0.98 ± 0.12
Confidence level			$0.68 (0.4\sigma)$	–
		$D_{K^+K^-\pi^0} K^+$		
LHCb	[449]	$\int \mathcal{L} dt = 3 \text{ fb}^{-1}$	$0.30 \pm 0.20 \pm 0.02$	$0.95 \pm 0.22 \pm 0.04$
		$D_{\pi^+\pi^-\pi^+\pi^-} K^+$		
LHCb	[450]	$\int \mathcal{L} dt = 3 \text{ fb}^{-1}$	$0.10 \pm 0.03 \pm 0.02$	$0.97 \pm 0.04 \pm 0.02$
		$D_{\pi^+\pi^-\pi^+\pi^-} K^{*+}$		
LHCb	[444]	$\int \mathcal{L} dt = 4.8 \text{ fb}^{-1}$	$0.02 \pm 0.11 \pm 0.01$	$1.08 \pm 0.13 \pm 0.03$

5.14.3 D decays to suppressed final states

For ADS analyses, all of *BABAR*, Belle, CDF and LHCb have studied the modes $B^+ \rightarrow DK^+$ and $B^+ \rightarrow D\pi^+$. *BABAR* has also analysed the $B^+ \rightarrow D^*K^+$ mode. There is an effective shift of π in the strong phase difference between the cases that the D^* is reconstructed as $D\pi^0$ and $D\gamma$ [313], therefore these modes are studied separately. In addition, *BABAR* has studied the $B^+ \rightarrow DK^{*+}$ mode, where K^{*+} is reconstructed as $K_s^0\pi^+$, and LHCb has studied the $B^+ \rightarrow DK^+\pi^+\pi^-$ mode. In all the above cases the suppressed decay $D \rightarrow K^-\pi^+$ has been used. *BABAR*, Belle and LHCb also have results using $B^+ \rightarrow DK^+$ with $D \rightarrow K^-\pi^+\pi^0$, while

LHCb has results using $B^+ \rightarrow DK^+$ with $D \rightarrow K^-\pi^+\pi^+\pi^-$. The results and averages are given in Table 53 and shown in Fig. 40.

Similar phenomenology as for $B \rightarrow DK$ decays holds for $B \rightarrow D\pi$ decays, although in this case the interference is between $b \rightarrow c\bar{u}d$ and $b \rightarrow u\bar{c}d$ transitions, and the ratio of suppressed to favoured amplitudes is expected to be much smaller, $\mathcal{O}(1\%)$. For most D meson final states this implies that the interference effect is too small to be of interest, but in the case of the ADS analysis it is possible that effects due to γ may be observable. Accordingly, the experiments now measure the corresponding observables in the $D\pi$ final states. The results and averages are given in Table 54 and shown in Fig. 41.

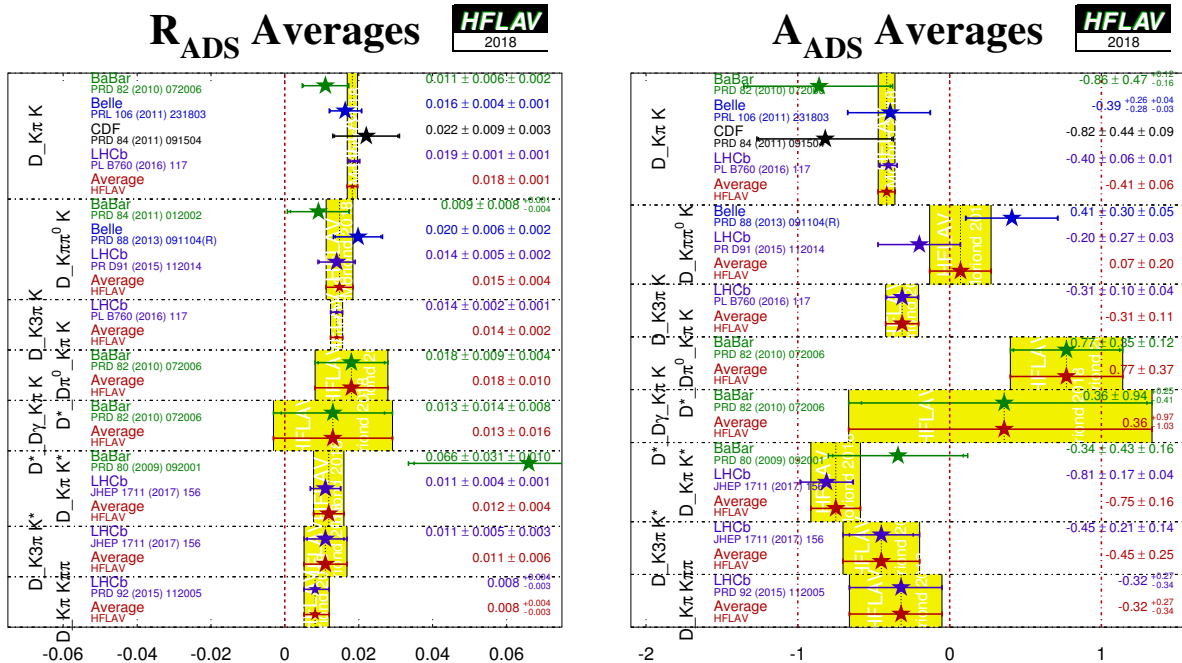


Figure 40: Averages of R_{ADS} and A_{ADS} for $B \rightarrow D^{(*)}K^{(*)}$ decays.

BABAR, *Belle* and *LHCb* have also presented results from a similar analysis method with self-tagging neutral B decays: $B^0 \rightarrow DK^{*0}$ with $D \rightarrow K^-\pi^+$ (all), $D \rightarrow K^-\pi^+\pi^0$ and $D \rightarrow K^-\pi^+\pi^+\pi^-$ (*BABAR* only). All these results are obtained with the $K^{*0} \rightarrow K^+\pi^-$ decay. Effects due to the natural width of the K^{*0} are handled using the parametrisation suggested by Gronau [309].

The following 95% CL limits are set by *BABAR* [456]:

$$R_{\text{ADS}}(K\pi) < 0.244 \quad R_{\text{ADS}}(K\pi\pi^0) < 0.181 \quad R_{\text{ADS}}(K\pi\pi\pi) < 0.391, \quad (168)$$

while *Belle* [457] obtain

$$R_{\text{ADS}}(K\pi) < 0.16. \quad (169)$$

The results from *LHCb*, which are presented in terms of the parameters R_+ and R_- instead of R_{ADS} and A_{ADS} , are given in Table 55.

Combining the results and using additional input from CLEO-c [458, 459] a limit on the ratio between the $b \rightarrow u$ and $b \rightarrow c$ amplitudes of $\bar{r}_B(DK^{*0}) \in [0.07, 0.41]$ at 95% CL limit

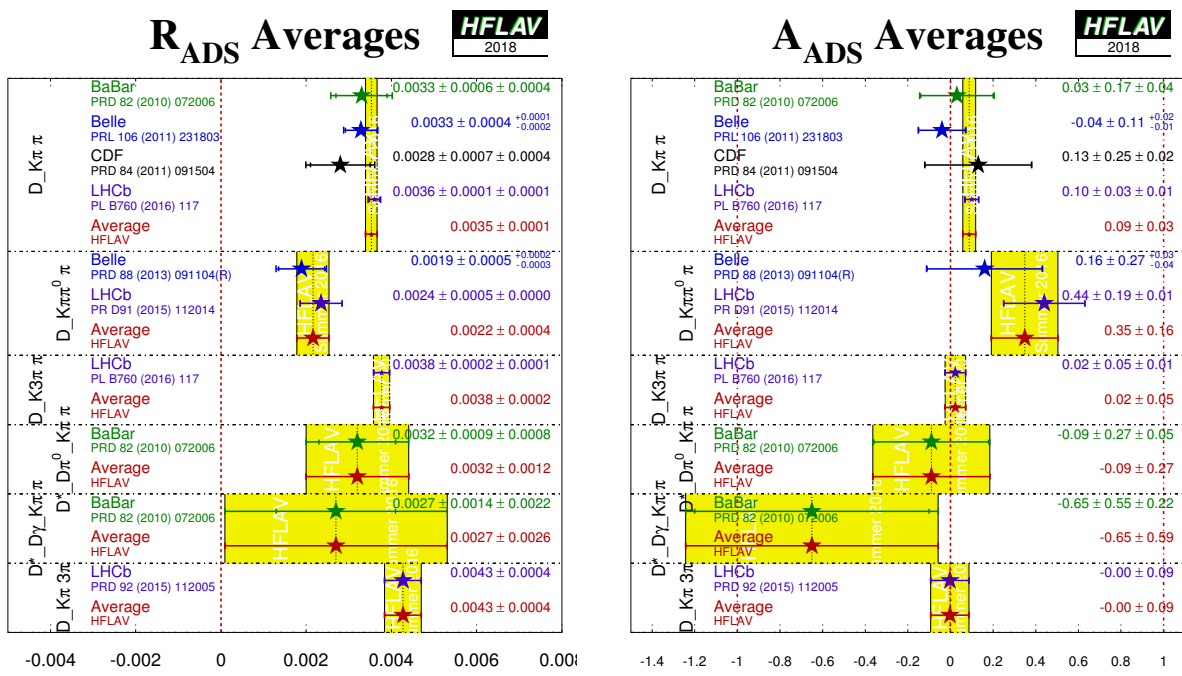


Figure 41: Averages of R_{ADS} and A_{ADS} for $B \rightarrow D^{(*)}\pi$ decays.

Table 53: Averages from ADS analyses of $b \rightarrow c\bar{s}/u\bar{s}$ modes.

Experiment		Sample size $N(B\bar{B})$ or $\int \mathcal{L} dt$	A_{ADS}	R_{ADS}
$DK^+, D \rightarrow K^-\pi^+$				
BABAR	[451]	467M	$-0.86 \pm 0.47^{+0.12}_{-0.16}$	$0.011 \pm 0.006 \pm 0.002$
Belle	[452]	772M	$-0.39^{+0.26}_{-0.28}{}^{+0.04}_{-0.03}$	$0.0163^{+0.0044}_{-0.0041}{}^{+0.0007}_{-0.0013}$
CDF	[453]	7 fb^{-1}	$-0.82 \pm 0.44 \pm 0.09$	$0.0220 \pm 0.0086 \pm 0.0026$
LHCb	[450]	3 fb^{-1}	$-0.403 \pm 0.056 \pm 0.011$	$0.0188 \pm 0.0011 \pm 0.0010$
Average			-0.415 ± 0.055	0.0183 ± 0.0014
Confidence level			$0.64 (0.5\sigma)$	$0.61 (0.5\sigma)$
$DK^+, D \rightarrow K^-\pi^+\pi^0$				
BABAR	[454]	474M	—	$0.0091^{+0.0082}_{-0.0076}{}^{+0.0014}_{-0.0037}$
Belle	[455]	772M	$0.41 \pm 0.30 \pm 0.05$	$0.0198 \pm 0.0062 \pm 0.0024$
LHCb	[449]	3 fb^{-1}	$-0.20 \pm 0.27 \pm 0.03$	$0.0140 \pm 0.0047 \pm 0.0019$
Average			0.07 ± 0.20	0.0148 ± 0.0036
Confidence level			$0.13 (1.5\sigma)$	$0.59 (0.5\sigma)$
$DK^+, D \rightarrow K^-\pi^+\pi^+\pi^-$				
LHCb	[450]	3 fb^{-1}	$-0.313 \pm 0.102 \pm 0.038$	$0.0140 \pm 0.0015 \pm 0.0006$
$D^*K^+, D^* \rightarrow D\pi^0, D \rightarrow K^-\pi^+$				
BABAR	[451]	467M	$0.77 \pm 0.35 \pm 0.12$	$0.018 \pm 0.009 \pm 0.004$
$D^*K^+, D^* \rightarrow D\gamma, D \rightarrow K^-\pi^+$				
BABAR	[451]	467M	$0.36 \pm 0.94^{+0.25}_{-0.41}$	$0.013 \pm 0.014 \pm 0.008$
$DK^{*+}, D \rightarrow K^-\pi^+, K^{*+} \rightarrow K_s^0\pi^+$				
BABAR	[443]	379M	$-0.34 \pm 0.43 \pm 0.16$	$0.066 \pm 0.031 \pm 0.010$
LHCb	[444]	4.8 fb^{-1}	$-0.81 \pm 0.17 \pm 0.04$	$0.011 \pm 0.004 \pm 0.001$
Average			-0.75 ± 0.16	0.012 ± 0.004
Confidence level			$0.34 (1.0\sigma)$	$0.09 (1.7\sigma)$
$DK^{*+}, D \rightarrow K^-\pi^+\pi^+\pi^-, K^{*+} \rightarrow K_s^0\pi^+$				
LHCb	[444]	4.8 fb^{-1}	$-0.45 \pm 0.21 \pm 0.14$	$0.011 \pm 0.005 \pm 0.003$
$DK^+\pi^+\pi^-, D \rightarrow K^-\pi^+$				
LHCb	[445]	3 fb^{-1}	$-0.32^{+0.27}_{-0.34}$	$0.0082^{+0.0038}_{-0.0030}$

Table 54: Averages from ADS analyses of $b \rightarrow c\bar{u}d/u\bar{c}d$ modes.

Experiment		Sample size $N(B\bar{B})$ or $\int \mathcal{L} dt$	A_{ADS}	R_{ADS}
$D\pi^+, D \rightarrow K^-\pi^+$				
BABAR	[451]	467M	$0.03 \pm 0.17 \pm 0.04$	$0.0033 \pm 0.0006 \pm 0.0004$
Belle	[452]	772M	$-0.04 \pm 0.11 {}^{+0.02}_{-0.01}$	$0.00328 {}^{+0.00038}_{-0.00036} {}^{+0.00012}_{-0.00018}$
CDF	[453]	7 fb^{-1}	$0.13 \pm 0.25 \pm 0.02$	$0.0028 \pm 0.0007 \pm 0.0004$
LHCb	[450]	3 fb^{-1}	$0.100 \pm 0.031 \pm 0.009$	$0.00360 \pm 0.00012 \pm 0.00009$
Average			0.088 ± 0.030	0.00353 ± 0.00014
Confidence level			0.66 (0.4σ)	0.68 (0.4σ)
$D\pi^+, D \rightarrow K^-\pi^+\pi^0$				
Belle	[455]	772M	$0.16 \pm 0.27 {}^{+0.03}_{-0.04}$	$0.00189 \pm 0.00054 {}^{+0.00022}_{-0.00025}$
LHCb	[449]	3 fb^{-1}	$0.44 \pm 0.19 \pm 0.01$	$0.00235 \pm 0.00049 \pm 0.00004$
Average			0.35 ± 0.16	0.00216 ± 0.00038
Confidence level			0.40 (0.8σ)	0.55 (0.6σ)
$D\pi^+, D \rightarrow K^-\pi^+\pi^+\pi^-$				
LHCb	[450]	3 fb^{-1}	$0.023 \pm 0.048 \pm 0.005$	$0.00377 \pm 0.00018 \pm 0.00006$
$D^*\pi^+, D^* \rightarrow D\pi^0, D \rightarrow K^-\pi^+$				
BABAR	[451]	467M	$-0.09 \pm 0.27 \pm 0.05$	$0.0032 \pm 0.0009 \pm 0.0008$
$D^*\pi^+, D^* \rightarrow D\gamma, D \rightarrow K^-\pi^+$				
BABAR	[451]	467M	$-0.65 \pm 0.55 \pm 0.22$	$0.0027 \pm 0.0014 \pm 0.0022$
$D\pi^+\pi^+\pi^-, D \rightarrow K^-\pi^+$				
LHCb	[445]	3 fb^{-1}	-0.003 ± 0.090	0.00427 ± 0.00043

 Table 55: Results from ADS analysis of $B^0 \rightarrow DK^{*0}, D \rightarrow K^-\pi^+$.

Experiment		Sample size	R_+	R_-
LHCb	[446]	$\int \mathcal{L} dt = 3 \text{ fb}^{-1}$	$0.06 \pm 0.03 \pm 0.01$	$0.06 \pm 0.03 \pm 0.01$

is set by *BABAR*. Belle set a limit of $\bar{r}_B < 0.4$ at 95% CL. LHCb take input from Sec. 9 and obtain $\bar{r}_B = 0.240^{+0.055}_{-0.048}$ (different from zero with 2.7σ significance).

5.14.4 D decays to multiparticle self-conjugate final states (model-dependent analysis)

For the model-dependent Dalitz plot analysis, both *BABAR* and Belle have studied the modes $B^+ \rightarrow DK^+$, $B^+ \rightarrow D^*K^+$ and $B^+ \rightarrow DK^{*+}$. For $B^+ \rightarrow D^*K^+$, both experiments have used both D^* decay modes, $D^* \rightarrow D\pi^0$ and $D^* \rightarrow D\gamma$, taking the effective shift in the strong phase difference into account.³³ In all cases the decay $D \rightarrow K_s^0\pi^+\pi^-$ has been used. *BABAR* also used the decay $D \rightarrow K_s^0K^+K^-$. LHCb has also studied $B^+ \rightarrow DK^+$ decays with $D \rightarrow K_s^0\pi^+\pi^-$. *BABAR* has also performed an analysis of $B^+ \rightarrow DK^+$ with $D \rightarrow \pi^+\pi^-\pi^0$. Results and averages are given in Table 56, and shown in Figs. 42 and 43. The third error on each measurement is due to D decay model uncertainty.

The parameters measured in the analyses are explained in Sec. 5.2.7. All experiments measure the Cartesian variables, defined in Eq. (152), and perform frequentist statistical procedures, to convert these into measurements of γ , r_B and δ_B . In the $B^+ \rightarrow DK^+$ with $D \rightarrow \pi^+\pi^-\pi^0$ analysis, the parameters (ρ^\pm, θ^\pm) are used instead.

In the $B^+ \rightarrow DK^{*+}$ analysis both *BABAR* and Belle experiments reconstruct K^{*+} as $K_s^0\pi^+$, but the treatment of possible nonresonant $K_s^0\pi^+$ differs: Belle assign an additional model uncertainty, while *BABAR* use a parametrisation suggested by Gronau [309] in which the parameters r_B and δ_B are replaced with effective parameters $\kappa\bar{r}_B$ and $\bar{\delta}_B$. In this case no attempt is made to extract the true hadronic parameters of the $B^+ \rightarrow DK^{*+}$ decay.

We perform averages using the following procedure, which is based on a set of reasonable, though imperfect, assumptions.

- It is assumed that effects due to differences in the D decay models used by the two experiments are negligible. Therefore, we do not rescale the results to a common model.
- It is further assumed that the D decay model uncertainty is 100% correlated between experiments. (This approximation is compromised by the fact that the *BABAR* results include $D \rightarrow K_s^0K^+K^-$ decays in addition to $D \rightarrow K_s^0\pi^+\pi^-$.) Other than the D decay model, we do not consider common sources of systematic uncertainty.
- We include in the average the effect of correlations within each experiment's set of measurements.
- At present it is unclear how to assign a model uncertainty to the average. We have not attempted to do so. An unknown amount of model uncertainty should be added to the final error.
- We follow the suggestion of Gronau [309] in making the DK^* averages. Explicitly, we assume that the selection of $K^{*+} \rightarrow K_s^0\pi^+$ is the same across experiments (so that κ, \bar{r}_B

³³ Belle [460] quote separate results for $B^+ \rightarrow D^*K^+$ with $D^* \rightarrow D\pi^0$ and $D^* \rightarrow D\gamma$. The results quoted in Table 56 are from our average, performed using the statistical correlations provided, and neglecting all systematic correlations; model uncertainties are not included. The first uncertainty on the quoted results is combined statistical and systematic, the second is the model error (taken from the Belle results on $B^+ \rightarrow D^*K^+$ with $D^* \rightarrow D\pi^0$).

and $\bar{\delta}_B$ are the same), and drop the additional source of model uncertainty assigned by Belle due to possible nonresonant decays.

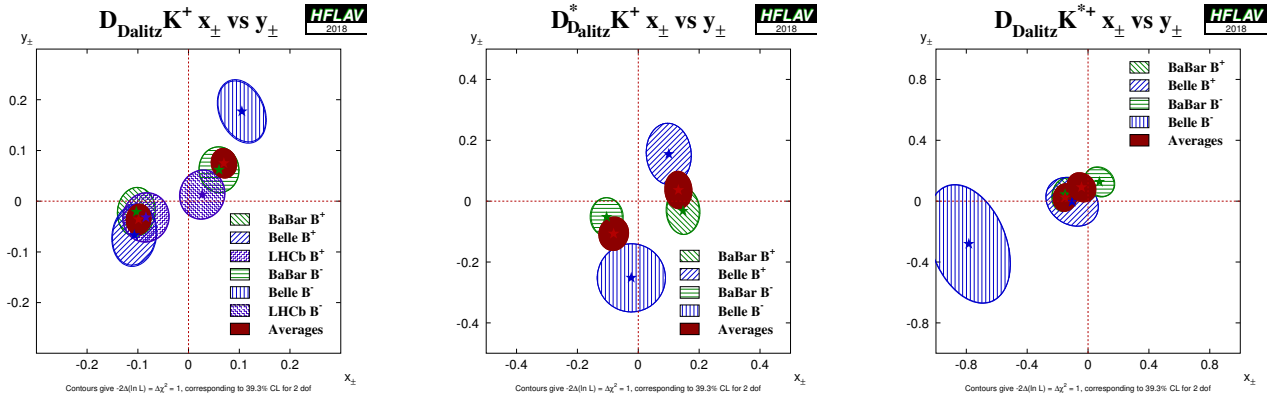


Figure 42: Contours in the (x_{\pm}, y_{\pm}) from model-dependent analysis of $B^+ \rightarrow D^{(*)}K^{(*)+}$, $D \rightarrow K_s^0 h^+ h^-$ ($h = \pi, K$). (Left) $B^+ \rightarrow DK^+$, (middle) $B^+ \rightarrow D^*K^+$, (right) $B^+ \rightarrow DK^{*+}$. Note that the uncertainties assigned to the averages given in these plots do not include model uncertainties.

Constraints on $\gamma \equiv \phi_3$

The measurements of (x_{\pm}, y_{\pm}) can be used to obtain constraints on $\gamma \equiv \phi_3$, as well as the hadronic parameters r_B and δ_B . BABAR [461], Belle [460, 463] and LHCb [462] have all done so using a frequentist procedure, with some differences in the details of the techniques used.

- BABAR obtain $\gamma = (68_{-14}^{+15} \pm 4 \pm 3)^\circ$ from DK^+ , D^*K^+ and DK^{*+} .
- Belle obtain $\phi_3 = (78_{-12}^{+11} \pm 4 \pm 9)^\circ$ from DK^+ and D^*K^+ .
- LHCb obtain $\gamma = (84_{-42}^{+49})^\circ$ from DK^+ using 1 fb^{-1} of data (a more precise result using 3 fb^{-1} and the model-independent method is reported below).
- The experiments also obtain values for the hadronic parameters as detailed in Table 57.
- In the BABAR analysis of $B^+ \rightarrow DK^+$ with $D \rightarrow \pi^+\pi^-\pi^0$ decays [320], a constraint of $-30^\circ < \gamma < 76^\circ$ is obtained at the 68% confidence level.
- The results discussed here are included in the HFLAV combination to obtain a world average value for $\gamma \equiv \phi_3$, as discussed in Sec. 5.14.7.

BABAR and LHCb have performed a similar analysis using the self-tagging neutral B decay $B^0 \rightarrow DK^{*0}$ (with $K^{*0} \rightarrow K^+\pi^-$). Effects due to the natural width of the K^{*0} are handled using the parametrisation suggested by Gronau [309]. LHCb [464] give results in terms of the Cartesian parameters, as shown in Table 56. BABAR [465] present results only in terms of γ and the hadronic parameters. The obtained constraints are:

- BABAR obtain $\gamma = (162 \pm 56)^\circ$;
- LHCb obtain $\gamma = (80_{-22}^{+21})^\circ$;
- Values for the hadronic parameters are given in Table 57.

Table 56: Averages from model-dependent Dalitz plot analyses of $b \rightarrow c\bar{u}s/u\bar{c}s$ modes. Note that the uncertainties assigned to the averages do not include model errors.

Experiment	Sample size	x_+	y_+	x_-	y_-
$DK^+, D \rightarrow K_s^0 \pi^+ \pi^-$					
BABAR [461]	$N(B\bar{B}) = 468M$	$-0.103 \pm 0.037 \pm 0.006 \pm 0.007$	$-0.021 \pm 0.048 \pm 0.004 \pm 0.009$	$0.060 \pm 0.039 \pm 0.007 \pm 0.006$	$0.062 \pm 0.045 \pm 0.004 \pm 0.006$
Belle [460]	$N(B\bar{B}) = 657M$	$-0.107 \pm 0.043 \pm 0.011 \pm 0.055$	$-0.067 \pm 0.059 \pm 0.018 \pm 0.063$	$0.105 \pm 0.047 \pm 0.011 \pm 0.064$	$0.177 \pm 0.060 \pm 0.018 \pm 0.054$
LHCb [462]	$\int \mathcal{L} dt = 1\text{fb}^{-1}$	$-0.084 \pm 0.045 \pm 0.009 \pm 0.005$	$-0.032 \pm 0.048^{+0.010}_{-0.009} \pm 0.008$	$0.027 \pm 0.044^{+0.010}_{-0.008} \pm 0.001$	$0.013 \pm 0.048^{+0.009}_{-0.007} \pm 0.003$
Average		-0.098 ± 0.024	-0.036 ± 0.030	0.070 ± 0.025	0.075 ± 0.029
Confidence level				$0.52 \text{ (0.7}\sigma)$	
$D^*K^+, D^* \rightarrow D\pi^0 \text{ or } D\gamma, D \rightarrow K_s^0 \pi^+ \pi^-$					
BABAR [461]	$N(B\bar{B}) = 468M$	$0.147 \pm 0.053 \pm 0.017 \pm 0.003$	$-0.032 \pm 0.077 \pm 0.008 \pm 0.006$	$-0.104 \pm 0.051 \pm 0.019 \pm 0.002$	$-0.052 \pm 0.063 \pm 0.009 \pm 0.007$
Belle [460]	$N(B\bar{B}) = 657M$	$0.100 \pm 0.074 \pm 0.081$	$0.155 \pm 0.101 \pm 0.063$	$-0.023 \pm 0.112 \pm 0.090$	$-0.252 \pm 0.112 \pm 0.049$
Average		0.132 ± 0.044	0.037 ± 0.061	-0.081 ± 0.049	-0.107 ± 0.055
Confidence level				$0.22 \text{ (1.2}\sigma)$	
$DK^{*+}, D \rightarrow K_s^0 \pi^+ \pi^-$					
BABAR [461]	$N(B\bar{B}) = 468M$	$-0.151 \pm 0.083 \pm 0.029 \pm 0.006$	$0.045 \pm 0.106 \pm 0.036 \pm 0.008$	$0.075 \pm 0.096 \pm 0.029 \pm 0.007$	$0.127 \pm 0.095 \pm 0.027 \pm 0.006$
Belle [463]	$N(B\bar{B}) = 386M$	$-0.105^{+0.177}_{-0.167} \pm 0.006 \pm 0.088$	$-0.004^{+0.164}_{-0.156} \pm 0.013 \pm 0.095$	$-0.784^{+0.249}_{-0.295} \pm 0.029 \pm 0.097$	$-0.281^{+0.440}_{-0.335} \pm 0.046 \pm 0.086$
Average		-0.152 ± 0.077	0.024 ± 0.091	-0.043 ± 0.094	0.091 ± 0.096
Confidence level				$0.011 \text{ (2.5}\sigma)$	
$DK^{*0}, D \rightarrow K_s^0 \pi^+ \pi^-, K^{*0} \rightarrow K^+ \pi^-$					
LHCb [464]	$\int \mathcal{L} dt = 3\text{ fb}^{-1}$	$0.05 \pm 0.24 \pm 0.04 \pm 0.01$	$-0.65^{+0.24}_{-0.23} \pm 0.08 \pm 0.01$	$-0.15 \pm 0.14 \pm 0.03 \pm 0.01$	$0.25 \pm 0.15 \pm 0.06 \pm 0.01$
$DK^+, D \rightarrow \pi^+ \pi^- \pi^0$					
Experiment	$N(B\bar{B})$	ρ^+	θ^+	ρ^-	θ^-
BABAR [320]	$324M$	$0.75 \pm 0.11 \pm 0.04$	$147 \pm 23 \pm 1$	$0.72 \pm 0.11 \pm 0.04$	$173 \pm 42 \pm 2$

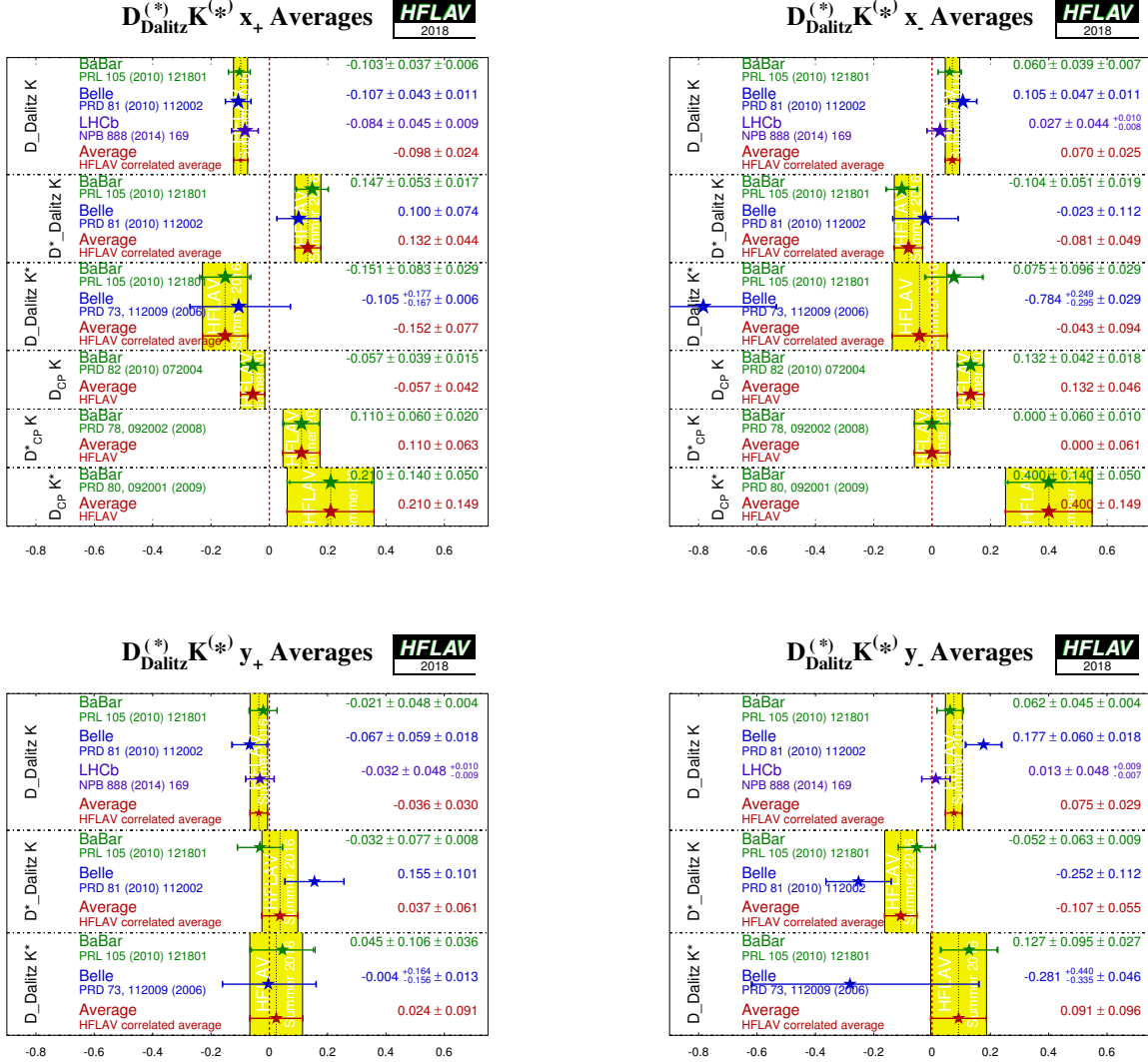


Figure 43: Averages of (x_{\pm}, y_{\pm}) from model-dependent analyses of $B^+ \rightarrow D^{(*)}K^{(*)+}$ with $D \rightarrow K_s h^+ h^-$ ($h = \pi, K$). (Top left) x_+ , (top right) x_- , (bottom left) y_+ , (bottom right) y_- . The top plots include constraints on x_{\pm} obtained from GLW analyses (see Sec. 5.14.1). Note that the uncertainties assigned to the averages given in these plots do not include model uncertainties.

5.14.5 D decays to multiparticle self-conjugate final states (model-independent analysis)

A model-independent approach to the analysis of $B^+ \rightarrow D^{(*)}K^+$ with multibody D decays was proposed by Giri, Grossman, Soffer and Zupan [306], and further developed by Bondar and Poluektov [317, 318]. The method relies on information on the average strong phase difference between D^0 and \bar{D}^0 decays in bins of Dalitz plot position that can be obtained from quantum-correlated $\psi(3770) \rightarrow D^0 \bar{D}^0$ events. This information is measured in the form of parameters c_i and s_i that are the weighted averages of the cosine and sine of the strong phase difference in a Dalitz plot bin labelled by i , respectively. These quantities have been obtained for $D \rightarrow$

Table 57: Summary of constraints on hadronic parameters from model-dependent analyses of $B^+ \rightarrow D^{(*)}K^{(*)+}$ and $B^0 \rightarrow DK^{*0}$ decays. Note the alternative parametrisation of the hadronic parameters used by *BABAR* in the DK^{*+} mode.

Experiment	Sample size	r_B	δ_B
In DK^+			
<i>BABAR</i> [461]	$N(B\bar{B}) = 468M$	$0.096 \pm 0.029 \pm 0.005 \pm 0.004$	$(119_{-20}^{+19} \pm 3 \pm 3)^\circ$
Belle [460]	$N(B\bar{B}) = 657M$	$0.160_{-0.038}^{+0.040} \pm 0.011_{-0.010}^{+0.05}$	$(138_{-16}^{+13} \pm 4 \pm 23)^\circ$
LHCb [462]	$\int \mathcal{L} dt = 1\text{fb}^{-1}$	0.06 ± 0.04	$(115_{-51}^{+41})^\circ$
In D^*K^+			
<i>BABAR</i> [461]	$N(B\bar{B}) = 468M$	$0.133_{-0.039}^{+0.042} \pm 0.014 \pm 0.003$	$(-82 \pm 21 \pm 5 \pm 3)^\circ$
Belle [460]	$N(B\bar{B}) = 657M$	$0.196_{-0.069}^{+0.072} \pm 0.012_{-0.012}^{+0.062}$	$(342_{-21}^{+19} \pm 3 \pm 23)^\circ$
\bar{r}_B			
In DK^{*+}			
<i>BABAR</i> [461]	$N(B\bar{B}) = 468M$	$\kappa\bar{r}_B = 0.149_{-0.062}^{+0.066} \pm 0.026 \pm 0.006$	$(111 \pm 32 \pm 11 \pm 3)^\circ$
Belle [463]	$N(B\bar{B}) = 386M$	$0.56_{-0.16}^{+0.22} \pm 0.04 \pm 0.08$	$(243_{-23}^{+20} \pm 3 \pm 50)^\circ$
In DK^{*0}			
<i>BABAR</i> [465]	$N(B\bar{B}) = 371M$	< 0.55 at 95% probability	$(62 \pm 57)^\circ$
LHCb [464]	$\int \mathcal{L} dt = 3\text{fb}^{-1}$	0.39 ± 0.13	$(197_{-20}^{+24})^\circ$

$K_s^0\pi^+\pi^-$ (and $D \rightarrow K_s^0K^+K^-$) decays by CLEO-c [258, 466].

Belle [467] and LHCb [468, 469] have used the model-independent Dalitz-plot analysis approach to study the mode $B^+ \rightarrow DK^+$. LHCb have presented results separately for two subsamples of their data, with the averaged result also given. Both Belle [470] and LHCb [471] have also used this approach to study $B^0 \rightarrow DK^*(892)^0$ decays. In both cases, the experiments use $D \rightarrow K_s^0\pi^+\pi^-$ decays, and LHCb has also included the $D \rightarrow K_s^0K^+K^-$ decay. The Cartesian variables (x_\pm, y_\pm) , defined in Eq. (152), were determined from the data. Note that due to the strong statistical and systematic correlations with the model-dependent results given in Sec. 5.14.4, these sets of results cannot be combined.

The results and averages are given in Table 58, and shown in Figs. 44. Most results have three sets of errors, which are, respectively, statistical, systematic, and the uncertainty coming from the knowledge of c_i and s_i . To perform the average, we first remove the last uncertainty, which should be 100% correlated between the measurements. Since the size of the uncertainty from c_i and s_i is found to depend on the size of the $B \rightarrow DK$ data sample, we assign the LHCb uncertainties (which are mostly the smaller of the Belle and LHCb values) to the averaged result. This procedure should be conservative. In the LHCb $B^0 \rightarrow DK^*(892)^0$ results [471], the values of c_i and s_i are constrained to their measured values within uncertainties in the fit to data, and hence the systematic uncertainties associated with the knowledge of these parameters is absorbed in their statistical uncertainties. The $B^0 \rightarrow DK^*(892)^0$ average is performed neglecting the model uncertainties on the Belle results.

Constraints on $\gamma \equiv \phi_3$

The measurements of (x_\pm, y_\pm) can be used to obtain constraints on γ , as well as the hadronic

Table 58: Averages from model-independent Dalitz plot analyses of $b \rightarrow c\bar{u}s/u\bar{c}s$ modes.

Experiment	Sample size	x_+	y_+	x_-	y_-
$DK^+, D \rightarrow K_s^0 \pi^+ \pi^-$					
Belle	[467] $N(B\bar{B}) = 772M$	$-0.110 \pm 0.043 \pm 0.014 \pm 0.007$	$-0.050^{+0.052}_{-0.055} \pm 0.011 \pm 0.007$	$0.095 \pm 0.045 \pm 0.014 \pm 0.010$	$0.137^{+0.053}_{-0.057} \pm 0.015 \pm 0.023$
LHCb Run 1	[468] $\int \mathcal{L} dt = 3\text{fb}^{-1}$	$-0.077 \pm 0.024 \pm 0.010 \pm 0.004$	$-0.022 \pm 0.025 \pm 0.004 \pm 0.010$	$0.025 \pm 0.025 \pm 0.010 \pm 0.005$	$0.075 \pm 0.029 \pm 0.005 \pm 0.014$
LHCb Run 2	[469] $\int \mathcal{L} dt = 2\text{fb}^{-1}$	$-0.077 \pm 0.019 \pm 0.007 \pm 0.004$	$-0.010 \pm 0.019 \pm 0.004 \pm 0.009$	$0.090 \pm 0.017 \pm 0.007 \pm 0.004$	$0.021 \pm 0.022 \pm 0.005 \pm 0.011$
LHCb combined	[469] $\int \mathcal{L} dt = 5\text{fb}^{-1}$	-0.078 ± 0.017	-0.014 ± 0.017	0.070 ± 0.017	0.041 ± 0.020
Average		$-0.081 \pm 0.015 \pm 0.004$	$-0.017 \pm 0.015 \pm 0.009$	$0.072 \pm 0.014 \pm 0.004$	$0.050 \pm 0.017 \pm 0.011$
Confidence level				$0.28 \text{ (1.1}\sigma)$	
$DK^{*0}, D \rightarrow K_s^0 \pi^+ \pi^-$					
Belle	[470] $N(B\bar{B}) = 772M$	$0.1^{+0.7+0.0}_{-0.4-0.1} \pm 0.1$	$0.3^{+0.5+0.0}_{-0.8-0.1} \pm 0.1$	$0.4^{+1.0+0.0}_{-0.6-0.1} \pm 0.0$	$-0.6^{+0.8+0.1}_{-1.0-0.0} \pm 0.1$
LHCb	[471] $\int \mathcal{L} dt = 3\text{fb}^{-1}$	$0.05 \pm 0.35 \pm 0.02$	$-0.81 \pm 0.28 \pm 0.06$	$-0.31 \pm 0.20 \pm 0.04$	$0.31 \pm 0.21 \pm 0.05$
Average		0.10 ± 0.30	-0.63 ± 0.26	-0.27 ± 0.20	0.27 ± 0.21
Confidence level				$0.38 \text{ (0.9}\sigma)$	

Table 59: Results from model-independent Dalitz plot analysis of $B^+ \rightarrow DK^+$, $D \rightarrow K_s^0 K^\pm \pi^\mp$.

Experiment	$\int \mathcal{L} dt$	R_{SS}	R_{OS}	$A_{\text{SS},DK}$	$A_{\text{OS},DK}$	$A_{\text{SS},D\pi}$	$A_{\text{OS},D\pi}$	
LHCb	[472]	3 fb^{-1}	$0.092 \pm 0.009 \pm 0.004$	$0.066 \pm 0.009 \pm 0.002$	$D \rightarrow K_s^0 K^\pm \pi^\mp$ (whole Dalitz plot) $0.040 \pm 0.091 \pm 0.018$	$0.233 \pm 0.129 \pm 0.024$	$-0.025 \pm 0.024 \pm 0.010$	$-0.052 \pm 0.029 \pm 0.017$
LHCb	[472]	3 fb^{-1}	$0.084 \pm 0.011 \pm 0.003$	$0.056 \pm 0.013 \pm 0.002$	$D \rightarrow K^*(892)^\pm K^\mp$ $0.026 \pm 0.109 \pm 0.029$	$0.336 \pm 0.208 \pm 0.026$	$-0.012 \pm 0.028 \pm 0.010$	$-0.054 \pm 0.043 \pm 0.017$

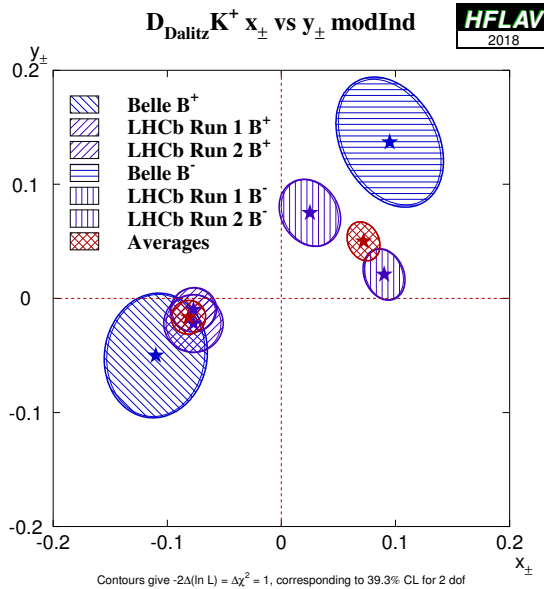


Figure 44: Contours in the (x_{\pm}, y_{\pm}) plane from model-independent analysis of $B^+ \rightarrow DK^+$ with $D \rightarrow K_s^0 h^+ h^-$ ($h = \pi, K$).

Table 60: Summary of constraints on hadronic parameters from model-independent analyses of $B^+ \rightarrow DK^+$ and $B^0 \rightarrow DK^{*0}$, $D \rightarrow K_s^0 h^+ h^-$ ($h = \pi, K$) decays.

Experiment	Sample size	$r_B(DK^+)$	$\delta_B(DK^+)$
Belle [467]	$N(B\bar{B}) = 772M$	$0.145 \pm 0.030 \pm 0.010 \pm 0.011$	$(129.9 \pm 15.0 \pm 3.8 \pm 4.7)^\circ$
LHCb [469]	$\int \mathcal{L} dt = 5\text{fb}^{-1}$	0.080 ± 0.011	$(110 \pm 10)^\circ$
$\bar{r}_B(DK^{*0})$			$\bar{\delta}_B(DK^{*0})$
Belle [470]	$N(B\bar{B}) = 772M$	< 0.87 at 68% confidence level	
LHCb [471]	$\int \mathcal{L} dt = 3\text{fb}^{-1}$	0.56 ± 0.17	$(204^{+21}_{-20})^\circ$

parameters r_B and δ_B . The experiments have done so using frequentist procedures, with some differences in the details of the techniques used.

- From $B^+ \rightarrow DK^+$, Belle [467] obtain $\phi_3 = (77.3^{+15.1}_{-14.9} \pm 4.1 \pm 4.3)^\circ$.
- From $B^+ \rightarrow DK^+$, LHCb [469] obtain $\gamma = (80^{+10}_{-9})^\circ$.
- From $B^0 \rightarrow DK^*(892)^0$, LHCb [471] obtain $\gamma = (71 \pm 20)^\circ$.
- The experiments also obtain values for the hadronic parameters as detailed in Table 60.
- The results discussed here are included in the HFLAV combination to obtain a world average value for $\gamma \equiv \phi_3$, as discussed in Sec. 5.14.7.

5.14.6 D decays to multiparticle non-self-conjugate final states (model-independent analysis)

Following the original suggestion of Grossman, Ligeti and Soffer [315], decays of D mesons to $K_s^0 K^\pm \pi^\mp$ can be used in a similar approach to that discussed above to determine $\gamma \equiv \phi_3$. Since these decays are less abundant, the event samples available to date have not been sufficient for a fine binning of the Dalitz plots, but the analysis can be performed using only an overall coherence factor and related strong phase difference for the decay. These quantities have been determined by CLEO-c [473] both for the full Dalitz plots and in a restricted region ± 100 MeV/ c^2 around the peak of the $K^*(892)^\pm$ resonance.

LHCb [472] has reported results of an analysis of $B^+ \rightarrow DK^+$ and $B^+ \rightarrow D\pi^+$ decays with $D \rightarrow K_s^0 K^\pm \pi^\mp$. The decays with different final states of the D meson are distinguished by the charge of the kaon from the decay of the D meson relative to the charge of the B meson, and are labelled “same sign” (SS) and “opposite sign” (OS). Six observables potentially sensitive to $\gamma \equiv \phi_3$ are measured: two ratios of rates for DK and $D\pi$ decays (one each for SS and OS) and four asymmetries (for DK and $D\pi$, SS and OS). This is done both for the full Dalitz plot of the D decay and for the $K^*(892)^\pm$ -dominated region (with the same boundaries as used by CLEO-c). Note that there is a significant overlap of events between the two samples. The results, shown in Table 59, do not yet have sufficient precision to set significant constraints on $\gamma \equiv \phi_3$.

5.14.7 Combinations of results on rates and asymmetries in $B \rightarrow D^{(*)} K^{(*)}$ decays to obtain constraints on $\gamma \equiv \phi_3$

BABAR and LHCb have both produced constraints on $\gamma \equiv \phi_3$ from combinations of their results on $B^+ \rightarrow DK^+$ and related processes. The experiments use a frequentist procedure, with some differences in the details of the techniques used.

- *BABAR* [474] use results from DK , D^*K and DK^* modes with GLW, ADS and GGSZ analyses, to obtain $\gamma = (69_{-16}^{+17})^\circ$.
- LHCb [475, 476] use results from the DK^+ mode with GLW, GLW-like, ADS, GGSZ ($K_s^0 h^+ h^-$) and GLS ($K_s^0 K^\pm \pi^\mp$) analyses, as well as DK^{*0} with GLW, ADS and GGSZ analyses, $DK^+ \pi^-$ GLW Dalitz plot analysis, $DK^+ \pi^- \pi^+$ with GLW and ADS analyses and $B_s^0 \rightarrow D_s^\mp K^\pm$ decays. The LHCb combination takes into account subleading effects due to charm mixing and CP violation [437]. The result is $\gamma = (74.0_{-5.8}^{+5.0})^\circ$.
- All the combinations use inputs determined from $\psi(3770) \rightarrow D^0 \bar{D}^0$ data samples (and/or from the HFLAV global fits on charm mixing parameters; see Sec. 9.1) to constrain the hadronic parameters in the charm system.
- Constraints are also obtained on the hadronic parameters involved in the decays. A summary of these is given in Table 61.
- The CKMfitter [244] and UTfit [337] groups perform similar combinations of all available results to obtain combined constraints on $\gamma \equiv \phi_3$.

Independently from the constraints on $\gamma \equiv \phi_3$ obtained by the experiments, the results summarised in Sec. 5.14 are statistically combined to produce world average constraints on $\gamma \equiv \phi_3$

Table 61: Summary of constraints on hadronic parameters obtained from global combinations of results in $B^+ \rightarrow D^{(*)}K^{(*)+}$ and $B^0 \rightarrow DK^{*0}$ decays. Results for parameters associated with the other decay modes discussed in this section are less precise and are not included in this summary.

Experiment		$r_B(DK^+)$	$\delta_B(DK^+)$	$r_B(D^*K^+)$	$\delta_B(D^*K^+)$
<i>BABAR</i>	[474]	$0.092^{+0.013}_{-0.012}$	$(105^{+16}_{-17})^\circ$	$0.106^{+0.019}_{-0.036}$	$(294^{+21}_{-31})^\circ$
<i>LHCb</i>	[476]	0.1019 ± 0.0056	$(142.6^{+5.7}_{-6.6})^\circ$	$0.191^{+0.045}_{-0.038}$	$(332^{+8}_{-10})^\circ$

and the hadronic parameters involved. The combination is performed with the GAMMA COMBO framework [428] and follows a frequentist procedure, identical to that used in Ref. [477].

The input measurements used in the combination are listed in Table 62. Individual measurements are used as inputs, rather than the averages presented in Sec. 5.14, in order to facilitate cross-checks and to ensure the most appropriate treatment of correlations. A combination based on our averages for each of the quantities measured by experiments gives consistent results.

All results from GLW and GLW-like analyses of $B^+ \rightarrow D^{(*)}K^{(*)+}$ modes, as listed in Tables 50 and 52, are used. All results from ADS analyses of $B^+ \rightarrow D^{(*)}K^{(*)+}$ as listed in Table 53 are also used. Regarding $B^0 \rightarrow DK^{*0}$ decays, the results of the $B^0 \rightarrow DK^+\pi^-$ GLW-Dalitz analysis (Table 51) are included, as are the LHCb results of the ADS analysis of $B^0 \rightarrow DK^{*0}$ (Table 55). Concerning results of GGSZ analyses of $B^+ \rightarrow D^{(*)}K^{(*)+}$ with $D \rightarrow K_s^0 h^+ h^-$, the model-dependent results, as listed in Table 56, are used for the *BABAR* and Belle experiments, whilst the model-independent results, as listed in Table 58, are used for LHCb. This choice is made in order to maintain consistency of the approach across experiments whilst maximising the size of the samples used to obtain inputs for the combination. For GGSZ analyses of $B^0 \rightarrow DK^{*0}$ with $D \rightarrow K_s^0 h^+ h^-$, the model-independent result from LHCb (given in Table 58) is used for consistency with the treatment of the LHCb $B^+ \rightarrow DK^+$ GGSZ result; the model-independent result by Belle is also included. Finally, results from the time-dependent analysis of $B_s^0 \rightarrow D_s^\mp K^\pm$ from LHCb (Table 49) are used.

Several results with sensitivity to γ are not included in the combination. Results from time-dependent analyses of $B^0 \rightarrow D^{(*)\mp}\pi^\pm$ and $D^\mp\rho^\pm$ (Table 48) are not used, as there are insufficient constraints on the associated hadronic parameters. Similarly, results from $B^0 \rightarrow D^\mp K_s^0 \pi^\pm$ (Sec. 5.13.1) are not used. Results from the LHCb $B^0 \rightarrow DK^{*0}$ GLW analysis (Table 50) are not used because of the statistical overlap with the GLW-Dalitz analysis, which is used instead. Limits on ADS parameters reported in Sec. 5.14.3 are not used. Results on $B^+ \rightarrow D\pi^+$ decays, given in Table 54, are not used, since the small value of $r_B(D\pi^+)$ means that these channels have less sensitivity to γ and are more vulnerable to biases from subleading effects [475]. Results from the *BABAR* Dalitz plot analysis of $B^+ \rightarrow DK^+$ with $D \rightarrow \pi^+\pi^-\pi^0$ (given in Table 56) are not included due to their limited sensitivity. Results from the $B^+ \rightarrow DK^+$, $D \rightarrow K_s^0\pi^+\pi^-$ GGSZ model-dependent analysis by LHCb (given in Table 56), and of the model-independent analysis of the same decay by Belle (given in Table 58) are not included due to the statistical overlap with results from model-(in)dependent analyses of the same data.

Table 62: List of measurements used in the γ combination.

B decay	D decay	Method	Experiment	Ref.
-----------	-----------	--------	------------	------

List of measurements used in the γ combination – continued from previous page.

$B^+ \rightarrow DK^+$	$D \rightarrow K^+K^-$, $D \rightarrow \pi^+\pi^-$, $D \rightarrow K_s^0\pi^0$, $D \rightarrow K_s^0\omega$, $D \rightarrow K_s^0\phi$	GLW	<i>BABAR</i>	[438]
$B^+ \rightarrow DK^+$	$D \rightarrow K^+K^-$, $D \rightarrow \pi^+\pi^-$, $D \rightarrow K_s^0\pi^0$, $D \rightarrow K_s^0\omega$, $D \rightarrow K_s^0\phi$	GLW	Belle	[439]
$B^+ \rightarrow DK^+$	$D \rightarrow K^+K^-$, $D \rightarrow \pi^+\pi^-$	GLW	CDF	[440]
$B^+ \rightarrow DK^+$	$D \rightarrow K^+K^-$, $D \rightarrow \pi^+\pi^-$	GLW	LHCb	[441]
$B^+ \rightarrow D^*K^+$	$D \rightarrow K^+K^-$, $D \rightarrow \pi^+\pi^-$	GLW	<i>BABAR</i>	[442]
$D^* \rightarrow D\gamma(\pi^0)$	$D \rightarrow K_s^0\pi^0$, $D \rightarrow K_s^0\omega$, $D \rightarrow K_s^0\phi$			
$B^+ \rightarrow D^*K^+$	$D \rightarrow K^+K^-$, $D \rightarrow \pi^+\pi^-$	GLW	Belle	[439]
$D^* \rightarrow D\gamma(\pi^0)$	$D \rightarrow K_s^0\pi^0$, $D \rightarrow K_s^0\omega$, $D \rightarrow K_s^0\phi$			
$B^+ \rightarrow D^*K^+$	$D \rightarrow K^+K^-$, $D \rightarrow \pi^+\pi^-$	GLW	LHCb	[441]
$D^* \rightarrow D\gamma(\pi^0)$				
$B^+ \rightarrow DK^{*+}$	$D \rightarrow K^+K^-$, $D \rightarrow \pi^+\pi^-$, $D \rightarrow K_s^0\pi^0$, $D \rightarrow K_s^0\omega$, $D \rightarrow K_s^0\phi$	GLW	<i>BABAR</i>	[443]
$B^+ \rightarrow DK^{*+}$	$D \rightarrow K^+K^-$, $D \rightarrow \pi^+\pi^-$	GLW	LHCb	[444]
$B^+ \rightarrow DK^+\pi^+\pi^-$	$D \rightarrow K^+K^-$, $D \rightarrow \pi^+\pi^-$	GLW	LHCb	[445]
$B^+ \rightarrow DK^+$	$D \rightarrow \pi^+\pi^-\pi^0$	GLW-like	<i>BABAR</i>	[320]
$B^+ \rightarrow DK^+$	$D \rightarrow K^+K^-\pi^0$, $D \rightarrow \pi^+\pi^-\pi^0$	GLW-like	LHCb	[449]
$B^+ \rightarrow DK^+$	$D \rightarrow \pi^+\pi^-\pi^+\pi^-$	GLW-like	LHCb	[450]
$B^+ \rightarrow DK^{*+}$	$D \rightarrow \pi^+\pi^-\pi^+\pi^-$	GLW-like	LHCb	[444]
$B^0 \rightarrow DK^+\pi^-$	$D \rightarrow K^+K^-$, $D \rightarrow \pi^+\pi^-$	GLW-Dalitz	LHCb	[447]
$B^+ \rightarrow DK^+$	$D \rightarrow K^\pm\pi^\mp$	ADS	<i>BABAR</i>	[451]
$B^+ \rightarrow DK^+$	$D \rightarrow K^\pm\pi^\mp$	ADS	Belle	[452]
$B^+ \rightarrow DK^+$	$D \rightarrow K^\pm\pi^\mp$	ADS	CDF	[453]
$B^+ \rightarrow DK^+$	$D \rightarrow K^\pm\pi^\mp$	ADS	LHCb	[450]
$B^+ \rightarrow DK^+$	$D \rightarrow K^\pm\pi^\mp\pi^0$	ADS	<i>BABAR</i>	[454]
$B^+ \rightarrow DK^+$	$D \rightarrow K^\pm\pi^\mp\pi^0$	ADS	Belle	[455]
$B^+ \rightarrow DK^+$	$D \rightarrow K^\pm\pi^\mp\pi^0$	ADS	LHCb	[449]
$B^+ \rightarrow DK^+$	$D \rightarrow K^\pm\pi^\mp\pi^+\pi^-$	ADS	LHCb	[450]
$B^+ \rightarrow D^*K^+$	$D \rightarrow K^\pm\pi^\mp$	ADS	<i>BABAR</i>	[451]
$D^* \rightarrow D\gamma(\pi^0)$				
$B^+ \rightarrow DK^{*+}$	$D \rightarrow K^\pm\pi^\mp$	ADS	<i>BABAR</i>	[443]
$B^+ \rightarrow DK^{*+}$	$D \rightarrow K^\pm\pi^\mp$	ADS	LHCb	[444]
$B^+ \rightarrow DK^{*+}$	$D \rightarrow K^\pm\pi^\mp\pi^+\pi^-$	ADS	LHCb	[444]
$B^0 \rightarrow DK^{*0}$	$D \rightarrow K^\pm\pi^\mp$	ADS	LHCb	[446]
$B^+ \rightarrow DK^+\pi^+\pi^-$	$D \rightarrow K^\pm\pi^\mp$	ADS	LHCb	[445]
$B^+ \rightarrow DK^+\pi^+\pi^-$	$D \rightarrow K_s^0\pi^+\pi^-$	GGSZ MD	<i>BABAR</i>	[461]
$B^+ \rightarrow DK^+$	$D \rightarrow K_s^0\pi^+\pi^-$	GGSZ MD	Belle	[460]
$B^+ \rightarrow DK^+$	$D \rightarrow K_s^0\pi^+\pi^-$, $D \rightarrow K_s^0K^+K^-$	GGSZ MI	LHCb	[468, 469]
$B^+ \rightarrow D^*K^+$	$D \rightarrow K_s^0\pi^+\pi^-$	GGSZ MD	<i>BABAR</i>	[461]
$D^* \rightarrow D\gamma(\pi^0)$				

List of measurements used in the γ combination – continued from previous page.

$B^+ \rightarrow D^* K^+$	$D \rightarrow K_s^0 \pi^+ \pi^-$	GGSZ MD	Belle	[460]
$D^* \rightarrow D\gamma (\pi^0)$				
$B^+ \rightarrow DK^{*+}$	$D \rightarrow K_s^0 \pi^+ \pi^-$	GGSZ MD	<i>BABAR</i>	[461]
$B^+ \rightarrow DK^{*+}$	$D \rightarrow K_s^0 \pi^+ \pi^-$	GGSZ MD	Belle	[463]
$B^0 \rightarrow DK^{*0}$	$D \rightarrow K_s^0 \pi^+ \pi^-$	GGSZ MI	Belle	[470]
$B^0 \rightarrow DK^{*0}$	$D \rightarrow K_s^0 \pi^+ \pi^-$, $D \rightarrow K_s^0 K^+ K^-$	GGSZ MI	LHCb	[471]
$B_s^0 \rightarrow D_s^\mp K^\pm$	$D_s^+ \rightarrow h^+ h^- \pi^+$	TD	LHCb	[293]

Auxiliary inputs are used in the combination in order to constrain the D system parameters and subsequently improve the determination of $\gamma \equiv \phi_3$. These include the ratio of suppressed to favoured decay amplitudes and the strong phase difference for $D \rightarrow K^\pm \pi^\mp$ decays, taken from the charm global fits (see Sec. 9). The amplitude ratios, strong phase differences and coherence factors of $D \rightarrow K^\pm \pi^\mp \pi^0$, $D \rightarrow K^\pm \pi^\mp \pi^+ \pi^-$ and $D \rightarrow K_s^0 K^\pm \pi^\pm$ decays are taken from CLEO-c and LHCb measurements [473, 478, 479]. The fraction of CP -even content for the GLW-like $D \rightarrow \pi^+ \pi^- \pi^+ \pi^-$, $D \rightarrow K^+ K^- \pi^0$ and $D \rightarrow \pi^+ \pi^- \pi^0$ decays are taken from CLEO-c measurements [448]. Constraints required to relate the hadronic parameters of the $B^0 \rightarrow DK^{*0}$ GLW-Dalitz analysis to the effective hadronic parameters of the Q2B approaches are taken from LHCb measurements [447]. Finally, the value of $-2\beta_s$ is taken from the HFLAV averages (see Sec. 4); this is required to obtain sensitivity to $\gamma \equiv \phi_3$ from the time-dependent analysis of $B_s^0 \rightarrow D_s^\mp K^\pm$ decays. A summary of the auxiliary constraints is given in Table 63.

The following reasonable, although imperfect, assumptions are made when performing the averages.

- CP violation in $D \rightarrow K^+ K^-$ and $D \rightarrow \pi^+ \pi^-$ decays is assumed to be zero. The results of Sec. 9 anyhow suggest such effects to be negligible.
- The combination is potentially sensitive to subleading effects from $D^0 - \bar{D}^0$ mixing [437, 480, 481], but these are expected to have little impact and are not accounted for.
- All $B^+ \rightarrow DK^{*+}$ modes are treated as two-body decays. In other words any dilution caused by non- K^{*+} contributions in the selected regions of the $DK_s^0 \pi^+$ or $DK^+ \pi^0$ Dalitz

Table 63: List of the auxiliary inputs used in the combinations.

Decay	Parameters	Source	Ref.
$D \rightarrow K^\pm \pi^\mp$	$r_D^{K\pi}, \delta_D^{K\pi}$	HFLAV	Sec. 9
$D \rightarrow K^\pm \pi^\mp \pi^+ \pi^-$	$\delta_D^{K3\pi}, \kappa_D^{K3\pi}, r_D^{K3\pi}$	CLEO+LHCb	[478]
$D \rightarrow \pi^+ \pi^- \pi^+ \pi^-$	$F_+(\pi^+ \pi^- \pi^+ \pi^-)$	CLEO	[448]
$D \rightarrow K^\pm \pi^\mp \pi^0$	$\delta_D^{K2\pi}, \kappa_D^{K2\pi}, r_D^{K2\pi}$	CLEO+LHCb	[478]
$D \rightarrow h^+ h^- \pi^0$	$F_+(\pi^+ \pi^- \pi^0), F_+(K^+ K^- \pi^0)$	CLEO	[448]
$D \rightarrow K_s^0 K^\pm \pi^\mp$	$\delta_D^{K_S K\pi}, \kappa_D^{K_S K\pi}, r_D^{K_S K\pi}$	CLEO	[473]
	$r_D^{K_S K\pi}$	LHCb	[479]
$B^0 \rightarrow DK^{*0}$	$\kappa_B(DK^{*0}), \bar{R}_B^{DK^{*0}}, \bar{\Delta}_B^{DK^{*0}}$	LHCb	[447]
$B_s^0 \rightarrow D_s^\mp K^\pm$	ϕ_s	HFLAV	Sec. 4

Table 64: Averages values obtained for the hadronic parameters in $B \rightarrow D^{(*)}K^{(*)}$ decays.

Parameter	Value
$r_B(DK^+)$	0.0993 ± 0.0046
$r_B(D^*K^+)$	0.140 ± 0.019
$r_B(DK^{*+})$	0.076 ± 0.020
$r_B(DK^{*0})$	$0.220^{+0.041}_{-0.047}$
$\delta_B(DK^+)$	$(129.6^{+5.0}_{-6.0})^\circ$
$\delta_B(D^*K^+)$	$(319^{+8}_{-9})^\circ$
$\delta_B(DK^{*+})$	$(98^{+18}_{-37})^\circ$
$\delta_B(DK^{*0})$	$(194^{+30}_{-22})^\circ$

Table 65: Averages of $\gamma \equiv \phi_3$ split by B meson decay mode.

Decay Mode	Value
$B_s^0 \rightarrow D_s^\mp K^\pm$	$(128^{+18}_{-22})^\circ$
$B^+ \rightarrow DK^{*+}$	$(45^{+16}_{-12})^\circ$
$B^+ \rightarrow D^*K^+$	$(55^{+11}_{-12})^\circ$
$B^0 \rightarrow DK^{*0}$	$(99^{+19}_{-21})^\circ$
$B^+ \rightarrow DK^+$	$(73.6^{+5.4}_{-6.2})^\circ$

plots is assumed to be negligible. As a check of this assumption, it was found that including a coherence factor for $B^+ \rightarrow DK^{*+}$ modes, $\kappa_B(DK^{*+}) = 0.9$, had negligible impact on the results.

- Each individual set of input measurements listed in Table 38 is assumed to be completely uncorrelated, though correlations between observables in a set are used if provided by the experiment. Whilst this assumption is true of the statistical uncertainties, it is not necessarily the case for systematic uncertainties. In particular, the model uncertainties for different model-dependent GGSZ analyses are fully correlated (when the same model is used). Similarly, the model-independent GGSZ analyses have correlated systematic uncertainties originating from the measurement of the strong phase variation across the Dalitz plot. The effect of including these correlations is estimated to be $< 1^\circ$.

In total, there are 136 observables and 29 free parameters. The combination has a χ^2 value of 123.4, which corresponds to a global p-value of 0.133. A coverage check with pseudoexperiments gives a p-value of $(11.4 \pm 0.3)\%$. The obtained world average for the Unitarity Triangle angle $\gamma \equiv \phi_3$ is

$$\gamma \equiv \phi_3 = (71.1^{+4.6}_{-5.3})^\circ. \quad (170)$$

An ambiguous solution at $\gamma \equiv \phi_3 \rightarrow \gamma \equiv \phi_3 + \pi$ also exists. The results for the hadronic parameters are listed in Table 64. Results for input analyses split by B meson decay mode are shown in Table 65 and Fig. 45. Results for input analyses split by the method are shown in Table 66 and Fig. 46. Results for the hadronic ratios, r_B , are shown in Fig. 47. A demonstration of how the various analyses contribute to the combination is shown in Fig. 48.

Table 66: Averages of $\gamma \equiv \phi_3$ split by method. For GLW method only the solution nearest the combined average is shown.

Method	Value
GLW	$(82.8^{+4.9}_{-12.3})^\circ$
ADS	$(73^{+12}_{-13})^\circ$
GGSZ	$(74.2^{+6.9}_{-6.8})^\circ$

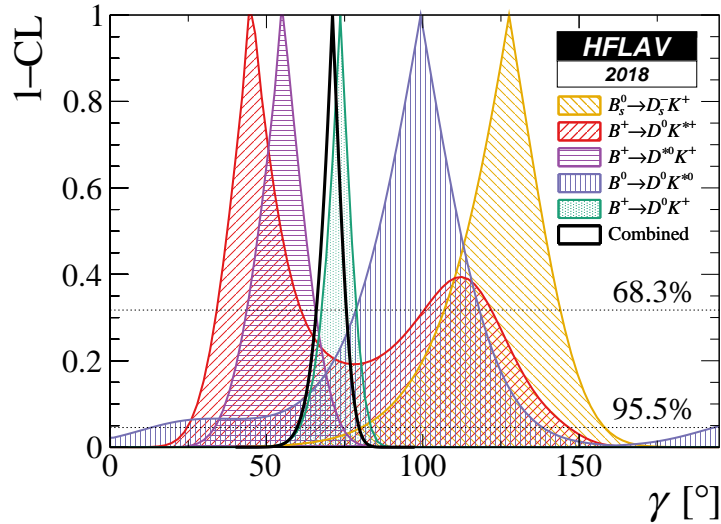


Figure 45: World average of $\gamma \equiv \phi_3$, in terms of $1-CL$, split by decay mode.

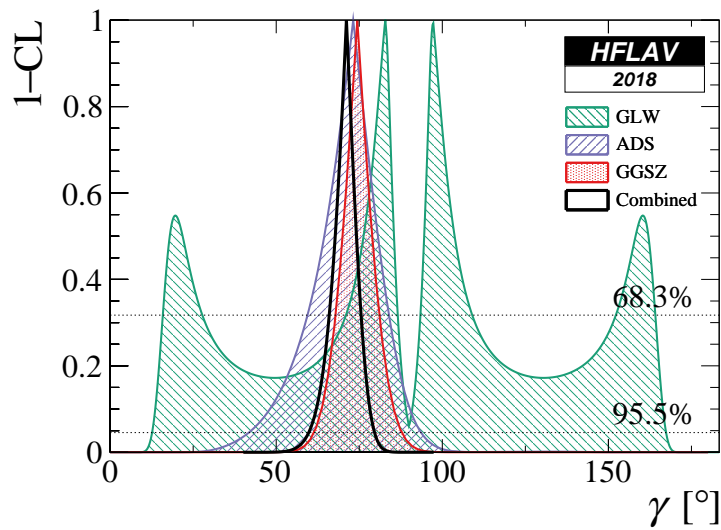


Figure 46: World average of $\gamma \equiv \phi_3$, in terms of $1-CL$, split by analysis method.

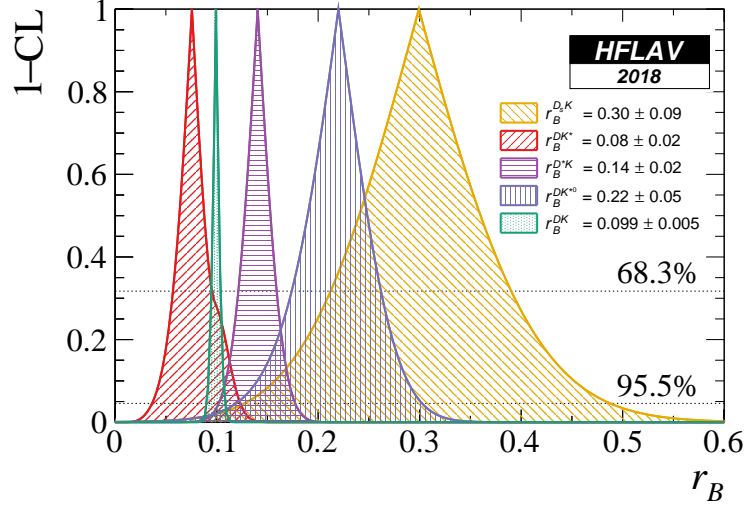


Figure 47: World averages for the hadronic parameters r_B in the different decay modes, in terms of 1-CL.

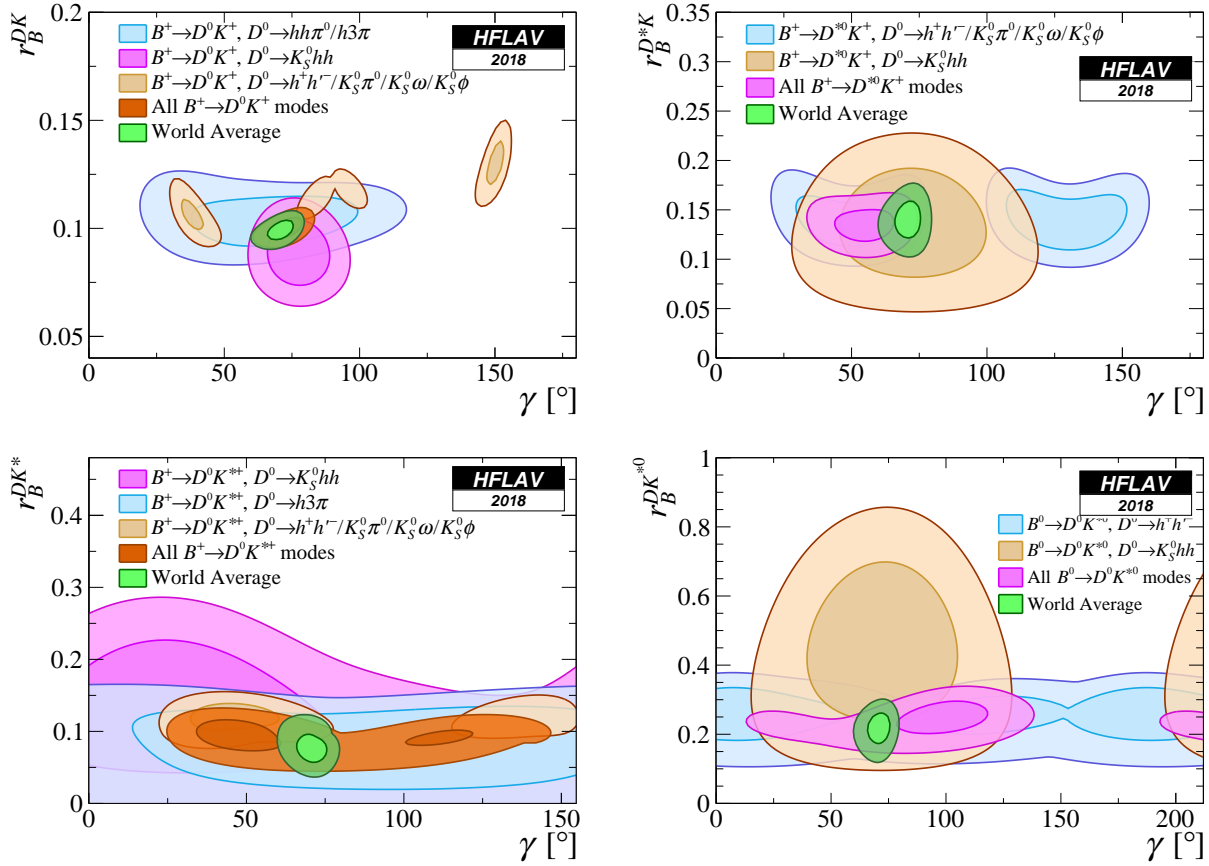


Figure 48: Contributions to the combination from different input measurements, shown in the plane of the relevant r_B parameter *vs.* $\gamma \equiv \phi_3$. From left to right, top to bottom: $B^+ \rightarrow DK^+$, $B^+ \rightarrow D^* K^+$, $B^+ \rightarrow DK^{*+}$ and $B^0 \rightarrow DK^{*0}$. Contours show the two-dimensional 68 % and 95 % CL regions.

5.15 Summary of the constraints on the angles of the Unitarity Triangle

World averages for the angles of the Unitarity Triangle $\beta \equiv \phi_1$, $\alpha \equiv \phi_2$ and $\gamma \equiv \phi_3$ are given in Sec. 5.4.1, Sec. 5.11.1 and Sec. 5.14.7, respectively. These constraints are summarised in Fig. 49 in terms of the CKM parameters $\bar{\rho}$ and $\bar{\eta}$ defined in Eq. (101) using the relations, $\tan \gamma = \bar{\eta}/\bar{\rho}$, $\tan \beta = \bar{\eta}/(1 - \bar{\rho})$, $\alpha = \tan^{-1}(\bar{\rho}/\bar{\eta}) + \tan^{-1}((1 - \bar{\rho})/\bar{\eta})$. The overlap of the constraints demonstrates agreement with the unitarity of the CKM matrix as predicted in the Standard Model. The obtained values of $\bar{\rho}$ and $\bar{\eta}$ from this angles only combination are

$$\bar{\rho} = 0.360 \pm 0.013, \quad \bar{\eta} = 0.119 \pm 0.022, \quad (171)$$

with a correlation of -0.42 .

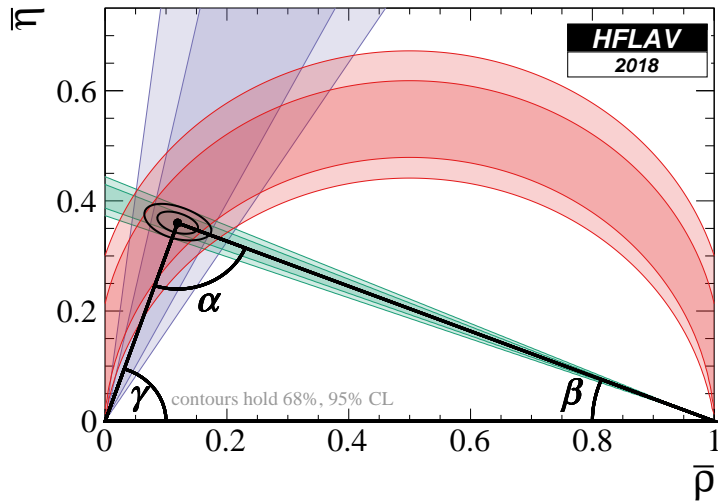


Figure 49: Summary of the constraints on the angles of the Unitarity Triangle.

6 Semileptonic B decays

This section contains averages for semileptonic B meson decays, *i.e.* decays of the type $B \rightarrow X\ell\nu_\ell$, where X refers to one or more hadrons, ℓ to a charged lepton and ν_ℓ to its associated neutrino. Unless otherwise stated, ℓ stands for an electron or a muon, lepton universality is assumed, and both charge conjugate states are combined. Some averages assume isospin symmetry, explicitly mentioned at every instance.

Averages are presented separately for CKM favored $b \rightarrow c$ quark transitions and CKM suppressed $b \rightarrow u$ transitions. We further distinguish *exclusive* decays involving a specific meson ($X = D, D^*, \pi, \rho, \dots$) from *inclusive* decay modes, *i.e.* the sum over all possible hadronic states. Semileptonic decays proceed via first order weak interactions and are well described in the framework of the SM. Their decay rates are sensitive to the magnitude squared of the CKM elements V_{cb} and V_{ub} , the determination of which is one of the primary goals for the study of these decays. Semileptonic decays involving the τ lepton might be more sensitive to beyond-SM processes, because the high τ mass might result in enhanced couplings to a hypothetical charged Higgs boson or leptoquarks.

The technique for obtaining the averages follows the general HFLAV procedure (Sec. 3) unless otherwise stated. More information on the averages, in particular on the common input parameters, is available on the HFLAV semileptonic webpage [482]. In general, averages in this section use experimental results available through September 2018. Some averages include more recent results and the corresponding figures are labeled *Spring 2019* for easier identification.

6.1 Exclusive CKM-favoured decays

6.1.1 $\overline{B} \rightarrow D^*\ell^-\bar{\nu}_\ell$

$\overline{B} \rightarrow D^*\ell^-\bar{\nu}_\ell$ decays are described in terms of the recoil variable $w = v_B \cdot v_{D^{(*)}}$, the product of the four-velocities of the initial and final state mesons. The differential decay rate for massless fermions as a function of w is given by (see, *e.g.*, [483])

$$\frac{d\Gamma(\overline{B} \rightarrow D^*\ell^-\bar{\nu}_\ell)}{dw} = \frac{G_F^2 m_{D^*}^3}{48\pi^3} (m_B - m_{D^*})^2 \chi(w) \eta_{EW}^2 \mathcal{F}^2(w) |V_{cb}|^2 , \quad (172)$$

where G_F is Fermi's constant, m_B and m_{D^*} are the B and D^* meson masses, $\chi(w)$ is a known phase-space factor, and η_{EW} is a small electroweak correction [484]. Some authors also include a long-distance EM radiation effect (Coulomb correction) in this factor. The form factor $\mathcal{F}(w)$ for the $\overline{B} \rightarrow D^*\ell^-\bar{\nu}_\ell$ decay contains three independent functions, $h_{A_1}(w)$, $R_1(w)$ and $R_2(w)$,

$$\begin{aligned} \chi(w)\mathcal{F}^2(w) = & \\ & h_{A_1}^2(w)\sqrt{w^2-1}(w+1)^2 \left\{ 2 \left[\frac{1-2wr+r^2}{(1-r)^2} \right] \left[1 + R_1^2(w) \frac{w^2-1}{w+1} \right] + \right. \\ & \left. \left[1 + (1-R_2(w)) \frac{w-1}{1-r} \right]^2 \right\} , \end{aligned} \quad (173)$$

where $r = m_{D^*}/m_B$.

Branching fraction

First, we perform separate one-dimensional averages of the $\bar{B}^0 \rightarrow D^{*+}\ell^-\bar{\nu}_\ell$ and $B^- \rightarrow D^{*0}\ell^-\bar{\nu}_\ell$ branching fractions. The measurements listed in Tables 67 and 68 are rescaled to the latest values of the input parameters (mainly branching fractions of charmed mesons) [485] and the following results are obtained

$$\mathcal{B}(\bar{B}^0 \rightarrow D^{*+}\ell^-\bar{\nu}_\ell) = (5.06 \pm 0.02 \pm 0.12)\%, \quad (174)$$

$$\mathcal{B}(B^- \rightarrow D^{*0}\ell^-\bar{\nu}_\ell) = (5.66 \pm 0.07 \pm 0.21)\%, \quad (175)$$

where the first uncertainty is statistical and the second one is systematic. The results of these two fits are also shown in Fig. 50.

Table 67: Average of the $\bar{B}^0 \rightarrow D^{*+}\ell^-\bar{\nu}_\ell$ branching fraction measurements.

Experiment	$\mathcal{B}(\bar{B}^0 \rightarrow D^{*+}\ell^-\bar{\nu}_\ell) [\%]$ (calculated)	$\mathcal{B}(\bar{B}^0 \rightarrow D^{*+}\ell^-\bar{\nu}_\ell) [\%]$ (published)
ALEPH [486]	$5.56 \pm 0.27_{\text{stat}} \pm 0.33_{\text{syst}}$	$5.53 \pm 0.26_{\text{stat}} \pm 0.52_{\text{syst}}$
OPAL incl [487]	$6.13 \pm 0.28_{\text{stat}} \pm 0.57_{\text{syst}}$	$5.92 \pm 0.27_{\text{stat}} \pm 0.68_{\text{syst}}$
OPAL excl [487]	$5.17 \pm 0.20_{\text{stat}} \pm 0.36_{\text{syst}}$	$5.11 \pm 0.19_{\text{stat}} \pm 0.49_{\text{syst}}$
DELPHI incl [488]	$4.96 \pm 0.14_{\text{stat}} \pm 0.35_{\text{syst}}$	$4.70 \pm 0.13_{\text{stat}} {}^{+0.36}_{-0.31} \text{syst}$
DELPHI excl [489]	$5.23 \pm 0.20_{\text{stat}} \pm 0.42_{\text{syst}}$	$5.90 \pm 0.22_{\text{stat}} \pm 0.50_{\text{syst}}$
CLEO [490]	$6.17 \pm 0.19_{\text{stat}} \pm 0.37_{\text{syst}}$	$6.09 \pm 0.19_{\text{stat}} \pm 0.40_{\text{syst}}$
Belle untagged [491]	$4.90 \pm 0.02_{\text{stat}} \pm 0.16_{\text{syst}}$	$4.90 \pm 0.02_{\text{stat}} \pm 0.16_{\text{syst}}$
Belle tagged [492]	$4.95 \pm 0.11_{\text{stat}} \pm 0.22_{\text{syst}}$	$4.95 \pm 0.11_{\text{stat}} \pm 0.22_{\text{syst}}$
<i>BABAR</i> untagged [493]	$4.52 \pm 0.04_{\text{stat}} \pm 0.33_{\text{syst}}$	$4.69 \pm 0.04_{\text{stat}} \pm 0.34_{\text{syst}}$
<i>BABAR</i> tagged [494]	$5.26 \pm 0.16_{\text{stat}} \pm 0.31_{\text{syst}}$	$5.49 \pm 0.16_{\text{stat}} \pm 0.25_{\text{syst}}$
Average	$5.06 \pm 0.02_{\text{stat}} \pm 0.12_{\text{syst}}$	$\chi^2/\text{dof} = 16.0/9$ (CL=6.61%)

Table 68: Average of the $B^- \rightarrow D^{*0}\ell^-\bar{\nu}_\ell$ branching fraction measurements.

Experiment	$\mathcal{B}(B^- \rightarrow D^{*0}\ell^-\bar{\nu}_\ell) [\%]$ (rescaled)	$\mathcal{B}(B^- \rightarrow D^{*0}\ell^-\bar{\nu}_\ell) [\%]$ (published)
CLEO [490]	$6.29 \pm 0.20_{\text{stat}} \pm 0.26_{\text{syst}}$	$6.50 \pm 0.20_{\text{stat}} \pm 0.43_{\text{syst}}$
<i>BABAR</i> tagged [494]	$5.35 \pm 0.15_{\text{stat}} \pm 0.33_{\text{syst}}$	$5.83 \pm 0.15_{\text{stat}} \pm 0.30_{\text{syst}}$
<i>BABAR</i> untagged [495]	$5.08 \pm 0.08_{\text{stat}} \pm 0.31_{\text{syst}}$	$5.56 \pm 0.08_{\text{stat}} \pm 0.41_{\text{syst}}$
Average	$5.66 \pm 0.07_{\text{stat}} \pm 0.21_{\text{syst}}$	$\chi^2/\text{dof} = 7.45/2$ (CL=2.41%)

Extraction of $|V_{cb}|$ based on the CLN form factor

To extract $|V_{cb}|$, we consider the parametrizations of the form factor functions $h_{A_1}(w)$, $R_1(w)$ and $R_2(w)$ by Caprini, Lellouch and Neubert (CLN) [496],

$$h_{A_1}(w) = h_{A_1}(1)[1 - 8\rho^2 z + (53\rho^2 - 15)z^2 - (231\rho^2 - 91)z^3], \quad (176)$$

$$R_1(w) = R_1(1) - 0.12(w-1) + 0.05(w-1)^2, \quad (177)$$

$$R_2(w) = R_2(1) + 0.11(w-1) - 0.06(w-1)^2, \quad (178)$$

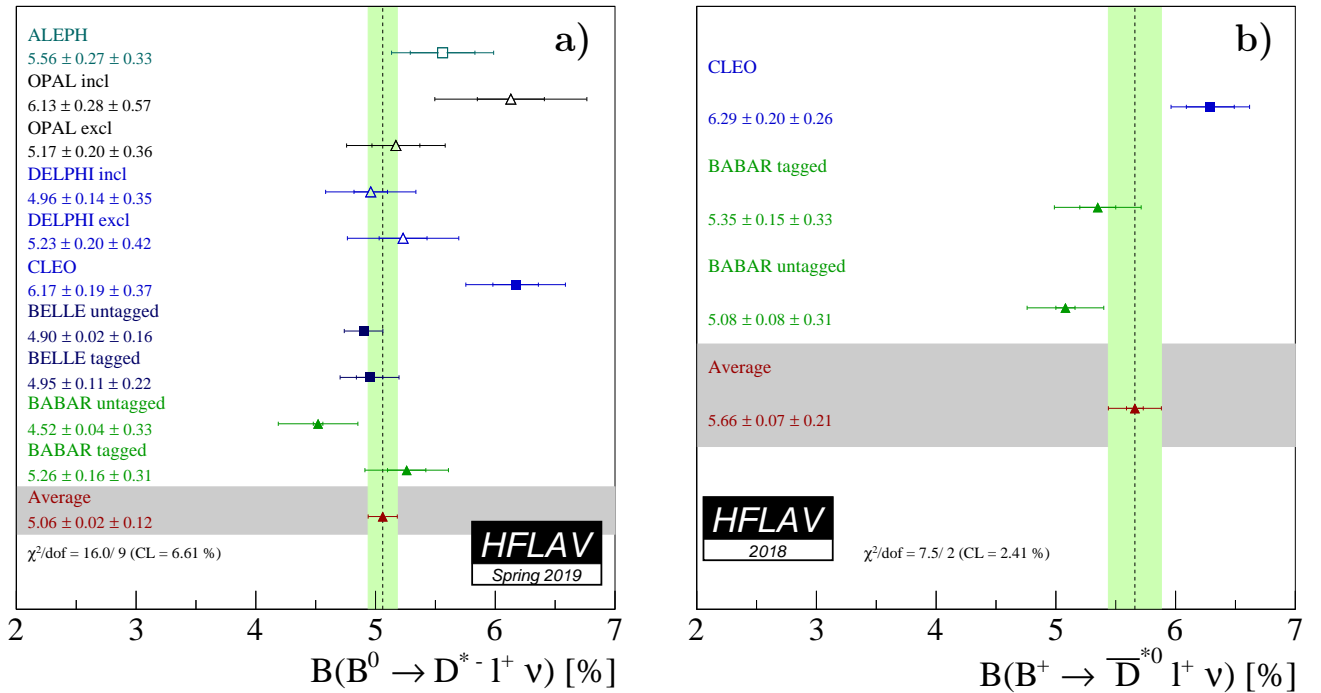


Figure 50: Branching fractions of exclusive semileptonic B decays: (a) $\bar{B}^0 \rightarrow D^{*+} l^- \bar{\nu}_l$ (Table 67) and (b) $B^- \rightarrow D^{*0} l^- \bar{\nu}_l$ (Table 68).

where $z = (\sqrt{w+1} - \sqrt{2})/(\sqrt{w+1} + \sqrt{2})$. The form factor $\mathcal{F}(w)$ in Eq. 172 is thus described by the slope ρ^2 and the ratios $R_1(1)$ and $R_2(1)$.

We use the measurements of these form factor parameters, shown in Table 69, and rescale them as described above. Most of the measurements in Table 69 are based on the decay $\bar{B}^0 \rightarrow D^{*+} l^- \bar{\nu}_l$. Some measurements [490, 497] are sensitive also to $B^- \rightarrow D^{*0} l^- \bar{\nu}_l$, and one measurement [495] is based on the decay $B^- \rightarrow D^{*0} l^- \bar{\nu}_l$. Isospin symmetry is assumed in this average. We note that the earlier results from the LEP experiments and CLEO required significant rescaling and have significantly larger uncertainties than the recent measurements by Belle and *BABAR*.

In the next step, we perform a four-parameter fit of $\eta_{\text{EW}} \mathcal{F}(1)|V_{cb}|$, ρ^2 , $R_1(1)$ and $R_2(1)$ to the rescaled measurements, taking into account correlated statistical and systematic uncertainties. Only two measurements constrain all four parameters [491, 493], and the remaining measurements determine only the normalization $\eta_{\text{EW}} \mathcal{F}(1)|V_{cb}|$ and the slope ρ^2 . The result of the fit is

$$\eta_{\text{EW}} \mathcal{F}(1)|V_{cb}| = (35.27 \pm 0.38) \times 10^{-3}, \quad (179)$$

$$\rho^2 = 1.122 \pm 0.024, \quad (180)$$

$$R_1(1) = 1.270 \pm 0.026, \quad (181)$$

$$R_2(1) = 0.852 \pm 0.018, \quad (182)$$

Table 69: Measurements of the Caprini, Lellouch and Neubert (CLN) [496] form factor parameters in $\bar{B} \rightarrow D^* \ell^- \bar{\nu}_\ell$ before and after rescaling. Most analyses (except [493]) measure only $\eta_{\text{EW}} \mathcal{F}(1)|V_{cb}|$, and ρ^2 , so only these two parameters are shown here.

Experiment	$\eta_{\text{EW}} \mathcal{F}(1) V_{cb} [10^{-3}]$ (rescaled) $\eta_{\text{EW}} \mathcal{F}(1) V_{cb} [10^{-3}]$ (published)	ρ^2 (rescaled) ρ^2 (published)
ALEPH [486]	$31.78 \pm 1.83_{\text{stat}} \pm 1.21_{\text{syst}}$ $31.9 \pm 1.8_{\text{stat}} \pm 1.9_{\text{syst}}$	$0.489 \pm 0.226_{\text{stat}} \pm 0.145_{\text{syst}}$ $0.37 \pm 0.26_{\text{stat}} \pm 0.14_{\text{syst}}$
CLEO [490]	$40.47 \pm 1.25_{\text{stat}} \pm 1.55_{\text{syst}}$ $43.1 \pm 1.3_{\text{stat}} \pm 1.8_{\text{syst}}$	$1.363 \pm 0.084_{\text{stat}} \pm 0.087_{\text{syst}}$ $1.61 \pm 0.09_{\text{stat}} \pm 0.21_{\text{syst}}$
OPAL excl [487]	$36.50 \pm 1.60_{\text{stat}} \pm 1.46_{\text{syst}}$ $36.8 \pm 1.6_{\text{stat}} \pm 2.0_{\text{syst}}$	$1.212 \pm 0.209_{\text{stat}} \pm 0.148_{\text{syst}}$ $1.31 \pm 0.21_{\text{stat}} \pm 0.16_{\text{syst}}$
OPAL partial reco [487]	$37.44 \pm 1.20_{\text{stat}} \pm 2.32_{\text{syst}}$ $37.5 \pm 1.2_{\text{stat}} \pm 2.5_{\text{syst}}$	$1.091 \pm 0.138_{\text{stat}} \pm 0.297_{\text{syst}}$ $1.12 \pm 0.14_{\text{stat}} \pm 0.29_{\text{syst}}$
DELPHI partial reco [488]	$35.64 \pm 1.41_{\text{stat}} \pm 2.29_{\text{syst}}$ $35.5 \pm 1.4_{\text{stat}} {}^{+2.3}_{-2.4}\text{syst}$	$1.144 \pm 0.123_{\text{stat}} \pm 0.381_{\text{syst}}$ $1.34 \pm 0.14_{\text{stat}} {}^{+0.24}_{-0.22}\text{syst}$
DELPHI excl [489]	$36.29 \pm 1.71_{\text{stat}} \pm 1.94_{\text{syst}}$ $39.2 \pm 1.8_{\text{stat}} \pm 2.3_{\text{syst}}$	$1.079 \pm 0.142_{\text{stat}} \pm 0.152_{\text{syst}}$ $1.32 \pm 0.15_{\text{stat}} \pm 0.33_{\text{syst}}$
Belle [491]	$35.07 \pm 0.15_{\text{stat}} \pm 0.56_{\text{syst}}$ $35.06 \pm 0.15_{\text{stat}} \pm 0.56_{\text{syst}}$	$1.106 \pm 0.031_{\text{stat}} \pm 0.008_{\text{syst}}$ $1.106 \pm 0.031_{\text{stat}} \pm 0.007_{\text{syst}}$
<i>BABAR</i> excl [493]	$33.77 \pm 0.29_{\text{stat}} \pm 0.98_{\text{syst}}$ $34.7 \pm 0.3_{\text{stat}} \pm 1.1_{\text{syst}}$	$1.184 \pm 0.048_{\text{stat}} \pm 0.029_{\text{syst}}$ $1.18 \pm 0.05_{\text{stat}} \pm 0.03_{\text{syst}}$
<i>BABAR</i> D^{*0} [495]	$34.81 \pm 0.58_{\text{stat}} \pm 1.06_{\text{syst}}$ $35.9 \pm 0.6_{\text{stat}} \pm 1.4_{\text{syst}}$	$1.125 \pm 0.058_{\text{stat}} \pm 0.053_{\text{syst}}$ $1.16 \pm 0.06_{\text{stat}} \pm 0.08_{\text{syst}}$
<i>BABAR</i> global fit [497]	$35.75 \pm 0.20_{\text{stat}} \pm 1.09_{\text{syst}}$ $35.7 \pm 0.2_{\text{stat}} \pm 1.2_{\text{syst}}$	$1.180 \pm 0.020_{\text{stat}} \pm 0.061_{\text{syst}}$ $1.21 \pm 0.02_{\text{stat}} \pm 0.07_{\text{syst}}$
Average	$35.27 \pm 0.11_{\text{stat}} \pm 0.36_{\text{syst}}$	$1.122 \pm 0.015_{\text{stat}} \pm 0.019_{\text{syst}}$

and the correlation coefficients are

$$\rho_{\eta_{\text{EW}} \mathcal{F}(1)|V_{cb}|, \rho^2} = 0.313 , \quad (183)$$

$$\rho_{\eta_{\text{EW}} \mathcal{F}(1)|V_{cb}|, R_1(1)} = -0.097 , \quad (184)$$

$$\rho_{\eta_{\text{EW}} \mathcal{F}(1)|V_{cb}|, R_2(1)} = -0.076 , \quad (185)$$

$$\rho_{\rho^2, R_1(1)} = 0.566 , \quad (186)$$

$$\rho_{\rho^2, R_2(1)} = -0.824 , \quad (187)$$

$$\rho_{R_1(1), R_2(1)} = -0.715 . \quad (188)$$

The uncertainties and correlations quoted here include both statistical and systematic contributions. The χ^2 of the fit is 42.3 for 23 degrees of freedom, which corresponds to a confidence level of 0.84%. The largest contribution to the χ^2 of the average is due to the ALEPH and CLEO measurements [486, 490]. An illustration of this fit result is given in Fig. 51.

To convert this result into $|V_{cb}|$, theory input for the form factor normalization is required.

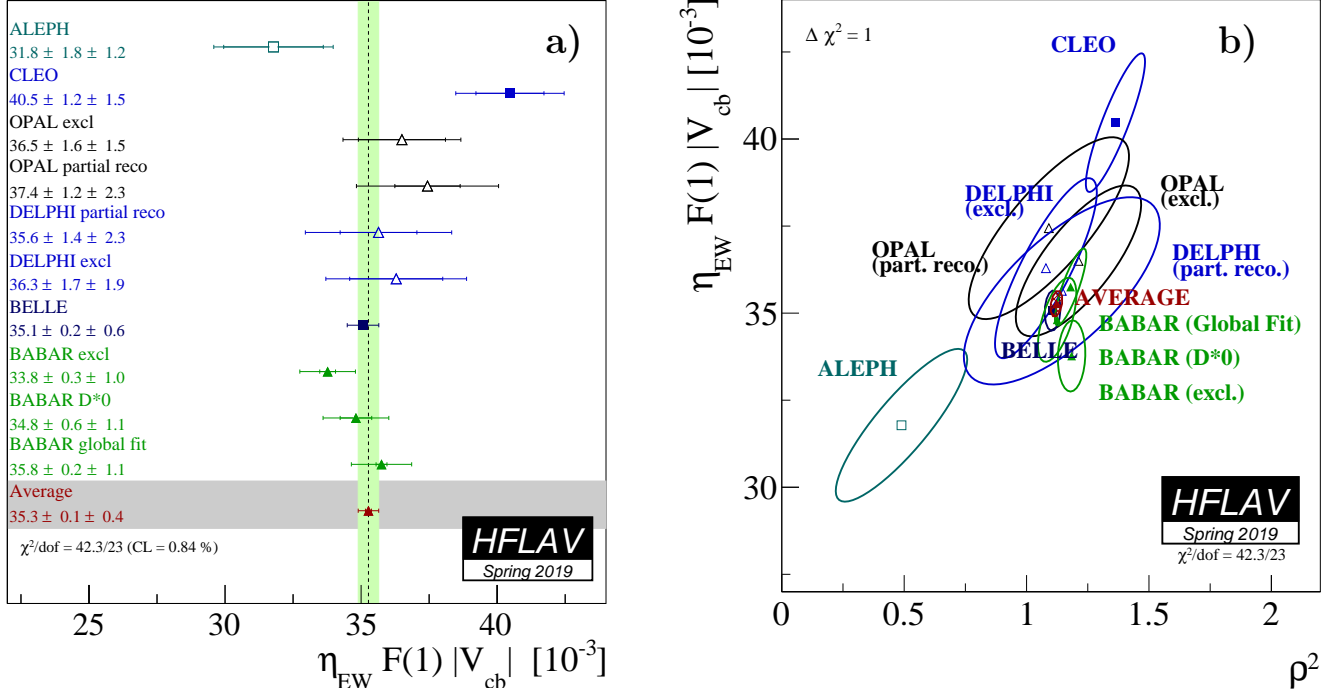


Figure 51: Illustration of the (a) the average and (b) the dependence of $\eta_{\text{EW}} \mathcal{F}(1) |V_{cb}|$ on ρ^2 . The error ellipses correspond to $\Delta\chi^2 = 1$ (CL=39%).

We use the result of the FLAG 2019 average [214],

$$\eta_{\text{EW}} \mathcal{F}(1) = 0.910 \pm 0.013 , \quad (189)$$

where $\eta_{\text{EW}} = 1.0066 \pm 0.0050$ has been used. The central value of the latter corresponds to the electroweak correction only. The uncertainty has been increased to accommodate the Coulomb effect [498]. With Eq. (179), this gives

$$|V_{cb}| = (38.76 \pm 0.42_{\text{exp}} \pm 0.55_{\text{th}}) \times 10^{-3} , \quad (190)$$

where the first uncertainty is experimental and the second is theoretical (lattice QCD calculation and electro-weak correction).

6.1.2 $\overline{B} \rightarrow D \ell^- \bar{\nu}_\ell$

The differential decay rate for massless fermions as a function of w (introduced in the previous section) is given by (see, *e.g.*, [483])

$$\frac{\overline{B} \rightarrow D \ell^- \bar{\nu}_\ell}{dw} = \frac{G_F^2 m_D^3}{48\pi^3} (m_B + m_D)^2 (w^2 - 1)^{3/2} \eta_{\text{EW}}^2 \mathcal{G}^2(w) |V_{cb}|^2 , \quad (191)$$

where G_F is Fermi's constant, and m_B and m_D are the B and D meson masses. Again, η_{EW} is the electroweak correction introduced in the previous section. In contrast to $\bar{B} \rightarrow D^* \ell^- \bar{\nu}_\ell$, $\mathcal{G}(w)$ contains a single form-factor function $f_+(w)$,

$$\mathcal{G}^2(w) = \frac{4r}{(1+r)^2} f_+^2(w) , \quad (192)$$

where $r = m_D/m_B$.

Branching fraction

Separate one-dimensional averages of the $\bar{B}^0 \rightarrow D^+ \ell^- \bar{\nu}_\ell$ and $B^- \rightarrow D^0 \ell^- \bar{\nu}_\ell$ branching fractions are shown in Tables 70 and 71. We obtain

$$\mathcal{B}(\bar{B}^0 \rightarrow D^+ \ell^- \bar{\nu}_\ell) = (2.31 \pm 0.04 \pm 0.09)\% , \quad (193)$$

$$\mathcal{B}(B^- \rightarrow D^0 \ell^- \bar{\nu}_\ell) = (2.35 \pm 0.03 \pm 0.09)\% , \quad (194)$$

where the first uncertainty is statistical and the second one is systematic. These fits are also shown in Fig. 52.

Table 70: Average of $\bar{B}^0 \rightarrow D^+ \ell^- \bar{\nu}_\ell$ branching fraction measurements.

Experiment	$\mathcal{B}(\bar{B}^0 \rightarrow D^+ \ell^- \bar{\nu}_\ell) [\%]$ (rescaled)	$\mathcal{B}(\bar{B}^0 \rightarrow D^+ \ell^- \bar{\nu}_\ell) [\%]$ (published)
ALEPH [486]	$2.32 \pm 0.18_{\text{stat}} \pm 0.36_{\text{syst}}$	$2.35 \pm 0.20_{\text{stat}} \pm 0.44_{\text{syst}}$
CLEO [499]	$2.15 \pm 0.13_{\text{stat}} \pm 0.16_{\text{syst}}$	$2.20 \pm 0.16_{\text{stat}} \pm 0.19_{\text{syst}}$
BABAR [500]	$2.19 \pm 0.11_{\text{stat}} \pm 0.14_{\text{syst}}$	$2.23 \pm 0.11_{\text{stat}} \pm 0.11_{\text{syst}}$
Belle [501]	$2.43 \pm 0.04_{\text{stat}} \pm 0.12_{\text{syst}}$	$2.39 \pm 0.04_{\text{stat}} \pm 0.11_{\text{syst}}$
Average	$2.31 \pm 0.04_{\text{stat}} \pm 0.09_{\text{syst}}$	$\chi^2/\text{dof} = 2.20/3$ (CL=53.1%)

Table 71: Average of $B^- \rightarrow D^0 \ell^- \bar{\nu}_\ell$ branching fraction measurements.

Experiment	$\mathcal{B}(B^- \rightarrow D^0 \ell^- \bar{\nu}_\ell) [\%]$ (rescaled)	$\mathcal{B}(B^- \rightarrow D^0 \ell^- \bar{\nu}_\ell) [\%]$ (published)
CLEO [499]	$2.19 \pm 0.13_{\text{stat}} \pm 0.17_{\text{syst}}$	$2.32 \pm 0.17_{\text{stat}} \pm 0.20_{\text{syst}}$
BABAR [500]	$2.19 \pm 0.08_{\text{stat}} \pm 0.13_{\text{syst}}$	$2.31 \pm 0.08_{\text{stat}} \pm 0.09_{\text{syst}}$
Belle [501]	$2.53 \pm 0.04_{\text{stat}} \pm 0.12_{\text{syst}}$	$2.54 \pm 0.04_{\text{stat}} \pm 0.13_{\text{syst}}$
Average	$2.35 \pm 0.03_{\text{stat}} \pm 0.09_{\text{syst}}$	$\chi^2/\text{dof} = 3.78/2$ (CL=15.1%)

Extraction of $|V_{cb}|$ based on the CLN form factor

As for $\bar{B} \rightarrow D^* \ell^- \bar{\nu}_\ell$ decays, we adopt the prescription by Caprini, Lellouch and Neubert [496], which describes the shape and normalization of the measured decay distributions in terms of two parameters: the normalization $\mathcal{G}(1)$ and the slope ρ^2 ,

$$\mathcal{G}(w) = \mathcal{G}(1) [1 - 8\rho^2 z + (51\rho^2 - 10)z^2 - (252\rho^2 - 84)z^3] , \quad (195)$$

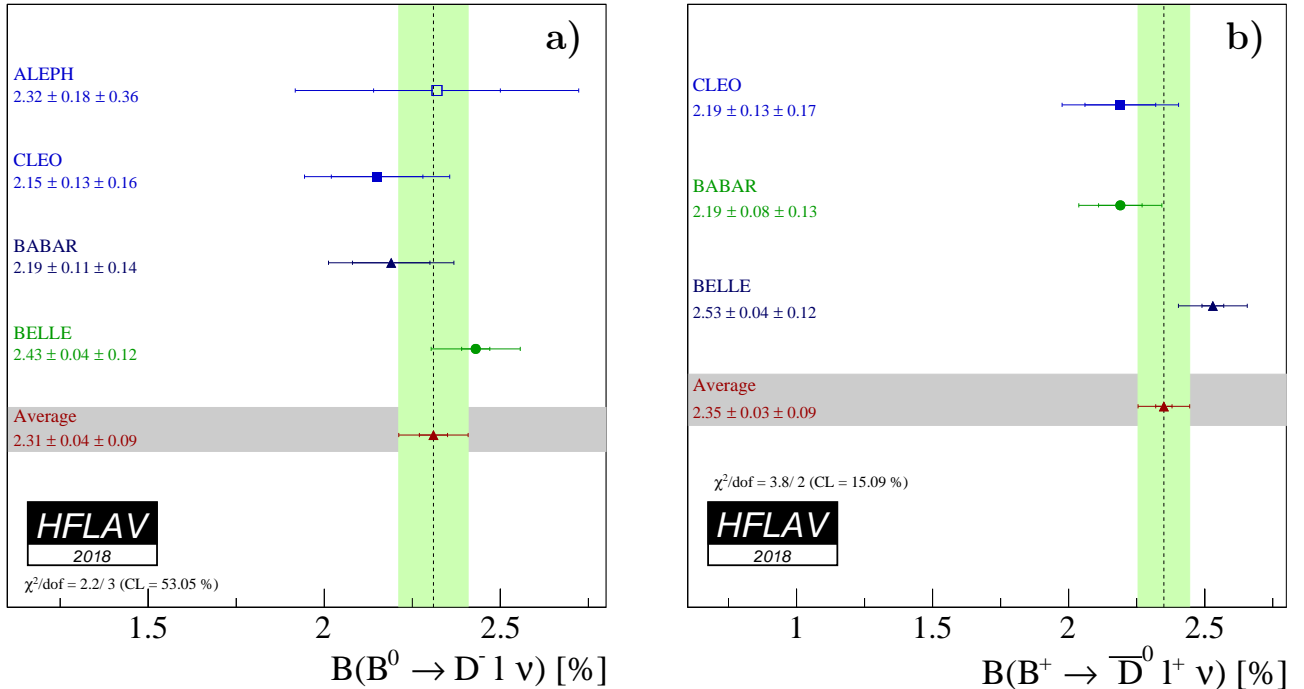


Figure 52: Branching fractions of exclusive semileptonic B decays: (a) $\bar{B}^0 \rightarrow D^+ \ell^- \bar{\nu}_\ell$ (Table 70) and (b) $B^- \rightarrow D^0 \ell^- \bar{\nu}_\ell$ (Table 71).

where $z = (\sqrt{w+1} - \sqrt{2})/(\sqrt{w+1} + \sqrt{2})$.

Table 72 shows experimental measurements of the two CLN parameters, which are corrected to match the latest values of the input parameters [485]. Both measurements of $\bar{B}^0 \rightarrow D^+ \ell^- \bar{\nu}_\ell$ and $B^- \rightarrow D^0 \ell^- \bar{\nu}_\ell$ are used and isospin symmetry is assumed in the analysis.

The form factor parameters are extracted by a two-parameter fit to the rescaled measurements of $\eta_{\text{EW}} \mathcal{G}(1) |V_{cb}|$ and ρ^2 taking into account correlated statistical and systematic uncertainties. The result of the fit is

$$\eta_{\text{EW}} \mathcal{G}(1) |V_{cb}| = (42.00 \pm 1.00) \times 10^{-3}, \quad (196)$$

$$\rho^2 = 1.131 \pm 0.033, \quad (197)$$

with a correlation of

$$\rho_{\eta_{\text{EW}} \mathcal{G}(1) |V_{cb}|, \rho^2} = 0.751. \quad (198)$$

The uncertainties and the correlation coefficient include both statistical and systematic contributions. The χ^2 of the fit is 5.0 for 8 degrees of freedom, which corresponds to a probability of 76.1%. An illustration of this fit result is given in Fig. 53.

The most recent lattice QCD result obtained for the form factor normalization is [498]

$$\mathcal{G}(1) = 1.0541 \pm 0.0083. \quad (199)$$

Using again $\eta_{\text{EW}} = 1.0066 \pm 0.0050$, we determine $|V_{cb}|$ from Eq. (196),

$$|V_{cb}| = (39.58 \pm 0.94_{\text{exp}} \pm 0.37_{\text{th}}) \times 10^{-3}, \quad (200)$$

where the first error is experimental and the second theoretical. This number is in excellent agreement with $|V_{cb}|$ obtained from $\bar{B} \rightarrow D^* \ell^- \bar{\nu}_\ell$ decays given in Eq. (190).

Table 72: Measurements of the Caprini, Lellouch and Neubert (CLN) [496] form factor parameters in $\bar{B} \rightarrow D\ell^-\bar{\nu}_\ell$ before and after rescaling.

Experiment	$\eta_{\text{EW}} \mathcal{G}(1) V_{cb} [10^{-3}]$ (rescaled) $\eta_{\text{EW}} \mathcal{G}(1) V_{cb} [10^{-3}]$ (published)	ρ^2 (rescaled) ρ^2 (published)
ALEPH [486]	$38.75 \pm 9.51_{\text{stat}} \pm 6.93_{\text{syst}}$ $31.1 \pm 9.9_{\text{stat}} \pm 8.6_{\text{syst}}$	$0.955 \pm 0.834_{\text{stat}} \pm 0.425_{\text{syst}}$ $0.70 \pm 0.98_{\text{stat}} \pm 0.50_{\text{syst}}$
CLEO [499]	$44.97 \pm 5.70_{\text{stat}} \pm 3.47_{\text{syst}}$ $44.8 \pm 6.1_{\text{stat}} \pm 3.7_{\text{syst}}$	$1.270 \pm 0.215_{\text{stat}} \pm 0.121_{\text{syst}}$ $1.30 \pm 0.27_{\text{stat}} \pm 0.14_{\text{syst}}$
Belle [501]	$42.22 \pm 0.60_{\text{stat}} \pm 1.21_{\text{syst}}$ 42.29 ± 1.37	$1.090 \pm 0.036_{\text{stat}} \pm 0.019_{\text{syst}}$ 1.09 ± 0.05
BABAR global fit [497]	$43.84 \pm 0.76_{\text{stat}} \pm 2.19_{\text{syst}}$ $43.1 \pm 0.8_{\text{stat}} \pm 2.3_{\text{syst}}$	$1.215 \pm 0.035_{\text{stat}} \pm 0.062_{\text{syst}}$ $1.20 \pm 0.04_{\text{stat}} \pm 0.07_{\text{syst}}$
BABAR tagged [500]	$42.76 \pm 1.71_{\text{stat}} \pm 1.26_{\text{syst}}$ $42.3 \pm 1.9_{\text{stat}} \pm 1.0_{\text{syst}}$	$1.200 \pm 0.088_{\text{stat}} \pm 0.043_{\text{syst}}$ $1.20 \pm 0.09_{\text{stat}} \pm 0.04_{\text{syst}}$
Average	$42.00 \pm 0.45_{\text{stat}} \pm 0.89_{\text{syst}}$	$1.131 \pm 0.024_{\text{stat}} \pm 0.023_{\text{syst}}$

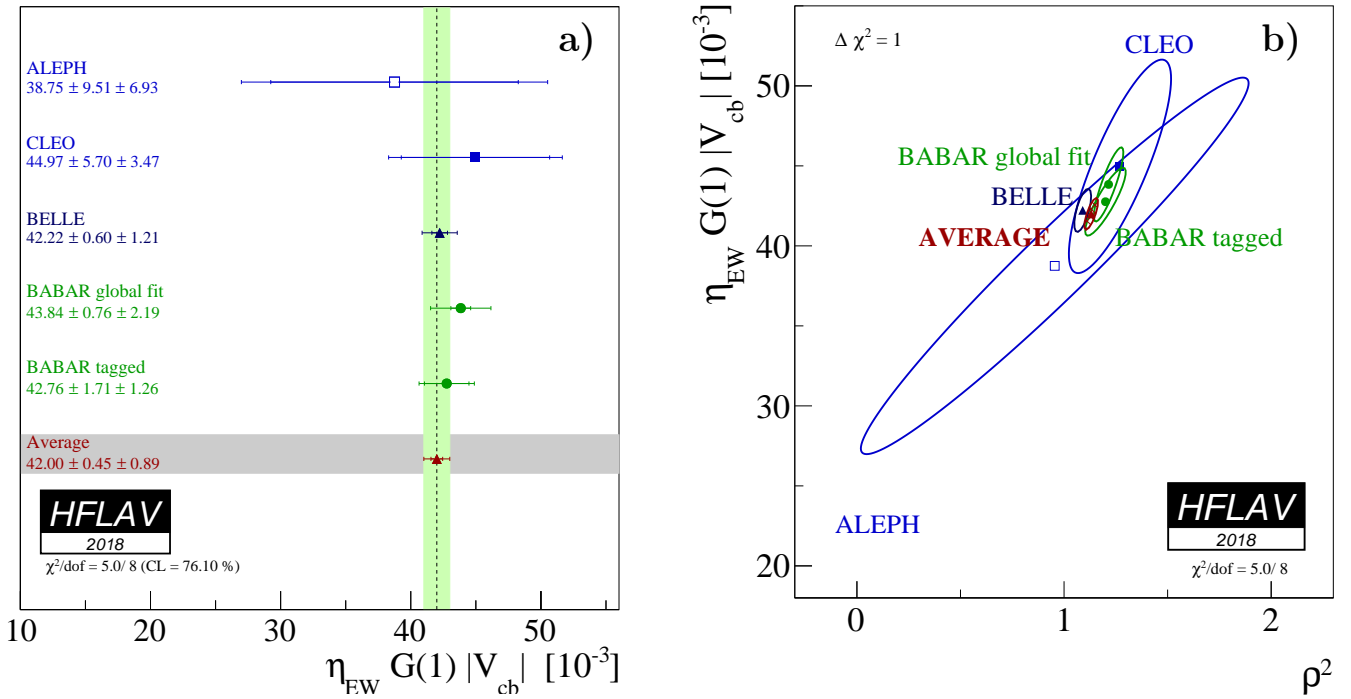


Figure 53: Illustration of the (a) the average and (b) dependence of $\eta_{\text{EW}} \mathcal{G}(w) |V_{cb}|$ on ρ^2 . The error ellipses correspond to $\Delta\chi^2 = 1$ (CL=39%).

6.1.3 $\bar{B} \rightarrow D^{(*)}\pi\ell^-\bar{\nu}_\ell$

The average inclusive branching fractions for $\bar{B} \rightarrow D^{(*)}\pi\ell^-\bar{\nu}_\ell$ decays, where no constraint is applied to the mass of the $D^{(*)}\pi$ system, are determined by the combination of the results provided in Table 73 for $\bar{B}^0 \rightarrow D^0\pi^+\ell^-\bar{\nu}_\ell$, $\bar{B}^0 \rightarrow D^{*0}\pi^+\ell^-\bar{\nu}_\ell$, $B^- \rightarrow D^+\pi^-\ell^-\bar{\nu}_\ell$, and $B^- \rightarrow D^{*+}\pi^-\ell^-\bar{\nu}_\ell$ decays. For the $\bar{B}^0 \rightarrow D^0\pi^+\ell^-\bar{\nu}_\ell$ decays a veto to reject the $D^{*+} \rightarrow D^0\pi^+$ decays is applied. The measurements included in the average are scaled to a consistent set of input parameters and their uncertainties [485]. For both the *BABAR* and *Belle* results, the B semileptonic signal yields are extracted from a fit to the missing mass squared distribution for a sample of fully reconstructed $B\bar{B}$ events. Figure 54 shows the measurements and the resulting average for the four decay modes.

Table 73: Averages of the $B \rightarrow D^{(*)}\pi^-\ell^-\bar{\nu}_\ell$ branching fractions and individual results.

Experiment	$\mathcal{B}(B^- \rightarrow D^+\pi^-\ell^-\bar{\nu}_\ell)[\%]$ (rescaled)	$\mathcal{B}(B^- \rightarrow D^+\pi^-\ell^-\bar{\nu}_\ell)[\%]$ (published)
Belle [502]	$0.455 \pm 0.027_{\text{stat}} \pm 0.039_{\text{syst}}$	$0.455 \pm 0.027_{\text{stat}} \pm 0.039_{\text{syst}}$
<i>BABAR</i> [494]	$0.415 \pm 0.060_{\text{stat}} \pm 0.031_{\text{syst}}$	$0.42 \pm 0.06_{\text{stat}} \pm 0.03_{\text{syst}}$
Average	0.443 ± 0.037	$\chi^2/\text{dof} = 0.25$ (CL=61.4%)
Experiment	$\mathcal{B}(B^- \rightarrow D^{*+}\pi^-\ell^-\bar{\nu}_\ell)[\%]$ (rescaled)	$\mathcal{B}(B^- \rightarrow D^{*+}\pi^-\ell^-\bar{\nu}_\ell)[\%]$ (published)
Belle [502]	$0.603 \pm 0.043_{\text{stat}} \pm 0.038_{\text{syst}}$	$0.604 \pm 0.043_{\text{stat}} \pm 0.038_{\text{syst}}$
<i>BABAR</i> [494]	$0.569 \pm 0.050_{\text{stat}} \pm 0.045_{\text{syst}}$	$0.59 \pm 0.05_{\text{stat}} \pm 0.04_{\text{syst}}$
Average	0.589 ± 0.044	$\chi^2/\text{dof} = 0.145$ (CL=70.3%)
Experiment	$\mathcal{B}(\bar{B}^0 \rightarrow D^0\pi^+\ell^-\bar{\nu}_\ell)[\%]$ (rescaled)	$\mathcal{B}(\bar{B}^0 \rightarrow D^0\pi^+\ell^-\bar{\nu}_\ell)[\%]$ (published)
Belle [502]	$0.405 \pm 0.036_{\text{stat}} \pm 0.041_{\text{syst}}$	$0.405 \pm 0.036_{\text{stat}} \pm 0.041_{\text{syst}}$
<i>BABAR</i> [494]	$0.410 \pm 0.080_{\text{stat}} \pm 0.035_{\text{syst}}$	$0.43 \pm 0.08_{\text{stat}} \pm 0.03_{\text{syst}}$
Average	0.406 ± 0.047	$\chi^2/\text{dof} = 0.002$ (CL=96.4%)
Experiment	$\mathcal{B}(\bar{B}^0 \rightarrow D^{*0}\pi^+\ell^-\bar{\nu}_\ell)[\%]$ (rescaled)	$\mathcal{B}(\bar{B}^0 \rightarrow D^{*0}\pi^+\ell^-\bar{\nu}_\ell)[\%]$ (published)
Belle [502]	$0.646 \pm 0.053_{\text{stat}} \pm 0.052_{\text{syst}}$	$0.646 \pm 0.053_{\text{stat}} \pm 0.052_{\text{syst}}$
<i>BABAR</i> [494]	$0.462 \pm 0.080_{\text{stat}} \pm 0.044_{\text{syst}}$	$0.48 \pm 0.08_{\text{stat}} \pm 0.04_{\text{syst}}$
Average	0.565 ± 0.061	$\chi^2/\text{dof} = 2.25$ (CL=13.3%)

6.1.4 $\bar{B} \rightarrow D^{**}\ell^-\bar{\nu}_\ell$

D^{**} mesons contain one charm quark and one light anti-quark with relative angular momentum $L = 1$. According to Heavy Quark Symmetry (HQS) [503], they form one doublet of states with angular momentum $j \equiv s_q + L = 3/2$ [$D_1(2420)$, $D_2^*(2460)$] and another doublet with $j = 1/2$ [$D_0^*(2400)$, $D_1'(2430)$], where s_q is the light quark spin. Parity and angular momentum conservation constrain the decays allowed for each state. The D_1 and D_2^* states decay via D-wave to $D^*\pi$ and $D^{(*)}\pi$, respectively, and have small decay widths, while the D_0^* and D_1' states decay via S-wave to $D\pi$ and $D^*\pi$ and are very broad. For the narrow states, the averages are determined by the combination of the results provided in Table 74 and 75 for $\mathcal{B}(B^- \rightarrow D_1^0\ell^-\bar{\nu}_\ell) \times \mathcal{B}(D_1^0 \rightarrow D^{*+}\pi^-)$ and $\mathcal{B}(B^- \rightarrow D_2^0\ell^-\bar{\nu}_\ell) \times \mathcal{B}(D_2^0 \rightarrow D^{*+}\pi^-)$. For the broad

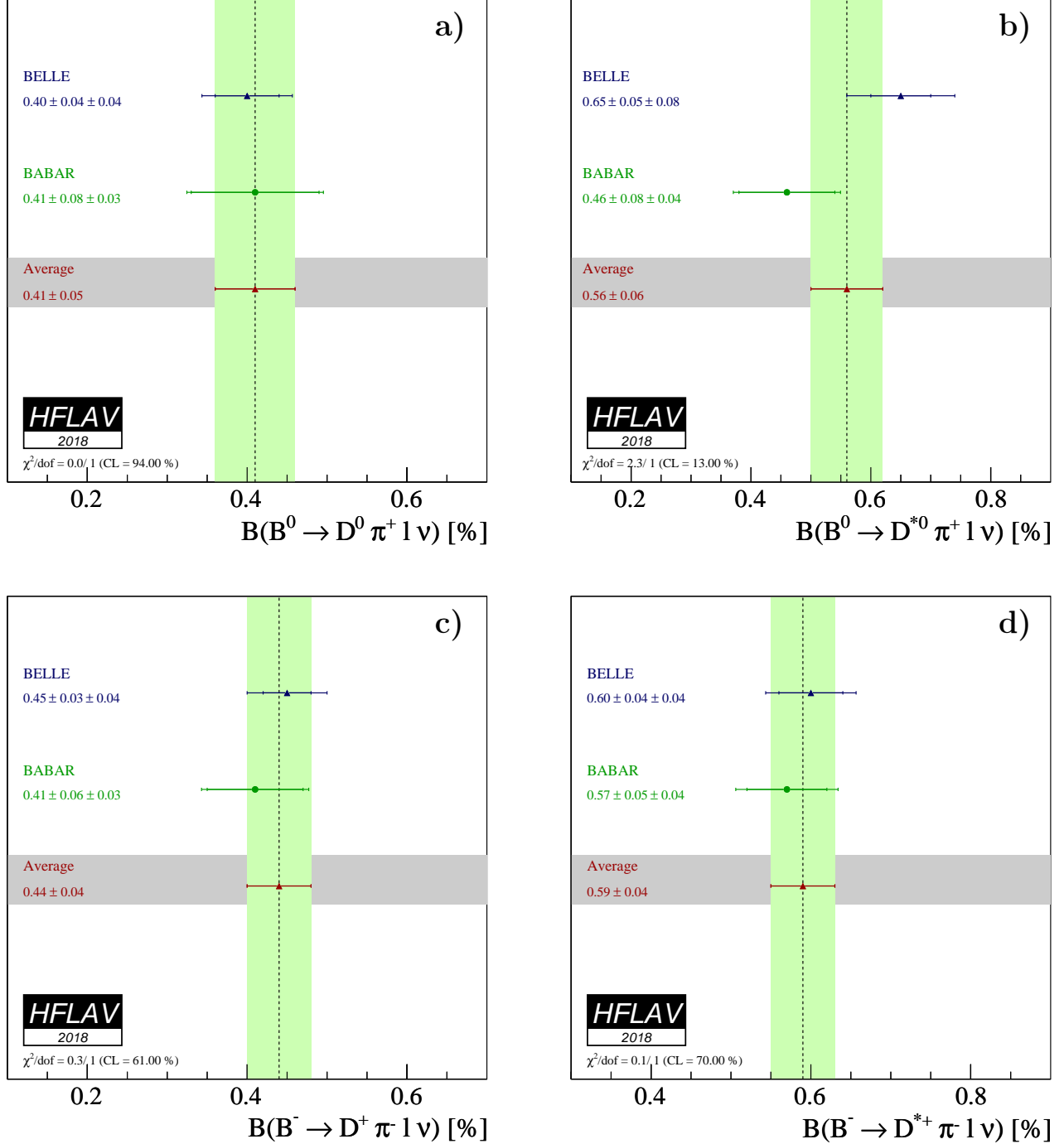


Figure 54: Average branching fraction of exclusive semileptonic B decays (a) $\overline{B}^0 \rightarrow D^0 \pi^+ \ell^- \bar{\nu}_\ell$, (b) $\overline{B}^0 \rightarrow D^{*0} \pi^+ \ell^- \bar{\nu}_\ell$, (c) $B^- \rightarrow D^+ \pi^- \ell^- \bar{\nu}_\ell$, and (d) $B^- \rightarrow D^{*+} \pi^- \ell^- \bar{\nu}_\ell$. The corresponding individual results are also shown.

states, the averages are determined by the combination of the results provided in Table 76 and 77 for $\mathcal{B}(B^- \rightarrow D_1'^0 \ell^- \bar{\nu}_\ell) \times \mathcal{B}(D_1'^0 \rightarrow D^{*+} \pi^-)$ and $\mathcal{B}(B^- \rightarrow D_0'^0 \ell^- \bar{\nu}_\ell) \times \mathcal{B}(D_0'^0 \rightarrow D^+ \pi^-)$. The

measurements are scaled to a consistent set of input parameters and their uncertainties [485].

For both the B-factory and the LEP and Tevatron results, the B semileptonic signal yields are extracted from a fit to the invariant mass distribution of the $D^{(*)+}\pi^-$ system. The LEP and Tevatron measurements are for the inclusive decays $\bar{B} \rightarrow D^{**}(D^*\pi^-)X\ell^-\bar{\nu}_\ell$. In the average with the results from the B-Factories, we use these measurements assuming that no particles are left in the X system. The *BABAR* tagged analysis of $\bar{B} \rightarrow D_2^*\ell^-\bar{\nu}_\ell$ was performed selecting $D_2^* \rightarrow D\pi$ decays. The *BABAR* result reported in Table 75 is translated in a branching fraction for the $D_2^* \rightarrow D^*\pi$ decay mode assuming $\mathcal{B}(D_2^* \rightarrow D\pi)/\mathcal{B}(D_2^* \rightarrow D^*\pi) = 1.54 \pm 0.15$ [21]. Figure 55 and 56 show the measurements and the resulting averages.

Table 74: Published and rescaled individual measurements and their averages for of the branching fraction $\mathcal{B}(B^- \rightarrow D_1^0\ell^-\bar{\nu}_\ell) \times \mathcal{B}(D_1^0 \rightarrow D^{*+}\pi^-)$.

Experiment	$\mathcal{B}(B^- \rightarrow D_1^0(D^{*+}\pi^-)\ell^-\bar{\nu}_\ell)[\%]$ (rescaled)	$\mathcal{B}(B^- \rightarrow D_1^0(D^{*+}\pi^-)\ell^-\bar{\nu}_\ell)[\%]$ (published)
ALEPH [504]	$0.436 \pm 0.085_{\text{stat}} \pm 0.056_{\text{syst}}$	$0.47 \pm 0.10_{\text{stat}} \pm 0.07_{\text{syst}}$
OPAL [505]	$0.568 \pm 0.210_{\text{stat}} \pm 0.100_{\text{syst}}$	$0.70 \pm 0.21_{\text{stat}} \pm 0.10_{\text{syst}}$
CLEO [506]	$0.349 \pm 0.085_{\text{stat}} \pm 0.056_{\text{syst}}$	$0.373 \pm 0.085_{\text{stat}} \pm 0.057_{\text{syst}}$
D0 [507]	$0.214 \pm 0.018_{\text{stat}} \pm 0.035_{\text{syst}}$	$0.219 \pm 0.018_{\text{stat}} \pm 0.035_{\text{syst}}$
Belle Tagged B^- [508]	$0.430 \pm 0.070_{\text{stat}} \pm 0.059_{\text{syst}}$	$0.42 \pm 0.07_{\text{stat}} \pm 0.07_{\text{syst}}$
Belle Tagged B^0 [508]	$0.593 \pm 0.200_{\text{stat}} \pm 0.076_{\text{syst}}$	$0.42 \pm 0.07_{\text{stat}} \pm 0.07_{\text{syst}}$
<i>BABAR</i> Tagged [509]	$0.277 \pm 0.030_{\text{stat}} \pm 0.029_{\text{syst}}$	$0.29 \pm 0.03_{\text{stat}} \pm 0.03_{\text{syst}}$
<i>BABAR</i> Untagged B^- [510]	$0.293 \pm 0.017_{\text{stat}} \pm 0.016_{\text{syst}}$	$0.30 \pm 0.02_{\text{stat}} \pm 0.02_{\text{syst}}$
<i>BABAR</i> Untagged B^0 [510]	$0.282 \pm 0.026_{\text{stat}} \pm 0.023_{\text{syst}}$	$0.30 \pm 0.02_{\text{stat}} \pm 0.02_{\text{syst}}$
Average	$0.281 \pm 0.010 \pm 0.015$	$\chi^2/\text{dof} = 12.3/8$ (CL=13.8%)

Table 75: Published and rescaled individual measurements and their averages for $\mathcal{B}(B^- \rightarrow D_2^0\ell^-\bar{\nu}_\ell) \times \mathcal{B}(D_2^0 \rightarrow D^{*+}\pi^-)$.

Experiment	$\mathcal{B}(B^- \rightarrow D_2^0(D^{*+}\pi^-)\ell^-\bar{\nu}_\ell)[\%]$ (rescaled)	$\mathcal{B}(B^- \rightarrow D_2^0(D^{*+}\pi^-)\ell^-\bar{\nu}_\ell)[\%]$ (published)
CLEO [506]	$0.055 \pm 0.066_{\text{stat}} \pm 0.011_{\text{syst}}$	$0.059 \pm 0.066_{\text{stat}} \pm 0.011_{\text{syst}}$
D0 [507]	$0.086 \pm 0.018_{\text{stat}} \pm 0.020_{\text{syst}}$	$0.088 \pm 0.018_{\text{stat}} \pm 0.020_{\text{syst}}$
Belle tagged [508]	$0.190 \pm 0.060_{\text{stat}} \pm 0.025_{\text{syst}}$	$0.18 \pm 0.06_{\text{stat}} \pm 0.03_{\text{syst}}$
<i>BABAR</i> tagged [509]	$0.075 \pm 0.013_{\text{stat}} \pm 0.009_{\text{syst}}$	$0.078 \pm 0.013_{\text{stat}} \pm 0.010_{\text{syst}}$
<i>BABAR</i> untagged B^- [510]	$0.087 \pm 0.009_{\text{stat}} \pm 0.007_{\text{syst}}$	$0.087 \pm 0.013_{\text{stat}} \pm 0.007_{\text{syst}}$
<i>BABAR</i> untagged B^0 [510]	$0.065 \pm 0.010_{\text{stat}} \pm 0.004_{\text{syst}}$	$0.087 \pm 0.013_{\text{stat}} \pm 0.007_{\text{syst}}$
Average	$0.077 \pm 0.006 \pm 0.004$	$\chi^2/\text{dof} = 5.4/5$ (CL=36.7%)

Table 76: Published and rescaled individual measurements and their averages for $\mathcal{B}(B^- \rightarrow D_1'^0 \ell^- \bar{\nu}_\ell) \times \mathcal{B}(D_1'^0 \rightarrow D^{*+} \pi^-)$.

Experiment	$\mathcal{B}(B^- \rightarrow D_1'^0(D^{*+} \pi^-) \ell^- \bar{\nu}_\ell)[\%]$ (rescaled)	$\mathcal{B}(B^- \rightarrow D_1'^0(D^{*+} \pi^-) \ell^- \bar{\nu}_\ell)[\%]$ (published)
DELPHI [511]	$0.73 \pm 0.17_{\text{stat}} \pm 0.18_{\text{syst}}$	$0.83 \pm 0.17_{\text{stat}} \pm 0.18_{\text{syst}}$
Belle [508]	$-0.03 \pm 0.06_{\text{stat}} \pm 0.07_{\text{syst}}$	$-0.03 \pm 0.06_{\text{stat}} \pm 0.07_{\text{syst}}$
BABAR [509]	$0.26 \pm 0.04_{\text{stat}} \pm 0.04_{\text{syst}}$	$0.27 \pm 0.04_{\text{stat}} \pm 0.05_{\text{syst}}$
Average	$0.19 \pm 0.03 \pm 0.04$	$\chi^2/\text{dof} = 11.9/2$ (CL=0.003%)

Table 77: Published and rescaled individual measurements and their averages for $\mathcal{B}(B^- \rightarrow D_0^{*0} \ell^- \bar{\nu}_\ell) \times \mathcal{B}(D_0^{*0} \rightarrow D^+ \pi^-)$.

Experiment	$\mathcal{B}(B^- \rightarrow D_0^{*0}(D^+ \pi^-) \ell^- \bar{\nu}_\ell)[\%]$ (rescaled)	$\mathcal{B}(B^- \rightarrow D_0^{*0}(D^+ \pi^-) \ell^- \bar{\nu}_\ell)[\%]$ (published)
Belle Tagged B^- [508]	$0.25 \pm 0.04_{\text{stat}} \pm 0.06_{\text{syst}}$	$0.24 \pm 0.04_{\text{stat}} \pm 0.06_{\text{syst}}$
Belle Tagged B^0 [508]	$0.22 \pm 0.08_{\text{stat}} \pm 0.06_{\text{syst}}$	$0.24 \pm 0.04_{\text{stat}} \pm 0.06_{\text{syst}}$
BABAR Tagged [509]	$0.32 \pm 0.04_{\text{stat}} \pm 0.05_{\text{syst}}$	$0.26 \pm 0.05_{\text{stat}} \pm 0.04_{\text{syst}}$
Average	$0.28 \pm 0.03 \pm 0.04$	$\chi^2/\text{dof} = 0.82/2$ (CL=66.4%)

6.2 Inclusive CKM-favored decays

6.2.1 Global analysis of $\overline{B} \rightarrow X_c \ell^- \bar{\nu}_\ell$

The semileptonic decay width $\Gamma(\overline{B} \rightarrow X_c \ell^- \bar{\nu}_\ell)$ has been calculated in the framework of the operator production expansion (OPE) [57–59]. The result is a double-expansion in Λ_{QCD}/m_b and α_s , which depends on a number of non-perturbative parameters. These parameters describe the dynamics of the b -quark inside the B hadron and can be measured using observables in $\overline{B} \rightarrow X_c \ell^- \bar{\nu}_\ell$ decays, such as the moments of the lepton energy and the hadronic mass spectrum.

Two renormalization schemes are commonly used to defined the b -quark mass and other theoretical quantities: the kinetic [512–515] and the 1S [516] schemes. An independent set of theoretical expressions is available for each, with several non-perturbative parameters. The non-perturbative parameters in the kinetic scheme are: the quark masses m_b and m_c , μ_π^2 and μ_G^2 at $O(1/m_b^2)$, and ρ_D^3 and ρ_{LS}^3 at $O(1/m_b^3)$. In the 1S scheme, the parameters are: m_b , λ_1 at $O(1/m_b^2)$, and ρ_1 , τ_1 , τ_2 and τ_3 at $O(1/m_b^3)$. Note that the numerical values of the kinetic and 1S b -quark masses cannot be compared without converting one or the other, or both, to the same renormalization scheme.

We use two sets of inclusive observables in $\overline{B} \rightarrow X_c \ell^- \bar{\nu}_\ell$ decays to constrain OPE parameters: the moments of the hadronic system effective mass $\langle M_X^n \rangle$ of order $n = 2, 4, 6$, and the moments of the charged lepton momentum $\langle E_\ell^n \rangle$ of order $n = 0, 1, 2, 3$. Moments are determined for different values of E_{cut} , the lower limit on the lepton momentum. Moments derived from the same spectrum with different value of E_{cut} are highly correlated. The list of measurements

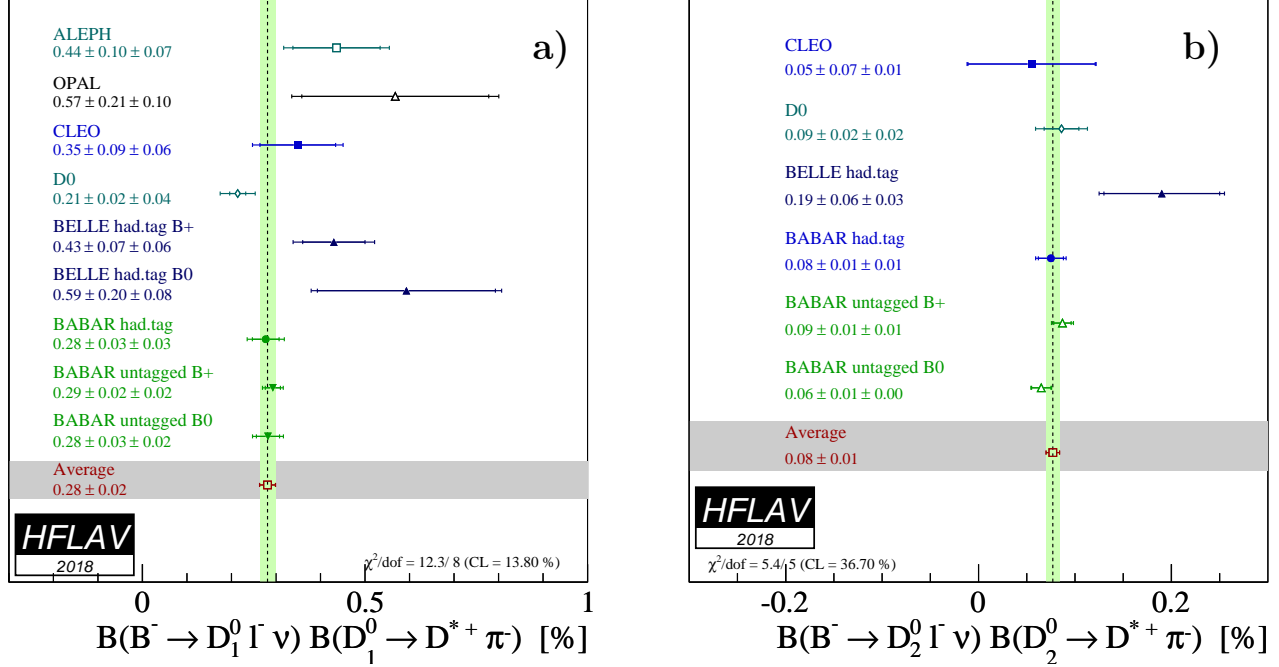


Figure 55: Rescaled individual measurements and their averages for (a) $\mathcal{B}(B^- \rightarrow D_1^0 \ell^- \bar{\nu}_\ell) \times \mathcal{B}(D_1^0 \rightarrow D^{*+} \pi^-)$ and (b) $\mathcal{B}(B^- \rightarrow D_2^0 \ell^- \bar{\nu}_\ell) \times \mathcal{B}(D_2^0 \rightarrow D^{*+} \pi^-)$.

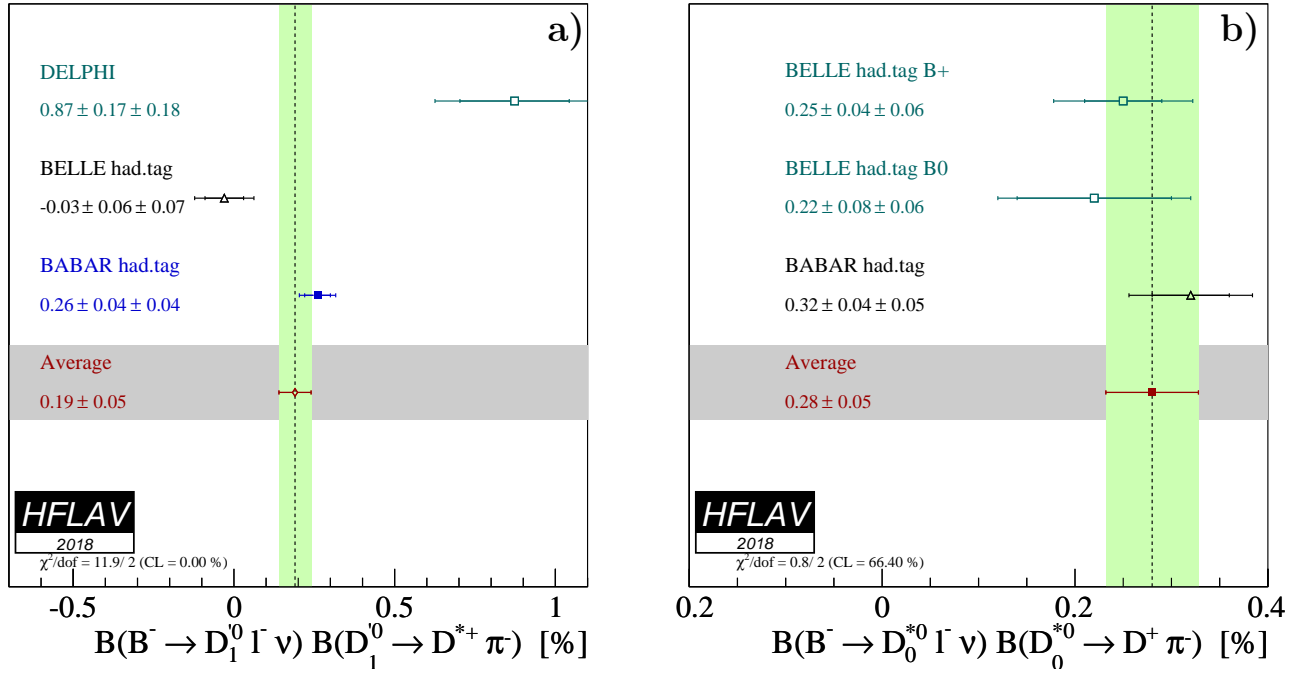


Figure 56: Rescaled individual measurements and their averages for (a) $\mathcal{B}(B^- \rightarrow D_1^0 \ell^- \bar{\nu}_\ell) \times \mathcal{B}(D_1^0 \rightarrow D^{*+} \pi^-)$ and (b) $\mathcal{B}(B^- \rightarrow D_0^{*0} \ell^- \bar{\nu}_\ell) \times \mathcal{B}(D_0^{*0} \rightarrow D^+ \pi^-)$.

used in our analysis is given in Table 78. The only external input is the average lifetime τ_B of neutral and charged B mesons, taken to be (1.579 ± 0.004) ps (Sec. 4).

Table 78: Experimental inputs used in the global analysis of $\bar{B} \rightarrow X_c \ell^- \bar{\nu}_\ell$. n is the order of the moment, c is the threshold value of the lepton momentum in GeV. In total, there are 23 measurements from *BABAR*, 15 measurements from *Belle* and 12 from other experiments.

Experiment	Hadron moments $\langle M_X^n \rangle$	Lepton moments $\langle E_\ell^n \rangle$
<i>BABAR</i>	$n = 2, c = 0.9, 1.1, 1.3, 1.5$	$n = 0, c = 0.6, 1.2, 1.5$
	$n = 4, c = 0.8, 1.0, 1.2, 1.4$	$n = 1, c = 0.6, 0.8, 1.0, 1.2, 1.5$
	$n = 6, c = 0.9, 1.3$ [517]	$n = 2, c = 0.6, 1.0, 1.5$ $n = 3, c = 0.8, 1.2$ [517, 518]
<i>Belle</i>	$n = 2, c = 0.7, 1.1, 1.3, 1.5$	$n = 0, c = 0.6, 1.4$
	$n = 4, c = 0.7, 0.9, 1.3$ [519]	$n = 1, c = 1.0, 1.4$ $n = 2, c = 0.6, 1.4$ $n = 3, c = 0.8, 1.2$ [520]
CDF	$n = 2, c = 0.7$ $n = 4, c = 0.7$ [521]	
CLEO	$n = 2, c = 1.0, 1.5$ $n = 4, c = 1.0, 1.5$ [522]	
DELPHI	$n = 2, c = 0.0$	$n = 1, c = 0.0$
	$n = 4, c = 0.0$	$n = 2, c = 0.0$
	$n = 6, c = 0.0$ [511]	$n = 3, c = 0.0$ [511]

In the kinetic and 1S schemes, the moments in $\bar{B} \rightarrow X_c \ell^- \bar{\nu}_\ell$ are not sufficient to determine the b -quark mass precisely. In the kinetic scheme analysis we constrain the c -quark mass (defined in the $\overline{\text{MS}}$ scheme) to the value of Ref. [523],

$$m_c^{\overline{\text{MS}}}(3 \text{ GeV}) = 0.986 \pm 0.013 \text{ GeV} . \quad (201)$$

In the 1S scheme analysis, the b -quark mass is constrained by measurements of the photon energy moments in $B \rightarrow X_s \gamma$ [524–527].

6.2.2 Analysis in the kinetic scheme

We obtain $|V_{cb}|$ and the six non-perturbative parameters mentioned above with a fit that follows closely the procedure described in Ref. [528] and relies on the calculations of the lepton energy and hadronic mass moments in $\bar{B} \rightarrow X_c \ell^- \bar{\nu}_\ell$ decays described in Ref. [514, 515]. The detailed fit result and the matrix of the correlation coefficients is given in Table 79. Projections of the fit onto the lepton energy and hadronic mass moments are shown in Figs. 57 and 58, respectively. The result in terms of the main parameters is

$$|V_{cb}| = (42.19 \pm 0.78) \times 10^{-3} , \quad (202)$$

$$m_b^{\text{kin}} = 4.554 \pm 0.018 \text{ GeV} , \quad (203)$$

$$\mu_\pi^2 = 0.464 \pm 0.076 \text{ GeV}^2 , \quad (204)$$

with a χ^2 of 15.6 for 43 degrees of freedom. The scale μ of the quantities in the kinematic scheme is 1 GeV.

Table 79: Fit result in the kinetic scheme, using a precise c -quark mass constraint. The error matrix of the fit contains experimental and theoretical contributions. In the lower part of the table, the correlation matrix of the parameters is given. The scale μ of the quantities in the kinematic scheme is 1 GeV.

	$ V_{cb} [10^{-3}]$	$m_b^{\text{kin}} [\text{GeV}]$	$m_c^{\overline{\text{MS}}} [\text{GeV}]$	$\mu_\pi^2 [\text{GeV}^2]$	$\rho_D^3 [\text{GeV}^3]$	$\mu_G^2 [\text{GeV}^2]$	$\rho_{LS}^3 [\text{GeV}^3]$
value	42.19	4.554	0.987	0.464	0.169	0.333	-0.153
error	0.78	0.018	0.015	0.076	0.043	0.053	0.096
$ V_{cb} $	1.000	-0.257	-0.078	0.354	0.289	-0.080	-0.051
m_b^{kin}		1.000	0.769	-0.054	0.097	0.360	-0.087
$m_c^{\overline{\text{MS}}}$			1.000	-0.021	0.027	0.059	-0.013
μ_π^2				1.000	0.732	0.012	0.020
ρ_D^3					1.000	-0.173	-0.123
μ_G^2						1.000	0.066
ρ_{LS}^3							1.000

The inclusive $\bar{B} \rightarrow X_c \ell^- \bar{\nu}_\ell$ branching fraction determined by this analysis is

$$\mathcal{B}(\bar{B} \rightarrow X_c \ell^- \bar{\nu}_\ell) = (10.65 \pm 0.16)\% . \quad (205)$$

Including the branching fraction of charmless semileptonic decays (Sec. 6.4), $\mathcal{B}(\bar{B} \rightarrow X_u \ell^- \bar{\nu}_\ell) = (2.13 \pm 0.30) \times 10^{-3}$, we obtain the semileptonic branching fraction,

$$\mathcal{B}(\bar{B} \rightarrow X \ell^- \bar{\nu}_\ell) = (10.86 \pm 0.16)\% . \quad (206)$$

6.2.3 Analysis in the 1S scheme

The fit relies on the same set of moment measurements and the calculations of the spectral moments described in Ref. [516]. The theoretical uncertainties are estimated as explained in Ref. [529]. Only trivial theory correlations, *i.e.* between the same moment at the same threshold are included in the analysis. The detailed result of the fit using the $B \rightarrow X_s \gamma$ constraint is given in Table 80. The result in terms of the main parameters is

$$|V_{cb}| = (41.98 \pm 0.45) \times 10^{-3} , \quad (207)$$

$$m_b^{1S} = 4.691 \pm 0.037 \text{ GeV} , \quad (208)$$

$$\lambda_1 = -0.362 \pm 0.067 \text{ GeV}^2 , \quad (209)$$

with a χ^2 of 23.0 for 59 degrees of freedom. We find a good agreement in the central values of $|V_{cb}|$ between the kinetic and 1S scheme analyses. No conclusion should, however, been drawn regarding the uncertainties in $|V_{cb}|$, as the two approaches are not equivalent in the number of higher-order corrections that are included.

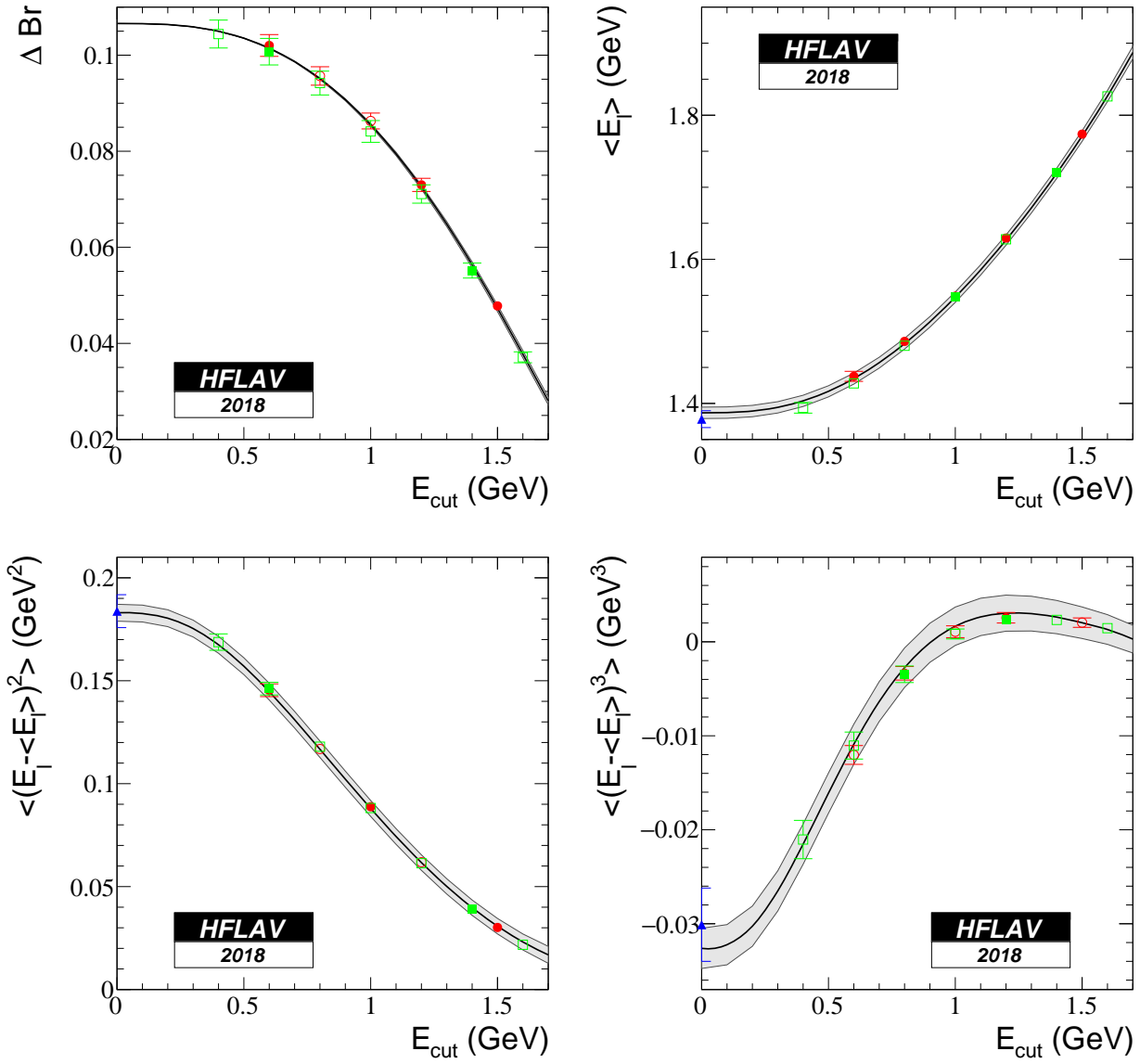


Figure 57: Fit to the inclusive partial semileptonic branching fractions and to the lepton energy moments in the kinetic mass scheme. In all plots, the grey band is the theory prediction with total theory error. *BABAR* data are shown by circles, *Belle* by squares and other experiments (DELPHI, CDF, CLEO) by triangles. Filled symbols mean that the point was used in the fit. Open symbols are measurements that were not used in the fit.

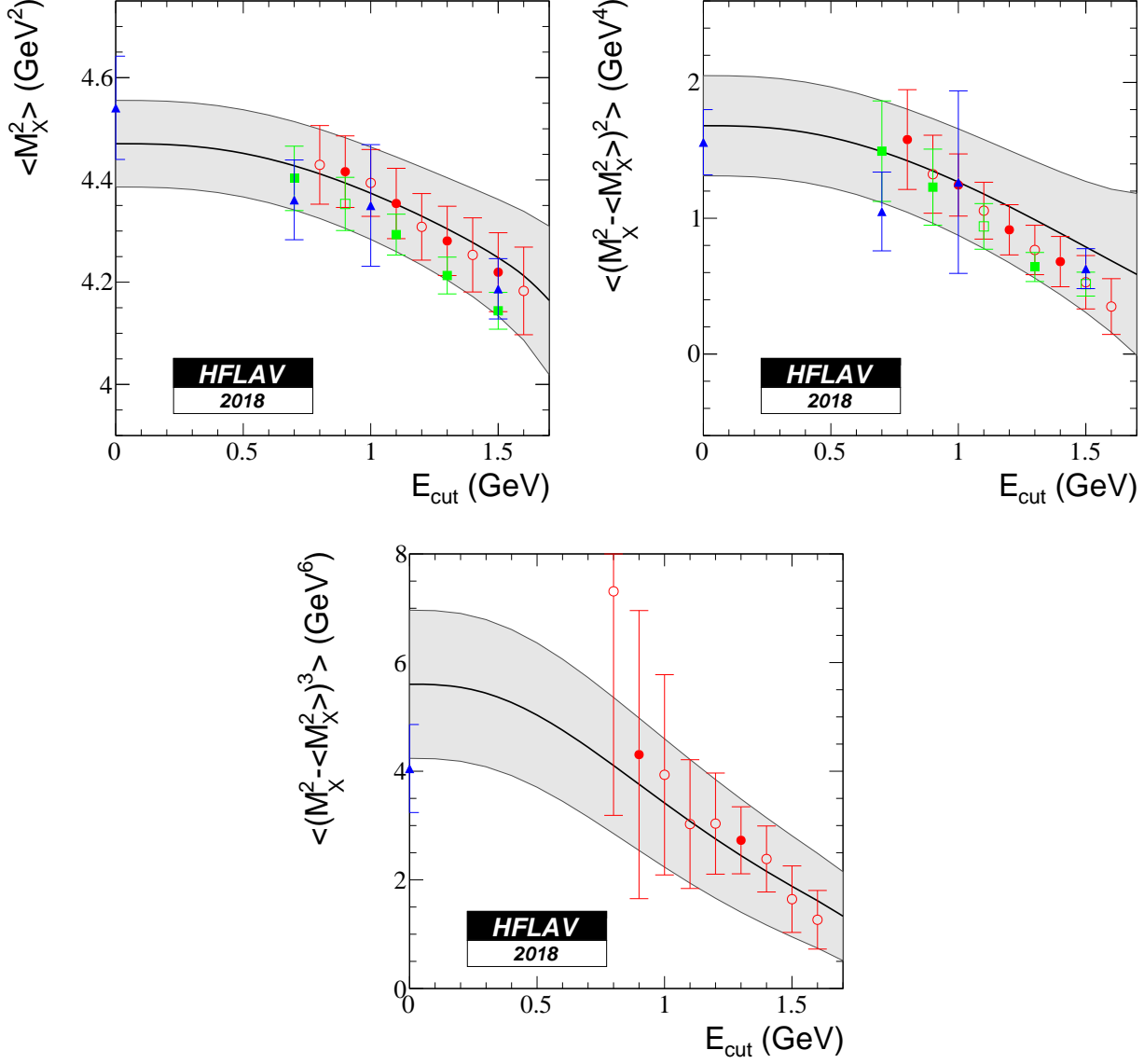


Figure 58: Same as Fig. 57 for the fit to the hadronic mass moments in the kinetic mass scheme.

6.3 Exclusive CKM-suppressed decays

In this section, we give results on exclusive charmless semileptonic branching fractions and the determination of $|V_{ub}|$ based on $B \rightarrow \pi \ell \nu$ decays. The measurements are based on two different event selections: tagged events, in which the second B meson in the event is fully (or partially) reconstructed, and untagged events, for which the momentum of the undetected neutrino is inferred from measurements of the total momentum sum of the detected particles and the knowledge of the initial state. The LHCb experiment has reported a direct measurement of $|V_{ub}|/|V_{cb}|$ [530], reconstructing the $\Lambda_b^0 \rightarrow p \mu \nu$ decays and normalizing the branching fraction to the $\Lambda_b^0 \rightarrow \Lambda_c^+ (\rightarrow p K \pi) \mu \nu$ decays. We show a combination of $|V_{ub}|$ and $|V_{cb}|$ using the LHCb constraint on $|V_{ub}|/|V_{cb}|$, the exclusive determination of $|V_{ub}|$ from $B \rightarrow \pi \ell \nu$, and $|V_{cb}|$ from both $B \rightarrow D^* \ell \nu$ and $B \rightarrow D \ell \nu$. We also present branching fraction averages for $B^0 \rightarrow \rho \ell^+ \nu$,

Table 80: Fit result in the 1S scheme, using $B \rightarrow X_s \gamma$ moments as a constraint. In the lower part of the table, the correlation matrix of the parameters is given.

	m_b^{1S} [GeV]	λ_1 [GeV 2]	ρ_1 [GeV 3]	τ_1 [GeV 3]	τ_2 [GeV 3]	τ_3 [GeV 3]	$ V_{cb} $ [10 $^{-3}$]
value	4.691	-0.362	0.043	0.161	-0.017	0.213	41.98
error	0.037	0.067	0.048	0.122	0.062	0.102	0.45
m_b^{1S}	1.000	0.434	0.213	-0.058	-0.629	-0.019	-0.215
λ_1		1.000	-0.467	-0.602	-0.239	-0.547	-0.403
ρ_1			1.000	0.129	-0.624	0.494	0.286
τ_1				1.000	0.062	-0.148	0.194
τ_2					1.000	-0.009	-0.145
τ_3						1.000	0.376
$ V_{cb} $							1.000

$B^+ \rightarrow \omega \ell^+ \nu$, $B^+ \rightarrow \eta \ell^+ \nu$ and $B^+ \rightarrow \eta' \ell^+ \nu$.

6.3.1 $B \rightarrow \pi \ell \nu$ branching fraction and q^2 spectrum

We use the four most precise measurements of the differential $B \rightarrow \pi \ell \nu$ decay rate as a function of the four-momentum transfer squared, q^2 , from *BABAR* and *Belle* [531–534] to obtain an average q^2 spectrum and an average for the total branching fraction. The measurements are presented in Fig. 59. From the two untagged *BABAR* analyses [533,534], the combined results for $B^0 \rightarrow \pi^- \ell^+ \nu$ and $B^+ \rightarrow \pi^0 \ell^+ \nu$ decays based on isospin symmetry are used. The hadronic-tag analysis by *Belle* [532] provides results for $B^0 \rightarrow \pi^- \ell^+ \nu$ and $B^+ \rightarrow \pi^0 \ell^+ \nu$ separately, but not for the combination of both channels. In the untagged analysis by *Belle* [531], only $B^0 \rightarrow \pi^- \ell^+ \nu$ decays were measured. The experimental measurements use different binnings in q^2 , but have matching bin edges, which allows them to be easily combined.

To arrive at an average q^2 spectrum, a binned maximum-likelihood fit to determine the average partial branching fraction in each q^2 interval is performed, differentiating between common and individual uncertainties and correlations for the various measurements. Shared sources of systematic uncertainty of all measurements are included in the likelihood as nuisance parameters constrained using normal distributions. The most important shared sources of uncertainty are due to continuum subtraction, branching fractions, the number of B -meson pairs (only correlated among measurement by the same experiment), tracking efficiency (only correlated among measurements by the same experiment), uncertainties from modelling the $b \rightarrow u \ell \bar{\nu}_\ell$ contamination, modelling of final state radiation, and contamination from $b \rightarrow c \ell \bar{\nu}_\ell$ decays.

The averaged q^2 spectrum is shown in Fig. 59. The probability of the average is computed as the χ^2 probability quantifying the agreement between the input spectra and the averaged spectrum and amounts to 6%. The partial branching fractions and the full covariance matrix obtained from the likelihood fit are given in Tables 81 and 82. The average for the total $B^0 \rightarrow \pi^- \ell^+ \nu_\ell$ branching fraction is obtained by summing up the partial branching fractions:

$$\mathcal{B}(B^0 \rightarrow \pi^- \ell^+ \nu_\ell) = (1.50 \pm 0.02_{\text{stat}} \pm 0.06_{\text{syst}}) \times 10^{-4}. \quad (210)$$

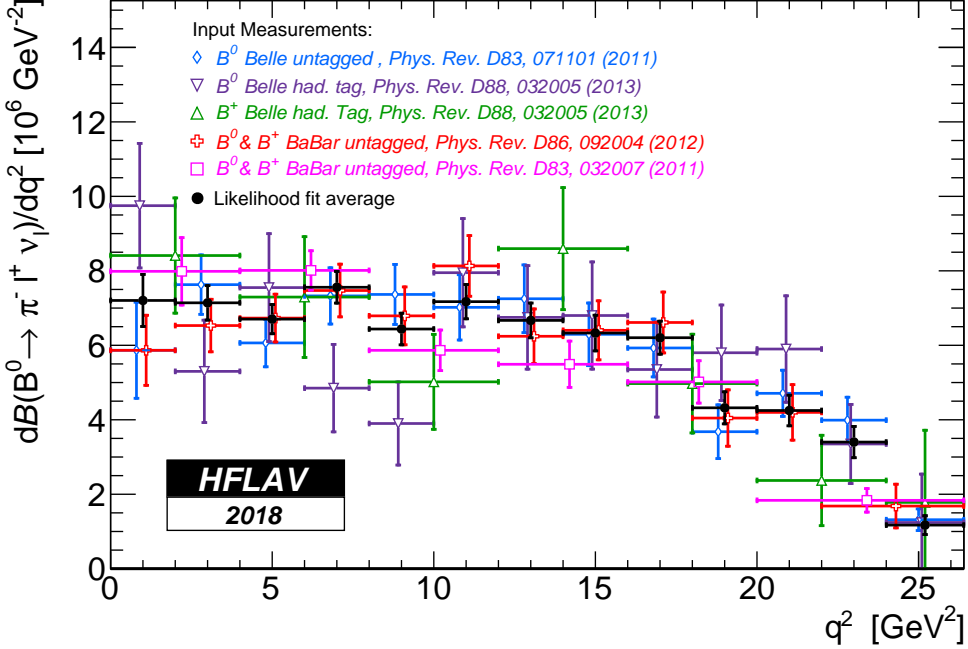


Figure 59: The $B \rightarrow \pi \ell \nu$ q^2 spectrum measurements and the average spectrum obtained from the likelihood combination (shown in black).

6.3.2 $|V_{ub}|$ from $B \rightarrow \pi \ell \nu$

The $|V_{ub}|$ average can be determined from the averaged q^2 spectrum in combination with a prediction for the normalization of the $B \rightarrow \pi$ form factor. The differential decay rate for light leptons (e, μ) is given by

$$\Delta\Gamma = \Delta\Gamma(q_{\text{low}}^2, q_{\text{high}}^2) = \int_{q_{\text{low}}^2}^{q_{\text{high}}^2} dq^2 \left[\frac{8 |\vec{p}_\pi| G_F^2 |V_{ub}|^2 q^2}{3 \cdot 256 \pi^3 m_B^2} H_0^2(q^2) \right], \quad (211)$$

where G_F is Fermi's constant, $|\vec{p}_\pi|$ is the absolute four-momentum of the final state π (a function of q^2), m_B the B^0 -meson mass, and $H_0(q^2)$ the only non-zero helicity amplitude. The helicity amplitude is a function of the form factor f_+ ,

$$H_0 = \frac{2m_B |\vec{p}_\pi|}{\sqrt{q^2}} f_+(q^2). \quad (212)$$

The form factor f_+ can be calculated with non-perturbative methods, but its general form can be constrained by the differential $B \rightarrow \pi \ell \nu$ spectrum. Here, we parametrize the form factor using the BCL parametrization [535].

The decay rate is proportional to $|V_{ub}|^2 |f_+(q^2)|^2$. Thus to extract $|V_{ub}|$ one needs to determine $f_+(q^2)$ (at least at one value of q^2). In order to enhance the precision, a binned χ^2 fit is performed using a χ^2 function of the form

$$\chi^2 = (\vec{\mathcal{B}} - \Delta\vec{\Gamma} \tau)^T C^{-1} (\vec{\mathcal{B}} - \Delta\vec{\Gamma} \tau) + \chi^2_{\text{LQCD}} + \chi^2_{\text{LCSR}} \quad (213)$$

Table 81: Partial $B^0 \rightarrow \pi^- \ell^+ \nu_\ell$ branching fractions per GeV^2 for the input measurements and the average obtained from the likelihood fit. The uncertainties are the combined statistical and systematic uncertainties.

Δq^2 [GeV 2]	$\Delta \mathcal{B}(B^0 \rightarrow \pi^- \ell^+ \nu_\ell) / \Delta q^2$ [10 $^{-7}$]						Average
	Belle untagged (B^0)	Belle tagged (B^0)	Belle tagged (B^+)	BABAR untagged ($B^{0,+}$, 12 bins)	BABAR untagged ($B^{0,+}$, 6 bins)		
0 – 2	58.7 ± 12.9	97.5 ± 16.7	84.1 ± 15.5	58.7 ± 9.4		79.9 ± 9.1	72.0 ± 7.0
2 – 4	76.3 ± 8.0	53.0 ± 13.8		65.3 ± 7.1			71.4 ± 4.6
4 – 6	60.6 ± 6.4	75.5 ± 14.5	73.0 ± 16.2	67.3 ± 6.4		80.1 ± 5.3	67.0 ± 3.9
6 – 8	73.3 ± 7.6	48.5 ± 11.8		74.7 ± 7.1			75.6 ± 4.3
8 – 10	73.7 ± 8.1	39.0 ± 11.2	50.2 ± 12.8	67.9 ± 7.8		58.7 ± 5.5	64.4 ± 4.3
10 – 12	70.2 ± 8.8	79.5 ± 14.6		81.3 ± 8.2			71.7 ± 4.6
12 – 14	72.5 ± 9.1	67.5 ± 13.9	86.0 ± 16.4	62.4 ± 7.4		54.9 ± 6.2	66.7 ± 4.7
14 – 16	63.0 ± 8.4	68.0 ± 14.4		64.0 ± 7.9			63.3 ± 4.8
16 – 18	59.3 ± 7.8	53.5 ± 12.8	49.7 ± 13.3	66.1 ± 8.2		50.2 ± 5.7	62.0 ± 4.4
18 – 20	36.8 ± 7.2	58.0 ± 12.8		40.5 ± 7.6			43.2 ± 4.3
20 – 22	47.1 ± 6.2	59.0 ± 14.3	23.7 ± 12.1	42.0 ± 7.5			42.5 ± 4.1
22 – 24	39.9 ± 6.2	33.5 ± 10.6			16.8 ± 5.9	18.4 ± 3.2	34.0 ± 4.2
24 – 26.4	13.2 ± 2.9	12.4 ± 13.0	17.8 ± 19.4				11.7 ± 2.6

Table 82: Covariance matrix of the averaged partial branching fractions per GeV^2 in units of 10 $^{-14}$.

Δq^2 [GeV 2]	0 – 2	2 – 4	4 – 6	6 – 8	8 – 10	10 – 12	12 – 14	14 – 16	16 – 18	18 – 20	20 – 22	22 – 24	24 – 26.4
0 – 2	49.091	1.164	8.461	7.996	7.755	9.484	7.604	9.680	8.868	7.677	7.374	7.717	2.877
2 – 4		21.487	-0.0971	7.155	4.411	5.413	4.531	4.768	4.410	3.442	3.597	3.388	1.430
4 – 6			15.489	-0.563	5.818	4.449	4.392	4.157	4.024	3.185	3.169	3.013	1.343
6 – 8				18.2	2.377	7.889	6.014	5.938	5.429	4.096	3.781	3.863	1.428
8 – 10					18.124	1.540	7.496	5.224	5.441	4.197	3.848	4.094	1.673
10 – 12						21.340	4.213	7.696	6.493	5.170	4.686	4.888	1.950
12 – 14							21.875	0.719	6.144	3.846	3.939	3.922	1.500
14 – 16								23.040	5.219	6.123	4.045	4.681	1.807
16 – 18									19.798	1.662	4.362	4.140	1.690
18 – 20										18.0629	2.621	3.957	1.438
20 – 22											16.990	1.670	1.127
22 – 24												17.774	-0.293
24 – 26.4													6.516

where C denotes the covariance matrix given in Table 82, $\vec{\mathcal{B}}$ is the vector of averaged branching fractions, and $\Delta \vec{\Gamma} \tau$ is the product of the vector of theoretical predictions of the partial decay rates and the B^0 -meson lifetime. The form factor normalization is included in the fit by the two extra terms in Eq. (213): χ_{LQCD} uses the latest FLAG lattice average [536] from two state-of-the-art unquenched lattice QCD calculations [537, 538]. The resulting constraints are quoted directly in terms of the coefficients b_j of the BCL parameterization and enter Eq. (213) as

$$\chi_{\text{LQCD}}^2 = \left(\vec{b} - \vec{b}_{\text{LQCD}} \right)^T C_{\text{LQCD}}^{-1} \left(\vec{b} - \vec{b}_{\text{LQCD}} \right), \quad (214)$$

with \vec{b} the vector containing the free parameters of the χ^2 fit constraining the form factor, \vec{b}_{LQCD} the averaged values from Ref. [536], and C_{LQCD} their covariance matrix. Additional information about the form factor can be obtained from light-cone sum rule calculations. The state-of-the-

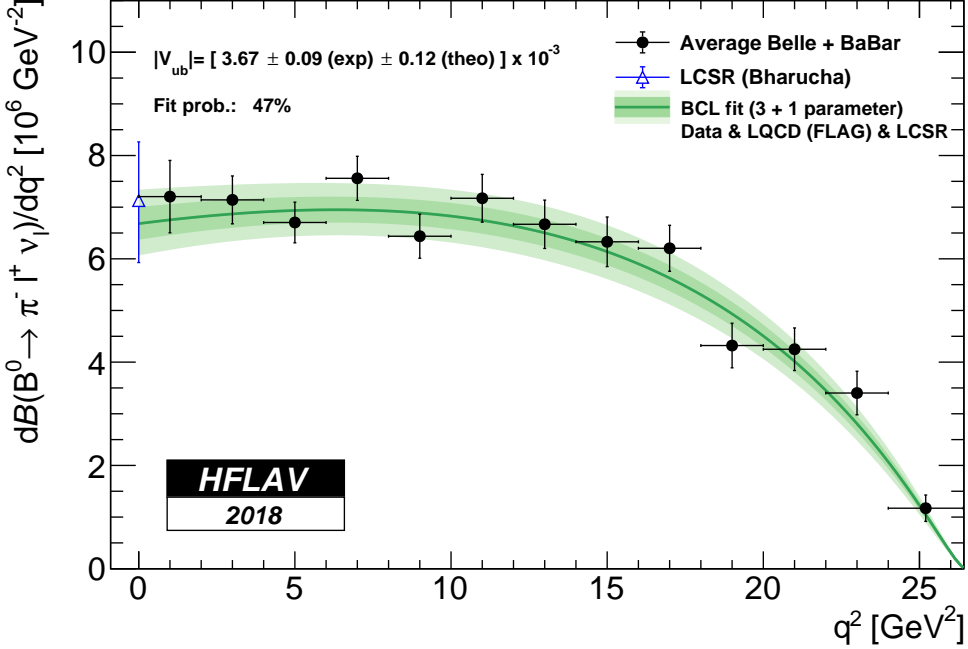


Figure 60: Fit of the BCL parametrization to the averaged q^2 spectrum from *BABAR* and *Belle* and the LQCD and LCSR calculations. The error bands represent the 1 σ (dark green) and 2 σ (light green) uncertainties of the fitted spectrum.

art calculation includes up to two-loop contributions [539]. It is included in Eq. (213) via

$$\chi^2_{\text{LQCD}} = \left(f_+^{\text{LCSR}} - f_+(q^2 = 0; \vec{b}) \right)^2 / \sigma_{f_+^{\text{LCSR}}}^2. \quad (215)$$

The $|V_{ub}|$ average is obtained for two versions: the first combines the data with the LQCD constraints and the second additionally includes the information from the LCSR calculation. The resulting values for $|V_{ub}|$ are

$$|V_{ub}| = (3.70 \pm 0.10 \text{ (exp)} \pm 0.12 \text{ (theo)}) \times 10^{-3} \text{ (data + LQCD)}, \quad (216)$$

$$|V_{ub}| = (3.67 \pm 0.09 \text{ (exp)} \pm 0.12 \text{ (theo)}) \times 10^{-3} \text{ (data + LQCD + LCSR)}, \quad (217)$$

for the first and second fit version, respectively. The result of the fit including both LQCD and LCSR is shown in Figure 60. The χ^2 probability of the fit is 47%. We quote the result of the fit including both LQCD and LCSR calculations as our average for $|V_{ub}|$. The best fit values for $|V_{ub}|$ and the BCL parameters and their covariance matrix are given in Tables 83 and 84.

6.3.3 Combined extraction of $|V_{ub}|$ and $|V_{cb}|$

The LHCb experiment reported the first observation of the CKM suppressed decay $\Lambda_b^0 \rightarrow p \mu \nu$ [530] and the measurement of the ratio of partial branching fractions at high q^2 for $\Lambda_b^0 \rightarrow p \mu \nu$ and $\Lambda_b^0 \rightarrow \Lambda_c^+ (\rightarrow p K \pi) \mu \nu$ decays,

$$R = \frac{\mathcal{B}(\Lambda_b^0 \rightarrow p \mu \nu)_{q^2 > 15 \text{ GeV}^2}}{\mathcal{B}(\Lambda_b^0 \rightarrow \Lambda_c^+ \mu \nu)_{q^2 > 7 \text{ GeV}^2}} = (1.00 \pm 0.04 \pm 0.08) \times 10^{-2}. \quad (218)$$

Table 83: Best fit values and uncertainties for the combined fit to data, LQCD and LCSR results.

Parameter	Value
$ V_{ub} $	$(3.67 \pm 0.15) \times 10^{-3}$
b_0	0.418 ± 0.012
b_1	-0.399 ± 0.033
b_2	-0.578 ± 0.130

Table 84: Covariance matrix for the combined fit to data, LQCD and LCSR results.

Parameter	$ V_{ub} $	b_0	b_1	b_2
$ V_{ub} $	2.064×10^{-8}	-1.321×10^{-6}	-1.881×10^{-6}	7.454×10^{-6}
b_0		1.390×10^{-4}	8.074×10^{-5}	-8.953×10^{-4}
b_1			1.053×10^{-3}	-2.879×10^{-3}
b_2				1.673×10^{-2}

The ratio R is proportional to $(|V_{ub}|/|V_{cb}|)^2$ and sensitive to the form factors of $\Lambda_b^0 \rightarrow p$ and $\Lambda_b^0 \rightarrow \Lambda_c^+ \rightarrow pK\pi$ transitions that have to be computed with non-perturbative methods, such as lattice QCD. The uncertainty on $\mathcal{B}(\Lambda_c^+ \rightarrow pK\pi)$ is the largest source of systematic uncertainties on R . Using the recent average of $\mathcal{B}(\Lambda_c^+ \rightarrow pK\pi) = (6.28 \pm 0.32)\%$ [21], the rescaled value for R is

$$R = (0.92 \pm 0.04 \pm 0.07) \times 10^{-2}. \quad (219)$$

Using the precise lattice QCD prediction [540] of the form factors in the experimentally interesting q^2 region considered, we obtain

$$\frac{|V_{ub}|}{|V_{cb}|} = 0.079 \pm 0.004_{Exp.} \pm 0.004_{F.F.} \quad (220)$$

where the first uncertainty is the total experimental uncertainty, and the second one is due to the knowledge of the form factors. A combined fit for $|V_{ub}|$ and $|V_{cb}|$ that includes the constraint from LHCb, and the determination of $|V_{ub}|$ and $|V_{cb}|$ from exclusive B meson decays, results in

$$|V_{ub}| = (3.49 \pm 0.13) \times 10^{-3} \quad (221)$$

$$|V_{cb}| = (39.25 \pm 0.56) \times 10^{-3} \quad (222)$$

$$\rho(|V_{ub}|, |V_{cb}|) = 0.14, \quad (223)$$

where the uncertainties in the inputs are considered uncorrelated. The χ^2 of the fit is 5.1 for 2 d.o.f., corresponding to a $P(\chi^2)$ of 7.7%. The fit result is shown in Fig. 61, where both the $\Delta\chi^2$ and the two-dimensional 68% C.L. contours are indicated. The $|V_{ub}|/|V_{cb}|$ value extracted from R is more compatible with the exclusive determinations of $|V_{ub}|$. Another calculation, by Faustov and Galkin [541], based on a relativistic quark model, gives a value of $|V_{ub}|/|V_{cb}|$ closer to the inclusive determinations.

6.3.4 Other exclusive charmless semileptonic B decays

We report the branching fraction average for $B^0 \rightarrow \rho\ell^+\nu$, $B^+ \rightarrow \omega\ell^+\nu$, $B^+ \rightarrow \eta\ell^+\nu$ and $B^+ \rightarrow \eta'\ell^+\nu$ decays. The measurements and their averages are listed in Tables 85, 86, 87, 88,

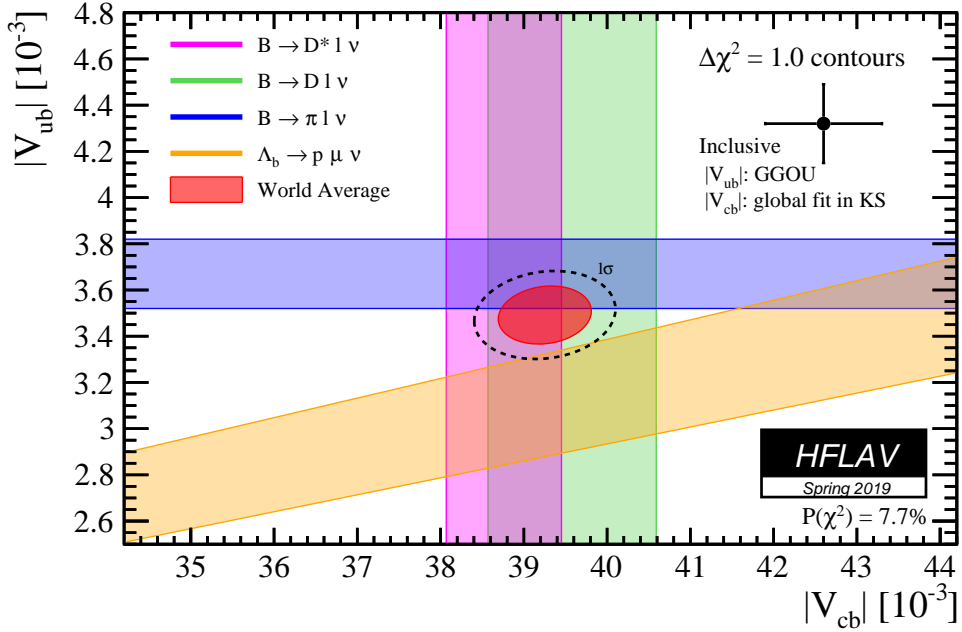


Figure 61: Combined average on $|V_{ub}|$ and $|V_{cb}|$ including the LHCb measurement of $|V_{ub}|/|V_{cb}|$, the exclusive $|V_{ub}|$ measurement from $B \rightarrow \pi \ell \nu$, and $|V_{cb}|$ measurements from both $B \rightarrow D^* \ell \nu$ and $B \rightarrow D \ell \nu$. The dashed ellipse corresponds to a 1σ two-dimensional contour (68% of CL). The point with the error bars corresponds to the inclusive $|V_{cb}|$ from the kinetic scheme (Sec. 6.2.2), and the inclusive $|V_{ub}|$ from GGOU calculation (Sec. 6.4.3).

and presented in Figures 62 and 63. In the $B^0 \rightarrow \rho^- \ell^+ \nu$ average, both the $B^0 \rightarrow \rho^- \ell^+ \nu$ and $B^+ \rightarrow \rho^0 \ell^+ \nu$ decays are used, where the $B^+ \rightarrow \rho^0 \ell^+ \nu$ are rescaled by $2\tau_{B^0}/\tau_{B^+}$ assuming the isospin symmetry. For $B^+ \rightarrow \omega \ell^+ \nu$ and $B^+ \rightarrow \eta \ell^+ \nu$ decays, the agreement between the different measurements is good. $B^+ \rightarrow \eta' \ell^+ \nu$ shows a discrepancy between the old CLEO measurement and the *BABAR* untagged analysis, but the statistical uncertainties of the CLEO measurement are large. The $B^0 \rightarrow \rho \ell^+ \nu$ results, instead, show significant differences, in particular the *BABAR* untagged analysis gives a branching fraction significantly lower (by about 2σ) than the Belle measurement based on the hadronic-tag. A possible reason for such discrepancy could be the broad nature of the ρ resonance that makes the control of the background under the ρ mass peak more difficult in the untagged analysis than in the hadronic-tag analysis.

We do not report $|V_{ub}|$ for these exclusive charmless decays, because the form factor calculations have not yet reached the precision achieved for $B \rightarrow \pi \ell \nu$ decays. Unquenched lattice QCD calculations of the form factors are not available for these decays, but LCSR calculations exist for all these decay modes. The most recent of these calculations for the $B \rightarrow \rho \ell \nu$ and $B \rightarrow \omega \ell \nu$ decays are reported in Ref. [542] and [543].

Table 85: Summary of exclusive determinations of $B^0 \rightarrow \rho\ell^+\nu$. The errors quoted correspond to statistical and systematic uncertainties, respectively.

	$\mathcal{B}[10^{-4}]$
CLEO (Untagged) ρ^+ [544]	$2.77 \pm 0.41 \pm 0.52$
CLEO (Untagged) ρ^+ [545]	$2.93 \pm 0.37 \pm 0.37$
Belle (Hadronic Tag) ρ^+ [532]	$3.22 \pm 0.27 \pm 0.24$
Belle (Hadronic Tag) ρ^0 [532]	$3.39 \pm 0.18 \pm 0.18$
Belle (Semileptonic Tag) ρ^+ [546]	$2.24 \pm 0.54 \pm 0.31$
Belle (Semileptonic Tag) ρ^0 [546]	$2.50 \pm 0.43 \pm 0.33$
<i>BABAR</i> (Untagged) ρ^+ [533]	$1.96 \pm 0.21 \pm 0.38$
<i>BABAR</i> (Untagged) ρ^0 [533]	$1.86 \pm 0.19 \pm 0.32$
Average	$2.937 \pm 0.093 \pm 0.178$

Table 86: Summary of exclusive determinations of $B^+ \rightarrow \omega\ell^+\nu$. The errors quoted correspond to statistical and systematic uncertainties, respectively.

	$\mathcal{B}[10^{-4}]$
Belle (Untagged) [547]	$1.30 \pm 0.40 \pm 0.36$
<i>BABAR</i> (Loose ν reco.) [534]	$1.19 \pm 0.16 \pm 0.09$
<i>BABAR</i> (Untagged) [548]	$1.21 \pm 0.14 \pm 0.08$
Belle (Hadronic Tag) [532]	$1.07 \pm 0.16 \pm 0.07$
<i>BABAR</i> (Semileptonic Tag) [549]	$1.35 \pm 0.21 \pm 0.11$
Average	$1.189 \pm 0.084 \pm 0.055$

Table 87: Summary of exclusive determinations of $B^+ \rightarrow \eta\ell^+\nu$. The errors quoted correspond to statistical and systematic uncertainties, respectively.

	$\mathcal{B}[10^{-4}]$
CLEO [550]	$0.45 \pm 0.23 \pm 0.11$
<i>BABAR</i> (Untagged) [551]	$0.31 \pm 0.06 \pm 0.08$
<i>BABAR</i> (Semileptonic Tag) [552]	$0.64 \pm 0.20 \pm 0.04$
<i>BABAR</i> (Loose ν -reco.) [534]	$0.38 \pm 0.05 \pm 0.05$
Belle (Hadronic Tag) [553]	$0.42 \pm 0.11 \pm 0.09$
Average	$0.44 \pm 0.02 \pm 0.05$

Table 88: Summary of exclusive determinations of $B^+ \rightarrow \eta' \ell^+ \nu$. The errors quoted correspond to statistical and systematic uncertainties, respectively.

	$\mathcal{B}[10^{-4}]$
CLEO [550]	$2.71 \pm 0.80 \pm 0.56$
BABAR (Semileptonic Tag) [552]	$0.04 \pm 0.22 \pm 0.04$, (< 0.47 @ 90% C.L.)
BABAR (Untagged) [534]	$0.24 \pm 0.08 \pm 0.03$
Belle (Hadronic Tag) [553]	$0.36 \pm 0.27 \pm 0.04$
Average	$0.24 \pm 0.07 \pm 0.03$

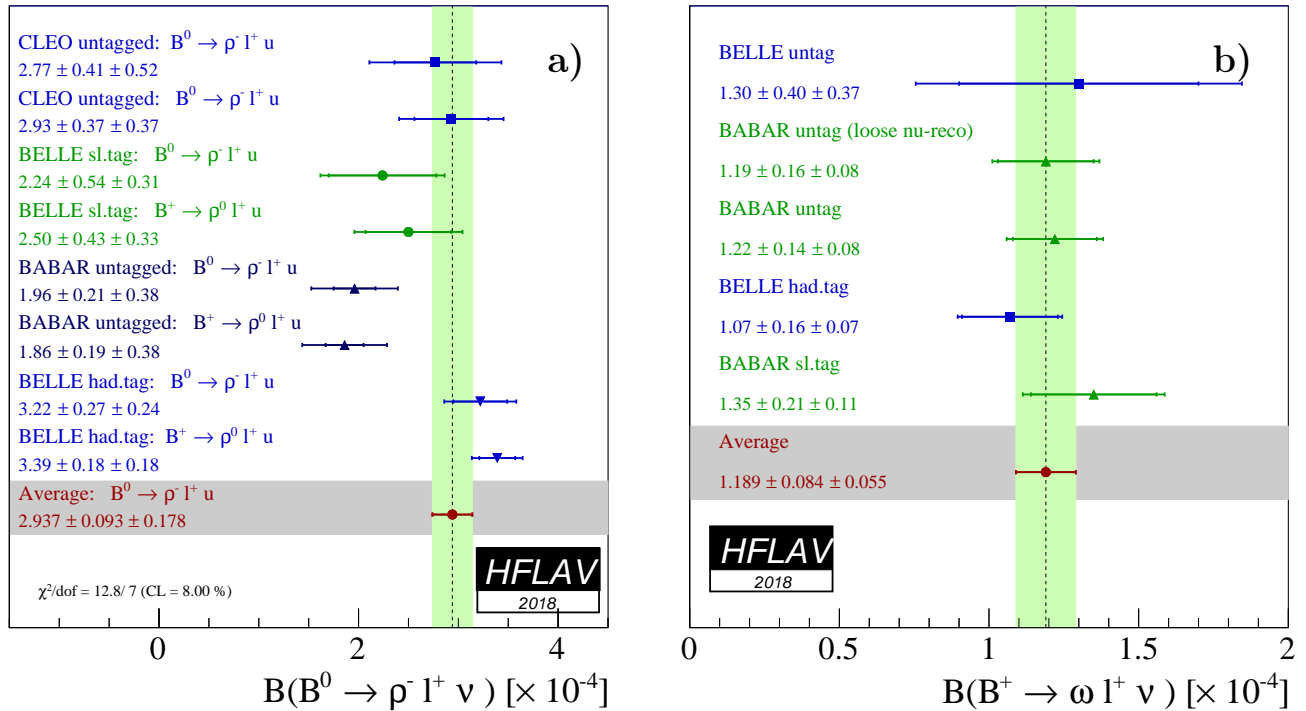


Figure 62: (a) Summary of exclusive determinations of $\mathcal{B}(B^0 \rightarrow \rho \ell^+ \nu)$ and their average. Measurements of $B^+ \rightarrow \rho^0 \ell^+ \nu$ branching fractions have been multiplied by $2\tau_{B^0}/\tau_{B^+}$ in accordance with isospin symmetry. (b) Summary of exclusive determinations of $B^+ \rightarrow \omega \ell^+ \nu$ and their average.

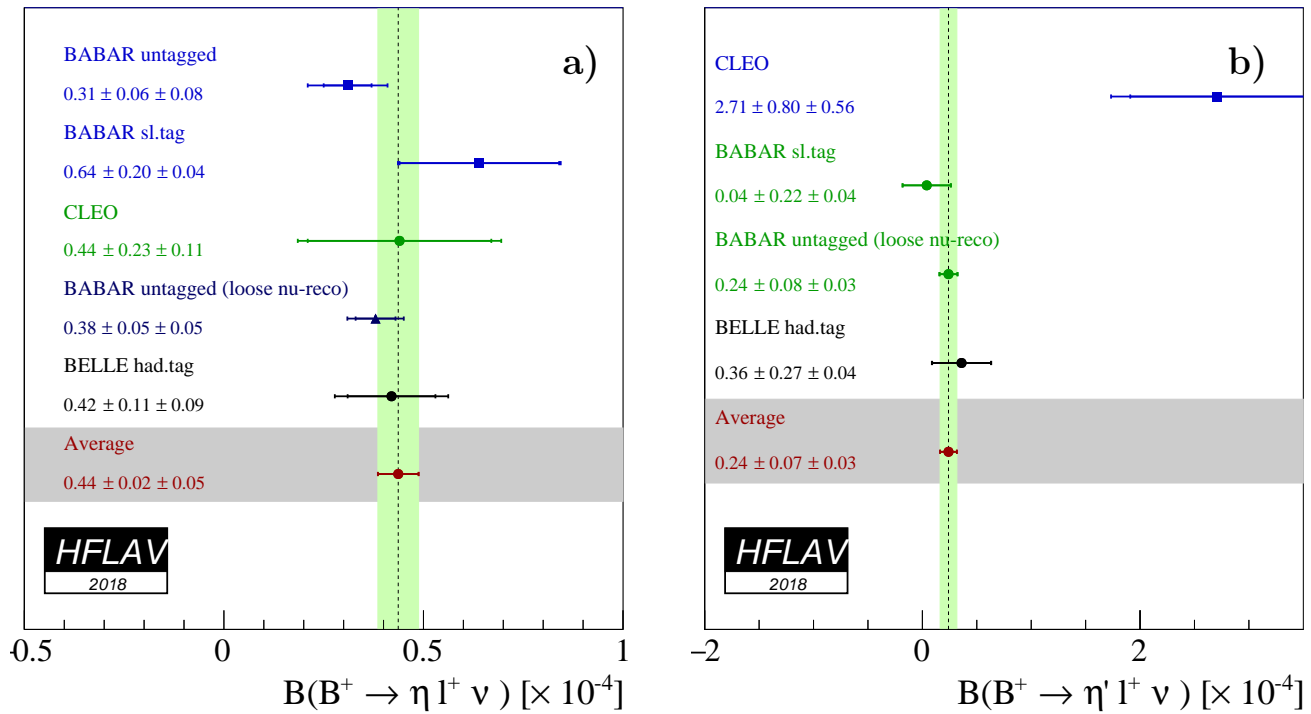


Figure 63: (a) Summary of exclusive determinations of $\mathcal{B}(B^+ \rightarrow \eta \ell^+ \nu)$ and their average. (b) Summary of exclusive determinations of $\mathcal{B}(B^+ \rightarrow \eta' \ell^+ \nu)$ and their average.

6.4 Inclusive CKM-suppressed decays

Measurements of $B \rightarrow X_u \ell^+ \nu$ decays are very challenging because of background from the Cabibbo-favoured $B \rightarrow X_c \ell^+ \nu$ decays, whose branching fraction is about 50 times larger than that of the signal. Cuts designed to suppress this dominant background severely complicate the perturbative QCD calculations required to extract $|V_{ub}|$. Tight cuts necessitate parameterization of the so-called shape functions in order to describe the unmeasured regions of phase space. We use several theoretical calculations to extract $|V_{ub}|$ and do not advocate the use of one method over another. The authors of the different calculations have provided codes to compute the partial rates in limited regions of phase space covered by the measurements. Belle [554] and *BABAR* [555] produced measurements that explore large portions of phase space, with consequent reduction of the theoretical uncertainties.

In the averages, the systematic uncertainties associated with the modeling of $B \rightarrow X_c \ell^+ \nu_\ell$ and $B \rightarrow X_u \ell^+ \nu_\ell$ decays and the theoretical uncertainties are taken as fully correlated among all measurements. Reconstruction-related uncertainties are taken as fully correlated within a given experiment. Measurements of partial branching fractions for $B \rightarrow X_u \ell^+ \nu_\ell$ transitions from $\Upsilon(4S)$ decays, together with the corresponding selected region, are given in Table 89. The signal yields for all the measurements shown in Table 89 are not rescaled to common input values of the B meson lifetime (see Sec. 4) and the semileptonic width [21]. We use all results published by *BABAR* in Ref. [555], since the statistical correlations are given. To make use of the theoretical calculations of Ref. [556], we restrict the kinematic range of the invariant mass of the hadronic system, M_X , and the square of the invariant mass of the lepton pair, q^2 . This reduces the size of the data sample significantly, but also the theoretical uncertainty, as stated by the authors [556]. The dependence of the quoted error on the measured value for each source of uncertainty is taken into account in the calculation of the averages.

It was first suggested by Neubert [557] and later detailed by Leibovich, Low, and Rothstein (LLR) [558] and Lange, Neubert and Paz (LNP) [559], that the uncertainty of the leading shape functions can be eliminated by comparing inclusive rates for $B \rightarrow X_u \ell^+ \nu_\ell$ decays with the inclusive photon spectrum in $B \rightarrow X_s \gamma$, based on the assumption that the shape functions for transitions to light quarks, u or s , are the same at first order. However, shape function uncertainties are only eliminated at the leading order and they still enter via the signal models used for the determination of efficiency.

In the following, the different theoretical methods and the resulting averages are described.

In a recent paper by *BABAR* [560], detailed studies are performed to assess the impact of four QCD-based theoretical predictions, used also below, on the measurements of the electron spectrum, the branching fraction, and the extraction of $|V_{ub}|$, where the lower limit on the electron momentum is varied from $0.8\text{GeV}/c$ to the kinematic endpoint. An important difference of this paper with respect to the other ones is that the dependency on the theoretical models enters primarily through the partial branching fractions, as the fit is sensitive to signal decays only in regions with good signal-to-noise such as the endpoint region. All other measurements instead determine a partial branching fraction by using a single model, and this partial branching fraction is then converted into a $|V_{ub}|$ measurement by taking the corresponding partial rate predicted by the theory calculations. Due to this difference, the $|V_{ub}|$ results obtained in this paper, with a lower limit of $0.8\text{GeV}/c$ on the electron momentum, are directly used as input to the BLNP, DGE and GGOU averages. These determinations supersede the previous *BABAR* endpoint measurement [561]. The partial branching ratio quoted in Table 89 for Ref. [560] is

taken as that obtained with the GGOU calculation.

Table 89: Summary of measurements of partial branching fractions for $B \rightarrow X_u \ell^+ \nu_\ell$ decays. The errors quoted on $\Delta\mathcal{B}$ correspond to statistical and systematic uncertainties. E_e is the electron energy in the B rest frame, p^* the lepton momentum in the B frame and m_X is the invariant mass of the hadronic system. The light-cone momentum P_+ is defined in the B rest frame as $P_+ = E_X - |\vec{p}_X|$. The s_h^{\max} variable is described in Refs. [562, 563].

Measurement	Accepted region	$\Delta\mathcal{B}[10^{-4}]$	Notes
CLEO [564]	$E_e > 2.1 \text{ GeV}$	$3.3 \pm 0.2 \pm 0.7$	
BABAR [563]	$E_e > 2.0 \text{ GeV}, s_h^{\max} < 3.5 \text{ GeV}^2$	$4.4 \pm 0.4 \pm 0.4$	
BABAR [560]	$E_e > 1.0 \text{ GeV}$	$1.55 \pm 0.08 \pm 0.09$	Using the GGOU model
Belle [565]	$E_e > 1.9 \text{ GeV}$	$8.5 \pm 0.4 \pm 1.5$	
BABAR [555]	$M_X < 1.7 \text{ GeV}/c^2, q^2 > 8 \text{ GeV}^2/c^4$	$6.9 \pm 0.6 \pm 0.4$	
Belle [566]	$M_X < 1.7 \text{ GeV}/c^2, q^2 > 8 \text{ GeV}^2/c^4$	$7.4 \pm 0.9 \pm 1.3$	
Belle [567]	$M_X < 1.7 \text{ GeV}/c^2, q^2 > 8 \text{ GeV}^2/c^4$	$8.5 \pm 0.9 \pm 1.0$	Used only in BLL average
BABAR [555]	$P_+ < 0.66 \text{ GeV}$	$9.9 \pm 0.9 \pm 0.8$	
BABAR [555]	$M_X < 1.7 \text{ GeV}/c^2$	$11.6 \pm 1.0 \pm 0.8$	
BABAR [555]	$M_X < 1.55 \text{ GeV}/c^2$	$10.9 \pm 0.8 \pm 0.6$	
Belle [554]	(M_X, q^2) fit, $p_\ell^* > 1 \text{ GeV}/c$	$19.6 \pm 1.7 \pm 1.6$	
BABAR [555]	(M_X, q^2) fit, $p_\ell^* > 1 \text{ GeV}/c$	$18.2 \pm 1.3 \pm 1.5$	
BABAR [555]	$p_\ell^* > 1.3 \text{ GeV}/c$	$15.5 \pm 1.3 \pm 1.4$	

6.4.1 BLNP

Bosch, Lange, Neubert and Paz (BLNP) [568–571] provide theoretical expressions for the triple differential decay rate for $B \rightarrow X_u \ell^+ \nu_\ell$ events, incorporating all known contributions, whilst smoothly interpolating between the “shape-function region” of large hadronic energy and small invariant mass, and the “OPE region” in which all hadronic kinematical variables scale with the b -quark mass. BLNP assign uncertainties to the b -quark mass, which enters through the leading shape function, to sub-leading shape function forms, to possible weak annihilation contribution, and to matching scales. The BLNP calculation uses the shape function renormalization scheme; the heavy quark parameters determined from the global fit in the kinetic scheme, described in 6.2.2, were therefore translated into the shape function scheme by using a prescription by Neubert [572, 573]. The resulting parameters are $m_b(\text{SF}) = (4.582 \pm 0.023 \pm 0.018) \text{ GeV}$, $\mu_\pi^2(\text{SF}) = (0.202 \pm 0.089^{+0.020}_{-0.040}) \text{ GeV}/c^2$, where the second uncertainty is due to the scheme translation. The extracted values of $|V_{ub}|$ for each measurement along with their average are given in Table 90 and illustrated in Fig. 64(a). The total uncertainty is $^{+5.6\%}_{-5.7\%}$ and is due to: statistics ($^{+1.8\%}_{-1.9\%}$), detector effects ($^{+1.7\%}_{-1.7\%}$), $B \rightarrow X_c \ell^+ \nu_\ell$ model ($^{+0.9\%}_{-1.0\%}$), $B \rightarrow X_u \ell^+ \nu_\ell$ model ($^{+1.5\%}_{-1.5\%}$), heavy quark parameters ($^{+2.7\%}_{-2.8\%}$), SF functional form ($^{+0.1\%}_{-0.3\%}$), sub-leading shape functions ($^{+0.8\%}_{-0.8\%}$), BLNP theory: matching scales μ, μ_i, μ_h ($^{+3.8\%}_{-3.8\%}$), and weak annihilation ($^{+0.0\%}_{-0.7\%}$). The error assigned to the matching scales is the source of the largest uncertainty, while the uncertainty due to HQE parameters (b -quark mass and μ_π^2) is second. The uncertainty due to weak annihilation is assumed to be asymmetric, *i.e.* it only tends to decrease $|V_{ub}|$.

Table 90: Summary of input parameters used by the different theory calculations, corresponding inclusive determinations of $|V_{ub}|$ and their average. The errors quoted on $|V_{ub}|$ correspond to experimental and theoretical uncertainties, respectively.

	BLNP	DGE	GGOU	ADFR	BLL
Input parameters					
scheme	SF	\overline{MS}	kinetic	\overline{MS}	$1S$
Ref.	[572, 573]	Ref. [574]	see Sec. 6.2.2	Ref. [575]	Ref. [556]
m_b (GeV)	4.582 ± 0.026	4.188 ± 0.043	4.554 ± 0.018	4.188 ± 0.043	4.704 ± 0.029
μ_π^2 (GeV 2)	$0.145^{+0.091}_{-0.097}$	-	0.414 ± 0.078	-	-
Ref.			$ V_{ub} $ values [10 $^{-3}$]		
CLEO E_e [564]	$4.22 \pm 0.49^{+0.29}_{-0.34}$	$3.86 \pm 0.45^{+0.25}_{-0.27}$	$4.23 \pm 0.49^{+0.22}_{-0.31}$	$3.42 \pm 0.40^{+0.17}_{-0.17}$	-
Belle M_X, q^2 [566]	$4.51 \pm 0.47^{+0.27}_{-0.29}$	$4.43 \pm 0.47^{+0.19}_{-0.21}$	$4.52 \pm 0.48^{+0.25}_{-0.28}$	$3.93 \pm 0.41^{+0.18}_{-0.17}$	$4.68 \pm 0.49^{+0.30}_{-0.30}$
Belle E_e [565]	$4.93 \pm 0.46^{+0.26}_{-0.29}$	$4.82 \pm 0.45^{+0.23}_{-0.23}$	$4.95 \pm 0.46^{+0.16}_{-0.21}$	$4.48 \pm 0.42^{+0.20}_{-0.20}$	-
$BABAR E_e$ [560]	$4.41 \pm 0.12^{+0.27}_{-0.27}$	$3.85 \pm 0.11^{+0.08}_{-0.07}$	$3.96 \pm 0.10^{+0.17}_{-0.17}$	-	-
$BABAR E_e, s_h^{\max}$ [563]	$4.71 \pm 0.32^{+0.33}_{-0.38}$	$4.35 \pm 0.29^{+0.28}_{-0.30}$	-	$3.81 \pm 0.19^{+0.19}_{-0.18}$	
Belle $p_\ell^*, (M_X, q^2)$ fit [554]	$4.50 \pm 0.27^{+0.20}_{-0.22}$	$4.62 \pm 0.28^{+0.13}_{-0.13}$	$4.62 \pm 0.28^{+0.09}_{-0.10}$	$4.50 \pm 0.30^{+0.20}_{-0.20}$	-
$BABAR M_X$ [555]	$4.24 \pm 0.19^{+0.25}_{-0.25}$	$4.47 \pm 0.20^{+0.19}_{-0.24}$	$4.30 \pm 0.20^{+0.20}_{-0.21}$	$3.83 \pm 0.18^{+0.20}_{-0.19}$	-
$BABAR M_X$ [555]	$4.03 \pm 0.22^{+0.22}_{-0.22}$	$4.22 \pm 0.23^{+0.21}_{-0.27}$	$4.10 \pm 0.23^{+0.16}_{-0.17}$	$3.75 \pm 0.21^{+0.18}_{-0.18}$	-
$BABAR M_X, q^2$ [555]	$4.32 \pm 0.23^{+0.26}_{-0.28}$	$4.24 \pm 0.22^{+0.18}_{-0.21}$	$4.33 \pm 0.23^{+0.24}_{-0.27}$	$3.75 \pm 0.20^{+0.17}_{-0.17}$	$4.50 \pm 0.24^{+0.29}_{-0.29}$
$BABAR P_+$ [555]	$4.09 \pm 0.25^{+0.25}_{-0.25}$	$4.17 \pm 0.25^{+0.28}_{-0.37}$	$4.25 \pm 0.26^{+0.26}_{-0.27}$	$3.57 \pm 0.22^{+0.19}_{-0.18}$	-
$BABAR p_\ell^*, (M_X, q^2)$ fit [555]	$4.33 \pm 0.24^{+0.19}_{-0.21}$	$4.45 \pm 0.24^{+0.12}_{-0.13}$	$4.44 \pm 0.24^{+0.09}_{-0.10}$	$4.33 \pm 0.24^{+0.19}_{-0.19}$	-
$BABAR p_\ell^*$ [555]	$4.34 \pm 0.27^{+0.20}_{-0.21}$	$4.43 \pm 0.27^{+0.13}_{-0.13}$	$4.43 \pm 0.27^{+0.09}_{-0.11}$	$4.28 \pm 0.27^{+0.19}_{-0.19}$	-
Belle M_X, q^2 [567]	-	-	-	-	$5.01 \pm 0.39^{+0.32}_{-0.32}$
Average	$4.44^{+0.13+0.21}_{-0.14-0.22}$	$3.99 \pm 0.10^{+0.09}_{-0.10}$	$4.32 \pm 0.12^{+0.12}_{-0.13}$	$3.99 \pm 0.13^{+0.18}_{-0.12}$	$4.62 \pm 0.20^{+0.29}_{-0.29}$

6.4.2 DGE

Andersen and Gardi (Dressed Gluon Exponentiation, DGE) [574] provide a framework where the on-shell b -quark calculation, converted into hadronic variables, is directly used as an approximation to the meson decay spectrum without the use of a leading-power non-perturbative function (or, in other words, a shape function). The on-shell mass of the b -quark within the B -meson (m_b) is required as input. The DGE calculation uses the \overline{MS} renormalization scheme. The heavy quark parameters determined from the global fit in the kinetic scheme, described in 6.2.2, were therefore translated into the \overline{MS} scheme by using code provided by Einan Gardi (based on Refs. [576, 577]), giving $m_b(\overline{MS}) = (4.188 \pm 0.043)$ GeV. The extracted values of $|V_{ub}|$ for each measurement along with their average are given in Table 90 and illustrated in Fig. 64(b). The total error is $^{+3.3\%}_{-3.4\%}$, whose breakdown is: statistics $(^{+1.8\%}_{-1.8\%})$, detector effects $(^{+1.7\%}_{-1.7\%})$, $B \rightarrow X_c \ell^+ \nu_\ell$ model $(^{+1.3\%}_{-1.3\%})$, $B \rightarrow X_u \ell^+ \nu_\ell$ model $(^{+2.1\%}_{-1.7\%})$, strong coupling α_s $(^{+0.5\%}_{-0.6\%})$, m_b $(^{+3.2\%}_{-2.9\%})$, weak annihilation $(^{+0.0\%}_{-1.1\%})$, matching scales in DGE $(^{+0.5\%}_{-0.4\%})$. The largest contribution to the total error is due to the effect of the uncertainty on m_b . The uncertainty due to weak annihilation has been assumed to be asymmetric, *i.e.* it only tends to decrease $|V_{ub}|$.

6.4.3 GGOU

Gambino, Giordano, Ossola and Uraltsev (GGOU) [578] compute the triple differential decay rates of $B \rightarrow X_u \ell^+ \nu_\ell$, including all perturbative and non-perturbative effects through $O(\alpha_s^2 \beta_0)$ and $O(1/m_b^3)$. The Fermi motion is parameterized in terms of a single light-cone function

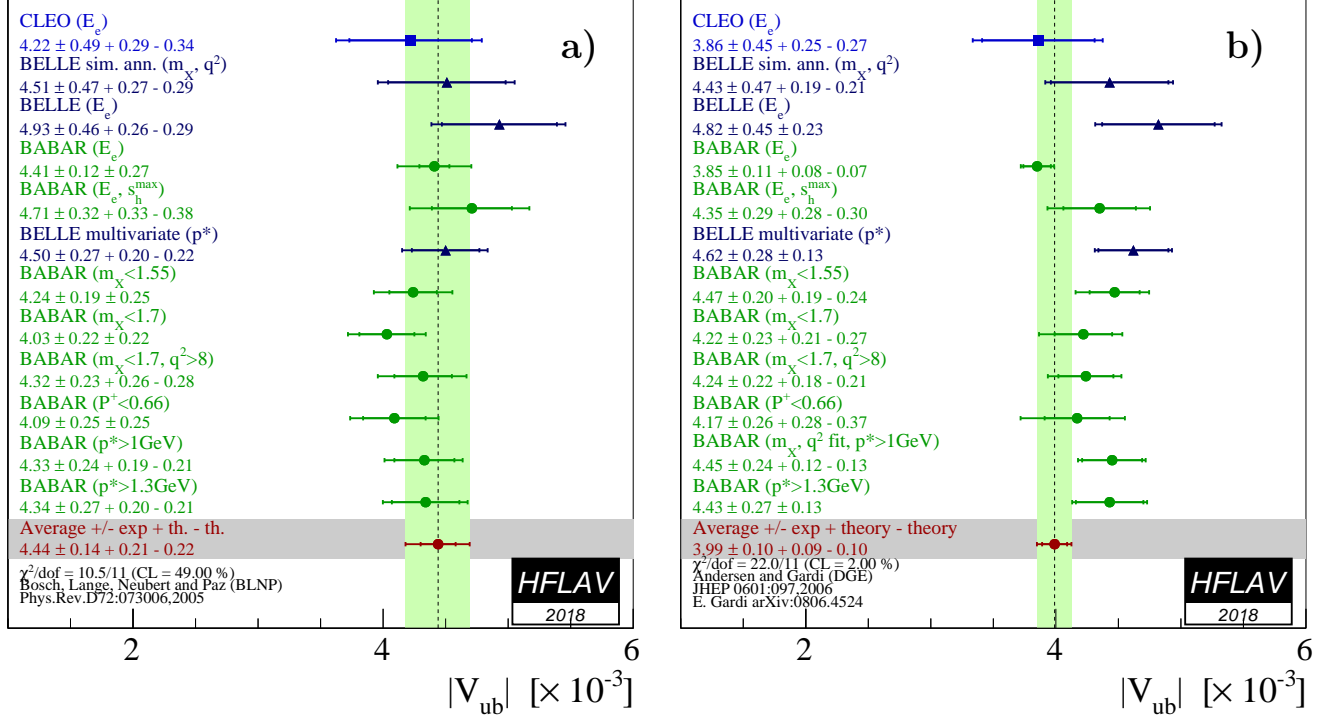


Figure 64: Measurements of $|V_{ub}|$ from inclusive semileptonic decays and their average based on the BLNP (a) and DGE (b) prescription. The labels indicate the variables and selections used to define the signal regions in the different analyses.

for each structure function and for any value of q^2 , accounting for all subleading effects. The calculations are performed in the kinetic scheme, a framework characterized by a Wilsonian treatment with a hard cutoff $\mu \sim 1$ GeV. GGOU have not included calculations for the “(E_e, s_h^{max})” analysis [563]. The heavy quark parameters determined from the global fit in the kinetic scheme, described in Section 6.2.2, are used as inputs: $m_b^{kin} = (4.554 \pm 0.018)$ GeV, $\mu_\pi^2 = (0.464 \pm 0.076)$ GeV/c^2 . The extracted values of $|V_{ub}|$ for each measurement along with their average are given in Table 90 and illustrated in Fig. 65(a). The total error is $^{+4.0\%}_{-4.0\%}$ whose breakdown is: statistics $(^{+1.6\%}_{-1.6\%})$, detector effects $(^{+1.6\%}_{-1.6\%})$, $B \rightarrow X_c \ell^+ \nu_\ell$ model $(^{+0.9\%}_{-0.9\%})$, $B \rightarrow X_u \ell^+ \nu_\ell$ model $(^{+1.5\%}_{-1.5\%})$, α_s , m_b and other non-perturbative parameters $(^{+1.9\%}_{-1.9\%})$, higher order perturbative and non-perturbative corrections $(^{+1.5\%}_{-1.5\%})$, modelling of the q^2 tail $(^{+1.3\%}_{-1.3\%})$, weak annihilations matrix element $(^{+0.0\%}_{-1.1\%})$, functional form of the distribution functions $(^{+0.1\%}_{-0.1\%})$. The leading uncertainties on $|V_{ub}|$ are both from theory, and are due to perturbative and non-perturbative parameters and the modelling of the q^2 tail. The uncertainty due to weak annihilation has been assumed to be asymmetric, *i.e.* it only tends to decrease $|V_{ub}|$.

6.4.4 ADFR

Aglietti, Di Lodovico, Ferrera and Ricciardi (ADFR) [579] use an approach to extract $|V_{ub}|$, that makes use of the ratio of the $B \rightarrow X_c \ell^+ \nu_\ell$ and $B \rightarrow X_u \ell^+ \nu_\ell$ widths. The normalized triple differential decay rate for $B \rightarrow X_u \ell^+ \nu_\ell$ [575, 580–582] is calculated with a model based on (i) soft-gluon resummation to next-to-next-leading order and (ii) an effective QCD coupling

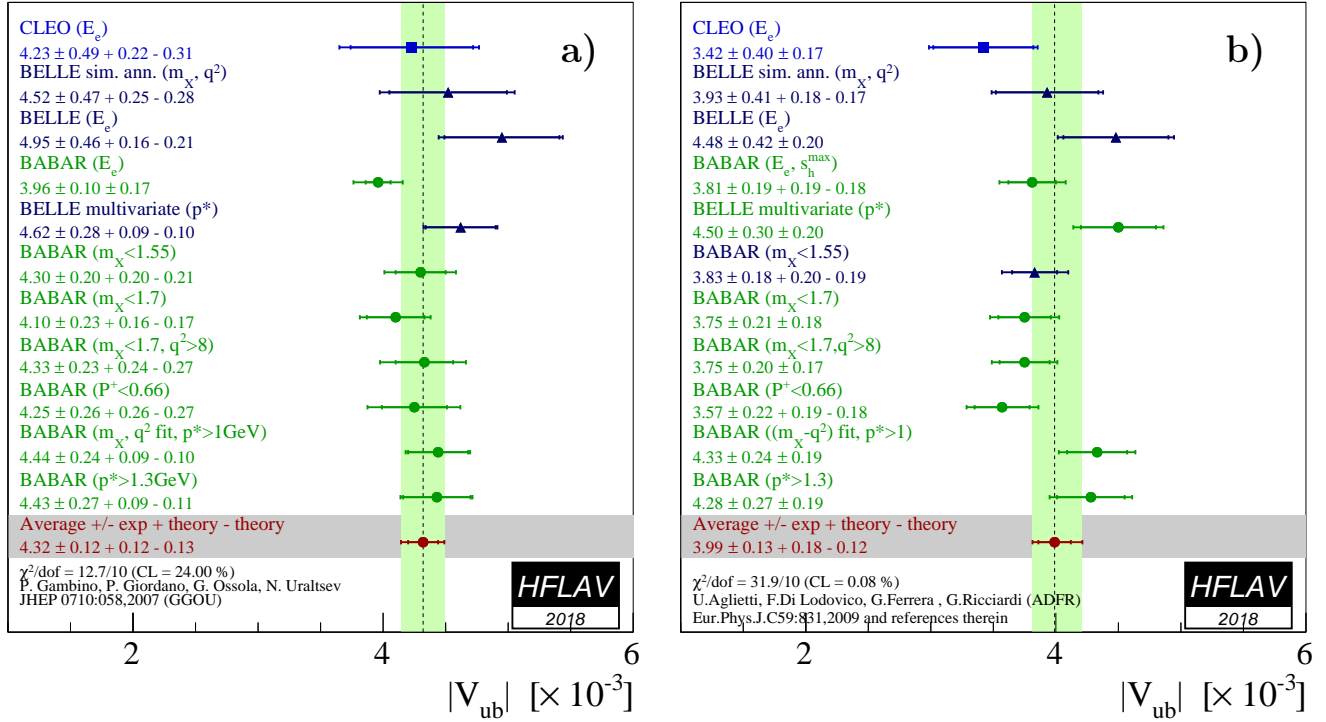


Figure 65: Measurements of $|V_{ub}|$ from inclusive semileptonic decays and their average based on the GGOU (a) and ADFR (b) prescription. The labels indicate the variables and selections used to define the signal regions in the different analyses .

without a Landau pole. This coupling is constructed by means of an extrapolation to low energy of the high-energy behaviour of the standard coupling. More technically, an analyticity principle is used. The lower cut on the electron energy for the endpoint analyses is 2.3 GeV [575]. The ADFR calculation uses the \overline{MS} renormalization scheme; the heavy quark parameters determined from the global fit in the kinetic scheme, described in 6.2.2, were therefore translated into the \overline{MS} scheme by using code provided by Einan Gardi (based on Refs. [576,577]), giving $m_b(\overline{MS}) = (4.188 \pm 0.043)$ GeV. The extracted values of $|V_{ub}|$ for each measurement along with their average are given in Table 90 and illustrated in Fig. 65(b). The total error is $^{+5.6\%}_{-5.6\%}$ whose breakdown is: statistics ($^{+1.9\%}_{-1.9\%}$), detector effects ($^{+1.7\%}_{-1.7\%}$), $B \rightarrow X_c \ell^+ \nu_\ell$ model ($^{+1.4\%}_{-1.4\%}$), $B \rightarrow X_u \ell^+ \nu_\ell$ model ($^{+1.5\%}_{-1.4\%}$), α_s ($^{+1.1\%}_{-1.0\%}$), $|V_{cb}|$ ($^{+1.9\%}_{-1.9\%}$), m_b ($^{+0.7\%}_{-0.7\%}$), m_c ($^{+1.3\%}_{-1.3\%}$), semileptonic branching fraction ($^{+0.8\%}_{-0.7\%}$), theory model ($^{+3.6\%}_{-3.6\%}$). The leading uncertainty is due to the theory model.

6.4.5 BLL

Bauer, Ligeti, and Luke (BLL) [556] give a HQET-based prescription that advocates combined cuts on the dilepton invariant mass, q^2 , and hadronic mass, m_X , to minimise the overall uncertainty on $|V_{ub}|$. In their reckoning a cut on m_X only, although most efficient at preserving phase space ($\sim 80\%$), makes the calculation of the partial rate untenable due to uncalculable corrections to the b -quark distribution function or shape function. These corrections are suppressed if events in the low q^2 region are removed. The cut combination used in measurements

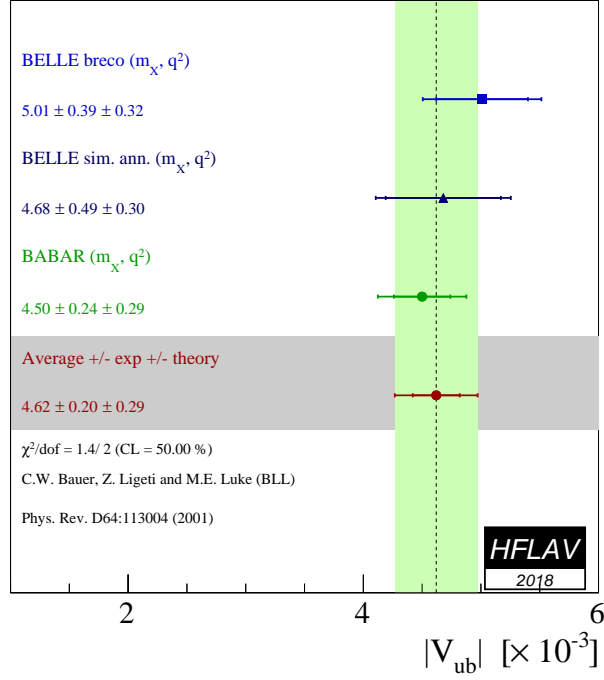


Figure 66: Measurements of $|V_{ub}|$ from inclusive semileptonic decays and their average in the BLL prescription.

is $M_x < 1.7 \text{ GeV}/c^2$ and $q^2 > 8 \text{ GeV}^2/c^4$. The extracted values of $|V_{ub}|$ for each measurement along with their average are given in Table 90 and illustrated in Fig. 66. The total error is $^{+7.7\%}_{-7.7\%}$ whose breakdown is: statistics $(^{+3.3\%}_{-3.3\%})$, detector effects $(^{+3.0\%}_{-3.0\%})$, $B \rightarrow X_c \ell^+ \nu_\ell$ model $(^{+1.6\%}_{-1.6\%})$, $B \rightarrow X_u \ell^+ \nu_\ell$ model $(^{+1.1\%}_{-1.1\%})$, spectral fraction (m_b) $(^{+3.0\%}_{-3.0\%})$, perturbative approach: strong coupling α_s $(^{+3.0\%}_{-3.0\%})$, residual shape function $(^{+2.5\%}_{-2.5\%})$, third order terms in the OPE $(^{+4.0\%}_{-4.0\%})$. The leading uncertainties, both from theory, are due to residual shape function effects and third order terms in the OPE expansion. The leading experimental uncertainty is due to statistics.

6.4.6 Summary

The averages presented in several different frameworks are presented in Table 91. In summary, we recognize that the experimental and theoretical uncertainties play out differently between the schemes and the theoretical assumptions for the theory calculations are different. Therefore, it is difficult to perform an average between the various determinations of $|V_{ub}|$. Since the methodology is similar to that used to determine the inclusive $|V_{cb}|$ average, we choose to quote as reference value the average determined by the GGOU calculation, which gives $|V_{ub}| = (4.32 \pm 0.12^{+0.12}_{-0.13}) \times 10^{-3}$.

6.5 $B \rightarrow D^{(*)} \tau \nu_\tau$ decays

In the SM the semileptonic decay are tree level processes which proceed via coupling to the W^\pm boson. These couplings are assumed to be universal for all leptons and are well understood theoretically, (see Section 5.1 and 5.2.). This universality has been tested in purely leptonic and

Table 91: Summary of inclusive determinations of $|V_{ub}|$. The errors quoted on $|V_{ub}|$ correspond to experimental and theoretical uncertainties.

Framework	$ V_{ub} [10^{-3}]$
BLNP	$4.44^{+0.13+0.21}_{-0.14-0.22}$
DGE	$4.52 \pm 0.10^{+0.09}_{-0.10}$
GGOU	$4.32 \pm 0.12^{+0.12}_{-0.13}$
ADFR	$3.99 \pm 0.13^{+0.18}_{-0.12}$
BLL (m_X/q^2 only)	$4.62 \pm 0.20 \pm 0.29$

semileptonic B meson decays involving a τ lepton, which might be sensitive to a hypothetical charged Higgs boson or other non-SM processes.

Compared to $B^+ \rightarrow \tau\nu_\tau$, the $B \rightarrow D^{(*)}\tau\nu_\tau$ decay has advantages: the branching fraction is relatively high, because it is not Cabibbo-suppressed, and it is a three-body decay allowing access to many observables besides the branching fraction, such as $D^{(*)}$ momentum, q^2 distributions, and measurements of the D^* and τ polarisations (see Ref. [583] and references therein for recent calculations).

Experiments have measured two ratios of branching fractions defined as

$$\mathcal{R}(D) = \frac{\mathcal{B}(B \rightarrow D\tau\nu_\tau)}{\mathcal{B}(B \rightarrow D\ell\nu_\ell)}, \quad (224)$$

$$\mathcal{R}(D^*) = \frac{\mathcal{B}(B \rightarrow D^*\tau\nu_\tau)}{\mathcal{B}(B \rightarrow D^*\ell\nu_\ell)} \quad (225)$$

where ℓ refers either to electron or μ . These ratios are independent of $|V_{cb}|$ and to a large extent, also of the $B \rightarrow D^{(*)}$ form factors. As a consequence, the SM predictions for these ratios are quite precise:

- $\mathcal{R}(D) = 0.299 \pm 0.003$, which is an average of the predictions from Refs. [584–586]. These predictions use as input the latest results on the $B \rightarrow D\ell\nu$ form factors from *BABAR* and *Belle*, and the most recent lattice calculations [498, 587].
- $\mathcal{R}(D^*) = 0.258 \pm 0.005$, which is an arithmetic average of the predictions from Refs. [585, 586, 588]. These calculations are in good agreement between each other, and consistent with the old prediction [589] extensively used in the past, but more robust. There are differences in the evaluation of the theoretical uncertainty associated mainly with assumptions on the pseudoscalar Form Factor.

Recently, in Ref. [590], Gambino, Jung and Schacht re-analysed the recent *Belle* results of $B \rightarrow D^*\ell\nu$ form factors [491], obtaining $\mathcal{R}(D) = 0.254^{+0.007}_{-0.006}$, compatible with the predictions mentioned before. Another calculation, based on the full angular analysis of $B \rightarrow D^*\ell\nu$ decay by *BABAR* [591], gives an independent prediction of $\mathcal{R}(D) = 0.253 \pm 0.005$.

On the experimental side, in the case of the leptonic τ decay, the ratios $\mathcal{R}(D^{(*)})$ can be directly measured, and many systematic uncertainties cancel in the measurement. The $B^0 \rightarrow D^{*+}\tau\nu_\tau$ decay was first observed by *Belle* [592] performing an "inclusive" reconstruction, which

is based on the reconstruction of the B_{tag} from all the particles of the events, other than the $D^{(*)}$ and the lepton candidate, without looking for any specific B_{tag} decay chain. Since then, both *BABAR* and *Belle* have published improved measurements and have observed the decays $B \rightarrow D\tau\nu_\tau$ decays [593, 594].

The most powerful way to study these decays at the B-Factories exploits the hadronic or semileptonic B_{tag} . Using the full dataset and an improved hadronic B_{tag} selection, *BABAR* measured [595]:

$$\mathcal{R}(D) = 0.440 \pm 0.058 \pm 0.042, \quad \mathcal{R}(D^*) = 0.332 \pm 0.024 \pm 0.018 \quad (226)$$

where decays to both e^\pm and μ^\pm were summed, and results for B^0 and B^- decays were combined in an isospin-constrained fit. The fact that the *BABAR* result exceeded SM predictions by 3.4σ raised considerable interest.

Belle, exploiting the full dataset, published several measurements using both the hadronic and the semileptonic tag. *Belle* also performed a combined measurement of $\mathcal{R}(D^*)$ and τ polarization by reconstructing the τ in the hadronic $\tau \rightarrow \pi\nu$ and $\tau \rightarrow \rho\nu$ decay modes [596]. LHCb measurements of $R(D^*)$ use both the muonic τ decay [597], and the three-prong hadronic $\tau \rightarrow 3\pi(\pi^0)\nu$ decays [598]. The latter is a direct measurement of the ratio $\mathcal{B}(B^0 \rightarrow D^{*-}\tau^+\nu_\tau)/\mathcal{B}(B^0 \rightarrow D^{*-}\pi^+\pi^-\pi^+)$, and is translated into a measurement of $R(D^*)$ using the independently measured branching fractions $\mathcal{B}(B^0 \rightarrow D^{*-}\pi^+\pi^-\pi^+)$ and $\mathcal{B}(B^0 \rightarrow D^{*-}\mu^+\nu_\mu)$.

The most important source of systematic uncertainties that are correlated among the different measurement is the $B \rightarrow D^{**}$ background components, which are difficult to disentangle from the signal. In our average, the systematic uncertainties due to the $B \rightarrow D^{**}$ composition and kinematics are considered fully correlated among the measurements.

The results of the individual measurements, their averages and correlations are presented in Table 92 and Fig.67. The combined results, projected separately on $\mathcal{R}(D)$ and $\mathcal{R}(D^*)$, are reported in Fig.68(a) and Fig.68(b) respectively.

The averaged $\mathcal{R}(D)$ and $\mathcal{R}(D^*)$ exceed the SM predictions by 1.4σ and 2.5σ respectively. Considering the $\mathcal{R}(D)$ and $\mathcal{R}(D^*)$ total correlation of -0.38 , the difference with respect to the SM is about 3.08σ , and the combined $\chi^2 = 12.33$ for 2 degrees of freedom corresponds to a p -value of 2.07×10^{-3} , assuming Gaussian error distributions.

Table 92: Measurements of $\mathcal{R}(D^*)$ and $\mathcal{R}(D)$, their correlations and the combined average.

Experiment	$\mathcal{R}(D^*)$	$\mathcal{R}(D)$	ρ
<i>BABAR</i> [595, 599]	$0.332 \pm 0.024_{\text{stat}} \pm 0.018_{\text{syst}}$	$0.440 \pm 0.058_{\text{stat}} \pm 0.042_{\text{syst}}$	-0.27
<i>Belle</i> [600]	$0.293 \pm 0.038_{\text{stat}} \pm 0.015_{\text{syst}}$	$0.375 \pm 0.064_{\text{stat}} \pm 0.026_{\text{syst}}$	-0.49
LHCb [597]	$0.336 \pm 0.027_{\text{stat}} \pm 0.030_{\text{syst}}$		
<i>Belle</i> [596]	$0.270 \pm 0.035_{\text{stat}}^{+0.028}_{-0.025_{\text{syst}}}$		
LHCb [598, 601]	$0.280 \pm 0.018_{\text{stat}} \pm 0.029_{\text{syst}}$		
<i>Belle</i> [602]	$0.283 \pm 0.018_{\text{stat}} \pm 0.014_{\text{syst}}$	$0.307 \pm 0.037_{\text{stat}} \pm 0.016_{\text{syst}}$	-0.51
Average	$0.295 \pm 0.011 \pm 0.008$	$0.340 \pm 0.027 \pm 0.013$	-0.38

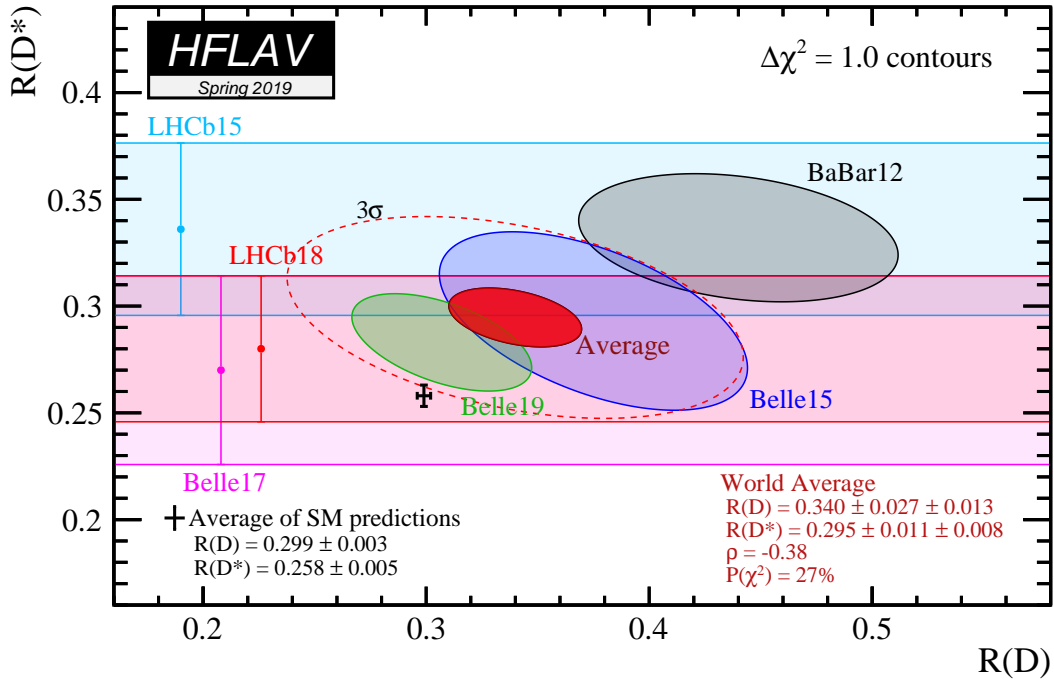


Figure 67: Measurements of $\mathcal{R}(D)$ and $\mathcal{R}(D^*)$ listed in Table 92 and their two-dimensional average. Contours correspond to $\Delta\chi^2 = 1$, *i.e.*, 68% CL for the bands and 39% CL for the ellipses. The black point with errors is the average of the SM predictions for $\mathcal{R}(D^*)$ and $\mathcal{R}(D)$ obtained from Refs. [584–586]. The prediction and the experimental average deviate from each other by 3.08σ . The dashed ellipse correspond to a 3σ contour (99.73% CL).

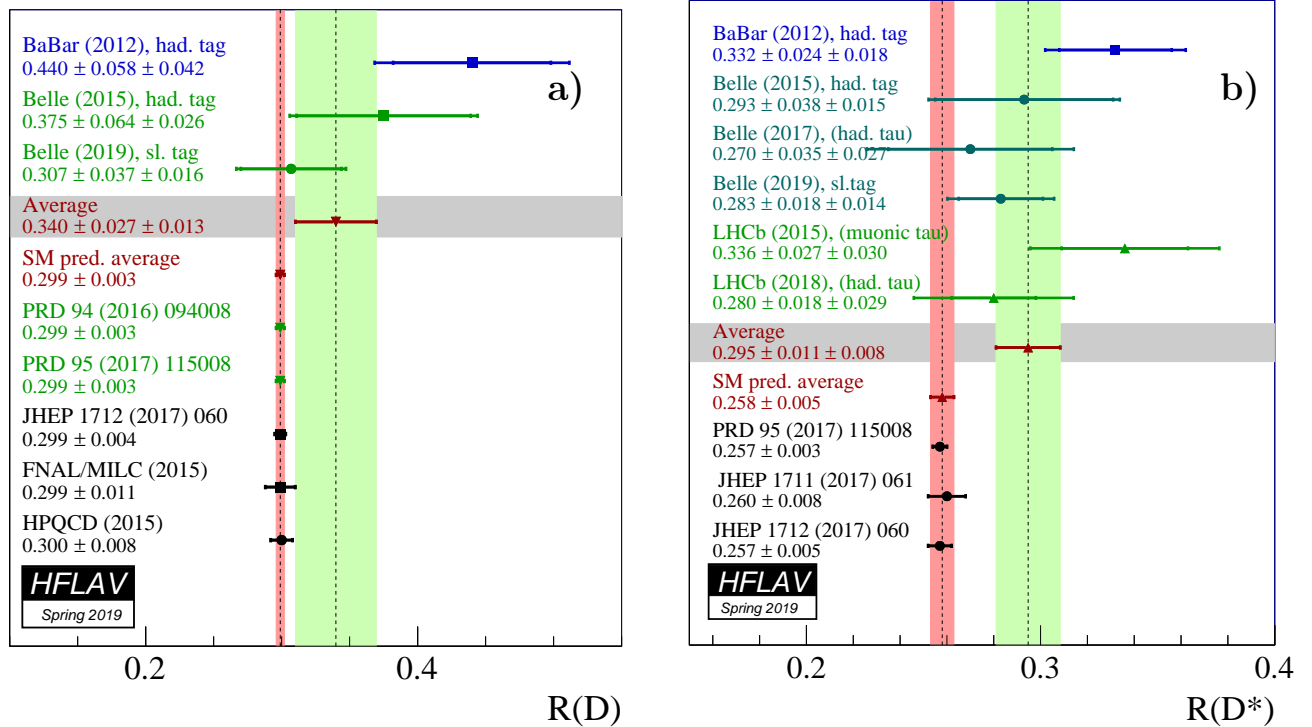


Figure 68: (a) Measurements of $\mathcal{R}(D)$ and (b) $\mathcal{R}(D^*)$. The average is the projection of the average obtained from the combined fit.

7 Decays of b -hadrons into open or hidden charm hadrons

Ground state B mesons and b baryons dominantly decay to particles containing a charm quark via the $b \rightarrow c$ quark transition. In this section, measurements of such decays to hadronic final states are summarized. The use of such decays for studying fundamental properties of the bottom hadrons and for obtaining parameters of the CKM matrix is discussed in Sections 4 and 5, respectively. The properties of certain b hadron decays to open or hidden charm hadrons, such as small Q values and similar topologies for different modes, allow the minimization of systematic uncertainties in these measurements.

The fact that decays to final states containing open or hidden charm hadrons dominate the b -hadron widths makes them a very important part of the experimental programme in heavy flavor physics. Understanding the rate of charm production in b -hadron decays is crucial for validation of the heavy-quark expansion (HQE) that underpins much of the theoretical framework for b physics (see, for example, Ref. [603] for a review). Moreover, such decays are often used as normalization modes for measurements of rarer decays. In addition, they are the dominant background in many analyses. To model accurately such backgrounds with simulated data, it is essential to have precise knowledge of the contributing decay modes. In particular, with the expected increase in the data samples at LHCb and Belle II, the enhanced statistical sensitivity has to be matched by low systematic uncertainties due to knowledge of the dominant b -hadron decay modes. For multibody decays, knowledge of the distribution of decays across the phase-space (*e.g.*, the Dalitz plot density for three-body decays or the polarization amplitudes for vector-vector final states) is required in addition to the total branching fraction.

The large yields of $b \rightarrow c$ decays to multibody final states make them ideal for studying the spectroscopy of both open and hidden charm hadrons. In particular, they have been used to both discover, and measure the properties of exotic particles, such as the $X(3872)$ [604, 605], $Z(4430)^+$ [606, 607] and $P_c(4450)^+$ [608] states. Similarly, $b \rightarrow c$ transitions are very useful for studying baryon-antibaryon pair production.

In addition to the dominant $b \rightarrow c$ decays, there are several decays in this category that are expected to be highly suppressed in the Standard Model. These are of interest for probing particular decay topologies (*e.g.*, the annihilation diagram, which dominates the $B^- \rightarrow D_s^- \phi$ decay), which thereby constrain effects in other hadronic decays, or for searching for new physics. There are also open charm production modes that involve $b \rightarrow u$ transitions, such as $\bar{B}^0 \rightarrow D_s^- \pi^+$, which are mediated by the W emission involving the $|V_{ub}|$ CKM matrix element. Finally, $b \rightarrow c$ decays involving lepton flavor or number violation are extremely suppressed in the Standard Model, and therefore provide highly sensitive tests of new physics.

In this section, we give an exhaustive list of measured branching ratios of decay modes to hadrons containing charm quarks. The averaging procedure follows the methodology described in Section 3. Where available, correlations between measurements are taken into account. If an insignificant measurement and a limit for the same parameter are provided, the former is quoted, so that it can be included in averages. In case of asymmetric uncertainties, a variable width Gaussian likelihood with linear variance in the range $[\sigma_-, \sigma_+]$ around the central value is assumed, following a suggestion in [609]. The confidence level of an average is quoted if it is below 1%. We provide averages of the polarization amplitudes of B meson decays to vector-vector states, but we do not currently provide detailed averages of quantities obtained from Dalitz plot analyses, due to the complications arising from the dependence on the model used.

The results are presented in subsections organized according to the type of decaying bottom

hadron: \bar{B}^0 (Sec. 7.1), B^- (Sec. 7.2), \bar{B}^0/B^- admixture (Sec. 7.3), \bar{B}_s^0 (Sec. 7.4), B_c^- (Sec. 7.5), b baryons (Sec. 7.6). For each subsection, the measurements are arranged according to the final state into the following groups: a single charmed meson, two charmed mesons, a charmonium state, a charm baryon, or other states, such as, e.g. the $X(3872)$. The individual measurements and averages are shown as numerical values in tables followed by a graphical representation of the averages. The symbol \mathcal{B} is used for branching ratios, f for production fractions (see Section 4), and σ for cross sections. The decay amplitudes for longitudinal, parallel, and perpendicular transverse polarization in pseudoscalar to vector-vector decays are denoted \mathcal{A}_0 , \mathcal{A}_{\parallel} , and \mathcal{A}_{\perp} , respectively, and the definitions $\delta_{\parallel} = \arg(\mathcal{A}_{\parallel}/\mathcal{A}_0)$ and $\delta_{\perp} = \arg(\mathcal{A}_{\perp}/\mathcal{A}_0)$ are used for their relative phases. The inclusion of charge conjugate modes is always implied.

Following the approach used by the PDG [21], for decays that involve neutral kaons we mainly quote results in terms of final states including either a K^0 or \bar{K}^0 meson (instead of a K_s^0 or K_L^0), although the flavor of the neutral kaon is never determined experimentally. The specification as K^0 or \bar{K}^0 simply follows the quark model expectation for the dominant decay and the inclusion of the conjugate final state neutral kaon is implied. An exception occurs for some B_s^0 decays, specifically those to CP eigenstates, where the width difference between the mass eigenstates (see Sec. 4) means that the measured branching fraction, integrated over decay time, is specific to the studied final state [610]. In such cases it is appropriate to quote the branching fraction for, *e.g.*, $\bar{B}_s^0 \rightarrow J/\psi K_S^0$ instead of $\bar{B}_s^0 \rightarrow J/\psi \bar{K}^0$.

Several measurements assume $\Gamma(Y(4S) \rightarrow B^+ B^-) = \Gamma(Y(4S) \rightarrow B^0 \bar{B}^0)$. While there is no evidence for isospin violation in $Y(4S)$ decays, deviations from this assumption can be of the order of a few percent, see Section 4.1.1 and Ref. [611]. As the effect is negligible for many averages, we take the quoted values without applying a correction or additional systematic uncertainty. However, we note that this can be relevant for averages with percent-level uncertainty.

7.1 Decays of \bar{B}^0 mesons

Measurements of \bar{B}^0 decays to charmed hadrons are summarized in Sections 7.1.1 to 7.1.5.

7.1.1 Decays to a single open charm meson

Averages of \bar{B}^0 decays to a single open charm meson are shown in Tables 93–107. In this section D^{**} refers to the sum of all the non-strange charm meson states with masses in the range $2.2 - 2.8 \text{ GeV}/c^2$.

Table 93: Branching fractions to a $D^{(*)}$ meson and one or more pions, I.

Parameter	Measurements	Average $[10^{-3}]$
$\mathcal{B}(\bar{B}^0 \rightarrow D^+ \pi^-)$	$BABAR$ [612]: $2.55 \pm 0.05 \pm 0.16$ $BABAR$ [613]: $3.03 \pm 0.23 \pm 0.23$	2.65 ± 0.15
$\mathcal{B}(\bar{B}^0 \rightarrow D^*(2010)^+ \pi^-)$	$Belle$ [614]: $2.22 \pm 0.04 \pm 0.19$ $BABAR$ [612]: $2.79 \pm 0.08 \pm 0.17$ $BABAR$ [613]: $2.99 \pm 0.23 \pm 0.24$	2.58 ± 0.13
$\mathcal{B}(\bar{B}^0 \rightarrow D^*(2010)^+ \pi^- \pi^+ \pi^-)$	$Belle$ [615]: $6.81 \pm 0.23 \pm 0.72$ $BABAR$ [616]: $7.26 \pm 0.11 \pm 0.31$	7.19 ± 0.30
$\mathcal{B}(\bar{B}^0 \rightarrow D^*(2007)^0 \pi^- \pi^+ \pi^- \pi^+)$	$Belle$ [615]: $2.60 \pm 0.47 \pm 0.37$	2.60 ± 0.60
$\mathcal{B}(\bar{B}^0 \rightarrow D^*(2010)^+ \pi^- \pi^+ \pi^- \pi^+ \pi^-)$	$Belle$ [615]: $4.72 \pm 0.59 \pm 0.71$	4.72 ± 0.92
$\mathcal{B}(\bar{B}^0 \rightarrow D^*(2010)^+ \omega(782) \pi^-)$	$Belle$ [617]: $2.31 \pm 0.11 \pm 0.14$ $BABAR$ [618]: $2.88 \pm 0.21 \pm 0.31$	2.41 ± 0.16

 Table 94: Branching fractions to a $D^{(*)}$ meson and one or more pions, II.

Parameter	Measurements	Average $[10^{-4}]$
$\mathcal{B}(\bar{B}^0 \rightarrow D^0 \pi^0)$	$Belle$ [619]: $2.25 \pm 0.14 \pm 0.35$ $BABAR$ [620]: $2.69 \pm 0.09 \pm 0.13$	2.62 ± 0.15
$\mathcal{B}(\bar{B}^0 \rightarrow D^*(2007)^0 \pi^0)$	$Belle$ [619]: $1.39 \pm 0.18 \pm 0.26$ $BABAR$ [620]: $3.05 \pm 0.14 \pm 0.28$	2.23 ± 0.22 <small>CL=0.2%</small>
$\mathcal{B}(\bar{B}^0 \rightarrow D^0 \pi^+ \pi^-)$	$LHCb$ [621]: $8.46 \pm 0.14 \pm 0.49$ $Belle$ [614]: $8.4 \pm 0.4 \pm 0.8$	8.45 ± 0.45
$\mathcal{B}(\bar{B}^0 \rightarrow D^*(2007)^0 \pi^+ \pi^-)$	$Belle$ [622]: $6.2 \pm 1.2 \pm 1.8$	6.2 ± 2.2

Table 95: Branching fractions to a $D^{(*)0}$ meson and a light neutral hadronic resonance.

Parameter	Measurements	Average [10 ⁻⁴]
$\mathcal{B}(\bar{B}^0 \rightarrow D^0 \rho(770)^0)$	Belle [614]: $3.19 \pm 0.20 \pm 0.45$	3.19 ± 0.49
$\mathcal{B}(\bar{B}^0 \rightarrow D^*(2007)^0 \rho(770)^0)$	Belle [622]: < 5.1	< 5.1
$\mathcal{B}(\bar{B}^0 \rightarrow D^0 \eta)$	Belle [619]: $1.77 \pm 0.16 \pm 0.21$ <i>BABAR</i> [620]: $2.53 \pm 0.09 \pm 0.11$	2.36 ± 0.13
$\mathcal{B}(\bar{B}^0 \rightarrow D^*(2007)^0 \eta)$	Belle [619]: $1.40 \pm 0.28 \pm 0.26$ <i>BABAR</i> [620]: $2.69 \pm 0.14 \pm 0.23$ CL=5.8%	2.26 ± 0.22
$\mathcal{B}(\bar{B}^0 \rightarrow D^0 \eta'(958))$	Belle [623]: $1.14 \pm 0.20^{+0.10}_{-0.13}$ <i>BABAR</i> [620]: $1.48 \pm 0.13 \pm 0.07$	1.38 ± 0.12
$\mathcal{B}(\bar{B}^0 \rightarrow D^*(2007)^0 \eta'(958))$	Belle [623]: $1.21 \pm 0.34 \pm 0.22$ <i>BABAR</i> [620]: $1.48 \pm 0.22 \pm 0.13$	1.40 ± 0.22
$\mathcal{B}(\bar{B}^0 \rightarrow D^0 \omega(782))$	LHCb [621]: $2.81 \pm 0.72^{+0.30}_{-0.33}$ Belle [619]: $2.37 \pm 0.23 \pm 0.28$ <i>BABAR</i> [620]: $2.57 \pm 0.11 \pm 0.14$	2.54 ± 0.16
$\mathcal{B}(\bar{B}^0 \rightarrow D^*(2007)^0 \omega(782))$	Belle [619]: $2.29 \pm 0.39 \pm 0.40$ <i>BABAR</i> [620]: $4.55 \pm 0.24 \pm 0.39$ CL=1.8%	3.64 ± 0.35
$\mathcal{B}(\bar{B}^0 \rightarrow D^0 f_2(1270))$	LHCb [621]: $1.61 \pm 0.11^{+0.19}_{-0.18}$ Belle [614]: $1.20 \pm 0.18 \pm 0.38$	1.57 ± 0.21

 Table 96: Branching fractions to a $D^{(*)+}$ meson and one or more kaons.

Parameter	Measurements	Average [10 ⁻³]
$\mathcal{B}(\bar{B}^0 \rightarrow D^+ K^-)$	LHCb [49]: $0.220 \pm 0.003 \pm 0.013$ Belle [624]: $0.204 \pm 0.045 \pm 0.034$	0.219 ± 0.013
$\mathcal{B}(\bar{B}^0 \rightarrow D^*(2010)^+ K^-)$	Belle [624]: $0.204 \pm 0.041 \pm 0.023$	0.204 ± 0.047
$\mathcal{B}(\bar{B}^0 \rightarrow D^+ K^*(892)^-)$	<i>BABAR</i> [625]: $0.46 \pm 0.06 \pm 0.05$	0.46 ± 0.08
$\mathcal{B}(\bar{B}^0 \rightarrow D^*(2010)^+ K^*(892)^-)$	<i>BABAR</i> [625]: $0.32 \pm 0.06 \pm 0.03$	0.32 ± 0.07
$\mathcal{B}(\bar{B}^0 \rightarrow D^+ K^0 \pi^-)$	<i>BABAR</i> [625]: $0.49 \pm 0.07 \pm 0.05$	0.49 ± 0.09
$\mathcal{B}(\bar{B}^0 \rightarrow D^*(2010)^+ K^0 \pi^-)$	<i>BABAR</i> [625]: $0.30 \pm 0.07 \pm 0.03$	0.30 ± 0.08
$\mathcal{B}(\bar{B}^0 \rightarrow D^+ K^- K^0)$	Belle [626]: < 0.31	< 0.31
$\mathcal{B}(\bar{B}^0 \rightarrow D^*(2010)^+ K^- K^0)$	Belle [626]: < 0.47	< 0.47
$\mathcal{B}(\bar{B}^0 \rightarrow D^+ K^- K^*(892)^0)$	Belle [626]: $0.88 \pm 0.11 \pm 0.15$	0.88 ± 0.19
$\mathcal{B}(\bar{B}^0 \rightarrow D^*(2010)^+ K^- K^*(892)^0)$	Belle [626]: $1.29 \pm 0.22 \pm 0.25$	1.29 ± 0.33

Table 97: Branching fractions to a $D^{(*)0}$ meson and a kaon.

Parameter	Measurements	Average $[10^{-4}]$
$\mathcal{B}(\bar{B}^0 \rightarrow D^0 \bar{K}^0)$	Belle [627]: $0.50^{+0.13}_{-0.12} \pm 0.06$ BABAR [628]: $0.53 \pm 0.07 \pm 0.03$	0.52 ± 0.07
$\mathcal{B}(\bar{B}^0 \rightarrow D^*(2007)^0 \bar{K}^0)$	Belle [627]: < 0.66 BABAR [628]: $0.36 \pm 0.12 \pm 0.03$	0.36 ± 0.12
$\mathcal{B}(\bar{B}^0 \rightarrow D^0 K^- \pi^+)$	BABAR [629]: $0.88 \pm 0.15 \pm 0.09$	0.88 ± 0.17
$\mathcal{B}(\bar{B}^0 \rightarrow D^0 \bar{K}^*(892)^0)$	Belle [627]: $0.48^{+0.11}_{-0.10} \pm 0.05$ BABAR [628]: $0.40 \pm 0.07 \pm 0.03$	0.42 ± 0.06
$\mathcal{B}(\bar{B}^0 \rightarrow D^0 \bar{K}^*(892)^0) \times \mathcal{B}(\bar{K}^*(892)^0 \rightarrow K^- \pi^+)$	BABAR [629]: $0.38 \pm 0.06 \pm 0.04$	0.38 ± 0.07
$\mathcal{B}(\bar{B}^0 \rightarrow D^*(2007)^0 \bar{K}^*(892)^0)$	Belle [627]: < 0.69	< 0.69
$\mathcal{B}(\bar{B}^0 \rightarrow \bar{D}^*(2007)^0 \bar{K}^*(892)^0)$	Belle [627]: < 0.40	< 0.40
$\mathcal{B}(\bar{B}^0 \rightarrow \bar{D}^0 K^- \pi^+)$	BABAR [629]: < 0.19	< 0.19
$\mathcal{B}(\bar{B}^0 \rightarrow \bar{D}^0 \bar{K}^*(892)^0)$	Belle [627]: < 0.18 BABAR [628]: $0.00 \pm 0.05 \pm 0.03$	0.00 ± 0.06

 Table 98: Branching fractions to a $D^{(*)0}$ meson and more than one kaon or a ϕ .

Parameter	Measurements	Average $[10^{-5}]$
$\mathcal{B}(\bar{B}^0 \rightarrow \bar{D}^0 K^- K^+)$	LHCb [630]: $6.1 \pm 0.4 \pm 0.4$	6.1 ± 0.6
$\mathcal{B}(\bar{B}^0 \rightarrow D^0 \phi(1020))$	LHCb [631]: < 0.20	< 0.20

Table 99: Branching fractions to a $D_s^{(*)}$ meson.

Parameter	Measurements	Average [10 ⁻⁴]
$\mathcal{B}(\bar{B}^0 \rightarrow D_s^- \pi^+)$	Belle [632]: $0.199 \pm 0.026 \pm 0.018$ BABAR [633]: $0.25 \pm 0.04 \pm 0.02$	0.216 ± 0.026
$\mathcal{B}(\bar{B}^0 \rightarrow D_s^{*-} \pi^+)$	Belle [634]: $0.175 \pm 0.034 \pm 0.020$ BABAR [633]: $0.26_{-0.04}^{+0.05} \pm 0.02$	0.214 ± 0.031
$\mathcal{B}(\bar{B}^0 \rightarrow D_s^- \rho(770)^+)$	BABAR [633]: $0.11_{-0.08}^{+0.09} \pm 0.03$	$0.11_{-0.09}^{+0.09}$
$\mathcal{B}(\bar{B}^0 \rightarrow D_s^{*-} \rho(770)^+)$	BABAR [633]: $0.41_{-0.12}^{+0.13} \pm 0.04$	$0.41_{-0.13}^{+0.14}$
$\mathcal{B}(\bar{B}^0 \rightarrow D_s^- a_0(980)^+)$	BABAR [635]: $0.06_{-0.11}^{+0.14} \pm 0.01$	$0.06_{-0.11}^{+0.14}$
$\mathcal{B}(\bar{B}^0 \rightarrow D_s^{*-} a_0(980)^+)$	BABAR [635]: $0.14_{-0.16}^{+0.21} \pm 0.03$	$0.14_{-0.16}^{+0.21}$
$\mathcal{B}(\bar{B}^0 \rightarrow D_s^- a_2(1320)^+)$	BABAR [635]: $0.64_{-0.57}^{+1.04} \pm 0.15$	$0.64_{-0.59}^{+1.05}$
$\mathcal{B}(\bar{B}^0 \rightarrow D_s^{*-} a_2(1320)^+)$	BABAR [635]: < 2.0	< 2.0
$\mathcal{B}(\bar{B}^0 \rightarrow D_s^+ K^-)$	Belle [632]: $0.191 \pm 0.024 \pm 0.017$ BABAR [633]: $0.29 \pm 0.04 \pm 0.02$	0.221 ± 0.025
$\mathcal{B}(\bar{B}^0 \rightarrow D_s^{*+} K^-)$	Belle [634]: $0.202 \pm 0.033 \pm 0.022$ BABAR [633]: $0.24 \pm 0.04 \pm 0.02$	0.219 ± 0.031
$\mathcal{B}(\bar{B}^0 \rightarrow D_s^+ K^*(892)^-)$	BABAR [633]: $0.35_{-0.09}^{+0.10} \pm 0.04$	$0.35_{-0.10}^{+0.11}$
$\mathcal{B}(\bar{B}^0 \rightarrow D_s^{*+} K^*(892)^-)$	BABAR [633]: $0.32_{-0.12}^{+0.14} \pm 0.04$	$0.32_{-0.13}^{+0.15}$
$\mathcal{B}(\bar{B}^0 \rightarrow D_s^+ K_S^0 \pi^-)$	BABAR [636]: $0.55 \pm 0.13 \pm 0.10$	0.55 ± 0.17
$\mathcal{B}(\bar{B}^0 \rightarrow D_s^{*+} K^0 \pi^-)$	BABAR [636]: < 0.55	< 0.55

Table 100: Branching fraction ratios, I.

Parameter	Measurements	Average
$\frac{\mathcal{B}(\bar{B}^0 \rightarrow D^0 \rho(770)^0)}{\mathcal{B}(\bar{B}^0 \rightarrow D^0 \omega(782))}$	Belle [622]: 1.6 ± 0.8	1.6 ± 0.8
$\frac{\mathcal{B}(\bar{B}^0 \rightarrow D^+ \pi^+ \pi^- \pi^-)}{\mathcal{B}(\bar{B}^0 \rightarrow D^+ \pi^-)}$	LHCb [637]: $2.38 \pm 0.11 \pm 0.21$	2.38 ± 0.24
$\frac{\mathcal{B}(\bar{B}^0 \rightarrow D^*(2010)^+ \pi^-)}{\mathcal{B}(\bar{B}^0 \rightarrow D^+ \pi^-)}$	BABAR [613]: $0.99 \pm 0.11 \pm 0.08$	0.99 ± 0.14
$\frac{\mathcal{B}(\bar{B}^0 \rightarrow D^{**+} \pi^-)}{\mathcal{B}(\bar{B}^0 \rightarrow D^+ \pi^-)}$	BABAR [613]: $0.77 \pm 0.22 \pm 0.29$	0.77 ± 0.36
$\frac{\mathcal{B}(\bar{B}^0 \rightarrow D_s^+ K^- \pi^+ \pi^-)}{\mathcal{B}(\bar{B}_s^0 \rightarrow D_s^+ K^- \pi^+ \pi^-)}$	LHCb [638]: $0.54 \pm 0.07 \pm 0.07$	0.54 ± 0.10
$\frac{\mathcal{B}(\bar{B}^0 \rightarrow D^*(2010)^+ \pi^+ \pi^- \pi^-)}{\mathcal{B}(\bar{B}^0 \rightarrow D^*(2010)^+ \pi^-)}$	LHCb [639]: $2.64 \pm 0.04 \pm 0.13$	2.64 ± 0.14

Table 101: Branching fraction ratios, II.

Parameter	Measurements	Average
$\frac{\mathcal{B}(\bar{B}^0 \rightarrow D^0 K^- \pi^+)}{\mathcal{B}(\bar{B}^0 \rightarrow D^0 \pi^- \pi^+)}$	LHCb [640]: $0.106 \pm 0.007 \pm 0.008$	0.106 ± 0.011
$\frac{\mathcal{B}(\bar{B}^0 \rightarrow \bar{D}^0 K^- K^+)}{\mathcal{B}(\bar{B}^0 \rightarrow \bar{D}^0 \pi^- \pi^+)}$	LHCb [630]: $0.069 \pm 0.004 \pm 0.003$	0.069 ± 0.005
$\frac{\mathcal{B}(\bar{B}^0 \rightarrow D^0 \phi(1020))}{\mathcal{B}(\bar{B}^0 \rightarrow D^0 \pi^+ \pi^-)}$	LHCb [631]: $0.0012 \pm 0.0007 \pm 0.0003$	0.0012 ± 0.0008
$\frac{\mathcal{B}(\bar{B}^0 \rightarrow D^+ K^-)}{\mathcal{B}(\bar{B}^0 \rightarrow D^+ \pi^-)}$	LHCb [49]: $0.0822 \pm 0.0011 \pm 0.0025$ Belle [624]: $0.068 \pm 0.015 \pm 0.007$	0.0818 ± 0.0027
$\frac{\mathcal{B}(\bar{B}^0 \rightarrow D^+ K^- \pi^+ \pi^-)}{\mathcal{B}(\bar{B}^0 \rightarrow D^+ \pi^+ \pi^- \pi^-)}$	LHCb [641]: $0.059 \pm 0.011 \pm 0.005$	0.059 ± 0.012
$\frac{\mathcal{B}(\bar{B}^0 \rightarrow D^*(2010)^+ K^-)}{\mathcal{B}(\bar{B}^0 \rightarrow D^*(2010)^+ \pi^-)}$	Belle [624]: $0.074 \pm 0.015 \pm 0.006$ <i>BABAR</i> [629]: $0.0776 \pm 0.0034 \pm 0.0029$	0.0773 ± 0.0043
$\frac{\mathcal{B}(\bar{B}^0 \rightarrow D_s^+ K^-)}{\mathcal{B}(\bar{B}^0 \rightarrow D_s^+ \pi^-)}$	LHCb [642]: $0.0129 \pm 0.0005 \pm 0.0008$	0.0129 ± 0.0009
$\mathcal{B}(\bar{B}^0 \rightarrow D^*(2010)^+ \pi^+ K^- \pi^-) / \mathcal{B}(\bar{B}^0 \rightarrow D^*(2010)^+ \pi^- \pi^- \pi^+)$	LHCb [639]: $0.0647 \pm 0.0037 \pm 0.0035$	0.0647 ± 0.0051
$[\mathcal{B}(\bar{B}^0 \rightarrow D_1(2420)^0 \pi^+ \pi^-) \times \mathcal{B}(D_1(2420)^0 \rightarrow D^*(2010)^+ \pi^-)] / \mathcal{B}(\bar{B}^0 \rightarrow D^*(2010)^+ \pi^- \pi^+ \pi^-)$	LHCb [639]: $0.0204 \pm 0.0042 \pm 0.0022$	0.0204 ± 0.0047

 Table 102: Product branching fractions to excited D mesons, I.

Parameter	Measurements	Average $[10^{-4}]$
$\mathcal{B}(\bar{B}^0 \rightarrow D_1(2420)^+ \pi^-) \times \mathcal{B}(D_1(2420)^+ \rightarrow D^+ \pi^- \pi^+)$		
	Belle [643]: $0.89 \pm 0.15 {}^{+0.17}_{-0.31}$	$0.89 {}^{+0.23}_{-0.34}$
$\mathcal{B}(\bar{B}^0 \rightarrow D_1^0(H) \omega(782)) \times \mathcal{B}(D_1^0(H) \rightarrow D^*(2010)^+ \pi^-)$		
	<i>BABAR</i> [618]: $4.1 \pm 1.2 \pm 1.1$	4.1 ± 1.6
$\mathcal{B}(\bar{B}^0 \rightarrow D_0^*(2400)^+ \pi^-) \times \mathcal{B}(D_0^*(2400)^+ \rightarrow D^0 \pi^+)$		
	Belle [614]: $0.60 \pm 0.13 \pm 0.27$	0.60 ± 0.30
$\mathcal{B}(\bar{B}^0 \rightarrow D_2^*(2460)^+ \pi^-) \times \mathcal{B}(D_2^*(2460)^+ \rightarrow D^0 \pi^+)$		
	Belle [614]: $2.15 \pm 0.17 \pm 0.31$	2.15 ± 0.36

Table 103: Product branching fractions to excited D mesons, II.

Parameter	Measurements	Average [10 ⁻⁵]
$\mathcal{B}(\bar{B}^0 \rightarrow D_1(2420)^+ \pi^-) \times \mathcal{B}(D_1(2420)^+ \rightarrow D^*(2010)^+ \pi^- \pi^+)$	Belle [643]: < 3.3	< 3.3
$\mathcal{B}(\bar{B}^0 \rightarrow D_2^*(2460)^+ \pi^-) \times \mathcal{B}(D_2^*(2460)^+ \rightarrow D^*(2010)^+ \pi^- \pi^+)$	Belle [643]: < 2.4	< 2.4
$\mathcal{B}(\bar{B}^0 \rightarrow D_2^*(2460)^+ K^-) \times \mathcal{B}(D_2^*(2460)^+ \rightarrow D^0 \pi^+)$	BABAR [629]: $1.83 \pm 0.40 \pm 0.31$	1.83 ± 0.51
$\mathcal{B}(\bar{B}^0 \rightarrow D_{sJ}(2460)^- \pi^+) \times \mathcal{B}(D_{sJ}(2460)^- \rightarrow D_s^- \gamma)$	Belle [644]: < 0.40	< 0.40
$\mathcal{B}(\bar{B}^0 \rightarrow D_{sJ}^+(2460) K^-) \times \mathcal{B}(D_{sJ}^+(2460) \rightarrow D_s^+ \gamma)$	Belle [644]: < 0.94	< 0.94
$\mathcal{B}(\bar{B}^0 \rightarrow D_{sJ}^*(2317)^- \pi^+) \times \mathcal{B}(D_{sJ}^*(2317)^- \rightarrow D_s^- \pi^0)$	Belle [644]: < 2.5	< 2.5
$\mathcal{B}(\bar{B}^0 \rightarrow D_{sJ}^*(2317)^+ K^-) \times \mathcal{B}(D_{sJ}^*(2317)^+ \rightarrow D_s^+ \pi^0)$	Belle [644]: $5.3^{+1.5}_{-1.3} \pm 1.6$	$5.3^{+2.2}_{-2.0}$

 Table 104: Branching fractions and ratios to excited D mesons.

Parameter	Measurements	Average [10 ⁻²]
$\mathcal{B}(\bar{B}^0 \rightarrow D^{**+} \pi^-)$	BABAR [613]: $0.234 \pm 0.065 \pm 0.088$	0.234 ± 0.109
$\frac{\mathcal{B}(\bar{B}^0 \rightarrow D_1^+ \pi^-) \times \mathcal{B}(D_1^+ \rightarrow D^+ \pi^+ \pi^-)}{\mathcal{B}(\bar{B}^0 \rightarrow D^+ \pi^+ \pi^- \pi^-)}$	LHCb [637]: $2.1 \pm 0.5^{+0.3}_{-0.5}$	$2.1^{+0.6}_{-0.7}$

Table 105: Branching fractions to baryonic decays, I.

Parameter	Measurements	Average [10 ⁻⁴]
$\mathcal{B}(\bar{B}^0 \rightarrow D^+ p\bar{p}\pi^-)$	BABAR [645]: $3.32 \pm 0.10 \pm 0.29$	3.32 ± 0.31
$\mathcal{B}(\bar{B}^0 \rightarrow D^*(2010)^+ p\bar{p}\pi^-)$	BABAR [645]: $4.55 \pm 0.16 \pm 0.39$	4.55 ± 0.42
$\mathcal{B}(\bar{B}^0 \rightarrow D^0 p\bar{p}\pi^-\pi^+)$	BABAR [645]: $2.99 \pm 0.21 \pm 0.45$	2.99 ± 0.50
$\mathcal{B}(\bar{B}^0 \rightarrow D^*(2007)^0 p\bar{p}\pi^-\pi^+)$	BABAR [645]: $1.91 \pm 0.36 \pm 0.29$	1.91 ± 0.46

Table 106: Branching fractions to baryonic decays, II.

Parameter	Measurements	Average [10 ⁻⁵]
$\mathcal{B}(\bar{B}^0 \rightarrow D^0 p\bar{p})$	Belle [646]: $11.8 \pm 1.5 \pm 1.6$ BABAR [645]: $10.2 \pm 0.4 \pm 0.6$	10.4 ± 0.7
$\mathcal{B}(\bar{B}^0 \rightarrow D^*(2007)^0 p\bar{p})$	Belle [646]: $12.0^{+3.3}_{-2.9} \pm 2.1$ BABAR [645]: $9.7 \pm 0.7 \pm 0.9$	9.9 ± 1.1
$\mathcal{B}(\bar{B}^0 \rightarrow D_s^+ \Lambda \bar{p})$	Belle [647]: $2.9 \pm 0.7 \pm 0.6$	2.9 ± 0.9
$\mathcal{B}(\bar{B}^0 \rightarrow D^0 \Lambda^0 \bar{\Lambda}^0)$	Belle [648]: $1.05^{+0.57}_{-0.44} \pm 0.14$ BABAR [649]: $0.98^{+0.29}_{-0.26} \pm 0.19$	1.00 ± 0.28
$\mathcal{B}(\bar{B}^0 \rightarrow D^0 \Sigma^0 \bar{\Lambda} + \bar{B}^0 \rightarrow D^0 \Lambda \bar{\Sigma}^0)$	BABAR [649]: $1.5^{+0.9}_{-0.8} \pm 0.3$	$1.5^{+0.9}_{-0.9}$
$\mathcal{B}(\bar{B}^0 \rightarrow D^+ \Lambda \bar{p})$	Belle [650]: $3.36 \pm 0.63 \pm 0.44$	3.36 ± 0.77
$\mathcal{B}(\bar{B}^0 \rightarrow D^{*+} \Lambda \bar{p})$	Belle [650]: $2.51 \pm 0.26 \pm 0.35$	2.51 ± 0.44

 Table 107: Baryonic decays II [10⁻⁵].

Parameter	Measurements	Average
$\mathcal{B}(\bar{B}^0 \rightarrow D^0 p\bar{p})$	Belle [646]: $11.8 \pm 1.5 \pm 1.6$ BABAR [645]: $10.2 \pm 0.4 \pm 0.6$	10.4 ± 0.7
$\mathcal{B}(\bar{B}^0 \rightarrow D^*(2007)^0 p\bar{p})$	Belle [646]: $12.0^{+3.3}_{-2.9} \pm 2.1$ BABAR [645]: $9.7 \pm 0.7 \pm 0.9$	9.9 ± 1.1
$\mathcal{B}(\bar{B}^0 \rightarrow D_s^+ \Lambda \bar{p})$	Belle [647]: $2.9 \pm 0.7 \pm 0.6$	2.9 ± 0.9
$\mathcal{B}(\bar{B}^0 \rightarrow D^0 \Lambda^0 \bar{\Lambda}^0)$	Belle [648]: $1.05^{+0.57}_{-0.44} \pm 0.14$ BABAR [649]: $0.98^{+0.29}_{-0.26} \pm 0.19$	1.00 ± 0.28
$\mathcal{B}(\bar{B}^0 \rightarrow D^0 \Sigma^0 \bar{\Lambda} + \bar{B}^0 \rightarrow D^0 \Lambda \bar{\Sigma}^0)$	BABAR [649]: $1.5^{+0.9}_{-0.8} \pm 0.3$	$1.5^{+0.9}_{-0.9}$
$\mathcal{B}(\bar{B}^0 \rightarrow D^+ \Lambda \bar{p})$	Belle [650]: $3.36 \pm 0.63 \pm 0.44$	3.36 ± 0.77
$\mathcal{B}(\bar{B}^0 \rightarrow D^{*+} \Lambda \bar{p})$	Belle [650]: $2.51 \pm 0.26 \pm 0.35$	2.51 ± 0.44

7.1.2 Decays to two open charm mesons

Averages of \bar{B}^0 decays to two open charm mesons are shown in Tables 108–117.

Table 108: Branching fractions to $D^{(*)+}D^{(*)-}$.

Parameter	Measurements	Average [10 ⁻³]
$\mathcal{B}(\bar{B}^0 \rightarrow D^+ D^-)$	Belle [282]: $0.212 \pm 0.016 \pm 0.018$ BABAR [651]: $0.28 \pm 0.04 \pm 0.05$	0.220 ± 0.023
$\mathcal{B}(\bar{B}^0 \rightarrow D^*(2010)^- D^+)$	Belle [282]: $0.614 \pm 0.029 \pm 0.050$ BABAR [651]: $0.57 \pm 0.07 \pm 0.07$	0.603 ± 0.050
$\mathcal{B}(\bar{B}^0 \rightarrow D^*(2010)^- D^*(2010)^+)$	Belle [354]: $0.782 \pm 0.038 \pm 0.060$ BABAR [651]: $0.81 \pm 0.06 \pm 0.10$	0.790 ± 0.061
$\mathcal{B}(\bar{B}^0 \rightarrow D^0 \bar{D}^0)$	Belle [652]: < 0.043 BABAR [651]: < 0.06	< 0.043
$\mathcal{B}(\bar{B}^0 \rightarrow D^0 \bar{D}^*(2007)^0)$	BABAR [651]: < 0.29	< 0.29
$\mathcal{B}(\bar{B}^0 \rightarrow D^*(2007)^0 \bar{D}^*(2007)^0)$	BABAR [651]: < 0.09	< 0.09

 Table 109: Branching fractions to two D mesons and a kaon, I.

Parameter	Measurements	Average [10 ⁻³]
$\mathcal{B}(\bar{B}^0 \rightarrow D^*(2010)^+ D^- \bar{K}^0)$	BABAR [653]: $6.41 \pm 0.36 \pm 0.39$	6.41 ± 0.53
$\mathcal{B}(\bar{B}^0 \rightarrow D^*(2010)^- D^*(2010)^+ \bar{K}^0)$	BABAR [653]: $8.26 \pm 0.43 \pm 0.67$	8.26 ± 0.80
$\mathcal{B}(\bar{B}^0 \rightarrow D^*(2010)^+ D^*(2010)^- K_S^0)$	Belle [261]: $3.4 \pm 0.4 \pm 0.7$ BABAR [260]: $4.4 \pm 0.4 \pm 0.7$	3.9 ± 0.6
$\mathcal{B}(\bar{B}^0 \rightarrow D^*(2010)^+ \bar{D}^0 K^-)$	BABAR [653]: $2.47 \pm 0.10 \pm 0.18$	2.47 ± 0.21
$\mathcal{B}(\bar{B}^0 \rightarrow D^+ \bar{D}^*(2007)^0 K^-)$	BABAR [653]: $3.46 \pm 0.18 \pm 0.37$	3.46 ± 0.41
$\mathcal{B}(\bar{B}^0 \rightarrow D^*(2010)^+ \bar{D}^*(2007)^0 K^-)$	BABAR [653]: $10.6 \pm 0.3 \pm 0.9$	10.6 ± 0.9
$\mathcal{B}(\bar{B}^0 \rightarrow D^0 \bar{D}^*(2007)^0 \bar{K}^0)$	BABAR [653]: $1.08 \pm 0.32 \pm 0.36$	1.08 ± 0.48
$\mathcal{B}(\bar{B}^0 \rightarrow D^*(2007)^0 \bar{D}^*(2007)^0 \bar{K}^0)$	BABAR [653]: $2.40 \pm 0.55 \pm 0.67$	2.40 ± 0.87

 Table 110: Branching fractions to two D mesons and a kaon, II.

Parameter	Measurements	Average [10 ⁻⁴]
$\mathcal{B}(\bar{B}^0 \rightarrow D^+ D^- \bar{K}^0)$	BABAR [653]: $7.5 \pm 1.2 \pm 1.2$	7.5 ± 1.7
$\mathcal{B}(\bar{B}^0 \rightarrow D^+ \bar{D}^0 K^-)$	BABAR [653]: $10.7 \pm 0.7 \pm 0.9$	10.7 ± 1.1
$\mathcal{B}(\bar{B}^0 \rightarrow D^0 \bar{D}^0 \bar{K}^0)$	BABAR [653]: $2.7 \pm 1.0 \pm 0.5$	2.7 ± 1.1
$\mathcal{B}(\bar{B}^0 \rightarrow D^0 \bar{D}^0 \pi^0 \bar{K}^0)$	Belle [654]: $1.73 \pm 0.70^{+0.31}_{-0.53}$	$1.73^{+0.77}_{-0.88}$

Table 111: Branching fractions to $D_s^{(*)-} D^{(*)+}$, I.

Parameter	Measurements	Average [10 ⁻³]
$\mathcal{B}(\bar{B}^0 \rightarrow D_s^- D^+)$	Belle [655]: $7.5 \pm 0.2 \pm 1.1$ BABAR [656]: $9.0 \pm 1.8 \pm 1.4$	7.8 ± 1.0
$\mathcal{B}(\bar{B}^0 \rightarrow D_s^- D^*(2010)^+)$	BABAR [656]: $5.7 \pm 1.6 \pm 0.9$ BABAR [657]: $10.3 \pm 1.4 \pm 2.9$	6.8 ± 1.6
$\mathcal{B}(\bar{B}^0 \rightarrow D_s^{*-} D^*(2010)^+)$	BABAR [656]: $16.5 \pm 2.3 \pm 1.9$ BABAR [658]: $18.8 \pm 0.9 \pm 1.7$ BABAR [657]: $19.7 \pm 1.5 \pm 5.7$	18.2 ± 1.6
$\mathcal{B}(\bar{B}^0 \rightarrow D_s^{*-} D^+)$	BABAR [656]: $6.7 \pm 2.0 \pm 1.1$	6.7 ± 2.3

 Table 112: Branching fractions to $D_s^{(*)-} D^{(*)+}$, II.

Parameter	Measurements	Average [10 ⁻⁴]
$\mathcal{B}(\bar{B}^0 \rightarrow D_s^- D^+) \times \mathcal{B}(D_s^- \rightarrow \phi(1020)\pi^-)$	BABAR [656]: $2.67 \pm 0.61 \pm 0.47$	2.67 ± 0.77
$\mathcal{B}(\bar{B}^0 \rightarrow D_s^- D^*(2010)^+) \times \mathcal{B}(D_s^- \rightarrow \phi(1020)\pi^-)$	BABAR [656]: $5.11 \pm 0.94 \pm 0.72$	5.11 ± 1.18
$\mathcal{B}(\bar{B}^0 \rightarrow D_s^{*-} D^+) \times \mathcal{B}(D_s^- \rightarrow \phi(1020)\pi^-)$	BABAR [656]: $4.14 \pm 1.19 \pm 0.94$	4.14 ± 1.52
$\mathcal{B}(\bar{B}^0 \rightarrow D_s^{*-} D^*(2010)^+) \times \mathcal{B}(D_s^- \rightarrow \phi(1020)\pi^-)$	BABAR [656]: $12.2 \pm 2.2 \pm 2.2$	12.2 ± 3.1

 Table 113: Branching fractions to $D_s^{(*)+} D_s^{(*)-}$.

Parameter	Measurements	Average [10 ⁻³]
$\mathcal{B}(\bar{B}^0 \rightarrow D_s^- D_s^+)$	Belle [655]: < 0.036 BABAR [659]: < 0.10	< 0.036
$\mathcal{B}(\bar{B}^0 \rightarrow D_s^- D_s^{*+})$	BABAR [659]: < 0.13	< 0.13
$\mathcal{B}(\bar{B}^0 \rightarrow D_s^{*+} D_s^{*-})$	BABAR [659]: < 0.24	< 0.24

Table 114: Branching fraction ratios.

Parameter	Measurements	Average [10 ⁻³]
$\frac{\mathcal{B}(\bar{B}^0 \rightarrow D^0 \bar{D}^0)}{\mathcal{B}(\bar{B}^- \rightarrow D^0 \bar{D}_s^-)}$	LHCb [660]: $1.4 \pm 0.6 \pm 0.2$	1.4 ± 0.6

Table 115: Branching fractions to excited D_s mesons.

Parameter	Measurements	Average $[10^{-3}]$
$\mathcal{B}(\bar{B}^0 \rightarrow D_{sJ}(2460)^- D^+)$	<i>BABAR</i> [656]: $2.6 \pm 1.5 \pm 0.7$	2.6 ± 1.7
$\mathcal{B}(\bar{B}^0 \rightarrow D_{sJ}(2460)^- D^*(2010)^+)$	<i>BABAR</i> [656]: $8.8 \pm 2.0 \pm 1.4$	8.8 ± 2.4
$\mathcal{B}(\bar{B}^0 \rightarrow D_{s1}(2536)^- D^*(2010)^+)$	<i>BABAR</i> [260]: $92 \pm 24 \pm 1$	92 ± 24

 Table 116: Product branching fractions to excited D_s mesons, I.

Parameter	Measurements	Average $[10^{-3}]$
$\mathcal{B}(\bar{B}^0 \rightarrow D^+ D_{sJ}(2460)^-) \times \mathcal{B}(D_{sJ}(2460)^- \rightarrow D_s^- \gamma)$		
<i>Belle</i> [661]: $0.82^{+0.22}_{-0.19} \pm 0.25$		0.81 ± 0.23
<i>BABAR</i> [662]: $0.8 \pm 0.2^{+0.3}_{-0.2}$		
$\mathcal{B}(\bar{B}^0 \rightarrow D^+ D_{sJ}(2460)^-) \times \mathcal{B}(D_{sJ}(2460)^- \rightarrow D_s^{*-} \pi^0)$		
<i>Belle</i> [661]: $2.27^{+0.73}_{-0.62} \pm 0.68$		2.48 ± 0.75
<i>BABAR</i> [662]: $2.8 \pm 0.8^{+1.1}_{-0.8}$		
$\mathcal{B}(\bar{B}^0 \rightarrow D_{sJ}(2460)^- D^*(2010)^+) \times \mathcal{B}(D_{sJ}(2460)^- \rightarrow D_s^{*-} \pi^0)$		
<i>BABAR</i> [662]: $5.5 \pm 1.2^{+2.1}_{-1.6}$		$5.5^{+2.5}_{-2.0}$
$\mathcal{B}(\bar{B}^0 \rightarrow D_{sJ}(2460)^- D^*(2010)^+) \times \mathcal{B}(D_{sJ}(2460)^- \rightarrow D_s^- \gamma)$		
<i>BABAR</i> [662]: $2.3 \pm 0.3^{+0.9}_{-0.6}$		$2.3^{+0.9}_{-0.7}$
$\mathcal{B}(\bar{B}^0 \rightarrow D_{sJ}^*(2317)^- D^*(2010)^+) \times \mathcal{B}(D_{sJ}^*(2317)^- \rightarrow D_s^- \pi^0)$		
<i>BABAR</i> [662]: $1.5 \pm 0.4^{+0.5}_{-0.4}$		$1.5^{+0.7}_{-0.5}$
$\mathcal{B}(\bar{B}^0 \rightarrow D^+ D_{sJ}^*(2317)^-) \times \mathcal{B}(D_{sJ}^*(2317)^- \rightarrow D_s^- \pi^0)$		
<i>Belle</i> [663]: $1.02^{+0.13}_{-0.12} \pm 0.11$		1.05 ± 0.16
<i>BABAR</i> [662]: $1.8 \pm 0.4^{+0.7}_{-0.5}$		
$\mathcal{B}(\bar{B}^0 \rightarrow D^+ D_{sJ}^*(2317)^-) \times \mathcal{B}(D_{sJ}^*(2317)^- \rightarrow D_s^{*-} \gamma)$		
<i>Belle</i> [661]: < 0.95		< 0.95

Table 117: Product branching fractions to excited D_s mesons, II.

Parameter	Measurements	Average [10 ⁻⁴]
$\mathcal{B}(\bar{B}^0 \rightarrow D_{s1}(2536)^- D^+) \times \mathcal{B}(D_{s1}(2536)^- \rightarrow D^*(2010)^- \bar{K}^0)$		
BABAR [664]: $2.61 \pm 1.03 \pm 0.31$	2.61 ± 1.08	
$\mathcal{B}(\bar{B}^0 \rightarrow D_{s1}(2536)^- D^+) \times \mathcal{B}(D_{s1}(2536)^- \rightarrow K^- \bar{D}^*(2007)^0)$		
BABAR [664]: $1.71 \pm 0.48 \pm 0.32$	1.71 ± 0.58	
$\mathcal{B}(\bar{B}^0 \rightarrow D_{s1}(2536)^- D^*(2010)^+) \times \mathcal{B}(D_{s1}(2536)^- \rightarrow D^*(2010)^- \bar{K}^0)$		
BABAR [664]: $5.00 \pm 1.51 \pm 0.67$	5.00 ± 1.65	
$\mathcal{B}(\bar{B}^0 \rightarrow D_{s1}(2536)^- D^*(2010)^+) \times \mathcal{B}(D_{s1}(2536)^- \rightarrow \bar{D}^*(2007)^0 K^+)$		
BABAR [664]: $3.32 \pm 0.88 \pm 0.66$	3.32 ± 1.10	
$\mathcal{B}(\bar{B}^0 \rightarrow D_{s1}(2536)^+ D^-) \times \mathcal{B}(D_{s1}(2536)^+ \rightarrow D^*(2007)^0 K^+ + D^*(2010)^+ K^0)$		
Belle [665]: $2.75 \pm 0.62 \pm 0.36$	2.75 ± 0.72	
$\mathcal{B}(\bar{B}^0 \rightarrow D_{s1}(2536)^+ D^*(2010)^-) \times \mathcal{B}(D_{s1}(2536)^+ \rightarrow D^*(2007)^0 K^+ + D^*(2010)^+ K^0)$		
Belle [665]: $5.01 \pm 1.21 \pm 0.70$	5.01 ± 1.40	
$\mathcal{B}(\bar{B}^0 \rightarrow D_{s1}(2536)^+ D^*(2010)^-) \times \mathcal{B}(D_{s1}(2536)^+ \rightarrow D^*(2010)^+ K_S^0)$		
Belle [261]: < 6.0	< 6.0	
$\mathcal{B}(\bar{B}^0 \rightarrow D^+ D_{sJ}(2460)^-) \times \mathcal{B}(D_{sJ}(2460)^- \rightarrow D_s^- \pi^+ \pi^-)$		
Belle [661]: < 2.0	< 2.0	
$\mathcal{B}(\bar{B}^0 \rightarrow D^+ D_{sJ}(2460)^-) \times \mathcal{B}(D_{sJ}(2460)^- \rightarrow D_s^- \pi^0)$		
Belle [661]: < 3.6	< 3.6	
$\mathcal{B}(\bar{B}^0 \rightarrow D^+ D_{sJ}(2460)^-) \times \mathcal{B}(D_{sJ}(2460)^- \rightarrow D_s^{*-} \gamma)$		
Belle [661]: < 6.0	< 6.0	

7.1.3 Decays to charmonium states

Averages of \bar{B}^0 decays to charmonium states are shown in Tables 118–127.

Table 118: Branching fractions to J/ψ and one kaon.

Parameter	Measurements	Average [10 ⁻³]
$\mathcal{B}(\bar{B}^0 \rightarrow J/\psi \bar{K}^0)$	CDF [666]: 1.15 ± 0.23 ± 0.17 Belle [667]: 0.79 ± 0.04 ± 0.09 <i>BABAR</i> [9]: 0.869 ± 0.022 ± 0.030	0.863 ± 0.035
$\mathcal{B}(\bar{B}^0 \rightarrow J/\psi K^- \pi^+)$	Belle [668]: 1.15 ± 0.01 ± 0.05	1.15 ± 0.05
$\mathcal{B}(\bar{B}^0 \rightarrow J/\psi \bar{K}^*(892)^0)$	CDF [669]: 1.74 ± 0.20 ± 0.18 Belle [668]: 1.19 ± 0.01 ± 0.08 <i>BABAR</i> [9]: 1.309 ± 0.026 ± 0.077	1.270 ± 0.056
$\mathcal{B}(\bar{B}^0 \rightarrow J/\psi \bar{K}^0 \pi^+ \pi^-)$	LHCb [670]: 0.430 ± 0.030 ± 0.037 CDF [671]: 1.03 ± 0.33 ± 0.15	0.440 ± 0.047
$\mathcal{B}(\bar{B}^0 \rightarrow J/\psi \bar{K}^0 \rho(770)^0)$	CDF [671]: 0.54 ± 0.29 ± 0.09	0.54 ± 0.30
$\mathcal{B}(\bar{B}^0 \rightarrow J/\psi K^*(892)^- \pi^+)$	CDF [671]: 0.77 ± 0.41 ± 0.13	0.77 ± 0.43
$\mathcal{B}(\bar{B}^0 \rightarrow J/\psi \omega(782) \bar{K}^0)$	<i>BABAR</i> [672]: 0.23 ± 0.03 ± 0.03	0.23 ± 0.04
$\mathcal{B}(\bar{B}^0 \rightarrow J/\psi \phi(1020) \bar{K}^0)$	<i>BABAR</i> [673]: 0.102 ± 0.038 ± 0.010	0.102 ± 0.039
$\mathcal{B}(\bar{B}^0 \rightarrow J/\psi \bar{K}_1^0(1270))$	Belle [674]: 1.30 ± 0.34 ± 0.31	1.30 ± 0.46
$\mathcal{B}(\bar{B}^0 \rightarrow J/\psi \eta K_S^0)$	Belle [675]: 0.0522 ± 0.0078 ± 0.0049 <i>BABAR</i> [676]: 0.084 ± 0.026 ± 0.027	0.0540 ± 0.0089
$\mathcal{B}(\bar{B}^0 \rightarrow J/\psi \bar{K}^*(892)^0 \pi^+ \pi^-)$	CDF [671]: 0.66 ± 0.19 ± 0.11	0.66 ± 0.22

Table 119: Branching fractions to charmonium other than J/ψ and one kaon, I.

Parameter	Measurements	Average [10 ⁻³]
$\mathcal{B}(\bar{B}^0 \rightarrow \psi(2S)\bar{K}^0)$	Belle [667]: 0.67 ± 0.11 BABAR [9]: $0.646 \pm 0.065 \pm 0.051$	0.655 ± 0.066
$\mathcal{B}(\bar{B}^0 \rightarrow \psi(2S)\bar{K}^*(892)^0)$	CDF [669]: $0.90 \pm 0.22 \pm 0.09$ BABAR [9]: $0.649 \pm 0.059 \pm 0.097$	0.696 ± 0.103
$\mathcal{B}(\bar{B}^0 \rightarrow \psi(2S)K^0)$	LHCb [670]: $0.47 \pm 0.07 \pm 0.07$	0.47 ± 0.10
$\mathcal{B}(\bar{B}^0 \rightarrow K^*(892)^0\psi(2S))$	Belle [677]: $0.552^{+0.035}_{-0.032}{}^{+0.053}_{-0.058}$	$0.552^{+0.064}_{-0.066}$
$\mathcal{B}(\bar{B}^0 \rightarrow \psi(2S)K^0) \times \mathcal{B}(\psi(2S) \rightarrow \chi_{c1}\gamma)$	Belle [678]: $0.68 \pm 0.10 \pm 0.07$	0.68 ± 0.12
$\mathcal{B}(\bar{B}^0 \rightarrow \psi(2S)K^0) \times \mathcal{B}(\psi(2S) \rightarrow \chi_{c2}\gamma)$	Belle [678]: $0.47 \pm 0.16 \pm 0.08$	0.47 ± 0.18
$\mathcal{B}(\bar{B}^0 \rightarrow \chi_{c0}\bar{K}^0)$	BABAR [679]: < 1.24	< 1.24
$\mathcal{B}(\bar{B}^0 \rightarrow \chi_{c0}\bar{K}^*(892)^0)$	BABAR [679]: < 0.77 BABAR [680]: $0.17 \pm 0.03 \pm 0.02$	0.17 ± 0.04
$\mathcal{B}(\bar{B}^0 \rightarrow \chi_{c1}\bar{K}^0)$	Belle [681]: $0.378^{+0.017}_{-0.016} \pm 0.033$ BABAR [682]: $0.42 \pm 0.03 \pm 0.03$	0.396 ± 0.028
$\mathcal{B}(\bar{B}^0 \rightarrow \chi_{c1}K^-\pi^+)$	Belle [683]: $0.497 \pm 0.012 \pm 0.028$ BABAR [684]: $0.511 \pm 0.014 \pm 0.058$	0.500 ± 0.027
$\mathcal{B}(\bar{B}^0 \rightarrow \chi_{c1}\bar{K}^*(892)^0)$	Belle [685]: $0.31 \pm 0.03 \pm 0.07$ BABAR [682]: $0.25 \pm 0.02 \pm 0.02$	0.26 ± 0.03
$\mathcal{B}(\bar{B}^0 \rightarrow \chi_{c1}K^-\pi^+\pi^0)$	Belle [683]: $0.352 \pm 0.052 \pm 0.024$	0.352 ± 0.057
$\mathcal{B}(\bar{B}^0 \rightarrow \chi_{c1}\bar{K}^0\pi^+\pi^-)$	Belle [683]: $0.316 \pm 0.035 \pm 0.032$	0.316 ± 0.047
$\mathcal{B}(\bar{B}^0 \rightarrow \eta_c\bar{K}^0)$	Belle [686]: $1.23 \pm 0.23^{+0.40}_{-0.41}$ BABAR [687]: $0.64^{+0.22}_{-0.20}{}^{+0.28}_{-0.16}$ BABAR [688]: $1.14 \pm 0.15 \pm 0.34$	0.88 ± 0.27
$\mathcal{B}(\bar{B}^0 \rightarrow \eta_c\bar{K}^*(892)^0)$	Belle [686]: $1.62 \pm 0.32^{+0.55}_{-0.60}$ BABAR [689]: $0.57 \pm 0.06 \pm 0.09$ BABAR [687]: $0.80^{+0.21}_{-0.19}{}^{+0.37}_{-0.23}$	0.62 ± 0.10
$\mathcal{B}(\bar{B}^0 \rightarrow \eta_c(2S)\bar{K}^*(892)^0)$	BABAR [689]: < 0.39	< 0.39
$\mathcal{B}(\bar{B}^0 \rightarrow h_c(1P)\bar{K}^*(892)^0) \times \mathcal{B}(h_c(1P) \rightarrow \eta_c\gamma)$	BABAR [689]: < 0.22	< 0.22
$\mathcal{B}(\bar{B}^0 \rightarrow \eta_cK^-\pi^+)$	LHCb [690]: $0.573 \pm 0.024 \pm 0.067$	0.573 ± 0.071

Table 120: Branching fractions to charmonium other than J/ψ and one kaon, II.

Parameter	Measurements	Average $[10^{-4}]$
$\mathcal{B}(\bar{B}^0 \rightarrow \psi(3770)\bar{K}^0) \times \mathcal{B}(\psi(3770) \rightarrow D^0\bar{D}^0)$	BABAR [664]: < 1.23	< 1.23
$\mathcal{B}(\bar{B}^0 \rightarrow \psi(3770)\bar{K}^0) \times \mathcal{B}(\psi(3770) \rightarrow D^+D^-)$	BABAR [664]: < 1.88	< 1.88
$\mathcal{B}(\bar{B}^0 \rightarrow \chi_{c2}\bar{K}^0)$	Belle [681]: < 0.15 BABAR [682]: $0.15 \pm 0.09 \pm 0.03$	0.15 ± 0.09
$\mathcal{B}(\bar{B}^0 \rightarrow \chi_{c2}\bar{K}^*(892)^0)$	BABAR [682]: $0.66 \pm 0.18 \pm 0.05$	0.66 ± 0.19
$\mathcal{B}(\bar{B}^0 \rightarrow \chi_{c2}K^-\pi^+)$	Belle [683]: $0.72 \pm 0.09 \pm 0.05$	0.72 ± 0.10

Table 121: Branching fractions to charmonium and light mesons, I.

Parameter	Measurements	Average $[10^{-5}]$
$\mathcal{B}(\bar{B}^0 \rightarrow J/\psi\pi^0)$	Belle [667]: $2.3 \pm 0.5 \pm 0.2$ BABAR [350]: $1.69 \pm 0.14 \pm 0.07$	1.74 ± 0.15
$\mathcal{B}(\bar{B}^0 \rightarrow J/\psi\pi^+\pi^-)$	BABAR [691]: < 1.2	< 1.2
$\mathcal{B}(\bar{B}^0 \rightarrow J/\psi\rho(770)^0)$	BABAR [691]: $2.7 \pm 0.3 \pm 0.2$	2.7 ± 0.4
$\mathcal{B}(\bar{B}^0 \rightarrow J/\psi\eta)$	Belle [692]: $1.23^{+0.18}_{-0.17} \pm 0.07$ BABAR [673]: < 2.7	$1.23^{+0.19}_{-0.18}$
$\mathcal{B}(\bar{B}^0 \rightarrow J/\psi\eta'(958))$	Belle [692]: < 0.74 BABAR [673]: < 6.3	< 0.74
$\mathcal{B}(\bar{B}^0 \rightarrow J/\psi f_2(1270))$	BABAR [691]: < 0.46	< 0.46
$\mathcal{B}(\bar{B}^0 \rightarrow J/\psi f_1(1285))$	LHCb [693]: $0.837 \pm 0.195^{+0.079}_{-0.075}$	$0.837^{+0.210}_{-0.209}$
$\mathcal{B}(\bar{B}^0 \rightarrow J/\psi K^0 K^\pm \pi^\mp)$	LHCb [670]: < 2.1	< 2.1
$\mathcal{B}(\bar{B}^0 \rightarrow J/\psi K^0 K^+ K^-)$	LHCb [670]: $2.02 \pm 0.43 \pm 0.19$	2.02 ± 0.47
$\mathcal{B}(\bar{B}^0 \rightarrow \chi_{c1}\pi^0)$	Belle [694]: $1.12 \pm 0.25 \pm 0.12$	1.12 ± 0.28

Table 122: Branching fractions to charmonium and light mesons, II.

Parameter	Measurements	Average [10 ⁻⁵]
$\mathcal{B}(\bar{B}^0 \rightarrow J/\psi a_0(980)) \times \mathcal{B}(a_0(980) \rightarrow K^+ K^-)$	LHCb [695]: < 0.090	< 0.090
$\mathcal{B}(\bar{B}^0 \rightarrow J/\psi f_0(980)) \times \mathcal{B}(f_0(980) \rightarrow \pi^+ \pi^-)$	LHCb [696]: < 0.11	< 0.11
$\mathcal{B}(\bar{B}^0 \rightarrow J/\psi f_1(1285)) \times \mathcal{B}(f_1(1285) \rightarrow \pi^+ \pi^- \pi^+ \pi^-)$	LHCb [693]: 0.0921 ± 0.0214 ± 0.0064	0.0921 ± 0.0223
$\mathcal{B}(\bar{B}^0 \rightarrow J/\psi K^+ K^-)$	LHCb [695]: 0.253 ± 0.031 ± 0.019	0.253 ± 0.036
$\mathcal{B}(\bar{B}^0 \rightarrow J/\psi \phi(1020))$	LHCb [695]: < 0.019 Belle [697]: < 0.094 <i>BABAR</i> [673]: < 0.9	< 0.019

 Table 123: Branching fractions to J/ψ and photons, baryons, or heavy mesons.

Parameter	Measurements	Average [10 ⁻⁵]
$\mathcal{B}(\bar{B}^0 \rightarrow J/\psi \gamma)$	LHCb [698]: < 0.15 <i>BABAR</i> [699]: < 0.16	< 0.15
$\mathcal{B}(\bar{B}^0 \rightarrow J/\psi \bar{p}p)$	LHCb [700]: < 0.052 Belle [701]: < 0.083 <i>BABAR</i> [702]: < 0.19	< 0.052
$\mathcal{B}(\bar{B}^0 \rightarrow J/\psi D^0)$	Belle [703]: < 2.0 <i>BABAR</i> [704]: < 1.3	< 1.3

Table 124: Branching fraction ratios, I.

Parameter	Measurements	Average
$\frac{\mathcal{B}(\bar{B}^0 \rightarrow J/\psi \bar{K}_1^0(1270))}{\mathcal{B}(B^- \rightarrow J/\psi K^-)}$	Belle [674]: $1.30 \pm 0.34 \pm 0.28$	1.30 ± 0.44
$\frac{\mathcal{B}(\bar{B}^0 \rightarrow J/\psi \bar{K}^*(892)^0)}{\mathcal{B}(\bar{B}^0 \rightarrow J/\psi K^0)}$	CDF [705]: $1.39 \pm 0.36 \pm 0.10$ BABAR [9]: $1.51 \pm 0.05 \pm 0.08$	1.50 ± 0.09
$\frac{\mathcal{B}(\bar{B}^0 \rightarrow J/\psi \omega(782))}{\mathcal{B}(\bar{B}^0 \rightarrow J/\psi \rho)}$	LHCb [706]: $0.89 \pm 0.19^{+0.07}_{-0.13}$	$0.89^{+0.20}_{-0.23}$
$\frac{\mathcal{B}(\bar{B}^0 \rightarrow J/\psi \omega(782) \bar{K}^0)}{\mathcal{B}(B^- \rightarrow J/\psi \omega(782) K^-)}$	BABAR [672]: $0.7 \pm 0.1 \pm 0.1$	0.7 ± 0.1
$\frac{\mathcal{B}(\bar{B}^0 \rightarrow J/\psi K_S^0 \pi^- \pi^+)}{\mathcal{B}(\bar{B}^0 \rightarrow J/\psi K_S^0)}$	LHCb [670]: $0.493 \pm 0.034 \pm 0.027$	0.493 ± 0.043
$[\mathcal{B}(\bar{B}^0 \rightarrow \psi(2S) K_S^0) \times \mathcal{B}(\psi(2S) \rightarrow J/\psi \pi^- \pi^+)] / \mathcal{B}(\bar{B}^0 \rightarrow J/\psi K_S^0)$	LHCb [670]: $0.183 \pm 0.027 \pm 0.015$	0.183 ± 0.031
$\frac{\mathcal{B}(\bar{B}^0 \rightarrow \psi(2S) \bar{K}^*(892)^0)}{\mathcal{B}(\bar{B}^0 \rightarrow \psi(2S) \bar{K}^0)}$	BABAR [9]: $1.00 \pm 0.14 \pm 0.09$	1.00 ± 0.17
$\frac{\mathcal{B}(\bar{B}^0 \rightarrow \psi(2S) \pi^+ \pi^-)}{\mathcal{B}(\bar{B}^0 \rightarrow J/\psi \pi^+ \pi^-)}$	LHCb [707]: $0.56 \pm 0.07 \pm 0.05$	0.56 ± 0.09
$\frac{\mathcal{B}(\bar{B}^0 \rightarrow \eta_c \bar{K}^0)}{\mathcal{B}(B^- \rightarrow \eta_c K^-)}$	BABAR [688]: $0.87 \pm 0.13 \pm 0.07$	0.87 ± 0.15
$\frac{\mathcal{B}(\bar{B}^0 \rightarrow \eta_c \bar{K}^0)}{\mathcal{B}(\bar{B}^0 \rightarrow J/\psi K^0)}$	BABAR [688]: $1.34 \pm 0.19 \pm 0.40$	1.34 ± 0.44
$\frac{\mathcal{B}(\bar{B}^0 \rightarrow \eta_c \bar{K}^*(892)^0)}{\mathcal{B}(B^- \rightarrow \eta_c K^-)}$	BABAR [689]: $0.62 \pm 0.06 \pm 0.05$	0.62 ± 0.08
$\frac{\mathcal{B}(\bar{B}^0 \rightarrow \eta_c \bar{K}^*(892)^0)}{\mathcal{B}(\bar{B}^0 \rightarrow \eta_c \bar{K}^0)}$	Belle [686]: $1.33 \pm 0.36^{+0.24}_{-0.33}$	$1.33^{+0.43}_{-0.49}$
$\frac{\mathcal{B}(\bar{B}^0 \rightarrow \chi_{c1} \bar{K}^*(892)^0)}{\mathcal{B}(\bar{B}^0 \rightarrow \chi_{c1} \bar{K}^0)}$	BABAR [9]: $0.72 \pm 0.11 \pm 0.12$	0.72 ± 0.16
$\frac{\mathcal{B}(\bar{B}^0 \rightarrow h_c(1P) \bar{K}^*(892)^0) \times \mathcal{B}(h_c(1P) \rightarrow \eta_c \gamma)}{\mathcal{B}(B^- \rightarrow \eta_c K^-)}$	BABAR [689]: < 0.236	< 0.236

Table 125: Branching fraction ratios, II.

Parameter	Measurements	Average
$\frac{\mathcal{B}(\bar{B}^0 \rightarrow \psi(2S) K(892)^{*0})}{\mathcal{B}(\bar{B}^0 \rightarrow J/\psi K(892)^{*0})}$	LHCb [708]: $0.476 \pm 0.014 \pm 0.016$	0.476 ± 0.021
$\frac{\mathcal{B}(\bar{B}^0 \rightarrow \chi_{c1} K^- \pi^+)}{\mathcal{B}(\bar{B}^0 \rightarrow J/\psi K^- \pi^+)}$	BABAR [684]: $0.474 \pm 0.013 \pm 0.054$	0.474 ± 0.056
$\frac{\mathcal{B}(\bar{B}^0 \rightarrow \eta_c K^- \pi^+)}{\mathcal{B}(\bar{B}^0 \rightarrow J/\psi K^- \pi^+)}$	LHCb [690]: $0.357 \pm 0.015 \pm 0.008$	0.357 ± 0.017

Table 126: Branching fraction ratios, III.

Parameter	Measurements	Average
$\frac{\mathcal{B}(\bar{B}^0 \rightarrow J/\psi \eta)}{\mathcal{B}(\bar{B}^0 \rightarrow J/\psi \eta)}$	LHCb [709]: $0.0185 \pm 0.0061 \pm 0.0014$	0.0185 ± 0.0063
$\frac{\mathcal{B}(\bar{B}^0 \rightarrow J/\psi \eta')}{\mathcal{B}(\bar{B}^0 \rightarrow J/\psi \eta')}$	LHCb [709]: $0.0228 \pm 0.0065 \pm 0.0016$	0.0228 ± 0.0067
$\frac{\mathcal{B}(\bar{B}^0 \rightarrow J/\psi K_S^0 K^\pm \pi^\mp)}{\mathcal{B}(\bar{B}^0 \rightarrow J/\psi K_S^0 \pi^+ \pi^-)}$	LHCb [670]: < 0.048	< 0.048
$\frac{\mathcal{B}(\bar{B}^0 \rightarrow J/\psi K_S^0 K^+ K^-)}{\mathcal{B}(\bar{B}^0 \rightarrow J/\psi K_S^0 \pi^+ \pi^-)}$	LHCb [670]: $0.047 \pm 0.010 \pm 0.004$	0.047 ± 0.011

Table 127: Polarization fractions.

Parameter	Measurements	Average
$ \mathcal{A}_0 ^2(B^0 \rightarrow J/\psi \bar{K}^*(892)^0)$	BABAR [710]: < 0.32	< 0.32
$ \mathcal{A}_0 ^2(\bar{B}^0 \rightarrow J/\psi \bar{K}^*(892)^0)$		
$ \mathcal{A}_0 ^2(\bar{B}^0 \rightarrow J/\psi K^*(892)^0)$	BABAR [710]: < 0.26	< 0.26

7.1.4 Decays to charm baryons

Averages of \bar{B}^0 decays to charm baryons are shown in Tables 128–131.

Table 128: Branching fractions, I.

Parameter	Measurements	Average $[10^{-4}]$
$\mathcal{B}(\bar{B}^0 \rightarrow \Lambda_c^+ \bar{p} \pi^0)$	BABAR [711]: $1.94 \pm 0.17 \pm 0.52$	1.94 ± 0.55
$\mathcal{B}(\bar{B}^0 \rightarrow \Lambda_c^+ \bar{p} \pi^+ \pi^-)$	Belle [712]: $11.0^{+1.2}_{-1.2} \pm 3.5$ BABAR [713]: $12.3 \pm 0.5 \pm 3.3$	11.9 ± 3.2
$\mathcal{B}(\bar{B}^0 \rightarrow \Sigma_c^{++} \bar{p} \pi^-)$	Belle [714]: $2.1 \pm 0.2 \pm 0.6$ BABAR [713]: $2.13 \pm 0.10 \pm 0.56$	2.13 ± 0.55
$\mathcal{B}(\bar{B}^0 \rightarrow \Sigma_c^{*++} \bar{p} \pi^-)$	Belle [714]: $1.2 \pm 0.1 \pm 0.4$ BABAR [713]: $1.15 \pm 0.10 \pm 0.30$	1.16 ± 0.32
$\mathcal{B}(\bar{B}^0 \rightarrow \Sigma_c^0 \bar{p} \pi^+)$	Belle [714]: $1.4 \pm 0.2 \pm 0.4$ BABAR [713]: $0.91 \pm 0.07 \pm 0.24$	0.77 ± 0.23
$\mathcal{B}(\bar{B}^0 \rightarrow \Lambda_c^+ \Lambda_c^- \bar{K}^0)$	Belle [715]: $7.9^{+2.9}_{-2.3} \pm 4.3$ BABAR [716]: $3.8 \pm 3.1 \pm 2.1$	4.9 ± 3.5
$\mathcal{B}(\bar{B}^0 \rightarrow \Lambda_c^+ \bar{p} \pi^+ \pi_{\text{non-}\Sigma_c}^-)$	BABAR [713]: $7.9 \pm 0.4 \pm 2.0$	7.9 ± 2.1

Table 129: Branching fractions, II.

Parameter	Measurements	Average [10 ⁻⁵]
$\mathcal{B}(\bar{B}^0 \rightarrow \Lambda_c^+ \bar{p} K^+ K^-)$	BABAR [717]: $2.5 \pm 0.4 \pm 0.6$	2.5 ± 0.7
$\mathcal{B}(\bar{B}^0 \rightarrow \Lambda_c^+ \bar{p} \phi(1020))$	BABAR [717]: < 1.2	< 1.2
$\mathcal{B}(\bar{B}^0 \rightarrow \Sigma_c^{*0} \bar{p} \pi^+)$	Belle [714]: < 3.3 BABAR [713]: $2.2 \pm 0.7 \pm 0.6$	2.2 ± 0.9
$\mathcal{B}(\bar{B}^0 \rightarrow \Lambda_c^+ \bar{p})$	Belle [718]: $2.19_{-0.49}^{+0.56} \pm 0.65$ BABAR [719]: $1.89 \pm 0.21 \pm 0.49$	1.90 ± 0.54
$\mathcal{B}(\bar{B}^0 \rightarrow \Lambda_c^+ \bar{p} \bar{K}^*(892)^0)$	BABAR [720]: $1.60 \pm 0.61 \pm 0.44$	1.60 ± 0.75
$\mathcal{B}(\bar{B}^0 \rightarrow \Sigma_c^{++} \bar{p} K^-)$	BABAR [720]: $1.11 \pm 0.30 \pm 0.30$	1.11 ± 0.43
$\mathcal{B}(\bar{B}^0 \rightarrow \Xi_c^+ \Lambda_c^-) \times \mathcal{B}(\Xi_c^+ \rightarrow \Xi^- \pi^+ \pi^+)$	Belle [721]: $9.3_{-2.8}^{+3.7} \pm 3.1$ BABAR [716]: $1.5 \pm 1.1 \pm 0.4$	1.7 ± 1.2
$\mathcal{B}(\bar{B}^0 \rightarrow \Lambda_c^+ \Lambda_c^-)$	Belle [722]: < 5.7	< 5.7
$\mathcal{B}(\bar{B}^0 \rightarrow \Lambda_c^+ \bar{\Lambda} K^-)$	BABAR [723]: $3.8 \pm 0.8 \pm 1.0$	3.8 ± 1.3
$\mathcal{B}(\bar{B}^0 \rightarrow \Lambda_c^+ \bar{p} K^- \pi^+)$	BABAR [720]: $4.33 \pm 0.82 \pm 1.18$	4.33 ± 1.43

Table 130: Branching fractions, III.

Parameter	Measurements	Average [10 ⁻⁶]
$\mathcal{B}(\bar{B}^0 \rightarrow \Sigma_c^+ \bar{p}) \times \mathcal{B}(\Lambda_c^+ \rightarrow p K^- \pi^+)$	BABAR [711]: < 1.5	< 1.5
$\mathcal{B}(\bar{B}^0 \rightarrow \Lambda_c^+ \bar{p} p \bar{p}) \times \mathcal{B}(\Lambda_c^+ \rightarrow p K^- \pi^+)$	BABAR [724]: < 0.14	< 0.14

Table 131: Branching fraction ratios.

Parameter	Measurements	Average [10 ⁻³]
$\frac{\mathcal{B}(\bar{B}^0 \rightarrow \Lambda_c^- \Lambda_c^+)}{\mathcal{B}(\bar{B}^0 \rightarrow D^+ D_s^-)}$	LHCb [725]: < 2	< 2

7.1.5 Decays to XYZ states

New charmonium-like states that are not clearly identified as charmonium with specific quantum numbers are often labeled by X , Y , or Z . Averages of \bar{B}^0 decays to such states are shown in Tables 132–137.

Table 132: Branching fractions to $X(3872)$.

Parameter	Measurements	Average $[10^{-5}]$
$\mathcal{B}(\bar{B}^0 \rightarrow X(3872)\bar{K}^0) \times \mathcal{B}(X(3872) \rightarrow J/\psi\pi^+\pi^-)$		
$BABAR$ [726]: $0.35 \pm 0.19 \pm 0.04$	0.35 ± 0.19	
$\mathcal{B}(\bar{B}^0 \rightarrow X(3872)\bar{K}^0) \times \mathcal{B}(X(3872) \rightarrow J/\psi\omega(782))$		
$BABAR$ [672]: $0.6 \pm 0.3 \pm 0.1$	0.6 ± 0.3	
$\mathcal{B}(\bar{B}^0 \rightarrow X(3872)\bar{K}^0) \times \mathcal{B}(X(3872) \rightarrow J/\psi\gamma)$		
Belle [681]: $0.24^{+0.13}_{-0.14} \pm 0.07$		0.25 ± 0.12
$BABAR$ [682]: $0.26 \pm 0.18 \pm 0.02$		
$\mathcal{B}(\bar{B}^0 \rightarrow X(3872)\bar{K}^*(892)^0) \times \mathcal{B}(X(3872) \rightarrow J/\psi\gamma)$		
$BABAR$ [682]: $0.07 \pm 0.14 \pm 0.01$	0.07 ± 0.14	
$\mathcal{B}(\bar{B}^0 \rightarrow X(3872)\bar{K}^0) \times \mathcal{B}(X(3872) \rightarrow \psi(2S)\gamma)$		
Belle [681]: $0.662^{+0.130}_{-0.140} \pm 0.070$		0.694 ± 0.145
$BABAR$ [682]: $1.14 \pm 0.55 \pm 0.10$		
$\mathcal{B}(\bar{B}^0 \rightarrow X(3872)\bar{K}^*(892)^0) \times \mathcal{B}(X(3872) \rightarrow \psi(2S)\gamma)$		
$BABAR$ [682]: $-0.13 \pm 0.31 \pm 0.03$	-0.13 ± 0.31	
$\mathcal{B}(\bar{B}^0 \rightarrow X(3872)K^0) \times \mathcal{B}(X(3872) \rightarrow \chi_{c1}\gamma)$		
Belle [678]: < 0.96		< 0.96
$\mathcal{B}(\bar{B}^0 \rightarrow X(3872)K^0) \times \mathcal{B}(X(3872) \rightarrow \chi_{c2}\gamma)$		
Belle [678]: < 1.22		< 1.22

 Table 133: Branching fractions to $X(3872)$ with $X(3872) \rightarrow D\bar{D}$.

Parameter	Measurements	Average $[10^{-4}]$
$\mathcal{B}(\bar{B}^0 \rightarrow X(3872)\bar{K}^0) \times \mathcal{B}(X(3872) \rightarrow \bar{D}^*(2007)^0 D^0)$		
$BABAR$ [664]: < 4.37	< 4.37	

Table 134: Branching fractions to neutral states other than $X(3872)$.

Parameter	Measurements	Average $[10^{-4}]$
$\mathcal{B}(\bar{B}^0 \rightarrow X(3823)K^0) \times \mathcal{B}(X(3823) \rightarrow \chi_{c1}\gamma)$	Belle [678]: < 0.099	< 0.099
$\mathcal{B}(\bar{B}^0 \rightarrow X(3823)K^0) \times \mathcal{B}(X(3823) \rightarrow \chi_{c2}\gamma)$	Belle [678]: < 0.228	< 0.228
$\mathcal{B}(\bar{B}^0 \rightarrow Y(3940)\bar{K}^0) \times \mathcal{B}(Y(3940) \rightarrow J/\psi\omega(782))$	BABAR [672]: $0.21 \pm 0.09 \pm 0.03$	0.21 ± 0.09
$\mathcal{B}(\bar{B}^0 \rightarrow Z_1(4050)K^-) \times \mathcal{B}(Z_1(4050) \rightarrow \chi_{c1}\pi^+)$	Belle [727]: $0.30^{+0.15}_{-0.08}{}^{+0.37}_{-0.16}$ BABAR [684]: < 0.18	$0.30^{+0.40}_{-0.18}$
$\mathcal{B}(\bar{B}^0 \rightarrow Z_2(4250)K^-) \times \mathcal{B}(Z_2(4250) \rightarrow \chi_{c1}\pi^+)$	Belle [727]: $0.40^{+0.23}_{-0.09}{}^{+1.97}_{-0.05}$ BABAR [684]: < 0.47	$0.40^{+1.98}_{-0.10}$

Table 135: Branching fractions to charged states, I.

Parameter	Measurements	Average $[10^{-4}]$
$\mathcal{B}(\bar{B}^0 \rightarrow X(3872)^+K^-)$	BABAR [728]: < 5.0	< 5.0

Table 136: Branching fractions to charged states, II.

Parameter	Measurements	Average $[10^{-5}]$
$\mathcal{B}(\bar{B}^0 \rightarrow X(3872)^+K^-) \times \mathcal{B}(X(3872)^+ \rightarrow J/\psi\pi^+\pi^0)$	BABAR [729]: < 0.54	< 0.54
$\mathcal{B}(\bar{B}^0 \rightarrow Z(4430)^+K^-) \times \mathcal{B}(Z(4430)^+ \rightarrow J/\psi\pi^+)$	Belle [668]: $0.54^{+0.40}_{-0.10}{}^{+0.11}_{-0.09}$ BABAR [730]: $-1.2 \pm 0.4 \pm 0.0$	0.38 ± 0.12 <small>CL=0.0%</small>
$\mathcal{B}(\bar{B}^0 \rightarrow Z(4430)^+K^-) \times \mathcal{B}(Z(4430)^+ \rightarrow \psi(2S)\pi^+)$	Belle [677]: $3.2^{+1.8}_{-0.9}{}^{+5.3}_{-1.6}$ BABAR [730]: $1.9 \pm 0.8 \pm 0.0$	2.0 ± 0.7
$\mathcal{B}(\bar{B}^0 \rightarrow Z_c(3900)^+K^-) \times \mathcal{B}(Z_c(3900)^+ \rightarrow J/\psi\pi^+)$	Belle [668]: < 0.09	< 0.09
$\mathcal{B}(\bar{B}^0 \rightarrow Z_c(4200)^+K^-) \times \mathcal{B}(Z_c(4200)^+ \rightarrow J/\psi\pi^+)$	Belle [668]: $2.2^{+0.7}_{-0.5}{}^{+1.1}_{-0.6}$	$2.2^{+1.3}_{-0.8}$

Table 137: Branching fraction ratios.

Parameter	Measurements	Average
$\frac{\mathcal{B}(\bar{B}^0 \rightarrow X(3872)\bar{K}^0)}{\mathcal{B}(B^- \rightarrow X(3872)K^-)}$	$BABAR$ [672]: $1.0^{+0.8}_{-0.6}{}^{+0.1}_{-0.2}$ $BABAR$ [726]: $0.41 \pm 0.24 \pm 0.05$	0.49 ± 0.23
$\frac{\mathcal{B}(\bar{B}^0 \rightarrow Y(3940)\bar{K}^0)}{\mathcal{B}(B^- \rightarrow Y(3940)K^-)}$	$BABAR$ [672]: $0.7^{+0.4}_{-0.3} \pm 0.1$	$0.7^{+0.4}_{-0.3}$

7.2 Decays of B^- mesons

Measurements of B^- decays to charmed hadrons are summarized in Sections 7.2.1 to 7.2.5.

7.2.1 Decays to a single open charm meson

Averages of B^- decays to a single open charm meson are shown in Tables 138–154. In this section D^{**} refers to the sum of all the non-strange charm meson states with masses in the range $2.2 - 2.8$ GeV/ c^2 .

 Table 138: Branching fractions to a $D^{(*)}$ meson and one or more pions.

Parameter	Measurements	Average $[10^{-2}]$
$\mathcal{B}(B^- \rightarrow D^*(2010)^-\pi^0)$	Belle [731]: < 0.00036	< 0.00036
	Belle [732]: $0.434 \pm 0.010 \pm 0.025$	
$\mathcal{B}(B^- \rightarrow D^0\pi^-)$	$BABAR$ [612]: $0.490 \pm 0.007 \pm 0.022$ $BABAR$ [613]: $0.449 \pm 0.021 \pm 0.023$	0.462 ± 0.015
$\mathcal{B}(B^- \rightarrow D^*(2007)^0\pi^-)$	Belle [732]: $0.482 \pm 0.012 \pm 0.035$ $BABAR$ [612]: $0.552 \pm 0.017 \pm 0.042$ $BABAR$ [613]: $0.513 \pm 0.022 \pm 0.028$	0.511 ± 0.022
$\mathcal{B}(B^- \rightarrow D^+\pi^-\pi^-)$	Belle [733]: $0.102 \pm 0.004 \pm 0.015$ $BABAR$ [734]: $0.108 \pm 0.003 \pm 0.005$	0.107 ± 0.005
$\mathcal{B}(B^- \rightarrow D^*(2010)^+\pi^-\pi^-)$	Belle [733]: $0.125 \pm 0.008 \pm 0.022$ $BABAR$ [735]: $0.122 \pm 0.005 \pm 0.018$	0.123 ± 0.015
$\mathcal{B}(B^- \rightarrow D^*(2007)^0\pi^-\pi^+\pi^-)$	Belle [615]: $1.055 \pm 0.047 \pm 0.129$	1.055 ± 0.137
$\mathcal{B}(B^- \rightarrow D^*(2010)^+\pi^-\pi^+\pi^-\pi^-)$	Belle [615]: $0.256 \pm 0.026 \pm 0.033$	0.256 ± 0.042
$\mathcal{B}(B^- \rightarrow D^*(2007)^0\pi^-\pi^+\pi^-\pi^+\pi^-)$	Belle [615]: $0.567 \pm 0.091 \pm 0.085$	0.567 ± 0.125

Table 139: Branching fractions to a $D^{(*)0}$ meson and one or more kaons.

Parameter	Measurements	Average [10 ⁻³]
$\mathcal{B}(B^- \rightarrow D^0 K^-)$	Belle [736]: $0.383 \pm 0.025 \pm 0.037$	0.383 ± 0.045
$\mathcal{B}(B^- \rightarrow D^*(2007)^0 K^-)$	Belle [624]: $0.359 \pm 0.087 \pm 0.051$	0.359 ± 0.101
$\mathcal{B}(B^- \rightarrow D^0 K^- K^0)$	Belle [626]: $0.55 \pm 0.14 \pm 0.08$	0.55 ± 0.16
$\mathcal{B}(B^- \rightarrow D^*(2007)^0 K^- K^0)$	Belle [626]: < 1.06	< 1.06
$\mathcal{B}(B^- \rightarrow D^0 K^- K^*(892)^0)$	Belle [626]: $0.75 \pm 0.13 \pm 0.11$	0.75 ± 0.17
$\mathcal{B}(B^- \rightarrow D^*(2007)^0 K^- K^*(892)^0)$	Belle [626]: $1.53 \pm 0.31 \pm 0.29$	1.53 ± 0.42
$\mathcal{B}(B^- \rightarrow D^0 K^*(892)^-)$	BABAR [737]: $0.529 \pm 0.030 \pm 0.034$	0.529 ± 0.045
$\mathcal{B}(B^- \rightarrow D^*(2007)^0 K^*(892)^-)$	BABAR [738]: $0.83 \pm 0.11 \pm 0.10$	0.83 ± 0.15
$\mathcal{B}(B^- \rightarrow D^+ K^- \pi^-)$	LHCb [739]: $0.0731 \pm 0.0019 \pm 0.0045$	0.0731 ± 0.0049

 Table 140: Branching fractions to a $D^{(*)-}$ meson and a neutral kaon or a kaon and a pion.

Parameter	Measurements	Average [10 ⁻⁶]
$\mathcal{B}(B^- \rightarrow D^- \bar{K}^0)$	BABAR [740]: $-3.8^{+2.2}_{-1.8} {}^{+1.2}_{-1.6}$	$-3.8^{+2.5}_{-2.4}$
$\mathcal{B}(B^- \rightarrow D^- \bar{K}^*(892)^0)$	BABAR [740]: $-5.3^{+2.3}_{-2.0} {}^{+1.4}_{-1.8}$	$-5.3^{+2.7}_{-2.7}$
$\mathcal{B}(B^- \rightarrow D^- K^- \pi^+)$	LHCb [741]: $5.31 \pm 0.90 \pm 0.59$	5.31 ± 1.08
$\mathcal{B}(B^- \rightarrow D^*(2010)^- \bar{K}^0)$	BABAR [742]: < 9	< 9

 Table 141: Branching fraction ratios to D^0 mesons, I.

Parameter	Measurements	Average
$\frac{\mathcal{B}(B^- \rightarrow D^0 \pi^-)}{\mathcal{B}(\bar{B}^0 \rightarrow D^+ \pi^-)}$	CDF [743]: $1.97 \pm 0.10 \pm 0.21$	1.97 ± 0.23
$\frac{\mathcal{B}(B^- \rightarrow D^0 \pi^+ \pi^- \pi^-)}{\mathcal{B}(B^- \rightarrow D^0 \pi^-)}$	LHCb [637]: $1.27 \pm 0.06 \pm 0.11$	1.27 ± 0.13

Table 142: Branching fraction ratios to D^0 mesons, II.

Parameter	Measurements	Average $[10^{-2}]$
$\frac{\mathcal{B}(B^- \rightarrow \bar{D}^0 K^-)}{\mathcal{B}(B^- \rightarrow D^0 K^-)}$	Belle [744]: < 19	< 19
	LHCb [450]: $7.79 \pm 0.06 \pm 0.19$	
$\frac{\mathcal{B}(B^- \rightarrow D^0 K^-)}{\mathcal{B}(B^- \rightarrow D^0 \pi^-)}$	Belle [744]: $6.77 \pm 0.23 \pm 0.30$	7.69 ± 0.16
	Belle [736]: $7.7 \pm 0.5 \pm 0.6$	<small>CL=3.5%</small>
	<i>BABAR</i> [745]: $8.31 \pm 0.35 \pm 0.20$	
$\frac{\mathcal{B}(B^- \rightarrow D^0 K^- \pi^+ \pi^-)}{\mathcal{B}(B^- \rightarrow D^0 \pi^+ \pi^- \pi^-)}$	LHCb [641]: $9.4 \pm 1.3 \pm 0.9$	9.4 ± 1.6

 Table 143: Branching fractions to excited D mesons.

Parameter	Measurements	Average $[10^{-3}]$
$\mathcal{B}(B^- \rightarrow D^{*0} \pi^-)$	<i>BABAR</i> [613]: $5.50 \pm 0.52 \pm 1.04$	5.50 ± 1.16

 Table 144: Product branching fractions to excited D mesons, I.

Parameter	Measurements	Average $[10^{-3}]$
$\mathcal{B}(B^- \rightarrow D_1^0(2420) \pi^-) \times \mathcal{B}(D_1^0(2420) \rightarrow D^*(2010)^+ \pi^-)$		
	Belle [733]: $0.68 \pm 0.07 \pm 0.13$	0.62 ± 0.09
	<i>BABAR</i> [735]: $0.59 \pm 0.03 \pm 0.11$	
$\mathcal{B}(B^- \rightarrow D_1^0(2420) \pi^-) \times \mathcal{B}(D_1^0(2420) \rightarrow D^0 \pi^- \pi^+)$		
	Belle [643]: $0.185 \pm 0.029 {}^{+0.035}_{-0.058}$	$0.185 {}^{+0.045}_{-0.065}$
$\mathcal{B}(B^- \rightarrow D_0^{*0} \pi^-) \times \mathcal{B}(D_0^{*0} \rightarrow D^+ \pi^-)$		
	Belle [733]: $0.61 \pm 0.06 \pm 0.18$	0.63 ± 0.19
	<i>BABAR</i> [734]: $0.68 \pm 0.03 \pm 0.20$	
$\mathcal{B}(B^- \rightarrow D_1^0(H) \pi^-) \times \mathcal{B}(D_1^0(H) \rightarrow D^*(2010)^+ \pi^-)$		
	Belle [733]: $0.50 \pm 0.04 \pm 0.11$	0.50 ± 0.11
$\mathcal{B}(B^- \rightarrow D_2^{*0}(2460) \pi^-) \times \mathcal{B}(D_2^{*0}(2460) \rightarrow D^*(2010)^+ \pi^-)$		
	Belle [733]: $0.18 \pm 0.03 \pm 0.04$	0.18 ± 0.04
	<i>BABAR</i> [735]: $0.18 \pm 0.03 \pm 0.05$	
$\mathcal{B}(B^- \rightarrow D_2^{*0}(2460) \pi^-) \times \mathcal{B}(D_2^{*0}(2460) \rightarrow D^+ \pi^-)$		
	Belle [733]: $0.34 \pm 0.03 \pm 0.07$	0.35 ± 0.05
	<i>BABAR</i> [734]: $0.35 \pm 0.02 \pm 0.04$	

Table 145: Product branching fractions to excited D mesons, II.

Parameter	Measurements	Average [10 ⁻⁵]
$\mathcal{B}(B^- \rightarrow D_1^0(2420)\pi^-) \times \mathcal{B}(D_1^0(2420) \rightarrow D^*(2007)^0\pi^-\pi^+)$	Belle [643]: < 0.6	< 0.6
$\mathcal{B}(B^- \rightarrow D_2^{*0}(2460)\pi^-) \times \mathcal{B}(D_2^{*0}(2460) \rightarrow D^*(2007)^0\pi^-\pi^+)$	Belle [643]: < 2.2	< 2.2

 Table 146: Branching fraction ratios to excited D mesons, I.

Parameter	Measurements	Average
$\frac{\mathcal{B}(B^- \rightarrow D^*(2007)^0\pi^-)}{\mathcal{B}(B^- \rightarrow D^0\pi^-)}$	BABAR [613]: $1.14 \pm 0.07 \pm 0.04$	1.14 ± 0.08
$\frac{\mathcal{B}(B^- \rightarrow D^{*0}\pi^-)}{\mathcal{B}(B^- \rightarrow D^0\pi^-)}$	BABAR [613]: $1.22 \pm 0.13 \pm 0.23$	1.22 ± 0.26
$\frac{\mathcal{B}(B^- \rightarrow D_2^{*0}(2460)\pi^-)}{\mathcal{B}(B^- \rightarrow D_1^0(2420)\pi^-)}$	BABAR [735]: $0.80 \pm 0.07 \pm 0.16$	0.80 ± 0.17

 Table 147: Branching fraction ratios to excited D mesons, II.

Parameter	Measurements	Average
$\frac{\mathcal{B}(B^- \rightarrow D^*(2007)^0K^-)}{\mathcal{B}(B^- \rightarrow D^*(2007)^0\pi^-)}$	Belle [624]: $0.078 \pm 0.019 \pm 0.009$ BABAR [746]: $0.0813 \pm 0.0040^{+0.0042}_{-0.0031}$	0.0811 ± 0.0052
$\mathcal{B}(B^- \rightarrow D^*(2010)^+K^-\pi^-)/\mathcal{B}(B^- \rightarrow D^*(2010)^+\pi^-\pi^-)$	LHCb [747]: $0.0639 \pm 0.0027 \pm 0.0048$	0.0639 ± 0.0055

 Table 148: Relative product branching fractions to excited D mesons.

Parameter	Measurements	Average
$[\mathcal{B}(B^- \rightarrow D_1^0\pi^-) \times \mathcal{B}(D_1^0 \rightarrow D^0\pi^+\pi^-)]/\mathcal{B}(B^- \rightarrow D^0\pi^+\pi^-\pi^-)$	LHCb [637]: $0.040 \pm 0.007 \pm 0.005$	0.040 ± 0.009
$[\mathcal{B}(B^- \rightarrow D_1^{*0}\pi^-) \times \mathcal{B}(D_1^{*0} \rightarrow D^{*+}\pi^-)]/\mathcal{B}(B^- \rightarrow D^0\pi^+\pi^-\pi^-)$	LHCb [637]: $0.093 \pm 0.016 \pm 0.009$	0.093 ± 0.018
$[\mathcal{B}(B^- \rightarrow D_1^{*0}\pi^-) \times \mathcal{B}(D_1^{*0} \rightarrow D^0\pi^+\pi^-)]/\mathcal{B}(B^- \rightarrow D^0\pi^+\pi^-\pi^-)$	LHCb [637]: $0.103 \pm 0.015 \pm 0.009$	0.103 ± 0.017
$[\mathcal{B}(B^- \rightarrow D_2^{*0}\pi^-) \times \mathcal{B}(D_2^{*0} \rightarrow D^{*+}\pi^-)]/\mathcal{B}(B^- \rightarrow D^0\pi^+\pi^-\pi^-)$	LHCb [637]: $0.039 \pm 0.012 \pm 0.004$	0.039 ± 0.013
$[\mathcal{B}(B^- \rightarrow D_2^{*0}\pi^-) \times \mathcal{B}(D_2^{*0} \rightarrow D^0\pi^+\pi^-)]/\mathcal{B}(B^- \rightarrow D^0\pi^+\pi^-\pi^-)$	LHCb [637]: $0.040 \pm 0.010 \pm 0.004$	0.040 ± 0.011
$[\mathcal{B}(B^- \rightarrow D_2^{*+}\pi^-) \times \mathcal{B}(D_2^{*+} \rightarrow D^0\pi^-\pi^+)]/\mathcal{B}(B^- \rightarrow D^0\pi^+\pi^-\pi^-)$	LHCb [637]: $0.014 \pm 0.006 \pm 0.002$	0.014 ± 0.006

Table 149: Branching fractions to $D_s^{(*)}$ mesons, I.

Parameter	Measurements	Average [10 ⁻⁴]
$\mathcal{B}(B^- \rightarrow D_s^+ K^- \pi^-)$	Belle [748]: $1.94^{+0.09}_{-0.08} {}^{+0.26}_{-0.26}$ BABAR [636]: $2.02 \pm 0.13 \pm 0.38$	1.97 ± 0.23
$\mathcal{B}(B^- \rightarrow D_s^{*+} K^- \pi^-)$	Belle [748]: $1.47^{+0.15}_{-0.14} {}^{+0.23}_{-0.23}$ BABAR [636]: $1.67 \pm 0.16 \pm 0.35$	1.54 ± 0.22

Table 150: Branching fractions to $D_s^{(*)}$ mesons, I.

Parameter	Measurements	Average [10 ⁻⁵]
$\mathcal{B}(B^- \rightarrow D_s^+ K^- K^-)$	BABAR [636]: $1.1 \pm 0.4 \pm 0.2$	1.1 ± 0.4
$\mathcal{B}(B^- \rightarrow D_s^{*+} K^- K^-)$	BABAR [636]: < 1.5	< 1.5
$\mathcal{B}(B^- \rightarrow D_s^- \pi^0)$	BABAR [749]: $1.5^{+0.5}_{-0.4} \pm 0.2$	$1.5^{+0.5}_{-0.5}$
$\mathcal{B}(B^- \rightarrow D_s^- \phi)$	LHCb [750]: $0.012^{+0.016}_{-0.014} \pm 0.008$ BABAR [751]: < 0.19	$0.012^{+0.018}_{-0.016}$
$\mathcal{B}(B^- \rightarrow D_s^{*-} \phi(1020))$	BABAR [751]: < 1.2	< 1.2

Table 151: Branching fraction ratios to $D_s^{(*)}$ mesons.

Parameter	Measurements	Average
$\mathcal{B}(B^- \rightarrow D_s^- K^+ K^-)/[\mathcal{B}(B^- \rightarrow D_s^- \bar{D}^0) \times \mathcal{B}(\bar{D}^0 \rightarrow K^+ K^-)]$	LHCb [750]: $0.197 \pm 0.015 \pm 0.017$	0.197 ± 0.023

Table 152: Branching fractions to baryonic decays, I.

Parameter	Measurements	Average [10 ⁻⁴]
$\mathcal{B}(B^- \rightarrow D^0 p\bar{p}\pi^-)$	BABAR [645]: $3.72 \pm 0.11 \pm 0.25$	3.72 ± 0.27
$\mathcal{B}(B^- \rightarrow D^*(2007)^0 p\bar{p}\pi^-)$	BABAR [645]: $3.73 \pm 0.17 \pm 0.27$	3.73 ± 0.32
$\mathcal{B}(B^- \rightarrow D^+ p\bar{p}\pi^-\pi^-)$	BABAR [645]: $1.66 \pm 0.13 \pm 0.27$	1.66 ± 0.30
$\mathcal{B}(B^- \rightarrow D^*(2010)^+ p\bar{p}\pi^-\pi^-)$	BABAR [645]: $1.86 \pm 0.16 \pm 0.19$	1.86 ± 0.25

Table 153: Branching fractions to baryonic decays, II.

Parameter	Measurements	Average [10 ⁻⁵]
$\mathcal{B}(B^- \rightarrow D^0 \Lambda \bar{p})$	Belle [752]: $1.43^{+0.28}_{-0.25} \pm 0.18$	$1.43^{+0.33}_{-0.31}$
$\mathcal{B}(B^- \rightarrow D^*(2007)^0 \Lambda \bar{p})$	Belle [752]: < 4.8	< 4.8
$\mathcal{B}(B^- \rightarrow D^- p \bar{p})$	Belle [646]: < 1.5	< 1.5
$\mathcal{B}(B^- \rightarrow D^*(2010)^- p \bar{p})$	Belle [646]: < 1.5	< 1.5

Table 154: Branching fractions to lepton number violating decays.

Parameter	Measurements	Average [10 ⁻⁶]
$\mathcal{B}(B^- \rightarrow D^- e^+ e^+)$	Belle [753]: < 2.6	< 2.6
$\mathcal{B}(B^- \rightarrow D^- e^+ \mu^+)$	Belle [753]: < 1.8	< 1.8
$\mathcal{B}(B^- \rightarrow D^- \mu^+ \mu^+)$	Belle [753]: < 1.0	< 1.0

7.2.2 Decays to two open charm mesons

Averages of B^- decays to two open charm mesons are shown in Tables 155–163.

Table 155: Branching fractions to $D^{(*)-} D^{(*)0}$.

Parameter	Measurements	Average [10 ⁻³]
$\mathcal{B}(B^- \rightarrow D^- D^0)$	Belle [652]: $0.385 \pm 0.031 \pm 0.038$ BABAR [651]: $0.38 \pm 0.06 \pm 0.05$	0.384 ± 0.042
$\mathcal{B}(B^- \rightarrow D^{*0} D^-)$	BABAR [651]: $0.63 \pm 0.14 \pm 0.10$	0.63 ± 0.17
$\mathcal{B}(B^- \rightarrow D^{*-}(2010)D^0)$	Belle [754]: $0.459 \pm 0.072 \pm 0.056$ BABAR [651]: $0.36 \pm 0.05 \pm 0.04$	0.393 ± 0.052
$\mathcal{B}(B^- \rightarrow D^*(2007)^0 D^*(2010)^-)$	BABAR [651]: $0.81 \pm 0.12 \pm 0.12$	0.81 ± 0.17

Table 156: Branching fractions to two D mesons and a kaon, I.

Parameter	Measurements	Average [10 ⁻²]
$\mathcal{B}(B^- \rightarrow D^*(2007)^0 \bar{D}^0 K^-)$	BABAR [653]: $0.226 \pm 0.016 \pm 0.017$	0.226 ± 0.023
$\mathcal{B}(B^- \rightarrow D^0 \bar{D}^*(2007)^0 K^-)$	BABAR [653]: $0.632 \pm 0.019 \pm 0.045$	0.632 ± 0.049
$\mathcal{B}(B^- \rightarrow \bar{D}^*(2007)^0 D^*(2007)^0 K^-)$	BABAR [653]: $1.123 \pm 0.036 \pm 0.126$	1.123 ± 0.131
$\mathcal{B}(B^- \rightarrow D^*(2007)^0 D^- \bar{K}^0)$	BABAR [653]: $0.206 \pm 0.038 \pm 0.030$	0.206 ± 0.048
$\mathcal{B}(B^- \rightarrow D^0 D^*(2010)^- \bar{K}^0)$	BABAR [653]: $0.381 \pm 0.031 \pm 0.023$	0.381 ± 0.039
$\mathcal{B}(B^- \rightarrow D^*(2007)^0 D^*(2010)^- \bar{K}^0)$	BABAR [653]: $0.917 \pm 0.083 \pm 0.090$	0.917 ± 0.122

 Table 157: Branching fractions to two D mesons and a kaon, II.

Parameter	Measurements	Average [10 ⁻³]
$\mathcal{B}(B^- \rightarrow D^0 \bar{D}^0 K^-)$	Belle [755]: $2.22 \pm 0.22^{+0.26}_{-0.24}$ BABAR [653]: $1.31 \pm 0.07 \pm 0.12$	1.45 ± 0.13
$\mathcal{B}(B^- \rightarrow D^0 \bar{D}^0 \pi^0 K^-)$	Belle [654]: $0.107 \pm 0.031^{+0.019}_{-0.033}$	$0.107^{+0.036}_{-0.045}$
$\mathcal{B}(B^- \rightarrow D^+ D^- K^-)$	Belle [756]: < 0.90 BABAR [653]: $0.22 \pm 0.05 \pm 0.05$	0.22 ± 0.07
$\mathcal{B}(B^- \rightarrow D^*(2010)^+ D^- K^-)$	BABAR [653]: $0.60 \pm 0.10 \pm 0.08$	0.60 ± 0.13
$\mathcal{B}(B^- \rightarrow D^+ D^*(2010)^- K^-)$	BABAR [653]: $0.63 \pm 0.09 \pm 0.06$	0.63 ± 0.11
$\mathcal{B}(B^- \rightarrow D^*(2010)^- D^*(2010)^+ K^-)$	BABAR [653]: $1.32 \pm 0.13 \pm 0.12$	1.32 ± 0.18
$\mathcal{B}(B^- \rightarrow D^0 D^- \bar{K}^0)$	BABAR [653]: $1.55 \pm 0.17 \pm 0.13$	1.55 ± 0.21

 Table 158: Branching fractions to $D_s^{(*)-} D^{(*)+}$.

Parameter	Measurements	Average [10 ⁻²]
$\mathcal{B}(B^- \rightarrow D_s^- D^0)$	BABAR [656]: $1.33 \pm 0.18 \pm 0.32$	1.33 ± 0.37
$\mathcal{B}(B^- \rightarrow D_s^- D^*(2007)^0)$	BABAR [656]: $1.21 \pm 0.23 \pm 0.20$	1.21 ± 0.30
$\mathcal{B}(B^- \rightarrow D_s^{*-} D^0)$	BABAR [656]: $0.93 \pm 0.18 \pm 0.19$	0.93 ± 0.26
$\mathcal{B}(B^- \rightarrow D_s^{*-} D^*(2007)^0)$	BABAR [656]: $1.70 \pm 0.26 \pm 0.24$	1.70 ± 0.35

Table 159: Product branching fractions to $D_s^{(*)-} D^{(*)+}$.

Parameter	Measurements	Average [10 ⁻⁴]
$\mathcal{B}(B^- \rightarrow D_s^- D^0) \times \mathcal{B}(D_s^- \rightarrow \phi(1020)\pi^-)$		
	BABAR [656]: $4.00 \pm 0.61 \pm 0.61$	4.00 ± 0.86
$\mathcal{B}(B^- \rightarrow D_s^- D^*(2007)^0) \times \mathcal{B}(D_s^- \rightarrow \phi(1020)\pi^-)$		
	BABAR [656]: $2.95 \pm 0.65 \pm 0.36$	2.95 ± 0.74
$\mathcal{B}(B^- \rightarrow D_s^{*-} D^0) \times \mathcal{B}(D_s^- \rightarrow \phi(1020)\pi^-)$		
	BABAR [656]: $3.13 \pm 1.19 \pm 0.58$	3.13 ± 1.32
$\mathcal{B}(B^- \rightarrow D_s^{*-} D^*(2007)^0) \times \mathcal{B}(D_s^- \rightarrow \phi(1020)\pi^-)$		
	BABAR [656]: $8.57 \pm 1.48 \pm 1.12$	8.57 ± 1.86

Table 160: Branching fraction ratios.

Parameter	Measurements	Average
$\mathcal{B}(B^- \rightarrow D_s^- D^0)/\mathcal{B}(\bar{B}^0 \rightarrow D_s^+ D^-)$		
	LHCb [660]: $1.22 \pm 0.02 \pm 0.07$	1.22 ± 0.07

Table 161: Branching fractions to excited D_s mesons.

Parameter	Measurements	Average [10 ⁻³]
$\mathcal{B}(B^- \rightarrow D_{sJ}(2460)^- D^0)$	BABAR [656]: $4.3 \pm 1.6 \pm 1.3$	4.3 ± 2.1
$\mathcal{B}(B^- \rightarrow D_{sJ}(2460)^- D^*(2007)^0)$	BABAR [656]: $11.2 \pm 2.6 \pm 2.0$	11.2 ± 3.3

Table 162: Product branching fractions to excited D_s mesons, I.

Parameter	Measurements	Average [10 ⁻³]
$\mathcal{B}(B^- \rightarrow D^0 D_{sJ}(2460)^-) \times \mathcal{B}(D_{sJ}(2460)^- \rightarrow D_s^{*-} \pi^0)$		
	Belle [661]: $1.19^{+0.61}_{-0.49} \pm 0.36$	1.65 ± 0.59
	BABAR [662]: $2.7 \pm 0.7^{+1.0}_{-0.8}$	
$\mathcal{B}(B^- \rightarrow D_{sJ}(2460)^- D^*(2007)^0) \times \mathcal{B}(D_{sJ}(2460)^- \rightarrow D_s^- \gamma)$		
	BABAR [662]: $1.4 \pm 0.4^{+0.6}_{-0.4}$	$1.4^{+0.7}_{-0.6}$
$\mathcal{B}(B^- \rightarrow D_{sJ}(2460)^- D^*(2007)^0) \times \mathcal{B}(D_{sJ}(2460)^- \rightarrow D_s^{*-} \pi^0)$		
	BABAR [662]: $7.6 \pm 1.7^{+3.2}_{-2.4}$	$7.6^{+3.6}_{-2.9}$

Table 163: Product branching fractions to excited D_s mesons, II.

Parameter	Measurements	Average [10 ⁻³]
$\mathcal{B}(B^- \rightarrow D^0 D_{sJ}^*(2317)^-) \times \mathcal{B}(D_{sJ}^*(2317)^- \rightarrow D_s^- \pi^0)$		
Belle [663]: $0.80^{+0.13}_{-0.12} \pm 0.12$		0.82 ± 0.16
BABAR [662]: $1.0 \pm 0.3^{+0.4}_{-0.2}$		
$\mathcal{B}(B^- \rightarrow D^0 D_{sJ}^*(2317)^-) \times \mathcal{B}(D_{sJ}^*(2317)^- \rightarrow D_s^{*-} \gamma)$		
Belle [661]: < 0.76		< 0.76
$\mathcal{B}(B^- \rightarrow D_{sJ}^*(2317)^- D^*(2007)^0) \times \mathcal{B}(D_{sJ}^*(2317)^- \rightarrow D_s^- \pi^0)$		
BABAR [662]: $0.9 \pm 0.6^{+0.4}_{-0.3}$		$0.9^{+0.7}_{-0.7}$
$\mathcal{B}(B^- \rightarrow D^0 D_{sJ}(2460)^-) \times \mathcal{B}(D_{sJ}(2460)^- \rightarrow D_s^- \gamma)$		
Belle [661]: $0.56^{+0.16}_{-0.15} \pm 0.17$		0.58 ± 0.17
BABAR [662]: $0.6 \pm 0.2^{+0.2}_{-0.1}$		
$\mathcal{B}(B^- \rightarrow D^0 D_{sJ}(2460)^-) \times \mathcal{B}(D_{sJ}(2460)^- \rightarrow D_s^{*-} \gamma)$		
Belle [661]: < 0.98		< 0.98
$\mathcal{B}(B^- \rightarrow D^0 D_{sJ}(2460)^-) \times \mathcal{B}(D_{sJ}(2460)^- \rightarrow D_s^- \pi^0)$		
Belle [661]: < 0.27		< 0.27
$\mathcal{B}(B^- \rightarrow D^0 D_{sJ}(2460)^-) \times \mathcal{B}(D_{sJ}(2460)^- \rightarrow D_s^- \pi^+ \pi^-)$		
Belle [661]: < 0.22		< 0.22
$\mathcal{B}(B^+ \rightarrow D_{s1}(2536)^+ \bar{D}^0) \times \mathcal{B}(D_{s1}(2536)^+ \rightarrow D^*(2007)^0 K^+ + D^*(2010)^+ K^0)$		
Belle [665]: $0.397 \pm 0.085 \pm 0.056$		0.397 ± 0.102
$\mathcal{B}(B^- \rightarrow D_{s1}(2536)^- D^0) \times \mathcal{B}(D_{s1}(2536)^- \rightarrow \bar{D}^*(2007)^0 K^-)$		
BABAR [664]: $0.216 \pm 0.052 \pm 0.045$		0.216 ± 0.069
$\mathcal{B}(B^- \rightarrow D_{s1}(2536)^- D^0) \times \mathcal{B}(D_{s1}(2536)^- \rightarrow D^*(2010)^- \bar{K}^0)$		
BABAR [664]: $0.230 \pm 0.098 \pm 0.043$		0.230 ± 0.107
$\mathcal{B}(B^- \rightarrow D_{s1}(2536)^- \bar{D}^*(2007)^0) \times \mathcal{B}(D_{s1}(2536)^- \rightarrow \bar{D}^*(2007)^0 K^-)$		
BABAR [664]: $0.546 \pm 0.117 \pm 0.104$		0.546 ± 0.157
$\mathcal{B}(B^- \rightarrow D_{s1}(2536)^- D^*(2007)^0) \times \mathcal{B}(D_{s1}(2536)^- \rightarrow D^*(2010)^- \bar{K}^0)$		
BABAR [664]: < 1.069		< 1.069

7.2.3 Decays to charmonium states

Averages of B^- decays to charmonium states are shown in Tables 164–175.

Table 164: Branching fractions to J/ψ and one kaon, I.

Parameter	Measurements	Average $[10^{-3}]$
$\mathcal{B}(B^- \rightarrow J/\psi K^-)$	Belle [732]: $0.89 \pm 0.06 \pm 0.05$ Belle [667]: $1.01 \pm 0.02 \pm 0.07$ <i>BABAR</i> [728]: $0.81 \pm 0.13 \pm 0.07$ <i>BABAR</i> [9]: $1.061 \pm 0.015 \pm 0.048$	0.999 ± 0.036
$\mathcal{B}(B^- \rightarrow J/\psi K^*(892)^-)$	CDF [666]: $1.58 \pm 0.47 \pm 0.27$ Belle [757]: $1.28 \pm 0.07 \pm 0.14$ <i>BABAR</i> [9]: $1.454 \pm 0.047 \pm 0.097$	1.404 ± 0.089
$\mathcal{B}(B^- \rightarrow J/\psi K_1(1270)^-)$	Belle [674]: $1.80 \pm 0.34 \pm 0.39$	1.80 ± 0.52
$\mathcal{B}(B^- \rightarrow J/\psi K^- \pi^+ \pi^-)$	CDF [758]: $0.69 \pm 0.18 \pm 0.12$ Belle [759]: $0.716 \pm 0.010 \pm 0.060$ <i>BABAR</i> [760]: $1.16 \pm 0.07 \pm 0.09$	0.807 ± 0.052 <small>CL=0.5%</small>

 Table 165: Branching fractions to J/ψ and one kaon, II.

Parameter	Measurements	Average $[10^{-4}]$
$\mathcal{B}(B^- \rightarrow J/\psi \eta K^-)$	Belle [675]: $1.27 \pm 0.11 \pm 0.11$ <i>BABAR</i> [676]: $1.08 \pm 0.23 \pm 0.24$	1.24 ± 0.14
$\mathcal{B}(B^- \rightarrow J/\psi \omega(782) K^-)$	<i>BABAR</i> [672]: $3.2 \pm 0.1^{+0.6}_{-0.3}$	$3.2^{+0.6}_{-0.3}$
$\mathcal{B}(B^- \rightarrow J/\psi \phi(1020) K^-)$	<i>BABAR</i> [673]: $0.44 \pm 0.14 \pm 0.05$	0.44 ± 0.15

Table 166: Branching fractions to charmonium other than J/ψ and one kaon, I.

Parameter	Measurements	Average $[10^{-3}]$
$\mathcal{B}(B^- \rightarrow \psi(2S)K^-)$	CDF [669]: $0.55 \pm 0.10 \pm 0.06$ Belle [732]: $0.64 \pm 0.10 \pm 0.04$ Belle [667]: 0.69 ± 0.06 <i>BABAR</i> [728]: $0.49 \pm 0.16 \pm 0.04$ <i>BABAR</i> [9]: $0.617 \pm 0.032 \pm 0.044$	0.633 ± 0.035
$\mathcal{B}(B^- \rightarrow \psi(2S)K^-) \times \mathcal{B}(\psi(2S) \rightarrow \chi_{c1}\gamma)$	Belle [678]: $0.77 \pm 0.08 \pm 0.09$	0.77 ± 0.12
$\mathcal{B}(B^- \rightarrow \psi(2S)K^-) \times \mathcal{B}(\psi(2S) \rightarrow \chi_{c2}\gamma)$	Belle [678]: $0.63 \pm 0.09 \pm 0.06$	0.63 ± 0.11
$\mathcal{B}(B^- \rightarrow \psi(2S)K^*(892)^-)$	<i>BABAR</i> [9]: $0.592 \pm 0.085 \pm 0.089$	0.592 ± 0.123
$\mathcal{B}(B^- \rightarrow \psi(2S)K^-\pi^+\pi^-)$	Belle [759]: $0.431 \pm 0.020 \pm 0.050$	0.431 ± 0.054
$\mathcal{B}(B^- \rightarrow \psi(3770)K^-)$	Belle [756]: $0.48 \pm 0.11 \pm 0.07$ Belle [732]: $-0.02 \pm 0.14 \pm 0.00$ <i>BABAR</i> [728]: $0.35 \pm 0.25 \pm 0.03$	0.26 ± 0.09 <small>CL=8.3%</small>
$\mathcal{B}(B^- \rightarrow \psi(3770)K^-) \times \mathcal{B}(\psi(3770) \rightarrow D^+D^-)$	<i>BABAR</i> [664]: $0.084 \pm 0.032 \pm 0.021$	0.084 ± 0.038
$\mathcal{B}(B^- \rightarrow \psi(3770)K^-) \times \mathcal{B}(\psi(3770) \rightarrow D^0\bar{D}^0)$	<i>BABAR</i> [664]: $0.141 \pm 0.030 \pm 0.022$	0.141 ± 0.037
$\mathcal{B}(B^- \rightarrow \chi_{c0}K^-)$	Belle [761]: $0.60^{+0.21}_{-0.18} \pm 0.11$ Belle [732]: $0.20 \pm 0.09 \pm 0.01$ <i>BABAR</i> [728]: < 0.18 <i>BABAR</i> [268]: $0.184 \pm 0.032 \pm 0.031$	0.201 ± 0.039
$\mathcal{B}(B^- \rightarrow \chi_{c0}K^*(892)^-)$	<i>BABAR</i> [679]: < 2.86 <i>BABAR</i> [680]: $0.14 \pm 0.05 \pm 0.02$	0.14 ± 0.05
$\mathcal{B}(B^- \rightarrow \chi_{c1}K^-)$	CDF [758]: $1.55 \pm 0.54 \pm 0.20$ Belle [681]: $0.494 \pm 0.011 \pm 0.033$ Belle [732]: $0.58 \pm 0.09 \pm 0.05$ <i>BABAR</i> [728]: $0.80 \pm 0.14 \pm 0.07$ <i>BABAR</i> [682]: $0.45 \pm 0.01 \pm 0.03$	0.484 ± 0.023 <small>CL=1.9%</small>
$\mathcal{B}(B^- \rightarrow \chi_{c1}K^*(892)^-)$	Belle [685]: $0.41 \pm 0.06 \pm 0.09$ <i>BABAR</i> [682]: $0.26 \pm 0.05 \pm 0.04$	0.30 ± 0.06
$\mathcal{B}(B^- \rightarrow \chi_{c1}K^-\pi^0)$	Belle [683]: $0.329 \pm 0.029 \pm 0.019$	0.329 ± 0.035
$\mathcal{B}(B^- \rightarrow \chi_{c1}\bar{K}^0\pi^-)$	Belle [683]: $0.575 \pm 0.026 \pm 0.032$ <i>BABAR</i> [684]: $0.552 \pm 0.026 \pm 0.061$	0.569 ± 0.035
$\mathcal{B}(B^- \rightarrow \chi_{c1}K^-\pi^+\pi^-)$	Belle [683]: $0.374 \pm 0.018 \pm 0.024$	0.374 ± 0.030
$\mathcal{B}(B^- \rightarrow \chi_{c2}\bar{K}^0\pi^-)$	Belle [683]: $0.116 \pm 0.022 \pm 0.012$	0.116 ± 0.025
$\mathcal{B}(B^- \rightarrow \chi_{c2}K^-\pi^+\pi^-)$	Belle [683]: $0.134 \pm 0.017 \pm 0.009$	0.134 ± 0.019
$\mathcal{B}(B^- \rightarrow \eta_c K^-)$	Belle [686]: $1.25 \pm 0.14^{+0.39}_{-0.40}$ Belle [732]: $1.20 \pm 0.08 \pm 0.07$ <i>BABAR</i> [728]: 0.87 ± 0.15 <i>BABAR</i> [688]: $1.29 \pm 0.09 \pm 0.38$	1.10 ± 0.08
$\mathcal{B}(B^- \rightarrow \eta_c K^*(892)^-)$	<i>BABAR</i> [687]: $1.21^{+0.43+0.64}_{-0.35-0.40}$	$1.21^{+0.77}_{-0.53}$
$\mathcal{B}(B^- \rightarrow \chi_{c0}^{\prime +} K^-)$	Belle [732]: $0.48 \pm 0.11 \pm 0.03$	0.44 ± 0.10

Table 167: Branching fractions to charmonium other than J/ψ and one kaon, II.

Parameter	Measurements	Average $[10^{-5}]$
$\mathcal{B}(B^- \rightarrow \chi_{c2} K^-)$	Belle [681]: $1.11^{+0.36}_{-0.34} \pm 0.09$ BABAR [682]: $1 \pm 1 \pm 0$	1.08 ± 0.31
$\mathcal{B}(B^- \rightarrow \chi_{c2} K^*(892)^-)$	BABAR [682]: $1.1 \pm 4.3 \pm 5.5$	1.1 ± 7.0
$\mathcal{B}(B^- \rightarrow h_c(1P) K^-) \times \mathcal{B}(h_c(1P) \rightarrow \eta_c \gamma)$	BABAR [689]: < 4.8	< 4.8

 Table 168: Branching fractions to charmonium other than J/ψ and one kaon, III.

Parameter	Measurements	Average $[10^{-6}]$
$\mathcal{B}(B^- \rightarrow \psi(2S) \phi(1020) K^-)$	CMS [762]: $4.0 \pm 0.4 \pm 0.6$	4.0 ± 0.7
$\mathcal{B}(B^- \rightarrow K^- \eta_c) \times \mathcal{B}(\eta_c \rightarrow K^0 K^+ \pi^+)$	Belle [763]: $0.267 \pm 0.014^{+0.057}_{-0.055}$	$0.267^{+0.059}_{-0.057}$
$\mathcal{B}(B^- \rightarrow \eta_c K^-) \times \mathcal{B}(\eta_c \rightarrow p\bar{p})$	Belle [764]: $1.42 \pm 0.11^{+0.16}_{-0.20}$ BABAR [765]: $1.8^{+0.3}_{-0.2} \pm 0.2$	1.54 ± 0.15
$\mathcal{B}(B^- \rightarrow \eta_c K^-) \times \mathcal{B}(\eta_c \rightarrow \Lambda\bar{\Lambda})$	Belle [764]: $0.95^{+0.25}_{-0.22}{}^{+0.08}_{-0.11}$	$0.95^{+0.26}_{-0.25}$
$\mathcal{B}(B^- \rightarrow K^- \eta_c(2S)) \times \mathcal{B}(\eta_c(2S) \rightarrow K^0 K^- \pi^+)$	Belle [763]: $0.034^{+0.022}_{-0.015}{}^{+0.005}_{-0.004}$	$0.034^{+0.023}_{-0.016}$
$\mathcal{B}(B^- \rightarrow h_c(1P) K^-)$	Belle [766]: < 3.8	< 3.8
$\mathcal{B}(B^- \rightarrow h_c(1P) K^-) \times \mathcal{B}(h_c(1P) \rightarrow J/\psi \pi^+ \pi^-)$	BABAR [760]: < 3.4	< 3.4

Table 169: Branching fractions to charmonium and light mesons.

Parameter	Measurements	Average $[10^{-5}]$
$\mathcal{B}(B^- \rightarrow J/\psi \pi^-)$	LHCb [767]: $3.88 \pm 0.11 \pm 0.15$ Belle [667]: $3.8 \pm 0.6 \pm 0.3$ BABAR [768]: $5.37 \pm 0.45 \pm 0.24$	4.04 ± 0.17 <small>CL=5.6%</small>
$\mathcal{B}(B^- \rightarrow J/\psi \pi^- \pi^0)$	BABAR [691]: < 0.73	< 0.73
$\mathcal{B}(B^- \rightarrow J/\psi \rho^-(770))$	BABAR [691]: $5 \pm 1 \pm 0$	5 ± 1
$\mathcal{B}(B^- \rightarrow \psi(2S) \pi^-)$	LHCb [767]: $2.52 \pm 0.26 \pm 0.15$	2.52 ± 0.30
$\mathcal{B}(B^- \rightarrow \chi_{c0} \pi^-)$	BABAR [769]: < 6.1	< 6.1
$\mathcal{B}(B^- \rightarrow \chi_{c1} \pi^-)$	Belle [770]: $2.2 \pm 0.4 \pm 0.3$	2.2 ± 0.5

Table 170: Branching fractions to J/ψ and a heavy mesons.

Parameter	Measurements	Average $[10^{-4}]$
$\mathcal{B}(B^- \rightarrow J/\psi D^-)$	BABAR [704]: < 1.2	< 1.2
$\mathcal{B}(B^- \rightarrow J/\psi D^0 \pi^-)$	Belle [703]: < 0.25 BABAR [760]: < 0.52	< 0.25

 Table 171: Branching fractions to J/ψ and baryons, I.

Parameter	Measurements	Average $[10^{-5}]$
$\mathcal{B}(B^- \rightarrow J/\psi \Lambda \bar{p})$	Belle [701]: $1.16 \pm 0.28^{+0.18}_{-0.23}$ BABAR [702]: $1.16^{+0.74+0.42}_{-0.53-0.18}$	1.16 ± 0.31
$\mathcal{B}(B^- \rightarrow J/\psi \Sigma^0 \bar{p})$	Belle [701]: < 1.1	< 1.1

 Table 172: Branching fractions to J/ψ and baryons, II.

Parameter	Measurements	Average $[10^{-6}]$
$\mathcal{B}(B^- \rightarrow J/\psi p \bar{p} \pi^-)$	LHCb [700]: < 0.50	< 0.50
$\mathcal{B}(B^- \rightarrow J/\psi K^-) \times \mathcal{B}(J/\psi \rightarrow \Lambda \bar{\Lambda})$	Belle [764]: $2.0^{+0.3}_{-0.3} \pm 0.3$	$2.0^{+0.5}_{-0.4}$
$\mathcal{B}(B^- \rightarrow J/\psi K^-) \times \mathcal{B}(J/\psi \rightarrow p \bar{p})$	Belle [764]: $2.21 \pm 0.13 \pm 0.10$ BABAR [765]: $2.2 \pm 0.2 \pm 0.1$	2.21 ± 0.13

Table 173: Branching fraction ratios, I.

Parameter	Measurements	Average
$\frac{\mathcal{B}(B^- \rightarrow J/\psi K^*(892)^-)}{\mathcal{B}(B^- \rightarrow J/\psi K^-)}$	CDF [705]: $1.92 \pm 0.60 \pm 0.17$ BABAR [9]: $1.37 \pm 0.05 \pm 0.08$	1.38 ± 0.09
$\frac{\mathcal{B}(B^- \rightarrow J/\psi K_1(1270)^-)}{\mathcal{B}(B^- \rightarrow J/\psi K^-)}$	Belle [674]: $1.80 \pm 0.34 \pm 0.34$	1.80 ± 0.48
$\frac{\mathcal{B}(B^- \rightarrow J/\psi K_1^-(1400))}{\mathcal{B}(B^- \rightarrow J/\psi K_1(1270)^-)}$	Belle [674]: < 0.30	< 0.30
$\frac{\mathcal{B}(B^- \rightarrow \psi(2S)K^-)}{\mathcal{B}(B^- \rightarrow J/\psi K^-)}$	LHCb [708]: $0.594 \pm 0.006 \pm 0.022$ D0 [771]: $0.65 \pm 0.04 \pm 0.08$	0.598 ± 0.022
$\frac{\mathcal{B}(B^- \rightarrow \psi(2S)K^*(892)^-)}{\mathcal{B}(B^- \rightarrow \psi(2S)K^-)}$	BABAR [9]: $0.96 \pm 0.15 \pm 0.09$	0.96 ± 0.17
$\frac{\mathcal{B}(B^- \rightarrow \chi_{c0}K^-)}{\mathcal{B}(B^- \rightarrow J/\psi K^-)}$	Belle [761]: $0.60^{+0.21}_{-0.18} \pm 0.09$	$0.60^{+0.23}_{-0.20}$
$\frac{\mathcal{B}(B^- \rightarrow \chi_{c1}K^*(892)^-)}{\mathcal{B}(B^- \rightarrow \chi_{c1}K^-)}$	BABAR [9]: $0.51 \pm 0.17 \pm 0.16$	0.51 ± 0.23
$\frac{\mathcal{B}(B^- \rightarrow \chi_{c1}\bar{K}^0\pi^-)}{\mathcal{B}(B^- \rightarrow J/\psi \bar{K}^0\pi^-)}$	BABAR [684]: $0.501 \pm 0.024 \pm 0.055$	0.501 ± 0.060
$\frac{\mathcal{B}(B^- \rightarrow \eta_c K^-)}{\mathcal{B}(B^- \rightarrow J/\psi K^-)}$	BABAR [728]: $1.06 \pm 0.23 \pm 0.04$ BABAR [688]: $1.28 \pm 0.10 \pm 0.38$	1.12 ± 0.20
$[\mathcal{B}(B^- \rightarrow \eta_c K^-) \times \mathcal{B}(\eta_c \rightarrow p\bar{p})]/[\mathcal{B}(B^- \rightarrow J/\psi K^-) \times \mathcal{B}(J/\psi \rightarrow p\bar{p})]$	LHCb [772]: $0.578 \pm 0.035 \pm 0.027$	0.578 ± 0.044

Table 174: Branching fraction ratios, II.

Parameter	Measurements	Average
$\frac{\mathcal{B}(B^- \rightarrow J/\psi \pi^-)}{\mathcal{B}(B^- \rightarrow J/\psi K^-)}$	CDF [773]: $0.050^{+0.019}_{-0.017} \pm 0.001$ CDF [774]: $0.0486 \pm 0.0082 \pm 0.0015$ BABAR [768]: $0.0537 \pm 0.0045 \pm 0.0011$	0.0524 ± 0.0040
$[\mathcal{B}(B^- \rightarrow \psi(2S)K^-) \times \mathcal{B}(\psi(2S) \rightarrow p\bar{p})]/[\mathcal{B}(B^- \rightarrow J/\psi K^-) \times \mathcal{B}(J/\psi \rightarrow p\bar{p})]$	LHCb [772]: $0.080 \pm 0.012 \pm 0.009$	0.080 ± 0.015
$\frac{\mathcal{B}(B^- \rightarrow \chi_{c1}\pi^-)}{\mathcal{B}(B^- \rightarrow \chi_{c1}K^-)}$	Belle [770]: $0.043 \pm 0.008 \pm 0.003$	0.043 ± 0.009
$\frac{\mathcal{B}(B^- \rightarrow h_c(1P)\bar{K}^-) \times \mathcal{B}(h_c(1P) \rightarrow \eta_c \gamma)}{\mathcal{B}(B^- \rightarrow \eta_c K^-)}$	BABAR [689]: < 0.052	< 0.052

Table 175: Direct CP violation parameters.

Parameter	Measurements	Average
$A_{CP}(B^- \rightarrow J/\psi K^-)$	D0 [775]: $0.0059 \pm 0.0036 \pm 0.0007$	0.0059 ± 0.0037
$A_{CP}(B^- \rightarrow J/\psi \pi^-)$	D0 [775]: $-0.042 \pm 0.044 \pm 0.009$	-0.042 ± 0.045

7.2.4 Decays to charm baryons

Averages of B^- decays to charm baryons are shown in Tables 176–178.

Table 176: (Product) branching fractions.

Parameter	Measurements	Average [10 ⁻⁴]
$\mathcal{B}(B^- \rightarrow \Lambda_c^+ \Lambda_c^- K^-)$	Belle [776]: $4.80 \pm 0.43 \pm 0.60$ BABAR [716]: $11.4 \pm 1.5 \pm 6.2$	4.89 ± 0.73
$\mathcal{B}(B^- \rightarrow \Xi_c^0 \Lambda_c^-) \times \mathcal{B}(\Xi_c^0 \rightarrow \Xi^- \pi^+)$	Belle [721]: $0.48^{+0.10}_{-0.09} \pm 0.16$ BABAR [716]: $0.208 \pm 0.065 \pm 0.061$	0.222 ± 0.089
$\mathcal{B}(B^- \rightarrow \Xi_c^0(2930) \Lambda_c^-) \times \mathcal{B}(\Xi_c^0(2930) \rightarrow \Lambda_c^+ K^-)$	Belle [776]: $1.73 \pm 0.45 \pm 0.21$	1.73 ± 0.50
$\mathcal{B}(B^- \rightarrow \Lambda_c^+ \bar{p} \pi^-)$	Belle [712]: $1.87^{+0.43}_{-0.40} \pm 0.56$ BABAR [719]: $3.38 \pm 0.12 \pm 0.89$	2.12 ± 0.70
$\mathcal{B}(B^- \rightarrow \Sigma_c^0 \bar{p})$	Belle [712]: $0.45^{+0.26}_{-0.19} \pm 0.14$	$0.45^{+0.29}_{-0.24}$
$\mathcal{B}(B^- \rightarrow \Sigma_c^{*0} \bar{p})$	Belle [712]: < 0.46	< 0.46
$\mathcal{B}(B^- \rightarrow \Sigma_c^{++} \bar{p} \pi^- \pi^-)$	BABAR [777]: $2.98 \pm 0.16 \pm 0.78$	2.98 ± 0.80

Table 177: Branching fraction ratios, I.

Parameter	Measurements	Average
$\frac{\mathcal{B}(B^- \rightarrow \Lambda_c^+ \bar{p} \pi^-)}{\mathcal{B}(B^- \rightarrow \Lambda_c^+ \bar{p})}$	BABAR [719]: $15.4 \pm 1.8 \pm 0.3$	15.4 ± 1.8

Table 178: Branching fraction ratios, II.

Parameter	Measurements	Average
$\frac{\mathcal{B}(B^- \rightarrow \Sigma_c(2455)^0 \bar{p})}{\mathcal{B}(B^- \rightarrow \Lambda_c^+ \bar{p} \pi^-)}$	BABAR [719]: $0.123 \pm 0.012 \pm 0.008$	0.123 ± 0.014
$\frac{\mathcal{B}(B^- \rightarrow \Sigma_c(2800)^0 \bar{p})}{\mathcal{B}(B^- \rightarrow \Lambda_c^+ \bar{p} \pi^-)}$	BABAR [719]: $0.117 \pm 0.023 \pm 0.024$	0.117 ± 0.033

7.2.5 Decays to other (XYZ) states

Averages of B^- decays to other (XYZ) states are shown in Tables 179–184.

Table 179: Branching fractions.

Parameter	Measurements	Average [10 ⁻⁴]
$\mathcal{B}(B^- \rightarrow X(3872) K^-)$	Belle [732]: $1.2 \pm 1.1 \pm 0.1$ BABAR [728]: < 3.2	1.2 ± 1.1
$\mathcal{B}(B^- \rightarrow X(3915) K^-)$	Belle [732]: $0.4 \pm 1.6 \pm 0.0$	0.4 ± 1.6

Table 180: Product branching fractions to $X(3872)$, I.

Parameter	Measurements	Average $[10^{-4}]$
$\mathcal{B}(B^- \rightarrow X(3872)K^-) \times \mathcal{B}(X(3872) \rightarrow \bar{D}^*(2007)^0 D^0)$		
BABAR [664]: $1.67 \pm 0.36 \pm 0.47$	1.67 ± 0.59	
$\mathcal{B}(B^- \rightarrow X(3872)K^-) \times \mathcal{B}(X(3872) \rightarrow D^0 \bar{D}^0 \pi^0)$		
Belle [756]: < 0.6	< 0.6	
$\mathcal{B}(B^- \rightarrow X(3872)K^-) \times \mathcal{B}(X(3872) \rightarrow D^0 \bar{D}^0)$		
Belle [756]: < 0.6	< 0.6	
$\mathcal{B}(B^- \rightarrow X(3872)K^-) \times \mathcal{B}(X(3872) \rightarrow D^+ D^-)$		
Belle [756]: < 0.4	< 0.4	

 Table 181: Product branching fractions to $X(3872)$, II.

Parameter	Measurements	Average $[10^{-5}]$
$\mathcal{B}(B^- \rightarrow K^- X(3872)) \times \mathcal{B}(X(3872) \rightarrow J/\psi \pi^+ \pi^-)$		
Belle [778]: $0.861 \pm 0.062 \pm 0.052$	0.857 ± 0.073	
BABAR [726]: $0.84 \pm 0.15 \pm 0.07$		
$\mathcal{B}(B^- \rightarrow X(3872)K^-) \times \mathcal{B}(X(3872) \rightarrow J/\psi \omega(782))$		
BABAR [672]: $0.6 \pm 0.2 \pm 0.1$	0.6 ± 0.2	
$\mathcal{B}(B^- \rightarrow X(3872)K^-) \times \mathcal{B}(X(3872) \rightarrow J/\psi \eta)$		
BABAR [676]: < 0.77	< 0.77	
$\mathcal{B}(B^- \rightarrow X(3872)K^-) \times \mathcal{B}(X(3872) \rightarrow J/\psi \gamma)$		
Belle [681]: $0.178^{+0.048}_{-0.044} \pm 0.012$	0.206 ± 0.042	
BABAR [682]: $0.28 \pm 0.08 \pm 0.01$		
$\mathcal{B}(B^- \rightarrow X(3872)K^*(892)^-) \times \mathcal{B}(X(3872) \rightarrow J/\psi \gamma)$		
BABAR [682]: $0.07 \pm 0.26 \pm 0.01$	0.07 ± 0.26	
$\mathcal{B}(B^- \rightarrow X(3872)K^-) \times \mathcal{B}(X(3872) \rightarrow \psi(2S) \gamma)$		
Belle [681]: < 0.345	0.95 ± 0.28	
BABAR [682]: $0.95 \pm 0.27 \pm 0.06$		
$\mathcal{B}(B^- \rightarrow X(3872)K^*(892)^-) \times \mathcal{B}(X(3872) \rightarrow \psi(2S) \gamma)$		
BABAR [682]: $0.64 \pm 0.98 \pm 0.96$	0.64 ± 1.37	
$\mathcal{B}(B^- \rightarrow X(3872)K^-) \times \mathcal{B}(X(3872) \rightarrow \chi_{c1} \gamma)$		
Belle [678]: < 0.19	< 0.19	
$\mathcal{B}(B^- \rightarrow X(3872)K^-) \times \mathcal{B}(X(3872) \rightarrow \chi_{c2} \gamma)$		
Belle [678]: < 0.67	< 0.67	

Table 182: Product branching fractions to neutral states other than $X(3872)$.

Parameter	Measurements	Average [10 ⁻⁵]
$\mathcal{B}(B^- \rightarrow X(3823)K^-) \times \mathcal{B}(X(3823) \rightarrow \chi_{c1}\gamma)$	Belle [678]: $0.97 \pm 0.28 \pm 0.11$	0.97 ± 0.30
$\mathcal{B}(B^- \rightarrow X(3823)K^-) \times \mathcal{B}(X(3823) \rightarrow \chi_{c2}\gamma)$	Belle [678]: < 0.36	< 0.36
$\mathcal{B}(B^- \rightarrow Y(3940)K^-) \times \mathcal{B}(Y(3940) \rightarrow J/\psi\gamma)$	BABAR [779]: < 1.4	< 1.4
$\mathcal{B}(B^- \rightarrow Y(3940)K^-) \times \mathcal{B}(Y(3940) \rightarrow J/\psi\omega(782))$	BABAR [672]: $3.0^{+0.7}_{-0.6}{}^{+0.5}_{-0.3}$	$3.0^{+0.9}_{-0.7}$
$\mathcal{B}(B^- \rightarrow Y(4260)K^-) \times \mathcal{B}(Y(4260) \rightarrow J/\psi\pi^+\pi^-)$	BABAR [780]: $2.0 \pm 0.7 \pm 0.2$	2.0 ± 0.7
$\mathcal{B}(B^- \rightarrow Y(4660)K^-) \times \mathcal{B}(Y(4660) \rightarrow \Lambda_c^+\Lambda_c^-)$	Belle [776]: < 12	< 12
$\mathcal{B}(B^- \rightarrow Y_\eta K^-) \times \mathcal{B}(Y_\eta \rightarrow \Lambda_c^+\Lambda_c^-)$	Belle [776]: < 20	< 20

 Table 183: Relative product branching fractions to states with $s\bar{s}$ component.

Parameter	Measurements	Average
$[\mathcal{B}(B^- \rightarrow X(4140)K^-) \times \mathcal{B}(X(4140) \rightarrow J/\psi\phi(1020))] / \mathcal{B}(B^- \rightarrow J/\psi\phi(1020)K^-)$	LHCb [781]: $0.130 \pm 0.032^{+0.047}_{-0.020}$ D0 [782]: $0.21 \pm 0.08 \pm 0.04$	0.148 ± 0.048
$[\mathcal{B}(B^- \rightarrow X(4274)K^-) \times \mathcal{B}(X(4274) \rightarrow J/\psi\phi(1020))] / \mathcal{B}(B^- \rightarrow J/\psi\phi(1020)K^-)$	LHCb [781]: $0.071 \pm 0.025^{+0.035}_{-0.024}$	$0.071^{+0.043}_{-0.035}$

Table 184: Product branching fractions to charged states.

Parameter	Measurements	Average [10 ⁻⁵]
$\mathcal{B}(B^- \rightarrow X(3872)^-\bar{K}^0) \times \mathcal{B}(X(3872)^- \rightarrow J/\psi\pi^-\pi^0)$	BABAR [729]: < 2.2	< 2.2
$\mathcal{B}(B^- \rightarrow Z(4430)^-\bar{K}^0) \times \mathcal{B}(Z(4430)^- \rightarrow J/\psi\pi^-)$	BABAR [730]: $-0.1 \pm 0.8 \pm 0.0$	-0.1 ± 0.8
$\mathcal{B}(B^- \rightarrow Z(4430)^-\bar{K}^0) \times \mathcal{B}(Z(4430)^- \rightarrow \psi(2S)\pi^-)$	BABAR [730]: $2.0 \pm 1.7 \pm 0.0$	2.0 ± 1.7

7.3 Decays of admixtures of \bar{B}^0/B^- mesons

Measurements of \bar{B}^0/B^- decays to charmed hadrons are summarized in Sections 7.3.1 to 7.3.3. These results reflect the \bar{B}^0/B^- production admixture in $\Upsilon(4S)$ decays.

7.3.1 Decays to two open charm mesons

Averages of \bar{B}^0/B^- decays to two open charm mesons are shown in Table 185.

Table 185: Branching fractions to double charm.

Parameter	Measurements	Average $[10^{-4}]$
$\mathcal{B}(B \rightarrow D^0 \bar{D}^0 \pi^0 K)$	Belle [654]: $1.27 \pm 0.31^{+0.22}_{-0.39}$	$1.27^{+0.38}_{-0.50}$

7.3.2 Decays to charmonium states

Averages of \bar{B}^0/B^- decays to charmonium states are shown in Tables 186–190.

Table 186: Decay amplitudes for parallel transverse polarization.

Parameter	Measurements	Average
$ \mathcal{A}_\parallel ^2(B \rightarrow J/\psi K^*)$	LHCb [324]: $0.227 \pm 0.004 \pm 0.011$ Belle [322]: $0.231 \pm 0.012 \pm 0.008$ BABAR [321]: $0.211 \pm 0.010 \pm 0.006$	0.222 ± 0.007
$ \mathcal{A}_\parallel ^2(B \rightarrow \chi_{c1} K^*)$	BABAR [321]: $0.20 \pm 0.07 \pm 0.04$	0.20 ± 0.08
$ \mathcal{A}_\parallel ^2(B \rightarrow \psi(2S) K^*)$	BABAR [321]: $0.22 \pm 0.06 \pm 0.02$	0.22 ± 0.06

Table 187: Decay amplitudes for perpendicular transverse polarization.

Parameter	Measurements	Average
$ \mathcal{A}_\perp ^2(B \rightarrow J/\psi K^*)$	LHCb [324]: $0.201 \pm 0.004 \pm 0.008$ Belle [322]: $0.195 \pm 0.012 \pm 0.008$ BABAR [321]: $0.233 \pm 0.010 \pm 0.005$	0.210 ± 0.006
$ \mathcal{A}_\perp ^2(B \rightarrow \chi_{c1} K^*)$	BABAR [321]: $0.03 \pm 0.04 \pm 0.02$	0.03 ± 0.04
$ \mathcal{A}_\perp ^2(B \rightarrow \psi(2S) K^*)$	BABAR [321]: $0.30 \pm 0.06 \pm 0.02$	0.30 ± 0.06

Table 188: Decay amplitudes for longitudinal polarization.

Parameter	Measurements	Average
$ \mathcal{A}_0 ^2(B \rightarrow J/\psi K^*)$	Belle [322]: $0.574 \pm 0.012 \pm 0.009$ BABAR [321]: $0.556 \pm 0.009 \pm 0.010$	0.564 ± 0.010
$ \mathcal{A}_0 ^2(B \rightarrow \chi_{c1} K^*)$	BABAR [321]: $0.77 \pm 0.07 \pm 0.04$	0.77 ± 0.08
$ \mathcal{A}_0 ^2(B \rightarrow \psi(2S) K^*)$	BABAR [321]: $0.48 \pm 0.05 \pm 0.02$	0.48 ± 0.05

Table 189: Relative phases of parallel transverse polarization decay amplitudes.

Parameter	Measurements	Average
$\delta_{\parallel}(B \rightarrow J/\psi K^*)$	LHCb [324]: $-2.94 \pm 0.02 \pm 0.03$ Belle [322]: $-2.887 \pm 0.090 \pm 0.008$ BABAR [321]: $-2.93 \pm 0.08 \pm 0.04$	-2.932 ± 0.031
$\delta_{\parallel}(B \rightarrow \chi_{c1} K^*)$	BABAR [321]: $0.0 \pm 0.3 \pm 0.1$	0.0 ± 0.3
$\delta_{\parallel}(B \rightarrow \psi(2S) K^*)$	BABAR [321]: $-2.8 \pm 0.4 \pm 0.1$	-2.8 ± 0.4

Table 190: Relative phases of perpendicular transverse polarization decay amplitudes.

Parameter	Measurements	Average
$\delta_{\perp}(B \rightarrow J/\psi K^*)$	LHCb [324]: $2.94 \pm 0.02 \pm 0.02$ Belle [322]: $2.938 \pm 0.064 \pm 0.010$ BABAR [321]: $2.91 \pm 0.05 \pm 0.03$	2.935 ± 0.024
$\delta_{\perp}(B \rightarrow \psi(2S) K^*)$	BABAR [321]: $2.8 \pm 0.3 \pm 0.1$	2.8 ± 0.3

7.3.3 Decays to other (XYZ) states

Averages of \bar{B}^0/B^- decays to other (XYZ) states are shown in Table 191.

Table 191: Branching fractions to X/Y states.

Parameter	Measurements	Average $[10^{-4}]$
$\mathcal{B}(B \rightarrow X(3872)K) \times \mathcal{B}(X(3872) \rightarrow D^*(2007)^0 \bar{D}^0)$	Belle [783]: $0.80 \pm 0.20 \pm 0.10$	0.80 ± 0.22
$\mathcal{B}(B \rightarrow Y(3940)K) \times \mathcal{B}(Y(3940) \rightarrow D^*(2007)^0 \bar{D}^0)$	Belle [783]: < 0.67	< 0.67
$\mathcal{B}(B \rightarrow KY(3940)) \times \mathcal{B}(Y(3940) \rightarrow J/\psi \omega(782))$	Belle [784]: $0.71 \pm 0.13 \pm 0.31$	0.71 ± 0.34

7.4 Decays of \bar{B}_s^0 mesons

Measurements of \bar{B}_s^0 decays to charmed hadrons are summarized in Sections 7.4.1 to 7.4.4. These measurements require knowledge of the production rates of \bar{B}_s^0 mesons, usually measured relative to those of \bar{B}^0 and B^- mesons, in the same experimental environment. Since these production fractions are reasonably well known, see Sec. 4.1, they can be corrected for allowing the results to be presented in terms of a \bar{B}_s^0 branching fraction. This is usually done in the publications; we do not attempt to rescale results according to more recent determinations of the relative production fractions. Ratios of branching fractions of two decays of the same hadron do not require any such correction.

7.4.1 Decays to a single open charm meson

Averages of \bar{B}_s^0 decays to a single open charm meson are shown in Tables 192–201.

Table 192: Branching fractions to a $D_s^{(*)}$ and a light meson, I.

Parameter	Measurements	Average [10 ⁻³]
$\mathcal{B}(\bar{B}_s^0 \rightarrow D_s^+ \pi^-)$	LHCb [785]: $2.95 \pm 0.05 {}^{+0.25}_{-0.28}$ Belle [31]: $3.67 {}^{+0.35 +0.65}_{-0.33 -0.65}$	3.03 ± 0.24
$\mathcal{B}(\bar{B}_s^0 \rightarrow D_s^{*+} \pi^-)$	Belle [786]: $2.4 {}^{+0.5}_{-0.4} \pm 0.4$	$2.4 {}^{+0.7}_{-0.6}$
$\mathcal{B}(\bar{B}_s^0 \rightarrow D_s^+ \rho^-(770))$	Belle [786]: $8.5 {}^{+1.3}_{-1.2} \pm 1.7$	$8.5 {}^{+2.1}_{-2.1}$
$\mathcal{B}(\bar{B}_s^0 \rightarrow D_s^{*+} \rho^-(770))$	Belle [786]: $11.8 {}^{+2.2}_{-2.0} \pm 2.5$	$11.8 {}^{+3.3}_{-3.2}$

Table 193: Branching fractions to a $D_s^{(*)}$ and a light meson, II.

Parameter	Measurements	Average [10 ⁻⁴]
$\mathcal{B}(\bar{B}_s^0 \rightarrow D_s^+ K^-)$	LHCb [785]: $1.90 \pm 0.12 {}^{+0.18}_{-0.19}$ Belle [31]: $2.4 {}^{+1.2}_{-1.0} \pm 0.4$	1.92 ± 0.21
$\mathcal{B}(\bar{B}_s^0 \rightarrow D_s^{*+} K^-)$	LHCb [787]: $1.63 \pm 0.12 {}^{+0.49}_{-0.48}$	$1.63 {}^{+0.50}_{-0.50}$

Table 194: Branching fractions to a $D^{(*)}$ and a light meson, I.

Parameter	Measurements	Average [10 ⁻⁴]
$\mathcal{B}(\bar{B}_s^0 \rightarrow D^0 K^0)$	LHCb [788]: $4.3 \pm 0.5 \pm 0.8$	4.3 ± 0.9
$\mathcal{B}(\bar{B}_s^0 \rightarrow D^{*0} K^0)$	LHCb [788]: $2.8 \pm 1.0 \pm 0.5$	2.8 ± 1.1
$\mathcal{B}(\bar{B}_s^0 \rightarrow D^0 K^{*0})$	LHCb [789]: $4.72 \pm 1.07 \pm 0.96$	4.72 ± 1.44

Table 195: Branching fractions to a $D^{(*)}$ and a light meson, II.

Parameter	Measurements	Average [10 ⁻⁵]
$\mathcal{B}(\bar{B}_s^0 \rightarrow D^0 \phi(1020))$	LHCb [631]: $3.0 \pm 0.3 \pm 0.3$	3.0 ± 0.4

Table 196: Branching fractions to a $D^{(*)}$ and a light meson, III.

Parameter	Measurements	Average [10 ⁻⁶]
$\mathcal{B}(\bar{B}_s^0 \rightarrow D^*(2010)^\pm \pi^\mp)$	LHCb [790]: < 6.1	< 6.1
$\mathcal{B}(\bar{B}_s^0 \rightarrow D^0 f_0(980))$	LHCb [791]: < 3.1	< 3.1
$\mathcal{B}(\bar{B}_s^0 \rightarrow D^*(2007)^0 \phi(1020))$	LHCb [631]: $37 \pm 5 \pm 4$	37 ± 6

Table 197: Branching fractions to a $D^{(*)0}$ meson and more than one light meson.

Parameter	Measurements	Average [10 ⁻⁵]
$\mathcal{B}(\bar{B}_s^0 \rightarrow D^0 K^+ K^-)$	LHCb [630]: $5.7 \pm 0.5 \pm 0.6$	5.7 ± 0.8

Table 198: Branching fraction ratios, I.

Parameter	Measurements	Average
$\frac{\mathcal{B}(\bar{B}_s^0 \rightarrow D_s^+ \pi^-)}{\mathcal{B}(\bar{B}^0 \rightarrow D^+ \pi^-)}$	CDF [792]: $1.13 \pm 0.08 \pm 0.23$	1.13 ± 0.25
$\frac{\mathcal{B}(\bar{B}_s^0 \rightarrow D_s^+ \pi^+ \pi^- \pi^-)}{\mathcal{B}(\bar{B}_s^0 \rightarrow D_s^+ \pi^-)}$	LHCb [637]: $2.01 \pm 0.37 \pm 0.20$	2.01 ± 0.42
$\frac{\mathcal{B}(\bar{B}_s^0 \rightarrow D_s^+ \pi^+ \pi^- \pi^-)}{\mathcal{B}(\bar{B}^0 \rightarrow D^+ \pi^+ \pi^- \pi^-)}$	CDF [792]: $1.05 \pm 0.10 \pm 0.22$	1.05 ± 0.24
$\frac{\mathcal{B}(\bar{B}_s^0 \rightarrow D^0 K^{*0})}{\mathcal{B}(\bar{B}^0 \rightarrow D^0 \rho^0)}$	LHCb [789]: $1.48 \pm 0.34 \pm 0.19$	1.48 ± 0.39
$\frac{\mathcal{B}(\bar{B}_s^0 \rightarrow D^0 K^{*0})}{\mathcal{B}(\bar{B}^0 \rightarrow D^0 \bar{K}^{*0})}$	LHCb [793]: $7.8 \pm 0.7 \pm 0.7$	7.8 ± 1.0
$\frac{\mathcal{B}(\bar{B}_s^0 \rightarrow D^0 K^+ \pi^-)}{\mathcal{B}(\bar{B}^0 \rightarrow D^0 \pi^- \pi^+)}$	LHCb [640]: $1.18 \pm 0.05 \pm 0.12$	1.18 ± 0.13
$\frac{\mathcal{B}(\bar{B}_s^0 \rightarrow D^*(2007)^0 \phi(1020))}{\mathcal{B}(\bar{B}_s^0 \rightarrow D^0 \phi(1020))}$	LHCb [631]: $1.23 \pm 0.20 \pm 0.06$	1.23 ± 0.21
$\frac{\mathcal{B}(\bar{B}_s^0 \rightarrow D^0 K^+ K^-)}{\mathcal{B}(\bar{B}^0 \rightarrow D^0 \pi^+ \pi^-)}$	LHCb [630]: $0.930 \pm 0.089 \pm 0.069$	0.930 ± 0.113

Table 199: Branching fraction ratios, II.

Parameter	Measurements	Average $[10^{-2}]$
$\frac{\mathcal{B}(\bar{B}_s^0 \rightarrow D_s^+ K^-)}{\mathcal{B}(\bar{B}_s^0 \rightarrow D_s^+ \pi^-)}$	LHCb [642]: $7.52 \pm 0.15 \pm 0.19$ CDF [794]: $9.7 \pm 1.8 \pm 0.9$	7.55 ± 0.24
$\frac{\mathcal{B}(\bar{B}_s^0 \rightarrow D_s^{*+} K^-)}{\mathcal{B}(\bar{B}_s^0 \rightarrow D_s^{*+} \pi^-)}$	LHCb [787]: $6.8 \pm 0.5^{+0.3}_{-0.2}$	$6.8^{+0.6}_{-0.5}$
$\frac{\mathcal{B}(\bar{B}_s^0 \rightarrow D_s^+ K^- \pi^+ \pi^-)}{\mathcal{B}(\bar{B}_s^0 \rightarrow D_s^+ \pi^- \pi^+ \pi^-)}$	LHCb [638]: $5.2 \pm 0.5 \pm 0.3$	5.2 ± 0.6
$\frac{\mathcal{B}(\bar{B}_s^0 \rightarrow D^0 \phi(1020))}{\mathcal{B}(\bar{B}_s^0 \rightarrow D^0 K^{*0})}$	LHCb [793]: $6.9 \pm 1.3 \pm 0.7$	6.9 ± 1.5
$\frac{\mathcal{B}(\bar{B}_s^0 \rightarrow D_{s1}^+ \pi^-) \times \mathcal{B}(D_{s1}^+ \rightarrow D_s^+ \pi^- \pi^+)}{\mathcal{B}(\bar{B}_s^0 \rightarrow D_s^+ \pi^- \pi^+ \pi^-)}$	LHCb [638]: $0.40 \pm 0.10 \pm 0.04$	0.40 ± 0.11

Table 200: Branching fraction ratios, III.

Parameter	Measurements	Average $[10^{-2}]$
$\frac{\mathcal{B}(\bar{B}_s^0 \rightarrow D^0 \phi(1020))}{\mathcal{B}(\bar{B}_s^0 \rightarrow D^0 \pi^+ \pi^-)}$	LHCb [631]: $3.4 \pm 0.4 \pm 0.2$	3.4 ± 0.4
$\frac{\mathcal{B}(\bar{B}_s^0 \rightarrow D^*(2007)^0 \phi(1020))}{\mathcal{B}(\bar{B}_s^0 \rightarrow D^0 \pi^+ \pi^-)}$	LHCb [631]: $4.2 \pm 0.5 \pm 0.4$	4.2 ± 0.6

Table 201: Longitudinal polarisation fraction.

Parameter	Measurements	Average
$f_L(\bar{B}_s^0 \rightarrow D^*(2007)^0 \phi(1020))$	LHCb [631]: $0.73 \pm 0.15 \pm 0.03$	0.73 ± 0.15

7.4.2 Decays to two open charm mesons

Averages of \bar{B}_s^0 decays to two open charm mesons are shown in Tables 202–204.

Table 202: Branching fractions.

Parameter	Measurements	Average [10 ⁻²]
$\mathcal{B}(\bar{B}_s^0 \rightarrow D_s^+ D_s^-)$	CDF [795]: $0.49 \pm 0.06 \pm 0.09$ Belle [18]: $0.58^{+0.11}_{-0.09} \pm 0.13$	0.52 ± 0.09
$\mathcal{B}(\bar{B}_s^0 \rightarrow D_s^+ D_s^{*-})$	LHCb [796]: $1.35 \pm 0.06 \pm 0.17$ CDF [795]: $1.13 \pm 0.12 \pm 0.21$ Belle [18]: $1.76^{+0.23}_{-0.22} \pm 0.40$	1.38 ± 0.17
$\mathcal{B}(\bar{B}_s^0 \rightarrow D_s^{*+} D_s^{*-})$	LHCb [796]: $1.27 \pm 0.08 \pm 0.17$ CDF [795]: $1.75 \pm 0.19 \pm 0.34$ Belle [18]: $1.98^{+0.33}_{-0.31} {}^{+0.51}_{-0.50}$	1.32 ± 0.18
$\mathcal{B}(\bar{B}_s^0 \rightarrow D_s^{(*)+} D_s^{(*)-})$	LHCb [796]: $3.05 \pm 0.10 \pm 0.39$ D0 [201]: $3.5 \pm 1.0 \pm 1.1$ CDF [795]: $3.38 \pm 0.25 \pm 0.64$ Belle [18]: $4.32^{+0.42}_{-0.39} {}^{+1.04}_{-1.03}$	3.19 ± 0.37

Table 203: Branching fraction ratios, I.

Parameter	Measurements	Average
$\frac{\mathcal{B}(\bar{B}_s^0 \rightarrow D^- D^+)}{\mathcal{B}(\bar{B}^0 \rightarrow D^- D^+)}$	LHCb [660]: $1.08 \pm 0.20 \pm 0.10$	1.08 ± 0.22
$\frac{\mathcal{B}(\bar{B}_s^0 \rightarrow D_s^- D_s^+)}{\mathcal{B}(\bar{B}^0 \rightarrow D_s^- D^+)}$	LHCb [660]: $0.56 \pm 0.03 \pm 0.04$	0.56 ± 0.05

Table 204: Branching fraction ratios, II.

Parameter	Measurements	Average [10 ⁻²]
$\frac{\mathcal{B}(\bar{B}_s^0 \rightarrow D_s^+ D^-)}{\mathcal{B}(B^0 \rightarrow D_s^+ D^-)}$	LHCb [660]: $5.0 \pm 0.8 \pm 0.4$	5.0 ± 0.9
$\frac{\mathcal{B}(\bar{B}_s^0 \rightarrow \bar{D}^0 D^0)}{\mathcal{B}(B^- \rightarrow D^0 D_s^-)}$	LHCb [660]: $1.9 \pm 0.3 \pm 0.3$	1.9 ± 0.4

7.4.3 Decays to charmonium states

Averages of \bar{B}_s^0 decays to charmonium states are shown in Tables 205–209.

Table 205: Branching fractions, I.

Parameter	Measurements	Average $[10^{-4}]$
$\mathcal{B}(\bar{B}_s^0 \rightarrow J/\psi\eta)$	Belle [797]: $5.10 \pm 0.50^{+1.17}_{-0.83}$	$5.10^{+1.27}_{-0.97}$
$\mathcal{B}(\bar{B}_s^0 \rightarrow J/\psi\eta')$	Belle [797]: $3.71 \pm 0.61^{+0.85}_{-0.60}$	$3.71^{+1.05}_{-0.85}$
$\mathcal{B}(\bar{B}_s^0 \rightarrow J/\psi\phi(1020))$	LHCb [798]: $10.5 \pm 0.1 \pm 1.0$ CDF [705]: $9.3 \pm 2.8 \pm 1.7$ Belle [799]: $12.5 \pm 0.7 \pm 2.3$	10.0 ± 0.9
$\mathcal{B}(\bar{B}_s^0 \rightarrow J/\psi K^0 K^\pm \pi^\mp)$	LHCb [670]: $9.1 \pm 0.6 \pm 0.7$	9.1 ± 0.9
$\mathcal{B}(\bar{B}_s^0 \rightarrow J/\psi f_0(980)) \times \mathcal{B}(f_0(980) \rightarrow \pi^+ \pi^-)$	Belle [30]: $1.16^{+0.31}_{-0.19} {}^{+0.30}_{-0.25}$	$1.16^{+0.43}_{-0.32}$

Table 206: Branching fractions, II.

Parameter	Measurements	Average $[10^{-5}]$
$\mathcal{B}(\bar{B}_s^0 \rightarrow J/\psi \bar{K}^0)$	LHCb [800]: $3.66 \pm 0.42 \pm 0.37$ CDF [801]: $3.5 \pm 0.6 \pm 0.6$	3.61 ± 0.46
$\mathcal{B}(\bar{B}_s^0 \rightarrow J/\psi K^{*0})$	LHCb [802]: $4.17 \pm 0.18 \pm 0.35$ CDF [801]: $8.3 \pm 1.2 \pm 3.6$	4.15 ± 0.40
$\mathcal{B}(\bar{B}_s^0 \rightarrow J/\psi p\bar{p})$	LHCb [700]: < 0.48	< 0.48
$\mathcal{B}(\bar{B}_s^0 \rightarrow J/\psi f_1(1285))$	LHCb [693]: $7.14 \pm 0.99^{+0.93}_{-1.00}$	$7.14^{+1.36}_{-1.41}$
$\mathcal{B}(\bar{B}_s^0 \rightarrow J/\psi K^0 \pi^+ \pi^-)$	LHCb [670]: < 4.4	< 4.4
$\mathcal{B}(\bar{B}_s^0 \rightarrow J/\psi K^0 K^+ K^-)$	LHCb [670]: < 1.2	< 1.2
$\mathcal{B}(\bar{B}_s^0 \rightarrow J/\psi f_0(1370)) \times \mathcal{B}(f_0(1370) \rightarrow \pi^+ \pi^-)$	Belle [30]: $3.4^{+1.1}_{-1.4} {}^{+0.9}_{-0.5}$	$3.4^{+1.4}_{-1.5}$
$\mathcal{B}(\bar{B}_s^0 \rightarrow J/\psi f_1(1285)) \times \mathcal{B}(f_1(1285) \rightarrow \pi^+ \pi^- \pi^+ \pi^-)$	LHCb [693]: $0.785 \pm 0.109^{+0.089}_{-0.101}$	$0.785^{+0.141}_{-0.149}$
$\mathcal{B}(\bar{B}_s^0 \rightarrow J/\psi \gamma)$	LHCb [698]: < 0.73	< 0.73

Table 207: Branching fraction ratios, I.

Parameter	Measurements	Average
$\frac{\mathcal{B}(\bar{B}_s^0 \rightarrow J/\psi\eta)}{\mathcal{B}(\bar{B}_s^0 \rightarrow J/\psi\rho)}$	LHCb [706]: $14.0 \pm 1.2^{+1.6}_{-1.8}$	$14.0^{+2.0}_{-2.2}$
$\frac{\mathcal{B}(\bar{B}_s^0 \rightarrow J/\psi\eta')}{\mathcal{B}(\bar{B}_s^0 \rightarrow J/\psi\rho)}$	LHCb [706]: $12.7 \pm 1.1^{+1.1}_{-0.9}$	$12.7^{+1.6}_{-1.4}$
$\frac{\mathcal{B}(\bar{B}_s^0 \rightarrow J/\psi K_S^0 K^\pm \pi^\mp)}{\mathcal{B}(\bar{B}_s^0 \rightarrow J/\psi \pi^+ \pi^-)}$	LHCb [670]: $2.12 \pm 0.15 \pm 0.18$	2.12 ± 0.23

Table 208: Branching fraction ratios, II.

Parameter	Measurements	Average
$\frac{\mathcal{B}(\bar{B}_s^0 \rightarrow J/\psi\eta)}{\mathcal{B}(\bar{B}_s^0 \rightarrow J/\psi\eta')}$	Belle [797]: $0.73 \pm 0.14 \pm 0.02$	0.73 ± 0.14
$\frac{\mathcal{B}(\bar{B}_s^0 \rightarrow J/\psi\eta')}{\mathcal{B}(\bar{B}_s^0 \rightarrow J/\psi\eta)}$	LHCb [706]: $0.90 \pm 0.09 {}^{+0.06}_{-0.02}$	$0.90 {}^{+0.11}_{-0.09}$
$\frac{\mathcal{B}(\bar{B}_s^0 \rightarrow J/\psi f'_2)}{\mathcal{B}(\bar{B}_s^0 \rightarrow J/\psi\phi(1020))}$	LHCb [803]: $0.264 \pm 0.027 \pm 0.024$ D0 [804]: $0.19 \pm 0.05 \pm 0.04$	0.246 ± 0.031
$\frac{\mathcal{B}(\bar{B}_s^0 \rightarrow J/\psi\pi^+\pi^-)}{\mathcal{B}(\bar{B}_s^0 \rightarrow J/\psi\phi(1020))}$	LHCb [805]: $0.162 \pm 0.022 \pm 0.016$	0.162 ± 0.027
$\frac{\mathcal{B}(\bar{B}_s^0 \rightarrow \psi(2S)\pi^+\pi^-)}{\mathcal{B}(\bar{B}_s^0 \rightarrow J/\psi\pi^+\pi^-)}$	LHCb [707]: $0.34 \pm 0.04 \pm 0.03$	0.34 ± 0.05
$\frac{\mathcal{B}(\bar{B}_s^0 \rightarrow \psi(2S)\phi(1020))}{\mathcal{B}(\bar{B}_s^0 \rightarrow J/\psi\phi(1020))}$	LHCb [708]: $0.489 \pm 0.026 \pm 0.024$ D0 [771]: $0.55 \pm 0.11 \pm 0.09$ CDF [806]: $0.52 \pm 0.13 \pm 0.07$	0.494 ± 0.034
$\frac{\mathcal{B}(\bar{B}_s^0 \rightarrow J/\psi K_S^0 \pi^+\pi^-)}{\mathcal{B}(\bar{B}_s^0 \rightarrow J/\psi\pi^+\pi^-)}$	LHCb [670]: < 0.10	< 0.10
$[\mathcal{B}(\bar{B}_s^0 \rightarrow J/\psi f_0(980)) \times \mathcal{B}(f_0(980) \rightarrow \pi^+\pi^-)] / [\mathcal{B}(\bar{B}_s^0 \rightarrow J/\psi\phi(1020)) \times \mathcal{B}(\phi \rightarrow K^+K^-)]$	LHCb [805]: $0.252 {}^{+0.046}_{-0.032} {}^{+0.027}_{-0.033}$ D0 [807]: $0.275 \pm 0.041 \pm 0.061$ CMS [808]: $0.140 \pm 0.008 \pm 0.023$ CDF [133]: $0.257 \pm 0.020 \pm 0.014$	0.208 ± 0.016 <small>CL=0.2%</small>
$\frac{\mathcal{B}(\bar{B}_s^0 \rightarrow \chi_{c2} K^+ K^-)}{\mathcal{B}(\bar{B}_s^0 \rightarrow \chi_{c1} K^+ K^-)}$	LHCb [809]: $0.171 \pm 0.031 \pm 0.010$	0.171 ± 0.033

Table 209: Branching fraction ratios, III.

Parameter	Measurements	Average [10^{-2}]
$\frac{\mathcal{B}(\bar{B}_s^0 \rightarrow J/\psi K_S^0)}{\mathcal{B}(\bar{B}_s^0 \rightarrow J/\psi K_S^0)}$	LHCb [800]: $4.20 \pm 0.49 \pm 0.40$	4.20 ± 0.63
$\frac{\mathcal{B}(\bar{B}_s^0 \rightarrow J/\psi\phi(1020)\phi(1020))}{\mathcal{B}(\bar{B}_s^0 \rightarrow J/\psi\phi(1020))}$	LHCb [810]: $1.15 \pm 0.12 {}^{+0.05}_{-0.09}$	$1.15 {}^{+0.13}_{-0.15}$
$\frac{\mathcal{B}(\bar{B}_s^0 \rightarrow \psi(2S)K^+\pi^-)}{\mathcal{B}(\bar{B}_s^0 \rightarrow \psi(2S)K^+\pi^-)}$	LHCb [811]: $5.38 \pm 0.36 \pm 0.38$	5.38 ± 0.52
$\frac{\mathcal{B}(\bar{B}_s^0 \rightarrow \psi(2S)K^{*0})}{\mathcal{B}(\bar{B}_s^0 \rightarrow \psi(2S)K^{*0})}$	LHCb [811]: $5.38 \pm 0.57 \pm 0.51$	5.38 ± 0.77
$\frac{\mathcal{B}(\bar{B}_s^0 \rightarrow J/\psi K_S^0 K^+ K^-)}{\mathcal{B}(\bar{B}_s^0 \rightarrow J/\psi\pi^+\pi^-)}$	LHCb [670]: < 2.7	< 2.7
$\frac{\mathcal{B}(\bar{B}_s^0 \rightarrow J/\psi f_0(500)) \times \mathcal{B}(f_0(500) \rightarrow \pi^+\pi^-)}{\mathcal{B}(\bar{B}_s^0 \rightarrow J/\psi f_0(980)) \times \mathcal{B}(f_0(500) \rightarrow \pi^+\pi^-)}$	LHCb [812]: < 3.4	< 3.4

7.4.4 Decays to charm baryons

Averages of \bar{B}_s^0 decays to charm baryons are shown in Tables 210–211.

Table 210: Branching fractions to one charm baryon.

Parameter	Measurements	Average [10 ⁻⁴]
$\mathcal{B}(\bar{B}_s^0 \rightarrow \Lambda_c^+ \bar{\Lambda} \pi^-)$	Belle [813]: $3.6 \pm 1.1^{+1.2}_{-1.2}$	$3.6^{+1.6}_{-1.7}$

Table 211: Branching fractions to two charm baryons.

Parameter	Measurements	Average
$\frac{\mathcal{B}(\bar{B}_s^0 \rightarrow \Lambda_c^- \Lambda_c^+)}{\mathcal{B}(\bar{B}_s^0 \rightarrow D^- D_s^+)}$	LHCb [725]: < 0.30	< 0.30

7.5 Decays of B_c^- mesons

Measurements of B_c^- decays to charmed hadrons are summarized in Sections 7.5.1 to 7.5.4. Since the absolute cross-section for B_c^- meson production in any production environment is currently not known, it is not possible to determine absolute branching fractions. Instead, results are presented either as ratios of branching fractions of different B_c^- decays, or are normalised to the branching fraction of the decay of a lighter B meson (usually B^-). In the latter case the measured quantity is the absolute or relative B_c^- branching fraction multiplied by the ratio of cross-sections (or, equivalently, production fractions) of the B_c^- and the lighter B meson.

It should be noted that the ratio of cross-sections for different b hadron species can depend on production environment, and on the fiducial region accessed by each experiment. While this has been studied for certain b hadron species (see Sec. 4.1), there is currently little published data that would allow to investigate the effect for B_c^- mesons. Therefore, we do not attempt to apply any correction for this effect.

7.5.1 Decays to a single open charm meson

Averages of B_c^- decays to a single open charm meson are shown in Table 212.

Table 212: Branching fractions to $D^{(*)0}$ meson and one or more kaons.

Parameter	Measurements	Average [10 ⁻⁷]
$\frac{f_c \times \mathcal{B}(B_c^- \rightarrow \bar{D}^0 K^-)}{f_u}$	LHCb [814]: $9.3^{+2.8}_{-2.5} \pm 0.6$	$9.3^{+2.9}_{-2.6}$

7.5.2 Decays to two open charm mesons

Averages of B_c^- decays to two open charm mesons are shown in Tables 213–216.

Table 213: Branching fraction ratios, I.

Parameter	Measurements	Average [10 ⁻⁴]
$\frac{f_c \times \mathcal{B}(B_c^- \rightarrow D_s^- D^0)}{f_u \times \mathcal{B}(B^- \rightarrow D_s^- D^0)}$	LHCb [815]: 3.0 ± 3.7	3.0 ± 3.7
$\frac{f_c \times \mathcal{B}(B_c^- \rightarrow D_s^- \bar{D}^0)}{f_u \times \mathcal{B}(B^- \rightarrow D_s^- D^0)}$	LHCb [815]: -3.8 ± 2.6	-3.8 ± 2.6

Table 214: Branching fraction ratios, II.

Parameter	Measurements	Average [10 ⁻³]
$\frac{f_c \times \mathcal{B}(B_c^- \rightarrow D^- D^0)}{f_u \times \mathcal{B}(B^- \rightarrow D^- D^0)}$	LHCb [815]: 8.0 ± 7.5	8.0 ± 7.5
$\frac{f_c \times \mathcal{B}(B_c^- \rightarrow D^- \bar{D}^0)}{f_u \times \mathcal{B}(B^- \rightarrow D^- D^0)}$	LHCb [815]: 2.9 ± 5.3	2.9 ± 5.3
$\frac{f_c \times (\mathcal{B}(B_c^- \rightarrow D_s^{*-} D^0) + \mathcal{B}(B_c^+ \rightarrow D_s^- D^{*0}))}{f_u \times \mathcal{B}(B^- \rightarrow D_s^- D^0)}$	LHCb [815]: -0.1 ± 1.5	-0.1 ± 1.5
$\frac{f_c \times (\mathcal{B}(B_c^- \rightarrow D_s^{*-} \bar{D}^0) + \mathcal{B}(B_c^+ \rightarrow D_s^- \bar{D}^{*0}))}{f_u \times \mathcal{B}(B^- \rightarrow D_s^- D^0)}$	LHCb [815]: -0.3 ± 1.9	-0.3 ± 1.9
$\frac{f_c \times \mathcal{B}(B_c^- \rightarrow D_s^{*-} D^{*0})}{f_u \times \mathcal{B}(B^- \rightarrow D_s^- D^0)}$	LHCb [815]: 3.2 ± 4.3	3.2 ± 4.3
$\frac{f_c \times \mathcal{B}(B_c^- \rightarrow D_s^{*-} \bar{D}^{*0})}{f_u \times \mathcal{B}(B^- \rightarrow D_s^- D^0)}$	LHCb [815]: 7.0 ± 9.2	7.0 ± 9.2

Table 215: Branching fraction ratios, III.

Parameter	Measurements	Average [10 ⁻²]
$[f_c \times (\mathcal{B}(B_c^- \rightarrow D^{*-} D^0) \times \mathcal{B}(D^{*-} \rightarrow D^-(\pi^0, \gamma)) + \mathcal{B}(B_c^- \rightarrow D^- D^{*0}))] / [f_u \times \mathcal{B}(B^- \rightarrow D^- D^0)]$ LHCb [815]: 0.2 ± 3.2	0.2 ± 3.2	0.2 ± 3.2
$[f_c \times (\mathcal{B}(B_c^- \rightarrow D^{*-} \bar{D}^0) \times \mathcal{B}(D^{*-} \rightarrow D^-(\pi^0, \gamma)) + \mathcal{B}(B_c^- \rightarrow D^- \bar{D}^{*0}))] / [f_u \times \mathcal{B}(B^- \rightarrow D^- D^0)]$ LHCb [815]: -1.5 ± 1.7	-1.5 ± 1.7	-1.5 ± 1.7
$\frac{f_c \times \mathcal{B}(B_c^- \rightarrow D_s^{*-} \bar{D}^{*0})}{f_u \times \mathcal{B}(B^- \rightarrow D^- D^0)}$ LHCb [815]: -4.1 ± 9.1	-4.1 ± 9.1	-4.1 ± 9.1

Table 216: Branching fraction ratios, IV.

Parameter	Measurements	Average [10 ⁻¹]
$\frac{f_c \times \mathcal{B}(B_c^- \rightarrow D_s^{*-} D^{*0})}{f_u \times \mathcal{B}(B^- \rightarrow D^- D^0)}$	LHCb [815]: 3.4 ± 2.3	3.4 ± 2.3

7.5.3 Decays to charmonium states

Averages of B_c^- decays to charmonium states are shown in Tables 217–220.

Table 217: Branching fraction ratios, I.

Parameter	Measurements	Average
$\frac{\mathcal{B}(B_c^- \rightarrow J/\psi D_s^-)}{\mathcal{B}(B_c^- \rightarrow J/\psi \pi^-)}$	LHCb [816]: $2.90 \pm 0.57 \pm 0.24$ ATLAS [817]: $3.8 \pm 1.1 \pm 0.4$	3.09 ± 0.55
$\frac{\mathcal{B}(B_c^- \rightarrow J/\psi D_s^{*-})}{\mathcal{B}(B_c^- \rightarrow J/\psi D_s^-)}$	ATLAS [817]: $2.8_{-0.8}^{+1.2} \pm 0.3$	$2.8_{-0.9}^{+1.2}$
$\frac{\mathcal{B}(B_c^- \rightarrow J/\psi D_s^{*-})}{\mathcal{B}(B_c^- \rightarrow J/\psi \pi^-)}$	ATLAS [817]: $10.4 \pm 3.1 \pm 1.6$	10.4 ± 3.5
$\frac{\mathcal{B}(B_c^- \rightarrow J/\psi \pi^+ \pi^- \pi^-)}{\mathcal{B}(B_c^- \rightarrow J/\psi \pi^-)}$	LHCb [818]: $2.41 \pm 0.30 \pm 0.33$ CMS [819]: $2.55 \pm 0.80_{-0.33}^{+0.33}$	2.44 ± 0.40
$\frac{\mathcal{B}(B_c^- \rightarrow J/\psi \bar{D}^{*0} K^-)}{\mathcal{B}(B_c^- \rightarrow J/\psi \bar{D}^0 K^-)}$	LHCb [820]: $5.1 \pm 1.8 \pm 0.4$	5.1 ± 1.8
$\frac{\mathcal{B}(B_c^- \rightarrow J/\psi D^{*-} \bar{K}^{*0})}{\mathcal{B}(B_c^- \rightarrow J/\psi \bar{D}^0 K^-)}$	LHCb [820]: $2.10 \pm 1.08 \pm 0.34$	2.10 ± 1.13

Table 218: Branching fraction ratios, II.

Parameter	Measurements	Average
$\frac{\mathcal{B}(B_c^- \rightarrow J/\psi K^-)}{\mathcal{B}(B_c^- \rightarrow J/\psi \pi^-)}$	LHCb [821]: $0.069 \pm 0.019 \pm 0.005$	0.069 ± 0.020
$\frac{\mathcal{B}(B_c^- \rightarrow J/\psi K^- K^+ \pi^-)}{\mathcal{B}(B_c^- \rightarrow J/\psi \pi^-)}$	LHCb [822]: $0.53 \pm 0.10 \pm 0.05$	0.53 ± 0.11
$\frac{\mathcal{B}(B_c^- \rightarrow \psi(2S) \pi^-)}{\mathcal{B}(B_c^- \rightarrow J/\psi \pi^-)}$	LHCb [823]: $0.268 \pm 0.032 \pm 0.009$	0.268 ± 0.033
$\frac{\mathcal{B}(B_c^- \rightarrow J/\psi \bar{D}^0 K^-)}{\mathcal{B}(B_c^- \rightarrow J/\psi \pi^-)}$	LHCb [820]: $0.432 \pm 0.136 \pm 0.028$	0.432 ± 0.139
$\frac{\mathcal{B}(B_c^- \rightarrow J/\psi D^- \bar{K}^{*0})}{\mathcal{B}(B_c^- \rightarrow J/\psi \bar{D}^0 K^-)}$	LHCb [820]: $0.63 \pm 0.39 \pm 0.08$	0.63 ± 0.40

Table 219: Production times branching fraction ratios.

Parameter	Measurements	Average $[10^{-3}]$
	LHCb [824]: $6.83 \pm 0.18 \pm 0.09$	
$\frac{\sigma(B_c^-) \times \mathcal{B}(B_c^- \rightarrow J/\psi \pi^-)}{\sigma(B^-) \times \mathcal{B}(B^- \rightarrow J/\psi K^-)}$	LHCb [825]: $6.8 \pm 1.0 \pm 0.6$ CMS [819]: $4.8 \pm 0.5 \pm 0.6$	6.72 ± 0.19

Table 220: Branching fractions times production ratios.

Parameter	Measurements	Average $[10^{-6}]$
$\frac{\sigma(B_c^-)}{\sigma(B^-)} \times \mathcal{B}(B_c^- \rightarrow \chi_{c0} \pi^-)$	LHCb [826]: $9.8_{-3.0}^{+3.4} \pm 0.8$	$9.8_{-3.1}^{+3.5}$

7.5.4 Decays to a B meson

Averages of B_c^- decays to a B meson are shown in Table 221.

Table 221: Branching fractions to B_s^0 meson.

Parameter	Measurements	Average $[10^{-3}]$
$\frac{\sigma(B_c^+)}{\sigma(B_s^0)} \times \mathcal{B}(B_c^+ \rightarrow B_s^0 \pi^+)$	LHCb [827]: $2.37 \pm 0.31^{+0.20}_{-0.17}$	$2.37^{+0.37}_{-0.35}$

7.6 Decays of b baryons

Measurements of b baryons decays to charmed hadrons are summarized in Sections 7.6.1 to 7.6.4. Comments regarding the production rates of \bar{B}_s^0 and B_c^- mesons relative to lighter B mesons, in Sec. 7.4 and Sec. 7.5 respectively, are also appropriate here. Specifically, since the cross-section for production of Λ_b^0 baryons is reasonably well-known, it is possible to determine absolute or relative branching fractions for its decays (although some older measurements are presented as products involving the cross-section). The cross-sections for production of heavier b baryons are not known, and therefore measured quantities are presented as absolute or relative branching fraction multiplied by a ratio of cross-sections (or, equivalently, production fractions).

7.6.1 Decays to a single open charm meson

Averages of b baryons decays to a single open charm meson are shown in Table 222.

Table 222: Branching fraction ratios to D^0 mesons.

Parameter	Measurements	Average
$\frac{\mathcal{B}(\Lambda_b^0 \rightarrow D^0 p K^-)}{\mathcal{B}(\Lambda_b^0 \rightarrow D^0 p \pi^-)}$	LHCb [828]: $0.073 \pm 0.008^{+0.005}_{-0.006}$	$0.073^{+0.009}_{-0.010}$
$[\mathcal{B}(\Lambda_b^0 \rightarrow D^0 p \pi^-) \times \mathcal{B}(D^0 \rightarrow K^+ \pi^-)] / [\mathcal{B}(\Lambda_b^0 \rightarrow \Lambda_c^+ \pi^-) \times \mathcal{B}(\Lambda_c^+ \rightarrow p K^- \pi^+)]$	LHCb [828]: $0.0806 \pm 0.0023 \pm 0.0035$	0.0806 ± 0.0042
$\frac{f_{\Xi_b^0} \times \mathcal{B}(\Xi_b^0 \rightarrow D^0 p K^-)}{f_{\Lambda_b^0} \times \mathcal{B}(\Lambda_b^0 \rightarrow D^0 p K^-)}$	LHCb [828]: $0.44 \pm 0.09 \pm 0.06$	0.44 ± 0.11

7.6.2 Decays to charmonium states

Averages of b baryons decays to charmonium states are shown in Tables 223–229.

Table 223: Λ_b^0 branching fractions to charmonium.

Parameter	Measurements	Average $[10^{-4}]$
$\mathcal{B}(\Lambda_b^0 \rightarrow J/\psi p K^-)$	LHCb [829]: $3.17 \pm 0.04^{+0.46}_{-0.29}$	$3.17^{+0.46}_{-0.29}$
$\mathcal{B}(\Lambda_b^0 \rightarrow J/\psi \Lambda)$	CDF [830]: $4.7 \pm 2.1 \pm 1.9$	4.7 ± 2.8

Table 224: Production times branching fraction to charmonium.

Parameter	Measurements	Average [10 ⁻⁵]
$f_{A_b} \times \mathcal{B}(\Lambda_b^0 \rightarrow J/\psi \Lambda)$	D0 [831]: $6.01 \pm 0.60 \pm 0.64$	6.01 ± 0.88

Table 225: Λ_b^0 branching fraction ratios, I.

Parameter	Measurements	Average
$\frac{\mathcal{B}(\Lambda_b^0 \rightarrow \psi(2S)\Lambda)}{\mathcal{B}(\Lambda_b^0 \rightarrow J/\psi\Lambda)}$	ATLAS [832]: $0.501 \pm 0.033 \pm 0.019$	0.501 ± 0.038
$\frac{\mathcal{B}(\Lambda_b^0 \rightarrow J/\psi p\pi^-)}{\mathcal{B}(\Lambda_b^0 \rightarrow J/\psi pK^-)}$	LHCb [833]: $0.0824 \pm 0.0025 \pm 0.0042$	0.0824 ± 0.0049
$\frac{\mathcal{B}(\Lambda_b^0 \rightarrow J/\psi \pi^+ \pi^- pK^-)}{\mathcal{B}(\Lambda_b^0 \rightarrow J/\psi pK^-)}$	LHCb [834]: $0.2086 \pm 0.0096 \pm 0.0134$	0.2086 ± 0.0165
$\frac{\mathcal{B}(\Lambda_b^0 \rightarrow \psi(2S)pK^-)}{\mathcal{B}(\Lambda_b^0 \rightarrow J/\psi pK^-)}$	LHCb [834]: $0.2070 \pm 0.0076 \pm 0.0059$	0.2070 ± 0.0096
$\frac{\mathcal{B}(\Lambda_b^0 \rightarrow \chi_{c1} pK^-)}{\mathcal{B}(\Lambda_b^0 \rightarrow J/\psi pK^-)}$	LHCb [835]: $0.242 \pm 0.014 \pm 0.016$	0.242 ± 0.021
$\frac{\mathcal{B}(\Lambda_b^0 \rightarrow \chi_{c2} pK^-)}{\mathcal{B}(\Lambda_b^0 \rightarrow J/\psi pK^-)}$	LHCb [835]: $0.248 \pm 0.020 \pm 0.017$	0.248 ± 0.026

Table 226: Λ_b^0 branching fraction ratios, II.

Parameter	Measurements	Average
$\frac{\mathcal{B}(\Lambda_b^0 \rightarrow \chi_{c2} pK^-)}{\mathcal{B}(\Lambda_b^0 \rightarrow \chi_{c1} pK^-)}$	LHCb [835]: $1.02 \pm 0.10 \pm 0.05$	1.02 ± 0.11

Table 227: Ξ_b^- and Ω_b^- production times branching fraction ratios to charmonium.

Parameter	Measurements	Average
$\frac{\sigma(\Xi_b^-) \times \mathcal{B}(\Xi_b^- \rightarrow J/\psi \Xi^-)}{\sigma(\Lambda_b^0) \times \mathcal{B}(\Lambda_b^0 \rightarrow J/\psi \Lambda)}$	CDF [47]: $0.167^{+0.037}_{-0.025} \pm 0.012$	$0.167^{+0.039}_{-0.028}$
$\frac{\sigma(\Omega_b^-) \times \mathcal{B}(\Omega_b^- \rightarrow J/\psi \Omega^-)}{\sigma(\Lambda_b^0) \times \mathcal{B}(\Lambda_b^0 \rightarrow J/\psi \Lambda)}$	CDF [47]: $0.045^{+0.017}_{-0.012} \pm 0.004$	$0.045^{+0.017}_{-0.013}$

Table 228: Transverse polarization in Λ_b^0 decays to charmonium.

Parameter	Measurements	Average
$\mathcal{P}_b(\Lambda_b^0 \rightarrow J/\psi \Lambda)$	LHCb [836]: $0.06 \pm 0.07 \pm 0.02$ CMS [837]: $0.00 \pm 0.06 \pm 0.06$	0.03 ± 0.06

Table 229: Parity-violating asymmetry in Λ_b^0 decays to charmonium.

Parameter	Measurements	Average
$\alpha_b(\Lambda_b^0 \rightarrow J/\psi \Lambda)$	LHCb [836]: $0.05 \pm 0.17 \pm 0.07$ CMS [837]: $-0.14 \pm 0.14 \pm 0.10$ ATLAS [838]: $0.30 \pm 0.16 \pm 0.06$	0.07 ± 0.10

7.6.3 Decays to charm baryons

Averages of b baryons decays to charm baryons are shown in Tables 230–234.

Table 230: Λ_b branching fractions.

Parameter	Measurements	Average [10^{-2}]
$\mathcal{B}(\Lambda_b^0 \rightarrow \Lambda_c^+ \pi^-)$	LHCb [50]: $0.430 \pm 0.003^{+0.036}_{-0.035}$	$0.430^{+0.036}_{-0.035}$
$\mathcal{B}(\Lambda_b^0 \rightarrow \Lambda_c^+ \pi^+ \pi^- \pi^-)$	CDF [839]: $2.68 \pm 0.29^{+1.15}_{-1.09}$	$2.68^{+1.19}_{-1.12}$

Table 231: Branching fraction ratios, I.

Parameter	Measurements	Average
$\frac{\mathcal{B}(\Lambda_b^0 \rightarrow \Lambda_c^+ \pi^-)}{\mathcal{B}(\bar{B}^0 \rightarrow D^+ \pi^-)}$	CDF [840]: $3.3 \pm 0.3 \pm 1.2$	3.3 ± 1.2
$\frac{\mathcal{B}(\Lambda_b^0 \rightarrow \Lambda_c^+ \pi^+ \pi^- \pi^-)}{\mathcal{B}(\Lambda_b^0 \rightarrow \Lambda_c^+ \pi^-)}$	LHCb [637]: $1.43 \pm 0.16 \pm 0.13$ CDF [839]: $3.04 \pm 0.33^{+0.70}_{-0.55}$	1.58 ± 0.20
$\frac{\mathcal{B}(\Xi_b^0 \rightarrow \Lambda_c^+ K^-) \times \mathcal{B}(\Lambda_c^+ \rightarrow p K^- \pi^+)}{\mathcal{B}(\Xi_b^0 \rightarrow D^0 p K^-) \times \mathcal{B}(D^0 \rightarrow K^+ \pi^-)}$	LHCb [828]: $0.57 \pm 0.22 \pm 0.21$	0.57 ± 0.30
$\frac{\mathcal{B}(\Lambda_b^0 \rightarrow \Lambda_c(2860)^+ \pi^-) \times \mathcal{B}(\Lambda_c(2860)^+ \rightarrow D^0 p)}{\mathcal{B}(\Lambda_b^0 \rightarrow \Lambda_c(2880)^+ \pi^-) \times \mathcal{B}(\Lambda_c(2880)^+ \rightarrow D^0 p)}$	LHCb [841]: $4.51^{+0.51}_{-0.39}{}^{+0.21}_{-0.45}$	$4.51^{+0.55}_{-0.59}$
$\frac{\mathcal{B}(\Lambda_b^0 \rightarrow \Lambda_c(2940)^+ \pi^-) \times \mathcal{B}(\Lambda_c(2940)^+ \rightarrow D^0 p)}{\mathcal{B}(\Lambda_b^0 \rightarrow \Lambda_c(2880)^+ \pi^-) \times \mathcal{B}(\Lambda_c(2880)^+ \rightarrow D^0 p)}$	LHCb [841]: $0.83^{+0.31}_{-0.10}{}^{+0.18}_{-0.43}$	$0.83^{+0.36}_{-0.45}$

Table 232: Branching fraction ratios, II.

Parameter	Measurements	Average [10^{-2}]
$\frac{\mathcal{B}(\Lambda_b^0 \rightarrow \Lambda_c^+ K^-)}{\mathcal{B}(\Lambda_b^0 \rightarrow \Lambda_c^+ \pi^-)}$	LHCb [828]: $7.31 \pm 0.16 \pm 0.16$	7.31 ± 0.23
$\frac{\mathcal{B}(\Lambda_b^0 \rightarrow \Lambda_c^+ D^-)}{\mathcal{B}(\Lambda_b^0 \rightarrow \Lambda_c^+ D_s^-)}$	LHCb [725]: $4.2 \pm 0.3 \pm 0.3$	4.2 ± 0.4
$\frac{\mathcal{B}(\Lambda_b^0 \rightarrow \Lambda_c^+ p\bar{p}\pi^-)}{\mathcal{B}(\Lambda_b^0 \rightarrow \Lambda_c^+ \pi^-)}$	LHCb [842]: $5.40 \pm 0.23 \pm 0.32$	5.40 ± 0.39
$\frac{\mathcal{B}(\Lambda_b^0 \rightarrow \Sigma_c(2455)^0 p\bar{p}) \times \mathcal{B}(\Sigma_c(2455)^0 \rightarrow \Lambda_c^+ \pi^-)}{\mathcal{B}(\Lambda_b^0 \rightarrow \Lambda_c^+ p\bar{p}\pi^-)}$	LHCb [842]: $8.9 \pm 1.5 \pm 0.6$	8.9 ± 1.6
$[\mathcal{B}(\Lambda_b^0 \rightarrow \Sigma_c(2520)^{*0} p\bar{p}) \times \mathcal{B}(\Sigma_c(2520)^{*0} \rightarrow \Lambda_c^+ \pi^-)] / \mathcal{B}(\Lambda_b^0 \rightarrow \Lambda_c^+ p\bar{p}\pi^-)$	LHCb [842]: $11.9 \pm 2.0 \pm 1.4$	11.9 ± 2.4

Table 233: Branching fraction ratios, III.

Parameter	Measurements	Average
$[\mathcal{B}(\Lambda_b^0 \rightarrow \Lambda_c(2595)^+ \pi^-) \times \mathcal{B}(\Lambda_c(2595)^+ \rightarrow \Lambda_c^+ \pi^+ \pi^-)] / \mathcal{B}(\Lambda_b^0 \rightarrow \Lambda_c^+ \pi^+ \pi^- \pi^-)$	LHCb [637]: $0.044 \pm 0.017^{+0.006}_{-0.004}$	$0.044^{+0.018}_{-0.017}$
$[\mathcal{B}(\Lambda_b^0 \rightarrow \Lambda_c(2625)^+ \pi^-) \times \mathcal{B}(\Lambda_c(2625)^+ \rightarrow \Lambda_c^+ \pi^+ \pi^-)] / \mathcal{B}(\Lambda_b^0 \rightarrow \Lambda_c^+ \pi^+ \pi^- \pi^-)$	LHCb [637]: $0.043 \pm 0.015 \pm 0.004$	0.043 ± 0.016
$[\mathcal{B}(\Lambda_b^0 \rightarrow \Sigma_c^0 \pi^+ \pi^-) \times \mathcal{B}(\Sigma_c^0 \rightarrow \Lambda_c^+ \pi^-)] / \mathcal{B}(\Lambda_b^0 \rightarrow \Lambda_c^+ \pi^+ \pi^- \pi^-)$	LHCb [637]: $0.074 \pm 0.024 \pm 0.012$	0.074 ± 0.027
$[\mathcal{B}(\Lambda_b^0 \rightarrow \Sigma_c^{++} \pi^- \pi^-) \times \mathcal{B}(\Sigma_c^{++} \rightarrow \Lambda_c^+ \pi^+)] / \mathcal{B}(\Lambda_b^0 \rightarrow \Lambda_c^+ \pi^+ \pi^- \pi^-)$	LHCb [637]: $0.042 \pm 0.018 \pm 0.007$	0.042 ± 0.019

 Table 234: Ξ_b branching fractions.

Parameter	Measurements	Average $[10^{-4}]$
$\frac{f_{\Xi_b^-}}{f_{\Lambda_b^0}} \times \mathcal{B}(\Xi_b^- \rightarrow \Lambda_b^0 \pi^-)$	LHCb [843]: $5.7 \pm 1.8^{+0.8}_{-0.9}$	$5.7^{+2.0}_{-2.0}$

7.6.4 Decays to other (XYZ) states

Averages of b baryons decays to other (XYZ) states are shown in Table 235.

Table 235: Branching fraction ratios involving pentaquarks.

Parameter	Measurements	Average
$\frac{\mathcal{B}(\Lambda_b^0 \rightarrow \pi^- P_c(4380)^+)}{\mathcal{B}(\Lambda_b^0 \rightarrow K^- P_c(4380)^+)}$	LHCb [844]: $0.050 \pm 0.016^{+0.036}_{-0.030}$	$0.050^{+0.039}_{-0.034}$
$\frac{\mathcal{B}(\Lambda_b^0 \rightarrow \pi^- P_c(4450)^+)}{\mathcal{B}(\Lambda_b^0 \rightarrow K^- P_c(4450)^+)}$	LHCb [844]: $0.033^{+0.016}_{-0.014} {}^{+0.014}_{-0.013}$	$0.033^{+0.021}_{-0.019}$
$\frac{\mathcal{B}(\Lambda_b^0 \rightarrow \pi^- P_c(4380)^+)}{\mathcal{B}(\Lambda_b^0 \rightarrow K^- J/\psi p)}$	LHCb [844]: $0.051 \pm 0.015^{+0.026}_{-0.016}$	$0.051^{+0.030}_{-0.022}$
$\frac{\mathcal{B}(\Lambda_b^0 \rightarrow \pi^- P_c(4450)^+)}{\mathcal{B}(\Lambda_b^0 \rightarrow K^- J/\psi p)}$	LHCb [844]: $0.016^{+0.008}_{-0.006} {}^{+0.006}_{-0.005}$	$0.016^{+0.010}_{-0.008}$
$\frac{\mathcal{B}(\Lambda_b^0 \rightarrow p Z_c(4200)^-)}{\mathcal{B}(\Lambda_b^0 \rightarrow K^- J/\psi p)}$	LHCb [844]: $0.077 \pm 0.028^{+0.034}_{-0.040}$	$0.077^{+0.044}_{-0.049}$

8 B decays to charmless final states

This section provides branching fractions (BF), polarization fractions, partial rate asymmetries (A_{CP}) and other observables of B decays to final states that do not contain charm hadrons or charmonia mesons. The order of entries in the tables corresponds to that in PDG2017 [5], and the quoted RPP numbers are the PDG numbers of the corresponding branching fractions. The asymmetry is defined as

$$A_{CP} = \frac{N_b - N_{\bar{b}}}{N_b + N_{\bar{b}}}, \quad (227)$$

where N_b ($N_{\bar{b}}$) is the number of hadrons containing a b (\bar{b}) quark decaying into a specific final state. This definition is consistent with that of Eq. (105) in Sec. 5.2.1. Four different B^0 and B^+ decay categories are considered: charmless mesonic (*i.e.*, final states containing only mesons), baryonic (only hadrons, but including a baryon-antibaryon pair), radiative (including a photon or a lepton-antilepton pair) and semileptonic/leptonic (including/only leptons). We also include measurements of B_s^0 , B_c^+ and b -baryon decays. Measurements supported with written documents are accepted in the averages; written documents include journal papers, conference contributed papers, preprints or conference proceedings. In all the tables of this section, values in red (blue) are new published (preliminary) results since PDG2017. Results from A_{CP} measurements obtained from time-dependent analyses are listed and described in Sec. 5.

Most of the branching fractions from *BABAR* and Belle assume equal production of charged and neutral B pairs. The best measurements to date show that this is still a reasonable approximation (see Sec. 4). For branching fractions, we provide either averages or the most stringent upper limits. If one or more experiments have measurements with a significance of more than three standard deviations (σ) for a decay channel, all available central values for that channel are used in the averaging. The most stringent limit will be used for branching fractions that do not satisfy this criterion. For A_{CP} we provide averages in all cases. At the end of some of the tables we give a list of results that were not included. Typical cases are the measurements of distributions, such as differential branching fractions or longitudinal polarizations, which are measured in different binning schemes by the different collaborations, and thus cannot be directly used to obtain averages.

Our averaging is performed by maximizing the likelihood, $\mathcal{L} = \prod_i \mathcal{P}_i(x)$, where \mathcal{P}_i is the probability density function (PDF) of the i^{th} measurement, and x is, *e.g.*, the branching fraction or A_{CP} . The PDF is modelled by an asymmetric Gaussian function with the measured central value as its most probable value and the quadratic sum of the statistical and systematic errors as the standard deviation. The experimental uncertainties are considered to be uncorrelated with each other when the averaging is performed. As mentioned in Sec. 3, no error scaling is applied when the fit χ^2 is greater than 1, except for cases of extreme disagreement (at present we have no such cases).

The largest improvement since the last report has come from the inclusion of a variety of new measurements from the LHC, especially LHCb. The measurements of B_s^0 decays are particularly noteworthy.

Sections 8.1 and 8.2 provide compilations of branching fractions of B^0 and B^+ to mesonic and baryonic charmless final states, respectively, while Sec. 8.3 gives branching fractions of b -baryon decays. In Secs. 8.4 and 8.5 various observables of interest are given in addition to branching

fractions: in the former, branching fractions of B_s^0 -meson charmless decays, and in the latter observables related to leptonic and radiative B^0 and B^+ meson decays, including processes in which the photon yields a pair of charged or neutral leptons. Section 8.5 also reports limits from searches for lepton-flavor/number-violating decays. Sections 8.6 and 8.7 give CP asymmetries and results of polarization measurements, respectively, in various b -hadron charmless decays. Finally, Sec. 8.8 gives branching fractions of B_c^+ meson decays to charmless final states.

8.1 Mesonic decays of B^0 and B^+ mesons

This section provides branching fractions of charmless mesonic decays: Tables 236 to 239 for B^+ and Tables 240 to 244 for B^0 mesons. The tables are separated according to the presence or absence of strange mesons in the final state. Finally, Table 245 details several relative branching fractions of B^0 decays.

Figure 69 gives a graphic representation of a selection of high-precision branching fractions given in this section. Footnote symbols indicate that the footnote in the corresponding table should be consulted.

Table 236: Branching fractions of charmless mesonic B^+ decays with strange mesons (part 1) in units of $\times 10^{-6}$. Upper limits are at 90% CL. Where values are shown in red (blue), this indicates that they are new published (preliminary) results since PDG2017.

RPP #	Mode	PDG2017 Avg.	B_{BABAR}	Belle	CLEO	CDF	LHCb	Our Avg.
327	$K^0\pi^+$	23.7 ± 0.8	$23.9 \pm 1.1 \pm 1.0$	[397]	$23.97 \pm 0.53 \pm 0.71$ [845]	$18.8^{+3.7+2.1}_{-3.3-1.8}$	[846]	23.79 ± 0.75
328	$K^+\pi^0$	12.9 ± 0.5	$13.6 \pm 0.6 \pm 0.7$	[847]	$12.62 \pm 0.31 \pm 0.56$ [845]	$12.9^{+2.4+1.2}_{-2.2-1.1}$	[846]	$12.94^{+0.52}_{-0.51}$
329	ηK^+	70.6 ± 2.5	$71.5 \pm 1.3 \pm 3.2$	[848]	$69.2 \pm 2.2 \pm 3.7$	[849]		70.6 ± 2.7
330	$\eta' K^{*+}$	$4.8^{+1.8}_{-1.6}$	$4.8^{+1.6}_{-1.4} \pm 0.8$	[850]	< 2.9	[851]		$4.8^{+1.8}_{-1.6}$
331	$\eta' K_0^*(1430)^+$	5.2 ± 2.1	$5.2 \pm 1.9 \pm 1.0$	[850]				5.2 ± 2.1
332	$\eta' K_2^*(1430)^+$	28 ± 5	$28.0^{+4.6}_{-4.3} \pm 2.6$	[850]				$28.0^{+5.3}_{-5.0}$
333	ηK^+	2.4 ± 0.4	$2.94^{+0.39}_{-0.34} \pm 0.21$	[848]	$2.12 \pm 0.23 \pm 0.11$ [852]	$2.2^{+2.8}_{-2.2}$	[853]	$2.36^{+0.22}_{-0.21}$
334	ηK^{*+}	19.3 ± 1.6	$18.9 \pm 1.8 \pm 1.3$	[854]	$19.3^{+2.0}_{-1.9} \pm 1.5$ [855]	$26.4^{+9.6}_{-8.2} \pm 3.3$ [853]		19.3 ± 1.6
335	$\eta K_0^*(1430)^+$	18 ± 4	$18.2 \pm 2.6 \pm 2.6$	[854]				18.2 ± 3.7
336	$\eta K_2^*(1430)^+$	9.1 ± 3.0	$9.1 \pm 2.7 \pm 1.4$	[854]				9.1 ± 3.0
337	$\eta(1295)K^+ \dagger$	$2.9^{+0.8}_{-0.7}$	$2.9^{+0.8}_{-0.7} \pm 0.2 \dagger$	[856]				$2.9^{+0.8}_{-0.7}$
339	$\eta(1405)K^+ \dagger$	< 1.2	< 1.2	[856]				< 1.2
340	$\eta(1475)K^+ \dagger$	$13.8^{+2.1}_{-1.8}$	$13.8^{+1.8+1.0}_{-1.7-0.6}$	[856]				$13.8^{+2.1}_{-1.8}$
341	$f_1(1285)K^+$	< 2.0	< 2.0	[856]				< 2.0
342	$f_1(1420)K^+ \dagger$	< 2.9	< 2.9	[856]				< 2.9
344	$\phi(1680)K^+ \dagger$	< 3.4	< 3.4	[856]				< 3.4
345	$f_0(1500)K^+$	3.7 ± 2.2	$3.7 \pm 2.2 \S$	[266, 273]				3.7 ± 2.2
346	ωK^+	6.5 ± 0.4	$6.3 \pm 0.5 \pm 0.3$	[857]	$6.8 \pm 0.4 \pm 0.4$ [387]	$3.2^{+2.4}_{-1.9} \pm 0.8$ [858]		6.5 ± 0.4
347	ωK^{*+}	< 7.4	< 7.4	[859]				< 7.4
348	$\omega(K\pi)^{*+}$	28 ± 4	$27.5^{+3.0}_{-2.6}$	[859]				$27.5^{+3.0}_{-2.6}$
349	$\omega K_0^*(1430)^+$	24 ± 5	$24.0 \pm 2.6 \pm 4.4$	[859]				24.0 ± 5.1
350	$\omega K_2^*(1430)^+$	21 ± 4	$21.5 \pm 3.6 \pm 2.4$	[859]				21.5 ± 4.3
351	$a_0(980)^+K^0 \dagger$	< 3.9	< 3.9	[860]				< 3.9
352	$a_0(980)^+K^+ \dagger$	< 2.5	< 2.5	[860]				< 2.5
353	$K^{*0}\pi^+$	10.1 ± 0.9	$10.8 \pm 0.6^{+1.2}_{-1.4}$	[273]	$9.7 \pm 0.6^{+0.8}_{-0.9}$	[271]		$10.1^{+0.8}_{-0.9}$
354	$K^{*+}\pi^0$	8.2 ± 1.9	$8.2 \pm 1.5 \pm 1.1$	[861]				8.2 ± 1.8
355	$K^{+}\pi^{+}\pi^{-}$	51 ± 2.9	$54.4 \pm 1.1 \pm 4.6$	[273]	$48.8 \pm 1.1 \pm 3.6$	[271]		51.0 ± 3.0
356	$K^{+}\pi^{+}\pi^{-} (NR)$	$16.3^{+2.1}_{-1.5}$	$9.3 \pm 1.0^{+6.9}_{-1.7}$	[273]	$16.9 \pm 1.3^{+1.7}_{-1.6}$	[271]		16.3 ± 2.0
357	$\omega(782)K^+ (K^+\pi^+\pi^-)$	6 ± 9	$5.9^{+8.8+0.5}_{-9.0-0.4}$	[273]				$5.9^{+8.8}_{-9.0}$
358	$f_0(980)K^+ (K^+\pi^+\pi^-)^\dagger$	$9.4^{+1.0}_{-1.2}$	$10.3 \pm 0.5^{+2.0}_{-1.4}$	[273]	$8.8 \pm 0.8^{+0.9}_{-1.8}$	[271]		$9.4^{+0.9}_{-1.0}$
359	$f_2(1270)^0K^+ (K^+\pi^+\pi^-)$	1.07 ± 0.27	$0.88^{+0.38+0.01}_{-0.33-0.03}$	[273]	$1.33 \pm 0.30^{+0.23}_{-0.34}$	[271]		1.07 ± 0.29
360	$f_0(1370)^0K^+ (K^+\pi^+\pi^-)^\dagger$	< 10.7	< 10.7	[272]				< 10.7
361	$\rho(1450)^0K^+ (K^+\pi^+\pi^-)$	< 11.7	< 11.7	[272]				< 11.7
362	$f_2'(1525)K^+ (K^+\pi^+\pi^-)$	< 3.4	< 3.4	[272]				< 3.4
363	$\rho^0 K^+ (K^+\pi^+\pi^-)$	3.7 ± 0.5	$3.56 \pm 0.45^{+0.57}_{-0.46}$	[273]	$3.89 \pm 0.47^{+0.43}_{-0.41}$	[271]		$3.74^{+0.49}_{-0.45}$

Results for LHCb are relative BFs converted to absolute BFs.

CLEO upper limits that have been greatly superseded are not shown.

[†] In this product of BFs, all daughter BFs not shown are set to 100%.

[‡] The value quoted is $\mathcal{B}(B^+ \rightarrow \eta(1295)K^+) \times \mathcal{B}(\eta(1295) \rightarrow \eta\pi\pi)$.

[§] Average of results in $K_S^0 K^+ K^-$, $K_S^0 K_S^0 K^+$ [266] and $K^+ \pi^+ \pi^-$ [273]. Includes an f_X resonance with parameters that are compatible with $f_0(1500)$.

Table 237: Branching fractions of charmless mesonic B^+ decays with strange mesons (part 2) in units of $\times 10^{-6}$. Upper limits are at 90% CL. Where values are shown in red (blue), this indicates that they are new published (preliminary) results since PDG2017.

RPP #	Mode	PDG2017 Avg.	BABAR	Belle	CLEO	CDF	LHCb	Our Avg.
364	$K_0^*(1430)^0\pi^+(K^+\pi^+\pi^-)$	45^{+9}_{-7}	$32.0 \pm 1.2^{+0.8}_{-6.0}$ [273]	$51.6 \pm 1.7^{+7.0}_{-7.5}$ [271]				45.1 ± 6.3
365	$K_2^*(1430)^0\pi^+(K^+\pi^+\pi^-)$	$5.6^{+2.2}_{-1.5}$	$5.6 \pm 1.2^{+1.8}_{-0.8}$ [273]	< 6.9 [267]				$5.6^{+2.2}_{-1.4}$
366	$K^*(1410)^0\pi^+(K^+\pi^+\pi^-)$	< 45		< 45 [267]				< 45
367	$K^*(1680)^0\pi^+(K^+\pi^+\pi^-)$	< 12	< 15 [272]	< 12 [267]				< 12
368	$K^+\pi^0\pi^0$	16.2 ± 1.9	$16.2 \pm 1.2 \pm 1.5$ [861]					16.2 ± 1.9
369	$f_0(980)K^+(K^+\pi^0\pi^0)$	2.8 ± 0.8	$2.8 \pm 0.6 \pm 0.5$ [861]					2.8 ± 0.8
370	$K^-\pi^+\pi^+$	< 0.046	< 0.95 [862]	< 4.5				< 0.046
371	$K^-\pi^+\pi^+ (NR)$	< 56						< 56
372	$K_1(1270)^0\pi^+$	< 40	< 40 [416]					< 40
373	$K_1(1400)^0\pi^+$	< 39	< 39 [416]					< 39
374	$K^0\pi^+\pi^0$	< 66						< 66
375	$\rho^+K^0(K^0\pi^+\pi^0)$	8.0 ± 1.5	$8.0^{+1.4}_{-1.3} \pm 0.6$ [867]					$8.0^{+1.5}_{-1.4}$
376	$K^{*+}\pi^+\pi^-$	75 ± 10	$75.3 \pm 6.0 \pm 8.1$ [868]					75.3 ± 10.1
377	$K^{*+}\rho^0$	4.6 ± 1.1	$4.6 \pm 1.0 \pm 0.4$ [869]					4.6 ± 1.1
378	$f_0(980)K^{*+} \dagger$	4.2 ± 0.7	$4.2 \pm 0.6 \pm 0.3$ [869]					4.2 ± 0.7
379	$a_1^+K^0$	35 ± 7	$34.9 \pm 5.0 \pm 4.4$ [870]					34.9 ± 6.7
380	$b_1^+K^0 \dagger$	9.6 ± 1.9	$9.6 \pm 1.7 \pm 0.9$ [871]					9.6 ± 1.9
381	$K^{*0}\rho^+$	9.2 ± 1.5	$9.6 \pm 1.7 \pm 1.5$ [872]					9.2 ± 1.5
382	$K_1(1400)^+\rho^0$	< 780	< 780 ¶ [874]					< 780 ¶
383	$K_2(1430)^+\rho^0$	< 1500	< 1500 ¶ [874]					< 1500 ¶
384	$b_1^0K^{*+} \dagger$	9.1 ± 2.0	$9.1 \pm 1.7 \pm 1.0$ [875]					9.1 ± 2.0
385	$b_1^+K^{*0} \dagger$	< 5.9	< 5.9 [876]					< 5.9
386	$b_1^0K^{*+} \dagger$	< 6.7	< 6.7 [876]					< 6.7
387	$K^+\overline{K}^0$	1.31 ± 0.17	$1.61 \pm 0.44 \pm 0.09$ [397]	$1.11 \pm 0.19 \pm 0.05$ [845]				$1.52 \pm 0.21 \pm 0.05$ [877]
388	$\overline{K}^0K^+\pi^0$	< 24						< 24
389	$K^+K_SK_S$	10.8 ± 0.6	$10.6 \pm 0.5 \pm 0.3$ [266]					< 24
390	$f_0(980)K^+(K^+K_SK_S)$	14.7 ± 3.3	$14.7 \pm 2.8 \pm 1.8$ [266]					10.62 ± 0.44
391	$f_0(1710)K^+(K^+K_SK_S)$	$0.48^{+0.40}_{-0.26}$	$0.48^{+0.40}_{-0.24} \pm 0.11$ [266]					14.7 ± 3.3
392	$K^+K_SK_S (NR)$	20 ± 4	$19.8 \pm 3.7 \pm 2.5$ [266]					$0.48^{+0.41}_{-0.26}$
393	$K_SK_S\pi^+$	< 0.51	< 0.51 [879]					19.8 ± 4.5
394	$K^+K^-\pi^+$	5.0 ± 0.7	$5.0 \pm 0.5 \pm 0.5$ [880]					< 0.51
395	$K^+K^-\pi^+ (NR)$	< 75						5.24 ± 0.42
396	$\overline{K}^{*0}K^+ (K^+K^-\pi^+)$	< 1.1	< 1.1 [882]					< 1.1
397	$\overline{K}_0^*(1430)^0K^+ (K^+K^-\pi^+)$	< 2.2	< 2.2 [882]					< 2.2
398	$K^+K^+\pi^-$	< 0.011	< 0.16 [862]					< 0.011
399	$K^+K^+\pi^- (NR)$	< 87.9						< 87.9

Results for CDF and LHCb are relative BFs converted to absolute BFs.

CLEO upper limits that have been greatly superseded are not shown.

† In this product of BFs, all daughter BFs not shown are set to 100%.

¶ Result from ARGUS. Cited in the BABAR column to avoid adding a column to the table.

Table 238: Branching fractions of charmless mesonic B^+ decays with strange mesons (part 3) in units of $\times 10^{-6}$. Upper limits are at 90% CL. Where values are shown in red (blue), this indicates that they are new published (preliminary) results since PDG2017.

RPP#	Mode	PDG2017 Avg.	BABAR	Belle	CLEO	CDF	LHCb	Our Avg.
400	$f'_2(1525)K^+$	1.8 ± 0.5	1.8 ± 0.5 [†]	[266]	< 8	[267]	1.8 ± 0.5	
401	$f_J(2220)K^+$	< 1.2		< 1.2	[883]	< 1.2		
402	$K^{*+}\pi^+K^-$	< 11.8	< 11.8	[868]	0.77 _{-0.30} ^{+0.35} ± 0.12	[885]	< 11.8	
403	$K^{*+}K^{*0}$	0.91 ± 0.29	1.2 ± 0.5 ± 0.1	[884]	0.91 _{-0.28} ^{+0.31}		0.91 _{-0.28} ^{+0.31}	
404	$K^{*+}K^+\pi^-$	< 6.1	< 6.1	[888]	< 6.1		< 6.1	
405	$K^+K^-K^+$	34.0 ± 1.4	34.6 ± 0.6 ± 0.9	[266]	30.6 ± 1.2 ± 2.3	[267]	34.0 ± 1.0	
406	$\phi K^+(K^+K^-K^+)$	8.8 _{-0.6} ^{+0.7}	9.2 ± 0.4 _{-0.5} ^{+0.7}	[266]	9.6 ± 0.9 _{-0.8} ^{+1.1}	[267]	8.8 ± 0.5	
407	$f_0(980)K^+(K^+K^-K^+)$	9.4 ± 3.2	9.4 _{-2.8} ^{+1.6}	[266]	< 1.1	[267]	9.4 _{-2.8} ^{+1.6}	
408	$a_2(1320)K^+(K^+K^-K^+)$	< 1.1		< 1.1			< 1.1	
409	$X_0(1550)K^+(K^+K^-K^+)$	4.3 ± 0.7	4.3 ± 0.60 ± 0.30	[888]	4.3 ± 0.60 ± 0.30	[888]	4.30 ± 0.67	
410	$\phi(1680)K^+(K^+K^-K^+)$	< 0.8		< 0.8			< 0.8	
411	$f_0(1710)K^+(K^+K^-K^+)$	1.1 ± 0.6	1.12 ± 0.25 ± 0.50	[266]	1.12 ± 0.25 ± 0.50	[266]	1.12 ± 0.56	
412	$K^+K^-K^+(NR)$	23.8 _{-5.0} ^{+2.8}	22.8 ± 2.7 ± 7.6	[266]	22.8 ± 2.7 ± 7.6	[266]	23.8 _{-6.1} ^{+2.9}	
413	$K^{*+}K^+K^-$	36 ± 5	36.2 ± 3.3 ± 3.6	[868]	36.2 ± 3.3 ± 3.6	[868]	36.2 ± 4.9	
414	ϕK^{*+}	10.0 ± 2.0	11.2 ± 1.0 ± 0.9	[890]	11.2 ± 1.0 ± 0.9	[890]	10.0 ± 1.1	
415	$\phi(K\pi)_0^{*+}$	8.3 ± 1.6	8.3 _{-0.8} ^{+1.4}	[891]	8.3 _{-0.8} ^{+1.4}	[891]	8.3 _{-0.8} ^{+1.4}	
416	$\phi K_1(1270)^+$	6.1 ± 1.9	6.1 ± 1.6 ± 1.1	[891]	6.1 ± 1.6 ± 1.1	[891]	6.1 ± 1.9	
417	$\phi K_1(1400)^+$	< 3.2	< 3.2	[891]	< 3.2	[891]	< 3.2	
418	$\phi K^*(1410)^+$	< 4.3	< 4.3	[891]	< 4.3	[891]	< 4.3	
419	$\phi K_0^*(1430)^+$	7.0 ± 1.6	7.0 ± 1.3 ± 0.9	[891]	7.0 ± 1.3 ± 0.9	[891]	7.0 ± 1.6	
420	$\phi K_2^*(1430)^+$	8.4 ± 2.1	8.4 ± 1.8 ± 1.0	[891]	8.4 ± 1.8 ± 1.0	[891]	8.4 ± 2.1	
421	$\phi K_2(1770)^+$	< 15	< 15	[891]	< 15	[891]	< 15	
422	$\phi K_2(1820)^+$	< 16.3	< 16.3	[891]	< 16.3	[891]	< 16.3	
423	$a_1^{+}K^{*0}$	< 3.6	< 3.6	[892]	< 3.6	[892]	< 3.6	
424	$\phi\phi K^+ \S$	5.0 ± 1.2	5.6 ± 0.5 ± 0.3	[893]	5.6 ± 0.5 ± 0.3	[893]	5.0 ± 0.5	
425	$\eta/\eta' K^+$	< 25	< 25	[894]	< 25	[894]	< 25	
426	$K^+\omega\phi$	< 1.9	< 1.9	[895]	< 1.9	[895]	< 1.9	
427	$K^+X(1812)^{\dagger}$	< 0.32	< 0.32	[895]	< 0.32	[895]	< 0.32	

Results for CDF and LHCb are relative BFs converted to absolute BFs.

CLEO upper limits that have been greatly superseded are not shown.

[†] In this product of BFs, all daughter BFs not shown are set to 100%.

[‡] Average of results in $K_S^0 K^+ K^-$, $K_S^0 K_S^0 K^+$ [266].

$\S M_{\phi\phi} < 2.85 \text{ GeV}/c^2$.

Table 239: Branching fractions of charmless mesonic B^+ decays without strange mesons in units of $\times 10^{-6}$. Upper limits are at 90% CL. Where values are shown in red (blue), this indicates that they are new published (preliminary) results since PDG2017.

RPP #	Mode	PDG2017 Avg.	BABAR	Belle	CLEO	CDF	LHCb	Our Avg.
446	$\pi^+\pi^0$	5.5 ± 0.4	5.02 ± 0.46 ± 0.29 [847]	5.86 ± 0.26 ± 0.38 [845]	4.6 ^{+1.8+0.6} _{-1.6-0.7} [846]			5.48 ^{+0.35} _{-0.34}
447	$\pi^+\pi^-\pi^-$	15.2 ± 1.4	15.2 ± 0.6 ± 1.3 [896]					15.2 ± 1.4
448	$\rho\pi^+$	8.3 ± 1.2	8.1 ± 0.7 ^{+1.3} _{-1.6} [896]	8.0 ^{+2.3} _{-2.0} ± 0.7 [897]	10.4 ^{+3.3} _{-3.4} ± 2.1 [858]			8.3 ^{+1.2} _{-1.3}
449	$f_0(980)\pi^+\dagger$	< 1.5		< 1.5 [896]				< 1.5
450	$f_2(1270)\pi^+$	1.6 ^{+0.7} _{-0.4}	1.57 ± 0.42 ^{+0.55} _{-0.25} [896]					1.57 ^{+0.69} _{-0.49}
451	$\rho(1450)^0\pi^+\dagger$	1.4 ^{+0.6} _{-0.9}	1.4 ± 0.4 ^{+0.5} _{-0.8} [896]					1.4 ^{+0.6} _{-0.9}
452	$f_0(1370)\pi^+\dagger$	< 4.0	< 4.0 [896]					< 4.0
454	$\pi^+\pi^-\pi^+(NR)$	5.3 ^{+1.5} _{-1.1}	5.3 ± 0.7 ^{+1.3} _{-0.8} [896]					5.3 ^{+1.5} _{-1.1}
455	$\pi^+\pi^0\pi^0$	< 890	< 890 [†] [898]					< 890 [‡]
456	$\rho^+\pi^0$	10.9 ± 1.4	10.2 ± 1.4 ± 0.9 [899]					10.9 ^{+1.4} _{-1.9}
458	$\rho^+\rho^0$	24.0 ± 1.9	23.7 ± 1.4 ± 1.4 [421]					24.0 ^{+1.9} _{-2.0}
459	$f_0(980)\rho^+\dagger$	< 2.0	< 2.0 [421]					< 2.0
460	$a_1^+\pi^0$	26 ± 7	26.4 ± 5.4 ± 4.1 [902]					26.4 ± 6.8
461	$a_1^0\pi^+$	20 ± 6	20.4 ± 4.7 ± 3.4 [902]					20.4 ± 5.8
462	$\omega\pi^+$	6.9 ± 0.5	6.7 ± 0.5 ± 0.4 [857]					6.9 ± 0.5
463	$\omega\rho^+$	15.9 ± 2.1	15.9 ± 1.6 ± 1.4 [859]					15.9 ± 2.1
464	$\eta\pi^+$	4.02 ± 0.27	4.00 ± 0.40 ± 0.24 [848]	4.07 ± 0.26 ± 0.21 [852]	1.2 ^{+2.8} _{-1.2} [853]			4.02 ± 0.27
465	$\eta\rho^+$	7.0 ± 2.9	9.9 ± 1.2 ± 0.8 [904]	4.1 ^{+1.4} _{-1.3} ± 0.4 [855]	4.8 ^{+5.2} _{-3.8} [853]			6.9 ± 1.0
466	$\eta'\pi^+$	2.7 ± 0.9	3.5 ± 0.6 ± 0.2 [848]	1.8 ^{+0.7} _{-0.6} ± 0.1 [849]	1.0 _{-1.0} ^{+5.8} [853]			2.7 ^{+0.5} _{-0.4}
467	$\eta'\rho^+$	9.7 ± 2.2	9.7 ^{+1.9} _{-1.8} ± 1.1 [850]	< 5.8 [851]				9.7 ^{+2.2} _{-2.1}
468	$\phi\pi^+$	< 0.15	< 0.24 [905]	< 0.33 [906]				< 0.15 [907]
469	$\phi\rho^+$	< 3.0	< 3.0 [908]					< 3.0
470	$a_0(980)^0\pi^+\dagger$	< 5.8	< 5.8 [860]					< 5.8
471	$a_0(980)^+\pi^0\dagger$	< 1.4	< 1.4 [909]					< 1.4
472	$\pi^+\pi^+\pi^-\pi^-$	< 860	< 860 [‡] [898]					< 860 [‡]
473	$\rho^0 a_1(1260)^+$	< 620						< 620
474	$\rho^0 a_2(1320)^+$	< 720						< 720
475	$b_1^0\pi^+\dagger$	6.7 ± 2.0	6.7 ± 1.7 ± 1.0 [875]					6.7 ± 2.0
476	$b_1^+\pi^0\dagger$	< 3.3	< 3.3 [871]					< 3.3
477	$\pi^+\pi^+\pi^-\pi^-$	< 6300	< 6300 [‡] [898]					< 6300 [‡]
478	$b_1^+\rho^0\dagger$	< 5.2	< 5.2 [876]					< 5.2
480	$b_1^0\rho^+\dagger$	< 3.3	< 3.3 [876]					< 3.3

Results for LHCb are relative BF_s converted to absolute BF_s.

CLEO upper limits that have been greatly superseded are not shown.

[†] In this product of BF_s, all daughter BF_s not shown are set to 100%.

[‡] Result from ARGUS. Cited in the BABAR column to avoid adding a column to the table.

Table 240: Branching fractions of charmless mesonic B^0 decays with strange mesons (part 1) in units of $\times 10^{-6}$. Upper limits are at 90% CL. Where values are shown in red (blue), this indicates that they are new published (preliminary) results since PDG2017.

RPP #	Mode	PDG2017 Avg.	BABAR	Belle	CLEO	CDF	LHCb	Our Avg.
257	$K^+\pi^-$	19.6 ± 0.5	$19.1 \pm 0.6 \pm 0.6$ [911]	$20.0 \pm 0.34 \pm 0.60$ [845]	$18.0^{+2.3+1.2}_{-2.1-0.9}$ [846]			$19.57^{+0.53}_{-0.52}$
258	$K^0\pi^0$	9.9 ± 0.5	$10.1 \pm 0.6 \pm 0.4$ [417]	$9.68 \pm 0.46 \pm 0.50$ [845]	$12.8^{+4.0+1.7}_{-3.3-1.4}$ [846]			9.93 ± 0.49
259	$\eta'K^0$	66 ± 4	$68.5 \pm 2.2 \pm 3.1$ [848]	$58.9^{+3.6}_{-3.5} \pm 4.3$ [849]	$89^{+18}_{-16} \pm 9$ [853]			66.1 ± 3.1
260	$\eta'K^{*0}$	2.8 ± 0.6	$3.1^{+0.9}_{-0.8} \pm 0.3$ [850]	$2.6 \pm 0.7 \pm 0.2$ [912]	$7.8^{+7.7}_{-5.7}$ [853]			$2.8^{+0.6}_{-0.5}$
261	$\eta'K_0^*(1430)^0$	6.3 ± 1.6	$6.3 \pm 1.3 \pm 0.9$ [850]					6.3 ± 1.6
262	$\eta'K_2^*(1430)^0$	13.7 ± 3.2	$13.7^{+3.0}_{-1.9} \pm 1.2$ [850]					$13.7^{+3.2}_{-2.2}$
263	ηK^0	$1.23^{+0.27}_{-0.24}$	$1.15^{+0.43}_{-0.38} \pm 0.09$ [848]	$1.27^{+0.33}_{-0.29} \pm 0.08$ [852]	$0.0^{+3.0}_{-0.0}$ [853]			$1.23^{+0.27}_{-0.24}$
264	ηK^{*0}	15.9 ± 1.0	$16.5 \pm 1.1 \pm 0.8$ [854]	$15.2 \pm 1.2 \pm 1.0$ [855]	$13.8^{+5.5}_{-4.6} \pm 1.6$ [853]			15.9 ± 1.0
265	$\eta K_0^*(1430)^0$	11.0 ± 2.2	$11.0 \pm 1.6 \pm 1.5$ [854]					11.0 ± 2.2
266	$\eta K_2^*(1430)^0$	9.6 ± 2.1	$9.6 \pm 1.8 \pm 1.1$ [854]					9.6 ± 2.1
267	ωK^0	4.8 ± 0.4	$5.4 \pm 0.8 \pm 0.3$ [857]	$4.5 \pm 0.4 \pm 0.3$ [387]	$10.0^{+5.4}_{-4.2} \pm 1.4$ [858]			4.8 ± 0.4
268	$a_0(980)^0 K^0$ †	< 7.8	< 7.8 [860]					< 7.8
269	$b_1^0 K^0$ †	< 7.8	< 7.8 [871]					< 7.8
270	$a_0(980)^- K^+$ †	< 1.9	< 1.9 [913]					< 1.9
271	$b_1^- K^+$ †	7.4 ± 1.4	$7.4 \pm 1.0 \pm 1.0$ [875]					7.4 ± 1.4
272	$b_1^0 K^{*0}$ †	< 8.0	< 8.0 [876]					< 8.0
273	$b_1^- K^{*+}$ †	< 5.0	< 5.0 [876]					< 5.0
274	$a_0(1450)^- K^{++}$ †	< 3.1	< 3.1 [913]					< 3.1
275	$K_S X^0$ (Familon) †	< 53			< 53 [914]			< 53
276	ωK^{*0}	2.0 ± 0.5	$2.2 \pm 0.6 \pm 0.2$ [859]	$1.8 \pm 0.7^{+0.3}_{-0.2}$ [915]				2.0 ± 0.5
277	$\omega(K\pi)_0^{*0}$	18.4 ± 2.5	$18.4^{+1.8}_{-1.7}$ [859]					$18.4^{+1.8}_{-1.7}$
278	$\omega K_0^*(1430)^0$	16.0 ± 3.4	$16.0 \pm 1.6 \pm 3.0$ [859]					16.0 ± 3.4
279	$\omega K_2^*(1430)^0$	10.1 ± 2.3	$10.1 \pm 2.0 \pm 1.1$ [859]					10.1 ± 2.3
280	$\omega K^+\pi^-(NR)$ †	5.1 ± 1.0						5.1 ± 1.0
281	$K^+\pi^-\pi^0$	37.8 ± 3.2	$38.5 \pm 1.0 \pm 3.9$ [916]	$5.1 \pm 0.7 \pm 0.7$ [915]				37.8 ± 3.2
282	$\rho^- K^+$	7.0 ± 0.9	$6.6 \pm 0.5 \pm 0.8$ [916]	$36.6^{+4.2}_{-4.3} \pm 3.0$ [917]				7.0 ± 0.9
283	$\rho(1450)^- K^+$	2.4 ± 1.2	$2.4 \pm 1.0 \pm 0.6$ [916]	$15.1^{+3.4+2.4}_{-3.3-2.6}$ [917]				2.4 ± 1.2
284	$\rho(1700)^- K^+$	0.6 ± 0.7	$0.6 \pm 0.6 \pm 0.4$ [916]					0.6 ± 0.7
285	$K^+\pi^-\pi^0$ (NR)	2.8 ± 0.6	$2.8 \pm 0.5 \pm 0.4$ [916]	< 9.4 [917]				2.8 ± 0.6
286	$(K\pi)_0^{**+}\pi^-$	34 ± 5	$34.2 \pm 2.4 \pm 4.1$ [916]					34.2 ± 4.8
287	$(K\pi)_0^{*+}\pi^0$	8.6 ± 1.7	$8.6^{+1.1}_{-1.3}$ [916]					$8.6^{+1.1}_{-1.3}$

Results for LHCb are relative BF_s converted to absolute BF_s.

CLEO upper limits that have been greatly superseded are not shown.

† In this product of BF_s, all daughter BF_s not shown are set to 100%.

$1.0755 < M(K\pi) < 1.250$ GeV/ c^2 .

Table 241: Branching fractions of charmless mesonic B^0 decays with strange mesons (part 2) in units of $\times 10^{-6}$. Upper limits are at 90% CL. Where values are shown in red (blue), this indicates that they are new published (preliminary) results since PDG2017.

RPP #	Mode	PDG2017 Avg.	BABAR	Belle	CLEO	CDF	LHCb	Our Avg.
288	$K_2^*(1430)^0\pi^0$	< 4.0	< 4.0	[918]				< 4.0
289	$K^*(1680)^0\pi^0$	< 7.5	< 7.5	[918]				< 7.5
290	$K^0\pi^0\pi^0$	6.1 ± 1.6	50.2 ± 1.5 ± 1.8	[269]	6.1 ± 1.6 ± 0.5	[919]	6.1 ± 1.6 ± 0.6	6.1 ± 1.6
291	$K^0\pi^+\pi^-$ (NR)	52.0 ± 2.4	14.7 ± 2.6	[269]	47.5 ± 2.4 ± 3.7	[919]	19.9 ± 2.5 ± 1.7	49.4 ± 1.7
292	$\rho^0 K^0$	4.7 ± 0.6	4.4 ± 0.7 ± 0.3	[269]	6.1 ± 1.0 ± 1.1	[919]	8.4 ± 1.1 ± 1.2	14.7 ± 2.0
293	$K^{*+}\pi^-$	8.4 ± 0.8	8.2 ± 0.9 ± 0.3	[269]	8.4 ± 1.1 ± 0.9	[919]	8.4 ± 0.8	8.4 ± 0.8
294	$K_0^*(1430)^+\pi^-$	33 ± 7	29.9 ± 2.3 ± 3.6	[269]	49.7 ± 3.8 ± 6.8	[919]	16 ± 6 ± 2	[866]
295	$K_x^*\pi^-\pi^-$	5.1 ± 1.6			5.1 ± 1.5 ± 0.6	[917]		33.5 ± 3.9
296	$K^*(1410)^+\pi^-$	< 3.8			< 3.8	[919]		5.1 ± 1.6
297	$f_0(980)K^0$ †	7.0 ± 0.9	6.9 ± 0.8 ± 0.6	[269]	7.6 ± 1.7 ± 0.9	[919]		< 3.8
298	$f_2(1270)^0K^0$	2.7 ± 1.3	2.7 ± 1.0 ± 0.9	[269]	< 2.5 †	[919]		7.0 ± 0.9
299	$f_x(1300)^0K^0$	1.8 ± 0.7	1.8 ± 0.55 ± 0.48	[269]				2.7 ± 1.3
300	$K^{*0}\pi^0$	3.3 ± 0.6	3.3 ± 0.5 ± 0.4	[916]	< 3.5	[917]		1.81 ± 0.73
301	$K_2^*(1430)^+\pi^-$	< 6	< 16.2	[918]	< 6.3	[919]		3.3 ± 0.6
302	$K^*(1680)^+\pi^-$	< 10	< 25	[918]	< 10.1	[919]		< 6.3
303	$K^+\pi^-\pi^+\pi^-$	< 230	< 230	[921]	2.8 ± 0.5 ± 0.5	[922]		< 10.1
304	$\rho^0 K^+\pi^-$	2.8 ± 0.7			1.4 ± 0.4 ± 0.3	[922]		< 230
305	$\rho^0 K^+\pi^-$	1.4 ± 0.5			1.4 ± 0.4 ± 0.4	[922]		2.8 ± 0.7
306	$f_0(980)K^+\pi^-$	< 2.1						1.4 ± 0.5
307	$K^+\pi^-\pi^-(NR)$	55 ± 5	54.5 ± 2.9 ± 4.3	[923]				< 0.6
308	$K^{*0}\pi^+\pi^-$	3.9 ± 1.3	5.1 ± 0.6 ± 0.6	[924]	2.1 ± 0.8 ± 0.9	[922]		54.5 ± 5.2
309	$K^{*0}\rho^0$	3.9 ± 1.8	5.7 ± 0.6 ± 0.4	[924]	1.4 ± 0.7 ± 0.5	[922]		3.9 ± 0.8
310	$f_0(980)K^0$ †	< 30	17 ± 6	[416]	1.4 ± 0.5 ± 0.4	[922]		3.9 ± 0.5
311	$K_1(1270)^+\pi^-$	< 27	16 ± 8	[416]				17 ± 6
312	$K_1(1400)^+\pi^-$	16 ± 4	16.3 ± 2.9 ± 2.3	[870]				16 ± 8
313	$a_1^- K^+$	10.3 ± 2.6	10.3 ± 2.3 ± 1.3	[924]				16.3 ± 24
314	$K^{*+}\rho^-$	28 ± 12	28 ± 10 ± 6	[924]				16.3 ± 3.7
315	$K_0(1430)^+\rho^-$	< 3000	28 ± 10 ± 6	[874]				10.3 ± 2.6
316	$K_1(1400)^0\rho^0$	27 ± 6	27 ± 4 ± 4	[924]				28 ± 11
317	$K_8^*(1430)^0\rho^0$	2.7 ± 0.9	2.7 ± 0.7 ± 0.6	[924]				27 ± 5
318	$K_0^*(1430)^0 f_0(980)$	8.6 ± 2.0	8.6 ± 1.7 ± 1.0	[924]				10.3 ± 2.6
319	$K_2^*(1430)^0 f_0(980)$	0.078 ± 0.015	< 0.5	[911]	0.10 ± 0.08 ± 0.04	[845]		2.7 ± 0.9
320	K^+K^-	1.21 ± 0.16	1.08 ± 0.28 ± 0.11	[397]	1.26 ± 0.19 ± 0.05	[845]		8.6 ± 2.0
321	$K^0\bar{K}^0$	6.5 ± 0.8	6.4 ± 1.0 ± 0.6	[927]	3.6 ± 0.33 ± 0.15	[928]		0.0803 ± 0.0147
322	$K^0K^-\pi^+$							0.0803 ± 0.0147
323	$K^{*0}K^\pm$	< 0.96	< 1.9	[930]	0.23 ± 0.10 ± 0.10	[925]	0.0780 ± 0.0127 ± 0.0084	[926]
324	$K^{*0}\bar{K}^0$ †	2.2 ± 0.6			2.17 ± 0.60 ± 0.24	[932]		0.21 ± 0.16
325	$K^+K^-a^0$	< 0.9	< 0.9	[933]				< 0.9
326	$K_S K_S \pi^0$	< 1.0	< 1.0	[933]				< 1.0
327	$K_S K_S \eta$	< 2.0	< 2.0	[933]				< 2.0
328	$K_S K_S \eta'$							
329	$K^+K^-K^0$	24.9 ± 3.1	26.5 ± 0.9 ± 0.8	[266]	28.3 ± 3.3 ± 4.0	[863]		26.8 ± 1.0
330	ϕK^0	7.3 ± 0.7	7.1 ± 0.6 ± 0.4	[266]	9.0 ± 2.6 ± 0.7	[890]	5.4 ± 3.7 ± 0.7	7.3 ± 0.7
331	$f_0(980)K^0$ †	7.0 ± 3.5	7.0 ± 2.6 ± 2.4	[266]				7.0 ± 3.0

Results for CDF and LHCb are relative BF_s converted to absolute BF_s.

CLEO upper limits that have been greatly superseded are not shown.

[†] In this product of BF_s, all daughter BF_s not shown are set to 100%.

[‡] Obtained from a fit to the ratios of BF_s measured by LHCb (Ref. [920]) and to the averages of the BF_s in their numerators, as measured by other experiments (RPP 322 and 329).

[§] Obtained from a fit to the ratios of BF_s measured by LHCb (Ref. [920]) and to the averages of the BF_s therein, as measured by other experiments (excluding the present line).

[¶] Result from DELPHI. Cited in the BABAR column to avoid adding a column to the table.

[§] Result from ARGUS. Cited in the BABAR column to avoid adding a column to the table.

Table 242: Branching fractions of charmless mesonic B^0 decays with strange mesons (part 3) in units of $\times 10^{-6}$. Upper limits are at 90% CL. Where values are shown in red (blue), this indicates that they are new published (preliminary) results since PDG2017.

RPP #	Mode	PDG2017 Avg.	<i>BABAR</i>	Belle	CLEO	CDF	LHCb	Our Avg.
332	$f_0(1500)K^0$ †	13^{+7}_{-5}	$13.3^{+5.8}_{-4.4} \pm 3.2$	[266]				$13.3^{+6.6}_{-5.4}$
333	$f_2'(1525)K^0$	$0.3^{+0.5}_{-0.4}$	$0.29^{+0.27}_{-0.18} \pm 0.36$	[266]				$0.29^{+0.45}_{-0.40}$
334	$f_0(1710)K^0$ †	4.4 ± 0.9	$4.4 \pm 0.7 \pm 0.5$					4.4 ± 0.9
335	$K^0K^+K^-$ (NR)	33 ± 10	$33 \pm 5 \pm 9$	[266]				33 ± 10
336	$K_S K_S K_S$	6.0 ± 0.5	$6.19 \pm 0.48 \pm 0.19$	[385]	$4.2^{+1.6}_{-1.3} \pm 0.8$			6.04 ± 0.50
337	$f_0(980)K_S$ †	2.7 ± 1.8	$2.7^{+1.3}_{-1.2} \pm 1.3$ †	[385]				2.7 ± 1.8
338	$f_0(1710)K_S$ †	$0.50^{+0.50}_{-0.26}$	$0.50^{+0.46}_{-0.24} \pm 0.11$ †	[385]				$0.50^{+0.47}_{-0.26}$
339	$f_0(2010)K_S$ †	0.5 ± 0.6	$0.54^{+0.21}_{-0.20} \pm 0.52$ †	[385]				0.54 ± 0.56
340	$K_S K_S K_S$ (NR)	13.3 ± 3.1	$13.3^{+2.2}_{-2.3} \pm 2.2$	[385]				$13.3^{+3.1}_{-3.2}$
341	$K_S K_S K_L$	< 16	< 16 ‡	[934]				< 16 ‡
342	$K^{*0}K^+K^-$	27.5 ± 2.6	$27.5 \pm 1.3 \pm 2.2$	[923]				27.5 ± 2.6
343	ϕK^{*0}	10.0 ± 0.5	$9.7 \pm 0.5 \pm 0.6$	[390]	$10.4 \pm 0.5 \pm 0.6$	[935]		$10.1^{+0.6}_{-0.5}$
344	$K^+\pi^-\pi^+K^-$ (NR)	< 71.7			< 71.7 ‡	[936]		< 71.7 ‡
345	$K^{*0}\pi^+K^-$	4.5 ± 1.3	$4.6 \pm 1.1 \pm 0.8$	[923]		< 13.9 ‡	[936]	4.6 ± 1.4
346	$K^{*0}\overline{K}^{*0}$	0.8 ± 0.5	$1.28^{+0.35}_{-0.30} \pm 0.11$	[937]	$0.26^{+0.33}_{-0.29} \pm 0.10$	[936]		0.81 ± 0.23
347	$K^+\pi^-K^+\pi^-$ (NR)	< 6.0			< 6.0 ‡	[936]		< 6.0 ‡
348	$K^{*0}K^+\pi^-$	< 2.2	< 2.2	[923]	< 7.6 ‡	[936]		< 2.2
349	$K^{*0}K^{*-}$	< 0.2	< 0.41	[937]	< 0.2	[936]		< 0.2
350	$K^{*+}K^{*-}$	< 2.0	< 2.0	[938]				< 2.0
351	$K_1^*(1400)^0\phi$	< 5000	< 5000 ‡	[874]				< 5000 ‡
352	$(K\pi)_0^{*0}\phi$	4.3 ± 0.4	$4.3 \pm 0.4 \pm 0.4$	[390]	$4.3 \pm 0.4 \pm 0.4$	[935]		4.3 ± 0.4
353	$(K\pi)_0^{*0}\phi$	< 1.7	< 1.7 ‡	[939]				< 1.7 ‡
354	$K_0^*(1430)^0\pi^+K^-$	< 31.8			< 31.8 ‡	[936]		< 31.8 ‡
355	$K_0^*(1430)^0\overline{K}^{*0}$	< 3.3			< 3.3	[936]		< 3.3
356	$K_0^*(1430)^0K^{*0}$	< 8.4			< 8.4	[936]		< 8.4
357	$\phi K_0^*(1430)^0$	3.9 ± 0.8	$3.9 \pm 0.5 \pm 0.6$	[390]	$4.3 \pm 0.4 \pm 0.4$	[935]		4.2 ± 0.5
358	$K_0^*(1430)^0K^{*0}$	< 1.7			< 1.7	[936]		< 1.7
359	$K_0^*(1430)^0K_0^*(1430)^0$	< 4.7			< 4.7	[936]		< 4.7
360	$\phi K_0^*(1680)^0$	< 3.5			< 3.5	[939]		< 3.5
361	$\phi K_3^*(1780)^0$	< 2.7			< 2.7	[939]		< 2.7
362	$\phi K_4^*(2045)^0$	< 15.3			< 15.3	[939]		< 15.3
363	$\rho^0 K_2^*(1430)^0$	< 1100			< 1100 ‡	[874]		< 1100 ‡
364	$\phi K_2^*(1430)^0$	6.8 ± 0.9	$7.5 \pm 0.9 \pm 0.5$	[390]	$5.5^{+0.9}_{-0.7} \pm 1.0$	[935]		6.8 ± 0.8
365	$\phi\phi K^0$ §	4.5 ± 0.9	$4.5 \pm 0.8 \pm 0.3$	[893]				4.5 ± 0.9
366	$\eta'\eta' K^0$	< 31	< 31	[894]				< 31

† In this product of BFs, all daughter BFs not shown are set to 100%. ‡ Result from ARGUS. Cited in the *BABAR* column to avoid adding a column to the table.

§ $M_{\phi\phi} < 2.85$ GeV/ c^2 .

‡ $0.75 < M(K\pi) < 1.20$ GeV/ c^2 .

‡ $0.70 < M(K\pi) < 1.70$ GeV/ c^2 .

‡ $1.60 < M(K\pi) < 2.15$ GeV/ c^2 .

Table 243: Branching fractions of charmless mesonic B^0 decays without strange mesons (part 1) in units of $\times 10^{-6}$. Upper limits are at 90% CL. Where values are shown in red (blue), this indicates that they are new published (preliminary) results since PDG2017.

RPP #	Mode	PDG2017 Avg.	B_{BABAR}	Belle	CLEO	CDF	LHCb	Our Avg.
387	$\pi^+\pi^-$	5.12 ± 0.19	5.5 ± 0.4 ± 0.3	[911]	5.04 ± 0.21 ± 0.18 [845]	4.5 ^{+1.4} _{-1.2} ^{0.5} [846]	5.02 ± 0.33 ± 0.35 [†] [940]	5.08 ± 0.17 ± 0.37 [941]
388	$\pi^0\pi^0$	1.91 ± 0.22	1.83 ± 0.21 ± 0.13	[417]	1.31 ± 0.19 ± 0.18 [429]	0.41 ^{+0.17} _{-0.15} ^{0.05} [942]	< 2.9 [853]	1.59 ± 0.18
389	$\eta\pi^0$	0.41 ± 0.17	< 1.5	[904]	0.41 ^{+0.17} _{-0.15} ^{0.07} [942]	0.76 ± 0.27 ± 0.14 [943]	< 2.9 [853]	0.41 ^{+0.18} _{-0.17}
390	$\eta\eta$	< 1.0	< 1.0	[848]	2.8 ± 1.0 ± 0.3	0.0 ^{+1.8} _{-0.0} [849]	< 6.5 [851]	0.76 ^{+0.30} _{-0.28}
391	$\eta'\pi^0$	1.2 ± 0.6	0.9 ± 0.4 ± 0.1	[904]	2.8 ± 1.0 ± 0.3	0.0 ^{+1.8} _{-0.0} [849]	< 4.5 [851]	1.2 ± 0.4
392	$\eta'\eta'$	< 1.7	< 1.7	[848]	< 6.5 [851]	< 4.5 [851]	< 1.7 [851]	< 1.7
393	$\eta'\eta$	< 1.2	< 1.2	[904]	< 4.5 [851]	< 4.5 [851]	< 1.2 [851]	< 1.2
394	$\eta'\rho^0$	< 1.3	< 2.8	[850]	< 1.3 [851]	< 1.3 [851]	< 1.3 [851]	< 1.3
395	$f_0(980)\eta'$	< 0.9	< 0.9	[850]	< 0.9 [851]	< 0.9 [851]	< 0.9 [851]	< 0.9
396	$\eta\rho^0$	< 1.5	< 1.5	[913]	< 1.9 [855]	< 1.9 [855]	< 1.5 [855]	< 1.5
397	$f_0(980)\eta$	< 0.4	< 0.4	[913]	< 0.4 [851]	< 0.4 [851]	< 0.4 [851]	< 0.4
398	$\omega\eta$	0.94 ^{+0.40} _{-0.31}	0.94 ^{+0.35} _{-0.30} ± 0.09	[848]	< 2.2 [851]	< 2.2 [851]	0.94 ^{+0.36} _{-0.31}	0.94 ^{+0.36} _{-0.31}
399	$\omega\eta'$	1.0 ^{+0.5} _{-0.4}	1.01 ^{+0.46} _{-0.38} ± 0.09	[848]	< 2.2 [851]	< 2.2 [851]	1.01 ^{+0.47} _{-0.39}	1.01 ^{+0.47} _{-0.39}
400	$\omega\rho^0$	< 1.6	< 1.6	[859]	< 1.6 [859]	< 1.6 [859]	< 1.6 [859]	< 1.6
401	$f_0(980)\omega$	< 1.5	< 1.5	[859]	< 1.5 [859]	< 1.5 [859]	< 1.5 [859]	< 1.5
402	$\omega\omega$	1.2 ± 0.4	1.2 ± 0.3 ^{+0.3} _{-0.2}	[944]	< 1.2 [944]	< 1.2 [944]	1.2 ± 0.4	1.2 ± 0.4
403	$\phi\pi^0$	< 0.15	< 0.28	[905]	< 0.15 [906]	< 0.15 [906]	< 0.15 [906]	< 0.15
404	$\phi\eta$	< 0.5	< 0.5	[848]	< 0.5 [848]	< 0.5 [848]	< 0.5 [848]	< 0.5
405	$\phi\eta'$	< 0.5	< 1.1	[848]	< 0.5 [851]	< 0.5 [851]	< 0.5 [851]	< 0.5
406	$\phi\pi^+\pi^-$	0.18 ± 0.05	< 0.33	[908]	< 0.33 [908]	< 0.33 [908]	0.182 ± 0.048 ± 0.014 [§] [945]	0.182 ± 0.050
407	$\phi\rho^0$	< 0.33	< 0.38	[908]	< 0.38 [908]	< 0.38 [908]	< 0.33 [908]	< 0.33
408	$f_0(980)\phi$	< 0.38	< 0.38	[908]	< 0.38 [908]	< 0.38 [908]	< 0.38 [908]	< 0.38
409	$\omega\phi$	< 0.7	< 0.7	[944]	< 0.7 [944]	< 0.7 [944]	< 0.7 [944]	< 0.7
410	$\phi\phi$	< 0.028	< 0.2	[908]	< 0.2 [908]	< 0.2 [908]	< 0.024 [396]	< 0.024
411	$a_0^\mp(980)\pi^\pm$	< 3.1	< 3.1	[913]	< 3.1 [913]	< 3.1 [913]	< 3.1 [913]	< 3.1
412	$a_0^\mp(1450)\pi^\pm$	< 2.3	< 2.3	[913]	< 2.3 [913]	< 2.3 [913]	< 2.3 [913]	< 2.3
413	$\pi^+\pi^-\pi^0$	< 720	< 720 [¶]	[898]	< 720 [¶] [898]	< 720 [¶] [898]	< 720 [¶] [898]	< 720 [¶]
414	$\rho^0\pi^0$	2.0 ± 0.5	1.4 ± 0.6 ± 0.3	[946]	3.0 ± 0.5 ± 0.7 [279]	1.6 ^{+2.0} _{-1.4} ^{± 0.8} [858]	2.0 ± 0.5 [279]	2.0 ± 0.5
415	$\rho^\mp\pi^\pm$	23.0 ± 2.3	22.6 ± 1.8 ± 2.2	[283]	22.6 ± 1.1 ± 4.4 [283]	22.6 ± 1.1 ± 4.4 [283]	23.0 ± 2.3 [283]	23.0 ± 2.3
416	$\pi^+\pi^-\pi^+\pi^-$	< 11.2	< 23.1	[411]	< 11.2 [411]	< 11.2 [411]	< 11.2 [411]	< 11.2
417	$\rho^0\pi^+\pi^-(NR)$	< 8.8	< 8.8	[411]	< 12 [411]	< 12 [411]	< 8.8 [411]	< 8.8
418	$\rho^0\rho^0$	0.96 ± 0.15	0.92 ± 0.32 ± 0.14	[411]	1.02 ± 0.30 ± 0.15 [412]	1.02 ± 0.30 ± 0.15 [412]	0.95 ± 0.16 [413]	0.95 ± 0.16
419	$f_0(980)\pi^+\pi^-(NR)$	< 3.0	< 3.0	[411]	< 3.0 [412]	< 3.0 [412]	< 3.0 [412]	< 3.0
420	$f_0(980)\rho^0$	0.78 ± 0.25	< 0.40	[411]	0.78 ± 0.22 ± 0.11 [412]	0.78 ± 0.22 ± 0.11 [412]	0.78 ± 0.25	0.78 ± 0.25
421	$f_0(980)f_0(980), 4\pi^+$	< 0.19	< 0.19	[411]	< 0.2 [412]	< 0.2 [412]	< 0.19	< 0.19
422	$f_0(980)f_0(980), 2\pi K^\pm$	< 0.23	< 0.23	[908]	< 0.23 [908]	< 0.23 [908]	< 0.23	< 0.23
423	$a_1^\mp\pi^\pm$	26 ± 5	33.2 ± 3.8 ± 3.0	[947]	22.2 ± 2.0 ± 2.8 [415]	22.2 ± 2.0 ± 2.8 [415]	25.9 ± 2.8	25.9 ± 2.8
424	$a_2^\mp\pi^\pm$	< 6.3	< 6.3	[415]	< 6.3 [415]	< 6.3 [415]	< 6.3	< 6.3
425	$\pi^+\pi^-\pi^0$	< 3100	< 3100 [¶]	[898]	< 3100 [¶] [898]	< 3100 [¶] [898]	< 3100 [¶]	< 3100 [¶]
426	$\rho^+\rho^-$	27.7 ± 1.9	25.5 ± 2.1 ^{+3.6} _{-3.9}	[409]	28.3 ± 1.5 ± 1.5 [410]	28.3 ± 1.5 ± 1.5 [410]	27.7 ± 1.9	27.7 ± 1.9
427	$a_1(1260)^0\pi^0$	< 1100	< 1100 [¶]	[898]	< 1100 [¶] [898]	< 1100 [¶] [898]	< 1100 [¶]	< 1100 [¶]
428	$\omega\pi^0$	< 0.5	< 0.5	[904]	< 0.5 [904]	< 0.5 [904]	< 0.5	< 0.5
429	$\pi^+\pi^-\pi^-\pi^-\pi^0$	< 9000	< 9000 [¶]	[898]	< 9000 [¶] [898]	< 9000 [¶] [898]	< 9000 [¶]	< 9000 [¶]
430	$a_1^\pm\rho^\mp$	< 61	< 61	[948]	< 61 [948]	< 61 [948]	< 61	< 61
431	$a_1^0\rho^0$	< 2400	< 2400 [¶]	[898]	< 2400 [¶] [898]	< 2400 [¶] [898]	< 2400 [¶]	< 2400 [¶]

Results for CDF and LHCb are relative BFs converted to absolute BFs.

CLEO upper limits that have been greatly superseded are not shown.

[†] In this product of BFs, all daughter BFs not shown are set to 100%.

[‡] Result given as $0.94 \pm 0.17 \pm 0.09 \pm 0.06$ where last error is from $\mathcal{B}(B^0 \rightarrow \phi K^{*0})$.

[§] In the mass range $400 < m(\pi^+\pi^-) < 1600 \text{ GeV}/c^2$.

[¶] Result from ARGUS. Cited in the BABAR column to avoid adding a column to the table.

◇ Both $f_0(980)$ decay into $\pi^+\pi^-K^+$.

[†] Using the final state $\pi^+\pi^-K^+$.

Table 244: Branching fractions of charmless mesonic B^0 decays without strange mesons (part 2) in units of $\times 10^{-6}$. Upper limits are at 90% CL. Where values are shown in red (blue), this indicates that they are new published (preliminary) results since PDG2017.

RPP#	Mode	PDG2017 Avg.	<i>BABAR</i>	Belle	CLEO	CDF	LHCb	Our Avg.
432	$b_1^\mp \pi^\pm$ †	10.9 ± 1.5	$10.9 \pm 1.2 \pm 0.9$ [875]					10.9 ± 1.5
433	$b_1^0 \pi^0$ †	< 1.9	< 1.9 [871]					< 1.9
434	$b_1^\pm \rho^\mp$ †	< 1.4	< 1.4 [876]					< 1.4
435	$b_1^0 \rho^0$ †	< 3.4	< 3.4 [876]					< 3.4
436	$\pi^+ \pi^+ \pi^+ \pi^- \pi^- \pi^-$	< 3000	< 3000 ‡ [898]					< 3000 ‡
437	$a_1^\pm a_1^\mp$	11.8 ± 2.6	11.8 ± 2.6 [949]					11.8 ± 2.6
438	$\pi^+ \pi^+ \pi^+ \pi^- \pi^- \pi^- \pi^0$	< 11000	< 11000 ‡ [898]					< 11000 ‡

Results for CDF and LHCb are relative BFs converted to absolute BFs.

CLEO upper limits that have been greatly superseded are not shown.

† In this product of BFs, all daughter BFs not shown are set to 100%.

‡ Result from ARGUS. Cited in the *BABAR* column to avoid adding a column to the table.

Table 245: Relative branching fractions of charmless mesonic B^0 decays. Upper limits are at 90% CL. Where values are shown in red (blue), this indicates that they are new published (preliminary) results since PDG2017.

RPP#	Mode	PDG2017 Avg.	CDF	LHCb	Our Avg.
320	$\mathcal{B}(B^0 \rightarrow K^+ K^-)/\mathcal{B}(B^0 \rightarrow K^+ \pi^-)$	$0.012 \pm 0.005 \pm 0.005$ [925]	$0.00398 \pm 0.00065 \pm 0.00042$ [926]	0.00416 ± 0.00099	
323	$\mathcal{B}(B^0 \rightarrow K^{*\mp} K^\pm)/\mathcal{B}(B^0 \rightarrow K^{*+} \pi^-)$		< 0.05 [929]		< 0.05
324	$\mathcal{B}(B^0 \rightarrow K_S^0 K^{*0})/\mathcal{B}(B^0 \rightarrow K_S^0 \pi^+ \pi^-)$ †		< 0.020 [931]		< 0.020
387	$\mathcal{B}(B^0 \rightarrow \pi^+ \pi^-)/\mathcal{B}(B^0 \rightarrow K^+ \pi^-)$	0.261 ± 0.015	$0.259 \pm 0.017 \pm 0.016$ [940]	$0.262 \pm 0.009 \pm 0.017$ [941]	0.261 ± 0.015

† Numerator includes two distinct decay processes: $\mathcal{B}(B^0 \rightarrow f) + \mathcal{B}(B^0 \rightarrow \bar{f})$.

High Precision Charmless Mesonic B BF Measurements

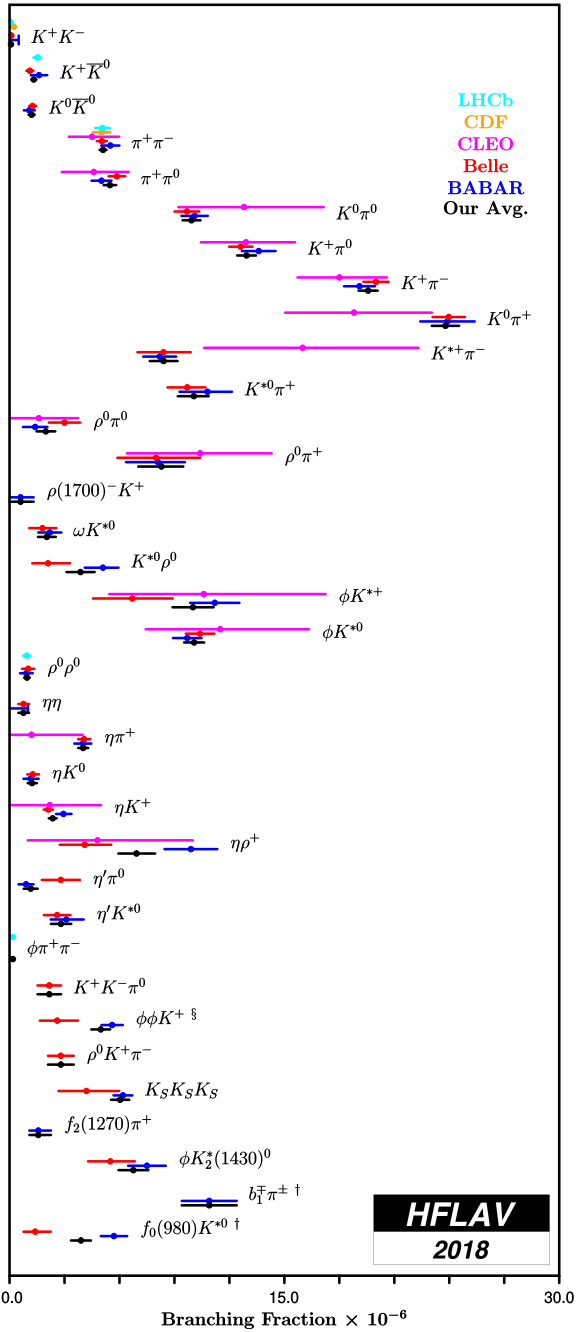


Figure 69: Selection of high-precision charmless mesonic B meson branching fraction measurements.

8.2 Baryonic decays of B^+ and B^0 mesons

This section provides branching fractions of charmless baryonic decays of B^+ and B^0 mesons in Tables 246 and 247, respectively. Relative branching fractions are given in Table 248.

Figures 70 and 71 show graphic representations of a selection of results given in this section. Footnote symbols indicate that the footnote in the corresponding table should be consulted.

Table 246: Branching fractions of charmless baryonic B^+ decays in units of $\times 10^{-6}$. Upper limits are at 90% CL. Where values are shown in red (blue), this indicates that they are new published (preliminary) results since PDG2017.

RPP#	Mode	PDG2017 Avg.	BABAR	Belle	LHCb	Our Avg.
484	$p\bar{p}\pi^+$	1.62 ± 0.20	$1.69 \pm 0.29 \pm 0.26$ [†] [687]	$1.60^{+0.22}_{-0.19} \pm 0.12$ [950]		$1.62^{+0.21}_{-0.20}$
484	$p\bar{p}\pi^+ \S$				$1.07 \pm 0.11 \pm 0.11$ [951]	1.07 ± 0.16
487	$p\bar{p}K^+$	5.9 ± 0.5	$6.7 \pm 0.5 \pm 0.4$ [†] [765]	$5.54^{+0.27}_{-0.25} \pm 0.36$ [950]	$4.46 \pm 0.21 \pm 0.27$ [¶] [772]	5.14 ± 0.25
488	$\Theta^{++}\bar{p}$ ¹	< 0.091	< 0.09 [765]	< 0.091 [952]		< 0.09
489	$f_J(2220)K^+$ ²	< 0.41		< 0.41 [952]		< 0.41
490	$p\bar{\Lambda}(1520)$	0.31 ± 0.06	< 1.5 [765]		$0.315 \pm 0.048 \pm 0.027$ [951]	0.315 ± 0.055
492	$p\bar{p}K^{*+}$	$3.6^{+0.8}_{-0.7}$	$5.3 \pm 1.5 \pm 1.3$ [†] [687]	$3.38^{+0.73}_{-0.60} \pm 0.39$ [‡] [953]		$3.64^{+0.79}_{-0.70}$
493	$f_J(2220)K^{*+}$ ²	< 0.77	< 0.77 [687]			< 0.77
494	$p\bar{\Lambda}$	< 0.32		< 0.32 [954]	$0.24^{+0.10}_{-0.08} \pm 0.03$ [955]	$0.24^{+0.10}_{-0.09}$
496	$p\bar{\Lambda}\pi^0$	$3.00^{+0.7}_{-0.6}$		$3.00^{+0.61}_{-0.53} \pm 0.33$ [956]		$3.00^{+0.69}_{-0.62}$
497	$p\bar{\Sigma}(1385)^0$	< 0.47		< 0.47 [956]		< 0.47
498	$\Delta^+\bar{\Lambda}$	< 0.82		< 0.82 [956]		< 0.82
500	$p\bar{\Lambda}\pi^+\pi^-$ (NR)	5.9 ± 1.1		$5.92^{+0.88}_{-0.84} \pm 0.69$ [957]		$5.92^{+1.12}_{-1.09}$
501	$p\bar{\Lambda}\rho^0$	4.8 ± 0.9		$4.78^{+0.67}_{-0.64} \pm 0.60$ [957]		$4.78^{+0.90}_{-0.88}$
502	$p\bar{\Lambda}f_2(1270)$	2.0 ± 0.8		$2.03^{+0.77}_{-0.72} \pm 0.27$ [957]		$2.03^{+0.82}_{-0.77}$
503	$\Lambda\bar{\Lambda}\pi^+$	< 0.94		< 0.94 [§] [648]		< 0.94 [§]
504	$\Lambda\bar{\Lambda}K^+$	3.4 ± 0.6		$3.38^{+0.41}_{-0.36} \pm 0.41$ [‡] [648]		$3.38^{+0.58}_{-0.55}$
505	$\Lambda\bar{\Lambda}K^{*+}$	$2.2^{+1.2}_{-0.9}$		$2.19^{+1.13}_{-0.88} \pm 0.33$ [§] [648]		$2.19^{+1.18}_{-0.94}$
506	$\bar{\Delta}^0 p$	< 1.38		< 1.38 [§] [950]		< 1.38 [§]
507	$\Delta^{++}\bar{p}$	< 0.14		< 0.14 [§] [950]		< 0.14 [§]
	$p\bar{\Lambda}K^+K^-$ (NR)			$4.10^{+0.45}_{-0.43} \pm 0.50$ [958]		$4.10^{+0.67}_{-0.66}$
	$\bar{p}\Lambda K^+K^-$ (NR)			$3.70^{+0.39}_{-0.37} \pm 0.44$ [958]		$3.70^{+0.59}_{-0.57}$
	$p\bar{\Lambda}\phi$			$0.795 \pm 0.209 \pm 0.077$ [958]		0.795 ± 0.223
	$\Lambda(1520)\bar{\Lambda}K^+$			$2.23 \pm 0.63 \pm 0.25$ [958]		2.23 ± 0.68
	$\bar{\Lambda}(1520)\Lambda K^+$			< 2.08 [958]		< 2.08

Channels with no RPP# were not included in PDG Live as of Dec. 31, 2017.

Results for LHCb are relative BFs converted to absolute BFs.

[†] Charmonium decays to $p\bar{p}$ have been statistically subtracted.

[‡] The charmonium mass region has been vetoed.

[§] Di-baryon mass is less than 2.85 GeV/ c^2 .

[¶] Includes contribution where $p\bar{p}$ is produced in charmonia decays.

¹ $\Theta(1540)^{++} \rightarrow K^+ p$ (pentaquark candidate).

² In this product of BFs, all daughter BFs not shown are set to 100%.

Table 247: Branching fractions of charmless baryonic B^0 decays in units of $\times 10^{-6}$. Upper limits are at 90% CL. Where values are shown in red (blue), this indicates that they are new published (preliminary) results since PDG2017.

RPP#	Mode	PDG2017 Avg.	BABAR		Belle		LHCb		Our Avg.
439	$p\bar{p}$	$0.015^{+0.007}_{-0.005}$	< 0.27	[959]	< 0.11	[954]	$0.0125 \pm 0.0027 \pm 0.0018$	[960]	0.0130 ± 0.0030
440	$p\bar{p}\pi^+\pi^-$	< 250					$2.7 \pm 0.1 \pm 0.1 \pm 0.2$	[961]	2.7 ± 0.2
441	$p\bar{p}K^0$	2.66 ± 0.32	$3.0 \pm 0.5 \pm 0.3$ †	[687]	$2.51^{+0.35}_{-0.29} \pm 0.21$ ‡	[953]			$2.66^{+0.34}_{-0.32}$
442	$\Theta^+\bar{p}$ §	< 0.05	< 0.05	[687]	< 0.23	[952]			< 0.05
443	$f_J(2220)K^0$ ¶	< 0.45	< 0.45	[687]					< 0.45
444	$p\bar{p}K^{*0}$	$1.24^{+0.28}_{-0.25}$	$1.47 \pm 0.45 \pm 0.40$ †	[687]	$1.18^{+0.29}_{-0.25} \pm 0.11$ ‡	[953]			$1.24^{+0.28}_{-0.25}$
445	$f_J(2220)K^{*0}$ ¶	< 0.15	< 0.15	[687]					< 0.15
446	$p\bar{\Lambda}\pi^-$	3.14 ± 0.29	$3.07 \pm 0.31 \pm 0.23$	[962]	$3.23^{+0.33}_{-0.29} \pm 0.29$	[956]			$3.14^{+0.29}_{-0.28}$
448	$p\bar{\Sigma}(1385)^-$	< 0.26			< 0.26	[956]			< 0.26
449	$\Delta^0\bar{\Lambda}$	< 0.93			< 0.93	[956]			< 0.93
450	$p\bar{\Lambda}K^-$	< 0.82			< 0.82	[963]			< 0.82
453	$p\bar{\Sigma}^0\pi^-$	< 3.8			< 3.8	[963]			< 3.8
454	$\bar{\Lambda}\Lambda$	< 0.32			< 0.32	[954]			< 0.32
455	$\bar{\Lambda}\Lambda K^0$	$4.8^{+1.0}_{-0.9}$			$4.76^{+0.84}_{-0.68} \pm 0.61$ ‡	[648]			$4.76^{+1.04}_{-0.91}$
456	$\Lambda\bar{\Lambda}K^{*0}$	$2.5^{+0.9}_{-0.8}$			$2.46^{+0.87}_{-0.72} \pm 0.34$ ‡	[648]			$2.46^{+0.93}_{-0.80}$
	$p\bar{p}K^+K^-$						$0.113 \pm 0.028 \pm 0.011 \pm 0.008$	[961]	0.113 ± 0.031
	$p\bar{p}K^+\pi^-$						$5.9 \pm 0.3 \pm 0.3 \pm 0.4$	[961]	5.9 ± 0.6
	$pp\bar{p}\bar{p}$		< 0.20	[964]					< 0.20

Channels with no RPP# were not included in PDG Live as of Dec. 31, 2017.

Results for LHCb are relative BFs converted to absolute BFs.

† Charmonium decays to $p\bar{p}$ have been statistically subtracted.

‡ The charmonium mass region has been vetoed.

§ $\Theta(1540)^+ \rightarrow pK^0$ (pentaquark candidate).

¶ In this product of BFs, all daughter BFs not shown are set to 100%.

Table 248: Relative branching fractions of charmless baryonic B decays. Where values are shown in red (blue), this indicates that they are new published (preliminary) results since PDG2017.

RPP#	Mode	PDG2017 Avg.	LHCb	Our Avg.
	$\mathcal{B}(B^+ \rightarrow p\bar{p}\pi^+, m_{p\bar{p}} < 2.85 \text{ GeV}/c^2)/\mathcal{B}(B^+ \rightarrow J/\psi(\rightarrow p\bar{p})\pi^+)$		$12.0 \pm 1.2 \pm 0.3$	[951] 12.0 ± 1.2
	$\mathcal{B}(B^+ \rightarrow p\bar{p}K^+)/\mathcal{B}(B^+ \rightarrow J/\psi(\rightarrow p\bar{p})K^+)$		$4.91 \pm 0.19 \pm 0.14$ †	[772] 4.91 ± 0.24
487	$\mathcal{B}(B^+ \rightarrow p\bar{p}K^+)/\mathcal{B}(B^+ \rightarrow J/\psi K^+)$	$0.0104 \pm 0.0005 \pm 0.0001$	$0.0104 \pm 0.0005 \pm 0.0001$ ‡	[772] 0.0100 ± 0.0010
	$\mathcal{B}(B^+ \rightarrow \bar{\Lambda}(1520)(\rightarrow K^+\bar{p})p)/\mathcal{B}(B^+ \rightarrow J/\psi(\rightarrow p\bar{p})\pi^+)$		$0.033 \pm 0.005 \pm 0.007$	[951] 0.033 ± 0.009
	$\mathcal{B}(B^0 \rightarrow p\bar{p}K^+K^-)/\mathcal{B}(B^0 \rightarrow p\bar{p}K^+\pi^-)$		$0.019 \pm 0.005 \pm 0.002$	[961] 0.019 ± 0.005
	$\mathcal{B}(B^0 \rightarrow p\bar{p}\pi^+\pi^-)/\mathcal{B}(B^0 \rightarrow p\bar{p}K^+\pi^-)$		$0.46 \pm 0.02 \pm 0.02$	[961] 0.46 ± 0.03

Channels with no RPP# were not included in PDG Live as of Dec. 31, 2017.

† Includes contribution where $p\bar{p}$ is produced in charmonia decays.

‡ Original experimental relative BF multiplied by the best values (PDG2014) of certain reference BFs. The first error is experimental, and the second is from the reference BFs.

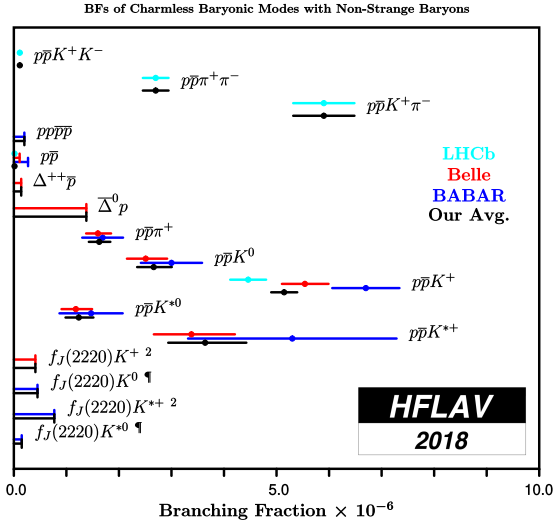


Figure 70: Branching fractions of charmless baryonic modes with non-strange baryons.

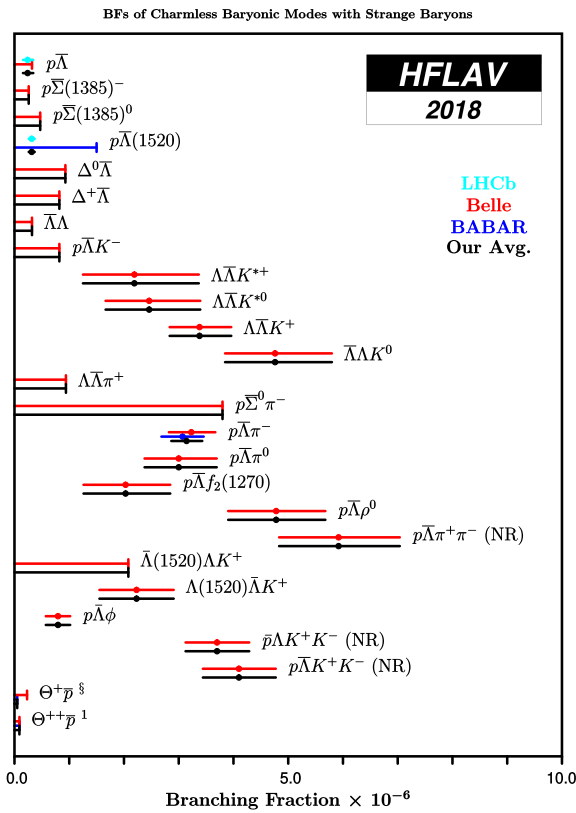


Figure 71: Branching fractions of charmless baryonic modes with strange baryons.

8.3 Decays of b baryons

A compilation of branching fractions of Λ_b^0 baryon decays is given in Table 249. Table 250 provides the partial branching fractions of $\Lambda_b^0 \rightarrow \Lambda\mu^+\mu^-$ decays. Compilations of branching fractions of Ξ_b^0 , Ξ_b^- and Ω_b^- baryon decays are given in Tables 251, 252, and 253, respectively.

Figure 72 shows a graphic representation of branching fractions of Λ_b^0 decays. Footnote symbols indicate that the footnote in the corresponding table should be consulted.

Table 249: Branching fractions of charmless Λ_b^0 decays in units of $\times 10^{-6}$. Upper limits are at 90% CL. Where values are shown in red (blue), this indicates that they are new [published](#) ([preliminary](#)) results since PDG2017.

RPP#	Mode	PDG2017 Avg.	CDF	LHCb	Our Avg.
12	$\bar{K}^0 p\pi^-$	13.0 ± 4.0		$12.6 \pm 1.9 \pm 0.9 \pm 3.4 \pm 0.5$ [§] [965]	12.6 ± 4.0
13	$K^0 pK^-$	< 3.5		< 3.5 [965]	< 3.5
33	$p\pi^-$	4.3 ± 0.8	$3.5 \pm 0.6 \pm 0.9$ [966]		3.5 ± 1.1
34	pK^-	5.1 ± 0.9	$5.6 \pm 0.8 \pm 1.5$ [966]		5.6 ± 1.7
37	$\Lambda\mu^+\mu^-$	1.08 ± 0.28	$1.73 \pm 0.42 \pm 0.55$ [967]	$0.96 \pm 0.16 \pm 0.25$ [968]	1.08 ± 0.27
38	$\Lambda\gamma$	< 1300	< 1300 [969]		< 1300
39	$\Lambda\eta$	9^{+7}_{-5}		$9.3^{+7.3}_{-5.3}$ ¶ [970]	$9.3^{+7.3}_{-5.3}$
40	$\Lambda\eta'$	< 3.1		< 3.1 [970]	< 3.1
41	$\Lambda\pi^+\pi^-$	4.7 ± 1.9		$4.6 \pm 1.2 \pm 1.4 \pm 0.6$ ^{† 2} [971]	4.6 ± 1.9
42	$\Lambda K^+\pi^-$	5.7 ± 1.3		$5.6 \pm 0.8 \pm 0.8 \pm 0.7$ ^{† 2} [971]	5.6 ± 1.3
43	ΛK^+K^-	16.1 ± 2.3		$15.9 \pm 1.2 \pm 1.2 \pm 2.0$ ^{† 2} [971]	15.9 ± 2.6
44	$\Lambda\phi$	2.0 ± 0.5		$5.18 \pm 1.04 \pm 0.35^{+0.67}_{-0.62} \pm 3$ [972]	$5.18^{+1.29}_{-1.26}$
	$p\pi^-\mu^+\mu^-$			$0.069 \pm 0.019 \pm 0.011^{+0.013}_{-0.010} \pm 1$ [973]	$0.069^{+0.026}_{-0.024}$
	$p\pi^-\pi^+\pi^-$			$19.0 \pm 0.6 \pm 1.0 \pm 1.6 \pm 0.7$ ¹ [974]	19.0 ± 2.1
	$pK^-\pi^+\pi^-$			$45.5 \pm 0.8 \pm 2.0 \pm 3.9 \pm 1.7$ ¹ [974]	45.5 ± 4.8
	$pK^-K^+\pi^-$			$3.7 \pm 0.3 \pm 0.4 \pm 0.3 \pm 0.1$ ¹ [974]	3.7 ± 0.6
	$pK^-K^+K^-$			$11.4 \pm 0.3 \pm 0.7 \pm 1.0 \pm 0.5$ ¹ [974]	11.4 ± 1.4
	$\Psi(2S)p\pi^-$			$7.17 \pm 0.82 \pm 0.33^{+1.30}_{-1.03} \pm 4$ [809]	$7.17^{+1.57}_{-1.36}$

Channels with no RPP# were not included in PDG Live as of Dec. 31, 2017.

Results for CDF and LHCb are relative BFs converted to absolute BFs.

[†] Last quoted uncertainty is due to the precision with which the normalization channel branching fraction is known.

[‡] Third uncertainty is related to external inputs.

[§] Third uncertainty is from the ratio of fragmentation fractions $f_{\Lambda_b^0}/f_d$, and the fourth is due to the uncertainty on $\mathcal{B}(B^0 \rightarrow K^0\pi^+\pi^-)$.

¶ Result at 68% CL.

¹ Third uncertainty is from $\mathcal{B}(\Lambda_b \rightarrow \Lambda_c^+\pi^-)$, and the fourth is due to the uncertainty on $\mathcal{B}(\Lambda_c^+ \rightarrow pK^-\pi^+)$.

² Normalization taken directly from LHCb paper.

³ Difference w.r.t. PDG value due to different values for the production rate ratio f_{Λ_b}/f_d .

⁴ Calculated using the value of $\mathcal{B}(\Lambda_b^0 \rightarrow \Psi(2S)pK^-) = (6.29 \pm 0.23 \pm 0.14^{+1.14}_{-0.90}) \times 10^{-6}$.

Table 250: Partial branching fractions of $\Lambda_b^0 \rightarrow \Lambda\mu^+\mu^-$ decays in intervals of $q^2 = m^2(\mu^+\mu^-)$ in units of $\times 10^{-7}$. Where values are shown in red (blue), this indicates that they are new published (preliminary) results since PDG2017.

Mode	q^2 [GeV $^2/c^4$]	\dagger	PDG2017 Avg.	CDF	LHCb	Our Avg.
$\Lambda\mu^+\mu^-$	< 2.0		0.71 ± 0.27	$0.15 \pm 2.01 \pm 0.05$ [967]	$0.72^{+0.24}_{-0.22} \pm 0.14$ [975]	$0.71^{+0.27}_{-0.26}$
$\Lambda\mu^+\mu^-$	[2.0, 4.3]		$0.28^{+0.28}_{-0.21}$	$1.8 \pm 1.7 \pm 0.6$	$0.253^{+0.276}_{-0.207} \pm 0.046$ [975]	$0.281^{+0.286}_{-0.218}$
$\Lambda\mu^+\mu^-$	[4.3, 8.68]		0.5 ± 0.7	$-0.2 \pm 1.6 \pm 0.1$	$0.66 \pm 0.72 \pm 0.16$ [968]	0.51 ± 0.67
$\Lambda\mu^+\mu^-$	[10.09, 12.86]		2.2 ± 0.6	$3.0 \pm 1.5 \pm 1.0$	$2.08^{+0.42}_{-0.39} \pm 0.42$ [975]	$2.17^{+0.57}_{-0.55}$
$\Lambda\mu^+\mu^-$	[14.18, 16.00]		1.7 ± 0.5	$1.0 \pm 0.7 \pm 0.3$	$2.04^{+0.35}_{-0.33} \pm 0.42$ [975]	1.70 ± 0.44
$\Lambda\mu^+\mu^-$	> 16.00		7.0 ± 2.9	$7.0 \pm 1.9 \pm 2.2$		7.0 ± 2.9

Results for CDF and LHCb are relative BFs converted to absolute BFs.

\dagger See the original paper for the exact $m^2(\mu^+\mu^-)$ selection.

\ddagger The two LHCb measurements include additional binning not reported here.

Table 251: Branching fractions of charmless Ξ_b^0 decays in units of $\times 10^{-6}$. Upper limits are at 90% CL. Where values are shown in red (blue), this indicates that they are new published (preliminary) results since PDG2017.

RPP#	Mode	PDG2017 Avg.	LHCb	Our Avg.
4	$f_{\Xi_b^0}/f_d \mathcal{B}(\Xi_b^0 \rightarrow \bar{K}^0 p\pi^-)$	< 1.6	< 1.6	[965] < 1.6
5	$f_{\Xi_b^0}/f_d \mathcal{B}(\Xi_b^0 \rightarrow \bar{K}^0 pK^-)$	< 1.1	< 1.1	[965] < 1.1
10	$f_{\Xi_b^0}/f_{\Lambda_b^0} \mathcal{B}(\Xi_b^0 \rightarrow \Lambda\pi^+\pi^-)$	< 1.7	< 1.7	[971] < 1.7
11	$f_{\Xi_b^0}/f_{\Lambda_b^0} \mathcal{B}(\Xi_b^0 \rightarrow \Lambda K^+\pi^-)$	< 0.8	< 0.8	[971] < 0.8
12	$f_{\Xi_b^0}/f_{\Lambda_b^0} \mathcal{B}(\Xi_b^0 \rightarrow \Lambda K^+K^-)$	< 0.3	< 0.3	[971] < 0.3
	$f_{\Xi_b^0}/f_{\Lambda_b^0} \mathcal{B}(\Xi_b^0 \rightarrow pK^-\pi^+\pi^-)$		$1.72 \pm 0.21 \pm 0.25 \pm 0.15 \pm 0.07$ [974]	1.72 ± 0.37
	$f_{\Xi_b^0}/f_{\Lambda_b^0} \mathcal{B}(\Xi_b^0 \rightarrow pK^-\pi^+K^-)$		$1.56 \pm 0.16 \pm 0.19 \pm 0.13 \pm 0.06$ [974]	1.56 ± 0.29
	$f_{\Xi_b^0}/f_{\Lambda_b^0} \mathcal{B}(\Xi_b^0 \rightarrow pK^-K^+K^-)$		< 0.25	[974] < 0.25

Channels with no RPP# were not included in PDG Live as of Dec. 31, 2017.

Results for LHCb are relative BFs converted to absolute BFs.

Table 252: Branching fractions of charmless Ξ_b^- decays in units of $\times 10^{-5}$. Upper limits are at 90% CL. Where values are shown in red (blue), this indicates that they are new published (preliminary) results since PDG2017.

RPP#	Mode	PDG2017 Avg.	LHCb	Our Avg.
6	$f_{\Xi_b^-} \mathcal{B}(\Xi_b^- \rightarrow pK^-K^-)/(f_u \mathcal{B}(B^- \rightarrow K^+K^-K^-))$	\dagger	$265 \pm 35 \pm 47$ [976]	265 ± 58
	$f_{\Xi_b^-} \mathcal{B}(\Xi_b^- \rightarrow pK^-\pi^-)/(f_u \mathcal{B}(B^- \rightarrow K^+K^-K^-))$		$259 \pm 64 \pm 49$ [976]	259 ± 80
8	$\mathcal{B}(\Xi_b^- \rightarrow p\pi^-\pi^-)/(\mathcal{B}(\Xi_b^- \rightarrow pK^-K^-))$	< 0.56	< 0.56	[976] < 0.56
	$f_{\Xi_b^-} \mathcal{B}(\Xi_b^- \rightarrow p\pi^-\pi^-)/(f_u \mathcal{B}(B^- \rightarrow K^+K^-K^-))$		< 147	[976] < 147
9	$\mathcal{B}(\Xi_b^- \rightarrow pK^-\pi^-)/(\mathcal{B}(\Xi_b^- \rightarrow pK^-K^-))$	$0.98 \pm 0.27 \pm 0.09$	$0.98 \pm 0.27 \pm 0.09$ [976]	0.98 ± 0.28

Channels with no RPP# were not included in PDG Live as of Dec. 31, 2017.

\dagger PDG reports results multiplied by $\mathcal{B}(B^+ \rightarrow K^+K^-K^+)$ and $\mathcal{B}(\bar{b} \rightarrow B^+)$.

Table 253: Branching fractions of charmless Ω_b^- decays in units of $\times 10^{-5}$. Upper limits are at 90% CL. Where values are shown in red (blue), this indicates that they are new published (preliminary) results since PDG2017.

RPP#	Mode	PDG2017 Avg.	LHCb	Our Avg.
2	$f_{\Omega_b^-} \mathcal{B}(\Omega_b^- \rightarrow pK^- K^-)/(f_u \mathcal{B}(B^- \rightarrow K^+ K^- K^-))$	†	< 18 [976]	< 18
3	$f_{\Omega_b^-} \mathcal{B}(\Omega_b^- \rightarrow pK^- \pi^-)/(f_u \mathcal{B}(B^- \rightarrow K^+ K^- K^-))$	†	< 51 [976]	< 51
4	$f_{\Omega_b^-} \mathcal{B}(\Omega_b^- \rightarrow p\pi^- \pi^-)/(f_u \mathcal{B}(B^- \rightarrow K^+ K^- K^-))$	†	< 109 [976]	< 109

† PDG reports results multiplied by $\mathcal{B}(B^+ \rightarrow K^+ K^- K^+)$ and $\mathcal{B}(\bar{b} \rightarrow B^+)$.

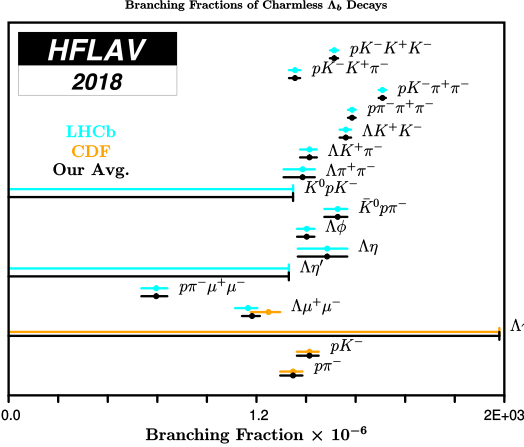


Figure 72: Branching fractions of charmless Λ_b^0 decays.

List of other measurements that are not included in the tables:

- In Ref. [975], LHCb provides a measurement of the differential $\Lambda_b^0 \rightarrow \Lambda \mu^+ \mu^-$ branching fraction. It is given in bins of $m^2(\mu^+ \mu^-)$ that are different from those used in the past by the LHCb and CDF collaborations (see table of differential branching fractions).
- In Ref. [977], LHCb measures angular observables of the decay $\Lambda_b^0 \rightarrow \Lambda \mu^+ \mu^-$, including the lepton-side, hadron-side and combined forward-backward asymmetries of the decay.
- In Ref. [978], LHCb measures the ratios

$$\frac{\sigma(pp \rightarrow \Xi_b'^- X) \mathcal{B}(\Xi_b'^- \rightarrow \Xi_b^0 \pi^-)}{\sigma(pp \rightarrow \Xi_b^0 X)}, \frac{\sigma(pp \rightarrow \Xi_b'^- X) \mathcal{B}(\Xi_b^{*-} \rightarrow \Xi_b^0 \pi^-)}{\sigma(pp \rightarrow \Xi_b^0 X)}.$$

- In Ref. [979], LHCb measures the ratio

$$\frac{\sigma(pp \rightarrow \Xi_b^{*-} X) \mathcal{B}(\Xi_b^{*-} \rightarrow \Xi_b^0 \pi^-)}{\sigma(pp \rightarrow \Xi_b^0 X)}.$$

- In Ref. [980], LHCb performs a search for baryon-number-violating Ξ_b^0 oscillations and set an upper limit of $\omega < 0.08 \text{ ps}^{-1}$ on the oscillation rate.

8.4 Decays of B_s^0 mesons

Tables 254 and 255 detail branching fractions and relative branching fractions of B_s^0 meson decays, respectively.

Figures 73 and 74 show graphic representations of a selection of results given in this section. Footnote symbols indicate that the footnote in the corresponding table should be consulted.

Table 254: Branching fractions of charmless B_s^0 decays in units of $\times 10^{-6}$. Upper limits are at 90% CL. Where values are shown in red (blue), this indicates that they are new published (preliminary) results since PDG2017.

RPP#	Mode	PDG2017 Avg.	Belle	CDF	D0	LHCb	CMS	ATLAS	Our Avg.
85	$\pi^+\pi^-$	0.68 ± 0.08	< 12	[981]	$0.60 \pm 0.17 \pm 0.04^\dagger$ [925]		$0.691 \pm 0.083 \pm 0.044^\dagger$ [926]		0.671 ± 0.083
90	$\eta'\eta'$	33 ± 7				$33.1 \pm 7.0 \pm 1.2^\dagger$ [982]			33.1 ± 7.1
91	$\phi f_0(980), f_0(980) \rightarrow \pi^+\pi^-$	1.12 ± 0.21				$1.12 \pm 0.18 \pm 0.11$ [945]			1.12 ± 0.21
92	$\phi f_2(1270), f_2(1270) \rightarrow \pi^+\pi^-$	$0.61^{+0.18}_{-0.15}$				$0.61^{+0.18}_{-0.14} \pm 0.06$ [945]			$0.61^{+0.19}_{-0.15}$
93	$\phi\bar{\rho}(770)$	0.27 ± 0.08				$0.27 \pm 0.07 \pm 0.02$ [945]			0.27 ± 0.07
94	$\phi\pi^+\pi^-$	3.5 ± 0.5				$3.48 \pm 0.29 \pm 0.35^3$ [945]			3.48 ± 0.46
95	$\phi\phi$	18.7 ± 1.5				$18.4 \pm 0.5 \pm 1.8^\S$ [984]			18.6 ± 1.6
96	π^+K^-	5.6 ± 0.6	< 26	[981]	$5.3 \pm 0.9 \pm 0.3^\dagger$ [966]		$5.6 \pm 0.6 \pm 0.3^\dagger$ [941]		5.5 ± 0.6
97	K^+K^-	25.4 ± 1.6		$38^{+10}_{-9} \pm 7$	[981]	$25.9 \pm 2.2 \pm 1.7^\dagger$ [940]		$23.7 \pm 1.6 \pm 1.5^\dagger$ [941]	24.8 ± 1.7
98	$K^0\bar{K}^0$	20 ± 6		$19.6^{+5.8}_{-5.1} \pm 1.0 \pm 2.0^\dagger$ [985]					$19.6^{+5.2}_{-5.6}$
99	$K^0\pi^+\pi^-$	15 ± 4				$9.5 \pm 1.3 \pm 1.5 \pm 0.4^\S$ [920]			9.5 ± 2.0
100	$K^0K^-\pi^+\P$	77 ± 10				$84.3 \pm 3.5 \pm 7.4 \pm 3.4^\S$ [920]			84.3 ± 8.9
101	$K^+\pi^-$	3.3 ± 1.2				$3.3 \pm 1.1 \pm 0.5$ [929]			3.3 ± 1.2
102	$K^+\bar{K}^\mp$	12.5 ± 2.6				$12.7 \pm 1.9 \pm 1.9$ [929]			12.7 ± 2.7
103	$K^0\bar{K}^0\P$	16 ± 4				$16.4 \pm 3.4 \pm 2.3$ [931]			16.4 ± 4.1
104	$K^0K^+K^-$	< 3.5				< 2.5 [920]			< 2.5
106	$K^{*0}\bar{K}^0$	11.1 ± 2.7				$10.8 \pm 2.1 \pm 1.4 \pm 0.6^\S$ [986]			10.8 ± 2.6
107	$\phi\bar{K}^0$	1.14 ± 0.3				$1.13 \pm 0.29 \pm 0.06^\dagger$ [987]			1.13 ± 0.30
108	$p\bar{p}$	$0.028^{+0.022}_{-0.017}$				< 0.015 [960]			< 0.015
111	$\gamma\gamma$	< 3.1	< 3.1	[988]					< 3.1
112	$\phi\gamma$	35.2 ± 3.4	$36 \pm 5 \pm 7$	[988]		$35.1 \pm 3.5 \pm 1.2^\dagger$ [989]			35.2 ± 3.4
113	$\mu^+\mu^-$	$0.0024^{+0.0009}_{-0.0007}$			$0.013^{+0.009}_{-0.007}$ [990]	< 0.012 [991]	$0.0030 \pm 0.0006^{+0.0003}_{-0.0002}$ [128]	$0.0028^{+0.0011}_{-0.0009}$ [992]	$0.0028^{+0.0008}_{-0.0007}$ [993]
114	e^+e^-	< 0.28		[994]					0.0031 ± 0.0006
	$\tau^+\tau^-$					< 5200 [995]			< 2.8
115	$\mu^+\mu^-\mu^+\mu^-$	< 0.012				$< 0.0025^1$ [996]			< 0.0025 ¹
117	$\phi\mu^+\mu^-$	0.83 ± 0.12				$0.797^{+0.045}_{-0.043} \pm 0.068$ [998]			$0.797^{+0.082}_{-0.080}$
118	$\pi^+\pi^-\mu^+\mu^-$	0.084 ± 0.017				$0.086 \pm 0.015 \pm 0.010^2$ [999]			0.086 ± 0.018
120	$e^+\mu^\mp$	< 0.011			< 0.20 [994]		< 0.0054 [1000]		< 0.0054
	$p\bar{K}^-\rightarrow p\bar{\lambda}K^+$					$5.46 \pm 0.61 \pm 0.57 \pm 0.50 \pm 0.32^4$ [1001]			5.46 ± 1.02
	$p\bar{p}K^+\pi^-$					$4.2 \pm 0.3 \pm 0.2 \pm 0.3 \pm 0.2^4$ [961]			4.2 ± 0.5
	$p\bar{p}\pi^+\pi^-$					$1.30 \pm 0.21 \pm 0.11 \pm 0.09 \pm 0.08^4$ [961]			1.30 ± 0.27
	$\eta'\phi$					< 0.66 [961]			< 0.66
	$\bar{K}^0\mu^+\mu^-$					< 0.82 [1002]			< 0.82
						$0.029 \pm 0.010 \pm 0.002 \pm 0.003^\S$ [1003]			0.029 ± 0.011

Channels with no RPP# were not included in PDG Live as of Dec. 31, 2017.

Results for CDF, D0, LHCb, CMS and ATLAS are relative BFs converted to absolute BFs.

[†] The first error is experimental, and the second is from the reference BF.

[‡] Last error represents the uncertainty due to the total number of $B_s^0\bar{B}_s^0$ pairs.

[§] Last error takes into account error the reference BF and f_d/f_s .

^P Includes two distinct decay processes: $\mathcal{B}(B_s^0 \rightarrow f) + \mathcal{B}(B_s^0 \rightarrow \bar{f})$.

¹ UL at 95% CL.

² Muon pairs do not originate from resonances and $0.5 < m(\pi^+\pi^-) < 1.3$ GeV/c².

³ In the mass range $400 < m(\pi^+\pi^-) < 1600$ GeV/c².

⁴ The third error is due to the reference BF and the fourth to f_d/f_s .

Table 255: Relative branching fractions of charmless B_s^0 decays. Upper limits are at 90% CL. Where values are shown in red (blue), this indicates that they are new published (preliminary) results since PDG2017.

RPP#	Mode	PDG2017 Avg.	CDF	LHCb	Our Avg.		
85/257	$f_s \mathcal{B}(B_s^0 \rightarrow \pi^+ \pi^-)/f_d \mathcal{B}(B^0 \rightarrow K^+ \pi^-)$	$0.008 \pm 0.002 \pm 0.001$	[925]	$0.00915 \pm 0.00071 \pm 0.00083$	[926]	0.00880 ± 0.00090	
85/387	$f_s \mathcal{B}(B_s^0 \rightarrow \pi^+ \pi^-)/f_d \mathcal{B}(B^0 \rightarrow \pi^+ \pi^-)$			$0.050^{+0.011}_{-0.009} \pm 0.004$	[941]	$0.050^{+0.012}_{-0.010}$	
95/46	$\mathcal{B}(B_s^0 \rightarrow \phi \phi)/\mathcal{B}(B_s^0 \rightarrow J/\psi \phi)$		$0.0178 \pm 0.0014 \pm 0.0020$	[983]		0.0180 ± 0.0020	
95/343	$\mathcal{B}(B_s^0 \rightarrow \phi \phi)/\mathcal{B}(B^0 \rightarrow \phi K^*)$				$1.84 \pm 0.05 \pm 0.13$	[999]	1.84 ± 0.14
96/257	$f_s \mathcal{B}(B_s^0 \rightarrow K^+ \pi^-)/f_d \mathcal{B}(B_d^0 \rightarrow K^+ \pi^-)$	$0.071 \pm 0.010 \pm 0.007$	[966]	$0.074 \pm 0.006 \pm 0.006$	[941]	0.073 ± 0.007	
97/257	$f_s \mathcal{B}(B_s^0 \rightarrow K^+ K^-)/f_d \mathcal{B}(B_d^0 \rightarrow K^+ \pi^-)$	$0.347 \pm 0.020 \pm 0.021$	[940]	$0.316 \pm 0.009 \pm 0.019$	[941]	0.327 ± 0.017	
99/291	$\mathcal{B}(B_s^0 \rightarrow K^0 \pi^+ \pi^-)/\mathcal{B}(B^0 \rightarrow K^0 \pi^+ \pi^-)$			$0.191 \pm 0.027 \pm 0.031 \pm 0.011$	[920]	0.191 ± 0.043	
100/322	$\mathcal{B}(B_s^0 \rightarrow K^0 K^- \pi^+)/\mathcal{B}(B^0 \rightarrow K^0 K^- \pi^+)$			$1.70 \pm 0.07 \pm 0.11 \pm 0.10$	[920]	1.70 ± 0.16	
101/294	$\mathcal{B}(B_s^0 \rightarrow K^{*-} \pi^+)/\mathcal{B}(B^0 \rightarrow K^{*-} \pi^-)$			$0.39 \pm 0.13 \pm 0.05$	[929]	0.39 ± 0.14	
102/294	$\mathcal{B}(B_s^0 \rightarrow K^{*-} K^+)/\mathcal{B}(B^0 \rightarrow K^{*-} \pi^-)$			$1.49 \pm 0.22 \pm 0.18$	[929]	1.49 ± 0.28	
103/291	$\mathcal{B}(B_s^0 \rightarrow K_s^0 K^{*0})/\mathcal{B}(B^0 \rightarrow K_s^0 \pi^+ \pi^-)$			$0.33 \pm 0.07 \pm 0.04$	[931]	0.33 ± 0.08	
104/329	$\mathcal{B}(B_s^0 \rightarrow K^0 K^+ K^-)/\mathcal{B}(B^0 \rightarrow K^0 K^+ K^-)$			< 0.051	[920]	< 0.051	
106/294	$\mathcal{B}(B_s^0 \rightarrow K^{*0} \bar{K}^{*0})/\mathcal{B}(B^0 \rightarrow K^{*+} \pi^-)$			$1.11 \pm 0.22 \pm 0.13$	[986]	1.11 ± 0.26	
107/343	$\mathcal{B}(B_s^0 \rightarrow \phi \bar{K}^{*0})/\mathcal{B}(B^0 \rightarrow \phi K^{*0})$			$0.113 \pm 0.024 \pm 0.016$	[987]	0.113 ± 0.029	
112/371	$\mathcal{B}(B_s^0 \rightarrow \phi \gamma)/\mathcal{B}(B^0 \rightarrow K^{*0} \gamma)$			$0.81 \pm 0.04 \pm 0.07$	[989]	0.81 ± 0.08	
117/46	$\mathcal{B}(B_s^0 \rightarrow \phi \mu^+ \mu^-)/\mathcal{B}(B_s^0 \rightarrow J/\psi \phi) \times 10^3$	$0.76 \pm 0.09^\diamond$	$1.13^{+0.19}_{-0.07}$	[967]	$0.741^{+0.042}_{-0.040} \pm 0.029$	[998]	0.876 ± 0.041
	$\mathcal{B}(B_s^0 \rightarrow p\bar{p} K^+ \pi^-)/\mathcal{B}(B^0 \rightarrow p\bar{p} K^+ \pi^-)$				$0.22 \pm 0.04 \pm 0.02 \pm 0.01$	[961]	0.22 ± 0.05
	$\mathcal{B}(B_s^0 \rightarrow p\bar{p} K^+ \pi^-)/\mathcal{B}(B_s^0 \rightarrow p\bar{p} K^+ K^-)$				$0.31 \pm 0.05 \pm 0.02$	[961]	0.31 ± 0.05
	$\mathcal{B}(B_s^0 \rightarrow \bar{K}^{*0} \mu^+ \mu^-)/\mathcal{B}(B_s^0 \rightarrow J/\psi \bar{K}^{*0})$				$0.014 \pm 0.004 \pm 0.001 \pm 0.001^\ddagger$	[1003]	0.014 ± 0.004
	$\mathcal{B}(B_s^0 \rightarrow \bar{K}^{*0} \mu^+ \mu^-)/(\mathcal{B}(\bar{B}^0 \rightarrow \bar{K}^{*0} \mu^+ \mu^-))$				$0.033 \pm 0.011 \pm 0.003 \pm 0.002^\S$	[1003]	0.033 ± 0.012

Channels with no RPP# were not included in PDG Live as of Dec. 31, 2017.

\dagger Numerator includes two distinct decay processes: $\mathcal{B}(B_s^0 \rightarrow f) + \mathcal{B}(B_s^0 \rightarrow \bar{f})$.

\ddagger The denominator is multiplied by $\mathcal{B}(J/\psi \rightarrow \mu^+ \mu^-)$.

\ddagger Last error is from the S-wave fraction in $B_s^0 \rightarrow \bar{K}^{*0} \mu^+ \mu^-$ and $B_s^0 \rightarrow J/\psi \bar{K}^{*0}$.

\S Last error is from the S-wave fraction in $B_s^0 \rightarrow \bar{K}^{*0} \mu^+ \mu^-$ and $\bar{B}^0 \rightarrow \bar{K}^{*0} \mu^+ \mu^-$, and f_d/f_s .

\diamond PDG also uses the denominator as input when computing the average.

List of other measurements that are not included in the tables:

- $B_s^0 \rightarrow \phi \mu^+ \mu^-$: LHCb measures the differential BF in bins of $m^2(\mu^+ \mu^-)$. It also performs an angular analysis and measures F_L , S_3 , S_4 , S_7 , A_5 , A_6 , A_8 and A_9 in bins of $m^2(\mu^+ \mu^-)$ [998].
- $B_s^0 \rightarrow \phi \gamma$: LHCb has measured the photon polarization [407].
- $B_s^0 \rightarrow \mu^+ \mu^-$: LHCb also measures the effective lifetime [128].

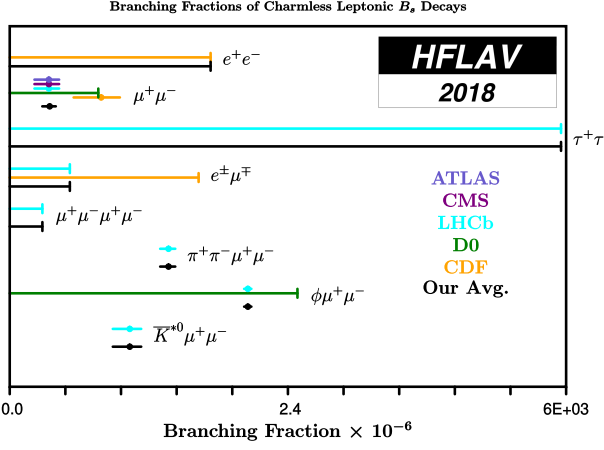


Figure 73: Branching fractions of charmless leptonic B_s^0 decays.

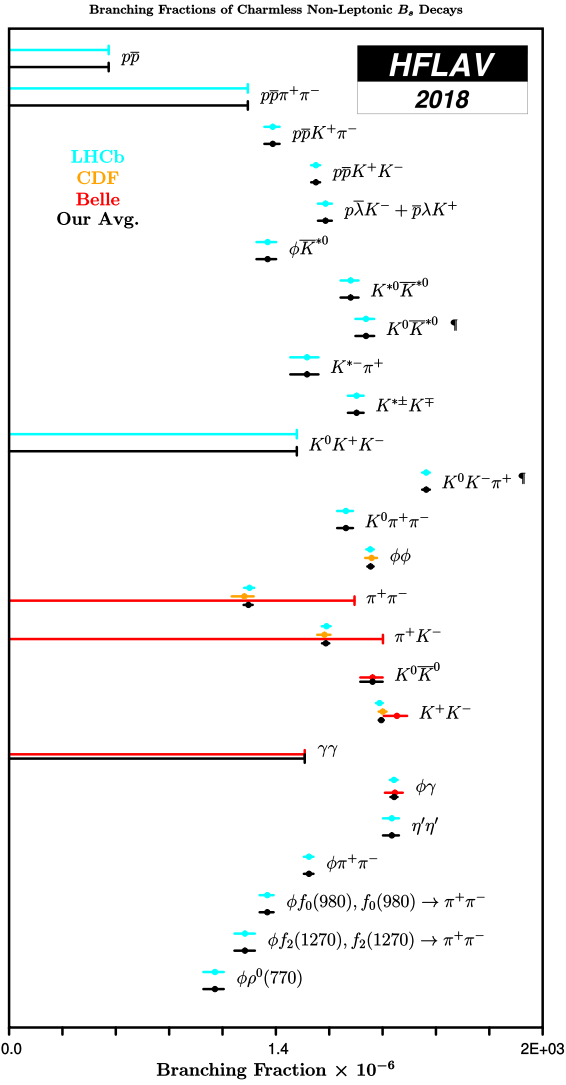


Figure 74: Branching fractions of charmless non-leptonic B_s^0 decays.

8.5 Radiative and leptonic decays of B^0 and B^+ mesons.

This section reports different observables for leptonic and radiative B^0 and B^+ meson decays. Throughout the section, “radiative decays” include processes in which a neutral boson yields a pair of charged or neutral leptons. Tables 256, 257 and 258 provide compilations of branching fractions of radiative decays of B^+ mesons, B^0 mesons and their admixture, respectively. Table 259, contains branching fractions of leptonic and radiative-leptonic B^+ and B^0 decays. It is followed by Tables 260 and 261, which give relative branching fractions of B^+ and B^0 decays and a compilations of inclusive decays, respectively. Table 262 contains isospin asymmetry measurements. Finally, Tables 263 and 264 provide compilations of branching fractions of B^+ and B^0 mesons to lepton-flavor/number-violating final states, respectively.

Figures 75 to 80 show graphic representations of a selection of results given in this section. Footnote symbols indicate that the footnote in the corresponding table should be consulted.

Table 256: Branching fractions of charmless radiative B^+ decays in units of $\times 10^{-6}$. Upper limits are at 90% CL. Where values are shown in red (blue), this indicates that they are new published (preliminary) results since PDG2017.

RPP #	Mode	PDG2017 Avg.	<i>BABAR</i>	Belle	LHCb	Our Avg.
428	$K^+\gamma$	42.1 ± 1.8	$42.2 \pm 1.4 \pm 1.6$ [1004]	$37.6 \pm 1.0 \pm 1.2$ [1005]		39.2 ± 1.3
429	$K_1^+(1270)\gamma$	44^{+7}_{-6}	$44.1^{+6.3}_{-4.4} \pm 5.8$ [†] [400]	$43 \pm 9 \pm 9$ [1006]		$43.8^{+7.1}_{-6.3}$
430	$K^+\eta\gamma$	7.9 ± 0.9	$7.7 \pm 1.0 \pm 0.4$ [404]	$8.4 \pm 1.5^{+1.2}_{-0.9}$ [1007]		7.9 ± 0.9
431	$K^+\eta'\gamma$	$2.9^{+1.0}_{-0.9}$	$1.9^{+1.5}_{-1.2} \pm 0.1$ [1008]	$3.6 \pm 1.2 \pm 0.4$ [1009]		$2.9^{+1.0}_{-0.9}$
432	$K^+\phi\gamma$	2.7 ± 0.4	$3.5 \pm 0.6 \pm 0.4$ [1010]	$2.48 \pm 0.30 \pm 0.24$ [406]		2.71 ± 0.34
433	$K^+\pi^-\pi^+\gamma$	25.8 ± 1.5	$25.9 \pm 0.7 \pm 1.0$ [¶] [400, 1011]	$25.0 \pm 1.8 \pm 2.2$ [‡] [1006]		25.8 ± 1.1
434	$K^{*0}\pi^+\gamma$ [§]	23.3 ± 1.2	$23.4 \pm 0.9^{+0.8}_{-0.7}$ [†] [400]	$20^{+7}_{-6} \pm 2$ [1012]		$23.3^{+1.2}_{-1.1}$
435	$K^+\rho^0\gamma$ [§]	$8.2 \pm 0.4 \pm 0.8$ [†]	$8.2 \pm 0.4 \pm 0.8$ [†] [400]	< 20 [1012]		8.2 ± 0.9
	$(K\pi)^0_0\pi^+\gamma$		$10.3^{+0.7+1.5}_{-0.8-2.0}$ [†] [400]			$10.3^{+1.7}_{-2.2}$
436	$K^+\pi^-\pi^+\gamma$ (N.R.) [§]	< 9.2	$9.9 \pm 0.7^{+1.5}_{-1.9}$ [†] [400]	< 9.2 [1012]		$9.9^{+1.7}_{-2.0}$
440	$K_0^*(1430)\pi^+\gamma$	$1.32^{+0.09+0.24}_{-0.10-0.30}$ [†]	$1.32^{+0.09+0.24}_{-0.10-0.30}$ [†] [400]			$1.32^{+0.26}_{-0.32}$
437	$K^0\pi^+\pi^0\gamma$	46 ± 5	$45.6 \pm 4.2 \pm 3.1$ [†] [1011]			45.6 ± 5.2
438	$K_1^+(1400)\gamma$	$9.7^{+4.6+2.9}_{-2.9-2.4}$ [†]	$9.7^{+4.6+2.9}_{-2.9-2.4}$ [†] [400]	< 15 [1006]		$9.7^{+5.4}_{-3.8}$
439	$K^*(1410)\gamma$	$27.1^{+5.4+5.9}_{-4.8-3.7}$ [†]	$27.1^{+5.4+5.9}_{-4.8-3.7}$ [†] [400]			$27.1^{+6.0}_{-6.1}$
441	$K_2^*(1430)^+\gamma$	14 ± 4	$13.8^{+3.5+1.5}_{-3.2-1.0}$ [†] [400, 1013]			$13.8^{+3.8}_{-3.4}$
442	$K^{*+}(1680)\gamma$	$66.7^{+9.3+14.4}_{-7.8-11.4}$ [†]	$66.7^{+9.3+14.4}_{-7.8-11.4}$ [†] [400]			$66.7^{+17.1}_{-13.8}$
443	$K_3^*(1780)^+\gamma$	< 39		< 39 [1007]		< 39
444	$K_3^*(2045)^+\gamma$	< 9900	< 9900 ^² [1014]			< 9900 ^²
445	$\rho^+\gamma$	0.98 ± 0.25	$1.20^{+0.42}_{-0.37} \pm 0.20$ [1015]	$0.87^{+0.29+0.09}_{-0.27-0.11}$ [1016]		$0.98^{+0.25}_{-0.24}$
495	$p\bar{A}\gamma$	$2.4^{+0.5}_{-0.4}$		$2.45^{+0.44}_{-0.38} \pm 0.22$ [956]		$2.45^{+0.49}_{-0.44}$
499	$p\bar{\Sigma}^0\gamma$	< 4.6		< 4.6 [1017]		< 4.6
534	$\pi^+\ell^+\ell^-$	< 0.049	< 0.066 [1018]	< 0.049 [1019]		< 0.049
535	$\pi^+e^+e^-$	< 0.080	< 0.125 [1018]	< 0.080 [1019]		< 0.080
536	$\pi^+\mu^+\mu^-$	$0.0179 \pm 0.0022 \pm 0.0005$	< 0.055 [1018]	< 0.069 [1019]	$0.0179 \pm 0.0022 \pm 0.0005$ [1020]	0.0180 ± 0.0020
537	$\pi^+\nu\bar{\nu}$	< 98	< 100 [1021]	< 98 [1022]		< 98
538	$K^+\ell^+\ell^-$	0.451 ± 0.023	$0.48 \pm 0.09 \pm 0.02$ [1023]	$0.53^{+0.06}_{-0.05} \pm 0.03$ [1024]		0.51 ± 0.05
539	$K^+e^+e^-$	0.55 ± 0.07	$0.51^{+0.12}_{-0.11} \pm 0.02$ [1023]	$0.57^{+0.09}_{-0.08} \pm 0.03$ [1024]		0.55 ± 0.07
540	$K^+\mu^+\mu^-$	0.443 ± 0.024	$0.41^{+0.16}_{-0.15} \pm 0.02$ [1023]	$0.53 \pm 0.08^{+0.07}_{-0.03}$ [1024]	$0.429 \pm 0.007 \pm 0.021$ [1025]	0.435 ± 0.021
541	$K^+\tau^+\tau^-$	< 2250	< 2250 [1026]			< 2250
542	$K^+\nu\bar{\nu}$	< 16	< 16 [1027]	< 16 [1028]		< 16
543	$\rho^+\nu\bar{\nu}$	< 213		< 30 [1028]		< 30
	$\pi^+\nu\bar{\nu}$			< 14 [1028]		< 14
544	$K^{*+}\ell^+\ell^-$	1.01 ± 0.11	$1.40^{+0.40}_{-0.37} \pm 0.09$ [1023]	$1.24^{+0.23}_{-0.21} \pm 0.13$ [1024]	$0.924 \pm 0.093 \pm 0.067$ [1029]	$1.009^{+0.101}_{-0.100}$
545	$K^{*+}e^+e^-$	$1.55^{+0.40}_{-0.31}$	$1.38^{+0.47}_{-0.40} \pm 0.08$ [1023]	$1.73^{+0.50}_{-0.46} \pm 0.20$ [1024]		$1.55^{+0.35}_{-0.32}$
546	$K^{*+}\mu^+\mu^-$	0.96 ± 0.10	$1.46^{+0.79}_{-0.75} \pm 0.12$ [1023]	$1.11^{+0.32}_{-0.27} \pm 0.10$ [1024]	$0.924 \pm 0.093 \pm 0.067$ [1029]	$0.958^{+0.107}_{-0.104}$
547	$K^{*+}\nu\bar{\nu}$	< 40	< 64 [1027]	< 40 [1022]		< 40
548	$K^+\pi^+\pi^-\mu^+\mu^-$	0.44 ± 0.04			$0.436^{+0.029}_{-0.027} \pm 0.028$ ^¹ [1030]	$0.436^{+0.040}_{-0.039}$
549	$K^+\phi\mu^+\mu^-$	$0.079^{+0.021}_{-0.017}$			$0.082^{+0.019+0.029}_{-0.017-0.027}$ [1030]	$0.082^{+0.035}_{-0.032}$
	$\Lambda\nu\bar{\nu}$		< 30 [1031]			< 30

Channels with no RPP# were not included in PDG Live as of Dec. 31, 2017.

Results for LHCb are relative BFs converted to absolute BFs.

CLEO upper limits that have been greatly superseded are not shown.

[†] $M_{K\pi\pi} < 1.8$ GeV/ c^2 .

[‡] $1.0 < M_{K\pi\pi} < 2.0$ GeV/ c^2 .

[§] $M_{K\pi\pi} < 2.4$ GeV/ c^2 .

[¶] Average of *BABAR* results from [400] and [1011].

[◊] Average of *BABAR* results from [400] and [1013].

^¹ Differential BF in bins of $m(\mu^+\mu^-)$ is also available.

^² Result from ARGUS. Cited in the *BABAR* column to avoid adding a column to the table.

Table 257: Branching fractions of charmless radiative B^0 decays in units of $\times 10^{-6}$. Upper limits are at 90% CL. Where values are shown in red (blue), this indicates that they are new published (preliminary) results since PDG2017.

RPP #	Mode	PDG2017 Avg.	BABAR	Belle	LHCb	Our Avg.
367	$K^0\eta\gamma$	7.6 ± 1.8	$7.1^{+2.1}_{-2.0} \pm 0.4$ [404]	$8.7^{+3.1+1.9}_{-2.7-1.6}$ [1007]		$7.6^{+1.7}_{-1.7}$
368	$K^0\eta'\gamma$	< 6.4	< 6.6 [1008]	< 6.4 [1009]		< 6.4
369	$K^0\rho'\gamma$	2.7 ± 0.7	< 2.7 [1010]	$2.74 \pm 0.60 \pm 0.32$ [406]		2.74 ± 0.68
370	$K^+\pi^-\gamma$ §	4.6 ± 1.4		$4.6^{+1.3+0.5}_{-1.2-0.7}$ [1012]		4.6 ± 1.4
371	$K^{*0}\gamma$	43.3 ± 1.5	$44.7 \pm 1.0 \pm 1.6$ [1004]	$39.6 \pm 0.7 \pm 1.4$ [1005]		41.7 ± 1.2
372	$K^*(1410)^0\gamma$	< 130		< 130 [1012]		< 130
373	$K^+\pi^-\gamma$ (N.R.) †	< 2.6		< 2.6 [1012]		< 2.6
374	$K^{*0}X(214), X(214) \rightarrow \mu^+\mu^-$	< 0.0226		< 0.0226 [1032]		< 0.0226
375	$K^*\pi^+\pi^-\gamma$	19.9 ± 1.8	$19.2 \pm 1.4 \pm 1.1$ § [400, 1011]	$24 \pm 4 \pm 3$ ¶ [1006]		19.7 ± 1.7
376	$K^+\pi^-\pi^0\gamma$	41 ± 4	$40.7 \pm 2.2 \pm 3.1$ † [1011]			40.7 ± 3.8
377	$K^0(1270)\gamma$	< 58		< 58 [1006]		< 58
378	$K_1^0(1400)\gamma$	< 12		< 12 [1006]		< 12
379	$K_2^*(1430)^0\gamma$	12.4 ± 2.4	$12.2 \pm 2.5 \pm 1.0$ [1013]	$13 \pm 5 \pm 1$ [1012]		12.4 ± 2.4
381	$K_3^*(1780)^0\gamma$	< 83		< 83 [1007]		< 83
383	$\rho^0\gamma$	0.86 ± 0.15	$0.97^{+0.24}_{-0.22} \pm 0.06$ [1015]	$0.78^{+0.17+0.09}_{-0.16-0.10}$ [1016]		$0.86^{+0.15}_{-0.14}$
384	$\rho^0X(214), X(214) \rightarrow \mu^+\mu^-$	< 0.0173		< 0.0173 [1032]		< 0.0173
385	$\omega\gamma$	$0.44^{+0.18}_{-0.16}$	$0.50^{+0.27}_{-0.23} \pm 0.09$ [1015]	$0.40^{+0.19}_{-0.16} \pm 0.13$ [1016]		$0.44^{+0.18}_{-0.16}$
386	$\phi\gamma$	< 0.1	< 0.85 [1033]	< 0.1 [1034]		< 0.1
447	$p\bar{A}\pi^-\gamma$			< 0.65 [1035]		< 0.65
503	$\pi^0\ell^+\ell^-$	< 0.053	< 0.053 [1018]	< 0.154 [1019]		< 0.053
504	$\pi^0e^+e^-$	< 0.084	< 0.084 [1018]	< 0.227 [1019]		< 0.084
505	$\pi^0\mu^+\mu^-$	< 0.069	< 0.069 [1018]	< 0.184 [1019]		< 0.069
506	$\eta\ell^+\ell^-$	< 0.064	< 0.064 [1018]			< 0.064
507	ηe^+e^-	< 0.108	< 0.108 [1018]			< 0.108
508	$\eta\mu^+\mu^-$	< 0.112	< 0.112 [1018]			< 0.112
509	$\pi^0\nu\bar{\nu}$	< 69		< 9 [1028]		< 9
510	$K^0\ell^+\ell^-$	$0.31^{+0.08}_{-0.07}$	$0.21^{+0.15}_{-0.13} \pm 0.02$ [1023]	$0.34^{+0.09}_{-0.08} \pm 0.02$ [1024]		$0.31^{+0.08}_{-0.07}$
511	$K^0e^+e^-$	$0.16^{+0.10}_{-0.08}$	$0.08^{+0.15}_{-0.12} \pm 0.01$ [1023]	$0.20^{+0.14}_{-0.10} \pm 0.01$ [1024]		$0.16^{+0.10}_{-0.08}$
512	$K^0\mu^+\mu^-$	0.339 ± 0.034	$0.49^{+0.27}_{-0.25} \pm 0.03$ [1023]	$0.44^{+0.19}_{-0.16} \pm 0.03$ [1024]	$0.327 \pm 0.034 \pm 0.017$ [1029]	$0.343^{+0.036}_{-0.035}$
513	$K^0\nu\bar{\nu}$	< 49	< 49 [1027]	< 26 [1028]		< 26
514	$\rho^0\nu\bar{\nu}$	< 208		< 40 [1028]		< 40
515	$K^{*0}\ell^+\ell^-$	$0.99^{+0.12}_{-0.11}$	$1.03^{+0.22}_{-0.21} \pm 0.07$ [1023]	$0.97^{+0.13}_{-0.11} \pm 0.07$ [1024]		$0.99^{+0.13}_{-0.11}$
516	$K^{*0}e^+e^-$	$1.03^{+0.19}_{-0.18}$	$0.86^{+0.26}_{-0.24} \pm 0.05$ [1023]	$1.18^{+0.27}_{-0.25} \pm 0.09$ [1024]		$1.03^{+0.19}_{-0.17}$
517	$K^{*0}\mu^+\mu^-$	1.03 ± 0.06	$1.35^{+0.40}_{-0.37} \pm 0.10$ [1023]	$1.06^{+0.19}_{-0.14} \pm 0.07$ [1024]	$1.036^{+0.018}_{-0.017} \pm 0.071$ ¹ [1036]	$1.049^{+0.067}_{-0.065}$
518	$K^{*0}X(214), X(214) \rightarrow \mu^+\mu^-$	< 0.001			< 0.001 [1037]	< 0.001
519	$\pi^+\pi^-\mu^+\mu^-$	$0.021 \pm 0.005 \pm 0.001$			$0.0211 \pm 0.0051 \pm 0.0022$ [◊] [999]	0.0210 ± 0.0060
520	$K^{*0}\nu\bar{\nu}$	< 55	< 120 [1027]	< 55 [1022]		< 55
523	$\phi\nu\bar{\nu}$	< 127		< 127 [1022]		< 127
525	$\pi^0e^\pm\mu^\mp$	< 0.14	< 0.14 [1038]			< 0.14
526	$K^0e^\pm\mu^\mp$	< 0.27	< 0.27 [1039]			< 0.27
527	$K^{*0}e^+\mu^-$	< 0.53	< 0.53 [1039]			< 0.53
528	$K^{*0}e^-\mu^+$	< 0.34	< 0.34 [1039]			< 0.34
529	$K^{*0}e^\pm\mu^\mp$	< 0.58	< 0.58 [1039]			< 0.58
532	$A_2^-\mu^-$	< 1.4	< 1.4 [1040]			< 1.4
533	$A_2^+e^-$	< 4	< 4 [1040]			< 4

Results for LHCb are relative BFs converted to absolute BFs.

CLEO upper limits that have been greatly superseded are not shown.

† $1.25 \text{ GeV}/c^2 < M_{K\pi} < 1.6 \text{ GeV}/c^2$.

‡ $M_{K\pi\pi} < 1.8 \text{ GeV}/c^2$.

§ Average of BABAR results from [400] and [1011].

¶ $1.0 < M_{K\pi\pi} < 2.0 \text{ GeV}/c^2$.

◊ This result takes into account the S-wave fraction in the $K\pi$ system.

¹ Muon pairs do not originate from resonances and $0.5 < m(\pi^+\pi^-) < 1.3 \text{ GeV}/c^2$.

Table 258: Branching fractions of charmless radiative decays of B^\pm/B^0 admixture in units of $\times 10^{-6}$. Upper limits are at 90% CL. Where values are shown in red (blue), this indicates that they are new published (preliminary) results since PDG2017.

RPP #	Mode	PDG2017 Avg.	BABAR	Belle	CLEO	CDF	Our Avg.
67	$K\eta\gamma$	$8.5^{+1.8}_{-1.6}$		$8.5^{+1.3}_{-1.2} \pm 0.9$	[1007]		$8.5^{+1.6}_{-1.5}$
68	$K_1(1400)\gamma$	< 1.27			< 1.27	[1041]	< 1.27
69	$K_2^*(1430)\gamma$	17^{+6}_{-5}			$17 \pm 6 \pm 1$	[1041]	17 ± 6
71	$K_3^*(1780)\gamma$	< 37		< 37 [§]	[1007]		< 37 [§]
78	$s\gamma$ [†]	349 ± 19	341^{+28}_{-28} [¶]	[1042–1044]	328^{+20}_{-20} [¶]	[526, 1045, 1046]	$329 \pm 44 \pm 29$ [527]
78	$s\gamma$ [◊]	308 ± 22 [¶]	[1042–1044]	305^{+16}_{-16} [¶]	[1045, 1046]		306 ± 12
79	$d\gamma$	9.2 ± 3.0	$9.2 \pm 2.0 \pm 2.3$	[1047]			9.2 ± 3.0
85	$\rho\gamma$	1.39 ± 0.25	$1.73^{+0.32}_{-0.32} \pm 0.17$	[1015]	$1.21^{+0.24}_{-0.22} \pm 0.12$	[1016]	$1.39^{+0.22}_{-0.21}$
86	$\rho/\omega\gamma$	1.30 ± 0.23	$1.63^{+0.30}_{-0.28} \pm 0.16$	[1015]	$1.14 \pm 0.20^{+0.10}_{-0.12}$	[1016]	$1.30^{+0.18}_{-0.19}$
121	se^+e^- [‡]	6.7 ± 1.7	$7.69^{+0.82+0.71}_{-0.77-0.60}$	[1048]	$4.05 \pm 1.30^{+0.87}_{-0.83}$	[1049]	6.67 ± 0.82
120	$s\mu^+\mu^-$ [‡]	4.3 ± 1.0	$4.41^{+1.31+0.63}_{-1.17-0.50}$	[1048]	$4.13 \pm 1.05^{+0.85}_{-0.81}$	[1049]	$4.27^{+0.98}_{-0.91}$
123	$s\ell^+\ell^-$ [‡]	5.8 ± 1.3	$6.73^{+0.70+0.60}_{-0.64-0.56}$	[1048]	$4.11 \pm 0.83^{+0.85}_{-0.81}$	[1049]	5.84 ± 0.69
124	$\pi\ell^+\ell^-$	< 0.059	< 0.059	[1018]	< 0.062	[1019]	< 0.059
125	πe^+e^-	< 0.110	< 0.110	[1018]			< 0.110
126	$\pi\mu^+\mu^-$	< 0.050	< 0.050	[1018]			< 0.050
127	Ke^+e^-	0.44 ± 0.06	$0.39^{+0.09}_{-0.08} \pm 0.02$	[1023]	$0.48^{+0.08}_{-0.07} \pm 0.03$	[1024]	0.44 ± 0.06
128	$K^*e^+e^-$	1.19 ± 0.20	$0.99^{+0.23}_{-0.22} \pm 0.06$	[1023]	$1.39^{+0.23}_{-0.20} \pm 0.12$	[1024]	$1.19^{+0.17}_{-0.16}$
129	$K\mu^+\mu^-$	0.44 ± 0.04	$0.41^{+0.13}_{-0.12} \pm 0.02$	[1023]	$0.50 \pm 0.06 \pm 0.03$	[1024]	$0.42 \pm 0.04 \pm 0.02$ [967]
130	$K^*\mu^+\mu^-$	1.06 ± 0.09	$1.39^{+0.35}_{-0.33} \pm 0.10$	[1023]	$1.10^{+0.16}_{-0.14} \pm 0.08$	[1024]	$1.01 \pm 0.10 \pm 0.05$ [967]
131	$K\ell^+\ell^-$	0.48 ± 0.04	$0.47 \pm 0.06 \pm 0.02$	[1050]	$0.48^{+0.04}_{-0.04} \pm 0.03$	[1024]	0.48 ± 0.04
132	$K^*\ell^+\ell^-$	1.05 ± 0.10	$1.02^{+0.14}_{-0.13} \pm 0.05$	[1050]	$1.07^{+0.11}_{-0.10} \pm 0.09$	[1024]	1.05 ± 0.10
133	$K\nu\bar{\nu}$	< 17	< 17	[1027]	< 16	[1028]	< 16
134	$K^*\nu\bar{\nu}$	< 76	< 76	[1027]	< 27	[1028]	< 27
	$\pi\nu\bar{\nu}$				< 9	[1028]	< 9
	$\rho\nu\bar{\nu}$				< 30	[1028]	< 30
136	$\pi e^\pm\mu^\mp$	< 0.092	< 0.092	[1038]			< 0.092
137	$\rho e^\pm\mu^\mp$	< 3.2			< 3.2	[1051]	< 3.2
138	$Ke^\pm\mu^\mp$	< 0.038	< 0.038	[1039]			< 0.038
139	$K^*e^\pm\mu^\mp$	< 0.51	< 0.51	[1039]			< 0.51

Channels with no RPP# were not included in PDG Live as of Dec. 31, 2017.

Results for CDF are relative BFs converted to absolute BFs.

CLEO upper limits that have been greatly superseded are not shown.

[†] Results extrapolated to $E_\gamma > 1.6$ GeV, using the method of Ref. [1052].

[‡] Belle: $m(\ell^+\ell^-) > 0.2$ GeV/c², BABAR: $m^2(\ell^+\ell^-) > 0.1$ GeV²/c⁴.

[§] The value quoted is $\mathcal{B}(B \rightarrow K_3^*\gamma) \times \mathcal{B}(K_3^* \rightarrow K\eta)$. PDG gives the BF assuming $\mathcal{B}(K_3^* \rightarrow K\eta) = 11^{+5}_{-4}\%$.

[¶] Average of several results, obtained with different methods.

[◊] Only results originally measured in the interval $E_\gamma > 1.9$ GeV (also taken into account in the previous line).

Table 259: Branching fractions of charmless leptonic and radiative-leptonic B^+ and B^0 decays in units of $\times 10^{-6}$. Upper limits are at 90% CL. Where values are shown in red (blue), this indicates that they are new published (preliminary) results since PDG2017.

RPP#	Mode	PDG2017 Avg.	BABAR	Belle	CDF	LHCb	CMS	ATLAS	Our Avg.
31	$e^+\nu$	< 0.98	< 1.9 [1053]	< 0.98 [†] [1054]					< 0.98 [†]
32	$\mu^+\nu$	< 1.0	< 1.0 [1053]	< 1.07 [1055]					< 1.0
33	$\tau^+\nu$	109 ± 24	179 ± 48 [1056]	91 ± 19 ± 11 [1057]					106 ± 19
34	$\ell^+\nu\gamma$	< 3.5	< 15.6 [1058]	< 3.0 [1059]					< 3.0
35	$e^+\nu_e\gamma$	< 6.1	< 17 [1058]	< 6.1 [1060]					< 6.1
36	$\mu^+\nu_\mu\gamma$	< 3.4	< 24 [1058]	< 3.4 [1060]					< 3.4
495	$\gamma\gamma$	< 0.32	< 0.32 [1061]	< 0.62 [1062]					< 0.32
458	e^+e^-	< 0.083	< 0.113 [1063]	< 0.19 [1064]	< 0.083 [994]				< 0.083
497	$e^-\gamma$	< 0.12	< 0.12 [1065]						< 0.12
498	$\mu^+\mu^-$	0.00018 ± 0.00031	< 0.052 [1063]	< 0.16 [1064]	< 0.0038 [990]	< 0.00034 [¶] [128]	< 0.00110 [¶] [1066]	< 0.00021 [¶] [993]	< 0.00021
499	$\mu^+\mu^-\gamma$	< 0.16	< 0.16 [1065]						< 0.16
500	$\mu^+\mu^-\mu^+\mu^-$	< 0.0053			< 0.0053 [¶] [996]				< 0.0053 [¶]
501	$SP, S \rightarrow \mu^+\mu^-, P \rightarrow \mu^+\mu^-$	< 0.0051			< 0.0051 [¶] [996]				< 0.0051 [¶]
502	$\tau^+\tau^-$	< 4100	< 4100 [1067]			< 1600 [995]			< 1600
524	$e^\pm\mu^\mp$	< 0.0028	< 0.092 [1063]	< 0.17 [1064]	< 0.064 [994]	< 0.001 [1000]			< 0.001
530	$e^+\tau^\mp$	< 28	< 28 [1068]						< 28
532	$\mu^+\tau^\mp$	< 22	< 22 [1068]						< 22
521	$\nu\bar{\nu}$	< 24	< 24 [1069]	< 130 [1070]					< 24
522	$\nu\bar{\nu}\gamma$	< 17	< 17 [1069]						< 17

Results for CDF, LHCb, CMS and ATLAS are relative BFs converted to absolute BFs.

[†] More recent results exist, with hadronic tagging [1071], that do not improve the limits (< 3.5 and < 2.7) for $e^+\nu$ and $\mu^+\nu$, respectively).

[¶] UL at 95% CL.

Table 260: Relative branching fractions of charmless radiative B^+ and B^0 decays. Where values are shown in red (blue), this indicates that they are new published (preliminary) results since PDG2017.

RPP#	Mode	PDG2017 AVG.	Belle	BABAR	LHCb	Our Avg.
548/298	$10^4 \times \mathcal{B}(K^+\pi^+\pi^-\mu^+\mu^-)/\mathcal{B}(\psi(2S)K^+)$	$6.95^{+0.46}_{-0.43} \pm 0.34$			$6.95^{+0.46}_{-0.43} \pm 0.24$ [1030]	$6.95^{+0.57}_{-0.55}$
549/274	$10^4 \times \mathcal{B}(K^+\mu^+\mu^-)/\mathcal{B}(\psi(2S)K^+)$	$1.58^{+0.36+0.19}_{-0.32-0.07}$			$1.58^{+0.33+0.19}_{-0.32-0.07}$ [1030]	$1.58^{+0.31}_{-0.33}$
536/540	$\mathcal{B}(\pi^+\mu^+\mu^-)/\mathcal{B}(K^+\mu^+\mu^-)$ [†]	$0.053 \pm 0.014 \pm 0.01$			$0.038 \pm 0.009 \pm 0.001$ [1020]	0.038 ± 0.009
	$\mathcal{B}(K^+\mu^+\mu^-)/\mathcal{B}(K^+e^+e^-)$ [‡]				$0.745^{+0.090}_{-0.074} \pm 0.036$ [1072]	$0.745^{+0.097}_{-0.082}$
	$\mathcal{B}(K^+\mu^+\mu^-)/\mathcal{B}(K^+e^+e^-)$ [‡]					$1.00^{+0.32}_{-0.26}$
	$\mathcal{B}(K^+\mu^+\mu^-)/\mathcal{B}(K^+e^+e^-)$ [§]		$1.03 \pm 0.19 \pm 0.06$ [1024]			1.03 ± 0.20
	$\mathcal{B}(K^*\mu^+\mu^-)/\mathcal{B}(K^*e^+e^-)$ [§]		$0.83 \pm 0.17 \pm 0.08$ [1024]			0.83 ± 0.19
	$\mathcal{B}(K^*\mu^+\mu^-)/\mathcal{B}(K^*e^+e^-)$ [¶]			$1.013^{+0.34}_{-0.26} \pm 0.010$ [1050]		$1.013^{+0.340}_{-0.260}$
	$\mathcal{B}(K^{*0}\mu^+\mu^-)/\mathcal{B}(K^{*0}e^+e^-)$ [○]				$0.66^{+0.11}_{-0.07} \pm 0.03$ [1073]	$0.66^{+0.11}_{-0.08}$
	$\mathcal{B}(K^{*0}\mu^+\mu^-)/\mathcal{B}(K^{*0}e^+e^-)$ [○]				$0.69^{+0.11}_{-0.07} \pm 0.05$ [1073]	$0.69^{+0.12}_{-0.09}$
	$\mathcal{B}(B^0 \rightarrow K^{*0}\gamma)/\mathcal{B}(B_s^0 \rightarrow \phi\gamma)$		$1.10 \pm 0.16 \pm 0.09 \pm 0.18$ [1005]		$1.23 \pm 0.06 \pm 0.11$ [989]	1.21 ± 0.11

Channels with no RPP# were not included in PDG Live as of Dec. 31, 2017.

[†] For $0.1 < m^2(\ell^+\ell^-) < 6.0 \text{ GeV}^2/c^4$.

[‡] For $1.0 < m^2(\ell^+\ell^-) < 6.0 \text{ GeV}^2/c^4$.

[§] For the full $m^2(\ell^+\ell^-)$ range.

[¶] For $0.10 < m^2(\ell^+\ell^-) < 8.12 \text{ GeV}^2/c^4$ and $m^2(\ell^+\ell^-) > 10.11 \text{ GeV}^2/c^4$.

[○] For $0.045 < m^2(\ell^+\ell^-) < 1.1 \text{ GeV}^2/c^4$.

¹ For $1.1 < m^2(\ell^+\ell^-) < 6.0 \text{ GeV}^2/c^4$.

Table 261: Branching fractions of $B^+/B^0 \rightarrow \bar{q}$ gluon decays in units of $\times 10^{-6}$. Upper limits are at 90% CL. Where values are shown in red (blue), this indicates that they are new published (preliminary) results since PDG2017.

RPP#	Mode	PDG2017 Avg.	<i>BABAR</i>	<i>Belle</i>	<i>CLEO</i>	Our Avg.
81	ηX	260^{+50}_{-80}		$261 \pm 30^{+44}_{-74} \S$ [1074]	< 440 [1075]	261^{+53}_{-79}
82	$\eta' X$	420 ± 90	$390 \pm 80 \pm 90 \dagger$ [1076]		$460 \pm 110 \pm 60 \dagger$ [1077]	423 ± 86
83	$K^+ X$	< 187	$< 187 \ddagger$ [1078]			$< 187 \ddagger$
84	$K^0 X$	190^{+70}_{-70}	$195^{+51}_{-45} \pm 50 \ddagger$ [1078]			195^{+71}_{-67}
95	$\pi^+ X$	370 ± 80	$372^{+50}_{-47} \pm 59 \P$ [1078]			372^{+77}_{-75}

\dagger $2.0 < p^*(\eta') < 2.7 \text{ GeV}/c$.

\ddagger $m_X < 1.69 \text{ GeV}/c^2$.

\S $0.4 < m_X < 2.6 \text{ GeV}/c^2$.

\P $m_X < 1.71 \text{ GeV}/c^2$.

Table 262: Isospin asymmetry in radiative B meson decays. The notations are those adopted by the PDG. Where values are shown in red (blue), this indicates that they are new published (preliminary) results since PDG2017.

Parameter	PDG2017 Avg.	<i>BABAR</i>	<i>Belle</i>	<i>LHCb</i>	Our Avg.
$\Delta_{0-}(X_s \gamma)$	-0.01 ± 0.06	$-0.01^{+0.06}_{-0.06} \ddagger$ [524, 1042]	$-0.0048 \pm 0.0149 \pm 0.0097 \pm 0.0115$ [1079]		-0.0055 ± 0.0198
$\Delta_{0+}(K^* \gamma)$	0.052 ± 0.026	$0.066 \pm 0.021 \pm 0.022$ [1004]	$0.062 \pm 0.015 \pm 0.006 \pm 0.012$ [1005]		0.063 ± 0.017
$\Delta_{\rho\gamma}$	-0.46 ± 0.17	$-0.43^{+0.25}_{-0.22} \pm 0.10$ [1015]	$-0.48^{+0.21+0.08}_{-0.19-0.09}$ [1016]		$-0.46^{+0.17}_{-0.16}$
$\Delta_{0-}(K \ell \ell) \dagger$	-0.13 ± 0.06	$-0.58^{+0.29}_{-0.37} \pm 0.02$ [1050]	$-0.31^{+0.17}_{-0.14} \pm 0.08$ [1024]	$-0.10^{+0.08}_{-0.09} \pm 0.02 \S$ [1029]	-0.17 ± 0.08
$\Delta_{0-}(K^* \ell \ell) \dagger$	-0.45 ± 0.17	$-0.64^{+0.15}_{-0.14} \pm 0.03$ [1050]	$0.30^{+0.12}_{-0.11} \pm 0.08$ [1024]	$0.00^{+0.12}_{-0.10} \pm 0.02 \S$ [1029]	-0.06 ± 0.07

In some of the B -factory results it is assumed that $\mathcal{B}(\Upsilon(4S) \rightarrow B^+ B^-) = \mathcal{B}(\Upsilon(4S) \rightarrow B^0 \bar{B}^0)$, and in others a measured value of the ratio of branching fractions is used. See original papers for details. The averages quoted above are computed naively and should be treated with caution.

\dagger Results given for the bin $1 < m^2(\ell^+ \ell^-) < 6 \text{ GeV}^2/c^4$, see references for the other bins.

\ddagger Average of two independent measurements from *BABAR* [524, 1042].

\S Only muons are used.

Table 263: Branching fractions of charmless semileptonic B^+ decays to LFV and LNV final states in units of $\times 10^{-6}$. Upper limits are at 90% CL. Where values are shown in red (blue), this indicates that they are new published (preliminary) results since PDG2017.

RPP#	Mode	PDG2017 Avg.	BABAR	BELLE	LHCb	Our Avg.
552	$\pi^+ e^\pm \mu^\mp$	< 0.17	< 0.17 [1038]			< 0.17
553	$\pi^+ e^+ \tau^-$	< 74	< 74 [1080]			< 74
554	$\pi^+ e^- \tau^+$	< 20	< 20 [1080]			< 20
555	$\pi^+ e^\pm \tau^\mp$	< 75	< 75 [1080]			< 75
556	$\pi^+ \mu^+ \tau^-$	< 62	< 62 [1080]			< 62
557	$\pi^+ \mu^- \tau^+$	< 45	< 45 [1080]			< 45
558	$\pi^+ \mu^\pm \tau^\mp$	< 72	< 72 [1080]			< 72
559	$K^+ e^+ \mu^-$	< 0.091	< 0.091 [1039]			< 0.091
560	$K^+ e^- \mu^+$	< 0.13	< 0.13 [1039]			< 0.13
561	$K^+ e^\pm \mu^\mp$	< 0.091	< 0.091 [1039]			< 0.091
562	$K^+ e^+ \tau^-$	< 43	< 43 [1080]			< 43
563	$K^+ e^- \tau^+$	< 15	< 15 [1080]			< 15
564	$K^+ e^\pm \tau^\mp$	< 30	< 30 [1080]			< 30
565	$K^+ \mu^+ \tau^-$	< 45	< 45 [1080]			< 45
566	$K^+ \mu^- \tau^+$	< 28	< 28 [1080]			< 28
567	$K^+ \mu^\pm \tau^\mp$	< 48	< 48 [1080]			< 48
568	$K^{*+} e^+ \mu^-$	< 1.3	< 1.3 [1039]			< 1.3
569	$K^{*+} e^- \mu^+$	< 0.99	< 0.99 [1039]			< 0.99
570	$K^{*+} e^\pm \mu^\mp$	< 1.4	< 1.4 [1039]			< 1.4
571	$\pi^- e^+ e^+$	< 0.023	< 0.023 [1081]			< 0.023
572	$\pi^- \mu^+ \mu^+$	< 0.013	< 0.107 [1081]		< 0.004 [†] [1082]	< 0.004 [†]
573	$\pi^- e^+ \mu^+$	< 0.15	< 0.15 [1083]			< 0.15
574	$\rho^- e^+ e^+$	< 0.17	< 0.17 [1083]			< 0.17
575	$\rho^- \mu^+ \mu^+$	< 0.42	< 0.42 [1083]			< 0.42
576	$\rho^- e^+ \mu^+$	< 0.47	< 0.47 [1083]			< 0.47
577	$K^- e^+ e^+$	< 0.03	< 0.03 [1081]			< 0.03
578	$K^- \mu^+ \mu^+$	< 0.041	< 0.067 [1081]		< 0.041 [1084]	< 0.041
579	$K^- e^+ \mu^+$	< 0.16	< 0.16 [1083]			< 0.16
580	$K^{*-} e^+ e^+$	< 0.40	< 0.40 [1083]			< 0.40
581	$K^{*-} \mu^+ \mu^+$	< 0.59	< 0.59 [1083]			< 0.59
582	$K^{*-} e^+ \mu^+$	< 0.30	< 0.30 [1083]			< 0.30
583	$D^- e^+ e^+$	< 2.6	< 2.6 [1083]	< 2.6 [753]		< 2.6
584	$D^- e^+ \mu^+$	< 1.8	< 2.1 [1083]	< 1.8 [753]		< 1.8
585	$D^- \mu^+ \mu^+$	< 0.69	< 1.7 [1083]	< 1.1 [753]	< 0.69 [1085]	< 0.69
586	$D_s^- \mu^+ \mu^+$	< 0.58			< 0.58 [1085]	< 0.58
587	$\bar{D}^0 \pi^- \mu^+ \mu^+$	< 1.5			< 1.5 [1085]	< 1.5
589	$\Lambda^0 \mu^+$	< 0.06	< 0.06 [1040]			< 0.06
590	$\Lambda^0 e^+$	< 0.032	< 0.032 [1040]			< 0.032
591	$\bar{\Lambda}^0 \mu^+$	< 0.06	< 0.06 [1040]			< 0.06
592	$\bar{\Lambda}^0 e^+$	< 0.08	< 0.08 [1040]			< 0.08

Results for LHCb are relative BFs converted to absolute BFs.

CLEO upper limits that have been greatly superseded are not shown.

[†] UL at 95% CL.

Table 264: Branching fractions of charmless semileptonic B^0 decays to LFV and LNV final states in units of $\times 10^{-6}$. Upper limits are at 90% CL. Where values are shown in red (blue), this indicates that they are new [published](#) ([preliminary](#)) results since PDG2017.

RPP#	Mode	PDG2017 Avg.	<i>BABAR</i>	<i>BELLE</i>	<i>LHCb</i>	Our Avg.
	$K^{*0}\mu^+e^-$			< 0.12 [1086]		< 0.12
	$K^{*0}\mu^-e^+$			< 0.16 [1086]		< 0.16
	$K^{*0}\mu^\pm e^\mp$			< 0.18 [1086]		< 0.18

Channels with no RPP# were not included in PDG Live as of Dec. 31, 2017.

List of other measurements that are not included in the tables:

- $B^+ \rightarrow K^+\pi^-\pi^+\gamma$: LHCb has measured the up-down asymmetries in bins of the $K\pi\pi\gamma$ mass [1087].
- In [1088], LHCb has also measured the branching fraction of $B^+ \rightarrow K^+e^-e^+$ in the $m^2(\ell\ell)$ bin [1, 6] GeV^2/c^4 .
- In the $B^+ \rightarrow \pi^+\mu^+\mu^-$ paper [1020], LHCb has also measured the differential branching fraction in bins of $m^2(\ell\ell)$.
- For $B \rightarrow K\ell^-\ell^+$, LHCb has measured F_H and A_{FB} in 17 (5) bins of $m^2(\ell\ell)$ for the K^+ (K_S^0) final state [1089]. Belle has measured F_L and A_{FB} in 6 $m^2(\ell\ell)$ bins [64].
- For the $B \rightarrow K^*\ell^-\ell^+$ analyses, partial branching fractions and angular observables in bins of $m^2(\ell\ell)$ are also available:
 - $B^0 \rightarrow K^{*0}e^-e^+$: LHCb has measured F_L , $A_T^{(2)}$, A_T^{Im} , A_T^{Re} in the [0.002, 1.120] GeV^2/c^4 bin of $m^2(\ell\ell)$ [1090], and has also determined the branching fraction in the dilepton mass region [10, 1000] MeV/c^2 [1088].
 - $B \rightarrow K^*\ell^-\ell^+$: Belle has measured F_L , A_{FB} , isospin asymmetry in 6 $m^2(\ell\ell)$ bins [1024] [41] and P'_4 , P'_5 , P'_6 , P'_8 in 4 $m^2(\ell\ell)$ bins [1091]. In a more recent paper [1092], they report measurements of P'_4 and P'_5 , separately for $\ell = \mu$ or e , in 4 $m^2(\ell\ell)$ bins and in the region [1, 6] GeV^2/c^4 bin of $m^2(\ell\ell)$. The measurements use both B^0 and B^+ decays. They also measure the LFV observables $Q_i = P_i^\mu - P_i^e$, for $i = 4, 5$. *BABAR* has measured F_L , A_{FB} , P_2 in 5 $m^2(\ell\ell)$ bins [1093].
 - $B^0 \rightarrow K^{*0}\mu^-\mu^+$: LHCb has measured F_L , A_{FB} , $S_3 - S_9$, $A_3 - A_9$, $P_1 - P_3$, $P'_4 - P'_8$ in 8 $m^2(\ell\ell)$ bins [1094]. CMS has measured F_L and A_{FB} in 7 $m^2(\ell\ell)$ bins [1095], and P_1, P'_5 in [1096]. ATLAS has measured F_L , $S_{3,4,5,7,8}$ and $P'_{1,4,5,6,8}$ in 6 $m^2(\ell\ell)$ bins [1097].
- For $B \rightarrow X_s\ell^-\ell^+$ (X_s is a hadronic system with an s quark), Belle has measured A_{FB} in bins of $m^2(\ell\ell)$ with a sum of 10 exclusive final states [1098].
- $B^0 \rightarrow K^+\pi^-\mu^+\mu^-$, with $1330 < m(K^+\pi^-) < 1530 \text{ GeV}/c^2$: LHCb has measured the partial branching fraction in bins of $m^2(\mu^+\mu^-)$ in the range [0.1, 8.0] GeV^2/c^4 , and has also determined angular moments [1099].
- In [1100], LHCb measures the phase difference between the short- and long-distance contributions to the $B^+ \rightarrow K^+\mu^+\mu^-$ decay. The measurement is based on the analysis of the dimuon mass distribution in the regions of the J/ψ and $\psi(2S)$ resonances and far from their poles, to probe long and short distance effects, respectively.
- In [1101] CMS studies the angular distribution of $B^+ \rightarrow K^+\mu^+\mu^-$ and measures, in 7 $m^2(\mu^+\mu^-)$ bins, A_{FB} and the contribution F_H from the pseudoscalar, scalar and tensor amplitudes to the decay.

- In [1102] LHCb performs a search for a hypothetical new scalar particle χ , assumed to have a narrow width, through the decay $B^+ \rightarrow \chi(\mu^+\mu^-)$ in the ranges of mass $250 < m(\chi) < 4700$ MeV/ c^2 and lifetime $0.1 < \tau(\chi) < 1000$ ps. Upper limits are given as a function of $m(\chi)$ and $\tau(\chi)$.

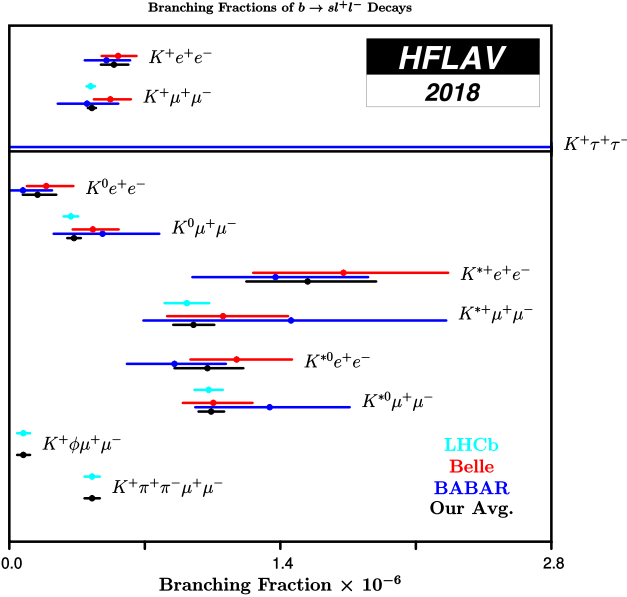


Figure 75: Branching fractions of $b \rightarrow s\ell^+\ell^-$ decays.

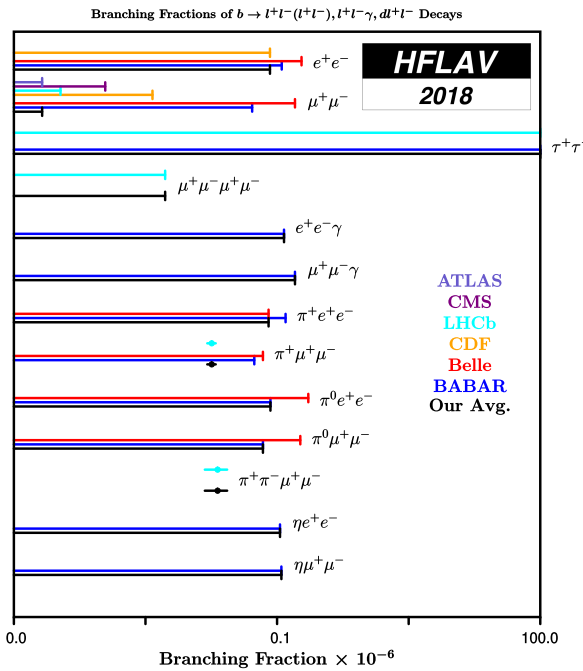


Figure 76: Branching fractions of $b \rightarrow \ell^+\ell^-(\ell^+\ell^-), \ell^+\ell^-\gamma$ and $b \rightarrow d\ell^+\ell^-$ decays.

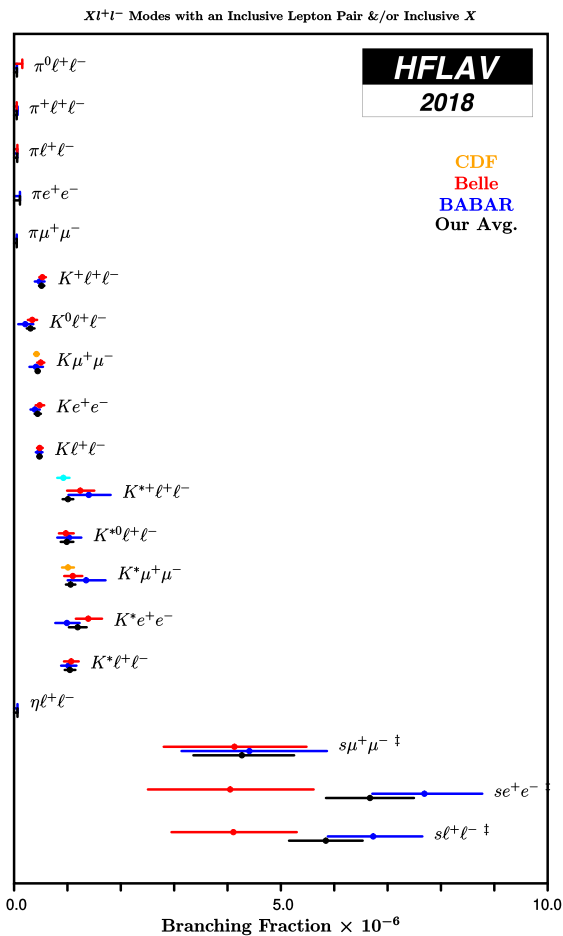


Figure 77: $X\ell^+\ell^-$ modes with an inclusive lepton pair and/or inclusive *X*.

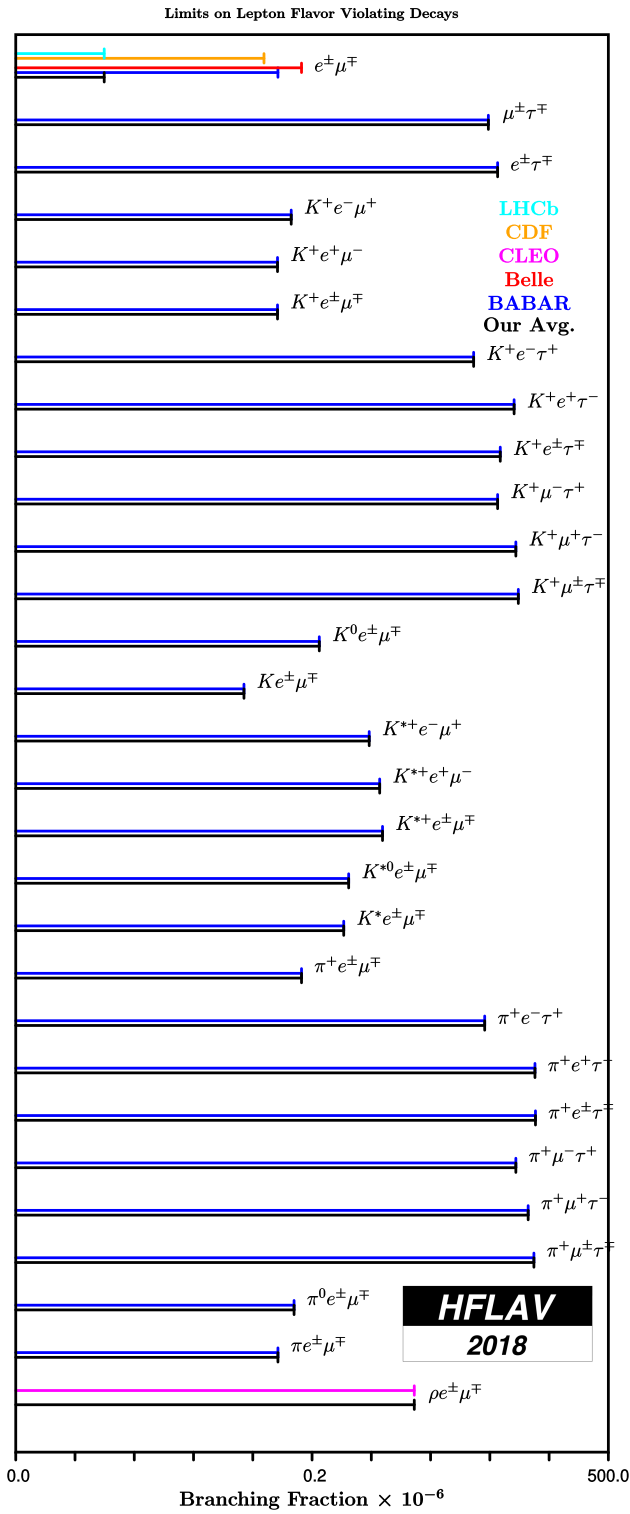


Figure 78: Limits on lepton-flavor-violating decays.

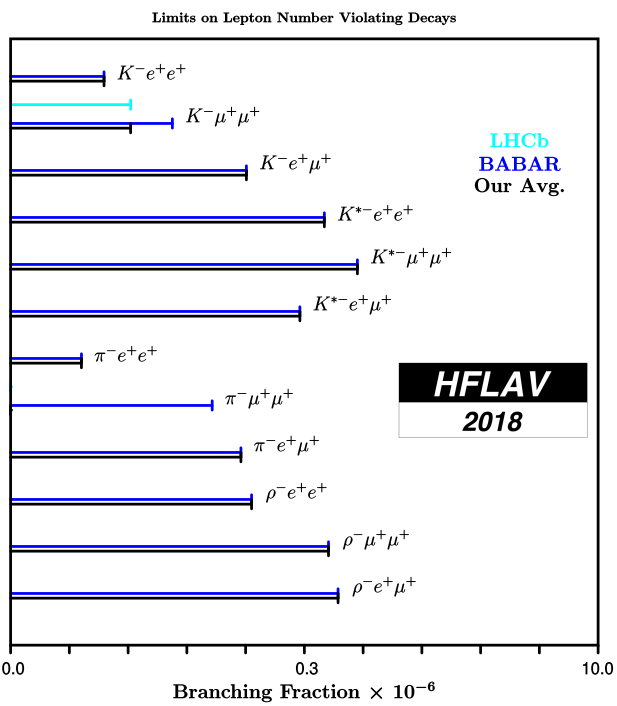


Figure 79: Limits on lepton-number-violating decays.

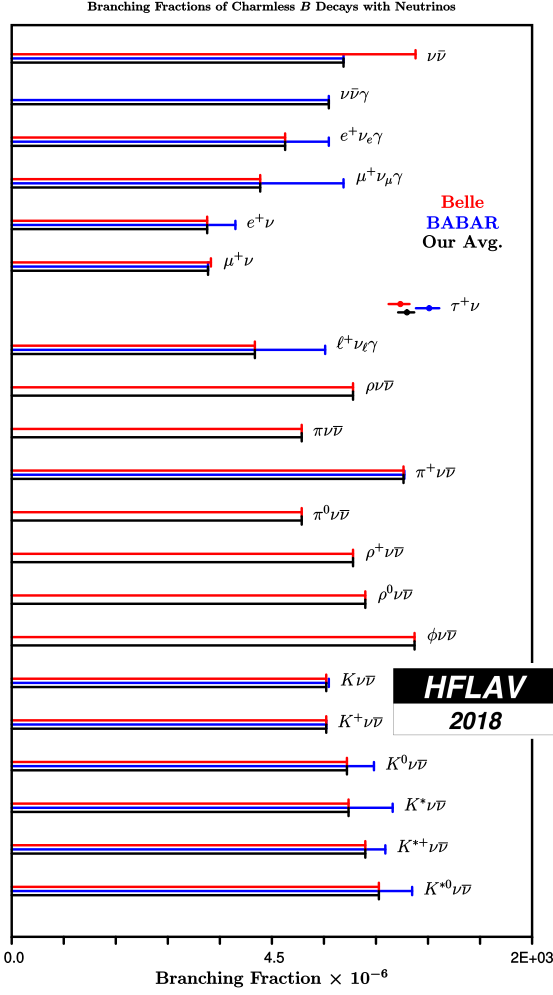


Figure 80: Branching fractions of charmless B decays with neutrinos.

8.6 Charge asymmetries in b -hadron decays

This section contains, in Tables 265 to 270, compilations of CP asymmetries in decays of various b -hadrons: B^+ , B^0 mesons, B^\pm/B^0 admixtures, B_s^0 mesons and finally Λ_b^0 baryons. Measurements of time-dependent CP asymmetries are not listed here but are discussed in Sec. 5.

Figure 81 shows a graphic representation of a selection of results given in this section. Footnote symbols indicate that the footnote in the corresponding table should be consulted.

Table 265: CP asymmetries of charmless hadronic B^+ decays (part 1). Where values are shown in red (blue), this indicates that they are new published (preliminary) results since PDG2017.

Mode	PDG2017 Avg.	BABAR	Belle	CDF	LHCb	Our Avg.
$K^+\pi^+$	-0.017 ± 0.016	$-0.029 \pm 0.039 \pm 0.010$ [397]	$-0.011 \pm 0.021 \pm 0.006$ [845]		$-0.022 \pm 0.025 \pm 0.010$ [877]	-0.017 ± 0.016
$K^+\pi^0$	$0.037 \pm 0.021^\ddagger$	$0.030 \pm 0.039 \pm 0.010$ [847]	$0.043 \pm 0.024 \pm 0.002$ [845]			0.040 ± 0.021
$\eta' K^+$	0.004 ± 0.011	$0.008^{+0.017}_{-0.018} \pm 0.009$ [848]	$0.028 \pm 0.028 \pm 0.021$ [849]		$-0.002 \pm 0.012 \pm 0.001 \pm 0.006$ [982]	0.003 ± 0.010
$\eta' K^{*+}$	-0.26 ± 0.27	$-0.26 \pm 0.27 \pm 0.02$ [850]				-0.26 ± 0.27
$\eta' K_0'(1430)^+$	0.06 ± 0.20	$0.06 \pm 0.20 \pm 0.02$ [850]				0.06 ± 0.20
$\eta' K_2'(1430)^+$	0.15 ± 0.13	$0.15 \pm 0.13 \pm 0.02$ [850]				0.15 ± 0.13
ηK^+	-0.37 ± 0.08	$-0.36 \pm 0.11 \pm 0.03$ [848]	$-0.38 \pm 0.11 \pm 0.01$ [852]			-0.37 ± 0.08
ηK^{*+}	0.02 ± 0.06	$0.01 \pm 0.08 \pm 0.02$ [854]	$0.03 \pm 0.10 \pm 0.01$ [855]			0.02 ± 0.06
$\eta K_0'(1430)^+$	$0.05 \pm 0.13 \pm 0.02$	$0.05 \pm 0.13 \pm 0.02$ [854]				0.05 ± 0.13
$\eta K_2'(1430)^+$	$-0.45 \pm 0.30 \pm 0.02$	$-0.45 \pm 0.30 \pm 0.02$ [854]				-0.45 ± 0.30
ωK^+	-0.02 ± 0.04	$-0.01 \pm 0.07 \pm 0.01$ [857]	$-0.03 \pm 0.04 \pm 0.01$ [1103]			-0.02 ± 0.04
ωK^{*+}	0.29 ± 0.35	$0.29 \pm 0.35 \pm 0.02$ [859]				0.29 ± 0.35
$\omega K_0'(1430)^+$	-0.10 ± 0.09	$-0.10 \pm 0.09 \pm 0.02$ [859]				-0.10 ± 0.09
$\omega K_2'(1430)^+$	0.14 ± 0.15	$0.14 \pm 0.15 \pm 0.02$ [859]				0.14 ± 0.15
$K^*\pi^+$	$-0.04 \pm 0.09^*$	$0.032 \pm 0.052^{+0.016}_{-0.013}$ [273]	$-0.149 \pm 0.064 \pm 0.022$ [271]			-0.038 ± 0.042
$K^{*+}\pi^0$	-0.06 ± 0.24	$-0.06 \pm 0.24 \pm 0.04$ [861]				-0.06 ± 0.24
$K^{*+}\pi^-$	0.027 ± 0.008	$0.028 \pm 0.020 \pm 0.023$ [273]	$0.049 \pm 0.026 \pm 0.020$ [271]	$0.025 \pm 0.004 \pm 0.008$ [1104]	0.027 ± 0.008	
$f_0(980)K^+$	$-0.08 \pm 0.09^\dagger$	$-0.106 \pm 0.050^{+0.036}_{-0.015}$ [273]	$-0.077 \pm 0.065^{+0.046}_{-0.026}$ [271]			$-0.095^{+0.049}_{-0.042}$
$f_2(1270)K^+$	$-0.68^{+0.10}_{-0.17}$	$-0.85 \pm 0.22^{+0.26}_{-0.13}$ [273]	$-0.59 \pm 0.22 \pm 0.04$ [271]			$-0.68^{+0.20}_{-0.18}$
$f_0(1370)K^+$	$0.28^{+0.30}_{-0.29}$	$0.28 \pm 0.26^{+0.15}_{-0.14}$ [273]				$0.28^{+0.36}_{-0.29}$
$\rho^0 K^+$	0.37 ± 0.10	$0.44 \pm 0.10^{+0.09}_{-0.08}$ [273]	$0.30 \pm 0.11^{+0.11}_{-0.05}$ [271]			0.37 ± 0.11
$K_0^*(1430)^0\pi^+$	0.055 ± 0.033	$0.032 \pm 0.035^{+0.034}_{-0.028}$ [273]	$0.076 \pm 0.038^{+0.028}_{-0.022}$ [271]			$0.055^{+0.034}_{-0.032}$
$K_2^*(1430)^0\pi^+$	$0.05^{+0.29}_{-0.24}$	$0.05 \pm 0.23^{+0.18}_{-0.08}$ [273]				$0.05^{+0.29}_{-0.24}$
$K^+\pi^0\pi^0$	-0.06 ± 0.07	$-0.06 \pm 0.06 \pm 0.04$ [861]				-0.06 ± 0.07
$\rho^+ K^0$	-0.12 ± 0.17	$-0.12 \pm 0.17 \pm 0.02$ [867]				-0.12 ± 0.17
$K^{*+}\pi^+\pi^-$	0.07 ± 0.08	$0.07 \pm 0.07 \pm 0.04$ [868]				0.07 ± 0.08
$K^{*+}\rho^0$	0.31 ± 0.13	$0.31 \pm 0.13 \pm 0.03$ [869]				0.31 ± 0.13
$f_0(980)K^{*+}$	-0.15 ± 0.12	$-0.15 \pm 0.12 \pm 0.03$ [869]				-0.15 ± 0.12
$a_1^+ K^0$	0.12 ± 0.11	$0.12 \pm 0.11 \pm 0.02$ [870]				0.12 ± 0.11
$b_1^+ K^0$	-0.03 ± 0.15	$-0.03 \pm 0.15 \pm 0.02$ [871]				-0.03 ± 0.15
$K^{*0}\rho^+$	-0.01 ± 0.16	$-0.01 \pm 0.16 \pm 0.02$ [872]				-0.01 ± 0.16
$b_1^0 K^+$	-0.46 ± 0.20	$-0.46 \pm 0.20 \pm 0.02$ [875]				-0.46 ± 0.20
$K^+ \bar{K}^0$	0.04 ± 0.14	$0.10 \pm 0.26 \pm 0.03$ [397]	$0.014 \pm 0.168 \pm 0.002$ [845]		$-0.21 \pm 0.14 \pm 0.01$ [877]	-0.087 ± 0.100
$K^+ K_S K_S$	$0.04^{+0.04}_{-0.05}$	$0.04^{+0.04}_{-0.02} \pm 0.02$ [266]	$-0.006 \pm 0.039 \pm 0.034^\ddagger$ [878]			$0.017^{+0.036}_{-0.039}$
$K^+ K^- \pi^+$	-0.12 ± 0.05	$0.00 \pm 0.10 \pm 0.03$ [880]	$-0.170 \pm 0.073 \pm 0.017^\ddagger$ [881]		$-0.123 \pm 0.017 \pm 0.014$ [1104]	-0.122 ± 0.021
$K^+ K^- K^+$	-0.033 ± 0.008	$-0.017^{+0.019}_{-0.014} \pm 0.014$ [266]			$-0.036 \pm 0.004 \pm 0.007$ [1104]	-0.033 ± 0.007
ϕK^+	$0.024 \pm 0.028^*$	$0.128 \pm 0.044 \pm 0.013$ [266]	$0.01 \pm 0.12 \pm 0.05$ [890]	$-0.07 \pm 0.17^{+0.03}_{-0.02}$ [887]	$0.017 \pm 0.011 \pm 0.002 \pm 0.006$ [982]	0.025 ± 0.012

* Errors from PDG include a scale factor.

† PDG takes the value from the BABAR amplitude analysis of $B^+ \rightarrow K^+ K^- K^+$, while our numbers are from amplitude analyses of $B^+ \rightarrow K^+ \pi^- \pi^+$.

‡ PDG uses also a result from CLEO.

§ CP asymmetry is also measured in different bins of $m_{K^+ K^-}$.

¶ CP asymmetry is also measured in different bins of $m_{K_S K_S}$.

Table 266: CP asymmetries of charmless hadronic B^+ decays (part 2). Where values are shown in red (blue), this indicates that they are new published (preliminary) results since PDG2017.

Mode	PDG2017 Avg.	<i>BABAR</i>		<i>Belle</i>		CDF	LHCb	Our Avg.
$K^{*+}K^+K^-$	0.11 ± 0.09	$0.11 \pm 0.08 \pm 0.03$	[868]					0.11 ± 0.09
ϕK^{*+}	-0.01 ± 0.08	$0.00 \pm 0.09 \pm 0.04$	[889]	$-0.02 \pm 0.14 \pm 0.03$	[1105]			-0.01 ± 0.08
$\phi K_1(1270)^+$	0.15 ± 0.20	$0.15 \pm 0.19 \pm 0.05$	[891]					0.15 ± 0.20
$\phi K_0^*(1430)^+$	0.04 ± 0.15	$0.04 \pm 0.15 \pm 0.04$	[891]					0.04 ± 0.15
$\phi K_2^*(1430)^+$	-0.23 ± 0.20	$-0.23 \pm 0.19 \pm 0.06$	[891]					-0.23 ± 0.20
$\phi\phi K^+$	-0.10 ± 0.08	-0.10 ± 0.08	[893]					-0.10 ± 0.08
$K^{*+}\gamma$	0.18 ± 0.29	$0.18 \pm 0.28 \pm 0.07$	[1004]	$0.011 \pm 0.023 \pm 0.003$	[1005]			0.012 ± 0.023
$K^+\eta\gamma$	-0.12 ± 0.07	$-0.09 \pm 0.10 \pm 0.01$	[404]	$-0.16 \pm 0.09 \pm 0.06$	[1007]			-0.12 ± 0.07
$K^+\phi\gamma$	$-0.13 \pm 0.11^*$	$-0.26 \pm 0.14 \pm 0.05$	[1010]	$-0.03 \pm 0.11 \pm 0.08$	[406]			-0.13 ± 0.10
$\rho^+\gamma$	-0.11 ± 0.33			$-0.11 \pm 0.32 \pm 0.09$	[1016]			-0.11 ± 0.33
$\pi^+\pi^0$	0.03 ± 0.04	$0.03 \pm 0.08 \pm 0.01$	[847]	$0.025 \pm 0.043 \pm 0.007$	[845]			0.026 ± 0.039
$\pi^+\pi^-\pi^+$	0.057 ± 0.013	$0.032 \pm 0.044^{+0.040}_{-0.037}$	[896]			$0.058 \pm 0.008 \pm 0.011$	[1104]	0.057 ± 0.014
$\rho^0\pi^+$	$0.18^{+0.09}_{-0.17}$	$0.18 \pm 0.07^{+0.05}_{-0.15}$	[896]					$0.18^{+0.09}_{-0.17}$
$f_2(1270)\pi^+$	$0.41^{+0.31}_{-0.29}$	$0.41 \pm 0.25^{+0.18}_{-0.15}$	[896]					$0.41^{+0.31}_{-0.29}$
$\rho(1450)^0\pi^+$	$-0.06^{+0.36}_{-0.42}$	$-0.06 \pm 0.28^{+0.23}_{-0.32}$	[896]					$-0.06^{+0.36}_{-0.42}$
$f_0(1370)\pi^+$	0.72 ± 0.22	$0.72 \pm 0.15 \pm 0.16$	[896]					0.72 ± 0.22
$\pi^+\pi^-\pi^+(NR)$	$-0.14^{+0.23}_{-0.16}$	$-0.14 \pm 0.14^{+0.18}_{-0.08}$	[896]					$-0.14^{+0.23}_{-0.16}$
$\rho^+\pi^0$	0.02 ± 0.11	$-0.01 \pm 0.13 \pm 0.02$	[899]	$0.06 \pm 0.17^{+0.04}_{-0.05}$	[900]			0.02 ± 0.11
$\rho^+\rho^0$	-0.05 ± 0.05	$-0.054 \pm 0.055 \pm 0.010$	[421]	$0.00 \pm 0.22 \pm 0.03$	[901]			-0.051 ± 0.054
$\omega\pi^+$	$-0.04 \pm 0.06^\dagger$	$-0.02 \pm 0.08 \pm 0.01$	[857]	$-0.02 \pm 0.09 \pm 0.01$	[903]			-0.02 ± 0.06
$\omega\rho^+$	-0.20 ± 0.09	$-0.20 \pm 0.09 \pm 0.02$	[859]					-0.20 ± 0.09
$\eta\pi^+$	$-0.14 \pm 0.07^*$	$-0.03 \pm 0.09 \pm 0.03$	[848]	$-0.19 \pm 0.06 \pm 0.01$	[852]			-0.14 ± 0.05
$\eta\rho^+$	0.11 ± 0.11	$0.13 \pm 0.11 \pm 0.02$	[904]	$-0.04^{+0.34}_{-0.32} \pm 0.01$	[855]			0.11 ± 0.11
$\eta'\pi^+$	0.06 ± 0.16	$0.03 \pm 0.17 \pm 0.02$	[848]	$0.20^{+0.37}_{-0.36} \pm 0.04$	[849]			0.06 ± 0.15
$\eta'\rho^+$	0.26 ± 0.17	$0.26 \pm 0.17 \pm 0.02$	[850]					0.26 ± 0.17
$b_1^0\pi^+$	0.05 ± 0.16	$0.05 \pm 0.16 \pm 0.02$	[875]					0.05 ± 0.16
$p\bar{p}\pi^+$	0.00 ± 0.04	$0.04 \pm 0.07 \pm 0.04$	[687]	$-0.17 \pm 0.10 \pm 0.02^\ddagger$	[950]	$-0.041 \pm 0.039 \pm 0.005$	[951]	-0.041 ± 0.033
$p\bar{p}K^+$	$0.00 \pm 0.04^*$	$-0.16 \pm 0.08 \pm 0.04$	[765]	$-0.02 \pm 0.05 \pm 0.02^\ddagger$	[950]	$-0.021 \pm 0.020 \pm 0.004$	[951]	-0.027 ± 0.018
$p\bar{p}K^{*+}$	$0.21 \pm 0.16^*$	$0.32 \pm 0.13 \pm 0.05$	[687]	$-0.01 \pm 0.19 \pm 0.02$	[953]			0.21 ± 0.11
$p\bar{A}\gamma$	0.17 ± 0.17			$0.17 \pm 0.16 \pm 0.05$	[956]			0.17 ± 0.17
$p\bar{A}\pi^0$	0.01 ± 0.17			$0.01 \pm 0.17 \pm 0.04$	[956]			0.01 ± 0.17
$K^+\ell\ell$	-0.02 ± 0.08	$-0.03 \pm 0.14 \pm 0.01^\S$	[1050]	$0.04 \pm 0.10 \pm 0.02$	[1024]			0.02 ± 0.08
$K^+e^+e^-$	0.14 ± 0.14			$0.14 \pm 0.14 \pm 0.03$	[1024]			0.14 ± 0.14
$K^+\mu^+\mu^-$	0.011 ± 0.017			$-0.05 \pm 0.13 \pm 0.03$	[1024]	$0.012 \pm 0.017 \pm 0.001^\P$	[1106]	0.011 ± 0.017
$\pi^+\mu^+\mu^-$	-0.11 ± 0.12					$-0.11 \pm 0.12 \pm 0.01$	[1020]	-0.11 ± 0.12
$K^{*+}\ell\ell$	-0.09 ± 0.14	$0.01^{+0.26}_{-0.24} \pm 0.02$	[1023]	$-0.13^{+0.17}_{-0.16} \pm 0.01$	[1024]			$-0.09^{+0.14}_{-0.13}$
$K^{*+}e^+e^-$	$-0.14^{+0.23}_{-0.22}$			$-0.14^{+0.23}_{-0.22} \pm 0.02$	[1024]			$-0.14^{+0.23}_{-0.22}$
$K^{*+}\mu^+\mu^-$	-0.12 ± 0.24			$-0.12 \pm 0.24 \pm 0.02$	[1024]	$-0.035 \pm 0.024 \pm 0.003^\P$	[1106]	-0.036 ± 0.024

* Errors from PDG include a scale factor.

† PDG uses also a result from CLEO.

‡ PDG swaps the Belle results corresponding to $A_{CP}(p\bar{p}\pi^+)$ and $A_{CP}(p\bar{p}K^+)$.

§ PDG uses also a previous result from *BABAR* ([1023]).

¶ LHCb also quotes results in bins of $m(\ell^+\ell^-)^2$.

Table 267: CP asymmetries of charmless hadronic B^0 decays. Where values are shown in red (blue), this indicates that they are new published (preliminary) results since PDG2017.

Mode	PDG2017 Avg.	BABAR	Belle	CDF	LHCb	Our Avg.
$K^+\pi^-$	-0.082 ± 0.006 [†]	$-0.107 \pm 0.016^{+0.006}_{-0.004}$ [417]	$-0.069 \pm 0.014 \pm 0.007$ [845]	$-0.083 \pm 0.013 \pm 0.004$ [1107]	$-0.084 \pm 0.004 \pm 0.003$	[393] -0.084 ± 0.004
$\eta' K^{*0}$	$-0.07 \pm 0.18 \pm 0.23$	$0.02 \pm 0.23 \pm 0.02$ [850]	$-0.22 \pm 0.29 \pm 0.07$ [912]			-0.07 ± 0.18
$\eta' K_0^*(1430)^0$	-0.19 ± 0.17	$-0.19 \pm 0.17 \pm 0.02$ [850]				-0.19 ± 0.17
$\eta' K_2^*(1430)^0$	0.14 ± 0.18	$0.14 \pm 0.18 \pm 0.02$ [850]				0.14 ± 0.18
ηK^{*0}	0.19 ± 0.05	$0.21 \pm 0.06 \pm 0.02$ [854]	$0.17 \pm 0.08 \pm 0.01$ [855]			0.19 ± 0.05
$\eta K_0^*(1430)^0$	0.06 ± 0.13	$0.06 \pm 0.13 \pm 0.02$ [854]				0.06 ± 0.13
$\eta K_2^*(1430)^0$	-0.07 ± 0.19	$-0.07 \pm 0.19 \pm 0.02$ [854]				-0.07 ± 0.19
$b_1^- K^+$	-0.07 ± 0.12	$-0.07 \pm 0.12 \pm 0.02$ [875]				-0.07 ± 0.12
ωK^{*0}	0.45 ± 0.25	$0.45 \pm 0.25 \pm 0.02$ [859]				0.45 ± 0.25
$\omega K_0^*(1430)^0$	-0.07 ± 0.09	$-0.07 \pm 0.09 \pm 0.02$ [859]				-0.07 ± 0.09
$\omega K_2^*(1430)^0$	-0.37 ± 0.17	$-0.37 \pm 0.17 \pm 0.02$ [859]				-0.37 ± 0.17
$K^+\pi^-\pi^0$	0.00 ± 0.06	$-0.030^{+0.045}_{-0.051} \pm 0.055$ [918]	$0.07 \pm 0.11 \pm 0.01$ [917]			$0.000^{+0.059}_{-0.061}$
$\rho^- K^+$	0.20 ± 0.11	$0.20 \pm 0.09 \pm 0.08$ [916]	$0.22^{+0.22+0.06}_{-0.23-0.02}$ [917]			0.20 ± 0.11
$\rho(1450)^-K^+$	-0.10 ± 0.33	$-0.10 \pm 0.32 \pm 0.09$ [916]				-0.10 ± 0.33
$\rho(1700)^-K^+$	-0.36 ± 0.61	$-0.36 \pm 0.57 \pm 0.23$ [916]				-0.36 ± 0.61
$K^+\pi^-\pi^0(NR)$	0.10 ± 0.18	$0.10 \pm 0.16 \pm 0.08$ [916]				0.10 ± 0.18
$K^0\pi^+\pi^-$	-0.01 ± 0.05	$-0.01 \pm 0.05 \pm 0.01$ [269]				-0.01 ± 0.05
$K^{*+}\pi^-$	-0.22 ± 0.06 [†]	$-0.24 \pm 0.07 \pm 0.02$ [‡] [916]	$-0.21 \pm 0.11 \pm 0.07$ [270]			$-0.308 \pm 0.060 \pm 0.011 \pm 0.012$ ¹ [1108]
$(K\pi)_0^+\pi^-$						-0.271 ± 0.044
$K_2^*(1430)^+\pi^-$						$-0.032 \pm 0.047 \pm 0.016 \pm 0.027$ ¹ [1108]
$K^*(1680)^+\pi^-$						$-0.032 \pm 0.037 \pm 0.005 \pm 0.057$
$f_0(980)K_s^0$						$-0.29 \pm 0.22 \pm 0.09 \pm 0.03$ ¹ [1108]
$K_0^*(1430)^+\pi^-$	0.09 ± 0.07	$0.09 \pm 0.07 \pm 0.03$ [269]				-0.29 ± 0.24
$K_0^*(1430)^0\pi^0$	-0.15 ± 0.11	$-0.15 \pm 0.10 \pm 0.04$ [916]				-0.07 ± 0.14
$K^{*0}\pi^0$	-0.15 ± 0.13	$-0.15 \pm 0.12 \pm 0.04$ [916]				0.28 ± 0.31
$K^{*0}\pi^+\pi^-$	0.07 ± 0.05	$0.07 \pm 0.04 \pm 0.03$ [923]				0.09 ± 0.08
$K^{*0}\rho^0$	-0.06 ± 0.09	$-0.06 \pm 0.09 \pm 0.02$ [924]				-0.15 ± 0.11
$f_0(980)K^{*0}$	0.07 ± 0.10	$0.07 \pm 0.10 \pm 0.02$ [924]				-0.15 ± 0.13
$K^{*+}\rho^-$	0.21 ± 0.15	$0.21 \pm 0.15 \pm 0.02$ [924]				0.07 ± 0.10
$K^{*0}K^{+}K^{-}$	0.01 ± 0.05	$0.01 \pm 0.05 \pm 0.02$ [923]				0.21 ± 0.15
$a_1^- K^+$	-0.16 ± 0.12	$-0.16 \pm 0.12 \pm 0.01$ [870]				0.01 ± 0.05
$K_2^* K^{+\pi^\pm}$		$-0.085 \pm 0.089 \pm 0.002$ [928]				-0.16 ± 0.12
ϕK^{*0}	0.00 ± 0.04	$0.01 \pm 0.06 \pm 0.03$ [390]	$-0.007 \pm 0.048 \pm 0.021$ [935]			-0.085 ± 0.089
$K^{*0}\pi^+K^-$	0.22 ± 0.39	$0.22 \pm 0.33 \pm 0.20$ [923]				-0.003 ± 0.038
$\phi K_0^*(1430)^0$	0.12 ± 0.08	$0.20 \pm 0.14 \pm 0.06$ [390]	$0.093 \pm 0.094 \pm 0.017$ [935]			0.22 ± 0.39
$\phi K_2^*(1430)^0$	-0.11 ± 0.10	$-0.08 \pm 0.12 \pm 0.05$ [390]	$-0.155^{+0.152}_{-0.133} \pm 0.033$ [935]			0.124 ± 0.081
$K^{*0}\gamma$	-0.002 ± 0.015	$-0.016 \pm 0.022 \pm 0.007$ [1004]	$-0.013 \pm 0.017 \pm 0.004$ [1005]			$-0.113^{+0.102}_{-0.096}$
$\pi^0\pi^0$	0.43 ± 0.24	$0.43 \pm 0.26 \pm 0.05$ [417]	$0.14 \pm 0.36 \pm 0.12$ [429]			0.33 ± 0.22
$a_1^\mp\pi^\pm$	-0.07 ± 0.06	$-0.07 \pm 0.07 \pm 0.02$ [875]	$-0.06 \pm 0.05 \pm 0.07$ [415]			-0.07 ± 0.06
$b_1^\mp\pi^\pm$	-0.05 ± 0.10	$-0.05 \pm 0.10 \pm 0.02$ [875]				-0.05 ± 0.10
$p\bar{p}K^{*0}$	0.05 ± 0.12	$0.11 \pm 0.13 \pm 0.06$ [687]	$-0.08 \pm 0.20 \pm 0.02$ [953]			0.05 ± 0.12
$p\bar{A}K^-$	0.04 ± 0.07	$-0.10 \pm 0.10 \pm 0.02$ [§] [962]	$-0.02 \pm 0.10 \pm 0.03$ [956]			-0.06 ± 0.07
$K^{*0}\ell\ell$	-0.05 ± 0.10	$0.02 \pm 0.20 \pm 0.02$ [1023]	$-0.08 \pm 0.12 \pm 0.02$ [1024]			-0.05 ± 0.10
$K^{*0}e^+e^-$	-0.21 ± 0.19		$-0.21 \pm 0.19 \pm 0.02$ [1024]			-0.21 ± 0.19
$K^{*0}\mu^+\mu^-$	-0.034 ± 0.024		$0.00 \pm 0.15 \pm 0.03$ [1024]			-0.034 ± 0.024
				$-0.035 \pm 0.024 \pm 0.003$ [°]	[1106]	

Measurements of time-dependent CP asymmetries are listed in the Unitarity Triangle home page. (<http://www.slac.stanford.edu/xorg/hfag/triangle/index.html>)

[†] PDG uses also a result from CLEO.

[‡] Average of BABAR results from $B^0 \rightarrow K^+\pi^-\pi^0$ and $B^0 \rightarrow K^0\pi^+\pi^-$.

[§] PDG quotes the opposite asymmetry.

[¶] Extracted from measured $\Delta A_{CP} = A_{CP}(\phi K^{*0}) - A_{CP}(J/\psi K^{*0}) = 0.015 \pm 0.032 \pm 0.005$.

[°] LHCb also quotes results in bins of $m(\ell^+\ell^-)^2$.

¹ Last error comes from the Dalitz plot model.

Table 268: CP asymmetries of charmless hadronic decays of B^\pm/B^0 admixture. Where values are shown in red (blue), this indicates that they are new published (preliminary) results since PDG2017.

Mode	PDG2017 Avg.	<i>BABAR</i>	<i>Belle</i>	Our Avg.
$K^*\gamma$	-0.003 ± 0.017 [†]	$-0.003 \pm 0.017 \pm 0.007$ [1004]	$-0.004 \pm 0.014 \pm 0.003$ ¹	-0.004 ± 0.011
$s\gamma$	0.015 ± 0.020	$0.017 \pm 0.019 \pm 0.010$ [‡] [1110]	$0.002 \pm 0.050 \pm 0.030$ [1111]	0.015 ± 0.020
$\Delta A_{CP}(s\gamma)$			$0.0369 \pm 0.0265 \pm 0.0076$ ² [1079]	0.0370 ± 0.0280
$(s+d)\gamma$	0.010 ± 0.031	$0.057 \pm 0.060 \pm 0.018$ [§] [1043]	$0.022 \pm 0.039 \pm 0.009$ [◊] [1103]	0.032 ± 0.034
$s\eta$	$-0.13^{+0.04}_{-0.05}$		$-0.13 \pm 0.04^{+0.02}_{-0.03}$ [1074]	$-0.13^{+0.04}_{-0.05}$
π^+X	0.10 ± 0.17	$0.10 \pm 0.16 \pm 0.05$ [1078]		0.10 ± 0.17
$s\ell\ell$	0.04 ± 0.11	$0.04 \pm 0.11 \pm 0.01$ [1048]		0.04 ± 0.11
$K^*e^+e^-$	-0.18 ± 0.15		$-0.18 \pm 0.15 \pm 0.01$ [1024]	-0.18 ± 0.15
$K^*\mu^+\mu^-$	-0.03 ± 0.13		$-0.03 \pm 0.13 \pm 0.02$ [1024]	-0.03 ± 0.13
$K\ell\ell$		$-0.03 \pm 0.14 \pm 0.01$ [1050]		-0.03 ± 0.14
$K^*\ell\ell$	-0.04 ± 0.07	$0.03 \pm 0.13 \pm 0.01$ [¶] [1050]	$-0.10 \pm 0.10 \pm 0.01$ [1024]	-0.05 ± 0.08

[†] PDG includes also a result from CLEO.

[‡] *BABAR* also measures the difference in direct CP asymmetry for charged and neutral B mesons: $\Delta A_{CP} = +(5.0 \pm 3.9 \pm 1.5)\%$.

[§] There is another *BABAR* result using the recoil method (Phys. Rev. D 77, 051103), and a CLEO result (Phys. Rev. Lett. 86, 5661) that are used in the PDG average.

[¶] Previous *BABAR* result is also included in the PDG Average.

[◊] Requires $E_\gamma > 2.1$ GeV.

¹ Belle also measures the difference in direct CP asymmetry for charged and neutral B mesons: $\Delta A_{CP} = +(2.4 \pm 2.8 \pm 0.5)\%$.

² $\Delta A_{CP}(s\gamma) = A_{CP}(B^+ \rightarrow X_s^+ \gamma) - A_{CP}(B^0 \rightarrow X_s^0 \gamma)$

Table 269: CP asymmetries of charmless hadronic B_s^0 decays. Where values are shown in red (blue), this indicates that they are new published (preliminary) results since PDG2017.

Mode	PDG2017 Avg.	CDF	LHCb	Our Avg.
π^+K^-	0.26 ± 0.04	$0.22 \pm 0.07 \pm 0.02$ [1107]	$0.213 \pm 0.015 \pm 0.007$ [393]	0.213 ± 0.017

Table 270: CP asymmetries of charmless hadronic A_b^0 decays. Where values are shown in red (blue), this indicates that they are new published (preliminary) results since PDG2017.

Mode	PDG2017 Avg.	CDF	LHCb	Our Avg.
$p\pi^-$	0.06 ± 0.08	$0.06 \pm 0.07 \pm 0.03$ [1107]	$-0.035 \pm 0.017 \pm 0.020$ [†] [1112]	-0.025 ± 0.024
pK^-	-0.10 ± 0.09	$-0.10 \pm 0.08 \pm 0.04$ [1107]	$-0.020 \pm 0.013 \pm 0.019$ [†] [1112]	-0.025 ± 0.022
$\bar{K}^0 p\pi^-$	0.22 ± 0.13		$0.22 \pm 0.13 \pm 0.03$ [965]	0.22 ± 0.13
$\Lambda K^+\pi^-$	-0.53 ± 0.25		$-0.53 \pm 0.23 \pm 0.11$ [971]	-0.53 ± 0.26
ΛK^+K^-	-0.28 ± 0.12		$-0.28 \pm 0.10 \pm 0.07$ [971]	-0.28 ± 0.12
$pK^-\mu^+\mu^-$			$-0.035 \pm 0.05 \pm 0.002$ [1113]	-0.035 ± 0.050

[†] LHCb also reports $\Delta A_{CP} = A_{CP}(A_b^0 \rightarrow pK^-) - A_{CP}(A_b^0 \rightarrow p\pi^-) = 0.014 \pm 0.022 \pm 0.010$.

List of other measurements that are not included in the tables:

- In [1114], LHCb has measured the triple-product asymmetries for the decays $\Lambda_b^0 \rightarrow p\pi^-\pi^+\pi^-$ and $\Lambda_b^0 \rightarrow p\pi^-K^+K^-$.
- In [1113], LHCb also measures $a_{CP}^{\hat{T}-odd}$ and $a_P^{\hat{T}-odd}$.
- In [881], Belle also measure the partial branching fraction and CP asymmetry in different bins of K^+K^- mass.
- In [1115], LHCb has measured the triple-product asymmetries for the decays $\Lambda_b^0 \rightarrow pK^-\pi^+\pi^-$, $\Lambda_b^0 \rightarrow pK^-K^+K^-$ and $\Xi_b^0 \rightarrow pK^-K^-\pi^+$.

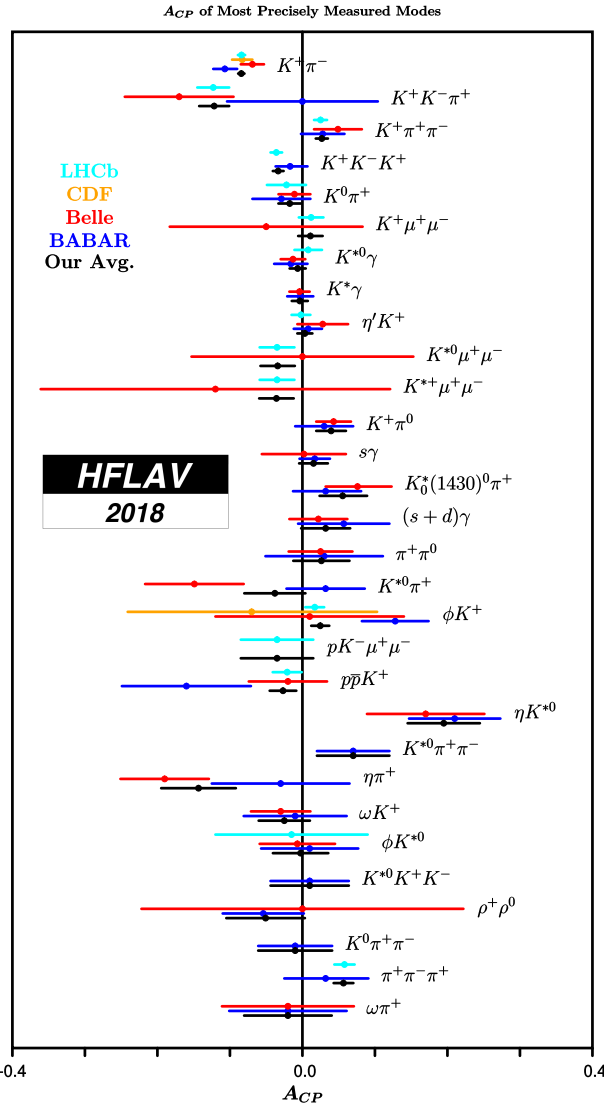


Figure 81: A_{CP} of most precisely measured modes.

8.7 Polarization measurements in b -hadron decays

In this section, compilations of polarization measurements in b -hadron decays are given. Table 271 (272) details measurements of the longitudinal fraction, f_L , in B^+ (B^0) decays, and Table 273 (274) the results of the full angular analyses of $B^+ (B^0) \rightarrow \phi K^*$ decays. Table 275 gives results of the full angular analysis of $B^0 \rightarrow \phi K_2^{*0}(1430)$ decays. Tables 276 to 278 detail quantities of B_s^0 decays: f_L measurements, and observables from full angular analyses of decays to $\phi\phi$ and $\phi\bar{K}^{*0}$.

Figures 82 and 83 show graphic representations of a selection of results shown in this section. Footnote symbols indicate that the footnote in the corresponding table should be consulted.

Table 271: Longitudinal polarization fraction f_L for B^+ decays. Where values are shown in red (blue), this indicates that they are new published (preliminary) results since PDG2017.

Mode	PDG2017 Avg.	<i>BABAR</i>		<i>Belle</i>		Our Avg.
ωK^{*+}	0.41 ± 0.19	$0.41 \pm 0.18 \pm 0.05$	[859]			0.41 ± 0.19
$\omega K_2^*(1430)^+$	0.56 ± 0.11	$0.56 \pm 0.10 \pm 0.04$	[859]			0.56 ± 0.11
$K^{*+}\bar{K}^{*0}$	$0.82^{+0.15}_{-0.21}$	$0.75^{+0.16}_{-0.26} \pm 0.03$	[884]	$1.06 \pm 0.30 \pm 0.14$	[885]	$0.82^{+0.13}_{-0.18}$
ϕK^{*+}	0.50 ± 0.05	$0.49 \pm 0.05 \pm 0.03$	[889]	$0.52 \pm 0.08 \pm 0.03$	[1105]	0.50 ± 0.05
$\phi K_1(1270)^+$	0.46 ± 0.14	$0.46^{+0.12+0.06}_{-0.13-0.07}$	[891]			$0.46^{+0.13}_{-0.15}$
$\phi K_2^*(1430)^+$	0.80 ± 0.10	$0.80^{+0.09}_{-0.10} \pm 0.03$	[891]			0.80 ± 0.10
$K^{*+}\rho^0$	0.78 ± 0.12	$0.78 \pm 0.12 \pm 0.03$	[869]			0.78 ± 0.12
$K^{*0}\rho^+$	0.48 ± 0.08	$0.52 \pm 0.10 \pm 0.04$	[872]	$0.43 \pm 0.11^{+0.05}_{-0.02}$	[873]	0.48 ± 0.08
$\rho^+\rho^0$	0.950 ± 0.016	$0.950 \pm 0.015 \pm 0.006$	[421]	$0.95 \pm 0.11 \pm 0.02$	[901]	0.950 ± 0.016
$\omega\rho^+$	0.90 ± 0.06	$0.90 \pm 0.05 \pm 0.03$	[859]			0.90 ± 0.06
$p\bar{p}K^{*+}$	0.32 ± 0.19			$0.32 \pm 0.17 \pm 0.09$	[953]	0.32 ± 0.19

Table 272: Longitudinal polarization fraction f_L for B^0 decays. Where values are shown in red (blue), this indicates that they are new published (preliminary) results since PDG2017.

Mode	PDG2017 Avg.	<i>BABAR</i>		<i>Belle</i>		<i>LHCb</i>	Our Avg.	
ωK^{*0}	0.69 ± 0.13	$0.72 \pm 0.14 \pm 0.02$	[859]	$0.56 \pm 0.29^{+0.18}_{-0.08}$	[915]		0.70 ± 0.13	
$\omega K_2^*(1430)^0$	0.45 ± 0.12	$0.45 \pm 0.12 \pm 0.02$	[859]				0.45 ± 0.12	
$K^{*0}\bar{K}^{*0}$	$0.80^{+0.12}_{-0.13}$	$0.80^{+0.10}_{-0.12} \pm 0.06$	[937]				$0.80^{+0.12}_{-0.13}$	
ϕK^{*0}	0.497 ± 0.017	$0.494 \pm 0.034 \pm 0.013$	[390]	$0.499 \pm 0.030 \pm 0.018$	[935]	$0.497 \pm 0.019 \pm 0.015$	[1109]	0.497 ± 0.017
$\phi K_2^*(1430)^0$	$0.913^{+0.028}_{-0.050}$	$0.901^{+0.046}_{-0.068} \pm 0.037$	[390]	$0.918^{+0.029}_{-0.060} \pm 0.012$	[935]		$0.913^{+0.029}_{-0.048}$	
$K^{*0}\rho^0$	0.40 ± 0.14	$0.40 \pm 0.08 \pm 0.11$	[924]				0.40 ± 0.14	
$K^{*+}\rho^-$	0.38 ± 0.13	$0.38 \pm 0.13 \pm 0.03$	[924]				0.38 ± 0.13	
$\rho^+\rho^-$	$0.990^{+0.021}_{-0.019}$	$0.992 \pm 0.024^{+0.026}_{-0.013}$	[409]	$0.988 \pm 0.012 \pm 0.023$	[410]		$0.990^{+0.021}_{-0.018}$	
$\rho^0\rho^0$	$0.71^{+0.08}_{-0.09}$	$0.75^{+0.11}_{-0.14} \pm 0.05$	[411]	$0.21^{+0.18}_{-0.22} \pm 0.15$	[412]	$0.745^{+0.048}_{-0.058} \pm 0.034$	[413]	$0.714^{+0.055}_{-0.062}$
$a_1^+a_1^-$	0.31 ± 0.24	$0.31 \pm 0.22 \pm 0.10$	[949]				0.31 ± 0.24	
$p\bar{p}K^{*0}$	1.01 ± 0.13			$1.01 \pm 0.13 \pm 0.03$	[953]		1.01 ± 0.13	
$\lambda\bar{\lambda}K^{*0}$	0.60 ± 0.23			$0.60 \pm 0.22 \pm 0.08$	[648]		0.60 ± 0.23	
$K^{*0}e^+e^-$	0.16 ± 0.07					$0.16 \pm 0.06 \pm 0.03$ †	[648]	0.16 ± 0.07

† $0.002 < q^2 < 1.120 \text{ GeV}^2/c^4$

Table 273: Results of the full angular analyses of $B^+ \rightarrow \phi K^{*+}$ decays. Where values are shown in red (blue), this indicates that they are new published (preliminary) results since PDG2017.

Parameter	PDG2017 Avg.	<i>BABAR</i>	<i>Belle</i>	Our Avg.
$f_\perp = A_{\perp\perp}$	0.20 ± 0.05	$0.21 \pm 0.05 \pm 0.02$ [889]	$0.19 \pm 0.08 \pm 0.02$ [1105]	0.20 ± 0.05
ϕ_{\parallel}	2.34 ± 0.18	$2.47 \pm 0.20 \pm 0.07$	$2.10 \pm 0.28 \pm 0.04$	2.34 ± 0.17
ϕ_{\perp}	2.58 ± 0.17	$2.69 \pm 0.20 \pm 0.03$	$2.31 \pm 0.30 \pm 0.07$	2.58 ± 0.17
δ_0	3.07 ± 19	$3.07 \pm 0.18 \pm 0.06$		3.07 ± 0.19
A_{CP}^0	0.17 ± 0.11	$0.17 \pm 0.11 \pm 0.02$		0.17 ± 0.11
A_{CP}^\perp	0.22 ± 0.25	$0.22 \pm 0.24 \pm 0.08$		0.22 ± 0.25
$\Delta\phi_{\parallel}$	0.07 ± 0.21	$0.07 \pm 0.20 \pm 0.05$		0.07 ± 0.21
$\Delta\phi_{\perp}$	0.19 ± 0.21	$0.19 \pm 0.20 \pm 0.07$		0.19 ± 0.21
$\Delta\delta_0$	0.20 ± 0.18	$0.20 \pm 0.18 \pm 0.03$		0.20 ± 0.18

Angles (ϕ, δ) are in radians. BF, f_L and A_{CP} are tabulated separately.

Table 274: Results of the full angular analyses of $B^0 \rightarrow \phi K^{*0}$ decays. Where values are shown in red (blue), this indicates that they are new published (preliminary) results since PDG2017.

Parameter	PDG2017 Avg.	<i>BABAR</i>	<i>Belle</i>	<i>LHCb</i>	Our Avg.
$f_\perp = A_{\perp\perp}$	0.224 ± 0.015	$0.212 \pm 0.032 \pm 0.013$ [390]	$0.238 \pm 0.026 \pm 0.008$ [935]	$0.221 \pm 0.016 \pm 0.013$ [1109]	0.225 ± 0.015
$f_S(K\pi)$				$0.143 \pm 0.013 \pm 0.012$	0.143 ± 0.018
$f_S(KK)$				$0.122 \pm 0.013 \pm 0.008$	0.122 ± 0.015
ϕ_{\parallel}	2.43 ± 0.11	$2.40 \pm 0.13 \pm 0.08$	$2.23 \pm 0.10 \pm 0.02$	$2.562 \pm 0.069 \pm 0.040$	2.430 ± 0.058
ϕ_{\perp}	2.53 ± 0.09	$2.35 \pm 0.13 \pm 0.09$	$2.37 \pm 0.10 \pm 0.04$	$2.633 \pm 0.062 \pm 0.037$	2.527 ± 0.056
δ_0	2.88 ± 0.10	$2.82 \pm 0.15 \pm 0.09$	$2.91 \pm 0.10 \pm 0.08$		2.88 ± 0.10
$\phi_S(K\pi)^{\dagger}$				$2.222 \pm 0.063 \pm 0.081$	2.222 ± 0.103
$\phi_S(KK)^{\dagger}$				$2.481 \pm 0.072 \pm 0.048$	2.481 ± 0.087
A_{CP}^0	-0.007 ± 0.030	$0.01 \pm 0.07 \pm 0.02$	$-0.03 \pm 0.06 \pm 0.01$	$-0.003 \pm 0.038 \pm 0.005$	-0.007 ± 0.030
A_{CP}^\perp	-0.02 ± 0.06	$-0.04 \pm 0.15 \pm 0.06$	$-0.14 \pm 0.11 \pm 0.01$	$0.047 \pm 0.072 \pm 0.009$	-0.014 ± 0.057
$A_{CP}^S(K\pi)$				$0.073 \pm 0.091 \pm 0.035$	0.073 ± 0.097
$A_{CP}^S(KK)$				$-0.209 \pm 0.105 \pm 0.012$	-0.209 ± 0.106
$\Delta\phi_{\parallel}$	0.05 ± 0.05	$0.22 \pm 0.12 \pm 0.08$	$-0.02 \pm 0.10 \pm 0.01$	$0.045 \pm 0.068 \pm 0.015$	0.051 ± 0.053
$\Delta\phi_{\perp}$	0.08 ± 0.05	$0.21 \pm 0.13 \pm 0.08$	$0.05 \pm 0.10 \pm 0.02$	$0.062 \pm 0.062 \pm 0.006$	0.075 ± 0.050
$\Delta\delta_0$	0.13 ± 0.09	$0.27 \pm 0.14 \pm 0.08$	$0.08 \pm 0.10 \pm 0.01$		0.13 ± 0.08
$\Delta\phi_S(K\pi)^{\dagger}$				$0.062 \pm 0.062 \pm 0.022$	0.062 ± 0.066
$\Delta\phi_S(KK)^{\dagger}$				$0.022 \pm 0.072 \pm 0.004$	0.022 ± 0.072

Angles (ϕ, δ) are in radians. BF, f_L and A_{CP} are tabulated separately.

\dagger Original LHCb notation adapted to match similar existing quantities.

Table 275: Results of the full angular analyses of $B^0 \rightarrow \phi K_2^{*0}(1430)$ decays. Where values are shown in red (blue), this indicates that they are new published (preliminary) results since PDG2017.

Parameter	PDG2017 Avg.	<i>BABAR</i>		<i>Belle</i>		Our Avg.
$f_\perp = A_{\perp\perp}$	$0.027^{+0.031}_{-0.025}$	$0.002^{+0.018}_{-0.002} \pm 0.031$	[390]	$0.056^{+0.050}_{-0.035} \pm 0.009$	[935]	$0.027^{+0.027}_{-0.024}$
ϕ_{\parallel}	4.0 ± 0.4	$3.96 \pm 0.38 \pm 0.06$		$3.76 \pm 2.88 \pm 1.32$		3.96 ± 0.38
ϕ_{\perp}	4.5 ± 0.4			$4.45^{+0.43}_{-0.38} \pm 0.13$		$4.45^{+0.45}_{-0.40}$
δ_0	3.46 ± 0.14	$3.41 \pm 0.13 \pm 0.13$		$3.53 \pm 0.11 \pm 0.19$		3.46 ± 0.14
A_{CP}^0	-0.03 ± 0.04	$-0.05 \pm 0.06 \pm 0.01$		$-0.016^{+0.066}_{-0.051} \pm 0.008$		$-0.032^{+0.043}_{-0.038}$
A_{CP}^{\perp}	$0.0^{+0.9}_{-0.7}$			$-0.01^{+0.85}_{-0.67} \pm 0.09$		$-0.01^{+0.85}_{-0.68}$
$\Delta\phi_{\parallel}$	-0.9 ± 0.4	$-1.00 \pm 0.38 \pm 0.09$		$-0.02 \pm 1.08 \pm 1.01$		-0.94 ± 0.38
$\Delta\phi_{\perp}$	-0.2 ± 0.4			$-0.19 \pm 0.42 \pm 0.11$		-0.19 ± 0.43
$\Delta\delta_0$	0.08 ± 0.09	$0.11 \pm 0.13 \pm 0.06$		$0.06 \pm 0.11 \pm 0.02$		0.08 ± 0.09

Angles (ϕ, δ) are in radians. BF, f_L and A_{CP} are tabulated separately.

Table 276: Longitudinal polarization fraction f_L for B_s^0 decays. Where values are shown in red (blue), this indicates that they are new published (preliminary) results since PDG2017.

Mode	PDG2017 Avg.	CDF	LHCb	Our Avg.
$\phi\phi$	0.362 ± 0.014	$0.348 \pm 0.041 \pm 0.021$ [983]	$0.382 \pm 0.008 \pm 0.011$ [396]	0.379 ± 0.013
$K^{*0}\bar{K}^{*0}$	0.20 ± 0.07		$0.208 \pm 0.032 \pm 0.046$ [1116]	0.208 ± 0.056
$\phi\bar{K}^{*0}$	0.51 ± 0.17		$0.51 \pm 0.15 \pm 0.07$ [987]	0.51 ± 0.17

Table 277: Results of the full angular analyses of $B_s^0 \rightarrow \phi\phi$ decays. Where values are shown in red (blue), this indicates that they are new published (preliminary) results since PDG2017.

Parameter	PDG2017 Avg.	CDF	LHCb	Our Avg.
$f_\perp = A_{\perp\perp}$	0.309 ± 0.015	$0.305 \pm 0.013 \pm 0.005$ [983]	$0.287 \pm 0.008 \pm 0.005$ [1117]	0.292 ± 0.008
ϕ_{\parallel}	2.55 ± 0.11	$2.71^{+0.31}_{-0.36} \pm 0.22$	$2.52 \pm 0.05 \pm 0.07$	2.53 ± 0.08
ϕ_{\perp}	2.67 ± 0.24		$2.81 \pm 0.21 \pm 0.10$	2.81 ± 0.23

The parameter ϕ is in radians. BF, f_L and A_{CP} are tabulated separately.

Table 278: Results of the full angular analyses of $B_s^0 \rightarrow \phi\bar{K}^{*0}$ decays. Where values are shown in red (blue), this indicates that they are new published (preliminary) results since PDG2017.

Parameter	PDG2017 Avg.	LHCb	Our Avg.
f_L	0.51 ± 0.17	$0.51 \pm 0.15 \pm 0.07$ [987]	0.51 ± 0.17
f_{\parallel}	0.21 ± 0.11	$0.21 \pm 0.11 \pm 0.02$	0.21 ± 0.11
$\phi_{\parallel}^{\dagger}$	1.8 ± 0.6	$1.75^{+0.59+0.38}_{-0.53-0.30}$	$1.75^{+0.70}_{-0.61}$

The parameter ϕ is in radians. BF, f_L and A_{CP} are tabulated separately.

[†] Converted from the measurement of $\cos(\phi_{\parallel})$. PDG takes the smallest resulting asymmetric error as parabolic.

Table 279: Results of the full angular analyses of $B_s^0 \rightarrow K^{*0} \bar{K}^{*0}$ decays. Where values are shown in red (blue), this indicates that they are new published (preliminary) results since PDG2017.

Parameter	PDG2017 Avg.	LHCb	Our Avg.
f_L	0.20 ± 0.07	$0.201 \pm 0.057 \pm 0.040$ [986]	0.201 ± 0.070
f_\perp	0.38 ± 0.12	$0.38 \pm 0.11 \pm 0.004$	0.380 ± 0.110
f_\parallel	0.21 ± 0.05	$0.215 \pm 0.046 \pm 0.015$	0.215 ± 0.048
$ A_s^+ ^2$		$0.114 \pm 0.037 \pm 0.023$	0.114 ± 0.044
$ A_s^- ^2$		$0.485 \pm 0.051 \pm 0.019$	0.485 ± 0.054
$ A_{ss} ^2$		$0.066 \pm 0.022 \pm 0.007$	0.066 ± 0.023
δ_\parallel	5.31 ± 0.28	$5.31 \pm 0.24 \pm 0.14$	5.31 ± 0.28
$\delta_\perp - \delta_s^+$		$1.95 \pm 0.21 \pm 0.04$	1.95 ± 0.21
δ_s^-		$1.79 \pm 0.19 \pm 0.19$	1.79 ± 0.27
δ_{ss}		$1.06 \pm 0.27 \pm 0.23$	1.06 ± 0.35

List of other measurements that are not included in the tables:

- In Ref. [1116], LHCb presents a flavour-tagged, decay-time-dependent amplitude analysis of $B_s^0 \rightarrow (K^+\pi^-)(K^-\pi^+)$ decays in the $K^\pm\pi^\mp$ mass range from 750 to 1600 MeV/ c^2 . The paper includes measurements of 19 CP -averaged amplitude parameters corresponding to scalar, vector and tensor final states.

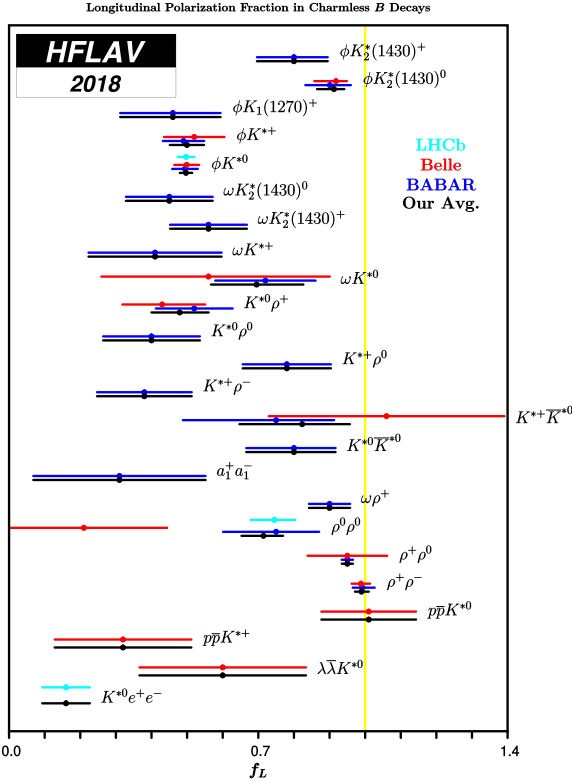


Figure 82: Longitudinal polarization fraction in charmless B decays.

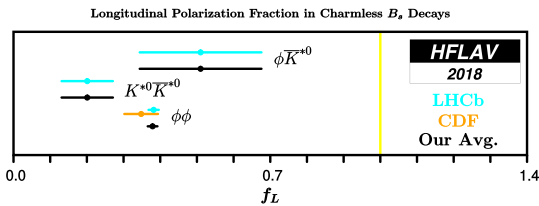


Figure 83: Longitudinal polarization fraction in charmless B_s^0 decays.

8.8 Decays of B_c^+ mesons

Table 280 details branching fractions of B_c^+ meson decays to charmless hadronic final states.

Table 280: Relative branching fractions of B_c^+ decays. Where values are shown in red (blue), this indicates that they are new published (preliminary) results since PDG2017.

RPP#	Mode	PDG2017 AVG.	LHCb	Our Avg.
18	$f_c \mathcal{B}(B_c^+ \rightarrow p\bar{p}\pi^+)/f_u$ [§]	3.6×10^{-8}	$< 2.8 \times 10^{-8}$ [1118]	$< 2.8 \times 10^{-8}$
25	$f_c \mathcal{B}(B_c^+ \rightarrow K^+ K^0)/f_u \mathcal{B}(B^+ \rightarrow K_S^0 \pi^+)$ $\sigma(B_c^+) \mathcal{B}(B_c^+ \rightarrow K^+ K^- \pi^+)/\sigma(B^+)$ [†]	[‡] $< 5.8 \times 10^{-2}$ [877]	$< 5.8 \times 10^{-2}$ [877]	$< 5.8 \times 10^{-2}$

Channels with no RPP# were not included in PDG Live as of Dec. 31, 2017.

[§] PDG result at 95% CL, LHCb at 90% CL.

[†] Measured in the annihilation region $m(K^-\pi^+) < 1.834 \text{ GeV}/c^2$.

[‡] PDG converts the LHCb result to $f_c \mathcal{B}(B_c^+ \rightarrow K^+ K^0) < 4.6 \times 10^{-7}$.

9 Charm physics

9.1 D^0 - \bar{D}^0 mixing and CP violation

9.1.1 Introduction

The first evidence for D^0 - \bar{D}^0 mixing was obtained in 2007 by Belle [1119] and *BABAR* [1120]. These results were confirmed by CDF [1121] and, much later, LHCb [1122]. There are now numerous measurements of D^0 - \bar{D}^0 mixing with various levels of sensitivity. HFLAV performs a global fit to all relevant measurements to determine world average values of mixing parameters, CP -violation (CPV) parameters, and strong phase differences.

Our notation is as follows. The mass eigenstates are denoted

$$D_1 = p|D^0\rangle - q|\bar{D}^0\rangle \quad (228)$$

$$D_2 = p|D^0\rangle + q|\bar{D}^0\rangle, \quad (229)$$

where we use the convention $CP|D^0\rangle = -|\bar{D}^0\rangle$ and $CP|\bar{D}^0\rangle = -|D^0\rangle$ [1123]. With this convention, D_1 is CP -even and D_2 is CP -odd in the absence of CP violation (i.e., $p = q$). The global fit determines central values and uncertainties for ten underlying parameters. These consist of the following:

- mixing parameters x and y , where $x = (m_1 - m_2)/\Gamma$, $y = (\Gamma_1 - \Gamma_2)/(2\Gamma)$, and m_1 , m_2 and Γ_1 , Γ_2 are the masses and decay widths of the mass eigenstates. The mean decay width $\Gamma \equiv (\Gamma_1 + \Gamma_2)/2$.
- CPV parameters $|q/p|$ and $\text{Arg}(q/p) \equiv \phi$; these give rise to *indirect CPV*.
- direct CPV asymmetries

$$\begin{aligned} A_D &\equiv \frac{\Gamma(D^0 \rightarrow K^+ \pi^-) - \Gamma(\bar{D}^0 \rightarrow K^- \pi^+)}{\Gamma(D^0 \rightarrow K^+ \pi^-) + \Gamma(\bar{D}^0 \rightarrow K^- \pi^+)} \\ A_K &\equiv \frac{\Gamma(D^0 \rightarrow K^+ K^-) - \Gamma(\bar{D}^0 \rightarrow K^- K^+)}{\Gamma(D^0 \rightarrow K^+ K^-) + \Gamma(\bar{D}^0 \rightarrow K^- K^+)} \\ A_\pi &\equiv \frac{\Gamma(D^0 \rightarrow \pi^+ \pi^-) - \Gamma(\bar{D}^0 \rightarrow \pi^- \pi^+)}{\Gamma(D^0 \rightarrow \pi^+ \pi^-) + \Gamma(\bar{D}^0 \rightarrow \pi^- \pi^+)}, \end{aligned}$$

where the decay rates corresponds to pure D^0 and \bar{D}^0 flavor eigenstates.

- the ratio of doubly Cabibbo-suppressed to Cabibbo-favored decay rates

$$R_D \equiv \frac{\Gamma(D^0 \rightarrow K^+ \pi^-) + \Gamma(\bar{D}^0 \rightarrow K^- \pi^+)}{\Gamma(D^0 \rightarrow K^- \pi^+) + \Gamma(\bar{D}^0 \rightarrow K^+ \pi^-)}$$

- the strong phase difference δ between the $\bar{D}^0 \rightarrow K^- \pi^+$ and $D^0 \rightarrow K^- \pi^+$ amplitudes; and
- the strong phase difference $\delta_{K\pi\pi}$ between $\bar{D}^0 \rightarrow K^- \rho^+$ and $D^0 \rightarrow K^- \rho^+$ amplitudes.

The fit uses 49 measurements of observables from the following³⁴ decays: $D^0 \rightarrow K^+ \ell^- \bar{\nu}$, $D^0 \rightarrow K^+ K^-$, $D^0 \rightarrow \pi^+ \pi^-$, $D^0 \rightarrow K^+ \pi^-$, $D^0 \rightarrow K^+ \pi^- \pi^0$, $D^0 \rightarrow K_S^0 \pi^+ \pi^-$, $D^0 \rightarrow \pi^0 \pi^+ \pi^-$, $D^0 \rightarrow K_S^0 K^+ K^-$, and $D^0 \rightarrow K^+ \pi^- \pi^+ \pi^-$. The fit also uses measurements of mixing parameters and strong phases obtained from double-tagged branching fractions measured at the $\psi(3770)$ resonance. The relationships between measured observables and fitted parameters are given in Table 281. Correlations among observables are accounted for by using covariance matrices provided by the experimental collaborations. Uncertainties are assumed to be Gaussian, and systematic uncertainties among different experiments are assumed to be uncorrelated unless specific correlations have been identified. We have compared this method with a second method that adds together three-dimensional log-likelihood functions for x , y , and δ obtained from several independent measurements; this combination accounts for non-Gaussian uncertainties. When both methods are applied to the same set of measurements, equivalent results are obtained.

Mixing in the B^0 , and B_s^0 heavy flavor systems is governed by a short-distance box diagram. In the D^0 system, this box diagram is both doubly-Cabibbo-suppressed and GIM-suppressed, and consequently the short-distance mixing rate is tiny. Thus, D^0 - \bar{D}^0 mixing is expected to be dominated by long-distance processes. These are difficult to calculate, and theoretical estimates for x and y range over three orders of magnitude, up to the percent level [1124–1127].

Almost all experimental analyses besides that of the $\psi(3770) \rightarrow \bar{D}D$ measurements [1128] identify the flavor of the D^0 or \bar{D}^0 when produced by reconstructing the decay $D^{*+} \rightarrow D^0 \pi^+$ or $D^{*-} \rightarrow \bar{D}^0 \pi^-$. The charge of the pion, which has low momentum in the lab frame relative to that of the D^0 and is often referred to as the “soft” pion, identifies the D^0 flavor. For $D^{*+} \rightarrow D^0 \pi^+$, $M_{D^*} - M_{D^0} - M_{\pi^+} \equiv Q \approx 6$ MeV, which is close to the kinematic threshold; thus analyses typically require that the reconstructed Q be small in order to suppress backgrounds. An LHCb measurement [1129] of the difference between time-integrated CP asymmetries $A_{CP}(K^+ K^-) - A_{CP}(\pi^+ \pi^-)$ identifies the flavor of the D^0 by partially reconstructing $\bar{B} \rightarrow D^0 \mu^- X$ and $B \rightarrow \bar{D}^0 \mu^+ X$ decays; in this case the charge of the μ^\pm identifies the flavor of the D^0 .

For time-dependent measurements, the D^0 decay time is calculated as $t = (\vec{d} \cdot \vec{p}) \times M_{D^0} / (cp^2)$, where \vec{d} is the displacement vector from the D^{*+} vertex to the D^0 decay vertex; \vec{p} is the reconstructed D^0 momentum; and p and M_{D^0} are in GeV. The D^{*+} vertex position is taken as the intersection of the D^0 momentum vector with the beamspot profile for $e^+ e^-$ experiments, and at the primary interaction vertex for pp and $\bar{p}p$ experiments [1121, 1122].

9.1.2 Input observables

The global fit determines central values and errors for ten parameters using a χ^2 statistic. The fitted parameters are x , y , R_D , A_D , $|q/p|$, ϕ , δ , $\delta_{K\pi\pi}$, A_K , and A_π . In the $D \rightarrow K^+ \pi^- \pi^0$ Dalitz plot analysis [1130], the phases of intermediate resonances in the $\bar{D}^0 \rightarrow K^+ \pi^- \pi^0$ decay amplitude are fitted relative to the phase for $\mathcal{A}(\bar{D}^0 \rightarrow K^+ \rho^-)$, and the phases of intermediate resonances for $D^0 \rightarrow K^+ \pi^- \pi^0$ are fitted relative to the phase for $\mathcal{A}(D^0 \rightarrow K^+ \rho^-)$. As the \bar{D}^0 and D^0 Dalitz plots are fitted independently, the phase difference $\delta_{K\pi\pi} = \text{Arg}[\mathcal{A}(\bar{D}^0 \rightarrow K^+ \rho^-)/\mathcal{A}(D^0 \rightarrow K^+ \rho^-)]$ between the reference amplitudes cannot be determined from these individual fits. However, this phase difference can be constrained in the global fit and thus is included as a fitted parameter.

³⁴Charge-conjugate modes are implicitly included.

Table 281: Left: decay modes used to determine the fitted parameters x , y , δ , $\delta_{K\pi\pi}$, R_D , A_D , A_K , A_π , $|q/p|$, and ϕ . Middle: measured observables for each decay mode. Right: relationships between the measured observables and the fitted parameters. The symbol $\langle t \rangle$ denotes the mean reconstructed decay time for $D^0 \rightarrow K^+ K^-$ or $D^0 \rightarrow \pi^+ \pi^-$ decays.

Decay Mode	Observables	Relationship
$D^0 \rightarrow K^+ K^- / \pi^+ \pi^-$	y_{CP} A_Γ	$2y_{CP} = (q/p + p/q) y \cos \phi - (q/p - p/q) x \sin \phi$ $2A_\Gamma = (q/p - p/q) y \cos \phi - (q/p + p/q) x \sin \phi$
$D^0 \rightarrow K_S^0 \pi^+ \pi^-$	x y $ q/p $ ϕ	
$D^0 \rightarrow K^+ \ell^- \bar{\nu}$	R_M	$R_M = (x^2 + y^2)/2$
$D^0 \rightarrow K^+ \pi^- \pi^0$ (Dalitz plot analysis)	x'' y''	$x'' = x \cos \delta_{K\pi\pi} + y \sin \delta_{K\pi\pi}$ $y'' = y \cos \delta_{K\pi\pi} - x \sin \delta_{K\pi\pi}$
“Double-tagged” branching fractions measured in $\psi(3770) \rightarrow DD$ decays	R_M y R_D $\sqrt{R_D} \cos \delta$	$R_M = (x^2 + y^2)/2$
$D^0 \rightarrow K^+ \pi^-$	x'^2, y' x'^{2+}, x'^{2-} y'^+, y'^-	$x' = x \cos \delta + y \sin \delta$ $y' = y \cos \delta - x \sin \delta$ $A_M \equiv (q/p ^4 - 1)/(q/p ^4 + 1)$ $x'^\pm = [(1 \pm A_M)/(1 \mp A_M)]^{1/4} \times (x' \cos \phi \pm y' \sin \phi)$ $y'^\pm = [(1 \pm A_M)/(1 \mp A_M)]^{1/4} \times (y' \cos \phi \mp x' \sin \phi)$
$D^0 \rightarrow K^+ \pi^- / K^- \pi^+$ (time-integrated)	R_D A_D	
$D^0 \rightarrow K^+ K^- / \pi^+ \pi^-$ (time-integrated)	$\frac{\Gamma(D^0 \rightarrow K^+ K^-) - \Gamma(\bar{D}^0 \rightarrow K^+ K^-)}{\Gamma(D^0 \rightarrow K^+ K^-) + \Gamma(\bar{D}^0 \rightarrow K^+ K^-)}$ $\frac{\Gamma(D^0 \rightarrow \pi^+ \pi^-) - \Gamma(\bar{D}^0 \rightarrow \pi^+ \pi^-)}{\Gamma(D^0 \rightarrow \pi^+ \pi^-) + \Gamma(\bar{D}^0 \rightarrow \pi^+ \pi^-)}$	$A_K + \frac{\langle t \rangle}{\tau_D} \mathcal{A}_{CP}^{\text{indirect}}$ ($\mathcal{A}_{CP}^{\text{indirect}} \approx -A_\Gamma$) $A_\pi + \frac{\langle t \rangle}{\tau_D} \mathcal{A}_{CP}^{\text{indirect}}$ ($\mathcal{A}_{CP}^{\text{indirect}} \approx -A_\Gamma$)

All input measurements are listed in Tables 282-284. There are three observables input to the fit that are world average values:

$$R_M = \frac{x^2 + y^2}{2} \quad (230)$$

$$y_{CP} = \frac{1}{2} \left(\left| \frac{q}{p} \right| + \left| \frac{p}{q} \right| \right) y \cos \phi - \frac{1}{2} \left(\left| \frac{q}{p} \right| - \left| \frac{p}{q} \right| \right) x \sin \phi \quad (231)$$

$$A_\Gamma = \frac{1}{2} \left(\left| \frac{q}{p} \right| - \left| \frac{p}{q} \right| \right) y \cos \phi - \frac{1}{2} \left(\left| \frac{q}{p} \right| + \left| \frac{p}{q} \right| \right) x \sin \phi. \quad (232)$$

These world averages are calculated using the COMBOS program [1131]. The observable R_M is measured in both $D^0 \rightarrow K^+ \ell^- \bar{\nu}$ and $D^0 \rightarrow K^+ \pi^- \pi^+ \pi^-$ [1132] decays, and it is for the first case (measured by several experiments) that the world average is used. The inputs used for this [1133–1136] are plotted in Fig. 84. The inputs used for world averages of y_{CP} and A_Γ are plotted in Figs. 85 and 86, respectively.

The $D^0 \rightarrow K^+ \pi^-$ measurements used are from Belle [1137, 1138], *BABAR* [1120], CDF [1139], and LHCb [1140]; earlier measurements are either superseded or have much less precision and are not used. The observables from $D^0 \rightarrow K_S^0 \pi^+ \pi^-$ decays are measured in two ways: assuming CP conservation (D^0 and \bar{D}^0 decays combined), and allowing for CP violation (D^0 and \bar{D}^0 decays fitted separately). The no- CPV measurements are from Belle [1141], *BABAR* [1142], and LHCb [1143]; for the CPV -allowed case, Belle [1141] and LHCb [1144] measurements are available. The $D^0 \rightarrow K^+ \pi^- \pi^0$, $D^0 \rightarrow K_S^0 K^+ K^-$, and $D^0 \rightarrow \pi^0 \pi^+ \pi^-$ results are from *BABAR* [1130, 1145]; the $D^0 \rightarrow K^+ \pi^- \pi^+ \pi^-$ results are from LHCb [1132]; and the $\psi(3770) \rightarrow \bar{D} D$ results are from CLEOc [1128].

As mentioned, Table 281 lists the relationships between the observables and the global-fit parameters. For each set of correlated observables, we use these relations to construct a difference vector \vec{V} between the measured values and those calculated from the fitted parameters. For example, for $D^0 \rightarrow K_S^0 \pi^+ \pi^-$ decays, $\vec{V} = (\Delta x, \Delta y, \Delta |q/p|, \Delta \phi)$, where $\Delta x \equiv x_{\text{measured}} - x_{\text{fitted}}$ (and similarly for Δy , $\Delta |q/p|$, and $\Delta \phi$). The contribution of a set of observables to the fit χ^2 is calculated as $\vec{V} \cdot (M^{-1}) \cdot \vec{V}^T$, where M^{-1} is the inverse of the covariance matrix for the measured observables. Covariance matrices are constructed from the correlation coefficients among the observables. These correlation coefficients are furnished by the experiments and listed in Tables 282-284.

9.1.3 Fit results

The global fitter uses MINUIT with the MIGRAD minimizer, and all uncertainties are obtained from MINOS [1162]. Four separate fits are performed:

1. assuming CP conservation, *i.e.*, fixing $A_D = 0$, $A_K = 0$, $A_\pi = 0$, $\phi = 0$, and $|q/p| = 1$;
2. assuming no direct CPV in doubly Cabibbo-suppressed (DCS) decays ($A_D = 0$) and fitting for the parameters $(x, y, |q/p|)$ or (x, y, ϕ) ;
3. assuming no direct CPV in DCS decays and fitting for alternative parameters [1163, 1164] $x_{12} = 2|M_{12}|/\Gamma$, $y_{12} = |\Gamma_{12}|/\Gamma$, and $\phi_{12} = \text{Arg}(M_{12}/\Gamma_{12})$, where M_{12} and Γ_{12} are the off-diagonal elements of the D^0 - \bar{D}^0 mass and decay matrices, respectively. The parameter

Table 282: Observables used in the global fit except those from time-dependent $D^0 \rightarrow K^+ \pi^-$ measurements, and those from direct CPV measurements. The $D^0 \rightarrow K^+ \pi^- \pi^0$ observables are $x'' = x \cos \delta_{K\pi\pi} + y \sin \delta_{K\pi\pi}$ and $y'' = -x \sin \delta_{K\pi\pi} + y \cos \delta_{K\pi\pi}$.

Mode	Observable	Values	Correlation coefficients
$D^0 \rightarrow K^+ K^- / \pi^+ \pi^-$, ϕK_S^0	y_{CP}	$(0.715 \pm 0.111)\%$	
	A_Γ	$(-0.032 \pm 0.026)\%$	
$D^0 \rightarrow K_S^0 \pi^+ \pi^-$ [1141] (Belle: no CPV)	x	$(0.56 \pm 0.19^{+0.067}_{-0.127})\%$	
	y	$(0.30 \pm 0.15^{+0.050}_{-0.078})\%$	+0.012
$D^0 \rightarrow K_S^0 \pi^+ \pi^-$ [1141] (Belle: no direct CPV)	$ q/p $	$0.90^{+0.16+0.078}_{-0.15-0.064}$	
	ϕ	$(-6 \pm 11^{+4.2}_{-5.0})$ degrees	
$D^0 \rightarrow K_S^0 \pi^+ \pi^-$ [1141] (Belle: direct CPV allowed)	x	$(0.58 \pm 0.19^{+0.0734})\%$	$\begin{Bmatrix} 1 & 0.054 & -0.074 & -0.031 \\ & 1 & 0.034 & -0.019 \\ & & 1 & 0.044 \\ & & & 1 \end{Bmatrix}$
	y	$(0.27 \pm 0.16^{+0.0546}_{-0.0854})\%$	
	$ q/p $	$0.82^{+0.20+0.0807}_{-0.18-0.0645}$	
	ϕ	$(-13^{+12+4.15}_{-13-4.77})$ degrees	
$D^0 \rightarrow K_S^0 \pi^+ \pi^-$ [1143] (LHCb: 1 fb^{-1} no CPV)	x	$(-0.86 \pm 0.53 \pm 0.17)\%$	
	y	$(0.03 \pm 0.46 \pm 0.13)\%$	+0.37
$D^0 \rightarrow K_S^0 \pi^+ \pi^-$ [1144] (LHCb: 3 fb^{-1} CPV allowed)	x_{CP}	$(0.27 \pm 0.16 \pm 0.04)\%$	$\begin{Bmatrix} 1 & (-0.17+0.15) & (0.04+0.01) & (-0.02-0.02) \\ & 1 & (-0.03-0.05) & (0.01-0.03) \\ & & 1 & (-0.13+0.14) \\ & & & 1 \end{Bmatrix}$
	y_{CP}	$(0.74 \pm 0.36 \pm 0.11)\%$	
	Δx	$(-0.053 \pm 0.070 \pm 0.022)\%$	
	Δy	$(0.06 \pm 0.16 \pm 0.03)\%$	
$D^0 \rightarrow K_S^0 \pi^+ \pi^-$ [1142] $K_S^0 K^+ K^-$ (BABAR: no CPV)	x	$(0.16 \pm 0.23 \pm 0.12 \pm 0.08)\%$	
	y	$(0.57 \pm 0.20 \pm 0.13 \pm 0.07)\%$	+0.0615
$D^0 \rightarrow \pi^0 \pi^+ \pi^-$ [1145] (BABAR: no CPV)	x	$(1.5 \pm 1.2 \pm 0.6)\%$	
	y	$(0.2 \pm 0.9 \pm 0.5)\%$	-0.006
$D^0 \rightarrow K^+ \ell^- \bar{\nu}$	$R_M = (x^2 + y^2)/2$	$(0.0130 \pm 0.0269)\%$	
$D^0 \rightarrow K^+ \pi^- \pi^0$ [1130]	x''	$(2.61^{+0.57}_{-0.68} \pm 0.39)\%$	
	y''	$(-0.06^{+0.55}_{-0.64} \pm 0.34)\%$	-0.75
$D^0 \rightarrow K^+ \pi^- \pi^+ \pi^-$ [1132]	$R_M/2$	$(4.8 \pm 1.8) \times 10^{-5}$	
$\psi(3770) \rightarrow \bar{D}D$ [1128] (CLEOc)	R_D	$(0.533 \pm 0.107 \pm 0.045)\%$	$\begin{Bmatrix} 1 & 0 & -0.42 & 0.01 \\ & 1 & -0.73 & 0.39 & 0.02 \\ & & 1 & -0.53 & -0.03 \\ & & & 1 & 0.04 \\ & & & & 1 \end{Bmatrix}$
	x^2	$(0.06 \pm 0.23 \pm 0.11)\%$	
	y	$(4.2 \pm 2.0 \pm 1.0)\%$	
	$\cos \delta$	$0.81^{+0.22+0.07}_{-0.18-0.05}$	
	$\sin \delta$	$-0.01 \pm 0.41 \pm 0.04$	

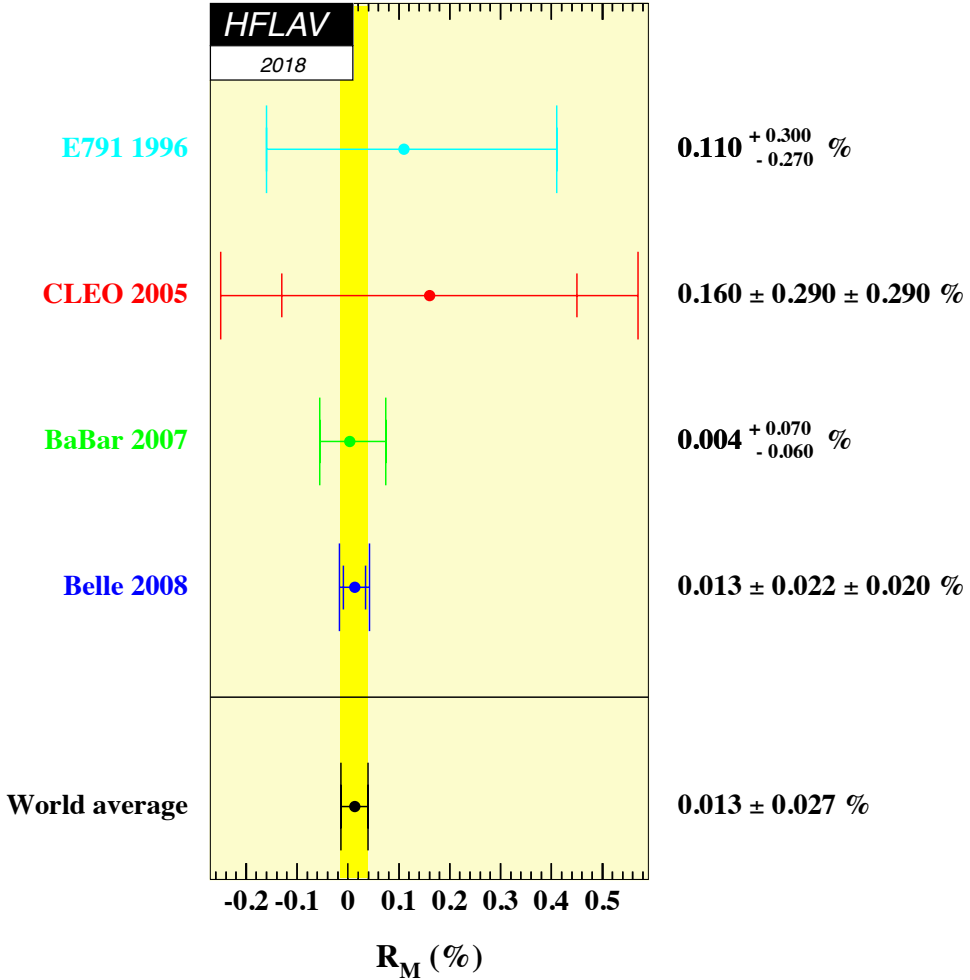


Figure 84: World average value of $R_M = (x^2 + y^2)/2$ as calculated from $D^0 \rightarrow K^+ \ell^- \bar{\nu}$ measurements [1133–1136].

ϕ_{12} is a weak phase that is responsible for CP violation in mixing. The conventional parameters $(x, y, |q/p|, \phi)$ can be derived from $(x_{12}, y_{12}, \phi_{12})$.

4. allowing full CPV , *i.e.*, floating all parameters.

For fit (2), in addition to fixing $A_D=0$, we reduce four independent parameters to three by imposing the relation [1164, 1165] $\tan \phi = (1 - |q/p|^2)/(1 + |q/p|^2) \times (x/y)$.³⁵ This constraint is imposed in two ways: in the first way we float parameters x , y , and ϕ and from these derive $|q/p|$; and in the second way we float x , y , and $|q/p|$ and from these derive ϕ . The central values returned by the two fits are identical, but the first fit yields MINOS errors for ϕ while the second fit yields MINOS errors for $|q/p|$. For the no-direct- CPV fit (3), we fit for parameters x_{12} , y_{12} , and ϕ_{12} , and from these derive x , y , $|q/p|$, and ϕ ; the latter parameters are used to calculate

³⁵One can also use Eq. (16) of Ref. [1163] to reduce four parameters to three.

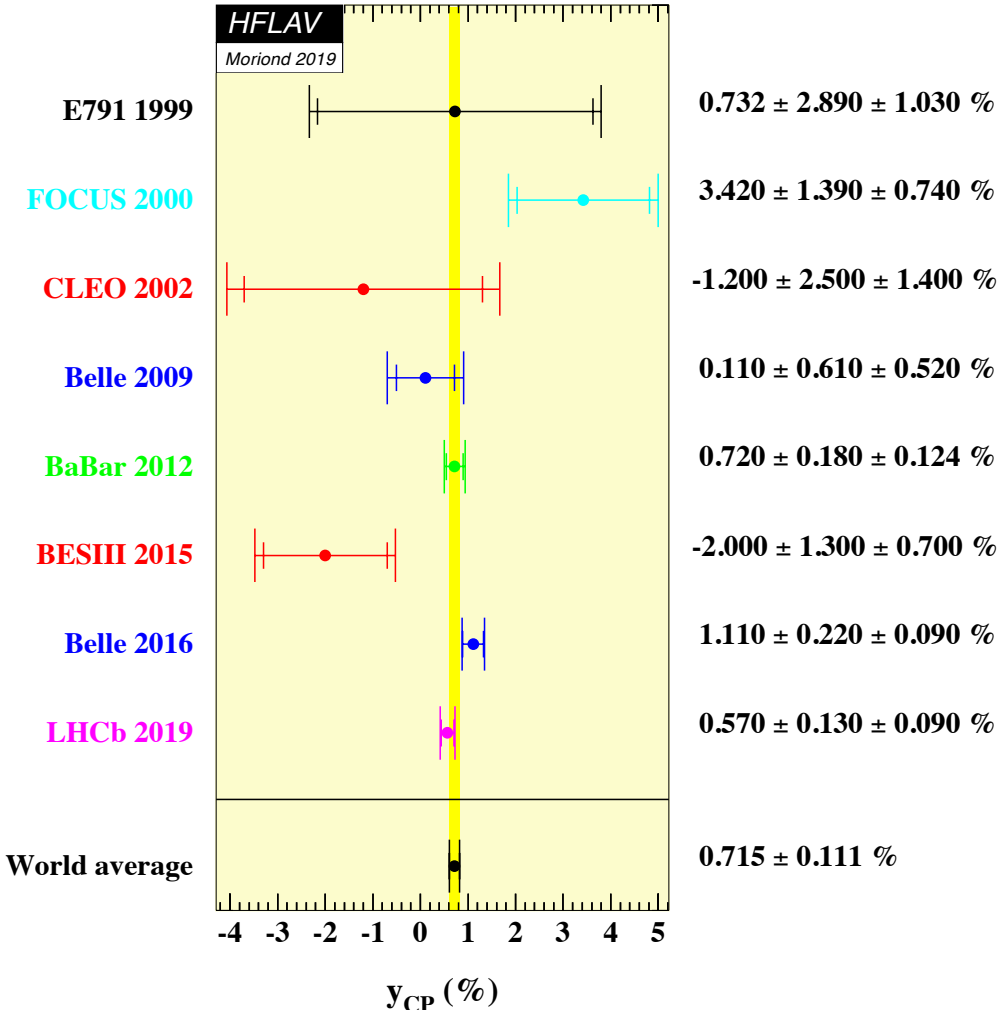


Figure 85: World average value of y_{CP} as calculated from $D^0 \rightarrow K^+K^-$, $\pi^+\pi^-$ measurements [1151–1158].

the fit χ^2 . All results are listed in Table 285. The overall χ^2 is 60.7 for $49 - 10 = 39$ degrees of freedom. Table 286 lists individual contributions to the χ^2 for the CPV -allowed fit (4).

Confidence contours in the two dimensions (x, y) or $(|q/p|, \phi)$ are obtained by finding the minimum χ^2 for each fixed point in the two-dimensional plane. The resulting 1σ – 5σ contours are shown in Fig. 87 for the CP -conserving fit (1); in Fig. 88 for the no-direct- CPV fit (3); and in Fig. 89 for the CPV -allowed fit (4). The contours are determined from the increase of the χ^2 above the minimum value. One observes that the (x, y) contours for the no- CPV fit are very similar to those for the CPV -allowed fit. In the latter fit, the χ^2 at the no-mixing point $(x, y) = (0, 0)$ is 2028 units above the minimum value, which, for two degrees of freedom, corresponds to a confidence level (C.L.) greater than 10σ . Thus, the no-mixing hypothesis is excluded at this high level. In the $(|q/p|, \phi)$ plot (Fig. 89 bottom), the no- CPV point $(1, 0)$ is

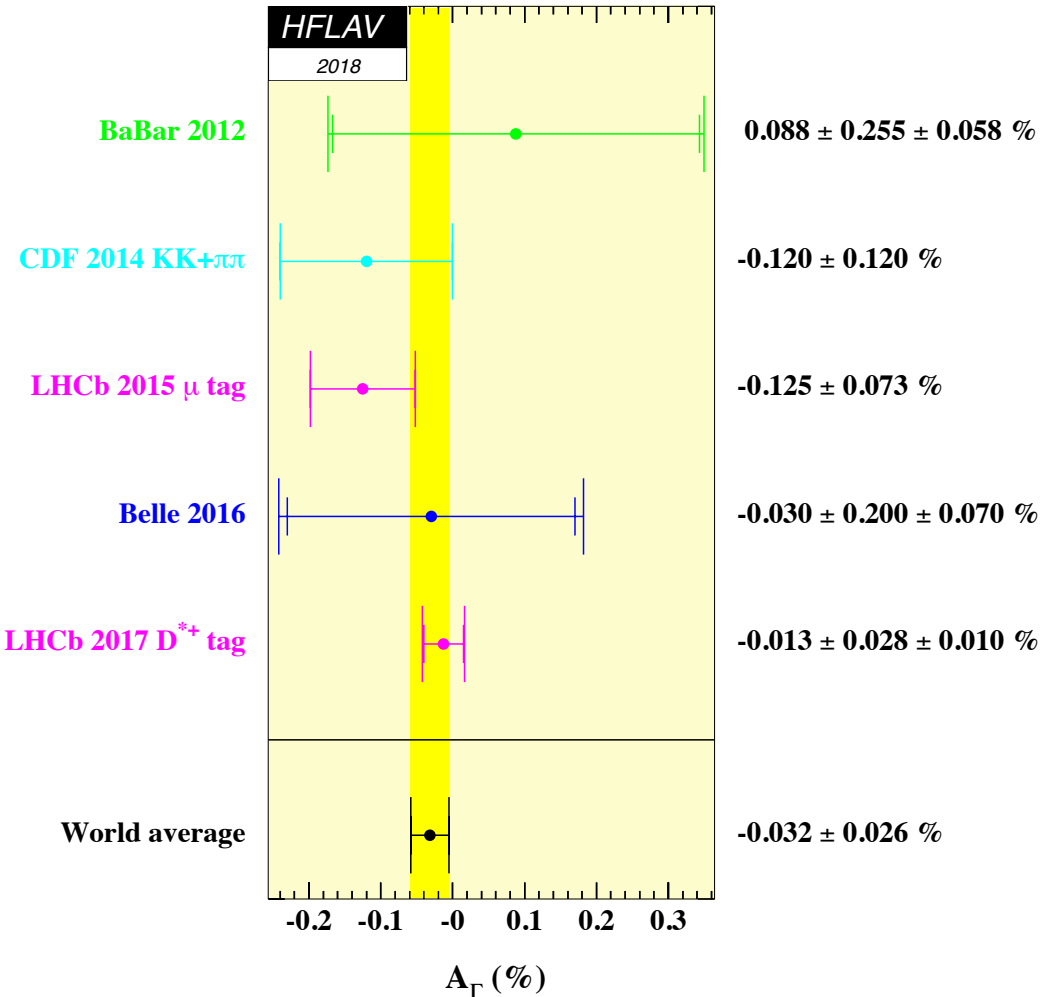


Figure 86: World average value of A_Γ as calculated from $D^0 \rightarrow K^+K^-$, $\pi^+\pi^-$ measurements [1155, 1157, 1159–1161].

within the 1σ contour, and thus the data is consistent with CP conservation.

One-dimensional likelihood curves for individual parameters are obtained by finding, for a fixed value of a parameter, the minimum χ^2 . The resulting functions $\Delta\chi^2 = \chi^2 - \chi_{\min}^2$, where χ_{\min}^2 is the minimum value, are shown in Fig. 90. The points where $\Delta\chi^2 = 3.84$ determine 95% C.L. intervals for the parameters. These intervals are listed in Table 285.

9.1.4 Conclusions

From the results listed in Table 285 and shown in Figs. 89 and 90, we conclude the following:

- The experimental data consistently indicate D^0 - \overline{D}^0 mixing. The no-mixing point $x = y = 0$ is excluded at $> 11.5\sigma$. The parameter x differs from zero by 3.1σ , and y differs from zero by $> 11.4\sigma$. This mixing is presumably dominated by long-distance processes, which are difficult to calculate.

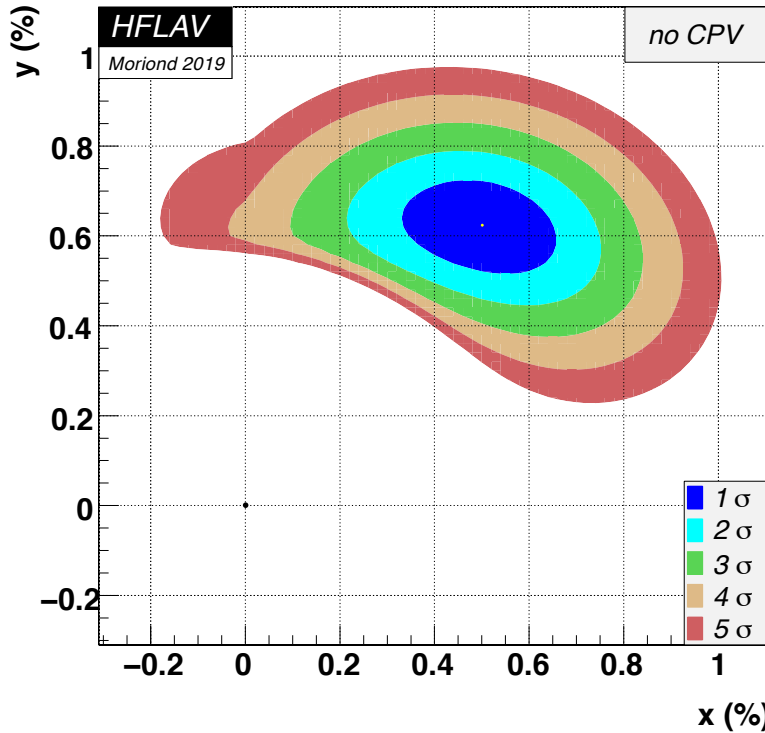


Figure 87: Two-dimensional contours for mixing parameters (x, y), for no CPV (fit 1).

- Since y_{CP} is positive, the CP -even state is shorter-lived, as in the K^0 - \bar{K}^0 system. However, since x also appears to be positive, the CP -even state is heavier, unlike in the K^0 - \bar{K}^0 system.
- There is no evidence for CPV arising from D^0 - \bar{D}^0 mixing ($|q/p| \neq 1$) or from a phase difference between the mixing amplitude and a direct decay amplitude ($\phi \neq 0$). However, *direct CP* violation has recently been observed by LHCb in time-integrated $D^0 \rightarrow K^+ K^-$, $\pi^+ \pi^-$ decays – see Ref. [1150]. The measured CP asymmetry is small, 0.15%, and thus it is unclear whether this asymmetry is consistent with the SM or indicates new physics.

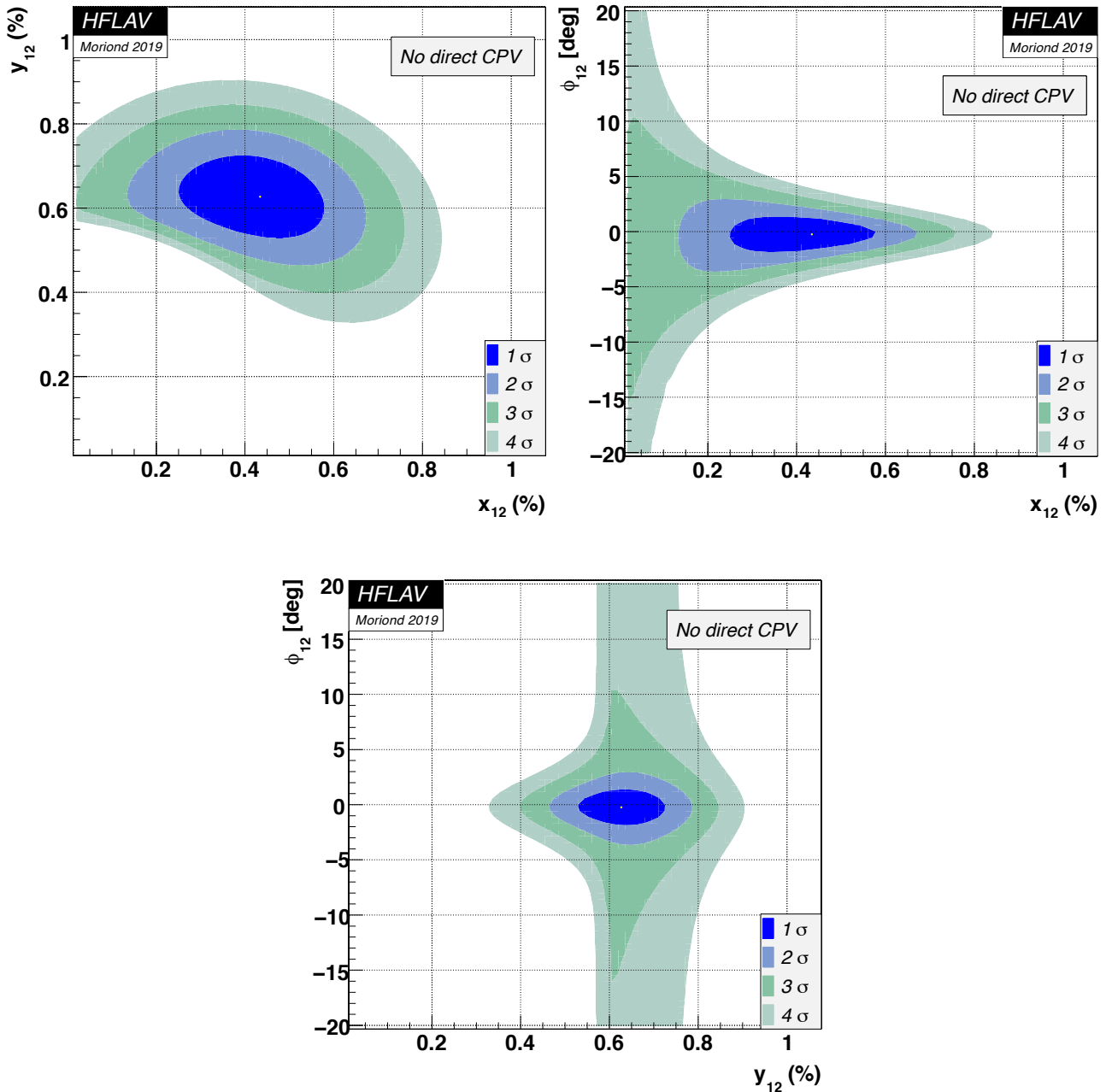


Figure 88: Two-dimensional contours for theoretical parameters (x_{12}, y_{12}) (top left), (x_{12}, ϕ_{12}) (top right), and (y_{12}, ϕ_{12}) (bottom), for no direct CPV in DCS decays (fit 3).

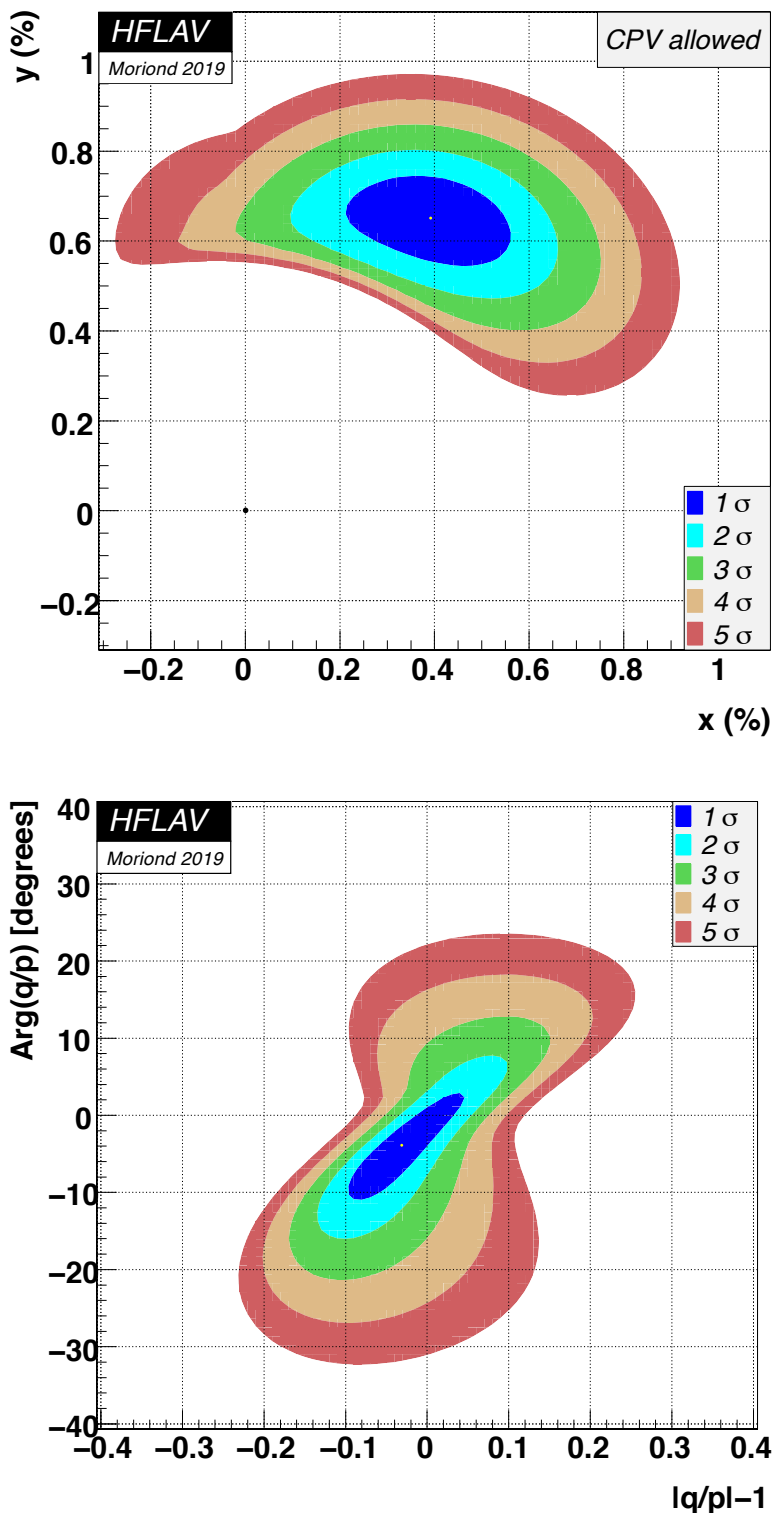


Figure 89: Two-dimensional contours for parameters (x, y) (top) and $(|q/p| - 1, \phi)$ (bottom), allowing for CPV (fit 4).

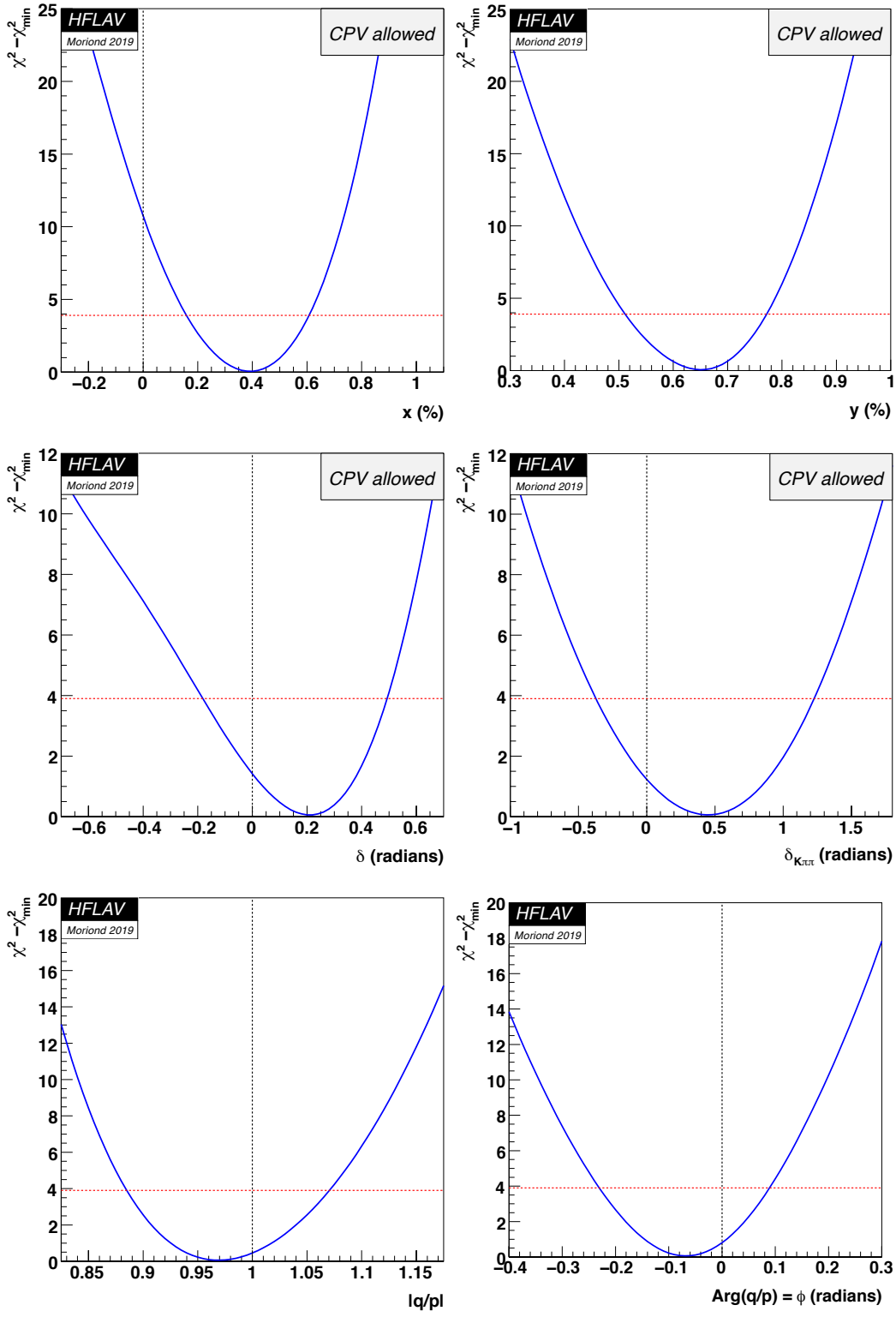


Figure 90: The function $\Delta\chi^2 = \chi^2 - \chi_{\min}^2$ for fitted parameters x , y , δ , $\delta_{K\pi\pi}$, $|q/p|$, and ϕ . The points where $\Delta\chi^2 = 3.84$ (denoted by dashed horizontal lines) determine 95% C.L. intervals.

Table 283: Time-dependent $D^0 \rightarrow K^+ \pi^-$ observables used for the global fit. The observables R_D^+ and R_D^- are related to parameters R_D and A_D via $R_D^\pm = R_D(1 \pm A_D)$.

Mode	Observable	Values	Correlation coefficients
$D^0 \rightarrow K^+ \pi^-$ [1120] (<i>BABAR</i> 384 fb $^{-1}$)	R_D	$(0.303 \pm 0.0189)\%$	$\begin{pmatrix} 1 & 0.77 & -0.87 \\ & 1 & -0.94 \\ & & 1 \end{pmatrix}$
	x'^{2+}	$(-0.024 \pm 0.052)\%$	
	y'^+	$(0.98 \pm 0.78)\%$	
$\bar{D}^0 \rightarrow K^- \pi^+$ [1120] (<i>BABAR</i> 384 fb $^{-1}$)	A_D	$(-2.1 \pm 5.4)\%$	same as above
	x'^{2-}	$(-0.020 \pm 0.050)\%$	
	y'^-	$(0.96 \pm 0.75)\%$	
$D^0 \rightarrow K^+ \pi^-$ [1138] (<i>Belle</i> 976 fb $^{-1}$ No <i>CPV</i>)	R_D	$(0.353 \pm 0.013)\%$	$\begin{pmatrix} 1 & 0.737 & -0.865 \\ & 1 & -0.948 \\ & & 1 \end{pmatrix}$
	x'^2	$(0.009 \pm 0.022)\%$	
	y'	$(0.46 \pm 0.34)\%$	
$D^0 \rightarrow K^+ \pi^-$ [1137] (<i>Belle</i> 400 fb $^{-1}$ <i>CPV</i> -allowed)	R_D	$(0.364 \pm 0.018)\%$	$\begin{pmatrix} 1 & 0.655 & -0.834 \\ & 1 & -0.909 \\ & & 1 \end{pmatrix}$
	x'^{2+}	$(0.032 \pm 0.037)\%$	
	y'^+	$(-0.12 \pm 0.58)\%$	
$\bar{D}^0 \rightarrow K^- \pi^+$ [1137] (<i>Belle</i> 400 fb $^{-1}$ <i>CPV</i> -allowed)	A_D	$(+2.3 \pm 4.7)\%$	same as above
	x'^{2-}	$(0.006 \pm 0.034)\%$	
	y'^-	$(0.20 \pm 0.54)\%$	
$D^0 \rightarrow K^+ \pi^-$ [1139] (<i>CDF</i> 9.6 fb $^{-1}$ No <i>CPV</i>)	R_D	$(0.351 \pm 0.035)\%$	$\begin{pmatrix} 1 & 0.90 & -0.97 \\ & 1 & -0.98 \\ & & 1 \end{pmatrix}$
	x'^2	$(0.008 \pm 0.018)\%$	
	y'	$(0.43 \pm 0.43)\%$	
$D^0 \rightarrow K^+ \pi^-$ [1140] (<i>LHCb</i> 5.0 fb $^{-1}$ <i>CPV</i> -allowed)	R_D^+	$(0.3454 \pm 0.0045)\%$	$\begin{pmatrix} 1 & 0.843 & -0.935 \\ & 1 & -0.963 \\ & & 1 \end{pmatrix}$
	x'^{2+}	$(0.0061 \pm 0.0037)\%$	
	y'^+	$(0.501 \pm 0.074)\%$	
$\bar{D}^0 \rightarrow K^- \pi^+$ [1140] (<i>LHCb</i> 5.0 fb $^{-1}$ <i>CPV</i> -allowed)	R_D^-	$(0.3454 \pm 0.0045)\%$	$\begin{pmatrix} 1 & 0.846 & -0.935 \\ & 1 & -0.964 \\ & & 1 \end{pmatrix}$
	x'^{2-}	$(0.0016 \pm 0.0039)\%$	
	y'^-	$(0.554 \pm 0.074)\%$	

Table 284: Measurements of time-integrated CP asymmetries. The observable $A_{CP}(f) = [\Gamma(D^0 \rightarrow f) - \Gamma(\bar{D}^0 \rightarrow f)] / [\Gamma(D^0 \rightarrow f) + \Gamma(\bar{D}^0 \rightarrow f)]$. The symbol $\Delta\langle t \rangle$ denotes the difference between the mean reconstructed decay times for $D^0 \rightarrow K^+K^-$ and $D^0 \rightarrow \pi^+\pi^-$ decays due to different trigger and reconstruction efficiencies.

Mode	Observable	Values	$\Delta\langle t \rangle/\tau_D$
$D^0 \rightarrow h^+h^-$ [1147] (<i>BABAR</i> 386 fb $^{-1}$)	$A_{CP}(K^+K^-)$	$(+0.00 \pm 0.34 \pm 0.13)\%$	0
	$A_{CP}(\pi^+\pi^-)$	$(-0.24 \pm 0.52 \pm 0.22)\%$	
$D^0 \rightarrow h^+h^-$ [1148, 1149] (<i>CDF</i> 9.7 fb $^{-1}$)	$A_{CP}(K^+K^-) - A_{CP}(\pi^+\pi^-)$	$(-0.62 \pm 0.21 \pm 0.10)\%$	
	$A_{CP}(K^+K^-)$	$(-0.32 \pm 0.21)\%$	0.27 ± 0.01
	$A_{CP}(\pi^+\pi^-)$	$(+0.31 \pm 0.22)\%$	
$D^0 \rightarrow h^+h^-$ [1150] (<i>LHCb</i> 9.0 fb $^{-1}$, $D^{*+} \rightarrow D^0\pi^+$ + $\bar{B} \rightarrow D^0\mu^-X$ tags combined)	$A_{CP}(K^+K^-) - A_{CP}(\pi^+\pi^-)$	$(-0.154 \pm 0.029)\%$	0.115 ± 0.002

Table 285: Results of the global fit for different assumptions regarding CPV .

Parameter	No CPV	No direct CPV	CPV -allowed	CPV -allowed
		in DCS decays		95% C.L. Interval
x (%)	$0.50^{+0.13}_{-0.14}$	$0.43^{+0.10}_{-0.11}$	$0.39^{+0.11}_{-0.12}$	[0.16, 0.61]
y (%)	0.62 ± 0.07	0.63 ± 0.06	$0.651^{+0.063}_{-0.069}$	[0.51, 0.77]
$\delta_{K\pi}$ ($^\circ$)	$8.9^{+8.2}_{-8.9}$	$9.3^{+8.3}_{-9.2}$	$12.1^{+8.6}_{-10.2}$	[-10.4, 28.2]
R_D (%)	0.344 ± 0.002	0.344 ± 0.002	0.344 ± 0.002	[0.339, 0.348]
A_D (%)	—	—	$-0.55^{+0.49}_{-0.51}$	[-1.5, 0.4]
$ q/p $	—	0.998 ± 0.008	$0.969^{+0.050}_{-0.045}$	[0.89, 1.07]
ϕ ($^\circ$)	—	0.08 ± 0.31	$-3.9^{+4.5}_{-4.6}$	[-13.2, 5.1]
$\delta_{K\pi\pi}$ ($^\circ$)	$18.5^{+22.7}_{-23.4}$	$22.1^{+22.6}_{-23.4}$	$25.8^{+23.0}_{-23.8}$	[-21.3, 70.3]
A_π (%)	—	0.05 ± 0.16	0.06 ± 0.16	[-0.25, 0.38]
A_K (%)	—	-0.11 ± 0.16	-0.09 ± 0.16	[-0.40, 0.22]
x_{12} (%)	—	$0.43^{+0.10}_{-0.11}$		[0.22, 0.63]
y_{12} (%)	—	0.63 ± 0.06		[0.50, 0.75]
ϕ_{12} ($^\circ$)	—	$-0.25^{+0.96}_{-0.99}$		[-2.5, 1.8]

Table 286: Individual contributions to the χ^2 for the CPV -allowed fit.

Observable	degrees of freedom	χ^2	$\sum \chi^2$
y_{CP} World Average (Fig. 85)	1	0.35	0.35
A_Γ World Average (Fig. 86)	1	2.07	2.41
$x_{K^0\pi^+\pi^-}$ Belle [1141]	1	0.71	3.12
$y_{K^0\pi^+\pi^-}$ Belle [1141]	1	4.42	7.54
$ q/p _{K^0\pi^+\pi^-}$ Belle [1141]	1	0.48	8.02
$\phi_{K^0\pi^+\pi^-}$ Belle [1141]	1	0.53	8.55
$x_{CP}(K^0\pi^+\pi^-)$ LHCb [1144]	1	0.55	9.10
$y_{CP}(K^0\pi^+\pi^-)$ LHCb [1144]	1	0.06	9.16
$\Delta x(K^0\pi^+\pi^-)$ LHCb [1144]	1	0.00	9.16
$\Delta y(K^0\pi^+\pi^-)$ LHCb [1144]	1	0.09	9.26
$x_{K^0h+h^-}$ BABAR [1142]	1	0.73	9.98
$y_{K^0h+h^-}$ BABAR [1142]	1	0.08	10.06
$x_{\pi^0\pi^+\pi^-}$ BABAR [1145]	1	0.68	10.74
$y_{\pi^0\pi^+\pi^-}$ BABAR [1145]	1	0.19	10.93
$(x^2 + y^2)_{K^+\ell^-\nu}$ World Average (Fig. 84)	1	0.14	11.07
$x_{K^+\pi^-\pi^0}$ BABAR [1130]	1	7.10	18.17
$y_{K^+\pi^-\pi^0}$ BABAR [1130]	1	3.91	22.08
CLEOc [1128]			
$(x/y/R_D/\cos\delta/\sin\delta)$	5	10.53	32.60
$R_D^+/x'^{2+}/y'^+$ BABAR [1120]	3	8.69	41.30
$R_D^-/x'^{2-}/y'^-$ BABAR [1120]	3	4.02	45.32
$R_D^+/x'^{2+}/y'^+$ Belle [1138]	3	1.88	47.20
$R_D^-/x'^{2-}/y'^-$ Belle [1138]	3	2.36	49.56
$R_D/x'^2/y'$ CDF [1139]	3	1.20	50.76
$R_D^+/x'^{2+}/y'^+$ LHCb [1140]	3	1.29	52.05
$R_D^-/x'^{2-}/y'^-$ LHCb [1140]	3	0.67	52.72
$A_{KK}/A_{\pi\pi}$ BABAR [1147]	2	0.35	53.08
$A_{KK}/A_{\pi\pi}$ CDF [1148]	2	4.07	57.14
$A_{KK} - A_{\pi\pi}$ LHCb [1150] ($D^*, B^0 \rightarrow D^0\mu X$ tags)	1	0.05	57.19
$(x^2 + y^2)_{K^+\pi^-\pi^+\pi^-}$ LHCb [1132]	1	3.47	60.67

9.2 CP asymmetries

One way CP violation manifests itself is in a difference between the decay rate for a particle and that of its CP -conjugate [1166]. Such phenomena can be classified into two broad categories, termed *direct* CP violation and *indirect* CP violation [1167]. Direct CP violation refers to charm changing $\Delta C=1$ processes and can occur in both charged and neutral charm hadron decays. It results from interference between two different decay amplitudes, *e.g.*, a penguin amplitude and a tree amplitude, that have different weak and strong phases. The weak phase difference ($\Delta\phi$) will have opposite sign for $D \rightarrow f$ and $\bar{D} \rightarrow \bar{f}$ decays, while the strong phase difference ($\Delta\delta$) will have the same sign. As a result, squaring the total amplitudes to obtain the decay rates gives an interference term proportional to $\cos(\Delta\phi + \Delta\delta)$ for $D \rightarrow f$ decays, and proportional to $\cos(-\Delta\phi + \Delta\delta)$ for $\bar{D} \rightarrow \bar{f}$ decays. Thus the decay rates will differ. This difference is unaffected when time-integrating the decay rates, and the overall branching fractions will differ.

In the Standard Model (SM), a difference in strong phases may arise due to final-state interactions (FSI) [1168], different isospin amplitudes, intermediate resonance contributions, or different partial waves. A difference in weak phases arises from different CKM vertex couplings, as is often the case for tree and penguin diagrams. Within the SM, direct CP violation is expected only in singly Cabibbo-suppressed (SCS) charm decays, as only these decays receive a non-negligible contribution from the penguin amplitude. This type of CP violation depends on the decay mode, and the CP asymmetries may reach a percent level. Indirect CP violation refers to $\Delta C=2$ processes and arises in D^0 decays due to $D^0-\bar{D}^0$ mixing. It can occur as an asymmetry in the mixing itself, or it can result from interference between a decay amplitude following mixing and a non-mixed amplitude. Within the SM, charm indirect CP violation is expected to be universal, *i.e.*, independent of final state. Current experimental limits on indirect CP violation are discussed in Sec. 9.1.

The time-integrated CP asymmetry A_{CP} is defined as the difference between D and \bar{D} partial widths divided by their sum:

$$A_{CP} = \frac{\Gamma(D) - \Gamma(\bar{D})}{\Gamma(D) + \Gamma(\bar{D})}. \quad (233)$$

In the case of D^+ and D_s^+ decays, A_{CP} measures direct CP violation; in the case of D^0 decays, A_{CP} measures direct and indirect CP violation combined (see also Sec. 9.4). Given experimental constraints on A_Γ , a contribution from indirect CP violation would be negligible compared to current A_{CP} sensitivities. Values of A_{CP} for D^+ , D^0 and D_s^+ decays are listed in Tables 287, 288, 289, 290 and 291 respectively. Modes with a single K_S meson in the final state can exhibit a CP asymmetry due to CP violation in $K^0-\bar{K}^0$ mixing [1169]; *i.e.*, the rate for $\bar{K}^0 \rightarrow K_S$ differs slightly from that for $K^0 \rightarrow K_S$. This small effect is visible thus far only in $D^+ \rightarrow K_S \pi^+$ decays (see Table 287). Modes with a K^0 or \bar{K}^0 in the final state have this effect already corrected for. The asymmetry for the DCS decay $D^0 \rightarrow K^+ \pi^-$ is not included in these tables, as it is a by-product of charm-mixing measurements and thus is discussed in Sec. 9.1 (where it is referred to as A_D).

In each experiment, care must be taken to correct for production and detection asymmetries, as they can reach the percent level. To take into account differences in production rates between D and \bar{D} , which would affect the number of respective decays observed, some experiments (such as E791 and FOCUS) normalize A_{CP} to that measured in a Cabibbo-favored mode. This method assumes there is negligible CP violation in the normalization mode. Explicitly, the CP

asymmetry is calculated as

$$A_{CP} = \frac{\eta(D) - \eta(\bar{D})}{\eta(D) + \eta(\bar{D})}, \quad (234)$$

where (considering, for example, $D^0 \rightarrow K^- K^+$)

$$\eta(D) = \frac{N(D^0 \rightarrow K^- K^+)}{N(D^0 \rightarrow K^- \pi^+)}, \quad (235)$$

$$\eta(\bar{D}) = \frac{N(\bar{D}^0 \rightarrow K^- K^+)}{N(\bar{D}^0 \rightarrow K^+ \pi^-)}. \quad (236)$$

In this method there is the additional advantage that most corrections due to reconstruction inefficiencies cancel out, reducing systematic uncertainties.

Other experiments (such as Belle and LHCb) determine A_{CP} via the relation

$$A_{\text{meas}} = A_{CP} + A_{\text{prod}} + A_{\text{det}}, \quad (237)$$

where A_{meas} is the measured (raw) asymmetry, A_{prod} is the asymmetry in the charm hadron production, and A_{det} is due to a difference in detection efficiencies between positively and negatively charged hadrons. The production asymmetry at the LHC arises from a charge asymmetry of the colliding particles: in pp collisions more charm baryons are produced than anti-baryons, and, as a result, charm mesons are less abundantly produced than anti-charm mesons. Such a production asymmetry is expected to be dependent on kinematics of the produced charm hadrons. The production asymmetry in e^+e^- collisions appears as a forward-backward (FB) asymmetry caused by an interference of the photon and off-shell Z^0 contributions. The detection asymmetries typically arise from differences in hadron interactions with detector material. In particular, the interaction cross sections for K^+ and K^- significantly differ, with the differences being dependent on the kaon momentum.

The B -factory strategy to separate the production and CP asymmetries relies on the former being odd, while the latter is even, with respect to the center-of-mass production polar angle (θ^*). The A_{meas} is measured in $|\cos \theta^*|$ bins and subsequently averaged; this removes the A_{prod} contribution. At LHCb, the production asymmetry is removed by measuring A_{CP} for D^* -tagged $D^0 \rightarrow K^- \pi^+$ decays; this also corrects for the soft π detection asymmetry. Subsequently, $D^+ \rightarrow K^- \pi^+ \pi^+$ decays are used to correct for the detection asymmetry introduced by the $K^- \pi^+$ system itself, and $D^+ \rightarrow K_S \pi^+$ decays are then used to remove the asymmetries in D^+ production and π^+ detection. Finally, the asymmetry related to the neutral kaon, *i.e.*, from regeneration and different interactions of K^0 and \bar{K}^0 with the detector, as well as from CP violation occurring in the K^0 - \bar{K}^0 mixing, is calculated. Put together, this gives

$$A_{CP}(K^+ K^-) = A_{\text{meas}}(K^+ K^-) - A_{\text{meas}}(K^- \pi^+) + A_{\text{meas}}(K^- \pi^+ \pi^+) - A_{\text{meas}}(K_S \pi^+) + A(\bar{K}^0 - K^0).$$

For some decays, typically the ones with lower statistics, one corrects for nuisance asymmetries by measuring A_{CP} relative to some well-measured reference channel, for instance

$$A_{CP}(D_s^+ \rightarrow \eta' \pi^+) = A_{\text{meas}}(D_s^+ \rightarrow \eta' \pi^+) - A_{\text{meas}}(D_s^+ \rightarrow \phi \pi^+) + A_{CP}(D_s^+ \rightarrow \phi \pi^+).$$

The uncertainty of the reference A_{CP} is treated as an external input error.

Much easier than individual A_{CP} measurements, and often easier for theoretical interpretation, are measurements of A_{CP} *differences*, defined as ΔA_{CP} . The most important one is that for $D^0 \rightarrow K^+K^-$ and $D^0 \rightarrow \pi^+\pi^-$ decays, which is discussed in Sec. 9.4. Its baryonic counterpart, ΔA_{CP} for $\Lambda_c^+ \rightarrow pK^+K^-$ and $\Lambda_c^+ \rightarrow p\pi^+\pi^-$ SCS decays, was recently measured by LHCb [1170]. We note that, in the limit of U-spin symmetry, direct CP violation in $D^0 \rightarrow K^+K^-$ and $D^0 \rightarrow \pi^+\pi^-$ decays is expected to have equal magnitude and opposite sign [1171]; thus the measurement of ΔA_{CP} “doubles” the effect. However, no such argument holds for baryonic $\Lambda_c^+ \rightarrow pK^+K^-$ and $\Lambda_c^+ \rightarrow p\pi^+\pi^-$ decays.

CP asymmetries arise from the interplay between weak and strong phases, and the latter change over the phase space of multi-body decays, which usually proceed via intermediate states. Therefore local CP asymmetries, *i.e.*, measured in the phase space of the multi-body decays, or asymmetries for individual strong amplitudes, can offer better sensitivity than a global asymmetry measurement, in which any effect can be diluted. Probing the multi-body phase space can be done in a model dependent way, by employing a Dalitz analysis or more general amplitude analysis separately for D and \bar{D} decays; a CP asymmetry is then measured for each contributing amplitude. The CP violating observables are asymmetries of magnitudes and phases of CP -conjugate amplitudes, as well as asymmetries of the amplitude fit fractions.

For multi-body decays, some experiments use model independent techniques to search for local CP asymmetries. The first technique (a.k.a the Miranda method) [1172] uses a binned χ^2 approach to compare the relative density in a bin of phase space of a decay with that of its CP conjugate. In the Energy Test technique [1173] two event samples are compared and a test statistic variable (T) is used to determine the average distances of events in phase space. If the distributions of events in both samples are identical (CP symmetric case), T will randomly fluctuate around a value close to zero. Such model-independent techniques allow to measure a p -value for a no- CP violation hypothesis and localize any CP asymmetric phase-space regions. As such methods serve as a discovery tool, any model-independent evidence for CP violation should be followed by a model-dependent measurement to allow its interpretation.

In Tables 287, 288, 289, 290, and 291, asymmetries for three- and four-body decays are reported for their actual final state, *i.e.*, resonant substructure is implicitly included but not considered separately. Most asymmetries measured for three- and four-body channels are still only global asymmetries. The reported model-independent tests, which attempt to probe the decay phase space, yield p -values typically at the level of a few percent or higher, thus consistent with no CP violation. The lowest p -value of 0.6%, corresponding to a significance for CP violation of 2.7σ , is obtained in the P -odd test of $D^0 \rightarrow \pi^+\pi^-\pi^+\pi^-$ decays [1174]. This implies that the effect originates from a P -odd amplitude, *e.g.*, $D^0 \rightarrow [\rho^0\rho^0]_{L=1}$. A model-dependent search for CP violation has been performed via an amplitude analysis of $D^0 \rightarrow K^+K^-\pi^+\pi^-$ decays [1175]. Asymmetries have been measured for 25 contributing amplitudes, with a total uncertainty ranging from 1% to 15%, dominated by the statistical uncertainty. No significant CP violation is found, and the highest fluctuation of 2.8σ is observed in the phase asymmetry for the P -odd amplitude $D^0 \rightarrow [\phi(1020)\rho(1450)]_{L=1}$. CP violation arising through P (parity) violation is discussed further in Sec. 9.3.

For the first time, A_{CP} has been measured for decays classified as rare: radiative modes $D^0 \rightarrow V\gamma$, with $V = \bar{K}^{*0}$, $\phi(1020)$, ρ^0 , as well as di-muon decays $D^0 \rightarrow \pi^+\pi^-\mu^+\mu^-$ and $D^0 \rightarrow K^+K^-\mu^+\mu^-$. For the di-muon modes, in addition to their global asymmetries listed in Table 290, A_{CP} has been measured in bins of di-muon invariant mass. Asymmetries for mass regions away from $\mu^+\mu^-$ production via η , ρ - ω or ϕ decays still have very limited sensitivities,

ranging from 12% to 26%. These non-resonance regions are particularly important for New Physics searches (see Sec. 9.11). Overall, CP asymmetries have been measured for more than 50 charm decay modes, and in several modes the sensitivity is well below 5×10^{-3} . There is currently no evidence for CP violation in the charm meson sector. The CP asymmetry observed for the mode $D^+ \rightarrow K_S\pi^+$ is consistent with that expected due to $K^0-\bar{K}^0$ mixing [1169], and thus it is not attributed to charm.

In the charm baryon sector, there is also no evidence of CP violation. Until recently, there had been only two measurements for Λ_c^+ ; these were performed by CLEO [1176] and FOCUS [1177] and had limited sensitivity. The former used the semileptonic $\Lambda_c^+ \rightarrow \Lambda e^+ \nu_e$ decays, while the latter the CF $\Lambda_c^+ \rightarrow \Lambda \pi^+$ decays; both have searched for CP violation through an angular analysis exploiting the Λ helicity angle. CP asymmetry is accessed through comparison of P asymmetry in decays of Λ_c^+ and Λ_c^- , measured with the weak-asymmetry parameters, respectively α_{Λ_c} and $\alpha_{\bar{\Lambda}_c}$. As $\alpha_{\Lambda_c} = -\alpha_{\bar{\Lambda}_c}$ under P -parity conservation, the CP -violating asymmetry is defined as

$$A_{CP}^\alpha = \frac{\alpha_{\Lambda_c} + \alpha_{\bar{\Lambda}_c}}{\alpha_{\Lambda_c} - \alpha_{\bar{\Lambda}_c}}. \quad (238)$$

The CLEO measurement [1176] gives

$$A_{CP}^\alpha(\Lambda_c^+ \rightarrow \Lambda e^+ \nu_e) = 0.00 \pm 0.03 \pm 0.01 \pm 0.02,$$

where the third error is related to the uncertainty of the Λ weak-asymmetry parameter. The asymmetry measured by FOCUS [1177] is

$$A_{CP}^\alpha(\Lambda_c^+ \rightarrow \Lambda \pi^+) = -0.07 \pm 0.19 \pm 0.12.$$

The first high-statistics CPV measurement of charm baryons comes from LHCb in the form of ΔA_{CP} for the $\Lambda_c^+ \rightarrow p K^+ K^-$ and $\Lambda_c^+ \rightarrow p \pi^+ \pi^-$ SCS decays [1170] where the result is

$$\Delta A_{CP}(\Lambda_c^+ \rightarrow ph^+ h^-) \equiv A_{CP}(p K^+ K^-) - A_{CP}(p \pi^+ \pi^-) = 0.003 \pm 0.009 \pm 0.006.$$

The measurement, performed in a phase-space integrated manner, has limited sensitivity and does not facilitate an interpretation. Given (potentially) rich dynamics of these decays in their five-dimensional phase space³⁶, ΔA_{CP} measured in phase-space regions or a model dependent measurement of individual asymmetries would be very much desirable. Taken together, the limits obtained for CP asymmetries in the charm sector pose tight constraints on New Physics models.

For charm decays one can build various SU(3)-based sum rules which, in addition to testing SU(3) symmetry itself, are also useful for performing model-independent tests of the SM. Particularly interesting are sums exploiting the SU(3) subgroups, U-spin or isospin (I), as they involve less decays and offer more precise tests. While U-spin symmetry in charm decays is broken by a non-negligible amount due to the s-quark mass, isospin symmetry holds at the $(m_u - m_d)$ level and thus is very precise. Important for our considerations are isospin sum rules that relate individual CP asymmetries of the isospin-related processes. Verifying such rules allows for tests to be performed with reduced uncertainty due to strong interaction effects. Such a sum rule has been proposed for $D \rightarrow \pi\pi$ decays in Ref. [1178].

³⁶For unpolarized Λ_c , its decay phase space reduces to a two-dimensional Dalitz distribution.

The isospin decomposition of $D \rightarrow \pi\pi$ amplitudes gives

$$\begin{aligned} A_{\pi^+\pi^-} &= \sqrt{2}\mathcal{A}_3 + \sqrt{2}\mathcal{A}_1, \\ A_{\pi^0\pi^0} &= 2\mathcal{A}_3 - \mathcal{A}_1, \\ A_{\pi^+\pi^0} &= 3\mathcal{A}_3, \end{aligned}$$

where \mathcal{A}_1 and \mathcal{A}_3 are amplitudes corresponding to the $\Delta I = 1/2$ and $\Delta I = 3/2$ transitions, respectively (*i.e.*, transitions to $\pi\pi$ final states with $I = 0$ and $I = 2$). From this, one can get an amplitude isospin sum rule

$$\frac{1}{\sqrt{2}}A_{\pi^+\pi^-} + A_{\pi^0\pi^0} - A_{\pi^+\pi^0} = 0. \quad (239)$$

Probing such a sum requires knowledge of strong phases, which are accessible only at charm-threshold experiments. However, without this knowledge the sum of differences of decay rates for D and \bar{D} decays can be measured:

$$|A_{\pi^+\pi^-}|^2 - |\bar{A}_{\pi^+\pi^-}|^2 + |A_{\pi^0\pi^0}|^2 - |\bar{A}_{\pi^0\pi^0}|^2 - \frac{2}{3}(|A_{\pi^+\pi^0}|^2 - |\bar{A}_{\pi^-\pi^0}|^2) = 3(|\mathcal{A}_1|^2 - |\bar{\mathcal{A}}_1|^2). \quad (240)$$

This equation suggests several SM tests. As the penguin amplitude is within the SM purely $\Delta I = 1/2$, any CP asymmetry observed in $D^+ \rightarrow \pi^+\pi^0$ would be a sign of New Physics in the $\Delta I = 3/2$ amplitude. If the sum in Eq. (240), depending only on \mathcal{A}_1 , is found to be non-zero, this would mean that CP violation arises from the $\Delta I = 1/2$ transitions. Moreover, a scenario in which the sum in Eq. (240) is zero and individual asymmetries are non-zero would suggest New Physics contributing to the $\Delta I = 3/2$ amplitude.

To facilitate an experimental test, the left-hand side of Eq. (240) is rewritten as a ratio [1179]:

$$R \equiv \frac{|A_{\pi^+\pi^-}|^2 - |\bar{A}_{\pi^+\pi^-}|^2 + |A_{\pi^0\pi^0}|^2 - |\bar{A}_{\pi^0\pi^0}|^2 - \frac{2}{3}(|A_{\pi^+\pi^0}|^2 - |\bar{A}_{\pi^-\pi^0}|^2)}{|A_{\pi^+\pi^-}|^2 + |\bar{A}_{\pi^+\pi^-}|^2 + |A_{\pi^0\pi^0}|^2 + |\bar{A}_{\pi^0\pi^0}|^2 + \frac{2}{3}(|A_{\pi^+\pi^0}|^2 + |\bar{A}_{\pi^-\pi^0}|^2)}. \quad (241)$$

Using the relations $|A|^2 \propto \mathcal{B}/\tau_D$ and $|A|^2 - |\bar{A}|^2 = A_{CP}(|A|^2 + |\bar{A}|^2)$, we rewrite Eq. (241) as

$$R = \frac{A_{CP}(D^0 \rightarrow \pi^+\pi^-)}{1 + \frac{\tau_{D^0}}{\mathcal{B}_{+-}}(\frac{\mathcal{B}_{00}}{\tau_{D^0}} + \frac{2}{3}\frac{\mathcal{B}_{+0}}{\tau_{D^+}})} + \frac{A_{CP}(D^0 \rightarrow \pi^0\pi^0)}{1 + \frac{\tau_{D^0}}{\mathcal{B}_{00}}(\frac{\mathcal{B}_{+-}}{\tau_{D^0}} + \frac{2}{3}\frac{\mathcal{B}_{+0}}{\tau_{D^+}})} + \frac{A_{CP}(D^+ \rightarrow \pi^+\pi^0)}{1 + \frac{3}{2}\frac{\tau_{D^+}}{\mathcal{B}_{+0}}(\frac{\mathcal{B}_{00}}{\tau_{D^0}} + \frac{\mathcal{B}_{+-}}{\tau_{D^0}})}, \quad (242)$$

where \mathcal{B}_{+-} , \mathcal{B}_{00} , and \mathcal{B}_{+0} denote the branching fractions for $D^0 \rightarrow \pi^+\pi^-$, $D^0 \rightarrow \pi^0\pi^0$, and $D^+ \rightarrow \pi^+\pi^0$, respectively. The sum R is calculated using our averages for CP asymmetries (Tables 287 and 289), and PDG averages [21] for branching fractions and lifetimes. The result is

$$R = (-3.05 \pm 2.65) \times 10^{-3}, \quad (243)$$

which is consistent with zero. In addition, all the individual asymmetries contributing to R are consistent with zero. The uncertainty on R is dominated by the uncertainties on individual asymmetries.

The sum rule for $D \rightarrow \bar{K}K$ decays involves full SU(3) considerations and thus is imprecise. Ref. [1178] proposes a set of isospin sum rules for $D \rightarrow \rho\pi$ or $D \rightarrow \bar{K}^{(*)}K^{(*)}\pi$, but to test these sum rules requires a number of not-yet-performed experimental measurements.

Table 287: CP asymmetries $A_{CP} = [\Gamma(D^+) - \Gamma(D^-)]/[\Gamma(D^+) + \Gamma(D^-)]$ for two-body D^\pm decays. In the individual asymmetries listed, the first uncertainties are statistical, and the second systematic, whereas the third uncertainty in $A_{CP}(D^+ \rightarrow \pi^+\eta')$ from LHCb is due to $A_{CP}(D^+ \rightarrow \pi^+K_S)$ used for calibration.

Mode	Year	Collaboration	A_{CP}
$D^+ \rightarrow \mu^+\nu$	2008	CLEO [1180]	$+0.08 \pm 0.08$
$D^+ \rightarrow \pi^+\pi^0$	2018	Belle [1179]	$+0.0231 \pm 0.0124 \pm 0.0023$
	2010	CLEO [1181]	$+0.029 \pm 0.029 \pm 0.003$
		HFLAV average	$+0.024 \pm 0.012$
$D^+ \rightarrow \pi^+\eta$	2011	Belle [1182]	$+0.0174 \pm 0.0113 \pm 0.0019$
	2010	CLEO [1181]	$-0.020 \pm 0.023 \pm 0.003$
		HFLAV average	$+0.010 \pm 0.010$
$D^+ \rightarrow \pi^+\eta'$	2017	LHCb [1183]	$-0.0061 \pm 0.0072 \pm 0.0053 \pm 0.0012$
	2011	Belle [1182]	$-0.0012 \pm 0.0112 \pm 0.0017$
	2010	CLEO [1181]	$-0.040 \pm 0.034 \pm 0.003$
		HFLAV average	-0.006 ± 0.007
$D^+ \rightarrow K^+\pi^0$	2010	CLEO [1181]	$-0.035 \pm 0.107 \pm 0.009$
$D^+ \rightarrow K_S\pi^+$	2014	CLEO [1184]	$-0.011 \pm 0.006 \pm 0.002$
	2012	Belle [1185]	$-0.00363 \pm 0.00094 \pm 0.00067$
	2011	BABAR [1186]	$-0.0044 \pm 0.0013 \pm 0.0010$
	2002	FOCUS [1187]	$-0.016 \pm 0.015 \pm 0.009$
		HFLAV average	-0.0041 ± 0.0009
$D^+ \rightarrow K_SK^+$	2013	BABAR [1188]	$+0.0013 \pm 0.0036 \pm 0.0025$
	2013	Belle [1189]	$-0.0025 \pm 0.0028 \pm 0.0014$
	2010	CLEO [1181]	$-0.002 \pm 0.015 \pm 0.009$
	2002	FOCUS [1187]	$+0.071 \pm 0.061 \pm 0.012$
		HFLAV average	-0.0011 ± 0.0025
$D^+ \rightarrow (\bar{K}^0/K^0)K^+$	2014	LHCb [1190]	$+0.0003 \pm 0.0017 \pm 0.0014$
	2013	BABAR [1188]	$+0.0046 \pm 0.0036 \pm 0.0025$
	2013	Belle [1189]	$-0.0008 \pm 0.0028 \pm 0.0014$
		HFLAV average	$+0.0011 \pm 0.0017$

Table 288: CP asymmetries $A_{CP} = [\Gamma(D^+) - \Gamma(D^-)]/[\Gamma(D^+) + \Gamma(D^-)]$ for three- and four-body D^\pm decays. In the individual asymmetries listed, the first uncertainties are statistical, and the second (if quoted) are systematic.

Mode	Year	Collaboration	A_{CP}
$D^+ \rightarrow \pi^+\pi^-\pi^+$	2014	LHCb [1191]	Model independent technique, no evidence for CPV
	1997	E791 [1192]	-0.017 ± 0.042 (stat.)
$D^+ \rightarrow K^-\pi^+\pi^+$	2014	D0 [1193]	$-0.0016 \pm 0.0015 \pm 0.0009$
	2014	CLEO [1184]	$-0.003 \pm 0.002 \pm 0.004$
		HFLAV average	-0.0018 ± 0.0016
$D^+ \rightarrow K_S\pi^+\pi^0$	2014	CLEO [1184]	$-0.001 \pm 0.007 \pm 0.002$
$D^+ \rightarrow K^+K^-\pi^+$	2014	CLEO [1184]	$-0.001 \pm 0.009 \pm 0.004$
	2013	BABAR [1194]	$+0.0037 \pm 0.0030 \pm 0.0015$
	2008	CLEO [1195]	Dalitz plot analysis, no evidence for CPV
	2000	FOCUS [1196]	$+0.006 \pm 0.011 \pm 0.005$
	1997	E791 [1192]	-0.014 ± 0.029 (stat.)
		HFLAV average	$+0.0032 \pm 0.0031$
$D^+ \rightarrow K^-\pi^+\pi^+\pi^0$	2014	CLEO [1184]	$-0.003 \pm 0.006 \pm 0.004$
$D^+ \rightarrow K_S\pi^+\pi^+\pi^-$	2014	CLEO [1184]	$+0.000 \pm 0.012 \pm 0.003$
$D^+ \rightarrow K_SK^+\pi^+\pi^-$	2005	FOCUS [1197]	$-0.042 \pm 0.064 \pm 0.022$

Table 289: CP asymmetries $A_{CP} = [\Gamma(D^0) - \Gamma(\bar{D}^0)]/[\Gamma(D^0) + \Gamma(\bar{D}^0)]$ for two-body D^0, \bar{D}^0 decays. In the individual asymmetries listed, the first uncertainties are statistical, and the second are systematic, unless explicitly stated that they have been combined. The third uncertainty in Belle $A_{CP}(D^0 \rightarrow K_S K_S)$ is due to $A_{CP}(D^0 \rightarrow K_S \pi^0)$ used for normalization.

Mode	Year	Collaboration	A_{CP}
$D^0 \rightarrow \pi^+ \pi^-$	2017	LHCb [1198]	+0.0007 ± 0.0014 ± 0.0011
	2012	CDF [1199]	+0.0022 ± 0.0024 ± 0.0011
	2008	BABAR [1147]	-0.0024 ± 0.0052 ± 0.0022
	2012	Belle [1200]	+0.0043 ± 0.0052 ± 0.0012
	2002	CLEO [1153]	+0.019 ± 0.032 ± 0.008
	2000	FOCUS [1196]	+0.048 ± 0.039 ± 0.025
	1998	E791 [1201]	-0.049 ± 0.078 ± 0.030
		HFLAV average	-0.0001 ± 0.0014
$D^0 \rightarrow \pi^0 \pi^0$	2014	Belle [1202]	-0.0003 ± 0.0064 ± 0.0010
	2001	CLEO [1203]	+0.001 ± 0.048 (stat. and syst. combined)
		HFLAV average	-0.0003 ± 0.0064
$D^0 \rightarrow K_S \pi^0$	2014	Belle [1202]	-0.0021 ± 0.0016 ± 0.0007
	2001	CLEO [1203]	+0.001 ± 0.013 (stat. and syst. combined)
		HFLAV average	-0.0020 ± 0.0017
$D^0 \rightarrow K_S \eta$	2011	Belle [1204]	+0.0054 ± 0.0051 ± 0.0016
$D^0 \rightarrow K_S \eta'$	2011	Belle [1204]	+0.0098 ± 0.0067 ± 0.0014
$D^0 \rightarrow K_S K_S$	2018	LHCb [1205]	+0.023 ± 0.028 ± 0.009
	2017	Belle [1206]	-0.0002 ± 0.0153 ± 0.0002 ± 0.0017
	2001	CLEO [1203]	-0.23 ± 0.19 (stat. and syst. combined)
		HFLAV average	+0.004 ± 0.014
$D^0 \rightarrow K^- \pi^+$	2014	CLEO [1184]	+0.003 ± 0.003 ± 0.006
$D^0 \rightarrow K^+ K^-$	2017	LHCb [1198]	+0.0004 ± 0.0012 ± 0.0010
	2012	CDF [1199]	-0.0024 ± 0.0022 ± 0.0009
	2008	BABAR [1147]	+0.0000 ± 0.0034 ± 0.0013
	2012	Belle [1200]	-0.0043 ± 0.0030 ± 0.0011
	2002	CLEO [1153]	+0.000 ± 0.022 ± 0.008
	2000	FOCUS [1196]	-0.001 ± 0.022 ± 0.015
	1998	E791 [1201]	-0.010 ± 0.049 ± 0.012
		HFLAV average	-0.0009 ± 0.0011

Table 290: CP asymmetries $A_{CP} = [\Gamma(D^0) - \Gamma(\bar{D}^0)]/[\Gamma(D^0) + \Gamma(\bar{D}^0)]$ for three- and four-body D^0, \bar{D}^0 decays. In the individual asymmetries listed, the first uncertainties are statistical, and the second are systematic, unless only the former is given, or explicitly stated that these two have been combined. The Belle study of $D^0 \rightarrow K^+K^-\pi^+\pi^-$ [1207] employs a T-odd method for P-even variables, which corresponds to measuring a global A_{CP} .

Mode	Year	Collaboration	A_{CP}
$D^0 \rightarrow \pi^+\pi^-\pi^0$	2015	LHCb [1208]	Model-independent method, no evidence for CPV
	2008	BABAR [1209]	+0.0031 ± 0.0041 ± 0.0017
	2008	Belle [1210]	+0.0043 ± 0.0130 (stat. and syst. combined)
	2005	CLEO [1211]	+0.01 ^{+0.09} _{-0.07} ± 0.05
		HFLAV average	+0.0032 ± 0.0042
$D^0 \rightarrow K^-\pi^+\pi^0$	2014	CLEO [1184]	+0.001 ± 0.003 ± 0.004
$D^0 \rightarrow K^+\pi^-\pi^0$	2005	Belle [1212]	-0.006 ± 0.053 (stat.)
	2001	CLEO [1213]	+0.09 ^{+0.25} _{-0.22} (stat.)
		HFLAV average	-0.0014 ± 0.0517
$D^0 \rightarrow K_S\pi^+\pi^-$	2012	CDF [1214]	-0.0005 ± 0.0057 ± 0.0054
	2004	CLEO [1215]	-0.009 ± 0.021 ^{+0.016} _{-0.057}
		HFLAV average	-0.0008 ± 0.0077
$D^0 \rightarrow K_SK^-\pi^+$	2016	LHCb [479]	Amplitude analysis, no evidence for CPV
$D^0 \rightarrow K_SK^+\pi^-$	2016	LHCb [479]	Amplitude analysis, no evidence for CPV
$D^0 \rightarrow K^+K^-\pi^0$	2008	BABAR [1209]	-0.0100 ± 0.0167 ± 0.0025
$D^0 \rightarrow \pi^-\pi^-\pi^+\pi^+$	2013	LHCb [1174]	Model-independent method, no evidence for CPV
$D^0 \rightarrow K^-\pi^+\pi^+\pi^-$	2014	CLEO [1184]	+0.002 ± 0.003 ± 0.004
$D^0 \rightarrow K^+\pi^-\pi^+\pi^-$	2005	Belle [1212]	-0.018 ± 0.044 (stat.)
$D^0 \rightarrow K^+K^-\pi^+\pi^-$	2018	Belle [1207]	+0.0034 ± 0.0036 ± 0.0006
	2018	LHCb [1175]	Amplitude analysis, no evidence for CPV
	2013	LHCb [1174]	Model-independent method, no evidence for CPV
	2012	CLEO [1216]	Amplitude analysis, no evidence for CPV
	2005	FOCUS [1197]	-0.082 ± 0.056 ± 0.047
		HFLAV average	+0.0032 ± 0.0036
$D^0 \rightarrow \bar{K}^{*0}[\rightarrow K^-\pi^+]\gamma$	2016	Belle [1217]	-0.003 ± 0.020 ± 0.000
$D^0 \rightarrow \phi[\rightarrow K^+K^-]\gamma$	2016	Belle [1217]	-0.094 ± 0.066 ± 0.001
$D^0 \rightarrow \rho^0[\rightarrow \pi^+\pi^-]\gamma$	2016	Belle [1217]	+0.056 ± 0.152 ± 0.006
$D^0 \rightarrow K^+K^-\mu^+\mu^-$	2018	LHCb [1218]	+0.00 ± 0.11 ± 0.02
$D^0 \rightarrow \pi^+\pi^-\mu^+\mu^-$	2018	LHCb [1218]	+0.049 ± 0.038 ± 0.007

Table 291: CP asymmetries $A_{CP} = [\Gamma(D_s^+) - \Gamma(D_s^-)]/[\Gamma(D_s^+) + \Gamma(D_s^-)]$ for D_s^\pm decays. In the individual asymmetries listed, the first uncertainties are statistical, and the second systematic, whereas the third uncertainty in $A_{CP}(D_s^+ \rightarrow \pi^+\eta')$ from LHCb is due to $A_{CP}(D^+ \rightarrow \pi^+\phi)$ used for calibration.

Mode	Year	Collaboration	A_{CP}
$D_s^+ \rightarrow \mu^+\nu$	2009	CLEO [1219]	$+0.048 \pm 0.061$
$D_s^+ \rightarrow \pi^+\eta$	2013	CLEO [1220]	$+0.011 \pm 0.030 \pm 0.008$
$D_s^+ \rightarrow \pi^+\eta'$	2017	LHCb [1183]	$-0.0082 \pm 0.0036 \pm 0.0022 \pm 0.002$
	2013	CLEO [1220]	$-0.022 \pm 0.022 \pm 0.006$
		HFLAV average	-0.0088 ± 0.0049
$D_s^+ \rightarrow K_S\pi^+$	2013	BABAR [1188]	$+0.006 \pm 0.020 \pm 0.003$
	2010	Belle [1221]	$+0.0545 \pm 0.0250 \pm 0.0033$
	2010	CLEO [1181]	$+0.163 \pm 0.073 \pm 0.003$
		HFLAV average	$+0.0311 \pm 0.0154$
$D_s^+ \rightarrow (\bar{K}^0/K^0)\pi^+$	2014	LHCb [1190]	$+0.0038 \pm 0.0046 \pm 0.0017$
	2013	BABAR [1188]	$+0.003 \pm 0.020 \pm 0.003$
		HFLAV average	$+0.0038 \pm 0.0048$
$D_s^+ \rightarrow K_SK^+$	2013	CLEO [1220]	$+0.026 \pm 0.015 \pm 0.006$
	2013	BABAR [1188]	$-0.0005 \pm 0.0023 \pm 0.0024$
	2010	Belle [1221]	$+0.0012 \pm 0.0036 \pm 0.0022$
		HFLAV average	$+0.0008 \pm 0.0026$
$D_s^+ \rightarrow K^+\pi^0$	2010	CLEO [1181]	$+0.266 \pm 0.228 \pm 0.009$
$D_s^+ \rightarrow K^+\eta$	2010	CLEO [1181]	$+0.093 \pm 0.152 \pm 0.009$
$D_s^+ \rightarrow K^+\eta'$	2010	CLEO [1181]	$+0.060 \pm 0.189 \pm 0.009$
$D_s^+ \rightarrow \pi^+\pi^+\pi^-$	2013	CLEO [1220]	$-0.007 \pm 0.030 \pm 0.006$
$D_s^+ \rightarrow \pi^+\pi^0\eta$	2013	CLEO [1220]	$-0.005 \pm 0.039 \pm 0.020$
$D_s^+ \rightarrow \pi^+\pi^0\eta'$	2013	CLEO [1220]	$-0.004 \pm 0.074 \pm 0.019$
$D_s^+ \rightarrow K_SK^+\pi^0$	2013	CLEO [1220]	$-0.016 \pm 0.060 \pm 0.011$
$D_s^+ \rightarrow K_SK_S\pi^+$	2013	CLEO [1220]	$+0.031 \pm 0.052 \pm 0.006$
$D_s^+ \rightarrow K^+\pi^+\pi^-$	2013	CLEO [1220]	$+0.045 \pm 0.048 \pm 0.006$
$D_s^+ \rightarrow K^+K^-\pi^+$	2013	CLEO [1220]	$-0.005 \pm 0.008 \pm 0.004$
$D_s^+ \rightarrow K_SK^-\pi^+\pi^+$	2013	CLEO [1220]	$+0.041 \pm 0.027 \pm 0.009$
$D_s^+ \rightarrow K_SK^+\pi^+\pi^-$	2013	CLEO [1220]	$-0.057 \pm 0.053 \pm 0.009$
$D_s^+ \rightarrow K^+K^-\pi^+\pi^0$	2013	CLEO [1220]	$+0.000 \pm 0.027 \pm 0.012$

9.3 T -odd asymmetries

Measuring T -odd asymmetries provides a complementary way to search for CP violation in the charm sector; it exploits CPT invariance. T -odd asymmetries are measured using triple-product correlations of the form $\vec{a} \cdot (\vec{b} \times \vec{c})$, where a , b , and c are spins or momenta; this combination is odd under time reversal (T). If a triple product is formed using *both* spin and momenta, *i.e.*,

$$\vec{s}_1 \cdot (\vec{p}_2 \times \vec{p}_3),$$

it is even under P -conjugation. However, if only momenta are used, *i.e.*,

$$\vec{p}_1 \cdot (\vec{p}_2 \times \vec{p}_3),$$

it becomes odd under P -conjugation. Thus, in this case the T -odd method becomes P -odd and allows one to probe CP violation occurring via P -violation. This type of CPV may arise only in P -odd amplitudes, which are allowed in decays of mesons into final states with at least four spinless particles. All the two- and three-body hadronic decays of charm mesons involve only P -even amplitudes³⁷, for which CP violation can arise only through C -violation.

Taking as an example the decay mode $D^0 \rightarrow K^+ K^- \pi^+ \pi^-$, involving spinless particles only, one forms a triple-product correlation using momenta of the final-state particles in the D^0 center-of-mass frame.³⁸ Defining the T -odd (and P -odd) correlation for D^0

$$C_T \equiv \vec{p}_{K^+} \cdot (\vec{p}_{\pi^+} \times \vec{p}_{\pi^-}), \quad (244)$$

and the corresponding quantity for \overline{D}^0

$$\overline{C}_T \equiv \vec{p}_{K^-} \cdot (\vec{p}_{\pi^-} \times \vec{p}_{\pi^+}), \quad (245)$$

one can construct the asymmetry for the D^0 decays as

$$A_T = \frac{\Gamma(C_T > 0) - \Gamma(C_T < 0)}{\Gamma(C_T > 0) + \Gamma(C_T < 0)}, \quad (246)$$

while for their CP -conjugate decays as

$$\overline{A}_T = \frac{\Gamma(-\overline{C}_T > 0) - \Gamma(-\overline{C}_T < 0)}{\Gamma(-\overline{C}_T > 0) + \Gamma(-\overline{C}_T < 0)}. \quad (247)$$

In these expressions, Γ represents a partial width, and the following applies:

$$P(C_T) = -C_T, \quad C(C_T) = \overline{C}_T, \quad CP(A_T) = \overline{A}_T. \quad (248)$$

The asymmetries A_T and \overline{A}_T depend on angular distributions of the daughter particles and may be nonzero due to final-state interactions or P -violation in weak decays. Given Eq. (248), one can construct the CP -violating, *i.e.* CP -odd (and P -odd, T -odd) asymmetry

$$\mathcal{A}_T \equiv \frac{A_T - \overline{A}_T}{2}; \quad (249)$$

³⁷ P -even amplitudes are accessed with P -even variables, like invariant masses or helicity angles.

³⁸ For momentum-only triple products, at least four-daughter final states are required to give a nonzero correlation, as only three out of four momenta are independent. For three-body decays, the daughters are in a plane and the triple product is zero.

where a nonzero value indicates CP violation (see Refs. [1222–1227]).

Values of \mathcal{A}_T for D^+ , D_s^+ , and D^0 decay modes are listed in Table 292. The first measurements were made by FOCUS, and subsequent *BABAR* measurements reached a sensitivity of $\sim 1\%$. Currently the best sensitivity is from LHCb. However, despite relatively high precision ($< 1\%$), there is no evidence for CP violation.

Table 292: Measurements of the T -odd CP asymmetry $\mathcal{A}_T = (A_T - \bar{A}_T)/2$.

Mode	Year	Collaboration	\mathcal{A}_T
$D^0 \rightarrow K^+ K^- \pi^+ \pi^-$	2018	Belle [1207]	$+0.0052 \pm 0.0037 \pm 0.0007$
	2014	LHCb [1228]	$+0.0018 \pm 0.0029 \pm 0.0004$
	2010	<i>BABAR</i> [1229]	$+0.0010 \pm 0.0051 \pm 0.0044$
	2005	FOCUS [1197]	$+0.010 \pm 0.057 \pm 0.037$
		HFLAV average	$+0.0035 \pm 0.0021$
$D^0 \rightarrow K_S \pi^+ \pi^- \pi^0$	2017	Belle [1230]	$-0.00028 \pm 0.00138^{+0.00023}_{-0.00076}$
$D^+ \rightarrow K_S K^+ \pi^+ \pi^-$	2011	<i>BABAR</i> [1231]	$-0.0120 \pm 0.0100 \pm 0.0046$
	2005	FOCUS [1197]	$+0.023 \pm 0.062 \pm 0.022$
		HFLAV average	-0.0110 ± 0.0109
$D_s^+ \rightarrow K_S K^+ \pi^+ \pi^-$	2011	<i>BABAR</i> [1231]	$-0.0136 \pm 0.0077 \pm 0.0034$
	2005	FOCUS [1197]	$-0.036 \pm 0.067 \pm 0.023$
		HFLAV average	-0.0139 ± 0.0084

All P -even contributions contributing to \mathcal{A}_T cancel out in the difference, thus it is only sensitive to P -odd amplitudes or interference between P -odd and P -even ones. The cancellation applies also to detection asymmetries and the production asymmetry (at least in the LHCb case); this is a big advantage of the T -odd method. Another way to probe P -odd amplitudes is through amplitude analysis using P -odd variables. Usually used is $\sin \Phi$, where Φ is the angle between the two decay planes formed with the $K^+ K^-$ and $\pi^+ \pi^-$ momenta in the $D^0 \rightarrow K^+ K^- \pi^+ \pi^-$ case [1175]; the $\sin \Phi$ corresponds to the triple product in fact. The model-independent technique used for the $D^0 \rightarrow \pi^+ \pi^- \pi^+ \pi^-$ decays [1174], has been carried out separately for P -odd and P -even contributions, separated out using a triple product. P -odd amplitudes in four-body decays of charm mesons are $D \rightarrow [VV]_{L=1}$, meaning a final state with two vector-mesons in a relative P -wave state, their contributions are however quite suppressed ($< 10\%$) [1175, 1232].

Decays of charm baryons offer an easier access to P -odd amplitudes. These are in particular Λ_c decays with a weakly-decaying baryon in their final states, for instance the $\Lambda_c^+ \rightarrow \Lambda \pi^+$ decays mentioned in Sec. 9.2. Moreover, for polarized charm baryons, e.g. Λ_c produced weakly in Λ_b decays, one can build a triple product using the Λ_c spin, however, this not yet been exploited.

Recently, the topic of symmetries has been revisited (see Refs. [1233, 1234]) with the suggestion to use other asymmetries constructed from triple products in multi-body decays to probe C , P , and CP symmetries. Up until now, experiments have measured only the asymmetry \mathcal{A}_T defined in Eq. (249); referred to in the literature by several names: $A_{T\text{viol}}$, a_{CP}^P , and $a_{CP}^{T-\text{odd}}$.

9.4 Interplay of direct and indirect CP violation

In decays of D^0 mesons, CP asymmetry measurements have contributions from both direct and indirect CP violation as discussed in Sec. 9.1. The contribution from indirect CP violation depends on the decay-time distribution of the data sample [1164]. This section describes a combination of measurements that allows the determination of the individual contributions of the two types of CP violation. At the same time, the level of agreement for a no- CP -violation hypothesis is tested. The observables are:

$$A_\Gamma \equiv \frac{\tau(\overline{D}^0 \rightarrow h^+ h^-) - \tau(D^0 \rightarrow h^+ h^-)}{\tau(\overline{D}^0 \rightarrow h^+ h^-) + \tau(D^0 \rightarrow h^+ h^-)}, \quad (250)$$

where $h^+ h^-$ can be $K^+ K^-$ or $\pi^+ \pi^-$, and

$$\Delta A_{CP} \equiv A_{CP}(K^+ K^-) - A_{CP}(\pi^+ \pi^-), \quad (251)$$

where A_{CP} are time-integrated CP asymmetries. The underlying theoretical parameters are:

$$\begin{aligned} a_{CP}^{\text{dir}} &\equiv \frac{|\mathcal{A}_{D^0 \rightarrow f}|^2 - |\mathcal{A}_{\overline{D}^0 \rightarrow f}|^2}{|\mathcal{A}_{D^0 \rightarrow f}|^2 + |\mathcal{A}_{\overline{D}^0 \rightarrow f}|^2}, \\ a_{CP}^{\text{ind}} &\equiv \frac{1}{2} \left[\left(\left| \frac{q}{p} \right| + \left| \frac{p}{q} \right| \right) x \sin \phi - \left(\left| \frac{q}{p} \right| - \left| \frac{p}{q} \right| \right) y \cos \phi \right], \end{aligned} \quad (252)$$

where $\mathcal{A}_{D \rightarrow f}$ is the amplitude for $D \rightarrow f$ [1235]. We use the relations [1236]

$$A_\Gamma = -a_{CP}^{\text{ind}} - a_{CP}^{\text{dir}} y_{CP}, \quad (253)$$

$$\begin{aligned} \Delta A_{CP} &= \Delta a_{CP}^{\text{dir}} \left(1 + y_{CP} \frac{\overline{\langle t \rangle}}{\tau} \right) + a_{CP}^{\text{ind}} \frac{\Delta \langle t \rangle}{\tau} + \overline{a_{CP}^{\text{dir}}} y_{CP} \frac{\Delta \langle t \rangle}{\tau}, \\ &\approx \Delta a_{CP}^{\text{dir}} \left(1 + y_{CP} \frac{\overline{\langle t \rangle}}{\tau} \right) + a_{CP}^{\text{ind}} \frac{\Delta \langle t \rangle}{\tau}. \end{aligned} \quad (254)$$

between the observables and the underlying parameters. Equation (253) constrains mostly indirect CP violation, and the direct CP violation contribution can differ for different final states. In Eq. (254), $\langle t \rangle / \tau$ denotes the mean decay time in units of the D^0 lifetime; ΔX denotes the difference in quantity X between $K^+ K^-$ and $\pi^+ \pi^-$ final states; and \overline{X} denotes the average for quantity X . We neglect the last term in this relation as all three factors are $\mathcal{O}(10^{-2})$ or smaller, and thus this term is negligible with respect to the other two terms. Note that $\Delta \langle t \rangle / \tau \ll \langle t \rangle / \tau$, and it is expected that $|a_{CP}^{\text{dir}}| < |\Delta a_{CP}^{\text{dir}}|$ because $a_{CP}^{\text{dir}}(K^+ K^-)$ and $a_{CP}^{\text{dir}}(\pi^+ \pi^-)$ are expected to have opposite signs in the Standard Model [1235].

A χ^2 fit is performed in the plane $\Delta a_{CP}^{\text{dir}}$ vs. a_{CP}^{ind} . For the *BABAR* result, the difference of the quoted values for $A_{CP}(K^+ K^-)$ and $A_{CP}(\pi^+ \pi^-)$ is calculated, adding all uncertainties in quadrature. This may overestimate the systematic uncertainty for the difference as it neglects correlated uncertainties; however, the result is conservative and the effect is small as all measurements are statistically limited. For all measurements, statistical and systematic uncertainties are added in quadrature when calculating the χ^2 . We use the HFLAV average value $y_{CP} = (0.715 \pm 0.111)\%$ (see Sec. 9.1) and the measurements listed in Table 293. In this fit,

Table 293: Inputs to the fit for direct and indirect CP violation. The first uncertainty listed is statistical and the second is systematic.

Year	Experiment	Results	$\Delta\langle t \rangle/\tau$	$\langle t \rangle/\tau$	Reference
2012	<i>BABAR</i>	$A_\Gamma = (+0.09 \pm 0.26 \pm 0.06)\%$	-	-	[1155]
2016	LHCb prompt	$A_\Gamma(KK) = (-0.030 \pm 0.032 \pm 0.010)\%$	-	-	[1161]
		$A_\Gamma(\pi\pi) = (+0.046 \pm 0.058 \pm 0.012)\%$	-	-	
2014	CDF	$A_\Gamma = (-0.12 \pm 0.12)\%$	-	-	[1159]
2015	LHCb SL	$A_\Gamma = (-0.125 \pm 0.073)\%$	-	-	[1160]
2015	Belle	$A_\Gamma = (-0.03 \pm 0.20 \pm 0.07)\%$	-	-	[1157]
2008	<i>BABAR</i>	$A_{CP}(KK) = (+0.00 \pm 0.34 \pm 0.13)\%$			
		$A_{CP}(\pi\pi) = (-0.24 \pm 0.52 \pm 0.22)\%$	0.00	1.00	[1147]
2012	CDF	$\Delta A_{CP} = (-0.62 \pm 0.21 \pm 0.10)\%$	0.25	2.58	[1149]
2014	LHCb SL	$\Delta A_{CP} = (+0.14 \pm 0.16 \pm 0.08)\%$	0.01	1.07	[1129]
2016	LHCb prompt	$\Delta A_{CP} = (-0.10 \pm 0.08 \pm 0.03)\%$	0.12	2.10	[1237]
2019	LHCb SL2	$\Delta A_{CP} = (-0.09 \pm 0.08 \pm 0.05)\%$	0.00	1.21	[1150]
2019	LHCb prompt2	$\Delta A_{CP} = (-0.18 \pm 0.03 \pm 0.09)\%$	0.13	1.74	[1150]

$A_\Gamma(KK)$ and $A_\Gamma(\pi\pi)$ are assumed to be identical. This assumption, which is expected in the SM, is supported by all measurements to date. A significant relative shift due to final-state dependent A_Γ values between ΔA_{CP} measurements with different mean decay times is excluded by these measurements.

The combination plot (see Fig. 91) shows the measurements listed in Table 293 for ΔA_{CP} and A_Γ . From the fit, the change in χ^2 from the minimum value for the no- CPV point $(0,0)$ is 33.5, which corresponds to a C.L. of 5.4×10^{-8} for two degrees of freedom or 5.4 standard deviations. The central values and $\pm 1\sigma$ uncertainties for the individual parameters are

$$\begin{aligned} a_{CP}^{\text{ind}} &= (+0.028 \pm 0.026)\% \\ \Delta a_{CP}^{\text{dir}} &= (-0.164 \pm 0.028)\%. \end{aligned} \quad (255)$$

This constitutes the first time that the average rejects the hypothesis of CP symmetry with a significance exceeding 5σ . The average clearly points at CP violation in the decays to two charged hadrons.

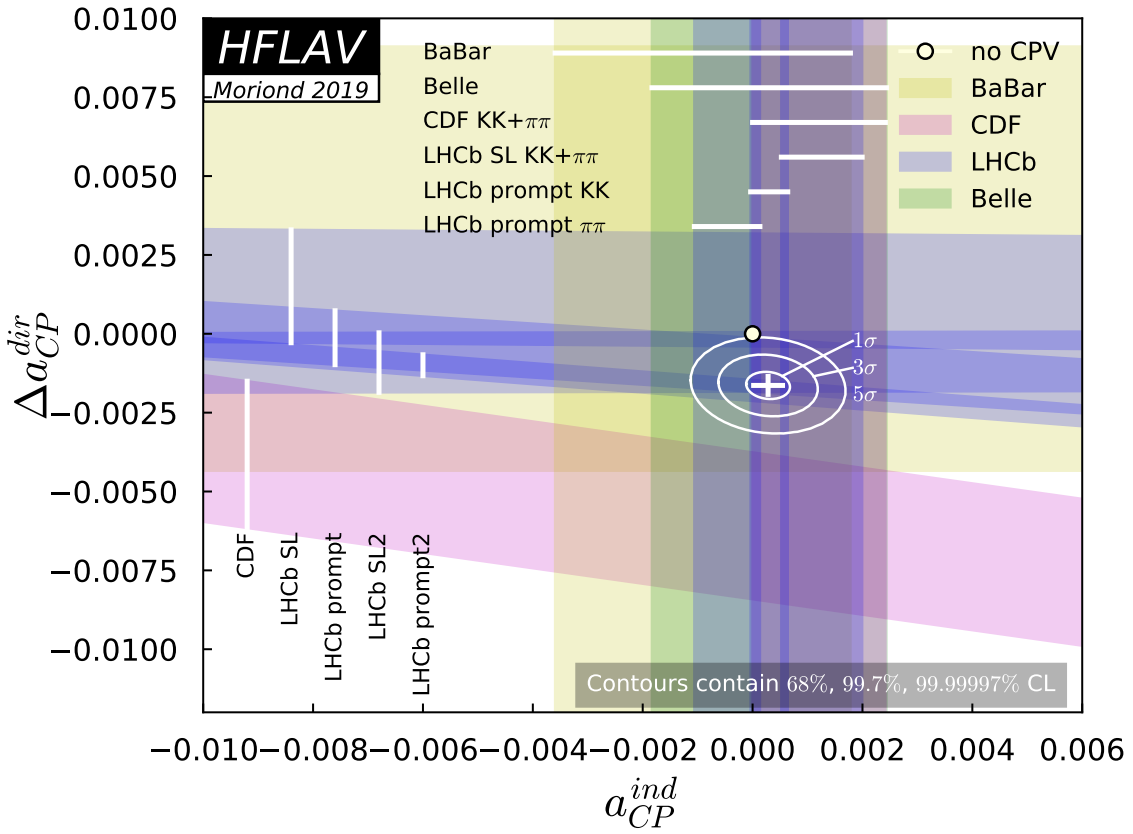


Figure 91: Plot of all data and the fit result. Individual measurements are plotted as bands showing their $\pm 1\sigma$ range. The no-CPV point (0,0) is shown as a filled circle, and the best fit value is indicated by a cross showing the one-dimensional uncertainties. Two-dimensional 68% C.L., 99.7% C.L., and 99.99997% C.L. regions are plotted as ellipses.

9.5 Semileptonic decays

9.5.1 Introduction

Semileptonic decays of D mesons involve the interaction of a leptonic current with a hadronic current. The latter is nonperturbative and cannot be calculated from first principles; thus it is usually parameterized in terms of form factors. The transition matrix element is written

$$\mathcal{M} = -i \frac{G_F}{\sqrt{2}} V_{cq} L^\mu H_\mu, \quad (256)$$

where G_F is the Fermi constant and V_{cq} is a CKM matrix element. The leptonic current L^μ is evaluated directly from the lepton spinors and has a simple structure; this allows one to extract information about the form factors (in H_μ) from data on semileptonic decays [1238]. Conversely, because there are no strong final-state interactions between the leptonic and hadronic systems, semileptonic decays for which the form factors can be calculated allow one to determine $|V_{cq}|$ [3].

9.5.2 $D \rightarrow P \bar{\ell} \nu_\ell$ decays

When the final state hadron is a pseudoscalar, the hadronic current is given by

$$H_\mu = \langle P(p) | \bar{q} \gamma_\mu q | D(p') \rangle = f_+(q^2) \left[(p' + p)_\mu - \frac{m_D^2 - m_P^2}{q^2} q_\mu \right] + f_0(q^2) \frac{m_D^2 - m_P^2}{q^2} q_\mu, \quad (257)$$

where m_D and p' are the mass and four momentum of the parent D meson, m_P and p are those of the daughter meson, $f_+(q^2)$ and $f_0(q^2)$ are form factors, and $q = p' - p$. Kinematics require that $f_+(0) = f_0(0)$. The contraction $q_\mu L^\mu$ results in terms proportional to m_ℓ [1239], and thus for $\ell = e$ the terms proportional to q_μ in Eq. (257) are negligible and only the $f_+(q^2)$ vector form factor is relevant. The corresponding differential partial width is

$$\frac{d\Gamma(D \rightarrow Pe\nu_e)}{dq^2 d\cos\theta_e} = \frac{G_F^2 |V_{cq}|^2}{32\pi^3} p^{*3} |f_+(q^2)|^2 \sin\theta_e^2, \quad (258)$$

where p^* is the magnitude of the momentum of the final state hadron in the D rest frame, and θ_e is the angle of the electron in the $e\nu$ rest frame with respect to the direction of the pseudoscalar meson in the D rest frame.

9.5.3 Form factor parameterizations

The form factor is traditionally parameterized with an explicit pole and a sum of effective poles:

$$f_+(q^2) = \frac{f_+(0)}{(1-\alpha)} \left[\left(\frac{1}{1-q^2/m_{\text{pole}}^2} \right) + \sum_{k=1}^N \frac{\rho_k}{1-q^2/(\gamma_k m_{\text{pole}}^2)} \right], \quad (259)$$

where ρ_k and γ_k are expansion parameters and α is a parameter that normalizes the form factor at $q^2 = 0$, $f_+(0)$. The parameter m_{pole} is the mass of the lowest-lying $c\bar{q}$ resonance with the vector quantum numbers; this is expected to provide the largest contribution to the form factor for the $c \rightarrow q$ transition. The sum over N gives the contribution of higher mass states. For example, for $D \rightarrow \pi$ transitions the dominant resonance is expected to be the $D^*(2010)$, and thus $m_{\text{pole}} = m_{D^*(2010)}$. For $D \rightarrow K$ transitions, the dominant resonance is expected to be the $D_s^*(2112)$, and thus $m_{\text{pole}} = m_{D_s^*(2112)}$.

9.5.4 Simple pole

Equation (259) can be simplified by neglecting the sum over effective poles, leaving only the explicit vector meson pole. This approximation is referred to as “nearest pole dominance” or “vector-meson dominance.” The resulting parameterization is

$$f_+(q^2) = \frac{f_+(0)}{(1 - q^2/m_{\text{pole}}^2)}. \quad (260)$$

However, values of m_{pole} that give a good fit to the data do not agree with the expected vector meson masses [1240]. To address this problem, the “modified pole” or Becirevic-Kaidalov (BK) parameterization [1241] was introduced. In this parameterization $m_{\text{pole}}/\sqrt{\alpha_{\text{BK}}}$ is interpreted as the mass of an effective pole higher than m_{pole} , i.e., it is expected that $\alpha_{\text{BK}} < 1$. The parameterization takes the form

$$f_+(q^2) = \frac{f_+(0)}{(1 - q^2/m_{\text{pole}}^2)} \frac{1}{\left(1 - \alpha_{\text{BK}} \frac{q^2}{m_{\text{pole}}^2}\right)}. \quad (261)$$

This parameterization is used by several experiments to determine form factor parameters. Measured values of m_{pole} and α_{BK} are listed in Tables 294 and 295 for $D \rightarrow K\ell\nu_\ell$ and $D \rightarrow \pi\ell\nu_\ell$ decays, respectively.

9.5.5 z expansion

Alternatively, a power series expansion around some value $q^2 = t_0$ can be used to parameterize $f_+(q^2)$ [1238, 1242–1244]. This parameterization is model-independent and satisfies general QCD constraints. The expansion is given in terms of a complex parameter z , which is the analytic continuation of q^2 into the complex plane:

$$z(q^2, t_0) = \frac{\sqrt{t_+ - q^2} - \sqrt{t_+ - t_0}}{\sqrt{t_+ - q^2} + \sqrt{t_+ - t_0}}, \quad (262)$$

where $t_0 = t_+(1 - \sqrt{1 - t_-/t_+})$ and $t_\pm \equiv (m_D \pm m_P)^2$. In this parameterization, $q^2 = t_0$ corresponds to $z = 0$, and the physical region extends in either direction up to $\pm|z|_{\text{max}} = \pm 0.051$ for $D \rightarrow K\ell\nu_\ell$ decays, and up to ± 0.17 for $D \rightarrow \pi\ell\nu_\ell$ decays.

The form factor is expressed as

$$f_+(q^2) = \frac{1}{P(q^2) \phi(q^2, t_0)} \sum_{k=0}^{\infty} a_k(t_0) [z(q^2, t_0)]^k, \quad (263)$$

where the $P(q^2)$ factor accommodates sub-threshold resonances via

$$P(q^2) \equiv \begin{cases} z(q^2, M_{D_s^*}^2) & (D \rightarrow K) \\ 1 & (D \rightarrow \pi). \end{cases} \quad (264)$$

The “outer” function $\phi(t, t_0)$ can be any analytic function, but a preferred choice (see, *e.g.*, Refs. [1242, 1243, 1245]), obtained from the Operator Product Expansion (OPE), is

$$\begin{aligned} \phi(q^2, t_0) = & \alpha \left(\sqrt{t_+ - q^2} + \sqrt{t_+ - t_0} \right) \times \\ & \frac{t_+ - q^2}{(t_+ - t_0)^{1/4}} \frac{(\sqrt{t_+ - q^2} + \sqrt{t_+ - t_-})^{3/2}}{(\sqrt{t_+ - q^2} + \sqrt{t_+})^5}, \end{aligned} \quad (265)$$

with $\alpha = \sqrt{\pi m_c^2/3}$. The OPE analysis provides a constraint upon the expansion coefficients, $\sum_{k=0}^N a_k^2 \leq 1$. These coefficients receive $1/M_D$ corrections, and thus the constraint is only approximate. However, the expansion is expected to converge rapidly since $|z| < 0.051$ (0.17) for $D \rightarrow K$ ($D \rightarrow \pi$) over the entire physical q^2 range, and Eq. (263) remains a useful parameterization. The main disadvantage as compared to phenomenological approaches is that there is no physical interpretation of the fitted coefficients a_K .

9.5.6 Three-pole formalism

An update of the vector pole dominance model has been developed for the $D \rightarrow \pi \ell \nu_\ell$ channel [1246]. It uses information of the residues of the semileptonic form factor at its first two poles, the $D^*(2010)$ and $D^{*'}(2600)$ resonances. The form factor is expressed as an infinite sum of residues from $J^P = 1^-$ states with masses $m_{D_n^*}$:

$$f_+(q^2) = \sum_{n=0}^{\infty} \frac{\text{Res}_{q^2=m_{D_n^*}^2} f_+(q^2)}{m_{D_n^*}^2 - q^2}, \quad (266)$$

with the residues given by

$$\text{Res}_{q^2=m_{D_n^*}^2} f_+(q^2) = \frac{1}{2} m_{D_n^*} f_{D_n^*} g_{D_n^* D \pi}. \quad (267)$$

Values of the f_{D^*} and $f_{D^{*'}(2600)}$ decay constants have been calculated relative to f_D via lattice QCD, with 2% and 28% precision, respectively [1246]. The couplings to the $D\pi$ state, $g_{D^* D \pi}$ and $g_{D^{*'} D \pi}$, are extracted from measurements of the $D^*(2010)$ and $D^{*'}(2600)$ widths by the BABAR and LHCb experiments [1247–1249]. This results in the contribution from the first pole being determined with 3% accuracy. The contribution from the $D^{*'}(2600)$ pole is determined with poorer accuracy, $\sim 30\%$, mainly due to lattice uncertainties. A *superconvergence* condition [1250]

$$\sum_{n=0}^{\infty} \text{Res}_{q^2=m_{D_n^*}^2} f_+(q^2) = 0 \quad (268)$$

is applied, protecting the form factor behavior at large q^2 . Within this model, the first two poles are not sufficient to describe the data, and a third effective pole needs to be included.

One of the advantages of this phenomenological model is that it can be extrapolated outside the charm physical region, providing a method to extract the magnitude of the CKM matrix element V_{ub} using the ratio of the form factors of the $D \rightarrow \pi \ell \nu$ and $B \rightarrow \pi \ell \nu$ decay channels. It will be used once lattice calculations provide the form factor ratio $f_{B\pi}^+(q^2)/f_{D\pi}^+(q^2)$ at the same pion energy.

This form factor description can be extended to the $D \rightarrow K \ell \nu$ decay channel, considering the contribution of several $c\bar{s}$ resonances with $J^P = 1^-$. The first two pole masses contributing to the form factor correspond to the $D_s^*(2112)$ and $D_{s1}^*(2700)$ resonant states [21]. A constraint on the first residue can be obtained using information of the f_K decay constant [21] and the g coupling extracted from the D^{*+} width [1247]. The contribution from the second pole can be evaluated using the decay constants from [1251], the measured total width, and the ratio of D^*K and DK decay branching fractions [21].

9.5.7 Experimental techniques and results

Various techniques have been used by several experiments to measure D semileptonic decays with a pseudoscalar particle in the final state. The most recent results are provided by the *BABAR* [1252] and *BES III* [1253, 1254] collaborations. *Belle* [1255], *BABAR* [1256], and *CLEO-c* [1257, 1258] have all previously reported results. *Belle* fully reconstructs $e^+e^- \rightarrow D\bar{D}X$ events from the continuum under the $\Upsilon(4S)$ resonance, achieving very good q^2 resolution (15 MeV 2) and a low background level but with a low efficiency. Using 282 fb $^{-1}$ of data, about 1300 $D \rightarrow K\ell^+\nu$ (Cabibbo-favored) and 115 $D \rightarrow \pi\ell^+\nu$ (Cabibbo-suppressed) decays are reconstructed, considering the electron and muon channels together. The *BABAR* experiment uses a partial reconstruction technique in which the semileptonic decays are tagged via $D^{*+} \rightarrow D^0\pi^+$ decays. The D direction and neutrino energy are obtained using information from the rest of the event. With 75 fb $^{-1}$ of data, 74000 signal events in the $D^0 \rightarrow K^-e^+\nu$ mode are obtained. This technique provides a large signal yield but also a high background level and a poor q^2 resolution (ranging from 66 to 219 MeV 2). In this case, the measurement of the branching fraction is obtained by normalizing to the $D^0 \rightarrow K^-\pi^+$ decay channel; thus the measurement would benefit from future improvements in the determination of the branching fraction for this reference channel. The Cabibbo-suppressed mode has been recently measured using the same technique and 350 fb $^{-1}$ data. For this measurement, 5000 $D^0 \rightarrow \pi^-e^+\nu$ signal events were reconstructed [1252].

The *CLEO-c* experiment uses two different methods to measure charm semileptonic decays. The *tagged* analyses [1257] rely on the full reconstruction of $\Psi(3770) \rightarrow D\bar{D}$ events. One of the D mesons is reconstructed in a hadronic decay mode, and the other in the semileptonic channel. The only missing particle is the neutrino, and thus the q^2 resolution is very good and the background level very low. With the entire *CLEO-c* data sample of 818 pb $^{-1}$, 14123 and 1374 signal events are reconstructed for the $D^0 \rightarrow K^-e^+\nu$ and $D^0 \rightarrow \pi^-e^+\nu$ channels, respectively, and 8467 and 838 are reconstructed for the $D^+ \rightarrow \bar{K}^0e^+\nu$ and $D^+ \rightarrow \pi^0e^+\nu$ decays, respectively. An alternative method that does not tag the D decay in a hadronic mode (referred to as *untagged* analyses) has also been used by *CLEO-c* [1258]. In this method, the entire missing energy and momentum in an event are associated with the neutrino four momentum, with the penalty of larger backgrounds as compared to the tagged method.

Using the tagged method, the *BES III* experiment measures the $D^0 \rightarrow K^-e^+\nu$ and $D^0 \rightarrow \pi^-e^+\nu$ decay channels. With 2.9 fb $^{-1}$ of data, they fully reconstruct 70700 and 6300 signal events, respectively, for the two channels [1253]. In a separate analysis, *BES III* measures the semileptonic decay $D^+ \rightarrow K_L^0e^+\nu$ [1254], with about 20100 semileptonic candidates. Since 2016, *BES III* has reported additional measurements of $D \rightarrow \bar{K}\ell^+\nu_\ell$ and $\pi\ell^+\nu_\ell$. The signal yields are 26008, 5013, 47100, 20714, 3402, 2265, and 1335 events for $D^+ \rightarrow \bar{K}^0(\pi^+\pi^-)e^+\nu_e$, $D^+ \rightarrow \bar{K}^0(\pi^0\pi^0)e^+\nu_e$, $D^0 \rightarrow K^-\mu^+\nu_\mu$, $D^+ \rightarrow \bar{K}^0(\pi\pi)\mu^+\nu_\mu$, $D^+ \rightarrow \pi^0e^+\nu_e$, $D^0 \rightarrow \pi^-\mu^+\nu_\mu$, and $D^+ \rightarrow \pi^0\mu^+\nu_\mu$ [1259–1263], respectively. The corresponding branching fractions are determined with good precision. In Refs. [1259, 1260], the products of the $c \rightarrow s(d)$ CKM matrix element and the semileptonic form factor are measured to be $|V_{cs}f_+^{D \rightarrow K}(0)| = 0.7053 \pm 0.0040 \pm 0.0112$, $|V_{cs}f_+^{D \rightarrow K}(0)| = 0.7133 \pm 0.0038 \pm 0.0030$, and $|V_{cd}f_+^{D \rightarrow \pi}(0)| = 0.1400 \pm 0.0026 \pm 0.0007$, respectively, based on a two-parameter series expansion.

Results of the hadronic form factor parameters, m_{pole} and α_{BK} , obtained from the measurements discussed above, are given in Tables 294 and 295. The z -expansion formalism has been used by *BABAR* [1252, 1256], *BES III* [1264] and *CLEO-c* [1257], [1258]. Their fits use the first

Table 294: Results for m_{pole} and α_{BK} from various experiments for $D^0 \rightarrow K^-\ell^+\nu$ and $D^+ \rightarrow \bar{K}^0\ell^+\nu$ decays. The last lines of the table has a comparison with recent results on other $c \rightarrow se^+\nu_e$ decays at BES III.

$D \rightarrow K\ell\nu_\ell$ Expt.	Mode	Ref.	m_{pole} (GeV/c 2)	α_{BK}
CLEO III	($D^0; \ell = e, \mu$)	[1265]	$1.89 \pm 0.05^{+0.04}_{-0.03}$	$0.36 \pm 0.10^{+0.03}_{-0.07}$
FOCUS	($D^0; \ell = \mu$)	[1266]	$1.93 \pm 0.05 \pm 0.03$	$0.28 \pm 0.08 \pm 0.07$
Belle	($D^0; \ell = e, \mu$)	[1255]	$1.82 \pm 0.04 \pm 0.03$	$0.52 \pm 0.08 \pm 0.06$
<i>BABAR</i>	($D^0; \ell = e$)	[1256]	$1.889 \pm 0.012 \pm 0.015$	$0.366 \pm 0.023 \pm 0.029$
CLEO-c (tagged)	($D^0, D^+; \ell = e$)	[1257]	$1.93 \pm 0.02 \pm 0.01$	$0.30 \pm 0.03 \pm 0.01$
CLEO-c (untagged)	($D^0; \ell = e$)	[1258]	$1.97 \pm 0.03 \pm 0.01$	$0.21 \pm 0.05 \pm 0.03$
CLEO-c (untagged)	($D^+; \ell = e$)	[1258]	$1.96 \pm 0.04 \pm 0.02$	$0.22 \pm 0.08 \pm 0.03$
BES III	($D^0; \ell = e$)	[1253]	$1.921 \pm 0.010 \pm 0.007$	$0.309 \pm 0.020 \pm 0.013$
BES III	($D^+; \ell = e$)	[1254]	$1.953 \pm 0.044 \pm 0.036$	$0.239 \pm 0.077 \pm 0.065$
BES III	$D^+ \rightarrow \bar{K}^0_{\pi^+\pi^-} e^+\nu_e$	[1259]	$1.935 \pm 0.017 \pm 0.006$	$0.294 \pm 0.031 \pm 0.010$
BES III	$D_s^+ \rightarrow \eta e^+\nu_e$	[1267]	$3.759 \pm 0.084 \pm 0.045$	$0.304 \pm 0.044 \pm 0.022$
BES III	$D_s^+ \rightarrow \eta' e^+\nu_e$	[1267]	$1.88 \pm 0.60 \pm 0.08$	$1.62 \pm 0.90 \pm 0.13$

three terms of the expansion, and the results for the ratios $r_1 \equiv a_1/a_0$ and $r_2 \equiv a_2/a_0$ are listed in Tables 296 and 297.

9.5.8 Combined results for the $D \rightarrow K\ell\nu_\ell$ and $D \rightarrow \pi\ell\nu_\ell$ channels

Results and world averages for the products $f_+^K(0)|V_{cs}|$ and $f_+^\pi(0)|V_{cd}|$ as measured by CLEO-c, Belle, BaBar, and BES III are summarized in Tables 298 and 299, respectively, and plotted in Figs. 92 and 93. When calculating these world averages, the systematic uncertainties of the BES III analyses are conservatively taken to be fully corrected.

9.5.9 Form factors of other $D_{(s)} \rightarrow P\ell\nu_\ell$ decays

In the past two decades, rapid progress in lattice QCD calculations of $f_+^{D \rightarrow K(\pi)}(0)$ has been achieved, motivated by much improved experimental measurements of $D \rightarrow \bar{K}\ell\nu_\ell$ and $D \rightarrow \pi\ell\nu_\ell$. However, in contrast, progress in theoretical calculations of form factors in other $D_{(s)} \rightarrow P\ell^+\nu_\ell$ decays has been slow, and experimental measurements sparse. Before BES III, only CLEO reported a measurement, that of $f_+^{D \rightarrow \eta}(0)$ [1268]. For this analysis both tagged and untagged methods were used. Recently, BES III reported measurements of $f_+^{D \rightarrow \eta}(0)$, $f_+^{D_s \rightarrow \eta}(0)$, $f_+^{D_s \rightarrow \eta'}(0)$ and $f_+^{D_s \rightarrow K}(0)$ using a tagged method [1267, 1269, 1270]. These measurements greatly expand experimental knowledge of hadronic form factors in $D \rightarrow P\ell^+\nu_\ell$ decays. To date, there is still no measurement of $f_+^{D \rightarrow \eta'}(0)$ due to the small amount of data available.

On the theory side, lattice QCD calculations of $f_+^{D_s \rightarrow \eta^{(\prime)}}(0)$ for $D_s^+ \rightarrow \eta^{(\prime)} e^+\nu_e$ were presented in Ref. [1271], but with no systematic uncertainties included. Other calculations of $f_+^{D_{(s)} \rightarrow \eta^{(\prime)}}(0)$ and $f_+^{D_s \rightarrow K}(0)$ have been reported based on QCD light-cone sum rules (LCSR) [1272–1274], three-point QCD sum rules (3PSR) [1275], a light-front quark model (LFQM) [1276, 1277], a constituent quark model (CQM) [1278], and a covariant confined quark model (CCQM) [1279].

Table 295: Results for m_{pole} and α_{BK} from various experiments for $D^0 \rightarrow \pi^- \ell^+ \nu$ and $D^+ \rightarrow \pi^0 \ell^+ \nu$ decays. The last lines of the table has a comparison with recent results from other $c \rightarrow d e^+ \nu_e$ decays at CLEO and BES III.

$D \rightarrow \pi \ell \nu_\ell$ Expt.	Mode	Ref.	m_{pole} (GeV/c ²)	α_{BK}
CLEO III	($D^0; \ell = e, \mu$)	[1265]	$1.86^{+0.10+0.07}_{-0.06-0.03}$	$0.37^{+0.20}_{-0.31} \pm 0.15$
FOCUS	($D^0; \ell = \mu$)	[1266]	$1.91^{+0.30}_{-0.15} \pm 0.07$	—
Belle	($D^0; \ell = e, \mu$)	[1255]	$1.97 \pm 0.08 \pm 0.04$	$0.10 \pm 0.21 \pm 0.10$
CLEO-c (tagged)	($D^0, D^+; \ell = e$)	[1257]	$1.91 \pm 0.02 \pm 0.01$	$0.21 \pm 0.07 \pm 0.02$
CLEO-c (untagged)	($D^0; \ell = e$)	[1258]	$1.87 \pm 0.03 \pm 0.01$	$0.37 \pm 0.08 \pm 0.03$
CLEO-c (untagged)	($D^+; \ell = e$)	[1258]	$1.97 \pm 0.07 \pm 0.02$	$0.14 \pm 0.16 \pm 0.04$
BES III	($D^0; \ell = e$)	[1253]	$1.911 \pm 0.012 \pm 0.004$	$0.279 \pm 0.035 \pm 0.011$
BABAR	($D^0; \ell = e$)	[1252]	$1.906 \pm 0.029 \pm 0.023$	$0.268 \pm 0.074 \pm 0.059$
BES III	$D^+ \rightarrow \pi^0 e^+ \nu_e$	[1259]	$1.898 \pm 0.020 \pm 0.003$	$0.285 \pm 0.057 \pm 0.010$
CLEO-c	$D^+ \rightarrow \eta e^+ \nu_e$	[1268]	$1.87 \pm 0.24 \pm 0.00$	$0.21 \pm 0.44 \pm 0.05$
BES III	$D^+ \rightarrow \eta e^+ \nu_e$	[1269]	$1.73 \pm 0.17 \pm 0.03$	$0.50 \pm 0.54 \pm 0.08$

Table 296: Results for r_1 and r_2 from various experiments for the $D \rightarrow K \ell \nu_\ell$ decay channel. The correlation coefficient between these parameters is larger than 0.9. And comparison with recent results on some $c \rightarrow s e^+ \nu_e$ decays at BES III, where only the first two terms of the expansion were used.

Expt. $D \rightarrow K \ell \nu_\ell$	Mode	Ref.	r_1	r_2
BABAR	($D^0; \ell = e$)	[1256]	$-2.5 \pm 0.2 \pm 0.2$	$0.6 \pm 6.0 \pm 5.0$
CLEO-c (tagged)	($D^0; \ell = e$)	[1257]	$-2.65 \pm 0.34 \pm 0.08$	$13 \pm 9 \pm 1$
CLEO-c (tagged)	($D^+; \ell = e$)	[1257]	$-1.66 \pm 0.44 \pm 0.10$	$-14 \pm 11 \pm 1$
CLEO-c (untagged)	($D^0; \ell = e$)	[1258]	$-2.4 \pm 0.4 \pm 0.1$	$21 \pm 11 \pm 2$
CLEO-c (untagged)	($D^+; \ell = e$)	[1258]	$-2.8 \pm 6 \pm 2$	$32 \pm 18 \pm 4$
BES III	($D^0; \ell = e$)	[1253]	$-2.334 \pm 0.159 \pm 0.080$	$3.42 \pm 3.91 \pm 2.41$
BES III	($D^+; \ell = e$)	[1254]	$-2.23 \pm 0.42 \pm 0.53$	$11.3 \pm 8.5 \pm 8.7$
BES III	$D^0 \rightarrow K^- \mu^+ \nu_\mu$	[1260]	$-1.90 \pm 0.21 \pm 0.07$	—
BES III	$D^+ \rightarrow \bar{K}_{\pi^+\pi^-}^0 e^+ \nu_e$	[1259]	$-1.76 \pm 0.25 \pm 0.06$	—
BES III	$D_s^+ \rightarrow \eta e^+ \nu_e$	[1267]	$-7.3 \pm 1.7 \pm 0.4$	—
BES III	$D_s^+ \rightarrow \eta' e^+ \nu_e$	[1267]	$-13.1 \pm 7.6 \pm 1.0$	—

Table 297: Results for r_1 and r_2 from various experiments, for $D \rightarrow \pi \ell \nu_\ell$. The correlation coefficient between these parameters is larger than 0.9. The last lines in the table has a comparison with recent results on $c \rightarrow d e^+ \nu_e$ decays at CLEO and BES III where only the first two terms of the expansion were used.

Expt. $D \rightarrow \pi \ell \nu_\ell$	Mode	Ref.	r_1	r_2
CLEO-c (tagged)	$(D^0; \ell = e)$	[1257]	$-2.80 \pm 0.49 \pm 0.04$	$6 \pm 3 \pm 0$
CLEO-c (tagged)	$(D^+; \ell = e)$	[1257]	$-1.37 \pm 0.88 \pm 0.24$	$-4 \pm 5 \pm 1$
CLEO-c (un-tagged)	$(D^0; \ell = e)$	[1258]	$-2.1 \pm 0.7 \pm 0.3$	$-1.2 \pm 4.8 \pm 1.7$
CLEO-c (un-tagged)	$(D^+; \ell = e)$	[1258]	$-0.2 \pm 1.5 \pm 0.4$	$-9.8 \pm 9.1 \pm 2.1$
BES III	$(D^0; \ell = e)$	[1253]	$-1.85 \pm 0.22 \pm 0.07$	$-1.4 \pm 1.5 \pm 0.5$
<i>BABAR</i>	$(D^0; \ell = e)$	[1252]	$-1.31 \pm 0.70 \pm 0.43$	$-4.2 \pm 4.0 \pm 1.9$
BES III	$D^+ \rightarrow \pi^0 e^+ \nu_e$	[1259]	$-2.23 \pm 0.42 \pm 0.06$	—
CLEO-c	$D^+ \rightarrow \eta e^+ \nu_e$	[1268]	$1.83 \pm 2.23 \pm 0.28$	—
BES III	$D^+ \rightarrow \eta e^+ \nu_e$	[1269]	$1.88 \pm 0.60 \pm 0.08$	—

Table 298: Results for $f_+^K(0)|V_{cs}|$ from various experiments.

$D \rightarrow K \ell \nu_\ell$ Measurement	Mode	$ V_{cs} f_+^K(0)$	Comment
BES III 2019 [1260]	$(D^0; \ell = \mu)$	0.7133(38)(30)	z expansion, 2 terms
BES III 2017 [1259]	$(D^+; \ell = e)$	0.6983(56)(112)	z expansion, 3 terms
BES III 2015B [1254]	$(D^+; \ell = e)$	0.7370(60)(90)	z expansion, 3 terms
BES III 2015A [1253]	$(D^0; \ell = e)$	0.7195(35)(41)	z expansion, 3 terms
CLEOc 2009 [1257]	$(D^0, D^+; \ell = e)$	0.7189(64)(48)	z expansion, 3 terms
<i>BABAR</i> 2007 [1256]	$(D^0; \ell = e)$	0.7211(69)(85)	Fitted pole mass + modified pole ansatze; $ V_{cs} = 0.9729 \pm 0.0003$; corrected for $\mathcal{B}(D^0 \rightarrow K^- \pi^+)$
Belle 2006 [1255]	$(D^0; \ell = e, \mu)$	0.6762(68)(214)	$ V_{cs} = 0.97296 \pm 0.00024$ (PDG 2006 w/unitarity)
World average		0.7180(33)	BES III syst. fully correlated

Table 299: Results for $f_+^\pi(0)|V_{cd}|$ from various experiments.

$D \rightarrow \pi \ell \nu_\ell$ Measurement	Mode	$ V_{cd} f_+^\pi(0)$	Comment
BES III 2017 [1259]	$(D^+; \ell = e)$	0.1413(35)(12)	z expansion, 3 terms
BES III 2015A [1253]	$(D^0; \ell = e)$	0.1420(24)(10)	z expansion, 3 terms
CLEOc 2009 [1257]	$(D^0, D^+; \ell = e)$	0.1500(40)(10)	z expansion, 3 terms
<i>BABAR</i> 2015 [1252]	$(D^0; \ell = e)$	0.1374(38)(24)	z expansion, 3 terms
Belle 2006 [1255]	$(D^0; \ell = e, \mu)$	0.1417(45)(68)	$ V_{cd} = 0.2271 \pm 0.0010$ (PDG 2006 w/unitarity)
World average		0.1426(18)	BES III syst. fully correlated

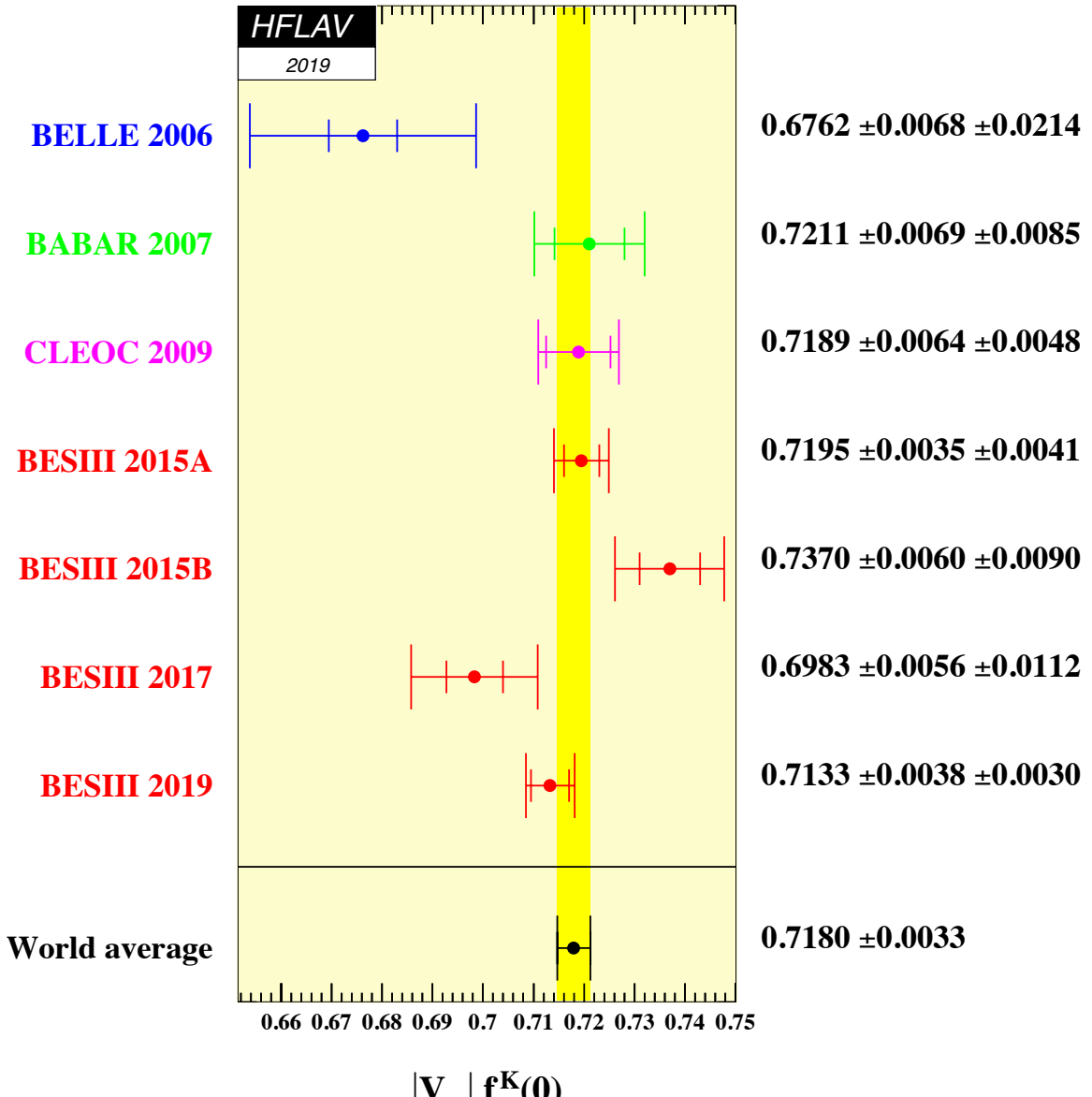


Figure 92: Comparison of the results of $f_+^K(0)|V_{cs}|$ measured by the Belle [1255], BaBar [1256], CLEO-c [1257], and BES III [1253, 1254, 1259, 1260] experiments.

Table 300 summarizes both experimental measurements and theoretical calculations of these form factors. The $f_+^{D_s \rightarrow K}(0)$ value measured by BES III is consistent with current theoretical calculations. The $f_+^{D_s \rightarrow \eta}(0)$ and $f_+^{D_s \rightarrow \eta'}(0)$ values measured by BES III tend to support the LCSR calculation of Ref. [1273]; however, the $f_+^{D \rightarrow \eta}(0)$ values measured at CLEO and BES III disfavor this calculation. More robust theoretical calculations of these form factors for both D^+ and D_s^+ semileptonic decays are still desired.

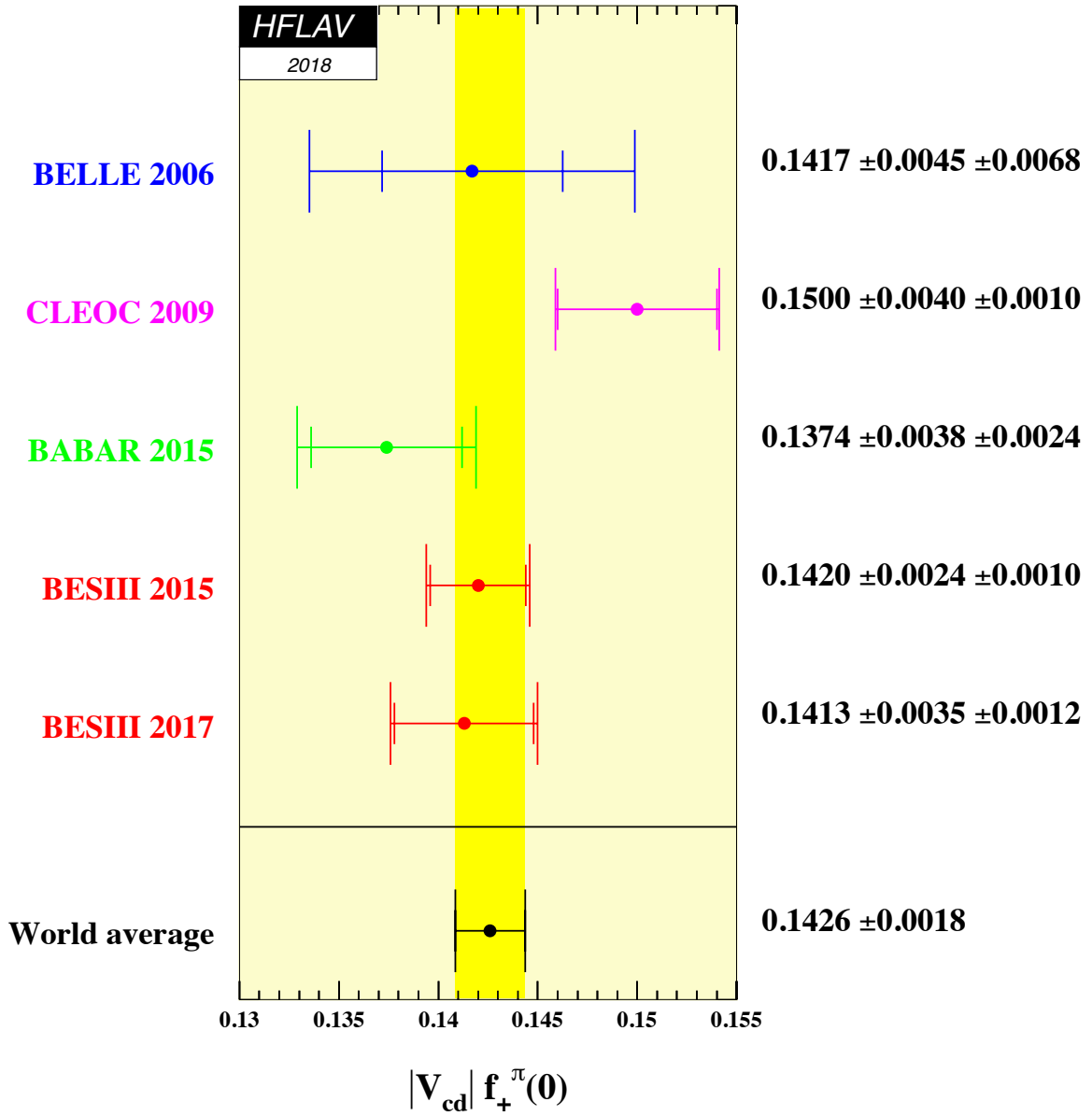


Figure 93: Comparison of the results of $f_+^\pi(0)|V_{cd}|$ measured by the Belle [1255], BaBar [1252], CLEO-c [1257], and BES III [1253, 1259] experiments.

9.5.10 Determinations of $|V_{cs}|$ and $|V_{cd}|$

Assuming unitarity of the CKM matrix, the values of the CKM matrix elements entering in charm semileptonic decays are evaluated from the V_{ud} , V_{td} and V_{cb} elements as [21]

$$\begin{aligned} |V_{cs}| &= 0.97359^{+0.00010}_{-0.00011}, \\ |V_{cd}| &= 0.22438 \pm 0.00044. \end{aligned} \quad (269)$$

Table 300: Comparison of the hadronic form factors for other $D_{(s)} \rightarrow P$ transitions from theoretical calculations and experiments. The BES III result of $f_+^{D \rightarrow \eta}(0)$ is obtained by dividing the product of $f_+^{D \rightarrow \eta}(0)|V_{cd}|$ by the world average of $|V_{cd}|$. The numbers in the first and second brackets are statistical and systematic uncertainties, respectively.

	$f_+^{D_s \rightarrow \eta}(0)$	$f_+^{D_s \rightarrow \eta'}(0)$	$f_+^{D \rightarrow \eta}(0)$	$f_+^{D \rightarrow \eta'}(0)$	$f_+^{D_s \rightarrow K}(0)$
CLEO	—	—	—	—	—
BES III	$0.458(05)(04)$ [1267]	$0.49(05)(01)$ [1267]	$0.38(03)(01)$ [1268] $0.35(03)(01)$ [1269]	—	$0.72(08)(01)$ [1270]
LQCD $m_\pi = 470$ MeV [1271]	0.564 ± 0.011	0.437 ± 0.018	—	—	—
LQCD $m_\pi = 370$ MeV [1271]	0.542 ± 0.013	0.404 ± 0.025	—	—	—
LCSR [1272]	$0.495^{+0.030}_{-0.029}$	$0.558^{+0.047}_{-0.045}$	$0.429^{+0.165}_{-0.141}$	$0.292^{+0.113}_{-0.104}$	—
LCSR [1273]	0.432 ± 0.033	0.520 ± 0.080	0.552 ± 0.051	0.458 ± 0.105	—
LCSR [1274]	0.45 ± 0.14	0.55 ± 0.18	—	—	—
3PSR [1275]	0.50 ± 0.04	—	—	—	—
LFQM [1276]	0.76	—	0.71	—	0.66
LFQM(I) [1277]	0.50	0.62	—	—	—
LFQM(II) [1277]	0.48	0.60	—	—	—
CQM [1278]	0.78	0.78	—	—	0.72
CCQM [1279]	0.78 ± 0.12	0.73 ± 11	0.67 ± 0.11	0.76 ± 0.11	0.60 ± 0.09

Using the world average values of $f_+^K(0)|V_{cs}|$ and $f_+^\pi(0)|V_{cd}|$ from Tables 298 and 299 leads to the form factor values

$$f_+^K(0) = 0.7361 \pm 0.0034,$$

$$f_+^\pi(0) = 0.6351 \pm 0.0081,$$

which are in agreement with present averages of lattice QCD calculations. Table 301 summarizes $f_+^{D \rightarrow \pi}(0)$ and $f_+^{D \rightarrow K}(0)$ results based on $N_f = 2 + 1 + 1$ flavor lattice QCD of the ETM collaboration [1280], and earlier results based on $N_f = 2 + 1$ flavor lattice QCD of the HPQCD collaboration [1281, 1282]. Recently, the Fermilab Lattice and MILC Collaborations released their preliminary results of $f_+^{D \rightarrow K}(0)$ and $f_+^{D \rightarrow \pi}(0)$ based on $N_f = 2 + 1 + 1$ flavor lattice QCD calculations [1283]. The weighted averages are $f_+^{D \rightarrow \pi}(0) = 0.634 \pm 0.015$ and $f_+^{D \rightarrow K}(0) = 0.760 \pm 0.011$, respectively. The experimental accuracy is at present better than that from lattice calculations.

Table 301: Summary of the latest LQCD calculations of $f_+^{D \rightarrow \pi}(0)$ and $f_+^{D \rightarrow K}(0)$ from the Fermilab/MILC, ETM, and HPQCD collaborations.

Collaboration	$f_+^{D \rightarrow \pi}(0)$	$f_+^{D \rightarrow K}(0)$
Fermilab Lattice and MILC [1283]	$0.625 \pm 0.017 \pm 0.013$	$0.768 \pm 0.012 \pm 0.011$
ETM(2+1+1) [1280]	0.612 ± 0.035	0.765 ± 0.031
HPQCD(2+1) [1281, 1282]	0.666 ± 0.029	0.747 ± 0.019
Average	0.634 ± 0.015	0.760 ± 0.011

Alternatively, if one assumes the lattice QCD form factor values, the averages in Tables 298 and 299 give

$$|V_{cs}| = 0.943 \pm 0.004(\text{exp.}) \pm 0.014(\text{LQCD}),$$

$$|V_{cd}| = 0.2249 \pm 0.0028(\text{exp.}) \pm 0.0055(\text{LQCD}),$$

which are compatible with unitarity of the CKM matrix. Here, the uncertainties are dominated by the LQCD calculations.

9.5.11 Test of e - μ lepton flavor universality

In the Standard Model (SM), the couplings between the three families of leptons and gauge bosons are expected to be equal; this is known as lepton flavor universality (LFU). The semileptonic decays of pseudoscalar mesons are well understood in the SM and thus offer a robust way to test LFU and search for new physics. Various tests of LFU with B semileptonic decays have been reported by BaBar, Belle, and LHCb. The average of the ratio of the branching fractions $\mathcal{B}_{B \rightarrow \bar{D}^{(*)}\tau^+\nu_\tau}/\mathcal{B}_{B \rightarrow \bar{D}^{(*)}\ell^+\nu_\ell}$ ($\ell = \mu, e$) deviates from the SM prediction by 3.1σ (see section 6.5). Precision measurements of D semileptonic decays also tests LFU, and in a manner complimentary to that of B decays [1284]. Within the SM, the ratios $\mathcal{B}_{D \rightarrow \bar{K}\mu^+\nu_\mu}/\mathcal{B}_{D \rightarrow \bar{K}e^+\nu_e}$ and $\mathcal{B}_{D \rightarrow \pi\mu^+\nu_\mu}/\mathcal{B}_{D \rightarrow \pi e^+\nu_e}$ are predicted to be 0.975 ± 0.001 and 0.985 ± 0.002 , respectively [1285]. Above $q^2 = 0.1 \text{ GeV}^2/c^4$, where q is the four momentum of the $\ell^+\nu_\ell$ system, the branching fraction ratios are expected to be close to unity with negligible uncertainty. This is due to the high correlation of the corresponding hadronic form factors [1285].

In 2016, BES III presented improved measurements of the branching fractions of $D^+ \rightarrow \bar{K}^0\mu^+\nu_\mu$ [1261], $D^0 \rightarrow \pi^-\mu^+\nu_\mu$ [1263], and $D^0 \rightarrow K^-\mu^+\nu_\mu$ [1260], and the first measurement of $D^+ \rightarrow \pi^0\mu^+\nu_\mu$ [1263]. All these analyses used the tagged method and 2.9 fb^{-1} of data taken at 3.773 GeV . Combining these results with previous BES III measurements of $\mathcal{B}(D^0 \rightarrow \pi^-e^+\nu_e)$, $\mathcal{B}(D^+ \rightarrow \pi^0e^+\nu_e)$, and $\mathcal{B}(D^0 \rightarrow K^-e^+\nu_e)$ using the same data sample, the ratios of branching fractions are

$$\frac{\mathcal{B}(D^0 \rightarrow \pi^-\mu^+\nu_\mu)}{\mathcal{B}(D^0 \rightarrow \pi^-e^+\nu_e)} = 0.922 \pm 0.030 \pm 0.022, \quad (270)$$

$$\frac{\mathcal{B}(D^+ \rightarrow \pi^0\mu^+\nu_\mu)}{\mathcal{B}(D^+ \rightarrow \pi^0e^+\nu_e)} = 0.964 \pm 0.037 \pm 0.026, \quad (271)$$

$$\frac{\mathcal{B}(D^0 \rightarrow K^-\mu^+\nu_\mu)}{\mathcal{B}(D^0 \rightarrow K^-e^+\nu_e)} = 0.974 \pm 0.007 \pm 0.012. \quad (272)$$

In addition, using the world average for $\mathcal{B}(D^+ \rightarrow \bar{K}^0e^+\nu_e)$ [21] gives

$$\frac{\mathcal{B}(D^+ \rightarrow \bar{K}^0\mu^+\nu_\mu)}{\mathcal{B}(D^+ \rightarrow \bar{K}^0e^+\nu_e)} = 1.00 \pm 0.03. \quad (273)$$

These results indicate that any e - μ LFU violation in D semileptonic decays has to be at the level of a few percent or less. BES III also tested e - μ LFU in separate q^2 intervals using $D^{0(+)} \rightarrow \pi^{-(0)}\ell^+\nu_\ell$ [1263] and $D^0 \rightarrow K^-\ell^+\nu_\ell$ [1260] decays. No indication of LFU above the 2σ level was found.

In 2018, using 0.482 fb^{-1} of data taken at a center-of-mass energy of 4.009 GeV , BES III reported measurements of the branching fractions for semileptonic decays $D_s^+ \rightarrow \phi\mu^+\nu_\mu$, $D_s^+ \rightarrow \eta\mu^+\nu_\mu$, and $D_s^+ \rightarrow \eta'\mu^+\nu_\mu$ [1286]. Combining these results with previous measurements of

$D_s^+ \rightarrow \phi e^+ \nu_e$ [1286], $D_s^+ \rightarrow \eta e^+ \nu_e$, and $D_s^+ \rightarrow \eta' e^+ \nu_e$ [1287] gives the ratios

$$\frac{\mathcal{B}(D_s^+ \rightarrow \phi \mu^+ \nu_\mu)}{\mathcal{B}(D_s^+ \rightarrow \phi e^+ \nu_e)} = 0.86 \pm 0.29, \quad (274)$$

$$\frac{\mathcal{B}(D_s^+ \rightarrow \eta \mu^+ \nu_\mu)}{\mathcal{B}(D_s^+ \rightarrow \eta e^+ \nu_e)} = 1.05 \pm 0.24, \quad (275)$$

$$\frac{\mathcal{B}(D_s^+ \rightarrow \eta' \mu^+ \nu_\mu)}{\mathcal{B}(D_s^+ \rightarrow \eta' e^+ \nu_e)} = 1.14 \pm 0.68. \quad (276)$$

These values are all consistent with unity. The uncertainties include both statistical and systematic uncertainties, the former of which dominates.

9.5.12 $D \rightarrow V \ell \nu_\ell$ decays

When the final state hadron is a vector meson, the decay can proceed through both vector and axial vector currents, and four form factors are needed. The hadronic current is $H_\mu = V_\mu + A_\mu$, where [1239]

$$V_\mu = \langle V(p, \varepsilon) | \bar{q} \gamma_\mu c | D(p') \rangle = \frac{2V(q^2)}{m_D + m_V} \varepsilon_{\mu\nu\rho\sigma} \varepsilon^{*\nu} p'^\rho p^\sigma \quad (277)$$

$$\begin{aligned} A_\mu = \langle V(p, \varepsilon) | -\bar{q} \gamma_\mu \gamma_5 c | D(p') \rangle &= -i(m_D + m_V) A_1(q^2) \varepsilon_\mu^* \\ &\quad + i \frac{A_2(q^2)}{m_D + m_V} (\varepsilon^* \cdot q)(p' + p)_\mu \\ &\quad + i \frac{2m_V}{q^2} (A_3(q^2) - A_0(q^2)) [\varepsilon^* \cdot (p' + p)] q_\mu. \end{aligned} \quad (278)$$

In this expression, m_V is the daughter meson mass and

$$A_3(q^2) = \frac{m_D + m_V}{2m_V} A_1(q^2) - \frac{m_D - m_V}{2m_V} A_2(q^2). \quad (279)$$

Kinematics require that $A_3(0) = A_0(0)$. Terms proportional to q_μ are only important for the case of τ leptons. Thus, only the three form factors $A_1(q^2)$, $A_2(q^2)$ and $V(q^2)$ are relevant in the decays involving muons and electrons.

The differential decay rate is

$$\begin{aligned} \frac{d\Gamma(D \rightarrow V \bar{\ell} \nu_\ell)}{dq^2 d\cos\theta_\ell} &= \frac{G_F^2 |V_{cq}|^2}{128\pi^3 m_D^2} p^* q^2 \times \\ &\quad \left[\frac{(1 - \cos\theta_\ell)^2}{2} |H_-|^2 + \frac{(1 + \cos\theta_\ell)^2}{2} |H_+|^2 + \sin^2\theta_\ell |H_0|^2 \right], \end{aligned} \quad (280)$$

where H_\pm and H_0 are helicity amplitudes, corresponding to helicities of the vector (V) meson

or virtual W . The helicity amplitudes can be expressed in terms of the form factors as

$$H_{\pm} = \frac{1}{m_D + m_V} [(m_D + m_V)^2 A_1(q^2) \mp 2m_D p^* V(q^2)] \quad (281)$$

$$\begin{aligned} H_0 &= \frac{1}{|q|} \frac{m_D^2}{2m_V(m_D + m_V)} \times \\ &\quad \left[\left(1 - \frac{m_V^2 - q^2}{m_D^2} \right) (m_D + m_V)^2 A_1(q^2) - 4p^{*2} A_2(q^2) \right]. \end{aligned} \quad (282)$$

Here p^* is the magnitude of the three-momentum of the V system as measured in the D rest frame, and θ_ℓ is the angle of the lepton momentum with respect to the direction opposite that of the D in the W rest frame (see Fig. 94 for the electron case, θ_e). The left-handed nature of the quark current manifests itself as $|H_-| > |H_+|$. The differential decay rate for $D \rightarrow V\ell\nu$ followed by the vector meson decaying into two pseudoscalars is

$$\begin{aligned} \frac{d\Gamma(D \rightarrow V\bar{\ell}\nu, V \rightarrow P_1 P_2)}{dq^2 d\cos\theta_V d\cos\theta_\ell d\chi} &= \frac{3G_F^2}{2048\pi^4} |V_{cq}|^2 \frac{p^*(q^2)q^2}{m_D^2} \mathcal{B}(V \rightarrow P_1 P_2) \times \\ &\quad \left\{ (1 + \cos\theta_\ell)^2 \sin^2\theta_V |H_+(q^2)|^2 \right. \\ &\quad + (1 - \cos\theta_\ell)^2 \sin^2\theta_V |H_-(q^2)|^2 \\ &\quad + 4\sin^2\theta_\ell \cos^2\theta_V |H_0(q^2)|^2 \\ &\quad - 4\sin\theta_\ell(1 + \cos\theta_\ell) \sin\theta_V \cos\theta_V \cos\chi H_+(q^2) H_0(q^2) \\ &\quad + 4\sin\theta_\ell(1 - \cos\theta_\ell) \sin\theta_V \cos\theta_V \cos\chi H_-(q^2) H_0(q^2) \\ &\quad \left. - 2\sin^2\theta_\ell \sin^2\theta_V \cos 2\chi H_+(q^2) H_-(q^2) \right\}, \end{aligned} \quad (283)$$

where the helicity angles θ_ℓ , θ_V , and acoplanarity angle χ are defined as shown in Fig. 94. Typically, the ratios of the form factors at $q^2 = 0$ are defined as

$$r_V \equiv \frac{V(0)}{A_1(0)}, \quad (284)$$

$$r_2 \equiv \frac{A_2(0)}{A_1(0)}. \quad (285)$$

9.5.13 Vector form factor measurements

In 2002 FOCUS reported an asymmetry in the observed $\cos(\theta_V)$ distribution in $D^+ \rightarrow K^-\pi^+\mu^+\nu$ decays [1288]. This was interpreted as evidence for an S -wave $K^-\pi^+$ component in the decay amplitude. Since H_0 typically dominates over H_{\pm} , the distribution given by Eq. (283) is, after integration over χ , roughly proportional to $\cos^2\theta_V$. Inclusion of a constant S -wave amplitude of the form $A e^{i\delta}$ leads to an interference term proportional to $|AH_0 \sin\theta_\ell \cos\theta_V|$ which then causes an asymmetry in $\cos(\theta_V)$. When FOCUS fit their data including this S -wave amplitude, they obtained $A = 0.330 \pm 0.022 \pm 0.015 \text{ GeV}^{-1}$ and $\delta = 0.68 \pm 0.07 \pm 0.05$ [1289]. Both *BABAR* [1290] and *CLEO-c* [1291] have also found evidence for an $f_0 \rightarrow K^+K^-$ component in semileptonic D_s decays.

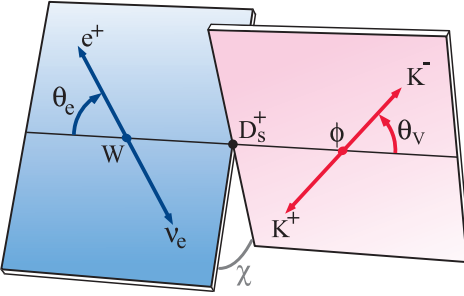


Figure 94: Decay angles θ_V , θ_ℓ and χ . Note that the angle χ between the decay planes is defined in the D -meson reference frame, whereas the angles θ_V and θ_ℓ are defined in the V meson and W reference frames, respectively.

The CLEO-c collaboration extracted the form factors $H_+(q^2)$, $H_-(q^2)$, and $H_0(q^2)$ from 11000 $D^+ \rightarrow K^-\pi^+\ell^+\nu_\ell$ events in a model-independent fashion directly as functions of q^2 [1292]. They also determined the S -wave form factor $h_0(q^2)$ via the interference term, despite the fact that the $K\pi$ mass distribution appears dominated by the vector $K^*(892)$ state. It is observed that $H_0(q^2)$ dominates over a wide range of q^2 , especially at low q^2 . The transverse form factor $H_t(q^2)$, which can be related to $A_3(q^2)$, is small compared to LQCD calculations and suggests that the form factor ratio $r_3 \equiv A_3(0)/A_1(0)$ is large and negative.

The *BABAR* collaboration selected a large sample of 244×10^3 $D^+ \rightarrow K^-\pi^+e^+\nu_e$ candidates with a ratio $S/B \sim 2.3$ from an integrated luminosity of 347 fb^{-1} [1293]. With four particles emitted in the final state, the differential decay rate depends on five variables. In addition to the four variables defined in previous sections there is also m^2 , the mass squared of the $K\pi$ system. To analyze the $D^+ \rightarrow K^-\pi^+e^+\nu_e$ decay channel, it was assumed that all form factors have a q^2 variation given by the simple pole model, and an effective pole mass of $m_A = (2.63 \pm 0.10 \pm 0.13) \text{ GeV}/c^2$ is fitted. This value is compatible with expectations when comparing to the mass of $J^P = 1^+$ charm mesons. For the mass dependence of the form factors, a Breit-Wigner with a mass dependent width and a Blatt-Weisskopf damping factor is used. For the S -wave amplitude, a polynomial below the $\bar{K}_0^*(1430)$, and a Breit-Wigner distribution above, are used. These are consistent with measurements of $D^+ \rightarrow K^-\pi^+\pi^+$ decays. For the polynomial part, a linear term is sufficient to fit the data. It is verified that the variation of the S -wave phase is compatible with expectations from elastic $K\pi$ scattering [341, 1294] (after correcting for $\delta^{3/2}$) according to the Watson theorem. At variance with elastic scattering, a negative relative sign between the S -wave and P -wave is measured; this is compatible with the Watson theorem. Contributions from other spin-1 and spin-2 resonances decaying into $K^-\pi^+$ are also considered.

Since 2016, several new measurements of form factors in $D_{(s)} \rightarrow Ve^+\nu_e$ decays have been reported by BES III. These measurements greatly increase the information available on $D \rightarrow V\ell^+\nu_e$ decays. The BES III data was recorded at center-of-mass energies of 3.773 GeV (2.9 fb^{-1}) and 4.178 GeV (3.2 fb^{-1}). The $D \rightarrow Ve^+\nu_e$ samples are reconstructed using a tagged method, and 18262, 3112, 978, 491, and 155 signal events, respectively, are obtained for the $D^+ \rightarrow \bar{K}^{*0}e^+\nu_e$, $D^0 \rightarrow K^{*-}e^+\nu_e$, $D^{0,+} \rightarrow \rho e^+\nu_e$, $D^+ \rightarrow \omega e^+\nu_e$, and $D_s^+ \rightarrow K^{*0}e^+\nu_e$ decay modes [1270, 1295–1298]. The form factor ratios r_V and r_2 are subsequently extracted.

Table 302 lists measurements of r_V and r_2 from several experiments. Most of the measure-

ments assume that the q^2 dependence of the form factors is given by the simple pole ansatz. Some of these measurements do not consider a separate S -wave contribution; in this case such a contribution is implicitly included in the measured values.

Table 302: Results for r_V and r_2 from various experiments.

Experiment	Ref.	r_V	r_2
$D^+ \rightarrow \bar{K}^{*0} \ell^+ \nu_\ell$			
E691	[1299]	$2.0 \pm 0.6 \pm 0.3$	$0.0 \pm 0.5 \pm 0.2$
E653	[1300]	$2.00 \pm 0.33 \pm 0.16$	$0.82 \pm 0.22 \pm 0.11$
E687	[1301]	$1.74 \pm 0.27 \pm 0.28$	$0.78 \pm 0.18 \pm 0.11$
E791 (e)	[1302]	$1.90 \pm 0.11 \pm 0.09$	$0.71 \pm 0.08 \pm 0.09$
E791 (μ)	[1303]	$1.84 \pm 0.11 \pm 0.09$	$0.75 \pm 0.08 \pm 0.09$
Beatrice	[1304]	$1.45 \pm 0.23 \pm 0.07$	$1.00 \pm 0.15 \pm 0.03$
FOCUS	[1289]	$1.504 \pm 0.057 \pm 0.039$	$0.875 \pm 0.049 \pm 0.064$
BES III (e)	[1295]	$1.406 \pm 0.058 \pm 0.022$	$0.784 \pm 0.041 \pm 0.024$
$D^0 \rightarrow \bar{K}^0 \pi^- \ell^+ \nu_\ell$			
FOCUS (μ)	[1305]	$1.706 \pm 0.677 \pm 0.342$	$0.912 \pm 0.370 \pm 0.104$
BABAR (μ)	[1293]	$1.493 \pm 0.014 \pm 0.021$	$0.775 \pm 0.011 \pm 0.011$
BES III (e)	[1296]	$1.46 \pm 0.07 \pm 0.02$	$0.67 \pm 0.06 \pm 0.01$
$D^+ \rightarrow \omega e^+ \nu_e$			
BES III	[1297]	$1.24 \pm 0.09 \pm 0.06$	$1.06 \pm 0.15 \pm 0.05$
$D^0, D^+ \rightarrow \rho e \nu_e$			
CLEO	[1306]	$1.40 \pm 0.25 \pm 0.03$	$0.57 \pm 0.18 \pm 0.06$
BES III	[1298]	$1.695 \pm 0.083 \pm 0.051$	$0.845 \pm 0.056 \pm 0.039$
$D_s^+ \rightarrow \phi e^+ \nu_e$			
BABAR	[1290]	$1.849 \pm 0.060 \pm 0.095$	$0.763 \pm 0.071 \pm 0.065$
$D_s^+ \rightarrow K^{*0} e^+ \nu_e$			
BES III	[1270]	$1.67 \pm 0.34 \pm 0.16$	$0.77 \pm 0.28 \pm 0.07$

9.5.14 $D \rightarrow S \ell^+ \nu_\ell$ decays

In 2018, BES III reported measurements of semileptonic D decays into a scalar meson. The experiment measured $D \rightarrow a_0(980) e^+ \nu_e$, with $a_0(980) \rightarrow \eta \pi$. Signal yields of $25.7_{-5.7}^{+6.4}$ events for $D^0 \rightarrow a_0(980)^- e^+ \nu_e$, and $10.2_{-4.1}^{+5.0}$ events for $D^+ \rightarrow a_0(980)^0 e^+ \nu_e$, were obtained, resulting in statistical significances of greater than 6.5σ and 3.0σ , respectively [1307]. As the branching fraction for $a_0(980) \rightarrow \eta \pi$ is not well-measured, BES III reports the product branching fractions

$$\mathcal{B}[D^0 \rightarrow a_0(980)^- e^+ \nu_e] \times \mathcal{B}[a_0(980)^- \rightarrow \eta \pi^-] = (1.33_{-0.29}^{+0.33} \pm 0.09) \times 10^{-4}, \quad (286)$$

$$\mathcal{B}[D^+ \rightarrow a_0(980)^0 e^+ \nu_e] \times \mathcal{B}[a_0(980)^0 \rightarrow \eta \pi^0] = (1.66_{-0.66}^{+0.81} \pm 0.11) \times 10^{-4}. \quad (287)$$

These values deviate by more than 2σ from predicted values based on QCD light-cone sum rules [1308]. Taking the lifetimes of the D^0 and D^+ into account, and assuming $\mathcal{B}[a_0(980)^- \rightarrow \eta\pi^-] = \mathcal{B}[a_0(980)^0 \rightarrow \eta\pi^0]$, the ratio of the partial widths is

$$\frac{\Gamma[D^0 \rightarrow a_0(980)^- e^+ \nu_e]}{\Gamma[D^+ \rightarrow a_0(980)^0 e^+ \nu_e]} = 2.03 \pm 0.95 \pm 0.06. \quad (288)$$

This value is consistent with isospin symmetry.

9.5.15 $D \rightarrow A\ell^+\nu_\ell$ decays

While semileptonic D decays into S -wave and D -wave states have been studied in both theory and experiment, there is a long-standing puzzle whether transitions into P -wave states have been established. Previously, CLEO-c reported evidence for $D^0 \rightarrow K_1(1270)^- e^+ \nu_e$ with a statistical significance of 4σ [1309]. The branching fraction was measured to be $\mathcal{B}[D^0 \rightarrow K_1(1270)^- e^+ \nu_e] = (7.6_{-3.0}^{+4.1} \pm 0.6 \pm 0.7) \times 10^{-4}$. Recently, BES III reported the first observation of $D^+ \rightarrow \bar{K}_1(1270)^0 e^+ \nu_e$, with a statistical significance greater than 10σ [1310]. The branching fraction was measured to be $\mathcal{B}[D^+ \rightarrow \bar{K}_1(1270)^0 e^+ \nu_e] = (23.0 \pm 2.6 \pm 1.8 \pm 2.5) \times 10^{-4}$, which is notably higher than the CLEO result. The third error listed arises from the branching fraction for $K_1(1270) \rightarrow K\pi\pi$. Taking the lifetimes of the D^0 and D^+ into account, the ratio of the partial widths is

$$\frac{\Gamma[D^+ \rightarrow \bar{K}_1(1270)^0 e^+ \nu_e]}{\Gamma[D^0 \rightarrow K_1(1270)^- e^+ \nu_e]} = 1.2_{-0.5}^{+0.7}. \quad (289)$$

This value, like that for $D \rightarrow a_0(980)\ell^+\nu_\ell$ decays, is consistent with isospin symmetry.

9.6 Leptonic decays

Purely leptonic decays of D^+ and D_s^+ mesons are among the simplest and best understood probes of $c \rightarrow d$ and $c \rightarrow s$ quark flavor-changing transitions. The amplitude of purely leptonic decays consists of the annihilation of the initial quark-antiquark pair ($c\bar{d}$ or $c\bar{s}$) into a virtual W^+ that subsequently materializes as an antilepton-neutrino pair ($\ell^+\nu_\ell$). The Standard Model branching fraction is given by

$$\mathcal{B}(D_q^+ \rightarrow \ell^+\nu_\ell) = \frac{G_F^2}{8\pi} \tau_{D_q} f_{D_q}^2 |V_{cq}|^2 m_{D_q} m_\ell^2 \left(1 - \frac{m_\ell^2}{m_{D_q}^2}\right)^2, \quad (290)$$

where m_{D_q} is the D_q meson mass, τ_{D_q} is its lifetime, m_ℓ is the charged lepton mass, $|V_{cq}|$ is the magnitude of the relevant CKM matrix element, and G_F is the Fermi coupling constant. The parameter f_{D_q} is the D_q meson decay constant and parameterizes the overlap of the wave functions of the constituent quark and anti-quark. The decay constants have been calculated using several theory methods, the most accurate and robust being that of lattice QCD (LQCD). Using the $N_f = 2 \pm 1 \pm 1$ flavor LQCD calculations of f_{D^+} and $f_{D_s^+}$ from the ETM [1311] and FNAL/MILC [1312] Collaborations, the Flavour Lattice Averaging Group (FLAG) calculates world average values [1313]

$$f_{D^+}^{\text{FLAG}} = 212.0 \pm 0.7 \text{ MeV}, \quad (291)$$

$$f_{D_s^+}^{\text{FLAG}} = 249.9 \pm 0.5 \text{ MeV}, \quad (292)$$

and the ratio

$$\left(\frac{f_{D_s^+}}{f_{D^+}}\right)^{\text{FLAG}} = 1.1783 \pm 0.0016. \quad (293)$$

These values are used within this section to determine the magnitudes $|V_{cd}|$ and $|V_{cs}|$ from the measured branching fractions of $D^+ \rightarrow \ell^+\nu_\ell$ and $D_s^+ \rightarrow \ell^+\nu_\ell$.

The leptonic decays of pseudoscalar mesons are helicity-suppressed, and thus their decay rates are proportional to the square of the charged lepton mass. Thus, decays to $\tau^+\nu_\tau$ are favored over decays to $\mu^+\nu_\mu$, and decays to $e^+\nu_e$, with an expected $\mathcal{B} \lesssim 10^{-7}$, are not yet experimentally observable. The ratio of $\tau^+\nu_\tau$ to $\mu^+\nu_\mu$ decays is given by

$$R_{\tau/\mu}^{D_q} \equiv \frac{\mathcal{B}(D_q^+ \rightarrow \tau^+\nu_\tau)}{\mathcal{B}(D_q^+ \rightarrow \mu^+\nu_\mu)} = \left(\frac{m_\tau^2}{m_\mu^2}\right) \frac{(m_{D_q}^2 - m_\tau^2)^2}{(m_{D_q}^2 - m_\mu^2)^2}, \quad (294)$$

and equals 9.74 ± 0.03 for D_s^+ decays and 2.67 ± 0.01 for D^+ decays, based on the well-measured values of m_μ , m_τ , and $m_{D_{(s)}}$ [21]. A significant deviation from this expectation would be interpreted as LFU violation in charged currents, which signifies new physics [1314].

In this section we present world average values for the product $f_{D_q}|V_{cq}|$, where $q = d, s$. For these averages, correlations between measurements and dependencies on input parameters are taken into account. Since our last report from 2016, there is one new experimental measurement: that of $\mathcal{B}(D_s^+ \rightarrow \mu^+\nu_\mu)$ by BES III [1315]. In addition, lattice QCD calculations of f_D and f_{D_s} have improved.

Table 303: Experimental results and world averages for $\mathcal{B}(D^+ \rightarrow \ell^+\nu_\ell)$ and $f_D|V_{cd}|$. The first uncertainty is statistical and the second is experimental systematic. The third uncertainty in the case of $f_{D^+}|V_{cd}|$ is due to external inputs (dominated by the uncertainty on τ_D). Here, we take the unconstrained result from CLEO-c.

Mode	$\mathcal{B} (10^{-4})$	$f_D V_{cd} $ (MeV)	Reference	
$\mu^+\nu_\mu$	$3.95 \pm 0.35 \pm 0.09$	$47.1 \pm 2.1 \pm 0.5 \pm 0.2$	CLEO-c	[1180]
	$3.71 \pm 0.19 \pm 0.06$	$45.7 \pm 1.2 \pm 0.4 \pm 0.2$	BES III	[1316]
	$3.77 \pm 0.17 \pm 0.05$	$46.1 \pm 1.0 \pm 0.3 \pm 0.2$	Average	
$e^+\nu_e$	< 0.088 at 90% C.L.		CLEO-c	[1180]
$\tau^+\nu_\tau$	< 12 at 90% C.L.		CLEO-c	[1180]

9.6.1 $D^+ \rightarrow \ell^+\nu_\ell$ decays and $|V_{cd}|$

We use measurements of the branching fraction $\mathcal{B}(D^+ \rightarrow \mu^+\nu_\mu)$ from CLEO-c [1180] and BES III [1316] to calculate the world average (WA) value. We obtain

$$\mathcal{B}^{\text{WA}}(D^+ \rightarrow \mu^+\nu_\mu) = (3.77 \pm 0.17) \times 10^{-4}, \quad (295)$$

from which we determine the product of the decay constant and the CKM matrix element to be

$$f_D|V_{cd}| = (46.1 \pm 1.1) \text{ MeV}. \quad (296)$$

The uncertainty listed includes the uncertainty on $\mathcal{B}^{\text{WA}}(D^+ \rightarrow \mu^+\nu_\mu)$, and also uncertainties on the external parameters m_μ , m_D , and τ_D [21] needed to extract $f_D|V_{cd}|$ from the branching fraction via Eq. (290). Using the LQCD value for f_D from FLAG [Eq. (291)], we calculate the magnitude of the CKM matrix element V_{cd} to be

$$|V_{cd}| = 0.2173 \pm 0.0051 \text{ (exp.)} \pm 0.0007 \text{ (LQCD)}, \quad (297)$$

where the uncertainties are from experiment and from LQCD, respectively. All input values and the resulting world average are summarized in Table 303 and plotted in Fig. 95. The upper limit on the ratio of branching fractions $R_{\tau/\mu}^D$ is 3.2 at 90% C.L.; this is slightly above the SM expected value.

9.6.2 $D_s^+ \rightarrow \ell^+\nu_\ell$ decays and $|V_{cs}|$

We use measurements of the branching fraction $\mathcal{B}(D_s^+ \rightarrow \mu^+\nu_\mu)$ from CLEO-c [1219], BABAR [1317], Belle [1318], and BES III [1315, 1319] to obtain a WA value of

$$\mathcal{B}^{\text{WA}}(D_s^+ \rightarrow \mu^+\nu_\mu) = (5.51 \pm 0.16) \times 10^{-3}. \quad (298)$$

The WA value for $\mathcal{B}(D_s^+ \rightarrow \tau^+\nu_\tau)$ is also calculated from CLEO-c, BABAR, Belle, and BES III measurements. CLEO-c made separate measurements using $\tau^+ \rightarrow e^+\nu_e\bar{\nu}_\tau$ [1320], $\tau^+ \rightarrow$

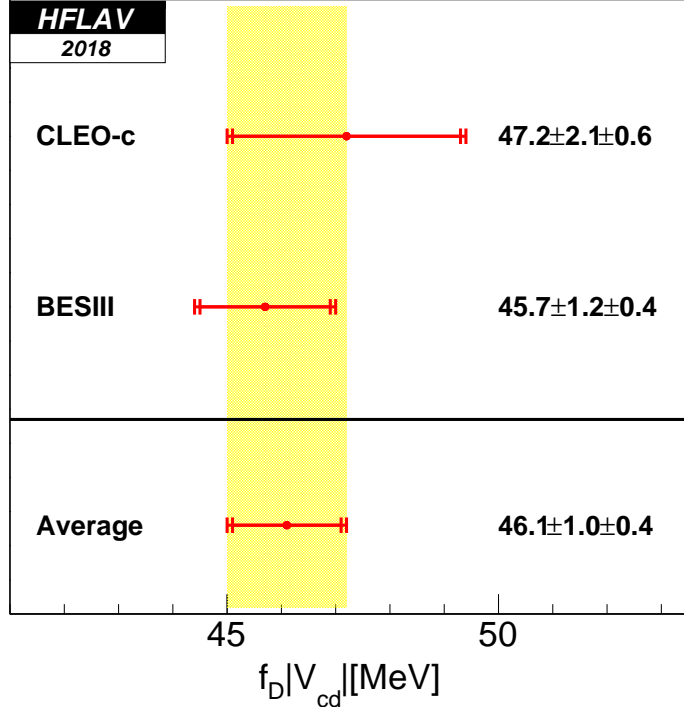


Figure 95: WA value for $f_D|V_{cd}|$. For each point, the first error listed is statistical and the second error is systematic.

$\pi^+\bar{\nu}_\tau$ [1219], and $\tau^+ \rightarrow \rho^+\bar{\nu}_\tau$ decays [1321]; *BABAR* made separate measurements using $\tau^+ \rightarrow e^+\nu_e\bar{\nu}_\tau$ and $\tau^+ \rightarrow \mu^+\nu_\mu\bar{\nu}_\tau$ decays [1317]; *Belle* made separate measurements using $\tau^+ \rightarrow e^+\nu_e\bar{\nu}_\tau$, $\tau^+ \rightarrow \mu^+\nu_\mu\bar{\nu}_\tau$, and $\tau^+ \rightarrow \pi^+\bar{\nu}_\tau$ decays [1318]; and *BES III* made measurements using only $\tau^+ \rightarrow \pi^+\bar{\nu}_\tau$ [1319] decays. Combining all these results and accounting for correlations, we obtain a WA value of

$$\mathcal{B}^{\text{WA}}(D_s^+ \rightarrow \tau^+\nu_\tau) = (5.52 \pm 0.24) \times 10^{-2}. \quad (299)$$

The ratio of branching fractions is found to be

$$R_{\tau/\mu}^{D_s} = 10.02 \pm 0.52, \quad (300)$$

which is consistent with the ratio expected in the SM.

Taking the average of $\mathcal{B}^{\text{WA}}(D_s^+ \rightarrow \mu^+\nu)$ and $\mathcal{B}^{\text{WA}}(D_s^+ \rightarrow \tau^+\nu)$ [Eqs. (298) and (299)], and using the most recent values for m_τ , m_{D_s} , and τ_D [21], we calculate the product of the D_s decay constant and $|V_{cs}|$. The result is

$$f_{D_s}|V_{cs}| = (247.8 \pm 3.1) \text{ MeV}, \quad (301)$$

where the uncertainty is due to the uncertainties on $\mathcal{B}^{\text{WA}}(D_s^+ \rightarrow \mu^+\nu_\mu)$, $\mathcal{B}^{\text{WA}}(D_s^+ \rightarrow \tau^+\nu_\tau)$, and the external inputs. All input values and the resulting world average are summarized in Table 304 and plotted in Fig. 96. To calculate this average, we take into account correlations within each experiment³⁹ for uncertainties related to normalization, tracking, particle identification, signal and background parameterizations, and peaking background contributions.

³⁹In the case of *BABAR*, we use the covariance matrix from the Errata of Ref. [1317].

Using the LQCD value for f_{D_s} from FLAG [Eq. (292)], we calculate the magnitude of the CKM matrix element V_{cs} to be

$$|V_{cs}| = 0.991 \pm 0.013 \text{ (exp.)} \pm 0.002 \text{ (LQCD)}, \quad (302)$$

where the uncertainties are from experiment and from lattice calculations, respectively.

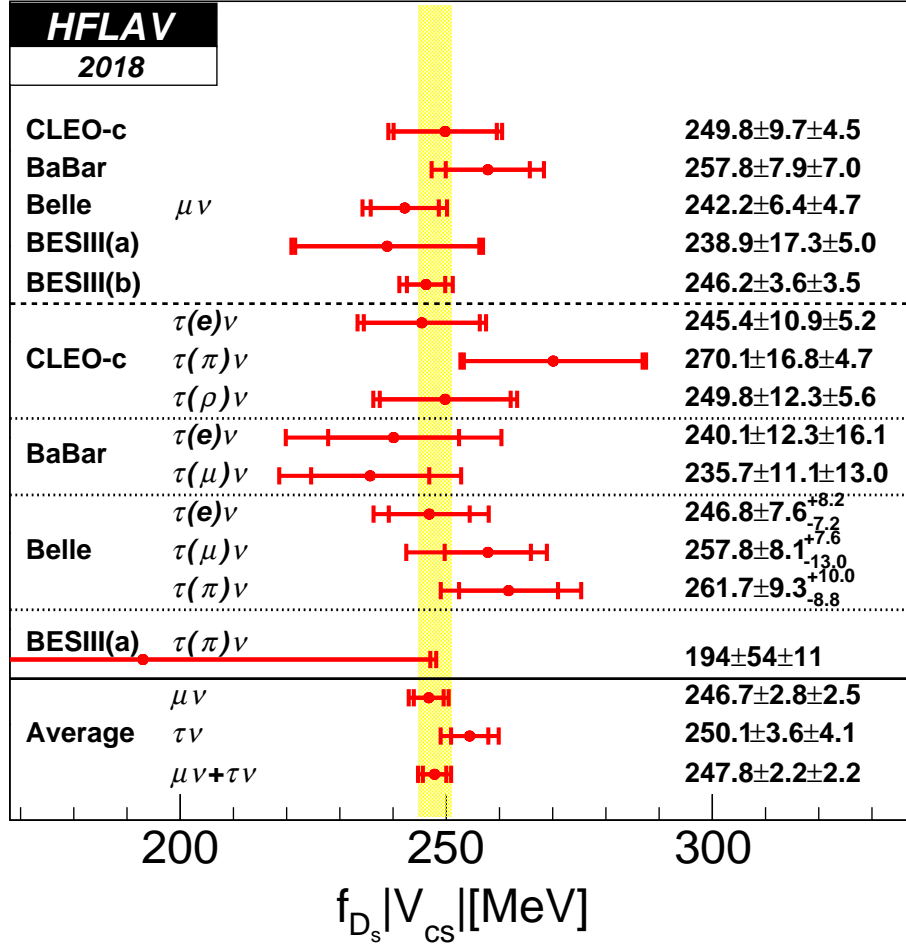


Figure 96: WA value for $f_{D_s} |V_{cs}|$. For each point, the first error listed is statistical and the second error listed is systematic. BES III(a) represents results based on 0.48 fb^{-1} of data recorded at $\sqrt{s} = 4.009 \text{ GeV}$ [1319], and BES III(b) represents results based on 3.19 fb^{-1} of data recorded at $\sqrt{s} = 4.178 \text{ GeV}$ [1315].

9.6.3 Comparison with other determinations of $|V_{cd}|$ and $|V_{cs}|$

Table 305 summarizes, and Fig. 97 displays, all determinations of the magnitudes $|V_{cd}|$ and $|V_{cs}|$. The table and figure show that, currently, the most precise direct determinations are from leptonic D^+ and D_s^+ decays. The values obtained are in agreement within uncertainties with those obtained from a global fit assuming CKM unitarity [244].

Table 304: Experimental results and world averages for $\mathcal{B}(D_s^+ \rightarrow \ell^+ \nu_\ell)$ and $f_{D_s} |V_{cs}|$. The first uncertainty is statistical and the second is experimental systematic. The third uncertainty in the case of $f_{D_s} |V_{cs}|$ is due to external inputs (dominated by the uncertainty on τ_{D_s}). We have adjusted the $\mathcal{B}(D_s^+ \rightarrow \tau^+ \nu_\tau)$ values quoted by CLEO-c and *BABAR* to account for the most recent values of $\mathcal{B}(\tau^+ \rightarrow \pi^+ \bar{\nu}_\tau)$, $\mathcal{B}(\tau^+ \rightarrow \mu^+ \nu_\mu \bar{\nu}_\tau)$, and $\mathcal{B}(\tau^+ \rightarrow e^+ \nu_e \bar{\nu}_\tau)$ [21]. CLEO-c and *BABAR* include the uncertainty in the number of D_s tags (denominator in the calculation of the branching fraction) in the statistical uncertainty of \mathcal{B} ; however, we subtract this uncertainty from the statistical one and include it in the systematic uncertainty.

Mode	$\mathcal{B} (10^{-2})$	$f_{D_s} V_{cs} $ (MeV)	Reference
$\mu^+ \nu_\mu$	$0.565 \pm 0.044 \pm 0.020$	$249.8 \pm 9.7 \pm 4.4 \pm 1.0$	CLEO-c [1219]
	$0.602 \pm 0.037 \pm 0.032$	$257.8 \pm 7.9 \pm 6.9 \pm 1.0$	<i>BABAR</i> [1317]
	$0.531 \pm 0.028 \pm 0.020$	$242.2 \pm 6.4 \pm 4.6 \pm 1.0$	Belle [1318]
	$0.517 \pm 0.075 \pm 0.021$	$238.9 \pm 17.3 \pm 4.9 \pm 0.9$	BES III [1319]
	$0.549 \pm 0.016 \pm 0.015$	$246.2 \pm 3.6 \pm 3.4 \pm 1.0$	BES III [1315]
$0.551 \pm 0.012 \pm 0.010$		$246.7 \pm 2.8 \pm 2.3 \pm 1.0$	Average
$\tau^+(e^+) \nu_\tau$	$5.32 \pm 0.47 \pm 0.22$	$245.4 \pm 10.9 \pm 5.1 \pm 1.0$	CLEO-c [1321]
$\tau^+(\pi^+) \nu_\tau$	$6.47 \pm 0.80 \pm 0.22$	$270.1 \pm 16.8 \pm 4.6 \pm 1.1$	CLEO-c [1219]
$\tau^+(\rho^+) \nu_\tau$	$5.50 \pm 0.54 \pm 0.24$	$249.8 \pm 12.3 \pm 5.5 \pm 1.0$	CLEO-c [1320]
$\tau^+ \nu_\tau$	$5.59 \pm 0.32 \pm 0.14$	$251.7 \pm 7.2 \pm 3.2 \pm 1.0$	CLEO-c
$\tau^+(e^+) \nu_\tau$	$5.09 \pm 0.52 \pm 0.68$	$240.1 \pm 12.3 \pm 16.1 \pm 1.0$	<i>BABAR</i> [1317]
$\tau^+(\mu^+) \nu_\tau$	$4.90 \pm 0.46 \pm 0.54$	$235.7 \pm 11.1 \pm 13.0 \pm 1.0$	
$\tau^+ \nu_\tau$	$4.96 \pm 0.37 \pm 0.57$	$237.1 \pm 8.8 \pm 13.6 \pm 1.0$	<i>BABAR</i>
$\tau^+(e^+) \nu_\tau$	$5.38 \pm 0.33^{+0.35}_{-0.31}$	$246.8 \pm 7.6^{+8.1}_{-7.1} \pm 1.0$	
$\tau^+(\mu^+) \nu_\tau$	$5.86 \pm 0.37^{+0.34}_{-0.59}$	$257.8 \pm 8.1^{+7.5}_{-13.0} \pm 1.0$	Belle [1318]
$\tau^+(\pi^+) \nu_\tau$	$6.05 \pm 0.43^{+0.46}_{-0.40}$	$261.7 \pm 9.3^{+10.0}_{-8.7} \pm 1.0$	
$\tau^+ \nu_\tau$	$5.70 \pm 0.21 \pm 0.31$	$254.1 \pm 4.7 \pm 6.9 \pm 1.0$	Belle
$\tau^+(\pi^+) \nu_\tau$	$3.28 \pm 1.83 \pm 0.37$	$193 \pm 54 \pm 11 \pm 1$	BES III [1319]
$5.52 \pm 0.16 \pm 0.18$		$250.1 \pm 3.6 \pm 4.0 \pm 1.0$	Average
$\mu^+ \nu_\mu + \tau^+ \nu_\tau$		$247.8 \pm 2.2 \pm 2.0 \pm 1.0$	Average
$e^+ \nu_e$	< 0.0083 at 90% C.L.		Belle [1318]

Table 305: Averages of the magnitudes of CKM matrix elements $|V_{cd}|$ and $|V_{cs}|$, as determined from leptonic and semileptonic $D_{(s)}^+$ decays. In calculating these averages, we conservatively assume that uncertainties due to LQCD are fully correlated. For comparison, values determined from neutrino scattering, from W decays, and from a global fit to the CKM matrix assuming unitarity [244] are also listed.

Method	Reference	Value
$ V_{cd} $		
$D \rightarrow \ell \nu_\ell$	This section	$0.2173 \pm 0.0051(\text{exp.}) \pm 0.0007(\text{LQCD})$
$D \rightarrow \pi \ell \nu_\ell$	Section 9.5	$0.2249 \pm 0.0028(\text{exp.}) \pm 0.0055(\text{LQCD})$
$ V_{cs} $		
$D_s \rightarrow \ell \nu_\ell$	Average	0.2204 ± 0.0040
$D \rightarrow K \ell \nu_\ell$		
νN	PDG [21]	0.230 ± 0.011
Global CKM Fit	CKMFitter [244]	$0.22529^{+0.00041}_{-0.00032}$
$D_s \rightarrow \ell \nu_\ell$	Average	0.969 ± 0.010
$D \rightarrow K \ell \nu_\ell$		
$W \rightarrow c \bar{s}$	PDG [21]	$0.94^{+0.32}_{-0.26} \pm 0.13$
Global CKM Fit	CKMFitter [244]	$0.973394^{+0.000074}_{-0.000096}$

9.6.4 Extraction of $D_{(s)}$ meson decay constants

As listed in Table 305 (and plotted in Fig. 97), the values of $|V_{cs}|$ and $|V_{cd}|$ can be determined from a global fit of the CKM matrix assuming unitarity [244]. These values can be used to extract the D^+ and D_s^+ decay constants from the world average values of $f_D |V_{cd}|$ and $f_{D_s} |V_{cs}|$ given in Eqs. (296) and (301). The results are

$$f_D^{\text{exp}} = (205.4 \pm 4.8) \text{ MeV}, \quad (303)$$

$$f_{D_s}^{\text{exp}} = (254.5 \pm 3.2) \text{ MeV}, \quad (304)$$

and the ratio of the decay constants is

$$\frac{f_{D_s}^{\text{exp}}}{f_D^{\text{exp}}} = 1.239 \pm 0.033. \quad (305)$$

These values are in agreement within their uncertainties with the LQCD values given by FLAG [Eqs. (291)-(293)]. The only discrepancy is in the ratio of decay constants; in this case the measurement is higher by 2.1σ than the LQCD prediction.

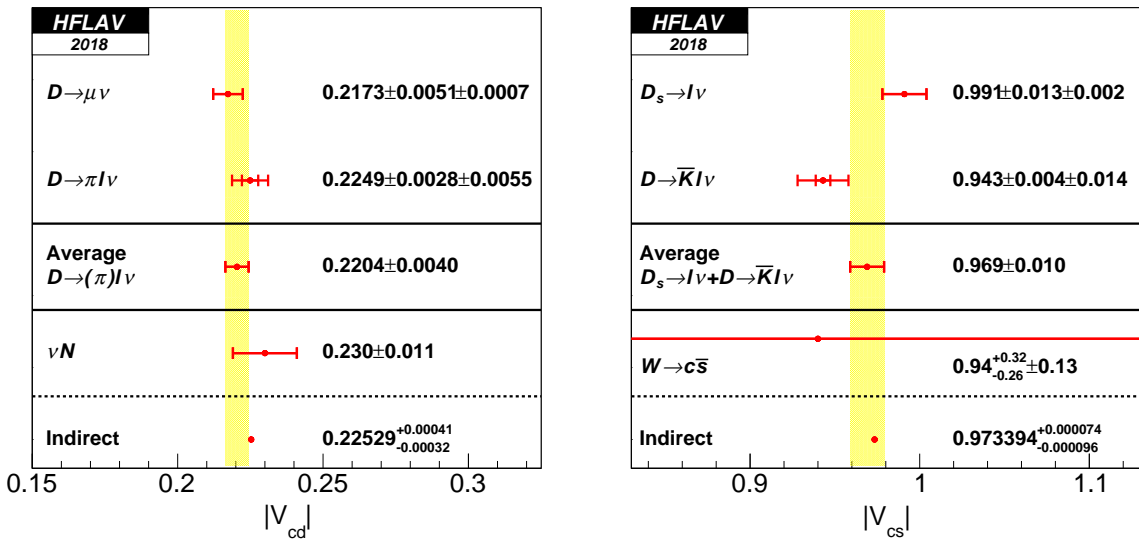


Figure 97: Comparison of magnitudes of CKM matrix elements $|V_{cd}|$ (left) and $|V_{cs}|$ (right), as determined from leptonic and semileptonic $D_{(s)}^+$ decays. Also listed are results from neutrino scattering, from W decays, and from a global fit of the CKM matrix assuming unitarity [244].

9.7 Hadronic D^0 decays and final state radiation

Measurements of the branching fractions for the decays $D^0 \rightarrow K^\mp\pi^\pm$, $D^0 \rightarrow \pi^+\pi^-$, and $D^0 \rightarrow K^+K^-$ have reached sufficient precision to allow averages with $\mathcal{O}(1\%)$ relative uncertainties. At this precision, Final State Radiation (FSR) must be treated correctly and consistently across the input measurements for the accuracy of the averages to match the precision. The sensitivity of measurements to FSR arises because of a tail in the distribution of radiated energy that extends to the kinematic limit. The tail beyond $\sum E_\gamma \approx 30$ MeV causes typical selection variables like the hadronic invariant mass to shift outside the selection range dictated by experimental resolution, as shown in Fig. 98. While the differential rate for the tail is small, the integrated rate amounts to several percent of the total $h^+h^-(n\gamma)$ rate because of the tail's extent. The tail therefore translates directly into a several percent loss in experimental efficiency.

All measurements that include an FSR correction have a correction based on the use of PHOTOS [1322–1326] within the experiment’s Monte Carlo simulation. PHOTOS itself, however, has evolved, over the period spanning the set of measurements [1325]. In particular, the incorporation of interference between radiation from the two separate mesons has proceeded in stages: it was first available for particle–antiparticle pairs in version 2.00 (1993), extended to any two-body, all-charged, final states in version 2.02 (1999), and further extended to multi-body final states in version 2.15 (2005). The effects of interference are clearly visible, as shown in Figure 98, and cause a roughly 30% increase in the integrated rate into the high energy photon tail. To evaluate the FSR correction incorporated into a given measurement, we must therefore note whether any correction was made, the version of PHOTOS used in correction, and whether the interference terms in PHOTOS were turned on. Also worth noting, an exponentiated multiple-photon mode was introduced in PHOTOS version 2.09, which allows PHOTOS to also simulate photons with low energies; this mode can be switched on or off.

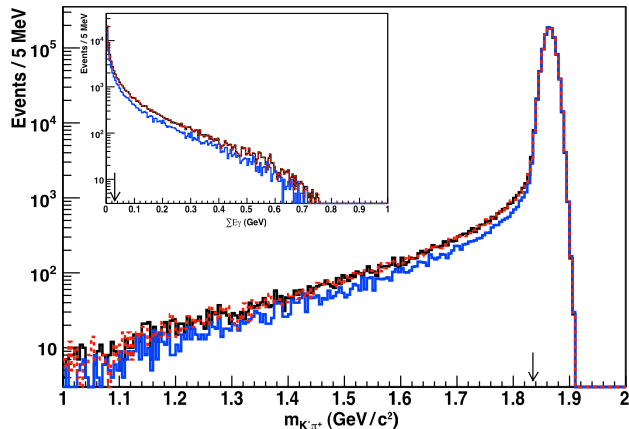


Figure 98: The $K\pi$ invariant mass distribution for $D^0 \rightarrow K^-\pi^+(n\gamma)$ decays. The 3 curves correspond to three different configurations of PHOTOS for modeling FSR: version 2.02 without interference (blue/grey), version 2.02 with interference (red dashed) and version 2.15 with interference (black). The true invariant mass has been smeared with a typical experimental resolution of 10 MeV/ c^2 . Inset: The corresponding spectrum of total energy radiated per event. The arrow indicates the $\sum E_\gamma$ value that begins to shift kinematic quantities outside of the range typically accepted in a measurement.

9.7.1 Updates to the branching fractions

Before averaging the measured branching fractions, the published results are updated, as necessary, to the FSR prediction of PHOTOS 2.15 with interference included and exponentiated multiple-photon mode turned on. The update will always shift a branching fraction to a higher value: with no FSR correction or an FSR correction suboptimally modeled, the experimental efficiency determination will be biased high, and therefore the branching fraction will be biased low.

Most of the branching fraction analyses used the kinematic quantity sensitive to FSR in the candidate selection criteria. For the analyses at the $\psi(3770)$, this variable was ΔE , the difference between the candidate D^0 energy and the beam energy (*e.g.*, $E_K + E_\pi - E_{\text{beam}}$ for $D^0 \rightarrow K^-\pi^+$). In the remainder of the analyses, the relevant quantity was the reconstructed hadronic two-body mass m_{h+h^-} . To make an FSR correction, we need to evaluate the fraction of decays that FSR moves outside of the range accepted for the analysis. The corrections were evaluated using an event generator (EVTGEN [1327,1328]) that incorporates PHOTOS to simulate the portions of the decay process most relevant to the correction.

We compared corrections determined both with and without smearing to account for experimental resolution; for the analyses using m_{h+h^-} as the kinematic quantity sensitive to FSR, the differences were negligible, typically of $\mathcal{O}(1\%)$ of the correction itself. The immunity of the correction to resolution effects comes about because most of the long FSR-induced tail in the m_{h+h^-} distribution resides well away from the selection boundaries. The smearing from resolution, on the other hand, mainly affects the distribution of events right at the boundary. For the analyses using ΔE however, events with low energy photons are found to substantially move events across the selection boundary; thus PHOTOS versions with exponentiated multiple-photon mode turned on and off, respectively, can give substantially different FSR corrections. In the case that this mode is on, smearing of the events with low energy photons increases the amount of the FSR correction by about 10%. This is well within the uncertainty on the FSR correction, as discussed later in this section, and thus ignored.

For measurements incorporating an FSR correction that did not include interference and/or use exponentiated multiple-photon mode, we update by assessing the FSR-induced efficiency loss for both the PHOTOS version and configuration used in the analysis and our nominal version 2.15 (with interference included and exponentiated multiple-photon mode turned on). For measurements that published their sensitivity to FSR, our generator-level predictions for the original efficiency loss agreed to within a few percent of the correction. This agreement lends additional credence to the procedure.

Once the event loss from FSR in the most sensitive kinematic quantity is accounted for, the event loss in other quantities is typically very small. For example, analyses using D^{*+} tags show very little sensitivity to FSR in the reconstructed $D^{*+} - D^0$ mass difference, *i.e.*, in $m_{h+h^-\pi^+} - m_{h+h^-}$. In this case, the effect of FSR tends to cancel in the difference of reconstructed masses. In the $\psi(3770)$ analyses, the beam-constrained mass distributions (*e.g.* $\sqrt{E_{\text{beam}}^2 - |\vec{p}_K + \vec{p}_\pi|^2}$) have some sensitivity, but provide negligible independent sensitivity after the ΔE selection.

The FOCUS [1329] analysis of the branching fraction ratios $\mathcal{B}(D^0 \rightarrow \pi^+\pi^-)/\mathcal{B}(D^0 \rightarrow K^-\pi^+)$ and $\mathcal{B}(D^0 \rightarrow K^+K^-)/\mathcal{B}(D^0 \rightarrow K^-\pi^+)$ obtained yields using fits to the two-body mass distributions. FSR will both distort the low end of the signal mass peak, and will contribute a signal component to the low side tail used to estimate the background. The fitting procedure is not sensitive to signal events out in the FSR tail, which would be counted as part of the

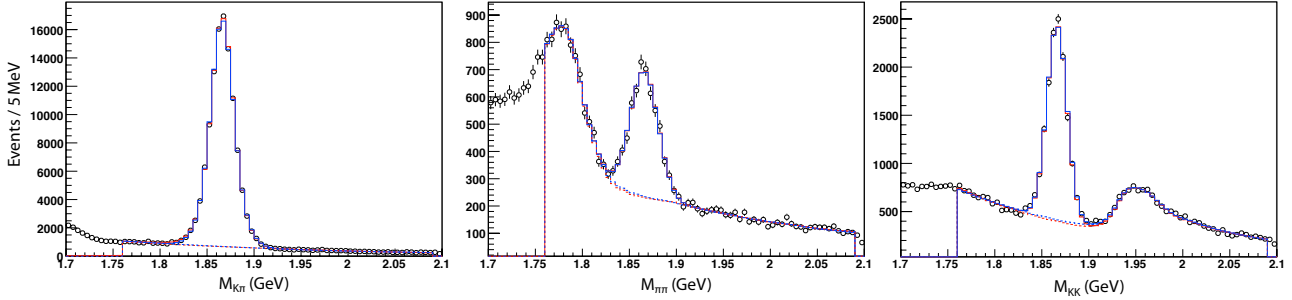


Figure 99: FOCUS data (dots), original fits (blue) and toy MC parameterization (red) for $D^0 \rightarrow K^-\pi^+$ (left), $D^0 \rightarrow \pi^+\pi^-$ (center), and $D^0 \rightarrow \pi^+\pi^-$ (right).

background.

A more complex toy Monte Carlo procedure was required to analyze the effect of FSR on the fitted yields, which were published with no FSR corrections applied. Determining the update involved an iterative procedure in which samples of similar size to the FOCUS sample were generated and then fit using the FOCUS signal and background parameterizations. The MC parameterizations were tuned based on differences between the fits to the toy MC data and the FOCUS fits, and the procedure was repeated. These steps were iterated until the fit parameters matched the original FOCUS parameters.

The toy MC samples for the first iteration were based on the generator-level distributions of $m_{K^-\pi^+}$, $m_{\pi^+\pi^-}$, and $m_{K^+K^-}$, including the effects of FSR, smeared according to the original FOCUS resolution function, and on backgrounds generated using the parameterization from the final FOCUS fits. For each iteration, 400 to 1600 individual data-sized samples were generated and fit. The central values of the parameters from these fits determined the corrections to the generator parameters for the following iteration. The ratio between the number of signal events generated and the final signal yield provides the required FSR correction in the final iteration. Only a few iterations were required in each mode. Figure 99 shows the FOCUS data, the published FOCUS fits, and the final toy MC parameterizations. The toy MC provides an excellent description of the data.

The corrections obtained to the individual FOCUS yields were 1.0298 ± 0.0001 for $K^-\pi^+$, 1.062 ± 0.001 for $\pi^+\pi^-$, and 1.0183 ± 0.0003 for K^+K^- . These corrections tend to cancel in the branching ratios, leading to corrections (update shifts) of 1.031 ± 0.001 (3.10%) for $\mathcal{B}(D^0 \rightarrow \pi^+\pi^-)/\mathcal{B}(D^0 \rightarrow K^-\pi^+)$, and 0.9888 ± 0.0003 (-1.12%) for $\mathcal{B}(D^0 \rightarrow K^+K^-)/\mathcal{B}(D^0 \rightarrow K^-\pi^+)$.

Table 306 summarizes the updated branching fractions. The published FSR-related modeling uncertainties have been replaced with a new, common estimate; this estimate is based on the assumption that the dominant uncertainty in the FSR corrections comes from the fact that the mesons are treated like structureless particles. No contributions from structure-dependent terms in the decay process (*e.g.*, radiation from individual quarks) are included in PHOTOS. Internal studies done by various experiments have indicated that in $K\pi$ decays, the PHOTOS corrections agree with data at the 20-30% level. We therefore attribute a 25% uncertainty to the (updated) FSR correction from potential structure-dependent contributions. For the other two modes, the only difference in structure is the final state valence quark content. While radiative corrections typically come in with a $1/M$ dependence, one would expect the additional contribution from the structure terms to come in on time scales shorter than the hadronization

Table 306: The experimental measurements relating to $\mathcal{B}(D^0 \rightarrow K^-\pi^+)$, $\mathcal{B}(D^0 \rightarrow \pi^+\pi^-)$, and $\mathcal{B}(D^0 \rightarrow K^+K^-)$ after updating them to the common version and configuration of PHOTOS. The uncertainties are statistical and total systematic, with the FSR-related systematic estimated in this procedure shown in parentheses. Also listed are the percent shifts in the results from those with the original correction (if any), in the case an update is applied here, as well as the original PHOTOS and interference configuration for each publication.

Experiment (acronym)	Result (rescaled)	Update shift [%]	PHOTOS
$D^0 \rightarrow K^-\pi^+$			
BES III 18 (BE18) [1330]	$3.931 \pm 0.006 \pm 0.067(44)\%$	1.25	2.03/Yes
CLEO-c 14 (CC14) [1184]	$3.934 \pm 0.021 \pm 0.061(31)\%$	–	2.15/Yes
<i>BABAR</i> 07 (BA07) [1331]	$4.035 \pm 0.037 \pm 0.074(24)\%$	0.69	2.02/No
CLEO II 98 (CL98) [1332]	$3.917 \pm 0.154 \pm 0.167(27)\%$	2.80	none
ALEPH 97 (AL97) [1333]	$3.931 \pm 0.091 \pm 0.124(27)\%$	0.79	2.0/No
ARGUS 94 (AR94) [1334]	$3.490 \pm 0.123 \pm 0.287(20)\%$	2.33	none
CLEO II 93 (CL93) [1335]	$3.965 \pm 0.080 \pm 0.171(13)\%$	0.38	2.0/No
ALEPH 91 (AL91) [1336]	$3.733 \pm 0.351 \pm 0.455(28)\%$	3.12	none
$D^0 \rightarrow \pi^+\pi^-$			
BES III 18 [1330]	$0.1529 \pm 0.0018 \pm 0.0032(23)\%$	1.39	2.03/Yes
$D^0 \rightarrow \pi^+\pi^-/D^0 \rightarrow K^-\pi^+$			
CLEO-c 10 (CC10) [1181]	$0.0370 \pm 0.0006 \pm 0.0009(02)$	–	2.15/Yes
CDF 05 (CD05) [1337]	$0.03594 \pm 0.00054 \pm 0.00043(15)$	–	2.15/Yes
FOCUS 02 (FO02) [1329]	$0.0364 \pm 0.0012 \pm 0.0006(02)$	3.10	none
$D^0 \rightarrow K^+K^-$			
BES III 18 [1330]	$0.4271 \pm 0.0021 \pm 0.0069(27)\%$	0.89	2.03/Yes
$D^0 \rightarrow K^+K^-/D^0 \rightarrow K^-\pi^+$			
CLEO-c 10 [1181]	$0.1041 \pm 0.0011 \pm 0.0012(03)$	–	2.15/Yes
CDF 05 [1337]	$0.0992 \pm 0.0011 \pm 0.0012(01)$	–	2.15/Yes
FOCUS 02 [1329]	$0.0982 \pm 0.0014 \pm 0.0014(01)$	-1.12	none

time scale. In this case, you might expect Λ_{QCD} to be the relevant scale, rather than the quark masses, and therefore that the amplitude is the same for the three modes. In treating the correlations among the measurements, this is what we assume. We also assume that the PHOTOS amplitudes and any missing structure amplitudes interfere constructively. The uncertainties largely cancel in the branching fraction ratios. For the final average branching fractions, the FSR uncertainty on $K\pi$ is as large as the uncertainty due to other systematic effects. Note that because of the relative sizes of FSR in the different modes, the $\pi\pi/K\pi$ branching ratio uncertainty from FSR is positively correlated with that for the $K\pi$ branching fraction, while the $KK/K\pi$ branching ratio FSR uncertainty is negatively correlated.

The $\mathcal{B}(D^0 \rightarrow K^-\pi^+)$ measurement of reference [1338], the $\mathcal{B}(D^0 \rightarrow \pi^+\pi^-)/\mathcal{B}(D^0 \rightarrow K^-\pi^+)$ measurements of references [1201] and [1153], and the $\mathcal{B}(D^0 \rightarrow K^+K^-)/\mathcal{B}(D^0 \rightarrow K^-\pi^+)$ measurement of reference [1153] are excluded from the branching fraction averages presented here. These measurements appear not to have incorporated any FSR corrections, and insufficient information is available to determine the 2-3% update shifts that would be required.

Table 307: The correlation matrix corresponding to the full covariance matrix. Subscripts $h \in \{\pi, K\}$ denote which of the $D^0 \rightarrow h^+ h^-$ decay results from a single experiment is represented in that row or column.

	BE18	CC14	BA07	CL98	AL97	AR94	CL93	AL91	BE18 $_{\pi}$	CC10 $_{\pi}$	CD05 $_{\pi}$	FO02 $_{\pi}$	BE18 $_K$	CC10 $_K$	CD05 $_K$	FO02 $_K$
BE18	1.0000	0.3143	0.1897	0.0777	0.1148	0.0419	0.0450	0.0319	0.6534	0.0930	0.1401	0.0948	0.5839	-0.1153	-0.0437	-0.0259
CC14	0.3143	1.0000	0.1394	0.0571	0.0844	0.0308	0.0331	0.0234	0.3023	0.0683	0.1029	0.0697	0.1788	-0.0847	-0.0321	-0.0191
BA07	0.1897	0.1394	1.0000	0.0345	0.0509	0.0186	0.0200	0.0141	0.1825	0.0413	0.0621	0.0421	0.1079	-0.0511	-0.0194	-0.0115
CL98	0.0777	0.0571	0.0345	1.0000	0.0209	0.0076	0.0082	0.0058	0.0748	0.0169	0.0255	0.0172	0.0442	-0.0209	-0.0079	-0.0047
AL97	0.1148	0.0844	0.0509	0.0209	1.0000	0.0112	0.0121	0.1156	0.1104	0.0250	0.0376	0.0254	0.0653	-0.0309	-0.0117	-0.0070
AR94	0.0419	0.0308	0.0186	0.0076	0.0112	1.0000	0.0044	0.0031	0.0403	0.0091	0.0137	0.0093	0.0238	-0.0113	-0.0043	-0.0025
CL93	0.0450	0.0331	0.0200	0.0082	0.0121	0.0044	1.0000	0.0034	0.0433	0.0098	0.0147	0.0100	0.0256	-0.0121	-0.0046	-0.0027
AL91	0.0319	0.0234	0.0141	0.0058	0.1156	0.0031	0.0034	1.0000	0.0306	0.0069	0.0104	0.0071	0.0181	-0.0086	-0.0033	-0.0019
BE18 $_{\pi}$	0.6534	0.3023	0.1825	0.0748	0.1104	0.0403	0.0433	0.0306	1.0000	0.0895	0.1347	0.0912	0.4334	-0.1109	-0.0421	-0.0249
CC10 $_{\pi}$	0.0930	0.0683	0.0413	0.0169	0.0250	0.0091	0.0098	0.0069	0.0895	1.0000	0.0305	0.0206	0.0529	-0.0251	-0.0095	-0.0056
CD05 $_{\pi}$	0.1401	0.1029	0.0621	0.0255	0.0376	0.0137	0.0147	0.0104	0.1347	0.0305	1.0000	0.0310	0.0797	-0.0378	-0.0143	-0.0085
FO02 $_{\pi}$	0.0948	0.0697	0.0421	0.0172	0.0254	0.0093	0.0100	0.0071	0.0912	0.0206	0.0310	1.0000	0.0539	-0.0255	-0.0097	-0.0057
BE18 $_K$	0.5839	0.1788	0.1079	0.0442	0.0653	0.0238	0.0256	0.0181	0.4334	0.0529	0.0797	0.0539	1.0000	-0.0656	-0.0249	-0.0148
CC10 $_K$	-0.1153	-0.0847	-0.0511	-0.0209	-0.0309	-0.0113	-0.0121	-0.0086	-0.1109	-0.0251	-0.0378	-0.0255	-0.0656	1.0000	0.0118	0.0070
CD05 $_K$	-0.0437	-0.0321	-0.0194	-0.0079	-0.0117	-0.0043	-0.0046	-0.0033	-0.0421	-0.0095	-0.0143	-0.0097	-0.0249	0.0118	1.0000	0.0027
FO02 $_K$	-0.0259	-0.0191	-0.0115	-0.0047	-0.0070	-0.0025	-0.0027	-0.0019	-0.0249	-0.0056	-0.0085	-0.0057	-0.0148	0.0070	0.0027	1.0000

9.7.2 Average branching fractions for $D^0 \rightarrow K^-\pi^+$, $D^0 \rightarrow \pi^+\pi^-$ and $D^0 \rightarrow K^+K^-$

The average branching fractions for $D^0 \rightarrow K^-\pi^+$, $D^0 \rightarrow \pi^+\pi^-$ and $D^0 \rightarrow K^+K^-$ decays are obtained from a single χ^2 minimization procedure, in which the three branching fractions are floating parameters. The central values are obtained from a fit in which the full covariance matrix, accounting for all statistical, systematic (excluding FSR), and FSR measurement uncertainties, is used. Table 307 presents the correlation matrix for this nominal fit. We then obtain the three reported uncertainties on those central values as follows: The statistical uncertainties are obtained from a fit using only the statistical covariance matrix. The systematic uncertainties are obtained by subtracting (in quadrature) the statistical uncertainties from the uncertainties determined via a fit using a covariance matrix that accounts for both statistical and systematic measurement uncertainties. The FSR uncertainties are obtained by subtracting (in quadrature) the uncertainties determined via a fit using a covariance matrix that accounts for both statistical and systematic measurement uncertainties from the uncertainties determined via the fit using the full covariance matrix.

In forming the full covariance matrix, the FSR uncertainties are treated as fully correlated (or anti-correlated) as described above. For the covariance matrices involving systematic measurement uncertainties, ALEPH's systematic uncertainties in the θ_{D^*} parameter are treated as fully correlated between the ALEPH 97 and ALEPH 91 measurements. Similarly, the tracking efficiency uncertainties in the CLEO II 98 and the CLEO II 93 measurements are treated as fully correlated. For the three BES III 18 results, both tracking and particle identification efficiencies for any particles shared between decay modes are treated as fully correlated. Finally, the BES III 18 results also have a fully correlated statistical dependence on the number of $D^0\bar{D}^0$ pairs produced.

The averaging procedure results in a final χ^2 of 36.0 for 13 (16 – 3) degrees of freedom. The branching fractions obtained are

$$\mathcal{B}(D^0 \rightarrow K^-\pi^+) = (3.999 \pm 0.006 \pm 0.031 \pm 0.032) \%, \quad (306)$$

$$\mathcal{B}(D^0 \rightarrow \pi^+\pi^-) = (0.1490 \pm 0.0012 \pm 0.0015 \pm 0.0019) \%, \quad (307)$$

$$\mathcal{B}(D^0 \rightarrow K^+K^-) = (0.4113 \pm 0.0017 \pm 0.0041 \pm 0.0025) \%. \quad (308)$$

The uncertainties, estimated as described above, are statistical, systematic (excluding FSR), and FSR modeling. The correlation coefficients from the fit using the total uncertainties are

	$K^-\pi^+$	$\pi^+\pi^-$	K^+K^-
$K^-\pi^+$	1.00	0.77	0.76
$\pi^+\pi^-$	0.77	1.00	0.58
K^+K^-	0.76	0.58	1.00

As Fig. 100 shows, the average value for $\mathcal{B}(D^0 \rightarrow K^-\pi^+)$ and the input branching fractions agree very well. For the $\mathcal{B}(D^0 \rightarrow K^-\pi^+)$ measurements only, the partial χ^2 is 4.9 in the final fit. With the estimated uncertainty in the FSR modeling used here, the FSR uncertainty dominates the statistical uncertainty in the average, suggesting that experimental work in the near future should focus on verification of FSR with $\sum E_\gamma \gtrsim 100$ MeV. Note that the systematic uncertainty excluding FSR has now approached the level of the FSR uncertainty; in the most precise measurements of these branching fractions, the competing uncertainty is the uncertainty on the tracking efficiency.

Table 308: Evolution of the $D^0 \rightarrow K^-\pi^+$ branching fraction from a fit with no FSR updates or correlations (similar to the average in the PDG 2018 update [21]) to the nominal fit presented here.

Modes fit	Description	$\mathcal{B}(D^0 \rightarrow K^-\pi^+)$ (%)	$\chi^2/\text{(deg. of freedom)}$
$K^-\pi^+$	PDG 2018 [21] equivalent	$3.931 \pm 0.017 \pm 0.041$	$4.5/(8-1) = 0.64$
$K^-\pi^+$	drop Ref. [1338]	$3.937 \pm 0.017 \pm 0.041$	$4.4/(7-1) = 0.73$
$K^-\pi^+$	add Ref. [1330]	$3.913 \pm 0.006 \pm 0.033$	$5.1/(8-1) = 0.73$
$K^-\pi^+$	add FSR updates	$3.948 \pm 0.006 \pm 0.032 \pm 0.019$	$3.5/(8-1) = 0.50$
$K^-\pi^+$	add FSR correlations	$3.949 \pm 0.006 \pm 0.032 \pm 0.033$	$3.7/(8-1) = 0.53$
all	add CLEO-c, CDF, and FOCUS h^+h^-	$3.956 \pm 0.006 \pm 0.032 \pm 0.033$	$11.1/(14-3) = 1.01$
all	add BES III h^+h^-	$3.999 \pm 0.006 \pm 0.031 \pm 0.032$	$36.0/(16-3) = 2.77$

The $\mathcal{B}(D^0 \rightarrow K^+K^-)$ and $\mathcal{B}(D^0 \rightarrow \pi^+\pi^-)$ measurements inferred from the branching ratio measurements do not agree as well (Fig. 101). There is some tension among the results when all measurements related to $\mathcal{B}(D^0 \rightarrow K^+K^-)$ and $\mathcal{B}(D^0 \rightarrow \pi^+\pi^-)$ are included in the average together. For the measurements related to $\mathcal{B}(D^0 \rightarrow K^+K^-)$ [$\mathcal{B}(D^0 \rightarrow \pi^+\pi^-)$] only, the partial χ^2 is 15.7 [6.0] in the final fit.

The $\mathcal{B}(D^0 \rightarrow K^-\pi^+)$ average obtained here is approximately four statistical standard deviations higher than the PDG 2018 update average [21]. Table 308 shows the evolution from a fit similar to the PDG fit (no FSR updates or correlations, reference [1338] included, reference [1330] not included) to the average presented here. There are three main contributions to the difference. The branching fraction in reference [1338] is low, and its exclusion shifts the result upwards. A large shift (-0.024%) is due to the precision of reference [1330] as it is added; reference [1330] is a considerably lower result than the PDG average before the FSR update. A subsequently larger shift ($+0.035\%$) is due to the FSR updates, which as expected shift the result upwards, and coincidentally back to compatible with the PDG average. The largest shift ($+0.050\%$) occurs as all of the measurements related to $\mathcal{B}(D^0 \rightarrow K^+K^-)$ and $\mathcal{B}(D^0 \rightarrow \pi^+\pi^-)$ are included in the average together with the $\mathcal{B}(D^0 \rightarrow K^-\pi^+)$ measurements.

9.7.3 Average branching fraction for $D^0 \rightarrow K^+\pi^-$

There is no reason to presume that the effects of FSR should be different in $D^0 \rightarrow K^+\pi^-$ and $D^0 \rightarrow K^-\pi^+$ decays, as both decay to one charged kaon and one charged pion; indeed, for the same version of PHOTOS the FSR simulations of these decays are identical. Measurements of the relative branching fraction ratio between the doubly Cabibbo-suppressed decay $D^0 \rightarrow K^+\pi^-$ and the Cabibbo-favored decay $D^0 \rightarrow K^-\pi^+$ (R_D , determined in Section 9.1) have now approached $\mathcal{O}(1\%)$ relative uncertainties. This makes it worthwhile to combine our R_D average with the $\mathcal{B}(D^0 \rightarrow K^-\pi^+)$ average obtained in Eq. (306), to provide a measurement of the branching fraction:

$$\mathcal{B}(D^0 \rightarrow K^+\pi^-) = (1.376 \pm 0.017) \times 10^{-4}. \quad (309)$$

Note that, by definition of R_D , these branching fractions do not include any contribution from Cabibbo-favored $\bar{D}^0 \rightarrow K^+\pi^-$ decays. In precision, our result compares favorably to the PDG 2018 update average of $\mathcal{B}(D^0 \rightarrow K^+\pi^-) = (1.366 \pm 0.028) \times 10^{-4}$ [21].

9.7.4 Consideration of PHOTOS++

The versions of PHOTOS that existing measurements were performed with are now well over a decade out of date. The newest version, PHOTOS++ 3.61 [1339], is now fully based on C++ instead of the original FORTRAN. None of the measurements used in our branching fraction averages use PHOTOS++, so we have not yet undertaken an effort to update all results to this newest version. However, at this time it is worth continuing our procedure to evaluate whether there is any continued low bias in the the branching fractions, due to sub-optimal modeling of FSR.

We find that the FSR spectra for PHOTOS 2.15, with interference included and exponentiated multiple-photon mode turned on, and PHOTOS++ (in its default mode) are compatible. The distributions of $m_{K\pi}$ for simulated D mesons from $B \rightarrow D^*X$ decays produced at $\Upsilon(4S)$ threshold appear to be identical. As an example, the *BABAR* 07 selection criteria was applied to decays simulated with PHOTOS++ and our nominal version of PHOTOS 2.15; both produce identical FSR corrections to within 0.01%.

The distributions of ΔE for simulated D mesons produced at $\psi(3770)$ threshold also appear to be identical. As an example, for the BES III 18 $D^0 \rightarrow K^-\pi^+$, $D^0 \rightarrow \pi^+\pi^-$, and $D^0 \rightarrow K^+K^-$ branching fraction results, the additional update shifts required to correct from our nominal version of PHOTOS 2.15 to PHOTOS++ are less than or equal to 0.02%. However, if smearing is applied with the BES III 18 ΔE resolution, while the update for $D^0 \rightarrow K^-\pi^+$ remains negligible, the update shifts for $D^0 \rightarrow \pi^+\pi^-$ and $D^0 \rightarrow K^+K^-$ are modest at -0.25% and 0.19%, respectively; this level of shifts are well within the systematic uncertainty of our averages.

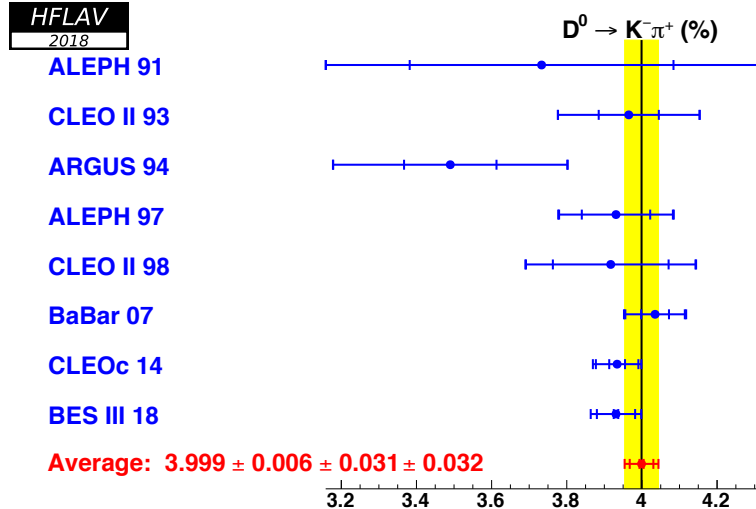


Figure 100: Comparison of measurements of $\mathcal{B}(D^0 \rightarrow K^- \pi^+)$ (blue) with the average branching fraction obtained here (red, and yellow band). For these measurements only, the partial χ^2 is 4.9 in the final fit.

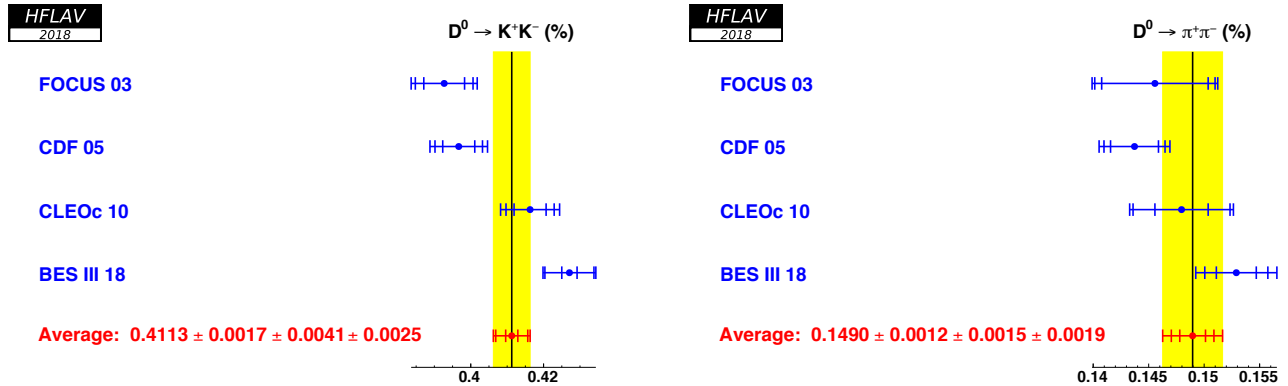


Figure 101: The $\mathcal{B}(D^0 \rightarrow K^+ K^-)$ (left) and $\mathcal{B}(D^0 \rightarrow \pi^+ \pi^-)$ (right) values obtained either from absolute measurements or by scaling the measured branching ratios with the $\mathcal{B}(D^0 \rightarrow K^- \pi^+)$ branching fraction average obtained here. For the measurements (blue points), the error bars correspond to the statistical, systematic and either the $K\pi$ normalization uncertainties or, in case of an absolute measurement, the FSR modeling uncertainty. The average obtained here (red point, yellow band) lists the statistical, systematics excluding FSR, and the FSR systematic. For the measurements related to $\mathcal{B}(D^0 \rightarrow K^+ K^-)$ [$\mathcal{B}(D^0 \rightarrow \pi^+ \pi^-)$] only, the partial χ^2 is 15.7 [6.0] in the final fit.

9.8 Hadronic D_s decays

For D_s^+ mesons, most branching fractions are measured relative to the normalizing channels $D_s^+ \rightarrow K^- K^+ \pi^+$ and $D_s^+ \rightarrow \bar{K}^0 K^+$. Thus, it is important to know the absolute branching fractions for these modes as precisely as possible. To achieve that, we calculate world average values using all relevant measurements and accounting for correlations among measurements. In addition, we calculate a world average branching fraction for $D_s^+ \rightarrow \eta \pi^+$, for which absolute branching fraction measurements exist. Other D_s^+ decay modes are either measured relative to one of the normalization modes above, or only a single measurement exists (e.g., Ref. [1340]). We note that the well-known two-body decay modes $D_s^+ \rightarrow \phi \pi^+$ and $D_s^+ \rightarrow \bar{K}^{*0} K^+$ are subsets of $D_s^+ \rightarrow K^- K^+ \pi^+$.

All measurements used are listed in Table 309 and plotted along with the resulting world averages in Figs. 102, 103, and 104. The measurements of $\mathcal{B}(D_s^+ \rightarrow K^- K^+ \pi^+)$ are integrated over phase space and thus have uncertainties arising from the contributions of intermediate resonances. These are accounted for in the systematic uncertainties. For $D_s^+ \rightarrow \bar{K}^0 K^+$, we use measurements of $\mathcal{B}(D_s^+ \rightarrow K_S^0 K^+)$ from CLEOc and BESIII, and a measurement of $\mathcal{B}(D_s^+ \rightarrow K_L^0 K^+)$ from BESIII, assuming $\mathcal{B}(D_s^+ \rightarrow \bar{K}^0 K^+) = 2 \times \mathcal{B}(D_s^+ \rightarrow K_S^0 K^+) = 2 \times \mathcal{B}(D_s^+ \rightarrow K_L^0 K^+)$. The two BESIII measurements are statistically independent but have correlated systematic uncertainties; we take these correlations into account when calculating the world average. We perform our averaging using COMBOS [1131], and the results are

$$\mathcal{B}^{\text{WA}}(D_s^+ \rightarrow K^- K^+ \pi^+) = (5.44 \pm 0.14)\%, \quad (310)$$

$$\mathcal{B}^{\text{WA}}(D_s^+ \rightarrow \bar{K}^0 K^+) = (2.94 \pm 0.05)\%, \quad (311)$$

$$\mathcal{B}^{\text{WA}}(D_s^+ \rightarrow \eta \pi^+) = (1.71 \pm 0.08)\%. \quad (312)$$

The uncertainties listed are total uncertainties, i.e., statistical plus systematic combined.

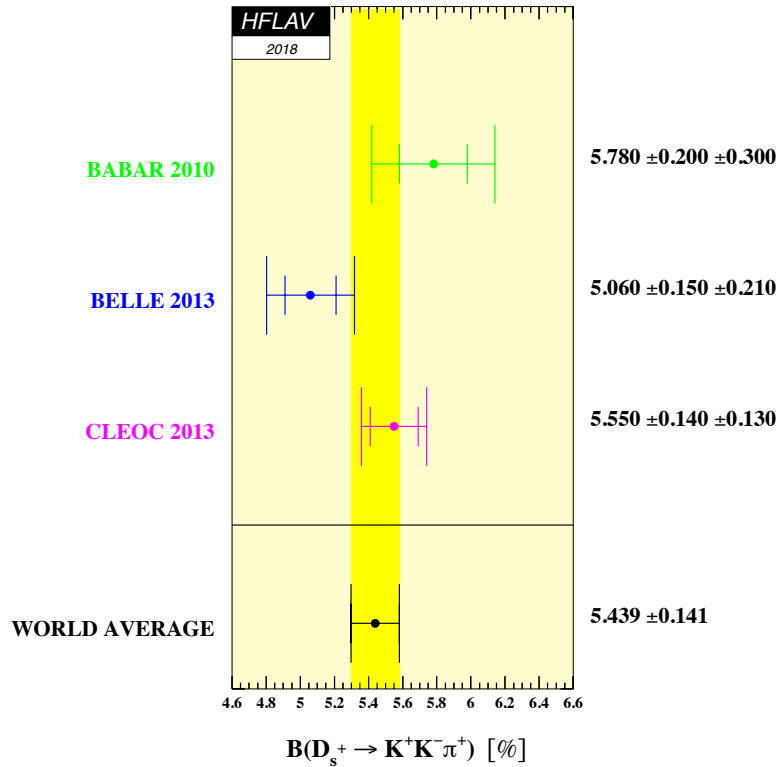


Figure 102: Input values and world average for $\mathcal{B}(D_s^+ \rightarrow K^- K^+ \pi^+)$. The first uncertainty listed is statistical, and the second is systematic.

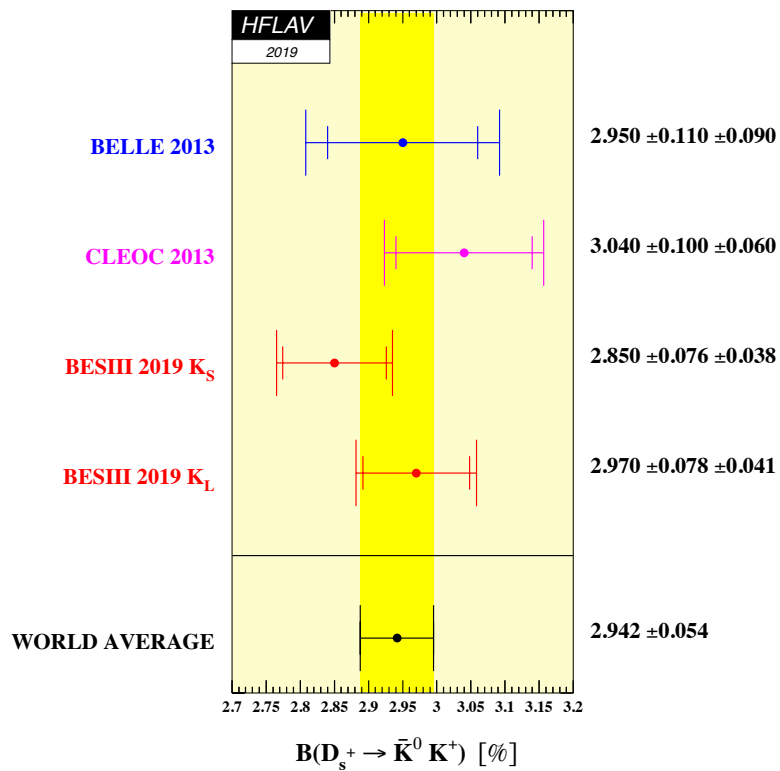


Figure 103: Input values and world average for $\mathcal{B}(D_s^+ \rightarrow \bar{K}^0 K^+)$. The first uncertainty listed is statistical, and the second is systematic.

Table 309: Experimental measurements and world averages for the branching fractions $\mathcal{B}(D_s^+ \rightarrow K^- K^+ \pi^+)$, $\mathcal{B}(D_s^+ \rightarrow \bar{K}^0 K^+)$, and $\mathcal{B}(D_s^+ \rightarrow \eta \pi^+)$. The first uncertainty listed is statistical, and the second is systematic.

Mode	Branching fraction (%)	Reference
$K^- K^+ \pi^+$	$5.78 \pm 0.20 \pm 0.30$	<i>BABAR</i> [1317]
$K^- K^+ \pi^+$	$5.06 \pm 0.15 \pm 0.21$	<i>Belle</i> [1318]
$K^- K^+ \pi^+$	$5.55 \pm 0.14 \pm 0.13$	<i>CLEOc</i> [1220]
	$5.44 \pm 0.09 \pm 0.11$	Average
$\bar{K}^0 K^+$	$2.95 \pm 0.11 \pm 0.09$	<i>Belle</i> [1318]
$\bar{K}^0 K^+$	$3.04 \pm 0.10 \pm 0.06$	<i>CLEOc</i> $D_s^+ \rightarrow K_S^0 K^+$ [1220]
$\bar{K}^0 K^+$	$2.850 \pm 0.076 \pm 0.038$	<i>BESIII</i> $D_s^+ \rightarrow K_S^0 K^+$ [1341]
$\bar{K}^0 K^+$	$2.970 \pm 0.078 \pm 0.041$	<i>BESIII</i> $D_s^+ \rightarrow K_L^0 K^+$ [1341]
	$2.94 \pm 0.04 \pm 0.03$	Average
$\eta \pi^+$	$1.67 \pm 0.08 \pm 0.06$	<i>CLEOc</i> [1220]
$\eta \pi^+$	$1.82 \pm 0.14 \pm 0.07$	<i>Belle</i> [1318]
	$1.71 \pm 0.07 \pm 0.05$	Average

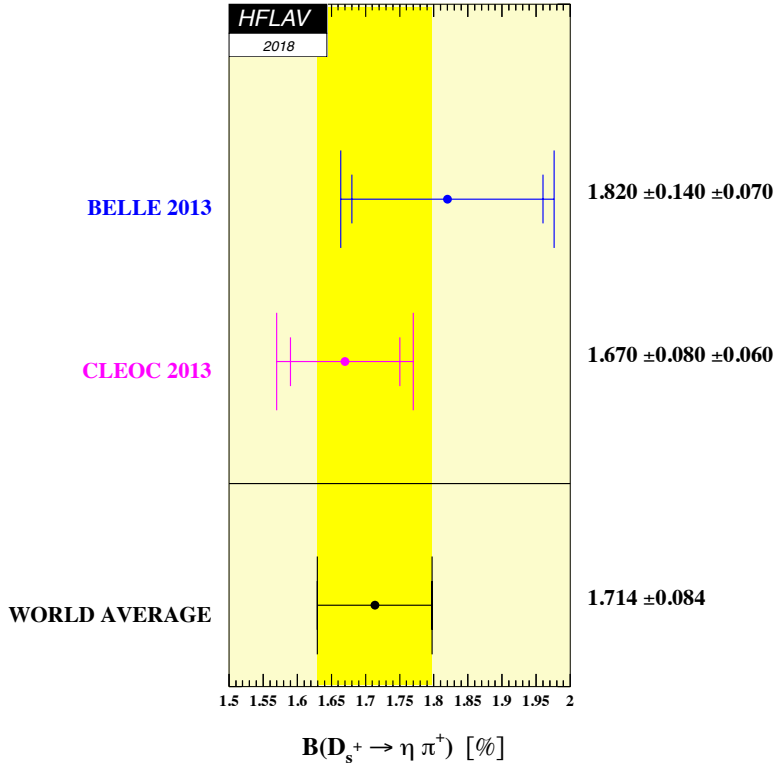


Figure 104: Input values and world average for $\mathcal{B}(D_s^+ \rightarrow \eta \pi^+)$. The first uncertainty listed is statistical, and the second is systematic.

9.9 Excited $D_{(s)}$ mesons

Excited charm meson states have received increased attention since the first observation of states that could not be accommodated by QCD predictions [1342–1345]. Their properties can be measured in both prompt analyses, as well as in amplitude analyses of multi-body B decays. Tables 310, 311 and 312 summarize the measurements of the masses and widths of excited D and D_s mesons, respectively. If a preferred assignment of spin and parity was measured, it is listed in the column J^P , where the label natural denotes $J^P = 0^-, 1^+, 2^- \dots$ and unnatural $J^P = 0^+, 1^-, 2^+ \dots$. In some studies, it was only possible to identify whether the state has natural or unnatural spin-parity, but not the exact values of the quantum numbers.

For states where multiple measurements are available, an average mass and width are calculated; these are listed in the gray shaded row. The calculation of the averages assumes no correlation between individual measurements. A summary of the averaged masses and widths is shown in Figure 105. The resonances are listed in the tables and figures as they appear in the respective publications. For some cases, it remains unclear whether all are in fact different states, or could be a measurement of the same resonance. An example is the recently observed $D_1^*(2680)^0$ [1346], which has parameters close to those of $D^*(2650)^0$. Further measurements are necessary in order to increase the precision.

The masses and widths of narrow ($\Gamma < 50$ MeV) orbitally excited D mesons (1P states), both neutral and charged, are well-established. Measurements of broad states ($\Gamma \sim 200\text{--}400$ MeV) are less abundant, as identifying the signal is more challenging. There is a slight discrepancy between the $D_0^*(2400)^0$ masses measured by the Belle [733] and FOCUS [1347] experiments. No data exist yet for the $D_1(2430)^\pm$ state. Dalitz plot analyses of $B \rightarrow \bar{D}^{(*)}\pi\pi$ decays strongly favor the assignments 0^+ and 1^+ for the spin-parity quantum numbers of the $D_0^*(2400)^0/D_0^*(2400)^\pm$ and $D_1(2430)^0$ states, respectively. The measured masses and widths, as well as the J^P values, are in agreement with theoretical predictions based on potential models [503, 1348–1350].

The spectroscopic assignment of heavier states remains less clear. Further theoretical studies suggest the identity of some 2S and 1D states [1351], [1352], and tentatively discuss possible 1F, 3S and 2P states. Possible new states to be found in the near future are suggested [1352].

Tables 313 and 314 summarize the branching fractions of B meson decays to excited D and D_s states, respectively. It is notable that the branching fractions for B mesons decaying to a narrow D^* state and a pion are similar for charged and neutral B initial states, while the branching fractions to a broad D^* state and π^+ are much larger for B^+ than for B^0 . This may be due to the fact that color-suppressed amplitudes contribute only to the B^+ decay and not to the B^0 decay (for a theoretical discussion, see Ref. [1353, 1354]). Measurements of individual branching fractions of D mesons are difficult due to the unknown fragmentation of a c quark to D^* or due to the unknown $B \rightarrow D^*X$ branching fractions.

The discoveries of the $D_{s0}^*(2317)^\pm$ and $D_{s1}(2460)^\pm$ have triggered increased interest in properties of, and searches for, excited D_s mesons. While the masses and widths of $D_{s1}(2536)^\pm$ and $D_{s2}^*(2573)^\pm$ states are in relatively good agreement with potential model predictions, the masses of $D_{s0}^*(2317)^\pm$ and $D_{s1}(2460)^\pm$ states are significantly lower than expected (see Ref. [1355] for a discussion of $c\bar{s}$ models). Moreover, the mass splitting between these two states greatly exceeds that between the $D_{s1}(2536)^\pm$ and $D_{s2}(2573)^\pm$. These unexpected properties have led to interpretations of the $D_{s0}^*(2317)^\pm$ and $D_{s1}(2460)^\pm$ as exotic four-quark states [1356, 1357].

While there are few measurements of the J^P values of $D_{s0}^*(2317)^\pm$ and $D_{s1}(2460)^\pm$, the available data favor 0^+ and 1^+ , respectively. A molecule-like (DK) interpretation of the $D_{s0}^*(2317)^\pm$

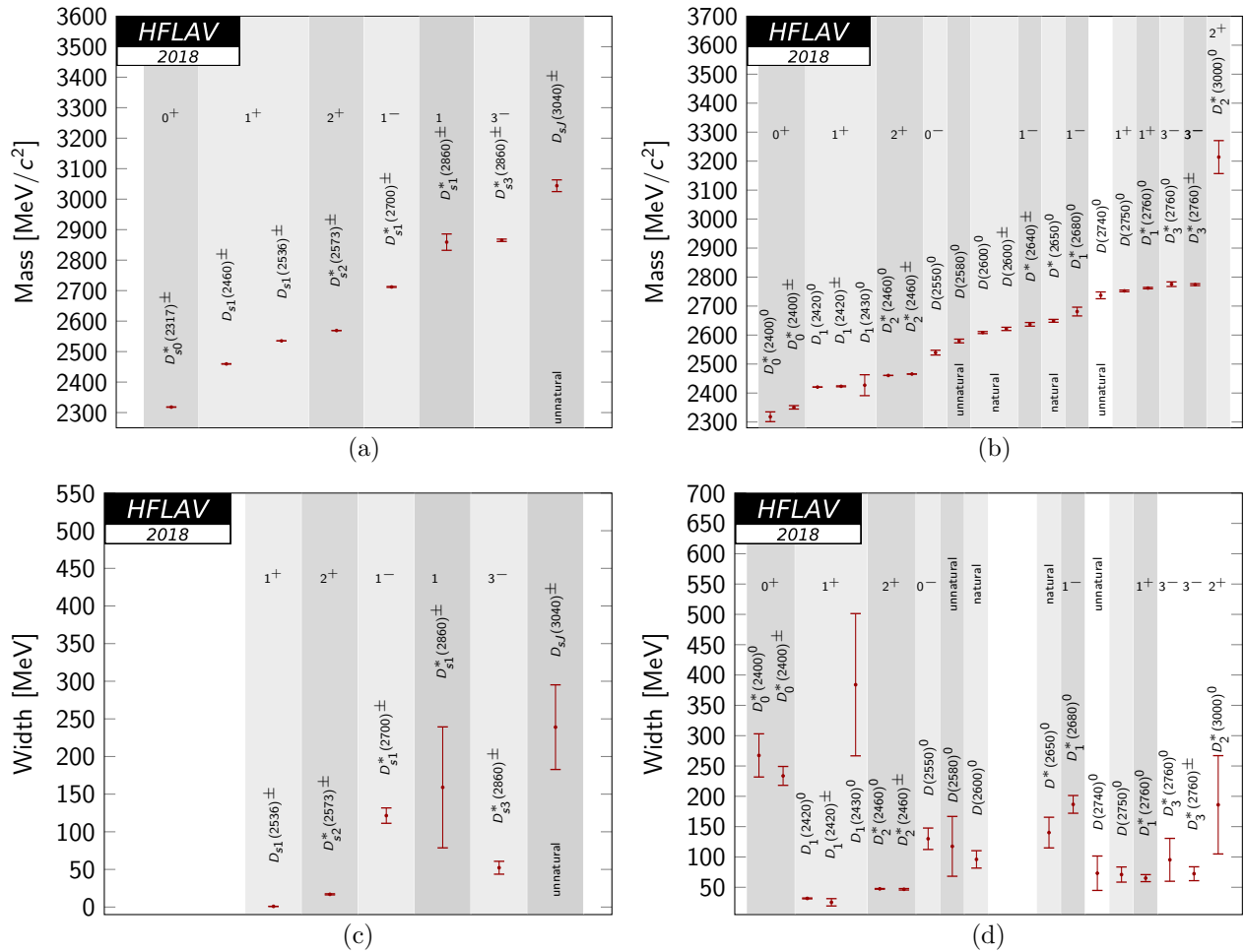


Figure 105: Averaged masses for excited D_s mesons are shown in subfigure (a) and for D mesons in subfigure (b). The average widths for excited D_s mesons are shown in subfigure (c) and for excited D mesons in subfigure (d). The vertical shaded regions distinguish between different spin parity states.

and $D_{s1}(2460)^\pm$ [1356, 1357] that can account for their low masses and isospin-breaking decay modes is tested by searching for charged and neutral isospin partners of these states; thus far such searches have yielded negative results. Therefore the models that predict equal production rates for different charged states are excluded. The molecular picture can also be tested by measuring the rates for the radiative processes $D_{s0}^*(2317)^\pm/D_{s1}(2460)^\pm \rightarrow D_s^{(*)}\gamma$ and comparing to theoretical predictions. The predicted rates, however, are below the sensitivity of current experiments.

Another model successful in explaining the total widths and the $D_{s0}^*(2317)^\pm - D_{s1}(2460)^\pm$ mass splitting is based on the assumption that these states are chiral partners of the ground states D_s^+ and D_s^* [1358]. While some measured branching fraction ratios agree with predicted values, further experimental tests with better sensitivity are needed to confirm or refute this scenario. A summary of the mass difference measurements is given in Table 315.

Measurements by *BABAR* [1359] and *LHCb* [1360] first indicated the existence of a strange-charm $D_{sJ}^*(2860)^\pm$ meson. An *LHCb* study of $B_s^0 \rightarrow \bar{D}^0 K^- \pi^+$ decays, in which they searched

for excited D_s mesons [1361], showed with 10σ significance that this state is comprised of two different particles, one of spin 1 and one of spin 3. This represents the first measurement of a heavy flavored spin-3 particle, and the first observation of B meson decays to spin 3 particles. A subsequent study of D_{sJ} mesons by the LHCb collaboration [1362] supports the natural parity assignment for this state ($J^P = 3^-$). This study also shows weak evidence for a further structure at a mass around 3040 MeV/ c^2 with unnatural parity, which was first hinted at by a *BABAR* analysis [1359]. The second observation of a spin-3 charm meson was a subsequent LHCb analysis of $B^0 \rightarrow \bar{D}^0\pi^+\pi^-$ decays, which measured the spin-parity assignment of the state $D_3^*(2760)^\pm$ to be $J^P = 3^-$. This resonance was in fact observed previously by *BABAR* [1248] and LHCb [1249]. The measurement suggests a spectroscopic assignment of 3D_3 . Recently, also the corresponding neutral state was observed by LHCb, the $D_3^*(2760)^0$ [1346].

Other observed excited D_s states include $D_{s1}^*(2700)^\pm$ and $D_{s2}^*(2573)^\pm$. The properties of both (mass, width, J^P) have been measured and determined in several analyses. A theoretical discussion [1363] investigates the possibility that the $D_{s1}(2700)^\pm$ could represent radial excitations of the $D_s^{*\pm}$. Similarly, the $D_{s1}^*(2860)^\pm$ and $D_{sJ}(3040)^\pm$ could be excitations of $D_{s0}^*(2317)^\pm$ and $D_{s1}(2460)^\pm$ or $D_{s1}(2536)^\pm$, respectively.

Table 316 summarizes measurements of the helicity parameter A_D (also referred to as polarization amplitude). In D^{**} meson decays to $D^{**} \rightarrow D^*\pi$, $D^* \rightarrow D\pi$, the helicity distribution varies like $1 + A_D \cos^2 \theta_H$, where θ_H is the angle in the D^* rest frame between the two pions emitted by decay $D^{**} \rightarrow D^*\pi$ and the $D^* \rightarrow D\pi$. The parameter is sensitive to possible S-wave contributions in the decay. In the case of a D meson decay decaying purely via D-wave, the helicity parameter is predicted to give $A_D = 3$. Studies of the $D_1(2420)^0$ meson by the ZEUS and *BABAR* collaborations suggest that there is an S-wave admixture in the decay, which is contrary to Heavy Quark Effective Theory calculations [483, 1364].

Table 310: Recent measurements of mass and width for different excited D_s mesons. The column J^P list the most significant assignment of spin and parity. If possible an average mass or width is calculated.

Resonance	J^P	Decay mode	Mass [MeV/ c^2]	Width [MeV]	Measured by	Reference
$D_{s0}^*(2317)^\pm$	0 ⁺	$D_s^+\pi^0$	$2319.6 \pm 0.2 \pm 1.4$		<i>BABAR</i>	[1365]
		$D_s^+\pi^0$	$2317.3 \pm 0.4 \pm 0.8$		<i>BABAR</i>	[1345]
		$D_s^+\pi^0$	$2318.3 \pm 1.2 \pm 1.2$		<i>BESIII</i>	[1366]
			2318.01 ± 0.69		Our average	
$D_{s1}(2460)^\pm$	1 ⁺	$D_s^{*+}\pi^0, D_s^+\pi^0\gamma, D_s^+\gamma, D_s^+\pi^+\pi^-$	$2460.1 \pm 0.2 \pm 0.8$		<i>BABAR</i>	[1365]
		$D_s^+\pi^0\gamma$	$2458 \pm 1.0 \pm 1.0$		<i>BABAR</i>	[1345]
			2459.6 ± 0.7		Our average	
$D_{s1}(2536)^\pm$	1 ⁺	$D^{*+}K_S^0$	$2535.7 \pm 0.6 \pm 0.5$		<i>D\O</i>	[1367]
		$D^{*+}K_S^0, D^{*0}K^+$	$2534.78 \pm 0.31 \pm 0.40$		<i>BABAR</i>	[664]
		$D_s^+\pi^+\pi^-$	$2534.6 \pm 0.3 \pm 0.7$		<i>BABAR</i>	[1365]
		$D^{*+}K_S^0, D^{*0}K^+$	$2535.0 \pm 0.6 \pm 1.0$		<i>E687</i>	[1368]
		$D^{*0}K^+$	$2535.3 \pm 0.2 \pm 0.5$		<i>CLEO</i>	[1369]
		$D^{*+}K_S^0$	$2534.8 \pm 0.6 \pm 0.6$		<i>CLEO</i>	[1369]
		$D^{*0}K^+$	$2535.2 \pm 0.5 \pm 1.5$		<i>ARGUS</i>	[1370]
		$D^{*+}K_S^0$	$2535.6 \pm 0.7 \pm 0.4$		<i>CLEO</i>	[1371]
		$D^{*+}K_S^0$	$2535.9 \pm 0.6 \pm 2.0$		<i>ARGUS</i>	[1372]
		$D^{*+}K_S^0$		$0.92 \pm 0.03 \pm 0.04$	<i>BABAR</i>	[1373]
			$2537.7 \pm 0.5 \pm 3.1$	$1.7 \pm 1.2 \pm 0.6$	<i>BESIII</i>	[1374]
			2535.12 ± 0.26	0.92 ± 0.05	Our average	
$D_{s2}(2573)^\pm$	2 ⁺	$D^0K^+, D^{*+}K_S^0$	$2568.39 \pm 0.29 \pm 0.26$	$16.9 \pm 0.5 \pm 0.6$	<i>LHCb</i>	[1375]
		$D^+K_S^0, D^0K^+$	$2569.4 \pm 1.6 \pm 0.5$	$12.1 \pm 4.5 \pm 1.6$	<i>LHCb</i>	[1376]
		$D^+K_S^0, D^0K^+$	$2572.2 \pm 0.3 \pm 1.0$	$27.1 \pm 0.6 \pm 5.6$	<i>BABAR</i>	[1377]
		D^0K^+	$2574.25 \pm 3.3 \pm 1.6$	$10.4 \pm 8.3 \pm 3.0$	<i>ARGUS</i>	[1378]
		D^0K^+	$2573.2^{+1.7}_{-1.6} \pm 0.9$	$16^{+5}_{-4} \pm 3$	<i>CLEO</i>	[1379]
			$2570.7 \pm 2.0 \pm 1.7$	$17.2 \pm 3.6 \pm 1.1$	<i>BESIII</i>	[1374]
			2569.10 ± 0.35	16.91 ± 0.74	Our average	
$D_{s1}^*(2700)^\pm$	1 ⁻	$D^{*+}K_S^0, D^{*0}K^+$	$2732.3 \pm 4.3 \pm 5.8$	$136 \pm 19 \pm 24$	<i>LHCb</i>	[1362]
		D^0K^+	2699^{+14}_{-7}	127^{+24}_{-19}	<i>BABAR</i>	[1380]
		$D^{*+}K_S^0, D^{*0}K^+$	$2709.2 \pm 1.9 \pm 4.5$	$115.8 \pm 7.3 \pm 12.1$	<i>LHCb</i>	[1360]
		DK, D^*K	$2710 \pm 2^{+12}_{-7}$	$149 \pm 7^{+39}_{-52}$	<i>BABAR</i>	[1359]
		D^0K^+	$2708 \pm 9^{+11}_{-10}$	$108 \pm 2^{+36}_{-31}$	<i>Belle</i>	[755]
			2712.0 ± 1.5	121.5 ± 10.2	Our average	
$D_{s1}^*(2860)^\pm$	1	D^0K^+	$2859 \pm 12 \pm 24$	$159 \pm 23 \pm 77$	<i>LHCb</i>	[1361]
$D_{s3}^*(2860)^\pm$	3 ⁻	$D^{*+}K_S^0, D^{*0}K^+$	$2867.1 \pm 4.3 \pm 1.9$	$50 \pm 11 \pm 13$	<i>LHCb</i>	[1362]
		D^0K^+	$2860.5 \pm 2.6 \pm 6.5$	$53 \pm 7 \pm 7$	<i>LHCb</i>	[1361]
			2865.0 ± 3.9	52.2 ± 8.6	Our average	
$D_{sJ}(3040)^\pm$	Unnatural	D^*K	$3044 \pm 8^{+30}_{-5}$	$239 \pm 35^{+46}_{-42}$	<i>BABAR</i> (m & Γ) + <i>LHCb</i> (J^P)	[1359] + [1362]

Table 311: Recent measurements of mass and width for different excited D mesons. The column J^P list the most significant assignment of spin and parity. If possible an average mass or width is calculated.

Resonance	J^P	Decay mode	Mass [MeV/ c^2]	Width [MeV]	Measured by	Reference
$D_0^*(2400)^0$	0^+	$D^+\pi^-$	$2297 \pm 8 \pm 20$	$273 \pm 12 \pm 48$	$BABAR$	[734]
		$D^+\pi^-$	$2308 \pm 17 \pm 32$	$276 \pm 21 \pm 63$	$Belle$	[733]
		$D^+\pi^-$	$2407 \pm 21 \pm 35$	$240 \pm 55 \pm 59$	$Focus$	[1347]
			2318.2 ± 16.9	267.4 ± 35.6	Our average	
$D_0^*(2400)^\pm$	0^+	$D^0\pi^+$	$2349 \pm 6 \pm 1 \pm 4$	$217 \pm 13 \pm 5 \pm 12$	$LHCb$	[621]
		$D^0\pi^+$	$2360 \pm 15 \pm 12 \pm 28$	$255 \pm 26 \pm 20 \pm 47$	$LHCb$	[1381]
		$D^0\pi^+$	$2403 \pm 14 \pm 35$	$283 \pm 24 \pm 34$	$Focus(m \& \Gamma) + Belle(J^P)$	[1347] + [614]
			2350.6 ± 5.9	233.7 ± 15.5	Our average	
$D_1(2420)^0$	1^+	$D^{*+}\pi^-$	$2419.6 \pm 0.1 \pm 0.7$	$35.2 \pm 0.4 \pm 0.9$	$LHCb$	[1249]
		$D^{*+}\pi^-$	$2423.1 \pm 1.5^{+0.4}_{-1.0}$	$38.8 \pm 5^{+1.9}_{-5.4}$	$Zeus$	[1382]
		$D^{*+}\pi^-$	$2420.1 \pm 0.1 \pm 0.8$	$31.4 \pm 0.5 \pm 1.3$	$BABAR$	[1248]
		$D^{*+}\pi^-$		$20.0 \pm 1.7 \pm 1.3$	CDF	[1383]
		$D^0\pi^+\pi^-$	$2426 \pm 3 \pm 1$	$24 \pm 7 \pm 8$	$Belle$	[643]
		$D^{*+}\pi^-$	$2421.4 \pm 1.5 \pm 0.9$	$23.7 \pm 2.7 \pm 4.0$	$Belle$	[733]
		$D^{*+}\pi^-$	$2421^{+1}_{-2} \pm 2$	20^{+6+3}_{-5-3}	$CLEO$	[1384]
		$D^{*+}\pi^-$	$2422 \pm 2 \pm 2$	$15 \pm 8 \pm 4$	$E687$	[1368]
		$D^{*+}\pi^-$	$2428 \pm 3 \pm 2$	23^{+8+10}_{-6-4}	$CLEO$	[1371]
		$D^{*+}\pi^-$	$2414 \pm 2 \pm 5$	$13 \pm 6^{+10}_{-5}$	$ARGUS$	[1385]
		$D^{*+}\pi^-$	$2428 \pm 8 \pm 5$	$58 \pm 14 \pm 10$	TPS	[1386]
			2420.5 ± 0.5	31.7 ± 0.7	Our average	
$D_1(2420)^\pm$	1^+	$D^{*0}\pi^+$	$2421.9 \pm 4.7^{+3.4}_{-1.2}$		$Zeus$	[1382]
		$D^+\pi^-\pi^+$	$2421 \pm 2 \pm 1$	$21 \pm 5 \pm 8$	$Belle$	[643]
		$D^{*0}\pi^+$	$2425 \pm 2 \pm 2$	$26^{+8}_{-7} \pm 4$	$CLEO$	[1387]
		$D^{*0}\pi^+$	$2443 \pm 7 \pm 5$	$41 \pm 19 \pm 8$	TPS	[1386]
			2423.2 ± 1.6	25.2 ± 6.0	Our average	
$D_1(2430)^0$	1^+	$D^{*+}\pi^-$	$2427 \pm 26 \pm 25$	$384^{+107}_{-75} \pm 74$	$Belle$	[733]
$D_2^*(2460)^0$	2^+	$D^{*+}\pi^-$	$2464.0 \pm 1.4 \pm 0.5 \pm 0.2$	$43.8 \pm 2.9 \pm 1.7 \pm 0.6$	$LHCb$	[739]
		$D^{*+}\pi^-$	$2460.4 \pm 0.4 \pm 1.2$	$43.2 \pm 1.2 \pm 3.0$	$LHCb$	[1249]
		$D^+\pi^-$	$2460.4 \pm 0.1 \pm 0.1$	$45.6 \pm 0.4 \pm 1.1$	$LHCb$	[1249]
		$D^{*+}\pi^-, D^+\pi^-$	$2462.5 \pm 2.4^{+1.3}_{-1.1}$	$46.6 \pm 8.1^{+5.9}_{-3.8}$	$Zeus$	[1382]
		$D^+\pi^-$	$2462.2 \pm 0.1 \pm 0.8$	$50.5 \pm 0.6 \pm 0.7$	$BABAR$	[1248]
		$D^+\pi^-$	$2460.4 \pm 1.2 \pm 2.2$	$41.8 \pm 2.5 \pm 2.9$	$BABAR$	[734]
		$D^+\pi^-$		$49.2 \pm 2.3 \pm 1.3$	CDF	[1383]
		$D^+\pi^-$	$2461.6 \pm 2.1 \pm 3.3$	$45.6 \pm 4.4 \pm 6.7$	$Belle$	[733]
		$D^+\pi^-$	$2464.5 \pm 1.1 \pm 1.9$	$38.7 \pm 5.3 \pm 2.9$	$Focus$	[1347]
		$D^+\pi^-$	$2465 \pm 3 \pm 3$	$28^{+8}_{-7} \pm 6$	$CLEO$	[1384]
		$D^+\pi^-$	$2453 \pm 3 \pm 2$	$25 \pm 10 \pm 5$	$E687$	[1368]
		$D^{*+}\pi^-$	$2461 \pm 3 \pm 1$	20^{+9+9}_{-12-10}	$CLEO$	[1371]
		$D^+\pi^-$	$2455 \pm 3 \pm 5$	15^{+13+5}_{-10-10}	$ARGUS$	[1388]
		$D^+\pi^-$	$2459 \pm 3 \pm 2$	$20 \pm 10 \pm 5$	TPS	[1386]
		$D^+\pi^-$	$2463.7 \pm 0.4 \pm 0.4 \pm 0.6$	$47.0 \pm 0.8 \pm 0.9 \pm 0.3$	$LHCb$	[1346]
			2460.58 ± 0.14	47.42 ± 0.57	Our average	

Table 312: Recent measurements of mass and width for different excited D mesons. The column J^P list the most significant assignment of spin and parity. If possible an average mass or width is calculated.

Resonance	J^P	Decay mode	Mass [MeV/ c^2]	Width [MeV]	Measured by	Reference
$D_2^*(2460)^{\pm}$	2 ⁺	$D^0\pi^+$	$2468.6 \pm 0.6 \pm 0.0 \pm 0.3$	$47.3 \pm 1.5 \pm 0.3 \pm 0.6$	LHCb	[621]
		$D^0\pi^+$	$2465.6 \pm 1.8 \pm 0.5 \pm 1.2$	$46.0 \pm 3.4 \pm 1.4 \pm 2.9$	LHCb	[1381]
		$D^0\pi^+$	$2463.1 \pm 0.2 \pm 0.6$	$48.6 \pm 1.3 \pm 1.9$	LHCb	[1249]
		$D^{*0}\pi^+, D^0\pi^+$	$2460.6 \pm 4.4^{+3.6}_{-0.8}$		Zeus	[1382]
		$D^0\pi^+$	$2465.4 \pm 0.2 \pm 1.1$		$BABAR$	[1248]
		$D^0\pi^+$	$2465.7 \pm 1.8^{+1.4}_{-4.8}$	$49.7 \pm 3.8 \pm 6.4$	Belle	[614]
		$D^0\pi^+$	$2467.6 \pm 1.5 \pm 0.8$	$34.1 \pm 6.5 \pm 4.2$	Focus	[1347]
		$D^0\pi^+$	$2463 \pm 3 \pm 3$	$27^{+11}_{-8} \pm 5$	CLEO	[1387]
		$D^0\pi^+$	$2453 \pm 3 \pm 2$	$23 \pm 9 \pm 5$	E687	[1368]
		$D^0\pi^+$	$2469 \pm 4 \pm 6$		ARGUS	[1389]
				2465.55 ± 0.40	46.7 ± 1.2	Our average
$D(2550)^0$	0 ⁻	$D^{*+}\pi^-$	$2539.4 \pm 4.5 \pm 6.8$	$130 \pm 12 \pm 13$	$BABAR$	[1248]
$D(2580)^0$	Unnatural	$D^{*+}\pi^-$	$2579.5 \pm 3.4 \pm 5.5$	$117.5 \pm 17.8 \pm 46.0$	LHCb	[1249]
$D(2600)^0$	Natural	$D^+\pi^-$	$2608.7 \pm 2.4 \pm 2.5$	$93 \pm 6 \pm 13$	$BABAR$	[1248]
$D(2600)^{\pm}$	Natural	$D^0\pi^+$	$2621.3 \pm 3.7 \pm 4.2$		$BABAR$	[1248]
$D^*(2640)^{\pm}$	1 ⁻	$D^{*+}\pi^+\pi^-$	$2637 \pm 2 \pm 6$		Delphi	[1390]
$D^*(2650)^0$	Natural	$D^{*+}\pi^-$	$2649.2 \pm 3.5 \pm 3.5$	$140.2 \pm 17.1 \pm 18.6$	LHCb	[1249]
$D_1^*(2680)^0$	1 ⁻	$D^+\pi^-$	$2681.1 \pm 5.6 \pm 4.9 \pm 13.1$	$186.7 \pm 8.5 \pm 8.6 \pm 8.2$	LHCb	[1346]
$D(2740)^0$	Unnatural	$D^{*+}\pi^-$	$2737.0 \pm 3.5 \pm 11.2$	$73.2 \pm 13.4 \pm 25.0$	LHCb	[1249]
$D(2750)^0$		$D^{*+}\pi^-$	$2752.4 \pm 1.7 \pm 2.7$	$71 \pm 6 \pm 11$	$BABAR$	[1248]
$D_1^*(2760)^0$	1 ⁺	$D^+\pi^-$	$2781 \pm 18 \pm 11 \pm 6$	$177 \pm 32 \pm 20 \pm 7$	LHCb	[739]
		$D^{*+}\pi^-$	$2761.1 \pm 5.1 \pm 6.5$	$74.4 \pm 3.4 \pm 37.0$	LHCb	[1249]
		$D^+\pi^-$	$2760.1 \pm 1.1 \pm 3.7$	$74.4 \pm 3.4 \pm 19.1$	LHCb	[1249]
		$D^+\pi^-$	$2763.3 \pm 2.3 \pm 2.3$	$60.9 \pm 5.1 \pm 3.6$	$BABAR$	[1248]
			2762.1 ± 2.4	65.1 ± 5.8	Our average	
$D_3^*(2760)^0$	3 ⁻	$D^+\pi^-$	$2775.5 \pm 4.5 \pm 4.5 \pm 4.7$	$95.3 \pm 9.6 \pm 7.9 \pm 33.1$	LHCb	[1346]
$D_3^*(2760)^{\pm}$	3 ⁻	$D^0\pi^+$	$2798 \pm 7 \pm 1 \pm 7$	$105 \pm 18 \pm 6 \pm 23$	LHCb	[621]
		$D^0\pi^+$	$2771.7 \pm 1.7 \pm 3.8$	$66.7 \pm 6.6 \pm 10.5$	LHCb	[1249]
		$D^0\pi^+$	$2769.7 \pm 3.8 \pm 1.5$		$BABAR$	[1248]
			2773.9 ± 3.3	72.3 ± 11.5	Our average	
$D_2^*(3000)^0$	2 ⁺	$D^+\pi^-$	$3214 \pm 29 \pm 33 \pm 36$	$186 \pm 38 \pm 34 \pm 63$	LHCb	[1346]

Table 313: Product of B meson branching fraction and (daughter) excited D meson branching fraction.

Resonance	Decay	$\mathcal{B} [10^{-4}]$	Measured by	Reference
$D_0^*(2400)^0$	$B^- \rightarrow D_0^*(2400)^0(\rightarrow D^+\pi^-)\pi^-$	$6.1 \pm 0.6 \pm 1.8$	Belle	[733]
		$6.8 \pm 0.3 \pm 2.0$	$B\bar{B}AR$	[734]
		6.4 ± 1.4	Our average	
$D_0^*(2400)^\pm$	$B^- \rightarrow D_0^*(2400)^0(\rightarrow D^+\pi^-)K^-$	$0.061 \pm 0.019 \pm 0.005 \pm 0.014 \pm 0.004$	LHCb	[739]
	$\bar{B}^0 \rightarrow D_0^*(2400)^+(\rightarrow D^0\pi^+)\pi^-$	$0.77 \pm 0.05 \pm 0.03 \pm 0.03 \pm 0.04$ $0.60 \pm 0.13 \pm 0.27$	LHCb Belle	[621] [614]
$D_1(2420)^0$		0.76 ± 0.07	Our average	
	$\bar{B}^0 \rightarrow D_0^*(2400)^+(\rightarrow D^0\pi^+)K^-$	$0.177 \pm 0.026 \pm 0.019 \pm 0.067 \pm 0.20$	LHCb	[1381]
	$B^- \rightarrow D_1(2420)^0(\rightarrow D^{*+}\pi^-)\pi^-$	$6.8 \pm 0.7 \pm 1.3$	Belle	[733]
$D_1(2420)^\pm$	$B^- \rightarrow D_1(2420)^0(\rightarrow D^0\pi^+\pi^-)\pi^-$	$1.85 \pm 0.29 \pm 0.27 \pm 0.41$	Belle	[643]
	$\bar{B}^0 \rightarrow D_1(2420)^0(\rightarrow D^{*+}\pi^-)\omega$	$0.7 \pm 0.2_{-0.0}^{+0.1} \pm 0.1$	Belle	[617]
	$\bar{B}^0 \rightarrow D_1(2420)^+(\rightarrow D^+\pi^-\pi^+)\pi^-$	$0.89 \pm 0.15 \pm 0.22$	Belle	[643]
$D_1(2430)^0$	$B^- \rightarrow D_1(2430)^0(\rightarrow D^{*+}\pi^-)\pi^-$	$5.0 \pm 0.4 \pm 1.08$	Belle	[733]
	$\bar{B}^0 \rightarrow D_1(2430)^0(\rightarrow D^{*+}\pi^-)\omega$	$2.5 \pm 0.4_{-0.2-0.1}^{+0.7+0.4}$	Belle	[617]
$D_2^*(2460)^0$		$3.4 \pm 0.3 \pm 0.7$	Belle	[733]
	$B^- \rightarrow D_2^*(2460)^0(\rightarrow D^+\pi^-)\pi^-$	$3.5 \pm 0.2 \pm 0.5$	$B\bar{B}AR$	[734]
		$3.62 \pm 0.06 \pm 0.14 \pm 0.09 \pm 0.25$	LHCb	[1346]
		3.58 ± 0.23	Our average	
	$B^- \rightarrow D_2^*(2460)^0(\rightarrow D^{*+}\pi^-)\pi^-$	$1.8 \pm 0.3 \pm 0.4$	Belle	[733]
$D_2^*(2460)^\pm$	$B^- \rightarrow D_2^*(2460)^0(\rightarrow D^{*+}\pi^-)\omega$	$0.4 \pm 0.1_{-0.1}^{+0.0} \pm 0.1$	Belle	[617]
	$B^- \rightarrow D_2^*(2460)^0(\rightarrow D^+\pi^-)K^-$	$0.232 \pm 0.011 \pm 0.006 \pm 0.010 \pm 0.016$	LHCb	[739]
	$\bar{B}^0 \rightarrow D_2^*(2460)^+(\rightarrow D^0\pi^+)\pi^-$	$2.44 \pm 0.07 \pm 0.10 \pm 0.04 \pm 0.12$ $2.15 \pm 0.17 \pm 0.31$	LHCb Belle	[621] [614]
$D_3^*(2680)^0$		2.38 ± 0.16	Our average	
	$\bar{B}^0 \rightarrow D_2^*(2460)^+(\rightarrow D^0\pi^+)K^-$	$0.212 \pm 0.010 \pm 0.011 \pm 0.011 \pm 0.25$	LHCb	[1381]
	$B^- \rightarrow D_1^*(2680)^0(\rightarrow D^+\pi^-)\pi^-$	$0.84 \pm 0.06 \pm 0.07 \pm 0.18 \pm 0.06$	LHCb	[1346]
$D_1^*(2760)^0$	$B^- \rightarrow D_1^*(2760)^0(\rightarrow D^+\pi^-)K^-$	$0.036 \pm 0.009 \pm 0.003 \pm 0.007 \pm 0.002$	LHCb	[739]
$D_3^*(2760)^0$	$\bar{B}^- \rightarrow D_3^*(2760)^0(\rightarrow D^+\pi^-)\pi^-$	$0.10 \pm 0.01 \pm 0.01 \pm 0.02 \pm 0.01$	LHCb	[1346]
$D_3^*(2760)^\pm$	$\bar{B}^0 \rightarrow D_3^*(2760)^+(\rightarrow D^0\pi^+)\pi^-$	$0.103 \pm 0.016 \pm 0.007 \pm 0.008 \pm 0.005$	LHCb	[621]
$D_2^*(3000)^0$	$\bar{B}^0 \rightarrow D_2^*(3000)^0(\rightarrow D^+\pi^-)\pi^-$	$0.02 \pm 0.01 \pm 0.01 \pm 0.01 \pm 0.00$	LHCb	[1346]

Table 314: Product of B meson branching fraction and (daughter) excited D_s meson branching fraction.

Resonance	Decay	$\mathcal{B} [10^{-4}]$	Measured by	Reference
$D_{s0}^*(2317)^{\pm}$	$B^0 \rightarrow D_{s0}^*(2317)^+(\rightarrow D_s^+\pi^0)D^-$	$8.6^{+3.3}_{-2.6} \pm 2.6$ $18.0 \pm 4.0^{+6.7}_{-5.0}$ $10.1^{+1.3}_{-1.2} \pm 1.0 \pm 0.4$	Belle <i>BABAR</i> Belle	[661] [662] [663]
		10.2 ± 1.5	Our average	
	$B^+ \rightarrow D_{s0}^*(2317)^+(\rightarrow D_s^+\pi^0)\bar{D}^0$	$8.0^{+1.3}_{-1.2} \pm 1.0 \pm 0.4$	Belle	[663]
	$B^0 \rightarrow D_{s0}^*(2317)^+(\rightarrow D_s^+\pi^0)K^-$	$0.53^{+0.15}_{-0.13} \pm 0.16$	Belle	[644]
	$B^0 \rightarrow D_{s1}(2460)^+(\rightarrow D_s^{*+}\pi^0)D^-$	$22.7^{+7.3}_{-6.2} \pm 6.8$ $28.0 \pm 8.0^{+11.2}_{-7.8}$	Belle <i>BABAR</i>	[661] [662]
		24.7 ± 7.6	Our average	
	$B^0 \rightarrow D_{s1}(2460)^+(\rightarrow D_s^{*+}\gamma)D^-$	$8.2^{+2.2}_{-1.9} \pm 2.5$ $8.0 \pm 2.0^{+3.2}_{-2.3}$	Belle <i>BABAR</i>	[661] [662]
		8.1 ± 2.3	Our average	
	$D_{s1}(2460)^+ \rightarrow D_s^{*+}\pi^0$	$(56 \pm 13 \pm 9)\%$	<i>BABAR</i>	[656]
	$D_{s1}(2460)^+ \rightarrow D_s^{*+}\gamma$	$(16 \pm 4 \pm 3)\%$	<i>BABAR</i>	[656]
$D_{s1}(2536)^{\pm}$	$B^0 \rightarrow D_{s1}(2536)^+(\rightarrow D^{*0}K^+)D^-$	$1.71 \pm 0.48 \pm 0.32$	<i>BABAR</i>	[664]
	$B^0 \rightarrow D_{s1}(2536)^+(\rightarrow D^{*+}K^0)D^-$	$2.61 \pm 1.03 \pm 0.31$	<i>BABAR</i>	[664]
	$B^0 \rightarrow D_{s1}(2536)^+(\rightarrow D^{*0}K^+)D^{*-}$	$3.32 \pm 0.88 \pm 0.66$	<i>BABAR</i>	[664]
	$B^0 \rightarrow D_{s1}(2536)^+(\rightarrow D^{*+}K^0)D^{*-}$	$5.00 \pm 1.51 \pm 0.67$	<i>BABAR</i>	[664]
	$B^+ \rightarrow D_{s1}(2536)^+(\rightarrow D^{*0}K^+)\bar{D}^0$	$2.16 \pm 0.52 \pm 0.45$	<i>BABAR</i>	[664]
	$B^+ \rightarrow D_{s1}(2536)^+(\rightarrow D^{*+}K^0)\bar{D}^0$	$2.30 \pm 0.98 \pm 0.43$	<i>BABAR</i>	[664]
	$B^+ \rightarrow D_{s1}(2536)^+(\rightarrow D^{*0}K^+)\bar{D}^{*0}$	$5.46 \pm 1.17 \pm 1.04$	<i>BABAR</i>	[664]
	$B^+ \rightarrow D_{s1}(2536)^+(\rightarrow D^{*+}K^0)\bar{D}^{*0}$	$3.92 \pm 2.46 \pm 0.83$	<i>BABAR</i>	[664]
	$B^0 \rightarrow D_{s2}^*(2573)(\rightarrow D^0K^+)D^-$	$0.34 \pm 0.17 \pm 0.05$	<i>BABAR</i>	[1380]
	$B^+ \rightarrow D_{s2}^*(2573)(\rightarrow D^0K^+)\bar{D}^0$	$0.08 \pm 14 \pm 0.05$	<i>BABAR</i>	[1380]
$D_{s1}^*(2700)^{\pm}$	$B^+ \rightarrow D_{s1}^*(2700)^+(\rightarrow D^0K^+)\bar{D}^0$	$11.3 \pm 2.2^{+1.4}_{-2.8}$ $5.02 \pm 0.71 \pm 0.93$	Belle <i>BABAR</i>	[755] [1380]
		5.83 ± 1.09	Our average	
	$B^0 \rightarrow D_{s1}^*(2700)^+(\rightarrow D^0K^+)D^-$	$7.14 \pm 0.96 \pm 0.69$	<i>BABAR</i>	[1380]

Table 315: Mass difference measurements for excited D mesons.

Resonance	Relative to	Δm [MeV/ c^2]	Measured by	Reference
$D_1^*(2420)^0$	D^{*+}	$410.2 \pm 2.1 \pm 0.9$	Zeus	[1391]
		$411.7 \pm 0.7 \pm 0.4$	CDF	[1383]
		411.5 ± 0.8	Our average	
$D_1(2420)^\pm$	$D_1^*(2420)^0$	$4_{-3}^{+2} \pm 3$	CLEO	[1387]
$D_2^*(2460)^0$	D^+	$593.9 \pm 0.6 \pm 0.5$	CDF	[1383]
	D^{*+}	$458.8 \pm 3.7_{-1.3}^{+1.2}$	Zeus	[1391]
$D_2^*(2460)^\pm$	$D_2^*(2460)^0$	$3.1 \pm 1.9 \pm 0.9$	Focus	[1347]
		$-2 \pm 4 \pm 4$	CLEO	[1387]
		$14 \pm 5 \pm 8$	ARGUS	[1389]
		3.0 ± 1.9	Our average	
$D_{s0}^*(2317)^\pm$	D_s^\pm	$348.7 \pm 0.5 \pm 0.7$	Belle	[1344]
		$350.0 \pm 1.2 \pm 1.0$	CLEO	[1343]
		$351.3 \pm 2.1 \pm 1.9$	Belle	[661]
$D_{s1}(2460)^\pm$	$D_s^{*\pm}$	349.2 ± 0.7	Our average	
		$344.1 \pm 1.3 \pm 1.1$	Belle	[1344]
		$351.2 \pm 1.7 \pm 1.0$	CLEO	[1343]
		$346.8 \pm 1.6 \pm 1.9$	Belle	[661]
$D_{s1}(2460)^\pm$	D_s^\pm	347.1 ± 1.1	Our average	
		$491.0 \pm 1.3 \pm 1.9$	Belle	[1344]
		$491.4 \pm 0.9 \pm 1.5$	Belle	[1344]
$D_{s1}(2536)^\pm$	$D^*(2010)^\pm$	491.3 ± 1.4	Our average	
		$524.83 \pm 0.01 \pm 0.04$	<i>BABAR</i>	[1373]
		$525.30_{-0.41}^{+0.44} \pm 0.10$	Zeus	[1391]
		$525.3 \pm 0.6 \pm 0.1$	ALEPH	[1392]
		524.84 ± 0.04	Our average	
$D^*(2007)^0$	$D^*(2010)^\pm$	$528.7 \pm 1.9 \pm 0.5$	ALEPH	[1392]
$D_{s2}^*(2573)^\pm$	D^0	$704 \pm 3 \pm 1$	ALEPH	[1392]

Table 316: Measurements of polarization amplitudes for excited D mesons.

Resonance	A_D	Measured by	Reference
$D_1(2420)^0$	$7.8^{+6.7+4.6}_{-2.7-1.8}$	ZEUS	[1382]
	5.72 ± 0.25	BABAR	[1248]
	$5.9^{+3.0+2.4}_{-1.7-1.0}$	ZEUS	[1391]
	$3.8 \pm 0.6 \pm 0.8$	BABAR	[510]
5.61 \pm 0.24		Our average	
$D_1(2420)^{\pm}$	$3.8 \pm 0.6 \pm 0.8$	BABAR	[510]
$D_2^*(2460)^0$	-1.16 ± 0.35	ZEUS	[1382]
$D(2750)^0$	-0.33 ± 0.28	BABAR	[1248]

9.10 Excited charm baryons

In this section we summarize the present status of excited charmed baryons, decaying strongly or electromagnetically. We list their masses (or the mass difference between the excited baryon and the corresponding ground state), natural widths, decay modes, and assigned quantum numbers. The present ground-state measurements are: $M(\Lambda_c^+) = 2286.46 \pm 0.14 \text{ MeV}/c^2$ measured by *BABAR* [1393], $M(\Xi_c^0) = (2470.85^{+0.28}_{-0.04}) \text{ MeV}/c^2$ and $M(\Xi_c^+) = (2467.93^{+0.28}_{-0.40}) \text{ MeV}/c^2$, both dominated by *CDF* [150], and $M(\Omega_c^0) = (2695.2 \pm 1.7) \text{ MeV}/c^2$, dominated by *Belle* [1394]. Should these values change, so will some of the values for the masses of the excited states.

Table 317 summarizes the excited Λ_c^+ baryons. The first two states listed, namely the $\Lambda_c(2595)^+$ and $\Lambda_c(2625)^+$, are well-established. The measured masses and decay patterns suggest that they are orbitally excited Λ_c^+ baryons with total angular momentum of the light quarks $L = 1$. Thus their quantum numbers are assigned to be $J^P = (\frac{1}{2})^-$ and $J^P = (\frac{3}{2})^-$, respectively. Their mass measurements are dominated by *CDF* [1395]: $M(\Lambda_c(2595)^+) = (2592.25 \pm 0.24 \pm 0.14) \text{ MeV}/c^2$ and $M(\Lambda_c(2625)^+) = (2628.11 \pm 0.13 \pm 0.14) \text{ MeV}/c^2$. Earlier measurements did not fully take into account the restricted phase-space of the $\Lambda_c(2595)^+$ decays.

The next two states, $\Lambda_c(2765)^+$ and $\Lambda_c(2880)^+$, were discovered by *CLEO* [1396] in the $\Lambda_c^+\pi^+\pi^-$ final state. *CLEO* found that a significant fraction of the $\Lambda_c(2880)^+$ decays proceeds via an intermediate $\Sigma_c(2445)^{++/0}\pi^{-/+}$. Later, *BABAR* [1397] observed that this state has also a $D^0 p$ decay mode. This was the first example of an excited charmed baryon decaying into a charm meson plus a baryon; previously all excited charmed baryon were found in their hadronic transitions into lower lying charmed baryons. In the same analysis, *BABAR* observed for the first time an additional state, $\Lambda_c(2940)^+$, decaying into $D^0 p$. Studying the $D^+ p$ final state, *BABAR* found no signal; this implies that the $\Lambda_c(2880)^+$ and $\Lambda_c(2940)^+$ are Λ_c^+ excited states rather than Σ_c excitations. *Belle* reported the result of an angular analysis that favors 5/2 for the $\Lambda_c(2880)^+$ spin hypothesis. Moreover, the measured ratio of branching fractions $\mathcal{B}(\Lambda_c(2880)^+ \rightarrow \Sigma_c(2520)\pi^\pm)/\mathcal{B}(\Lambda_c(2880)^+ \rightarrow \Sigma_c(2455)\pi^\pm) = (0.225 \pm 0.062 \pm 0.025)$, combined with theoretical predictions based on HQS [503,1398], favor even parity. However this prediction is only valid if the P-wave portion of $\Sigma_c(2520)\pi$ is suppressed. *LHCb* [841] have analyzed the $D^0 p$ system in the resonant substructure of Λ_b decays. They confirm the 5/2 identification of the $\Lambda_c(2880)^+$. In addition they find evidence for a further, wider, state they name the $\Lambda_c(2860)^+$, with $J^P = 3/2^+$ (with the parity measured with respect to that of the $\Lambda_c(2880)^+$). The explanation for these states in the heavy quark-light diquark model is that they are a pair of orbital D-wave excitations. Furthermore, *LHCb* [841] find evidence for the spin-parity of the $\Lambda_c(2940)^+$ to be 3/2⁻, and improve the world average measurements of both the mass and width of this particle.

A current open question concerns the nature of the $\Lambda_c(2765)^+$ state, or even whether it is an excited Σ_c^+ or Λ_c^+ . However, there is no doubt that the state exists, as it is clearly visible in *Belle* [1399] and *LHCb* [1400] data.

Table 318 summarizes the excited $\Sigma_c^{++,+,0}$ baryons. The ground iso-triplets of $\Sigma_c(2455)^{++,+,0}$ and $\Sigma_c(2520)^{++,+,0}$ baryons are well-established. *Belle* [1401] precisely measured the mass differences and widths of the doubly charged and neutral members of this triplet. The short list of excited Σ_c baryons is completed by the triplet of $\Sigma_c(2800)$ states observed by *Belle* [1402]. Based on the measured masses and theoretical predictions [1403,1404], these states are assumed to be members of the predicted Σ_{c2} 3/2⁻ triplet. From a study of resonant substructure in

Table 317: Summary of excited Λ_c^+ baryons.

Charmed baryon excited state	Mode	Mass (MeV/ c^2)	Natural width (MeV)	J^P
$\Lambda_c(2595)^+$	$\Lambda_c^+ \pi^+ \pi^-$, $\Sigma_c(2455)\pi$	2592.25 ± 0.28	$2.59 \pm 0.30 \pm 0.47$	$1/2^-$
$\Lambda_c(2625)^+$	$\Lambda_c^+ \pi^+ \pi^-$	2628.11 ± 0.19	< 0.97	$3/2^-$
$\Lambda_c(2765)^+$	$\Lambda_c^+ \pi^+ \pi^-$, $\Sigma_c(2455)\pi$	2766.6 ± 2.4	50	?
$\Lambda_c(2860)^+$	$D^0 p$	$2856.1^{+2.0}_{-1.7} \pm 0.5^{+1.1}_{-5.6}$	$67.6^{+10.1}_{-8.1} \pm 1.4^{+5.9}_{-20.0}$	$3/2^+$
$\Lambda_c(2880)^+$	$\Lambda_c^+ \pi^+ \pi^-$, $\Sigma_c(2455)\pi$, $\Sigma_c(2520)\pi$, $D^0 p$	2881.63 ± 0.24	$5.6^{+0.8}_{-0.6} 0.8$	$5/2^+$
$\Lambda_c(2940)^+$	$D^0 p$, $\Sigma_c(2455)\pi$	$2939.6^{+1.3}_{-1.5}$	20^{+6}_{-5}	?

$B^- \rightarrow \Lambda_c^+ \bar{p} \pi^-$ decays, *BABAR* found a significant signal in the $\Lambda_c^+ \pi^-$ final state with a mean value higher than measured for the $\Sigma_c(2800)$ by *Belle* by about 3σ (Table 318). The decay widths measured by *Belle* and *BABAR* are consistent, but it is an open question if the observed state is the same as the *Belle* state.

 Table 318: Summary of the excited $\Sigma_c^{++,+,0}$ baryon family.

Charmed baryon excited state	Mode	ΔM (MeV/ c^2)	Natural width (MeV)	J^P
$\Sigma_c(2455)^{++}$	$\Lambda_c^+ \pi^+$	167.510 ± 0.17	$1.89^{+0.09}_{-0.18}$	$1/2^+$
$\Sigma_c(2455)^+$	$\Lambda_c^+ \pi^0$	166.4 ± 0.4	< 4.6 @ 90% C.L.	$1/2^+$
$\Sigma_c(2455)^0$	$\Lambda_c^+ \pi^-$	167.29 ± 0.17	$1.83^{+0.11}_{-0.19}$	$1/2^+$
$\Sigma_c(2520)^{++}$	$\Lambda_c^+ \pi^+$	$231.95^{+0.17}_{-0.12}$	$14.78^{+0.30}_{-0.40}$	$3/2^+$
$\Sigma_c(2520)^+$	$\Lambda_c^+ \pi^0$	231.0 ± 2.3	< 17 @ 90% C.L.	$3/2^+$
$\Sigma_c(2520)^0$	$\Lambda_c^+ \pi^-$	$232.02^{+0.15}_{-0.14}$	$15.3^{+0.4}_{-0.5}$	$3/2^+$
$\Sigma_c(2800)^{++}$	$\Lambda_c^+ \pi^+$	514^{+4}_{-6}	75^{+18+12}_{-13-11}	$3/2^-$
$\Sigma_c(2800)^+$	$\Lambda_c^+ \pi^0$	505^{+15}_{-5}	62^{+37+52}_{-23-38}	
$\Sigma_c(2800)^0$	$\Lambda_c^+ \pi^-$	519^{+5}_{-7}	72^{+22}_{-15}	
	$\Lambda_c^+ \pi^-$	$560 \pm 8 \pm 10$	86^{+33}_{-22}	

Table 319 summarizes the excited $\Xi_c^{+,0}$. The list of excited Ξ_c baryons has several states, of unknown quantum numbers, having masses above 2900 MeV/ c^2 and decaying into three different types of decay modes: $\Lambda_c/\Sigma_c n \pi$, $\Xi_c n \pi$ and the most recently observed AD . Some of these states ($\Xi_c(2970)^+$, $\Xi_c(3055)$ and $\Xi_c(3080)^{+,0}$) have been observed by both *Belle* [1405–1407] and *BABAR* [716], are produced in the charm continuum, and are considered well-established. The $\Xi_c(2930)^0$ state decaying into $\Lambda_c^+ K^-$, first reported by *BABAR* [1408] in B decays, has now

been observed by Belle [776]. The latter analysis includes a study of the effects of possible interference and other resonances in the mass distribution, and these are reflected in the large negative systematic uncertainty. As the *BABAR* [1408] paper only "suggests the presence of a Ξ_c^0 resonance", we quote the mass and width measured by Belle [776] rather than a weighted sum of the two measurements. Furthermore, Belle [1409] have reported evidence of its charged partner. It is unclear if the fact that it has been seen in B decays rather than charm continuum can be used to help identify the state.

The $\Xi_c(3123)^+$ reported by *BABAR* [716] in the $\Sigma_c(2520)^{++}\pi^-$ final state has not been confirmed by Belle [1406] with twice the statistics; thus its existence is in doubt and it is omitted from Tab. 319.

Several of the width and mass measurements for the $\Xi_c(3055)$ and $\Xi_c(3080)$ iso-doublets are only in marginal agreement between experiments and decay modes. However, there seems little doubt that the differing measurements are of the same particle.

Belle [1410] has recently analyzed large samples of Ξ'_c , $\Xi_c(2645)$, $\Xi_c(2790)$, $\Xi_c(2815)$ and $\Xi_c(2970)$ decays. From this analysis they obtain the most precise mass measurements of all five iso-doublets, and the first significant width measurements of the $\Xi_c(2645)$, $\Xi_c(2790)$ and $\Xi_c(2815)$. The level of agreement in the different measurements of the mass and width of the $\Xi_c(2970)$, formerly named by the PDG as the $\Xi_c(2980)$, is not satisfactory. This leaves open the possibility of there being other resonances nearby or that threshold effects have not been fully understood. The present situation in the excited Ξ_c sector is summarized in Table 319.

The Ω_c^{*0} doubly-strange charmed baryon has been seen by both *BABAR* [1411] and Belle [1394]. The mass differences $\delta M = M(\Omega_c^{*0}) - M(\Omega_c^0)$ measured by the experiments are in good agreement and are also consistent with most theoretical predictions [1412–1415]. Recently LHCb [1416] have found a family of 5 excited Ω_c^0 baryons decaying into $\Xi_c^+ K^-$. The natural explanation is that they are the 5 states with $L=1$ between the heavy quark and the light (ss) di-quark; however, there is no consensus as to which state is which, and this overall interpretation is controversial. Four of the five states have been confirmed by Belle [1417] and, although the Belle dataset is much smaller than that of LHCb, these mass measurements do contribute to the world averages. There is evidence for a further, wider, state at higher mass in the LHCb data. Belle show a small excess in the same region, but it is of low significance.

Figure 106 shows the levels of excited charm baryons along with corresponding transitions between them, and also transitions to the ground states. We note that Belle and *BABAR* recently discovered that transitions between families are possible, *i.e.*, between the Ξ_c and Λ_c^+ families of excited charmed baryons [716, 1405] and that highly excited states are found to decay into a non-charmed baryons and a D meson [1397, 1407].

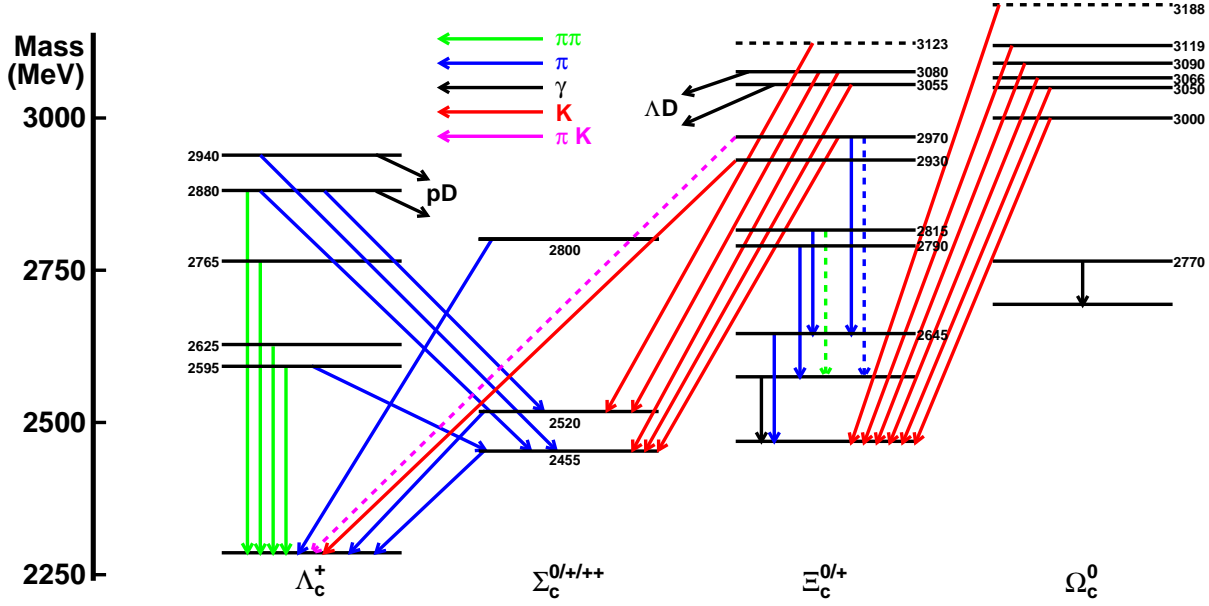


Figure 106: Level diagram for multiplets and transitions for excited charm baryons.

Table 319: Summary of excited $\Xi_c^{+,0}$ states. For the first four iso-doublets, the mass difference with respect to the ground state is given, as the uncertainties are dominated by the uncertainty in the ground state mass. In the remaining cases, the uncertainty on the measurement of the excited state itself dominates.

Charmed baryon excited state	Mode	Mass difference (MeV/ c^2)	Natural width (MeV)	J^P
$\Xi_c'^+$	$\Xi_c^+ \gamma$	110.5 ± 0.4		$1/2^+$
$\Xi_c'^0$	$\Xi_c^0 \gamma$	108.3 ± 0.4		$1/2^+$
$\Xi_c(2645)^+$	$\Xi_c^0 \pi^+$	178.5 ± 0.1	2.1 ± 0.2	$3/2^+$
$\Xi_c(2645)^0$	$\Xi_c^+ \pi^-$	174.7 ± 0.1	2.4 ± 0.2	$3/2^+$
$\Xi_c(2790)^+$	$\Xi_c'^0 \pi^+$	320.7 ± 0.5	9 ± 1	$1/2^-$
$\Xi_c(2790)^0$	$\Xi_c'^+ \pi^-$	323.8 ± 0.5	10 ± 1	$1/2^-$
$\Xi_c(2815)^+$	$\Xi_c(2645)^0 \pi^+$	348.8 ± 0.1	2.43 ± 0.23	$3/2^-$
$\Xi_c(2815)^0$	$\Xi_c(2645)^+ \pi^-$	349.4 ± 0.1	2.54 ± 0.23	$3/2^-$
Charmed baryon excited state	Mode	Mass (MeV/ c^2)	Natural width (MeV)	J^P
$\Xi_c(2930)^+$	$\Lambda_c^+ K_S^0$	$2942.3 \pm 4.4 \pm 1.5$	$14.8 \pm 8.8 \pm 2.5$?
$\Xi_c(2930)^0$	$\Lambda_c^+ K^-$	$2928.6 \pm 3_{-12.0}^{+0.9}$	$19.5 \pm 8.4_{-7.9}^{+5.9}$?
$\Xi_c(2970)^+$	$\Lambda_c^+ K^- \pi^+, \Sigma_c^{++} K^-, \Xi_c(2645)^0 \pi^+$	2967.2 ± 0.8	21 ± 3	?
$\Xi_c(2970)^0$	$\Xi_c(2645)^+ \pi^-$	2970.4 ± 0.8	28 ± 3	?
$\Xi_c(3055)^+$	$\Sigma_c^{++} K^-, \Delta D$	3055.7 ± 0.4	8.0 ± 1.9	?
$\Xi_c(3055)^0$	ΔD	3059.0 ± 0.8	6.2 ± 2.4	?
$\Xi_c(3080)^+$	$\Lambda_c^+ K^- \pi^+, \Sigma_c^{++} K^-, \Sigma_c(2520)^{++} K^-, \Delta D$	3077.8 ± 0.3	3.6 ± 0.7	?
$\Xi_c(3080)^0$	$\Lambda_c^+ K_S^0 \pi^-, \Sigma_c^0 K_S^0, \Sigma_c(2520)^0 K_S^0$	3079.9 ± 1.0	5.6 ± 2.2	?

Table 320: Summary of excited Ω_c^0 baryons. For the $\Omega_c(2770)^0$, the mass difference with respect to the ground state is given, as the uncertainty is dominated by the uncertainty in the ground state mass. In the remaining cases the total mass is shown, though the uncertainty in the Ξ_c^+ mass makes an important contribution to the total uncertainty.

Charmed baryon excited state	Mode	Mass difference (MeV/ c^2)	Natural width (MeV)	J^P
$\Omega_c(2770)^0$	$\Omega_c^0\gamma$	$70.7^{+0.8}_{-0.9}$		$3/2^+$
Charmed baryon excited state	Mode	Mass (MeV/ c^2)	Natural width (MeV)	J^P
$\Omega_c(3000)^0$	$\Xi_c^+K^-$	3000.4 ± 0.4	4.5 ± 0.7	?
$\Omega_c(3050)^0$	$\Xi_c^+K^-$	3050.2 ± 0.3	< 1.2	?
$\Omega_c(3065)^0$	$\Xi_c^+K^-$	3065.5 ± 0.4	3.5 ± 0.5	?
$\Omega_c(3090)^0$	$\Xi_c^+K^-$	3090.0 ± 0.6	8.7 ± 1.4	?
$\Omega_c(3120)^0$	$\Xi_c^+K^-$	3119.1 ± 1.0	< 2.6	?

9.11 Rare and forbidden decays

This section provides a summary of searches for rare and forbidden charm decays in tabular form. The decay modes can be categorized as flavor-changing neutral currents and radiative, lepton-flavor-violating, lepton-number-violating, and both baryon- and lepton-number-violating decays. Figures 107-109 plot the upper limits for D^0 , D^+ , D_s^+ , and A_c^+ decays. Tables 321-324 give the corresponding numerical results. Some theoretical predictions are given in Refs. [1418–1425].

Some D^0 decay modes have been observed and are quoted as a branching fraction with uncertainties in the tables and shown as a symbol with a line representing the 68% C.L. interval in the plots.

In several cases the rare-decay final states have been observed with the di-lepton pair being the decay product of a vector meson. For these measurements the quoted limits are those expected for the non-resonant di-lepton spectrum. For the extrapolation to the full spectrum a phase-space distribution of the non-resonant component has been assumed. This applies to the CLEO measurement of the decays $D_{(s)}^+ \rightarrow (K^+, \pi^+)e^+e^-$ [1426], to the D0 measurements of the decays $D_{(s)}^+ \rightarrow \pi^+\mu^+\mu^-$ [1427], and to the *BABAR* measurements of the decays $D_{(s)}^+ \rightarrow (K^+, \pi^+)e^+e^-$ and $D_{(s)}^+ \rightarrow (K^+, \pi^+)\mu^+\mu^-$, where the contribution from $\phi \rightarrow l^+l^-$ ($l = e, \mu$) has been excluded. In the case of the LHCb measurements of the decays $D^0 \rightarrow \pi^+\pi^-\mu^+\mu^-$ [1428] as well as the decays $D_{(s)}^+ \rightarrow \pi^+\mu^+\mu^-$ [1429] the contributions from $\phi \rightarrow l^+l^-$ as well as from $\rho, \omega \rightarrow l^+l^-$ ($l = e, \mu$) have been excluded.

Table 321: Upper limits for branching fractions at 90% C.L. for D^0 decays.

Where values are quoted with uncertainties, these refer to observed branching fractions with the first uncertainty being statistical and all others systematic as detailed in the corresponding reference.

Decay	$BF \times 10^6$	Experiment	Reference
$\gamma\gamma$	26.0	CLEO II	[1430]
	3.8	BESIII	[1431]
	2.2	BaBar	[1432]
	0.85	Belle	[1433]
e^+e^-	220.0	CLEO	[1434]
	170.0	Argus	[1435]
	130.0	Mark3	[1436]
	13.0	CLEO II	[1437]
	8.19	E789	[1438]
	6.2	E791	[1439]
	1.2	BaBar	[1440]
	0.079	Belle	[1441]
$\mu^+\mu^-$	70.0	Argus	[1435]
	44.0	E653	[1442]
	34.0	CLEO II	[1437]
	15.6	E789	[1438]
	5.2	E791	[1439]

Table 321 – continued from previous page

Decay	$\text{BF} \times 10^6$	Experiment	Reference
$\pi^0 e^+ e^-$	2.0	HERAb	[1443]
	1.3	BaBar	[1440]
	0.21	CDF	[1444]
	0.14	Belle	[1441]
	0.0062	LHCb	[1445]
$\pi^0 \mu^+ \mu^-$	45.0	CLEO II	[1437]
	4.0	BESIII	[1446]
$\pi^0 \eta \mu^+ \mu^-$	540.0	CLEO II	[1437]
	180.0	E653	[1442]
$\eta e^+ e^-$	110.0	CLEO II	[1437]
	3.0	BESIII	[1446]
$\eta \mu^+ \mu^-$	530.0	CLEO II	[1437]
$\pi^+ \pi^- e^+ e^-$	370.0	E791	[1447]
	7.0	BESIII	[1446]
$K_S e^+ e^-$	12.0	BESIII	[1446]
$\rho^0 e^+ e^-$	450.0	CLEO	[1434]
	124.0	E791	[1447]
	100.0	CLEO II	[1437]
$\pi^+ \pi^- \mu^+ \mu^-$	30.0	E791	[1447]
	$0.964 \pm 0.048 \pm 0.051 \pm 0.097$	LHCb	[1448]
$\rho^0 \mu^+ \mu^-$	810.0	CLEO	[1434]
	490.0	CLEO II	[1437]
	230.0	E653	[1442]
	22.0	E791	[1447]
$\omega e^+ e^-$	180.0	CLEO II	[1437]
	6.0	BESIII	[1446]
$\omega \mu^+ \mu^-$	830.0	CLEO II	[1437]
$K^+ K^- e^+ e^-$	315.0	E791	[1447]
	11.0	BESIII	[1446]
$\phi e^+ e^-$	59.0	E791	[1447]
	52.0	CLEO II	[1437]
$K^+ K^- \mu^+ \mu^-$	33.0	E791	[1447]
	$0.154 \pm 0.027 \pm 0.009 \pm 0.016$	LHCb	[1448]
$\phi \mu^+ \mu^-$	410.0	CLEO II	[1437]
	31.0	E791	[1447]
$\bar{K}^0 e^+ e^-$	1700.0	Mark3	[1449]
	110.0	CLEO II	[1437]
$\bar{K}^0 \mu^+ \mu^-$	670.0	CLEO II	[1437]
	260.0	E653	[1442]
$K^- \pi^+ e^+ e^-$	385.0	E791	[1447]

Table 321 – continued from previous page

Decay	$\text{BF} \times 10^6$	Experiment	Reference
	41.0	BESIII	[1446]
$\bar{K}^*(892)^0 e^+ e^-$	140.0	CLEO II	[1437]
	47.0	E791	[1447]
$K^- \pi^+ \mu^+ \mu^-$	360.0	E791	[1447]
$\bar{K}^*(892)^0 \mu^+ \mu^-$	1180.0	CLEO II	[1437]
	24.0	E791	[1447]
$\pi^+ \pi^- \pi^0 \mu^+ \mu^-$	810.0	E653	[1442]
$\rho^0 \gamma$	240.0	CLEO II	[1450]
	$17.7 \pm 3.0 \pm 0.7$	Belle	[1217]
$\omega \gamma$	240.0	CLEO II	[1450]
$\bar{K}^*(892)^0 \gamma$	760.0	CLEO II	[1450]
	$322.0 \pm 20.0 \pm 27.0$	BaBar	[1451]
$\phi \gamma$	190.0	CLEO II	[1450]
	$27.3 \pm 3.0 \pm 2.6$	BaBar	[1451]
$\mu^\pm e^\mp$	270.0	CLEO	[1434]
	120.0	Mark3	[1452]
	100.0	Argus	[1435]
	19.0	CLEO II	[1437]
	17.2	E789	[1438]
	8.1	E791	[1439]
	0.81	BaBar	[1440]
	0.26	Belle	[1441]
	0.016	LHCb	[1453]
$\pi^0 e^\pm \mu^\mp$	86.0	CLEO II	[1437]
$\eta e^\pm \mu^\mp$	100.0	CLEO II	[1437]
$\pi^+ \pi^- e^\pm \mu^\mp$	15.0	E791	[1447]
$\rho^0 e^\pm \mu^\mp$	66.0	E791	[1447]
	49.0	CLEO II	[1437]
$\omega e^\pm \mu^\mp$	120.0	CLEO II	[1437]
$K^+ K^- e^\pm \mu^\mp$	180.0	E791	[1447]
$\phi e^\pm \mu^\mp$	47.0	E791	[1447]
	34.0	CLEO II	[1437]
$\bar{K}^0 e^\pm \mu^\mp$	100.0	CLEO II	[1437]
$K^- \pi^+ e^\pm \mu^\mp$	550.0	E791	[1447]
$\bar{K}^*(892)^0 e^\pm \mu^\mp$	100.0	CLEO II	[1437]
	83.0	E791	[1447]
$\pi^\mp \pi^\mp e^\pm e^\pm$	112.0	E791	[1447]
$\pi^\mp \pi^\mp \mu^\pm \mu^\pm$	29.0	E791	[1447]
$K^\mp \pi^\mp e^\pm e^\pm$	206.0	E791	[1447]

Table 321 – continued from previous page

Decay	$\text{BF} \times 10^6$	Experiment	Reference
$K^\mp\pi^\mp\mu^\pm\mu^\pm$	390.0	E791	[1447]
$K^\mp K^\mp e^\pm e^\pm$	152.0	E791	[1447]
$K^\mp K^\mp\mu^\pm\mu^\pm$	94.0	E791	[1447]
$\pi^\mp\pi^\mp e^\pm\mu^\pm$	79.0	E791	[1447]
$K^\mp\pi^\mp e^\pm\mu^\pm$	218.0	E791	[1447]
$K^\mp K^\mp e^\pm\mu^\pm$	57.0	E791	[1447]
$p e^-$	10.0	CLEO	[1454]
$\bar{p} e^+$	11.0	CLEO	[1454]

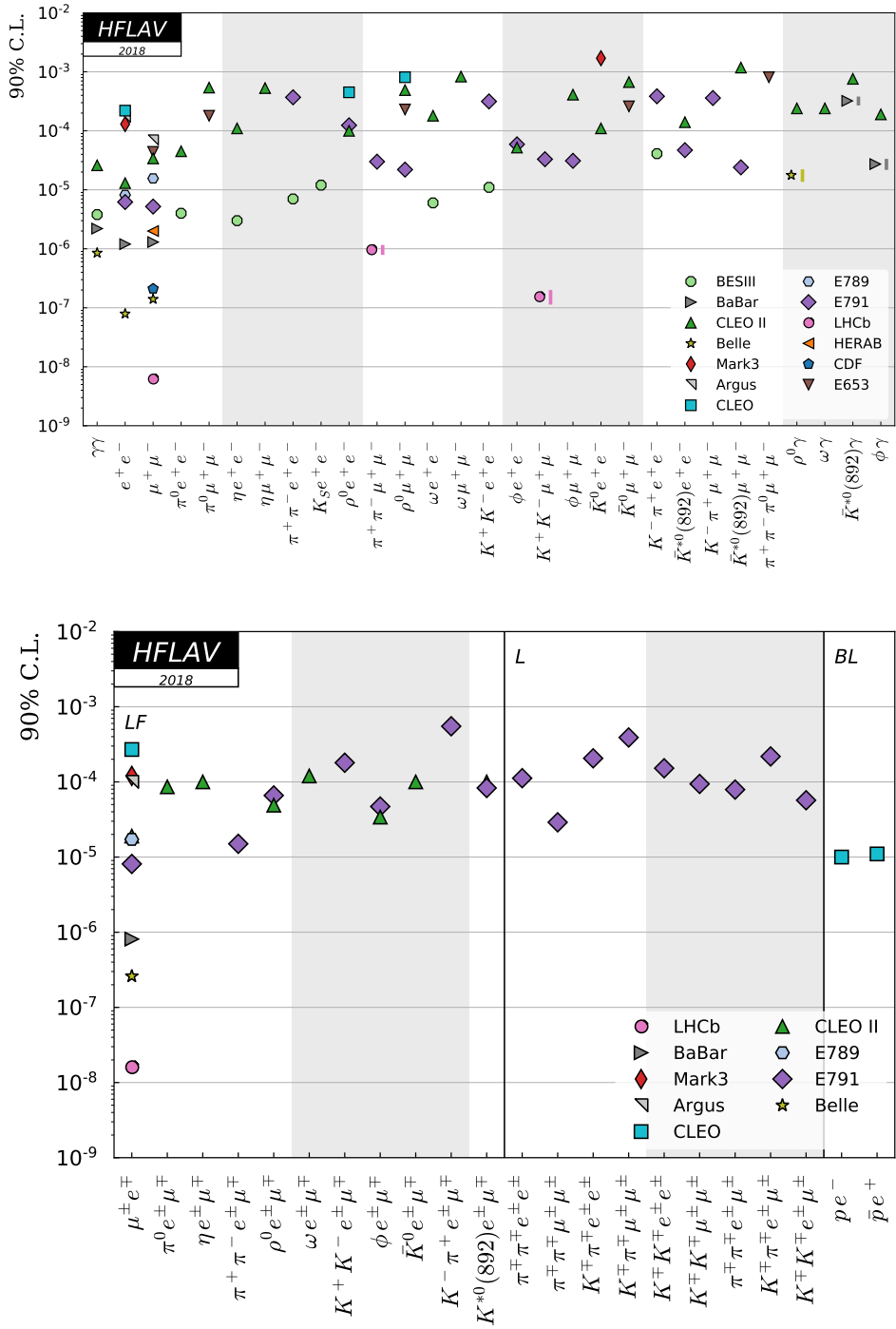


Figure 107: Upper limits at 90% C.L. for D^0 decays. The top plot shows flavor-changing neutral current decays, and the bottom plot shows lepton-flavor-changing (LF), lepton-number-changing (L), and both baryon- and lepton-number-changing (BL) decays.

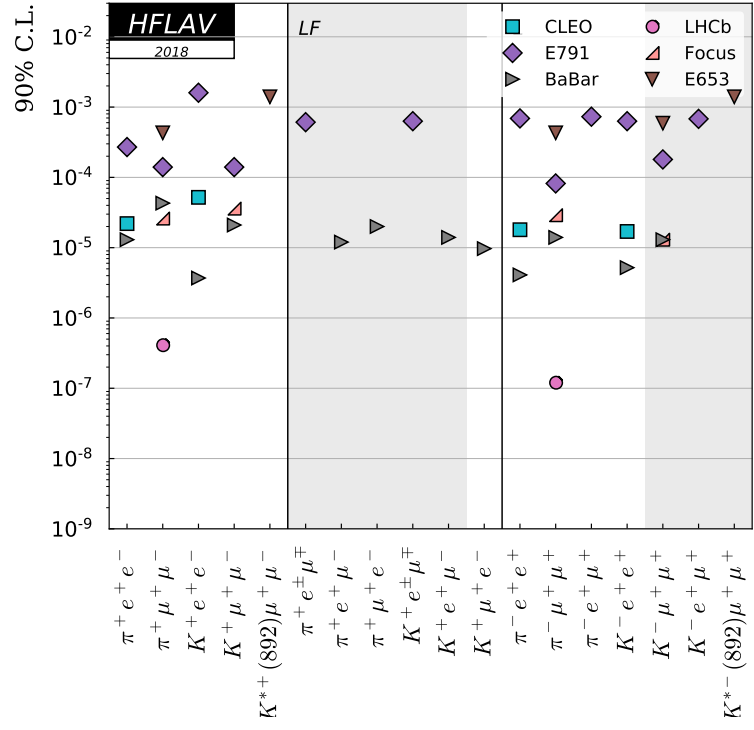
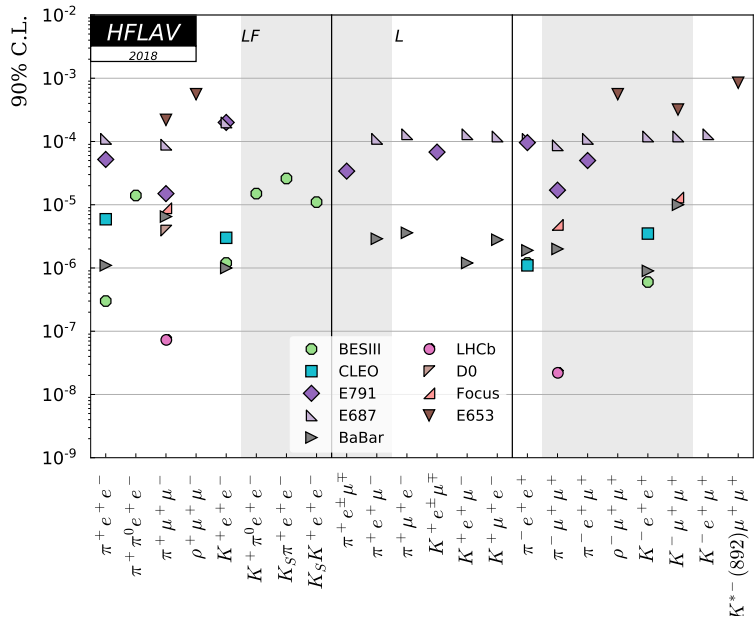


Figure 108: Upper limits at 90% C.L. for D^+ (top) and D_s^+ (bottom) decays. Each plot shows flavor-changing neutral current decays, lepton-flavor-changing decays (LF), and lepton-number-changing (L) decays.

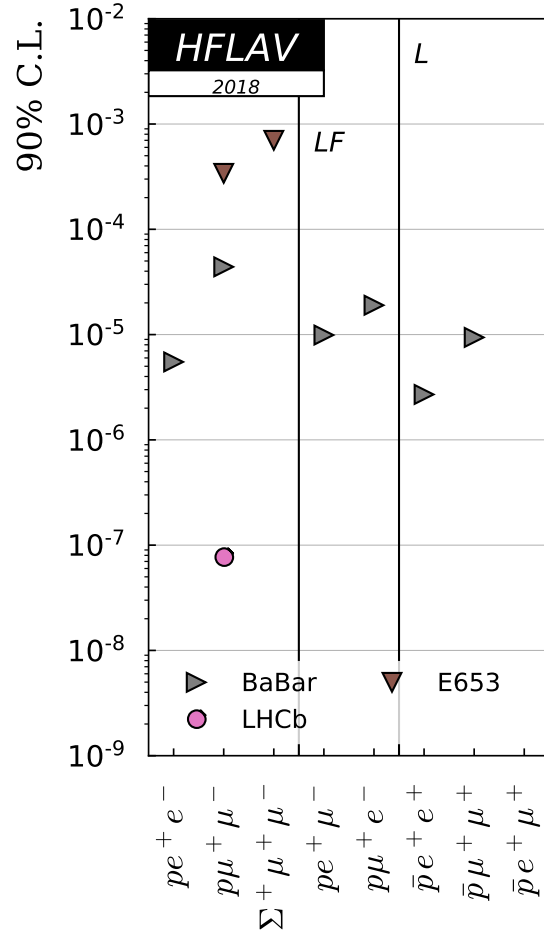


Figure 109: Upper limits at 90% C.L. for A_c^+ decays. Shown are flavor-changing neutral current decays, lepton-flavor-changing (LF) decays, and lepton-number-changing (L) decays.

Table 322: Upper limits at 90% C.L. for D^+ decays.

Decay	Limit $\times 10^6$	Experiment	Reference
$\pi^+ e^+ e^-$	110.0	E687	[1455]
	52.0	E791	[1439]
	5.9	CLEO	[1426]
	1.1	BaBar	[1456]
	0.3	BESIII	[1457]
$\pi^+ \pi^0 e^+ e^-$	14.0	BESIII	[1446]
$\pi^+ \mu^+ \mu^-$	220.0	E653	[1442]
	89.0	E687	[1455]
	15.0	E791	[1439]
	8.8	Focus	[1458]

Table 322 – continued from previous page

Decay	Limit $\times 10^6$	Experiment	Reference
$K^+\mu^+\mu^-$	6.5	BaBar	[1456]
	3.9	D0	[1427]
	0.073	LHCb	[1429]
$K^+\mu^+\mu^-$	97.0	E687	[1455]
	44.0	E791	[1439]
	9.2	Focus	[1458]
	4.3	BaBar	[1456]
$\rho^+\mu^+\mu^-$	560.0	E653	[1442]
$K^+e^+e^-$	200.0	E687	[1455]
	3.0	CLEO	[1426]
	1.2	BESIII	[1457]
	1.0	BaBar	[1456]
$K^+\pi^0e^+e^-$	15.0	BESIII	[1446]
$K_S\pi^+e^+e^-$	26.0	BESIII	[1446]
$K_SK^+e^+e^-$	11.0	BESIII	[1446]
$\pi^+e^\pm\mu^\mp$	34.0	E791	[1439]
$\pi^+e^+\mu^-$	110.0	E687	[1455]
	2.9	BaBar	[1456]
$\pi^+\mu^+e^-$	130.0	E687	[1455]
	3.6	BaBar	[1456]
$K^+e^\pm\mu^\mp$	68.0	E791	[1439]
$K^+e^+\mu^-$	130.0	E687	[1455]
	1.2	BaBar	[1456]
$K^+\mu^+e^-$	120.0	E687	[1455]
	2.8	BaBar	[1456]
$\pi^-e^+e^+$	110.0	E687	[1455]
	96.0	E791	[1439]
	1.9	BaBar	[1456]
	1.2	BESIII	[1457]
	1.1	CLEO	[1426]
$\pi^-\mu^+\mu^+$	87.0	E687	[1455]
	17.0	E791	[1439]
	4.8	Focus	[1458]
	2.0	BaBar	[1456]
	0.022	LHCb	[1429]
$\pi^-e^+\mu^+$	110.0	E687	[1455]
	50.0	E791	[1439]
	2.0	BaBar	[1456]
$\rho^-\mu^+\mu^+$	560.0	E653	[1442]
$K^-e^+e^+$	120.0	E687	[1455]

Table 322 – continued from previous page

Decay	Limit $\times 10^6$	Experiment	Reference
$K^- \mu^+ \mu^+$	3.5	CLEO	[1426]
	0.9	BaBar	[1456]
	0.6	BESIII	[1457]
$K^- e^+ \mu^+$	320.0	E653	[1442]
	120.0	E687	[1455]
	13.0	Focus	[1458]
	10.0	BaBar	[1456]
$K^*(892)^- \mu^+ \mu^+$	130.0	E687	[1455]
$K^*(892)^- \mu^+ \mu^+$	850.0	E653	[1442]

Table 323: Upper limits at 90% C.L. for D_s^+ decays.

Decay	Limit $\times 10^6$	Experiment	Reference
$\pi^+ e^+ e^-$	270.0	E791	[1439]
	22.0	CLEO	[1426]
	13.0	BaBar	[1456]
$\pi^+ \mu^+ \mu^-$	430.0	E653	[1442]
	140.0	E791	[1439]
	43.0	BaBar	[1456]
	26.0	Focus	[1458]
	0.41	LHCb	[1429]
$K^+ e^+ e^-$	1600.0	E791	[1439]
	52.0	CLEO	[1426]
	3.7	BaBar	[1456]
$K^+ \mu^+ \mu^-$	140.0	E791	[1439]
	36.0	Focus	[1458]
	21.0	BaBar	[1456]
$K^*(892)^+ \mu^+ \mu^-$	1400.0	E653	[1442]
$\pi^+ e^\pm \mu^\mp$	610.0	E791	[1439]
$\pi^+ e^+ \mu^-$	12.0	BaBar	[1456]
$\pi^+ \mu^+ e^-$	20.0	BaBar	[1456]
$K^+ e^\pm \mu^\mp$	630.0	E791	[1439]
$K^+ e^+ \mu^-$	14.0	BaBar	[1456]
$K^+ \mu^+ e^-$	9.7	BaBar	[1456]
$\pi^- e^+ e^+$	690.0	E791	[1439]
	18.0	CLEO	[1426]
	4.1	BaBar	[1456]
$\pi^- \mu^+ \mu^+$	430.0	E653	[1442]
	82.0	E791	[1439]
	29.0	Focus	[1458]

Table 323 – continued from previous page

Decay	Limit $\times 10^6$	Experiment	Reference
$\pi^- e^+ \mu^+$	14.0	BaBar	[1456]
	0.12	LHCb	[1429]
$K^- e^+ e^+$	730.0	E791	[1439]
	8.4	BaBar	[1456]
$K^- \mu^+ \mu^+$	630.0	E791	[1439]
	17.0	CLEO	[1426]
	5.2	BaBar	[1456]
$K^- e^+ \mu^+$	590.0	E653	[1442]
	180.0	E791	[1439]
	13.0	BaBar	[1456]
$K^*(892)^- \mu^+ \mu^+$	680.0	E791	[1439]
	6.1	BaBar	[1456]
$K^*(892)^- \mu^+ \mu^+$	1400.0	E653	[1442]

Table 324: Upper limits at 90% C.L. for Λ_c^+ decays.

Decay	Limit $\times 10^6$	Experiment	Reference
pe^+e^-	5.5	BaBar	[1456]
$p\mu^+\mu^-$	340.0	E653	[1442]
	44.0	BaBar	[1456]
	0.077	LHCb	[1459]
$\Sigma^+\mu^+\mu^-$	700.0	E653	[1442]
$pe^+\mu^-$	9.9	BaBar	[1456]
$p\mu^+e^-$	19.0	BaBar	[1456]
$\bar{p}e^+e^+$	2.7	BaBar	[1456]
$\bar{p}\mu^+\mu^+$	9.4	BaBar	[1456]
$\bar{p}e^+\mu^+$	16.0	BaBar	[1456]

10 Tau lepton properties

This section reports averages and elaborations of τ branching fractions, and combinations of upper limits on τ branching fractions to lepton-flavour-violating τ decay modes.

Branching fractions averages are obtained with a fit of τ branching fractions measurements aimed at optimally exploiting the available experimental information and described in Section 10.1. The fit results are used in Section 10.2 to test the lepton-flavor universality of the charged-current weak interaction. The “universality-improved” [1460] branching fraction $\mathcal{B}_e = \mathcal{B}(\tau \rightarrow e\nu\bar{\nu})$ and the ratio between the hadronic branching fraction and \mathcal{B}_e , are obtained in Section 10.3. The value of the Cabibbo-Kobayashi-Maskawa (CKM) matrix element $|V_{us}|$ from τ decays is given in Section 10.4. Combinations of upper limits on lepton-flavour-violating τ branching fractions are computed in Section 10.5. All results are obtained from inputs available through the end of 2018.

10.1 Branching fraction fit

A fit of the available experimental measurements is used to determine the τ branching fractions, together with their uncertainties and correlations.

All relevant published statistical and systematic correlations among the measurements are used. In addition, for a selection of measurements, particularly the most precise and the most recent ones, the documented systematic uncertainty contributions are examined to consider systematic dependencies from external parameters. The measurements are updated to reflect updates of their relevant external parameters, and implicit correlations due to the fact that multiple measurements depend on a common external parameter are used in the fit.

Both the measurements and the fitted quantities consist of either τ decay branching fractions, labelled as \mathcal{B}_i , or ratios of two τ decay branching fractions, labelled as $\mathcal{B}_i/\mathcal{B}_j$. Some branching fractions are sums of other branching fractions, for instance $\mathcal{B}_8 = \mathcal{B}(\tau \rightarrow h^-\nu_\tau)$ is the sum of $\mathcal{B}_9 = \mathcal{B}(\tau \rightarrow \pi^-\nu_\tau)$ and $\mathcal{B}_{10} = \mathcal{B}(\tau \rightarrow K^-\nu_\tau)$. The symbol h is used to mean either a π or a K . The fit χ^2 is minimized while respecting a list of constraints on the fitted quantities:

- quantities corresponding to ratios like $\mathcal{B}_i/\mathcal{B}_j$ must be equal to the ratio of the respective quantities \mathcal{B}_i and \mathcal{B}_j ;
- quantities corresponding to branching fractions that are sum of other branching fractions must be equal to the sum of the quantities corresponding to the summed branching fractions.

Section 10.1.7 lists all equations relating one quantity to other quantities.

10.1.1 Technical implementation of the fit procedure

The fit computes the quantities q_i by minimizing a χ^2 while respecting a series of equality constraints on the q_i . The χ^2 is computed using the measurements x_i and their covariance matrix V_{ij} as

$$\chi^2 = (x_i - A_{ik}q_k)^t V_{ij}^{-1} (x_j - A_{jl}q_l) , \quad (313)$$

where the model matrix A_{ij} is used to get the vector of the predicted measurements x'_i from the vector of the fit parameters q_j as $x'_i = A_{ij}q_j$. In this particular implementation, the

measurements are grouped according to the measured quantity, and all quantities with at least one measurement correspond to a fit parameter. Therefore, the matrix A_{ij} has one row per measurement x_i and one column per fitted quantity q_j , with unity coefficients for the rows and column that identify a measurement x_i of the quantity q_j . In summary, the χ^2 given in Eq. (313) is minimized subject to the constraints

$$f_r(q_s) - c_r = 0 , \quad (314)$$

where Eq. (314) corresponds to the constraint equations, written as a set of “constraint expressions” that are equated to zero. Using the method of Lagrange multipliers, a set of equations is obtained by taking the derivatives with respect to the fitted quantities q_k and the Lagrange multipliers λ_r of the sum of the χ^2 and the constraint expressions multiplied by the Lagrange multipliers λ_r , one for each constraint:

$$\min [h = (A_{ik}q_k - x_i)^t V_{ij}^{-1} (A_{jl}q_l - x_j) + 2\lambda_r (f_r(q_s) - c_r)] \quad (315)$$

$$(\partial/\partial q_k, \partial/\partial \lambda_r) h = 0 . \quad (316)$$

Equation (316) defines a set of equations for the vector of the unknowns (q_k, λ_r) , some of which may be non-linear, in case of non-linear constraints. An iterative minimization procedure approximates at each step the non-linear constraint expressions by their first order Taylor expansion around the current values of the fitted quantities, \bar{q}_s :

$$f_r(q_s) - c_r \simeq f_r(\bar{q}_s) + \frac{\partial f_r(q_s)}{\partial q_s} \Big|_{\bar{q}_s} (q_s - \bar{q}_s) - c_r , \quad (317)$$

which can be written as

$$B_{rs}q_s - c'_r , \quad (318)$$

where c'_r are the resulting constant known terms, independent of q_s at first order. After linearization, the differentiation by q_k and λ_r is trivial and leads to a set of linear equations

$$A_{ki}^t V_{ij}^{-1} A_{jl} q_l + B_{kr}^t \lambda_r = A_{ki}^t V_{ij}^{-1} x_j \quad (319)$$

$$B_{rs}q_s = c'_r , \quad (320)$$

which can be expressed as:

$$F_{ij}u_j = v_i , \quad (321)$$

where $u_j = (q_k, \lambda_r)$ and v_i is the vector of the known constant terms running over the index k and then r in the right terms of Eq. (319) and Eq. (320). Solving the equation set in Eq. (321) gives the fitted quantities and their covariance matrix, using the measurements and their covariance matrix. The fit procedure starts by computing the linear approximation of the non-linear constraint expressions around the quantities seed values. With an iterative procedure, the unknowns are updated at each step by solving the equations and the equations are then linearized around the updated values, until the RMS average of relative variation of the fitted unknowns is reduced below 10^{-12} .

10.1.2 Fit results

Although the fit treats all quantities in the same way, for the purpose of describing the results we select a set of 47 “basis quantities” from which all remaining quantities can be calculated using the definitions listed in Section 10.1.7.

The fit output consists of 136 fitted quantities that correspond to either branching fractions or ratios of branching fractions. The fitted quantities values and uncertainties are listed in Table 327. The off-diagonal correlation terms between the basis quantities are listed in Section 10.1.6.

Furthermore we define (see Section 10.1.7) $\mathcal{B}_{110} = \mathcal{B}(\tau^- \rightarrow X_s^- \nu_\tau)$, the total branching fraction of the τ decays to final states with the strangeness quantum number equal to one, and \mathcal{B}_{All} , the branching fraction of the τ into any measured final state, which should be equal to 1 within the experimental uncertainty. We define the unitarity residual as $\mathcal{B}_{998} = 1 - \mathcal{B}_{\text{All}}$.

The fit has $\chi^2/\text{d.o.f.} = 142/129$, corresponding to a confidence level $\text{CL} = 20.13\%$. We use a total of 176 measurements to fit the above mentioned 136 quantities subjected to 89 constraints. Although the unitarity constraint is not applied, the fit is statistically consistent with unitarity, where the residual is $\mathcal{B}_{998} = 1 - \mathcal{B}_{\text{All}} = (0.0274 \pm 0.1026) \cdot 10^{-2}$.

A scale factor of 5.44 has been applied to the published uncertainties of the two severely inconsistent measurements of $\mathcal{B}_{96} = \tau \rightarrow K K K \nu$ by *BABAR* and *Belle*. The scale factor has been determined using the PDG procedure, *i.e.*, to the proper size in order to obtain a reduced χ^2 equal to 1 when fitting just the two \mathcal{B}_{96} measurements.

10.1.3 Changes with respect to the previous report

The following changes have been introduced with respect to the previous HFLAV report [1].

We added the *BABAR* 2018 result [1461] for the τ branching fraction

$$\mathcal{B}_{37} = K^- K^0 \nu_\tau \quad (14.78 \pm 0.22 \pm 0.40) \cdot 10^{-4},$$

and the 2018 *BABAR* preliminary results [1462] for the τ branching fractions

$$\begin{aligned} \mathcal{B}_{10} &= K^- \nu_\tau & (7.17 \pm 0.031 \pm 0.21) \cdot 10^{-3} \\ \mathcal{B}_{16} &= K^- \pi^0 \nu_\tau & (5.05 \pm 0.02 \pm 0.15) \cdot 10^{-3} \\ \mathcal{B}_{23} &= K^- 2\pi^0 \nu_\tau \text{ (ex. } K^0) & (6.15 \pm 0.12 \pm 0.34) \cdot 10^{-4} \\ \mathcal{B}_{27} &= \pi^- 3\pi^0 \nu_\tau \text{ (ex. } K^0) & (1.168 \pm 0.006 \pm 0.038) \cdot 10^{-2} \\ \mathcal{B}_{28} &= K^- 3\pi^0 \nu_\tau \text{ (ex. } K^0, \eta) & (1.25 \pm 0.16 \pm 0.24) \cdot 10^{-4} \\ \mathcal{B}_{809} &= \pi^- 4\pi^0 \nu_\tau \text{ (ex. } K^0, \eta) & (9.02 \pm 0.40 \pm 0.65) \cdot 10^{-4}. \end{aligned}$$

The above \mathcal{B}_{16} result supersedes the previous *BABAR* result in Ref. [1463].

The parameters used to update the measurements’ systematic biases and the parameters appearing in the constraint equations in Section 10.1.7 have been updated to the PDG 2018 averages [21].

10.1.4 Differences between the HFLAV 2018 fit and the PDG 2018 fit

As is standard for the PDG branching fraction fits, the PDG 2018 τ branching fraction fit is unitarity constrained, while the HFLAV 2018 fit is unconstrained.

The HFLAV-Tau fit uses an elaboration of the measurements reported on the main ALEPH paper on τ branching fractions [1464] to obtain branching fractions to inclusive final states with “hadrons” (where a hadron is either a pion or a kaon), since this set of results is closer to the actual experimental measurements and facilitates a more appropriate and comprehensive treatment of the experimental results correlations. The PDG 2018 fit on the other hand continues to use – as in the past editions – the published ALEPH measurements of branching fractions to exclusive final states with pions [1464].

As in 2016, HFLAV uses the ALEPH estimate for $\mathcal{B}_{805} = \mathcal{B}(\tau \rightarrow a_1^- (\rightarrow \pi^-\gamma)\nu_\tau)$, which is not a direct measurement, and the PDG 2018 fit uses the PDG average of $\mathcal{B}(a_1 \rightarrow \pi\gamma)$ as a parameter and defines $\mathcal{B}_{805} = \mathcal{B}(a_1 \rightarrow \pi\gamma) \times \mathcal{B}(\tau \rightarrow 3\pi\nu)$. As a consequence, the PDG fit procedure does not take into account the large uncertainty on $\mathcal{B}(a_1 \rightarrow \pi\gamma)$, resulting in an underestimated fit uncertainty on \mathcal{B}_{805} . Therefore, in this case an appropriate correction has been applied after the fit.

Finally, the HFLAV 2018 τ branching fraction fit includes measurements that appeared after the deadline for inclusion in the PDG, and preliminary measurements that are not included in the PDG.

10.1.5 Branching ratio fit results and experimental inputs

Table 327 reports the τ branching ratio fit results and experimental inputs.

Table 327: HFLAV 2018 branching fractions fit results.

τ lepton branching fraction	Experiment	Reference
$\mathcal{B}_1 = (\text{particles})^- \geq 0 \text{ neutrals} \geq 0 K^0 \nu_\tau$		
0.8521 ± 0.0011	average	
$\mathcal{B}_2 = (\text{particles})^- \geq 0 \text{ neutrals} \geq 0 K_L^0 \nu_\tau$		
0.8455 ± 0.0010	average	
$\mathcal{B}_3 = \mu^- \bar{\nu}_\mu \nu_\tau$		
0.17392 ± 0.00039	average	
$0.17319 \pm 0.00070 \pm 0.00032$	ALEPH	[1464]
$0.17325 \pm 0.00095 \pm 0.00077$	DELPHI	[1465]
$0.17342 \pm 0.00110 \pm 0.00067$	L3	[1466]
$0.17340 \pm 0.00090 \pm 0.00060$	OPAL	[1467]
$\frac{\mathcal{B}_3}{\mathcal{B}_5} = \frac{\mu^- \bar{\nu}_\mu \nu_\tau}{e^- \bar{\nu}_e \nu_\tau}$		
0.9761 ± 0.0028	average	
$0.9970 \pm 0.0350 \pm 0.0400$	ARGUS	[1468]
$0.9796 \pm 0.0016 \pm 0.0036$	BABAR	[1469]
$0.9777 \pm 0.0063 \pm 0.0087$	CLEO	[1470]

Table 327 – continued from previous page

τ lepton branching fraction	Experiment	Reference
$\mathcal{B}_5 = e^- \bar{\nu}_e \nu_\tau$		
0.17817 ± 0.00041	average	
$0.17837 \pm 0.00072 \pm 0.00036$	ALEPH	[1464]
$0.17760 \pm 0.00060 \pm 0.00170$	CLEO	[1470]
$0.17877 \pm 0.00109 \pm 0.00110$	DELPHI	[1465]
$0.17806 \pm 0.00104 \pm 0.00076$	L3	[1466]
$0.17810 \pm 0.00090 \pm 0.00060$	OPAL	[1471]
$\mathcal{B}_7 = h^- \geq 0 K_L^0 \nu_\tau$		
0.12019 ± 0.00053	average	
$0.12400 \pm 0.00700 \pm 0.00700$	DELPHI	[1472]
$0.12470 \pm 0.00260 \pm 0.00430$	L3	[1473]
$0.12100 \pm 0.00700 \pm 0.00500$	OPAL	[1474]
$\mathcal{B}_8 = h^- \nu_\tau$		
0.11502 ± 0.00053	average	
$0.11524 \pm 0.00070 \pm 0.00078$	ALEPH	[1464]
$0.11520 \pm 0.00050 \pm 0.00120$	CLEO	[1470]
$0.11571 \pm 0.00120 \pm 0.00114$	DELPHI	[1475]
$0.11980 \pm 0.00130 \pm 0.00160$	OPAL	[1476]
$\frac{\mathcal{B}_8}{\mathcal{B}_5} = \frac{h^- \nu_\tau}{e^- \bar{\nu}_e \nu_\tau}$		
0.6456 ± 0.0033	average	
$\mathcal{B}_9 = \pi^- \nu_\tau$		
0.10804 ± 0.00052	average	
$\frac{\mathcal{B}_9}{\mathcal{B}_5} = \frac{\pi^- \nu_\tau}{e^- \bar{\nu}_e \nu_\tau}$		
0.6064 ± 0.0032	average	
$0.5945 \pm 0.0014 \pm 0.0061$	BABAR	[1469]
$\mathcal{B}_{10} = K^- \nu_\tau$		
$(0.6986 \pm 0.0085) \cdot 10^{-2}$	average	
$(0.6960 \pm 0.0250 \pm 0.0140) \cdot 10^{-2}$	ALEPH	[1477]
$(0.7170 \pm 0.0031 \pm 0.0210) \cdot 10^{-2}$	BABAR	[1462]
$(0.6600 \pm 0.0700 \pm 0.0900) \cdot 10^{-2}$	CLEO	[1478]
$(0.8500 \pm 0.1800 \pm 0.0000) \cdot 10^{-2}$	DELPHI	[1479]

Table 327 – continued from previous page

τ lepton branching fraction	Experiment	Reference
$(0.6580 \pm 0.0270 \pm 0.0290) \cdot 10^{-2}$	OPAL	[1480]
$\frac{\mathcal{B}_{10}}{\mathcal{B}_5} = \frac{K^- \nu_\tau}{e^- \bar{\nu}_e \nu_\tau}$		
$(3.921 \pm 0.048) \cdot 10^{-2}$	average	
$(3.882 \pm 0.032 \pm 0.057) \cdot 10^{-2}$	BABAR	[1469]
$\frac{\mathcal{B}_{10}}{\mathcal{B}_9} = \frac{K^- \nu_\tau}{\pi^- \nu_\tau}$		
$(6.467 \pm 0.084) \cdot 10^{-2}$	average	
$\mathcal{B}_{11} = h^- \geq 1 \text{ neutrals } \nu_\tau$		
0.36996 ± 0.00094	average	
$\mathcal{B}_{12} = h^- \geq 1 \pi^0 \nu_\tau \text{ (ex. } K^0)$		
0.36495 ± 0.00094	average	
$\mathcal{B}_{13} = h^- \pi^0 \nu_\tau$		
0.25938 ± 0.00090	average	
$0.25924 \pm 0.00097 \pm 0.00085$	ALEPH	[1464]
$0.25670 \pm 0.00010 \pm 0.00390$	Belle	[1481]
$0.25870 \pm 0.00120 \pm 0.00420$	CLEO	[1482]
$0.25740 \pm 0.00201 \pm 0.00138$	DELPHI	[1475]
$0.25050 \pm 0.00350 \pm 0.00500$	L3	[1473]
$0.25890 \pm 0.00170 \pm 0.00290$	OPAL	[1476]
$\mathcal{B}_{14} = \pi^- \pi^0 \nu_\tau$		
0.25447 ± 0.00091	average	
$\mathcal{B}_{16} = K^- \pi^0 \nu_\tau$		
$(0.4904 \pm 0.0092) \cdot 10^{-2}$	average	
$(0.4440 \pm 0.0260 \pm 0.0240) \cdot 10^{-2}$	ALEPH	[1477]
$(0.5050 \pm 0.0020 \pm 0.0150) \cdot 10^{-2}$	BABAR	[1462]
$(0.5100 \pm 0.1000 \pm 0.0700) \cdot 10^{-2}$	CLEO	[1478]
$(0.4710 \pm 0.0590 \pm 0.0230) \cdot 10^{-2}$	OPAL	[1483]
$\mathcal{B}_{17} = h^- \geq 2 \pi^0 \nu_\tau$		
0.10793 ± 0.00091	average	
$0.09910 \pm 0.00310 \pm 0.00270$	OPAL	[1476]
$\mathcal{B}_{18} = h^- 2\pi^0 \nu_\tau$		
$(9.421 \pm 0.092) \cdot 10^{-2}$	average	

Table 327 – continued from previous page

τ lepton branching fraction	Experiment	Reference
$\mathcal{B}_{19} = h^- 2\pi^0 \nu_\tau$ (ex. K^0) $(9.270 \pm 0.092) \cdot 10^{-2}$	average	
$(9.295 \pm 0.084 \pm 0.088) \cdot 10^{-2}$	ALEPH	[1464]
$(9.498 \pm 0.320 \pm 0.275) \cdot 10^{-2}$	DELPHI	[1475]
$(8.880 \pm 0.370 \pm 0.420) \cdot 10^{-2}$	L3	[1473]
$\frac{\mathcal{B}_{19}}{\mathcal{B}_{13}} = \frac{h^- 2\pi^0 \nu_\tau \text{ (ex. } K^0\text{)}}{h^- \pi^0 \nu_\tau}$ 0.3574 ± 0.0042	average	
$0.3420 \pm 0.0060 \pm 0.0160$	CLEO	[1484]
$\mathcal{B}_{20} = \pi^- 2\pi^0 \nu_\tau$ (ex. K^0) $(9.211 \pm 0.092) \cdot 10^{-2}$	average	
$\mathcal{B}_{23} = K^- 2\pi^0 \nu_\tau$ (ex. K^0) $(0.0585 \pm 0.0027) \cdot 10^{-2}$	average	
$(0.0560 \pm 0.0200 \pm 0.0150) \cdot 10^{-2}$	ALEPH	[1477]
$(0.0615 \pm 0.0012 \pm 0.0034) \cdot 10^{-2}$	BABAR	[1462]
$(0.0900 \pm 0.1000 \pm 0.0300) \cdot 10^{-2}$	CLEO	[1478]
$\mathcal{B}_{24} = h^- \geq 3\pi^0 \nu_\tau$ $(1.372 \pm 0.034) \cdot 10^{-2}$	average	
$\mathcal{B}_{25} = h^- \geq 3\pi^0 \nu_\tau$ (ex. K^0) $(1.288 \pm 0.034) \cdot 10^{-2}$	average	
$(1.403 \pm 0.214 \pm 0.224) \cdot 10^{-2}$	DELPHI	[1475]
$\mathcal{B}_{26} = h^- 3\pi^0 \nu_\tau$ $(1.236 \pm 0.030) \cdot 10^{-2}$	average	
$(1.082 \pm 0.071 \pm 0.059) \cdot 10^{-2}$	ALEPH	[1464]
$(1.700 \pm 0.240 \pm 0.380) \cdot 10^{-2}$	L3	[1473]
$\frac{\mathcal{B}_{26}}{\mathcal{B}_{13}} = \frac{h^- 3\pi^0 \nu_\tau}{h^- \pi^0 \nu_\tau}$ $(4.764 \pm 0.118) \cdot 10^{-2}$	average	
$(4.400 \pm 0.300 \pm 0.500) \cdot 10^{-2}$	CLEO	[1484]
$\mathcal{B}_{27} = \pi^- 3\pi^0 \nu_\tau$ (ex. K^0) $(1.1381 \pm 0.0292) \cdot 10^{-2}$	average	
$(1.1680 \pm 0.0060 \pm 0.0380) \cdot 10^{-2}$	BABAR	[1462]
$\mathcal{B}_{28} = K^- 3\pi^0 \nu_\tau$ (ex. K^0, η)		

Table 327 – continued from previous page

τ lepton branching fraction	Experiment	Reference
$(1.127 \pm 0.263) \cdot 10^{-4}$	average	
$(3.700 \pm 2.100 \pm 1.100) \cdot 10^{-4}$	ALEPH	[1477]
$(1.250 \pm 0.160 \pm 0.240) \cdot 10^{-4}$	BABAR	[1462]
$\mathcal{B}_{29} = h^- 4\pi^0 \nu_\tau$ (ex. K^0)		
$(0.1333 \pm 0.0071) \cdot 10^{-2}$	average	
$(0.1600 \pm 0.0500 \pm 0.0500) \cdot 10^{-2}$	CLEO	[1484]
$\mathcal{B}_{30} = h^- 4\pi^0 \nu_\tau$ (ex. K^0, η)		
$(0.0864 \pm 0.0067) \cdot 10^{-2}$	average	
$(0.1120 \pm 0.0370 \pm 0.0350) \cdot 10^{-2}$	ALEPH	[1464]
$\mathcal{B}_{31} = K^- \geq 0 \pi^0 \geq 0 K^0 \geq 0 \gamma \nu_\tau$		
$(1.568 \pm 0.018) \cdot 10^{-2}$	average	
$(1.700 \pm 0.120 \pm 0.190) \cdot 10^{-2}$	CLEO	[1478]
$(1.540 \pm 0.240 \pm 0.000) \cdot 10^{-2}$	DELPHI	[1479]
$(1.528 \pm 0.039 \pm 0.040) \cdot 10^{-2}$	OPAL	[1480]
$\mathcal{B}_{32} = K^- \geq 1 (\pi^0 \text{ or } K^0 \text{ or } \gamma) \nu_\tau$		
$(0.8729 \pm 0.0141) \cdot 10^{-2}$	average	
$\mathcal{B}_{33} = K_S^0 (\text{particles})^- \nu_\tau$		
$(0.9366 \pm 0.0292) \cdot 10^{-2}$	average	
$(0.9700 \pm 0.0580 \pm 0.0620) \cdot 10^{-2}$	ALEPH	[1485]
$(0.9700 \pm 0.0900 \pm 0.0600) \cdot 10^{-2}$	OPAL	[1486]
$\mathcal{B}_{34} = h^- \bar{K}^0 \nu_\tau$		
$(0.9860 \pm 0.0138) \cdot 10^{-2}$	average	
$(0.8550 \pm 0.0360 \pm 0.0730) \cdot 10^{-2}$	CLEO	[1487]
$\mathcal{B}_{35} = \pi^- \bar{K}^0 \nu_\tau$		
$(0.8378 \pm 0.0139) \cdot 10^{-2}$	average	
$(0.9280 \pm 0.0450 \pm 0.0340) \cdot 10^{-2}$	ALEPH	[1477]
$(0.8320 \pm 0.0025 \pm 0.0150) \cdot 10^{-2}$	Belle	[1488]
$(0.9500 \pm 0.1500 \pm 0.0600) \cdot 10^{-2}$	L3	[1489]
$(0.9330 \pm 0.0680 \pm 0.0490) \cdot 10^{-2}$	OPAL	[1490]
$\mathcal{B}_{37} = K^- K^0 \nu_\tau$		
$(0.1483 \pm 0.0034) \cdot 10^{-2}$	average	
$(0.1580 \pm 0.0420 \pm 0.0170) \cdot 10^{-2}$	ALEPH	[1485]

Table 327 – continued from previous page

τ lepton branching fraction	Experiment	Reference
$(0.1620 \pm 0.0210 \pm 0.0110) \cdot 10^{-2}$	ALEPH	[1477]
$(0.1478 \pm 0.0022 \pm 0.0040) \cdot 10^{-2}$	BABAR	[1461]
$(0.1480 \pm 0.0013 \pm 0.0055) \cdot 10^{-2}$	Belle	[1488]
$(0.1510 \pm 0.0210 \pm 0.0220) \cdot 10^{-2}$	CLEO	[1487]
$\mathcal{B}_{38} = K^- K^0 \geq 0 \pi^0 \nu_\tau$		
$(0.2977 \pm 0.0073) \cdot 10^{-2}$	average	
$(0.3300 \pm 0.0550 \pm 0.0390) \cdot 10^{-2}$	OPAL	[1490]
$\mathcal{B}_{39} = h^- \bar{K}^0 \pi^0 \nu_\tau$		
$(0.5302 \pm 0.0134) \cdot 10^{-2}$	average	
$(0.5620 \pm 0.0500 \pm 0.0480) \cdot 10^{-2}$	CLEO	[1487]
$\mathcal{B}_{40} = \pi^- \bar{K}^0 \pi^0 \nu_\tau$		
$(0.3807 \pm 0.0129) \cdot 10^{-2}$	average	
$(0.2940 \pm 0.0730 \pm 0.0370) \cdot 10^{-2}$	ALEPH	[1485]
$(0.3470 \pm 0.0530 \pm 0.0370) \cdot 10^{-2}$	ALEPH	[1477]
$(0.3860 \pm 0.0031 \pm 0.0135) \cdot 10^{-2}$	Belle	[1488]
$(0.4100 \pm 0.1200 \pm 0.0300) \cdot 10^{-2}$	L3	[1489]
$\mathcal{B}_{42} = K^- \pi^0 K^0 \nu_\tau$		
$(0.1494 \pm 0.0070) \cdot 10^{-2}$	average	
$(0.1520 \pm 0.0760 \pm 0.0210) \cdot 10^{-2}$	ALEPH	[1485]
$(0.1430 \pm 0.0250 \pm 0.0150) \cdot 10^{-2}$	ALEPH	[1477]
$(0.1496 \pm 0.0019 \pm 0.0073) \cdot 10^{-2}$	Belle	[1488]
$(0.1450 \pm 0.0360 \pm 0.0200) \cdot 10^{-2}$	CLEO	[1487]
$\mathcal{B}_{43} = \pi^- \bar{K}^0 \geq 1 \pi^0 \nu_\tau$		
$(0.4042 \pm 0.0260) \cdot 10^{-2}$	average	
$(0.3240 \pm 0.0740 \pm 0.0660) \cdot 10^{-2}$	OPAL	[1490]
$\mathcal{B}_{44} = \pi^- \bar{K}^0 2\pi^0 \nu_\tau$ (ex. K^0)		
$(2.346 \pm 2.306) \cdot 10^{-4}$	average	
$(2.600 \pm 2.400 \pm 0.000) \cdot 10^{-4}$	ALEPH	[1491]
$\mathcal{B}_{46} = \pi^- K^0 \bar{K}^0 \nu_\tau$		
$(0.1516 \pm 0.0247) \cdot 10^{-2}$	average	
$\mathcal{B}_{47} = \pi^- K_S^0 \bar{K}_S^0 \nu_\tau$		
$(2.342 \pm 0.065) \cdot 10^{-4}$	average	

Table 327 – continued from previous page

τ lepton branching fraction	Experiment	Reference
$(2.600 \pm 1.000 \pm 0.500) \cdot 10^{-4}$	ALEPH	[1485]
$(2.310 \pm 0.040 \pm 0.080) \cdot 10^{-4}$	BABAR	[1492]
$(2.330 \pm 0.033 \pm 0.093) \cdot 10^{-4}$	Belle	[1488]
$(2.300 \pm 0.500 \pm 0.300) \cdot 10^{-4}$	CLEO	[1487]
$\mathcal{B}_{48} = \pi^- K_S^0 K_L^0 \nu_\tau$		
$(0.1048 \pm 0.0247) \cdot 10^{-2}$	average	
$(0.1010 \pm 0.0230 \pm 0.0130) \cdot 10^{-2}$	ALEPH	[1485]
$\mathcal{B}_{49} = \pi^- K^0 \bar{K}^0 \pi^0 \nu_\tau$		
$(3.543 \pm 1.193) \cdot 10^{-4}$	average	
$\mathcal{B}_{50} = \pi^- \pi^0 K_S^0 K_L^0 \nu_\tau$		
$(1.816 \pm 0.207) \cdot 10^{-5}$	average	
$(1.600 \pm 0.200 \pm 0.220) \cdot 10^{-5}$	BABAR	[1492]
$(2.000 \pm 0.216 \pm 0.202) \cdot 10^{-5}$	Belle	[1488]
$\mathcal{B}_{51} = \pi^- \pi^0 K_S^0 K_L^0 \nu_\tau$		
$(3.179 \pm 1.192) \cdot 10^{-4}$	average	
$(3.100 \pm 1.100 \pm 0.500) \cdot 10^{-4}$	ALEPH	[1485]
$\mathcal{B}_{53} = \bar{K}^0 h^- h^- h^+ \nu_\tau$		
$(2.220 \pm 2.024) \cdot 10^{-4}$	average	
$(2.300 \pm 1.900 \pm 0.700) \cdot 10^{-4}$	ALEPH	[1485]
$\mathcal{B}_{54} = h^- h^- h^+ \geq 0 \text{ neutrals} \geq 0 K_L^0 \nu_\tau$		
0.15206 ± 0.00061	average	
$0.15000 \pm 0.00400 \pm 0.00300$	CELLO	[1493]
$0.14400 \pm 0.00600 \pm 0.00300$	L3	[1494]
$0.15100 \pm 0.00800 \pm 0.00600$	TPC	[1495]
$\mathcal{B}_{55} = h^- h^- h^+ \geq 0 \text{ neutrals} \nu_\tau \text{ (ex. } K^0)$		
0.14558 ± 0.00056	average	
$0.14556 \pm 0.00105 \pm 0.00076$	L3	[1496]
$0.14960 \pm 0.00090 \pm 0.00220$	OPAL	[1497]
$\mathcal{B}_{56} = h^- h^- h^+ \nu_\tau$		
$(9.769 \pm 0.053) \cdot 10^{-2}$	average	
$\mathcal{B}_{57} = h^- h^- h^+ \nu_\tau \text{ (ex. } K^0)$		
$(9.428 \pm 0.053) \cdot 10^{-2}$	average	

Table 327 – continued from previous page

τ lepton branching fraction	Experiment	Reference
$(9.510 \pm 0.070 \pm 0.200) \cdot 10^{-2}$	CLEO	[1498]
$(9.317 \pm 0.090 \pm 0.082) \cdot 10^{-2}$	DELPHI	[1475]
$\frac{\mathcal{B}_{57}}{\mathcal{B}_{55}} = \frac{h^- h^- h^+ \nu_\tau \text{ (ex. } K^0\text{)}}{h^- h^- h^+ \geq 0 \text{ neutrals } \nu_\tau \text{ (ex. } K^0\text{)}}$		
0.6476 ± 0.0029	average	
$0.6600 \pm 0.0040 \pm 0.0140$	OPAL	[1497]
$\mathcal{B}_{58} = h^- h^- h^+ \nu_\tau \text{ (ex. } K^0, \omega\text{)}$		
$(9.397 \pm 0.053) \cdot 10^{-2}$	average	
$(9.469 \pm 0.062 \pm 0.073) \cdot 10^{-2}$	ALEPH	[1464]
$\mathcal{B}_{59} = \pi^- \pi^+ \pi^- \nu_\tau$		
$(9.279 \pm 0.051) \cdot 10^{-2}$	average	
$\mathcal{B}_{60} = \pi^- \pi^+ \pi^- \nu_\tau \text{ (ex. } K^0\text{)}$		
$(8.990 \pm 0.051) \cdot 10^{-2}$	average	
$(8.830 \pm 0.010 \pm 0.130) \cdot 10^{-2}$	BABAR	[1499]
$(8.420 \pm 0.000^{+0.260}_{-0.250}) \cdot 10^{-2}$	Belle	[1500]
$(9.130 \pm 0.050 \pm 0.460) \cdot 10^{-2}$	CLEO3	[1501]
$\mathcal{B}_{62} = \pi^- \pi^- \pi^+ \nu_\tau \text{ (ex. } K^0, \omega\text{)}$		
$(8.960 \pm 0.051) \cdot 10^{-2}$	average	
$\mathcal{B}_{63} = h^- h^- h^+ \geq 1 \text{ neutrals } \nu_\tau$		
$(5.327 \pm 0.049) \cdot 10^{-2}$	average	
$\mathcal{B}_{64} = h^- h^- h^+ \geq 1 \pi^0 \nu_\tau \text{ (ex. } K^0\text{)}$		
$(5.122 \pm 0.049) \cdot 10^{-2}$	average	
$\mathcal{B}_{65} = h^- h^- h^+ \pi^0 \nu_\tau$		
$(4.791 \pm 0.052) \cdot 10^{-2}$	average	
$\mathcal{B}_{66} = h^- h^- h^+ \pi^0 \nu_\tau \text{ (ex. } K^0\text{)}$		
$(4.607 \pm 0.051) \cdot 10^{-2}$	average	
$(4.734 \pm 0.059 \pm 0.049) \cdot 10^{-2}$	ALEPH	[1464]
$(4.230 \pm 0.060 \pm 0.220) \cdot 10^{-2}$	CLEO	[1498]
$(4.545 \pm 0.106 \pm 0.103) \cdot 10^{-2}$	DELPHI	[1475]
$\mathcal{B}_{67} = h^- h^- h^+ \pi^0 \nu_\tau \text{ (ex. } K^0, \omega\text{)}$		
$(2.821 \pm 0.070) \cdot 10^{-2}$	average	
$\mathcal{B}_{68} = \pi^- \pi^+ \pi^- \pi^0 \nu_\tau$		

Table 327 – continued from previous page

τ lepton branching fraction	Experiment	Reference
$(4.652 \pm 0.053) \cdot 10^{-2}$	average	
$\mathcal{B}_{69} = \pi^- \pi^+ \pi^- \pi^0 \nu_\tau$ (ex. K^0)		
$(4.520 \pm 0.052) \cdot 10^{-2}$	average	
$(4.190 \pm 0.100 \pm 0.210) \cdot 10^{-2}$	CLEO	[1502]
$\mathcal{B}_{70} = \pi^- \pi^- \pi^+ \pi^0 \nu_\tau$ (ex. K^0, ω)		
$(2.770 \pm 0.071) \cdot 10^{-2}$	average	
$\mathcal{B}_{74} = h^- h^- h^+ \geq 2 \pi^0 \nu_\tau$ (ex. K^0)		
$(0.5148 \pm 0.0311) \cdot 10^{-2}$	average	
$(0.5610 \pm 0.0680 \pm 0.0950) \cdot 10^{-2}$	DELPHI	[1475]
$\mathcal{B}_{75} = h^- h^- h^+ 2\pi^0 \nu_\tau$		
$(0.5037 \pm 0.0309) \cdot 10^{-2}$	average	
$\mathcal{B}_{76} = h^- h^- h^+ 2\pi^0 \nu_\tau$ (ex. K^0)		
$(0.4937 \pm 0.0309) \cdot 10^{-2}$	average	
$(0.4350 \pm 0.0300 \pm 0.0350) \cdot 10^{-2}$	ALEPH	[1464]
$\mathcal{B}_{76} = \frac{h^- h^- h^+ 2\pi^0 \nu_\tau}{h^- h^- h^+ \geq 0 \text{ neutrals} \geq 0 K_L^0 \nu_\tau}$ (ex. K^0)		
$(3.247 \pm 0.202) \cdot 10^{-2}$	average	
$(3.400 \pm 0.200 \pm 0.300) \cdot 10^{-2}$	CLEO	[1503]
$\mathcal{B}_{77} = h^- h^- h^+ 2\pi^0 \nu_\tau$ (ex. K^0, ω, η)		
$(9.812 \pm 3.555) \cdot 10^{-4}$	average	
$\mathcal{B}_{78} = h^- h^- h^+ 3\pi^0 \nu_\tau$		
$(2.114 \pm 0.299) \cdot 10^{-4}$	average	
$(2.200 \pm 0.300 \pm 0.400) \cdot 10^{-4}$	CLEO	[1504]
$\mathcal{B}_{79} = K^- h^- h^+ \geq 0 \text{ neutrals} \nu_\tau$		
$(0.6293 \pm 0.0140) \cdot 10^{-2}$	average	
$\mathcal{B}_{80} = K^- \pi^- h^+ \nu_\tau$ (ex. K^0)		
$(0.4361 \pm 0.0072) \cdot 10^{-2}$	average	
$\mathcal{B}_{80} = \frac{K^- \pi^- h^+ \nu_\tau}{\pi^- \pi^+ \pi^- \nu_\tau}$ (ex. K^0)		
$(4.851 \pm 0.080) \cdot 10^{-2}$	average	
$(5.440 \pm 0.210 \pm 0.530) \cdot 10^{-2}$	CLEO	[1505]
$\mathcal{B}_{81} = K^- \pi^- h^+ \pi^0 \nu_\tau$ (ex. K^0)		

Table 327 – continued from previous page

τ lepton branching fraction	Experiment	Reference
$(8.727 \pm 1.177) \cdot 10^{-4}$	average	
$\frac{\mathcal{B}_{81}}{\mathcal{B}_{69}} = \frac{K^-\pi^-h^+\pi^0\nu_\tau \text{ (ex. } K^0\text{)}}{\pi^-\pi^+\pi^-\pi^0\nu_\tau \text{ (ex. } K^0\text{)}}$		
$(1.931 \pm 0.266) \cdot 10^{-2}$	average	
$(2.610 \pm 0.450 \pm 0.420) \cdot 10^{-2}$	CLEO	[1505]
$\mathcal{B}_{82} = K^-\pi^-\pi^+ \geq 0 \text{ neutrals } \nu_\tau$		
$(0.4779 \pm 0.0137) \cdot 10^{-2}$	average	
$(0.5800^{+0.1500}_{-0.1300} \pm 0.1200) \cdot 10^{-2}$	TPC	[1506]
$\mathcal{B}_{83} = K^-\pi^-\pi^+ \geq 0 \pi^0 \nu_\tau \text{ (ex. } K^0\text{)}$		
$(0.3741 \pm 0.0135) \cdot 10^{-2}$	average	
$\mathcal{B}_{84} = K^-\pi^-\pi^+\nu_\tau$		
$(0.3442 \pm 0.0068) \cdot 10^{-2}$	average	
$\mathcal{B}_{85} = K^-\pi^+\pi^-\nu_\tau \text{ (ex. } K^0\text{)}$		
$(0.2929 \pm 0.0067) \cdot 10^{-2}$	average	
$(0.2140 \pm 0.0370 \pm 0.0290) \cdot 10^{-2}$	ALEPH	[1507]
$(0.2730 \pm 0.0020 \pm 0.0090) \cdot 10^{-2}$	BABAR	[1499]
$(0.3300 \pm 0.0010^{+0.0160}_{-0.0170}) \cdot 10^{-2}$	Belle	[1500]
$(0.3840 \pm 0.0140 \pm 0.0380) \cdot 10^{-2}$	CLEO3	[1501]
$(0.4150 \pm 0.0530 \pm 0.0400) \cdot 10^{-2}$	OPAL	[1483]
$\frac{\mathcal{B}_{85}}{\mathcal{B}_{60}} = \frac{K^-\pi^+\pi^-\nu_\tau \text{ (ex. } K^0\text{)}}{\pi^-\pi^+\pi^-\nu_\tau \text{ (ex. } K^0\text{)}}$		
$(3.258 \pm 0.074) \cdot 10^{-2}$	average	
$\mathcal{B}_{87} = K^-\pi^-\pi^+\pi^0\nu_\tau$		
$(0.1329 \pm 0.0119) \cdot 10^{-2}$	average	
$\mathcal{B}_{88} = K^-\pi^-\pi^+\pi^0\nu_\tau \text{ (ex. } K^0\text{)}$		
$(8.116 \pm 1.168) \cdot 10^{-4}$	average	
$(6.100 \pm 3.900 \pm 1.800) \cdot 10^{-4}$	ALEPH	[1507]
$(7.400 \pm 0.800 \pm 1.100) \cdot 10^{-4}$	CLEO3	[1508]
$\mathcal{B}_{89} = K^-\pi^-\pi^+\pi^0\nu_\tau \text{ (ex. } K^0, \eta\text{)}$		
$(7.762 \pm 1.168) \cdot 10^{-4}$	average	
$\mathcal{B}_{92} = \pi^-K^-K^+ \geq 0 \text{ neutrals } \nu_\tau$		
$(0.1493 \pm 0.0033) \cdot 10^{-2}$	average	
$(0.1590 \pm 0.0530 \pm 0.0200) \cdot 10^{-2}$	OPAL	[1509]

Table 327 – continued from previous page

τ lepton branching fraction	Experiment	Reference
$(0.1500^{+0.0900}_{-0.0700} \pm 0.0300) \cdot 10^{-2}$	TPC	[1506]
$\mathcal{B}_{93} = \pi^- K^- K^+ \nu_\tau$		
$(0.1431 \pm 0.0027) \cdot 10^{-2}$	average	
$(0.1630 \pm 0.0210 \pm 0.0170) \cdot 10^{-2}$	ALEPH	[1507]
$(0.1346 \pm 0.0010 \pm 0.0036) \cdot 10^{-2}$	BABAR	[1499]
$(0.1550 \pm 0.0010^{+0.0060}_{-0.0050}) \cdot 10^{-2}$	Belle	[1500]
$(0.1550 \pm 0.0060 \pm 0.0090) \cdot 10^{-2}$	CLEO3	[1501]
$\frac{\mathcal{B}_{93}}{\mathcal{B}_{60}} = \frac{\pi^- K^- K^+ \nu_\tau}{\pi^- \pi^+ \pi^- \nu_\tau \text{ (ex. } K^0)}$		
$(1.592 \pm 0.030) \cdot 10^{-2}$	average	
$(1.600 \pm 0.150 \pm 0.300) \cdot 10^{-2}$	CLEO	[1505]
$\mathcal{B}_{94} = \pi^- K^- K^+ \pi^0 \nu_\tau$		
$(0.611 \pm 0.183) \cdot 10^{-4}$	average	
$(7.500 \pm 2.900 \pm 1.500) \cdot 10^{-4}$	ALEPH	[1507]
$(0.550 \pm 0.140 \pm 0.120) \cdot 10^{-4}$	CLEO3	[1508]
$\frac{\mathcal{B}_{94}}{\mathcal{B}_{69}} = \frac{\pi^- K^- K^+ \pi^0 \nu_\tau}{\pi^- \pi^+ \pi^- \pi^0 \nu_\tau \text{ (ex. } K^0)}$		
$(0.1353 \pm 0.0405) \cdot 10^{-2}$	average	
$(0.7900 \pm 0.4400 \pm 0.1600) \cdot 10^{-2}$	CLEO	[1505]
$\mathcal{B}_{96} = K^- K^- K^+ \nu_\tau$		
$(2.169 \pm 0.800) \cdot 10^{-5}$	average	
$(1.578 \pm 0.130 \pm 0.123) \cdot 10^{-5}$	BABAR	[1499]
$(3.290 \pm 0.170^{+0.190}_{-0.200}) \cdot 10^{-5}$	Belle	[1500]
$\mathcal{B}_{102} = 3h^- 2h^+ \geq 0 \text{ neutrals } \nu_\tau \text{ (ex. } K^0)$		
$(0.0990 \pm 0.0037) \cdot 10^{-2}$	average	
$(0.0970 \pm 0.0050 \pm 0.0110) \cdot 10^{-2}$	CLEO	[1510]
$(0.1020 \pm 0.0290 \pm 0.0000) \cdot 10^{-2}$	HRS	[1511]
$(0.1700 \pm 0.0220 \pm 0.0260) \cdot 10^{-2}$	L3	[1496]
$\mathcal{B}_{103} = 3h^- 2h^+ \nu_\tau \text{ (ex. } K^0)$		
$(8.260 \pm 0.314) \cdot 10^{-4}$	average	
$(7.200 \pm 0.900 \pm 1.200) \cdot 10^{-4}$	ALEPH	[1464]
$(6.400 \pm 2.300 \pm 1.000) \cdot 10^{-4}$	ARGUS	[1512]
$(7.700 \pm 0.500 \pm 0.900) \cdot 10^{-4}$	CLEO	[1510]
$(9.700 \pm 1.500 \pm 0.500) \cdot 10^{-4}$	DELPHI	[1475]

Table 327 – continued from previous page

τ lepton branching fraction	Experiment	Reference
$(5.100 \pm 2.000 \pm 0.000) \cdot 10^{-4}$	HRS	[1511]
$(9.100 \pm 1.400 \pm 0.600) \cdot 10^{-4}$	OPAL	[1513]
$\mathcal{B}_{104} = 3h^- 2h^+ \pi^0 \nu_\tau$ (ex. K^0)		
$(1.641 \pm 0.114) \cdot 10^{-4}$	average	
$(2.100 \pm 0.700 \pm 0.900) \cdot 10^{-4}$	ALEPH	[1464]
$(1.700 \pm 0.200 \pm 0.200) \cdot 10^{-4}$	CLEO	[1504]
$(1.600 \pm 1.200 \pm 0.600) \cdot 10^{-4}$	DELPHI	[1475]
$(2.700 \pm 1.800 \pm 0.900) \cdot 10^{-4}$	OPAL	[1513]
$\mathcal{B}_{106} = (5\pi)^- \nu_\tau$		
$(0.7532 \pm 0.0356) \cdot 10^{-2}$	average	
$\mathcal{B}_{110} = X_s^- \nu_\tau$		
$(2.931 \pm 0.041) \cdot 10^{-2}$	average	
$\mathcal{B}_{126} = \pi^- \pi^0 \eta \nu_\tau$		
$(0.1386 \pm 0.0072) \cdot 10^{-2}$	average	
$(0.1800 \pm 0.0400 \pm 0.0200) \cdot 10^{-2}$	ALEPH	[1514]
$(0.1350 \pm 0.0030 \pm 0.0070) \cdot 10^{-2}$	Belle	[1515]
$(0.1700 \pm 0.0200 \pm 0.0200) \cdot 10^{-2}$	CLEO	[1516]
$\mathcal{B}_{128} = K^- \eta \nu_\tau$		
$(1.543 \pm 0.080) \cdot 10^{-4}$	average	
$(2.900^{+1.300}_{-1.200} \pm 0.700) \cdot 10^{-4}$	ALEPH	[1514]
$(1.420 \pm 0.110 \pm 0.070) \cdot 10^{-4}$	BABAR	[1517]
$(1.580 \pm 0.050 \pm 0.090) \cdot 10^{-4}$	Belle	[1515]
$(2.600 \pm 0.500 \pm 0.500) \cdot 10^{-4}$	CLEO	[1518]
$\mathcal{B}_{130} = K^- \pi^0 \eta \nu_\tau$		
$(0.483 \pm 0.116) \cdot 10^{-4}$	average	
$(0.460 \pm 0.110 \pm 0.040) \cdot 10^{-4}$	Belle	[1515]
$(1.770 \pm 0.560 \pm 0.710) \cdot 10^{-4}$	CLEO	[1519]
$\mathcal{B}_{132} = \pi^- \bar{K}^0 \eta \nu_\tau$		
$(0.936 \pm 0.149) \cdot 10^{-4}$	average	
$(0.880 \pm 0.140 \pm 0.060) \cdot 10^{-4}$	Belle	[1515]
$(2.200 \pm 0.700 \pm 0.220) \cdot 10^{-4}$	CLEO	[1519]
$\mathcal{B}_{136} = \pi^- \pi^+ \pi^- \eta \nu_\tau$ (ex. K^0)		

Table 327 – continued from previous page

τ lepton branching fraction	Experiment	Reference
$(2.196 \pm 0.129) \cdot 10^{-4}$	average	
$\mathcal{B}_{149} = h^- \omega \geq 0 \text{ neutrals } \nu_\tau$		
$(2.402 \pm 0.075) \cdot 10^{-2}$	average	
$\mathcal{B}_{150} = h^- \omega \nu_\tau$		
$(1.996 \pm 0.064) \cdot 10^{-2}$	average	
$(1.910 \pm 0.070 \pm 0.060) \cdot 10^{-2}$	ALEPH	[1514]
$(1.600 \pm 0.270 \pm 0.410) \cdot 10^{-2}$	CLEO	[1520]
$\frac{\mathcal{B}_{150}}{\mathcal{B}_{66}} = \frac{h^- \omega \nu_\tau}{h^- h^- h^+ \pi^0 \nu_\tau \text{ (ex. } K^0)}$		
0.4331 ± 0.0139	average	
$0.4310 \pm 0.0330 \pm 0.0000$	ALEPH	[1521]
$0.4640 \pm 0.0160 \pm 0.0170$	CLEO	[1498]
$\mathcal{B}_{151} = K^- \omega \nu_\tau$		
$(4.100 \pm 0.922) \cdot 10^{-4}$	average	
$(4.100 \pm 0.600 \pm 0.700) \cdot 10^{-4}$	CLEO3	[1508]
$\mathcal{B}_{152} = h^- \pi^0 \omega \nu_\tau$		
$(0.4066 \pm 0.0419) \cdot 10^{-2}$	average	
$(0.4300 \pm 0.0600 \pm 0.0500) \cdot 10^{-2}$	ALEPH	[1514]
$\frac{\mathcal{B}_{152}}{\mathcal{B}_{54}} = \frac{h^- \omega \pi^0 \nu_\tau}{h^- h^- h^+ \geq 0 \text{ neutrals } \geq 0 K_L^0 \nu_\tau}$		
$(2.674 \pm 0.275) \cdot 10^{-2}$	average	
$\frac{\mathcal{B}_{152}}{\mathcal{B}_{76}} = \frac{h^- \omega \pi^0 \nu_\tau}{h^- h^- h^+ 2\pi^0 \nu_\tau \text{ (ex. } K^0)}$		
0.8236 ± 0.0757	average	
$0.8100 \pm 0.0600 \pm 0.0600$	CLEO	[1503]
$\mathcal{B}_{167} = K^- \phi \nu_\tau$		
$(4.409 \pm 1.626) \cdot 10^{-5}$	average	
$\mathcal{B}_{168} = K^- \phi \nu_\tau \ (\phi \rightarrow K^+ K^-)$		
$(2.169 \pm 0.800) \cdot 10^{-5}$	average	
$\mathcal{B}_{169} = K^- \phi \nu_\tau \ (\phi \rightarrow K_S^0 K_L^0)$		
$(1.499 \pm 0.553) \cdot 10^{-5}$	average	
$\mathcal{B}_{800} = \pi^- \omega \nu_\tau$		

Table 327 – continued from previous page

τ lepton branching fraction	Experiment	Reference
$(1.955 \pm 0.065) \cdot 10^{-2}$	average	
$\mathcal{B}_{802} = K^- \pi^- \pi^+ \nu_\tau$ (ex. K^0, ω)		
$(0.2923 \pm 0.0067) \cdot 10^{-2}$	average	
$\mathcal{B}_{803} = K^- \pi^- \pi^+ \pi^0 \nu_\tau$ (ex. K^0, ω, η)		
$(4.105 \pm 1.429) \cdot 10^{-4}$	average	
$\mathcal{B}_{804} = \pi^- K_L^0 K_L^0 \nu_\tau$		
$(2.342 \pm 0.065) \cdot 10^{-4}$	average	
$\mathcal{B}_{805} = a_1^- (\rightarrow \pi^- \gamma) \nu_\tau$		
$(4.000 \pm 2.000) \cdot 10^{-4}$	average	
$(4.000 \pm 2.000 \pm 0.000) \cdot 10^{-4}$	ALEPH	[1464]
$\mathcal{B}_{806} = \pi^- \pi^0 K_L^0 K_L^0 \nu_\tau$		
$(1.816 \pm 0.207) \cdot 10^{-5}$	average	
$\mathcal{B}_{809} = \pi^- 4\pi^0 \nu_\tau$ (ex. K^0, η)		
$(8.640 \pm 0.670) \cdot 10^{-4}$	average	
$(9.020 \pm 0.400 \pm 0.650) \cdot 10^{-4}$	BABAR	[1462]
$\mathcal{B}_{810} = 2\pi^- \pi^+ 3\pi^0 \nu_\tau$ (ex. K^0)		
$(1.931 \pm 0.298) \cdot 10^{-4}$	average	
$\mathcal{B}_{811} = \pi^- 2\pi^0 \omega \nu_\tau$ (ex. K^0)		
$(7.139 \pm 1.586) \cdot 10^{-5}$	average	
$(7.300 \pm 1.200 \pm 1.200) \cdot 10^{-5}$	BABAR	[1522]
$\mathcal{B}_{812} = 2\pi^- \pi^+ 3\pi^0 \nu_\tau$ (ex. K^0, η, ω, f_1)		
$(1.325 \pm 2.682) \cdot 10^{-5}$	average	
$(1.000 \pm 0.800 \pm 3.000) \cdot 10^{-5}$	BABAR	[1522]
$\mathcal{B}_{820} = 3\pi^- 2\pi^+ \nu_\tau$ (ex. K^0, ω)		
$(8.242 \pm 0.313) \cdot 10^{-4}$	average	
$\mathcal{B}_{821} = 3\pi^- 2\pi^+ \nu_\tau$ (ex. K^0, ω, f_1)		
$(7.719 \pm 0.295) \cdot 10^{-4}$	average	
$(7.680 \pm 0.040 \pm 0.400) \cdot 10^{-4}$	BABAR	[1522]
$\mathcal{B}_{822} = K^- 2\pi^- 2\pi^+ \nu_\tau$ (ex. K^0)		
$(0.594 \pm 1.208) \cdot 10^{-6}$	average	

Table 327 – continued from previous page

τ lepton branching fraction	Experiment	Reference
$(0.600 \pm 0.500 \pm 1.100) \cdot 10^{-6}$	<i>BABAR</i>	[1522]
$\mathcal{B}_{830} = 3\pi^- 2\pi^+ \pi^0 \nu_\tau$ (ex. K^0)		
$(1.630 \pm 0.113) \cdot 10^{-4}$	average	
$\mathcal{B}_{831} = 2\pi^- \pi^+ \omega \nu_\tau$ (ex. K^0)		
$(8.400 \pm 0.624) \cdot 10^{-5}$	average	
$(8.400 \pm 0.400 \pm 0.600) \cdot 10^{-5}$	<i>BABAR</i>	[1522]
$\mathcal{B}_{832} = 3\pi^- 2\pi^+ \pi^0 \nu_\tau$ (ex. K^0, η, ω, f_1)		
$(3.775 \pm 0.874) \cdot 10^{-5}$	average	
$(3.600 \pm 0.300 \pm 0.900) \cdot 10^{-5}$	<i>BABAR</i>	[1522]
$\mathcal{B}_{833} = K^- 2\pi^- 2\pi^+ \pi^0 \nu_\tau$ (ex. K^0)		
$(1.108 \pm 0.566) \cdot 10^{-6}$	average	
$(1.100 \pm 0.400 \pm 0.400) \cdot 10^{-6}$	<i>BABAR</i>	[1522]
$\mathcal{B}_{910} = 2\pi^- \pi^+ \eta \nu_\tau$ ($\eta \rightarrow 3\pi^0$) (ex. K^0)		
$(7.176 \pm 0.422) \cdot 10^{-5}$	average	
$(8.270 \pm 0.880 \pm 0.810) \cdot 10^{-5}$	<i>BABAR</i>	[1522]
$\mathcal{B}_{911} = \pi^- 2\pi^0 \eta \nu_\tau$ ($\eta \rightarrow \pi^+ \pi^- \pi^0$) (ex. K^0)		
$(4.444 \pm 0.867) \cdot 10^{-5}$	average	
$(4.570 \pm 0.770 \pm 0.500) \cdot 10^{-5}$	<i>BABAR</i>	[1522]
$\mathcal{B}_{920} = \pi^- f_1 \nu_\tau$ ($f_1 \rightarrow 2\pi^- 2\pi^+$)		
$(5.225 \pm 0.444) \cdot 10^{-5}$	average	
$(5.200 \pm 0.310 \pm 0.370) \cdot 10^{-5}$	<i>BABAR</i>	[1522]
$\mathcal{B}_{930} = 2\pi^- \pi^+ \eta \nu_\tau$ ($\eta \rightarrow \pi^+ \pi^- \pi^0$) (ex. K^0)		
$(5.033 \pm 0.296) \cdot 10^{-5}$	average	
$(5.390 \pm 0.270 \pm 0.410) \cdot 10^{-5}$	<i>BABAR</i>	[1522]
$\mathcal{B}_{944} = 2\pi^- \pi^+ \eta \nu_\tau$ ($\eta \rightarrow \gamma\gamma$) (ex. K^0)		
$(8.654 \pm 0.509) \cdot 10^{-5}$	average	
$(8.260 \pm 0.350 \pm 0.510) \cdot 10^{-5}$	<i>BABAR</i>	[1522]
$\mathcal{B}_{945} = \pi^- 2\pi^0 \eta \nu_\tau$		
$(1.939 \pm 0.378) \cdot 10^{-4}$	average	
$\mathcal{B}_{998} = 1 - \mathcal{B}_{\text{All}}$		
$(0.0274 \pm 0.1026) \cdot 10^{-2}$	average	

10.1.6 Correlation terms between basis branching fractions uncertainties

The following tables report the correlation coefficients between basis quantities that were obtained from the τ branching fractions fit, in percent.

Table 328: Basis quantities correlation coefficients in percent, subtable 1.

\mathcal{B}_5	22													
\mathcal{B}_9	6	4												
\mathcal{B}_{10}	2	4	2											
\mathcal{B}_{14}	-13	-14	-13	-7										
\mathcal{B}_{16}	-2	-1	-3	35	-13									
\mathcal{B}_{20}	-7	-7	-12	-4	-42	-16								
\mathcal{B}_{23}	-3	-2	-5	14	-9	66	-18							
\mathcal{B}_{27}	-4	-4	-7	3	-9	61	-23	72						
\mathcal{B}_{28}	-2	-1	-3	2	-4	32	-10	28	37					
\mathcal{B}_{30}	-3	-3	-6	-1	-6	34	-14	41	52	23				
\mathcal{B}_{35}	0	0	0	0	0	0	0	0	0	0	0	0	0	
\mathcal{B}_{37}	0	-1	1	0	0	0	0	0	0	-1	0	0	-15	
\mathcal{B}_{40}	0	0	0	0	0	0	0	0	-1	0	0	-12	2	
\mathcal{B}_3	\mathcal{B}_5	\mathcal{B}_9	\mathcal{B}_{10}	\mathcal{B}_{14}	\mathcal{B}_{16}	\mathcal{B}_{20}	\mathcal{B}_{23}	\mathcal{B}_{27}	\mathcal{B}_{28}	\mathcal{B}_{30}	\mathcal{B}_{35}	\mathcal{B}_{37}	\mathcal{B}_{40}	

Table 329: Basis quantities correlation coefficients in percent, subtable 2.

\mathcal{B}_{42}	0	0	0	-2	1	-5	1	-4	-4	-2	-2	-1	-15	-20
\mathcal{B}_{44}	0	0	0	0	0	0	0	0	0	0	0	-1	0	-4
\mathcal{B}_{47}	0	-1	2	1	-1	2	-1	1	1	0	0	-1	2	-4
\mathcal{B}_{48}	0	0	0	0	0	0	0	0	0	0	0	-3	0	-2
\mathcal{B}_{50}	0	0	0	0	0	0	0	0	0	0	0	1	5	0
\mathcal{B}_{51}	0	0	0	0	0	0	0	0	0	0	0	-1	0	-1
\mathcal{B}_{53}	0	0	0	0	0	0	0	0	0	0	0	0	0	0
\mathcal{B}_{62}	-4	-5	6	2	-4	1	-11	-1	-2	-2	-3	-1	3	0
\mathcal{B}_{70}	-5	-6	-7	-2	-8	-1	-1	-1	-1	0	0	0	-1	0
\mathcal{B}_{77}	0	0	-2	0	-2	1	0	1	2	1	1	0	0	0
\mathcal{B}_{93}	-1	-1	2	1	-1	1	-2	0	0	0	0	0	1	0
\mathcal{B}_{94}	0	0	0	0	0	0	0	0	0	0	0	0	0	0
\mathcal{B}_{126}	0	0	0	0	0	0	-1	0	0	0	0	0	0	0
\mathcal{B}_{128}	0	0	1	0	0	0	0	0	0	0	0	0	1	0
\mathcal{B}_3	\mathcal{B}_5	\mathcal{B}_9	\mathcal{B}_{10}	\mathcal{B}_{14}	\mathcal{B}_{16}	\mathcal{B}_{20}	\mathcal{B}_{23}	\mathcal{B}_{27}	\mathcal{B}_{28}	\mathcal{B}_{30}	\mathcal{B}_{35}	\mathcal{B}_{37}	\mathcal{B}_{40}	

Table 330: Basis quantities correlation coefficients in percent, subtable 3.

\mathcal{B}_{130}	0	0	0	0	0	0	0	0	0	0	0	0	0	0
\mathcal{B}_{132}	0	0	0	0	0	0	0	0	0	0	0	0	0	0
\mathcal{B}_{136}	0	0	1	1	0	1	-1	0	0	0	0	0	1	0
\mathcal{B}_{151}	0	0	0	0	0	0	0	0	0	0	0	0	0	0
\mathcal{B}_{152}	0	0	-3	0	-2	1	0	1	2	1	2	0	0	0
\mathcal{B}_{167}	0	0	0	0	0	0	0	0	0	0	0	0	0	0
\mathcal{B}_{800}	-1	-1	-2	0	-3	0	0	0	0	0	0	0	0	0
\mathcal{B}_{802}	-1	-1	0	0	-1	-1	-3	-1	-2	-1	-1	0	0	0
\mathcal{B}_{803}	0	0	0	0	0	0	0	0	0	0	0	0	0	0
\mathcal{B}_{805}	0	0	0	0	0	0	0	0	0	0	0	0	0	0
\mathcal{B}_{811}	0	0	0	0	0	0	0	0	0	0	0	0	0	0
\mathcal{B}_{812}	1	1	0	0	0	0	0	0	0	0	0	0	0	0
\mathcal{B}_{821}	0	0	2	1	0	1	-2	0	0	0	0	0	1	0
\mathcal{B}_{822}	0	0	0	0	0	0	0	0	0	0	0	0	0	0
\mathcal{B}_3	\mathcal{B}_5	\mathcal{B}_9	\mathcal{B}_{10}	\mathcal{B}_{14}	\mathcal{B}_{16}	\mathcal{B}_{20}	\mathcal{B}_{23}	\mathcal{B}_{27}	\mathcal{B}_{28}	\mathcal{B}_{30}	\mathcal{B}_{35}	\mathcal{B}_{37}	\mathcal{B}_{40}	

Table 331: Basis quantities correlation coefficients in percent, subtable 4.

\mathcal{B}_{831}	0	0	1	0	0	0	-1	0	0	0	0	0	1	0
\mathcal{B}_{832}	0	0	0	0	0	0	0	0	0	0	0	0	0	0
\mathcal{B}_{833}	0	0	0	0	0	0	0	0	0	0	0	0	0	0
\mathcal{B}_{920}	0	0	1	0	0	0	-1	0	0	0	0	0	0	0
\mathcal{B}_{945}	0	0	0	0	0	0	0	0	0	0	0	0	0	0
\mathcal{B}_3	\mathcal{B}_5	\mathcal{B}_9	\mathcal{B}_{10}	\mathcal{B}_{14}	\mathcal{B}_{16}	\mathcal{B}_{20}	\mathcal{B}_{23}	\mathcal{B}_{27}	\mathcal{B}_{28}	\mathcal{B}_{30}	\mathcal{B}_{35}	\mathcal{B}_{37}	\mathcal{B}_{40}	

Table 332: Basis quantities correlation coefficients in percent, subtable 5.

\mathcal{B}_{44}	0													
\mathcal{B}_{47}	1	0												
\mathcal{B}_{48}	-1	-6	0											
\mathcal{B}_{50}	6	0	-7	0										
\mathcal{B}_{51}	0	-3	0	-6	0									
\mathcal{B}_{53}	0	0	0	0	0	0								
\mathcal{B}_{62}	-1	0	5	0	1	0	0							
\mathcal{B}_{70}	0	0	-1	0	0	0	0	-19						
\mathcal{B}_{77}	0	0	0	0	0	0	0	-1	-7					
\mathcal{B}_{93}	0	0	2	0	0	0	0	14	-4	0				
\mathcal{B}_{94}	0	0	0	0	0	0	0	0	-2	0	0			
\mathcal{B}_{126}	0	0	0	0	0	0	0	0	0	-5	0	0		
\mathcal{B}_{128}	0	0	1	0	0	0	0	2	0	0	1	0	4	
\mathcal{B}_{42}	\mathcal{B}_{44}	\mathcal{B}_{47}	\mathcal{B}_{48}	\mathcal{B}_{50}	\mathcal{B}_{51}	\mathcal{B}_{53}	\mathcal{B}_{62}	\mathcal{B}_{70}	\mathcal{B}_{77}	\mathcal{B}_{93}	\mathcal{B}_{94}	\mathcal{B}_{126}	\mathcal{B}_{128}	

Table 333: Basis quantities correlation coefficients in percent, subtable 6.

\mathcal{B}_{130}	0	0	0	0	0	0	0	0	-1	0	0	1	1
\mathcal{B}_{132}	0	0	0	0	0	0	0	0	0	0	0	2	1
\mathcal{B}_{136}	0	0	1	0	0	0	2	-1	0	1	0	0	0
\mathcal{B}_{151}	0	0	0	0	0	0	0	12	0	0	0	0	0
\mathcal{B}_{152}	0	0	0	0	0	0	-1	-11	-64	0	0	0	0
\mathcal{B}_{167}	0	0	0	0	0	0	-1	0	0	1	0	0	0
\mathcal{B}_{800}	0	0	0	0	0	0	-8	-69	-2	-1	0	0	0
\mathcal{B}_{802}	0	0	0	0	0	0	16	-6	0	0	0	0	0
\mathcal{B}_{803}	0	0	0	0	0	0	-1	-19	0	0	-2	0	-1
\mathcal{B}_{805}	0	0	0	0	0	0	0	0	0	0	0	0	0
\mathcal{B}_{811}	0	0	0	0	0	0	0	-1	0	0	0	0	0
\mathcal{B}_{812}	0	0	0	0	-1	0	0	-1	-1	0	0	0	0
\mathcal{B}_{821}	0	0	2	0	0	0	3	-1	0	1	0	0	1
\mathcal{B}_{822}	0	0	0	0	0	0	0	0	0	0	0	0	0
\mathcal{B}_{42}	\mathcal{B}_{44}	\mathcal{B}_{47}	\mathcal{B}_{48}	\mathcal{B}_{50}	\mathcal{B}_{51}	\mathcal{B}_{53}	\mathcal{B}_{62}	\mathcal{B}_{70}	\mathcal{B}_{77}	\mathcal{B}_{93}	\mathcal{B}_{94}	\mathcal{B}_{126}	\mathcal{B}_{128}

Table 334: Basis quantities correlation coefficients in percent, subtable 7.

\mathcal{B}_{831}	0	0	1	0	0	0	0	1	-1	0	1	0	0
\mathcal{B}_{832}	0	0	0	0	0	0	0	0	0	0	0	0	0
\mathcal{B}_{833}	0	0	0	0	0	0	0	0	0	0	0	0	0
\mathcal{B}_{920}	0	0	1	0	0	0	0	1	-1	0	1	0	0
\mathcal{B}_{945}	0	0	0	0	0	0	0	0	0	0	0	0	0
\mathcal{B}_{42}	\mathcal{B}_{44}	\mathcal{B}_{47}	\mathcal{B}_{48}	\mathcal{B}_{50}	\mathcal{B}_{51}	\mathcal{B}_{53}	\mathcal{B}_{62}	\mathcal{B}_{70}	\mathcal{B}_{77}	\mathcal{B}_{93}	\mathcal{B}_{94}	\mathcal{B}_{126}	\mathcal{B}_{128}

Table 335: Basis quantities correlation coefficients in percent, subtable 8.

\mathcal{B}_{132}	0												
\mathcal{B}_{136}	0	0											
\mathcal{B}_{151}	0	0	0										
\mathcal{B}_{152}	0	0	0	0									
\mathcal{B}_{167}	0	0	0	0	0								
\mathcal{B}_{800}	0	0	0	-14	-3	0							
\mathcal{B}_{802}	0	0	0	-2	0	1	-1						
\mathcal{B}_{803}	0	0	0	-58	0	0	9	1					
\mathcal{B}_{805}	0	0	0	0	0	0	0	0	0				
\mathcal{B}_{811}	0	-1	20	0	0	0	0	0	0	0	0		
\mathcal{B}_{812}	0	-2	-8	0	0	0	0	0	0	0	0	-16	
\mathcal{B}_{821}	0	0	46	0	0	0	0	0	0	0	8	-4	
\mathcal{B}_{822}	0	0	-1	0	0	0	0	0	0	0	0	0	-1
\mathcal{B}_{130}	\mathcal{B}_{132}	\mathcal{B}_{136}	\mathcal{B}_{151}	\mathcal{B}_{152}	\mathcal{B}_{167}	\mathcal{B}_{800}	\mathcal{B}_{802}	\mathcal{B}_{803}	\mathcal{B}_{805}	\mathcal{B}_{811}	\mathcal{B}_{812}	\mathcal{B}_{821}	\mathcal{B}_{822}

Table 336: Basis quantities correlation coefficients in percent, subtable 9.

\mathcal{B}_{831}	0	0	38	0	0	0	0	0	0	14	-4	39	-1
\mathcal{B}_{832}	0	0	3	0	0	0	0	0	0	2	0	3	0
\mathcal{B}_{833}	0	0	-1	0	0	0	0	0	0	0	0	-1	0
\mathcal{B}_{920}	0	0	20	0	0	0	0	0	0	3	-2	34	-1
\mathcal{B}_{945}	0	-1	25	0	0	0	0	0	0	10	-11	10	0
\mathcal{B}_{130}	\mathcal{B}_{132}	\mathcal{B}_{136}	\mathcal{B}_{151}	\mathcal{B}_{152}	\mathcal{B}_{167}	\mathcal{B}_{800}	\mathcal{B}_{802}	\mathcal{B}_{803}	\mathcal{B}_{805}	\mathcal{B}_{811}	\mathcal{B}_{812}	\mathcal{B}_{821}	\mathcal{B}_{822}

Table 337: Basis quantities correlation coefficients in percent, subtable 10.

\mathcal{B}_{832}	-2			
\mathcal{B}_{833}	-1	-1		
\mathcal{B}_{920}	17	1	0	
\mathcal{B}_{945}	17	2	0	4
\mathcal{B}_{831}	\mathcal{B}_{832}	\mathcal{B}_{833}	\mathcal{B}_{920}	\mathcal{B}_{945}

10.1.7 Equality constraints

The constraints on the τ branching fractions fitted quantities are listed in the following. The constraint equations include as coefficients the values of some non-tau branching fractions, denoted *e.g.*, with the self-describing notation $\mathcal{B}_{K_S \rightarrow \pi^0 \pi^0}$. Some coefficients are probabilities corresponding to the modulus square of amplitudes describing quantum mixtures of states such as K^0 , \bar{K}^0 , K_S , K_L , denoted with *e.g.*, $\mathcal{B}_{\langle K^0 | K_S \rangle} = |\langle K^0 | K_S \rangle|^2$. All non-tau quantities are taken from the PDG 2018 [21] averages. The fit procedure does not account for their uncertainties, which are generally small with respect to the uncertainties on the τ branching fractions. Please note that, in the following table, when a quantity like $\mathcal{B}_3/\mathcal{B}_5$ appears on the left side of the equation, it represents a fitted quantity, and when it appears on the right side it represents the ratio of two separate fitted quantities.

$$\begin{aligned}
 \mathcal{B}_1 = & \mathcal{B}_3 + \mathcal{B}_5 + \mathcal{B}_9 + \mathcal{B}_{10} + \mathcal{B}_{14} + \mathcal{B}_{16} \\
 & + \mathcal{B}_{20} + \mathcal{B}_{23} + \mathcal{B}_{27} + \mathcal{B}_{28} + \mathcal{B}_{30} + \mathcal{B}_{35} \\
 & + \mathcal{B}_{40} + \mathcal{B}_{44} + \mathcal{B}_{37} + \mathcal{B}_{42} + \mathcal{B}_{47} + \mathcal{B}_{48} \\
 & + \mathcal{B}_{804} + \mathcal{B}_{50} + \mathcal{B}_{51} + \mathcal{B}_{806} + \mathcal{B}_{126} \cdot \mathcal{B}_{\eta \rightarrow \text{neutral}} \\
 & + \mathcal{B}_{128} \cdot \mathcal{B}_{\eta \rightarrow \text{neutral}} + \mathcal{B}_{130} \cdot \mathcal{B}_{\eta \rightarrow \text{neutral}} + \mathcal{B}_{132} \cdot \mathcal{B}_{\eta \rightarrow \text{neutral}} \\
 & + \mathcal{B}_{800} \cdot \mathcal{B}_{\omega \rightarrow \pi^0 \gamma} + \mathcal{B}_{151} \cdot \mathcal{B}_{\omega \rightarrow \pi^0 \gamma} + \mathcal{B}_{152} \cdot \mathcal{B}_{\omega \rightarrow \pi^0 \gamma} \\
 & + \mathcal{B}_{167} \cdot \mathcal{B}_{\phi \rightarrow K_S K_L}
 \end{aligned}$$

$$\begin{aligned}
& \mathcal{B}_2 = \mathcal{B}_3 + \mathcal{B}_5 + \mathcal{B}_9 + \mathcal{B}_{10} + \mathcal{B}_{14} + \mathcal{B}_{16} \\
& + \mathcal{B}_{20} + \mathcal{B}_{23} + \mathcal{B}_{27} + \mathcal{B}_{28} + \mathcal{B}_{30} + \mathcal{B}_{35} \cdot (\mathcal{B}_{<\overline{K}^0|K_S>} \cdot \mathcal{B}_{K_S \rightarrow \pi^0 \pi^0} \\
& + \mathcal{B}_{<\overline{K}^0|K_L>} + \mathcal{B}_{40} \cdot (\mathcal{B}_{<\overline{K}^0|K_S>} \cdot \mathcal{B}_{K_S \rightarrow \pi^0 \pi^0} + \mathcal{B}_{<\overline{K}^0|K_L>})) + \mathcal{B}_{44} \cdot (\mathcal{B}_{<\overline{K}^0|K_S>} \cdot \mathcal{B}_{K_S \rightarrow \pi^0 \pi^0} \\
& + \mathcal{B}_{<\overline{K}^0|K_L>} + \mathcal{B}_{37} \cdot (\mathcal{B}_{<\overline{K}^0|K_S>} \cdot \mathcal{B}_{K_S \rightarrow \pi^0 \pi^0} + \mathcal{B}_{<\overline{K}^0|K_L>})) + \mathcal{B}_{42} \cdot (\mathcal{B}_{<\overline{K}^0|K_S>} \cdot \mathcal{B}_{K_S \rightarrow \pi^0 \pi^0} \\
& + \mathcal{B}_{<\overline{K}^0|K_L>} + \mathcal{B}_{47} \cdot (\mathcal{B}_{K_S \rightarrow \pi^0 \pi^0} \cdot \mathcal{B}_{K_S \rightarrow \pi^0 \pi^0}) + \mathcal{B}_{48} \cdot \mathcal{B}_{K_S \rightarrow \pi^0 \pi^0} \\
& + \mathcal{B}_{804} + \mathcal{B}_{50} \cdot (\mathcal{B}_{K_S \rightarrow \pi^0 \pi^0} \cdot \mathcal{B}_{K_S \rightarrow \pi^0 \pi^0}) + \mathcal{B}_{51} \cdot \mathcal{B}_{K_S \rightarrow \pi^0 \pi^0} \\
& + \mathcal{B}_{806} + \mathcal{B}_{126} \cdot \mathcal{B}_{\eta \rightarrow \text{neutral}} + \mathcal{B}_{128} \cdot \mathcal{B}_{\eta \rightarrow \text{neutral}} + \mathcal{B}_{130} \cdot \mathcal{B}_{\eta \rightarrow \text{neutral}} \\
& + \mathcal{B}_{132} \cdot (\mathcal{B}_{\eta \rightarrow \text{neutral}} \cdot (\mathcal{B}_{<\overline{K}^0|K_S>} \cdot \mathcal{B}_{K_S \rightarrow \pi^0 \pi^0} + \mathcal{B}_{<\overline{K}^0|K_L>})) + \mathcal{B}_{800} \cdot \mathcal{B}_{\omega \rightarrow \pi^0 \gamma} \\
& + \mathcal{B}_{151} \cdot \mathcal{B}_{\omega \rightarrow \pi^0 \gamma} + \mathcal{B}_{152} \cdot \mathcal{B}_{\omega \rightarrow \pi^0 \gamma} + \mathcal{B}_{167} \cdot (\mathcal{B}_{\phi \rightarrow K_S K_L} \cdot \mathcal{B}_{K_S \rightarrow \pi^0 \pi^0})
\end{aligned}$$

$$\frac{\mathcal{B}_3}{\mathcal{B}_5} = \frac{\mathcal{B}_3}{\mathcal{B}_5}$$

$$\begin{aligned} \mathcal{B}_7 = & \mathcal{B}_{35} \cdot \mathcal{B}_{<\overline{K}^0|K_L>} + \mathcal{B}_9 + \mathcal{B}_{804} + \mathcal{B}_{37} \cdot \mathcal{B}_{$$

$$\mathcal{B}_8 = \mathcal{B}_9 + \mathcal{B}_{10}$$

$$\frac{\mathcal{B}_8}{\mathcal{B}_5} = \frac{\mathcal{B}_8}{\mathcal{B}_5}$$

$$\frac{\mathcal{B}_9}{\mathcal{B}_5} = \frac{\mathcal{B}_9}{\mathcal{B}_5}$$

$$\frac{\mathcal{B}_{10}}{\mathcal{B}_5} = \frac{\mathcal{B}_{10}}{\mathcal{B}_5}$$

$$\frac{\mathcal{B}_{10}}{\mathcal{B}_9} = \frac{\mathcal{B}_{10}}{\mathcal{B}_9}$$

$$\begin{aligned}
\mathcal{B}_{11} = & \mathcal{B}_{14} + \mathcal{B}_{16} + \mathcal{B}_{20} + \mathcal{B}_{23} + \mathcal{B}_{27} + \mathcal{B}_{28} \\
& + \mathcal{B}_{30} + \mathcal{B}_{35} \cdot (\mathcal{B}_{<K^0|K_S>} \cdot \mathcal{B}_{K_S \rightarrow \pi^0 \pi^0}) + \mathcal{B}_{37} \cdot (\mathcal{B}_{<K^0|K_S>} \cdot \mathcal{B}_{K_S \rightarrow \pi^0 \pi^0}) \\
& + \mathcal{B}_{40} \cdot (\mathcal{B}_{<K^0|K_S>} \cdot \mathcal{B}_{K_S \rightarrow \pi^0 \pi^0}) + \mathcal{B}_{42} \cdot (\mathcal{B}_{<K^0|K_S>} \cdot \mathcal{B}_{K_S \rightarrow \pi^0 \pi^0}) \\
& + \mathcal{B}_{47} \cdot (\mathcal{B}_{K_S \rightarrow \pi^0 \pi^0} \cdot \mathcal{B}_{K_S \rightarrow \pi^0 \pi^0}) + \mathcal{B}_{50} \cdot (\mathcal{B}_{K_S \rightarrow \pi^0 \pi^0} \cdot \mathcal{B}_{K_S \rightarrow \pi^0 \pi^0}) \\
& + \mathcal{B}_{126} \cdot \mathcal{B}_{\eta \rightarrow \text{neutral}} + \mathcal{B}_{128} \cdot \mathcal{B}_{\eta \rightarrow \text{neutral}} + \mathcal{B}_{130} \cdot \mathcal{B}_{\eta \rightarrow \text{neutral}} \\
& + \mathcal{B}_{132} \cdot (\mathcal{B}_{<K^0|K_S>} \cdot \mathcal{B}_{K_S \rightarrow \pi^0 \pi^0} \cdot \mathcal{B}_{\eta \rightarrow \text{neutral}}) + \mathcal{B}_{151} \cdot \mathcal{B}_{\omega \rightarrow \pi^0 \gamma} \\
& + \mathcal{B}_{152} \cdot \mathcal{B}_{\omega \rightarrow \pi^0 \gamma} + \mathcal{B}_{800} \cdot \mathcal{B}_{\omega \rightarrow \pi^0 \gamma}
\end{aligned}$$

$$\begin{aligned} \mathcal{B}_{12} = & \mathcal{B}_{128} \cdot \mathcal{B}_{\eta \rightarrow 3\pi^0} + \mathcal{B}_{30} + \mathcal{B}_{23} + \mathcal{B}_{28} + \mathcal{B}_{14} \\ & + \mathcal{B}_{16} + \mathcal{B}_{20} + \mathcal{B}_{27} + \mathcal{B}_{126} \cdot \mathcal{B}_{\eta \rightarrow 3\pi^0} + \mathcal{B}_{130} \cdot \mathcal{B}_{\eta \rightarrow 3\pi^0} \end{aligned}$$

$$\mathcal{B}_{13} = \mathcal{B}_{14} + \mathcal{B}_{16}$$

$$\begin{aligned} \mathcal{B}_{17} = & \mathcal{B}_{128} \cdot \mathcal{B}_{\eta \rightarrow 3\pi^0} + \mathcal{B}_{30} + \mathcal{B}_{23} + \mathcal{B}_{28} + \mathcal{B}_{35} \cdot (\mathcal{B}_{<K^0|K_S>} \cdot \mathcal{B}_{K_S \rightarrow \pi^0\pi^0}) \\ & + \mathcal{B}_{40} \cdot (\mathcal{B}_{<K^0|K_S>} \cdot \mathcal{B}_{K_S \rightarrow \pi^0\pi^0}) + \mathcal{B}_{42} \cdot (\mathcal{B}_{<K^0|K_S>} \cdot \mathcal{B}_{K_S \rightarrow \pi^0\pi^0}) \\ & + \mathcal{B}_{20} + \mathcal{B}_{27} + \mathcal{B}_{47} \cdot (\mathcal{B}_{K_S \rightarrow \pi^0\pi^0} \cdot \mathcal{B}_{K_S \rightarrow \pi^0\pi^0}) + \mathcal{B}_{50} \cdot (\mathcal{B}_{K_S \rightarrow \pi^0\pi^0} \cdot \mathcal{B}_{K_S \rightarrow \pi^0\pi^0}) \\ & + \mathcal{B}_{126} \cdot \mathcal{B}_{\eta \rightarrow 3\pi^0} + \mathcal{B}_{37} \cdot (\mathcal{B}_{<K^0|K_S>} \cdot \mathcal{B}_{K_S \rightarrow \pi^0\pi^0}) + \mathcal{B}_{130} \cdot \mathcal{B}_{\eta \rightarrow 3\pi^0} \end{aligned}$$

$$\mathcal{B}_{18} = \mathcal{B}_{23} + \mathcal{B}_{35} \cdot (\mathcal{B}_{<K^0|K_S>} \cdot \mathcal{B}_{K_S \rightarrow \pi^0 \pi^0}) + \mathcal{B}_{20} + \mathcal{B}_{37} \cdot (\mathcal{B}_{<K^0|K_S>} \cdot \mathcal{B}_{K_S \rightarrow \pi^0 \pi^0})$$

$$\mathcal{B}_{19} = \mathcal{B}_{23} + \mathcal{B}_{20}$$

$$\frac{\mathcal{B}_{19}}{\mathcal{B}_{13}} = \frac{\mathcal{B}_{19}}{\mathcal{B}_{13}}$$

$$\begin{aligned}\mathcal{B}_{24} = & \mathcal{B}_{27} + \mathcal{B}_{28} + \mathcal{B}_{30} + \mathcal{B}_{40} \cdot (\mathcal{B}_{<K^0|K_S>} \cdot \mathcal{B}_{K_S \rightarrow \pi^0 \pi^0}) \\ & + \mathcal{B}_{42} \cdot (\mathcal{B}_{<K^0|K_S>} \cdot \mathcal{B}_{K_S \rightarrow \pi^0 \pi^0}) + \mathcal{B}_{47} \cdot (\mathcal{B}_{K_S \rightarrow \pi^0 \pi^0} \cdot \mathcal{B}_{K_S \rightarrow \pi^0 \pi^0}) \\ & + \mathcal{B}_{50} \cdot (\mathcal{B}_{K_S \rightarrow \pi^0 \pi^0} \cdot \mathcal{B}_{K_S \rightarrow \pi^0 \pi^0}) + \mathcal{B}_{126} \cdot \mathcal{B}_{\eta \rightarrow 3\pi^0} + \mathcal{B}_{128} \cdot \mathcal{B}_{\eta \rightarrow 3\pi^0} \\ & + \mathcal{B}_{130} \cdot \mathcal{B}_{\eta \rightarrow 3\pi^0} + \mathcal{B}_{132} \cdot (\mathcal{B}_{<K^0|K_S>} \cdot \mathcal{B}_{K_S \rightarrow \pi^0 \pi^0} \cdot \mathcal{B}_{\eta \rightarrow 3\pi^0})\end{aligned}$$

$$\begin{aligned}\mathcal{B}_{25} = & \mathcal{B}_{128} \cdot \mathcal{B}_{\eta \rightarrow 3\pi^0} + \mathcal{B}_{30} + \mathcal{B}_{28} + \mathcal{B}_{27} + \mathcal{B}_{126} \cdot \mathcal{B}_{\eta \rightarrow 3\pi^0} \\ & + \mathcal{B}_{130} \cdot \mathcal{B}_{\eta \rightarrow 3\pi^0}\end{aligned}$$

$$\begin{aligned}\mathcal{B}_{26} = & \mathcal{B}_{128} \cdot \mathcal{B}_{\eta \rightarrow 3\pi^0} + \mathcal{B}_{28} + \mathcal{B}_{40} \cdot (\mathcal{B}_{<K^0|K_S>} \cdot \mathcal{B}_{K_S \rightarrow \pi^0 \pi^0}) \\ & + \mathcal{B}_{42} \cdot (\mathcal{B}_{<K^0|K_S>} \cdot \mathcal{B}_{K_S \rightarrow \pi^0 \pi^0}) + \mathcal{B}_{27}\end{aligned}$$

$$\frac{\mathcal{B}_{26}}{\mathcal{B}_{13}} = \frac{\mathcal{B}_{26}}{\mathcal{B}_{13}}$$

$$\mathcal{B}_{29} = \mathcal{B}_{30} + \mathcal{B}_{126} \cdot \mathcal{B}_{\eta \rightarrow 3\pi^0} + \mathcal{B}_{130} \cdot \mathcal{B}_{\eta \rightarrow 3\pi^0}$$

$$\begin{aligned}\mathcal{B}_{31} = & \mathcal{B}_{128} \cdot \mathcal{B}_{\eta \rightarrow \text{neutral}} + \mathcal{B}_{23} + \mathcal{B}_{28} + \mathcal{B}_{42} + \mathcal{B}_{16} \\ & + \mathcal{B}_{37} + \mathcal{B}_{10} + \mathcal{B}_{167} \cdot (\mathcal{B}_{\phi \rightarrow K_S K_L} \cdot \mathcal{B}_{K_S \rightarrow \pi^0 \pi^0})\end{aligned}$$

$$\begin{aligned}\mathcal{B}_{32} = & \mathcal{B}_{16} + \mathcal{B}_{23} + \mathcal{B}_{28} + \mathcal{B}_{37} + \mathcal{B}_{42} + \mathcal{B}_{128} \cdot \mathcal{B}_{\eta \rightarrow \text{neutral}} \\ & + \mathcal{B}_{130} \cdot \mathcal{B}_{\eta \rightarrow \text{neutral}} + \mathcal{B}_{167} \cdot (\mathcal{B}_{\phi \rightarrow K_S K_L} \cdot \mathcal{B}_{K_S \rightarrow \pi^0 \pi^0})\end{aligned}$$

$$\begin{aligned}\mathcal{B}_{33} = & \mathcal{B}_{35} \cdot \mathcal{B}_{<\bar{K}^0|K_S>} + \mathcal{B}_{40} \cdot \mathcal{B}_{<\bar{K}^0|K_S>} + \mathcal{B}_{42} \cdot \mathcal{B}_{<K^0|K_S>} \\ & + \mathcal{B}_{47} + \mathcal{B}_{48} + \mathcal{B}_{50} + \mathcal{B}_{51} + \mathcal{B}_{37} \cdot \mathcal{B}_{<K^0|K_S>} \\ & + \mathcal{B}_{132} \cdot (\mathcal{B}_{<\bar{K}^0|K_S>} \cdot \mathcal{B}_{\eta \rightarrow \text{neutral}}) + \mathcal{B}_{44} \cdot \mathcal{B}_{<\bar{K}^0|K_S>} + \mathcal{B}_{167} \cdot \mathcal{B}_{\phi \rightarrow K_S K_L}\end{aligned}$$

$$\mathcal{B}_{34} = \mathcal{B}_{35} + \mathcal{B}_{37}$$

$$\mathcal{B}_{38} = \mathcal{B}_{42} + \mathcal{B}_{37}$$

$$\mathcal{B}_{39} = \mathcal{B}_{40} + \mathcal{B}_{42}$$

$$\mathcal{B}_{43} = \mathcal{B}_{40} + \mathcal{B}_{44}$$

$$\mathcal{B}_{46} = \mathcal{B}_{48} + \mathcal{B}_{47} + \mathcal{B}_{804}$$

$$\mathcal{B}_{49} = \mathcal{B}_{50} + \mathcal{B}_{51} + \mathcal{B}_{806}$$

$$\begin{aligned}\mathcal{B}_{66} = & \mathcal{B}_{70} + \mathcal{B}_{94} + \mathcal{B}_{128} \cdot \mathcal{B}_{\eta \rightarrow \pi^+ \pi^- \pi^0} + \mathcal{B}_{151} \cdot \mathcal{B}_{\omega \rightarrow \pi^+ \pi^- \pi^0} \\ & + \mathcal{B}_{152} \cdot \mathcal{B}_{\omega \rightarrow \pi^+ \pi^-} + \mathcal{B}_{800} \cdot \mathcal{B}_{\omega \rightarrow \pi^+ \pi^- \pi^0} + \mathcal{B}_{803}\end{aligned}$$

$$\mathcal{B}_{67} = \mathcal{B}_{70} + \mathcal{B}_{94} + \mathcal{B}_{128} \cdot \mathcal{B}_{\eta \rightarrow \pi^+ \pi^- \pi^0} + \mathcal{B}_{803}$$

$$\begin{aligned}\mathcal{B}_{68} = & \mathcal{B}_{40} \cdot (\mathcal{B}_{<K^0|K_S>} \cdot \mathcal{B}_{K_S \rightarrow \pi^+ \pi^-}) + \mathcal{B}_{70} + \mathcal{B}_{152} \cdot \mathcal{B}_{\omega \rightarrow \pi^+ \pi^-} \\ & + \mathcal{B}_{800} \cdot \mathcal{B}_{\omega \rightarrow \pi^+ \pi^- \pi^0}\end{aligned}$$

$$\mathcal{B}_{69} = \mathcal{B}_{152} \cdot \mathcal{B}_{\omega \rightarrow \pi^+ \pi^-} + \mathcal{B}_{70} + \mathcal{B}_{800} \cdot \mathcal{B}_{\omega \rightarrow \pi^+ \pi^- \pi^0}$$

$$\begin{aligned}\mathcal{B}_{74} = & \mathcal{B}_{152} \cdot \mathcal{B}_{\omega \rightarrow \pi^+ \pi^- \pi^0} + \mathcal{B}_{78} + \mathcal{B}_{77} + \mathcal{B}_{126} \cdot \mathcal{B}_{\eta \rightarrow \pi^+ \pi^- \pi^0} \\ & + \mathcal{B}_{130} \cdot \mathcal{B}_{\eta \rightarrow \pi^+ \pi^- \pi^0}\end{aligned}$$

$$\begin{aligned}\mathcal{B}_{75} = & \mathcal{B}_{152} \cdot \mathcal{B}_{\omega \rightarrow \pi^+ \pi^- \pi^0} + \mathcal{B}_{47} \cdot (2 \cdot \mathcal{B}_{K_S \rightarrow \pi^+ \pi^-} \cdot \mathcal{B}_{K_S \rightarrow \pi^0 \pi^0}) \\ & + \mathcal{B}_{77} + \mathcal{B}_{126} \cdot \mathcal{B}_{\eta \rightarrow \pi^+ \pi^- \pi^0} + \mathcal{B}_{130} \cdot \mathcal{B}_{\eta \rightarrow \pi^+ \pi^- \pi^0}\end{aligned}$$

$$\mathcal{B}_{76} = \mathcal{B}_{152} \cdot \mathcal{B}_{\omega \rightarrow \pi^+ \pi^- \pi^0} + \mathcal{B}_{77} + \mathcal{B}_{126} \cdot \mathcal{B}_{\eta \rightarrow \pi^+ \pi^- \pi^0} + \mathcal{B}_{130} \cdot \mathcal{B}_{\eta \rightarrow \pi^+ \pi^- \pi^0}$$

$$\frac{\mathcal{B}_{76}}{\mathcal{B}_{54}} = \frac{\mathcal{B}_{76}}{\mathcal{B}_{54}}$$

$$\mathcal{B}_{78} = \mathcal{B}_{810} + \mathcal{B}_{50} \cdot (2 \cdot \mathcal{B}_{K_S \rightarrow \pi^+ \pi^-} \cdot \mathcal{B}_{K_S \rightarrow \pi^0 \pi^0}) + \mathcal{B}_{132} \cdot (\mathcal{B}_{<\bar{K}^0|K_S>} \cdot \mathcal{B}_{K_S \rightarrow \pi^+ \pi^-} \cdot \mathcal{B}_{\eta \rightarrow 3\pi^0})$$

$$\begin{aligned}\mathcal{B}_{79} = & \mathcal{B}_{37} \cdot (\mathcal{B}_{<K^0|K_S>} \cdot \mathcal{B}_{K_S \rightarrow \pi^+ \pi^-}) + \mathcal{B}_{42} \cdot (\mathcal{B}_{<K^0|K_S>} \cdot \mathcal{B}_{K_S \rightarrow \pi^+ \pi^-}) \\ & + \mathcal{B}_{93} + \mathcal{B}_{94} + \mathcal{B}_{128} \cdot \mathcal{B}_{\eta \rightarrow \text{charged}} + \mathcal{B}_{151} \cdot (\mathcal{B}_{\omega \rightarrow \pi^+ \pi^- \pi^0} \\ & + \mathcal{B}_{\omega \rightarrow \pi^+ \pi^-}) + \mathcal{B}_{168} + \mathcal{B}_{802} + \mathcal{B}_{803}\end{aligned}$$

$$\mathcal{B}_{80} = \mathcal{B}_{93} + \mathcal{B}_{802} + \mathcal{B}_{151} \cdot \mathcal{B}_{\omega \rightarrow \pi^+ \pi^-}$$

$$\frac{\mathcal{B}_{80}}{\mathcal{B}_{60}} = \frac{\mathcal{B}_{80}}{\mathcal{B}_{60}}$$

$$\mathcal{B}_{81} = \mathcal{B}_{128} \cdot \mathcal{B}_{\eta \rightarrow \pi^+ \pi^- \pi^0} + \mathcal{B}_{94} + \mathcal{B}_{803} + \mathcal{B}_{151} \cdot \mathcal{B}_{\omega \rightarrow \pi^+ \pi^- \pi^0}$$

$$\frac{\mathcal{B}_{81}}{\mathcal{B}_{69}} = \frac{\mathcal{B}_{81}}{\mathcal{B}_{69}}$$

$$\begin{aligned}\mathcal{B}_{82} = & \mathcal{B}_{128} \cdot \mathcal{B}_{\eta \rightarrow \text{charged}} + \mathcal{B}_{42} \cdot (\mathcal{B}_{<K^0|K_S>} \cdot \mathcal{B}_{K_S \rightarrow \pi^+ \pi^-}) + \mathcal{B}_{802} \\ & + \mathcal{B}_{803} + \mathcal{B}_{151} \cdot (\mathcal{B}_{\omega \rightarrow \pi^+ \pi^- \pi^0} + \mathcal{B}_{\omega \rightarrow \pi^+ \pi^-}) + \mathcal{B}_{37} \cdot (\mathcal{B}_{<K^0|K_S>} \cdot \mathcal{B}_{K_S \rightarrow \pi^+ \pi^-})\end{aligned}$$

$$\begin{aligned}\mathcal{B}_{83} = & \mathcal{B}_{128} \cdot \mathcal{B}_{\eta \rightarrow \pi^+ \pi^- \pi^0} + \mathcal{B}_{802} + \mathcal{B}_{803} + \mathcal{B}_{151} \cdot (\mathcal{B}_{\omega \rightarrow \pi^+ \pi^- \pi^0} \\ & + \mathcal{B}_{\omega \rightarrow \pi^+ \pi^-})\end{aligned}$$

$$\mathcal{B}_{84} = \mathcal{B}_{802} + \mathcal{B}_{151} \cdot \mathcal{B}_{\omega \rightarrow \pi^+ \pi^-} + \mathcal{B}_{37} \cdot (\mathcal{B}_{<K^0|K_S>} \cdot \mathcal{B}_{K_S \rightarrow \pi^+ \pi^-})$$

$$\mathcal{B}_{85} = \mathcal{B}_{802} + \mathcal{B}_{151} \cdot \mathcal{B}_{\omega \rightarrow \pi^+ \pi^-}$$

$$\frac{\mathcal{B}_{85}}{\mathcal{B}_{60}} = \frac{\mathcal{B}_{85}}{\mathcal{B}_{60}}$$

$$\begin{aligned}\mathcal{B}_{87} = & \mathcal{B}_{42} \cdot (\mathcal{B}_{<K^0|K_S>} \cdot \mathcal{B}_{K_S \rightarrow \pi^+ \pi^-}) + \mathcal{B}_{128} \cdot \mathcal{B}_{\eta \rightarrow \pi^+ \pi^- \pi^0} + \mathcal{B}_{151} \cdot \mathcal{B}_{\omega \rightarrow \pi^+ \pi^- \pi^0} \\ & + \mathcal{B}_{803}\end{aligned}$$

$$\mathcal{B}_{88} = \mathcal{B}_{128} \cdot \mathcal{B}_{\eta \rightarrow \pi^+ \pi^- \pi^0} + \mathcal{B}_{803} + \mathcal{B}_{151} \cdot \mathcal{B}_{\omega \rightarrow \pi^+ \pi^- \pi^0}$$

$$\mathcal{B}_{89} = \mathcal{B}_{803} + \mathcal{B}_{151} \cdot \mathcal{B}_{\omega \rightarrow \pi^+ \pi^- \pi^0}$$

$$\mathcal{B}_{92} = \mathcal{B}_{94} + \mathcal{B}_{93}$$

$$\frac{\mathcal{B}_{93}}{\mathcal{B}_{60}} = \frac{\mathcal{B}_{93}}{\mathcal{B}_{60}}$$

$$\frac{\mathcal{B}_{94}}{\mathcal{B}_{69}} = \frac{\mathcal{B}_{94}}{\mathcal{B}_{69}}$$

$$\mathcal{B}_{96} = \mathcal{B}_{167} \cdot \mathcal{B}_{\phi \rightarrow K^+ K^-}$$

$$\mathcal{B}_{102} = \mathcal{B}_{103} + \mathcal{B}_{104}$$

$$\mathcal{B}_{103} = \mathcal{B}_{820} + \mathcal{B}_{822} + \mathcal{B}_{831} \cdot \mathcal{B}_{\omega \rightarrow \pi^+ \pi^-}$$

$$\mathcal{B}_{104} = \mathcal{B}_{830} + \mathcal{B}_{833}$$

$$\begin{aligned} \mathcal{B}_{106} = & \mathcal{B}_{30} + \mathcal{B}_{44} \cdot \mathcal{B}_{<\bar{K}^0|K_S>} + \mathcal{B}_{47} + \mathcal{B}_{53} \cdot \mathcal{B}_{} \\ & + \mathcal{B}_{77} + \mathcal{B}_{103} + \mathcal{B}_{126} \cdot (\mathcal{B}_{\eta \rightarrow 3\pi^0} + \mathcal{B}_{\eta \rightarrow \pi^+ \pi^- \pi^0}) + \mathcal{B}_{152} \cdot \mathcal{B}_{\omega \rightarrow \pi^+ \pi^- \pi^0} \end{aligned}$$

$$\begin{aligned} \mathcal{B}_{110} = & \mathcal{B}_{10} + \mathcal{B}_{16} + \mathcal{B}_{23} + \mathcal{B}_{28} + \mathcal{B}_{35} + \mathcal{B}_{40} \\ & + \mathcal{B}_{128} + \mathcal{B}_{802} + \mathcal{B}_{803} + \mathcal{B}_{151} + \mathcal{B}_{130} + \mathcal{B}_{132} \\ & + \mathcal{B}_{44} + \mathcal{B}_{53} + \mathcal{B}_{168} + \mathcal{B}_{169} + \mathcal{B}_{822} + \mathcal{B}_{833} \end{aligned}$$

$$\mathcal{B}_{149} = \mathcal{B}_{152} + \mathcal{B}_{800} + \mathcal{B}_{151}$$

$$\mathcal{B}_{150} = \mathcal{B}_{800} + \mathcal{B}_{151}$$

$$\frac{\mathcal{B}_{150}}{\mathcal{B}_{66}} = \frac{\mathcal{B}_{150}}{\mathcal{B}_{66}}$$

$$\frac{\mathcal{B}_{152}}{\mathcal{B}_{54}} = \frac{\mathcal{B}_{152}}{\mathcal{B}_{54}}$$

$$\frac{\mathcal{B}_{152}}{\mathcal{B}_{76}} = \frac{\mathcal{B}_{152}}{\mathcal{B}_{76}}$$

$$\mathcal{B}_{168} = \mathcal{B}_{167} \cdot \mathcal{B}_{\phi \rightarrow K^+ K^-}$$

$$\mathcal{B}_{169} = \mathcal{B}_{167} \cdot \mathcal{B}_{\phi \rightarrow K_S K_L}$$

$$\mathcal{B}_{804} = \mathcal{B}_{47} \cdot ((\mathcal{B}_{<K^0|K_L>} \cdot \mathcal{B}_{<\bar{K}^0|K_L>}) / (\mathcal{B}_{<K^0|K_S>} \cdot \mathcal{B}_{<\bar{K}^0|K_S>}))$$

$$\mathcal{B}_{806} = \mathcal{B}_{50} \cdot ((\mathcal{B}_{<K^0|K_L>} \cdot \mathcal{B}_{<\bar{K}^0|K_L>}) / (\mathcal{B}_{<K^0|K_S>} \cdot \mathcal{B}_{<\bar{K}^0|K_S>}))$$

$$\mathcal{B}_{809} = \mathcal{B}_{30}$$

$$\mathcal{B}_{810} = \mathcal{B}_{910} + \mathcal{B}_{911} + \mathcal{B}_{811} \cdot \mathcal{B}_{\omega \rightarrow \pi^+ \pi^- \pi^0} + \mathcal{B}_{812}$$

$$\mathcal{B}_{820} = \mathcal{B}_{920} + \mathcal{B}_{821}$$

$$\mathcal{B}_{830} = \mathcal{B}_{930} + \mathcal{B}_{831} \cdot \mathcal{B}_{\omega \rightarrow \pi^+ \pi^- \pi^0} + \mathcal{B}_{832}$$

$$\mathcal{B}_{910} = \mathcal{B}_{136} \cdot \mathcal{B}_{\eta \rightarrow 3\pi^0}$$

$$\mathcal{B}_{911} = \mathcal{B}_{945} \cdot \mathcal{B}_{\eta \rightarrow \pi^+ \pi^- \pi^0}$$

$$\mathcal{B}_{930} = \mathcal{B}_{136} \cdot \mathcal{B}_{\eta \rightarrow \pi^+ \pi^- \pi^0}$$

$$\mathcal{B}_{944} = \mathcal{B}_{136} \cdot \mathcal{B}_{\eta \rightarrow \gamma\gamma}$$

$$\begin{aligned} \mathcal{B}_{\text{All}} = & \mathcal{B}_3 + \mathcal{B}_5 + \mathcal{B}_9 + \mathcal{B}_{10} + \mathcal{B}_{14} + \mathcal{B}_{16} \\ & + \mathcal{B}_{20} + \mathcal{B}_{23} + \mathcal{B}_{27} + \mathcal{B}_{28} + \mathcal{B}_{30} + \mathcal{B}_{35} \\ & + \mathcal{B}_{37} + \mathcal{B}_{40} + \mathcal{B}_{42} + \mathcal{B}_{47} \cdot (1 + ((\mathcal{B}_{<K^0|K_L>} \cdot \mathcal{B}_{<\bar{K}^0|K_L>} / (\mathcal{B}_{<K^0|K_S>} \cdot \mathcal{B}_{<\bar{K}^0|K_S>}))) \\ & + \mathcal{B}_{48} + \mathcal{B}_{62} + \mathcal{B}_{70} + \mathcal{B}_{77} + \mathcal{B}_{811} + \mathcal{B}_{812} \\ & + \mathcal{B}_{93} + \mathcal{B}_{94} + \mathcal{B}_{832} + \mathcal{B}_{833} + \mathcal{B}_{126} + \mathcal{B}_{128} \\ & + \mathcal{B}_{802} + \mathcal{B}_{803} + \mathcal{B}_{800} + \mathcal{B}_{151} + \mathcal{B}_{130} + \mathcal{B}_{132} \\ & + \mathcal{B}_{44} + \mathcal{B}_{53} + \mathcal{B}_{50} \cdot (1 + ((\mathcal{B}_{<K^0|K_L>} \cdot \mathcal{B}_{<\bar{K}^0|K_L>} / (\mathcal{B}_{<K^0|K_S>} \cdot \mathcal{B}_{<\bar{K}^0|K_S>}))) \\ & + \mathcal{B}_{51} + \mathcal{B}_{167} \cdot (\mathcal{B}_{\phi \rightarrow K^+ K^-} + \mathcal{B}_{\phi \rightarrow K_S K_L}) + \mathcal{B}_{152} + \mathcal{B}_{920} \\ & + \mathcal{B}_{821} + \mathcal{B}_{822} + \mathcal{B}_{831} + \mathcal{B}_{136} + \mathcal{B}_{945} + \mathcal{B}_{805} \end{aligned}$$

10.2 Tests of lepton universality

Lepton universality tests probe the Standard Model prediction that the charged weak current interaction has the same coupling for all lepton generations. The precision of such tests has been significantly improved since the 2014 edition by the addition of the Belle τ lifetime measurement [1523], while improvements from the τ branching fraction fit are negligible. We compute the universality tests by using ratios of the partial widths of a heavier lepton λ decaying to a lighter lepton ρ [1524],

$$\Gamma(\lambda \rightarrow \nu_\lambda \rho \bar{\nu}_\rho(\gamma)) = \frac{\mathcal{B}(\lambda \rightarrow \nu_\lambda \rho \bar{\nu}_\rho)}{\tau_\lambda} = \frac{G_\lambda G_\rho m_\lambda^5}{192\pi^3} f\left(\frac{m_\rho^2}{m_\lambda^2}\right) R_W^\lambda R_\gamma^\lambda ,$$

where

$$\begin{aligned} G_\rho &= \frac{g_\rho^2}{4\sqrt{2}M_W^2} , & f(x) &= 1 - 8x + 8x^3 - x^4 - 12x^2 \ln x , \\ R_W^\lambda &= 1 + \frac{3}{5} \frac{m_\lambda^2}{M_W^2} + \frac{9}{5} \frac{m_\rho^2}{M_W^2} \quad [1525-1527] , & R_\gamma^\lambda &= 1 + \frac{\alpha(m_\lambda)}{2\pi} \left(\frac{25}{4} - \pi^2 \right) . \end{aligned}$$

We use $R_\gamma^\tau = 1 - 43.2 \cdot 10^{-4}$ and $R_\gamma^\mu = 1 - 42.4 \cdot 10^{-4}$ [1524] and M_W from PDG 2018 [21]. We use HFLAV 2018 averages and PDG 2018 for the other quantities. Using pure leptonic processes we obtain

$$\left(\frac{g_\tau}{g_\mu} \right) = 1.0010 \pm 0.0014 , \quad \left(\frac{g_\tau}{g_e} \right) = 1.0029 \pm 0.0014 , \quad \left(\frac{g_\mu}{g_e} \right) = 1.0018 \pm 0.0014 .$$

Using the expressions for the τ semi-hadronic partial widths, we obtain

$$\left(\frac{g_\tau}{g_\mu}\right)^2 = \frac{\mathcal{B}(\tau \rightarrow h\nu_\tau)}{\mathcal{B}(h \rightarrow \mu\bar{\nu}_\mu)} \frac{2m_h m_\mu^2 \tau_h}{(1 + \delta R_{\tau/h}) m_\tau^3 \tau_\tau} \left(\frac{1 - m_\mu^2/m_h^2}{1 - m_h^2/m_\tau^2}\right)^2 ,$$

where $h = \pi$ or K and the radiative corrections are $\delta R_{\tau/\pi} = (0.16 \pm 0.14)\%$ and $\delta R_{\tau/K} = (0.90 \pm 0.22)\%$ [1528–1531]. We measure:

$$\left(\frac{g_\tau}{g_\mu}\right)_\pi = 0.9958 \pm 0.0026 , \quad \left(\frac{g_\tau}{g_\mu}\right)_K = 0.9879 \pm 0.0063 .$$

Similar tests could be performed with decays to electrons, however they are less precise because the hadron two body decays to electrons are helicity-suppressed. Averaging the three g_τ/g_μ ratios we obtain

$$\left(\frac{g_\tau}{g_\mu}\right)_{\tau+\pi+K} = 0.9999 \pm 0.0014 ,$$

accounting for correlations. Table 338 reports the correlation coefficients for the fitted coupling ratios.

Table 338: Universality coupling ratios correlation coefficients (%).

$\left(\frac{g_\tau}{g_e}\right)$	51			
$\left(\frac{g_\mu}{g_e}\right)$	-50	49		
$\left(\frac{g_\tau}{g_\mu}\right)_\pi$	23	25	2	
$\left(\frac{g_\tau}{g_\mu}\right)_K$	11	10	-1	6
	$\left(\frac{g_\tau}{g_\mu}\right)$	$\left(\frac{g_\tau}{g_e}\right)$	$\left(\frac{g_\mu}{g_e}\right)$	$\left(\frac{g_\tau}{g_\mu}\right)_\pi$

Since there is 100% correlation between g_τ/g_μ , g_τ/g_e and g_μ/g_e , the correlation matrix is expected to be positive semi-definite, with one eigenvalue equal to zero. Due to numerical inaccuracies, one eigenvalue is expected to be close to zero rather than exactly zero.

10.3 Universality-improved $\mathcal{B}(\tau \rightarrow e\nu\bar{\nu})$ and R_{had}

We compute two quantities that are used in this report and that have been traditionally used for further elaborations and tests involving the τ branching fractions:

- the “universality-improved” experimental determination of $\mathcal{B}_e = \mathcal{B}(\tau \rightarrow e\nu\bar{\nu})$, which relies on the assumption that the Standard Model and lepton universality hold;
- the ratio R_{had} between the total branching fraction of the τ to hadrons, \mathcal{B}_{had} and the universality-improved \mathcal{B}_e , which is the same as the ratio of the two respective partial widths, $\Gamma(\tau \rightarrow \text{had})$ and $\Gamma(\tau \rightarrow e\nu\bar{\nu})$.

Following Ref. [1460], we obtain a more precise experimental determination of \mathcal{B}_e using the τ branching fraction to $\mu\nu\bar{\nu}$, \mathcal{B}_μ , and the τ lifetime. We average:

- the \mathcal{B}_e fit value \mathcal{B}_5 ,
- the \mathcal{B}_e determination from the $\mathcal{B}_\mu = \mathcal{B}(\tau \rightarrow \mu\nu\bar{\nu})$ fit value \mathcal{B}_3 assuming that $g_\mu/g_e = 1$, hence (see also Section 10.2)

$$\mathcal{B}_e = \mathcal{B}_\mu \cdot f(m_e^2/m_\tau^2)/f(m_\mu^2/m_\tau^2) ,$$

- the \mathcal{B}_e determination from the τ lifetime assuming that $g_\tau/g_\mu = 1$, hence

$$\mathcal{B}_e = \mathcal{B}(\mu \rightarrow e\bar{\nu}_e\nu_\mu) \cdot (\tau/\tau_\mu) \cdot (m_\tau/m_\mu)^5 \cdot f(m_e^2/m_\tau^2)/f(m_\mu^2/m_\tau^2) \cdot (R_\gamma^\tau R_W^\tau)/(R_\gamma^\mu R_W^\mu) ,$$

where $\mathcal{B}(\mu \rightarrow e\bar{\nu}_e\nu_\mu) = 1$.

Accounting for correlations, we obtain

$$\mathcal{B}_e^{\text{uni}} = (17.814 \pm 0.022)\%.$$

We use $\mathcal{B}_e^{\text{uni}}$ to obtain the ratio

$$R_{\text{had}} = \frac{\Gamma(\tau \rightarrow \text{hadrons})}{\Gamma(\tau \rightarrow e\nu\bar{\nu})} = \frac{\mathcal{B}_{\text{had}}}{\mathcal{B}_e^{\text{uni}}} = 3.6355 \pm 0.0081 .$$

We define \mathcal{B}_{had} as the sum of all *measured* branching fractions to hadrons, which corresponds to the sum of all branching fractions minus the leptonic branching fractions, $\mathcal{B}_{\text{had}} = \mathcal{B}_{\text{All}} - \mathcal{B}_3 - \mathcal{B}_5 = (64.76 \pm 0.10)\%$ (see Section 10.1 and Table 327 for the definitions of \mathcal{B}_{All} , \mathcal{B}_3 , \mathcal{B}_5). It is worth noting that other authors use the alternative definition of \mathcal{B}_{had} as the total branching fraction, $\mathcal{B}_{\text{tot}} = 1$, minus the leptonic branching fractions, resulting in $\mathcal{B}_{\text{had}}^{\text{uni}} = 1 - \mathcal{B}_3 - \mathcal{B}_5$.

10.4 $|V_{us}|$ measurement

The CKM matrix element magnitude $|V_{us}|$ is most precisely determined from kaon decays [1532] (see Figure 110), and its precision is limited by the uncertainties of the lattice QCD estimates of the meson decay constants $f_+^{K\pi}(0)$ and $f_{K\pm}/f_{\pi\pm}$. Using the τ branching fractions, it is possible to determine $|V_{us}|$ in an alternative way [1533, 1534] that does not depend on lattice QCD and has small theory uncertainties (as discussed in Section 10.4.1). Moreover, $|V_{us}|$ can be determined using the τ branching fractions similarly to the kaon case, using the same meson decay constants from lattice QCD.

10.4.1 $|V_{us}|$ from $\mathcal{B}(\tau \rightarrow X_s\nu)$

The τ hadronic partial width is the sum of the τ partial widths to strange and to non-strange hadronic final states, $\Gamma_{\text{had}} = \Gamma_s + \Gamma_{\text{VA}}$. The suffix “VA” traditionally denotes the sum of the τ partial widths to non-strange final states, which proceed through either vector or axial-vector currents.

Dividing any partial width Γ_x by the electronic partial width, Γ_e , we obtain partial width ratios R_x (which are equal to the respective branching fraction ratios $\mathcal{B}_x/\mathcal{B}_e$) for which $R_{\text{had}} = R_s + R_{\text{VA}}$. In terms of such ratios, $|V_{us}|$ can be measured as [1533, 1534]

$$|V_{us}|_{\tau s} = \sqrt{R_s / \left[\frac{R_{\text{VA}}}{|V_{ud}|^2} - \delta R_{\text{theory}} \right]} ,$$

where δR_{theory} can be determined in the context of low energy QCD theory, partly relying on experimental low energy scattering data. The literature reports several calculations [1535–1537]. In this report we use Ref. [1535], whose estimated uncertainty size is intermediate between the two other ones. We use the information in that paper and the PDG 2018 value for the s -quark mass $m_s = 95.00 \pm 6.70$ MeV [21] to calculate $\delta R_{\text{theory}} = 0.242 \pm 0.033$.

We proceed following the same procedure of the 2012 HFLAV report [226]. We sum the relevant τ branching fractions to compute \mathcal{B}_{VA} and \mathcal{B}_s and we use the universality-improved $\mathcal{B}_e^{\text{uni}}$ (see Section 10.3) to compute the R_{VA} and R_s ratios. In past determinations of $|V_{us}|$, for example in the 2009 HFLAV report [420], the total hadronic branching fraction has been computed using unitarity as $\mathcal{B}_{\text{had}}^{\text{uni}} = 1 - \mathcal{B}_e - \mathcal{B}_\mu$, obtaining then \mathcal{B}_s from the sum of the strange branching fractions and \mathcal{B}_{VA} from $\mathcal{B}_{\text{had}}^{\text{uni}} - \mathcal{B}_s$. We prefer to use the more direct experimental determination of \mathcal{B}_{VA} for two reasons. First, both methods result in comparable uncertainties on $|V_{us}|$, since the better precision on $\mathcal{B}_{\text{had}}^{\text{uni}} = 1 - \mathcal{B}_e - \mathcal{B}_\mu$ is vanquished by increased correlations in the expressions $(1 - \mathcal{B}_e - \mathcal{B}_\mu)/\mathcal{B}_e^{\text{uni}}$ and $\mathcal{B}_s/(\mathcal{B}_{\text{had}} - \mathcal{B}_s)$ in the $|V_{us}|$ calculation. Second, if there are unobserved τ hadronic decay modes, they would affect \mathcal{B}_{VA} and \mathcal{B}_s in a more asymmetric way when using unitarity.

Using the τ branching fraction fit results with their uncertainties and correlations (Section 10.1), we compute $\mathcal{B}_s = (2.931 \pm 0.041)\%$ (see also Table 339) and $\mathcal{B}_{\text{VA}} = \mathcal{B}_{\text{had}} - \mathcal{B}_s = (61.83 \pm 0.10)\%$, where \mathcal{B}_{had} has been defined in section 10.3. PDG 2018 averages are used for non- τ quantities; $|V_{ud}| = 0.97420 \pm 0.00021$ [1538, 1539].

We obtain $|V_{us}|_{\tau s} = 0.2195 \pm 0.0019$, which is 2.9σ lower than the unitarity CKM prediction $|V_{us}|_{\text{uni}} = 0.22565 \pm 0.00089$, from $(|V_{us}|_{\text{uni}})^2 = 1 - |V_{ud}|^2 - |V_{ub}|^2$. The $|V_{us}|_{\tau s}$ uncertainty includes a systematic error contribution of 0.0011 from the theory uncertainty on δR_{theory} . The 2018 *BABAR* preliminary results improved the $|V_{us}|$ precision by about 10% and reduced the discrepancy by about 6.5%.

10.4.2 $|V_{us}|$ from $\mathcal{B}(\tau \rightarrow K\nu)/\mathcal{B}(\tau \rightarrow \pi\nu)$

We compute $|V_{us}|$ from the ratio of branching fractions $\mathcal{B}(\tau \rightarrow K^-\nu_\tau)/\mathcal{B}(\tau \rightarrow \pi^-\nu_\tau) = (6.467 \pm 0.084) \cdot 10^{-2}$ from the equation [1540]:

$$\frac{\mathcal{B}(\tau \rightarrow K^-\nu_\tau)}{\mathcal{B}(\tau \rightarrow \pi^-\nu_\tau)} = \frac{f_{K\pm}^2 |V_{us}|^2}{f_{\pi\pm}^2 |V_{ud}|^2} \frac{(m_\tau^2 - m_K^2)^2}{(m_\tau^2 - m_\pi^2)^2} \frac{1 + \delta R_{\tau/K}}{1 + \delta R_{\tau/\pi}} (1 + \delta R_{K/\pi})$$

We use $f_{K\pm}/f_{\pi\pm} = 1.1932 \pm 0.0019$ from the FLAG 2019 lattice QCD averages with $N_f = 2 + 1 + 1$ [214, 1541–1543],

$$\begin{aligned} \frac{1 + \delta R_{\tau/K}}{1 + \delta R_{\tau/\pi}} &= \frac{1 + (0.90 \pm 0.22)\%}{1 + (0.16 \pm 0.14)\%} \quad [1528–1531] , \\ 1 + \delta R_{K/\pi} &= 1 + (-0.69 \pm 0.17)\% \quad [1525, 1544, 1545] . \end{aligned}$$

The value of $\delta R_{K/\pi}$ in the Spring 2017 HFLAV-Tau report [1] incorrectly included a strong isospin-breaking correction that is not needed when using $f_{K\pm}/f_{\pi\pm}$ rather than its isospin-limit variant. We compute $|V_{us}|_{\tau K/\pi} = 0.2236 \pm 0.0015$, 1.2σ below the CKM unitarity prediction.

Table 339: HFLAV 2018 τ branching fractions to strange final states.

Branching fraction	HFLAV 2018 fit (%)
$K^-\nu_\tau$	0.6986 ± 0.0085
$K^-\pi^0\nu_\tau$	0.4904 ± 0.0092
$K^-2\pi^0\nu_\tau$ (ex. K^0)	0.0585 ± 0.0027
$K^-3\pi^0\nu_\tau$ (ex. K^0, η)	0.0113 ± 0.0026
$\pi^-\bar{K}^0\nu_\tau$	0.8378 ± 0.0139
$\pi^-\bar{K}^0\pi^0\nu_\tau$	0.3807 ± 0.0129
$\pi^-\bar{K}^02\pi^0\nu_\tau$ (ex. K^0)	0.0235 ± 0.0231
$\bar{K}^0h^-h^-h^+\nu_\tau$	0.0222 ± 0.0202
$K^-\eta\nu_\tau$	0.0154 ± 0.0008
$K^-\pi^0\eta\nu_\tau$	0.0048 ± 0.0012
$\pi^-\bar{K}^0\eta\nu_\tau$	0.0094 ± 0.0015
$K^-\omega\nu_\tau$	0.0410 ± 0.0092
$K^-\phi\nu_\tau$ ($\phi \rightarrow K^+K^-$)	0.0022 ± 0.0008
$K^-\phi\nu_\tau$ ($\phi \rightarrow K_S^0K_L^0$)	0.0015 ± 0.0006
$K^-\pi^-\pi^+\nu_\tau$ (ex. K^0, ω)	0.2923 ± 0.0067
$K^-\pi^-\pi^+\pi^0\nu_\tau$ (ex. K^0, ω, η)	0.0410 ± 0.0143
$K^-2\pi^-2\pi^+\nu_\tau$ (ex. K^0)	0.0001 ± 0.0001
$K^-2\pi^-2\pi^+\pi^0\nu_\tau$ (ex. K^0)	0.0001 ± 0.0001
$X_s^-\nu_\tau$	2.9308 ± 0.0412

10.4.3 $|V_{us}|$ from $\mathcal{B}(\tau \rightarrow K\nu)$

We determine $|V_{us}|$ from the branching fraction $\mathcal{B}(\tau^- \rightarrow K^-\nu_\tau)$ using

$$\mathcal{B}(\tau^- \rightarrow K^-\nu_\tau) = \frac{G_F^2}{16\pi\hbar} f_{K\pm}^2 |V_{us}|^2 \tau_\tau m_\tau^3 \left(1 - \frac{m_K^2}{m_\tau^2}\right)^2 (1 + \delta R_{\tau/K})(1 + \delta R_{K\mu 2}) .$$

We use $f_{K\pm} = 155.7 \pm 0.3$ MeV from the FLAG 2019 lattice QCD averages with $N_f = 2 + 1 + 1$ [214, 1541, 1542, 1546], $\delta R_{\tau/K} = (0.90 \pm 0.22)\%$ [1528–1531] and $\delta R_{K\mu 2} = (1.07 \pm 0.21)\%$ [21, 1544, 1547], which includes short and long-distance radiative corrections. We obtain $|V_{us}|_{\tau K} = 0.2234 \pm 0.0015$, which is 1.3σ below the CKM unitarity prediction. The physical constants have been taken from PDG 2018 (which uses CODATA 2014 [1548]).

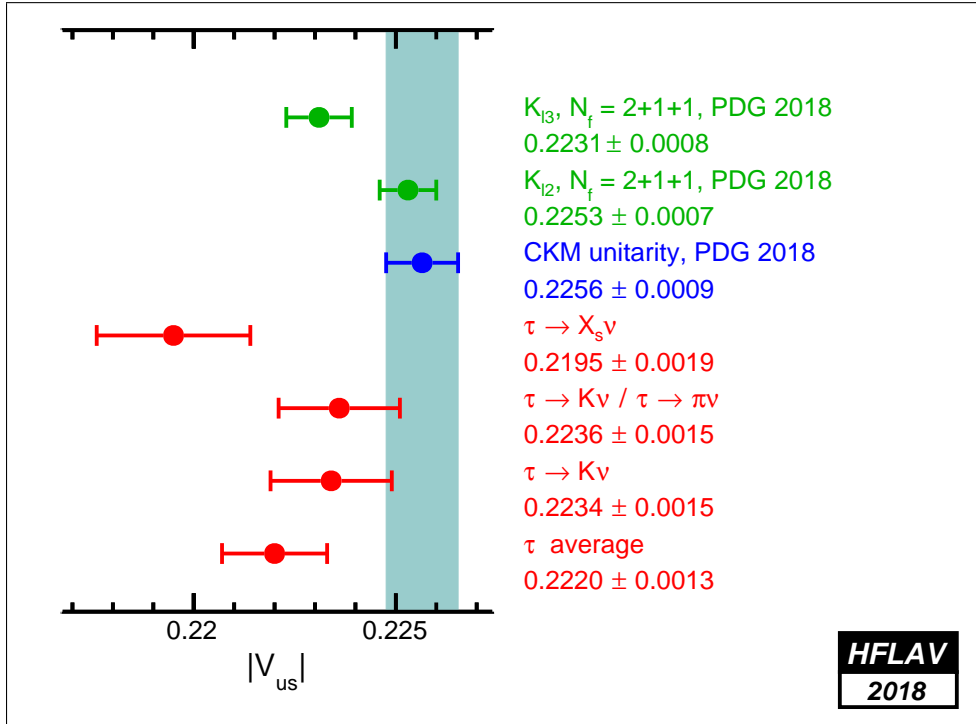


Figure 110: $|V_{us}|$ averages.

10.4.4 $|V_{us}|$ from τ summary

We summarize the $|V_{us}|$ results reporting the values, the discrepancy with respect to the $|V_{us}|$ determination from CKM unitarity, and an illustration of the measurement method:

$$\begin{aligned}
 |V_{us}|_{\text{uni}} &= 0.22565 \pm 0.00089 && [\text{from } \sqrt{1 - |V_{ud}|^2 - |V_{ub}|^2} \quad (\text{CKM unitarity})] , \\
 |V_{us}|_{\tau s} &= 0.2195 \pm 0.0019 && - 2.9\sigma \quad [\text{from } \mathcal{B}(\tau^- \rightarrow X_s^- \nu_\tau)] , \\
 |V_{us}|_{\tau K/\pi} &= 0.2236 \pm 0.0015 && - 1.2\sigma \quad [\text{from } \mathcal{B}(\tau^- \rightarrow K^- \nu_\tau) / \mathcal{B}(\tau^- \rightarrow \pi^- \nu_\tau)] , \\
 |V_{us}|_{\tau K} &= 0.2234 \pm 0.0015 && - 1.3\sigma \quad [\text{from } \mathcal{B}(\tau^- \rightarrow K^- \nu_\tau)] .
 \end{aligned}$$

Averaging the three above $|V_{us}|$ determinations that rely on the τ branching fractions (taking into account all correlations due to the τ HFLAV and other mentioned inputs) we obtain, for $|V_{us}|$ and its discrepancy:

$$|V_{us}|_\tau = 0.2221 \pm 0.0013 \quad - 2.2\sigma \quad [\text{average of 3 } |V_{us}| \tau \text{ measurements}] .$$

The correlation between $f_{K\pm}$ and $f_{K\pm}/f_{\pi\pm}$ has been assumed to be zero.

All $|V_{us}|$ determinations based on measured τ branching fractions are lower than both the kaon and the CKM-unitarity determinations. This is correlated with the fact that the direct measurements of the three major τ branching fractions to kaons [$\mathcal{B}(\tau \rightarrow K^- \nu_\tau)$, $\mathcal{B}(\tau \rightarrow K^-\pi^0 \nu_\tau)$ and $\mathcal{B}(\tau \rightarrow \pi^-\bar{K}^0 \nu_\tau)$] are lower than their determinations from the kaon branching fractions into final states with leptons within the SM [1525, 1549, 1550].

Alternative determinations of $|V_{us}|$ from $\mathcal{B}(\tau \rightarrow X_s \nu)$ [1551, 1552], based on partially different sets of experimental inputs, report $|V_{us}|$ values consistent with the unitarity determination.

Figure 110 reports the HFLAV $|V_{us}|$ determinations that use the τ branching fractions, compared to two $|V_{us}|$ determinations based on kaon data [21] and to $|V_{us}|$ obtained from $|V_{ud}|$ and the CKM matrix unitarity [21].

10.5 Combination of upper limits on τ lepton-flavour-violating branching fractions

The Standard Model predicts that the τ lepton-flavour-violating (LFV) branching fractions are too small to be measured with the available experimental precision. We report in Table 340 and Figure 111 the experimental upper limits on these branching fractions that have been published by the B -factories *BABAR* and *Belle* and later experiments. We omit previous weaker upper limits (mainly from CLEO) and all preliminary results older than a few years. Presently, no preliminary result is included.

Combining upper limits is a delicate issue, since there is no standard and generally agreed procedure. Furthermore, the τ LFV searches published limits are extracted from the data with a variety of methods, and cannot be directly combined with a uniform procedure. It is however possible to use a single and effective upper limit combination procedure for all modes by re-computing the published upper limits with just one extraction method, using the published information that documents the upper limit determination: number of observed candidates, expected background, signal efficiency and number of analyzed τ decays.

We chose to use the CL_s method [1553] to re-compute the τ LFV upper limits, since it is well known and widely used (see the Statistics review of PDG 2018 [21]), and since the limits computed with the CL_s method can be combined in a straightforward way (see below). The CL_s method is based on two hypotheses: signal plus background and background only. We calculate the observed confidence levels for the two hypotheses:

$$CL_{s+b} = P_{s+b}(Q \leq Q_{obs}) = \int_{-\infty}^{Q_{obs}} \frac{dP_{s+b}}{dQ} dQ, \quad (322)$$

$$CL_b = P_b(Q \leq Q_{obs}) = \int_{-\infty}^{Q_{obs}} \frac{dP_b}{dQ} dQ, \quad (323)$$

where CL_{s+b} is the confidence level observed for the signal plus background hypotheses, CL_b is the confidence level observed for the background only hypothesis, $\frac{dP_{s+b}}{dQ}$ and $\frac{dP_b}{dQ}$ are the probability distribution functions (PDFs) for the two corresponding hypothesis and Q is called the test statistic. The CL_s value is defined as the ratio between the confidence level for the signal plus background hypothesis and the confidence level for the background hypothesis:

$$CL_s = \frac{CL_{s+b}}{CL_b}. \quad (324)$$

When multiple results are combined, the PDFs in Eqs. (322) and (323) are the product of the individual PDFs,

$$CL_s = \frac{\prod_{i=1}^N \sum_{n=0}^{n_i} \frac{e^{-(s_i+b_i)}(s_i+b_i)^n}{n!} \prod_{j=1}^N [s_i S_i(x_{ij}) + b_i B_i(x_{ij})]}{\prod_{i=1}^N \sum_{n=0}^{n_i} \frac{e^{-b_i} b_i^n}{n!} \prod_{j=1}^N B_i(x_{ij})}, \quad (325)$$

where N is the number of results (or channels), and, for each channel i , n_i is the number of observed candidates, x_{ij} are the values of the discriminating variables (with index j), s_i and b_i are the number of signal and background events and S_i , B_i are the probability distribution functions of the discriminating variables. The discriminating variables x_{ij} are assumed to be uncorrelated. The expected signal s_i is related to the τ lepton branching fraction $\mathcal{B}(\tau \rightarrow f_i)$ into the searched final state f_i by $s_i = N_i \epsilon_i \mathcal{B}(\tau \rightarrow f_i)$, where N_i is the number of produced τ leptons and ϵ_i is the detection efficiency for observing the decay $\tau \rightarrow f_i$. For e^+e^- experiments, $N_i = 2\mathcal{L}_i \sigma_{\tau\tau}$, where \mathcal{L}_i is the integrated luminosity and $\sigma_{\tau\tau}$ is the τ pair production cross section $\sigma(e^+e^- \rightarrow \tau^+\tau^-)$ [1554]. In experiments where τ leptons are produced in more complex multiple reactions, the effective N_i is typically estimated with Monte Carlo simulations calibrated with related data yields.

The extraction of the upper limits is performed using the code provided by Tom Junk [1555]. The systematic uncertainties are modeled in the Monte Carlo toy experiments by convolving the S_i and B_i PDFs with Gaussian distributions corresponding to the nuisance parameters.

Table 340 reports the HFLAV combinations of the τ LFV limits. Since there is negligible gain in combining limits of very different strength, the combinations do not include the CLEO searches and do not include results where the single event sensitivity is more than a factor of 5 lower than the value for the search with the best limit.

Figure 112 reports a graphical representation of the τ LFV limits combinations listed in Table 340. The published information that has been used to obtain these limits is reported in Table 341. In the previous HFLAV reports, the determination of combined limit $\mathcal{B}_{183} = \mu^-\mu^+\mu^-$ erroneously counted twice the systematic uncertainty of the LHCb limit. That has been fixed now, and the combination of the upper limits on $\mathcal{B}_{183} = \mu^-\mu^+\mu^-$ has changed from $< 1.2 \cdot 10^{-8}$ to $< 1.1 \cdot 10^{-8}$.

Table 340: Experimental upper limits on lepton flavour violating τ decays. The modes are grouped according to the properties of their final states. Modes with baryon number violation are labelled with “BNV”. The experiment “HFLAV” denotes the combinations of upper limits computed by HFLAV.

Decay mode	Category	90% CL Limit	Experiment	References
$\mathcal{B}_{156} = e^-\gamma$	$\ell\gamma$	$3.3 \cdot 10^{-8}$	<i>BABAR</i>	[1556]
		$1.2 \cdot 10^{-7}$	<i>Belle</i>	[1557]
		$5.4 \cdot 10^{-8}$	HFLAV	[1556, 1557]
$\mathcal{B}_{157} = \mu^-\gamma$		$4.4 \cdot 10^{-8}$	<i>BABAR</i>	[1556]
		$4.5 \cdot 10^{-8}$	<i>Belle</i>	[1557]
		$5.0 \cdot 10^{-8}$	HFLAV	[1556, 1557]
$\mathcal{B}_{158} = e^-\pi^0$	ℓP^0	$1.3 \cdot 10^{-7}$	<i>BABAR</i>	[1558]
		$8.0 \cdot 10^{-8}$	<i>Belle</i>	[1559]
		$4.9 \cdot 10^{-8}$	HFLAV	[1558, 1559]
$\mathcal{B}_{159} = \mu^-\pi^0$		$1.1 \cdot 10^{-7}$	<i>BABAR</i>	[1558]
		$1.2 \cdot 10^{-7}$	<i>Belle</i>	[1559]

Table 340 – continued from previous page

Decay mode	Category	90% CL Limit	Experiment	References
$\mathcal{B}_{160} = e^- K_S^0$		$3.6 \cdot 10^{-8}$	HFLAV	[1558, 1559]
$\mathcal{B}_{161} = \mu^- K_S^0$		$3.3 \cdot 10^{-8}$	BABAR	[1560]
		$2.6 \cdot 10^{-8}$	Belle	[1561]
		$1.4 \cdot 10^{-8}$	HFLAV	[1560, 1561]
$\mathcal{B}_{162} = e^- \eta$		$4.0 \cdot 10^{-8}$	BABAR	[1560]
		$2.3 \cdot 10^{-8}$	Belle	[1561]
		$1.5 \cdot 10^{-8}$	HFLAV	[1560, 1561]
$\mathcal{B}_{163} = \mu^- \eta$		$1.6 \cdot 10^{-7}$	BABAR	[1558]
		$9.2 \cdot 10^{-8}$	Belle	[1559]
		$5.5 \cdot 10^{-8}$	HFLAV	[1558, 1559]
$\mathcal{B}_{172} = e^- \eta'(958)$		$1.5 \cdot 10^{-7}$	BABAR	[1558]
		$6.5 \cdot 10^{-8}$	Belle	[1559]
		$3.8 \cdot 10^{-8}$	HFLAV	[1558, 1559]
$\mathcal{B}_{173} = \mu^- \eta'(958)$		$2.4 \cdot 10^{-7}$	BABAR	[1558]
		$1.6 \cdot 10^{-7}$	Belle	[1559]
		$9.9 \cdot 10^{-8}$	HFLAV	[1558, 1559]
$\mathcal{B}_{164} = e^- \rho^0$	ℓV^0	$4.6 \cdot 10^{-8}$	BABAR	[1562]
		$1.8 \cdot 10^{-8}$	Belle	[1563]
		$1.5 \cdot 10^{-8}$	HFLAV	[1562, 1563]
$\mathcal{B}_{165} = \mu^- \rho^0$		$2.6 \cdot 10^{-8}$	BABAR	[1562]
		$1.2 \cdot 10^{-8}$	Belle	[1563]
		$1.5 \cdot 10^{-8}$	HFLAV	[1562, 1563]
$\mathcal{B}_{166} = e^- \omega$		$1.1 \cdot 10^{-7}$	BABAR	[1564]
		$4.8 \cdot 10^{-8}$	Belle	[1563]
		$3.3 \cdot 10^{-8}$	HFLAV	[1563, 1564]
$\mathcal{B}_{167} = \mu^- \omega$		$1.0 \cdot 10^{-7}$	BABAR	[1564]
		$4.7 \cdot 10^{-8}$	Belle	[1563]
		$4.0 \cdot 10^{-8}$	HFLAV	[1563, 1564]
$\mathcal{B}_{168} = e^- K^*(892)$		$5.9 \cdot 10^{-8}$	BABAR	[1562]
		$3.2 \cdot 10^{-8}$	Belle	[1563]
		$2.3 \cdot 10^{-8}$	HFLAV	[1562, 1563]
$\mathcal{B}_{169} = \mu^- K^*(892)$		$1.7 \cdot 10^{-7}$	BABAR	[1562]
		$7.2 \cdot 10^{-8}$	Belle	[1563]
		$6.0 \cdot 10^{-8}$	HFLAV	[1562, 1563]
$\mathcal{B}_{170} = e^- \bar{K}^*(892)$		$4.6 \cdot 10^{-8}$	BABAR	[1562]

Table 340 – continued from previous page

Decay mode	Category	90% CL Limit	Experiment	References
$\mathcal{B}_{171} = \mu^- \bar{K}^*(892)$		$3.4 \cdot 10^{-8}$	Belle	[1563]
		$2.2 \cdot 10^{-8}$	HFLAV	[1562, 1563]
		$7.3 \cdot 10^{-8}$	<i>BABAR</i>	[1562]
		$7.0 \cdot 10^{-8}$	Belle	[1563]
$\mathcal{B}_{176} = e^- \phi$		$4.2 \cdot 10^{-8}$	HFLAV	[1562, 1563]
		$3.1 \cdot 10^{-8}$	<i>BABAR</i>	[1562]
		$3.1 \cdot 10^{-8}$	Belle	[1563]
		$2.0 \cdot 10^{-8}$	HFLAV	[1562, 1563]
$\mathcal{B}_{177} = \mu^- \phi$		$1.9 \cdot 10^{-7}$	<i>BABAR</i>	[1562]
		$8.4 \cdot 10^{-8}$	Belle	[1563]
		$6.8 \cdot 10^{-8}$	HFLAV	[1562, 1563]
$\mathcal{B}_{174} = e^- f_0(980)$	ℓS^0	$3.2 \cdot 10^{-8}$	Belle	[1565]
$\mathcal{B}_{175} = \mu^- f_0(980)$		$3.4 \cdot 10^{-8}$	Belle	[1565]
$\mathcal{B}_{178} = e^- e^+ e^-$	$\ell \ell \ell$	$2.9 \cdot 10^{-8}$	<i>BABAR</i>	[1566]
		$2.7 \cdot 10^{-8}$	Belle	[1567]
		$1.4 \cdot 10^{-8}$	HFLAV	[1566, 1567]
$\mathcal{B}_{179} = e^- \mu^+ \mu^-$		$3.2 \cdot 10^{-8}$	<i>BABAR</i>	[1566]
		$2.7 \cdot 10^{-8}$	Belle	[1567]
		$1.6 \cdot 10^{-8}$	HFLAV	[1566, 1567]
$\mathcal{B}_{180} = \mu^- e^+ \mu^-$		$2.6 \cdot 10^{-8}$	<i>BABAR</i>	[1566]
		$1.7 \cdot 10^{-8}$	Belle	[1567]
		$9.8 \cdot 10^{-9}$	HFLAV	[1566, 1567]
$\mathcal{B}_{181} = \mu^- e^+ e^-$		$2.2 \cdot 10^{-8}$	<i>BABAR</i>	[1566]
		$1.8 \cdot 10^{-8}$	Belle	[1567]
		$1.1 \cdot 10^{-8}$	HFLAV	[1566, 1567]
$\mathcal{B}_{182} = e^- \mu^+ e^-$		$1.8 \cdot 10^{-8}$	<i>BABAR</i>	[1566]
		$1.5 \cdot 10^{-8}$	Belle	[1567]
		$8.4 \cdot 10^{-9}$	HFLAV	[1566, 1567]
$\mathcal{B}_{183} = \mu^- \mu^+ \mu^-$		$3.8 \cdot 10^{-7}$	ATLAS	[1568]
		$3.3 \cdot 10^{-8}$	<i>BABAR</i>	[1566]
		$2.1 \cdot 10^{-8}$	Belle	[1567]
		$4.6 \cdot 10^{-8}$	LHCb	[1569]
		$1.1 \cdot 10^{-8}$	HFLAV	[1566, 1567, 1569]
$\mathcal{B}_{184} = e^- \pi^+ \pi^-$	$\ell h h$	$1.2 \cdot 10^{-7}$	<i>BABAR</i>	[1570]
		$2.3 \cdot 10^{-8}$	Belle	[1571]
$\mathcal{B}_{185} = e^+ \pi^- \pi^-$		$2.7 \cdot 10^{-7}$	<i>BABAR</i>	[1570]
		$2.0 \cdot 10^{-8}$	Belle	[1571]
$\mathcal{B}_{186} = \mu^- \pi^+ \pi^-$		$2.9 \cdot 10^{-7}$	<i>BABAR</i>	[1570]

Table 340 – continued from previous page

Decay mode	Category	90% CL Limit	Experiment	References
$\mathcal{B}_{187} = \mu^+ \pi^- \pi^-$		$2.1 \cdot 10^{-8}$	Belle	[1571]
$\mathcal{B}_{187} = \mu^+ \pi^- \pi^-$		$7.0 \cdot 10^{-8}$	<i>BABAR</i>	[1570]
$\mathcal{B}_{188} = e^- \pi^+ K^-$		$3.9 \cdot 10^{-8}$	Belle	[1571]
$\mathcal{B}_{188} = e^- \pi^+ K^-$		$3.2 \cdot 10^{-7}$	<i>BABAR</i>	[1570]
$\mathcal{B}_{189} = e^- K^+ \pi^-$		$3.7 \cdot 10^{-8}$	Belle	[1571]
$\mathcal{B}_{189} = e^- K^+ \pi^-$		$1.7 \cdot 10^{-7}$	<i>BABAR</i>	[1570]
$\mathcal{B}_{190} = e^+ \pi^- K^-$		$3.1 \cdot 10^{-8}$	Belle	[1571]
$\mathcal{B}_{190} = e^+ \pi^- K^-$		$1.8 \cdot 10^{-7}$	<i>BABAR</i>	[1570]
$\mathcal{B}_{191} = e^- K_S^0 K_S^0$		$3.2 \cdot 10^{-8}$	Belle	[1571]
$\mathcal{B}_{192} = e^- K^+ K^-$		$7.1 \cdot 10^{-8}$	<i>BABAR</i>	[1561]
$\mathcal{B}_{193} = e^+ K^- K^-$		$1.4 \cdot 10^{-7}$	Belle	[1570]
$\mathcal{B}_{193} = e^+ K^- K^-$		$3.4 \cdot 10^{-8}$	<i>BABAR</i>	[1571]
$\mathcal{B}_{194} = \mu^- \pi^+ K^-$		$1.5 \cdot 10^{-7}$	Belle	[1570]
$\mathcal{B}_{194} = \mu^- \pi^+ K^-$		$3.3 \cdot 10^{-8}$	<i>BABAR</i>	[1571]
$\mathcal{B}_{195} = \mu^- K^+ \pi^-$		$8.6 \cdot 10^{-8}$	Belle	[1571]
$\mathcal{B}_{195} = \mu^- K^+ \pi^-$		$3.2 \cdot 10^{-7}$	<i>BABAR</i>	[1570]
$\mathcal{B}_{196} = \mu^+ \pi^- K^-$		$4.5 \cdot 10^{-8}$	Belle	[1571]
$\mathcal{B}_{196} = \mu^+ \pi^- K^-$		$2.2 \cdot 10^{-7}$	<i>BABAR</i>	[1570]
$\mathcal{B}_{197} = \mu^- K_S^0 K_S^0$		$4.8 \cdot 10^{-8}$	Belle	[1571]
$\mathcal{B}_{198} = \mu^- K^+ K^-$		$8.0 \cdot 10^{-8}$	<i>BABAR</i>	[1561]
$\mathcal{B}_{198} = \mu^- K^+ K^-$		$2.5 \cdot 10^{-7}$	Belle	[1570]
$\mathcal{B}_{199} = \mu^+ K^- K^-$		$4.4 \cdot 10^{-8}$	<i>BABAR</i>	[1571]
$\mathcal{B}_{199} = \mu^+ K^- K^-$		$4.8 \cdot 10^{-7}$	Belle	[1570]
$\mathcal{B}_{199} = \mu^+ K^- K^-$		$4.7 \cdot 10^{-8}$	<i>BABAR</i>	[1571]
$\mathcal{B}_{211} = \pi^- \Lambda$	BNV	$7.2 \cdot 10^{-8}$	Belle	[1572]
$\mathcal{B}_{212} = \pi^- \bar{\Lambda}$		$1.4 \cdot 10^{-7}$	Belle	[1572]
$\mathcal{B}_{215} = p \mu^- \mu^-$		$4.4 \cdot 10^{-7}$	LHCb	[1573]
$\mathcal{B}_{216} = \bar{p} \mu^+ \mu^-$		$3.3 \cdot 10^{-7}$	LHCb	[1573]

Table 341: Published information that has been used to re-compute upper limits with the CL_s method, *i.e.* the number of τ leptons produced, the signal detection efficiency and its uncertainty, the number of expected background events and its uncertainty, and the number of observed events. The uncertainty on the efficiency includes the minor uncertainty contribution on the number of τ leptons (typically originating on the uncertainties on the integrated luminosity and on the production cross-section). The additional limit used in the combinations (from LHCb) has been originally determined with the CL_s method.

Decay mode	Exp.	Ref.	N_τ (millions)	efficiency (%)	N_{bkg}	N_{obs}
$\mathcal{B}_{156} = e^-\gamma$	BABAR	[1556]	963	3.90 ± 0.30	1.60 ± 0.40	0
$\mathcal{B}_{156} = e^-\gamma$	Belle	[1557]	983	3.00 ± 0.10	5.14 ± 3.30	5
$\mathcal{B}_{157} = \mu^-\gamma$	BABAR	[1556]	963	6.10 ± 0.50	3.60 ± 0.70	2
$\mathcal{B}_{157} = \mu^-\gamma$	Belle	[1557]	983	5.07 ± 0.20	13.90 ± 5.00	10
$\mathcal{B}_{158} = e^-\pi^0$	BABAR	[1558]	339	2.83 ± 0.25	0.17 ± 0.04	0
$\mathcal{B}_{158} = e^-\pi^0$	Belle	[1559]	401	3.93 ± 0.18	0.20 ± 0.20	0
$\mathcal{B}_{159} = \mu^-\pi^0$	BABAR	[1558]	339	4.75 ± 0.37	1.33 ± 0.15	1
$\mathcal{B}_{159} = \mu^-\pi^0$	Belle	[1559]	401	4.53 ± 0.20	0.58 ± 0.34	1
$\mathcal{B}_{160} = e^-K_S^0$	BABAR	[1560]	862	9.10 ± 1.73	0.59 ± 0.25	1
$\mathcal{B}_{160} = e^-K_S^0$	Belle	[1561]	1274	10.20 ± 0.67	0.18 ± 0.18	0
$\mathcal{B}_{161} = \mu^-K_S^0$	BABAR	[1560]	862	6.14 ± 0.20	0.30 ± 0.18	1
$\mathcal{B}_{161} = \mu^-K_S^0$	Belle	[1561]	1274	10.70 ± 0.73	0.35 ± 0.21	0
$\mathcal{B}_{162} = e^-\eta$	BABAR	[1558]	339	2.12 ± 0.20	0.22 ± 0.05	0
$\mathcal{B}_{162} = e^-\eta$	Belle	[1559]	401	2.87 ± 0.20	0.78 ± 0.78	0
$\mathcal{B}_{163} = \mu^-\eta$	BABAR	[1558]	339	3.59 ± 0.41	0.75 ± 0.08	1
$\mathcal{B}_{163} = \mu^-\eta$	Belle	[1559]	401	4.08 ± 0.28	0.64 ± 0.04	0
$\mathcal{B}_{172} = e^-\eta'(958)$	BABAR	[1558]	339	1.53 ± 0.16	0.12 ± 0.03	0
$\mathcal{B}_{172} = e^-\eta'(958)$	Belle	[1559]	401	1.59 ± 0.13	0.01 ± 0.41	0
$\mathcal{B}_{173} = \mu^-\eta'(958)$	BABAR	[1558]	339	2.18 ± 0.26	0.49 ± 0.26	0
$\mathcal{B}_{173} = \mu^-\eta'(958)$	Belle	[1559]	401	2.47 ± 0.20	0.23 ± 0.46	0
$\mathcal{B}_{164} = e^-\rho^0$	BABAR	[1562]	829	7.31 ± 0.20	1.32 ± 0.17	1
$\mathcal{B}_{164} = e^-\rho^0$	Belle	[1563]	1554	7.58 ± 0.41	0.29 ± 0.15	0
$\mathcal{B}_{165} = \mu^-\rho^0$	BABAR	[1562]	829	4.52 ± 0.40	2.04 ± 0.19	0
$\mathcal{B}_{165} = \mu^-\rho^0$	Belle	[1563]	1554	7.09 ± 0.37	1.48 ± 0.35	0
$\mathcal{B}_{166} = e^-\omega$	BABAR	[1564]	829	2.96 ± 0.13	0.35 ± 0.06	0
$\mathcal{B}_{166} = e^-\omega$	Belle	[1563]	1554	2.92 ± 0.18	0.30 ± 0.14	0
$\mathcal{B}_{167} = \mu^-\omega$	BABAR	[1564]	829	2.56 ± 0.16	0.73 ± 0.03	0
$\mathcal{B}_{167} = \mu^-\omega$	Belle	[1563]	1554	2.38 ± 0.14	0.72 ± 0.18	0
$\mathcal{B}_{168} = e^-K^*(892)$	BABAR	[1562]	829	8.00 ± 0.20	1.65 ± 0.23	2
$\mathcal{B}_{168} = e^-K^*(892)$	Belle	[1563]	1554	4.37 ± 0.24	0.29 ± 0.14	0
$\mathcal{B}_{169} = \mu^-K^*(892)$	BABAR	[1562]	829	4.60 ± 0.40	1.79 ± 0.21	4
$\mathcal{B}_{169} = \mu^-K^*(892)$	Belle	[1563]	1554	3.39 ± 0.19	0.53 ± 0.20	1
$\mathcal{B}_{170} = e^-\bar{K}^*(892)$	BABAR	[1562]	829	7.80 ± 0.20	2.76 ± 0.28	2
$\mathcal{B}_{170} = e^-\bar{K}^*(892)$	Belle	[1563]	1554	4.41 ± 0.25	0.08 ± 0.08	0
$\mathcal{B}_{171} = \mu^-\bar{K}^*(892)$	BABAR	[1562]	829	4.10 ± 0.30	1.72 ± 0.17	1
$\mathcal{B}_{171} = \mu^-\bar{K}^*(892)$	Belle	[1563]	1554	3.60 ± 0.20	0.45 ± 0.17	1
$\mathcal{B}_{176} = e^-\phi$	BABAR	[1562]	829	6.40 ± 0.20	0.68 ± 0.12	0
$\mathcal{B}_{176} = e^-\phi$	Belle	[1563]	1554	4.18 ± 0.25	0.47 ± 0.19	0

Table 341 – continued from previous page

Decay mode	Exp.	Ref.	N_τ (millions)	efficiency (%)	N_{bkg}	N_{obs}
$\mathcal{B}_{177} = \mu^- \phi$	BABAR	[1562]	829	5.20 ± 0.30	2.76 ± 0.16	6
$\mathcal{B}_{177} = \mu^- \phi$	Belle	[1563]	1554	3.21 ± 0.19	0.06 ± 0.06	1
$\mathcal{B}_{178} = e^- e^+ e^-$	BABAR	[1566]	868	8.60 ± 0.20	0.12 ± 0.02	0
$\mathcal{B}_{178} = e^- e^+ e^-$	Belle	[1567]	1437	6.00 ± 0.59	0.21 ± 0.15	0
$\mathcal{B}_{179} = e^- \mu^+ \mu^-$	BABAR	[1566]	868	6.40 ± 0.40	0.54 ± 0.14	0
$\mathcal{B}_{179} = e^- \mu^+ \mu^-$	Belle	[1567]	1437	6.10 ± 0.58	0.10 ± 0.04	0
$\mathcal{B}_{180} = \mu^- e^+ \mu^-$	BABAR	[1566]	868	10.20 ± 0.60	0.03 ± 0.02	0
$\mathcal{B}_{180} = \mu^- e^+ \mu^-$	Belle	[1567]	1437	10.10 ± 0.77	0.02 ± 0.02	0
$\mathcal{B}_{181} = \mu^- e^+ e^-$	BABAR	[1566]	868	8.80 ± 0.50	0.64 ± 0.19	0
$\mathcal{B}_{181} = \mu^- e^+ e^-$	Belle	[1567]	1437	9.30 ± 0.73	0.04 ± 0.04	0
$\mathcal{B}_{182} = e^- \mu^+ e^-$	BABAR	[1566]	868	12.70 ± 0.70	0.34 ± 0.12	0
$\mathcal{B}_{182} = e^- \mu^+ e^-$	Belle	[1567]	1437	11.50 ± 0.89	0.01 ± 0.01	0
$\mathcal{B}_{183} = \mu^- \mu^+ \mu^-$	BABAR	[1566]	868	6.60 ± 0.60	0.44 ± 0.17	0
$\mathcal{B}_{183} = \mu^- \mu^+ \mu^-$	Belle	[1567]	1437	7.60 ± 0.56	0.13 ± 0.20	0

11 Acknowledgments

We are grateful for the strong support of the ATLAS, *BABAR*, Belle, BESIII, CLEO(c), CDF, CMS, D0 and LHCb collaborations, without whom this compilation of results and world averages would not have been possible. The success of these experiments in turn would not have been possible without the excellent operations of the BEPC, CESR, KEKB, LHC, PEP-II, and Tevatron accelerators. We also recognise the interplay between theoretical and experimental communities that has provided a stimulus for many of the measurements in this document.

Our averages and this compilation have benefitted greatly from contributions to the Heavy Flavor Averaging Group from numerous individuals. In particular, we would like to thank Yinghui Guan for contributions to the charm physics chapter, and Paolo Gambino and Andreas Kronfeld for discussions regarding the averages in the semileptonic chapter. We also thank all past members of the HFLAV. Finally, we thank the SLAC National Accelerator Laboratory for providing crucial computing resources and support to HFLAV in past years and CERN for taking this over from 2018.

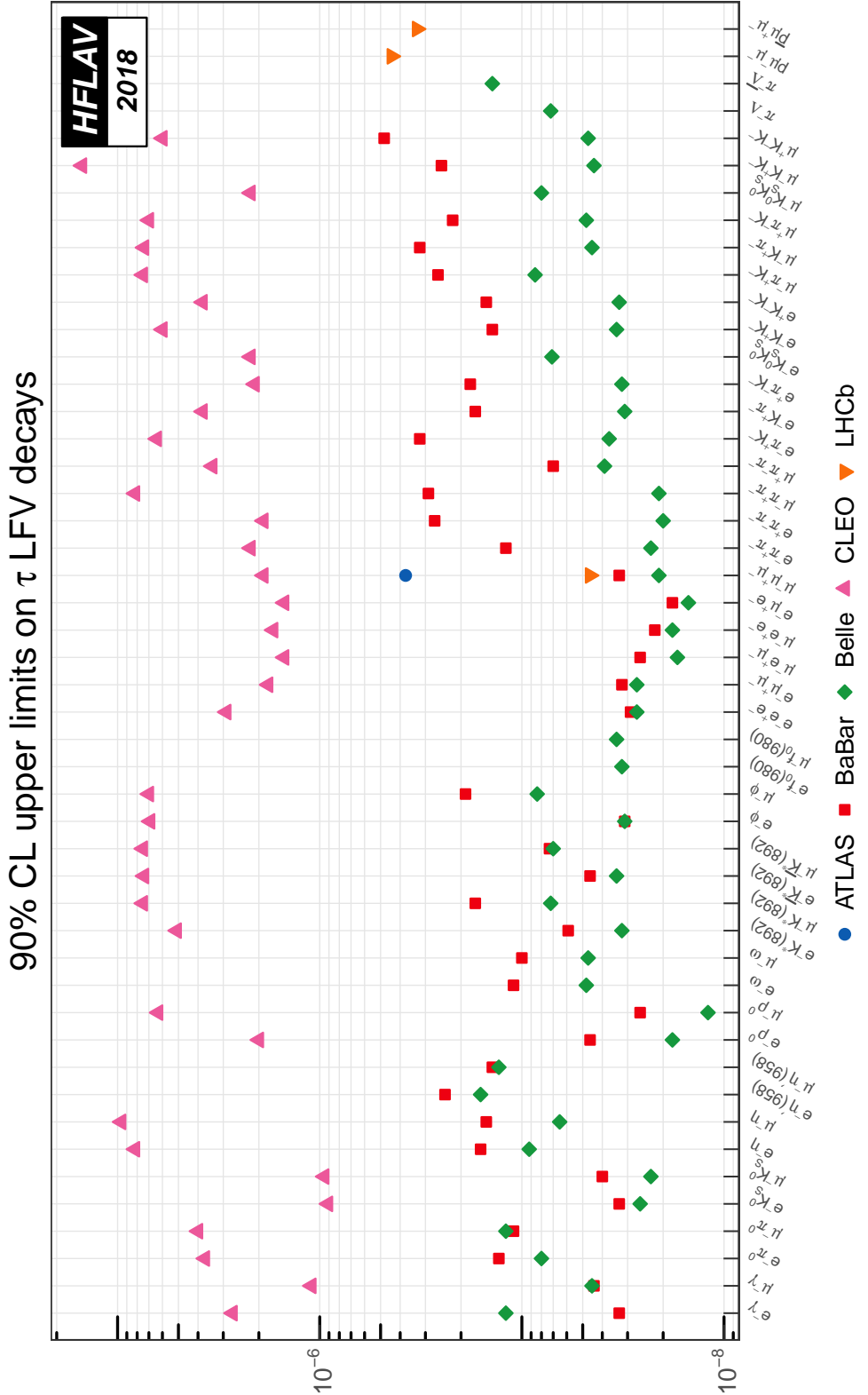


Figure 111: Tau lepton-flavor-violating branching fraction upper limits summary plot. In order to appreciate the physics reach improvement over time, the plot includes also the CLEO upper limits reported by PDG 2016 [21].

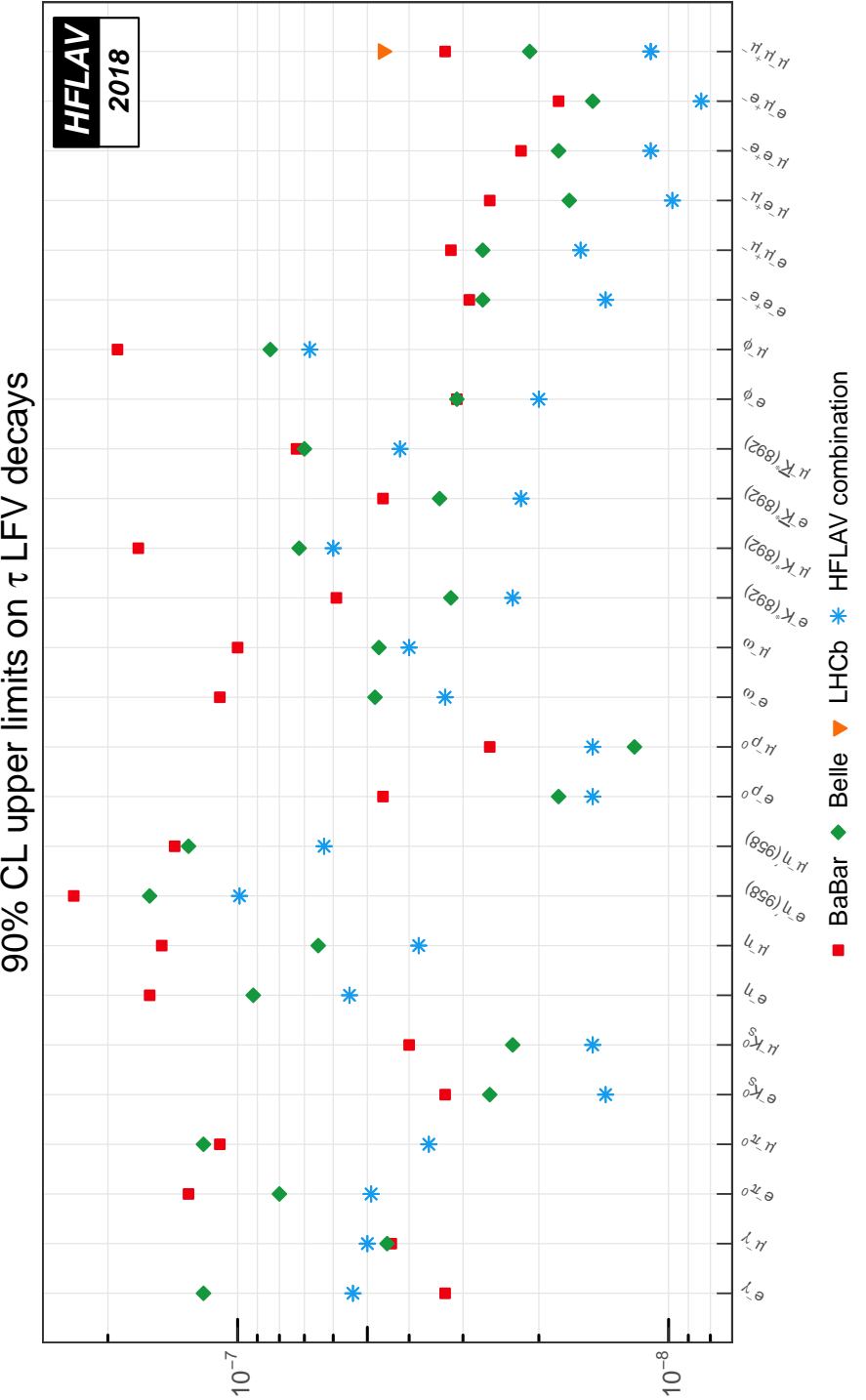


Figure 112: Tau lepton-flavour-violating branching fraction upper limits combinations summary plot. For each channel we report the HFLAV combined limit, and the experimental published limits. In some cases, the combined limit is weaker than the limit published by a single experiment. This arises since the CL_s method used in the combination can be more conservative compared to other legitimate methods, especially when the number of observed events fluctuates below the expected background.

References

- [1] Heavy Flavor Averaging Group, Y. Amhis *et al.*, Eur. Phys. J. **C77**, 895 (2017), [arXiv:1612.07233 \[hep-ex\]](https://arxiv.org/abs/1612.07233).
- [2] N. Cabibbo, Phys. Rev. Lett. **10**, 531 (1963).
- [3] M. Kobayashi and T. Maskawa, Prog. Theor. Phys. **49**, 652 (1973).
- [4] ALEPH, CDF, DELPHI, L3, OPAL, and SLD collaborations, D. Abbaneo *et al.*, [arXiv:hep-ex/0009052](https://arxiv.org/abs/hep-ex/0009052) (2000), CERN-EP-2000-096; [arXiv:hep-ex/0112028](https://arxiv.org/abs/hep-ex/0112028) (2001), CERN-EP-2001-050.
- [5] Particle Data Group, C. Patrignani *et al.*, Chin. Phys. **C40**, 100001 (2016).
- [6] CLEO collaboration, J. P. Alexander *et al.*, Phys. Rev. Lett. **86**, 2737 (2001), [arXiv:hep-ex/0006002 \[hep-ex\]](https://arxiv.org/abs/hep-ex/0006002).
- [7] CLEO collaboration, S. B. Athar *et al.*, Phys. Rev. **D66**, 052003 (2002), [arXiv:hep-ex/0202033 \[hep-ex\]](https://arxiv.org/abs/hep-ex/0202033).
- [8] Belle collaboration, N. C. Hastings *et al.*, Phys. Rev. **D67**, 052004 (2003), [arXiv:hep-ex/0212033 \[hep-ex\]](https://arxiv.org/abs/hep-ex/0212033).
- [9] BABAR collaboration, B. Aubert *et al.*, Phys. Rev. Lett. **94**, 141801 (2005), [arXiv:hep-ex/0412062 \[hep-ex\]](https://arxiv.org/abs/hep-ex/0412062).
- [10] CLEO collaboration, B. Barish *et al.*, Phys. Rev. **D51**, 1014 (1995), [arXiv:hep-ex/9406005 \[hep-ex\]](https://arxiv.org/abs/hep-ex/9406005).
- [11] BABAR collaboration, B. Aubert *et al.*, Phys. Rev. Lett. **95**, 042001 (2005), [arXiv:hep-ex/0504001 \[hep-ex\]](https://arxiv.org/abs/hep-ex/0504001).
- [12] BABAR collaboration, B. Aubert *et al.*, Phys. Rev. Lett. **96**, 232001 (2006), [arXiv:hep-ex/0604031 \[hep-ex\]](https://arxiv.org/abs/hep-ex/0604031).
- [13] Belle collaboration, A. Sokolov *et al.*, Phys. Rev. **D75**, 071103 (2007), [arXiv:hep-ex/0611026 \[hep-ex\]](https://arxiv.org/abs/hep-ex/0611026).
- [14] BABAR collaboration, B. Aubert *et al.*, Phys. Rev. **D78**, 112002 (2008), [arXiv:0807.2014 \[hep-ex\]](https://arxiv.org/abs/0807.2014).
- [15] Belle collaboration, E. Guido *et al.*, Phys. Rev. Lett. **121**, 062001 (2018), [arXiv:1803.10303 \[hep-ex\]](https://arxiv.org/abs/1803.10303).
- [16] CLEO collaboration, B. Barish *et al.*, Phys. Rev. Lett. **76**, 1570 (1996).
- [17] Belle collaboration, A. Drutskoy *et al.*, Phys. Rev. **D81**, 112003 (2010), [arXiv:1003.5885 \[hep-ex\]](https://arxiv.org/abs/1003.5885).
- [18] Belle collaboration, S. Esen *et al.*, Phys. Rev. **D87**, 031101 (2013), [arXiv:1208.0323](https://arxiv.org/abs/1208.0323).
- [19] Belle collaboration, A. Drutskoy *et al.*, Phys. Rev. Lett. **98**, 052001 (2007), [arXiv:hep-ex/0608015 \[hep-ex\]](https://arxiv.org/abs/hep-ex/0608015).

- [20] CLEO collaboration, G. S. Huang *et al.*, Phys. Rev. **D75**, 012002 (2007), [arXiv:hep-ex/0610035](https://arxiv.org/abs/hep-ex/0610035) [hep-ex].
- [21] Particle Data Group collaboration, M. Tanabashi *et al.*, Phys. Rev. **D98**, 030001 (2018).
- [22] CLEO collaboration, M. Artuso *et al.*, Phys. Rev. Lett. **95**, 261801 (2005), [arXiv:hep-ex/0508047](https://arxiv.org/abs/hep-ex/0508047).
- [23] Belle collaboration, K. F. Chen *et al.*, Phys. Rev. Lett. **100**, 112001 (2008), [arXiv:0710.2577](https://arxiv.org/abs/0710.2577) [hep-ex].
- [24] Belle collaboration, A. Garmash *et al.*, Phys. Rev. **D91**, 072003 (2015), [arXiv:1403.0992](https://arxiv.org/abs/1403.0992) [hep-ex].
- [25] Belle collaboration, I. Adachi *et al.*, Phys. Rev. Lett. **108**, 032001 (2012), [arXiv:1103.3419](https://arxiv.org/abs/1103.3419) [hep-ex].
- [26] Belle collaboration, P. Krokovny *et al.*, Phys. Rev. **D88**, 052016 (2013), [arXiv:1308.2646](https://arxiv.org/abs/1308.2646) [hep-ex].
- [27] Belle collaboration, U. Tamponi *et al.*, Eur. Phys. J. **C78**, 633 (2018), [arXiv:1803.03225](https://arxiv.org/abs/1803.03225) [hep-ex].
- [28] R. Louvot, PhD thesis #5213, EPFL, Lausanne, 2012, <http://dx.doi.org/10.5075/epfl-thesis-5213>.
- [29] BABAR collaboration, J. P. Lees *et al.*, Phys. Rev. **D85**, 011101 (2012), [arXiv:1110.5600](https://arxiv.org/abs/1110.5600) [hep-ex].
- [30] Belle collaboration, J. Li *et al.*, Phys. Rev. Lett. **106**, 121802 (2011), [arXiv:1102.2759](https://arxiv.org/abs/1102.2759) [hep-ex].
- [31] Belle collaboration, R. Louvot *et al.*, Phys. Rev. Lett. **102**, 021801 (2009), [arXiv:0809.2526](https://arxiv.org/abs/0809.2526) [hep-ex].
- [32] DELPHI collaboration, P. Abreu *et al.*, Phys. Lett. **B289**, 199 (1992).
- [33] OPAL collaboration, P. D. Acton *et al.*, Phys. Lett. **B295**, 357 (1992).
- [34] ALEPH collaboration, D. Buskulic *et al.*, Phys. Lett. **B361**, 221 (1995).
- [35] DELPHI collaboration, P. Abreu *et al.*, Z. Phys. **C68**, 375 (1995).
- [36] ALEPH collaboration, R. Barate *et al.*, Eur. Phys. J. **C2**, 197 (1998).
- [37] ALEPH collaboration, D. Buskulic *et al.*, Phys. Lett. **B384**, 449 (1996).
- [38] DELPHI collaboration, J. Abdallah *et al.*, Eur. Phys. J. **C44**, 299 (2005), [arXiv:hep-ex/0510023](https://arxiv.org/abs/hep-ex/0510023) [hep-ex].
- [39] ALEPH collaboration, R. Barate *et al.*, Eur. Phys. J. **C5**, 205 (1998).
- [40] DELPHI collaboration, J. Abdallah *et al.*, Phys. Lett. **B576**, 29 (2003), [arXiv:hep-ex/0311005](https://arxiv.org/abs/hep-ex/0311005) [hep-ex].
- [41] CDF collaboration, T. Affolder *et al.*, Phys. Rev. Lett. **84**, 1663 (2000), [arXiv:hep-ex/9909011](https://arxiv.org/abs/hep-ex/9909011) [hep-ex].

- [42] CDF collaboration, T. Aaltonen *et al.*, Phys. Rev. **D77**, 072003 (2008), [arXiv:0801.4375 \[hep-ex\]](https://arxiv.org/abs/0801.4375).
- [43] CDF collaboration, T. Aaltonen *et al.*, Phys. Rev. **D79**, 032001 (2009), [arXiv:0810.3213 \[hep-ex\]](https://arxiv.org/abs/0810.3213).
- [44] CDF collaboration, F. Abe *et al.*, Phys. Rev. **D60**, 092005 (1999).
- [45] D0 collaboration, V. M. Abazov *et al.*, Phys. Rev. Lett. **99**, 052001 (2007), [arXiv:0706.1690 \[hep-ex\]](https://arxiv.org/abs/0706.1690).
- [46] D0 collaboration, V. M. Abazov *et al.*, Phys. Rev. Lett. **101**, 232002 (2008), [arXiv:0808.4142 \[hep-ex\]](https://arxiv.org/abs/0808.4142).
- [47] CDF collaboration, T. Aaltonen *et al.*, Phys. Rev. **D80**, 072003 (2009), [arXiv:0905.3123 \[hep-ex\]](https://arxiv.org/abs/0905.3123).
- [48] LHCb collaboration, R. Aaij *et al.*, Phys. Rev. **D85**, 032008 (2012), [arXiv:1111.2357 \[hep-ex\]](https://arxiv.org/abs/1111.2357), with numerical results and full covariance matrix available at <https://cdsweb.cern.ch/record/1390838>.
- [49] LHCb collaboration, R. Aaij *et al.*, JHEP **04**, 001 (2013), [arXiv:1301.5286 \[hep-ex\]](https://arxiv.org/abs/1301.5286), with numerical results and full covariance matrix available at <http://cdsweb.cern.ch/record/1507868>.
- [50] LHCb collaboration, R. Aaij *et al.*, JHEP **08**, 143 (2014), [arXiv:1405.6842 \[hep-ex\]](https://arxiv.org/abs/1405.6842).
- [51] ATLAS collaboration, G. Aad *et al.*, Phys. Rev. Lett. **115**, 262001 (2015), [arXiv:1507.08925 \[hep-ex\]](https://arxiv.org/abs/1507.08925).
- [52] X. Liu, W. Wang, and Y. Xie, Phys. Rev. **D89**, 094010 (2014), [arXiv:1309.0313 \[hep-ph\]](https://arxiv.org/abs/1309.0313).
- [53] ALEPH, CDF, DELPHI, L3, OPAL, and SLD collaborations, LEP electroweak working group, SLD electroweak and heavy flavour working groups, S. Schael *et al.*, Phys. Rept. **427**, 257 (2006), [arXiv:hep-ex/0509008 \[hep-ex\]](https://arxiv.org/abs/hep-ex/0509008).
- [54] D0 collaboration, V. M. Abazov *et al.*, Phys. Rev. **D74**, 092001 (2006), [arXiv:hep-ex/0609014 \[hep-ex\]](https://arxiv.org/abs/hep-ex/0609014).
- [55] CDF collaboration, D. Acosta *et al.*, Phys. Rev. **D69**, 012002 (2004), [arXiv:hep-ex/0309030 \[hep-ex\]](https://arxiv.org/abs/hep-ex/0309030).
- [56] LHCb collaboration, LHCb-CONF-2013-011, 2013, <https://cdsweb.cern.ch/record/1559262>.
- [57] M. A. Shifman and M. B. Voloshin, Sov. Phys. JETP **64**, 698 (1986).
- [58] J. Chay, H. Georgi, and B. Grinstein, Phys. Lett. **B247**, 399 (1990).
- [59] I. I. Bigi, N. G. Uraltsev, and A. I. Vainshtein, Phys. Lett. **B293**, 430 (1992), [arXiv:hep-ph/9207214 \[hep-ph\]](https://arxiv.org/abs/hep-ph/9207214), Erratum *ibid.* **B297**, 477 (1992).
- [60] M. A. Shifman, [arXiv:hep-ph/0009131 \[hep-ph\]](https://arxiv.org/abs/hep-ph/0009131) (2000).
- [61] I. I. Y. Bigi and N. Uraltsev, Int. J. Mod. Phys. **A16**, 5201 (2001), [arXiv:hep-ph/0106346 \[hep-ph\]](https://arxiv.org/abs/hep-ph/0106346).

- [62] T. Jubb, M. Kirk, A. Lenz, and G. Tetlalmatzi-Xolocotzi, Nucl. Phys. **B915**, 431 (2017), [arXiv:1603.07770 \[hep-ph\]](#).
- [63] K. G. Wilson, Phys. Rev. **179**, 1499 (1969).
- [64] M. Ciuchini, E. Franco, V. Lubicz, and F. Mescia, Nucl. Phys. **B625**, 211 (2002), [arXiv:hep-ph/0110375 \[hep-ph\]](#).
- [65] M. Beneke, G. Buchalla, C. Greub, A. Lenz, and U. Nierste, Nucl. Phys. **B639**, 389 (2002), [arXiv:hep-ph/0202106 \[hep-ph\]](#).
- [66] E. Franco, V. Lubicz, F. Mescia, and C. Tarantino, Nucl. Phys. **B633**, 212 (2002), [arXiv:hep-ph/0203089 \[hep-ph\]](#).
- [67] C. Tarantino, Eur. Phys. J. **C33**, S895 (2004), [arXiv:hep-ph/0310241 \[hep-ph\]](#).
- [68] F. Gabbiani, A. I. Onishchenko, and A. A. Petrov, Phys. Rev. **D68**, 114006 (2003), [arXiv:hep-ph/0303235 \[hep-ph\]](#).
- [69] F. Gabbiani, A. I. Onishchenko, and A. A. Petrov, Phys. Rev. **D70**, 094031 (2004), [arXiv:hep-ph/0407004 \[hep-ph\]](#).
- [70] A. Lenz, Int. J. Mod. Phys. **A30**, 1543005 (2015).
- [71] A. Lenz, [arXiv:1405.3601 \[hep-ph\]](#) (2014).
- [72] ALEPH collaboration, D. Buskulic *et al.*, Phys. Lett. **B314**, 459 (1993).
- [73] DELPHI collaboration, P. Abreu *et al.*, Z. Phys. **C63**, 3 (1994).
- [74] DELPHI collaboration, P. Abreu *et al.*, Phys. Lett. **B377**, 195 (1996).
- [75] DELPHI collaboration, J. Abdallah *et al.*, Eur. Phys. J. **C33**, 307 (2004), [arXiv:hep-ex/0401025 \[hep-ex\]](#).
- [76] L3 collaboration, M. Acciarri *et al.*, Phys. Lett. **B416**, 220 (1998).
- [77] OPAL collaboration, K. Ackerstaff *et al.*, Z. Phys. **C73**, 397 (1997).
- [78] SLD collaboration, K. Abe *et al.*, Phys. Rev. Lett. **75**, 3624 (1995), [arXiv:hep-ex/9511005 \[hep-ex\]](#).
- [79] ALEPH collaboration, D. Buskulic *et al.*, Phys. Lett. **B369**, 151 (1996).
- [80] OPAL collaboration, P. D. Acton *et al.*, Z. Phys. **C60**, 217 (1993).
- [81] CDF collaboration, F. Abe *et al.*, Phys. Rev. **D57**, 5382 (1998).
- [82] ALEPH collaboration, R. Barate *et al.*, Phys. Lett. **B492**, 275 (2000), [arXiv:hep-ex/0008016 \[hep-ex\]](#).
- [83] ALEPH collaboration, D. Buskulic *et al.*, Z. Phys. **C71**, 31 (1996).
- [84] DELPHI collaboration, P. Abreu *et al.*, Z. Phys. **C68**, 13 (1995).
- [85] DELPHI collaboration, W. Adam *et al.*, Z. Phys. **C68**, 363 (1995).
- [86] DELPHI collaboration, P. Abreu *et al.*, Z. Phys. **C74**, 19 (1997).

- [87] L3 collaboration, M. Acciarri *et al.*, Phys. Lett. **B438**, 417 (1998).
- [88] OPAL collaboration, R. Akers *et al.*, Z. Phys. **C67**, 379 (1995).
- [89] OPAL collaboration, G. Abbiendi *et al.*, Eur. Phys. J. **C12**, 609 (2000),
[arXiv:hep-ex/9901017 \[hep-ex\]](https://arxiv.org/abs/hep-ex/9901017).
- [90] OPAL collaboration, G. Abbiendi *et al.*, Phys. Lett. **B493**, 266 (2000),
[arXiv:hep-ex/0010013 \[hep-ex\]](https://arxiv.org/abs/hep-ex/0010013).
- [91] SLD collaboration, K. Abe *et al.*, Phys. Rev. Lett. **79**, 590 (1997).
- [92] CDF collaboration, F. Abe *et al.*, Phys. Rev. **D58**, 092002 (1998), [arXiv:hep-ex/9806018 \[hep-ex\]](https://arxiv.org/abs/hep-ex/9806018).
- [93] CDF collaboration, D. Acosta *et al.*, Phys. Rev. **D65**, 092009 (2002).
- [94] CDF collaboration, T. Aaltonen *et al.*, Phys. Rev. Lett. **106**, 121804 (2011),
[arXiv:1012.3138 \[hep-ex\]](https://arxiv.org/abs/1012.3138).
- [95] D0 collaboration, V. M. Abazov *et al.*, Phys. Rev. Lett. **102**, 032001 (2009),
[arXiv:0810.0037 \[hep-ex\]](https://arxiv.org/abs/0810.0037).
- [96] D0 collaboration, V. M. Abazov *et al.*, Phys. Rev. **D85**, 112003 (2012), [arXiv:1204.2340 \[hep-ex\]](https://arxiv.org/abs/1204.2340).
- [97] D0 collaboration, V. M. Abazov *et al.*, Phys. Rev. Lett. **114**, 062001 (2015),
[arXiv:1410.1568 \[hep-ex\]](https://arxiv.org/abs/1410.1568).
- [98] BABAR collaboration, B. Aubert *et al.*, Phys. Rev. Lett. **87**, 201803 (2001),
[arXiv:hep-ex/0107019 \[hep-ex\]](https://arxiv.org/abs/hep-ex/0107019).
- [99] BABAR collaboration, B. Aubert *et al.*, Phys. Rev. Lett. **89**, 011802 (2002),
[arXiv:hep-ex/0202005 \[hep-ex\]](https://arxiv.org/abs/hep-ex/0202005), Erratum ibid. **89**, 169903, (2002).
- [100] BABAR collaboration, B. Aubert *et al.*, Phys. Rev. **D67**, 072002 (2003),
[arXiv:hep-ex/0212017 \[hep-ex\]](https://arxiv.org/abs/hep-ex/0212017).
- [101] BABAR collaboration, B. Aubert *et al.*, Phys. Rev. **D67**, 091101 (2003),
[arXiv:hep-ex/0212012 \[hep-ex\]](https://arxiv.org/abs/hep-ex/0212012).
- [102] BABAR collaboration, B. Aubert *et al.*, Phys. Rev. **D73**, 012004 (2006),
[arXiv:hep-ex/0507054 \[hep-ex\]](https://arxiv.org/abs/hep-ex/0507054).
- [103] Belle collaboration, K. Abe *et al.*, Phys. Rev. **D71**, 072003 (2005), [arXiv:hep-ex/0408111 \[hep-ex\]](https://arxiv.org/abs/hep-ex/0408111), Erratum ibid. **D71**, 079903, (2005).
- [104] ATLAS collaboration, G. Aad *et al.*, Phys. Rev. **D87**, 032002 (2013), [arXiv:1207.2284 \[hep-ex\]](https://arxiv.org/abs/1207.2284).
- [105] CMS collaboration, A. M. Sirunyan *et al.*, Eur. Phys. J. **C78**, 457 (2018), [arXiv:1710.08949 \[hep-ex\]](https://arxiv.org/abs/1710.08949), Erratum ibid. **C78**, 561 (2018).
- [106] LHCb collaboration, R. Aaij *et al.*, JHEP **04**, 114 (2014), [arXiv:1402.2554 \[hep-ex\]](https://arxiv.org/abs/1402.2554).
- [107] LHCb collaboration, R. Aaij *et al.*, Phys. Lett. **B736**, 446 (2014), [arXiv:1406.7204 \[hep-ex\]](https://arxiv.org/abs/1406.7204).

- [108] CDF collaboration, T. Aaltonen *et al.*, Phys. Rev. **D83**, 032008 (2011), [arXiv:1004.4855 \[hep-ex\]](#).
- [109] D0 collaboration, V. M. Abazov *et al.*, Phys. Rev. Lett. **94**, 182001 (2005), [arXiv:hep-ex/0410052 \[hep-ex\]](#).
- [110] LHCb collaboration, R. Aaij *et al.*, Phys. Rev. Lett. **108**, 241801 (2012), [arXiv:1202.4717 \[hep-ex\]](#).
- [111] M. Artuso, G. Borissov, and A. Lenz, Rev. Mod. Phys. **88**, 045002 (2016), [arXiv:1511.09466 \[hep-ph\]](#).
- [112] S. Laplace, Z. Ligeti, Y. Nir, and G. Perez, Phys. Rev. **D65**, 094040 (2002), [arXiv:hep-ph/0202010 \[hep-ph\]](#).
- [113] M. Ciuchini, E. Franco, V. Lubicz, F. Mescia, and C. Tarantino, JHEP **08**, 031 (2003), [arXiv:hep-ph/0308029 \[hep-ph\]](#).
- [114] M. Beneke, G. Buchalla, A. Lenz, and U. Nierste, Phys. Lett. **B576**, 173 (2003), [arXiv:hep-ph/0307344 \[hep-ph\]](#).
- [115] R. Fleischer and R. Knegjens, Eur. Phys. J. **C71**, 1789 (2011), [arXiv:1109.5115 \[hep-ph\]](#).
- [116] ALEPH collaboration, R. Barate *et al.*, Eur. Phys. J. **C4**, 367 (1998).
- [117] DELPHI collaboration, P. Abreu *et al.*, Eur. Phys. J. **C18**, 229 (2000), [arXiv:hep-ex/0105077 \[hep-ex\]](#).
- [118] OPAL collaboration, K. Ackerstaff *et al.*, Eur. Phys. J. **C2**, 407 (1998), [arXiv:hep-ex/9708023 \[hep-ex\]](#).
- [119] ALEPH collaboration, D. Buskulic *et al.*, Phys. Lett. **B377**, 205 (1996).
- [120] CDF collaboration, F. Abe *et al.*, Phys. Rev. **D59**, 032004 (1999), [arXiv:hep-ex/9808003 \[hep-ex\]](#).
- [121] DELPHI collaboration, P. Abreu *et al.*, Eur. Phys. J. **C16**, 555 (2000), [arXiv:hep-ex/0107077 \[hep-ex\]](#).
- [122] OPAL collaboration, K. Ackerstaff *et al.*, Phys. Lett. **B426**, 161 (1998), [arXiv:hep-ex/9802002 \[hep-ex\]](#).
- [123] CDF collaboration, T. Aaltonen *et al.*, Phys. Rev. Lett. **107**, 272001 (2011), [arXiv:1103.1864 \[hep-ex\]](#).
- [124] LHCb collaboration, R. Aaij *et al.*, Phys. Rev. Lett. **112**, 111802 (2014), [arXiv:1312.1217 \[hep-ex\]](#).
- [125] LHCb collaboration, R. Aaij *et al.*, Phys. Rev. Lett. **113**, 172001 (2014), [arXiv:1407.5873 \[hep-ex\]](#).
- [126] LHCb collaboration, R. Aaij *et al.*, Phys. Rev. Lett. **119**, 101801 (2017), [arXiv:1705.03475 \[hep-ex\]](#).
- [127] D0 collaboration, V. M. Abazov *et al.*, Phys. Rev. Lett. **94**, 042001 (2005), [arXiv:hep-ex/0409043 \[hep-ex\]](#).

- [128] LHCb collaboration, R. Aaij *et al.*, Phys. Rev. Lett. **118**, 191801 (2017), [arXiv:1703.05747 \[hep-ex\]](#).
- [129] ALEPH collaboration, R. Barate *et al.*, Phys. Lett. **B486**, 286 (2000).
- [130] LHCb collaboration, R. Aaij *et al.*, Phys. Lett. **B707**, 349 (2012), [arXiv:1111.0521 \[hep-ex\]](#).
- [131] LHCb collaboration, R. Aaij *et al.*, Phys. Lett. **B762**, 484 (2016), [arXiv:1607.06314 \[hep-ex\]](#).
- [132] LHCb collaboration, R. Aaij *et al.*, Nucl. Phys. **B873**, 275 (2013), [arXiv:1304.4500 \[hep-ex\]](#).
- [133] CDF collaboration, T. Aaltonen *et al.*, Phys. Rev. **D84**, 052012 (2011), [arXiv:1106.3682 \[hep-ex\]](#).
- [134] D0 collaboration, V. M. Abazov *et al.*, Phys. Rev. **D94**, 012001 (2016), [arXiv:1603.01302 \[hep-ex\]](#).
- [135] LHCb collaboration, R. Aaij *et al.*, Phys. Rev. **D87**, 112010 (2013), [arXiv:1304.2600 \[hep-ex\]](#).
- [136] K. Hartkorn and H. G. Moser, Eur. Phys. J. **C8**, 381 (1999).
- [137] LHCb collaboration, R. Aaij *et al.*, Phys. Lett. **B739**, 218 (2014), [arXiv:1408.0275 \[hep-ex\]](#).
- [138] CDF collaboration, F. Abe *et al.*, Phys. Rev. Lett. **81**, 2432 (1998), [arXiv:hep-ex/9805034 \[hep-ex\]](#).
- [139] CDF collaboration, A. Abulencia *et al.*, Phys. Rev. Lett. **97**, 012002 (2006), [arXiv:hep-ex/0603027 \[hep-ex\]](#).
- [140] D0 collaboration, V. M. Abazov *et al.*, Phys. Rev. Lett. **102**, 092001 (2009), [arXiv:0805.2614 \[hep-ex\]](#).
- [141] CDF collaboration, T. Aaltonen *et al.*, Phys. Rev. **D87**, 011101 (2013), [arXiv:1210.2366 \[hep-ex\]](#).
- [142] LHCb collaboration, R. Aaij *et al.*, Eur. Phys. J. **C74**, 2839 (2014), [arXiv:1401.6932 \[hep-ex\]](#).
- [143] LHCb collaboration, R. Aaij *et al.*, Phys. Lett. **B742**, 29 (2015), [arXiv:1411.6899 \[hep-ex\]](#).
- [144] DELPHI collaboration, P. Abreu *et al.*, Eur. Phys. J. **C10**, 185 (1999).
- [145] DELPHI collaboration, P. Abreu *et al.*, Z. Phys. **C71**, 199 (1996).
- [146] OPAL collaboration, R. Akers *et al.*, Z. Phys. **C69**, 195 (1996).
- [147] CDF collaboration, F. Abe *et al.*, Phys. Rev. Lett. **77**, 1439 (1996).
- [148] D0 collaboration, V. M. Abazov *et al.*, Phys. Rev. Lett. **99**, 182001 (2007), [arXiv:0706.2358 \[hep-ex\]](#).

- [149] CDF collaboration, T. Aaltonen *et al.*, Phys. Rev. Lett. **104**, 102002 (2010), arXiv:0912.3566 [hep-ex].
- [150] CDF collaboration, T. A. Aaltonen *et al.*, Phys. Rev. **D89**, 072014 (2014), arXiv:1403.8126 [hep-ex].
- [151] CMS collaboration, S. Chatrchyan *et al.*, JHEP **07**, 163 (2013), arXiv:1304.7495 [hep-ex].
- [152] LHCb collaboration, R. Aaij *et al.*, Phys. Lett. **B734**, 122 (2014), arXiv:1402.6242 [hep-ex].
- [153] DELPHI collaboration, P. Abreu *et al.*, Z. Phys. **C68**, 541 (1995).
- [154] LHCb collaboration, R. Aaij *et al.*, Phys. Lett. **B736**, 154 (2014), arXiv:1405.1543 [hep-ex].
- [155] LHCb collaboration, R. Aaij *et al.*, Phys. Rev. Lett. **113**, 242002 (2014), arXiv:1409.8568 [hep-ex].
- [156] LHCb collaboration, R. Aaij *et al.*, Phys. Rev. Lett. **113**, 032001 (2014), arXiv:1405.7223 [hep-ex].
- [157] LHCb collaboration, R. Aaij *et al.*, Phys. Rev. **D93**, 092007 (2016), arXiv:1604.01412 [hep-ex].
- [158] M. Beneke, G. Buchalla, and I. Dunietz, Phys. Rev. **D54**, 4419 (1996), arXiv:hep-ph/9605259 [hep-ph], Erratum ibid. **D83**, 119902, (2011).
- [159] Y.-Y. Keum and U. Nierste, Phys. Rev. **D57**, 4282 (1998), arXiv:hep-ph/9710512 [hep-ph].
- [160] M. B. Voloshin, Phys. Rept. **320**, 275 (1999), arXiv:hep-ph/9901445 [hep-ph]; B. Guberina, B. Melic, and H. Stefancic, Phys. Lett. **B469**, 253 (1999), arXiv:hep-ph/9907468 [hep-ph]; M. Neubert and C. T. Sachrajda, Nucl. Phys. **B483**, 339 (1997), arXiv:hep-ph/9603202 [hep-ph]; I. I. Y. Bigi, M. A. Shifman, and N. Uraltsev, Ann. Rev. Nucl. Part. Sci. **47**, 591 (1997), arXiv:hep-ph/9703290 [hep-ph].
- [161] N. G. Uraltsev, Phys. Lett. **B376**, 303 (1996), arXiv:hep-ph/9602324 [hep-ph]; D. Pirjol and N. Uraltsev, Phys. Rev. **D59**, 034012 (1999), arXiv:hep-ph/9805488 [hep-ph]; P. Colangelo and F. De Fazio, Phys. Lett. **B387**, 371 (1996), arXiv:hep-ph/9604425 [hep-ph]; UKQCD collaboration, M. Di Pierro, C. T. Sachrajda, and C. Michael, Phys. Lett. **B468**, 143 (1999), arXiv:hep-lat/9906031 [hep-lat], Erratum ibid. **D525**, 360, (2002).
- [162] ALEPH collaboration, D. Buskulic *et al.*, Z. Phys. **C75**, 397 (1997).
- [163] DELPHI collaboration, P. Abreu *et al.*, Z. Phys. **C76**, 579 (1997).
- [164] DELPHI collaboration, J. Abdallah *et al.*, Eur. Phys. J. **C28**, 155 (2003), arXiv:hep-ex/0303032 [hep-ex].
- [165] L3 collaboration, M. Acciarri *et al.*, Eur. Phys. J. **C5**, 195 (1998).
- [166] OPAL collaboration, K. Ackerstaff *et al.*, Z. Phys. **C76**, 417 (1997), arXiv:hep-ex/9707010 [hep-ex].
- [167] OPAL collaboration, K. Ackerstaff *et al.*, Z. Phys. **C76**, 401 (1997), arXiv:hep-ex/9707009 [hep-ex].

- [168] OPAL collaboration, G. Alexander *et al.*, Z. Phys. **C72**, 377 (1996).
- [169] CDF collaboration, F. Abe *et al.*, Phys. Rev. Lett. **80**, 2057 (1998), [arXiv:hep-ex/9712004 \[hep-ex\]](#); CDF collaboration, F. Abe *et al.*, Phys. Rev. **D59**, 032001 (1999), [arXiv:hep-ex/9806026 \[hep-ex\]](#).
- [170] CDF collaboration, F. Abe *et al.*, Phys. Rev. **D60**, 051101 (1999).
- [171] CDF collaboration, F. Abe *et al.*, Phys. Rev. **D60**, 072003 (1999), [arXiv:hep-ex/9903011 \[hep-ex\]](#).
- [172] CDF collaboration, T. Affolder *et al.*, Phys. Rev. **D60**, 112004 (1999), [arXiv:hep-ex/9907053 \[hep-ex\]](#).
- [173] D0 collaboration, V. M. Abazov *et al.*, Phys. Rev. **D74**, 112002 (2006), [arXiv:hep-ex/0609034 \[hep-ex\]](#).
- [174] BABAR collaboration, B. Aubert *et al.*, Phys. Rev. Lett. **88**, 221802 (2002), [arXiv:hep-ex/0112044 \[hep-ex\]](#); BABAR collaboration, B. Aubert *et al.*, Phys. Rev. **D66**, 032003 (2002), [arXiv:hep-ex/0201020 \[hep-ex\]](#).
- [175] BABAR collaboration, B. Aubert *et al.*, Phys. Rev. Lett. **88**, 221803 (2002), [arXiv:hep-ex/0112045 \[hep-ex\]](#).
- [176] Belle collaboration, Y. Zheng *et al.*, Phys. Rev. **D67**, 092004 (2003), [arXiv:hep-ex/0211065 \[hep-ex\]](#).
- [177] LHCb collaboration, R. Aaij *et al.*, Phys. Lett. **B709**, 177 (2012), [arXiv:1112.4311 \[hep-ex\]](#).
- [178] LHCb collaboration, R. Aaij *et al.*, Phys. Lett. **B719**, 318 (2013), [arXiv:1210.6750 \[hep-ex\]](#).
- [179] LHCb collaboration, R. Aaij *et al.*, Eur. Phys. J. **C73**, 2655 (2013), [arXiv:1308.1302 \[hep-ex\]](#).
- [180] LHCb collaboration, R. Aaij *et al.*, Eur. Phys. J. **C76**, 412 (2016), [arXiv:1604.03475 \[hep-ex\]](#).
- [181] ARGUS collaboration, H. Albrecht *et al.*, Z. Phys. **C55**, 357 (1992); ARGUS collaboration, H. Albrecht *et al.*, Phys. Lett. **B324**, 249 (1994).
- [182] CLEO collaboration, J. E. Bartelt *et al.*, Phys. Rev. Lett. **71**, 1680 (1993).
- [183] CLEO collaboration, B. H. Behrens *et al.*, Phys. Lett. **B490**, 36 (2000), [arXiv:hep-ex/0005013 \[hep-ex\]](#).
- [184] BABAR collaboration, B. Aubert *et al.*, Phys. Rev. Lett. **92**, 181801 (2004), [arXiv:hep-ex/0311037 \[hep-ex\]](#); BABAR collaboration, B. Aubert *et al.*, Phys. Rev. **D70**, 012007 (2004), [arXiv:hep-ex/0403002 \[hep-ex\]](#).
- [185] Belle collaboration, T. Higuchi *et al.*, Phys. Rev. **D85**, 071105 (2012), [arXiv:1203.0930 \[hep-ex\]](#).
- [186] T. Gershon, J. Phys. **G38**, 015007 (2011), [arXiv:1007.5135 \[hep-ph\]](#), Erratum ibid. **G42**, 119501, (2015).

- [187] ATLAS collaboration, M. Aaboud *et al.*, JHEP **06**, 081 (2016), [arXiv:1605.07485 \[hep-ex\]](https://arxiv.org/abs/1605.07485).
- [188] CKMfitter group, J. Charles *et al.*, Phys. Rev. **D84**, 033005 (2011), [arXiv:1106.4041 \[hep-ph\]](https://arxiv.org/abs/1106.4041), with updated results and plots available at <http://ckmfitter.in2p3.fr>; UTfit collaboration, M. Bona *et al.*, JHEP **10**, 081 (2006), [arXiv:hep-ph/0606167 \[hep-ph\]](https://arxiv.org/abs/hep-ph/0606167), with similar updated results and plots available at <http://www.utfit.org>.
- [189] D0 collaboration, V. M. Abazov *et al.*, Phys. Rev. **D89**, 012002 (2014), [arXiv:1310.0447 \[hep-ex\]](https://arxiv.org/abs/1310.0447).
- [190] U. Nierste, talk presented at the 8th International Workshop on the CKM unitarity Triangle (CKM 2014), 2014, <http://indico.cern.ch/event/253826/contributions/567426/>.
- [191] CDF collaboration, T. Aaltonen *et al.*, Phys. Rev. Lett. **109**, 171802 (2012), [arXiv:1208.2967 \[hep-ex\]](https://arxiv.org/abs/1208.2967).
- [192] D0 collaboration, V. M. Abazov *et al.*, Phys. Rev. **D85**, 032006 (2012), [arXiv:1109.3166 \[hep-ex\]](https://arxiv.org/abs/1109.3166).
- [193] ATLAS collaboration, G. Aad *et al.*, Phys. Rev. **D90**, 052007 (2014), [arXiv:1407.1796 \[hep-ex\]](https://arxiv.org/abs/1407.1796).
- [194] ATLAS collaboration, G. Aad *et al.*, JHEP **08**, 147 (2016), [arXiv:1601.03297 \[hep-ex\]](https://arxiv.org/abs/1601.03297).
- [195] CMS collaboration, V. Khachatryan *et al.*, Phys. Lett. **B757**, 97 (2016), [arXiv:1507.07527 \[hep-ex\]](https://arxiv.org/abs/1507.07527).
- [196] LHCb collaboration, R. Aaij *et al.*, Phys. Rev. Lett. **114**, 041801 (2015), [arXiv:1411.3104 \[hep-ex\]](https://arxiv.org/abs/1411.3104).
- [197] LHCb collaboration, R. Aaij *et al.*, JHEP **08**, 037 (2017), [arXiv:1704.08217 \[hep-ex\]](https://arxiv.org/abs/1704.08217).
- [198] LHCb collaboration, R. Aaij *et al.*, Phys. Lett. **B762**, 253 (2016), [arXiv:1608.04855 \[hep-ex\]](https://arxiv.org/abs/1608.04855).
- [199] A. Lenz, [arXiv:1205.1444 \[hep-ph\]](https://arxiv.org/abs/1205.1444) (2012).
- [200] Belle collaboration, S. Esen *et al.*, Phys. Rev. Lett. **105**, 201802 (2010), [arXiv:1005.5177 \[hep-ex\]](https://arxiv.org/abs/1005.5177).
- [201] D0 collaboration, V. Abazov *et al.*, Phys. Rev. Lett. **102**, 091801 (2009), [arXiv:0811.2173 \[hep-ex\]](https://arxiv.org/abs/0811.2173).
- [202] CDF collaboration, T. Aaltonen *et al.*, Phys. Rev. Lett. **100**, 021803 (2008).
- [203] A. Lenz and U. Nierste, [arXiv:1102.4274 \[hep-ph\]](https://arxiv.org/abs/1102.4274) (2011); A. Lenz and U. Nierste, JHEP **06**, 072 (2007), [arXiv:hep-ph/0612167 \[hep-ph\]](https://arxiv.org/abs/hep-ph/0612167).
- [204] ALEPH collaboration, A. Heister *et al.*, Eur. Phys. J. **C29**, 143 (2003).
- [205] DELPHI collaboration, J. Abdallah *et al.*, Eur. Phys. J. **C35**, 35 (2004), [arXiv:hep-ex/0404013 \[hep-ex\]](https://arxiv.org/abs/hep-ex/0404013).
- [206] OPAL collaboration, G. Abbiendi *et al.*, Eur. Phys. J. **C11**, 587 (1999), [arXiv:hep-ex/9907061 \[hep-ex\]](https://arxiv.org/abs/hep-ex/9907061).

- [207] OPAL collaboration, G. Abbiendi *et al.*, Eur. Phys. J. **C19**, 241 (2001), [arXiv:hep-ex/0011052 \[hep-ex\]](#).
- [208] SLD collaboration, K. Abe *et al.*, Phys. Rev. **D67**, 012006 (2003), [arXiv:hep-ex/0209002 \[hep-ex\]](#).
- [209] SLD collaboration, K. Abe *et al.*, Phys. Rev. **D66**, 032009 (2002), [arXiv:hep-ex/0207048 \[hep-ex\]](#).
- [210] CDF collaboration, F. Abe *et al.*, Phys. Rev. Lett. **82**, 3576 (1999).
- [211] D0 collaboration, V. M. Abazov *et al.*, Phys. Rev. Lett. **97**, 021802 (2006), [arXiv:hep-ex/0603029 \[hep-ex\]](#).
- [212] CDF collaboration, A. Abulencia *et al.*, Phys. Rev. Lett. **97**, 242003 (2006), [arXiv:hep-ex/0609040 \[hep-ex\]](#).
- [213] LHCb collaboration, R. Aaij *et al.*, New J. Phys. **15**, 053021 (2013), [arXiv:1304.4741 \[hep-ex\]](#).
- [214] FLAG collaboration, S. Aoki *et al.*, [arXiv:1902.08191 \[hep-lat\]](#).
- [215] Fermilab Lattice and MILC collaborations, A. Bazavov *et al.*, Phys. Rev. **D93**, 113016 (2016), [arXiv:1602.03560 \[hep-lat\]](#).
- [216] CLEO collaboration, D. E. Jaffe *et al.*, Phys. Rev. Lett. **86**, 5000 (2001), [arXiv:hep-ex/0101006 \[hep-ex\]](#).
- [217] BABAR collaboration, J. P. Lees *et al.*, Phys. Rev. Lett. **114**, 081801 (2015), [arXiv:1411.1842 \[hep-ex\]](#).
- [218] CDF collaboration, F. Abe *et al.*, Phys. Rev. **D55**, 2546 (1997).
- [219] ALEPH collaboration, R. Barate *et al.*, Eur. Phys. J. **C20**, 431 (2001).
- [220] BABAR collaboration, J. P. Lees *et al.*, Phys. Rev. Lett. **111**, 101802 (2013), [arXiv:1305.1575 \[hep-ex\]](#), Erratum *ibid.* **111**, 159901, (2013).
- [221] BABAR collaboration, B. Aubert *et al.*, Phys. Rev. Lett. **96**, 251802 (2006), [arXiv:hep-ex/0603053 \[hep-ex\]](#).
- [222] Belle collaboration, E. Nakano *et al.*, Phys. Rev. **D73**, 112002 (2006), [arXiv:hep-ex/0505017 \[hep-ex\]](#).
- [223] M. Beneke, G. Buchalla, and I. Dunietz, Phys. Lett. **B393**, 132 (1997), [arXiv:hep-ph/9609357 \[hep-ph\]](#); I. Dunietz, Eur. Phys. J. **C7**, 197 (1999), [arXiv:hep-ph/9806521 \[hep-ph\]](#).
- [224] D0 collaboration, V. M. Abazov *et al.*, Phys. Rev. **D86**, 072009 (2012), [arXiv:1208.5813 \[hep-ex\]](#).
- [225] LHCb collaboration, R. Aaij *et al.*, Phys. Rev. Lett. **114**, 041601 (2015), [arXiv:1409.8586 \[hep-ex\]](#).
- [226] Heavy Flavor Averaging Group, Y. Amhis *et al.*, [arXiv:1207.1158 \[hep-ex\]](#) (2012).

- [227] D0 collaboration, V. M. Abazov *et al.*, Phys. Rev. Lett. **110**, 011801 (2013), [arXiv:1207.1769 \[hep-ex\]](https://arxiv.org/abs/1207.1769).
- [228] LHCb collaboration, R. Aaij *et al.*, Phys. Rev. Lett. **117**, 061803 (2016), [arXiv:1605.09768 \[hep-ex\]](https://arxiv.org/abs/1605.09768).
- [229] A. Lenz, private communication, 2017.
- [230] S. Descotes-Genon and J. F. Kamenik, Phys. Rev. **D87**, 074036 (2013), [arXiv:1207.4483 \[hep-ph\]](https://arxiv.org/abs/1207.4483), Erratum *ibid.* **D92**, 079903, (2015).
- [231] ATLAS collaboration, M. Aaboud *et al.*, JHEP **02**, 071 (2017), [arXiv:1610.07869 \[hep-ex\]](https://arxiv.org/abs/1610.07869).
- [232] LHCb collaboration, R. Aaij *et al.*, Phys. Lett. **B736**, 186 (2014), [arXiv:1405.4140 \[hep-ex\]](https://arxiv.org/abs/1405.4140).
- [233] LHCb collaboration, R. Aaij *et al.*, Phys. Rev. **D86**, 052006 (2012), [arXiv:1204.5643 \[hep-ex\]](https://arxiv.org/abs/1204.5643).
- [234] LHCb collaboration, R. Aaij *et al.*, Phys. Rev. Lett. **113**, 211801 (2014), [arXiv:1409.4619 \[hep-ex\]](https://arxiv.org/abs/1409.4619).
- [235] LHCb collaboration, R. Aaij *et al.*, Phys. Lett. **B741**, 1 (2015), [arXiv:1408.4368 \[hep-ex\]](https://arxiv.org/abs/1408.4368).
- [236] L.-L. Chau and W.-Y. Keung, Phys. Rev. Lett. **53**, 1802 (1984).
- [237] L. Wolfenstein, Phys. Rev. Lett. **51**, 1945 (1983).
- [238] A. J. Buras, M. E. Lautenbacher, and G. Ostermaier, Phys. Rev. **D50**, 3433 (1994), [arXiv:hep-ph/9403384](https://arxiv.org/abs/hep-ph/9403384).
- [239] C. Jarlskog, Phys. Rev. Lett. **55**, 1039 (1985).
- [240] C. Jarlskog, Phys. Lett. **B615**, 207 (2005), [arXiv:hep-ph/0503199](https://arxiv.org/abs/hep-ph/0503199).
- [241] P. F. Harrison, S. Dallison, and W. G. Scott, Phys. Lett. **B680**, 328 (2009), [arXiv:0904.3077 \[hep-ph\]](https://arxiv.org/abs/0904.3077).
- [242] P. H. Frampton and X.-G. He, Phys. Lett. **B688**, 67 (2010), [arXiv:1003.0310 \[hep-ph\]](https://arxiv.org/abs/1003.0310).
- [243] P. H. Frampton and X.-G. He, Phys. Rev. **D82**, 017301 (2010), [arXiv:1004.3679 \[hep-ph\]](https://arxiv.org/abs/1004.3679).
- [244] CKMfitter group, J. Charles *et al.*, Eur. Phys. J. **C41**, 1 (2005), [arXiv:hep-ph/0406184](https://arxiv.org/abs/hep-ph/0406184), see also online updates, <http://ckmfitter.in2p3.fr/>.
- [245] BABAR collaboration, B. Aubert *et al.*, Phys. Rev. Lett. **86**, 2515 (2001), [arXiv:hep-ex/0102030](https://arxiv.org/abs/hep-ex/0102030).
- [246] LHCb collaboration, R. Aaij *et al.*, Phys. Lett. **B721**, 24 (2013), [arXiv:1211.6093 \[hep-ex\]](https://arxiv.org/abs/1211.6093).
- [247] Belle collaboration, K. Abe *et al.*, Phys. Rev. Lett. **87**, 091802 (2001), [arXiv:hep-ex/0107061](https://arxiv.org/abs/hep-ex/0107061).
- [248] A. B. Carter and A. I. Sanda, Phys. Rev. **D23**, 1567 (1981).
- [249] I. I. Y. Bigi and A. I. Sanda, Nucl. Phys. **B193**, 85 (1981).

- [250] I. Dunietz, R. Fleischer, and U. Nierste, Phys. Rev. **D63**, 114015 (2001), [arXiv:hep-ph/0012219 \[hep-ph\]](#).
- [251] LHCb collaboration, R. Aaij *et al.*, Phys. Lett. **B742**, 38 (2015), [arXiv:1411.1634 \[hep-ex\]](#).
- [252] *BABAR* collaboration, B. Aubert *et al.*, Phys. Rev. **D79**, 032002 (2009), [arXiv:0808.1866 \[hep-ex\]](#).
- [253] Belle collaboration, P. Krokovny *et al.*, Phys. Rev. Lett. **97**, 081801 (2006), [arXiv:hep-ex/0605023](#).
- [254] *BABAR* collaboration, B. Aubert *et al.*, Phys. Rev. Lett. **99**, 231802 (2007), [arXiv:0708.1544 \[hep-ex\]](#).
- [255] *BABAR* and Belle collaborations, I. Adachi *et al.*, Phys. Rev. Lett. **121**, 261801 (2018), [arXiv:1804.06152 \[hep-ex\]](#).
- [256] *BABAR* and Belle collaborations, I. Adachi *et al.*, Phys. Rev. **D98**, 112012 (2018), [arXiv:1804.06153 \[hep-ex\]](#).
- [257] Belle collaboration, V. Vorobyev *et al.*, Phys. Rev. **D94**, 052004 (2016), [arXiv:1607.05813 \[hep-ex\]](#).
- [258] CLEO collaboration, J. Libby *et al.*, Phys. Rev. **D82**, 112006 (2010), [arXiv:1010.2817 \[hep-ex\]](#).
- [259] T. E. Browder, A. Datta, P. J. O'Donnell, and S. Pakvasa, Phys. Rev. **D61**, 054009 (2000), [arXiv:hep-ph/9905425](#).
- [260] *BABAR* collaboration, B. Aubert *et al.*, Phys. Rev. **D74**, 091101 (2006), [arXiv:hep-ex/0608016 \[hep-ex\]](#).
- [261] Belle collaboration, J. Dalseno *et al.*, Phys. Rev. **D76**, 072004 (2007), [arXiv:0706.2045 \[hep-ex\]](#).
- [262] LHCb collaboration, R. Aaij *et al.*, Phys. Rev. **D90**, 012003 (2014), [arXiv:1404.5673 \[hep-ex\]](#).
- [263] J. R. Pelaez, Phys. Rept. **658**, 1 (2016), [arXiv:1510.00653 \[hep-ph\]](#).
- [264] *BABAR* collaboration, B. Aubert *et al.*, Phys. Rev. Lett. **99**, 161802 (2007), [arXiv:0706.3885 \[hep-ex\]](#).
- [265] Belle collaboration, Y. Nakahama *et al.*, Phys. Rev. **D82**, 073011 (2010), [arXiv:1007.3848 \[hep-ex\]](#).
- [266] *BABAR* collaboration, J. P. Lees *et al.*, Phys. Rev. **D85**, 112010 (2012), [arXiv:1201.5897 \[hep-ex\]](#).
- [267] Belle collaboration, A. Garmash *et al.*, Phys. Rev. **D71**, 092003 (2005), [arXiv:hep-ex/0412066 \[hep-ex\]](#).
- [268] *BABAR* collaboration, B. Aubert *et al.*, Phys. Rev. **D74**, 032003 (2006), [arXiv:hep-ex/0605003 \[hep-ex\]](#).

- [269] *BABAR* collaboration, B. Aubert *et al.*, Phys. Rev. **D80**, 112001 (2009), [arXiv:0905.3615 \[hep-ex\]](#).
- [270] *Belle* collaboration, J. Dalseno *et al.*, Phys. Rev. **D79**, 072004 (2009), [arXiv:0811.3665 \[hep-ex\]](#).
- [271] *Belle* collaboration, A. Garmash *et al.*, Phys. Rev. Lett. **96**, 251803 (2006), [arXiv:hep-ex/0512066 \[hep-ex\]](#).
- [272] *BABAR* collaboration, B. Aubert *et al.*, Phys. Rev. **D72**, 072003 (2005), [arXiv:hep-ex/0507004 \[hep-ex\]](#), Erratum ibid. **D74**, 099903, (2006).
- [273] *BABAR* collaboration, B. Aubert *et al.*, Phys. Rev. **D78**, 012004 (2008), [arXiv:0803.4451 \[hep-ex\]](#).
- [274] A. E. Snyder and H. R. Quinn, Phys. Rev. **D48**, 2139 (1993).
- [275] H. R. Quinn and J. P. Silva, Phys. Rev. **D62**, 054002 (2000), [arXiv:hep-ph/0001290](#).
- [276] *BABAR* collaboration, B. Aubert *et al.*, Phys. Rev. **D76**, 012004 (2007), [arXiv:hep-ex/0703008](#).
- [277] *BABAR* collaboration, J. P. Lees *et al.*, Phys. Rev. **D88**, 012003 (2013), [arXiv:1304.3503 \[hep-ex\]](#).
- [278] *Belle* collaboration, A. Kusaka *et al.*, Phys. Rev. Lett. **98**, 221602 (2007), [arXiv:hep-ex/0701015](#).
- [279] *Belle* collaboration, A. Kusaka *et al.*, Phys. Rev. **D77**, 072001 (2008), [arXiv:0710.4974 \[hep-ex\]](#).
- [280] *BABAR* collaboration, B. Aubert *et al.*, Phys. Rev. Lett. **99**, 071801 (2007), [arXiv:0705.1190 \[hep-ex\]](#).
- [281] *Belle* collaboration, T. Aushev *et al.*, Phys. Rev. Lett. **93**, 201802 (2004), [arXiv:hep-ex/0408051](#).
- [282] *Belle* collaboration, M. Rohrken *et al.*, Phys. Rev. **D85**, 091106 (2012), [arXiv:1203.6647 \[hep-ex\]](#).
- [283] *BABAR* collaboration, B. Aubert *et al.*, Phys. Rev. Lett. **91**, 201802 (2003), [arXiv:hep-ex/0306030 \[hep-ex\]](#).
- [284] *Belle* collaboration, C. C. Wang *et al.*, Phys. Rev. Lett. **94**, 121801 (2005), [arXiv:hep-ex/0408003](#).
- [285] *BABAR* collaboration, B. Aubert *et al.*, Phys. Rev. **D73**, 111101 (2006), [arXiv:hep-ex/0602049](#).
- [286] *BABAR* collaboration, B. Aubert *et al.*, Phys. Rev. **D71**, 112003 (2005), [arXiv:hep-ex/0504035](#).
- [287] O. Long, M. Baak, R. N. Cahn, and D. Kirkby, Phys. Rev. **D68**, 034010 (2003), [arXiv:hep-ex/0303030](#).

- [288] Belle collaboration, S. Bahinipati *et al.*, Phys. Rev. **D84**, 021101 (2011), arXiv:1102.0888 [hep-ex].
- [289] Belle collaboration, F. J. Ronga *et al.*, Phys. Rev. **D73**, 092003 (2006), arXiv:hep-ex/0604013.
- [290] R. Fleischer, Nucl. Phys. **B671**, 459 (2003), arXiv:hep-ph/0304027.
- [291] LHCb collaboration, R. Aaij *et al.*, JHEP **06**, 084 (2018), arXiv:1805.03448 [hep-ex].
- [292] LHCb collaboration, R. Aaij *et al.*, JHEP **11**, 060 (2014), arXiv:1407.6127 [hep-ex].
- [293] LHCb collaboration, R. Aaij *et al.*, JHEP **03**, 059 (2018), arXiv:1712.07428 [hep-ex].
- [294] D. Atwood, M. Gronau, and A. Soni, Phys. Rev. Lett. **79**, 185 (1997), arXiv:hep-ph/9704272.
- [295] D. Atwood, T. Gershon, M. Hazumi, and A. Soni, Phys. Rev. **D71**, 076003 (2005), arXiv:hep-ph/0410036.
- [296] B. Grinstein, Y. Grossman, Z. Ligeti, and D. Pirjol, Phys. Rev. **D71**, 011504 (2005), arXiv:hep-ph/0412019.
- [297] B. Grinstein and D. Pirjol, Phys. Rev. **D73**, 014013 (2006), arXiv:hep-ph/0510104.
- [298] M. Matsumori and A. I. Sanda, Phys. Rev. **D73**, 114022 (2006), arXiv:hep-ph/0512175.
- [299] P. Ball and R. Zwicky, Phys. Lett. **B642**, 478 (2006), arXiv:hep-ph/0609037.
- [300] F. Muheim, Y. Xie, and R. Zwicky, Phys. Lett. **B664**, 174 (2008), arXiv:0802.0876 [hep-ph].
- [301] I. I. Y. Bigi and A. I. Sanda, Phys. Lett. **B211**, 213 (1988).
- [302] M. Gronau and D. London., Phys. Lett. **B253**, 483 (1991).
- [303] M. Gronau and D. Wyler, Phys. Lett. **B265**, 172 (1991).
- [304] D. Atwood, I. Dunietz, and A. Soni, Phys. Rev. Lett. **78**, 3257 (1997), arXiv:hep-ph/9612433.
- [305] D. Atwood, I. Dunietz, and A. Soni, Phys. Rev. **D63**, 036005 (2001), arXiv:hep-ph/0008090.
- [306] A. Giri, Y. Grossman, A. Soffer, and J. Zupan, Phys. Rev. **D68**, 054018 (2003), arXiv:hep-ph/0303187.
- [307] Belle collaboration, A. Poluektov *et al.*, Phys. Rev. **D70**, 072003 (2004), arXiv:hep-ex/0406067.
- [308] J. Brod and J. Zupan, JHEP **01**, 051 (2014), arXiv:1308.5663 [hep-ph].
- [309] M. Gronau, Phys. Lett. **B557**, 198 (2003), arXiv:hep-ph/0211282.
- [310] R. Aleksan, T. C. Petersen, and A. Soffer, Phys. Rev. **D67**, 096002 (2003), arXiv:hep-ph/0209194 [hep-ph].
- [311] T. Gershon, Phys. Rev. **D79**, 051301 (2009), arXiv:0810.2706 [hep-ph].
- [312] T. Gershon and M. Williams, Phys. Rev. **D80**, 092002 (2009), arXiv:0909.1495 [hep-ph].

- [313] A. Bondar and T. Gershon, Phys. Rev. **D70**, 091503 (2004), [arXiv:hep-ph/0409281](#).
- [314] D. Atwood and A. Soni, Phys. Rev. **D68**, 033003 (2003), [arXiv:hep-ph/0304085](#).
- [315] Y. Grossman, Z. Ligeti, and A. Soffer, Phys. Rev. **D67**, 071301 (2003),
[arXiv:hep-ph/0210433](#) [hep-ph].
- [316] M. Nayak *et al.*, Phys. Lett. **B740**, 1 (2014), [arXiv:1410.3964](#) [hep-ex].
- [317] A. Bondar and A. Poluektov, Eur. Phys. J. **C47**, 347 (2006), [arXiv:hep-ph/0510246](#).
- [318] A. Bondar and A. Poluektov, Eur. Phys. J. **C55**, 51 (2008), [arXiv:0801.0840](#) [hep-ex].
- [319] T. Gershon, J. Libby, and G. Wilkinson, Phys. Lett. **B750**, 338 (2015), [arXiv:1506.08594](#) [hep-ph].
- [320] *BABAR* collaboration, B. Aubert *et al.*, Phys. Rev. Lett. **99**, 251801 (2007),
[arXiv:hep-ex/0703037](#).
- [321] *BABAR* collaboration, B. Aubert *et al.*, Phys. Rev. **D76**, 031102 (2007), [arXiv:0704.0522](#) [hep-ex].
- [322] Belle collaboration, R. Itoh *et al.*, Phys. Rev. Lett. **95**, 091601 (2005), [arXiv:hep-ex/0504030](#) [hep-ex].
- [323] CDF collaboration, D. Acosta *et al.*, Phys. Rev. Lett. **94**, 101803 (2005),
[arXiv:hep-ex/0412057](#).
- [324] LHCb collaboration, R. Aaij *et al.*, Phys. Rev. **D88**, 052002 (2013), [arXiv:1307.2782](#) [hep-ex].
- [325] M. Jung, Phys. Rev. **D86**, 053008 (2012), [arXiv:1206.2050](#) [hep-ph].
- [326] K. De Bruyn and R. Fleischer, JHEP **03**, 145 (2015), [arXiv:1412.6834](#) [hep-ph].
- [327] P. Frings, U. Nierste, and M. Wiebusch, Phys. Rev. Lett. **115**, 061802 (2015),
[arXiv:1503.00859](#) [hep-ph].
- [328] *BABAR* collaboration, B. Aubert *et al.*, Phys. Rev. **D79**, 072009 (2009), [arXiv:0902.1708](#) [hep-ex].
- [329] Belle collaboration, I. Adachi *et al.*, Phys. Rev. Lett. **108**, 171802 (2012), [arXiv:1201.4643](#) [hep-ex].
- [330] LHCb collaboration, R. Aaij *et al.*, Phys. Rev. Lett. **115**, 031601 (2015), [arXiv:1503.07089](#) [hep-ex].
- [331] LHCb collaboration, R. Aaij *et al.*, JHEP **11**, 170 (2017), [arXiv:1709.03944](#) [hep-ex].
- [332] *BABAR* collaboration, B. Aubert *et al.*, Phys. Rev. **D69**, 052001 (2004),
[arXiv:hep-ex/0309039](#).
- [333] ALEPH collaboration, R. Barate *et al.*, Phys. Lett. **B492**, 259 (2000),
[arXiv:hep-ex/0009058](#).
- [334] OPAL collaboration, K. Ackerstaff *et al.*, Eur. Phys. J. **C5**, 379 (1998),
[arXiv:hep-ex/9801022](#).

- [335] CDF collaboration, A. A. Affolder *et al.*, Phys. Rev. **D61**, 072005 (2000), [arXiv:hep-ex/9909003](https://arxiv.org/abs/hep-ex/9909003).
- [336] Belle collaboration, Y. Sato *et al.*, Phys. Rev. Lett. **108**, 171801 (2012), [arXiv:1201.3502](https://arxiv.org/abs/1201.3502) [hep-ex].
- [337] UTfit collaboration, M. Bona *et al.*, JHEP **07**, 028 (2005), [arXiv:hep-ph/0501199](https://arxiv.org/abs/hep-ph/0501199), see also online updates, <http://www.utfit.org/>.
- [338] E. Lunghi and A. Soni, Phys. Lett. **B666**, 162 (2008), [arXiv:0803.4340](https://arxiv.org/abs/0803.4340) [hep-ph].
- [339] G. Eigen, G. Dubois-Felsmann, D. Hitlin, and F. Porter, Phys. Rev. **D89**, 033004 (2014), [arXiv:1301.5867](https://arxiv.org/abs/1301.5867) [hep-ex].
- [340] I. Dunietz, H. R. Quinn, A. Snyder, W. Toki, and H. J. Lipkin, Phys. Rev. **D43**, 2193 (1991).
- [341] D. Aston *et al.*, Nucl. Phys. **B296**, 493 (1988).
- [342] M. Suzuki, Phys. Rev. **D64**, 117503 (2001), [arXiv:hep-ph/0106354](https://arxiv.org/abs/hep-ph/0106354).
- [343] *BABAR* collaboration, B. Aubert *et al.*, Phys. Rev. **D71**, 032005 (2005), [arXiv:hep-ex/0411016](https://arxiv.org/abs/hep-ex/0411016).
- [344] Y. Grossman and M. P. Worah, Phys. Lett. **B395**, 241 (1997), [arXiv:hep-ph/9612269](https://arxiv.org/abs/hep-ph/9612269).
- [345] R. Fleischer, Phys. Lett. **B562**, 234 (2003), [arXiv:hep-ph/0301255](https://arxiv.org/abs/hep-ph/0301255).
- [346] R. Fleischer, Nucl. Phys. **B659**, 321 (2003), [arXiv:hep-ph/0301256](https://arxiv.org/abs/hep-ph/0301256).
- [347] *BABAR* and *Belle* collaborations, A. Abdesselam *et al.*, Phys. Rev. Lett. **115**, 121604 (2015), [arXiv:1505.04147](https://arxiv.org/abs/1505.04147) [hep-ex].
- [348] A. Bondar, T. Gershon, and P. Krokovny, Phys. Lett. **B624**, 1 (2005), [arXiv:hep-ph/0503174](https://arxiv.org/abs/hep-ph/0503174).
- [349] F. Botella and J. Silva, Phys. Rev. **D71**, 094008 (2005), [arXiv:hep-ph/0503136](https://arxiv.org/abs/hep-ph/0503136) [hep-ph].
- [350] *BABAR* collaboration, B. Aubert *et al.*, Phys. Rev. Lett. **101**, 021801 (2008), [arXiv:0804.0896](https://arxiv.org/abs/0804.0896) [hep-ex].
- [351] *Belle* collaboration, B. Pal *et al.*, Phys. Rev. **D98**, 112008 (2018), [arXiv:1810.01356](https://arxiv.org/abs/1810.01356) [hep-ex].
- [352] LHCb collaboration, R. Aaij *et al.*, Phys. Rev. Lett. **117**, 261801 (2016), [arXiv:1608.06620](https://arxiv.org/abs/1608.06620) [hep-ex].
- [353] *BABAR* collaboration, J. P. Lees *et al.*, Phys. Rev. **D86**, 112006 (2012), [arXiv:1208.1282](https://arxiv.org/abs/1208.1282) [hep-ex].
- [354] *Belle* collaboration, B. Kronenbitter *et al.*, Phys. Rev. **D86**, 071103 (2012), [arXiv:1207.5611](https://arxiv.org/abs/1207.5611) [hep-ex].
- [355] *Belle* collaboration, S. Fratina *et al.*, Phys. Rev. Lett. **98**, 221802 (2007), [arXiv:hep-ex/0702031](https://arxiv.org/abs/hep-ex/0702031).
- [356] R. Fleischer, Eur. Phys. J. **C10**, 299 (1999), [arXiv:hep-ph/9903455](https://arxiv.org/abs/hep-ph/9903455) [hep-ph].

- [357] K. De Bruyn, R. Fleischer, and P. Koppenburg, Eur. Phys. J. **C70**, 1025 (2010), arXiv:1010.0089 [hep-ph].
- [358] LHCb collaboration, R. Aaij *et al.*, JHEP **06**, 131 (2015), arXiv:1503.07055 [hep-ex].
- [359] R. Fleischer, Int. J. Mod. Phys. **A12**, 2459 (1997), arXiv:hep-ph/9612446.
- [360] D. London and A. Soni, Phys. Lett. **B407**, 61 (1997), arXiv:hep-ph/9704277.
- [361] M. Ciuchini, E. Franco, G. Martinelli, A. Masiero, and L. Silvestrini, Phys. Rev. Lett. **79**, 978 (1997), arXiv:hep-ph/9704274.
- [362] S. Okubo, Phys. Lett. **5**, 165–168 (1963).
- [363] G. Zweig, CERN-TH-412, 1964.
- [364] J. Iizuka, Prog. Theor. Phys. Suppl. **37**, 21–34 (1966).
- [365] T. Gershon and M. Hazumi, Phys. Lett. **B596**, 163 (2004), arXiv:hep-ph/0402097.
- [366] Y. Grossman, Z. Ligeti, Y. Nir, and H. Quinn, Phys. Rev. **D68**, 015004 (2003), arXiv:hep-ph/0303171.
- [367] M. Gronau and J. L. Rosner, Phys. Lett. **B564**, 90 (2003), arXiv:hep-ph/0304178.
- [368] M. Gronau, Y. Grossman, and J. L. Rosner, Phys. Lett. **B579**, 331 (2004), arXiv:hep-ph/0310020.
- [369] M. Gronau, J. L. Rosner, and J. Zupan, Phys. Lett. **B596**, 107 (2004), arXiv:hep-ph/0403287.
- [370] H.-Y. Cheng, C.-K. Chua, and A. Soni, Phys. Rev. **D72**, 014006 (2005), arXiv:hep-ph/0502235.
- [371] M. Gronau and J. L. Rosner, Phys. Rev. **D71**, 074019 (2005), arXiv:hep-ph/0503131.
- [372] G. Buchalla, G. Hiller, Y. Nir, and G. Raz, JHEP **09**, 074 (2005), arXiv:hep-ph/0503151.
- [373] M. Beneke, Phys. Lett. **B620**, 143 (2005), arXiv:hep-ph/0505075.
- [374] G. Engelhard, Y. Nir, and G. Raz, Phys. Rev. **D72**, 075013 (2005), arXiv:hep-ph/0505194.
- [375] H.-Y. Cheng, C.-K. Chua, and A. Soni, Phys. Rev. **D72**, 094003 (2005), arXiv:hep-ph/0506268.
- [376] G. Engelhard and G. Raz, Phys. Rev. **D72**, 114017 (2005), arXiv:hep-ph/0508046.
- [377] M. Gronau, J. L. Rosner, and J. Zupan, Phys. Rev. **D74**, 093003 (2006), arXiv:hep-ph/0608085.
- [378] L. Silvestrini, Ann. Rev. Nucl. Part. Sci. **57**, 405 (2007), arXiv:0705.1624 [hep-ph].
- [379] R. Dutta and S. Gardner, Phys. Rev. **D78**, 034021 (2008), arXiv:0805.1963 [hep-ph].
- [380] Belle collaboration, M. Fujikawa *et al.*, Phys. Rev. **D81**, 011101 (2010), arXiv:0809.4366 [hep-ex].
- [381] Belle collaboration, K. Abe *et al.*, Phys. Rev. **D76**, 091103 (2007), arXiv:hep-ex/0609006.

- [382] *BABAR* collaboration, B. Aubert *et al.*, Phys. Rev. **D71**, 091102 (2005), [arXiv:hep-ex/0502019](https://arxiv.org/abs/hep-ex/0502019).
- [383] *BABAR* collaboration, B. Aubert *et al.*, Phys. Rev. **D79**, 052003 (2009), [arXiv:0809.1174 \[hep-ex\]](https://arxiv.org/abs/0809.1174).
- [384] *Belle* collaboration, L. Šantelj *et al.*, JHEP **10**, 165 (2014), [arXiv:1408.5991 \[hep-ex\]](https://arxiv.org/abs/1408.5991).
- [385] *BABAR* collaboration, J. P. Lees *et al.*, Phys. Rev. **D85**, 054023 (2012), [arXiv:1111.3636 \[hep-ex\]](https://arxiv.org/abs/1111.3636).
- [386] *Belle* collaboration, K. F. Chen *et al.*, Phys. Rev. Lett. **98**, 031802 (2007), [arXiv:hep-ex/0608039](https://arxiv.org/abs/hep-ex/0608039).
- [387] *Belle* collaboration, V. Chobanova *et al.*, Phys. Rev. **D90**, 012002 (2014), [arXiv:1311.6666 \[hep-ex\]](https://arxiv.org/abs/1311.6666).
- [388] *BABAR* collaboration, B. Aubert *et al.*, Phys. Rev. **D76**, 071101 (2007), [arXiv:hep-ex/0702010](https://arxiv.org/abs/hep-ex/0702010).
- [389] *Belle* collaboration, Y. Yusa *et al.*, Phys. Rev. **D99**, 011102 (2019), [arXiv:1810.03336 \[hep-ex\]](https://arxiv.org/abs/1810.03336).
- [390] *BABAR* collaboration, B. Aubert *et al.*, Phys. Rev. **D78**, 092008 (2008), [arXiv:0808.3586 \[hep-ex\]](https://arxiv.org/abs/0808.3586).
- [391] I. Dunietz, FERMILAB-CONF-93-090-T, 1993.
- [392] R. Fleischer, Phys. Lett. **B459**, 306 (1999), [arXiv:hep-ph/9903456 \[hep-ph\]](https://arxiv.org/abs/hep-ph/9903456).
- [393] LHCb collaboration, R. Aaij *et al.*, Phys. Rev. **D98**, no. 3, 032004 (2018), [arXiv:1805.06759 \[hep-ex\]](https://arxiv.org/abs/1805.06759).
- [394] LHCb collaboration, R. Aaij *et al.*, JHEP **10**, 183 (2013), [arXiv:1308.1428 \[hep-ex\]](https://arxiv.org/abs/1308.1428).
- [395] M. Raidal, Phys. Rev. Lett. **89**, 231803 (2002), [arXiv:hep-ph/0208091 \[hep-ph\]](https://arxiv.org/abs/hep-ph/0208091).
- [396] LHCb collaboration, R. Aaij *et al.*, [arXiv:1907.10003 \[hep-ex\]](https://arxiv.org/abs/1907.10003).
- [397] *BABAR* collaboration, B. Aubert *et al.*, Phys. Rev. Lett. **97**, 171805 (2006), [arXiv:hep-ex/0608036 \[hep-ex\]](https://arxiv.org/abs/hep-ex/0608036).
- [398] *Belle* collaboration, Y. Nakahama *et al.*, Phys. Rev. Lett. **100**, 121601 (2008), [arXiv:0712.4234 \[hep-ex\]](https://arxiv.org/abs/0712.4234).
- [399] S. Akar, PhD thesis, LPNHE, Université Pierre et Marie Curie - Paris VI, 2013, <https://tel.archives-ouvertes.fr/tel-00998252>.
- [400] *BABAR* collaboration, P. del Amo Sanchez *et al.*, Phys. Rev. **D93**, 052013 (2016), [arXiv:1512.03579 \[hep-ex\]](https://arxiv.org/abs/1512.03579).
- [401] *Belle* collaboration, J. Li *et al.*, Phys. Rev. Lett. **101**, 251601 (2008), [arXiv:0806.1980 \[hep-ex\]](https://arxiv.org/abs/0806.1980).
- [402] *BABAR* collaboration, B. Aubert *et al.*, Phys. Rev. **D78**, 071102 (2008), [arXiv:0807.3103 \[hep-ex\]](https://arxiv.org/abs/0807.3103).

- [403] Belle collaboration, Y. Ushiroda *et al.*, Phys. Rev. **D74**, 111104 (2006), [arXiv:hep-ex/0608017](#).
- [404] *BABAR* collaboration, B. Aubert *et al.*, Phys. Rev. **D79**, 011102 (2009), [arXiv:0805.1317 \[hep-ex\]](#).
- [405] Belle collaboration, H. Nakano *et al.*, Phys. Rev. **D97**, 092003 (2018), [arXiv:1803.07774 \[hep-ex\]](#).
- [406] Belle collaboration, H. Sahoo *et al.*, Phys. Rev. **D84**, 071101 (2011), [arXiv:1104.5590 \[hep-ex\]](#).
- [407] LHCb collaboration, R. Aaij *et al.*, Phys. Rev. Lett. **118**, 021801 (2017), [arXiv:1609.02032 \[hep-ex\]](#).
- [408] Belle collaboration, Y. Ushiroda *et al.*, Phys. Rev. Lett. **100**, 021602 (2008), [arXiv:0709.2769 \[hep-ex\]](#).
- [409] *BABAR* collaboration, B. Aubert *et al.*, Phys. Rev. **D76**, 052007 (2007), [arXiv:0705.2157 \[hep-ex\]](#).
- [410] Belle collaboration, P. Vanhoefer *et al.*, Phys. Rev. **D93**, no. 3, 032010 (2016), [arXiv:1510.01245 \[hep-ex\]](#), [addendum: Phys. Rev.D94,no.9,099903(2016)].
- [411] *BABAR* collaboration, B. Aubert *et al.*, Phys. Rev. **D78**, 071104 (2008), [arXiv:0807.4977 \[hep-ex\]](#).
- [412] Belle collaboration, I. Adachi *et al.*, Phys. Rev. **D89**, 072008 (2014), [arXiv:1212.4015 \[hep-ex\]](#), addendum ibid. **D89**, 119903, (2014).
- [413] LHCb collaboration, R. Aaij *et al.*, Phys. Lett. **B747**, 468 (2015), [arXiv:1503.07770 \[hep-ex\]](#).
- [414] *BABAR* collaboration, B. Aubert *et al.*, Phys. Rev. Lett. **98**, 181803 (2007), [arXiv:hep-ex/0612050](#).
- [415] Belle collaboration, J. Dalseno *et al.*, Phys. Rev. **D86**, 092012 (2012), [arXiv:1205.5957 \[hep-ex\]](#).
- [416] *BABAR* collaboration, B. Aubert *et al.*, Phys. Rev. **D81**, 052009 (2010), [arXiv:0909.2171 \[hep-ex\]](#).
- [417] *BABAR* collaboration, J. P. Lees *et al.*, Phys. Rev. **D87**, 052009 (2013), [arXiv:1206.3525 \[hep-ex\]](#).
- [418] Belle collaboration, I. Adachi *et al.*, Phys. Rev. **D88**, 092003 (2013), [arXiv:1302.0551 \[hep-ex\]](#).
- [419] M. Gronau and D. London, Phys. Rev. Lett. **65**, 3381 (1990).
- [420] Heavy Flavor Averaging Group, D. Asner *et al.*, [arXiv:1010.1589 \[hep-ex\]](#) (2010).
- [421] *BABAR* collaboration, B. Aubert *et al.*, Phys. Rev. Lett. **102**, 141802 (2009), [arXiv:0901.3522 \[hep-ex\]](#).
- [422] H. J. Lipkin, Y. Nir, H. R. Quinn, and A. Snyder, Phys. Rev. **D44**, 1454 (1991).

- [423] M. Gronau and J. Zupan, Phys. Rev. **D73**, 057502 (2006), [arXiv:hep-ph/0512148](https://arxiv.org/abs/hep-ph/0512148).
- [424] *BABAR* and Belle collaborations, A. Bevan *et al.*, Eur. Phys. J. **C74**, 3026 (2014), [arXiv:1406.6311 \[hep-ex\]](https://arxiv.org/abs/1406.6311).
- [425] M. Gronau and J. Zupan, Phys. Rev. **D71**, 074017 (2005), [arXiv:hep-ph/0502139 \[hep-ph\]](https://arxiv.org/abs/hep-ph/0502139).
- [426] S. Gardner, Phys. Rev. **D72**, 034015 (2005), [arXiv:hep-ph/0505071 \[hep-ph\]](https://arxiv.org/abs/hep-ph/0505071).
- [427] J. Charles, O. Deschamps, S. Descotes-Genon, and V. Niess, Eur. Phys. J. **C77**, 574 (2017), [arXiv:1705.02981 \[hep-ph\]](https://arxiv.org/abs/1705.02981).
- [428] GammaCombo framework for combinations of measurements and computation of confidence intervals, CERN, <http://gammacombo.github.io/>.
- [429] Belle collaboration, T. Julius *et al.*, [arXiv:1705.02083 \[hep-ex\]](https://arxiv.org/abs/1705.02083) (2017).
- [430] I. Dunietz, Phys. Lett. **B427**, 179 (1998), [arXiv:hep-ph/9712401 \[hep-ph\]](https://arxiv.org/abs/hep-ph/9712401).
- [431] M.A. Baak, PhD thesis, Vrije U., Amsterdam, 2007, <http://www-public.slac.stanford.edu/sciDoc/docMeta.aspx?slacPubNumber=slac-r-858>.
- [432] K. De Bruyn, R. Fleischer, R. Knegjens, M. Merk, M. Schiller, and N. Tuning, Nucl. Phys. **B868**, 351 (2013), [arXiv:1208.6463 \[hep-ph\]](https://arxiv.org/abs/1208.6463).
- [433] M. Kenzie, M. Martinelli, and N. Tuning, Phys. Rev. **D94**, 054021 (2016), [arXiv:1606.09129 \[hep-ph\]](https://arxiv.org/abs/1606.09129).
- [434] *BABAR* collaboration, B. Aubert *et al.*, Phys. Rev. **D77**, 071102 (2008), [arXiv:0712.3469 \[hep-ex\]](https://arxiv.org/abs/0712.3469).
- [435] I. Dunietz and R. G. Sachs, Phys. Rev. **D37**, 3186 (1988), Erratum *ibid.* **D39**, 3515, (1989).
- [436] R. Aleksan, I. Dunietz, and B. Kayser, Z. Phys. **C54**, 653 (1992).
- [437] M. Rama, Phys. Rev. **D89**, 014021 (2014), [arXiv:1307.4384 \[hep-ex\]](https://arxiv.org/abs/1307.4384).
- [438] *BABAR* collaboration, P. del Amo Sanchez *et al.*, Phys. Rev. **D82**, 072004 (2010), [arXiv:1007.0504 \[hep-ex\]](https://arxiv.org/abs/1007.0504).
- [439] Belle collaboration, K. Abe *et al.*, Phys. Rev. **D73**, 051106 (2006), [arXiv:hep-ex/0601032](https://arxiv.org/abs/hep-ex/0601032).
- [440] CDF collaboration, T. Aaltonen *et al.*, Phys. Rev. **D81**, 031105 (2010), [arXiv:0911.0425 \[hep-ex\]](https://arxiv.org/abs/0911.0425).
- [441] LHCb collaboration, R. Aaij *et al.*, Phys. Lett. **B777**, 16–30 (2018), [arXiv:1708.06370 \[hep-ex\]](https://arxiv.org/abs/1708.06370).
- [442] *BABAR* collaboration, B. Aubert *et al.*, Phys. Rev. **D78**, 092002 (2008), [arXiv:0807.2408 \[hep-ex\]](https://arxiv.org/abs/0807.2408).
- [443] *BABAR* collaboration, B. Aubert *et al.*, Phys. Rev. **D80**, 092001 (2009), [arXiv:0909.3981 \[hep-ex\]](https://arxiv.org/abs/0909.3981).
- [444] LHCb collaboration, R. Aaij *et al.*, JHEP **11**, 156 (2017), [arXiv:1709.05855 \[hep-ex\]](https://arxiv.org/abs/1709.05855), Erratum *ibid.* **05**, 067, (2018).

- [445] LHCb collaboration, R. Aaij *et al.*, Phys. Rev. **D92**, 112005 (2015), [arXiv:1505.07044 \[hep-ex\]](#).
- [446] LHCb collaboration, R. Aaij *et al.*, Phys. Rev. **D90**, 112002 (2014), [arXiv:1407.8136 \[hep-ex\]](#).
- [447] LHCb collaboration, R. Aaij *et al.*, Phys. Rev. **D93**, 112018 (2016), [arXiv:1602.03455 \[hep-ex\]](#).
- [448] S. Malde *et al.*, Phys. Lett. **B747**, 9 (2015), [arXiv:1504.05878 \[hep-ex\]](#).
- [449] LHCb collaboration, R. Aaij *et al.*, Phys. Rev. **D91**, 112014 (2015), [arXiv:1504.05442 \[hep-ex\]](#).
- [450] LHCb collaboration, R. Aaij *et al.*, Phys. Lett. **B760**, 117 (2016), [arXiv:1603.08993 \[hep-ex\]](#).
- [451] *BABAR* collaboration, P. del Amo Sanchez *et al.*, Phys. Rev. **D82**, 072006 (2010), [arXiv:1006.4241 \[hep-ex\]](#).
- [452] Belle collaboration, Y. Horii *et al.*, Phys. Rev. Lett. **106**, 231803 (2011), [arXiv:1103.5951 \[hep-ex\]](#).
- [453] CDF collaboration, T. Aaltonen *et al.*, Phys. Rev. **D84**, 091504 (2011), [arXiv:1108.5765 \[hep-ex\]](#).
- [454] *BABAR* collaboration, J. P. Lees *et al.*, Phys. Rev. **D84**, 012002 (2011), [arXiv:1104.4472 \[hep-ex\]](#).
- [455] Belle collaboration, M. Nayak *et al.*, Phys. Rev. **D88**, 091104 (2013), [arXiv:1310.1741 \[hep-ex\]](#).
- [456] *BABAR* collaboration, B. Aubert *et al.*, Phys. Rev. **D80**, 031102 (2009), [arXiv:0904.2112 \[hep-ex\]](#).
- [457] Belle collaboration, K. Negishi *et al.*, Phys. Rev. **D86**, 011101 (2012), [arXiv:1205.0422 \[hep-ex\]](#).
- [458] CLEO collaboration, D. M. Asner *et al.*, Phys. Rev. **D78**, 012001 (2008), [arXiv:0802.2268 \[hep-ex\]](#).
- [459] CLEO collaboration, N. Lowrey *et al.*, Phys. Rev. **D80**, 031105 (2009), [arXiv:0903.4853 \[hep-ex\]](#).
- [460] Belle collaboration, A. Poluektov *et al.*, Phys. Rev. **D81**, 112002 (2010), [arXiv:1003.3360 \[hep-ex\]](#).
- [461] *BABAR* collaboration, P. del Amo Sanchez *et al.*, Phys. Rev. Lett. **105**, 121801 (2010), [arXiv:1005.1096 \[hep-ex\]](#).
- [462] LHCb collaboration, R. Aaij *et al.*, Nucl. Phys. **B888**, 169 (2014), [arXiv:1407.6211 \[hep-ex\]](#).
- [463] Belle collaboration, A. Poluektov *et al.*, Phys. Rev. **D73**, 112009 (2006), [arXiv:hep-ex/0604054](#).

- [464] LHCb collaboration, R. Aaij *et al.*, JHEP **08**, 137 (2016), arXiv:1605.01082 [hep-ex].
- [465] BABAR collaboration, B. Aubert *et al.*, Phys. Rev. **D79**, 072003 (2009), arXiv:0805.2001 [hep-ex].
- [466] CLEO collaboration, R. A. Briere *et al.*, Phys. Rev. **D80**, 032002 (2009), arXiv:0903.1681 [hep-ex].
- [467] Belle collaboration, H. Aihara *et al.*, Phys. Rev. **D85**, 112014 (2012), arXiv:1204.6561 [hep-ex].
- [468] LHCb collaboration, R. Aaij *et al.*, JHEP **10**, 97 (2014), arXiv:1408.2748 [hep-ex].
- [469] LHCb collaboration, R. Aaij *et al.*, JHEP **08**, 176 (2018), arXiv:1806.01202 [hep-ex], Erratum *ibid.* **10**, 107, (2018).
- [470] Belle collaboration, K. Negishi *et al.*, PTEP **2016**, 043C01 (2016), arXiv:1509.01098 [hep-ex].
- [471] LHCb collaboration, R. Aaij *et al.*, JHEP **06**, 131 (2016), arXiv:1604.01525 [hep-ex].
- [472] LHCb collaboration, R. Aaij *et al.*, Phys. Lett. **B733**, 36 (2014), arXiv:1402.2982 [hep-ex].
- [473] CLEO collaboration, J. Insler *et al.*, Phys. Rev. **D85**, 092016 (2012), arXiv:1203.3804 [hep-ex].
- [474] BABAR collaboration, J. P. Lees *et al.*, Phys. Rev. **D87**, 052015 (2013), arXiv:1301.1029 [hep-ex].
- [475] LHCb collaboration, R. Aaij *et al.*, JHEP **12**, 087 (2016), arXiv:1611.03076 [hep-ex].
- [476] LHCb collaboration, LHCb-CONF-2018-002, 2018.
- [477] LHCb collaboration, R. Aaij *et al.*, Phys. Lett. **B726**, 151 (2013), arXiv:1305.2050 [hep-ex].
- [478] T. Evans, S. Harnew, J. Libby, S. Malde, J. Rademacker, and G. Wilkinson, Phys. Lett. **B757**, 520 (2016), arXiv:1602.07430 [hep-ex].
- [479] LHCb collaboration, R. Aaij *et al.*, Phys. Rev. **D93**, 052018 (2016), arXiv:1509.06628 [hep-ex].
- [480] J. P. Silva and A. Soffer, Phys. Rev. **D61**, 112001 (2000), arXiv:hep-ph/9912242 [hep-ph].
- [481] Y. Grossman, A. Soffer, and J. Zupan, Phys. Rev. **D72**, 031501 (2005), arXiv:hep-ph/0505270 [hep-ph].
- [482] HFLAV averages of semileptonic B decays,
<https://hflav.web.cern.ch/content/semileptonic-b-decays>.
- [483] M. Neubert, Phys. Rept. **245**, 259 (1994), arXiv:hep-ph/9306320 [hep-ph].
- [484] A. Sirlin, Nucl. Phys. **B196**, 83 (1982).
- [485] B semileptonic decays common input parameters, <https://hflav-eos.web.cern.ch/hflav-eos/semi/spring19/common/common.param.writeup18>.

- [486] ALEPH collaboration, D. Buskulic *et al.*, Phys. Lett. **B395**, 373 (1997).
- [487] OPAL collaboration, G. Abbiendi *et al.*, Phys. Lett. **B482**, 15 (2000), [arXiv:hep-ex/0003013](#).
- [488] DELPHI collaboration, P. Abreu *et al.*, Phys. Lett. **B510**, 55 (2001), [arXiv:hep-ex/0104026](#).
- [489] DELPHI collaboration, J. Abdallah *et al.*, Eur. Phys. J. **C33**, 213 (2004), [arXiv:hep-ex/0401023](#).
- [490] CLEO collaboration, N. E. Adam *et al.*, Phys. Rev. **D67**, 032001 (2003), [arXiv:hep-ex/0210040](#).
- [491] Belle collaboration, A. Abdesselam *et al.*, [arXiv:1809.03290 \[hep-ex\]](#).
- [492] Belle collaboration, A. Abdesselam *et al.*, [arXiv:1702.01521 \[hep-ex\]](#).
- [493] BABAR collaboration, B. Aubert *et al.*, Phys. Rev. **D77**, 032002 (2008), [arXiv:0705.4008 \[hep-ex\]](#).
- [494] BABAR collaboration, B. Aubert *et al.*, Phys. Rev. Lett. **100**, 151802 (2008), [arXiv:0712.3503 \[hep-ex\]](#).
- [495] BABAR collaboration, B. Aubert *et al.*, Phys. Rev. Lett. **100**, 231803 (2008), [arXiv:0712.3493 \[hep-ex\]](#).
- [496] I. Caprini, L. Lellouch, and M. Neubert, Nucl. Phys. **B530**, 153 (1998), [arXiv:hep-ph/9712417](#).
- [497] BABAR collaboration, B. Aubert *et al.*, Phys. Rev. **D79**, 012002 (2009), [arXiv:0809.0828 \[hep-ex\]](#).
- [498] MILC collaboration, J. A. Bailey *et al.*, Phys. Rev. **D92**, 034506 (2015), [arXiv:1503.07237 \[hep-lat\]](#).
- [499] CLEO collaboration, J. E. Bartelt *et al.*, Phys. Rev. Lett. **82**, 3746 (1999), [arXiv:hep-ex/9811042](#).
- [500] BABAR collaboration, B. Aubert *et al.*, Phys. Rev. Lett. **104**, 011802 (2010), [arXiv:0904.4063 \[hep-ex\]](#).
- [501] Belle collaboration, R. Glattauer *et al.*, Phys. Rev. **D93**, 032006 (2016), [arXiv:1510.03657 \[hep-ex\]](#).
- [502] Belle collaboration, A. Vossen *et al.*, Phys. Rev. **D98**, no. 1, 012005 (2018), [arXiv:1803.06444 \[hep-ex\]](#).
- [503] N. Isgur and M. B. Wise, Phys. Rev. Lett. **66**, 1130 (1991).
- [504] ALEPH collaboration, D. Buskulic *et al.*, Z. Phys. **C73**, 601 (1997).
- [505] OPAL collaboration, G. Abbiendi *et al.*, Eur. Phys. J. **C30**, 467 (2003), [arXiv:hep-ex/0301018](#).
- [506] CLEO collaboration, A. Anastassov *et al.*, Phys. Rev. Lett. **80**, 4127 (1998), [arXiv:hep-ex/9708035](#).

- [507] D0 collaboration, V. M. Abazov *et al.*, Phys. Rev. Lett. **95**, 171803 (2005),
[arXiv:hep-ex/0507046](https://arxiv.org/abs/hep-ex/0507046).
- [508] Belle collaboration, D. Liventsev *et al.*, Phys. Rev. **D77**, 091503 (2008), [arXiv:0711.3252](https://arxiv.org/abs/0711.3252) [hep-ex].
- [509] BABAR collaboration, B. Aubert *et al.*, Phys. Rev. Lett. **101**, 261802 (2008),
[arXiv:0808.0528](https://arxiv.org/abs/0808.0528) [hep-ex].
- [510] BABAR collaboration, B. Aubert *et al.*, Phys. Rev. Lett. **103**, 051803 (2009),
[arXiv:0808.0333](https://arxiv.org/abs/0808.0333) [hep-ex].
- [511] DELPHI collaboration, J. Abdallah *et al.*, Eur. Phys. J. **C45**, 35 (2006),
[arXiv:hep-ex/0510024](https://arxiv.org/abs/hep-ex/0510024).
- [512] D. Benson, I. I. Bigi, T. Mannel, and N. Uraltsev, Nucl. Phys. **B665**, 367 (2003),
[arXiv:hep-ph/0302262](https://arxiv.org/abs/hep-ph/0302262).
- [513] P. Gambino and N. Uraltsev, Eur. Phys. J. **C34**, 181 (2004), [arXiv:hep-ph/0401063](https://arxiv.org/abs/hep-ph/0401063).
- [514] P. Gambino, JHEP **09**, 055 (2011), [arXiv:1107.3100](https://arxiv.org/abs/1107.3100) [hep-ph].
- [515] A. Alberti, P. Gambino, K. J. Healey, and S. Nandi, Phys. Rev. Lett. **114**, 061802 (2015),
[arXiv:1411.6560](https://arxiv.org/abs/1411.6560) [hep-ph].
- [516] C. W. Bauer, Z. Ligeti, M. Luke, A. V. Manohar, and M. Trott, Phys. Rev. **D70**, 094017 (2004), [arXiv:hep-ph/0408002](https://arxiv.org/abs/hep-ph/0408002).
- [517] BABAR collaboration, B. Aubert *et al.*, Phys. Rev. **D81**, 032003 (2010), [arXiv:0908.0415](https://arxiv.org/abs/0908.0415) [hep-ex].
- [518] BABAR collaboration, B. Aubert *et al.*, Phys. Rev. **D69**, 111104 (2004),
[arXiv:hep-ex/0403030](https://arxiv.org/abs/hep-ex/0403030).
- [519] Belle collaboration, C. Schwanda *et al.*, Phys. Rev. **D75**, 032005 (2007),
[arXiv:hep-ex/0611044](https://arxiv.org/abs/hep-ex/0611044).
- [520] Belle collaboration, P. Urquijo *et al.*, Phys. Rev. **D75**, 032001 (2007), [arXiv:hep-ex/0610012](https://arxiv.org/abs/hep-ex/0610012).
- [521] CDF collaboration, D. E. Acosta *et al.*, Phys. Rev. **D71**, 051103 (2005),
[arXiv:hep-ex/0502003](https://arxiv.org/abs/hep-ex/0502003).
- [522] CLEO collaboration, S. E. Csorna *et al.*, Phys. Rev. **D70**, 032002 (2004),
[arXiv:hep-ex/0403052](https://arxiv.org/abs/hep-ex/0403052).
- [523] K. Chetyrkin *et al.*, Phys. Rev. **D80**, 074010 (2009), [arXiv:0907.2110](https://arxiv.org/abs/0907.2110) [hep-ph].
- [524] BABAR collaboration, B. Aubert *et al.*, Phys. Rev. **D72**, 052004 (2005),
[arXiv:hep-ex/0508004](https://arxiv.org/abs/hep-ex/0508004) [hep-ex].
- [525] BABAR collaboration, B. Aubert *et al.*, Phys. Rev. Lett. **97**, 171803 (2006),
[arXiv:hep-ex/0607071](https://arxiv.org/abs/hep-ex/0607071) [hep-ex].
- [526] Belle collaboration, A. Limosani *et al.*, Phys. Rev. Lett. **103**, 241801 (2009),
[arXiv:0907.1384](https://arxiv.org/abs/0907.1384) [hep-ex].

- [527] CLEO collaboration, S. Chen *et al.*, Phys. Rev. Lett. **87**, 251807 (2001), [arXiv:hep-ex/0108032](https://arxiv.org/abs/hep-ex/0108032) [hep-ex].
- [528] P. Gambino and C. Schwanda, Phys. Rev. **D89**, 014022 (2014), [arXiv:1307.4551](https://arxiv.org/abs/1307.4551) [hep-ph].
- [529] Belle collaboration, C. Schwanda *et al.*, Phys. Rev. **D78**, 032016 (2008), [arXiv:0803.2158](https://arxiv.org/abs/0803.2158) [hep-ex].
- [530] LHCb collaboration, R. Aaij *et al.*, Nature Phys. **11**, 743 (2015), [arXiv:1504.01568](https://arxiv.org/abs/1504.01568) [hep-ex].
- [531] Belle collaboration, H. Ha *et al.*, Phys. Rev. **D83**, 071101 (2011), [arXiv:1012.0090](https://arxiv.org/abs/1012.0090) [hep-ex].
- [532] Belle collaboration, A. Sibidanov *et al.*, Phys. Rev. **D88**, 032005 (2013), [arXiv:1306.2781](https://arxiv.org/abs/1306.2781) [hep-ex].
- [533] BABAR collaboration, P. del Amo Sanchez *et al.*, Phys. Rev. **D83**, 032007 (2011), [arXiv:1005.3288](https://arxiv.org/abs/1005.3288) [hep-ex].
- [534] BABAR collaboration, J. P. Lees *et al.*, Phys. Rev. **D86**, 092004 (2012), [arXiv:1208.1253](https://arxiv.org/abs/1208.1253) [hep-ex].
- [535] C. Bourrely, I. Caprini, and L. Lellouch, Phys. Rev. **D79**, 013008 (2009), [arXiv:0807.2722](https://arxiv.org/abs/0807.2722) [hep-ph], erratum *ibid.* **D82**, 099902, (2010).
- [536] FLAG, S. Aoki *et al.*, Eur. Phys. J. **C77**, 112 (2017), [arXiv:1607.00299](https://arxiv.org/abs/1607.00299) [hep-lat], see also <http://flag.unibe.ch/>.
- [537] Fermilab Lattice and MILC collaborations, J. A. Bailey *et al.*, Phys. Rev. **D92**, 014024 (2015), [arXiv:1503.07839](https://arxiv.org/abs/1503.07839) [hep-lat].
- [538] RBC and UKQCD collaborations, J. M. Flynn, T. Izubuchi, T. Kawanai, C. Lehner, A. Soni, R. S. Van de Water, and O. Witzel, Phys. Rev. **D91**, 074510 (2015), [arXiv:1501.05373](https://arxiv.org/abs/1501.05373) [hep-lat].
- [539] A. Bharucha, JHEP **05**, 092 (2012), [arXiv:1203.1359](https://arxiv.org/abs/1203.1359) [hep-ph].
- [540] W. Detmold, C. Lehner, and S. Meinel, Phys. Rev. **D92**, 034503 (2015), [arXiv:1503.01421](https://arxiv.org/abs/1503.01421) [hep-lat].
- [541] R. N. Faustov and V. O. Galkin, Phys. Rev. **D94**, 073008 (2016), [arXiv:1609.00199](https://arxiv.org/abs/1609.00199) [hep-ph].
- [542] P. Ball and R. Zwicky, Phys. Rev. **D71**, 014015 (2005), [arXiv:hep-ph/0406232](https://arxiv.org/abs/hep-ph/0406232).
- [543] A. Bharucha, D. M. Straub, and R. Zwicky, JHEP **08**, 098 (2016), [arXiv:1503.05534](https://arxiv.org/abs/1503.05534) [hep-ph].
- [544] CLEO collaboration, B. H. Behrens *et al.*, Phys. Rev. **D61**, 052001 (2000), [arXiv:hep-ex/9905056](https://arxiv.org/abs/hep-ex/9905056).
- [545] CLEO collaboration, N. E. Adam *et al.*, Phys. Rev. Lett. **99**, 041802 (2007), [arXiv:hep-ex/0703041](https://arxiv.org/abs/hep-ex/0703041).
- [546] Belle collaboration, T. Hokuue *et al.*, Phys. Lett. **B648**, 139 (2007), [arXiv:hep-ex/0604024](https://arxiv.org/abs/hep-ex/0604024).

- [547] Belle collaboration, C. Schwanda *et al.*, Phys. Rev. Lett. **93**, 131803 (2004), [arXiv:hep-ex/0402023 \[hep-ex\]](#).
- [548] *BABAR* collaboration, J. P. Lees *et al.*, Phys. Rev. **D87**, 032004 (2013), [arXiv:1205.6245 \[hep-ex\]](#).
- [549] *BABAR* collaboration, J. P. Lees *et al.*, Phys. Rev. **D88**, 072006 (2013), [arXiv:1308.2589 \[hep-ex\]](#).
- [550] CLEO collaboration, R. Gray *et al.*, Phys. Rev. **D76**, 012007 (2007), [arXiv:hep-ex/0703042](#).
- [551] *BABAR* collaboration, B. Aubert *et al.*, Phys. Rev. **D79**, 052011 (2009), [arXiv:0808.3524 \[hep-ex\]](#).
- [552] *BABAR* collaboration, B. Aubert *et al.*, Phys. Rev. Lett. **101**, 081801 (2008), [arXiv:0805.2408 \[hep-ex\]](#).
- [553] Belle collaboration, C. Belén̄o *et al.*, Phys. Rev. **D96**, no. 9, 091102 (2017), [arXiv:1703.10216 \[hep-ex\]](#).
- [554] Belle collaboration, P. Urquijo *et al.*, Phys. Rev. Lett. **104**, 021801 (2010), [arXiv:0907.0379 \[hep-ex\]](#).
- [555] *BABAR* collaboration, J. P. Lees *et al.*, Phys. Rev. **D86**, 032004 (2012), [arXiv:1112.0702 \[hep-ex\]](#).
- [556] C. W. Bauer, Z. Ligeti, and M. E. Luke, Phys. Rev. **D64**, 113004 (2001), [arXiv:hep-ph/0107074](#).
- [557] M. Neubert, Phys. Rev. **D49**, 4623 (1994), [arXiv:hep-ph/9312311](#).
- [558] A. K. Leibovich, I. Low, and I. Z. Rothstein, Phys. Rev. **D61**, 053006 (2000), [arXiv:hep-ph/9909404](#).
- [559] B. O. Lange, M. Neubert, and G. Paz, JHEP **10**, 084 (2005), [arXiv:hep-ph/0508178](#).
- [560] *BABAR* collaboration, J. P. Lees *et al.*, Phys. Rev. **D95**, 072001 (2017), [arXiv:1611.05624 \[hep-ex\]](#).
- [561] *BABAR* collaboration, B. Aubert *et al.*, Phys. Rev. **D73**, 012006 (2006), [arXiv:hep-ex/0509040](#).
- [562] R. V. Kowalewski and S. Menke, Phys. Lett. **B541**, 29 (2002), [arXiv:hep-ex/0205038](#).
- [563] *BABAR* collaboration, B. Aubert *et al.*, Phys. Rev. Lett. **95**, 111801 (2005), [arXiv:hep-ex/0506036](#).
- [564] CLEO collaboration, A. Bornheim *et al.*, Phys. Rev. Lett. **88**, 231803 (2002), [arXiv:hep-ex/0202019](#).
- [565] Belle collaboration, A. Limosani *et al.*, Phys. Lett. **B621**, 28 (2005), [arXiv:hep-ex/0504046](#).
- [566] Belle collaboration, H. Kakuno *et al.*, Phys. Rev. Lett. **92**, 101801 (2004), [arXiv:hep-ex/0311048](#).
- [567] Belle collaboration, I. Bizjak *et al.*, Phys. Rev. Lett. **95**, 241801 (2005), [arXiv:hep-ex/0505088](#).

- [568] B. O. Lange, M. Neubert, and G. Paz, Phys. Rev. **D72**, 073006 (2005), [arXiv:hep-ph/0504071](#).
- [569] S. W. Bosch, B. O. Lange, M. Neubert, and G. Paz, Nucl. Phys. **B699**, 335 (2004), [arXiv:hep-ph/0402094](#).
- [570] S. W. Bosch, M. Neubert, and G. Paz, JHEP **11**, 073 (2004), [arXiv:hep-ph/0409115](#).
- [571] M. Neubert, Eur. Phys. J. **C44**, 205 (2005), [arXiv:hep-ph/0411027](#).
- [572] M. Neubert, Phys. Lett. **B612**, 13 (2005), [arXiv:hep-ph/0412241](#) [hep-ph].
- [573] M. Neubert, Phys. Rev. **D72**, 074025 (2005), [arXiv:hep-ph/0506245](#) [hep-ph].
- [574] J. R. Andersen and E. Gardi, JHEP **01**, 097 (2006), [arXiv:hep-ph/0509360](#).
- [575] U. Aglietti, G. Ferrera, and G. Ricciardi, Nucl. Phys. **B768**, 85 (2007), [arXiv:hep-ph/0608047](#).
- [576] I. R. Blokland, A. Czarnecki, M. Misiak, M. Slusarczyk, and F. Tkachov, Phys. Rev. **D72**, 033014 (2005), [arXiv:hep-ph/0506055](#) [hep-ph].
- [577] P. Gambino and P. Giordano, Phys. Lett. **B669**, 69–73 (2008), [arXiv:0805.0271](#) [hep-ph].
- [578] P. Gambino, P. Giordano, G. Ossola, and N. Uraltsev, JHEP **10**, 058 (2007), [arXiv:0707.2493](#) [hep-ph].
- [579] U. Aglietti, F. Di Lodovico, G. Ferrera, and G. Ricciardi, Eur. Phys. J. **C59**, 831 (2009), [arXiv:0711.0860](#) [hep-ph].
- [580] U. Aglietti, G. Ricciardi, and G. Ferrera, Phys. Rev. **D74**, 034004 (2006), [arXiv:hep-ph/0507285](#).
- [581] U. Aglietti, G. Ricciardi, and G. Ferrera, Phys. Rev. **D74**, 034005 (2006), [arXiv:hep-ph/0509095](#).
- [582] U. Aglietti, G. Ricciardi, and G. Ferrera, Phys. Rev. **D74**, 034006 (2006), [arXiv:hep-ph/0509271](#).
- [583] M. Duraisamy, P. Sharma, and A. Datta, Phys. Rev. **D90**, 074013 (2014), [arXiv:1405.3719](#) [hep-ph].
- [584] D. Bigi and P. Gambino, Phys. Rev. **D94**, 094008 (2016), [arXiv:1606.08030](#) [hep-ph].
- [585] F. U. Bernlochner, Z. Ligeti, M. Papucci, and D. J. Robinson, Phys. Rev. **D95**, no. 11, 115008 (2017), [arXiv:1703.05330](#) [hep-ph], erratum *ibid* **D97**, 059902 (2018)].
- [586] S. Jaiswal, S. Nandi, and S. K. Patra, JHEP **12**, 060 (2017), [arXiv:1707.09977](#) [hep-ph].
- [587] HPQCD collaboration, H. Na, C. M. Bouchard, G. P. Lepage, C. Monahan, and J. Shigemitsu, Phys. Rev. **D92**, 054510 (2015), [arXiv:1505.03925](#) [hep-lat], erratum *ibid*. **D93**, 119906, (2016).
- [588] D. Bigi, P. Gambino, and S. Schacht, JHEP **11**, 061 (2017), [arXiv:1707.09509](#) [hep-ph].
- [589] S. Fajfer, J. F. Kamenik, and I. Nisandzic, Phys. Rev. **D85**, 094025 (2012), [arXiv:1203.2654](#) [hep-ph].

- [590] P. Gambino, M. Jung, and S. Schacht, Phys. Lett. **B795**, 386–390 (2019), [arXiv:1905.08209 \[hep-ph\]](#).
- [591] BaBar collaboration, J. P. Lees *et al.*, [arXiv:1903.10002 \[hep-ex\]](#).
- [592] Belle collaboration, A. Matyja *et al.*, Phys. Rev. Lett. **99**, 191807 (2007), [arXiv:0706.4429 \[hep-ex\]](#).
- [593] BABAR collaboration, B. Aubert *et al.*, Phys. Rev. Lett. **100**, 021801 (2008), [arXiv:0709.1698 \[hep-ex\]](#).
- [594] Belle collaboration, A. Bozek *et al.*, Phys. Rev. **D82**, 072005 (2010), [arXiv:1005.2302 \[hep-ex\]](#).
- [595] BABAR collaboration, J. P. Lees *et al.*, Phys. Rev. Lett. **109**, 101802 (2012), [arXiv:1205.5442 \[hep-ex\]](#).
- [596] Belle collaboration, S. Hirose *et al.*, Phys. Rev. Lett. **118**, no. 21, 211801 (2017), [arXiv:1612.00529 \[hep-ex\]](#).
- [597] LHCb collaboration, R. Aaij *et al.*, Phys. Rev. Lett. **115**, 111803 (2015), [arXiv:1506.08614 \[hep-ex\]](#), addendum ibid. **115**, 159901, (2015).
- [598] LHCb collaboration, R. Aaij *et al.*, Phys. Rev. Lett. **120**, no. 17, 171802 (2018), [arXiv:1708.08856 \[hep-ex\]](#).
- [599] BABAR collaboration, J. P. Lees *et al.*, Phys. Rev. **D88**, 072012 (2013), [arXiv:1303.0571 \[hep-ex\]](#).
- [600] Belle collaboration, M. Huschle *et al.*, Phys. Rev. **D92**, 072014 (2015), [arXiv:1507.03233 \[hep-ex\]](#).
- [601] LHCb collaboration, R. Aaij *et al.*, Phys. Rev. **D97**, no. 7, 072013 (2018), [arXiv:1711.02505 \[hep-ex\]](#).
- [602] Belle collaboration, A. Abdesselam *et al.*, [arXiv:1904.08794 \[hep-ex\]](#).
- [603] A. J. Lenz, J. Phys. **G41**, 103001 (2014), [arXiv:1404.6197 \[hep-ph\]](#).
- [604] Belle collaboration, S. Choi *et al.*, Phys. Rev. Lett. **91**, 262001 (2003), [arXiv:hep-ex/0309032 \[hep-ex\]](#).
- [605] LHCb collaboration, R. Aaij *et al.*, Phys. Rev. Lett. **110**, 222001 (2013), [arXiv:1302.6269 \[hep-ex\]](#).
- [606] Belle collaboration, S. Choi *et al.*, Phys. Rev. Lett. **100**, 142001 (2008), [arXiv:0708.1790 \[hep-ex\]](#).
- [607] LHCb collaboration, R. Aaij *et al.*, Phys. Rev. Lett. **112**, 222002 (2014), [arXiv:1404.1903 \[hep-ex\]](#).
- [608] LHCb collaboration, R. Aaij *et al.*, Phys. Rev. Lett. **115**, 072001 (2015), [arXiv:1507.03414 \[hep-ex\]](#).
- [609] R. Barlow, [arXiv:physics/0406120 \[physics\]](#) (2004).

- [610] K. De Bruyn *et al.*, Phys. Rev. **D86**, 014027 (2012), arXiv:1204.1735 [hep-ph].
- [611] M. Jung, Phys. Lett. **B753**, 187 (2016), arXiv:1510.03423 [hep-ph].
- [612] *BABAR* collaboration, B. Aubert *et al.*, Phys. Rev. **D75**, 031101 (2007), arXiv:hep-ex/0610027 [hep-ex].
- [613] *BABAR* collaboration, B. Aubert *et al.*, Phys. Rev. **D74**, 111102 (2006), arXiv:hep-ex/0609033 [hep-ex].
- [614] Belle collaboration, A. Kuzmin *et al.*, Phys. Rev. **D76**, 012006 (2007), arXiv:hep-ex/0611054 [hep-ex].
- [615] Belle collaboration, G. Majumder *et al.*, Phys. Rev. **D70**, 111103 (2004), arXiv:hep-ex/0409008 [hep-ex].
- [616] *BABAR* collaboration, J. P. Lees *et al.*, Phys. Rev. **D94**, 091101 (2016), arXiv:1609.06802 [hep-ex].
- [617] Belle collaboration, D. Matvienko *et al.*, Phys. Rev. **D92**, 012013 (2015), arXiv:1505.03362 [hep-ex].
- [618] *BABAR* collaboration, B. Aubert *et al.*, Phys. Rev. **D74**, 012001 (2006), arXiv:hep-ex/0604009 [hep-ex].
- [619] Belle collaboration, S. Blyth *et al.*, Phys. Rev. **D74**, 092002 (2006), arXiv:hep-ex/0607029 [hep-ex].
- [620] *BABAR* collaboration, J. P. Lees *et al.*, Phys. Rev. **D84**, 112007 (2011), arXiv:1107.5751 [hep-ex], Erratum ibid. **D87**, 039901, (2013).
- [621] LHCb collaboration, R. Aaij *et al.*, Phys. Rev. **D92**, 032002 (2015), arXiv:1505.01710 [hep-ex].
- [622] Belle collaboration, A. Satpathy *et al.*, Phys. Lett. **B553**, 159 (2003), arXiv:hep-ex/0211022 [hep-ex].
- [623] Belle collaboration, J. Schumann *et al.*, Phys. Rev. **D72**, 011103 (2005), arXiv:hep-ex/0501013 [hep-ex].
- [624] Belle collaboration, K. Abe *et al.*, Phys. Rev. Lett. **87**, 111801 (2001), arXiv:hep-ex/0104051 [hep-ex].
- [625] *BABAR* collaboration, B. Aubert *et al.*, Phys. Rev. Lett. **95**, 171802 (2005), arXiv:hep-ex/0412040 [hep-ex].
- [626] Belle collaboration, A. Drutskoy *et al.*, Phys. Lett. **B542**, 171 (2002), arXiv:hep-ex/0207041 [hep-ex].
- [627] Belle collaboration, P. Krokovny *et al.*, Phys. Rev. Lett. **90**, 141802 (2003), arXiv:hep-ex/0212066 [hep-ex].
- [628] *BABAR* collaboration, B. Aubert *et al.*, Phys. Rev. **D74**, 031101 (2006), arXiv:hep-ex/0604016 [hep-ex].

- [629] *BABAR* collaboration, B. Aubert *et al.*, Phys. Rev. Lett. **96**, 011803 (2006), [arXiv:hep-ex/0509036 \[hep-ex\]](#).
- [630] LHCb collaboration, R. Aaij *et al.*, [arXiv:1807.01891 \[hep-ex\]](#).
- [631] LHCb collaboration, R. Aaij *et al.*, [arXiv:1807.01892 \[hep-ex\]](#).
- [632] Belle collaboration, A. Das *et al.*, Phys. Rev. **D82**, 051103 (2010), [arXiv:1007.4619 \[hep-ex\]](#).
- [633] *BABAR* collaboration, B. Aubert *et al.*, Phys. Rev. **D78**, 032005 (2008), [arXiv:0803.4296 \[hep-ex\]](#).
- [634] Belle collaboration, N. Joshi *et al.*, Phys. Rev. **D81**, 031101 (2010), [arXiv:0912.2594 \[hep-ex\]](#).
- [635] *BABAR* collaboration, B. Aubert *et al.*, Phys. Rev. **D73**, 071103 (2006), [arXiv:hep-ex/0512031 \[hep-ex\]](#).
- [636] *BABAR* collaboration, B. Aubert *et al.*, Phys. Rev. Lett. **100**, 171803 (2008), [arXiv:0707.1043 \[hep-ex\]](#).
- [637] LHCb collaboration, R. Aaij *et al.*, Phys. Rev. **D84**, 092001 (2011), [arXiv:1109.6831 \[hep-ex\]](#), Erratum *ibid.* **D85**, 039904, (2011).
- [638] LHCb collaboration, R. Aaij *et al.*, Phys. Rev. **D86**, 112005 (2012), [arXiv:1211.1541 \[hep-ex\]](#).
- [639] LHCb collaboration, R. Aaij *et al.*, Phys. Rev. **D87**, 092001 (2013), [arXiv:1303.6861 \[hep-ex\]](#).
- [640] LHCb collaboration, R. Aaij *et al.*, Phys. Rev. **D87**, 112009 (2013), [arXiv:1304.6317 \[hep-ex\]](#).
- [641] LHCb collaboration, R. Aaij *et al.*, Phys. Rev. Lett. **108**, 161801 (2012), [arXiv:1201.4402 \[hep-ex\]](#).
- [642] LHCb collaboration, R. Aaij *et al.*, JHEP **05**, 019 (2015), [arXiv:1412.7654 \[hep-ex\]](#).
- [643] Belle collaboration, K. Abe *et al.*, Phys. Rev. Lett. **94**, 221805 (2005), [arXiv:hep-ex/0410091 \[hep-ex\]](#).
- [644] Belle collaboration, A. Drutskoy *et al.*, Phys. Rev. Lett. **94**, 061802 (2005), [arXiv:hep-ex/0409026 \[hep-ex\]](#).
- [645] *BABAR* collaboration, P. del Amo Sanchez *et al.*, Phys. Rev. **D85**, 092017 (2012), [arXiv:1111.4387 \[hep-ex\]](#).
- [646] Belle collaboration, K. Abe *et al.*, Phys. Rev. Lett. **89**, 151802 (2002), [arXiv:hep-ex/0205083 \[hep-ex\]](#).
- [647] Belle collaboration, T. Medvedeva *et al.*, Phys. Rev. **D76**, 051102 (2007), [arXiv:0704.2652 \[hep-ex\]](#).
- [648] Belle collaboration, Y. W. Chang *et al.*, Phys. Rev. **D79**, 052006 (2009), [arXiv:0811.3826 \[hep-ex\]](#).

- [649] *BABAR* collaboration, J. P. Lees *et al.*, Phys. Rev. **D89**, 112002 (2014), [arXiv:1401.5990 \[hep-ex\]](#).
- [650] *Belle* collaboration, Y. Y. Chang *et al.*, Phys. Rev. Lett. **115**, 221803 (2015), [arXiv:1509.03034 \[hep-ex\]](#).
- [651] *BABAR* collaboration, B. Aubert *et al.*, Phys. Rev. **D73**, 112004 (2006), [arXiv:hep-ex/0604037 \[hep-ex\]](#).
- [652] *Belle* collaboration, I. Adachi *et al.*, Phys. Rev. **D77**, 091101 (2008), [arXiv:0802.2988 \[hep-ex\]](#).
- [653] *BABAR* collaboration, P. del Amo Sanchez *et al.*, Phys. Rev. **D83**, 032004 (2011), [arXiv:1011.3929 \[hep-ex\]](#).
- [654] *Belle* collaboration, G. Gokhroo *et al.*, Phys. Rev. Lett. **97**, 162002 (2006), [arXiv:hep-ex/0606055 \[hep-ex\]](#).
- [655] *Belle* collaboration, A. Zupanc *et al.*, Phys. Rev. **D75**, 091102 (2007), [arXiv:hep-ex/0703040 \[hep-ex\]](#).
- [656] *BABAR* collaboration, B. Aubert *et al.*, Phys. Rev. **D74**, 031103 (2006), [arXiv:hep-ex/0605036 \[hep-ex\]](#).
- [657] *BABAR* collaboration, B. Aubert *et al.*, Phys. Rev. **D67**, 092003 (2003), [arXiv:hep-ex/0302015 \[hep-ex\]](#).
- [658] *BABAR* collaboration, B. Aubert *et al.*, Phys. Rev. **D71**, 091104 (2005), [arXiv:hep-ex/0502041 \[hep-ex\]](#).
- [659] *BABAR* collaboration, B. Aubert *et al.*, Phys. Rev. **D72**, 111101 (2005), [arXiv:hep-ex/0510051 \[hep-ex\]](#).
- [660] LHCb collaboration, R. Aaij *et al.*, Phys. Rev. **D87**, 092007 (2013), [arXiv:1302.5854 \[hep-ex\]](#).
- [661] *Belle* collaboration, P. Krokovny *et al.*, Phys. Rev. Lett. **91**, 262002 (2003), [arXiv:hep-ex/0308019 \[hep-ex\]](#).
- [662] *BABAR* collaboration, B. Aubert *et al.*, Phys. Rev. Lett. **93**, 181801 (2004), [arXiv:hep-ex/0408041 \[hep-ex\]](#).
- [663] *Belle* collaboration, S. K. Choi *et al.*, Phys. Rev. **D91**, 092011 (2015), [arXiv:1504.02637 \[hep-ex\]](#), Addendum *ibid.* **D92**, 039905, (2015).
- [664] *BABAR* collaboration, B. Aubert *et al.*, Phys. Rev. **D77**, 011102 (2008), [arXiv:0708.1565 \[hep-ex\]](#).
- [665] *Belle* collaboration, T. Aushev *et al.*, Phys. Rev. **D83**, 051102 (2011), [arXiv:1102.0935 \[hep-ex\]](#), Erratum *ibid.* **D83**, 051102, (2011).
- [666] CDF collaboration, F. Abe *et al.*, Phys. Rev. Lett. **76**, 2015 (1996).
- [667] *Belle* collaboration, K. Abe *et al.*, Phys. Rev. **D67**, 032003 (2003), [arXiv:hep-ex/0211047 \[hep-ex\]](#).

- [668] Belle collaboration, K. Chilikin *et al.*, Phys. Rev. **D90**, 112009 (2014), [arXiv:1408.6457 \[hep-ex\]](#).
- [669] CDF collaboration, F. Abe *et al.*, Phys. Rev. **D58**, 072001 (1998), [arXiv:hep-ex/9803013 \[hep-ex\]](#).
- [670] LHCb collaboration, R. Aaij *et al.*, JHEP **07**, 140 (2014), [arXiv:1405.3219 \[hep-ex\]](#).
- [671] CDF collaboration, T. Affolder *et al.*, Phys. Rev. Lett. **88**, 071801 (2002), [arXiv:hep-ex/0108022 \[hep-ex\]](#).
- [672] *BABAR* collaboration, P. del Amo Sanchez *et al.*, Phys. Rev. **D82**, 011101 (2010), [arXiv:1005.5190 \[hep-ex\]](#).
- [673] *BABAR* collaboration, B. Aubert *et al.*, Phys. Rev. Lett. **91**, 071801 (2003), [arXiv:hep-ex/0304014 \[hep-ex\]](#).
- [674] Belle collaboration, K. Abe *et al.*, Phys. Rev. Lett. **87**, 161601 (2001), [arXiv:hep-ex/0105014 \[hep-ex\]](#).
- [675] Belle collaboration, T. Iwashita *et al.*, PTEP **2014**, 043C01 (2014), [arXiv:1310.2704 \[hep-ex\]](#).
- [676] *BABAR* collaboration, B. Aubert *et al.*, Phys. Rev. Lett. **93**, 041801 (2004), [arXiv:hep-ex/0402025 \[hep-ex\]](#).
- [677] Belle collaboration, R. Mizuk *et al.*, Phys. Rev. **D80**, 031104 (2009), [arXiv:0905.2869 \[hep-ex\]](#).
- [678] Belle collaboration, V. Bhardwaj *et al.*, Phys. Rev. Lett. **111**, 032001 (2013), [arXiv:1304.3975 \[hep-ex\]](#).
- [679] *BABAR* collaboration, B. Aubert *et al.*, Phys. Rev. Lett. **94**, 171801 (2005), [arXiv:hep-ex/0501061 \[hep-ex\]](#).
- [680] *BABAR* collaboration, B. Aubert *et al.*, Phys. Rev. **D78**, 091101 (2008), [arXiv:0808.1487 \[hep-ex\]](#).
- [681] Belle collaboration, V. Bhardwaj *et al.*, Phys. Rev. Lett. **107**, 091803 (2011), [arXiv:1105.0177 \[hep-ex\]](#).
- [682] *BABAR* collaboration, B. Aubert *et al.*, Phys. Rev. Lett. **102**, 132001 (2009), [arXiv:0809.0042 \[hep-ex\]](#).
- [683] Belle collaboration, V. Bhardwaj *et al.*, Phys. Rev. **D93**, 052016 (2016), [arXiv:1512.02672 \[hep-ex\]](#).
- [684] *BABAR* collaboration, J. P. Lees *et al.*, Phys. Rev. **D85**, 052003 (2012), [arXiv:1111.5919 \[hep-ex\]](#).
- [685] Belle collaboration, N. Soni *et al.*, Phys. Lett. **B634**, 155 (2006), [arXiv:hep-ex/0508032 \[hep-ex\]](#).
- [686] Belle collaboration, F. Fang *et al.*, Phys. Rev. Lett. **90**, 071801 (2003), [arXiv:hep-ex/0208047 \[hep-ex\]](#).

- [687] *BABAR* collaboration, B. Aubert *et al.*, Phys. Rev. **D76**, 092004 (2007), [arXiv:0707.1648 \[hep-ex\]](#).
- [688] *BABAR* collaboration, B. Aubert *et al.*, Phys. Rev. **D70**, 011101 (2004), [arXiv:hep-ex/0403007 \[hep-ex\]](#).
- [689] *BABAR* collaboration, B. Aubert *et al.*, Phys. Rev. **D78**, 012006 (2008), [arXiv:0804.1208 \[hep-ex\]](#).
- [690] LHCb collaboration, R. Aaij *et al.*, Submitted to: Eur. Phys. J. (2018), [arXiv:1809.07416 \[hep-ex\]](#).
- [691] *BABAR* collaboration, B. Aubert *et al.*, Phys. Rev. **D76**, 031101 (2007), [arXiv:0704.1266 \[hep-ex\]](#).
- [692] Belle collaboration, M. Chang *et al.*, Phys. Rev. **D85**, 091102 (2012), [arXiv:1203.3399 \[hep-ex\]](#).
- [693] LHCb collaboration, R. Aaij *et al.*, Phys. Rev. Lett. **112**, 091802 (2014), [arXiv:1310.2145 \[hep-ex\]](#).
- [694] Belle collaboration, R. Kumar *et al.*, Phys. Rev. **D78**, 091104 (2008), [arXiv:0809.1778 \[hep-ex\]](#).
- [695] LHCb collaboration, R. Aaij *et al.*, Phys. Rev. **D88**, 072005 (2013), [arXiv:1308.5916 \[hep-ex\]](#).
- [696] LHCb collaboration, R. Aaij *et al.*, Phys. Rev. **D87**, 052001 (2013), [arXiv:1301.5347 \[hep-ex\]](#).
- [697] Belle collaboration, Y. Liu *et al.*, Phys. Rev. **D78**, 011106 (2008), [arXiv:0805.3225 \[hep-ex\]](#).
- [698] LHCb collaboration, R. Aaij *et al.*, Phys. Rev. **D92**, 112002 (2015), [arXiv:1510.04866 \[hep-ex\]](#).
- [699] *BABAR* collaboration, B. Aubert *et al.*, Phys. Rev. **D70**, 091104 (2004), [arXiv:hep-ex/0408018 \[hep-ex\]](#).
- [700] LHCb collaboration, R. Aaij *et al.*, JHEP **09**, 006 (2013), [arXiv:1306.4489 \[hep-ex\]](#).
- [701] Belle collaboration, Q. Xie *et al.*, Phys. Rev. **D72**, 051105 (2005), [arXiv:hep-ex/0508011 \[hep-ex\]](#).
- [702] *BABAR* collaboration, B. Aubert *et al.*, Phys. Rev. Lett. **90**, 231801 (2003), [arXiv:hep-ex/0303036 \[hep-ex\]](#).
- [703] Belle collaboration, L. Zhang *et al.*, Phys. Rev. **D71**, 091107 (2005), [arXiv:hep-ex/0503037 \[hep-ex\]](#).
- [704] *BABAR* collaboration, B. Aubert *et al.*, Phys. Rev. **D71**, 091103 (2005), [arXiv:hep-ex/0503021 \[hep-ex\]](#).
- [705] CDF collaboration, F. Abe *et al.*, Phys. Rev. **D54**, 6596 (1996), [arXiv:hep-ex/9607003 \[hep-ex\]](#).

- [706] LHCb collaboration, R. Aaij *et al.*, Nucl. Phys. **B867**, 547 (2013), arXiv:1210.2631 [hep-ex].
- [707] LHCb collaboration, R. Aaij *et al.*, Nucl. Phys. **B871**, 403 (2013), arXiv:1302.6354 [hep-ex].
- [708] LHCb collaboration, R. Aaij *et al.*, Eur. Phys. J. **C72**, 2118 (2012), arXiv:1205.0918 [hep-ex].
- [709] LHCb collaboration, R. Aaij *et al.*, JHEP **01**, 024 (2015), arXiv:1411.0943 [hep-ex].
- [710] BABAR collaboration, B. Aubert *et al.*, Phys. Rev. Lett. **93**, 081801 (2004), arXiv:hep-ex/0404005 [hep-ex].
- [711] BABAR collaboration, B. Aubert *et al.*, Phys. Rev. **D82**, 031102 (2010), arXiv:1007.1370 [hep-ex].
- [712] Belle collaboration, N. Gabyshev *et al.*, Phys. Rev. **D66**, 091102 (2002), arXiv:hep-ex/0208041 [hep-ex].
- [713] BABAR collaboration, J. P. Lees *et al.*, Phys. Rev. **D87**, 092004 (2013), arXiv:1302.0191 [hep-ex].
- [714] Belle collaboration, K. Park *et al.*, Phys. Rev. **D75**, 011101 (2007), arXiv:hep-ex/0608025 [hep-ex].
- [715] Belle collaboration, K. Abe *et al.*, Phys. Rev. Lett. **97**, 202003 (2006), arXiv:hep-ex/0508015 [hep-ex].
- [716] BABAR collaboration, B. Aubert *et al.*, Phys. Rev. **D77**, 012002 (2008), arXiv:0710.5763 [hep-ex].
- [717] BABAR collaboration, J. P. Lees *et al.*, Phys. Rev. **D91**, 031102 (2015), arXiv:1410.3644 [hep-ex].
- [718] Belle collaboration, N. Gabyshev *et al.*, Phys. Rev. Lett. **90**, 121802 (2003), arXiv:hep-ex/0212052 [hep-ex].
- [719] BABAR collaboration, B. Aubert *et al.*, Phys. Rev. **D78**, 112003 (2008), arXiv:0807.4974 [hep-ex].
- [720] BABAR collaboration, B. Aubert *et al.*, Phys. Rev. **D80**, 051105 (2009), arXiv:0907.4566 [hep-ex].
- [721] Belle collaboration, R. Chistov *et al.*, Phys. Rev. **D74**, 111105 (2006), arXiv:hep-ex/0510074 [hep-ex].
- [722] Belle collaboration, Y. Uchida *et al.*, Phys. Rev. **D77**, 051101 (2008), arXiv:0708.1105 [hep-ex].
- [723] BABAR collaboration, J. P. Lees *et al.*, Phys. Rev. **D84**, 071102 (2011), arXiv:1108.3211 [hep-ex], Erratum ibid. **D85**, 039903, (2012).
- [724] BABAR collaboration, J. P. Lees *et al.*, Phys. Rev. **D89**, 071102 (2014), arXiv:1312.6800 [hep-ex].

- [725] LHCb collaboration, R. Aaij *et al.*, Phys. Rev. Lett. **112**, 202001 (2014), [arXiv:1403.3606 \[hep-ex\]](#).
- [726] BABAR collaboration, B. Aubert *et al.*, Phys. Rev. **D77**, 111101 (2008), [arXiv:0803.2838 \[hep-ex\]](#).
- [727] Belle collaboration, R. Mizuk *et al.*, Phys. Rev. **D78**, 072004 (2008), [arXiv:0806.4098 \[hep-ex\]](#).
- [728] BABAR collaboration, B. Aubert *et al.*, Phys. Rev. Lett. **96**, 052002 (2006), [arXiv:hep-ex/0510070 \[hep-ex\]](#).
- [729] BABAR collaboration, B. Aubert *et al.*, Phys. Rev. **D71**, 031501 (2005), [arXiv:hep-ex/0412051 \[hep-ex\]](#).
- [730] BABAR collaboration, B. Aubert *et al.*, Phys. Rev. **D79**, 112001 (2009), [arXiv:0811.0564 \[hep-ex\]](#).
- [731] Belle collaboration, M. Iwabuchi *et al.*, Phys. Rev. Lett. **101**, 041601 (2008), [arXiv:0804.0831 \[hep-ex\]](#).
- [732] Belle collaboration, Y. Kato *et al.*, Phys. Rev. **D97**, 012005 (2018), [arXiv:1709.06108 \[hep-ex\]](#).
- [733] Belle collaboration, K. Abe *et al.*, Phys. Rev. **D69**, 112002 (2004), [arXiv:hep-ex/0307021 \[hep-ex\]](#).
- [734] BABAR collaboration, B. Aubert *et al.*, Phys. Rev. **D79**, 112004 (2009), [arXiv:0901.1291 \[hep-ex\]](#).
- [735] BABAR collaboration, B. Aubert *et al.*, [arXiv:hep-ex/0308026 \[hep-ex\]](#) (2003).
- [736] Belle collaboration, S. Swain *et al.*, Phys. Rev. **D68**, 051101 (2003), [arXiv:hep-ex/0304032 \[hep-ex\]](#).
- [737] BABAR collaboration, B. Aubert *et al.*, Phys. Rev. **D73**, 111104 (2006), [arXiv:hep-ex/0604017 \[hep-ex\]](#).
- [738] BABAR collaboration, B. Aubert *et al.*, Phys. Rev. Lett. **92**, 141801 (2004), [arXiv:hep-ex/0308057 \[hep-ex\]](#).
- [739] LHCb collaboration, R. Aaij *et al.*, Phys. Rev. **D91**, 092002 (2015), [arXiv:1503.02995 \[hep-ex\]](#), Erratum *ibid.* **D93**, 119901, (2016).
- [740] BABAR collaboration, P. del Amo Sanchez *et al.*, Phys. Rev. **D82**, 092006 (2010), [arXiv:1005.0068 \[hep-ex\]](#).
- [741] LHCb collaboration, R. Aaij *et al.*, Phys. Rev. **D93**, 051101 (2016), [arXiv:1512.02494 \[hep-ex\]](#), Erratum *ibid.* **D93**, 119902, (2016).
- [742] BABAR collaboration, B. Aubert *et al.*, Phys. Rev. **D72**, 011102 (2005), [arXiv:hep-ex/0505099 \[hep-ex\]](#).
- [743] CDF collaboration, A. Abulencia *et al.*, Phys. Rev. Lett. **96**, 191801 (2006), [arXiv:hep-ex/0508014 \[hep-ex\]](#).

- [744] Belle collaboration, Y. Horii *et al.*, Phys. Rev. **D78**, 071901 (2008), arXiv:0804.2063 [hep-ex].
- [745] BABAR collaboration, B. Aubert *et al.*, Phys. Rev. Lett. **92**, 202002 (2004), arXiv:hep-ex/0311032 [hep-ex].
- [746] BABAR collaboration, B. Aubert *et al.*, Phys. Rev. **D71**, 031102 (2005), arXiv:hep-ex/0411091 [hep-ex].
- [747] LHCb collaboration, R. Aaij *et al.*, Phys. Rev. **D96**, 011101 (2017), arXiv:1704.07581 [hep-ex].
- [748] Belle collaboration, J. Wiechczynski *et al.*, Phys. Rev. **D80**, 052005 (2009), arXiv:0903.4956 [hep-ex].
- [749] BABAR collaboration, B. Aubert *et al.*, Phys. Rev. Lett. **98**, 171801 (2007), arXiv:hep-ex/0611030 [hep-ex].
- [750] LHCb collaboration, R. Aaij *et al.*, JHEP **01**, 131 (2018), arXiv:1711.05637 [hep-ex].
- [751] BABAR collaboration, B. Aubert *et al.*, Phys. Rev. **D73**, 011103 (2006), arXiv:hep-ex/0512028 [hep-ex].
- [752] Belle collaboration, P. Chen *et al.*, Phys. Rev. **D84**, 071501 (2011), arXiv:1108.4271 [hep-ex].
- [753] BELLE collaboration, O. Seon *et al.*, Phys. Rev. **D84**, 071106 (2011), arXiv:1107.0642 [hep-ex].
- [754] Belle collaboration, G. Majumder *et al.*, Phys. Rev. Lett. **95**, 041803 (2005), arXiv:hep-ex/0502038 [hep-ex].
- [755] Belle collaboration, J. Brodzicka *et al.*, Phys. Rev. Lett. **100**, 092001 (2008), arXiv:0707.3491 [hep-ex].
- [756] Belle collaboration, K. Abe *et al.*, Phys. Rev. Lett. **93**, 051803 (2004), arXiv:hep-ex/0307061 [hep-ex].
- [757] Belle collaboration, K. Abe *et al.*, Phys. Lett. **B538**, 11 (2002), arXiv:hep-ex/0205021 [hep-ex].
- [758] CDF collaboration, D. Acosta *et al.*, Phys. Rev. **D66**, 052005 (2002).
- [759] Belle collaboration, H. Guler *et al.*, Phys. Rev. **D83**, 032005 (2011), arXiv:1009.5256 [hep-ex].
- [760] BABAR collaboration, B. Aubert *et al.*, Phys. Rev. **D71**, 071103 (2005), arXiv:hep-ex/0406022 [hep-ex].
- [761] Belle collaboration, K. Abe *et al.*, Phys. Rev. Lett. **88**, 031802 (2002), arXiv:hep-ex/0111069 [hep-ex].
- [762] CMS collaboration, V. Khachatryan *et al.*, Phys. Lett. **B764**, 66 (2017), arXiv:1607.02638 [hep-ex].

- [763] Belle collaboration, A. Vinokurova *et al.*, Phys. Lett. **B706**, 139 (2011), [arXiv:1105.0978 \[hep-ex\]](https://arxiv.org/abs/1105.0978).
- [764] Belle collaboration, C.-H. Wu *et al.*, Phys. Rev. Lett. **97**, 162003 (2006), [arXiv:hep-ex/0606022 \[hep-ex\]](https://arxiv.org/abs/hep-ex/0606022).
- [765] *BABAR* collaboration, B. Aubert *et al.*, Phys. Rev. **D72**, 051101 (2005), [arXiv:hep-ex/0507012 \[hep-ex\]](https://arxiv.org/abs/hep-ex/0507012).
- [766] Belle collaboration, F. Fang *et al.*, Phys. Rev. **D74**, 012007 (2006), [arXiv:hep-ex/0605007 \[hep-ex\]](https://arxiv.org/abs/hep-ex/0605007).
- [767] LHCb collaboration, R. Aaij *et al.*, Phys. Rev. **D85**, 091105 (2012), [arXiv:1203.3592 \[hep-ex\]](https://arxiv.org/abs/1203.3592).
- [768] *BABAR* collaboration, B. Aubert *et al.*, Phys. Rev. Lett. **92**, 241802 (2004), [arXiv:hep-ex/0401035 \[hep-ex\]](https://arxiv.org/abs/hep-ex/0401035).
- [769] *BABAR* collaboration, B. Aubert *et al.*, Phys. Rev. **D72**, 052002 (2005), [arXiv:hep-ex/0507025 \[hep-ex\]](https://arxiv.org/abs/hep-ex/0507025).
- [770] Belle collaboration, R. Kumar *et al.*, Phys. Rev. **D74**, 051103 (2006), [arXiv:hep-ex/0607008 \[hep-ex\]](https://arxiv.org/abs/hep-ex/0607008).
- [771] D0 collaboration, V. Abazov *et al.*, Phys. Rev. **D79**, 111102 (2009), [arXiv:0805.2576 \[hep-ex\]](https://arxiv.org/abs/0805.2576).
- [772] LHCb collaboration, R. Aaij *et al.*, Eur. Phys. J. **C73**, 2462 (2013), [arXiv:1303.7133 \[hep-ex\]](https://arxiv.org/abs/1303.7133).
- [773] CDF collaboration, F. Abe *et al.*, Phys. Rev. Lett. **77**, 5176 (1996).
- [774] CDF collaboration, A. Abulencia, Phys. Rev. **D79**, 112003 (2009), [arXiv:0905.2146 \[hep-ex\]](https://arxiv.org/abs/0905.2146).
- [775] D0 collaboration, V. M. Abazov *et al.*, Phys. Rev. Lett. **110**, 241801 (2013), [arXiv:1304.1655 \[hep-ex\]](https://arxiv.org/abs/1304.1655).
- [776] Belle collaboration, Y. B. Li *et al.*, Eur. Phys. J. **C78**, no. 3, 252 (2018), [arXiv:1712.03612 \[hep-ex\]](https://arxiv.org/abs/1712.03612).
- [777] *BABAR* collaboration, J. P. Lees *et al.*, Phys. Rev. **D86**, 091102 (2012), [arXiv:1208.3086 \[hep-ex\]](https://arxiv.org/abs/1208.3086).
- [778] Belle collaboration, S. K. Choi *et al.*, Phys. Rev. **D84**, 052004 (2011), [arXiv:1107.0163 \[hep-ex\]](https://arxiv.org/abs/1107.0163).
- [779] *BABAR* collaboration, B. Aubert *et al.*, Phys. Rev. **D74**, 071101 (2006), [arXiv:hep-ex/0607050 \[hep-ex\]](https://arxiv.org/abs/hep-ex/0607050).
- [780] *BABAR* collaboration, B. Aubert *et al.*, Phys. Rev. **D73**, 011101 (2006), [arXiv:hep-ex/0507090 \[hep-ex\]](https://arxiv.org/abs/hep-ex/0507090).
- [781] LHCb collaboration, R. Aaij *et al.*, Phys. Rev. Lett. **118**, 022003 (2017), [arXiv:1606.07895 \[hep-ex\]](https://arxiv.org/abs/1606.07895).

- [782] D0 collaboration, V. M. Abazov *et al.*, Phys. Rev. **D89**, 012004 (2014), [arXiv:1309.6580 \[hep-ex\]](#).
- [783] Belle collaboration, T. Aushev *et al.*, Phys. Rev. **D81**, 031103 (2010), [arXiv:0810.0358 \[hep-ex\]](#).
- [784] Belle collaboration, K. Abe *et al.*, Phys. Rev. Lett. **94**, 182002 (2005), [arXiv:hep-ex/0408126 \[hep-ex\]](#).
- [785] LHCb collaboration, R. Aaij *et al.*, JHEP **06**, 115 (2012), [arXiv:1204.1237 \[hep-ex\]](#).
- [786] Belle collaboration, R. Louvot *et al.*, Phys. Rev. Lett. **104**, 231801 (2010), [arXiv:1003.5312 \[hep-ex\]](#).
- [787] LHCb collaboration, R. Aaij *et al.*, JHEP **06**, 130 (2015), [arXiv:1503.09086 \[hep-ex\]](#).
- [788] LHCb collaboration, R. Aaij *et al.*, Phys. Rev. Lett. **116**, 161802 (2016), [arXiv:1603.02408 \[hep-ex\]](#).
- [789] LHCb collaboration, R. Aaij *et al.*, Phys. Lett. **B706**, 32 (2011), [arXiv:1110.3676 \[hep-ex\]](#).
- [790] LHCb collaboration, R. Aaij *et al.*, Phys. Rev. **D87**, 071101 (2013), [arXiv:1302.6446 \[hep-ex\]](#).
- [791] LHCb collaboration, R. Aaij *et al.*, JHEP **08**, 005 (2015), [arXiv:1505.01654 \[hep-ex\]](#).
- [792] CDF collaboration, A. Abulencia *et al.*, Phys. Rev. Lett. **98**, 061802 (2007), [arXiv:hep-ex/0610045 \[hep-ex\]](#).
- [793] LHCb collaboration, R. Aaij *et al.*, Phys. Lett. **B727**, 403 (2013), [arXiv:1308.4583 \[hep-ex\]](#).
- [794] CDF collaboration, T. Aaltonen *et al.*, Phys. Rev. Lett. **103**, 191802 (2009), [arXiv:0809.0080 \[hep-ex\]](#).
- [795] CDF collaboration, T. Aaltonen *et al.*, Phys. Rev. Lett. **108**, 201801 (2012), [arXiv:1204.0536 \[hep-ex\]](#).
- [796] LHCb collaboration, R. Aaij *et al.*, Phys. Rev. **D93**, 092008 (2016), [arXiv:1602.07543 \[hep-ex\]](#).
- [797] Belle collaboration, J. Li *et al.*, Phys. Rev. Lett. **108**, 181808 (2012), [arXiv:1202.0103 \[hep-ex\]](#).
- [798] LHCb collaboration, R. Aaij *et al.*, Phys. Rev. **D87**, 072004 (2013), [arXiv:1302.1213 \[hep-ex\]](#).
- [799] Belle collaboration, F. Thorne *et al.*, Phys. Rev. **D88**, 114006 (2013), [arXiv:1309.0704 \[hep-ex\]](#).
- [800] LHCb collaboration, R. Aaij *et al.*, Phys. Lett. **B713**, 172 (2012), [arXiv:1205.0934 \[hep-ex\]](#).
- [801] CDF collaboration, T. Aaltonen *et al.*, Phys. Rev. **D83**, 052012 (2011), [arXiv:1102.1961 \[hep-ex\]](#).

- [802] LHCb collaboration, R. Aaij *et al.*, JHEP **11**, 082 (2015), [arXiv:1509.00400 \[hep-ex\]](#).
- [803] LHCb collaboration, R. Aaij *et al.*, Phys. Rev. Lett. **108**, 151801 (2012), [arXiv:1112.4695 \[hep-ex\]](#).
- [804] D0 collaboration, V. M. Abazov *et al.*, Phys. Rev. **D86**, 092011 (2012), [arXiv:1204.5723 \[hep-ex\]](#).
- [805] LHCb collaboration, R. Aaij *et al.*, Phys. Lett. **B698**, 115 (2011), [arXiv:1102.0206 \[hep-ex\]](#).
- [806] CDF collaboration, A. Abulencia *et al.*, Phys. Rev. Lett. **96**, 231801 (2006), [arXiv:hep-ex/0602005 \[hep-ex\]](#).
- [807] D0 collaboration, V. M. Abazov *et al.*, Phys. Rev. **D85**, 011103 (2012), [arXiv:1110.4272 \[hep-ex\]](#).
- [808] CMS collaboration, V. Khachatryan *et al.*, Phys. Lett. **B756**, 84 (2016), [arXiv:1501.06089 \[hep-ex\]](#).
- [809] LHCb collaboration, R. Aaij *et al.*, JHEP **08**, 131 (2018), [arXiv:1806.08084 \[hep-ex\]](#).
- [810] LHCb collaboration, R. Aaij *et al.*, JHEP **03**, 040 (2016), [arXiv:1601.05284 \[hep-ex\]](#).
- [811] LHCb collaboration, R. Aaij *et al.*, Phys. Lett. **B747**, 484 (2015), [arXiv:1503.07112 \[hep-ex\]](#).
- [812] LHCb collaboration, R. Aaij *et al.*, Phys. Rev. **D89**, 092006 (2014), [arXiv:1402.6248 \[hep-ex\]](#).
- [813] Belle collaboration, E. Solovieva *et al.*, Phys. Lett. **B726**, 206 (2013), [arXiv:1304.6931 \[hep-ex\]](#).
- [814] LHCb collaboration, R. Aaij *et al.*, Phys. Rev. Lett. **118**, 111803 (2017), [arXiv:1701.01856 \[hep-ex\]](#).
- [815] LHCb collaboration, R. Aaij *et al.*, [arXiv:1712.04702 \[hep-ex\]](#).
- [816] LHCb collaboration, R. Aaij *et al.*, Phys. Rev. **D87**, 112012 (2013), [arXiv:1304.4530 \[hep-ex\]](#).
- [817] ATLAS collaboration, G. Aad *et al.*, Eur. Phys. J. **C76**, 4 (2016), [arXiv:1507.07099 \[hep-ex\]](#).
- [818] LHCb collaboration, R. Aaij *et al.*, Phys. Rev. Lett. **108**, 251802 (2012), [arXiv:1204.0079 \[hep-ex\]](#).
- [819] CMS collaboration, V. Khachatryan *et al.*, JHEP **01**, 063 (2015), [arXiv:1410.5729 \[hep-ex\]](#).
- [820] LHCb collaboration, R. Aaij *et al.*, Phys. Rev. **D95**, 032005 (2017), [arXiv:1612.07421 \[hep-ex\]](#).
- [821] LHCb collaboration, R. Aaij *et al.*, JHEP **09**, 075 (2013), [arXiv:1306.6723 \[hep-ex\]](#).
- [822] LHCb collaboration, R. Aaij *et al.*, JHEP **11**, 094 (2013), [arXiv:1309.0587 \[hep-ex\]](#).

- [823] LHCb collaboration, R. Aaij *et al.*, Phys. Rev. **D92**, 072007 (2015), [arXiv:1507.03516 \[hep-ex\]](#).
- [824] LHCb collaboration, R. Aaij *et al.*, Phys. Rev. Lett. **114**, 132001 (2015), [arXiv:1411.2943 \[hep-ex\]](#).
- [825] LHCb collaboration, R. Aaij *et al.*, Phys. Rev. Lett. **109**, 232001 (2012), [arXiv:1209.5634 \[hep-ex\]](#).
- [826] LHCb collaboration, R. Aaij *et al.*, Phys. Rev. **D94**, 091102 (2016), [arXiv:1607.06134 \[hep-ex\]](#).
- [827] LHCb collaboration, R. Aaij *et al.*, Phys. Rev. Lett. **111**, 181801 (2013), [arXiv:1308.4544 \[hep-ex\]](#).
- [828] LHCb collaboration, R. Aaij *et al.*, Phys. Rev. **D89**, 032001 (2014), [arXiv:1311.4823 \[hep-ex\]](#).
- [829] LHCb collaboration, R. Aaij *et al.*, Chin. Phys. **C40**, 011001 (2016), [arXiv:1509.00292 \[hep-ex\]](#).
- [830] CDF collaboration, F. Abe *et al.*, Phys. Rev. **D55**, 1142 (1997).
- [831] D0 collaboration, V. M. Abazov *et al.*, Phys. Rev. **D84**, 031102 (2011), [arXiv:1105.0690 \[hep-ex\]](#).
- [832] ATLAS collaboration, G. Aad *et al.*, Phys. Lett. **B751**, 63 (2015), [arXiv:1507.08202 \[hep-ex\]](#).
- [833] LHCb collaboration, R. Aaij *et al.*, JHEP **07**, 103 (2014), [arXiv:1406.0755 \[hep-ex\]](#).
- [834] LHCb collaboration, R. Aaij *et al.*, JHEP **05**, 132 (2016), [arXiv:1603.06961 \[hep-ex\]](#).
- [835] LHCb collaboration, R. Aaij *et al.*, Phys. Rev. Lett. **119**, 062001 (2017), [arXiv:1704.07900 \[hep-ex\]](#).
- [836] LHCb collaboration, R. Aaij *et al.*, Phys. Lett. **B724**, 27 (2013), [arXiv:1302.5578 \[hep-ex\]](#).
- [837] CMS collaboration, A. M. Sirunyan *et al.*, Phys. Rev. **D97**, 072010 (2018), [arXiv:1802.04867 \[hep-ex\]](#).
- [838] ATLAS collaboration, G. Aad *et al.*, Phys. Rev. **D89**, 092009 (2014), [arXiv:1404.1071 \[hep-ex\]](#).
- [839] CDF collaboration, T. Aaltonen *et al.*, Phys. Rev. **D85**, 032003 (2012), [arXiv:1112.3334 \[hep-ex\]](#).
- [840] CDF collaboration, A. Abulencia *et al.*, Phys. Rev. Lett. **98**, 122002 (2007), [arXiv:hep-ex/0601003 \[hep-ex\]](#).
- [841] LHCb collaboration, R. Aaij *et al.*, JHEP **05**, 030 (2017), [arXiv:1701.07873 \[hep-ex\]](#).
- [842] LHCb collaboration, R. Aaij *et al.*, Submitted to: Phys. Lett. (2018), [arXiv:1804.09617 \[hep-ex\]](#).
- [843] LHCb collaboration, R. Aaij *et al.*, Phys. Rev. Lett. **115**, 241801 (2015), [arXiv:1510.03829 \[hep-ex\]](#).

- [844] LHCb collaboration, R. Aaij *et al.*, Phys. Rev. Lett. **117**, 082003 (2016), [arXiv:1606.06999 \[hep-ex\]](#), addendum: Phys. Rev. Lett. **118**, 119901 (2017).
- [845] Belle collaboration, Y. T. Duh *et al.*, Phys. Rev. **D87**, 031103 (2013), [arXiv:1210.1348 \[hep-ex\]](#).
- [846] CLEO collaboration, A. Bornheim *et al.*, Phys. Rev. **D68**, 052002 (2003), [arXiv:hep-ex/0302026 \[hep-ex\]](#), Erratum ibid. **D75**, 119907, (2007).
- [847] *BABAR* collaboration, B. Aubert *et al.*, Phys. Rev. **D76**, 091102 (2007), [arXiv:0707.2798 \[hep-ex\]](#).
- [848] *BABAR* collaboration, B. Aubert *et al.*, Phys. Rev. **D80**, 112002 (2009), [arXiv:0907.1743 \[hep-ex\]](#).
- [849] Belle collaboration, J. Schumann *et al.*, Phys. Rev. Lett. **97**, 061802 (2006), [arXiv:hep-ex/0603001 \[hep-ex\]](#).
- [850] *BABAR* collaboration, P. del Amo Sanchez *et al.*, Phys. Rev. **D82**, 011502 (2010), [arXiv:1004.0240 \[hep-ex\]](#).
- [851] Belle collaboration, J. Schumann *et al.*, Phys. Rev. **D75**, 092002 (2007), [arXiv:hep-ex/0701046 \[hep-ex\]](#).
- [852] Belle collaboration, C. T. Hoi *et al.*, Phys. Rev. Lett. **108**, 031801 (2012), [arXiv:1110.2000 \[hep-ex\]](#).
- [853] CLEO collaboration, S. J. Richichi *et al.*, Phys. Rev. Lett. **85**, 520 (2000), [arXiv:hep-ex/9912059 \[hep-ex\]](#).
- [854] *BABAR* collaboration, B. Aubert *et al.*, Phys. Rev. Lett. **97**, 201802 (2006), [arXiv:hep-ex/0608005 \[hep-ex\]](#).
- [855] Belle collaboration, C. H. Wang *et al.*, Phys. Rev. **D75**, 092005 (2007), [arXiv:hep-ex/0701057 \[hep-ex\]](#).
- [856] *BABAR* collaboration, B. Aubert *et al.*, Phys. Rev. Lett. **101**, 091801 (2008), [arXiv:0804.0411 \[hep-ex\]](#).
- [857] *BABAR* collaboration, B. Aubert *et al.*, Phys. Rev. **D76**, 031103 (2007), [arXiv:0706.3893 \[hep-ex\]](#).
- [858] CLEO collaboration, C. P. Jessop *et al.*, Phys. Rev. Lett. **85**, 2881 (2000), [arXiv:hep-ex/0006008 \[hep-ex\]](#).
- [859] *BABAR* collaboration, B. Aubert *et al.*, Phys. Rev. **D79**, 052005 (2009), [arXiv:0901.3703 \[hep-ex\]](#).
- [860] *BABAR* collaboration, B. Aubert *et al.*, Phys. Rev. **D70**, 111102 (2004), [arXiv:hep-ex/0407013 \[hep-ex\]](#).
- [861] *BABAR* collaboration, J. P. Lees *et al.*, Phys. Rev. **D84**, 092007 (2011), [arXiv:1109.0143 \[hep-ex\]](#).
- [862] *BABAR* collaboration, B. Aubert *et al.*, Phys. Rev. **D78**, 091102 (2008), [arXiv:0808.0900 \[hep-ex\]](#).

- [863] Belle collaboration, A. Garmash *et al.*, Phys. Rev. **D69**, 012001 (2004),
arXiv:hep-ex/0307082 [hep-ex].
- [864] LHCb collaboration, R. Aaij *et al.*, Phys. Lett. **B765**, 307 (2017), arXiv:1608.01478
[hep-ex].
- [865] CLEO collaboration, T. Bergfeld *et al.*, Phys. Rev. Lett. **77**, 4503 (1996).
- [866] CLEO collaboration, E. Eckhart *et al.*, Phys. Rev. Lett. **89**, 251801 (2002),
arXiv:hep-ex/0206024 [hep-ex].
- [867] BABAR collaboration, B. Aubert *et al.*, Phys. Rev. **D76**, 011103 (2007),
arXiv:hep-ex/0702043 [hep-ex].
- [868] BABAR collaboration, B. Aubert *et al.*, Phys. Rev. **D74**, 051104 (2006),
arXiv:hep-ex/0607113 [hep-ex].
- [869] BABAR collaboration, P. del Amo Sanchez *et al.*, Phys. Rev. **D83**, 051101 (2011),
arXiv:1012.4044 [hep-ex].
- [870] BABAR collaboration, B. Aubert *et al.*, Phys. Rev. Lett. **100**, 051803 (2008),
arXiv:0709.4165 [hep-ex].
- [871] BABAR collaboration, B. Aubert *et al.*, Phys. Rev. **D78**, 011104 (2008), arXiv:0805.1217
[hep-ex].
- [872] BABAR collaboration, B. Aubert *et al.*, Phys. Rev. Lett. **97**, 201801 (2006),
arXiv:hep-ex/0607057 [hep-ex].
- [873] Belle collaboration, J. Zhang *et al.*, Phys. Rev. Lett. **95**, 141801 (2005),
arXiv:hep-ex/0408102 [hep-ex].
- [874] ARGUS collaboration, H. Albrecht *et al.*, Phys. Lett. **B254**, 288 (1991).
- [875] BABAR collaboration, B. Aubert *et al.*, Phys. Rev. Lett. **99**, 241803 (2007), arXiv:0707.4561
[hep-ex].
- [876] BABAR collaboration, B. Aubert *et al.*, Phys. Rev. **D80**, 051101 (2009), arXiv:0907.3485
[hep-ex].
- [877] LHCb collaboration, R. Aaij *et al.*, Phys. Lett. **B726**, 646 (2013), arXiv:1308.1277
[hep-ex].
- [878] Belle collaboration, A. Abdesselam *et al.*, arXiv:1808.00174 [hep-ex].
- [879] BABAR collaboration, B. Aubert *et al.*, Phys. Rev. **D79**, 051101 (2009), arXiv:0811.1979
[hep-ex].
- [880] BABAR collaboration, B. Aubert *et al.*, Phys. Rev. Lett. **99**, 221801 (2007), arXiv:0708.0376
[hep-ex].
- [881] Belle collaboration, C. L. Hsu *et al.*, Phys. Rev. **D96**, no. 3, 031101 (2017),
arXiv:1705.02640 [hep-ex].
- [882] BABAR collaboration, B. Aubert *et al.*, Phys. Rev. **D76**, 071103 (2007), arXiv:0706.1059
[hep-ex].

- [883] Belle collaboration, H. C. Huang *et al.*, Phys. Rev. Lett. **91**, 241802 (2003), [arXiv:hep-ex/0305068 \[hep-ex\]](#).
- [884] *BABAR* collaboration, B. Aubert *et al.*, Phys. Rev. **D79**, 051102 (2009), [arXiv:0901.1223 \[hep-ex\]](#).
- [885] Belle collaboration, Y. M. Goh *et al.*, Phys. Rev. **D91**, 071101 (2015), [arXiv:1502.00381 \[hep-ex\]](#).
- [886] CLEO collaboration, R. A. Briere *et al.*, Phys. Rev. Lett. **86**, 3718 (2001), [arXiv:hep-ex/0101032 \[hep-ex\]](#).
- [887] CDF collaboration, D. Acosta *et al.*, Phys. Rev. Lett. **95**, 031801 (2005), [arXiv:hep-ex/0502044 \[hep-ex\]](#).
- [888] CDF collaboration, A. Abulencia *et al.*, Phys. Rev. **D73**, 032003 (2006), [arXiv:hep-ex/0510048 \[hep-ex\]](#).
- [889] *BABAR* collaboration, B. Aubert *et al.*, Phys. Rev. Lett. **99**, 201802 (2007), [arXiv:0705.1798 \[hep-ex\]](#).
- [890] Belle collaboration, K. F. Chen *et al.*, Phys. Rev. Lett. **91**, 201801 (2003), [arXiv:hep-ex/0307014 \[hep-ex\]](#).
- [891] *BABAR* collaboration, B. Aubert *et al.*, Phys. Rev. Lett. **101**, 161801 (2008), [arXiv:0806.4419 \[hep-ex\]](#).
- [892] *BABAR* collaboration, P. del Amo Sanchez *et al.*, Phys. Rev. **D82**, 091101 (2010), [arXiv:1007.2732 \[hep-ex\]](#).
- [893] *BABAR* collaboration, J. P. Lees *et al.*, Phys. Rev. **D84**, 012001 (2011), [arXiv:1105.5159 \[hep-ex\]](#).
- [894] *BABAR* collaboration, B. Aubert *et al.*, Phys. Rev. **D74**, 031105 (2006), [arXiv:hep-ex/0605008 \[hep-ex\]](#).
- [895] Belle collaboration, C. Liu *et al.*, Phys. Rev. **D79**, 071102 (2009), [arXiv:0902.4757 \[hep-ex\]](#).
- [896] *BABAR* collaboration, B. Aubert *et al.*, Phys. Rev. **D79**, 072006 (2009), [arXiv:0902.2051 \[hep-ex\]](#).
- [897] Belle collaboration, A. Gordon *et al.*, Phys. Lett. **B542**, 183 (2002), [arXiv:hep-ex/0207007 \[hep-ex\]](#).
- [898] ARGUS collaboration, H. Albrecht *et al.*, Phys. Lett. **B241**, 278 (1990).
- [899] *BABAR* collaboration, B. Aubert *et al.*, Phys. Rev. **D75**, 091103 (2007), [arXiv:hep-ex/0701035 \[hep-ex\]](#).
- [900] Belle collaboration, J. Zhang *et al.*, Phys. Rev. Lett. **94**, 031801 (2005), [arXiv:hep-ex/0406006 \[hep-ex\]](#).
- [901] Belle collaboration, J. Zhang *et al.*, Phys. Rev. Lett. **91**, 221801 (2003), [arXiv:hep-ex/0306007 \[hep-ex\]](#).

- [902] *BABAR* collaboration, B. Aubert *et al.*, Phys. Rev. Lett. **99**, 261801 (2007), arXiv:0708.0050 [hep-ex].
- [903] *Belle* collaboration, C. M. Jen *et al.*, Phys. Rev. **D74**, 111101 (2006), arXiv:hep-ex/0609022 [hep-ex].
- [904] *BABAR* collaboration, B. Aubert *et al.*, Phys. Rev. **D78**, 011107 (2008), arXiv:0804.2422 [hep-ex].
- [905] *BABAR* collaboration, B. Aubert *et al.*, Phys. Rev. **D74**, 011102 (2006), arXiv:hep-ex/0605037 [hep-ex].
- [906] *Belle* collaboration, J. H. Kim *et al.*, Phys. Rev. **D86**, 031101 (2012), arXiv:1206.4760 [hep-ex].
- [907] *LHCb* collaboration, R. Aaij *et al.*, Phys. Lett. **B728**, 85 (2014), arXiv:1309.3742 [hep-ex].
- [908] *BABAR* collaboration, B. Aubert *et al.*, Phys. Rev. Lett. **101**, 201801 (2008), arXiv:0807.3935 [hep-ex].
- [909] *BABAR* collaboration, B. Aubert *et al.*, Phys. Rev. **D77**, 011101 (2008), arXiv:0708.0963 [hep-ex].
- [910] *CLEO* collaboration, D. Bortoletto *et al.*, Phys. Rev. Lett. **62**, 2436 (1989).
- [911] *BABAR* collaboration, B. Aubert *et al.*, Phys. Rev. **D75**, 012008 (2007), arXiv:hep-ex/0608003 [hep-ex].
- [912] *Belle* collaboration, S. Sato *et al.*, Phys. Rev. **D90**, 072009 (2014), arXiv:1408.6343 [hep-ex].
- [913] *BABAR* collaboration, B. Aubert *et al.*, Phys. Rev. **D75**, 111102 (2007), arXiv:hep-ex/0703038 [hep-ex].
- [914] *CLEO* collaboration, R. Ammar *et al.*, Phys. Rev. Lett. **87**, 271801 (2001), arXiv:hep-ex/0106038 [hep-ex].
- [915] *Belle* collaboration, P. Goldenzweig *et al.*, Phys. Rev. Lett. **101**, 231801 (2008), arXiv:0807.4271 [hep-ex].
- [916] *BABAR* collaboration, J. P. Lees *et al.*, Phys. Rev. **D83**, 112010 (2011), arXiv:1105.0125 [hep-ex].
- [917] *Belle* collaboration, P. Chang *et al.*, Phys. Lett. **B599**, 148 (2004), arXiv:hep-ex/0406075 [hep-ex].
- [918] *BABAR* collaboration, B. Aubert *et al.*, Phys. Rev. **D78**, 052005 (2008), arXiv:0711.4417 [hep-ex].
- [919] *Belle* collaboration, A. Garmash *et al.*, Phys. Rev. **D75**, 012006 (2007), arXiv:hep-ex/0610081 [hep-ex].
- [920] *LHCb* collaboration, R. Aaij *et al.*, JHEP **11**, 027 (2017), arXiv:1707.01665 [hep-ex].
- [921] *DELPHI* collaboration, W. Adam *et al.*, Z. Phys. **C72**, 207–220 (1996).

- [922] Belle collaboration, S. H. Kyeong *et al.*, Phys. Rev. **D80**, 051103 (2009), arXiv:0905.0763 [hep-ex].
- [923] BABAR collaboration, B. Aubert *et al.*, Phys. Rev. **D76**, 071104 (2007), arXiv:0708.2543 [hep-ex].
- [924] BABAR collaboration, J. P. Lees *et al.*, Phys. Rev. **D85**, 072005 (2012), arXiv:1112.3896 [hep-ex].
- [925] CDF collaboration, T. Aaltonen *et al.*, Phys. Rev. Lett. **108**, 211803 (2012), arXiv:1111.0485 [hep-ex].
- [926] LHCb collaboration, R. Aaij *et al.*, Phys. Rev. Lett. **118**, 081801 (2017), arXiv:1610.08288 [hep-ex].
- [927] BABAR collaboration, P. del Amo Sanchez *et al.*, Phys. Rev. **D82**, 031101 (2010), arXiv:1003.0640 [hep-ex].
- [928] Belle collaboration, A. Abdesselam *et al.*, arXiv:1807.06782 [hep-ex] (2018).
- [929] LHCb collaboration, R. Aaij *et al.*, New J. Phys. **16**, 123001 (2014), arXiv:1407.7704 [hep-ex].
- [930] BABAR collaboration, B. Aubert *et al.*, Phys. Rev. **D74**, 072008 (2006), arXiv:hep-ex/0606050 [hep-ex].
- [931] LHCb collaboration, R. Aaij *et al.*, JHEP **01**, 012 (2016), arXiv:1506.08634 [hep-ex].
- [932] Belle collaboration, V. Gaur *et al.*, Phys. Rev. **D87**, 091101 (2013), arXiv:1304.5312 [hep-ex].
- [933] BABAR collaboration, B. Aubert *et al.*, Phys. Rev. **D80**, 011101 (2009), arXiv:0905.0868 [hep-ex].
- [934] BABAR collaboration, B. Aubert *et al.*, Phys. Rev. **D74**, 032005 (2006), arXiv:hep-ex/0606031 [hep-ex].
- [935] Belle collaboration, M. Prim *et al.*, Phys. Rev. **D88**, 072004 (2013), arXiv:1308.1830 [hep-ex].
- [936] Belle collaboration, C. C. Chiang *et al.*, Phys. Rev. **D81**, 071101 (2010), arXiv:1001.4595 [hep-ex].
- [937] BABAR collaboration, B. Aubert *et al.*, Phys. Rev. Lett. **100**, 081801 (2008), arXiv:0708.2248 [hep-ex].
- [938] BABAR collaboration, B. Aubert *et al.*, Phys. Rev. **D78**, 051103 (2008), arXiv:0806.4467 [hep-ex].
- [939] BABAR collaboration, B. Aubert *et al.*, Phys. Rev. **D76**, 051103 (2007), arXiv:0705.0398 [hep-ex].
- [940] CDF collaboration, T. Aaltonen *et al.*, Phys. Rev. Lett. **106**, 181802 (2011), arXiv:1103.5762 [hep-ex].
- [941] LHCb collaboration, R. Aaij *et al.*, JHEP **10**, 037 (2012), arXiv:1206.2794 [hep-ex].

- [942] Belle collaboration, B. Pal *et al.*, Phys. Rev. **D92**, 011101 (2015), arXiv:1504.00957 [hep-ex].
- [943] Belle collaboration, A. Abdesselam *et al.*, arXiv:1609.03267 [hep-ex] (2016).
- [944] BABAR collaboration, J. P. Lees *et al.*, Phys. Rev. **D89**, 051101 (2014), arXiv:1312.0056 [hep-ex].
- [945] LHCb collaboration, R. Aaij *et al.*, Phys. Rev. **D95**, 012006 (2017), arXiv:1610.05187 [hep-ex].
- [946] BABAR collaboration, B. Aubert *et al.*, Phys. Rev. Lett. **93**, 051802 (2004), arXiv:hep-ex/0311049 [hep-ex].
- [947] BABAR collaboration, B. Aubert *et al.*, Phys. Rev. Lett. **97**, 051802 (2006), arXiv:hep-ex/0603050 [hep-ex].
- [948] BABAR collaboration, B. Aubert *et al.*, Phys. Rev. **D74**, 031104 (2006), arXiv:hep-ex/0605024 [hep-ex].
- [949] BABAR collaboration, B. Aubert *et al.*, Phys. Rev. **D80**, 092007 (2009), arXiv:0907.1776 [hep-ex].
- [950] Belle collaboration, J. T. Wei *et al.*, Phys. Lett. **B659**, 80 (2008), arXiv:0706.4167 [hep-ex].
- [951] LHCb collaboration, R. Aaij *et al.*, Phys. Rev. Lett. **113**, 141801 (2014), arXiv:1407.5907 [hep-ex].
- [952] Belle collaboration, M. Z. Wang *et al.*, Phys. Lett. **B617**, 141 (2005), arXiv:hep-ex/0503047 [hep-ex].
- [953] Belle collaboration, J. H. Chen *et al.*, Phys. Rev. Lett. **100**, 251801 (2008), arXiv:0802.0336 [hep-ex].
- [954] Belle collaboration, Y. T. Tsai *et al.*, Phys. Rev. **D75**, 111101 (2007), arXiv:hep-ex/0703048 [hep-ex].
- [955] LHCb collaboration, R. Aaij *et al.*, JHEP **04**, 162 (2017), arXiv:1611.07805 [hep-ex].
- [956] Belle collaboration, M. Z. Wang *et al.*, Phys. Rev. **D76**, 052004 (2007), arXiv:0704.2672 [hep-ex].
- [957] Belle collaboration, P. Chen *et al.*, Phys. Rev. **D80**, 111103 (2009), arXiv:0910.5817 [hep-ex].
- [958] Belle collaboration, P. C. Lu *et al.*, Phys. Rev. **D99**, no. 3, 032003 (2019), arXiv:1807.10503 [hep-ex].
- [959] BABAR collaboration, B. Aubert *et al.*, Phys. Rev. **D69**, 091503 (2004), arXiv:hep-ex/0403003 [hep-ex].
- [960] LHCb collaboration, R. Aaij *et al.*, Phys. Rev. Lett. **119**, no. 23, 232001 (2017), arXiv:1709.01156 [hep-ex].

- [961] LHCb collaboration, R. Aaij *et al.*, Phys. Rev. **D96**, no. 5, 051103 (2017), [arXiv:1704.08497 \[hep-ex\]](#).
- [962] BABAR collaboration, B. Aubert *et al.*, Phys. Rev. **D79**, 112009 (2009), [arXiv:0904.4724 \[hep-ex\]](#).
- [963] Belle collaboration, M. Z. Wang *et al.*, Phys. Rev. Lett. **90**, 201802 (2003), [arXiv:hep-ex/0302024 \[hep-ex\]](#).
- [964] BaBar collaboration, J. P. Lees *et al.*, Phys. Rev. **D98**, no. 7, 071102 (2018), [arXiv:1803.10378 \[hep-ex\]](#).
- [965] LHCb collaboration, R. Aaij *et al.*, JHEP **04**, 087 (2014), [arXiv:1402.0770 \[hep-ex\]](#).
- [966] CDF collaboration, T. Aaltonen *et al.*, Phys. Rev. Lett. **103**, 031801 (2009), [arXiv:0812.4271 \[hep-ex\]](#).
- [967] CDF collaboration, T. Aaltonen *et al.*, Phys. Rev. Lett. **107**, 201802 (2011), [arXiv:1107.3753 \[hep-ex\]](#).
- [968] LHCb collaboration, R. Aaij *et al.*, Phys. Lett. **B725**, 25 (2013), [arXiv:1306.2577 \[hep-ex\]](#).
- [969] CDF collaboration, D. Acosta *et al.*, Phys. Rev. **D66**, 112002 (2002), [arXiv:hep-ex/0208035 \[hep-ex\]](#).
- [970] LHCb collaboration, R. Aaij *et al.*, JHEP **09**, 006 (2015), [arXiv:1505.03295 \[hep-ex\]](#).
- [971] LHCb collaboration, R. Aaij *et al.*, JHEP **05**, 081 (2016), [arXiv:1603.00413 \[hep-ex\]](#).
- [972] LHCb collaboration, R. Aaij *et al.*, Phys. Lett. **B759**, 282 (2016), [arXiv:1603.02870 \[hep-ex\]](#).
- [973] LHCb collaboration, R. Aaij *et al.*, JHEP **04**, 029 (2017), [arXiv:1701.08705 \[hep-ex\]](#).
- [974] LHCb collaboration, R. Aaij *et al.*, JHEP **02**, 098 (2018), [arXiv:1711.05490 \[hep-ex\]](#).
- [975] LHCb collaboration, R. Aaij *et al.*, JHEP **06**, 115 (2015), [arXiv:1503.07138 \[hep-ex\]](#).
- [976] LHCb collaboration, R. Aaij *et al.*, Phys. Rev. Lett. **118**, no. 7, 071801 (2017), [arXiv:1612.02244 \[hep-ex\]](#).
- [977] LHCb collaboration, R. Aaij *et al.*, JHEP **09**, 146 (2018), [arXiv:1808.00264 \[hep-ex\]](#).
- [978] LHCb collaboration, R. Aaij *et al.*, Phys. Rev. Lett. **114**, 062004 (2015), [arXiv:1411.4849 \[hep-ex\]](#).
- [979] LHCb collaboration, R. Aaij *et al.*, JHEP **05**, 161 (2016), [arXiv:1604.03896 \[hep-ex\]](#).
- [980] LHCb collaboration, R. Aaij *et al.*, [arXiv:1708.05808 \[hep-ex\]](#) (2017).
- [981] Belle collaboration, C. C. Peng *et al.*, Phys. Rev. **D82**, 072007 (2010), [arXiv:1006.5115 \[hep-ex\]](#).
- [982] LHCb collaboration, R. Aaij *et al.*, Phys. Rev. Lett. **115**, 051801 (2015), [arXiv:1503.07483 \[hep-ex\]](#).

- [983] CDF collaboration, T. Aaltonen *et al.*, Phys. Rev. Lett. **107**, 261802 (2011), [arXiv:1107.4999 \[hep-ex\]](#).
- [984] LHCb collaboration, R. Aaij *et al.*, JHEP **10**, 053 (2015), [arXiv:1508.00788 \[hep-ex\]](#).
- [985] Belle collaboration, B. Pal *et al.*, Phys. Rev. Lett. **116**, 161801 (2016), [arXiv:1512.02145 \[hep-ex\]](#).
- [986] LHCb collaboration, R. Aaij *et al.*, JHEP **07**, 166 (2015), [arXiv:1503.05362 \[hep-ex\]](#).
- [987] LHCb collaboration, R. Aaij *et al.*, JHEP **11**, 092 (2013), [arXiv:1306.2239 \[hep-ex\]](#).
- [988] Belle collaboration, D. Dutta *et al.*, Phys. Rev. **D91**, 011101 (2015), [arXiv:1411.7771 \[hep-ex\]](#).
- [989] LHCb collaboration, R. Aaij *et al.*, Nucl. Phys. **B867**, 1 (2013), [arXiv:1209.0313 \[hep-ex\]](#).
- [990] CDF collaboration, T. Aaltonen *et al.*, Phys. Rev. **D87**, 072003 (2013), [arXiv:1301.7048 \[hep-ex\]](#).
- [991] D0 collaboration, V. M. Abazov *et al.*, Phys. Rev. **D87**, 072006 (2013), [arXiv:1301.4507 \[hep-ex\]](#).
- [992] CMS and LHCb collaborations, V. Khachatryan *et al.*, Nature **522**, 68 (2015), [arXiv:1411.4413 \[hep-ex\]](#).
- [993] ATLAS collaboration, M. Aaboud *et al.*, Submitted to: JHEP (2018), [arXiv:1812.03017 \[hep-ex\]](#).
- [994] CDF collaboration, T. Aaltonen *et al.*, Phys. Rev. Lett. **102**, 201801 (2009), [arXiv:0901.3803 \[hep-ex\]](#).
- [995] LHCb collaboration, R. Aaij *et al.*, Phys. Rev. Lett. **118**, no. 25, 251802 (2017), [arXiv:1703.02508 \[hep-ex\]](#).
- [996] LHCb collaboration, R. Aaij *et al.*, JHEP **03**, 001 (2017), [arXiv:1611.07704 \[hep-ex\]](#).
- [997] D0 collaboration, V. M. Abazov *et al.*, Phys. Rev. **D74**, 031107 (2006), [arXiv:hep-ex/0604015 \[hep-ex\]](#).
- [998] LHCb collaboration, R. Aaij *et al.*, JHEP **09**, 179 (2015), [arXiv:1506.08777 \[hep-ex\]](#).
- [999] LHCb collaboration, R. Aaij *et al.*, Phys. Lett. **B743**, 46 (2015), [arXiv:1412.6433 \[hep-ex\]](#).
- [1000] LHCb collaboration, R. Aaij *et al.*, JHEP **03**, 078 (2018), [arXiv:1710.04111 \[hep-ex\]](#).
- [1001] LHCb collaboration, R. Aaij *et al.*, Phys. Rev. Lett. **119**, no. 4, 041802 (2017), [arXiv:1704.07908 \[hep-ex\]](#).
- [1002] LHCb collaboration, R. Aaij *et al.*, JHEP **05**, 158 (2017), [arXiv:1612.08110 \[hep-ex\]](#).
- [1003] LHCb collaboration, R. Aaij *et al.*, JHEP **07**, 020 (2018), [arXiv:1804.07167 \[hep-ex\]](#).
- [1004] BABAR collaboration, B. Aubert *et al.*, Phys. Rev. Lett. **103**, 211802 (2009), [arXiv:0906.2177 \[hep-ex\]](#).

- [1005] Belle collaboration, T. Horiguchi *et al.*, Phys. Rev. Lett. **119**, no. 19, 191802 (2017), [arXiv:1707.00394 \[hep-ex\]](#).
- [1006] Belle collaboration, H. Yang *et al.*, Phys. Rev. Lett. **94**, 111802 (2005), [arXiv:hep-ex/0412039 \[hep-ex\]](#).
- [1007] Belle collaboration, S. Nishida *et al.*, Phys. Lett. **B610**, 23 (2005), [arXiv:hep-ex/0411065 \[hep-ex\]](#).
- [1008] *BABAR* collaboration, B. Aubert *et al.*, Phys. Rev. **D74**, 031102 (2006), [arXiv:hep-ex/0603054 \[hep-ex\]](#).
- [1009] Belle collaboration, R. Wedd *et al.*, Phys. Rev. **D81**, 111104 (2010), [arXiv:0810.0804 \[hep-ex\]](#).
- [1010] *BABAR* collaboration, B. Aubert *et al.*, Phys. Rev. **D75**, 051102 (2007), [arXiv:hep-ex/0611037 \[hep-ex\]](#).
- [1011] *BABAR* collaboration, B. Aubert *et al.*, Phys. Rev. Lett. **98**, 211804 (2007), [arXiv:hep-ex/0507031 \[hep-ex\]](#), Erratum *ibid.* **100**, 199905, (2008).
- [1012] Belle collaboration, S. Nishida *et al.*, Phys. Rev. Lett. **89**, 231801 (2002), [arXiv:hep-ex/0205025 \[hep-ex\]](#).
- [1013] *BABAR* collaboration, B. Aubert *et al.*, Phys. Rev. **D70**, 091105 (2004), [arXiv:hep-ex/0409035 \[hep-ex\]](#).
- [1014] ARGUS collaboration, H. Albrecht *et al.*, Phys. Lett. **B229**, 304–308 (1989).
- [1015] *BABAR* collaboration, B. Aubert *et al.*, Phys. Rev. **D78**, 112001 (2008), [arXiv:0808.1379 \[hep-ex\]](#).
- [1016] Belle collaboration, N. Taniguchi *et al.*, Phys. Rev. Lett. **101**, 111801 (2008), [arXiv:0804.4770 \[hep-ex\]](#), Erratum *ibid.* **101**, 129904, (2008).
- [1017] Belle collaboration, Y. J. Lee *et al.*, Phys. Rev. Lett. **95**, 061802 (2005), [arXiv:hep-ex/0503046 \[hep-ex\]](#).
- [1018] *BABAR* collaboration, J. P. Lees *et al.*, Phys. Rev. **D88**, 032012 (2013), [arXiv:1303.6010 \[hep-ex\]](#).
- [1019] Belle collaboration, J. T. Wei *et al.*, Phys. Rev. **D78**, 011101 (2008), [arXiv:0804.3656 \[hep-ex\]](#).
- [1020] LHCb collaboration, R. Aaij *et al.*, JHEP **10**, 034 (2015), [arXiv:1509.00414 \[hep-ex\]](#).
- [1021] *BABAR* collaboration, B. Aubert *et al.*, Phys. Rev. Lett. **94**, 101801 (2005), [arXiv:hep-ex/0411061 \[hep-ex\]](#).
- [1022] Belle collaboration, O. Lutz *et al.*, Phys. Rev. **D87**, 111103 (2013), [arXiv:1303.3719 \[hep-ex\]](#).
- [1023] *BABAR* collaboration, B. Aubert *et al.*, Phys. Rev. Lett. **102**, 091803 (2009), [arXiv:0807.4119 \[hep-ex\]](#).

- [1024] Belle collaboration, J. T. Wei *et al.*, Phys. Rev. Lett. **103**, 171801 (2009), arXiv:0904.0770 [hep-ex].
- [1025] LHCb collaboration, R. Aaij *et al.*, JHEP **02**, 105 (2013), arXiv:1209.4284 [hep-ex].
- [1026] BABAR collaboration, J. P. Lees *et al.*, Phys. Rev. Lett. **118**, 031802 (2017), arXiv:1605.09637 [hep-ex].
- [1027] BABAR collaboration, J. P. Lees *et al.*, Phys. Rev. **D87**, 112005 (2013), arXiv:1303.7465 [hep-ex].
- [1028] Belle collaboration, J. Grygier *et al.*, Phys. Rev. **D96**, no. 9, 091101 (2017), arXiv:1702.03224 [hep-ex].
- [1029] LHCb collaboration, R. Aaij *et al.*, JHEP **06**, 133 (2014), arXiv:1403.8044 [hep-ex].
- [1030] LHCb collaboration, R. Aaij *et al.*, JHEP **10**, 064 (2014), arXiv:1408.1137 [hep-ex].
- [1031] BABAR collaboration, (CKM, 2018), <https://indico.cern.ch/event/686555/contributions/2986950/attachments/1680649/2699988/talk.pdf>.
- [1032] Belle collaboration, H. J. Hyun *et al.*, Phys. Rev. Lett. **105**, 091801 (2010), arXiv:1005.1450 [hep-ex].
- [1033] BABAR collaboration, B. Aubert *et al.*, Phys. Rev. **D72**, 091103 (2005), arXiv:hep-ex/0501038 [hep-ex].
- [1034] Belle collaboration, Z. King *et al.*, Phys. Rev. **D93**, 111101 (2016), arXiv:1603.06546 [hep-ex].
- [1035] Belle collaboration, Y. T. Lai *et al.*, Phys. Rev. **D89**, 051103 (2014), arXiv:1312.4228 [hep-ex].
- [1036] LHCb collaboration, R. Aaij *et al.*, JHEP **11**, 047 (2016), arXiv:1606.04731 [hep-ex].
- [1037] LHCb collaboration, R. Aaij *et al.*, Phys. Rev. Lett. **115**, no. 16, 161802 (2015), arXiv:1508.04094 [hep-ex].
- [1038] BABAR collaboration, B. Aubert *et al.*, Phys. Rev. Lett. **99**, 051801 (2007), arXiv:hep-ex/0703018 [hep-ex].
- [1039] BABAR collaboration, B. Aubert *et al.*, Phys. Rev. **D73**, 092001 (2006), arXiv:hep-ex/0604007 [hep-ex].
- [1040] BaBar collaboration, P. del Amo Sanchez *et al.*, Phys. Rev. **D83**, 091101 (2011), arXiv:1101.3830 [hep-ex].
- [1041] CLEO collaboration, T. E. Coan *et al.*, Phys. Rev. Lett. **84**, 5283 (2000), arXiv:hep-ex/9912057 [hep-ex].
- [1042] BABAR collaboration, B. Aubert *et al.*, Phys. Rev. **D77**, 051103 (2008), arXiv:0711.4889 [hep-ex].
- [1043] BABAR collaboration, J. P. Lees *et al.*, Phys. Rev. Lett. **109**, 191801 (2012), arXiv:1207.2690 [hep-ex].

- [1044] *BABAR* collaboration, J. P. Lees *et al.*, Phys. Rev. **D86**, 052012 (2012), [arXiv:1207.2520 \[hep-ex\]](#).
- [1045] *Belle* collaboration, T. Saito *et al.*, Phys. Rev. **D91**, 052004 (2015), [arXiv:1411.7198 \[hep-ex\]](#).
- [1046] *Belle* collaboration, A. Abdesselam *et al.*, [arXiv:1608.02344 \[hep-ex\]](#) (2016).
- [1047] *BABAR* collaboration, P. del Amo Sanchez *et al.*, Phys. Rev. **D82**, 051101 (2010), [arXiv:1005.4087 \[hep-ex\]](#).
- [1048] *BABAR* collaboration, J. P. Lees *et al.*, Phys. Rev. Lett. **112**, 211802 (2014), [arXiv:1312.5364 \[hep-ex\]](#).
- [1049] *Belle* collaboration, M. Iwasaki *et al.*, Phys. Rev. **D72**, 092005 (2005), [arXiv:hep-ex/0503044 \[hep-ex\]](#).
- [1050] *BABAR* collaboration, J. P. Lees *et al.*, Phys. Rev. **D86**, 032012 (2012), [arXiv:1204.3933 \[hep-ex\]](#).
- [1051] CLEO collaboration, K. W. Edwards *et al.*, Phys. Rev. **D65**, 111102 (2002), [arXiv:hep-ex/0204017 \[hep-ex\]](#).
- [1052] O. Buchmuller and H. Flacher, Phys. Rev. **D73**, 073008 (2006), [arXiv:hep-ph/0507253 \[hep-ph\]](#).
- [1053] *BABAR* collaboration, B. Aubert *et al.*, Phys. Rev. **D79**, 091101 (2009), [arXiv:0903.1220 \[hep-ex\]](#).
- [1054] *Belle* collaboration, N. Satoyama *et al.*, Phys. Lett. **B647**, 67 (2007), [arXiv:hep-ex/0611045 \[hep-ex\]](#).
- [1055] *Belle* collaboration, A. Sibidanov *et al.*, [arXiv:1712.04123 \[hep-ex\]](#) (2017).
- [1056] *BABAR* collaboration, J. P. Lees *et al.*, Phys. Rev. **D88**, 031102 (2013), [arXiv:1207.0698 \[hep-ex\]](#).
- [1057] *Belle* collaboration, B. Kronenbitter *et al.*, Phys. Rev. **D92**, 051102 (2015), [arXiv:1503.05613 \[hep-ex\]](#).
- [1058] *BABAR* collaboration, B. Aubert *et al.*, Phys. Rev. **D80**, 111105 (2009), [arXiv:0907.1681 \[hep-ex\]](#).
- [1059] *Belle* collaboration, M. Gelb *et al.*, [arXiv:1810.12976 \[hep-ex\]](#).
- [1060] *Belle* collaboration, A. Heller *et al.*, Phys. Rev. **D91**, 112009 (2015), [arXiv:1504.05831 \[hep-ex\]](#).
- [1061] *BABAR* collaboration, P. del Amo Sanchez *et al.*, Phys. Rev. **D83**, 032006 (2011), [arXiv:1010.2229 \[hep-ex\]](#).
- [1062] *Belle* collaboration, S. Villa *et al.*, Phys. Rev. **D73**, 051107 (2006), [arXiv:hep-ex/0507036 \[hep-ex\]](#).
- [1063] *BABAR* collaboration, B. Aubert *et al.*, Phys. Rev. **D77**, 032007 (2008), [arXiv:0712.1516 \[hep-ex\]](#).

- [1064] Belle collaboration, M. C. Chang *et al.*, Phys. Rev. **D68**, 111101 (2003), arXiv:hep-ex/0309069 [hep-ex].
- [1065] *BABAR* collaboration, B. Aubert *et al.*, Phys. Rev. **D77**, 011104 (2008), arXiv:0706.2870 [hep-ex].
- [1066] CMS collaboration, S. Chatrchyan *et al.*, Phys. Rev. Lett. **111**, 101804 (2013), arXiv:1307.5025 [hep-ex].
- [1067] *BABAR* collaboration, B. Aubert *et al.*, Phys. Rev. Lett. **96**, 241802 (2006), arXiv:hep-ex/0511015 [hep-ex].
- [1068] *BABAR* collaboration, B. Aubert *et al.*, Phys. Rev. **D77**, 091104 (2008), arXiv:0801.0697 [hep-ex].
- [1069] *BABAR* collaboration, J. P. Lees *et al.*, Phys. Rev. **D86**, 051105 (2012), arXiv:1206.2543 [hep-ex].
- [1070] Belle collaboration, C. L. Hsu *et al.*, Phys. Rev. **D86**, 032002 (2012), arXiv:1206.5948 [hep-ex].
- [1071] Belle collaboration, Y. Yook *et al.*, Phys. Rev. **D91**, 052016 (2015), arXiv:1406.6356 [hep-ex].
- [1072] LHCb collaboration, R. Aaij *et al.*, Phys. Rev. Lett. **113**, 151601 (2014), arXiv:1406.6482 [hep-ex].
- [1073] LHCb collaboration, R. Aaij *et al.*, arXiv:1705.05802 [hep-ex] (2017).
- [1074] Belle collaboration, K. Nishimura *et al.*, Phys. Rev. Lett. **105**, 191803 (2010), arXiv:0910.4751 [hep-ex].
- [1075] CLEO collaboration, T. E. Browder *et al.*, Phys. Rev. Lett. **81**, 1786 (1998), arXiv:hep-ex/9804018 [hep-ex].
- [1076] *BABAR* collaboration, B. Aubert *et al.*, Phys. Rev. Lett. **93**, 061801 (2004), arXiv:hep-ex/0401006 [hep-ex].
- [1077] CLEO collaboration, G. Bonvicini *et al.*, Phys. Rev. **D68**, 011101 (2003), arXiv:hep-ex/0303009 [hep-ex].
- [1078] *BABAR* collaboration, P. del Amo Sanchez *et al.*, Phys. Rev. **D83**, 031103 (2011), arXiv:1012.5031 [hep-ex].
- [1079] Belle collaboration, S. Watanuki *et al.*, Phys. Rev. **D99**, no. 3, 032012 (2019), arXiv:1807.04236 [hep-ex].
- [1080] *BABAR* collaboration, J. P. Lees *et al.*, Phys. Rev. **D86**, 012004 (2012), arXiv:1204.2852 [hep-ex].
- [1081] *BABAR* collaboration, J. P. Lees *et al.*, Phys. Rev. **D85**, 071103 (2012), arXiv:1202.3650 [hep-ex].
- [1082] LHCb collaboration, R. Aaij *et al.*, Phys. Rev. Lett. **112**, 131802 (2014), arXiv:1401.5361 [hep-ex].

- [1083] *BABAR* collaboration, J. P. Lees *et al.*, Phys. Rev. **D89**, 011102 (2014), [arXiv:1310.8238 \[hep-ex\]](#).
- [1084] *LHCb* collaboration, R. Aaij *et al.*, Phys. Rev. Lett. **108**, 101601 (2012), [arXiv:1110.0730 \[hep-ex\]](#).
- [1085] *LHCb* collaboration, R. Aaij *et al.*, Phys. Rev. **D85**, 112004 (2012), [arXiv:1201.5600 \[hep-ex\]](#).
- [1086] *Belle* collaboration, S. Sandilya *et al.*, Phys. Rev. **D98**, no. 7, 071101 (2018), [arXiv:1807.03267 \[hep-ex\]](#).
- [1087] *LHCb* collaboration, R. Aaij *et al.*, Phys. Rev. Lett. **112**, 161801 (2014), [arXiv:1402.6852 \[hep-ex\]](#).
- [1088] *LHCb* collaboration, R. Aaij *et al.*, JHEP **05**, 159 (2013), [arXiv:1304.3035 \[hep-ex\]](#).
- [1089] *LHCb* collaboration, R. Aaij *et al.*, JHEP **05**, 082 (2014), [arXiv:1403.8045 \[hep-ex\]](#).
- [1090] *LHCb* collaboration, R. Aaij *et al.*, JHEP **04**, 064 (2015), [arXiv:1501.03038 \[hep-ex\]](#).
- [1091] *Belle* collaboration, A. Abdesselam *et al.*, [arXiv:1604.04042 \[hep-ex\]](#) (2016).
- [1092] *Belle* collaboration, S. Wehle *et al.*, Phys. Rev. Lett. **118**, no. 11, 111801 (2017), [arXiv:1612.05014 \[hep-ex\]](#).
- [1093] *BABAR* collaboration, J. P. Lees *et al.*, Phys. Rev. **D93**, 052015 (2016), [arXiv:1508.07960 \[hep-ex\]](#).
- [1094] *LHCb* collaboration, R. Aaij *et al.*, JHEP **02**, 104 (2016), [arXiv:1512.04442 \[hep-ex\]](#).
- [1095] *CMS* collaboration, V. Khachatryan *et al.*, Phys. Lett. **B753**, 424 (2016), [arXiv:1507.08126 \[hep-ex\]](#).
- [1096] *CMS* collaboration, A. M. Sirunyan *et al.*, Phys. Lett. **B781**, 517 (2018), [arXiv:1710.02846 \[hep-ex\]](#).
- [1097] *ATLAS* collaboration, ATLAS-CONF-2017-023, 2017.
- [1098] *Belle* collaboration, Y. Sato *et al.*, Phys. Rev. **D93**, 032008 (2016), [arXiv:1402.7134 \[hep-ex\]](#), addendum *ibid.* **D93**, 059901, (2016).
- [1099] *LHCb* collaboration, R. Aaij *et al.*, JHEP **12**, 065 (2016), [arXiv:1609.04736 \[hep-ex\]](#).
- [1100] *LHCb* collaboration, R. Aaij *et al.*, Eur. Phys. J. **C77**, no. 3, 161 (2017), [arXiv:1612.06764 \[hep-ex\]](#).
- [1101] *CMS* collaboration, A. M. Sirunyan *et al.*, Phys. Rev. **D98**, no. 11, 112011 (2018), [arXiv:1806.00636 \[hep-ex\]](#).
- [1102] *LHCb* collaboration, R. Aaij *et al.*, Phys. Rev. **D95**, no. 7, 071101 (2017), [arXiv:1612.07818 \[hep-ex\]](#).
- [1103] *Belle* collaboration, L. Pesáñez *et al.*, Phys. Rev. Lett. **114**, 151601 (2015), [arXiv:1501.01702 \[hep-ex\]](#).

- [1104] LHCb collaboration, R. Aaij *et al.*, Phys. Rev. **D90**, 112004 (2014), arXiv:1408.5373 [hep-ex].
- [1105] Belle collaboration, K. F. Chen *et al.*, Phys. Rev. Lett. **94**, 221804 (2005), arXiv:hep-ex/0503013 [hep-ex].
- [1106] LHCb collaboration, R. Aaij *et al.*, JHEP **09**, 177 (2014), arXiv:1408.0978 [hep-ex].
- [1107] CDF collaboration, T. A. Aaltonen *et al.*, Phys. Rev. Lett. **113**, 242001 (2014), arXiv:1403.5586 [hep-ex].
- [1108] LHCb collaboration, R. Aaij *et al.*, Phys. Rev. Lett. **120**, no. 26, 261801 (2018), arXiv:1712.09320 [hep-ex].
- [1109] LHCb collaboration, R. Aaij *et al.*, JHEP **05**, 069 (2014), arXiv:1403.2888 [hep-ex].
- [1110] BABAR collaboration, J. P. Lees *et al.*, Phys. Rev. **D90**, 092001 (2014), arXiv:1406.0534 [hep-ex].
- [1111] Belle collaboration, S. Nishida *et al.*, Phys. Rev. Lett. **93**, 031803 (2004), arXiv:hep-ex/0308038 [hep-ex].
- [1112] LHCb collaboration, R. Aaij *et al.*, Phys. Lett. **B787**, 124–133 (2018), arXiv:1807.06544 [hep-ex].
- [1113] LHCb collaboration, R. Aaij *et al.*, JHEP **06**, 108 (2017), arXiv:1703.00256 [hep-ex].
- [1114] LHCb collaboration, R. Aaij *et al.*, Nature Phys. **13**, 391 (2017), arXiv:1609.05216 [hep-ex].
- [1115] LHCb collaboration, R. Aaij *et al.*, arXiv:1805.03941 [hep-ex].
- [1116] LHCb collaboration, R. Aaij *et al.*, JHEP **03**, 140 (2018), arXiv:1712.08683 [hep-ex].
- [1117] LHCb collaboration, LHCb-CONF-2018-001, 2018.
- [1118] LHCb collaboration, R. Aaij *et al.*, Phys. Lett. **B759**, 313 (2016), arXiv:1603.07037 [hep-ex].
- [1119] Belle collaboration, M. Staric *et al.*, Phys. Rev. Lett. **98**, 211803 (2007), arXiv:hep-ex/0703036.
- [1120] BABAR collaboration, B. Aubert *et al.*, Phys. Rev. Lett. **98**, 211802 (2007), arXiv:hep-ex/0703020.
- [1121] CDF collaboration, T. Aaltonen *et al.*, Phys. Rev. Lett. **100**, 121802 (2008), arXiv:0712.1567 [hep-ex].
- [1122] LHCb collaboration, R. Aaij *et al.*, Phys. Rev. Lett. **111**, 251801 (2013), arXiv:1309.6534 [hep-ex].
- [1123] S. Bergmann, Y. Grossman, Z. Ligeti, Y. Nir, and A. A. Petrov, Phys. Lett. **B486**, 418 (2000), arXiv:hep-ph/0005181 [hep-ph].
- [1124] I. I. Y. Bigi and N. G. Uraltsev, Nucl. Phys. **B592**, 92 (2001), arXiv:hep-ph/0005089.
- [1125] A. A. Petrov, arXiv:hep-ph/0311371 (2003).

- [1126] A. A. Petrov, Nucl. Phys. Proc. Suppl. **142**, 333 (2005), [arXiv:hep-ph/0409130](https://arxiv.org/abs/hep-ph/0409130).
- [1127] A. F. Falk, Y. Grossman, Z. Ligeti, Y. Nir, and A. A. Petrov, Phys. Rev. **D69**, 114021 (2004), [arXiv:hep-ph/0402204](https://arxiv.org/abs/hep-ph/0402204).
- [1128] CLEO collaboration, D. Asner *et al.*, Phys. Rev. **D86**, 112001 (2012), [arXiv:1210.0939 \[hep-ex\]](https://arxiv.org/abs/1210.0939).
- [1129] LHCb collaboration, R. Aaij *et al.*, JHEP **07**, 041 (2014), [arXiv:1405.2797 \[hep-ex\]](https://arxiv.org/abs/1405.2797).
- [1130] BABAR collaboration, B. Aubert *et al.*, Phys. Rev. Lett. **103**, 211801 (2009), [arXiv:0807.4544 \[hep-ex\]](https://arxiv.org/abs/0807.4544).
- [1131] Documentation available at, 1999,
<http://www.slac.stanford.edu/xorg/hflav/docs/combos.ps>.
- [1132] LHCb collaboration, R. Aaij *et al.*, Phys. Rev. Lett. **116**, 241801 (2016), [arXiv:1602.07224 \[hep-ex\]](https://arxiv.org/abs/1602.07224).
- [1133] Fermilab E791 collaboration, E. M. Aitala *et al.*, Phys. Rev. Lett. **77**, 2384 (1996), [arXiv:hep-ex/9606016](https://arxiv.org/abs/hep-ex/9606016).
- [1134] CLEO collaboration, C. Cawfield *et al.*, Phys. Rev. **D71**, 077101 (2005), [arXiv:hep-ex/0502012](https://arxiv.org/abs/hep-ex/0502012).
- [1135] BABAR collaboration, B. Aubert *et al.*, Phys. Rev. **D76**, 014018 (2007), [arXiv:0705.0704 \[hep-ex\]](https://arxiv.org/abs/0705.0704).
- [1136] Belle collaboration, U. Bitenc *et al.*, Phys. Rev. **D77**, 112003 (2008), [arXiv:0802.2952 \[hep-ex\]](https://arxiv.org/abs/0802.2952).
- [1137] Belle collaboration, L. M. Zhang *et al.*, Phys. Rev. Lett. **96**, 151801 (2006), [arXiv:hep-ex/0601029](https://arxiv.org/abs/hep-ex/0601029).
- [1138] Belle collaboration, B. R. Ko *et al.*, Phys. Rev. Lett. **112**, 111801 (2014), [arXiv:1401.3402 \[hep-ex\]](https://arxiv.org/abs/1401.3402).
- [1139] CDF collaboration, T. A. Aaltonen *et al.*, Phys. Rev. Lett. **111**, 231802 (2013), [arXiv:1309.4078 \[hep-ex\]](https://arxiv.org/abs/1309.4078).
- [1140] LHCb collaboration, R. Aaij *et al.*, Phys. Rev. **D97**, no. 3, 031101 (2018), [arXiv:1712.03220 \[hep-ex\]](https://arxiv.org/abs/1712.03220).
- [1141] Belle collaboration, T. Peng *et al.*, Phys. Rev. **D89**, 091103 (2014), [arXiv:1404.2412 \[hep-ex\]](https://arxiv.org/abs/1404.2412).
- [1142] BABAR collaboration, P. del Amo Sanchez *et al.*, Phys. Rev. Lett. **105**, 081803 (2010), [arXiv:1004.5053 \[hep-ex\]](https://arxiv.org/abs/1004.5053).
- [1143] LHCb collaboration, R. Aaij *et al.*, JHEP **04**, 033 (2016), [arXiv:1510.01664 \[hep-ex\]](https://arxiv.org/abs/1510.01664).
- [1144] LHCb collaboration, R. Aaij *et al.*, Submitted to: Phys. Rev. Lett. (2019), [arXiv:1903.03074 \[hep-ex\]](https://arxiv.org/abs/1903.03074).
- [1145] BABAR collaboration, J. P. Lees *et al.*, Phys. Rev. **D93**, 112014 (2016), [arXiv:1604.00857 \[hep-ex\]](https://arxiv.org/abs/1604.00857).

- [1146] A. Di Canto, J. Garra Ticó, T. Gershon, N. Jurik, M. Martinelli, T. Pilař, S. Stahl, and D. Tonelli, Phys. Rev. **D99**, 012007 (2019), [arXiv:1811.01032 \[hep-ex\]](https://arxiv.org/abs/1811.01032).
- [1147] *BABAR* collaboration, B. Aubert *et al.*, Phys. Rev. Lett. **100**, 061803 (2008), [arXiv:0709.2715 \[hep-ex\]](https://arxiv.org/abs/0709.2715).
- [1148] CDF collaboration, CDF note 10784, 2012,
<http://www-cdf.fnal.gov/physics/new/bottom/120216.blessed-CPVcharm10fb/>.
- [1149] CDF collaboration, T. Aaltonen *et al.*, Phys. Rev. Lett. **109**, 111801 (2012), [arXiv:1207.2158 \[hep-ex\]](https://arxiv.org/abs/1207.2158).
- [1150] LHCb collaboration, R. Aaij *et al.*, [arXiv:1903.08726 \[hep-ex\]](https://arxiv.org/abs/1903.08726).
- [1151] Fermilab E791 collaboration, E. M. Aitala *et al.*, Phys. Rev. Lett. **83**, 32 (1999), [arXiv:hep-ex/9903012](https://arxiv.org/abs/hep-ex/9903012).
- [1152] FOCUS collaboration, J. M. Link *et al.*, Phys. Lett. **B485**, 62 (2000), [arXiv:hep-ex/0004034](https://arxiv.org/abs/hep-ex/0004034).
- [1153] CLEO collaboration, S. E. Csorna *et al.*, Phys. Rev. **D65**, 092001 (2002), [arXiv:hep-ex/0111024](https://arxiv.org/abs/hep-ex/0111024).
- [1154] Belle collaboration, A. Zupanc *et al.*, Phys. Rev. **D80**, 052006 (2009), [arXiv:0905.4185 \[hep-ex\]](https://arxiv.org/abs/0905.4185).
- [1155] *BABAR* collaboration, J. P. Lees *et al.*, Phys. Rev. **D87**, 012004 (2013), [arXiv:1209.3896 \[hep-ex\]](https://arxiv.org/abs/1209.3896).
- [1156] BESIII collaboration, M. Ablikim *et al.*, Phys. Lett. **B744**, 339 (2015), [arXiv:1501.01378 \[hep-ex\]](https://arxiv.org/abs/1501.01378).
- [1157] Belle collaboration, M. Staric *et al.*, Phys. Lett. **B753**, 412–418 (2016), [arXiv:1509.08266 \[hep-ex\]](https://arxiv.org/abs/1509.08266).
- [1158] LHCb collaboration, R. Aaij *et al.*, Phys. Rev. Lett. **122**, no. 1, 011802 (2019), [arXiv:1810.06874 \[hep-ex\]](https://arxiv.org/abs/1810.06874).
- [1159] CDF collaboration, T. A. Aaltonen *et al.*, Phys. Rev. **D90**, 111103 (2014), [arXiv:1410.5435 \[hep-ex\]](https://arxiv.org/abs/1410.5435).
- [1160] LHCb collaboration, R. Aaij *et al.*, JHEP **04**, 043 (2015), [arXiv:1501.06777 \[hep-ex\]](https://arxiv.org/abs/1501.06777).
- [1161] LHCb collaboration, R. Aaij *et al.*, Phys. Rev. Lett. **118**, 261803 (2017), [arXiv:1702.06490 \[hep-ex\]](https://arxiv.org/abs/1702.06490).
- [1162] CERN Program Library Long Writeup D506, 1994,
<http://wwwasdoc.web.cern.ch/wwwasdoc/minuit/minmain.html>.
- [1163] Y. Grossman, Y. Nir, and G. Perez, Phys. Rev. Lett. **103**, 071602 (2009), [arXiv:0904.0305 \[hep-ph\]](https://arxiv.org/abs/0904.0305).
- [1164] A. L. Kagan and M. D. Sokoloff, Phys. Rev. **D80**, 076008 (2009), [arXiv:0907.3917 \[hep-ph\]](https://arxiv.org/abs/0907.3917).
- [1165] M. Ciuchini *et al.*, Phys. Lett. **B655**, 162 (2007), [arXiv:hep-ph/0703204 \[hep-ph\]](https://arxiv.org/abs/hep-ph/0703204).

- [1166] I. I. Y. Bigi and A. I. Sanda, Camb. Monogr. Part. Phys. Nucl. Phys. Cosmol. **9**, 1 (2000).
- [1167] Y. Nir, arXiv:hep-ph/9911321 (1999).
- [1168] F. Buccella, M. Lusignoli, G. Miele, A. Pugliese, and P. Santorelli, Phys. Rev. **D51**, 3478 (1995), arXiv:hep-ph/9411286.
- [1169] Y. Grossman and Y. Nir, JHEP **04**, 002 (2012), arXiv:1110.3790 [hep-ph].
- [1170] LHCb collaboration, R. Aaij *et al.*, JHEP **03**, 182 (2018), arXiv:1712.07051 [hep-ex].
- [1171] J. Brod, Y. Grossman, A. L. Kagan, and J. Zupan, JHEP **10**, 161 (2012), arXiv:1203.6659 [hep-ph].
- [1172] I. Bediaga, I. I. Bigi, A. Gomes, G. Guerrer, J. Miranda, and A. C. d. Reis, Phys. Rev. **D80**, 096006 (2009), arXiv:0905.4233 [hep-ph].
- [1173] B. Aslan and G. Zech, Journal of Statistical Computation and Simulation **75**, 109 (2005).
- [1174] LHCb collaboration, R. Aaij *et al.*, Phys. Lett. **B726**, 623 (2013), arXiv:1308.3189 [hep-ex].
- [1175] LHCb collaboration, R. Aaij *et al.*, JHEP **02**, 126 (2019), arXiv:1811.08304 [hep-ex].
- [1176] CLEO collaboration, J. W. Hinson *et al.*, Phys. Rev. Lett. **94**, 191801 (2005), arXiv:hep-ex/0501002 [hep-ex].
- [1177] FOCUS collaboration, J. M. Link *et al.*, Phys. Lett. **B634**, 165 (2006), arXiv:hep-ex/0509042 [hep-ex].
- [1178] Y. Grossman, A. L. Kagan, and J. Zupan, Phys. Rev. **D85**, 114036 (2012), arXiv:1204.3557 [hep-ph].
- [1179] Belle collaboration, V. Babu *et al.*, Phys. Rev. **D97**, 011101 (2018), arXiv:1712.00619 [hep-ex].
- [1180] CLEO collaboration, B. I. Eisenstein *et al.*, Phys. Rev. **D78**, 052003 (2008), arXiv:0806.2112 [hep-ex].
- [1181] CLEO collaboration, H. Mendez *et al.*, Phys. Rev. **D81**, 052013 (2010), arXiv:0906.3198 [hep-ex].
- [1182] Belle collaboration, E. Won *et al.*, Phys. Rev. Lett. **107**, 221801 (2011), arXiv:1107.0553 [hep-ex].
- [1183] LHCb collaboration, R. Aaij *et al.*, Phys. Lett. **B771**, 21 (2017), arXiv:1701.01871 [hep-ex].
- [1184] CLEO collaboration, G. Bonvicini *et al.*, Phys. Rev. **D89**, 072002 (2014), arXiv:1312.6775 [hep-ex].
- [1185] Belle collaboration, B. R. Ko *et al.*, Phys. Rev. Lett. **109**, 021601 (2012), arXiv:1203.6409 [hep-ex].
- [1186] BABAR collaboration, P. del Amo Sanchez *et al.*, Phys. Rev. **D83**, 071103 (2011), arXiv:1011.5477 [hep-ex].

- [1187] FOCUS collaboration, J. M. Link *et al.*, Phys. Rev. Lett. **88**, 041602; 159903(E) (2002), [arXiv:hep-ex/0109022](#).
- [1188] BABAR collaboration, J. P. Lees *et al.*, Phys. Rev. **D87**, 052012 (2013), [arXiv:1212.3003 \[hep-ex\]](#).
- [1189] Belle collaboration, B. R. Ko *et al.*, JHEP **02**, 098 (2013), [arXiv:1212.6112 \[hep-ex\]](#).
- [1190] LHCb collaboration, R. Aaij *et al.*, JHEP **10**, 25 (2014), [arXiv:1406.2624 \[hep-ex\]](#).
- [1191] LHCb collaboration, R. Aaij *et al.*, Phys. Lett. **B728**, 585 (2014), [arXiv:1310.7953 \[hep-ex\]](#).
- [1192] Fermilab E791 collaboration, E. M. Aitala *et al.*, Phys. Lett. **B403**, 377 (1997), [arXiv:hep-ex/9612005](#).
- [1193] D0 collaboration, V. M. Abazov *et al.*, Phys. Rev. **D90**, 111102 (2014), [arXiv:1408.6848 \[hep-ex\]](#).
- [1194] BABAR collaboration, J. P. Lees *et al.*, Phys. Rev. **D87**, 052010 (2013), [arXiv:1212.1856 \[hep-ex\]](#).
- [1195] CLEO collaboration, P. Rubin *et al.*, Phys. Rev. **D78**, 072003 (2008), [arXiv:0807.4545 \[hep-ex\]](#).
- [1196] FOCUS collaboration, J. M. Link *et al.*, Phys. Lett. **B491**, 232 (2000), [arXiv:hep-ex/0005037](#).
- [1197] FOCUS collaboration, J. M. Link *et al.*, Phys. Lett. **B622**, 239 (2005), [arXiv:hep-ex/0506012](#).
- [1198] LHCb collaboration, R. Aaij *et al.*, Phys. Lett. **B767**, 177–187 (2017), [arXiv:1610.09476 \[hep-ex\]](#).
- [1199] CDF collaboration, T. Aaltonen *et al.*, Phys. Rev. **D85**, 012009 (2012), [arXiv:1111.5023 \[hep-ex\]](#).
- [1200] Belle collaboration, M. Staric *et al.*, Phys. Lett. **B670**, 190 (2008), [arXiv:0807.0148 \[hep-ex\]](#).
- [1201] Fermilab E791 collaboration, E. M. Aitala *et al.*, Phys. Lett. **B421**, 405 (1998), [arXiv:hep-ex/9711003](#).
- [1202] Belle collaboration, N. K. Nisar *et al.*, Phys. Rev. Lett. **112**, 211601 (2014), [arXiv:1404.1266 \[hep-ex\]](#).
- [1203] CLEO collaboration, G. Bonvicini *et al.*, Phys. Rev. **D63**, 071101 (2001), [arXiv:hep-ex/0012054](#).
- [1204] Belle collaboration, B. R. Ko *et al.*, Phys. Rev. Lett. **106**, 211801 (2011), [arXiv:1101.3365 \[hep-ex\]](#).
- [1205] LHCb collaboration, R. Aaij *et al.*, JHEP **11**, 048 (2018), [arXiv:1806.01642 \[hep-ex\]](#).
- [1206] N. Dash *et al.*, Phys. Rev. Lett. **119**, no. 17, 171801 (2017), [arXiv:1705.05966 \[hep-ex\]](#).

- [1207] Belle collaboration, J. B. Kim *et al.*, [arXiv:1810.06457 \[hep-ex\]](#).
- [1208] LHCb collaboration, R. Aaij *et al.*, Phys. Lett. **B740**, 158 (2015), [arXiv:1410.4170 \[hep-ex\]](#).
- [1209] BABAR collaboration, B. Aubert *et al.*, Phys. Rev. **D78**, 051102 (2008), [arXiv:0802.4035 \[hep-ex\]](#).
- [1210] Belle collaboration, K. Arinstein, Phys. Lett. **B662**, 102 (2008), [arXiv:0801.2439 \[hep-ex\]](#).
- [1211] CLEO collaboration, D. Cronin-Hennessy *et al.*, Phys. Rev. **D72**, 031102 (2005), [arXiv:hep-ex/0503052](#).
- [1212] Belle collaboration, X. C. Tian *et al.*, Phys. Rev. Lett. **95**, 231801 (2005), [arXiv:hep-ex/0507071](#).
- [1213] CLEO collaboration, G. Brandenburg *et al.*, Phys. Rev. Lett. **87**, 071802 (2001), [arXiv:hep-ex/0105002](#).
- [1214] CDF collaboration, T. Aaltonen *et al.*, Phys. Rev. **D86**, 032007 (2012), [arXiv:1207.0825 \[hep-ex\]](#).
- [1215] CLEO collaboration, D. M. Asner *et al.*, Phys. Rev. **D70**, 091101 (2004), [arXiv:hep-ex/0311033](#).
- [1216] CLEO collaboration, M. Artuso *et al.*, Phys. Rev. **D85**, 122002 (2012), [arXiv:1201.5716 \[hep-ex\]](#).
- [1217] Belle collaboration, A. Abdesselam *et al.*, Phys. Rev. Lett. **118**, no. 5, 051801 (2017), [arXiv:1603.03257 \[hep-ex\]](#).
- [1218] LHCb collaboration, R. Aaij *et al.*, Phys. Rev. Lett. **121**, no. 9, 091801 (2018), [arXiv:1806.10793 \[hep-ex\]](#).
- [1219] CLEO collaboration, J. Alexander *et al.*, Phys. Rev. **D79**, 052001 (2009), [arXiv:0901.1216 \[hep-ex\]](#).
- [1220] CLEO collaboration, P. Onyisi *et al.*, Phys. Rev. **D88**, 032009 (2013), [arXiv:1306.5363 \[hep-ex\]](#).
- [1221] Belle collaboration, B. R. Ko *et al.*, Phys. Rev. Lett. **104**, 181602 (2010), [arXiv:1001.3202 \[hep-ex\]](#).
- [1222] E. Golowich and G. Valencia, Phys. Rev. **D40**, 112 (1989).
- [1223] I. I. Y. Bigi, [arXiv:hep-ph/0107102](#) (2001).
- [1224] W. Bensalem, A. Datta, and D. London, Phys. Rev. **D66**, 094004 (2002), [arXiv:hep-ph/0208054](#).
- [1225] W. Bensalem and D. London, Phys. Rev. **D64**, 116003 (2001), [arXiv:hep-ph/0005018](#).
- [1226] W. Bensalem, A. Datta, and D. London, Phys. Lett. **B538**, 309 (2002), [arXiv:hep-ph/0205009](#).
- [1227] M. Gronau and J. L. Rosner, Phys. Rev. **D84**, 096013 (2011), [arXiv:1107.1232 \[hep-ph\]](#).

- [1228] LHCb collaboration, R. Aaij *et al.*, JHEP **10**, 005 (2014), [arXiv:1408.1299 \[hep-ex\]](#).
- [1229] BABAR collaboration, P. del Amo Sanchez *et al.*, Phys. Rev. **D81**, 111103 (2010), [arXiv:1003.3397 \[hep-ex\]](#).
- [1230] Belle collaboration, K. Prasanth *et al.*, Phys. Rev. **D95**, no. 9, 091101 (2017), [arXiv:1703.05721 \[hep-ex\]](#).
- [1231] BABAR collaboration, J. P. Lees *et al.*, Phys. Rev. **D84**, 031103 (2011), [arXiv:1105.4410 \[hep-ex\]](#).
- [1232] LHCb collaboration, R. Aaij *et al.*, Eur. Phys. J. **C78**, no. 6, 443 (2018), [arXiv:1712.08609 \[hep-ex\]](#).
- [1233] A. J. Bevan, [arXiv:1506.04246 \[hep-ex\]](#) (2015).
- [1234] G. Durieux and Y. Grossman, Phys. Rev. **D92**, 076013 (2015), [arXiv:1508.03054 \[hep-ph\]](#).
- [1235] Y. Grossman, A. L. Kagan, and Y. Nir, Phys. Rev. **D75**, 036008 (2007), [arXiv:hep-ph/0609178 \[hep-ph\]](#).
- [1236] M. Gersabeck, M. Alexander, S. Borghi, V. Gligorov, and C. Parkes, J. Phys. **G39**, 045005 (2012), [arXiv:1111.6515 \[hep-ex\]](#).
- [1237] LHCb collaboration, R. Aaij *et al.*, Phys. Rev. Lett. **116**, 191601 (2016), [arXiv:1602.03160 \[hep-ex\]](#).
- [1238] T. Becher and R. J. Hill, Phys. Lett. **B633**, 61 (2006), [arXiv:hep-ph/0509090 \[hep-ph\]](#).
- [1239] F. J. Gilman and R. L. Singleton, Phys. Rev. **D41**, 142 (1990).
- [1240] R. J. Hill, eConf **C060409**, 027 (2006), [arXiv:hep-ph/0606023 \[hep-ph\]](#) (2006).
- [1241] D. Becirevic and A. B. Kaidalov, Phys. Lett. **B478**, 417 (2000), [arXiv:hep-ph/9904490 \[hep-ph\]](#).
- [1242] C. G. Boyd, B. Grinstein, and R. F. Lebed, Phys. Rev. Lett. **74**, 4603 (1995), [arXiv:hep-ph/9412324 \[hep-ph\]](#).
- [1243] C. G. Boyd and M. J. Savage, Phys. Rev. **D56**, 303 (1997), [arXiv:hep-ph/9702300 \[hep-ph\]](#).
- [1244] M. C. Arnesen, B. Grinstein, I. Z. Rothstein, and I. W. Stewart, Phys. Rev. Lett. **95**, 071802 (2005).
- [1245] C. Bourrely, B. Machet, and E. de Rafael, Nucl. Phys. **B189**, 157 (1981).
- [1246] D. Becirevic, A. L. Yaouanc, A. Oyanguren, P. Roudeau, and F. Sanfilippo, [arXiv:1407.1019 \[hep-ph\]](#) (2014).
- [1247] BABAR collaboration, J. P. Lees *et al.*, Phys. Rev. **D88**, 052003 (2013), [arXiv:1304.5009 \[hep-ex\]](#), Erratum ibid. **D88**, 079902, (2013).
- [1248] BABAR collaboration, P. del Amo Sanchez *et al.*, Phys. Rev. **D82**, 111101 (2010), [arXiv:1009.2076 \[hep-ex\]](#).
- [1249] LHCb collaboration, R. Aaij *et al.*, JHEP **09**, 145 (2013), [arXiv:1307.4556](#).

- [1250] G. Burdman and J. Kambor, Phys. Rev. **D55**, 2817 (1997), [arXiv:hep-ph/9602353 \[hep-ph\]](#).
- [1251] D. Becirevic, A. Le Yaouanc, L. Oliver, J.-C. Raynal, P. Roudeau, and J. Serrano, Phys. Rev. **D87**, 054007 (2013), [arXiv:1206.5869 \[hep-ph\]](#).
- [1252] *BABAR* collaboration, J. P. Lees *et al.*, Phys. Rev. **D91**, 052022 (2015), [arXiv:1412.5502 \[hep-ex\]](#).
- [1253] *BESIII* collaboration, M. Ablikim *et al.*, Phys. Rev. **D92**, 072012 (2015), [arXiv:1508.07560 \[hep-ex\]](#).
- [1254] *BESIII* collaboration, M. Ablikim *et al.*, Phys. Rev. **D92**, 112008 (2015), [arXiv:1510.00308 \[hep-ex\]](#).
- [1255] Belle collaboration, L. Widhalm *et al.*, Phys. Rev. Lett. **97**, 061804 (2006), [arXiv:hep-ex/0604049 \[hep-ex\]](#).
- [1256] *BABAR* collaboration, B. Aubert *et al.*, Phys. Rev. **D76**, 052005 (2007), [arXiv:0704.0020 \[hep-ex\]](#).
- [1257] CLEO collaboration, D. Besson *et al.*, Phys. Rev. **D80**, 032005 (2009), [arXiv:0906.2983 \[hep-ex\]](#).
- [1258] CLEO collaboration, S. Dobbs *et al.*, Phys. Rev. **D77**, 112005 (2008), [arXiv:0712.1020 \[hep-ex\]](#).
- [1259] *BESIII* collaboration, M. Ablikim *et al.*, Phys. Rev. D **96**, 012002 (2017), [arXiv:1703.09084 \[hep-ex\]](#).
- [1260] *BESIII* collaboration, M. Ablikim *et al.*, Phys. Rev. Lett. **122**, 011804 (2019), [arXiv:1810.03127 \[hep-ex\]](#).
- [1261] *BESIII* collaboration, M. Ablikim *et al.*, Eur. Phys. J. C **76**, 369 (2016), [arXiv:1605.00068 \[hep-ex\]](#).
- [1262] *BESIII* collaboration, M. Ablikim *et al.*, Chin. Phys. C **40**, 113001 (2016), [arXiv:1605.00208 \[hep-ex\]](#).
- [1263] *BESIII* collaboration, M. Ablikim *et al.*, Phys. Rev. Lett. **121**, 171803 (2018), [arXiv:1802.05492 \[hep-ex\]](#).
- [1264] Y. Zheng, *BESIII* collaboration. presented at the 37th International Conference on High Energy Physics (ICHEP 2014), 2014.
- [1265] CLEO collaboration, G. Huang *et al.*, Phys. Rev. Lett. **94**, 011802 (2005), [arXiv:hep-ex/0407035 \[hep-ex\]](#).
- [1266] FOCUS collaboration, J. Link *et al.*, Phys. Lett. **B607**, 233 (2005), [arXiv:hep-ex/0410037 \[hep-ex\]](#).
- [1267] *BESIII* collaboration, M. Ablikim *et al.*, Phys. Rev. Lett. **122**, 121801 (2019), [arXiv:1901.02133 \[hep-ex\]](#).
- [1268] CLEO collaboration, J. Yelton *et al.*, Phys. Rev. D **84**, 032001 (2011), [arXiv:1011.1195 \[hep-ex\]](#).

- [1269] BESIII collaboration, M. Ablikim *et al.*, Phys. Rev. D **97**, 092009 (2018), arXiv:1512.08627 [hep-ex].
- [1270] BESIII collaboration, M. Ablikim *et al.*, Phys. Rev. Lett. **122**, 061801 (2019), arXiv:1811.02911 [hep-ex].
- [1271] G. S. Bali *et al.*, Phys. Rev. D **91**, 014503 (2015), arXiv:1406.5449 [hep-ph].
- [1272] G. Duplancic *et al.*, JHEP **1511**, 138 (2015), arXiv:1508.05287 [hep-ph].
- [1273] N. Offen *et al.*, Phys. Rev. D **88**, 034023 (2013), arXiv:1307.2797 [hep-ph].
- [1274] K. Azizi *et al.*, J. Phys. G **38**, 095001 (2011), arXiv:1011.6046 [hep-ph].
- [1275] P. Colangelo *et al.*, Phys. Lett. B **520**, 78 (2001), arXiv:0107137 [hep-ph].
- [1276] R. C. Verma, J. Phys. G **39**, 025005 (2012), arXiv:1103.2973 [hep-ph].
- [1277] Z. T. Wei *et al.*, Phys. Rev. D **80**, 015022 (2009), arXiv:0905.3069 [hep-ph].
- [1278] D. Melikhov *et al.*, Phys. Rev. D **62**, 014006 (2000), arXiv:0001113 [hep-ph].
- [1279] N. R. Soni *et al.*, Phys. Rev. D **98**, 114031 (2018), arXiv:1810.11907 [hep-ph].
- [1280] ETM collaboration, V. Lubicz *et al.*, Phys. Rev. D **96**, 054514 (2017), arXiv:1706.03017 [hep-lat].
- [1281] HPQCD collaboration, H. Na *et al.*, Phys. Rev. D **82**, 114506 (2010), arXiv:1008.4562 [hep-lat].
- [1282] HPQCD collaboration, H. Na *et al.*, Phys. Rev. D **84**, 114505 (2011), arXiv:1109.1501 [hep-lat].
- [1283] Fermilab Lattice and MILC collaboration, R. Li *et al.*, Lattice 2018 (2019), arXiv:1901.08989 [hep-lat].
- [1284] S. Fajfer *et al.*, Phys. Rev. D91 (2015) no.9, 094009 **91**, 094009 (2015), arXiv:1502.07488 [hep-lat].
- [1285] L. Riggio *et al.*, Eur. Phys. J. C **78**, 501 (2018), arXiv:1706.03657 [hep-lat].
- [1286] BESIII collaboration, M. Ablikim *et al.*, Phys. Rev. D **97**, 012006 (2018), arXiv:1709.03680 [hep-ex].
- [1287] BESIII collaboration, M. Ablikim *et al.*, Phys. Rev. D **94**, 112003 (2016), arXiv:1608.06484 [hep-ex].
- [1288] FOCUS collaboration, J. Link *et al.*, Phys. Lett. **B535**, 43 (2002), arXiv:hep-ex/0203031 [hep-ex].
- [1289] FOCUS collaboration, J. Link *et al.*, Phys. Lett. **B544**, 89 (2002), arXiv:hep-ex/0207049 [hep-ex].
- [1290] BABAR collaboration, B. Aubert *et al.*, Phys. Rev. **D78**, 051101 (2008), arXiv:0807.1599 [hep-ex].

- [1291] CLEO collaboration, K. M. Ecklund *et al.*, Phys. Rev. **D80**, 052009 (2009), [arXiv:0907.3201 \[hep-ex\]](#).
- [1292] CLEO collaboration, R. A. Briere *et al.*, Phys. Rev. **D81**, 112001 (2010), [arXiv:1004.1954 \[hep-ex\]](#).
- [1293] BABAR collaboration, P. del Amo Sanchez *et al.*, Phys. Rev. **D83**, 072001 (2011), [arXiv:1012.1810 \[hep-ex\]](#).
- [1294] P. Estabrooks *et al.*, Nucl. Phys. **B133**, 490 (1978).
- [1295] BESIII collaboration, M. Ablikim *et al.*, Phys. Rev. D **94**, 032001 (2016), [arXiv:1512.08627 \[hep-ex\]](#).
- [1296] BESIII collaboration, M. Ablikim *et al.*, Phys. Rev. D **99**, 011103 (2019), [arXiv:1811.11349 \[hep-ex\]](#).
- [1297] BESIII collaboration, M. Ablikim *et al.*, Phys. Rev. D **92**, 071101 (2016), [arXiv:1508.00151 \[hep-ex\]](#).
- [1298] BESIII collaboration, M. Ablikim *et al.*, Phys. Rev. Lett. **122**, 062001 (2019), [arXiv:1809.06496 \[hep-ex\]](#).
- [1299] Fermilab E691 collaboration, J. Anjos *et al.*, Phys. Rev. Lett. **65**, 2630 (1990).
- [1300] Fermilab E653 collaboration, K. Kodama *et al.*, Phys. Lett. **B274**, 246 (1992).
- [1301] Fermilab E687 collaboration, P. Frabetti *et al.*, Phys. Lett. **B307**, 262 (1993).
- [1302] Fermilab E791 collaboration, E. Aitala *et al.*, Phys. Rev. Lett. **80**, 1393 (1998), [arXiv:hep-ph/9710216 \[hep-ph\]](#).
- [1303] Fermilab E791 collaboration, E. Aitala *et al.*, Phys. Lett. **B440**, 435 (1998), [arXiv:hep-ex/9809026 \[hep-ex\]](#).
- [1304] BEATRICE collaboration, M. Adamovich *et al.*, Eur. Phys. J. **C6**, 35 (1999).
- [1305] FOCUS collaboration, J. Link *et al.*, Phys. Lett. **B607**, 67 (2005), [arXiv:hep-ex/0410067 \[hep-ex\]](#).
- [1306] H. Mahlke, eConf **C0610161**, 014 (2006), [arXiv:hep-ex/0702014 \[hep-ex\]](#).
- [1307] BESIII collaboration, M. Ablikim *et al.*, Phys. Rev. Lett. **121**, 081802 (2018), [arXiv:1803.02166 \[hep-ex\]](#).
- [1308] ARGUS collaboration, X. D. Cheng *et al.*, Phys. Rev. **D96**, 033002 (2017), [arXiv:hep-ph/1706.01019 \[hep-ph\]](#).
- [1309] CLEO collaboration, M. Artuso *et al.*, Phys. Rev. Lett. **99**, 191801 (2007), [arXiv:0705.4276 \[hep-ex\]](#).
- [1310] BESIII collaboration, M. Ablikim *et al.*, (2019), [arXiv:1907.11370 \[hep-ex\]](#).
- [1311] ETM collaboration, N. Carrasco *et al.*, Phys. Rev. **D91**, 054507 (2015), [arXiv:1411.7908 \[hep-lat\]](#).

- [1312] ETM collaboration, A. Bazavov *et al.*, Phys. Rev. **D98**, 074512 (2018), [arXiv:1712.09262](https://arxiv.org/abs/1712.09262) [hep-lat].
- [1313] FLAG collaboration, S. Aoki *et al.*, (2019), [arXiv:1902.08191](https://arxiv.org/abs/1902.08191) [hep-lat].
- [1314] A. Filipuzzi, J. Portoles, and M. Gonzalez-Alonso, Phys. Rev. **D85**, 116010 (2012), [arXiv:1203.2092](https://arxiv.org/abs/1203.2092) [hep-ph].
- [1315] BESIII collaboration, M. Ablikim *et al.*, Phys. Rev. Lett. **122**, no. 7, 071802 (2019), [arXiv:1811.10890](https://arxiv.org/abs/1811.10890) [hep-ex].
- [1316] BESIII collaboration, M. Ablikim *et al.*, Phys. Rev. **D89**, 051104 (2014), [arXiv:1312.0374](https://arxiv.org/abs/1312.0374) [hep-ex].
- [1317] BABAR collaboration, P. del Amo Sanchez *et al.*, Phys. Rev. **D82**, 091103 (2010), [arXiv:1008.4080](https://arxiv.org/abs/1008.4080) [hep-ex], Erratum ibid. **D91**, 019901 (2015).
- [1318] Belle collaboration, A. Zupanc *et al.*, JHEP **09**, 139 (2013), [arXiv:1307.6240](https://arxiv.org/abs/1307.6240) [hep-ex].
- [1319] BESIII collaboration, M. Ablikim *et al.*, Phys. Rev. **D94**, 072004 (2016), [arXiv:1608.06732](https://arxiv.org/abs/1608.06732) [hep-ex].
- [1320] CLEO collaboration, P. Naik *et al.*, Phys. Rev. **D80**, 112004 (2009), [arXiv:0910.3602](https://arxiv.org/abs/0910.3602) [hep-ex].
- [1321] CLEO collaboration, P. Onyisi *et al.*, Phys. Rev. **D79**, 052002 (2009), [arXiv:0901.1147](https://arxiv.org/abs/0901.1147) [hep-ex].
- [1322] E. Barberio, B. van Eijk, and Z. Was, Comput. Phys. Commun. **66**, 115 (1991).
- [1323] E. Barberio and Z. Was, Comput. Phys. Commun. **79**, 291 (1994).
- [1324] P. Golonka and Z. Was, Eur. Phys. J. **C45**, 97 (2006), [arXiv:hep-ph/0506026](https://arxiv.org/abs/hep-ph/0506026).
- [1325] P. Golonka, B. Kersevan, T. Pierzchala, E. Richter-Was, Z. Was, and M. Worek, Comput. Phys. Commun. **174**, 818–835 (2006), [arXiv:hep-ph/0312240](https://arxiv.org/abs/hep-ph/0312240) [hep-ph].
- [1326] P. Golonka and Z. Was, Eur. Phys. J. **C50**, 53 (2007), [arXiv:hep-ph/0604232](https://arxiv.org/abs/hep-ph/0604232).
- [1327] EVTGEN-V00-11-07, 2005, <http://inspirehep.net/record/707695>.
- [1328] D. J. Lange, Nucl. Instrum. Meth. **A462**, 152–155 (2001).
- [1329] FOCUS collaboration, J. M. Link *et al.*, Phys. Lett. **B555**, 167 (2003), [arXiv:hep-ex/0212058](https://arxiv.org/abs/hep-ex/0212058).
- [1330] BESIII collaboration, M. Ablikim *et al.*, Phys. Rev. **D97**, no. 7, 072004 (2018), [arXiv:1802.03119](https://arxiv.org/abs/1802.03119) [hep-ex].
- [1331] BABAR collaboration, B. Aubert *et al.*, Phys. Rev. Lett. **100**, 051802 (2008), [arXiv:0704.2080](https://arxiv.org/abs/0704.2080) [hep-ex].
- [1332] CLEO collaboration, M. Artuso *et al.*, Phys. Rev. Lett. **80**, 3193 (1998), [arXiv:hep-ex/9712023](https://arxiv.org/abs/hep-ex/9712023).
- [1333] ALEPH collaboration, R. Barate *et al.*, Phys. Lett. **B403**, 367 (1997).

- [1334] ARGUS collaboration, H. Albrecht *et al.*, Phys. Lett. **B340**, 125 (1994).
- [1335] CLEO collaboration, D. S. Akerib *et al.*, Phys. Rev. Lett. **71**, 3070 (1993).
- [1336] ALEPH collaboration, D. Decamp *et al.*, Phys. Lett. **B266**, 218 (1991).
- [1337] CDF collaboration, D. E. Acosta *et al.*, Phys. Rev. Lett. **94**, 122001 (2005),
[arXiv:hep-ex/0504006](https://arxiv.org/abs/hep-ex/0504006).
- [1338] CLEO collaboration, T. E. Coan *et al.*, Phys. Rev. Lett. **80**, 1150 (1998),
[arXiv:hep-ex/9710028](https://arxiv.org/abs/hep-ex/9710028).
- [1339] N. Davidson, T. Przedzinski, and Z. Was, Comput. Phys. Commun. **199**, 86–101 (2016),
[arXiv:1011.0937 \[hep-ph\]](https://arxiv.org/abs/1011.0937).
- [1340] BESIII collaboration, M. Ablikim *et al.*, [arXiv:1903.04118 \[hep-ex\]](https://arxiv.org/abs/1903.04118).
- [1341] BESIII collaboration, M. Ablikim *et al.*, Phys. Rev. **D99**, no. 11, 112005 (2019),
[arXiv:1903.04164 \[hep-ex\]](https://arxiv.org/abs/1903.04164).
- [1342] BABAR collaboration, B. Aubert *et al.*, Phys. Rev. Lett. **90**, 242001 (2003),
[arXiv:hep-ex/0304021 \[hep-ex\]](https://arxiv.org/abs/hep-ex/0304021).
- [1343] CLEO collaboration, D. Besson *et al.*, Phys. Rev. **D68**, 032002 (2003),
[arXiv:hep-ex/0305100 \[hep-ex\]](https://arxiv.org/abs/hep-ex/0305100), Erratum *ibid.* **D75**, 119908 (2007).
- [1344] Belle collaboration, K. Abe *et al.*, Phys. Rev. Lett. **92**, 012002 (2004), [arXiv:hep-ex/0307052 \[hep-ex\]](https://arxiv.org/abs/hep-ex/0307052).
- [1345] BABAR collaboration, B. Aubert *et al.*, Phys. Rev. **D69**, 031101 (2004),
[arXiv:hep-ex/0310050 \[hep-ex\]](https://arxiv.org/abs/hep-ex/0310050).
- [1346] LHCb collaboration, R. Aaij *et al.*, Phys. Rev. **D94**, 072001 (2016), [arXiv:1608.01289 \[hep-ex\]](https://arxiv.org/abs/1608.01289).
- [1347] FOCUS collaboration, J. M. Link *et al.*, Phys. Lett. **B586**, 11 (2004), [arXiv:hep-ex/0312060 \[hep-ex\]](https://arxiv.org/abs/hep-ex/0312060).
- [1348] S. Godfrey and N. Isgur, Phys. Rev. **D32**, 189 (1985).
- [1349] S. Godfrey and R. Kokoski, Phys. Rev. **D43**, 1679 (1991).
- [1350] P. Schweitzer, S. Boffi, and M. Radici, Phys. Rev. **D66**, 114004 (2002),
[arXiv:hep-ph/0207230 \[hep-ph\]](https://arxiv.org/abs/hep-ph/0207230).
- [1351] B. Chen, X. Liu, and A. Zhang, Phys. Rev. **D92**, 034005 (2015), [arXiv:1507.02339 \[hep-ph\]](https://arxiv.org/abs/1507.02339).
- [1352] S. Godfrey and K. Moats, Phys. Rev. **D93**, 034035 (2016), [arXiv:1510.08305 \[hep-ph\]](https://arxiv.org/abs/1510.08305).
- [1353] F. Jugeau, A. Le Yaouanc, L. Oliver, and J.-C. Raynal, Phys. Rev. **D72**, 094010 (2005),
[arXiv:hep-ph/0504206 \[hep-ph\]](https://arxiv.org/abs/hep-ph/0504206).
- [1354] P. Colangelo, F. De Fazio, and R. Ferrandes, Mod. Phys. Lett. **A19**, 2083 (2004),
[arXiv:hep-ph/0407137 \[hep-ph\]](https://arxiv.org/abs/hep-ph/0407137).

- [1355] R. N. Cahn and J. D. Jackson, Phys. Rev. **D68**, 037502 (2003), [arXiv:hep-ph/0305012 \[hep-ph\]](#).
- [1356] T. Barnes, F. E. Close, and H. J. Lipkin, Phys. Rev. **D68**, 054006 (2003), [arXiv:hep-ph/0305025 \[hep-ph\]](#).
- [1357] H. Lipkin, Phys. Lett. **B580**, 50 (2004), [arXiv:hep-ph/0306204 \[hep-ph\]](#).
- [1358] W. A. Bardeen, E. J. Eichten, and C. T. Hill, Phys. Rev. **D68**, 054024 (2003), [arXiv:hep-ph/0305049 \[hep-ph\]](#).
- [1359] *BABAR* collaboration, B. Aubert *et al.*, Phys. Rev. **D80**, 092003 (2009), [arXiv:0908.0806 \[hep-ex\]](#).
- [1360] LHCb collaboration, R. Aaij *et al.*, JHEP **10**, 151 (2012), [arXiv:1207.6016 \[hep-ex\]](#).
- [1361] LHCb collaboration, R. Aaij *et al.*, Phys. Rev. Lett. **113**, 162001 (2014), [arXiv:1407.7574 \[hep-ex\]](#).
- [1362] LHCb collaboration, R. Aaij *et al.*, JHEP **02**, 133 (2016), [arXiv:1601.01495 \[hep-ex\]](#).
- [1363] T. Matsuki, T. Morii, and K. Sudoh, Eur. Phys. J. **A31**, 701 (2007), [arXiv:hep-ph/0610186 \[hep-ph\]](#).
- [1364] N. Isgur and M. B. Wise, Phys. Lett. **B232**, 113 (1989).
- [1365] *BABAR* collaboration, B. Aubert *et al.*, Phys. Rev. **D74**, 032007 (2006), [arXiv:hep-ex/0604030 \[hep-ex\]](#).
- [1366] BESIII collaboration, M. Ablikim *et al.*, Phys. Rev. **D97**, 051103 (2018), [arXiv:1711.08293 \[hep-ex\]](#).
- [1367] D0 collaboration, V. M. Abazov *et al.*, Phys. Rev. Lett. **102**, 051801 (2009), [arXiv:0712.3789 \[hep-ex\]](#).
- [1368] Fermilab E687 collaboration, P. L. Frabetti *et al.*, Phys. Rev. Lett. **72**, 324 (1994).
- [1369] CLEO collaboration, J. P. Alexander *et al.*, Phys. Lett. **B303**, 377 (1993).
- [1370] ARGUS collaboration, H. Albrecht *et al.*, Phys. Lett. **B297**, 425 (1992).
- [1371] CLEO collaboration, P. Avery *et al.*, Phys. Rev. **D41**, 774 (1990).
- [1372] ARGUS collaboration, H. Albrecht *et al.*, Phys. Lett. **B230**, 162 (1989).
- [1373] *BABAR* collaboration, J. P. Lees *et al.*, Phys. Rev. **D83**, 072003 (2011), [arXiv:1103.2675 \[hep-ex\]](#).
- [1374] BESIII collaboration, M. Ablikim *et al.*, [arXiv:1812.09800 \[hep-ex\]](#).
- [1375] LHCb collaboration, R. Aaij *et al.*, Phys. Rev. **D90**, 072003 (2014), [arXiv:1407.7712 \[hep-ex\]](#).
- [1376] LHCb collaboration, R. Aaij *et al.*, Phys. Lett. **B698**, 14 (2011), [arXiv:1102.0348 \[hep-ex\]](#).
- [1377] *BABAR* collaboration, B. Aubert *et al.*, Phys. Rev. Lett. **97**, 222001 (2006), [arXiv:hep-ex/0607082 \[hep-ex\]](#).

- [1378] ARGUS collaboration, H. Albrecht *et al.*, Z. Phys. **C69**, 405 (1996).
- [1379] CLEO collaboration, Y. Kubota *et al.*, Phys. Rev. Lett. **72**, 1972 (1994),
[arXiv:hep-ph/9403325](https://arxiv.org/abs/hep-ph/9403325) [hep-ph].
- [1380] BABAR collaboration, J. P. Lees *et al.*, Phys. Rev. **D91**, 052002 (2015), [arXiv:1412.6751](https://arxiv.org/abs/1412.6751) [hep-ex].
- [1381] LHCb collaboration, R. Aaij *et al.*, Phys. Rev. **D92**, 012012 (2015), [arXiv:1505.01505](https://arxiv.org/abs/1505.01505) [hep-ex].
- [1382] ZEUS collaboration, H. Abramowicz *et al.*, Nucl. Phys. **B866**, 229 (2013), [arXiv:1208.4468](https://arxiv.org/abs/1208.4468) [hep-ex].
- [1383] CDF collaboration, A. Abulencia *et al.*, Phys. Rev. **D73**, 051104 (2006),
[arXiv:hep-ex/0512069](https://arxiv.org/abs/hep-ex/0512069) [hep-ex].
- [1384] CLEO collaboration, P. Avery *et al.*, Phys. Lett. **B331**, 236 (1994), [arXiv:hep-ph/9403359](https://arxiv.org/abs/hep-ph/9403359) [hep-ph].
- [1385] ARGUS collaboration, H. Albrecht *et al.*, Phys. Lett. **B232**, 398 (1989).
- [1386] Tagged Photon Spectrometer collaboration, J. C. Anjos *et al.*, Phys. Rev. Lett. **62**, 1717 (1989).
- [1387] CLEO collaboration, T. Bergfeld *et al.*, Phys. Lett. **B340**, 194 (1994).
- [1388] ARGUS collaboration, H. Albrecht *et al.*, Phys. Lett. **B221**, 422 (1989).
- [1389] ARGUS collaboration, H. Albrecht *et al.*, Phys. Lett. **B231**, 208 (1989).
- [1390] DELPHI collaboration, P. Abreu *et al.*, Phys. Lett. **B426**, 231 (1998).
- [1391] ZEUS collaboration, S. Chekanov *et al.*, Eur. Phys. J. **C60**, 25 (2009), [arXiv:0807.1290](https://arxiv.org/abs/0807.1290) [hep-ex].
- [1392] ALEPH collaboration, A. Heister *et al.*, Phys. Lett. **B526**, 34 (2002), [arXiv:hep-ex/0112010](https://arxiv.org/abs/hep-ex/0112010) [hep-ex].
- [1393] BABAR collaboration, B. Aubert *et al.*, Phys. Rev. **D72**, 052006 (2005),
[arXiv:hep-ex/0507009](https://arxiv.org/abs/hep-ex/0507009) [hep-ex].
- [1394] Belle collaboration, E. Solovieva *et al.*, Phys. Lett. **B672**, 1 (2009), [arXiv:0808.3677](https://arxiv.org/abs/0808.3677) [hep-ex].
- [1395] CDF collaboration, T. Aaltonen *et al.*, Phys. Rev. **D84**, 012003 (2011), [arXiv:1105.5995](https://arxiv.org/abs/1105.5995) [hep-ex].
- [1396] CLEO collaboration, M. Artuso *et al.*, Phys. Rev. Lett. **86**, 4479 (2001),
[arXiv:hep-ex/0010080](https://arxiv.org/abs/hep-ex/0010080) [hep-ex].
- [1397] BABAR collaboration, B. Aubert *et al.*, Phys. Rev. Lett. **98**, 012001 (2007),
[arXiv:hep-ex/0603052](https://arxiv.org/abs/hep-ex/0603052) [hep-ex].
- [1398] H.-Y. Cheng and C.-K. Chua, Phys. Rev. **D75**, 014006 (2007), [arXiv:hep-ph/0610283](https://arxiv.org/abs/hep-ph/0610283) [hep-ph].

- [1399] C. W. Joo, Y. Kato, K. Tanida, and Y. Kato, PoS **Hadron2013**, 201 (2013).
- [1400] LHCb collaboration, R. Aaij *et al.*, Phys. Rev. **D96**, no. 11, 112005 (2017), [arXiv:1709.01920 \[hep-ex\]](#).
- [1401] Belle collaboration, S. H. Lee *et al.*, Phys. Rev. **D89**, 091102 (2014), [arXiv:1404.5389 \[hep-ex\]](#).
- [1402] Belle collaboration, R. Mizuk *et al.*, Phys. Rev. Lett. **94**, 122002 (2005), [arXiv:hep-ex/0412069 \[hep-ex\]](#).
- [1403] L. Copley, N. Isgur, and G. Karl, Phys. Rev. **D20**, 768 (1979), Erratum ibid. **D23**, 817, (1981).
- [1404] D. Pirjol and T.-M. Yan, Phys. Rev. **D56**, 5483 (1997), [arXiv:hep-ph/9701291 \[hep-ph\]](#).
- [1405] Belle collaboration, R. Chistov *et al.*, Phys. Rev. Lett. **97**, 162001 (2006), [arXiv:hep-ex/0606051 \[hep-ex\]](#).
- [1406] Belle collaboration, Y. Kato *et al.*, Phys. Rev. **D89**, 052003 (2014), [arXiv:1312.1026 \[hep-ex\]](#).
- [1407] Belle collaboration, Y. Kato *et al.*, Phys. Rev. **D94**, 032002 (2016), [arXiv:1605.09103 \[hep-ex\]](#).
- [1408] BABAR collaboration, B. Aubert *et al.*, Phys. Rev. **D77**, 031101 (2008), [arXiv:0710.5775 \[hep-ex\]](#).
- [1409] Belle collaboration, Y. B. Li *et al.*, Eur. Phys. J. **C78**, no. 11, 928 (2018), [arXiv:1806.09182 \[hep-ex\]](#).
- [1410] Belle collaboration, J. Yelton *et al.*, Phys. Rev. **D94**, 052011 (2016), [arXiv:1607.07123 \[hep-ex\]](#).
- [1411] BABAR collaboration, B. Aubert *et al.*, Phys. Rev. Lett. **97**, 232001 (2006), [arXiv:hep-ex/0608055 \[hep-ex\]](#).
- [1412] J. L. Rosner, Phys. Rev. **D52**, 6461 (1995), [arXiv:hep-ph/9508252 \[hep-ph\]](#).
- [1413] L. Y. Glozman and D. Riska, Nucl. Phys. **A603**, 326 (1996), [arXiv:hep-ph/9509269 \[hep-ph\]](#), Erratum ibid. **A620**, 510, (1997).
- [1414] E. E. Jenkins, Phys. Rev. **D54**, 4515 (1996), [arXiv:hep-ph/9603449 \[hep-ph\]](#).
- [1415] L. Burakovsky, J. T. Goldman, and L. Horwitz, Phys. Rev. **D56**, 7124 (1997), [arXiv:hep-ph/9706464 \[hep-ph\]](#).
- [1416] LHCb collaboration, R. Aaij *et al.*, Phys. Rev. Lett. **118**, no. 18, 182001 (2017), [arXiv:1703.04639 \[hep-ex\]](#).
- [1417] Belle collaboration, J. Yelton *et al.*, Phys. Rev. **D97**, no. 5, 051102 (2018), [arXiv:1711.07927 \[hep-ex\]](#).
- [1418] G. Burdman, E. Golowich, J. L. Hewett, and S. Pakvasa, Phys. Rev. **D66**, 014009 (2002), [arXiv:hep-ph/0112235 \[hep-ph\]](#).

- [1419] S. Fajfer, A. Prapotnik, S. Prelovsek, P. Singer, and J. Zupan, Nucl. Phys. Proc. Suppl. **115**, 93 (2003), [arXiv:hep-ph/0208201 \[hep-ph\]](#).
- [1420] S. Fajfer, N. Kosnik, and S. Prelovsek, Phys. Rev. **D76**, 074010 (2007), [arXiv:0706.1133 \[hep-ph\]](#).
- [1421] E. Golowich, J. Hewett, S. Pakvasa, and A. A. Petrov, Phys. Rev. **D79**, 114030 (2009), [arXiv:0903.2830 \[hep-ph\]](#).
- [1422] A. Paul, I. I. Bigi, and S. Recksiegel, Phys. Rev. **D82**, 094006 (2010), [arXiv:1008.3141 \[hep-ph\]](#), Erratum ibid. **D83**, 019901, (2011).
- [1423] A. Borisov, [arXiv:1112.3269 \[hep-ph\]](#) (2011).
- [1424] R.-M. Wang, J.-H. Sheng, J. Zhu, Y.-Y. Fan, and Y. Gao, Int. J. Mod. Phys. **A29**, 1450169 (2014).
- [1425] S. de Boer and G. Hiller, Phys. Rev. **D93**, 074001 (2016), [arXiv:1510.00311 \[hep-ph\]](#).
- [1426] CLEO collaboration, P. Rubin *et al.*, Phys. Rev. **D82**, 092007 (2010), [arXiv:1009.1606 \[hep-ex\]](#).
- [1427] D0 collaboration, V. Abazov *et al.*, Phys. Rev. Lett. **100**, 101801 (2008), [arXiv:0708.2094 \[hep-ex\]](#).
- [1428] LHCb collaboration, R. Aaij *et al.*, Phys. Lett. **B728**, 234 (2014), [arXiv:1310.2535 \[hep-ex\]](#).
- [1429] LHCb collaboration, R. Aaij *et al.*, Phys. Lett. **B724**, 203 (2013), [arXiv:1304.6365 \[hep-ex\]](#).
- [1430] CLEO collaboration, T. Coan *et al.*, Phys. Rev. Lett. **90**, 101801 (2003), [arXiv:hep-ex/0212045 \[hep-ex\]](#).
- [1431] BESIII collaboration, M. Ablikim *et al.*, Phys. Rev. **D91**, 112015 (2015), [arXiv:1505.03087 \[hep-ex\]](#).
- [1432] BABAR collaboration, J. P. Lees *et al.*, Phys. Rev. **D85**, 091107 (2012), [arXiv:1110.6480 \[hep-ex\]](#).
- [1433] Belle collaboration, N. K. Nisar *et al.*, Phys. Rev. **D93**, 051102 (2016), [arXiv:1512.02992 \[hep-ex\]](#).
- [1434] CLEO collaboration, P. Haas *et al.*, Phys. Rev. Lett. **60**, 1614 (1988).
- [1435] ARGUS collaboration, H. Albrecht *et al.*, Phys. Lett. **B209**, 380 (1988).
- [1436] MARK-III collaboration, J. Adler *et al.*, Phys. Rev. **D37**, 2023 (1988), Erratum ibid. **D40**, 3788, (1989).
- [1437] CLEO collaboration, A. Freyberger *et al.*, Phys. Rev. Lett. **76**, 3065 (1996).
- [1438] Fermilab E789 collaboration, D. Pripstein *et al.*, Phys. Rev. **D61**, 032005 (2000), [arXiv:hep-ex/9906022 \[hep-ex\]](#).
- [1439] Fermilab E791 collaboration, E. Aitala *et al.*, Phys. Lett. **B462**, 401 (1999), [arXiv:hep-ex/9906045 \[hep-ex\]](#).

- [1440] *BABAR* collaboration, B. Aubert *et al.*, Phys. Rev. Lett. **93**, 191801 (2004), [arXiv:hep-ex/0408023 \[hep-ex\]](#).
- [1441] *Belle* collaboration, M. Petric *et al.*, Phys. Rev. **D81**, 091102 (2010), [arXiv:1003.2345 \[hep-ex\]](#).
- [1442] Fermilab E653 collaboration, K. Kodama *et al.*, Phys. Lett. **B345**, 85 (1995).
- [1443] HERA-B collaboration, I. Abt *et al.*, Phys. Lett. **B596**, 173 (2004), [arXiv:hep-ex/0405059 \[hep-ex\]](#).
- [1444] CDF collaboration, T. Aaltonen *et al.*, Phys. Rev. **D82**, 091105 (2010), [arXiv:1008.5077 \[hep-ex\]](#).
- [1445] LHCb collaboration, R. Aaij *et al.*, Phys. Lett. **B725**, 15 (2013), [arXiv:1305.5059 \[hep-ex\]](#).
- [1446] BESIII collaboration, M. Ablikim *et al.*, Phys. Rev. **D97**, no. 7, 072015 (2018), [arXiv:1802.09752 \[hep-ex\]](#).
- [1447] Fermilab E791 collaboration, E. Aitala *et al.*, Phys. Rev. Lett. **86**, 3969 (2001), [arXiv:hep-ex/0011077 \[hep-ex\]](#).
- [1448] LHCb collaboration, R. Aaij *et al.*, Phys. Rev. Lett. **119**, no. 18, 181805 (2017), [arXiv:1707.08377 \[hep-ex\]](#).
- [1449] MARK-III collaboration, J. Adler *et al.*, Phys. Rev. **D40**, 906 (1989).
- [1450] CLEO collaboration, D. M. Asner *et al.*, Phys. Rev. **D58**, 092001 (1998), [arXiv:hep-ex/9803022 \[hep-ex\]](#).
- [1451] BaBar collaboration, B. Aubert *et al.*, Phys. Rev. **D78**, 071101 (2008), [arXiv:0808.1838 \[hep-ex\]](#).
- [1452] MARK-III collaboration, J. Becker *et al.*, Phys. Lett. **B193**, 147 (1987).
- [1453] LHCb collaboration, R. Aaij *et al.*, Phys. Lett. **B754**, 167 (2016), [arXiv:1512.00322 \[hep-ex\]](#).
- [1454] CLEO collaboration, P. Rubin *et al.*, Phys. Rev. **D79**, 097101 (2009), [arXiv:0904.1619 \[hep-ex\]](#).
- [1455] Fermilab E687 collaboration, P. Frabetti *et al.*, Phys. Lett. **B398**, 239 (1997).
- [1456] *BABAR* collaboration, J. P. Lees *et al.*, Phys. Rev. **D84**, 072006 (2011), [arXiv:1107.4465 \[hep-ex\]](#).
- [1457] BESIII collaboration, M.-G. Zhao, [arXiv:1605.08952 \[hep-ex\]](#) (2016).
- [1458] FOCUS collaboration, J. Link *et al.*, Phys. Lett. **B572**, 21 (2003), [arXiv:hep-ex/0306049 \[hep-ex\]](#).
- [1459] LHCb collaboration, R. Aaij *et al.*, Phys. Rev. **D97**, no. 9, 091101 (2018), [arXiv:1712.07938 \[hep-ex\]](#).
- [1460] M. Davier, A. Hocker, and Z. Zhang, Rev. Mod. Phys. **78**, 1043 (2006), [arXiv:hep-ph/0507078 \[hep-ph\]](#).

- [1461] BaBar collaboration, J. P. Lees *et al.*, Phys. Rev. **D98**, 032010 (2018), arXiv:1806.10280 [hep-ex].
- [1462] A. Lusiani, EPJ Web Conf. **212**, 08001 (2019), arXiv:1906.02626 [hep-ex].
- [1463] BABAR collaboration, B. Aubert *et al.*, Phys. Rev. **D76**, 051104 (2007), arXiv:0707.2922 [hep-ex].
- [1464] ALEPH collaboration, S. Schael *et al.*, Phys. Rept. **421**, 191 (2005), arXiv:hep-ex/0506072 [hep-ex], HFLAV-tau uses measurements of $\tau \rightarrow hX$ and $\tau \rightarrow KX$ and obtains $\tau \rightarrow \pi X$ by difference; the measurement of $\mathcal{B}(\tau^- \rightarrow 3h^- 2h^+ \pi^0 \nu_\tau (\text{ex. } K^0))$ has been read as $(2.1 \pm 0.7 \pm 0.6) \times 10^{-4}$ whereas PDG11 uses $(2.1 \pm 0.7 \pm 0.9) \times 10^{-4}$.
- [1465] DELPHI collaboration, P. Abreu *et al.*, Eur. Phys. J. **C10**, 201 (1999).
- [1466] L3 collaboration, M. Acciarri *et al.*, Phys. Lett. **B507**, 47 (2001), arXiv:hep-ex/0102023 [hep-ex].
- [1467] OPAL collaboration, G. Abbiendi *et al.*, Phys. Lett. **B551**, 35 (2003), arXiv:hep-ex/0211066 [hep-ex].
- [1468] ARGUS collaboration, H. Albrecht *et al.*, Z. Phys. **C53**, 367 (1992).
- [1469] BABAR collaboration, B. Aubert *et al.*, Phys. Rev. Lett. **105**, 051602 (2010), arXiv:0912.0242 [hep-ex].
- [1470] CLEO collaboration, A. Anastassov *et al.*, Phys. Rev. **D55**, 2559 (1997), Erratum ibid. **D58**, 119903, (1998).
- [1471] OPAL collaboration, G. Abbiendi *et al.*, Phys. Lett. **B447**, 134 (1999), arXiv:hep-ex/9812017 [hep-ex].
- [1472] DELPHI collaboration, P. Abreu *et al.*, Z. Phys. **C55**, 555 (1992).
- [1473] L3 collaboration, M. Acciarri *et al.*, Phys. Lett. **B345**, 93 (1995).
- [1474] OPAL collaboration, G. Alexander *et al.*, Phys. Lett. **B266**, 201 (1991).
- [1475] DELPHI collaboration, J. Abdallah *et al.*, Eur. Phys. J. **C46**, 1 (2006), arXiv:hep-ex/0603044 [hep-ex].
- [1476] OPAL collaboration, K. Ackerstaff *et al.*, Eur. Phys. J. **C4**, 193 (1998), arXiv:hep-ex/9801029 [hep-ex].
- [1477] ALEPH collaboration, R. Barate *et al.*, Eur. Phys. J. **C10**, 1 (1999), arXiv:hep-ex/9903014 [hep-ex].
- [1478] CLEO collaboration, M. Battle *et al.*, Phys. Rev. Lett. **73**, 1079 (1994), arXiv:hep-ph/9403329 [hep-ph].
- [1479] DELPHI collaboration, P. Abreu *et al.*, Phys. Lett. **B334**, 435 (1994).
- [1480] OPAL collaboration, G. Abbiendi *et al.*, Eur. Phys. J. **C19**, 653 (2001), arXiv:hep-ex/0009017 [hep-ex].
- [1481] Belle collaboration, M. Fujikawa *et al.*, Phys. Rev. **D78**, 072006 (2008), arXiv:0805.3773 [hep-ex].

- [1482] CLEO collaboration, M. Artuso *et al.*, Phys. Rev. Lett. **72**, 3762 (1994),
[arXiv:hep-ph/9404310](https://arxiv.org/abs/hep-ph/9404310) [hep-ph].
- [1483] OPAL collaboration, G. Abbiendi *et al.*, Eur. Phys. J. **C35**, 437 (2004),
[arXiv:hep-ex/0406007](https://arxiv.org/abs/hep-ex/0406007) [hep-ex].
- [1484] CLEO collaboration, M. Procario *et al.*, Phys. Rev. Lett. **70**, 1207 (1993).
- [1485] ALEPH collaboration, R. Barate *et al.*, Eur. Phys. J. **C4**, 29 (1998),
<http://cdsweb.cern.ch/record/346304>.
- [1486] OPAL collaboration, R. Akers *et al.*, Phys. Lett. **B339**, 278 (1994).
- [1487] CLEO collaboration, T. Coan *et al.*, Phys. Rev. **D53**, 6037 (1996).
- [1488] Belle collaboration, S. Ryu *et al.*, Phys. Rev. **D89**, 072009 (2014), [arXiv:1402.5213](https://arxiv.org/abs/1402.5213) [hep-ex].
- [1489] L3 collaboration, M. Acciarri *et al.*, Phys. Lett. **B352**, 487 (1995).
- [1490] OPAL collaboration, G. Abbiendi *et al.*, Eur. Phys. J. **C13**, 213 (2000),
[arXiv:hep-ex/9911029](https://arxiv.org/abs/hep-ex/9911029) [hep-ex].
- [1491] ALEPH collaboration, R. Barate *et al.*, Eur. Phys. J. **C11**, 599 (1999),
[arXiv:hep-ex/9903015](https://arxiv.org/abs/hep-ex/9903015) [hep-ex].
- [1492] BABAR collaboration, J. P. Lees *et al.*, Phys. Rev. **D86**, 092013 (2012), [arXiv:1208.0376](https://arxiv.org/abs/1208.0376) [hep-ex].
- [1493] CELLO collaboration, H. Behrend *et al.*, Phys. Lett. **B222**, 163 (1989).
- [1494] L3 collaboration, B. Adeva *et al.*, Phys. Lett. **B265**, 451 (1991).
- [1495] TPC/Two Gamma collaboration, H. Aihara *et al.*, Phys. Rev. **D35**, 1553 (1987).
- [1496] L3 collaboration, P. Achard *et al.*, Phys. Lett. **B519**, 189 (2001), [arXiv:hep-ex/0107055](https://arxiv.org/abs/hep-ex/0107055) [hep-ex].
- [1497] OPAL collaboration, R. Akers *et al.*, Z. Phys. **C68**, 555 (1995).
- [1498] CLEO collaboration, R. Balest *et al.*, Phys. Rev. Lett. **75**, 3809 (1995).
- [1499] BABAR collaboration, B. Aubert *et al.*, Phys. Rev. Lett. **100**, 011801 (2008),
[arXiv:0707.2981](https://arxiv.org/abs/0707.2981) [hep-ex].
- [1500] Belle collaboration, M. Lee *et al.*, Phys. Rev. **D81**, 113007 (2010), [arXiv:1001.0083](https://arxiv.org/abs/1001.0083) [hep-ex].
- [1501] CLEO collaboration, R. A. Briere *et al.*, Phys. Rev. Lett. **90**, 181802 (2003),
[arXiv:hep-ex/0302028](https://arxiv.org/abs/hep-ex/0302028) [hep-ex].
- [1502] CLEO collaboration, K. Edwards *et al.*, Phys. Rev. **D61**, 072003 (2000),
[arXiv:hep-ex/9908024](https://arxiv.org/abs/hep-ex/9908024) [hep-ex].
- [1503] CLEO collaboration, D. Bortoletto *et al.*, Phys. Rev. Lett. **71**, 1791 (1993).

- [1504] CLEO collaboration, A. Anastassov *et al.*, Phys. Rev. Lett. **86**, 4467 (2001), [arXiv:hep-ex/0010025 \[hep-ex\]](#).
- [1505] CLEO collaboration, S. Richichi *et al.*, Phys. Rev. **D60**, 112002 (1999), [arXiv:hep-ex/9810026 \[hep-ex\]](#).
- [1506] TPC/Two Gamma collaboration, D. A. Bauer *et al.*, Phys. Rev. **D50**, 13 (1994).
- [1507] ALEPH collaboration, R. Barate *et al.*, Eur. Phys. J. **C1**, 65 (1998).
- [1508] CLEO collaboration, K. E. Arms *et al.*, Phys. Rev. Lett. **94**, 241802 (2005), [arXiv:hep-ex/0501042 \[hep-ex\]](#).
- [1509] OPAL collaboration, G. Abbiendi *et al.*, Eur. Phys. J. **C13**, 197 (2000), [arXiv:hep-ex/9908013 \[hep-ex\]](#).
- [1510] CLEO collaboration, D. Gibaut *et al.*, Phys. Rev. Lett. **73**, 934 (1994).
- [1511] B. Bylsma *et al.*, Phys. Rev. **D35**, 2269 (1987).
- [1512] ARGUS collaboration, H. Albrecht *et al.*, Phys. Lett. **B202**, 149 (1988).
- [1513] OPAL collaboration, K. Ackerstaff *et al.*, Eur. Phys. J. **C8**, 183 (1999), [arXiv:hep-ex/9808011 \[hep-ex\]](#).
- [1514] ALEPH collaboration, D. Buskulic *et al.*, Z. Phys. **C74**, 263 (1997).
- [1515] Belle collaboration, K. Inami *et al.*, Phys. Lett. **B672**, 209 (2009), [arXiv:0811.0088 \[hep-ex\]](#).
- [1516] CLEO collaboration, M. Artuso *et al.*, Phys. Rev. Lett. **69**, 3278 (1992).
- [1517] BABAR collaboration, P. del Amo Sanchez *et al.*, Phys. Rev. **D83**, 032002 (2011), [arXiv:1011.3917 \[hep-ex\]](#).
- [1518] CLEO collaboration, J. E. Bartelt *et al.*, Phys. Rev. Lett. **76**, 4119 (1996).
- [1519] CLEO collaboration, M. Bishai *et al.*, Phys. Rev. Lett. **82**, 281 (1999), [arXiv:hep-ex/9809012 \[hep-ex\]](#).
- [1520] CLEO collaboration, P. S. Baringer *et al.*, Phys. Rev. Lett. **59**, 1993 (1987).
- [1521] ALEPH collaboration, D. Buskulic *et al.*, Z. Phys. **C70**, 579 (1996).
- [1522] BABAR collaboration, J. P. Lees *et al.*, Phys. Rev. **D86**, 092010 (2012), [arXiv:1209.2734 \[hep-ex\]](#).
- [1523] Belle collaboration, K. Belous *et al.*, Phys. Rev. Lett. **112**, 031801 (2014), [arXiv:1310.8503 \[hep-ex\]](#).
- [1524] W. Marciano and A. Sirlin, Phys. Rev. Lett. **61**, 1815 (1988).
- [1525] A. Pich, Prog. Part. Nucl. Phys. **75**, 41 (2014), [arXiv:1310.7922 \[hep-ph\]](#).
- [1526] A. Ferroglio, C. Greub, A. Sirlin, and Z. Zhang, Phys. Rev. **D88**, 033012 (2013), [arXiv:1307.6900 \[hep-ph\]](#).

- [1527] M. Fael, L. Mercolli, and M. Passera, Phys. Rev. **D88**, 093011 (2013), [arXiv:1310.1081 \[hep-ph\]](https://arxiv.org/abs/1310.1081).
- [1528] W. J. Marciano and A. Sirlin, Phys. Rev. Lett. **71**, 3629 (1993).
- [1529] R. Decker and M. Finkemeier, Phys. Lett. **B334**, 199 (1994).
- [1530] R. Decker and M. Finkemeier, Nucl. Phys. **B438**, 17 (1995), [arXiv:hep-ph/9403385](https://arxiv.org/abs/hep-ph/9403385).
- [1531] R. Decker and M. Finkemeier, Nucl. Phys. Proc. Suppl. **40**, 453 (1995), [arXiv:hep-ph/9411316 \[hep-ph\]](https://arxiv.org/abs/hep-ph/9411316).
- [1532] FlaviaNet working group on kaon decays, M. Antonelli *et al.*, Eur. Phys. J. **C69**, 399 (2010), [arXiv:1005.2323 \[hep-ph\]](https://arxiv.org/abs/1005.2323).
- [1533] E. Gamiz, M. Jamin, A. Pich, J. Prades, and F. Schwab, JHEP **01**, 060 (2003), [arXiv:hep-ph/0212230 \[hep-ph\]](https://arxiv.org/abs/hep-ph/0212230).
- [1534] E. Gamiz, M. Jamin, A. Pich, J. Prades, and F. Schwab, Phys. Rev. Lett. **94**, 011803 (2005), [arXiv:hep-ph/0408044 \[hep-ph\]](https://arxiv.org/abs/hep-ph/0408044).
- [1535] E. Gamiz, M. Jamin, A. Pich, J. Prades, and F. Schwab, Nucl. Phys. Proc. Suppl. **169**, 85 (2007), [arXiv:hep-ph/0612154](https://arxiv.org/abs/hep-ph/0612154).
- [1536] E. Gamiz, M. Jamin, A. Pich, J. Prades, and F. Schwab, PoS **KAON**, 008 (2008), [arXiv:0709.0282 \[hep-ph\]](https://arxiv.org/abs/0709.0282).
- [1537] K. Maltman, Nucl. Phys. Proc. Suppl. **218**, 146 (2011), [arXiv:1011.6391 \[hep-ph\]](https://arxiv.org/abs/1011.6391).
- [1538] J. C. Hardy and I. S. Towner, Phys. Rev. **C91**, 025501 (2015), [arXiv:1411.5987 \[nucl-ex\]](https://arxiv.org/abs/1411.5987).
- [1539] J. Hardy and I. S. Towner, PoS **CKM2016**, 028 (2016).
- [1540] BaBar collaboration, S. Banerjee, [arXiv:0811.1429 \[hep-ex\]](https://arxiv.org/abs/0811.1429) (2008), <http://www-public.slac.stanford.edu/sciDoc/docMeta.aspx?slacPubNumber=SLAC-PUB-14714>.
- [1541] R. J. Dowdall, C. T. H. Davies, G. P. Lepage, and C. McNeile, Phys. Rev. **D88**, 074504 (2013), [arXiv:1303.1670 \[hep-lat\]](https://arxiv.org/abs/1303.1670).
- [1542] N. Carrasco *et al.*, Phys. Rev. **D91**, 054507 (2015), [arXiv:1411.7908 \[hep-lat\]](https://arxiv.org/abs/1411.7908).
- [1543] A. Bazavov *et al.*, Phys. Rev. **D98**, 074512 (2018), [arXiv:1712.09262 \[hep-lat\]](https://arxiv.org/abs/1712.09262).
- [1544] V. Cirigliano and H. Neufeld, Phys. Lett. **B700**, 7 (2011), [arXiv:1102.0563 \[hep-ph\]](https://arxiv.org/abs/1102.0563).
- [1545] W. J. Marciano, Phys. Rev. Lett. **93**, 231803 (2004), [arXiv:hep-ph/0402299](https://arxiv.org/abs/hep-ph/0402299).
- [1546] Fermilab Lattice, MILC collaboration, A. Bazavov *et al.*, Phys. Rev. **D90**, 074509 (2014), [arXiv:1407.3772 \[hep-lat\]](https://arxiv.org/abs/1407.3772).
- [1547] J. L. Rosner, S. Stone, and R. S. Van de Water, [arXiv:1509.02220 \[hep-ph\]](https://arxiv.org/abs/1509.02220) (2015).
- [1548] P. J. Mohr, D. B. Newell, and B. N. Taylor, Rev. Mod. Phys. **88**, 035009 (2016), [arXiv:1507.07956](https://arxiv.org/abs/1507.07956).
- [1549] M. Jamin, A. Pich, and J. Portoles, Phys. Lett. **B664**, 78 (2008), [arXiv:0803.1786 \[hep-ph\]](https://arxiv.org/abs/0803.1786).

- [1550] M. Antonelli, V. Cirigliano, A. Lusiani, and E. Passemar, JHEP **10**, 070 (2013), [arXiv:1304.8134 \[hep-ph\]](https://arxiv.org/abs/1304.8134).
- [1551] R. J. Hudspith, R. Lewis, K. Maltman, and J. Zanotti, Phys. Lett. **B781**, 206–212 (2018), [arXiv:1702.01767 \[hep-ph\]](https://arxiv.org/abs/1702.01767).
- [1552] RBC, UKQCD collaboration, P. Boyle, R. J. Hudspith, T. Izubuchi, A. Jüttner, C. Lehner, R. Lewis, K. Maltman, H. Ohki, A. Portelli, and M. Spraggs, Phys. Rev. Lett. **121**, 202003 (2018), [arXiv:1803.07228 \[hep-lat\]](https://arxiv.org/abs/1803.07228).
- [1553] A. L. Read, J. Phys. **G28**, 2693 (2002).
- [1554] S. Banerjee, B. Pietrzyk, J. M. Roney, and Z. Was, Phys. Rev. **D77**, 054012 (2008), [arXiv:0706.3235 \[hep-ph\]](https://arxiv.org/abs/0706.3235).
- [1555] CDF collaboration, CDF note 8128, 2007, http://www-cdf.fnal.gov/physics/statistics/notes/cdf8128_mclimit_csm_v2.pdf.
- [1556] BABAR collaboration, B. Aubert *et al.*, Phys. Rev. Lett. **104**, 021802 (2010), [arXiv:0908.2381 \[hep-ex\]](https://arxiv.org/abs/0908.2381).
- [1557] Belle collaboration, K. Hayasaka *et al.*, Phys. Lett. **B666**, 16 (2008), [arXiv:0705.0650 \[hep-ex\]](https://arxiv.org/abs/0705.0650).
- [1558] BABAR collaboration, B. Aubert *et al.*, Phys. Rev. Lett. **98**, 061803 (2007), [arXiv:hep-ex/0610067 \[hep-ex\]](https://arxiv.org/abs/hep-ex/0610067).
- [1559] Belle collaboration, Y. Miyazaki *et al.*, Phys. Lett. **B648**, 341 (2007), [arXiv:hep-ex/0703009 \[hep-ex\]](https://arxiv.org/abs/hep-ex/0703009).
- [1560] BABAR collaboration, B. Aubert *et al.*, Phys. Rev. **D79**, 012004 (2009), [arXiv:0812.3804 \[hep-ex\]](https://arxiv.org/abs/0812.3804).
- [1561] Belle collaboration, Y. Miyazaki *et al.*, Phys. Lett. **B692**, 4 (2010), [arXiv:1003.1183 \[hep-ex\]](https://arxiv.org/abs/1003.1183).
- [1562] BABAR collaboration, B. Aubert *et al.*, Phys. Rev. Lett. **103**, 021801 (2009), [arXiv:0904.0339 \[hep-ex\]](https://arxiv.org/abs/0904.0339).
- [1563] Belle collaboration, Y. Miyazaki, Phys. Lett. **B699**, 251 (2011), [arXiv:1101.0755 \[hep-ex\]](https://arxiv.org/abs/1101.0755).
- [1564] BABAR collaboration, B. Aubert *et al.*, Phys. Rev. Lett. **100**, 071802 (2008), [arXiv:0711.0980 \[hep-ex\]](https://arxiv.org/abs/0711.0980).
- [1565] Belle collaboration, Y. Miyazaki *et al.*, Phys. Lett. **B672**, 317 (2009), [arXiv:0810.3519 \[hep-ex\]](https://arxiv.org/abs/0810.3519).
- [1566] BABAR collaboration, J. P. Lees *et al.*, Phys. Rev. **D81**, 111101 (2010), [arXiv:1002.4550 \[hep-ex\]](https://arxiv.org/abs/1002.4550).
- [1567] Belle collaboration, K. Hayasaka *et al.*, Phys. Lett. **B687**, 139 (2010), [arXiv:1001.3221 \[hep-ex\]](https://arxiv.org/abs/1001.3221).
- [1568] ATLAS collaboration, G. Aad *et al.*, Eur. Phys. J. **C76**, 232 (2016), [arXiv:1601.03567 \[hep-ex\]](https://arxiv.org/abs/1601.03567).

- [1569] LHCb collaboration, R. Aaij *et al.*, JHEP **02**, 121 (2015), arXiv:1409.8548 [hep-ex].
- [1570] *BABAR* collaboration, B. Aubert *et al.*, Phys. Rev. Lett. **95**, 191801 (2005), arXiv:hep-ex/0506066 [hep-ex].
- [1571] Belle collaboration, Y. Miyazaki *et al.*, Phys. Lett. **B719**, 346 (2013), arXiv:1206.5595 [hep-ex].
- [1572] Belle collaboration, Y. Miyazaki *et al.*, Phys. Lett. **B632**, 51 (2006), arXiv:hep-ex/0508044 [hep-ex].
- [1573] LHCb collaboration, R. Aaij *et al.*, Phys. Lett. **B724**, 36 (2013), arXiv:1304.4518 [hep-ex].